

**Antagonizing the Adhesion of Type 1 Fimbriae-
Mediated *Escherichia coli* – A Novel Therapy for
Urinary Tract Infections**

Inauguraldissertation

zur

Erlangung der Würde eines Doktors der Philosophie

vorgelegt der

Philosophisch-Naturwissenschaftlichen Fakultät

der Universität Basel

von

Lijuan Pang

aus Beijing, China

Basel, 2015

Genehmigt von der Philosophisch-Naturwissenschaftlichen Fakultät

auf Antrag von:

Prof. Dr. Beat Ernst, Institut für Molekulare Pharmazie, Universität Basel,
Klingelbergstrasse 50/70, CH-4055 Basel

Prof. Dr. Armin Buschauer, Institut für Pharmazie, Pharm./Med. Chem. II, Universität
Regensburg, D-93040 Regensburg, Germany

Basel, den 25 März 2014

Signature of the Faculty Representative

Prof. Dr. Jörg Schibler
The Dean of Faculty

Acknowledgements

First of all I would like to thank Prof. Dr. Beat Ernst for giving me the great opportunity to do my doctoral dissertation in his group, and for his confidence and long-term supports during my work on the fascinating projects.

I further would like to thank Prof. Dr. Armin Buschauer for accepting to be the co-referee of my thesis.

I would also like to especially thank Bea Wagner, Claudia Huber, Gabi Lichtenhahn, Dr. Oliver Schwardt, Dr. Said Rabbani, Dr. Brian Cutting, and Dr. Brigitte Fiege for their administrative and technical supports in the last four years.

Many thanks to all current and former members of the Institute of Molecular Pharmacy for the great working atmosphere, the outstanding research environment, and everyday help and support during my PhD study. I had the great pleasure to work with many excellent group members on the FimH project, thank Dr. Xiaohua Jiang, Dr. Simon Kleeb, Dr. Adam Zalewski, Jacqueline Bezencon, Deniz Eris, Pascal Zihlmann, Dr. Sameh Eid, Dr. Katrin Lemme, Dr. Meike Scharenberg, Dr. Daniela Abgottspon, and Dr. Martin Smiesko for giving me so much information and support to my work. Furthermore, I would like to thank the members of Lab4007, Mirko, Kathi, Florian, Norbert and Blijke, for the enjoyable working environment and their kind help and support. Thanks to all the rest group members for the wonderful time we spent together in and outside the institute.

Additionally, I would like to thank the Association of Chinese Students and Scholars in Basel for providing me the opportunities to attend the fantastic events and to meet many new friends in Switzerland. I want to thank my friends Yingsi, Zhenquan, Yanlei, Shyanhuey, Irene, Eva, Ken, Valentina, especially Xiaohua and her family, Laura and her family, Jiayun and her family for the many good memories.

Finally, I would like to thank my parents who always believe in me and support me. Many thanks to my dearest husband Dr. Fan Yang for being with me through all the good and tough times.

Abstract

Urinary tract infections (UTIs), primarily caused by uropathogenic *E. coli* (UPEC), affect millions of people and account for significant morbidity and high medical costs. The key step in the pathogenesis of UTIs is the bacterial adhesion to urothelial cells, which is mediated by the virulence factor FimH located on type 1 pili. Blocking FimH and therefore the adhesion with FimH antagonists offers a new therapeutic approach for the prevention and treatment of UTIs. However, the antagonists developed so far have hardly met the requirements for clinical applications due to poor pharmacokinetic (PK) properties. In vivo studies indicated that with biphenyl α -D-mannosides as FimH antagonists, high doses were necessary to achieve the minimal concentrations required for anti-adhesive effects in the bladder. Additionally, the binding mode of an antagonist to the carbohydrate recognition domain of FimH can switch from an “in-docking mode” to an “out-docking mode”, depending on the structure of the antagonist. Further studies indicated that the existence of the high- and low-affinity state of FimH could complicate the binding affinity.

To achieve oral bioavailability, to improve binding affinity, and to explore the binding mode, we chemically modified the biphenyl FimH antagonists with diverse strategies. To establish the designed compound libraries, traditional synthesis and dynamic combinatorial techniques were applied. The binding affinity and the thermodynamic profile of the antagonists were evaluated by a cell-free competitive binding assay, a competitive fluorescence polarization assay, a cell-based flow cytometry assay, and isothermal titration calorimetry (ITC). Furthermore, the PK properties were determined by in vitro and in vivo assays. As results, structure-activity and structure-property relationships were established for structurally diversified FimH antagonists. The reported strategies led to FimH antagonists with significantly improved PD/PK profile regarding effectiveness of the anti-adhesive treatment.

Abbreviations

AcOH	acetic acid
ADMET	absorption, distribution, metabolism, excretion, toxicity
aq.	aqueous
AUC	area under the curve
BBB	blood brain barrier
BSA	bovine serum albumin
Caco-2	cells human colorectal adenocarcinoma cells
DCC	dynamic combinatorial chemistry
DCL	dynamic combinatorial library
DCM	dichloromethane
CES	carboxylesterase
CL'_{int}	intrinsic clearance
CRD	carbohydrate recognition domain
<i>D</i>	distribution coefficient
DIBAL-H	diisobutylaluminium hydride
DMAP	4-dimethylaminopyridine
DME	dimethoxyethane
DMF	<i>N,N</i> -dimethylformamide
DMSO	dimethylsulfoxide
HEPES	4-(2-hydroxyethyl)-1-piperazineethanesulfonic acid
HPLC	high performance liquid chromatography
Hz	Hertz
IC ₅₀	half maximal inhibitory concentration
K_a	acid dissociation constant
LC-MS	liquid chromatography-mass spectrometry
Log <i>P</i>	octanol-water partition coefficient

Me	methyl
MeCN	acetonitrile
MeOH	methanol
MP	melting point
NaOH	sodium hydroxide
μ W	microwave irradiation
NMR	nuclear magnetic resonance
PAMPA	parallel artificial membrane permeability assay
P_{app}	apparent permeability
PDB	protein data bank
P_e	effective permeability
PPB	plasma protein binding
PSA	polar surface area
RLM	rat liver microsomes
rIC ₅₀	relative IC ₅₀
RT	room temperature
<i>S</i>	solubility
Sat.	Saturated
$t_{1/2}$	half-life
TBAF	tert-butyl ammonium fluoride
Tf	triflate (Trifluoromethanesulfonate)
TFA	trifluoroacetic acid
THF	tetrahydrofuran
TRIS	tris(hydroxymethyl)aminomethane
TLC	thin-layer chromatography
UPEC	uropathogenic Escherichia coli
UTI	urinary tract infection

Table of Contents

<i>Chapter 1. Introduction</i>	1
1.1 Urinary tract infection	
1	
1.1.1 Infection cycle of UPEC	2
1.1.2 Uropathogenic agent – type 1 fimbria (pilus)	2
1.2 Anti-adhesive therapy	3
1.3 The bacterial adhesin FimH	4
1.3.1 FimH catch bonds	4
1.3.2 Natural ligands for FimH	6
1.3.3 FimH CRD	7
1.4 FimH antagonists	9
1.5 Pharmacokinetic aspects	11
1.6 Protein-directed dynamic combinatorial chemistry	13
1.7 Aims of this thesis	14
<i>Chapter 2. Results and Discussion</i>	30
2.1 Outline	30
2.2 FimH antagonists for the oral treatment of urinary tract infections: from design and synthesis to in vitro and in vivo evaluation (Paper 1)	34
2.3 FimH antagonists: structure-activity and structure-property relationships for biphenyl α -D-mannopyranosides (Paper 2)	50
2.4 FimH antagonists: bioisosteres to improve the in vitro and in vivo PK/PD profile (Paper 3)	170
2.5 Manuscript: FimH antagonists – solubility vs. oral availability (Manuscript)	222
2.6 Kinetic properties of carbohydrate – lectin interactions: FimH antagonists (Paper 4)	342
2.7 Combinatorial library screening of FimH antagonists: an application of protein-directed dynamic strategy	354
2.7.1 Introduction	355
2.7.2 <i>In silico</i> docking and structural design	357
2.7.3 Chemical synthesis	359
2.7.4 Biological evaluation	363

2.7.5 Dynamic combinatorial screening	366
2.7.6 Conclusion	372
2.7.7 Experimental section	373
2.8 Synthesis and evaluation of 6-modified mannosides as FimH antagonists	407
2.8.1 Introduction	408
2.8.2 Chemical synthesis	409
2.8.3 Structural characterization - Mosher's analysis	411
2.8.4 Biological evaluation	412
2.8.5 Conclusion	413
2.8.6 Experimental section	413
<i>Chapter 3. Summary and Outlook</i>	424
<i>Chapter 4. Formula Index</i>	427
<i>Chapter 5. Curriculum Vitae</i>	433

1. Introduction

1.1 Urinary tract infection

Urinary tract infection (UTI), among the most prevalent infectious diseases worldwide, affects millions of people and accounts for significant morbidity and high medical costs each year.¹⁻³ About 50% of women will experience a UTI at some points in their life and about 60% of them will experience recurrent infections within six months following the treatment of initial UTIs.^{4, 5} The leading cause of UTI is gram-negative uropathogenic *Escherichia coli* (UPEC), which make up to 90% of all diagnosed UTIs.^{6, 7} About 5-15% of UTIs are caused by *Staphylococcus saprophyticus*,⁸ and only a small number is caused by *Klebsiella pneumoniae* or *Proteus mirabilis*.³ Clinically, it is known as cystitis (a bladder infection) when UTI affects lower urinary tract, and it is known as pyelonephritis (a kidney infection) when UTI affects upper urinary tract.⁹ For uncomplicated lower urinary tract infections, the first-line treatment is a three-day treatment with trimethoprim, trimethoprim-sulfamethoxazole (TMP/SMX) or a fluoroquinolone (e.g. ciprofloxacin).^{10,}

¹¹ For pyelonephritis, more aggressive treatment has to be applied by using longer course of oral/intravenous antibiotics.¹² However, recurrent infections of UPEC with repeated antibiotic exposure often lead to the emergence of multi-drug resistance, and consequently to treatment failure.¹³⁻¹⁵ Since the number of antibiotics is limited and the antibiotic resistance of UPEC is increasing,^{16, 17} a novel approach for the prevention and treatment of UTI is urgently needed.

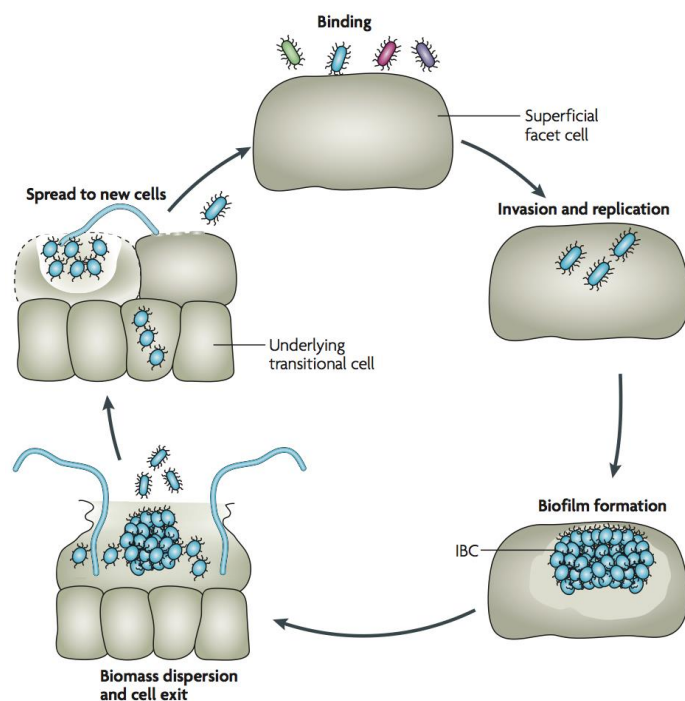


Figure 1.1. Infection cycle of uropathogenic *E. coli* (UPEC) in the lower urinary tract (adopted from Ref.7)

1.1.1 Infection cycle of UPEC

The infection cycle of UPEC involves a well-defined multi-step cascade examined in mouse cystitis models and human UTIs (Figure 1.1).¹⁸⁻²² Virtually all clinical UPEC isolates express type 1 fimbriae (pili).²³ In the initial step of infection, the pili bind to mannoseylated glycoprotein receptors, mainly uroplakin-Ia (UPIa), on the surface of urinary bladder mucosa.^{24, 25} This adhesion prevents UPEC from being removed by the flow of urine and initiates the invasion of bacteria into the bladder epithelial cells.^{19, 26} After entering the host cells, UPEC start replicating to form biofilm-like intracellular bacterial community (IBC), which can protect them from antibiotics treatment and host innate immune responses.^{18, 27} After an acute infection, UPEC can persist for many weeks to months in a quiescent bladder reservoir, regardless the antibiotic treatment, and re-emerge to cause recurrent UTIs.^{28, 29} Eventually, UPEC detach and disperse from the IBC to initiate a new round of infection in other cells. Some of the dispersing UPEC can form filaments, invade neutrophil phagocytosis and facilitate bacteria survival.^{20, 21}

1.1.2 Uropathogenic agent – type 1 fimbria (pilus)

Type 1 fimbriae (pili) are expressed by a large number of *E. coli* strains, and are found in more than 95% of *E. coli* isolates from intestinal and extra-intestinal infections.^{23, 30} Pili act as highly efficient adhesion tools for bacterial inhabiting in diverse environments, including biotic and abiotic surfaces.³¹⁻³³

On the surface of UPEC, type 1 pili are uniformly distributed, commonly 100 to 400 per cell.³⁴ Structurally, type 1 pili are 7 nm wide and several

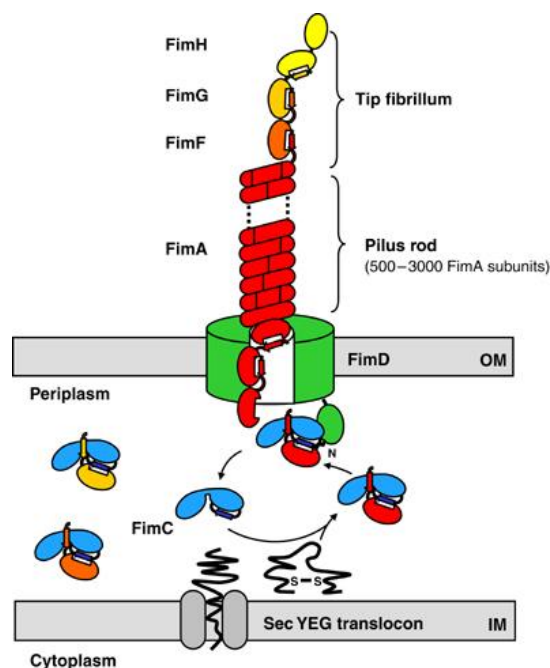


Figure 1.2. Schematic representation of type 1 pilus and its assembly through the chaperone-usher pathway (adopted from Ref.36). Pilus subunits are assembled via “donor strand exchange”, in which the immunoglobulin-like fold is completed by the insertion of an anti-parallel β -sheet of the following subunit.

micrometers long rod-like fibers (Figure 1.2).^{35, 36} The pili rods are composed of immunoglobulin like (Ig) FimA pilin subunits that are anchored into a chain, and the chain is further coiled into a helix.^{37, 38} FimA helix is joined to a short 3 nm thick distal tip fibrillum that consists of two adaptor proteins, FimF and FimG. At the tip of each pilus is a single mannose-specific adhesin – FimH. The pilus rod is assembled by the chaperone/usher pathway³⁹⁻⁴¹ and in their mature form the Ig fold of each subunit is completed by an amino-terminal extension from a neighboring subunit in a process termed “donor-strand exchange” (Figure 1.2).^{36, 42, 43}

1.2 Anti-adhesive therapy

More than three decades ago, Sharon and his co-workers reported the first sugar anti-adhesive study on protecting animals against experimental infection in a UTI mouse model.⁴⁴ They found that co-administration of methyl α -D-mannoside with type 1 fimbriated *E. coli* into the urinary bladder of the mice reduced the rate of UTI by two thirds, while methyl α -D-glucoside, which is not a ligand of lectin FimH, was not effective. Since the first attachment is a crucial step in the colonization of pathogenic bacteria, blocking lectins with carbohydrates or analogues thereof prevents the bacterial adhesion to host cells and therefore offers a potential therapeutic approach for prevention and treatment of UTIs (Figure 1.3).³⁴

The validity of this approach has been further demonstrated in a variety of studies with different pathogenic bacteria and animals.^{32, 45-48} Since anti-adhesive carbohydrate or analogues do not function by killing or interfering the growth of the pathogens, the bacterial strains are unlikely to emerge resistance to such agents.⁴⁹

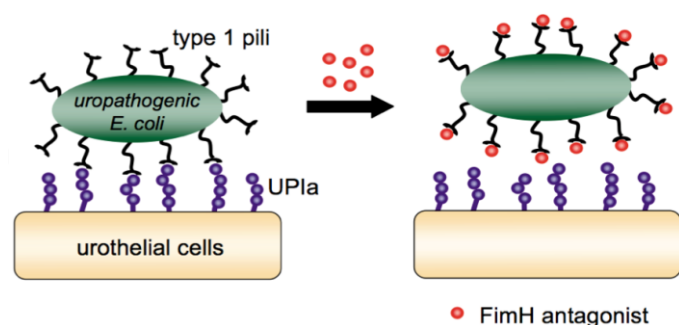


Figure 1.3. The illustration of anti-adhesive therapy with FimH antagonists (adopted from Ref. 46). In the presence of FimH antagonists, UPEC cannot attach to urothelial cells and are therefore being washed away by a bulk flow of urine. As a consequence, the infection cycle cannot be established.

Therefore, the inhibition of bacterial adhesion by FimH antagonists provides a promising approach to tackle the issues of the current antibiotic treatments.

1.3 The bacterial adhesin FimH

The adhesin FimH (M.W. 29 KDa), located at the tip of type 1 pilus, consists two Ig-like domains: the lectin domain (residues 1-156) at the N-terminus, which contains the carbohydrate recognition domain (CRD), and the pilin domain (residues 160-279), which connects FimH to the pilus rod and regulates the switch between high- and low-affinity states of the lectin domain.⁵⁰⁻⁵²

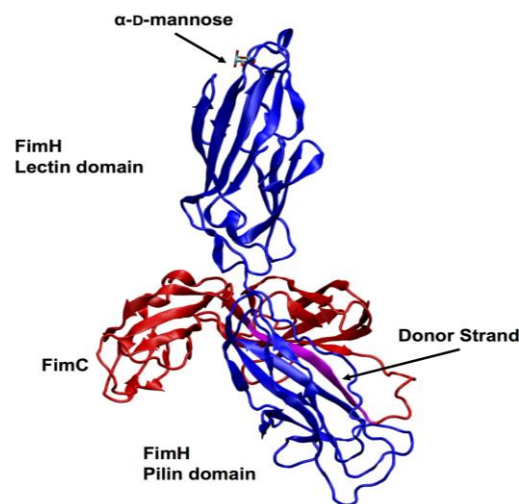


Figure 1.4. Structure of FimH_{LD}-FimH_{PD}-FimC in complex with D-mannose (PDB code 1KLF).⁵² FimH (blue) is wedged apart by FimC (red), which provides the donor strand (magenta). The carbohydrate-binding site is located at the very tip of FimH.

While the lectin domain alone is stable, the full-length FimH in solution is only stable in presence of FimC. The first structure of FimC-FimH complex was solved in 1999,⁵⁰ and three years later Hung and his coworkers reported the first co-crystallized structure of FimC-FimH with a mannose ligand (Figure 1.4, PDB code 1KLF),⁵² which gave important insight into the binding site. Later, numerous structures of the FimH lectin domain alone or in complex with diverse mannoside ligands were published,^{51, 53-56} greatly facilitating the discovery of high-affinity FimH antagonists for the treatment of UTIs.

1.3.1 FimH catch bonds

The term “catch bonds”, first proposed in 1988, has been defined as a stronger or longer-lived molecular interaction under tensile mechanical forces.⁵⁷ Recently, catch bonds were observed with two types of adhesive proteins, selectins and FimH.^{58, 59} Further flow chamber assays⁶⁰⁻⁶³ and atomic force microscopy (AFM) studies⁶⁴ experimentally supported the allosteric catch bond for FimH. However, the structural mechanism of FimH catch bond behavior was just a putative model until recently the crystal structure of native full-length FimH was published.⁵¹

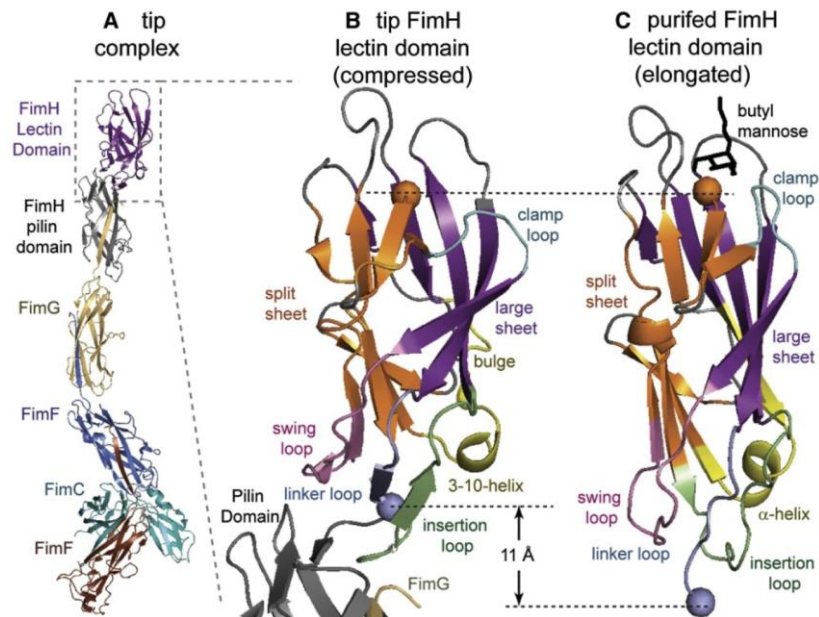


Figure 1.5. Structure of lectin FimH integrated in the fimbrial tips (A). In the fimbrial tips the lectin domain of FimH is docked to the pilin domain (black) (B) and this causes conformational changes across a large-sheet (violet) that makes the lectin domain more compressed and the mannose-binding pocket wider, than it is seen in the isolated lectin domain bound to butyl mannoside (black) (C). (Picture adopted from Ref.51)

The crystal structure elucidates that the pilin domain of FimH, which anchors the lectin to the fimbrial shaft, interacts with the lectin domain such that a twist in its β -sandwich fold is caused (Figure 1.5).⁵¹ The twisted β -sheet loosens the mannose-binding pocket of FimH, which is located on the opposite end of the lectin domain, thus leading to a low-affinity state of the lectin. When tensile forces are applied, the pilin and lectin domains separate, and the lectin domain untwists and elongates, resulting in a tight mannose-binding pocket therefore a high-affinity state of FimH. This mechanism, as summarized in Figure 1.6, has been called as “page-turning” mechanism, which forms the basis of an allosteric regulation in the ligand-receptor interaction under mechanical forces.⁵¹

Furthermore, it has been found that the purified lectin domain is in the elongated high-affinity conformation regardless of the presence of mannose (Figure 1.5, C). When the FimH lectin domain is included in the fimbrial tip, it is maintained in the compressed low-affinity conformation without mannose, but can switch to the elongated high-affinity conformation upon binding to ligand.⁶⁵ However, this ligand-induced change might not

occur every time, and when it does occur, the change is transient because the pilin domain can re-dock and cause the reversion to the compressed conformation (Figure 1.5, B). In this case, FimH affinity and bond lifetime would remain low.⁵¹

In natural environment, bacteria have to combat ubiquitous shear forces in order to successfully establish adhesion to their host cells. Therefore, catch bonds provide a way for bacteria to stabilize their attachment, particularly in the presence of flowing fluid.⁶⁶ Based on evolutionary analysis, more weakly binding variants, such as FimH from *E. coli* F18, are evolutionarily predominant, suggesting that allosteric inhibition and corresponding catch-bond behavior could be beneficial for bacterial transmission or survival.⁶⁶ Moreover, physiological advantage of allosteric catch-bond adhesion could include resistance to soluble inhibitors^{58, 61}, and rapid surface colonization.⁶⁷

1.3.2 Natural ligands for FimH

As stated above, FimH mediates the adhesion of UPEC by interacting with the high-mannosylated glycoprotein receptors, among which are uroplakin Ia (UPIa),²⁵ Tamm-Horsfall glycoprotein (THP)⁶⁸ and β 1- and α 3-integrins.⁶⁹ UPIa is a major glycoprotein existing on the large superficial epithelial cells in the bladder.⁷⁰ Mouse UPIa4 presents high mannose glycans on Asn169 with a heterogeneity ranging from $\text{Man}_6\text{GlcNAc}_2$ to $\text{Man}_9\text{GlcNAc}_2$.²⁴ The same high-mannose type glycans decorate β 1- and α 3-integrins.⁷¹ THP is secreted in the urine as a natural inhibitor of type 1-mediated bacterial adhesion

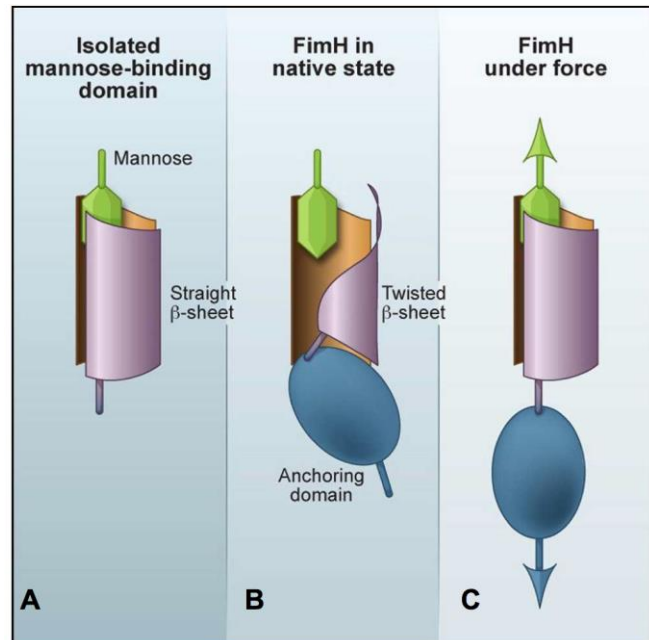


Figure 1.6. Schematic representation of FimH catch-bond behavior (adopted from the graphic abstract of Ref 51). A) The conformation of the isolated lectin domain of FimH (violet) exhibits a high-affinity state of FimH. B) The native interaction of the pilin domain and the lectin domain of FimH induces β -sheet twisting therefore a low-affinity state of FimH. C) Shear force-induced untwisting in the mannose-binding domain of FimH enables FimH to bind mannose more strongly *via* catch bonds.

through its high-mannosylated Asn251 residue.^{72, 73}

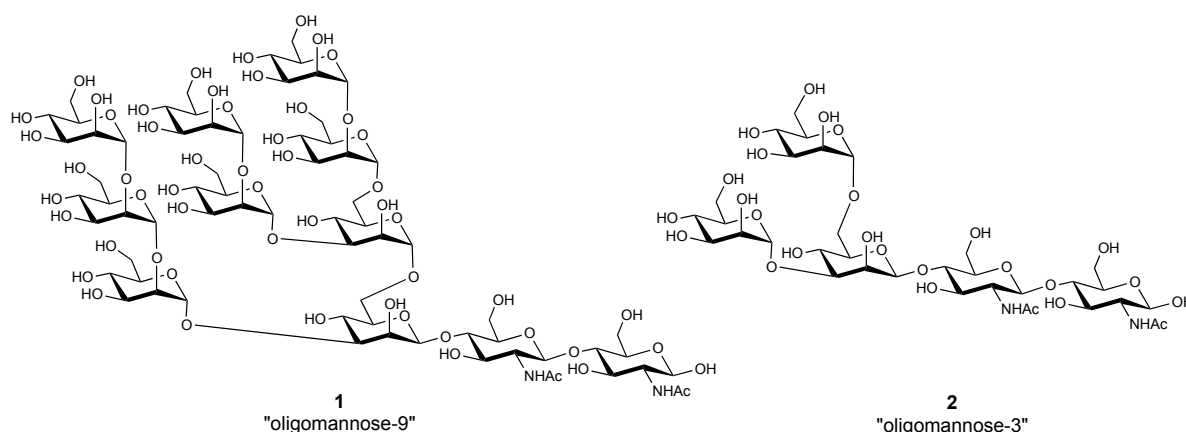


Figure 1.7. The structures of oligomannose-9 (**1**) and oligomannose-3 (**2**), as a part of the glycoprotein uroplakin Ia (UPIa) presented on urothelial cells, represent the natural ligands of FimH.

Previous epitope mapping on high-mannose glycan receptors revealed high affinity of the FimH receptor-binding domain for oligomannose-3, a part of the high mannose glycan.⁷⁴ Thermodynamics of FimH binding were determined for oligomannose-9 and oligomannose-3 (**1**, **2** respectively, in Figure 1.7) by surface plasmon resonance (SPR) solution affinity measurements, which showed a higher affinity of **2** (K_d 20 nM) than **1** (K_d 420 nM).⁵⁴ The data are in accordance with the early studies carried out by Sharon and co-workers.⁷⁵ Further studies indicated that the chitobiose unit that bridges the mannosides to the asparagines in the Asn-X-Ser/Thr motif of the glycoprotein receptor contributes significantly to the interaction with FimH.⁷⁴

1.3.3 FimH CRD

Crystal structures of lectins provide important insights into the binding modes of interactions that mediate carbohydrate recognition.^{76, 77} Frequently, it has been observed that the lectin with a carbohydrate ligand is complexed in a well-defined network of hydrogen bonds, involving hydrogen-bond donors and acceptors of the ligand and the side chains of asparagine or glutamine residues, carboxylate groups from aspartates or glutamates, hydroxyl groups in serine side chains and amino groups from lysine, tryptophan or histidine residues of the lectin carbohydrate recognition domain (CRD). Water molecules can mediate the hydrogen bonding between carbohydrates and the

protein surface. In some cases divalent metal ions, such as Ca^{2+} or Mn^{2+} , are also involved in carbohydrate binding, e.g. Ca^{2+} stabilizes the binding site of C-type lectins and fix the positions of amino acids that interact with sugar ligands. Additionally, carbohydrate ligand can be sandwiched between aromatic amino acid side chains, leading to a relevant contribution of CH- π interaction and improved binding affinity.

Since the first crystal structure of FimH was solved in 1999,⁵⁰ numerous crystallographic studies on FimH CRD have been reported. The crystal structure of the FimC/FimH chaperone-adhesin complexed with α -D-mannose (PDB code 1KLF, Figure 1.4), reported by Hung and co-workers, revealed the crucial amino acids for mannose recognition in great details.⁵² More recently, the reported structure of FimH co-crystallized with *n*-butyl α -D-mannopyranoside⁵³ (PDB

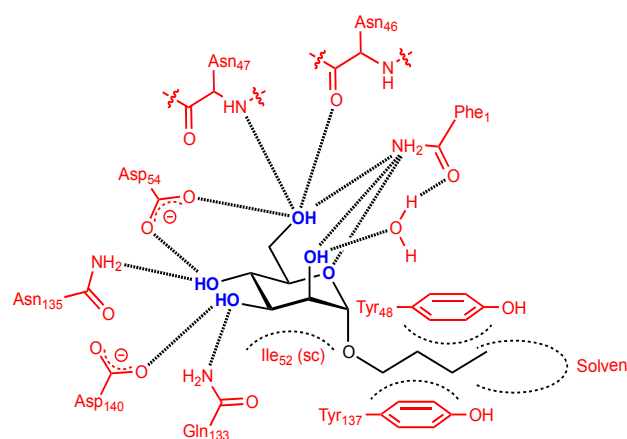


Figure 1.8. Schematic representation of the binding site of *n*-butyl α -D-mannopyranoside according to X-ray crystallography (PDB code 1UWF⁴⁷, picture provided by Dr. Roland C. Preston).

code 1UWF, Figure 1.8) represented the main features of FimH CRD-ligand interaction, and also revealed the importance of the hydrophobic interaction between the alkyl aglycone and the binding site. Being accommodated in a deep and negatively charged pocket, the mannose makes ten direct hydrogen bonds to the mannose binding site as well as indirect water-mediated hydrogen bonds. All hydroxyl groups on mannose, except the one at the anomeric position, interact extensively with FimH CRD, especially with residues Phe1, Asn46, Asp47, Asp54, Gln133, Asn135, and Asp140 (as shown in Figure 1.8). Additionally, the entrance of the binding site, formed by three hydrophobic amino acids (Tyr48, Ile52, Tyr137), referred to as the “tyrosine gate”, can host aliphatic and aromatic aglycones and provide hydrophobic interactions.^{52, 55, 74, 78, 79} Above observations further lightened the way for the development of carbohydrate ligands as anti-adhesive therapeutics.

1.4 FimH antagonists

As numerous crystal structures of type 1 fimbrial lectin FimH became available, a rational, computer-aided design of FimH antagonists for the inhibition of bacterial adhesion to mucosal surfaces has been largely facilitated. So far, the reported rational studies lead to three classes of FimH antagonists: (i) long-chain alkyl mannosides,⁵³ (ii) mannosides with substituted aromatic aglycone moieties,⁸⁰ and (iii) mannosides with extended aglycone moieties.^{32, 45, 47, 56, 78, 79, 81-84}

Since the anti-adhesion affinity of methyl α -D-mannoside (**3**, Figure 1.9) was identified in micro-^{53, 85-87} to millimolar^{80, 88} range, most drug discovery studies for FimH antagonists have been focusing on affinity improvement by modifying the aglycones of α -D-mannosides. In 2005, Bouckaert and co-workers reported a series of alkyl α -D-mannosides as potent FimH antagonists.⁵³ Van der Waals contacts of the alkyl chain to the phenyl rings of the lectin's "tyrosine gate" (Tyr48, Tyr 137 and Ile52) were found in the crystal structure of butyl α -D-mannoside complexed with FimH-CRD (Figure 1.8). Compared with the crystal structure of oligomannose-3 in complex with FimH, the butyl chain mimics the hydrophobic face of oligomannose-3, therefore, maintains the binding affinity.⁵⁴ Additionally, the affinity of alkyl α -D-mannosides for FimH increases with the length of the alkyl aglycone; as a result, the optimal length of the alkyl chain was found to be seven carbon atoms. Later, the high affinity of heptyl α -D-mannoside (**4**, Figure 1.9) was also demonstrated in other studies.^{45, 47, 83, 86, 89-91}

Other than alkyl aglycones, aromatic aglycones were designed to reach the hydrophobic rim at the entrance of the FimH binding site. As early as 1980s, aromatic aglycone moieties were found to be able to enhance the affinity of the respective mannosides for FimH by a factor of 600 or more.⁸⁰ Such findings could also be rationalized on the basis of the FimH crystal structures, i.e. the π - π stacking of the aromatic ring with the amino acid side chains of Tyr48 and Tyr137 of the binding site improves the binding affinity of carbohydrate ligands.⁵⁶ Furthermore, a favorable effect of *o*-substitution on the aromatic ring was also observed, as introduction of a chlorine in the *ortho* position of the phenyl ring (**5a** \rightarrow **5b**, Figure 1.9) increased the affinity by a factor of 10,⁸⁰ and further evidence

were also found with extended aromatic aglycones (**6e-f** and **8**, Figure 1.9).^{45, 79, 83}

As stated above, the crystal structure of butyl α -D-mannoside with FimH shows the interactions of the alkyl aglycone with both Tyr48 and Tyr137 of the tyrosine gate,⁵³ which is termed as “in-docking mode” (Figure 1.10, Left).⁸² Whereas an unexpected docking mode was discovered upon co-crystallization of FimH with biphenyl mannoside **6a** (Figure 1.9),⁵⁶ a representative of FimH antagonists with extended aromatic aglycones. As shown in the crystal structure of FimH with **6a** (Figure 1.10, Right),⁵⁶ the biphenyl aglycone adopts an “out-docking mode”⁸²; that is, it interacts only with Tyr48, probably due to insufficient flexibility; π - π stacking of the outer aromatic ring of the biphenyl aglycone with Tyr48 is effected by induced fit, causing a substantial movement of Tyr48. *In silico* docking studies with biphenyl derivatives also suggested a similar “out-docking mode”.⁸³ Further stabilization of the protein-ligand complex by a polar interaction between the ester in the *meta* position of mannoside and the side chain of Arg98 was also proposed.⁵⁶ Further studies on FimH antagonists with extended aromatic moieties lead to a series of modified biphenyl (**6b-f**, Figure 1.9),^{32, 48, 83, 84} indolinyphenyl⁴⁷ (**7**, Figure 1.9) and squaric acid^{92, 93} (**8**, Figure 1.9) derivatives, showing the affinities in the low nanomolar range.

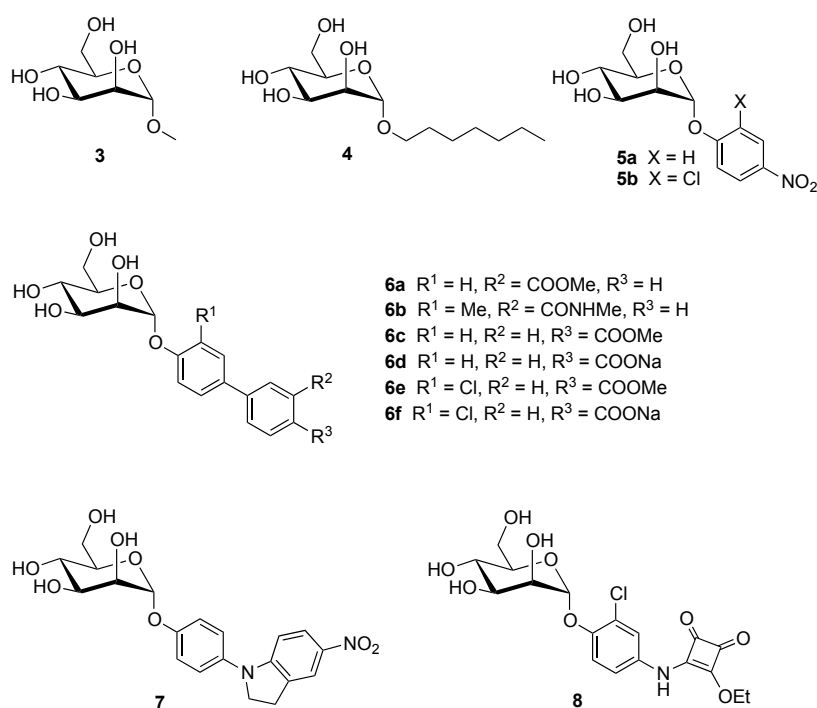


Figure 1.9. List of representatives of three classes of FimH antagonists: alkyl mannosides (**3-4**);

mannosides with aromatic aglycones (**5a-b**); mannosides with extended aglycones, including biphenyl mannosides (**6a-f**), indolinyphenyl mannoside (**7**), and squaric acid derivative (**8**).

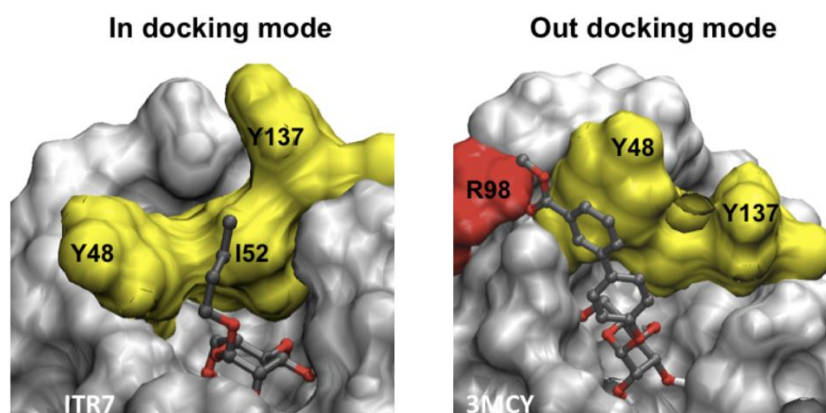


Figure 1.10. “In” and “out” docking modes of FimH antagonists. Left: crystal structure of butyl mannoside (PDB code: ITR7⁵³) bound to the FimH CRD, as a representative of “in-docking mode”. Right: crystal structure of biphenyl mannoside **6a** bound to the FimH CRD (PDB code: 3MCY⁵⁶), as a representative of “out-docking mode”.

Besides mono-valence FimH antagonists, carbohydrate-centered cluster mannosides and carbohydrate dendrimers were also developed and extensively studied for FimH inhibition. Hartmann and Imberty have summarized the recent development of glycodendrimers as FimH antagonists in their reviews.^{94, 95} Although these multi-valence mannosides have shown high affinities for FimH due to their cluster effects upon binding, their size and polarity make them unlikely exhibit drug-like properties for oral application.^{96, 97}

1.5 Pharmacokinetic aspects

The “quality” of small-molecule drug candidates, encompassing potency, selectivity and pharmacokinetic (PK) properties, is a key factor for successful *in vivo* application.⁹⁶⁻⁹⁹ Although the development of FimH antagonists traces back to the late 1980’s, only a few PK studies have been reported. Recently, Ernst and co-workers published for the first time *in vitro* and *in vivo* PK data of a series of biphenyl α -D-mannosides, which laid a foundation for further lead optimization of FimH antagonists.⁴⁵

As extensively studied, a prerequisite of oral bioavailability is intestinal absorption, which requires an optimal balance between solubility and permeability.^{100, 101} In addition,

since the target FimH is located in the bladder, metabolic stability and fast renal elimination are also required. But because intestinal absorption and renal elimination are related to opposed properties, i.e. lipophilicity for intestinal absorption and hydrophilicity for renal elimination, a prodrug approach was applied.^{45, 83} For example, with high intestinal absorption, ester **6e** was firstly hydrolyzed by esterases in the enterocytes and in the liver (“first pass”) to release the active principle, acid **6f**, which underwent fast renal elimination and reached the target FimH in the bladder to realize the therapeutic effect (Figure 1.12).⁴⁵

Although the above prodrug approach has been demonstrated the effectiveness in a UTI mouse model, the low solubility limits the dosage of the ester pro-drugs and their further *in vivo* evaluation.^{45, 83} Later, further structural modifications on FimH antagonists, such as methyl amide-substituted biphenyl **6b**⁸⁴ and indolinyphenyl **7**⁴⁷ (Figure 1.9), were carried out to increase oral bioavailability. Among these modified structures, the indolinyphenyls have shown high therapeutic potentials, resulting from optimized PK properties, and a substantial reduction of the dosage, i.e. a successful treatment of UTI with a low dosage of 1 mg/kg without any additional administration of antibiotics.⁴⁷ However, a major drawback of these indolinyphenyl antagonists is their low solubility, limiting their further *in vivo* applications.

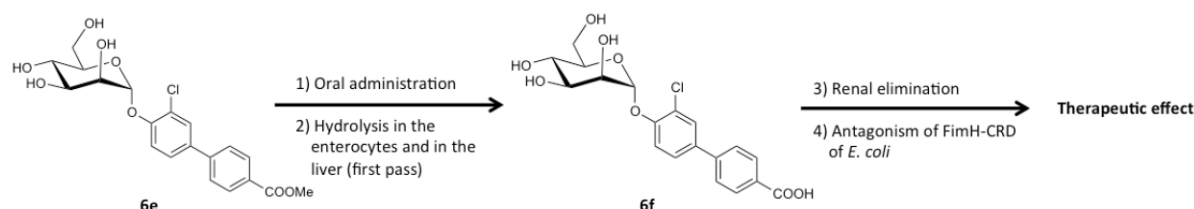


Figure 1.12. Schematic representation of the prodrug approach for the therapeutic application of FimH antagonists.⁴⁵ (1-2) After orally dosing, the ester prodrug **6e** was firstly hydrolyzed in the enterocytes and then in the liver to release the active principle **6f**. (3-4) **6f** underwent renal elimination, reached the target in the bladder and finally realized the anti-adhesive effect.

Since low-solubility of compounds could cause other problems in drug discovery, such as artificially low activity values from bioassays, development challenges for formulation, increased development time, high-dose administration and et al,^{96, 102} it became an important PK issue for the development of FimH antagonists.^{45, 47, 83} Structural modifications (e.g. disruption of the molecular planarity^{103, 104}) and appropriate formulations was considered as promising solutions.¹⁰²

1.6 Protein-directed dynamic combinatorial chemistry

Dynamic combinatorial chemistry (DCC), an emerging approach in drug discovery, produces combinatorial libraries by reversible inter-conversion of the library constituents.¹⁰⁵⁻¹⁰⁷ Virtually, DCC generates all possible combinations through reversible chemical reactions, and allows for the target-driven amplification of the active constituents, thus performing a self-screening process by which the active species is preferentially expressed (Figure 1.13). Unlike the parallel synthesis or resin-based combinatorial libraries, DCC approach doesn't require the preparation of individual compound over synthetic steps and characterization; therefore, DCC has been recognized as a fast and adaptive paradigm in modern drug discovery.¹⁰⁵

Since the first report appeared in the late 1990s,¹⁰⁸ the protein-directed DCC has been largely developed. In a protein-directed dynamic combinatorial library (DCL), the library population distribution is under thermodynamic control, therefore, the amplification of the best binder is at expense of other (nonbinding) species, generating hit structures that can be identified through analysis of the DCL population distribution. By this means, protein-directed DCC bridges the chemical synthesis and biological evaluation, meshing the two operations into a single process whereby the target protein directs the assembly of its best binder *in situ*.

Because of high sensitivity to pH, temperature and chemical reagents, proteins are challenging templates that place restraint on the optional reversible reactions.¹⁰⁵ Accordingly, the DCLs must be assembled under physiological conditions, and many of the reversible bond formations used to generate DCL, such as S-S or C=N, are fundamental to biological chemistry.^{109, 110} Furthermore, the reversible reaction used in DCC should allow the potential fixation, that is the freezing of the exchange process either by changing the surrounding conditions (e.g. pH, temperature, solvent composition), or by adding quenching reagents (e.g. oxidation/reduction reagents). In this way, the DCLs can be easily analyzed with various analytical schemes.¹¹¹

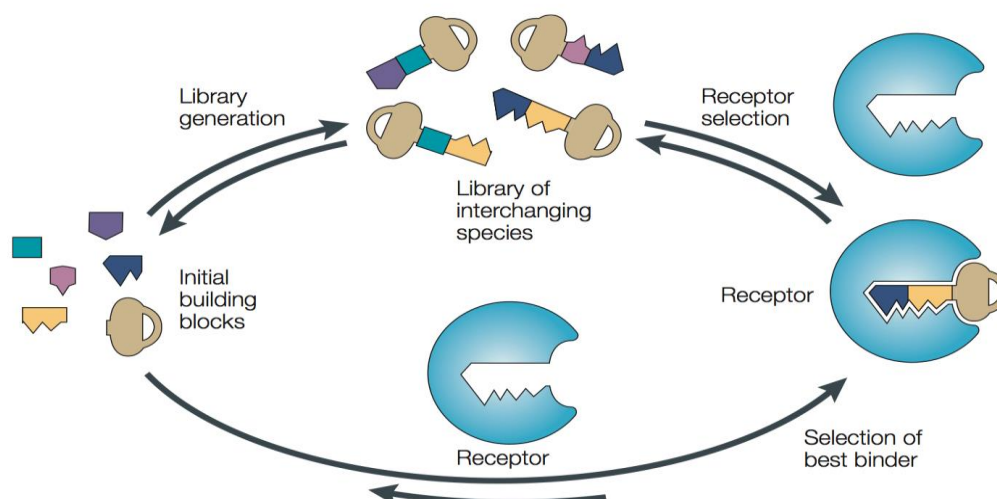


Figure 1.13. Schematic representation of the concepts behind DCC and virtual DCLs. (Figure adopted from Ref. 107) Top: a true DCL is formed through reversible exchange of initial “keys” (building blocks). A molecular “lock” (e.g. protein target) favors the best binder, forcing the DCL to rearrange to produce more of this member. Bottom: generation of a virtual DCL, the constituents of which become detectable only in the presence of the selector.

So far, the most commonly used bond formation reactions in protein-directed DCC include imine formation,^{108, 112-118} hydrazone formation¹¹⁹⁻¹²³ and disulfide bond formation.^{124, 125} Rather than attempting to review all the reported DCC cases in drug discovery, the present text focuses on the representative examples of the protein-directed DCL. As listed in Table 1 (on Page 16), the reaction conditions, analytical methods, advantages and drawbacks are summarized for comparison between varied reversible reactions. Among these examples, a striking case was reported by Campopiano, Greaney and co-workers, they used aniline as a nucleophilic catalyst, which allowed for conducting reversible hydrazone chemistry at pH 6.2 (last entry in Table 1).¹²³ Inspired by their work, we designed DCLs for FimH antagonists screening (detailed in Chapter 2).

1.7 Aims of this thesis

The present thesis is aiming at further understanding the binding mode of FimH antagonists, optimization of lead structures, and development of highly active and bioavailable FimH antagonists.

The four goals of this thesis are: 1) Structure-based drug design of novel FimH antagonists; 2) chemical synthesis of designed structures; 3) application of dynamic combinatorial chemistry in lead discovery and optimization; 4) improvement of pharmacodynamic (PD) and pharmacokinetic (PK) properties with medicinal chemistry strategies, such as heterocyclic replacement and bioisostere approaches. Diverse chemical synthesis, i.e. traditional synthesis and *in situ* dynamic combinatorial approaches, were implemented aiming for both structural diversity and lead identification. Based on the results of *in vitro* and *in vivo* evaluation, structure-activity and structure-property relationships were established and further guided the development of FimH antagonists towards the final goal – “drug-likeness”.

Table 1. Representative examples of DCC in drug lead discovery (imine, hydrazone and disulfide formation as reversible reactions).

Target protein	Reversible chemistry	Analysis method	Advantage	Drawback
Carbonic anhydrase (CA) ^{108, 112}	Imine formation (NaBH ₃ CN as reducing agent)	HPLC-UV	<ul style="list-style-type: none"> Large excess of amine limited cross-reactivity with nucleophilic amino acid residues on protein surface. Slow reduction with reducing agents produces sturdy amines, which are stable for analysis. 	<ul style="list-style-type: none"> The imines taking part in the templating and amplification process in DCL are not represented in final analysis. The reducing agent reduces the starting aldehyde and erodes the aldehyde concentration in the DCL and produces benzylic alcohol as side products.
Acetylcholine esterase (ACE) ¹¹⁹ <i>Bacillus subtilis</i> HPt kinase ¹²⁰	Acylhydrazone formation at pH4	HPLC-UV Enzyme assay Deconvolution strategy	<ul style="list-style-type: none"> The formed acyl hydrazones are robust and readily amenable to analysis. A “pre-equilibrated” DCC approach was applied to allow an efficient equilibration of DCL at acidic pH. The separation of DCL and templating processes allows a greater range of reversible reactions to be used. 	<ul style="list-style-type: none"> The separation of DCL and templating removes the adaptive and amplification processes of DCC. A conventional screening of a combinatorial mixture library is required.
Neuraminidase ^{113, 114}	Imine formation (NH ₄ BH ₃ CN as reducing agent)	HPLC-MS	<ul style="list-style-type: none"> The DCL is theoretically very large; over 40,000 components are possible at equilibrium. The transient components were present at very low concentration; only in the presence of target, amplification of the best binders could afford detectable amounts of compound that could be detected by HPLC-MS. 	A separation of the molecular recognition events, namely binding of the transient imines to the protein and binding of the product amines to the protein, could bring false positive/negative results.
Hen egg-white lysozyme (HEWL) D-GlcNAc-binding glycosidase ¹¹⁵ Glycosyltransferases (GTs) ¹¹⁶⁻¹¹⁸	Carbohydrate-based imine formation (NaBH ₃ CN as reducing agent)	HPLC-UV	The HPLC analysis is aided by chromophore appended to the carbohydrate moiety.	The amplification process required stoichiometric amounts of the target protein, however, GTs are typically available in very small amount. If the binding affinity of the amine products were significantly weaker than the transient imines, constant amplification of the reduced amine products could be realized in the presence of sub-stoichiometric amount of target protein, e.g. GTs.

Cyclin-dependent kinase 2 (CDK-2) ¹²¹	Hydrazone formation	<ul style="list-style-type: none"> X-ray crystallography LC-MS 	<ul style="list-style-type: none"> Only very small amount of protein is needed. The protein structure influences equilibrium distribution of hydrazone in microcosm within the crystal. 	<ul style="list-style-type: none"> The total amount of protein in the crystals was too small to cause any gross changes in the outcome of the reaction. The crystal effect could also occur under kinetic control other than expected thermodynamic control in DCL.
Concavavalin A (Con A) ¹²⁴	Disulfide bond formation	HPLC-UV	<ul style="list-style-type: none"> The DCL was isoenergetic and without significant kinetic disparity. Con A target was attached to sepharose beads. By applying acidic quench to the DCL, bound components could be washed off the resin beads. 	<ul style="list-style-type: none"> HPLC-resolution issues hampered analysis of the DCL solution at equilibrium. Quenching and elution showed the Man dimers bound to the immobilized protein. The amplification of the DCL by Con A was relatively weak.
Calistum transducer calmodulin (CaM) ¹²⁵	Disulfide bond formation	HPLC-MS	<ul style="list-style-type: none"> Denaturation and filtration afforded a mixture of all peptides that had bound to CaM in the course of DCL. Centrifugation filtration step separated protein/bound components from free components in solution. 	<ul style="list-style-type: none"> The filtration membrane affected the composition of the library, complicating HPLC analysis.
Carbonic anhydrase (CA) ¹²²	Hydrazone formation	ESI-FTMS (electrospray ionization Fourier transform mass spectrometry)	<ul style="list-style-type: none"> No denaturation of the protein. No chromatography or synthesis of sub-libraries. The DCL can be analyzed directly and fast. 	<ul style="list-style-type: none"> High requirement of sample preparation: nonvolatile buffers, salts, and detergents can suppress the ion abundance, leading to poor mass spectrum result. MS parameters need to be carefully adjusted before measurement.
Glutathione S-transferase (GST) ¹²³	Acylhydrazone formation at pH 6.2	HPLC-UV	<ul style="list-style-type: none"> Aniline was used as a nucleophilic catalyst, which allowed for conducting reversible hydrazone chemistry at pH6.2. Good kinetic and thermodynamic properties lead to ease of analysis. The DCLs are truly adaptive, allowing amplification effects to be simply and directly related to structures present at equilibrium. 	<ul style="list-style-type: none"> The building blocks of DCL are limited to the ones with chromophores, which is required for UV-detection at low concentrations. The size of the DCL is limited by the separation capacity of HPLC. Sub-libraries were needed to identify the components.

REFERENCES

1. Foxman, B. Recurring urinary tract infection: incidence and risk factors. *Am. J. Public Health* **1990**, *80*, 331-333.
2. Foxman, B.; Barlow, R.; D'Arcy, H.; Gillespie, B.; Sobel, J. D. Urinary tract infection: Self reported incidence and associated costs. *Ann. Epidemiol.* **2000**, *10*, 509-515.
3. Ronald, A. The etiology of urinary tract infection: Traditional and emerging pathogens. *Am. J. Med.* **2002**, *113 (Suppl 1A)*, 14S-19S.
4. Foxman, B.; Somsel, P.; Tallman, P.; Gillespie, B.; Raz, R.; Colodner, R.; Kandula, D.; Sobel, J. D. Urinary tract infection among women aged 40 to 65: Behavioral and sexual risk factors. *J. Clin. Epidemiol.* **2001**, *54*, 710-718.
5. Hooton, T. M.; Scholes, D.; Hughes, J. P.; Winter, C.; Roberts, P. L.; Stapleton, A. E.; Stergachis, A.; Stamm, W. E. A prospective study of risk factors for symptomatic urinary tract infection in young women. *N. Engl. J. Med.* **1996**, *335*, 468-474.
6. Zhang, L.; Foxman, B. Molecular epidemiology of Escherichia coli mediated urinary tract infections. *Front Biosci.* **2003**, *8*, E235-E244.
7. Cegelski, L.; Marshall, G. R.; Eldridge, G. R.; Hultgren, S. J. The biology and future prospects of antivirulence therapies. *Nat. Rev. Microbiol.* **2008**, *6*, 17-27.
8. Kuroda, M.; Yamashita, A.; Hirakawa, H.; Kumano, M.; Morikawa, K.; Higashide, M.; Maruyama, A.; Inose, Y.; Matoba, K.; Toh, H.; Kuhara, S.; Hattori, M.; Ohta, T. Whole genome sequence of Staphylococcus saprophyticus reveals the pathogenesis of uncomplicated urinary tract infection. *Proc. Natl. Acad. Sci. U.S.A.* **2005**, *102*, 13272-13277.
9. Nicolle, L. E. Uncomplicated urinary tract infection in adults including uncomplicated pyelonephritis. *Urol. Clin. North Am.* **2008**, *35*, 1-12.
10. Hooton, T. Fluoroquinolones and resistance in the treatment of uncomplicated urinary tract infection. *Int J Antimicrob Agents.* **2003**, *22*, S65-S72.
11. Hooton, T. The current management strategies for community-acquired urinary tract infection. *Infect. Dis. Clin. North Am.* **2003**, *17*, 303-332.
12. Colgan, R.; Williams, M.; Johnson, J. R. Diagnosis and treatment of acute pyelonephritis in women. *Am. Fam. Physician* **2011**, *84*, 519-526.

13. Franco, A. V. M. Recurrent urinary tract infections. *Best Pract. Res. Clin. Obstet. Gynaecol.* **2005**, *19*, 861-873.
14. Sanchez, G. V.; Master, R. N.; Bordon, J. Trimethoprim-sulfamethoxazole may no longer be acceptable for the treatment of acute uncomplicated cystitis in the United States. *Clin. Infect. Dis.* **2011**, *53*, 316-317.
15. Sanchez, G. V.; Master, R. N.; Karlowsky, J. A.; Bordon, J. M. In vitro antimicrobial resistance of urinary Escherichia coli isolates among U.S. outpatients from 2000 to 2010. *Antimicrob. Agents Chemother.* **2012**, *56*, 2181-2183.
16. Nicolle, L.; Anderson, P. A. M.; Conly, J.; Mainprize, T. C.; Meuser, J.; Nickel, J. C.; Senikas, V. M.; Zhanel, G. G. Uncomplicated urinary tract infection in women - Current practice and the effect of antibiotic resistance on empiric treatment. *Can. Fam. Physician.* **2006**, *52*, 612-618.
17. Gupta, K.; Hooton, T. M.; Naber, K. G.; Wullt, B.; Colgan, R.; Miller, L. G.; Moran, G. J.; Nicolle, L. E.; Raz, R.; Schaeffer, A. J.; Soper, D. E.; American, I. D. S. o.; Diseases, E. S. f. M. a. I. International clinical practice guidelines for the treatment of acute uncomplicated cystitis and pyelonephritis in women: A 2010 update by the Infectious Diseases Society of America and the European Society for Microbiology and Infectious Diseases. *Clin. Infect Dis.* **2011**, *52*, e103-e120.
18. Anderson, G. G.; Dodson, K. W.; Hooton, T. M.; Hultgren, S. J. Intracellular bacterial communities of uropathogenic Escherichia coli in urinary tract pathogenesis. *Trends Microbiol.* **2004**, *12*, 424-430.
19. Martinez, J. J.; Mulvey, M. A.; Schilling, J. D.; Pinkner, J. S.; Hultgren, S. J. Type 1 pilus-mediated bacterial invasion of bladder epithelial cells. *EMBO J.* **2000**, *19*, 2803-2812.
20. Wiles, T. J.; Kulesus, R. R.; Mulvey, M. A. Origins and virulence mechanisms of uropathogenic Escherichia coli. *Exp. Mol. Pathol.* **2008**, *85*, 11-19.
21. Justice, S.; Hung, C.; Theriot, J.; Fletcher, D.; Anderson, G.; Footer, M.; Hultgren, S. Differentiation and developmental pathways of uropathogenic Escherichia coli in urinary tract pathogenesis. *Proc. Natl. Acad. Sci. U.S.A.* **2004**, *101*, 1333-1338.
22. Abgottspon, D.; Rölli, G.; Hosch, L.; Steinhuber, A.; Jiang, X.; Schwardt, O.; Cutting, B.; Smiesko, M.; Jenal, U.; Ernst, B.; Trampuz, A. Development of an aggregation assay to screen FimH antagonists. *J Microbiol. Methods* **2010**, *82*, 249-255.

23. Soto, G. E.; Hultgren, S. J. Bacterial adhesins: common themes and variations in architecture and assembly. *J. Bacteriol.* **1999**, *181*, 1059-1071.
24. Xie, B.; Zhou, G.; Chan, S. Y.; Shapiro, E.; Kong, X. P.; Wu, X. R.; Sun, T. T.; Costello, C. E. Distinct glycan structures of uroplakins Ia and Ib - Structural basis for the selective binding of FimH adhesin to uroplakin Ia. *J. Biol. Chem.* **2006**, *281*, 14644-14653.
25. Zhou, G.; Mo, W. J.; Sebbel, P.; Min, G. W.; Neubert, T. A.; Glockshuber, R.; Wu, X. R.; Sun, T. T.; Kong, X. P. Uroplakin Ia is the urothelial receptor for uropathogenic Escherichia coli: evidence from in vitro FimH binding. *J. Cell Sci.* **2001**, *114*, 4095-4103.
26. Mulvey, M. A. Adhesion and entry of uropathogenic Escherichia coli. *Cell. Microbiol* **2002**, *4*, 257-271.
27. Mulvey, M. A.; Lopez-Boado, Y. S.; Wilson, C. L.; Roth, R.; Parks, W. C.; Heuser, J.; Hultgren, S. J. Induction and evasion of host defenses by type 1-piliated uropathogenic Escherichia coli. *Science* **1998**, *282*, 1494-1497.
28. Mysorekar, I.; Hultgren, S. Mechanisms of uropathogenic Escherichia coli persistence and eradication from the urinary tract. *Proc. Natl. Acad. Sci. U.S.A.* **2006**, *103*, 14170-14175.
29. Blango, M.; Mulvey, M. Persistence of uropathogenic Escherichia coli in the face of multiple antibiotics. *Antimicrob. Agents. Chemother.* **2010**, *54*, 1855-1863.
30. Bahrani-Mougeot, F. K.; Buckles, E. L.; Lockatell, C. V.; Hebel, J. R.; Johnson, D. E.; Tang, C. M.; Sonnenberg, M. S. Type 1 fimbriae and extracellular polysaccharides are preeminent uropathogenic Escherichia coli virulence determinants in the murine urinary tract. *Mol. Microbiol.* **2002**, *45*, 1079-1093.
31. Knight, S. D.; Berglund, J.; Choudhury, D. Bacterial adhesins: structural studies reveal chaperone function and pilus biogenesis. *Curr. Opin. Chem. Biol.* **2000**, *4*, 653-660.
32. Cusumano, C. K.; Pinkner, J. S.; Han, Z.; Greene, S. E.; Ford, B. A.; Crowley, J. R.; Henderson, J. P.; Janetka, J. W.; Hultgren, S. J. Treatment and prevention of urinary tract infection with orally active FimH inhibitors. *Sci. Transl. Med.* **2011**, *3*, 109-115.
33. Guiton, P.; Cusumano, C.; Kline, K.; Dodson, K.; Han, Z.; Janetka, J.; Henderson, J.; Caparon, M.; Hultgren, S. Combinatorial small-molecule therapy prevents

- uropathogenic *Escherichia coli* catheter-associated urinary tract infections in mice. *Antimicrob. Agents Chemother.* **2012**, *56*, 4738-4745.
34. Sharon, N. Carbohydrates as future anti-adhesion drugs for infectious diseases. *Biochim. Biophys. Acta* **2006**, *1760*, 527-537.
 35. Russell, P. W.; Orndorff, P. E. Lesions in 2 *Escherichia coli* type-1 pilus genes alter pilus number and length without affecting receptor-binding. *J. Bacteriol.* **1992**, *174*, 5923-5935.
 36. Capitani, G.; Eidam, O.; Glockshuber, R.; Grütter, M. G. Structural and functional insights into the assembly of type 1 pili from *Escherichia coli*. *Microbes Infect.* **2006**, *8*, 2284-2290.
 37. Schilling, J. D.; Mulvey, M. A.; Hultgren, S. J. Structure and function of *Escherichia coli* type 1 pili: new insight into the pathogenesis of urinary tract infections. *J. Infect. Dis.* **2001**, *183* (Suppl 1), S36-S40.
 38. Hahn, E.; Wild, P.; Hermanns, U.; Sebbel, P.; Glockshuber, R.; Haner, M.; Taschner, N.; Burkhard, P.; Aebi, U.; Müller, S. A. Exploring the 3D molecular architecture of *Escherichia coli* type 1 pili. *J. Mol. Biol.* **2002**, *323*, 845-857.
 39. Waksman, G.; Hultgren, S. J. Structural biology of the chaperone-usher pathway of pilus biogenesis. *Nat. Rev. Microbiol.* **2009**, *7*, 765-74.
 40. Sauer, F. G.; Barnhart, M.; Choudhury, D.; Knights, S. D.; Waksman, G.; Hultgren, S. J. Chaperone-assisted pilus assembly and bacterial attachment. *Curr. Opin. Struct. Biol.* **2000**, *10*, 548-556.
 41. Hung, D. L.; Hultgren, S. J. Pilus biogenesis via the chaperone/usher pathway: An integration of structure and function. *J. Struct. Biol.* **1998**, *124*, 201-220.
 42. Nishiyama, M.; Glockshuber, R. The outer membrane usher guarantees the formation of functional pili by selectively catalyzing donor-strand exchange between subunits that are adjacent in the mature pilus. *J. Mol. Biol.* **2010**, *396*, 1-8.
 43. Puorger, C.; Eidam, O.; Capitani, G.; Erilov, D.; Grutter, M. G.; Glockshuber, R. Infinite kinetic stability against dissociation of supramolecular protein complexes through donor strand complementation. *Structure* **2008**, *16*, 631-642.
 44. Aronson, M.; Medalia, O.; Schori, L.; Mirelman, D.; Sharon, N.; Ofek, I. Prevention of colonization of the urinary tract of mice with *Escherichia coli* by blocking of bacterial adherence with methyl α -D-mannopyranoside. *J. Infect. Dis.* **1979**, *139*, 329-332.

45. Klein, T.; Abgottspon, D.; Wittwer, M.; Rabbani, S.; Herold, J.; Jiang, X. H.; Kleeb, S.; Luthi, C.; Scharenberg, M.; Bezencon, J.; Gubler, E.; Pang, L. J.; Smiesko, M.; Cutting, B.; Schwaradt, O.; Ernst, B. FimH Antagonists for the oral treatment of urinary tract infections: from design and synthesis to in vitro and in vivo evaluation. *J. Med. Chem.* **2010**, *53*, 8627-8641.
46. Abgottspon, D.; Ernst, B. In vivo evaluation of FimH antagonists - a novel class of antimicrobials for the treatment of urinary tract infection. *Chimia (Aarau)* **2012**, *66*, 166-9.
47. Jiang, X. H.; Abgottspon, D.; Kleeb, S.; Rabbani, S.; Scharenberg, M.; Wittwer, M.; Haug, M.; Schwaradt, O.; Ernst, B. Antiadhesion therapy for urinary tract infections- A balanced PK/PD profile proved to be key for success. *J. Med. Chem.* **2012**, *55*, 4700-4713.
48. Schwartz, D. J.; Kalas, V.; Pinkner, J. S.; Chen, S. L.; Spaulding, C. N.; Dodson, K. W.; Hultgren, S. J. Positively selected FimH residues enhance virulence during urinary tract infection by altering FimH conformation. *Proc. Natl. Acad. Sci. U.S.A.* **2013**, *110*, 15530-15537.
49. Ofek, I.; Hasy, D.; Sharon, N. Anti-adhesion therapy of bacterial diseases: prospects and problems. *FEMS Immunol. Med. Microbiol.* **2003**, *38*, 181-191.
50. Choudhury, D.; Thompson, A.; Stojanoff, V.; Langermann, S.; Pinkner, J.; Hultgren, S. J.; Knight, S. D. X-ray structure of the FimC-FimH chaperone-adhesin complex from uropathogenic *Escherichia coli*. *Science* **1999**, *285*, 1061-1066.
51. Le Trong, I.; Aprikian, P.; Kidd, B. A.; Forero-Shelton, M.; Tchesnokova, V.; Rajagopal, P.; Rodriguez, V.; Interlandi, G.; Klevit, R.; Vogel, V.; Stenkamp, R. E.; Sokurenko, E. V.; Thomas, W. E. Structural basis for mechanical force regulation of the adhesin FimH via finger trap-like β -sheet twisting. *Cell* **2010**, *141*, 645-655.
52. Hung, C. S.; Bouckaert, J.; Hung, D.; Pinkner, J.; Widberg, C.; DeFusco, A.; Auguste, C. G.; Strouse, R.; Langermann, S.; Waksman, G.; Hultgren, S. J. Structural basis of tropism of *Escherichia coli* to the bladder during urinary tract infection. *Mol. Microbiol.* **2002**, *44*, 903-915.
53. Bouckaert, J.; Berglund, J.; Schembri, M.; De Genst, E.; Cools, L.; Wuhler, M.; Hung, C. S.; Pinkner, J.; Slattegard, R.; Zavialov, A.; Choudhury, D.; Langermann, S.; Hultgren, S. J.; Wyns, L.; Klemm, P.; Oscarson, S.; Knight, S. D.; De Greve, H.

- Receptor binding studies disclose a novel class of high-affinity inhibitors of the *Escherichia coli* FimH adhesin. *Mol. Microbiol.* **2005**, *55*, 441-455.
54. Wellens, A.; Garofalo, C.; Nguyen, H.; Van Gerven, N.; Slattegard, R.; Hernalsteens, J. P.; Wyns, L.; Oscarson, S.; De Greve, H.; Hultgren, S.; Bouckaert, J. Intervening with urinary tract infections using anti-adhesives based on the crystal structure of the FimH-oligomannose-3 complex. *PLoS One* **2008**, *3*, e2040
 55. Wellens, A.; Lahmann, M.; Touaibia, M.; Vaucher, J.; Oscarson, S.; Roy, R.; Remaut, H.; Bouckaert, J. The tyrosine gate as a potential entropic lever in the receptor-binding site of the bacterial adhesin FimH. *Biochemistry* **2012**, *51*, 4790-4799.
 56. Han, Z. F.; Pinkner, J. S.; Ford, B.; Obermann, R.; Nolan, W.; Wildman, S. A.; Hobbs, D.; Ellenberger, T.; Cusumano, C. K.; Hultgren, S. J.; Janetka, J. W. Structure-based drug design and optimization of mannoside bacterial FimH antagonists. *J. Med. Chem.* **2010**, *53*, 4779-4792.
 57. Dembo, M.; Torney, D. C.; Saxman, K.; Hammer, D. The reaction-limited kinetics of membrane-to-surface adhesion and detachment. *Proc. R. Soc. Lond. B Biol. Sci.* **1988**, *234*, 55-83.
 58. Thomas, W. E.; Trintchina, E.; Forero, M.; Vogel, V.; Sokurenko, E. V. Bacterial adhesion to target cells enhanced by shear force. *Cell* **2002**, *109*, 913-23.
 59. Thomas, W. Catch bonds in adhesion. *Annu. Rev. Biomed. Eng.* **2008**, *10*, 39-57.
 60. Nilsson, L. M.; Thomas, W. E.; Trintchina, E.; Vogel, V.; Sokurenko, E. V. Catch bond-mediated adhesion without a shear threshold: trimannose versus monomannose interactions with the FimH adhesin of *Escherichia coli*. *J. Biol. Chem.* **2006**, *281*, 16656-16663.
 61. Nilsson, L. M.; Thomas, W. E.; Sokurenko, E. V.; Vogel, V. Elevated shear stress protects *Escherichia coli* cells adhering to surfaces via catch bonds from detachment by soluble inhibitors. *Appl. Environ. Microbiol.* **2006**, *72*, 3005-3010.
 62. Aprikian, P.; Tchesnokova, V.; Kidd, B.; Yakovenko, O.; Yarov-Yarovoy, V.; Trinchina, E.; Vogel, V.; Thomas, W.; Sokurenko, E. Interdomain interaction in the FimH adhesin of *Escherichia coli* regulates the affinity to mannose. *J. Biol. Chem.* **2007**, *282*, 23437-23446.
 63. Nilsson, L. M.; Yakovenko, O.; Tchesnokova, V.; Thomas, W. E.; Schembri, M. A.; Vogel, V.; Klemm, P.; Sokurenko, E. V. The cysteine bond in the *Escherichia coli*

- FimH adhesin is critical for adhesion under flow conditions. *Mol. Microbiol.* **2007**, *65*, 1158-1169.
64. Yakovenko, O.; Tchesnokova, V.; Aprikian, P.; Forero, M.; Vogel, V.; Sokurenko, E.; Thomas, W. Mechanical force activates an adhesion protein through allosteric regulation. *J. Biol. Chem.* **2008**, *283*, 11596-11605.
 65. Thomas, W. E.; Vogel, V.; Sokurenko, E. Biophysics of catch bonds. *Annu. Rev. Biophys.* **2008**, *37*, 399-416.
 66. Sokurenko, E. V.; Feldgarden, M.; Trintchina, E.; Weissman, S. J.; Avagyan, S.; Chattopadhyay, S.; Johnson, J. R.; Dykhuizen, D. E. Selection footprint in the FimH adhesin shows pathoadaptive niche differentiation in *Escherichia coli*. *Mol. Biol. Evol.* **2004**, *21*, 1373-1383.
 67. Anderson, B. N.; Ding, A. M.; Nilsson, L. M.; Kusuma, K.; Tchesnokova, V.; Vogel, V.; Sokurenko, E. V.; Thomas, W. E. Weak rolling adhesion enhances bacterial surface colonization. *J. Bacteriol.* **2007**, *189*, 1794-802.
 68. Pak, J.; Pu, Y.; Zhang, Z. T.; Hasty, D. L.; Wu, X. R. Tamm-Horsfall protein binds to type 1 fimbriated *Escherichia coli* and prevents *E. coli* from binding to uroplakin Ia and Ib receptors. *J. Biol. Chem.* **2001**, *276*, 9924-9930.
 69. Eto, D. S.; Jones, T. A.; Sundsbak, J. L.; Mulvey, M. A. Integrin-mediated host cell invasion by type 1-piliated uropathogenic *Escherichia coli*. *PLoS Pathog.* **2007**, *3*, e100.
 70. Yu, J.; Lin, J. H.; Wu, X. R.; Sun, T. T. Uroplakins Ia and Ib, two major differentiation products of bladder epithelium, belong to a family of four transmembrane domain (4TM) proteins. *J. Cell. Biol.* **1994**, *125*, 171-182.
 71. Lityńska, A.; Pocheć, E.; Hoja-Lukowicz, D.; Kremser, E.; Laidler, P.; Amoresano, A.; Monti, C. The structure of the oligosaccharides of $\alpha 3\beta 1$ integrin from human ureter epithelium (HCV29) cell line. *Acta Biochim. Pol.* **2002**, *49*, 491-500.
 72. Saemann, M. D.; Weichhart, T.; Horl, W. H.; Zlabinger, G. J. Tamm-Horsfall protein: a multilayered defence molecule against urinary tract infection. *Eur. J. Clin. Invest.* **2005**, *35*, 227-235.
 73. Serafini-Cessi, F.; Monti, A.; Cavallone, D. N-Glycans carried by Tamm-Horsfall glycoprotein have a crucial role in the defense against urinary tract diseases. *Glycoconj. J.* **2005**, *22*, 383-94.

74. Bouckaert, J.; Mackenzie, J.; de Paz, J. L.; Chipwaza, B.; Choudhury, D.; Zavialov, A.; Mannerstedt, K.; Anderson, J.; Pierard, D.; Wyns, L.; Seeberger, P. H.; Oscarson, S.; De Greve, H.; Knight, S. D. The affinity of the FimH fimbrial adhesin is receptor-driven and quasi-independent of Escherichia coli pathotypes. *Mol. Microbiol.* **2006**, *61*, 1556-1568.
75. Sharon, N. Bacterial lectins, cell-cell recognition and infectious disease. *FEBS Lett.* **1987**, *217*, 145-157.
76. Weis, W. I.; Drickamer, K. Structural basis of lectin-carbohydrate recognition. *Annu. Rev. Biochem.* **1996**, *65*, 441-473.
77. Lis, H.; Sharon, N. Lectins: Carbohydrate-specific proteins that mediate cellular recognition. *Chem. Rev.* **1998**, *98*, 637-674.
78. Roos, G.; Wellens, A.; Touaibia, M.; Yamakawa, N.; Geerlings, P.; Roy, R.; Wyns, L.; Bouckaert, J. Validation of reactivity descriptors to assess the aromatic stacking within the tyrosine gate of FimH. *ACS Med. Chem. Lett.* **2013**, *4*, 1085-1090.
79. Sperling, O.; Fuchs, A.; Lindhorst, T. K. Evaluation of the carbohydrate recognition domain of the bacterial adhesin FimH: Design, synthesis and binding properties of mannoside ligands. *Org. Biomol. Chem.* **2006**, *4*, 3913-3922.
80. Firon, N.; Ashkenazi, S.; Mirelman, D.; Ofek, I.; Sharon, N. Aromatic α -glycosides of mannose are powerful inhibitors of the adherence of type-1 fimbriated escherichia-coli to yeast and intestinal epithelial-cells. *Infect. Immun.* **1987**, *55*, 472-476.
81. Lindhorst, T.; Kotter, S.; Kubisch, J.; Krallmann-Wenzel, U.; Ehlers, S.; Kren, V. Effect of p-substitution of aryl α -D-mannosides on inhibiting mannose-sensitive adhesion of Escherichia coli - Syntheses and testing. *Eur. J. Org. Chem.* **1998**, 1669-1674.
82. Schwardt, O.; Rabbani, S.; Hartmann, M.; Abgottspon, D.; Wittwer, M.; Kleeb, S.; Zalewski, A.; Smieško, M.; Cutting, B.; Ernst, B. Design, synthesis and biological evaluation of mannosyl triazoles as FimH antagonists. *Bioorg. Med. Chem.* **2011**, *19*, 6454-6673.
83. Pang, L. J.; Kleeb, S.; Lemme, K.; Rabbani, S.; Scharenberg, M.; Zalewski, A.; Schadler, F.; Schwardt, O.; Ernst, B. FimH antagonists: structure-activity and structure-property relationships for biphenyl α -D-Mannopyranosides. *ChemMedChem* **2012**, *7*, 1404-1422.

84. Han, Z. F.; Pinkner, J. S.; Ford, B.; Chorell, E.; Crowley, J. M.; Cusumano, C. K.; Campbell, S.; Henderson, J. P.; Hultgren, S. J.; Janetka, J. W. Lead optimization studies on FimH antagonists: discovery of potent and orally bioavailable ortho-substituted biphenyl mannosides. *J. Med. Chem.* **2012**, *55*, 3945-3959.
85. Ofek, I.; Mirelman, D.; Sharon, N. Adherence of *Escherichia coli* to human mucosal cells mediated by mannose receptors. *Nature* **1977**, *265*, 623-625.
86. Rabbani, S.; Jiang, X. H.; Schwaradt, O.; Ernst, B. Expression of the carbohydrate recognition domain of FimH and development of a competitive binding assay. *Anal Biochem.* **2010**, *407*, 188-195.
87. Horst, A. K.; Kotter, S.; Lindhorst, T. K.; Ludwig, A.; Brandt, E.; Wagener, C. Binding inhibition of type 1 fimbriae to human granulocytes: a flow cytometric inhibition assay using trivalent cluster mannosides. *Med. Microbiol. Immunol.* **2001**, *190*, 145-149.
88. Lindhorst, T. K.; Kieburg, C.; Krallmann-Wenzel, U. Inhibition of the type 1 fimbriae-mediated adhesion of *Escherichia coli* to erythrocytes by multiantennary α -mannosyl clusters: The effect of multivalency. *Glycoconj. J.* **1998**, *15*, 605-613.
89. Abgottspon, D.; Rolli, G.; Hosch, L.; Steinhuber, A.; Jiang, X. H.; Schwaradt, O.; Cutting, B.; Smiesko, M.; Jenal, U.; Ernst, B.; Trampuz, A. Development of an aggregation assay to screen FimH antagonists. *J. Microbiol. Methods.* **2010**, *82*, 249-255.
90. Scharenberg, M.; Abgottspon, D.; Cicek, E.; Jiang, X.; Schwaradt, O.; Rabbani, S.; Ernst, B. A flow cytometry-based assay for screening FimH antagonists. *Assay Drug Dev. Technol.* **2011**, *9*, 455-464.
91. Scharenberg, M.; Schwaradt, O.; Rabbani, S.; Ernst, B. Target selectivity of FimH antagonists. *J. Med. Chem.* **2012**, *55*, 9810-9816.
92. Sperling, O.; Dubber, M.; Lindhorst, T. K. Functionalization of oligosaccharide mimetics and multimerization using squaric diester-mediated coupling. *Carbohydr. Res.* **2007**, *342*, 696-703.
93. Grabosch, C.; Hartmann, M.; Schmidt-Lassen, J.; Lindhorst, T. K. Squaric acid monoamide mannosides as ligands for the bacterial lectin FimH: covalent inhibition or not? *Chembiochem* **2011**, *12*, 1066-1074.

94. Hartmann, M.; Lindhorst, T. K. The bacterial lectin FimH, a target for drug discovery – carbohydrate inhibitors of type 1 fimbriae-mediated bacterial adhesion. *Eur. J. Org Chem.* **2011**, 3583-3609.
95. Imberty, A.; Chabre, Y. M.; Roy, R. Glycomimetics and glycodendrimers as high affinity microbial anti-adhesins. *Chem. Eur. J.* **2008**, *14*, 7490-7499.
96. Lipinski, C. A. Drug-like properties and the causes of poor solubility and poor permeability. *J. Pharmacol. Toxicol. Methods* **2000**, *44*, 235-249.
97. Lipinski, C.; Lombardo, F.; Dominy, B.; Feeney, P. Experimental and computational approaches to estimate solubility and permeability in drug discovery and development settings. *Adv. Drug Deliv. Rev.* **2001**, *46*, 3-26.
98. Van de Waterbeemd, H.; Gifford, E. ADMET in silico modelling: Towards prediction paradise? *Nat. Rev. Drug Discov.* **2003**, *2*, 192-204.
99. Cumming, J.; Davis, A.; Muresan, S.; Haeberlein, M.; Chen, H. Chemical predictive modelling to improve compound quality. *Nat. Rev. Drug Discov.* **2013**, *12*, 948-962.
100. van de Waterbeemd, H.; Smith, D.; Beaumont, K.; Walker, D. Property-based design: Optimization of drug absorption and pharmacokinetics. *J. Med. Chem.* **2001**, *44*, 1313-1333.
101. Burton, P.; Goodwin, J.; Vidmar, T.; Amore, B. Predicting drug absorption: How nature made it a difficult problem. *J. Pharmacol. Exp. Ther.* **2002**, *303*, 889-895.
102. Williams, H.; Trevaskis, N.; Charman, S.; Shanker, R.; Charman, W.; Pouton, C.; Porter, C. Strategies to address low drug solubility in discovery and development. *Pharmacol Rev.* **2013**, *65*, 315-499.
103. Lovering, F.; Bikker, J.; Humblet, C. Escape from flatland: increasing saturation as an approach to improving clinical success. *J. Med. Chem.* **2009**, *52*, 6752-6756.
104. Ishikawa, M.; Hashimoto, Y. Improvement in aqueous solubility in small molecule drug discovery programs by disruption of molecular planarity and symmetry. *J. Med. Chem.* **2011**, *54*, 1539-1554.
105. Ramstrom, O.; Lehn, J. Drug discovery by dynamic combinatorial libraries. *Nat. Rev. Drug Discov.* **2002**, *1*, 26-36.
106. Corbett, P.; Leclaire, J.; Vial, L.; West, K.; Wieter, J.; Sanders, J.; Otto, S. Dynamic combinatorial chemistry. *Chem. Rev.* **2006**, *106*, 3652-3711.
107. Li, J.; Nowak, P.; Otto, S. Dynamic Combinatorial Libraries: From exploring molecular recognition to systems chemistry. *J. Am. Chem. Soc.* **2013**, *135*, 9222-9239.

108. Huc, I.; Lehn, J. M. Virtual combinatorial libraries: dynamic generation of molecular and supramolecular diversity by self-assembly. *Proc. Natl. Acad. Sci. U.S.A.* **1997**, *94*, 2106-2110.
109. Godoy-Alcantar, C.; Yatsimirsky, A.; Lehn, J. Structure-stability correlations for imine formation in aqueous solution. *J. Phys. Org. Chem.* **2005**, *18*, 979-985.
110. Szajewski, R.; Whitesides, G. Rate constants and equilibrium constants for thiol-disulfide interchange reactions involving oxidized glutathione. *J. Am. Chem. Soc.* **1980**, *102*, 2011-2026.
111. Ladame, S. Dynamic combinatorial chemistry: on the road to fulfilling the promise. *Org. Biomol. Chem.* **2008**, *6*, 219-226.
112. Lehn, J. Dynamic combinatorial chemistry and virtual combinatorial libraries. *Chem. Eur. J.* **1999**, *5*, 2455-2463.
113. Hochgurtel, M.; Kroth, H.; Piecha, D.; Hofmann, M.; Nicolau, C.; Krause, S.; Schaaf, O.; Sonnenmoser, G.; Eliseev, A. Target-induced formation of neuraminidase inhibitors from in vitro virtual combinatorial libraries. *Proc. Natl. Acad. Sci. U.S.A.* **2002**, *99*, 3382-3387.
114. Hochgurtel, M.; Biesinger, R.; Kroth, H.; Piecha, D.; Hofmann, M.; Krause, S.; Schaaf, O.; Nicolau, C.; Eliseev, A. Ketones as building blocks for dynamic combinatorial libraries: Highly active neuraminidase inhibitors generated via selection pressure of the biological target. *J. Med. Chem.* **2003**, *46*, 356-358.
115. Zameo, S.; Vauzeilles, B.; Beau, J. Dynamic combinatorial chemistry: Lysozyme selects an aromatic motif that mimics a carbohydrate residue. *Angew. Chem. Int. Ed.* **2005**, *44*, 965-969.
116. Zameo, S.; Vauzeilles, B.; Beau, J. Direct composition analysis of a dynamic library of imines in an aqueous medium. *Eur. J. Org. Chem.* **2006**, 5441-5444.
117. Valade, A.; Urban, D.; Beau, J. Target-assisted selection of galactosyltransferase binders from dynamic combinatorial libraries. An unexpected solution with restricted amounts of the enzyme. *Chembiochem* **2006**, *7*, 1023-1027.
118. Valade, A.; Urban, D.; Beau, J. Two galactosyltransferases' selection of different binders from the same uridine-based dynamic combinatorial library. *J. Comb. Chem.* **2007**, *9*, 1-4.
119. Bunyapaiboonsri, T.; Ramstrom, O.; Lohmann, S.; Lehn, J.; Peng, L.; Goeldner, M. Dynamic deconvolution of a pre-equilibrated dynamic combinatorial library of acetylcholinesterase inhibitors. *Chembiochem* **2001**, *2*, 438-444.

120. Bunyapaiboonsri, T.; Ramstrom, H.; Ramstrom, O.; Haiech, J.; Lehn, J. Generation of Bis-cationic heterocyclic inhibitors of Bacillus subtilis HPr kinase/phosphatase from a ditopic dynamic combinatorial library. *J. Med. Chem.* **2003**, *46*, 5803-5811.
121. Congreve, M.; Davis, D.; Devine, L.; Granata, C.; O'Reilly, M.; Wyatt, P.; Jhoti, H. Detection of ligands from a dynamic combinatorial library by X-ray crystallography. *Angew. Chem. Int. Ed.* **2003**, *42*, 4479-4482.
122. Poulsen, S. Direct screening of a dynamic combinatorial library using mass spectrometry. *J. Am. Soc. Mass Spectrom.* **2006**, *17*, 1074-1080.
123. Bhat, V.; Caniard, A.; Luksch, T.; Brenk, R.; Campopiano, D.; Greaney, M. Nucleophilic catalysis of acylhydrazone equilibration for protein-directed dynamic covalent chemistry. *Nat. Chem.* **2010**, *2*, 490-497.
124. Ramstrom, O.; Lehn, J. In situ generation and screening of a dynamic combinatorial carbohydrate library against concanavalin A. *Chembiochem* **2000**, *1*, 41-48.
125. Milanesi, L.; Hunter, C.; Sedelnikova, S.; Waltho, J. Amplification of bifunctional ligands for calmodulin from a dynamic combinatorial library. *Chem. Eur. J.* **2006**, *12*, 1081-1087.

2. Results and discussion

2.1 Outline

Optimization of biphenyl FimH antagonists to improve potency, aqueous solubility and oral bioavailability. Since the binding mode of an antagonist to the CRD of FimH can switch from an “in-docking mode” to an “out-docking mode”, depending on the structure of antagonist, different substitution patterns, such as the *ortho*-substituent on ring A and *para*-substituent on ring B, were introduced to explore the binding mode and therefore improve binding affinity. Furthermore, based on the lead structure **6d** and its ester prodrug **6c**, structural modifications were implemented to improve potency, aqueous solubility and oral bioavailability of biphenyl FimH antagonists. Although the prodrug strategy was proved to be effective in an UTI mouse model, the major drawback of the ester prodrugs developed until then was their low solubility, which hampered their *in vivo* application. To solve the solubility issue, different strategies were applied, including disruption of molecular symmetry by diverse substitution patterns and introduction of aromatic heterocycles. Additionally, bioisosteric replacement of the carboxylic acid moiety was carried out to increase the anti-adhesive efficacy, and at the same time the metabolically stable bioisosteres were expected to exhibit improved oral bioavailability. To summarize, the optimization of the lead structure **6d** towards optimal anti-adhesive potency, aqueous solubility and oral bioavailability relies on diverse modifications depicted in Figure 2.1.1 and described in the following publications and manuscript:

- 1) Introduction of methyl ester prodrug to mask the carboxylic acid moiety on ring B (*Chapter 2.2 - Paper1*).
- 2) Optimization of the *ortho*-substituent on ring A of the biphenyl aglycone and introduction of flexible aglycones (*Chapter 2.3 - Paper2*).
- 3) Bioisosteric replacement of the carboxylic acid moiety on ring B (*Chapter 2.4 - Paper3*).
- 4) Introduction of aromatic heterocycles as ring B of the biaryl aglycone (*Chapter 2.5 - Manuscript*).

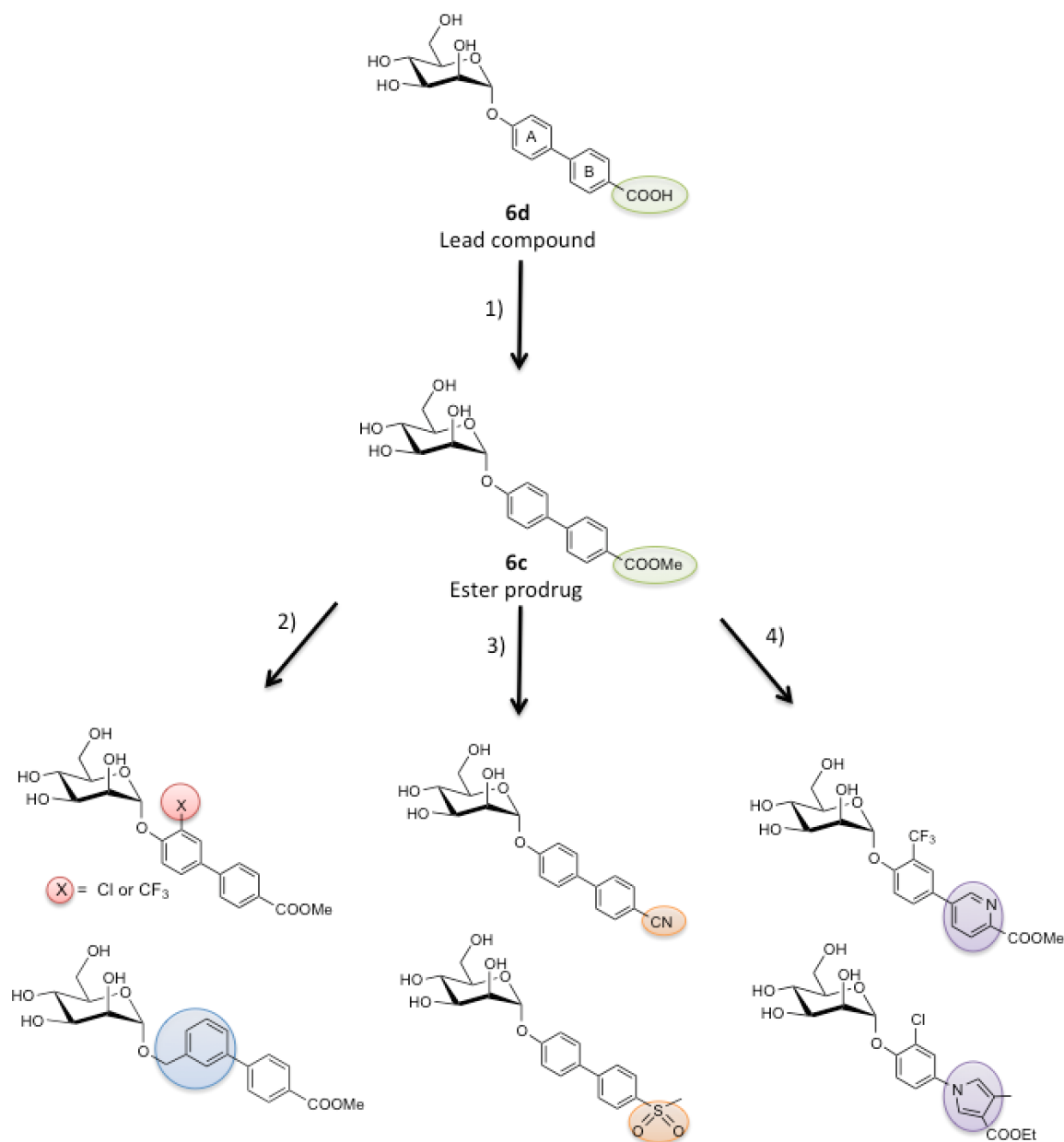


Figure 2.1.1. Modifications on biphenyl α -D-mannopyranoside lead structure **6d** : 1) introduction of methyl ester to mask the polar carboxylic acid substituent on ring B and therefore improve intestinal absorption; 2) optimization of the substitution patterns of ring A and B to study the binding mode, and to improve solubility by disruption of molecular symmetry; 3) replacement of ring B with aromatic heterocycles to improve solubility; 4) Bioisosteric replacement of the carboxylic acid moiety on ring B to improve oral bioavailability.

Studies on the kinetic properties of FimH-ligand interactions. As part of the preclinical development process, kinetic properties of FimH antagonists were examined. With an amide linker the FimH antagonists were immobilized to sensor chips, and then analyzed with surface plasmon resonance (SPR), as described in *Chapter 2.6 - Paper 4*.

Combinatorial libraries against *FimH*. As another lead structure, heptyl mannoside was recognized as a highly potent *FimH* antagonist, which adopts an “in-docking mode” upon binding. Although numerous *FimH* antagonists have been developed so far, mannose is always an indispensable part of the structure and few modifications have been done on mannose ring. Additionally, in the last decade, the structures of the aglycone were mostly limited to the long-chain alkyls, phenyls, and biphenyls. In fact, the switch between the high- and low-affinity states of *FimH* provides a natural selection opportunity for discovery of diversified structures as *FimH* antagonists. Therefore, a combinatorial strategy was implemented by carrying out modifications on 2-position of mannose and on the aglycones. By doing so, the optimized precursor was chosen and adopted for *in situ* generation of dynamic combinatorial libraries and screening against *FimH*. The modifications on mannose and aglycones were summarized in Figure 2.1.2 and described in Chapter 2.7.

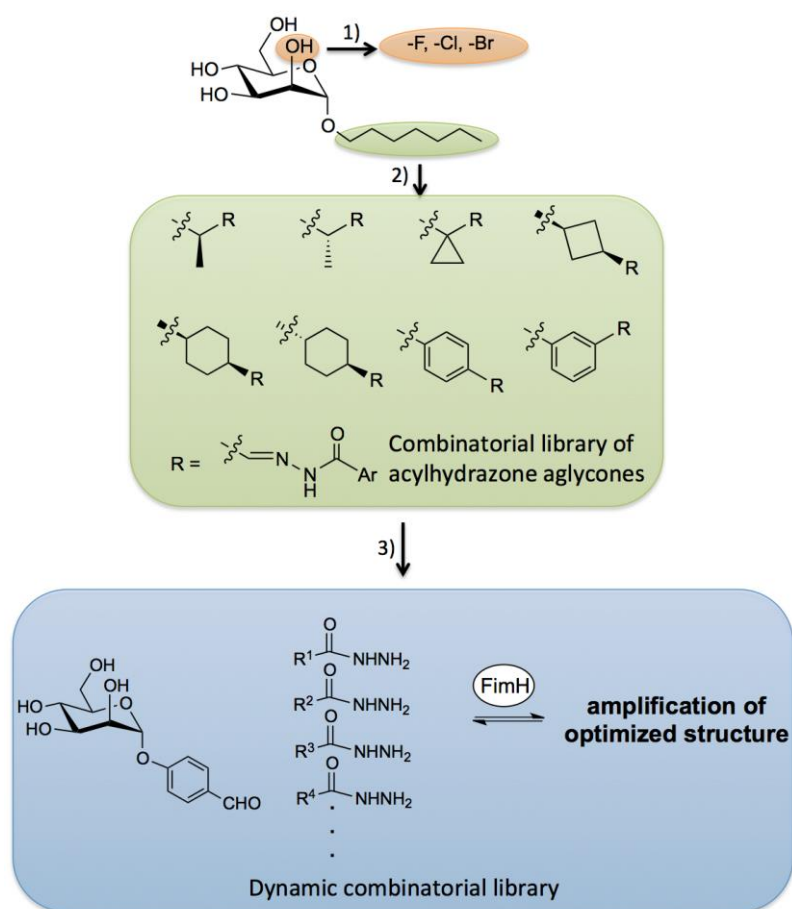


Figure 2.1.2. Combinatorial strategy for lead discovery and lead optimization: combinatorial library of α -D-mannopyranosides with 1) halogen modifications on the 2-position of mannose and 2) diversified aglycones

to optimize the structural combinations; 3) *in situ* generation and screening of dynamic combinatorial libraries against FimH protein.

Locking the 6-hydroxyl of mannose and conformational studies. Although the aglycones of FimH antagonists were extensively modified, few studies on the sugar moiety were reported. To further extend the structural scope and to study the conformational factors upon FimH binding, we modified the mannose moiety by either stereochemically locking 6-hydroxyl group with a cyclopropane unit or introducing a methyl group at C-6 (Figure 2.1.3). Here I used NMR-based methods and Mosher's analysis to characterize the chemical structures of 6-modified ligands and fluorescence polarization assay to evaluate their binding affinities, as described in *Chapter 2.8*.

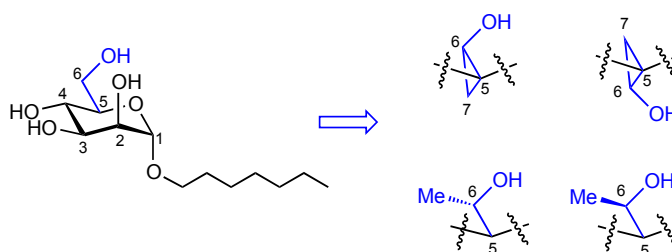


Figure 2.1.3. Conformational studies on modified *n*-heptyl mannosides.

2.2 Paper 1: FimH Antagonists for the Oral Treatment of Urinary Tract Infections: From Design and Synthesis to *in Vitro* and *in Vivo* Evaluation

This article describes the identification of biphenyl α -D-mannopyranosides as FimH antagonists. The anti-adhesion efficacy of the synthesized compounds was evaluated with *in vitro* and *in vivo* experiments. Furthermore, an ester prodrug approach was applied for achieving oral bioavailability.

Contribution to the project:

Lijuan Pang synthesized compound **5**, **6c** and **7c**.

This paper was published in the *Journal of Medicinal Chemistry*:

Klein, T.*; Abgottspon, D.*; Wittwer, M.*; Rabbani, S.*; Herold, J.*; Jiang, X.; Kleeb, S.; Luethi, C.; Scharenberg, M.; Bezençon, J.; Gubler, E.; Pang, L.; Smiesko, M.; Cutting, B.; Schwardt, O.; Ernst, B. FimH antagonists for the oral treatment of urinary tract infections: from design and synthesis to *in vitro* and *in vivo* evaluation. *J. Med. Chem.* **2010**, *53*, 8627-8641.

* These authors contributed equally to the project.

© 2010 American Chemical Society

FimH Antagonists for the Oral Treatment of Urinary Tract Infections: From Design and Synthesis to in Vitro and in Vivo Evaluation

Tobias Klein,[†] Daniela Abgottspon,[†] Matthias Wittwer,[†] Said Rabbani,[†] Jano Herold,[†] Xiaohua Jiang, Simon Kleeb, Christine Lüthi, Meike Scharenberg, Jacqueline Bezençon, Erich Gubler, Lijuan Pang, Martin Smiesko, Brian Cutting, Oliver Schwardt, and Beat Ernst*

Institute of Molecular Pharmacy, Pharmacenter, University of Basel, Klingelbergstrasse 50, CH-4056 Basel, Switzerland.

[†]These authors contributed equally to the project

Received August 4, 2010

Urinary tract infection (UTI) by uropathogenic *Escherichia coli* (UPEC) is one of the most common infections, particularly affecting women. The interaction of FimH, a lectin located at the tip of bacterial pili, with high mannose structures is critical for the ability of UPEC to colonize and invade the bladder epithelium. We describe the synthesis and the in vitro/in vivo evaluation of α -D-mannosides with the ability to block the bacteria/host cell interaction. According to the pharmacokinetic properties, a prodrug approach for their evaluation in the UTI mouse model was explored. As a result, an orally available, low molecular weight FimH antagonist was identified with the potential to reduce the colony forming units (CFU) in the urine by 2 orders of magnitude and in the bladder by 4 orders of magnitude. With FimH antagonist **16b**, the great potential for the effective treatment of urinary tract infections with a new class of orally available antiinfectives could be demonstrated.

Introduction

Urinary tract infection (UTI^a) is one of the most common infections, affecting millions of people each year. Particularly affected are women, who have a 40–50% risk to experience at least one symptomatic UTI episode at some time during their life. In addition, more than half of them experience a relapse of the infection within 6 months.^{1,2}

Although UTIs rarely cause severe diseases such as pyelonephritis or urosepsis, they are associated with high incidence rate and consume considerable healthcare resources.³ Uropathogenic *Escherichia coli* (UPEC) are the primary cause of UTIs, accounting for 70–95% of the reported cases. Symptomatic UTIs require antimicrobial treatment, often resulting in the emergence of resistant microbial flora. As a consequence, treatment of consecutive infections becomes increasingly difficult because the number of antibiotics is limited and the resistance of *E. coli* is increasing, especially in patients with diabetes, urinary tract anomaly, paraplegy, and those with permanent urinary catheter. Therefore, a new approach for the prevention and treatment of UTI with inexpensive, orally

applicable therapeutics with a low potential for resistance would have a great impact on patient care, public health care, and medical expenses.

UPEC strains express a number of well-studied virulence factors used for a successful colonization of their host.^{3–5} One important virulence factor is located on type 1 pili, allowing UPEC to adhere and invade host cells within the urinary tract. It enables UPEC to attach to oligomannosides, which are part of the glycoprotein uroplakin Ia on the urinary bladder mucosa. This initial step prevents the rapid clearance of *E. coli* from the urinary tract by the bulk flow of urine and at the same time enables the invasion of the host cells.^{3,6}

Type 1 pili are the most prevalent fimbriae encoded by UPEC, consisting of the four subunits FimA, FimF, FimG, and FimH, the latter located at the tip of the pili.⁷ As a part of the FimH subunit, a carbohydrate-recognizing domain (CRD) is responsible for bacterial interactions with the host cells within the urinary tract.⁶ The crystal structure of the FimH-CRD was solved⁸ and its complexes with *n*-butyl α -D-mannopyranoside⁹ and Man α (1–3)[Man α (1–6)]Man¹⁰ recently became available.

Previous studies showed that vaccination with FimH adhesin inhibits colonization and subsequent *E. coli* infection of the urothelium in humans.^{11,12} In addition, adherence and invasion of host cells by *E. coli* can also be prevented by α -D-mannopyranosides, which are potent antagonists of interactions mediated by type 1 pili.¹³ Whereas α -D-mannopyranosides efficiently prevent adhesion of *E. coli* to human urothelium, they are not exhibiting a selection pressure to induce antimicrobial resistance. Furthermore, environmental contamination is less problematic compared to antibiotics.¹⁴

More than two decades ago, Sharon and co-workers have investigated various mannosides and oligomannosides as

*To whom correspondence should be addressed. Phone: +41 61 267 1551. Fax: +41 61 267 1552. E-mail: beat.ernst@unibas.ch.

^a Abbreviations: AUC, area under the curve; Caco-2 cells, Caucasian colon adenocarcinoma cells; CFU, colony forming units; CRD, carbohydrate recognition domain; DC-SIGN, dendritic cell-specific intercellular adhesion molecule-3-grabbing nonintegrin; CES, carboxylesterase; IC₅₀, half maximal inhibitory concentration; iv, intravenous; D, distribution coefficient; GPE, guinea pig erythrocytes; LC-MS, liquid chromatography–mass spectrometry; MBP, mannose-binding protein; PAMPA, parallel artificial membrane permeation assay; P_{app} , apparent permeability; P_e , effective permeation; po, peroral; PPB, plasma protein binding; PSA, polar surface area; S, solubility; SAR, structure–activity relationship; sGF, simulated gastric fluid; sIF, simulated intestinal fluid; TEER, transepithelial resistance; UPEC, uropathogenic *E. coli*; UTI, urinary tract infection.

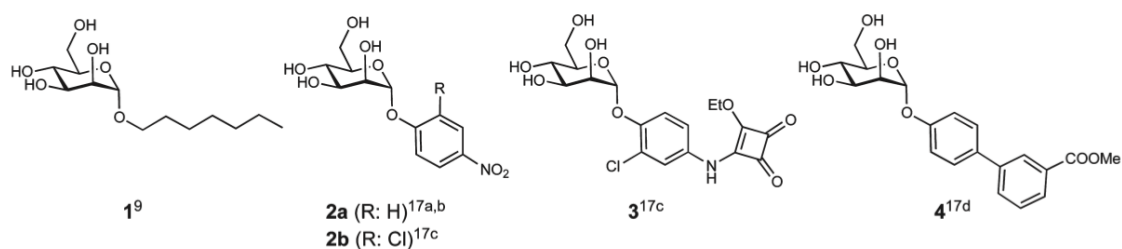
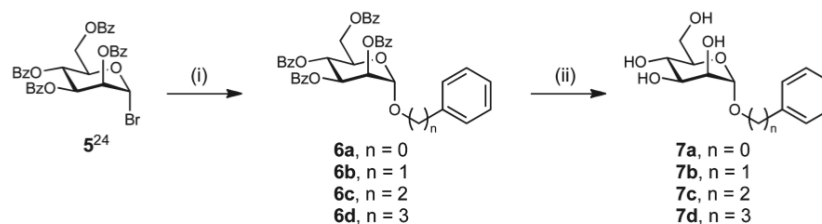


Figure 1. Known alkyl (1) and aryl (2–4) α -D-mannosides exhibiting nanomolar affinities.

Scheme 1. Phenyl α -D-Mannosides **7a–7d** with Spacers of Different Lengths between the Carbohydrate Moiety and the Phenyl Substituent^a



^a (i) $\text{Ph}(\text{CH}_2)_n\text{OH}$, $\text{Hg}(\text{CN})_2$, HgBr_2 , DCM, 2 h to 7 d, rt, 57–99%; (ii) NaOMe, MeOH, 6–16 h, rt, 48–91%.

potential antagonists for type 1 fimbriae-mediated bacterial adhesion.¹⁵ However, for these mannosides, only weak interactions in the milli- to micromolar range were observed. In contrast, numerous reports on glycoconjugate dendrimers with nanomolar affinities have been published.¹⁶ However, on the basis of their large molecular weight and high polarity, they are predicted to exhibit only poor intestinal absorption and are therefore not amenable for oral dosing. Recently, some isolated reports on high affinity monovalent FimH antagonists were published¹⁷ and, in one case, a systematic structure–activity relationship (SAR) profile was established.^{17d} In summary,^{8,9,15–19} long chain alkyl and aryl mannosides (selected examples are presented in Figure 1) displayed the highest affinity, likely due to hydrophobic interactions with two tyrosines and one isoleucine forming the entrance to the binding site, the so-called “tyrosine gate”.¹⁸ Because binding affinities were obtained from diverse assay formats,^{9,17c,20} a direct comparison of the affinities is difficult. On the basis of various crystal structures of methyl-⁸ and *n*-butyl α -D-mannoside¹⁸ as well as oligomannose-3⁹ bound to FimH, Han et al. recently presented a rationale for the design of aryl mannosides with increased affinities.^{17d}

To date, a few reports on the *in vivo* potential of methyl α -D-mannoside^{10,21,22} and *n*-heptyl α -D-mannoside (**1**)¹⁰ are available. In all cases, the FimH antagonists were directly instilled into the bladder concomitantly with uropathogenic *E. coli* (UPEC). In this communication, we present for the first time nanomolar FimH antagonists exhibiting appropriate pharmacokinetic properties for *iv* and oral treatment of urinary tract infections.

Results and Discussion

Identification of Lead Mannoside. In most of the reported FimH antagonists, aromatic aglycones have been applied.¹⁷ However, only limited information on the optimal spacer length between the mannose moiety and the aromatic substituent is available. Generally, the aromatic moiety is directly fused to the anomeric oxygen.^{17a–d} Extended spacers containing one^{17b,d} or two^{17c} methylene moieties were also reported,

however, the corresponding antagonists are not really comparable to each other because different assay formats were used for their evaluation. For the identification of the optimal spacer length, we therefore synthesized mannosides **7a–d** (Scheme 1). In a competitive binding assay,²³ mannoside **7a** showed a slightly higher affinity (Table 1, entry 2) compared with **7b–7d** (see Table 1, entries 3–5), confirming recent data for **7a** and **7b**.^{17d}

From the crystal structure of *n*-butyl α -D-mannoside bound to FimH,¹⁸ it becomes obvious that the hydrophobic rim formed by Tyr48, Tyr137, and Ile52 is not reached by an anomeric phenyl group. An extension by a second aromatic ring, i.e. a biphenyl α -D-mannoside, however, should be compatible for π – π stacking. Indeed, some recently published representatives of this compound class show excellent affinities.^{17d}

To achieve an optimal fit with the hydrophobic binding site of FimH, the conformation of the biphenyl aglycone in **1** was modified by different substitution patterns on ring A (Figure 2). Because electron poor aromatic rings substantially improve the binding affinities of FimH antagonists (a 10-fold improvement is reported for **2B** vs **2A**^{17c}), chloro substituents on ring A were used for the spatial exploration of the binding site. With substituents in *ortho*-position, only a minor change of the dihedral angle Φ_1 is observed (-3.3° to -0.7°). However, by an increased rotational barrier, the conformational flexibility is limited. The dihedral angle Φ_2 between the conjugated aromatic rings results from an interplay between π -conjugation and steric effects.^{24,25} By migrating the substituent to the *meta*-position, the torsion angle Φ_2 is substantially influenced. Whereas unsubstituted biphenyls show a global twisted minimum at a torsion angle Φ_2 of approximately 39° ,²⁶ substituents in the *meta*-position favor an increase of Φ_2 to 60° . Details of the conformational analyses are summarized in the Supporting Information.

Design Strategy for Intestinal Absorption and Renal Elimination. Besides high affinity, drug-like pharmacokinetic properties are a prerequisite for a successful *in vivo* application. In the present case, orally available FimH antagonists

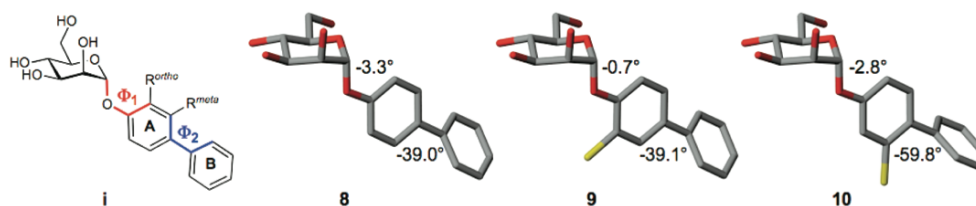


Figure 2. Conformational changes of the biphenyl aglycone by chloro substitutions in *ortho*- and *meta*-position of ring A.

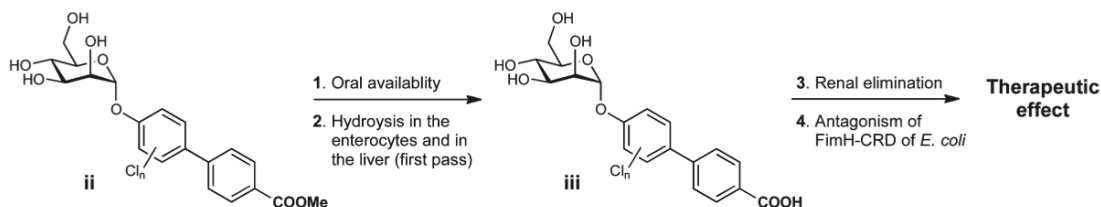


Figure 3. FimH antagonists with the pharmacodynamic and pharmacokinetic properties required for a therapeutic application. (1) For the prediction of oral availability, the PAMPA³⁰ and the Caco-2 cell assay³¹ are applied. (2) The hydrolysis of ester **ii** to carboxylate **iii** is evaluated by mouse liver microsomes. (3) Renal excretion is estimated based on a positive correlation with polar descriptors (polar surface area, H-bond donors, H-bond acceptors, rotatable bonds).³² (4) The potential of FimH antagonists is assessed with a target-based assay²³ and a function-based cellular assay.³³ For the evaluation of the therapeutic effect, a urinary tract infection mouse model (UTI mouse model in C3H/HeN mice) is applied.

that, once in circulation, are metabolically stable and undergo fast renal elimination, are required. This pharmacokinetic profile results from various serial and/or simultaneous processes that include dissolution, intestinal absorption, plasma protein binding, metabolic clearance, body distribution as well as renal and other clearance mechanisms. Because intestinal absorption and renal elimination are related to opposed properties, i.e. lipophilicity for intestinal absorption and hydrophilicity for renal elimination, a prodrug approach²⁷ was envisaged (Figure 3). Ester **ii** is expected to undergo intestinal absorption²⁸ and, later on, efficient hydrolysis to carboxylate **iii** by esterases²⁹ present in enterocytes lining the small intestine and in the liver.

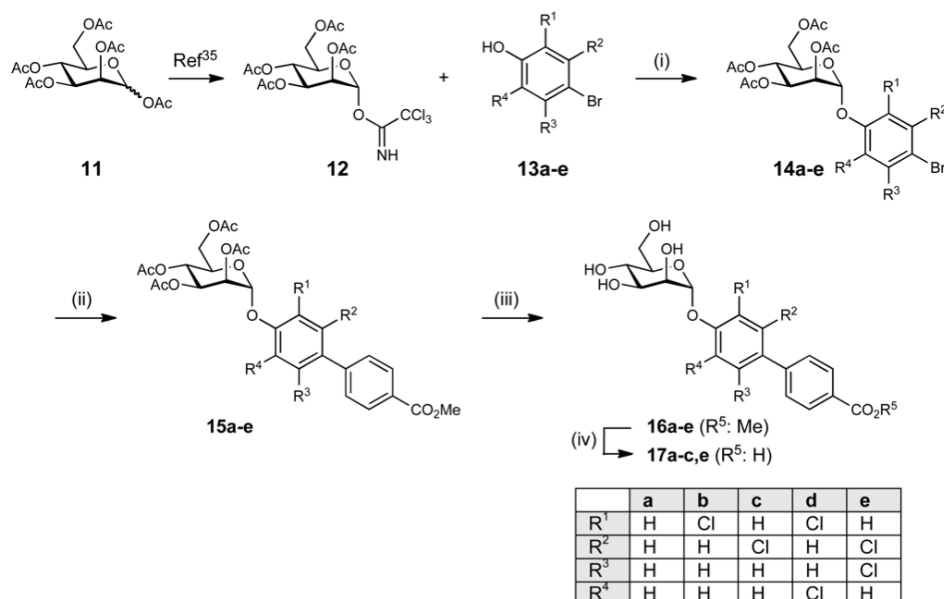
For renal clearance, the net result of glomerular filtration, active tubular secretion, and reabsorption, carboxylate **iii** should exhibit low lipophilicity ($\log D_{7.4}$) and favorable polar descriptor values (polar surface area (PSA), H-bond capacity and rotatable bonds).³² By contrast, lipophilic compounds are efficiently reabsorbed (as the passive reabsorption process occurs throughout the length of the nephron, whereas the secretion predominantly occurs at the proximal tubule). The estimated negative $\log D_{7.4}$ for antagonists of type **iii** is expected to fulfill these specifications for an efficient renal elimination and a low reabsorption. Finally, once arrived at the site of action in the bladder, the antagonist binds to the carbohydrate recognition domain (CRD) located on the bacterial pili, thus interfering with the adhesion of *E. coli* to oligosaccharide structures on urothelial cells.³⁴ To identify antagonists with the pharmacokinetic properties required for oral absorption and fast renal elimination, it was planned to determine PK parameters such as $\log D_{7.4}$, pK_a , solubility, plasma protein binding, metabolic stability, and oral availability using the parallel artificial membrane permeation assay (PAMPA)³⁰ and the Caco-2 cell assay.³¹

Synthesis of FimH Antagonists. The aglycone in the α -1-position of D-mannose plays a ternary role, i.e. it mediates the lipophilic contact with the hydrophobic tyrosine gate, contains the elements required for intestinal absorption and, after metabolic cleavage of the prodrug, for a fast renal elimination.

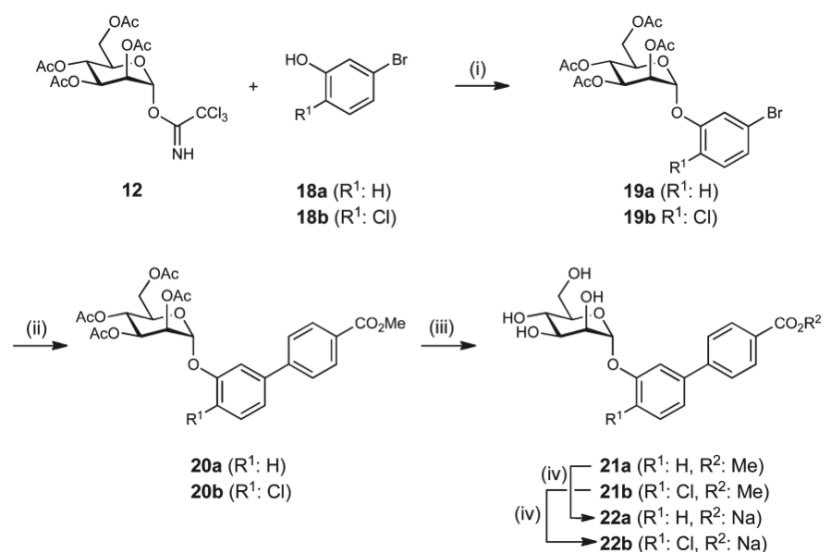
The syntheses of the *para*-substituted biphenyls **16a–e** and **17a–c,e** are outlined in Scheme 2. Lewis acid promoted glycosylation of the halogenated phenols **13a–e** with trichloroacetimidate **12**³⁵ yielded the phenyl α -D-mannosides **14a–e**. In a palladium-catalyzed Suzuki coupling with 4-methoxycarbonylphenylboronic acid, the biphenyls **15a–e** were obtained. For the deprotection of the mannose moiety, Zemplén conditions were applied (\rightarrow **16a–e**). Finally, the methyl esters were saponified, yielding the sodium salts **17a–c,e**.

In a similar approach, two *meta*-substituted biphenyls in their ester form (\rightarrow **21a,b**) and as free acids (\rightarrow **22a,b**) were obtained (see Scheme 3).

Binding Affinities and Activities. For the biological in vitro evaluation of the FimH antagonists, two assay formats have been developed. For an initial characterization, a cell-free competitive binding assay²³ and, later on, a cell-based aggregation assay,³³ were applied. Whereas in the cell-free competitive binding assay only the CRD of the pili was used, the complete pili are present in the cell-based assay format. Furthermore, both formats are competitive assays, i.e. the analyzed antagonists compete with mannosides for the binding site. In the cell-free competitive binding assay, the competitors are polymer-bound trimannosides, whereas in the aggregation assay, the antagonist competes with more potent oligo- and polysaccharide chains present on the surface of erythrocytes.³⁶ Therefore, lower IC_{50} values are expected for the cell-free competitive binding assay. In addition, switching from the cell-free target-based assay to the function-based assay generally leads to a reduction of potency by several orders of magnitude. The interaction is further complicated by the existence of a high- and a low-affinity state of the CRD of FimH. Aprikian et al. experimentally demonstrated that in full-length fimbriae the pilin domain stabilizes the CRD domain in the low-affinity state, whereas the CRD domain alone adopts the high-affinity state.³⁷ It was recently shown that the pilin domain allosterically causes a twist in the β -sandwich fold of the CRD domain, resulting in a loosening of the binding pocket.³⁸ On

Scheme 2^a

^a(i) TMSOTf, toluene, rt, 5 h (42–77%); (ii) 4-methoxycarbonylphenylboronic acid, Cs₂CO₃, Pd(PPh₃)₄, dioxane, 120°C, 8 h (28–85%); (iii) NaOMe, MeOH, rt, 4–24 h (22–86%); (iv) NaOMe, MeOH, rt, then NaOH/H₂O, rt, 16–24 h (63–94%).

Scheme 3^a

^a(i) TMSOTf, toluene, rt, 5 h (67–70%); (ii) 4-methoxycarbonylphenylboronic acid, Cs₂CO₃, Pd(PPh₃)₄, dioxane, 120°C, 8 h or Pd₂(dba)₃, S-Phos, dioxane, 80°C, overnight (46–56%); (iii) NaOMe, MeOH, rt, 24 h (52–67%); (iv) NaOMe, MeOH, rt, then NaOH/H₂O, rt, 24 h (75–95%).

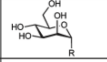
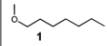
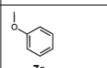
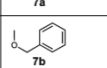
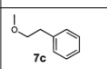
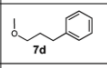
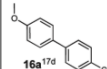
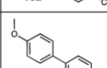
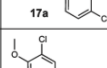
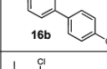
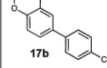
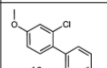
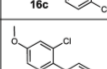
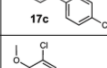
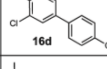
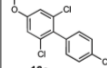
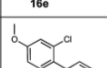
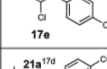
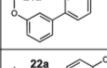
the basis of these findings, we expect a loss of affinity of our antagonists toward full-length fimbriae, when compared to the CRD domain alone.

Cell-Free Competitive Binding Assay. The cell-free inhibition assay is based on the interaction of a biotinylated polyacrylamide glycopolymer with the FimH-CRD as previously reported.²³ A recombinant protein consisting of the carbohydrate recognition domain of FimH linked with a thrombin cleavage site to a 6His-tag (FimH-CRD-Th-6His) was expressed in *E. coli* strain HM125 and purified by affinity chromatography. The IC₅₀ values of the test compounds were determined in microtiter plates coated with

FimH-CRD-Th-6His. Complexation of the biotinylated glycopolymer with streptavidin coupled to horseradish peroxidase allowed the quantification of the binding properties of FimH antagonists (Figure 4a). To ensure comparability with different antagonists, the reference compound *n*-heptyl α-D-mannopyranoside (**1**)³³ was tested in parallel in each individual microtiter plate. The affinities are reported relative to *n*-heptyl α-D-mannopyranoside (**1**) as rIC₅₀ in Table 1.

The most active representatives from the ester group are **16a** (Table 1, entry 6) and **16b** (entry 8) with affinities in the low nanomolar range, which is an approximately 10-fold improvement compared to reference compound **1**. The

Table 1. Pharmacodynamic and Pharmacokinetic Parameters of FimH Antagonists^{a,b}

		IC ₅₀ binding assay [nM]	rIC ₅₀	IC ₅₀ Aggrego- metry assay [μM]	PAMPA log P _e [log10 ⁶ cm/s/ %Mm]	Caco-2 P _{app} [10 ⁶ cm/s]	log D _s	pK _a	log S [μg/ml.]/ pH	PPB [%]
1		73±7.9	1.0	77.14±8.7	-4.89/21	nd	1.65	-	>3000	81
2		150±11.5	1.9	nd	nd/nd	nd	nd	-	>3000	nd
3		364±16.8	4.6	nd	nd/nd	nd	nd	-	nd	nd
4		210±11.2	2.6	nd	nd/nd	nd	nd	-	nd	nd
5		253±13.4	3.2	nd	nd/nd	nd	nd	-	nd	nd
6		10.4±1.2	0.14	42±7	-4.7/<20%	4.23	2.14	-	33.8/6.51	93
7		17.1±2.2	0.15	45±8	np	nd	<-1.5	3.88	>3000/6.61	73
8		4.8±1.2	0.06	9±2.7	-4.6/41.00	2.05	2.32	-	11.9/6.53	94
9		6.7±2.1	0.09	10±2.3	np/3.5	nd	-0.77	3.98	>3000/6.50	89
10		22.0±8.4	0.30	41 ¹⁾	-4.72/67.6	nd	2.42	-	11.5/6.50	95
11		27.6±3.9	0.38	17 ¹⁾	np	nd	-1.33	3.95	>3000/6.50	83
12		16.0±0.8	0.22	14 ¹⁾	-4.29/54.3	3.32	2.31	-	4.6/6.53	98
13		15.3±0.4	0.07	nd	-4.40/70.2	5.81	3.10	-	22.7/6.53	94
14		23.9±2.2	0.19	nd	nd/nd	nd	nd	nd	nd	nd
15		20.0±4.3	0.27	33 ¹⁾	-5.01/60.7	4.88	2.02	-	37.6/6.52	92
16		38.7±5.2	0.53	45 ¹⁾	np/9.7	nd	<-1.5	3.60	>3000/6.50	81
17		11.8±0.1	0.16	31 ¹⁾	-4.69/51.7	1.63	1.70	-	24.3/6.54	96
18		29.2±0.7	0.40	nd	np/nr	0.55	<-1.5	3.41	>3000/6.5	87

^aSingle determination; P_e, effective permeation; P_{app}, apparent permeability; np, no permeation; nr, no retention; nd, not determined. ^bThe IC₅₀s were determined with the cell-free competitive binding assay.²³ The rIC₅₀ of each substance was calculated by dividing the IC₅₀ of the compound of interest by the IC₅₀ of the reference compound **1** (entry 1). This leads to rIC₅₀ values below 1.00 for derivatives binding better than **1** and rIC₅₀ values above 1.00 for compounds with a lower affinity than **1**. The aggregation of *E. coli* and GPE were determined in the aggregometry assay.³⁵ Passive permeation through an artificial membrane and retention therein was determined by PAMPA (parallel artificial membrane permeation assay).³⁰ The permeation through cell monolayers was assessed by a Caco-2 assay.³¹ Distribution coefficients (log *D* values) were measured by a miniaturized shake flask procedure.⁴⁴ pK_a values were determined by NMR spectroscopy.⁴⁵ Plasma protein binding (PPB) was assessed by a miniaturized equilibrium dialysis protocol.⁴⁶ Thermodynamic solubility (*S*) was measured by an equilibrium shake flask approach.⁴⁷

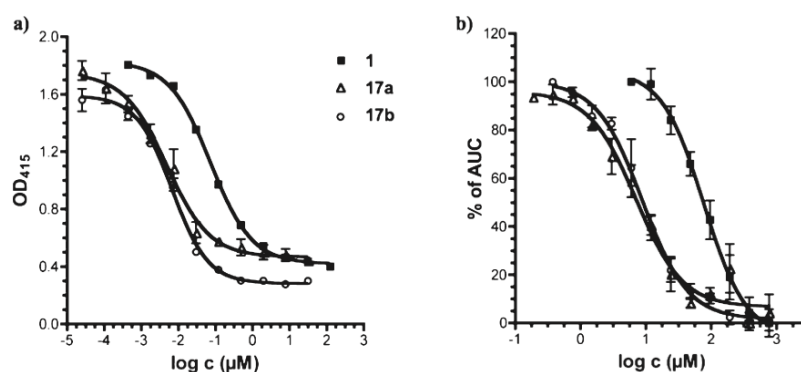


Figure 4. Affinities were determined in two different competitive assay formats. (a) a cell-free competitive binding assay²³ and (b) a cell-based aggregometry assay.³³ For antagonists **17a**, **17b**, and the reference compound **1**, IC₅₀ values in the nM and μM range, respectively, were obtained. The 1000-fold difference between the two assay formats is due to the different competitors used as well as the different affinity states present in FimH, i.e. the high-affinity state present in the CRD used in the cell-free competitive binding assay and the low-affinity state present in the pili of *E. coli* used in the aggregometry assay.

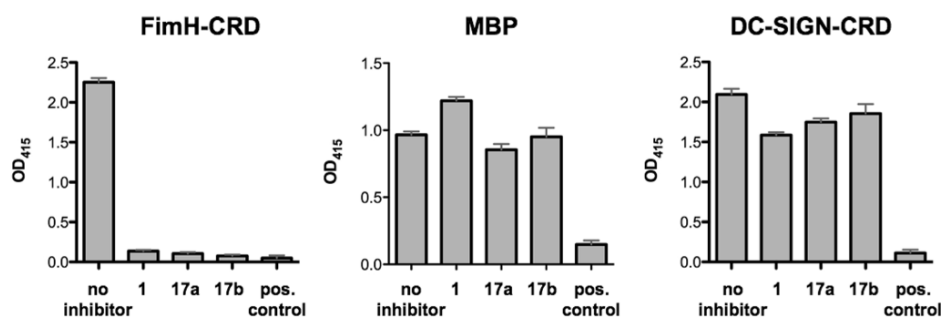


Figure 5. Competitive binding assay using FimH-CRD-Th-6His, DC-SIGN-CRD-IgG-Fc,⁴³ and MBP to evaluate the selectivity of compounds **1**, **17a**, and **17b**. Inhibitory capacities of the compounds were tested at a concentration of 1 mM. As positive control, D-mannose at a concentration of 50 mM was used.

corresponding carboxylic acids **17a** (entry 7) and **17b** (entry 9) exhibited a small reduction in affinity but are still 5-fold more active than reference compound **1**. All the remaining antagonists listed in Table 1 are slightly less active. For the in vivo examination, antagonists **17a** and **17b** were therefore foreseen for iv application and the prodrug **16b** for oral application.

Target selectivity is a further important issue. Mammalian mannose receptors are part of various biological processes, e.g. in cell–cell adhesion (DC-SIGN, dendritic cell-specific intercellular adhesion molecule-3-grabbing nonintegrin),³⁹ in the regulation of serum glycoprotein homeostasis (mannose receptor)⁴⁰ or in the innate and adaptive immune system by recognizing molecular patterns on pathogens (e.g., mannose-binding protein, mannose receptor, DC-SIGN).^{39,41,42} Non-specific interactions to the various mannose receptors by FimH inhibitors would have a profound impact on these processes. We therefore determined the affinity of reference compound **1** and the two antagonists **17a** and **17b** for two additional mannose binding proteins, DC-SIGN,^{39,43} and MBP (mannose-binding protein)⁴² (Figure 5). In both cases, affinities above 1 mM, i.e. a decrease of more than 5 orders of magnitude, was detected.

Aggregometry Assay. The potential of the biphenyl mannosides to disaggregate *E. coli* from guinea pig erythrocytes (GPE) was determined by a function-based aggregometry assay.³³ Antagonists were measured in triplicates, and the corresponding IC₅₀ values were calculated by plotting the

area under the curve (AUC) of disaggregation against the concentration of the antagonists. *n*-Heptyl α-D-mannopyranoside (**1**) was used again as reference compound and exhibits an IC₅₀ of 77.14 ± 8.7 μM. Antagonists **17a** and **17b** showed IC₅₀ values of 45 ± 8 μM and 10 ± 2.3 μM, respectively (Figure 4b). In general, the activities obtained from the aggregometry assay are approximately 1000-fold lower than the affinities determined in the target-based competitive assay (discussion see above).

In Vitro Pharmacokinetic Characterization of FimH Antagonists. For an application in the UTI mouse model, iv or po available FimH antagonists are required that, once absorbed to circulation, are metabolically stable and undergo fast renal elimination. Sufficient bioavailability requires a combination of high solubility and permeability to maximize absorption and low hepatic clearance to minimize first pass extraction. Furthermore, for efficient renal elimination, active and/or passive membrane permeability and low reabsorption in the renal tubuli is required. From the series of FimH antagonists with nanomolar in vitro activities (see Table 1), representatives with appropriate pharmacokinetic properties were selected for in vivo experiments based on the parameters shown below.

Oral Absorption and Renal Excretion. For the evaluation of oral absorption and renal excretion of the esters **16** and **21** as well as the acids **17** and **22** physicochemical parameters such as pK_a values, lipophilicity (distribution coefficients, log D_{7.4}), solubility, and permeability were determined

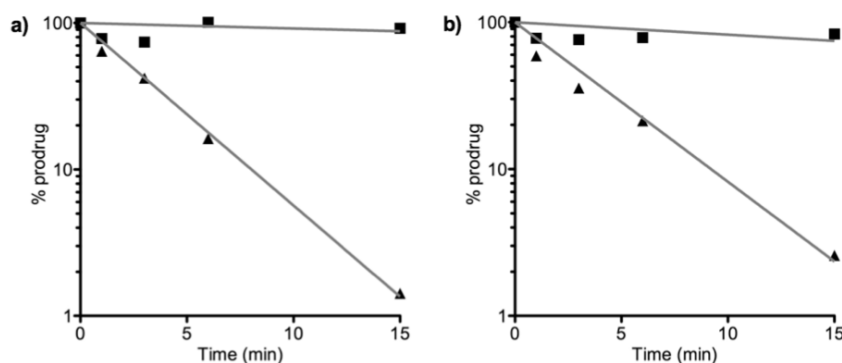


Figure 6. Incubation of (a) **16a** and (b) **16b** with pooled mouse liver microsomes (0.25 mg of protein/mL), in absence (▲) and in presence (■) of the specific carboxylesterase inhibitor bis(4-nitrophenyl) phosphate (BNPP).

(Table 1). Not surprisingly, the acids **17** and **22** showed $\log D_{7.4}$ values in the range of -1 to -2 and $\text{p}K_a$ values of approximately 4. While these parameters are beneficial for renal excretion,³² oral absorption by passive diffusion seems unlikely. Indeed, when the permeation through an artificial membrane (PAMPA³⁰) was studied, neither significant permeation ($\log P_e$, P_e : effective permeation) nor membrane retention could be detected. Whereas for a successful oral absorption $\log P_e$ should be above -5.7 and/or the membrane retention above 80%,⁴⁸ the corresponding values for the carboxylic acids **17** and **22** are far from being in this range (see Table 1, e.g. entries 7 and 9). However, $\log D_{7.4}$ values and PAMPA results were markedly improved for the esters **16** and **21** (Table 1, e.g. entries 6 and 8), suggesting that these FimH antagonists are orally absorbed. This assumption was fully confirmed in a cell-based permeation assay with Caco-2 cells.³¹ For renal excretion, Varma et al.³¹ correlated low lipophilicity and the presence of a charged state at physiological pH positively with enhanced elimination. On the basis of $\log D_{7.4}$ and $\text{p}K_a$ summarized in Table 1, the carboxylates **17** and **22** fulfill these requirements. Overall, these results support the prodrug approach: (i) oral application of the esters **16** and **21** and (ii) renal elimination of the corresponding acids **17** and **22**.

Solubility. A major problem of the antagonists **16** and **21** is their insufficient solubility, ranging from 4.6 to 37.6 $\mu\text{g}/\text{mL}$. Even though the solubility issue can be addressed by appropriate formulations, further structural modifications to improve solubility are necessary. Opposite to the esters, the corresponding carboxylates **17** and **22** showed excellent solubility ($> 3 \text{ mg}/\text{mL}$). This enables their iv application in physiological solutions (PBS) in the UTI model without further needs to develop suitable formulations (see below).

Stability in Simulated Gastrointestinal Fluids. To exclude degradation in the gastrointestinal tract prior to absorption, the stability of **1**, **16b**, and **17b** in simulated gastric fluid (sGF) and simulated intestinal fluid (sIF) was determined. All three antagonists proved to be sufficiently stable with more than 80% of the initial concentrations found after two hours.

Metabolic Stability. Because the prodrug approach is only applicable when the esters **16a** and **16b** are rapidly metabolically cleaved into the corresponding acids, their propensity to enzymatic hydrolysis by carboxylesterase (CES) was studied. Mammalian CESs are localized in the endoplasmic reticulum of the liver and most other organs.²⁹ Because of the excellent affinity of the corresponding acids **17a** and

17b to FimH, we concentrated our metabolic studies on the ester prodrugs **16a** and **16b**, which were incubated with pooled male mouse liver microsomes to study the hydrolysis and the release of the metabolites. Preliminary experiments involving low substrate concentrations (2 μM) and a concentration of the microsomal protein of 0.25 mg/mL showed a fast degradation of the ester prodrugs (Figure 6). Addition of the specific CES inhibitor bis(4-nitrophenyl) phosphate (BNPP) prevented ester degradation, suggesting that the metabolic transformation can be attributed to CESs.⁴⁹

On the basis of these *in vitro* results, we also expect fast hydrolysis of the esters *in vivo* at the first liver passage. Current studies are focusing on the kinetic parameters of the enzymatic ester cleavage.

To reach the minimal therapeutic concentration in the bladder (approximately 1 $\mu\text{g}/\text{mL}$, as estimated from a cell-based infection assay⁵⁰), the FimH antagonists **17a** and **17b** should be efficiently renally eliminated and not further metabolically processed. Therefore, the metabolic fate of the free carboxylic acids **17a** and **17b** was examined. A common method to predict a compound's propensity to phase I metabolism is its incubation with liver microsomes in presence of NADPH.⁵¹ Under these conditions, *in vitro* incubations of the free carboxylic acids **17a** and **17b** with pooled male mouse liver microsomes (0.5 mg microsomal protein/mL) did not show significant compound depletion over a period of 30 min, suggesting a high stability against cytochrome P450 mediated metabolism *in vivo*. However, phase II metabolic pathways such as glucuronidation remain to be studied in details.

Plasma Protein Binding (PPB). Compared to the corresponding esters **16** and **21**, the antagonists **17** and **22** exhibit 5–20% lower plasma protein binding, typically in the range of 73–89%. This rather low PPB beneficially influences renal excretion because, in line with the free drug hypothesis,⁵² molecules bound to plasma proteins evade metabolism and excretion. However, for a concluding statement, the kinetics of PPB, i.e. association and dissociation rate constants, have to be determined because PPB alone is not necessarily predictive for distribution, metabolism, and clearance.^{53,54}

In Vivo Pharmacokinetics and Treatment Studies. The two mannose derivatives methyl α -D-mannoside and *n*-heptyl α -D-mannoside (**1**) were previously tested in the UTI mouse model.^{10,21,22} In all three studies, the FimH antagonists were first preincubated with the bacterial suspension, followed by transurethral inoculation. To efficiently reduce infection,

Antagonist	Compartment	C_{max} ($\mu\text{g/mL}$)	AUC_{0-24} ($\mu\text{g} \times \text{h/mL}$)	PPB
1	plasma	35 ± 14.1	34.3 ± 33.3	81%
	urine	951.4 ± 249.6	2469.3 ± 636.4	
17a	plasma	34.4 ± 11.8	19.3 ± 6.2	73%
	urine	509.6 ± 427.5	139.9 ± 118.8	
17b	plasma	39.4 ± 15.7	20.8 ± 7.3	89%
	urine	588.4 ± 218.2	209.6 ± 72.3	

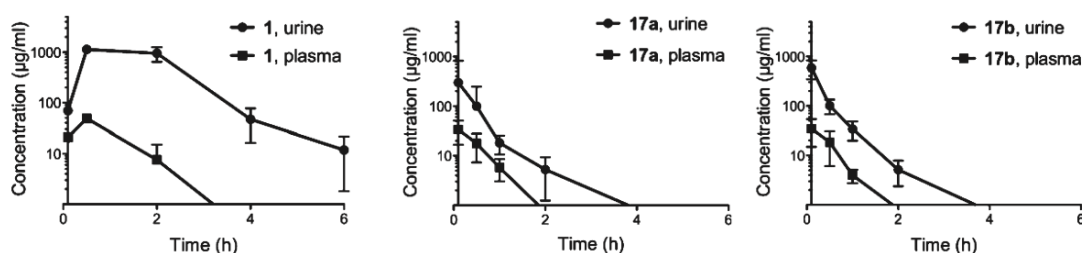


Figure 7. Determination of antagonist concentration in urine and plasma after a single iv application of 50 mg/kg. The data (table and graphs) show time-dependent urine and plasma concentrations of **1**, **17a**, and **17b**.

large amounts of methyl α -D-mannoside had to be applied (up to 1 M).²¹ For *n*-heptyl α -D-mannoside (**1**), an approximately one \log_{10} unit reduction of bacterial counts in the bladder was reached with lower, but still millimolar, concentration.¹⁰ In the previously presented studies, the FimH antagonists were exclusively instilled into the bladder, which is obviously not suitable for a therapeutic application. The aim of our project was therefore the identification of FimH antagonists suitable for iv or preferably po applications. Before infection studies in a mouse disease model could be performed, the in vivo pharmacokinetic parameters (C_{max} , AUC) had to be determined to ensure the antagonists availability in the target organ (bladder).

Pharmacokinetics of a Single iv Application in C3H/HeN Mice. Plasma and urine concentrations of the FimH antagonists **1**, **17a**, and **17b** after iv application were determined. With a single dose of 50 mg/kg, the control compound **1** exhibited availability in the bladder over a period of 6 h after administration ($n = 4$), whereas at similar doses, **17a** and **17b** showed lower urine concentrations over a reduced time period (max 2 h) ($n = 6$). In Figure 7, the pharmacokinetic parameters are summarized. Overall, for all three compounds, higher availability of the antagonists in the urine was observed compared to the plasma. Because plasma protein binding is of comparable scale for the three compounds (see Table 1 and Figure 7), it similarly influences urine concentrations.

Pharmacokinetics of a Single po Application in C3H/HeN Mice. Aiming for an orally available FimH antagonist, the prodrug **16b** and its metabolite **17b** were tested. Because of the in vitro pharmacokinetic properties of **17b** (Table 1, entry 9), its low oral bioavailability after the administration of a single po dose (50 mg/kg) was not surprising. For the determination of the availability of a similar dose of **16b** at the target organ (bladder), plasma and urine concentrations were determined over a period of 24 h ($n = 6$) (Figure 8). Because **16b** was designed as a prodrug expected to be rapidly

Antagonist applied	Antagonist detected	Compartment	$AUC_{0-24 \text{ p.o.}}$ ($\mu\text{g} \times \text{h/mL}$)
17b	17b	Plasma	n.d.
	17b	Urine	2.7 ± 3.2
16b	16b	Plasma	1.02 ± 0.32
		Urine	1.89 ± 0.37
	17b	Plasma	2.1 ± 0.61
		Urine	21.69 ± 3.88

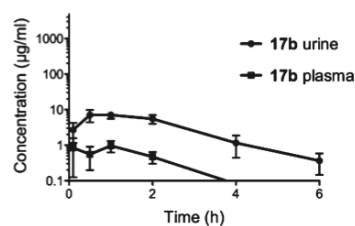


Figure 8. Determination of antagonist concentration in urine and plasma after a single po application of 50 mg/kg of antagonists **16b** and **17b**. The data (table and graph) show their time-dependent urine and plasma concentrations. When **17b** was orally applied, its plasma concentration was below the detection level, and only a small portion was present in the urine. However, after the application of the prodrug **16b**, metabolite **17b** was predominantly detected due to fast metabolic hydrolysis of **16b**. However, minor amounts of **16b** are still traceable in plasma as well as urine; nd, not detectable.

hydrolyzed, plasma and urine samples were analyzed not only for **16b** but also for its metabolite **17b**. **16b** was present only in minor concentrations in both plasma and urine. However, although the AUC of metabolite **17b** in urine is reduced by 90% compared to the iv application, its minimal therapeutic concentration can be maintained over a period of 2 to 3 h.

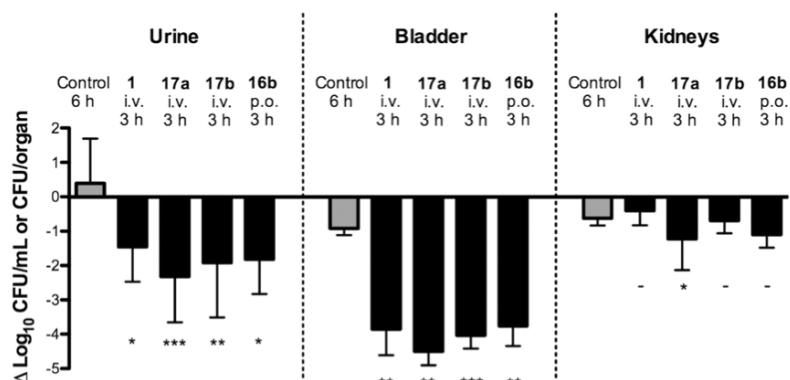


Figure 9. Treatment efficacy of the reference compound (**1**) and three FimH antagonists (**17a**, **17b**, **16b**) at a dosage of 50 mg/kg in the UTI mouse model after 3 h of infection, compared to a 6 h infection study ($n = 6$). **1**, **17a**, and **17b** were applied iv into the tail vein, whereas **16b** was applied orally. As baseline (reference), the mean counts of the 3 h infection were subtracted from the results of the tested antagonists and the 6 h control group. P values were calculated by comparing the treatment groups with the 3 h control group. (*) $P < 0.05$, (**) $P < 0.01$, (***) $P < 0.001$, (-) not significant (determined by Mann–Whitney test).

UTI Mouse Model: Treatment Study. Before treatment studies were started, the optimal infection profile was established. A 3 h infection exhibited the highest infection level in the C3H/HeN mouse strain. At longer infection times, e.g. 6 h, the control group showed indeed higher bacterial counts in the urine, however, the bladder and kidney counts already decreased due to self-clearance of the infection in the UTI mouse model.⁵⁵ For the in vivo UTI treatment studies (Figure 9), antagonists **1**, **17a**, **17b**, and **16b** were applied followed by infection with UPEC (UTI89). For each antagonist, a group of six animals was used. The animals were sacrificed 3 h after inoculation and urine and homogenized organs (bladder, kidneys) were examined for bacterial counts. The mean value in the untreated reference group ($n = 6$) showed 1.8×10^6 CFU/mL in the urine, 1.4×10^8 CFU in the bladder and 9.7×10^6 CFU in the kidneys. The bar diagram in Figure 9 summarizes the bacterial counts after iv (**1**, **17a**, and **17b**) and po (**16b**) treatment. The baseline represents the values obtained for the control group after 3 h and was used as reference for CFU reductions. **1** showed the lowest inhibition of growth in the urine with $1.5 \log_{10}$ CFU reduction and an approximately $4 \log_{10}$ reduction of bacterial counts in the bladder. After iv application of **17a**, a substantial decrease in the bacterial count was obtained ($>2 \log_{10}$ CFU reduction in the urine and $4.5 \log_{10}$ reduction in the bladder). A slightly lower reduction was observed when **17b** was applied iv (a decrease of $2 \log_{10}$ CFU in the urine and $4 \log_{10}$ for bladder counts). Interestingly, almost the same reduction of the bacterial count was detected with orally applied **16b**.

In general, urine samples showed higher bacterial counts compared to the bladder. This could be due to the difficulties during urine sampling. We observed that infected C3H/HeN mice void considerably less urine ($5\text{--}50 \mu\text{L}$) compared to healthy mice ($50\text{--}100 \mu\text{L}$). As a consequence, the lower urine volume leads to a higher concentration of bacteria in the collected urine and therefore to higher bacterial counts compared to the bladder.

In all treated animals, bacterial counts were only marginally reduced in the kidneys. This lower response to the treatment with FimH antagonists is probably due to different bacterial adhesion mechanisms in bladder and kidney. Whereas in the bladder adhesion is mediated by type I pili (via the CRD of FimH), P pili-dependent interactions are crucial for the adhesion in the kidneys.⁶

Summary and Conclusions

With the objective to develop an oral treatment of urinary tract infections, we have synthesized a series of potent small molecular weight FimH antagonists. Starting from the known antagonist phenyl α -D-mannopyranoside (**7a**), two equally potent classes of biphenyl α -D-mannopyranoside, those with an ester function (**16** and **21**) and those with a carboxylate (**17** and **22**) on the terminal aromatic ring, were synthesized. According to their pharmacokinetic properties, the acids **17** and **22** were not expected to be orally absorbed, a prediction that was also confirmed by an in vivo PK study. Therefore, a prodrug approach was envisaged. On the basis of permeation assays (PAMPA and Caco-2), the esters **16** and **22** were expected to exhibit oral availability. Moreover, metabolic studies with mouse liver microsomes proposed fast in vivo hydrolysis of orally applied **16b** to the corresponding carboxylate **17b**. In vivo PK studies in mice finally confirmed the in vitro prediction of a fast renal elimination of **17b** to the target organ, the bladder. When orally applied **16b** was tested in the UTI mouse model, it reduced the colony forming units (CFU) in the urine by 2 orders of magnitude and in the bladder by 4 orders of magnitude. As a result, a low molecular weight FimH antagonist suitable for the oral treatment of urinary tract infections was identified.

However, a number of parameters remain to be improved. Because the solubilities of the esters **16** and **22** are in the low $\mu\text{g/mL}$ range, an iv application was impossible and the suspension in DMSO/1% Tween 80 used for oral dosing is not optimal. In addition, due to fast renal elimination, the minimal therapeutic concentration of **17b** in the bladder could only be maintained for 2–3 h. Because high plasma protein binding was observed, an unfavorable kinetic of dissociation of the active principle from plasma proteins followed by fast renal elimination might be the reason for these findings. An improvement of the corresponding pharmacokinetic parameters should positively influence the duration of action. Furthermore, a detailed analysis of the metabolic pathway of **16b** and its metabolite **17b** will elucidate their overall metabolic fate. Finally, a detailed PK/PD profile in the mouse model will elucidate the full potential of FimH antagonists for the therapy of urinary tract infections (UTI).

Experimental Section

General Methods. NMR spectra were recorded on a Bruker Avance DMX-500 (500 MHz) spectrometer. Assignment of ^1H

and ^{13}C NMR spectra was achieved using 2D methods (COSY, HSQC, TOCSY). Chemical shifts are expressed in ppm using residual CHCl_3 , CHD_2OD , and H_2O as references. Optical rotations were measured using Perkin-Elmer polarimeter 341. Electron spray ionization mass spectra (ESI-MS) were obtained on a Waters micromass ZQ. HRMS analysis were carried out using a Bruker Daltonics micrOTOF spectrometer equipped with a TOF hexapole detector. Microanalyses were performed at the Department of Chemistry, University of Basel, Switzerland. Microwave-assisted reactions were carried out with a CEM Discover and Explorer. Reactions were monitored by TLC using glass plates coated with silica gel 60 F₂₅₄ (Merck) and visualized by using UV light and/or by heating to 140 °C for 5 min with a molybdate solution (a 0.02 M solution of ammonium cerium sulfate dihydrate and ammonium molybdate tetrahydrate in aqueous 10% H_2SO_4). Column chromatography was performed on a CombiFlash Companion (Teledyne-ISCO, Inc.) using RediSep normal phase disposable flash columns (silica gel). Reversed phase chromatography was performed on LiChroprepRP-18 (Merck, 40–63 μm). Commercially available reagents were purchased from Fluka, Aldrich, Merck, AKSci, ASDI, or Alfa Aesar. Methanol (MeOH) was dried by refluxing with sodium methoxide and distilled immediately before use. Toluene was dried by filtration over Al_2O_3 (Fluka, type 5016 A basic). Dioxane was dried by distillation from sodium/benzophenone.

4-Bromophenyl 2,3,4,6-Tetra-O-acetyl- α -D-mannopyranoside (14a). To a stirred solution of **12** (1.17 g, 3.00 mmol) and 4-bromophenol (**13a**, 623 mg, 3.60 mmol) in toluene (12 mL), TMSOTf (65 μL , 0.36 mmol) was added dropwise under argon. The mixture was stirred at rt for 5 h and then diluted with toluene (15 mL) and washed with satd aq NaHCO_3 . The organic layer was separated, and the aqueous layer was extracted three times with toluene. The combined organic layers were dried over Na_2SO_4 and concentrated in vacuo. The residue was purified by flash chromatography on silica (petroleum ether/EtOAc, 19:1 to 1.5:1) to yield **14a** (1.17 g, 74%) as a white solid.

^1H NMR (500 MHz, CDCl_3): δ 2.06 (s, 9H, 3 COCH_3), 2.19 (s, 3H, COCH_3), 4.06 (m, 2H, H-5, H-6a), 4.27 (dd, $J = 5.6$, 12.4 Hz, 1H, H-6b), 5.36 (t, $J = 10.2$ Hz, 1H, H-4), 5.43 (dd, $J = 1.8$, 3.5 Hz, 1H, H-2), 5.48 (d, $J = 1.7$ Hz, 1H, H-1), 5.53 (dd, $J = 3.5$, 10.1 Hz, 1H, H-3), 6.98, 7.41 (AA', BB' of AA'BB', $J = 9.0$ Hz, 4H, C_6H_4). ^{13}C NMR (125 MHz, CDCl_3): δ 20.71, 20.73, 20.74, 20.9 (4 COCH_3), 62.1 (C-6), 65.9 (C-4), 68.8 (C-3), 69.2 (C-2), 69.3 (C-5), 95.9 (C-1), 115.6, 118.3, 132.6, 154.7 (6C, C_6H_4), 170.0 (4C, 4 CO).

4-Bromo-2-chlorophenyl 2,3,4,6-tetra-O-acetyl- α -D-mannopyranoside (14b). According to the procedure described for **14a**, compound **12** (2.38 g, 4.84 mmol) and 4-bromo-2-chlorophenol (**13b**, 1.20 g, 5.80 mmol) were treated with TMSOTf (107 mg, 0.484 mmol) to yield **14b** (1.54 g, 59%) as a white solid.

$[\alpha]_D +60.6$ (c 0.40, CHCl_3). ^1H NMR (500 MHz, CDCl_3): δ 2.02, 2.04, 2.18 (3s, 12H, 4 COCH_3), 4.05 (dd, $J = 2.3$, 12.2 Hz, 1H, H-6a), 4.10 (ddd, $J = 2.7$, 5.3, 9.6 Hz, 1H, H-5), 4.24 (dd, $J = 5.4$, 12.2 Hz, 1H, H-6b), 5.35 (t, $J = 10.1$ Hz, 1H, H-4), 5.48 (m, 2H, H-1, H-2), 5.56 (dd, $J = 3.2$, 10.1 Hz, 1H, H-3), 7.03 (d, $J = 8.8$ Hz, 1H, C_6H_3), 7.30 (dd, $J = 2.4$, 8.8 Hz, 1H, C_6H_3), 7.53 (d, $J = 2.4$ Hz, 1H, C_6H_3). ^{13}C NMR (125 MHz, CDCl_3): δ 20.9, 21.1 (4C, 4 COCH_3), 62.3 (C-6), 65.9 (C-4), 68.9 (C-3), 69.4 (C-2), 70.1 (C-5), 96.9 (C-1), 115.9, 118.4, 125.7, 130.8, 133.3, 150.6 (C_6H_3), 169.9, 170.0, 170.1, 170.7 (4 CO). ESI-MS calcd for $\text{C}_{20}\text{H}_{22}\text{BrClNaO}_{10}$ [$\text{M} + \text{Na}$] $^+$ 559.0; found 559.0; Anal. Calcd for $\text{C}_{20}\text{H}_{22}\text{BrClO}_{10}$: C 44.67, H 4.12. Found: C 45.08, H 4.14.

Methyl 4'-(2,3,4,6-Tetra-O-acetyl- α -D-mannopyranosyloxy)-biphenyl-4-carboxylate (15a). A Schlenk tube was charged with **14a** (503 mg, 1.00 mmol), 4-methoxycarbonylbiphenylboronic acid (224 mg, 1.24 mmol), *S*-Phos (20.5 mg, 0.05 mmol), cesium carbonate (1.17 g, 3.6 mmol), $\text{Pd}_2(\text{dba})_3$ (10.4 mg, 0.01 mmol), and a stirring bar. The tube was closed with a rubber septum and was evacuated and flushed with argon. This procedure was

repeated once, and then freshly degassed dioxane (5 mL) was added under a stream of argon. The reaction tube was quickly sealed and the contents were stirred at 80 °C overnight. The reaction mixture was cooled to rt, diluted with EtOAc (10 mL), washed with satd aq NaHCO_3 (5 mL) and brine (5 mL), and dried over Na_2SO_4 . The solvents were removed in vacuo, and the residue was purified by flash chromatography on silica (petroleum ether/EtOAc, 3:1 to 3:2) to give **15a** (474 mg, 85%) as a white solid.

$[\alpha]_D +80.8$ (c 1.00, CHCl_3). ^1H NMR (500 MHz, CDCl_3): δ 2.02, 2.03, 2.04, 2.19 (4s, 12H, COCH_3), 3.91 (s, 3H, OCH_3), 4.08 (m, 2H, H-6a, H-5), 4.27 (dd, $J = 5.2$, 12.2 Hz, 1H, H-6b), 5.37 (t, $J = 10.1$ Hz, 1H, H-4), 5.45 (dd, $J = 1.8$, 3.4 Hz, 1H, H-2), 5.56 (m, 2H, H-1, H-3), 7.16 (AA' of AA'BB', $J = 8.7$ Hz, 2H, C_6H_4), 7.57 (m, 4H, C_6H_4), 8.07 (BB' of AA'BB', $J = 8.4$ Hz, 2H, C_6H_4). ^{13}C NMR (125 MHz, CDCl_3): δ 20.74, 20.75, 20.77, 21.0 (4 COCH_3), 52.2 (OCH_3), 62.1 (C-6), 65.9 (C-4), 68.9 (C-3), 69.3, 69.4 (C-2, C-5), 95.8 (C-1), 116.9, 126.7, 128.5, 128.7, 130.2, 134.8, 144.8, 155.7 (12C, 2 C_6H_4), 167.0, 169.8, 170.0, 170.1, 170.6 (5 CO). ESI-MS calcd for $\text{C}_{28}\text{H}_{30}\text{NaO}_{12}$ [$\text{M} + \text{Na}$] $^+$ 581.2; found 581.0.

Methyl 4'-(2,3,4,6-Tetra-O-acetyl- α -D-mannopyranosyloxy)-3'-chlorobiphenyl-4-carboxylate (15b). A microwave tube was charged with bromide **14b** (720 mg, 1.34 mmol), 4-methoxycarbonylbiphenylboronic acid (289 mg, 1.61 mmol), cesium carbonate (1.31 g, 4.02 mmol), and $\text{Pd}(\text{PPh}_3)_4$ (77.4 mg, 0.067 mmol). The tube was sealed with a Teflon septum, evacuated through a needle, and flushed with argon. Degassed dioxane (1.5 mL) was added and the closed tube was degassed in an ultrasonic bath for 15 min, flushed again with argon for 20 min, and exposed to microwave irradiation at 120 °C for 500 min. The solvent was evaporated in vacuo. The residue was dissolved in DCM (10 mL), washed with brine (2 \times 10 mL), dried over Na_2SO_4 , and concentrated in vacuo. The residue was purified by flash chromatography on silica (petroleum ether/EtOAc, 5:1 to 0.5:1) to yield **15b** (333 mg, 42%) as a white foam.

$[\alpha]_D +66.3$ (c 1.06, CHCl_3). ^1H NMR (500 MHz, CDCl_3): δ 2.03, 2.06, 2.20 (3s, 12H, COCH_3), 3.92 (s, 3H, OCH_3), 4.08 (dd, $J = 2.4$, 12.3 Hz, 1H, H-6a), 4.17 (m, 1H, H-5), 4.28 (dd, $J = 5.4$, 12.3 Hz, 1H, H-6b), 5.39 (t, $J = 10.6$ Hz, 1H, H-4), 5.54 (dd, $J = 1.9$, 3.4 Hz, 1H, H-2), 5.59 (d, $J = 1.8$ Hz, 1H, H-1), 5.62 (dd, $J = 3.5$, 10.1 Hz, 1H, H-3), 7.24 (s, 1H, C_6H_3), 7.24 (dd, $J = 2.2$, 8.5 Hz, 1H, C_6H_3), 7.57 (AA' of AA'BB', $J = 8.5$ Hz, 2H, C_6H_4), 7.65 (d, $J = 2.2$ Hz, 1H, C_6H_3), 8.08 (BB' of AA'BB', $J = 8.5$ Hz, 2H, C_6H_4). ^{13}C NMR (125 MHz, CDCl_3): δ 20.9, 21.0, 21.1 (4C, 4 COCH_3), 52.5 (OCH_3), 62.3 (C-6), 66.0 (C-4), 69.0 (C-3), 69.5 (C-2), 70.0 (C-5), 96.8 (C-1), 117.4, 126.7, 126.9, 129.5, 130.5, 136.4, 143.6, 151.3 (12C, C_6H_3 , C_6H_4), 167.0, 169.9, 170.0, 170.2, 170.7 (5 CO). ESI-MS calcd for $\text{C}_{28}\text{H}_{29}\text{ClNaO}_{12}$ [$\text{M} + \text{Na}$] $^+$ 615.1; found 615.2. Anal. Calcd for $\text{C}_{28}\text{H}_{29}\text{ClO}_{12}$: C 56.71, H 4.93. Found: C 56.79, H 4.92.

Methyl 4'-(α -D-Mannopyranosyloxy)-biphenyl-4-carboxylate (16a).^{17d} To a solution of **15a** (170 mg, 0.304 mmol) in MeOH (3 mL) was added freshly prepared 1 M NaOMe in MeOH (100 μL) under argon. The mixture was stirred at rt until the reaction was complete (monitored by TLC), then neutralized with Amberlyst-15 (H^+) ion-exchange resin, filtered, and concentrated in vacuo. The residue was purified by reversed-phase chromatography (RP-18, $\text{H}_2\text{O}/\text{MeOH}$, 1:0–1:1) to give **16a** (90 mg, 76%) as white solid.

$[\alpha]_D +82.8$ (c 0.2, MeOH). ^1H NMR (500 MHz, CD_3OD): δ 3.62 (m, 1H, H-5), 3.72 (m, 3H, H-4, H-6a, H-6b), 3.92 (m, 4H, H-3, OCH_3), 4.03 (s, 1H, H-2), 5.55 (s, 1H, H-1), 7.24 (AA' of AA'BB', $J = 8.0$ Hz, 2H, C_6H_4), 7.64 (AA' of AA'BB', $J = 7.5$ Hz, 2H, C_6H_4), 7.71 (BB' of AA'BB', $J = 8.0$ Hz, 2H, C_6H_4), 8.07 (BB' of AA'BB', $J = 7.5$ Hz, 2H, C_6H_4). ^{13}C NMR (125 MHz, CD_3OD): δ 52.6 (OCH_3), 62.7 (C-6), 68.3 (C-4), 72.0 (C-2), 72.4 (C-3), 75.5 (C-5), 100.1 (C-1), 118.2, 127.7, 131.1, 135.1, 146.6, 158.2, 160.3 (12C, 2 C_6H_4), 166.1 (CO). HR-MS calcd for $\text{C}_{20}\text{H}_{22}\text{NaO}_8$ [$\text{M} + \text{Na}$] $^+$ 413.1212; found 413.1218.

Methyl 3'-Chloro-4'-(α -D-mannopyranosyloxy)-biphenyl-4-carboxylate (16b). According to the procedure described for **16a**, compound **16b** was prepared from **15b** (764 mg, 1.29 mmol). Yield: 69 mg, 12%.

$[\alpha]_D^{25} +97.4$ (*c* 1.01, MeOH). $^1\text{H NMR}$ (500 MHz, CD_3OD): δ 3.64 (m, 1H, H-5), 3.72 (m, 1H, H-6a), 3.78 (m, 2H, H-4, H-6b), 3.91 (s, 3H, OCH_3), 4.00 (dd, $J = 3.4, 9.5$ Hz, 1H, H-3), 4.11 (dd, $J = 1.8, 3.1$ Hz, 1H, H-2), 5.60 (d, $J = 1.1$ Hz, 1H, H-1), 7.46 (d, $J = 8.6$ Hz, 1H, C_6H_3), 7.58 (dd, $J = 2.2, 8.6$ Hz, 1H, C_6H_3), 7.69 (AA' of AA'BB', $J = 8.4$ Hz, 2H, C_6H_4), 7.72 (d, $J = 2.2$ Hz, 1H, C_6H_3), 8.08 (BB' of AA'BB', $J = 8.4$ Hz, 2H, C_6H_4). $^{13}\text{C NMR}$ (125 MHz, CD_3OD): δ 52.7 (OCH_3), 62.8 (C-6), 68.3 (C-4), 71.9 (C-2), 72.5 (C-3), 76.2 (C-5), 100.8 (C-1), 118.7, 125.58, 127.8, 127.9, 129.9, 130.3, 131.3, 136.4, 145.3, 153.5 (12C, C_6H_3 , C_6H_4), 168.4 (CO). HR-MS calcd for $\text{C}_{20}\text{H}_{21}\text{ClNaO}_8$ [$\text{M} + \text{Na}$] $^+$ 447.0823; found 447.082.

Sodium 4'-(α -D-Mannopyranosyloxy)-biphenyl-4-carboxylate (17a). To a solution of **15a** (228 mg, 0.408 mmol) in MeOH (6.0 mL) was added 1 M NaOMe in MeOH (60 μL) at rt. The reaction mixture was stirred at rt for 4 h, and then NaOH (82 mg) in water (6 mL) was added and stirring was continued at rt overnight. The reaction mixture was concentrated in vacuo, and the residue was purified by reversed-phase chromatography (RP-18, $\text{H}_2\text{O}/\text{MeOH}$, 1:0–1:1) to afford **17a** (96 mg, 63%) as a white solid.

$[\alpha]_D^{25} +103$ (*c* 0.10, MeOH). $^1\text{H NMR}$ (500 MHz, CD_3OD): δ 3.60 (m, 1H, H-5), 3.72 (m, 3H, H-6a, H-6b, H-4), 3.89 (dd, $J = 3.4, 9.5$ Hz, 1H, H-3), 4.00 (dd, $J = 1.8, 3.3$ Hz, 1H, H-2), 5.51 (s, 1H, H-1), 7.19, 7.60 (AA', BB' of AA'BB', $J = 8.7$ Hz, 4H, C_6H_4), 8.01 (d, $J = 8.2$ Hz, 2H, C_6H_3), 8.46 (s, 2H, C_6H_4). $^{13}\text{C NMR}$ (125 MHz, CD_3OD): δ 63.2 (C-6), 68.9 (C-4), 72.6 (C-2), 73.0 (C-3), 76.1 (C-5), 100.7 (C-1), 118.7, 128.0, 129.9, 131.8 (12C, 2 C_6H_4). HR-MS calcd for $\text{C}_{19}\text{H}_{20}\text{NaO}_8$ [$\text{M} + \text{H}$] $^+$ 399.1056; found 399.1052.

Sodium 3'-Chloro-4'-(α -D-mannopyranosyloxy)-biphenyl-4-carboxylate (17b). To a solution of **15b** (380 mg, 0.641 mmol) in MeOH (10 mL) was added 1 M NaOMe in MeOH (300 μL). After stirring at rt for 24 h, 0.5 M aq NaOH (18 mL) was added and stirring continued for another 24 h. The solution was concentrated in vacuo and the residue was purified by reversed-phase chromatography (RP-18, $\text{H}_2\text{O}/\text{MeOH}$, 1:0–1:1) to yield **17b** (222 mg, 80%) as a white solid.

$[\alpha]_D^{25} +61.6$ (*c* 1.00, H_2O). $^1\text{H NMR}$ (500 MHz, D_2O): δ 3.66 (m, 1H, H-5), 3.73 (m, 2H, H-6a, H-6b), 3.79 (t, $J = 9.8$ Hz, 1H, H-4), 4.07 (dd, $J = 3.4, 9.8$ Hz, 1H, H-3), 4.14 (d, $J = 1.4$ Hz, 1H, H-2), 5.47 (bs, 1H, H-1), 7.04 (d, $J = 8.6$ Hz, 1H, C_6H_3), 7.24 (d, $J = 8.6$ Hz, 1H, C_6H_3), 7.37 (AA' of AA'BB', $J = 8.1$ Hz, 2H, C_6H_4), 7.41 (bs, 1H, C_6H_3), 7.86 (BB' of AA'BB', $J = 8.1$ Hz, 2H, C_6H_4). $^{13}\text{C NMR}$ (125 MHz, D_2O): δ 60.6 (C-6), 66.5 (C-4), 69.0 (C-2), 70.5 (C-3), 73.9 (C-5), 98.6 (C-1), 117.5, 123.9, 126.2, 126.4, 128.4, 129.6, 135.2, 135.3, 141.0, 150.4 (12C, C_6H_3 , C_6H_4), 175.0 (CO). HR-MS calcd for $\text{C}_{19}\text{H}_{18}\text{ClNaO}_8$ [$\text{M} + \text{H}$] $^+$ 433.0666; found 433.0670.

Competitive Binding Assay. A recombinant protein consisting of the CRD of FimH linked with a thrombin cleavage site to a 6His-tag (FimH-CRD-Th-6His) was expressed in *E. coli* strain HM125 and purified by affinity chromatography.²³ To determine the affinity of the various FimH antagonists, a competitive binding assay described previously²³ was applied. Microtiter plates (F96 MaxiSorp, Nunc) were coated with 100 $\mu\text{L}/\text{well}$ of a 10 $\mu\text{g}/\text{mL}$ solution of FimH-CRD-Th-6His in 20 mM HEPES, 150 mM NaCl, and 1 mM CaCl_2 , pH 7.4 (assay buffer) overnight at 4 $^\circ\text{C}$. The coating solution was discarded and the wells were blocked with 150 $\mu\text{L}/\text{well}$ of 3% BSA in assay buffer for 2 h at 4 $^\circ\text{C}$. After three washing steps with assay buffer (150 $\mu\text{L}/\text{well}$), a 4-fold serial dilution of the test compound (50 $\mu\text{L}/\text{well}$) in assay buffer containing 5% DMSO and streptavidin-peroxidase coupled Man- α (1-3)-[Man- α (1-6)]-Man- β (1-4)-GlcNAc- β (1-4)-GlcNAc β polyacrylamide (TM-PAA) polymer (50 $\mu\text{L}/\text{well}$ of a 0.5 $\mu\text{g}/\text{mL}$ solution) were added. On each individual microtiter plate, *n*-heptyl α -D-mannopyranoside (**1**) was tested in parallel.

The plates were incubated for 3 h at 25 $^\circ\text{C}$ and 350 rpm and then carefully washed four times with 150 $\mu\text{L}/\text{well}$ assay buffer. After the addition of 100 $\mu\text{L}/\text{well}$ of 2,2'-azino-di-(3-ethylbenzthiazoline-6-sulfonic acid) (ABTS)-substrate, the colorimetric reaction was allowed to develop for 4 min and then stopped by the addition of 2% aqueous oxalic acid before the optical density (OD) was measured at 415 nm on a microplate-reader (Spectramax 190, Molecular Devices, California, USA). The IC_{50} values of the compounds tested in duplicates were calculated with prism software (GraphPad Software, Inc., La Jolla, California, USA). The IC_{50} defines the molar concentration of the test compound that reduces the maximal specific binding of TM-PAA polymer to FimH-CRD by 50%. The relative IC_{50} (rIC_{50}) is the ratio of the IC_{50} of the test compound to the IC_{50} of *n*-heptyl α -D-mannopyranoside (**1**).

Selectivity for FimH vs Mannose-Binding Protein and DC-SIGN. Recombinant FimH-CRD-Th-6His (10 $\mu\text{g}/\text{mL}$), DC-SIGN-CRD-Fc-IgG³⁹ (2.5 $\mu\text{g}/\text{mL}$), and mannose-binding protein⁴² (MBP, 10 $\mu\text{g}/\text{mL}$, R&D Systems, Minneapolis, MN) were each diluted in assay buffer (20 mM HEPES, pH 7.4, 150 mM NaCl, and 10 mM CaCl_2) and were coated on microtiter plates (F96 MaxiSorp, Nunc) with 100 $\mu\text{L}/\text{well}$ overnight at 4 $^\circ\text{C}$. The further steps were performed as described above.

Aggregometry Assay. The aggregometry assay was carried out as previously described.³³ In short, the percentage of aggregation of *E. coli* UTI89 with guinea pig erythrocytes (GPE) was quantitatively determined by measuring the optical density at 740 nm and 37 $^\circ\text{C}$ under stirring at 1000 rpm using an APACT 4004 aggregometer (Endotell AG, Allschwil, Switzerland). Bacteria were cultivated as described below (see in vivo models). GPE were separated from guinea pig blood (Charles River Laboratories, Sulzfeld, Germany) using Histopaque (density of 1.077 g/mL at 24 $^\circ\text{C}$, Sigma-Aldrich, Buchs, Switzerland). Prior to the measurements, the cell densities of *E. coli* and GPE were adjusted to an OD_{600} of 4, corresponding to 1.9×10^8 CFU/mL and 2.2×10^6 cells/mL, respectively. For the calibration of the instrument, the aggregation of protein-poor plasma (PPP) using PBS alone was set as 100% and the aggregation of protein-rich plasma (PRP) using GPE as 0%. After calibration, measurements were performed with 250 μL of GPE and 50 μL of bacterial suspension and the aggregation monitored over 600 s. After the aggregation phase of 600 s, 25 μL of antagonist in PBS was added to each cuvette and disaggregation was monitored for 1400 s. UTI89 $\Delta\text{fimA-H}$ was used as negative control.

Determination of the Pharmacokinetic Parameters. Materials. Dimethyl sulfoxide (DMSO), 1-octanol, pepsin, pancreatin, reduced nicotinamide adenine dinucleotide phosphate (NADPH), Dulbecco's Modified Eagle's Medium (DMEM) high glucose, and bis(4-nitrophenyl) phosphate (BNPP) were purchased from Sigma-Aldrich (Sigma-Aldrich, St. Louis MO, USA). PAMPA System Solution, GIT-0 Lipid Solution, and Acceptor Sink Buffer were ordered from pIon (pIon, Woburn MA, USA). L-Glutamine-200 mM (100 \times) solution, MEM nonessential amino acid (MEM-NEAA) solution, fetal bovine serum (FBS), and DMEM without sodium pyruvate and phenol red were bought from Invitrogen (Invitrogen, Carlsbad CA, USA). Human plasma was bought from Biopredic (Biopredic, Rennes, France) and acetonitrile (MeCN) from Acros (Acros Organics, Geel, Belgium). Pooled male mouse liver microsomes were purchased from BD Bioscience (BD Bioscience, Woburn, MA, USA). Magnesium chloride was bought from Fluka (Fluka Chemie GmbH, Buchs, Switzerland). Tris(hydroxymethyl)-aminomethane (TRIS) was obtained from AppliChem (AppliChem, Darmstadt, Germany). The Caco-2 cells were kindly provided by Prof G. Imanidis, FHNW, Muttentz, and originated from the American Type Culture Collection (Rockville, MD, USA).

log $D_{7.4}$ Determination. The in silico prediction tool ALOGPS 2.1⁵⁶ was used to estimate the log *P* values of the compounds. Depending on these values, the compounds were classified into three categories: hydrophilic compounds (log *P*

Table 2

compound type	log <i>P</i>	ratios (1-octanol:buffer)
hydrophilic	< 0	30:140, 40:130
moderately lipophilic	0–1	70:110, 110:70
lipophilic	> 1	3:180, 4:180

below zero), moderately lipophilic compounds (log *P* between zero and one) and lipophilic compounds (log *P* above one). For each category, two different ratios (volume of 1-octanol to volume of buffer) were defined as experimental parameters (Table 2):

Equal amounts of phosphate buffer (0.1 M, pH 7.4) and 1-octanol were mixed and shaken vigorously for 5 min to saturate the phases. The mixture was left until separation of the two phases occurred, and the buffer was retrieved. Stock solutions of the test compounds were diluted with buffer to a concentration of 1 μM. For each compound, six determinations, i.e., three determinations per 1-octanol:buffer ratio, were performed in different wells of a 96-well plate. The respective volumes of buffer containing analyte (1 μM) were pipetted to the wells and covered by saturated 1-octanol according to the chosen volume ratio. The plate was sealed with aluminum foil, shaken (1350 rpm, 25 °C, 2 h) on a Heidolph Titramax 1000 plate-shaker (Heidolph Instruments GmbH & Co. KG, Schwabach, Germany) and centrifuged (2000 rpm, 25 °C, 5 min, 5804 R Eppendorf centrifuge, Hamburg, Germany). The aqueous phase was transferred to a 96-well plate for analysis by liquid chromatography–mass spectrometry (LC-MS).

log *D*_{7.4} was calculated from the 1-octanol:buffer ratio (*o:b*), the initial concentration of the analyte in buffer (1 μM), and the concentration of the analyte in buffer (*c*_B) with equilibration:

$$\log D_{7.4} = \log \left(\frac{1 \mu\text{M} - c_B}{c_B} \times \frac{1}{o:b} \right)$$

The average of the three log *D*_{7.4} values per 1-octanol:buffer ratio was calculated. If the two mean values obtained for a compound did not differ by more than 0.1 unit, the results were accepted.

Parallel Artificial Membrane Permeation Assay (PAMPA). log *P*_e was determined in a 96-well format with the PAMPA³⁰ permeation assay. For each compound, measurements were performed at three pH values (5.0, 6.2, 7.4) in quadruplicates. For this purpose, 12 wells of a deep well plate, i.e., four wells per pH value, were filled with 650 μL of System Solution. Samples (150 μL) were withdrawn from each well to determine the blank spectra by UV-spectroscopy (SpectraMax 190, Molecular Devices, Silicon Valley CA, USA). Then, analyte dissolved in DMSO was added to the remaining System Solution to yield 50 μM solutions. To exclude precipitation, the optical density was measured at 650 nm, with 0.01 being the threshold value. Solutions exceeding this threshold were filtrated. Afterward, samples (150 μL) were withdrawn to determine the reference spectra. A further 200 μL were transferred to each well of the donor plate of the PAMPA sandwich (pIon, Woburn MA, USA, P/N 110 163). The filter membranes at the bottom of the acceptor plate were impregnated with 5 μL of GIT-0 Lipid Solution and 200 μL of Acceptor Sink Buffer were filled into each acceptor well. The sandwich was assembled, placed in the GutBox, and left undisturbed for 16 h. Then, it was disassembled and samples (150 μL) were transferred from each donor and acceptor well to UV-plates. Quantification was performed by both UV-spectroscopy and LC-MS. log *P*_e values were calculated with the aid of the PAMPA Explorer Software (pIon, version 3.5).

Colorectal Adenocarcinoma Cells (Caco-2 Cells) Permeation Assay. The cells were cultivated in tissue culture flasks (BD Biosciences, Franklin Lakes NJ, USA) with DMEM high glucose medium, containing 1% L-glutamine solution, 1% MEM-NEAA solution, and 10% FBS. The cells were kept at

37 °C in humidified air containing 8% CO₂, and the medium was changed every second to third day. When approximately 90% confluence was reached, the cells were split in a 1:10 ratio and distributed to new tissue culture flasks. At passage numbers between 60 and 65, they were seeded at a density of 5.33 × 10⁵ cells per well to Transwell 6-well plates (Corning Inc., Corning NY, USA) with 2.5 mL of culture medium in the basolateral compartment and 1.5 mL (days 1–10) or 1.8 mL (from day 10 on) in the basolateral compartment. The medium was renewed on alternate days. Experiments were performed between days 19 and 21 postseeding. DMEM without sodium pyruvate and phenol red was used as transport medium for experiments. Previous to the experiment, the integrity of the Caco-2 monolayers was evaluated by measuring the transepithelial resistance (TEER) in transport medium (37 °C) with an Endohm tissue resistance instrument (World Precision Instruments Inc., Sarasota, FL, USA). Only wells with TEER values higher than 300 Ωcm² were used. Experiments were performed in triplicates. Transport medium (10 μL) from the apical compartments of three wells were replaced by the same volume of compound stock solutions (10 mM). The Transwell plate was then shaken (250 rpm) in the incubator. Samples (100 μL) were withdrawn after 5, 15, 30, 60, and 120 min from the basolateral compartment and concentrations were analyzed by HPLC. Apparent permeability coefficients (*P*_{app}) were calculated according to the following equation

$$P_{\text{app}} = \frac{dQ}{dt} \times \frac{1}{A \times c_0}$$

where *dQ/dt* is the permeability rate, *A* the surface area of the monolayer, and *c*₀ the initial concentration in the donor compartment.³¹ After the experiment, TEER values were assessed again for every well and results from wells with values below 300 Ωcm² were discarded.

p*K*_a Values. The p*K*_a values were determined as described elsewhere.⁴⁵ Briefly, the pH of a sample solution was gradually changed and the chemical shift of protons adjacent to ionizable centers was monitored by ¹H nuclear magnetic resonance (NMR) spectroscopy. The shift was plotted against the pH of the respective sample, and the p*K*_a was read out from the inflection point of the resulting sigmoidal curve.

Plasma Protein Binding (PPB). The dialysis membranes (HTDialysis LCC, Gales Ferry, CT, USA; MWCO 12–14 K) were prepared according to company instructions. The human plasma was centrifuged (5800 rpm, 25 °C, 10 min), the pH of the centrifugate (without floating plasma lipids) was adjusted to 7.5, and analyte was added to yield 10 μM solutions. Equal volumes (150 μL) of phosphate buffer (0.1 M, pH 7.5) and analyte-containing plasma were transferred to the separated compartments of the assembled 96-well high throughput dialysis block (HTDialysis LCC, Gales Ferry, CT, USA). Measurements were performed in triplicates. The plate was covered with a sealing film and incubated (5 h, 37 °C). Buffer and plasma compartment were processed separately. From the buffer compartments, 90 μL were withdrawn and 10 μL of blank plasma were added. From the plasma compartments, 10 μL were withdrawn and 90 μL of blank buffer were added. After protein precipitation with 300 μL ice-cooled MeCN, the solutions were mixed, centrifuged (3600 rpm, 4 °C, 11 min), and 50 μL of the supernatant were retrieved. Analyte concentrations were determined by LC-MS. The fraction bound (*f*_b) was calculated as follows:

$$f_b = 1 - \frac{c_b}{c_p}$$

where *c*_b is the concentration in the buffer and *c*_p the concentration in the plasma compartment. Values were accepted if the recovery of analyte was between 80 and 120%.

Thermodynamic Solubility. Microanalysis tubes (Labo-Tech J. Stofer LTS AG, MuttENZ, Switzerland) were charged with

1 mg of solid substance and 250 μL of phosphate buffer (50 mM, pH 6.5). The samples were briefly shaken by hand and then sonicated for 15 min and vigorously shaken (600 rpm, 25 $^{\circ}\text{C}$, 2 h) on a Eppendorf Thermomixer Comfort. Afterward, the samples were left undisturbed for 24 h. After measuring the pH, the saturated solutions were filtered through a filtration plate (MultiScreen HTS, Millipore, Billerica MA, USA) by centrifugation (1500 rpm, 25 $^{\circ}\text{C}$, 3 min). Prior to concentration determination by LC-MS, the filtrates were diluted (1:1, 1:10 and 1:100 or, if the results were outside of the calibration range, 1:1000 and 1:10000). The calibration was based on six values ranging from 0.1 to 10 $\mu\text{g}/\text{mL}$.

Stability in Simulated Gastrointestinal Fluids. Simulated gastric fluid (sGF) and simulated intestinal fluid (sIF) were prepared according to the United States Pharmacopeia (USP 28). sGF contained sodium chloride (200 mg), pepsin (320 mg), and 37% aq HCl (0.7 mL) in bidistilled water (100 mL). sIF consisted of monopotassium phosphate (680 mg), 0.2 M NaOH (7.7 mL), and pancreatin (1 g) in bidistilled water (100 mL). sIF was adjusted to pH 6 by adding 0.2 M NaOH. sGF and sIF were preheated (37 $^{\circ}\text{C}$), and the compounds were added to yield 10 μM solutions. Incubations were performed on a Eppendorf Thermomixer Comfort (500 rpm, 37 $^{\circ}\text{C}$). Before starting the experiment ($t = 0$ min) and after an incubation time of 15, 30, 60, and 120 min, samples (20 μL) were withdrawn, precipitated with ice-cooled MeCN, and centrifuged (3600 rpm, 4 $^{\circ}\text{C}$, 10 min). The concentrations of analyte in the supernatant were analyzed by LC-MS. Stability was expressed as percentage remaining compound relative to the initial concentration.

In Vitro Metabolism: Ester Hydrolysis. Incubations were performed in a 96-well format on a Eppendorf Thermomixer Comfort. Each compound was incubated with a reaction mixture (270 μL) consisting of pooled male mouse liver microsomes in the presence of TRIS buffer (0.1 M, pH 7.4) and MgCl_2 (2 mM). After preheating (37 $^{\circ}\text{C}$, 500 rpm, 10 min), the incubation was initiated by adding 30 μL of compound solution (20 μM) in TRIS buffer. The final concentration of the compounds was 2 μM , and the microsomal concentration was 0.25 mg/mL. At the beginning of the experiment ($t = 0$ min) and after an incubation time of 1, 3, 6, and 15 min, samples (50 μL) were transferred to 150 μL of ice-cooled MeCN, centrifuged (3600 rpm, 4 $^{\circ}\text{C}$, 10 min), and 80 μL of supernatant were transferred to a 96-well plate for LC-MS analysis. Metabolic degradation was assessed as percentage remaining compound versus incubation time. Control experiments were performed in parallel by preincubating the microsomes with the specific carboxylesterase inhibitor BNPP (1 mM) for 5 min before addition of the antagonists.

In Vitro Metabolism: Cytochrome P450-Mediated Metabolism. Incubations consisted of pooled male mouse liver microsomes (0.5 mg microsomal protein/mL), compounds (2 μM), MgCl_2 (2 mM), and NADPH (1 mM) in a total volume of 300 μL TRIS buffer (0.1 M, pH 7.4) and were performed in a 96-well plate on a Thermomixer Comfort. Compounds and microsomes were preincubated (37 $^{\circ}\text{C}$, 700 rpm, 10 min) before NADPH was added. Samples (50 μL) at $t = 0$ min and after an incubation time of 5, 10, 20, and 30 min were quenched with 150 μL of ice-cooled acetonitrile, centrifuged (3600 rpm, 4 $^{\circ}\text{C}$, 10 min), and 80 μL of each supernatant were transferred to a 96-well plate for LC-MS analysis. Control experiments without NADPH were performed in parallel.

LC-MS Measurements. Analyses were performed using a 1100/1200 series HPLC system coupled to a 6410 triple quadrupole mass detector (Agilent Technologies, Inc., Santa Clara, CA, USA) equipped with electrospray ionization. The system was controlled with the Agilent MassHunter Workstation Data Acquisition software (version B.01.04). The column used was an Atlantis T3 C18 column (2.1 mm \times 50 mm) with a 3 μm particle size (Waters Corp., Milford, MA, USA). The mobile phase consisted of two eluents: solvent A (H_2O , containing 0.1%

formic acid, v/v) and solvent B (acetonitrile, containing 0.1% formic acid, v/v), both delivered at 0.6 mL/min. The gradient was ramped from 95% A/5% B to 5% A/95% B over 1 min, and then held at 5% A/95% B for 0.1 min. The system was then brought back to 95% A/5% B, resulting in a total duration of 4 min. MS parameters such as fragmentor voltage, collision energy, polarity were optimized individually for each drug, and the molecular ion was followed for each compound in the multiple reaction monitoring mode. The concentrations of the analytes were quantified by the Agilent Mass Hunter Quantitative Analysis software (version B.01.04).

In Vivo Pharmacokinetic and Disease Model. Bacteria. The clinical *E. coli* isolate UTI89⁵⁵ (UTI89wt) were kindly provided by the group of Prof. Urs Jenal, Biocenter, University of Basel. Microorganisms were stored at -70 $^{\circ}\text{C}$ and before experiment incubated for 24 h under static conditions at 37 $^{\circ}\text{C}$ in 10 mL of Luria–Bertani broth (Becton, Dickinson and Company, Le Pont de Claix, France) using 50 mL tubes. Prior to each experiment, the microorganisms were washed twice and resuspended in phosphate buffered saline (PBS, Hospital Pharmacy at the University Hospital Basel, Switzerland). Bacterial concentrations were determined by plating serial 1:10 dilutions on blood agar, followed by colony counting with 20–200 colonies after overnight incubation at 37 $^{\circ}\text{C}$.

Animals. Female C3H/HeN mice weighting between 19 and 25 g were obtained from Charles River (Sulzfeld, Germany) and were housed four to a cage. Mice were kept under specific-pathogen-free conditions in the Animal House of the Department of Biomedicine, University Hospital Basel, and animal experimentation guidelines according to the regulations of Swiss veterinary law were followed. After seven days of acclimatization, 9- to 10-week old mice were used for the PK and infection studies. During the studies, animals were allowed free access to chow and water. Three days before infection studies and during infection, 5% D-(+)-glucose (AppliChem, Baden-Dättwil, Switzerland) was added to the drinking water to increase the number of bacterial counts in the urine and kidneys.⁵⁷

Pharmacokinetic Studies. Single-dose pharmacokinetic studies were performed by iv and po application of the FimH antagonists at a concentration of 50 mg/kg followed by urine and plasma sampling. For iv application, the antagonists (**1**, **17a**, **17b**) were diluted in 100 μL of PBS and injected into the tail vein. For po application, antagonist **1** was diluted in 200 μL of PBS and antagonists **17b** and **16b** were first dissolved in DMSO (20 \times) and then slowly diluted to the final concentration (1 \times) in 1% Tween-80/PBS to obtain a suspension. Antagonists were applied iv by injection into the tail vein and po using a gavage followed by blood and urine sampling (10 μL) after 6 min, 30 min, 1 h, 2 h, 4 h, 6 h, 8 h, and 24 h. Before analysis, proteins in blood and urine samples were precipitated using methanol (Acros Organics, Basel, Switzerland) and centrifuged for 11 min at 13000 rpm. The supernatant was transferred into a 96-well plate (0.5 mL, polypropylene, Agilent Technologies, Basel, Switzerland) and analyzed by LC-MS as described above.

UTI Mouse Model. Mice were infected as previously described.⁵⁷ In brief, before infection, all remaining urine was depleted from the bladder by gentle pressure on the abdomen. Mice were anesthetized with 2.5 vol% isoflurane/oxygen mixture (Attane, Minrad Inc., Buffalo, NY, USA) and placed on their back. Anesthetized mice were inoculated transurethraly with the bacterial suspension by use of a 2 cm polyethylene catheter (Intramedic polyethylene tubing, inner diameter 0.28 mm, outer diameter 0.61 mm, Beckton Dickinson, Allschwil, Switzerland), which was placed on a syringe (Hamilton Gastight Syringe 50 μL , removable 30G needle, BGB Analytik AG, Boeckten, Switzerland). The catheter was gently inserted through the urethra until it reached the top of the bladder, followed by slow injection of 50 μL of bacterial suspension at a concentration of approximately 10^9 to 10^{10} CFU/mL.

Antagonist Treatment Studies. FimH antagonists were applied iv in 100 μL of PBS into the tail vein or po as a suspension by the help

of a gavage, 10 min (17a, 17b, 16b) or 1 h before infection (1). Three h after the onset of infection, urine was collected by gentle pressure on the abdomen and then the mouse was sacrificed with CO₂. Organs were removed aseptically and homogenized in 1 mL of PBS by using a tissue lyser (Retsch, Haan, Germany). Serial dilutions of urine, bladder, and kidneys were plated on Levine Eosin Methylene Blue Agar plates (Beckton Dickinson, Le Pont de Claix, France). CFU counts were determined after overnight incubation at 37 °C and expressed as CFU/mL for the urine and CFU/bladder and CFU/2 kidneys for the organs.

Acknowledgment. We thank Professor Rudi Glockshuber (ETH Zürich, Switzerland) for gratefully providing the plasmid pNT-FimH used for the cloning of the FimH CRD and *E. coli* strain HM 125. We thank Dr. Manfred Kansy and Dr. Christoph Funk, F. Hoffmann-La Roche AG, Basel, Switzerland, for supporting us with their expertise when we established the PADMET platform, and to Prof. Angelo Vedani, University of Basel, Switzerland, for fruitful discussions on conformational issues. We further appreciate the support by Prof. Dr. med. Radek Skoda, Department of Biomedicine, University Hospital Basel, Switzerland, for giving us access to the animal facility and Prof. Niels Frimodt-Møller, Statens Serum Institut, Copenhagen, Denmark for the introduction to the in vivo model. We thank Prof G. Imanidis, FHNW, Muttenz, Switzerland, for providing the Caco-2 cells, and Dr. M. Schneider, Department of Pharmaceutical Sciences, University of Basel, Switzerland, for his help during the assay build-up. We are grateful to Prof. Urs Jenal, Biocenter of the University of Basel, Switzerland, for the clinical *E. coli* isolate UTI89 and the FimH knock out strain UTI89Δ*fimA-H*. Finally, we thank the Swiss National Science Foundation (project K-32K1-120904) for their financial support.

Supporting Information Available: ¹H NMR spectra and HPLC traces for the target compounds 16a–e, 17a–c,e, 21a,b, and 22a,b and experimental and spectroscopic details for compounds 6a–d, 7a–d, 14c–e, 15c–e, 16c–e, 17c,e, 19a,b, 20a,b, and 21a,b. This material is available free of charge via the Internet at <http://pubs.acs.org>.

References

- (1) Fihn, S. D. Clinical practice. Acute uncomplicated urinary tract infection in women. *N. Engl. J. Med.* **2003**, *349*, 259–266.
- (2) Hooton, T. M. Recurrent urinary tract infection in women. *Int. J. Antimicrob. Agents* **2001**, *17*, 259–268.
- (3) Wiles, T. J.; Kulesus, R. R.; Mulvey, M. A. Origins and virulence mechanisms of uropathogenic *Escherichia coli*. *Exp. Mol. Pathol.* **2008**, *85*, 11–19.
- (4) Gouin, S. G.; Wellens, A.; Bouckaert, J.; Kovensky, J. Synthetic Multimeric Heptyl Mannosides as Potent Antiadhesives of Uropathogenic *Escherichia coli*. *ChemMedChem* **2009**, *4*, 749–755.
- (5) Rosen, D. A.; Hung, C. S.; Kline, K. A.; Hultgren, S. J. Streptozocin-induced diabetic mouse model of urinary tract infection. *Infect. Immun.* **2008**, *76*, 4290–4298.
- (6) Mulvey, M. A. Adhesion and entry of uropathogenic *Escherichia coli*. *Cell Microbiol.* **2002**, *4*, 257–271.
- (7) Capitani, G.; Eidam, O.; Glockshuber, R.; Grutter, M. G. Structural and functional insights into the assembly of type 1 pili from *Escherichia coli*. *Microbes Infect.* **2006**, *8*, 2284–2290.
- (8) Choudhury, D.; Thompson, A.; Stojanoff, V.; Langermann, S.; Pinkner, J.; Hultgren, S. J.; Knight, S. D. X-ray structure of the FimC–FimH chaperone–adhesin complex from uropathogenic *Escherichia coli*. *Science* **1999**, *285*, 1061–1066.
- (9) Bouckaert, J.; Berglund, J.; Schembri, M.; Genst, E. D.; Cools, L.; Wuhrer, M.; Hung, C. S.; Pinkner, J.; Slättergard, R.; Zavalov, A.; Choudhury, D.; Langermann, S.; Hultgren, S. J.; Wyns, L.; Klemm, P.; Oscarson, S.; Knight, S. D.; Greve, H. D. Receptor binding studies disclose a novel class of high-affinity inhibitors of the *Escherichia coli* FimH adhesin. *Mol. Microbiol.* **2005**, *55*, 441–455.
- (10) Wellens, A.; Garofalo, C.; Nguyen, H.; Van Gerven, N.; Slättergard, R.; Hernalsteens, J.-P.; Wyns, L.; Oscarson, S.; De Greve, H.; Hultgren, S.; Bouckaert, J. Intervening with urinary tract infections using anti-adhesives based on the crystal structure of the FimH–oligomannose-3 complex. *PLoS ONE* **2008**, *3*, 4–13.
- (11) Langermann, S.; Mollby, R.; Burlein, J. E.; Palaszynski, S. R.; Auguste, C. G.; DeFusco, A.; Strouse, R.; Schenerman, M. A.; Hultgren, S. J.; Pinkner, J. S.; Winberg, J.; Guldevall, L.; Soderhall, M.; Ishikawa, K.; Normark, S.; Koenig, S. Vaccination with FimH adhesin protects cynomolgus monkeys from colonization and infection by uropathogenic *Escherichia coli*. *J. Infect. Dis.* **2000**, *181*, 774–778.
- (12) Langermann, S.; Palaszynski, S.; Barnhart, M.; Auguste, G.; Pinkner, J. S.; Burlein, J.; Barren, P.; Koenig, S.; Leath, S.; Jones, C. H.; Hultgren, S. J. Prevention of mucosal *Escherichia coli* infection by FimH-adhesin-based systemic vaccination. *Science* **1997**, *276*, 607–611.
- (13) Bouckaert, J.; Mackenzie, J.; de Paz, J. L.; Chipwaza, B.; Choudhury, D.; Zavalov, A.; Mannerstedt, K.; Anderson, J.; Pierard, D.; Wyns, L.; Seeburger, P. H.; Oscarson, S.; De Greve, H.; Knight, S. D. The affinity of the FimH fimbrial adhesin is receptor-driven and quasi-independent of *Escherichia coli* pathotypes. *Mol. Microbiol.* **2006**, *61*, 1556–1568.
- (14) Sharon, N. Carbohydrates as future anti-adhesion drugs for infectious diseases. *Biochim. Biophys. Acta* **2006**, *1760*, 527–537.
- (15) (a) Firon, N.; Ofek, I.; Sharon, N. Interaction of mannose-containing oligosaccharides with the fimbrial lectin of *Escherichia coli*. *Biochem. Biophys. Res. Commun.* **1982**, *105*, 1426–1432. (b) Firon, N.; Ofek, I.; Sharon, N. Carbohydrate specificity of the surface lectins of *Escherichia coli*, *Klebsiella pneumoniae* and *Salmonella typhimurium*. *Carbohydr. Res.* **1983**, *120*, 235–249. (c) Sharon, N. Bacterial lectins, cell–cell recognition and infectious disease. *FEBS Lett.* **1987**, *217*, 145–157.
- (16) (a) Neeser, J.-R.; Koellreutter, B.; Wuersch, P. Oligomannoside-type glycopeptides inhibiting adhesion of *Escherichia coli* strains mediated by type 1 pili: preparation of potent inhibitors from plant glycoproteins. *Infect. Immun.* **1986**, *52*, 428–436. (b) Lindhorst, T. K. Artificial multivalent sugar ligands to understand and manipulate carbohydrate–protein interactions. *Top. Curr. Chem.* **2002**, *218*, 201–235 (review); (c) Patel, A.; Lindhorst, T. K. A modular approach for the synthesis of oligosaccharide mimetics. *Carbohydr. Res.* **2006**, *341*, 1657–1668. (d) Nagahori, N.; Lee, R. T.; Nishimura, S.-L.; Pagé, S.; Roy, R.; Lee, Y. C. Inhibition of adhesion of type 1 fimbriated *Escherichia coli* to highly mannose-sylated ligands. *ChemBioChem* **2002**, *3*, 836–844. (e) Appeldoorn, C. C. M.; Joosten, J. A. F.; Maate, F. A.; Dobrindt, U.; Hacker, J.; Liskamp, R. M. J.; Khan, A. S.; Pieters, R. J. Novel multivalent mannose compounds and their inhibition of the adhesion of type 1 fimbriated uropathogenic *E. coli*. *Tetrahedron Asymmetry* **2005**, *16*, 361–372. (f) Touaibia, M.; Wellens, A.; Shiao, T. C.; Wang, Q.; Sirois, S.; Bouckaert, J.; Roy, R. Mannosylated G(0) dendrimers with nanomolar affinities to *Escherichia coli* FimH. *ChemMedChem* **2007**, *2*, 1190–1201.
- (17) (a) Firon, N.; Ashkenazi, S.; Mirelman, D.; Ofek, I.; Sharon, N. Aromatic alpha-glycosides of mannose are powerful inhibitors of the adherence of type 1 fimbriated *Escherichia coli* to yeast and intestinal epithelial cells. *Infect. Immun.* **1987**, *55*, 472–476. (b) Lindhorst, T. K.; Köster, S.; Kubisch, J.; Krallmann-Wenzel, U.; Ehlers, S.; Kren, V. Effect of p-substitution of aryl α-D-mannosides on inhibiting mannose-sensitive adhesion of *Escherichia coli*—synthesis and testing. *Eur. J. Org. Chem.* **1998**, 1669–1674. (c) Sperling, O.; Fuchs, A.; Lindhorst, T. K. Evaluation of the carbohydrate recognition domain of the bacterial adhesin FimH: design, synthesis and binding properties of mannoside ligands. *Org. Biomol. Chem.* **2006**, *4*, 3913–3922. (d) Han, Z.; Pinker, J. S.; Ford, B.; Obermann, R.; Nolan, W.; Wildman, S. A.; Hobbs, D.; Ellenberger, T.; Cusumano, C. K.; Hultgren, S. J.; Janetka, J. W. Structure-Based Drug Design and Optimization of Mannoside Bacterial FimH Antagonists. *J. Med. Chem.* **2010**, *53*, 4779–4792. (e) Berglund, J.; Bouckaert, J.; De Greve, H.; Knight, S. Anti-adhesive compounds to prevent and treat bacterial infections. International Patent Application PCT/US 2005/089733, 2005.
- (18) Hung, C. S.; Bouckaert, J.; Hultgren, S. J.; Widberg, C.; Defusco, A.; Auguste, C. G.; Strouse, R.; Langermann, S.; Waksman, G.; Hultgren, S. J. Structural basis of tropism of *Escherichia coli* to the bladder during urinary tract infection. *Mol. Microbiol.* **2002**, *44*, 903–918.
- (19) Ernst, B.; Magnani, J. L. From carbohydrate leads to glycomimetic drugs. *Nature Rev. Drug Discovery* **2009**, *8*, 661–677.
- (20) (a) Lindhorst, T. K.; Kieburg, C.; Krallmann-Wenzel, U. Inhibition of the type 1 fimbriae-mediated adhesion of *Escherichia coli* to erythrocytes by multiantennary α-mannosyl clusters: the effect of multivalency. *Glycoconjugate J.* **1998**, *15*, 605–613. (b) Dubber, M.; Sperling, O.; Lindhorst, T. K. Oligomannoside mimetics by glycosylation of 'octopus glycosides' and their investigation as inhibitors of type 1

- fimbriae-mediated adhesion of *Escherichia coli*. *Org. Biomol. Chem.* **2006**, *4*, 3901–3912. (c) Touaibia, M.; Wellens, A.; Shiao, T. C.; Wang, Q.; Sirois, S.; Bouckaert, J.; Roy, R. Mannosylated G0 dendrimers with nanomolar affinities to *Escherichia coli* FimH. *ChemMedChem* **2007**, *2*, 1190–1201.
- (21) Aronson, M.; Medalia, O.; Schori, L.; Mirelman, D.; Sharon, N.; Ofek, I. Prevention of colonization of the urinary tract of mice with *Escherichia coli* by blocking of bacterial adherence with methyl α -D-mannopyranoside. *J. Infect. Dis.* **1979**, *139*, 329–332.
- (22) Svanborg Eden, C.; Freter, R.; Hagberg, L.; Hull, R.; Leffer, H.; Schoolnik, G. Inhibition of experimental ascending urinary tract infection by an epithelial cell-surface receptor analog. *Nature* **1982**, *298*, 560–562.
- (23) Rabbani, S.; Jiang, X.; Schwardt, O.; Ernst, B. Expression of the carbohydrate recognition domain of FimH and development of a competitive binding assay. *Anal. Biochem.* **2010**, *407*, 188–195.
- (24) Ness, R. K.; Fletcher, H. G.; Hudson, C. S. Reaction of 2,3,4,6-tetrabenzoyl- α -D-glucopyranosyl bromide and 2,3,4,6-tetrabenzoyl- α -D-mannopyranosyl bromide with methanol. Certain benzoylated derivatives of D-glucose and D-mannose. *J. Am. Chem. Soc.* **1950**, *72*, 2200–2205.
- (25) Sancho-Garcia, J. C.; Cornil, J. Anchoring the Torsional Potential of Biphenyl at the ab Initio Level: The Role of Basis Set versus Correlation Effects. *J. Chem. Theory Comput.* **2005**, *1*, 581–589.
- (26) Eaton, V. J.; Steele, D. Dihedral angle of biphenyl in solution and the molecular force field. *J. Chem. Soc., Faraday Trans. 2* **1973**, 1601–1608.
- (27) Albert, A. Chemical aspects of selective toxicity. *Nature* **1958**, *182*, 421–422.
- (28) Winiwarter, S.; Bonham, N. M.; Ax, F.; Hallberg, A.; Lennernäs, H.; Karlén, A. Correlation of Human Jejunal Permeability (in Vivo) of Drugs with Experimentally and Theoretically Derived Parameters. A Multivariate Data Analysis Approach. *J. Med. Chem.* **1998**, *41*, 4939–4949.
- (29) Taketani, M.; Shii, M.; Ohura, K.; Ninomiya, S.; Imai, T. Carboxylesterase in the liver and small intestine of experimental animals and human. *Life Sci.* **2007**, *81*, 924–932.
- (30) Kansy, M.; Senner, F.; Gubernator, K. Physicochemical High Throughput Screening: Parallel Artificial Membrane Permeation Assay in the Description of Passive Absorption Processes. *J. Med. Chem.* **1998**, *41*, 1007–1010.
- (31) Artursson, P.; Karlsson, J. Correlation between oral drug absorption in humans and apparent drug permeability coefficients in human intestinal epithelial (Caco-2) cells. *Biochem. Biophys. Res. Com.* **1991**, *175*, 880–885.
- (32) Varma, M. V. S.; Feng, B.; Obach, R. S.; Troutman, M. D.; Chupka, J.; Miller, H. R.; El-Kattan, A. Physicochemical Determinants of Human Renal Clearance. *J. Med. Chem.* **2009**, *52*, 4844–4852.
- (33) Abgottspon, D.; Rölli, G.; Hosch, L.; Steinhuber, A.; Jiang, X.; Schwardt, O.; Cutting, B.; Smiesko, M.; Jenal, U.; Ernst, B.; Trampuz, A. Development of an Aggregation Assay to Screen FimH Antagonists. *J. Microbiol. Methods* **2010**, *82*, 249–255.
- (34) Zhou, G.; Mo, W.-J.; Sebbel, P.; Min, G.; Neubert, T. A.; Glockshuber, R.; Wu, X.-R.; Sun, T.-T.; Kong, X.-P. Uroplakin Ia is the urothelial receptor for uropathogenic *Escherichia coli*: evidence from in vitro FimH binding. *J. Cell Sci.* **2001**, *114*, 4095–4103.
- (35) (a) Kartha, K. P. R.; Field, R. A. Iodine: a versatile reagent in carbohydrate chemistry. IV. Per-O-acetylation, regioselective acylation and acetolysis. *Tetrahedron* **1997**, *53*, 11753–11766. (b) Chittaboina, S.; Hodges, B.; Wang, Q. A facile route for the regioselective deacetylation of peracetylated carbohydrates at anomeric position. *Lett. Org. Chem.* **2006**, *3*, 35–38. (c) Mori, M.; Ito, Y.; Ogawa, T. Total synthesis of the mollu-series glycosyl ceramides α -D-Manp-(1 \rightarrow 3)- β -D-Manp-(1 \rightarrow 4)- β -D-Glcp-(1 \rightarrow 1)-Cer and α -D-Manp-(1 \rightarrow 3)-[β -D-Xylp-(1 \rightarrow 2)]- β -D-Manp-(1 \rightarrow 4)- β -D-Glcp-(1 \rightarrow 1)-Cer. *Carbohydr. Res.* **1990**, *195*, 199–224. (d) Egusa, K.; Kusumoto, S.; Fukase, K. Solid-phase synthesis of a phytoalexin elicitor pentasaccharide using a 4-azido-3-chlorobenzyl group as the key for temporary protection and catch-and-release purification. *Eur. J. Org. Chem.* **2003**, 3435–3445.
- (36) Giampapa, C. S.; Abraham, S. N.; Chiang, T. M.; Beachey, E. H. Isolation and characterization of a receptor for type 1 fimbriae of *Escherichia coli* from guinea pig erythrocytes. *J. Biol. Chem.* **1988**, *263*, 5362–5367.
- (37) Aprikian, P.; Tchesnokova, V.; Kidd, B.; Yakovenko, O.; Yarov-Yarovoy, V.; Trinchina, E.; Vogel, V.; Thomas, W.; Sokurenko, E. Interdomain interaction in the FimH adhesin of *Escherichia coli* regulates the affinity to mannose. *J. Biol. Chem.* **2007**, *282*, 23437–23446.
- (38) Trong, I. L.; Aprikian, P.; Kidd, B. A.; Forero-Shelton, M.; Tchesnokova, V.; Rajagopal, P.; Rodriguez, V.; Interlandi, G.; Klevit, R.; Vogel, V.; Stenkamp, R. E.; Sokurenko, E. V.; Thomas, W. E. Structural basis for mechanical force regulation of the adhesin FimH via finger trap-like beta sheet twisting. *Cell* **2010**, *141*, 645–655.
- (39) Khoo, U. S.; Chan, K. Y. K.; Chan, V. S. F.; Lin, C. L. S. DC-SIGN and L-SIGN: the SIGNs for infection. *J. Mol. Med.* **2008**, *86*, 861–874.
- (40) Lee, S. J.; Evers, S.; Roeder, D.; Parlow, A. F.; Risteli, J.; Risteli, L.; Lee, Y. C.; Feizi, T.; Langen, H.; Nussenzweig, M. C. Mannose receptor-mediated regulation of serum glycoprotein homeostasis. *Science* **2002**, *295*, 1898–1901.
- (41) East, L.; Isacke, C. M. The mannose receptor family. *Biochim. Biophys. Acta* **2002**, *1572*, 364–386.
- (42) Dommett, R. M.; Klein, N.; Turner, M. W. Mannose-binding lectin in innate immunity: past, present and future. *Tissue Antigens* **2006**, *68*, 193–209.
- (43) Scharenberg, M. Expression and purification of DC-SIGN-CRD-Fc-IgG. Unpublished results.
- (44) Dearden, J. C.; Bresnen, J. G. M. The measurement of partition coefficients. *QSAR Comb. Sci.* **1988**, *7*, 133–144.
- (45) Wittwer, M.; Bezençon, J.; Cutting, B.; Wagner, B.; Kansy, M.; Ernst, B. pK_a determination by ¹H-NMR spectroscopy—an old methodology revisited. Unpublished results.
- (46) Banker, M. J.; Clark, T. H.; Williams, J. A. Development and validation of a 96-well equilibrium dialysis apparatus for measuring plasma protein binding. *J. Pharm. Sci.* **2003**, *92*, 967–974.
- (47) Kerns, E. H. High throughput physicochemical profiling for drug discovery. *J. Pharm. Sci.* **2001**, *90*, 1838–1858.
- (48) Avdeef, A.; Bendels, S.; Di, L.; Faller, B.; Kansy, M.; Sugano, K.; Yamauchi, Y. Parallel artificial membrane permeability assay (PAMPA)-critical factors for better predictions of absorption. *J. Pharm. Sci.* **2007**, *96*, 2893–2909.
- (49) Brandt, E.; Heymann, E.; Mentlein, R. Selective inhibition of rat liver carboxylesterases by various organophosphorus diesters in vivo and in vitro. *Biochem. Pharmacol.* **1980**, *29*, 1927–1931.
- (50) Scharenberg, M.; Abgottspon, D. Personal communication.
- (51) Obach, R. S. Prediction of human clearance of twenty-nine drugs from hepatic microsomal intrinsic clearance data: an examination of in vitro half-life approach and nonspecific binding to microsomes. *Drug Metab. Dispos.* **1999**, *27*, 1350–1359.
- (52) Trainor, G. L. The importance of plasma protein binding in drug discovery. *Expert Opin. Drug Discovery* **2007**, *2*, 51–64.
- (53) Weisiger, R. A. Dissociation from albumin: a potentially rate-limiting step in the clearance of substances by the liver. *Proc. Natl. Acad. Sci. U.S.A.* **1985**, *82*, 1563–1567.
- (54) Urien, S.; Tillement, J.-P.; Barre, J., The significance of plasma protein binding in drug research. In *Pharmacokinetic Optimization in Drug Research: Biological, Physicochemical, and Computational Strategies*; Wiley-VCH: Weinheim, Germany, 2001; pp 189–197.
- (55) Mulvey, M. A.; Schilling, J. D.; Hultgren, S. J. Establishment of a persistent *Escherichia coli* reservoir during the acute phase of a bladder infection. *Infect. Immun.* **2001**, *69*, 4572–4579.
- (56) (a) VCCLAB, *Virtual Computational Chemistry Laboratory*; <http://www.vccclab.org>, 2005; (b) Tetko, I. V.; Gasteiger, J.; Todeschini, R.; Mauri, A.; Livingston, D.; Ertl, P.; Palyulin, V. A.; Radchenko, E. V.; Zefirov, N. S.; Makarenko, A. S.; Tanchuk, V. Y.; Prokopenko, V. V. Virtual computational chemistry laboratory—design and description. *J. Comput.-Aided Mol. Des.* **2005**, *19*, 453–463.
- (57) Kern, M. B.; Frimodt-Møller, N.; Espersen, F. Effects of Sulfamethazole and Amdinocillin against *Escherichia coli* Strains (with Various Susceptibilities) in an Ascending Urinary Tract Infection Model. *Antimicrob. Agents Chemother.* **2003**, *47*, 1002–1009.

2.3 Paper 2: FimH Antagonists: Structure-Activity and Structure-Property Relationships for Biphenyl α -D-Mannopyranosides

This article reports the optimization of biphenyl FimH antagonists with diverse structural modifications, notably the introduction of *ortho*-substituents on the phenyl ring adjacent to the sugar moiety, the introduction of a methylene spacer between the anomeric oxygen and the biphenyl moiety, and the extension of the *para*-substituent on the terminal phenyl ring. The structural design was based on the co-crystal structure of a biphenyl antagonist with FimH and guided by computational modeling results. Both of the designed ester prodrugs and their active principles (the acids) were chemically synthesized and evaluated for *in vitro* binding affinities. Furthermore, the pharmacokinetic (PK) properties were analyzed for the ester prodrugs. Finally, structure-activity and structure-property relationships were established for a series of biphenyl FimH antagonists.

Contribution to the project:

Lijuan Pang performed all experiments regarding the chemical synthesis. Furthermore, She participated in drug design by collaborating with Dr. Adam Zalewski. She was responsible for writing the respective sections as well as the introduction and the summary of the paper. Moreover, She designed a backcover for the same issue of *ChemMedChem*, regarding this paper.

This paper was published in *ChemMedChem* as a Very Important Paper:

Pang, L. *; Kleeb, S. *; Lemme, K. *; Rabbani, S. *; Scharenberg, M.; Zalewski, A.; Schaedler, F.; Schwardt, O.; Ernst, B. FimH antagonists: structure-activity and structure-property relationships for biphenyl α -D-mannopyranosides. *ChemMedChem* **2012**, *7*, 1404-1422.

* These authors contributed equally to the project.

DOI: 10.1002/cmdc.201200125

VIP FimH Antagonists: Structure–Activity and Structure–Property Relationships for Biphenyl α -D-Mannopyranosides

Lijuan Pang, Simon Kleeb, Katrin Lemme, Said Rabbani, Meike Scharenberg, Adam Zalewski, Florentina Schädler, Oliver Schwardt, and Beat Ernst^{*,[a]}

Urinary tract infections (UTIs) are caused primarily by uropathogenic *Escherichia coli* (UPEC), which encode filamentous surface-adhesive organelles called type 1 pili. FimH is located at the tips of these pili. The initial attachment of UPEC to host cells is mediated by the interaction of the carbohydrate recognition domain (CRD) of FimH with oligomannosides on urothelial cells. Blocking these lectins with carbohydrates or analogues thereof prevents bacterial adhesion to host cells and therefore offers a potential therapeutic approach for prevention and/or treatment of UTIs. Although numerous FimH antagonists have been developed so far, few of them meet the requirement for clinical application due to poor pharmacokinetics. Additionally, the binding mode of an antagonist to the

CRD of FimH can switch from an in-docking mode to an out-docking mode, depending on the structure of the antagonist. In this communication, biphenyl α -D-mannosides were modified to improve their binding affinity, to explore their binding mode, and to optimize their pharmacokinetic properties. The inhibitory potential of the FimH antagonists was measured in a cell-free competitive binding assay, a cell-based flow cytometry assay, and by isothermal titration calorimetry. Furthermore, pharmacokinetic properties such as $\log D$, solubility, and membrane permeation were analyzed. As a result, a structure–activity and structure–property relationships were established for a series of biphenyl α -D-mannosides.

Introduction

Urinary tract infections (UTIs), the most prevalent series of infectious diseases worldwide, affect millions of people and account for significant morbidity as well as high medical costs.^[1] The primary cause of UTIs are strains of uropathogenic *Escherichia coli* (UPEC), which make up 70–95% of reported cases.^[1a,2] UTIs are treated with antibiotics; however, recurrent infections by UPEC with subsequent antibiotic exposure can lead to the emergence of antimicrobial resistance.^[3]

Adhesion to host cells is the initial step of microbial infection. To gain an initial foothold within the bladder, UPEC strains encode filamentous surface-adhesive organelles called type 1 pili (fimbriae).^[4] They mediate bacterial attachment to uroplakin Ia, a glycoprotein located on urothelial cells. This initial step prevents the clearance of *E. coli* by the bulk flow of urine and facilitates the invasion of host cells.^[1b,5] A bacterial lectin known as FimH is located at the tips of type 1 pili. The carbohydrate recognition domain (CRD) of this lectin is responsible for binding to the complementary carbohydrate epitope of the host tissue. Blocking this lectin by a carbohydrate or a glycomimetic thereof offers a potential therapeutic approach for prevention and/or treatment of UTIs.^[6]

More than two decades ago, Sharon and co-workers explored various mannosides and oligomannosides as potential antagonists for type 1 pili-mediated bacterial adhesion and observed interactions in the micro- to millimolar range.^[7] The first crystal structure of FimH was solved in 1999,^[8] and since then, numerous crystallographic studies have been reported, greatly facilitating the design of high-affinity ligands.^[9] In summary,

the reported affinities can be rationalized on the basis of the structure of FimH: First, the binding pocket accommodates the mannose with the hydroxy groups forming an extended hydrogen bond network. Second, the entrance to the binding site, referred to as the “tyrosine gate”, is formed by three hydrophobic amino acids (Tyr48, Tyr137, and Ile52)^[9a] and can host aliphatic and aromatic aglycones.

As a consequence of hydrophobic contacts of the alkyl aglycone, *n*-heptyl α -D-mannopyranoside (**1**) exhibits nanomolar affinity.^[9b] With aromatic aglycones such as **2–5** (Figure 1), further improvements in affinity were observed.^[10] To explore the binding mode and to improve affinity as well as ADME properties, a series of biphenyl FimH antagonists were synthesized.

Results and Discussion

An unexpected docking mode was discovered upon co-crystallization of biphenyl mannoside **3** with the FimH CRD.^[10d] Whereas the alkyl aglycone of *n*-butyl α -D-mannopyranoside^[9b]

[a] L. Pang,^{*} S. Kleeb,^{*} Dr. K. Lemme,^{*} Dr. S. Rabbani,^{*} Dr. M. Scharenberg, A. Zalewski, F. Schädler, Dr. O. Schwardt, Prof. Dr. B. Ernst
Institute of Molecular Pharmacy, Pharmazentrum, University of Basel
Klingelbergstrasse 50, 4056 Basel (Switzerland)
E-mail: beat.ernst@unibas.ch

[*] These authors contributed equally to this work.

Supporting information for this article is available on the WWW under <http://dx.doi.org/10.1002/cmdc.201200125>.

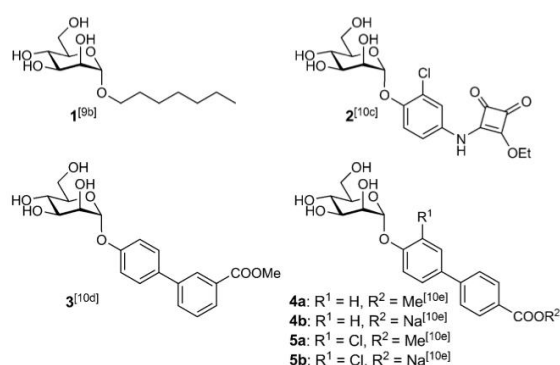


Figure 1. FimH antagonists: *n*-heptyl α -D-mannopyranoside (**1**) is used as reference compound; the squaric acid derivative **2** and biphenyl derivatives **3–5** exhibit nanomolar affinities.

interacts with both Tyr48 and Tyr137 of the tyrosine gate (in-docking mode),^[10f] the biphenyl aglycone adopts the out-docking mode; that is, it interacts only with Tyr48 (Figure 2 A), probably due to insufficient flexibility; π - π stacking of the outer aromatic ring of the biphenyl aglycone (ring B) with Tyr48 is effected by induced fit: a substantial move of Tyr48. Moreover, further stabilization of the protein–ligand complex by polar interaction between the ester in the *meta* position of **3** and the side chain of Arg98 was proposed.^[10d]

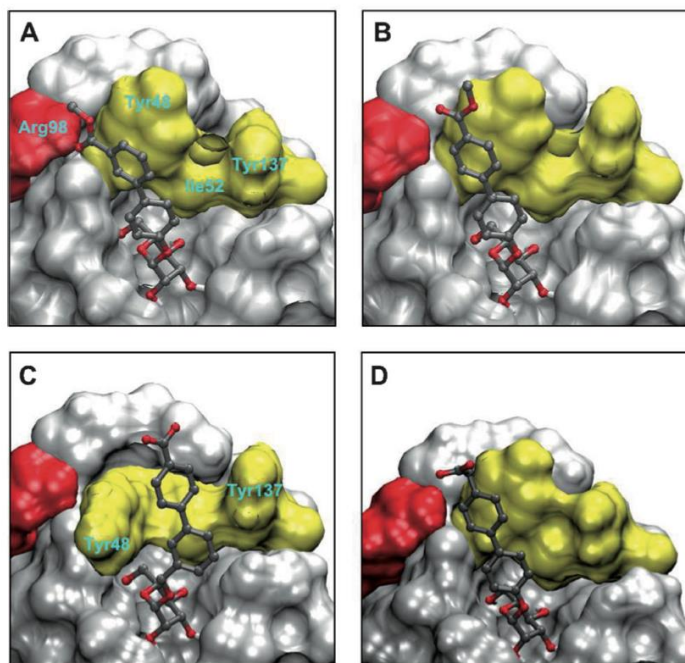


Figure 2. A) Crystal structure of biphenyl **3** (PDB ID: 3MCY)^[10d] bound to the FimH CRD. B–D) In silico docking studies obtained with flexible docking (Glide software package)^[11] to the same FimH CRD structure; top-scored binding mode of B) **4a**, C) **6**, and D) **7**.

In silico docking studies with biphenyl derivative **4a**^[10e] suggested a similar out-docking mode (Figure 2 B). A close inspection revealed empty space between the *ortho* position of the aromatic ring adjacent to the anomeric center (ring A) and the protein surface. Indeed, with an *ortho*-chloro substituent (\rightarrow **5a**, Figure 1), affinity was substantially improved. Further studies with FimH antagonists that exhibit enhanced flexibility (e.g., compound **6**; Figure 2 C and Figure 3) indicated a switch from the out-docking mode to the in-docking mode. However, whether an optimal π - π stacking within the tyrosine gate can be realized remains to be determined. Finally, docking studies also indicated that elongation of the carboxylate-bearing *para* substituent enables a polar interaction between the carboxylate and Arg98 (e.g., compound **7**; Figure 2 D and Figure 3).

Starting from antagonist **4**, we explored three types of modifications (Figure 3):

- 1) For optimizing the van der Waals contact between the *ortho* position of ring A and the binding pocket, a series of substituents — F, CH₃, CF₃, OCH₃, cyclopropyl, and CN — were introduced as depicted in Scheme 1.
- 2) To determine whether the out-docking mode reported for **3**^[10d] results from insufficient flexibility, we increased the aglycone flexibility by introducing a methylene spacer between the anomeric oxygen and ring A of the biphenyl moiety (Scheme 2). This should decrease the conformational constraints to allow an optimized spatial arrangement of the aglycone in the tyrosine gate (\rightarrow **6**, Figure 2 C); at the same time, water solubility should be improved as a result of the decreased stacking tendency derived from disruption of the symmetry of the aglycone.^[15]
- 3) To enable a polar interaction between the carboxylate substituent on ring B with Arg98 of FimH, we extended the *para* substituent of **4**, that is, we replaced it with either a flexible methyl ethanolate or a rigid methyl cyclopropanecarboxylate (Scheme 3). Biphenyl α -D-mannoside **24**^[10d] shows a three- to eightfold lower affinity for FimH than its counterparts with a methoxycarbonyl substituent at the *meta* (\rightarrow **3**)^[10d] or *para* positions (\rightarrow **4**)^[10e] of ring B (Table 1). Han et al. assigned the increased affinity of compound **3** to a polar interaction of the ester with Arg98 of FimH.^[10d] Because for spatial reasons the ester in the

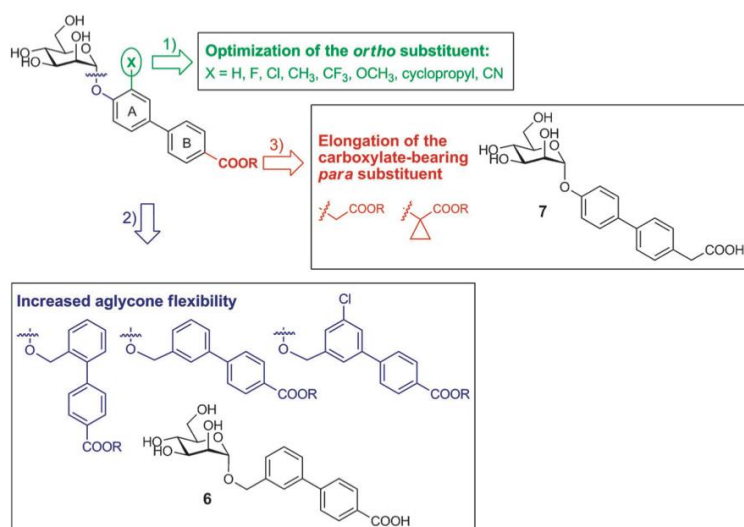


Figure 3. Modifications to the aglycone of FimH antagonists by 1) optimization of the *ortho* substituent, 2) an increase in the flexibility of the aglycone, and 3) elongation of the carboxylate-bearing *para* substituent.

para-substituted derivative **4** cannot establish a similar interaction with Arg98, the substantial improvement in affinity may result from solvation effects.

Synthesis

Optimization of *ortho* substituents (Scheme 1)

Mannosylation of phenols **9a–f** with mannosyl fluoride **8** and $\text{BF}_3 \cdot \text{OEt}_2$ as promoter yielded α -mannosides **10a–f** stereospecifically.^[12] Whereas the phenols **9a–d** and **9f** are commercially available, the cyclopropyl derivative **9e** was prepared via tandem carbolithiation/1,3-elimination according to Ocasio and Scanlan.^[13] In a palladium-catalyzed Miyaura–Suzuki coupling^[14] of **10a–f** with 4-methoxycarbonylphenylboronic acid (**11**), biphenyls **12a–f** were obtained in good to excellent yields. Deacetylation using Zemplén conditions (\rightarrow **13a–f**) followed by saponification of the methyl esters gave the test compounds **14a–e**. Owing to the instability of the cyano group under aqueous basic conditions, **14f** was synthesized by coupling **10f** with 4-carboxyphenylboronic acid pinacol ester (**15**) followed by transesterification under Zemplén conditions to avoid the final saponification with aqueous sodium hydroxide.

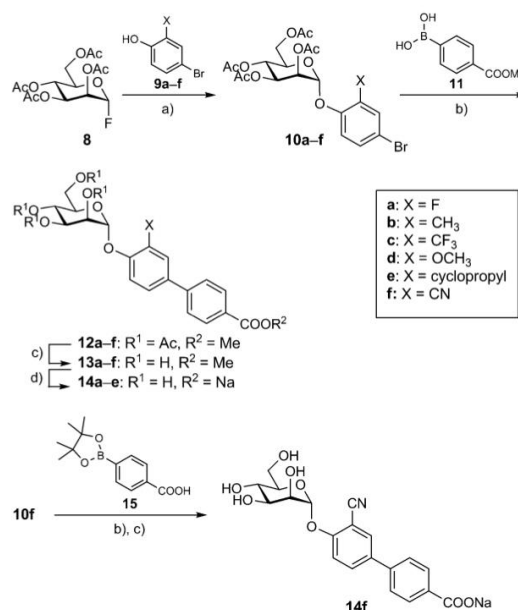
Increase in aglycone flexibility (Scheme 2)

Benzyl alcohols **16a–c** were first mannosylated with donor **8**^[12] to yield the benzyloxy mannosides **17a–c**. Subsequent cross-coupling with 4-methoxycarbonylphenylboronic acid (**11**) afforded acetates **18a,b** and **21**. Deacetylation of the mannose moiety

(\rightarrow **19a,b** and **22**) followed by saponification of the methyl esters gave compounds **6**, **20**, and **23**.

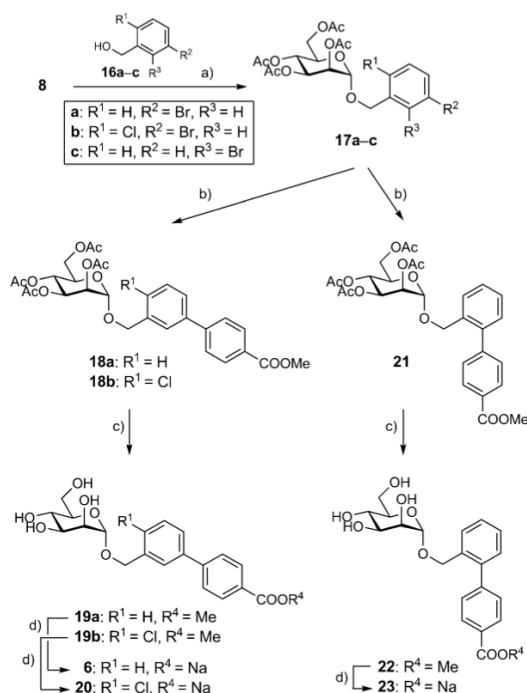
Elongation of the carboxylate-bearing *para* substituent (Scheme 3)

Peracetylated mannoside **25** was treated with 4-iodophenol in the presence of $\text{BF}_3 \cdot \text{Et}_2 \cdot \text{O}$. The resulting iodide **26** was transformed into boronic acid pinacol ester **27**, which was coupled with 4-bromophenylacetic acid methyl ester (**28**) and 4-bromophenylcyclopropylcarboxylic acid methyl ester (**32**) under Miyaura–Suzuki coupling conditions^[14] to yield biphenyls **29** and **33**. Deacetylation with sodium methoxide (\rightarrow

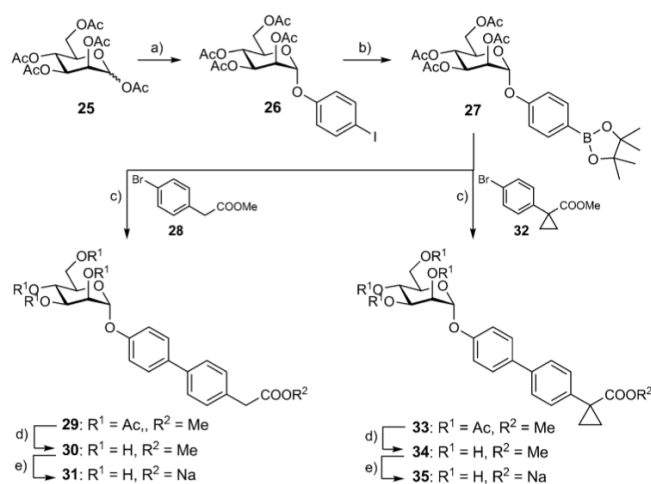


Scheme 1. Reagents and conditions: a) $\text{BF}_3 \cdot \text{Et}_2 \cdot \text{O}$, CH_2Cl_2 , 0°C , 3 h (**10a–f**, 73–86%); b) $\text{Pd}(\text{Cl}_2)\text{dppf} \cdot \text{CH}_2\text{Cl}_2$, K_3PO_4 , DMF, 80°C , overnight (**12a–f**, 55–91%); c) NaOMe, MeOH, RT, 4 h (**13a–e**, **14f**, 52–73%); d) 1.0.2 N $\text{NaOH}_{(\text{aq})}$, MeOH, RT, overnight; 2. Dowex (Na^+), size-exclusion chromatography (P-2 gel) (**14a–e**, 15–74%).

30 and **34**) followed by saponification of the methyl ester yielded the sodium salts **31** and **35**.



Scheme 2. Reagents and conditions: a) $BF_3 \cdot Et_2O$, CH_2Cl_2 , $0^\circ C$, 3 h (**17a-c**, 34–48%); b) 4-methoxycarbonylphenylboronic acid (**11**), $Pd(Cl_2)dppf \cdot CH_2Cl_2$, K_3PO_4 , DMF, $80^\circ C$, overnight (**18a,b** and **21**, 73–94%); c) NaOMe, MeOH, RT, 4 h (**19a,b** and **22**, 47–90%); d) 1. 0.2 N NaOH_(aq), MeOH, RT, overnight; 2. Dowex (Na^+), size-exclusion chromatography (P-2 gel) (**6**, **20** and **23**, 10–96%).



Scheme 3. Reagents and conditions: a) 4-iodophenol, $BF_3 \cdot Et_2O$, CH_2Cl_2 , $40^\circ C$, overnight (70%); b) bis(pinacolato)diboron, $Pd(Cl_2)dppf \cdot CH_2Cl_2$, KOAc, DMF, MW $120^\circ C$, 2 h (50%); c) $Pd(Cl_2)dppf \cdot CH_2Cl_2$, K_3PO_4 , DMF, $80^\circ C$, overnight (34–56%); d) NaOMe, MeOH, RT, 4 h (33–95%); e) 1. 0.2 N NaOH_(aq), MeOH, RT, overnight; 2. Dowex (Na^+), size-exclusion chromatography (P-2 gel) (**31**: 40%; **35**: 23%).

Binding affinity and activity

The biphenyl α -D-mannosides with varying *ortho* substituents (**5a–b**, **13a–f**, **14a–f**), increased aglycone flexibility (**6**, **19**, **20**, **22**, **23**), and elongated carboxylate-bearing *para* substituents (**30**, **31**, **34**, **35**) were evaluated in vitro by two competitive assay formats (Table 1). All antagonists were tested in a cell-free competitive binding assay.^[16] Subsequently, the best candidates were investigated in a cell-based flow cytometry assay.^[17]

The cell-free competitive binding assay is based on the interaction of a biotinylated polyacrylamide glycopolymer as competitor with the isolated CRD of FimH. In contrast, the cell-based flow cytometry assay involves the infection of human urinary bladder epithelial carcinoma cells with GFP-labeled UPECs expressing the complete type 1 pili (see the Experimental Section below for details). The competitors in the former assay are thus polymer-bound trimannosides, whereas in the latter the antagonists compete with more potent high-mannose oligosaccharides present on uroplakin Ia, which is located on the surface of human urinary bladder cells.^[18,19] The interaction is further affected by the presence of high- and low-affinity states of the CRD of FimH. Aprikian et al. experimentally demonstrated that in full-length fimbriae, the pilin domain stabilizes the CRD domain in the low-affinity state, whereas the CRD domain alone adopts the high-affinity state.^[20] Furthermore, it was recently shown that shear stress can induce a conformational switch (twist in the β -sandwich fold of the CRD domain), resulting in improved affinity.^[21] Therefore, differing affinities were expected in the cell-based flow cytometry assay, in which full-length fimbriae are present, relative to the cell-free competitive binding assay.

Cell-free competitive binding assays^[16]

These assays were performed twice for every compound with each concentration in duplicate. To ensure comparability between various antagonists, the reference compound *n*-heptyl α -D-mannopyranoside **1**^[22] was tested each time in parallel. The affinities are reported relative to **1** as rIC_{50} in Table 1. A comparison of the affinities of compounds **4a** and **4b** with the *ortho*-substituted analogues **5a**, **13a–f** and **5b**, **14a–f** clearly demonstrates that *ortho* substituents on ring A indeed improve binding. However, the differences between the various substituted FimH antagonists are small. For a better understanding of these results, a more detailed analysis of the thermodynamic profile by isothermal titration calorimetry (ITC) was performed (see below). By increasing the flexibility of the aglycone, we expected a switch from the out-docking mode as present for antagonists **3** and **4** (Figure 2A,B) to the in-docking mode (represented by antagonist **6** in Figure 2C).^[10] However, affinities for all six representatives with increased spacer length between carbohydrate and aglycone (Table 1: **6**–**19**, **20**, **22**, and **23**) were dramatically decreased. A similar tendency was observed

Table 1. Pharmacodynamic parameters of FimH antagonists.

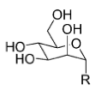
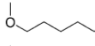
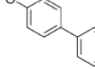
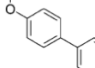
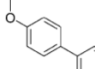
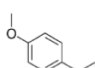
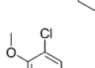
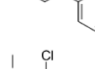
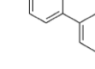
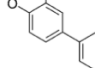
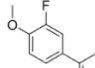
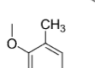
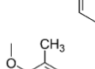
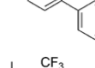
Compd		Binding assay		Flow cytometry
		IC ₅₀ [nM] ^[a]	rIC ₅₀ ^[b]	IC ₅₀ [μM] ^[a,c]
1 ^[10e]		73 ± 7.9	1	3.9 ± 1.6
24 ^[10d]		84.9	1.47	n.d.
3 ^[10d]		28.6	0.55	n.d.
4a ^[10e]		10.4 ± 1.2	0.14	n.d.
4b ^[10e]		17.1 ± 2.2	0.15	n.d.
5a		4.8 ± 1.2	0.06	n.d.
5b		6.7 ± 2.1	0.09	0.33 ± 0.05
13a		8.0	0.14	n.d.
14a		33.5	0.58	1.54 ± 0.31
13b		23.3	0.40	n.d.
14b		9.2	0.16	1.83 ± 0.14
13c		2.6	0.04	n.d.
14c		8.9	0.15	0.89 ± 0.10

Table 1. (Continued)

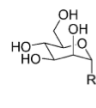
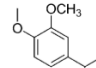
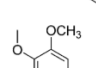

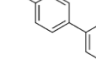
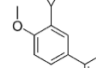
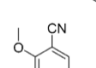
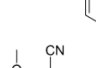
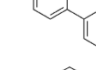
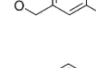
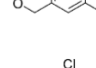
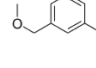
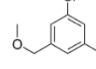
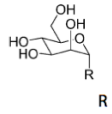
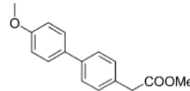
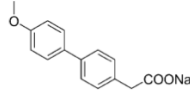
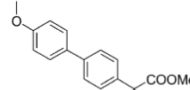
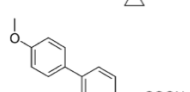
Compd		Binding assay		Flow cytometry
		IC ₅₀ [nM] ^[a]	rIC ₅₀ ^[b]	IC ₅₀ [μM] ^[a,c]
13d		3.5	0.06	n.d.
14d		4.8	0.08	1.95 ± 0.36
13e		31.7	0.55	n.d.
14e		63.0	1.09	4.85 ± 0.79
13f		22.5	0.39	n.d.
14f		33.9	0.58	n.d.
19a		56.1	0.97	n.d.
6		107.9	1.87	n.d.
19b		98.9	1.7	n.d.
20		142.2	2.44	n.d.
22		85.8	1.49	n.d.
23		642.0	11.14	n.d.

Table 1. (Continued)				
Compd		Binding assay		Flow cytometry
		IC ₅₀ [nM] ^[a]	rIC ₅₀ ^[b]	IC ₅₀ [μM] ^[a,c]
30		63.2	1.09	n.d.
31		70.5	1.21	n.d.
34		49.5	0.85	n.d.
35		62.5	1.07	n.d.

[a] IC₅₀ values were determined in a cell-free competitive binding assay.^[16]
 [b] The rIC₅₀ values were calculated by dividing the IC₅₀ of the compound of interest by that of reference compound 1; this leads to rIC₅₀ values < 1 for derivatives that bind better than reference 1, and rIC₅₀ values > 1 for compounds with lower affinity than 1. [c] The anti-adhesion potential to human epithelial bladder cells was determined in the flow cytometry assay.^[17] n.d. = not determined.

for the biphenyls with an elongated carboxylate-bearing *para* substituent (Table 1: **30**, **31**, **34**, and **35**). It was previously described that the ester of **3** is placed within hydrogen bonding distance to form a polar interaction with Arg98 and Glu50.^[10d] However, an improvement of affinity provided by a similar polar interaction between Arg98 and the antagonists **31** and **35** could not be achieved, probably due to the high desolvation penalty of Arg98. Finally, it is important to note that the free acids (sodium salt) of the antagonists in general showed slightly lower affinities than their methyl ester counterparts, with the only exceptions of **13b** and **14b** (Table 1). However, because the esters are thought to act as prodrugs and to be rapidly cleaved after oral application,^[10e] the affinities of the carboxylates are relevant with regard to the therapeutic potential of the present FimH antagonists.

Cell-based flow cytometry assay^[17]

These assays were performed in duplicate/triplicate, and *n*-heptyl α -D-mannopyranoside **1** was used as reference compound with an IC₅₀ value of $3.9 \pm 1.6 \mu\text{M}$. The most potent antagonists **5b** and **14c** (Table 1) showed respective IC₅₀ values of 0.33 ± 0.05 and $0.89 \pm 0.10 \mu\text{M}$. In general, the activities obtained from the flow cytometry assay were ~50-fold lower than the affinities determined in the target-based competitive assay (see above).

Isothermal titration calorimetry

Because the biological *in vitro* evaluation only revealed small differences between affinities, ITC experiments were carried out to study the thermodynamic profile of the variously *ortho*-substituted biphenyl compounds **5b** and **14a–f** in binding to FimH. ITC directly measures the heat of interaction (change in enthalpy, ΔH) at a constant temperature on titrating two compounds of known concentration that form an equilibrium complex.^[23] It includes contributions from all equilibria that occur as the interacting molecules go from the free to the bound state, including those associated with solvent interactions and macromolecular conformational changes. The noncovalent interaction between a protein and a ligand can be quantified by the change in free energy (ΔG), consisting of the change in enthalpy (ΔH) and change in entropy (ΔS) [Eq. (1)].^[24] The binding energy under standard conditions (ΔG°), in which all reactants and products are at a concentration of 1 M, can be calculated from the dissociation constant, K_D [Eq. (2)]. With ITC, K_D and ΔH can be measured directly, whereas ΔG and the entropy term $T\Delta S$ are calculated according to Equations (1) and (2).

$$\Delta G = \Delta H - T\Delta S \quad (1)$$

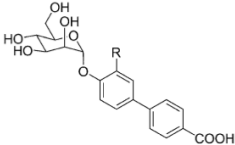
$$\Delta G = RT \ln K_D \quad (2)$$

A favorable enthalpy term ΔH is associated with hydrogen bond formation, electrostatic, and dipole–dipole interactions at the overcompensation of the desolvation penalty.^[25] The entropy term ΔS reflects the overall change in the degrees of freedom of a system. It can be dissected into translational and rigid body rotational entropy,^[26] solvation entropy,^[27] and entropy costs related to conformational changes of protein and ligand [Eq. (3)].^[28] Whereas the formation of a protein–ligand complex is always associated with a decrease in translational and rotational freedom and therefore with entropy costs, the entropic contribution involving changes in solvation (ΔS_{solv}) and changes in rotational and vibrational entropy due to the loss of conformational flexibility (ΔS_{conf}) can differ both in sign and magnitude.^[29]

$$\Delta S = \Delta S_{\text{solv}} + \Delta S_{\text{trans/rot}} + \Delta S_{\text{conf}} \quad (3)$$

The FimH CRD was used for the ITC experiments. It was prepared from FimH-CRD-Th-His₆ (see *Competitive binding assay*, Experimental Section below) by incubation with thrombin, as described earlier.^[16]

The thermodynamic fingerprints of the various biphenyl derivatives (Table 2, Figure 4) reveal a significant improvement in the enthalpic term ($\Delta\Delta H$ -4.3 to $-11.2 \text{ kJ mol}^{-1}$) for all substituted biphenyls (**5b**, **14a–f**) in comparison with the unsubstituted derivative **4b**. The largest enthalpy improvement was observed for the trifluoromethyl group (**14c**; Table 2). Interestingly, these largely improved enthalpic contributions are mostly compensated by entropic penalties ($-T\Delta\Delta S$ $+3.2$ to $+7.5 \text{ kJ mol}^{-1}$), resulting in only marginally improved K_D values. In the best case, the trifluoromethyl derivative **14c**, a fourfold improvement in K_D was measured. Similar, but less pronounced

Table 2. Binding thermodynamics of FimH antagonists determined by ITC.


Compd	R	K_D [nM]	ΔG° [kJ mol ⁻¹]	ΔH° [kJ mol ⁻¹]	$-T\Delta S^\circ$ [kJ mol ⁻¹]	$N^{[a]}$	V_{vdW} [Å ³] ^[b]
4b	H	14.1	-44.8	-47.3	+2.5	1.00	7.2
5b	Cl	3.7	-48.1	-55.5	+7.4	1.01	22.4
14a	F	9.2	-45.9	-51.6	+5.7	1.00	13.3
14b	Me	4.8	-47.5	-56.2	+8.7	1.01	26.7
14c	CF ₃	3.2	-48.5	-58.5	+10.0	1.02	41.4
14d	OMe	7.7	-46.3	-52.5	+6.2	1.02	34.8
14e	cPr	6.9	-46.6	-46.7	+0.1	1.01	52.5
14f	CN	7.4	-46.4	-55.0	+8.6	1.01	29.7

[a] Molar ratio of protein/ligand. [b] van der Waals volumes (V_{vdW}) of the *ortho* substituent were calculated with the Phase volCalc utility.^[30]

cific *ortho* substituent and varies between -2.39 kJ mol⁻¹ for CH₃ and 19.31 kJ mol⁻¹ for CN.^[25] Finally, depending on the surface area of the *ortho* substituent, the entropy of solvation may change. In summary, the various effects are superimposed and of opposing contributions to the free binding energy ΔG .

Physicochemical and in vitro pharmacokinetic characterization

To estimate the oral bioavailability and renal elimination of acids **4b**, **5b**, **6**, **14a–f**, **20**, **23**, **31**, **35**, and the methyl esters **4a**, **5a**,

effects were observed for most other *ortho* substituents. This trend was broken only by the cyclopropyl derivative **14e** ($\Delta\Delta H$ +0.7 kJ mol⁻¹, $-T\Delta\Delta S$ -2.4 kJ mol⁻¹; Table 2).

The influence of the *ortho* substituent on binding can be attributed to three factors. First, *ortho* substituents of appropriate volume establish an improved shape complementarity within the binding pocket, leading to a better van der Waals (vdW) contact and therefore an improvement in the enthalpy term ΔH . The improvement in enthalpy ($\Delta\Delta H$) correlates well with increasing vdW volumes of spherical *ortho* substituents (**5b**, **14a–c**; Figure 5). For non-spherical substituents (OMe, **14d**; cyclopropyl, **14e**; and CN, **14f**), the shape complementarity is not optimal, leading to only a decreased enthalpy contribution. However, better vdW contacts also lead to decreased conformational flexibility and therefore an entropic compensation by a less favorable ΔS_{conf} value. A second parameter is the desolvation enthalpy, which depends on the polarity of a spe-

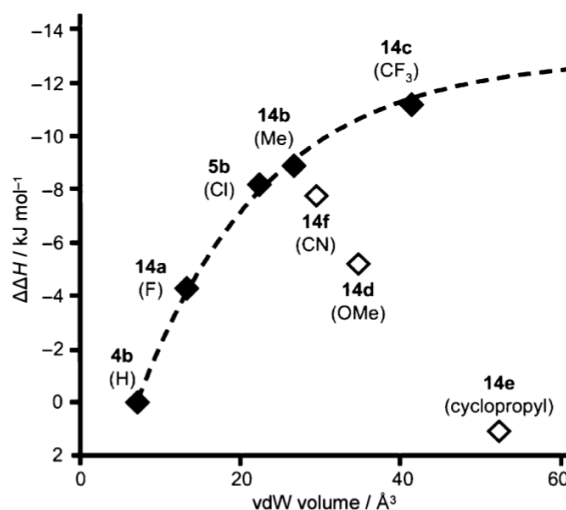


Figure 5. Correlation of $\Delta\Delta H$ (relative to antagonist **4b**) with the van der Waals volumes^[30] of *ortho* substituents.

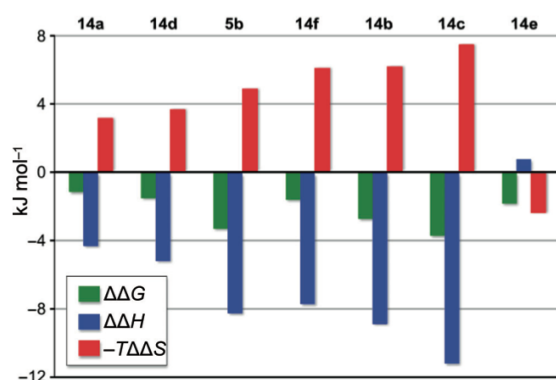


Figure 4. Enthalpy–entropy compensation, a property often reported for carbohydrate–lectin interactions,^[31] for *ortho*-substituted biphenyl α -D-mannopyranosides; $\Delta\Delta G$, $\Delta\Delta H$, and $T\Delta\Delta S$ values for **5b** and **14a–f** are plotted relative to the unsubstituted derivative **4b**.

13a–f, **19a–b**, **22**, **30** and **34**, several physicochemical parameters (lipophilicity, solubility) as well as permeability through an artificial membrane and a cell monolayer were determined (Table 3). The free acids of the antagonists assessed in this study (**4b**, **5b**, **6**, **14a–f**, **20**, **23**, **31**, and **35**) are generally hydrophilic and soluble at pH values >5 . All acids showed $\log D_{7.4}$ values below zero and are therefore thought to undergo considerable renal clearance,^[32] a prerequisite for FimH antagonists to reach their target in the urinary bladder. Permeation studies through an artificial membrane (PAMPA^[33]) indicated for all acids except **14a** effective permeation values ($\log P_e$) below -6.7 , suggesting low absorption in the small intestine by passive permeation.^[34] However, the high absorption potential of the fluoro-substituted biphenyl **14a** predicted by

Table 3. Physicochemical and in vitro pharmacokinetic parameters of FimH antagonists.

Compd	PAMPA $\log P_c$ [$\log 10^{-6} \text{ cm s}^{-1}$]/pH ^[a]	Caco-2 P_{app} [$10^{-6} \text{ cm s}^{-1}$] ^[b]			$\log D_{7.4}$ ^[c]	Solubility [$\mu\text{g mL}^{-1}$]/pH ^[d]
		a→b	b→a	(b→a)/(a→b)		
1	-4.9	7.0±0.6	9.4±0.2	1.3	1.7	> 3000/6.5
24	-5.0±0.1/5.0	10.0±0.9	19.0±1.2	1.9	2.1±0.1	22±0/3.0
	-4.9±0.1/6.2					22±1/5.0
	-4.7±0.1/7.4					21±1/7.4
3	-4.9±0.0/5.0	2.2±0.2	17.6±0.4	8.0	2.0±0.0	> 150/3.0
	-4.9±0.0/6.2					> 150/5.0
	-4.9±0.0/7.4					> 150/7.4
4a	-4.7	1.5±0.0	6.4±0.4	4.3	2.1	14±1/3.0
						13±1/5.0
						12±1/7.4
4b	n.p.	n.d.	n.d.	n.d.	< -1.5	> 3000/6.6
5a	-4.6	5.3±0.6	17.5±1.3	3.3	2.3	16±2/3.0
						15±0/5.0
						17±2/7.4
5b	n.p.	0.2±0.0	0.4±0.0	1.6	-0.8	> 3000/6.5
13a	-4.8±0.0/5.0	5.6±0.7	22.0±0.6	4.0	2.7±0.1	22±1/3.0
	-4.8±0.0/6.2					24±3/5.0
	-4.8±0.0/7.4					17±6/7.4
14a	-5.8±0.1/5.0	0.2±0.1	0.2±0.0	0.8	< -1.5	30±3/3.0
	-6.3±0.1/6.2					> 100/5.0
	-7.4±0.1/7.4					> 100/7.4
13b	-4.5±0.1/5.0	6.2±1.3	22.7±1.2	3.6	2.4±0.2	7±0/3.0
	-4.5±0.0/6.2					7±0/5.0
	-4.6±0.1/7.4					7±0/7.4
14b	-8.6±1.7/5.0	n.d.	n.d.	n.d.	-0.6±0.1	34±3/3.0
	-8.8±1.4/6.2					> 200/5.0
	-8.7±1.5/7.4					> 200/7.4
13c	-4.4±0.0/5.0	9.2±0.1	16.9±1.5	1.8	2.8±0.1	17±1/3.0
	-4.4±0.0/6.2					15±1/5.0
	-4.5±0.1/7.4					16±1/7.4
14c	-8.4±1.3/5.0	n.d.	n.d.	n.d.	-0.8±0.1	15±1/3.0
	-9.3±1.4/6.2					140±6/5.0
	-8.6±1.6/7.4					> 200/7.4
13d	-5.4±0.0/5.0	4.2±0.7	16.4±1.2	3.9	1.8±0.1	24±0/3.0
	-5.4±0.0/6.2					24±1/5.0
	-5.4±0.0/7.4					26±1/7.4
14d	-8.5±0.6/5.0	n.d.	n.d.	n.d.	< -1.5	127±4/3.0
	-9.1±0.2/6.2					> 200/5.0
	-9.2±0.4/7.4					> 200/7.4
13e	-4.5±0.2/5.0	6.1±0.6	17.9±1.2	3.0	2.9±0.1	14±2/3.0
	-4.4±0.0/6.2					13±0/5.0
	-4.4±0.1/7.4					14±1/7.4
14e	-9.3±1.3/5.0	n.d.	n.d.	n.d.	-0.8±0.1	31±2/3.0
	-8.7±1.5/6.2					> 200/5.0
	-8.7±1.5/7.4					> 200/7.4
13f	-6.5±0.0/5.0	0.9±0.7	18.1±0.6	19.7	1.7±0.0	22±2/3.0
	-6.5±0.1/6.2					24±1/5.0
	-6.3±0.1/7.4					23±1/7.4
14f	-8.5±1.7/5.0	n.d.	n.d.	n.d.	< -1.5	35±11/3.0
	-7.3±0.3/6.2					> 200/5.0
	-7.8±1.5/7.4					> 200/7.4
19a	-4.9±0.0/5.0	4.4±0.1	18.8±1.7	4.3	1.9±0.1	103±8/3.0
	-4.9±0.0/6.2					100±6/5.0
	-4.9±0.1/7.4					95±5/7.4
6	-8.6±1.6/5.0	n.d.	n.d.	n.d.	< -1.5	> 130/3.0
	-9.3±1.4/6.2					> 130/5.0
	-8.7±1.5/7.4					> 130/7.4
19b	-5.3±0.1/5.0	n.d.	n.d.	n.d.	2.4±0.1	30±0/3.0
	-5.6±0.1/6.2					29±1/5.0
	-5.1±0.2/7.4					31±1/7.4
20	-8.6±1.6/5.0	n.d.	n.d.	n.d.	-1.2±0.2	> 130/3.0
	-9.3±1.4/6.2					> 130/5.0
	-10/7.4					> 130/7.4

Table 3. (Continued)

Compd	PAMPA $\log P_e$ [$\log 10^{-6} \text{ cm s}^{-1}$]/pH ^[a]	Caco-2 P_{app} [$10^{-6} \text{ cm s}^{-1}$] ^[b]			$\log D_{7.4}$ ^[c]	Solubility [$\mu\text{g mL}^{-1}$]/pH ^[d]
		a→b	b→a	(b→a)/(a→b)		
22	$-5.1 \pm 0.0/5.0$	n.d.	n.d.	n.d.	1.7 ± 0.1	> 130/3.0
	$-5.1 \pm 0.0/6.2$					> 130/5.0
	$-5.1 \pm 0.0/7.4$					> 130/7.4
23	$-7.3 \pm 1.8/5.0$	n.d.	n.d.	n.d.	< -1.5	> 130/3.0
	$-8.1 \pm 2.2/6.2$					> 130/5.0
	-10/7.4					> 130/7.4
30	$-5.5 \pm 0.0/5.0$	n.d.	n.d.	n.d.	1.6 ± 0.1	> 130/3.0
	$-5.5 \pm 0.0/6.2$					> 130/5.0
	$-5.4 \pm 0.1/7.4$					> 130/7.4
31	$-7.7 \pm 1.6/5.0$	n.d.	n.d.	n.d.	< -1.5	> 130/3.0
	$-8.1 \pm 1.3/6.2$					> 130/5.0
	-10/7.4					> 130/7.4
34	$-5.3 \pm 0.1/5.0$	n.d.	n.d.	n.d.	2.2 ± 0.1	> 130/3.0
	$-5.6 \pm 0.0/6.2$					> 130/5.0
	$-5.3 \pm 0.2/7.4$					> 130/7.4
35	$-8.0 \pm 1.3/5.0$	n.d.	n.d.	n.d.	n.d.	63 ± 8/3.0
	$-8.6 \pm 1.6/6.2$					> 130/5.0
	-10/7.4					> 130/7.4

[a] P_e =effective permeation: passive permeation through an artificial membrane was determined by parallel artificial membrane permeation assay (PAMPA); values represent the mean ± SD of quadruplicate measurements taken at three pH values (pH 5.0, 6.2, and 7.4).^[33] [b] P_{app} =apparent permeability: permeation through cell monolayers was assessed by a Caco-2 assay in the absorptive (a→b) and secretory (b→a) directions in triplicate.^[42] n.p.=no permeation, n.d.=not determined. [c] Distribution coefficients ($\log D$) were measured by a miniaturized shake-flask procedure at pH 7.4. [d] Kinetic solubility was measured in a 96-well format using the μSOL Explorer solubility analyzer at three pH values (pH 3.0, 5.0, and 7.4) in triplicate.

PAMPA could not be confirmed by the colorectal adenocarcinoma (Caco-2) cell permeation assay. In contrast, the methyl esters (**3**, **4a**, **5a**, **13a–f**, **19a–b**, **22**, **30**, and **34**) showed $\log D_{7.4}$ values > 1.5, that is, they are more lipophilic and hence more permeable than the corresponding acids, as shown by the PAMPA and Caco-2 permeation assay. Despite this high absorption potential, the ratios between the apparent permeability coefficients (P_{app}) in the basolateral-to-apical (b→a, secretory) and apical-to-basolateral (a→b, absorptive) directions revealed active efflux processes as an additional issue of all the assessed compounds. Moreover, the methyl esters must be readily hydrolyzed after absorption to become more polar and to be renally eliminated. Rapid metabolic turnover by the enzyme carboxylesterase was previously shown for the methyl esters **4a** and **5a**.^[10e]

The different substituents at the *ortho* position of ring A (**5a**, **5b**, **13a–f**, **14a–f**; Table 3) only have a minor influence on the physicochemical properties. The addition of chloro, fluoro, methyl, trifluoromethyl, or cyclopropyl substituents slightly increases the lipophilicity of the respective acids and methyl esters, whereas methoxy and cyano substituents render the compounds more hydrophilic and less permeable. Moreover, the substituents at the *ortho* position have negligible effects on the low aqueous solubility, which is a major drawback of all methyl esters.^[35] In contrast, the modifications with increased spacer length between carbohydrate and aglycone (**6**, **19a–b**, **20**, **22**, and **23**; Table 3) show higher aqueous solubility. Extending the spacer and linking it at the *ortho* or *meta* positions of the biaryl moiety disrupts the symmetry of the molecular structure, leading to increased solubility.^[15,36] However, an additional chloro substituent at the 4-position (**19b**, **20**; Table 3) restores the symmetrical character of the structure, which in turn

lowers the solubility of the compound. Disrupted structural symmetry might also hold true for the enhanced solubility of the biphenyls with an elongated carboxylate-bearing *para* substituent (**30**, **31**, **34**, and **35**; Table 3). The introduction of a methylene or cyclopropylene group between the biphenyl and the carboxylate moiety markedly improved the aqueous solubility of the methyl esters, whereas the absorption potential was only slightly decreased.

Summary and Conclusions

In this study, we investigated the structure–affinity relationship for *ortho* substituents on ring A of the biphenyl aglycone of the FimH antagonists **13** and **14**. The correlation between vdW volumes of these substituents and the enthalpy term clearly indicates the importance of shape complementarity. This interpretation is further supported by the fact that the electronic character of the substituent [Cl in **5a** (Table 2), CF_3 in **14c** versus CH_3 in **14b**] is less important. The correlation of enthalpic improvements ($\Delta\Delta H$) with vdW volumes offers a potent tool for guiding further structural optimization.

The successful oral application using a prodrug approach was recently demonstrated with the ester **5a**.^[10e] A major drawback of the biphenyl methyl esters is their insufficient solubility, which is mostly in the range of 15–35 $\mu\text{g mL}^{-1}$. As expected,^[15] solubility could be substantially improved when the symmetry of the aglycone was disrupted. Thus, the solubility of **3** (> 150 $\mu\text{g mL}^{-1}$; Table 3), **19a** (100 $\mu\text{g mL}^{-1}$), and **22** (> 130 $\mu\text{g mL}^{-1}$) was improved by a factor of ~10. However, for these more flexible derivatives, the expected optimized fit leading to improved affinities in the in-docking mode could not be observed. In fact, the affinities for the members of this

family of compounds are drastically decreased, for example, compounds **20** or **23** (Table 1).

Finally, the elongation of the ester-bearing *para* substituent (Table 1; compounds **31** and **35**) did not lead to the expected additional polar interaction with Arg98. Instead, a five- to sevenfold decrease in affinity was observed. Clearly, the desolvation penalty for the guanidinium group could not be matched by the geometrically possible salt bridge with the carboxylate of the antagonists **31** and **35**.

In summary, our study confirms the earlier selection of the FimH antagonists **5a** for oral and **5b** for intravenous application. However, the methoxy derivative **13d** (Table 1) shows slightly improved pharmacokinetic properties and therefore represents an additional candidate for future *in vivo* studies.

Experimental Section

General methods: NMR spectra were recorded on a Bruker Avance DMX-500 (500.1 MHz) spectrometer. Assignment of ^1H and ^{13}C NMR spectra was achieved using 2D methods (COSY, HSQC, HMBC). Chemical shifts are expressed in ppm using residual CHCl_3 , CHD_2OD , or H_2O as references. Optical rotations were measured with a PerkinElmer Polarimeter 341. Electrospray ionization mass spectrometry (ESI-MS) data were obtained on a Waters Micromass ZQ instrument. LC–HRMS analyses were carried out using an Agilent 1100 LC equipped with a photodiode array detector and a Micromass QTOF I equipped with a 4 GHz digital time converter. Microwave-assisted reactions were carried out with a CEM Discover and Explorer. Reactions were monitored by TLC using glass plates coated with silica gel 60 F_{254} (Merck) and visualized by UV light and/or by charring with a molybdate solution (0.02 M solution of ammonium cerium sulfate dihydrate and ammonium molybdate tetrahydrate in aqueous 10% H_2SO_4). MPLC separations were carried out on a CombiFlash Companion or R_f from Teledyne Isco equipped with RediSep normal-phase or RP-18 reversed-phase flash columns. LC–MS separations were carried out on a Waters system equipped with sample manager 2767, pump 2525, PDA 2525, and Micromass ZQ. Size-exclusion chromatography was performed on Bio-Gel P-2 Gel (45–90 mm) from Bio-Rad (Reinach, Switzerland). All compounds used for biological assays are at least of 98% purity based on analytical HPLC results. Commercially available reagents were purchased from Fluka, Aldrich, Alfa Aesar or Iris Biotech (Germany). Solvents were purchased from Sigma–Aldrich (Buchs, Switzerland) or Acros Organics (Geel, Belgium) and were dried prior to use where indicated. MeOH was dried by reflux with sodium methoxide and distilled immediately before use. CH_2Cl_2 was dried by filtration over Al_2O_3 (Fluka, type 5016 A basic). Molecular sieves (4 Å) were activated *in vacuo* at 500 °C for 1 h immediately before use.

General procedure A for the synthesis of mannosides 10a–f and 17a–c: To an ice-cold suspension of **8**^[12] (200 mg, 0.57 mmol, 1.1 equiv), phenol **9a–f** or benzyl alcohol **16a–c** (0.52 mmol, 1.0 equiv), and molecular sieves (4 Å, 600 mg) in dry CH_2Cl_2 (5 mL), $\text{BF}_3\cdot\text{Et}_2\text{O}$ (0.3 mL, 2.44 mmol, 4.7 equiv) was added dropwise under argon. The mixture was stirred at 0 °C for 3 h, and then at RT overnight. The reaction mixture was filtered over Celite, and the filtrate was diluted with CH_2Cl_2 (50 mL), extracted with 0.5 N $\text{NaOH}_{(\text{aq})}$ (50 mL), H_2O (50 mL), and brine (50 mL). The organic layer was dried over Na_2SO_4 and concentrated *in vacuo*. The residue was purified by MPLC on silica gel (petroleum ether (PE)/EtOAc) to yield **10a–f** or **17a–c**.

General procedure B for the synthesis of mannosylated biphenyls: A Schlenk tube was charged with aryl bromide (1.0 equiv), boronic acid or boronate (1.1 equiv), $\text{Pd}(\text{dppf})\text{Cl}_2\cdot\text{CH}_2\text{Cl}_2$ (0.03 equiv), K_3PO_4 (1.5 equiv) and a stirring bar. The tube was closed with a rubber septum and was evacuated and flushed with argon. This procedure was repeated once, then anhydrous DMF (2 mL) was added under a stream of argon. The mixture was degassed in an ultrasonic bath and flushed with argon for 5 min, and then stirred at 80 °C overnight. The reaction mixture was cooled to RT, diluted with EtOAc (50 mL), and washed with H_2O (50 mL) and brine (50 mL). The organic layer was dried over Na_2SO_4 and concentrated *in vacuo*. The residue was purified by MPLC on silica gel (PE/EtOAc) to afford biphenyls **12a–f**, **18a,b**, **21**, **29** or **33**.

General procedure C for deacetylation: To a solution of **12a–f**, **18a,b**, **21**, **29** or **33** (1.0 equiv) in dry MeOH (5 mL) was added freshly prepared 1 M NaOMe/MeOH (0.1 equiv) under argon. The mixture was stirred at RT until the reaction was complete (monitored by TLC), then neutralized with Amberlyst-15 (H^+) ion-exchange resin, filtered and concentrated *in vacuo*. The residue was purified by MPLC on silica gel ($\text{CH}_2\text{Cl}_2/\text{MeOH}$, 10:1–8:1) to afford **13a–f**, **19a,b**, **22**, **30** or **34** as white solids.

General procedure D for saponification: To a solution of **12a–e**, **18a,b**, **21**, **29** or **33** (1.0 equiv) in MeOH (5 mL) was added 1 M NaOMe/MeOH (0.1 equiv) at RT. The reaction mixture was stirred at RT for 4 h and concentrated. The residue was treated with 0.5 M $\text{NaOH}_{(\text{aq})}$ (1 mL) for 24 h at RT. The solution was then adjusted to pH 3–4 with Amberlyst-15 (H^+), and the mixture was filtered and concentrated. The crude product was transformed into the sodium salt by passing through a small column of Dowex 50X8 (Na^+ form) ion-exchange resin. After concentration, the residue was purified by MPLC (RP-18, $\text{H}_2\text{O}/\text{MeOH}$, 1:0–2:1) followed by size-exclusion chromatography (P-2 gel, H_2O) to give **14a–e**, **6**, **20**, **23**, **31** or **35** as white solids after final lyophilization from H_2O .

4-Bromo-2-fluorophenyl 2,3,4,6-tetra-O-acetyl- α -D-mannopyranoside (10a): Prepared according to general procedure A from **8**^[12] and 4-bromo-2-fluorophenol (**9a**). Yield: 220 mg (74%) as white solid. $R_f=0.48$ (PE/EtOAc, 2:1); $[\alpha]_D^{20}+83.0$ ($c=0.70$, EtOAc); ^1H NMR (500 MHz, CDCl_3): $\delta=7.30$ (dd, $J=2.3$, 10.1 Hz, 1H, Ar-H), 7.21 (dt, $J=1.7$, 8.8 Hz, 1H, Ar-H), 7.08 (t, $J=8.6$ Hz, 1H, Ar-H), 5.54 (dd, $J=3.5$, 10.0 Hz, 1H, H-3), 5.50 (dd, $J=1.8$, 3.4 Hz, 1H, H-2), 5.46 (d, $J=1.5$ Hz, 1H, H-1), 5.36 (t, $J=10.0$ Hz, 1H, H-4), 4.26 (dd, $J=5.5$, 12.2 Hz, 1H, H-6a), 4.17 (ddd, $J=2.1$, 5.5, 10.0 Hz, 1H, H-5), 4.10 (dd, $J=2.2$, 12.2 Hz, 1H, H-6b), 2.20, 2.07, 2.05, 2.04 ppm (4 s, 12H, 4 OAc); ^{13}C NMR (125 MHz, CDCl_3): $\delta=170.51$, 169.95, 169.82, 169.76 (4 CO), 153.28 (d, $J=251.4$ Hz, Ar-C), 142.64 (d, $J=11.1$ Hz, Ar-C), 127.58 (d, $J=4.0$ Hz, Ar-C), 120.4 (d, $J=21.5$ Hz, Ar-C), 120.28 (d, $J=0.9$ Hz, Ar-C), 115.73 (d, $J=8.1$ Hz, Ar-C), 97.49 (C-1), 69.76 (C-5), 69.15 (C-2), 68.60 (C-3), 65.76 (C-4), 62.09 (C-6), 20.87, 20.71, 20.69, 20.67 ppm (4 COCH_3); elemental analysis calcd (%) for $\text{C}_{20}\text{H}_{22}\text{BrFO}_{10}$: C 46.08, H 4.25, found: C 46.11, H 4.26.

4-Bromo-2-methylphenyl 2,3,4,6-tetra-O-acetyl- α -D-mannopyranoside (10b): Prepared according to general procedure A from **8**^[12] and 4-bromo-2-methylphenol (**9b**). Yield: 254 mg (86%) as white solid. $R_f=0.60$ (PE/EtOAc, 2:1); $[\alpha]_D^{20}+61.8$ ($c=1.00$, EtOAc); ^1H NMR (500 MHz, CDCl_3): $\delta=7.31$ (d, $J=1.9$ Hz, 1H, Ar-H), 7.24 (dd, $J=2.3$, 8.7 Hz, 1H, Ar-H), 6.97 (d, $J=8.8$ Hz, 1H, Ar-H), 5.53 (dd, $J=3.4$, 10.0 Hz, 1H, H-3), 5.47 (d, $J=1.7$ Hz, 1H, H-1), 5.45 (dd, $J=2.0$, 3.4 Hz, 1H, H-2), 5.37 (t, $J=10.0$ Hz, 1H, H-4), 4.28 (dd, $J=5.6$, 12.3 Hz, 1H, H-6a), 4.10–4.03 (m, 2H, H-5, H-6b), 2.27 (s, 3H, CH_3), 2.20, 2.06, 2.05, 2.04 ppm (4 s, 12H, 4 OAc); ^{13}C NMR (125 MHz, CDCl_3): $\delta=170.53$, 170.04, 169.96, 169.73 (4 CO), 152.96, 133.78,

129.88, 129.61, 115.81, 115.23 (Ar-C), 95.91 (C-1), 69.39 (C-5), 69.38 (C-2), 68.88 (C-3), 65.76 (C-4), 62.12 (C-6), 20.88, 20.70, 20.68 (4C, 4 COCH₃), 16.07 ppm (CH₃); elemental analysis calcd (%) for C₂₁H₂₅BrO₁₀: C 48.76, H 4.87, found: C 48.84, H 4.91.

4-Bromo-2-trifluoromethyl-phenyl 2,3,4,6-tetra-O-acetyl- α -D-mannopyranoside (10c): Prepared according to general procedure A from **8**^[12] and 4-bromo-2-trifluoromethylphenol (**9c**). Yield: 260 mg (80%) as white solid. $R_f=0.50$ (PE/EtOAc, 2:1); $[\alpha]_D^{20} + 64.6$ ($c=1.00$, EtOAc); ¹H NMR (500 MHz, CDCl₃): $\delta=7.74$ (d, $J=2.3$ Hz, 1H, Ar-H), 7.61 (dd, $J=2.4, 8.9$ Hz, 1H, Ar-H), 7.15 (d, $J=8.9$ Hz, 1H, Ar-H), 5.60 (d, $J=1.6$ Hz, 1H, H-1), 5.51 (dd, $J=3.5, 10.1$ Hz, 1H, H-3), 5.45 (dd, $J=2.0, 3.3$ Hz, 1H, H-2), 5.39 (t, $J=10.1$ Hz, 1H, H-4), 4.27 (dd, $J=5.3, 12.4$ Hz, 1H, H-6a), 4.08–4.00 (m, 2H, H-5, H-6b), 2.21, 2.06, 2.05, 2.04 ppm (4 s, 12H, 4 OAc); ¹³C NMR (125 MHz, CDCl₃): $\delta=170.41, 169.91, 169.74, 169.62$ (4 CO), 152.16 (d, $J=1.7$ Hz, Ar-C), 136.07 (Ar-C), 130.35 (t, $J=5.3$ Hz, Ar-C), 122.30 (d, $J=271.4$ Hz, CF₃), 121.72 (d, $J=31.7$ Hz, Ar-C), 117.08, 114.88 (Ar-C), 95.75 (C-1), 69.96 (C-5), 69.02 (C-2), 68.45 (C-3), 65.44 (C-4), 61.95 (C-6), 20.84, 20.70, 20.67, 20.63 ppm (4 COCH₃); elemental analysis calcd (%) for C₂₁H₂₅BrF₃O₁₀: C 44.15, H 3.88, found: C 44.10, H 3.88.

4-Bromo-2-methoxyphenyl 2,3,4,6-tetra-O-acetyl- α -D-mannopyranoside (10d): Prepared according to general procedure A from **8**^[12] and 4-bromo-2-methoxyphenol (**9d**). Yield: 234 mg (77%) as white solid. $R_f=0.32$ (PE/acetone, 4:1); $[\alpha]_D^{20} + 70.3$ ($c=0.70$, EtOAc); ¹H NMR (500 MHz, CDCl₃): $\delta=7.03$ –6.95 (m, 3H, Ar-H), 5.58 (dd, $J=3.5, 10.0$ Hz, 1H, H-3), 5.52 (dd, $J=1.8, 3.4$ Hz, 1H, H-2), 5.42 (d, $J=1.8$ Hz, 1H, H-1), 5.34 (t, $J=10.0$ Hz, 1H, H-4), 4.28–4.24 (m, 2H, H-5, H-6a), 4.10 (m, 1H, H-6b), 3.84 (s, 3H, OCH₃), 2.19, 2.07, 2.05, 2.04 ppm (4 s, 12H, 4 OAc); ¹³C NMR (125 MHz, CDCl₃): $\delta=170.58, 169.98, 169.89, 169.80$ (4 CO), 151.52, 143.91, 123.49, 120.37, 116.69, 115.94 (Ar-C), 97.52 (C-1), 69.45 (C-5), 69.36 (C-2), 68.80 (C-3), 66.06 (C-4), 62.27 (C-6), 56.04 (OCH₃), 20.91, 20.73, 20.71, 20.69 ppm (4 COCH₃); elemental analysis calcd (%) for C₂₁H₂₅BrO₁₁: C 47.29, H 4.72, found: C 47.20, H 4.70.

4-Bromo-2-cyclopropylphenyl 2,3,4,6-tetra-O-acetyl- α -D-mannopyranoside (10e): Prepared according to general procedure A from **8**^[12] and 4-bromo-2-cyclopropylphenol (**9e**). Yield: 235 mg (76%) as white solid. $R_f=0.30$ (PE/EtOAc, 3:1); $[\alpha]_D^{20} + 64.7$ ($c=0.40$, EtOAc); ¹H NMR (500 MHz, CDCl₃): $\delta=7.20$ (d, $J=8.7$ Hz, 1H, Ar-H), 7.00–6.69 (m, 2H, Ar-H), 5.58 (d, $J=10.1$ Hz, 1H, H-3), 5.50 (s, 2H, H-1, H-2), 5.39 (t, $J=10.1$ Hz, 1H, H-4), 4.28 (dd, $J=5.4, 12.2$ Hz, 1H, H-6a), 4.14–4.08 (m, 2H, H-5, H-6b), 2.21, 2.09, 2.04 (3 s, 12H, 4 OAc), 1.02 (d, $J=8.1$ Hz, 2H, CH₂-cPr), 0.65 ppm (d, $J=4.6$ Hz, 2H, CH₂-cPr); ¹³C NMR (125 MHz, CDCl₃): $\delta=170.54, 170.03, 170.15, 169.75$ (4 CO), 153.64, 135.64, 129.11, 128.94, 116.29, 115.79 (Ar-C), 96.15 (C-1), 69.46 (C-5), 69.39 (C-2), 68.93 (C-3), 65.78 (C-4), 62.16 (C-6), 21.07, 20.89, 20.70 (4C, 4 COCH₃), 9.73, 7.88, 7.82 ppm (cPr); elemental analysis calcd (%) for C₂₃H₂₇BrFO₁₀: C 50.84, H 5.01, found: C 50.82, H 5.00.

4-Bromo-2-cyanophenyl 2,3,4,6-tetra-O-acetyl- α -D-mannopyranoside (10f): Prepared according to general procedure A from **8**^[12] and 4-bromo-2-cyanophenol (**9f**). Yield: 220 mg (73%) as white solid. $R_f=0.51$ (PE/EtOAc, 2:3); $[\alpha]_D^{20} + 54.3$ ($c=0.60$, EtOAc); IR (KBr): $\nu=2232$ (s, C \equiv N), 1749 cm⁻¹ (vs, C=O); ¹H NMR (500 MHz, CDCl₃): $\delta=7.73$ (d, $J=2.5$ Hz, 1H, Ar-H), 7.66 (dd, $J=2.5, 9.0$ Hz, 1H, Ar-H), 7.15 (d, $J=9.0$ Hz, 1H, Ar-H), 5.62 (d, $J=1.7$ Hz, 1H, H-1), 5.56 (dd, $J=3.5, 10.0$ Hz, 1H, H-3), 5.51 (dd, $J=2.0, 3.4$ Hz, 1H, H-2), 5.41 (t, $J=10.0$ Hz, 1H, H-4), 4.28 (dd, $J=4.9, 12.1$ Hz, 1H, H-6a), 4.13–4.08 (m, 2H, H-5, H-6b), 2.21, 2.07, 2.05, 2.04 ppm (4 s, 12H, 4 OAc); ¹³C NMR (125 MHz, CDCl₃): $\delta=169.37, 168.93, 168.71, 168.48$ (4 CO), 155.18, 136.28, 135.00, 116.12, 114.41, 112.97, 104.62 (Ar-C,

CN), 95.68 (C-1), 69.26 (C-5), 68.02 (C-2), 67.35 (C-3), 64.38 (C-4), 60.85 (C-6), 19.81, 19.67, 19.64, 19.58 ppm (4 COCH₃); elemental analysis calcd (%) for C₂₁H₂₂BrNO₁₀: C 47.74, H 4.02, N 2.65, found: C 47.78, H 4.29, N 2.67.

Methyl 4'-(2,3,4,6-tetra-O-acetyl- α -D-mannopyranosyloxy)-3'-fluorobiphenyl-4-carboxylate (12a): Prepared according to general procedure B from **10a** (100 mg, 0.192 mmol), 4-methoxycarbonylphenylboronic acid (**11**, 38.0 mg, 0.211 mmol), Pd(dppf)Cl₂·CH₂Cl₂ (4.7 mg, 5.8 μ mol) and K₃PO₄ (61.1 mg, 0.288 mmol). Yield: 83 mg (75%) as white solid. $R_f=0.26$ (PE/EtOAc, 2:1); $[\alpha]_D^{20} + 93.0$ ($c=0.60$, EtOAc); ¹H NMR (500 MHz, CDCl₃): $\delta=8.03$ –8.02 (m, 2H, Ar-H), 7.53–7.52 (m, 2H, Ar-H), 7.33 (dd, $J=2.1, 11.8$ Hz, 1H, Ar-H), 7.27 (dd, $J=1.5, 8.9$ Hz, 1H, Ar-H), 7.20 (t, $J=8.3$ Hz, 1H, Ar-H), 5.53 (dd, $J=3.4, 10.0$ Hz, 1H, H-3), 5.49–5.47 (m, 2H, H-1, H-2), 5.32 (t, $J=10.0$ Hz, 1H, H-4), 4.22 (dd, $J=5.4, 12.1$ Hz, 1H, H-6a), 4.17 (m, 1H, H-5), 4.05 (dd, $J=1.8, 12.1$ Hz, 1H, H-6b), 3.87 (s, 3H, OCH₃), 2.15, 2.01, 1.98, 1.97 ppm (4 s, 12H, 4OAc); ¹³C NMR (125 MHz, CDCl₃): $\delta=170.54, 170.00, 169.86, 169.79, 166.82$ (5 CO), 153.50 (d, $J=247.0$ Hz, Ar-C), 143.56 (d, $J=1.8$ Hz, Ar-C), 143.22 (d, $J=11.2$ Hz, Ar-C), 136.48 (d, $J=6.7$ Hz, Ar-C), 130.27, 129.29, 126.75 (5C, Ar-C), 123.16 (d, $J=3.4$ Hz, Ar-C), 119.32 (Ar-C), 115.64 (d, $J=19.4$ Hz, Ar-C), 97.42 (C-1), 69.71 (C-5), 69.26 (C-2), 68.70 (C-3), 65.83 (C-4), 62.10 (C-6), 52.24 (OMe), 20.91, 20.74, 20.72, 20.70 ppm (4 COCH₃); HRMS: m/z : calcd for C₂₈H₂₉FO₁₂ [M+Na]⁺: 599.1535, found: 599.1536.

Methyl 4'-(2,3,4,6-tetra-O-acetyl- α -D-mannopyranosyloxy)-3'-methylbiphenyl-4-carboxylate (12b): Prepared according to general procedure B from **10b** (100 mg, 0.193 mmol), **11** (38.2 mg, 0.212 mmol), Pd(dppf)Cl₂·CH₂Cl₂ (4.7 mg, 5.8 μ mol) and K₃PO₄ (61.5 mg, 0.290 mmol). Yield: 87 mg (79%) as white solid. $R_f=0.41$ (PE/EtOAc, 1:0.9); $[\alpha]_D^{20} + 85.4$ ($c=0.80$, EtOAc); ¹H NMR (500 MHz, CDCl₃): $\delta=8.09$ –8.07 (m, 2H, Ar-H), 7.61 (m, 2H, Ar-H), 7.46 (d, $J=1.8$ Hz, 1H, Ar-H), 7.40 (dd, $J=2.3, 8.5$ Hz, 1H, Ar-H), 7.18 (d, $J=8.5$ Hz, 1H, Ar-H), 5.61–5.58 (m, 2H, H-1, H-3), 5.50 (dd, $J=2.0, 3.5$ Hz, 1H, H-2), 5.41 (t, $J=10.0$ Hz, 1H, H-4), 4.31 (dd, $J=5.9, 12.8$ Hz, 1H, H-6a), 4.14–4.09 (m, 2H, H-5, H-6b), 3.94 (s, 3H, OCH₃), 2.37 (s, 3H, CH₃), 2.22, 2.08, 2.05, 2.04 ppm (4 s, 12H, 4 OAc); ¹³C NMR (125 MHz, CDCl₃): $\delta=170.55, 170.06, 169.98, 169.75, 167.00$ (5 CO), 154.05, 144.94, 134.54, 130.10, 130.02, 128.54, 128.05, 126.66, 125.76, 114.46 (12C, Ar-C), 95.84 (C-1), 69.48 (C-5), 69.37 (C-2), 68.98 (C-3), 65.81 (C-4), 62.13 (C-6), 52.12 (OCH₃), 21.06, 20.91, 20.72, 20.70 (4 COCH₃), 16.40 ppm (CH₃); HRMS: m/z : calcd for C₂₉H₃₂NaO₁₂ [M+Na]⁺: 595.1786, found: 595.1786; elemental analysis calcd (%) for C₂₉H₃₂O₁₂: C 60.84, H 5.63, found: C 60.76, H 5.80.

Methyl 4'-(2,3,4,6-tetra-O-acetyl- α -D-mannopyranosyloxy)-3'-trifluoromethylbiphenyl-4-carboxylate (12c): Prepared according to general procedure B from **10c** (100 mg, 0.175 mmol), **11** (34.6 mg, 0.193 mmol), Pd(dppf)Cl₂·CH₂Cl₂ (4.3 mg, 5.3 μ mol) and K₃PO₄ (55.7 mg, 0.263 mmol). Yield: 100 mg (91%) as white solid. $R_f=0.25$ (PE/EtOAc, 2:1); $[\alpha]_D^{20} + 43.3$ ($c=1.00$, EtOAc); ¹H NMR (500 MHz, CDCl₃): $\delta=8.13$ –8.11 (m, 2H, Ar-H), 7.87 (d, $J=2.1$ Hz, 1H, Ar-H), 7.75 (dd, $J=2.2, 8.7$ Hz, 1H, Ar-H), 7.63–7.61 (m, 2H, Ar-H), 7.35 (d, $J=8.7$ Hz, 1H, Ar-H), 5.70 (d, $J=1.7$ Hz, 1H, H-1), 5.57 (dd, $J=3.5, 10.1$ Hz, 1H, H-3), 5.50 (dd, $J=2.0, 3.4$ Hz, 1H, H-2), 5.43 (t, $J=10.0$ Hz, 1H, H-4), 4.30 (dd, $J=5.6, 12.8$ Hz, 1H, H-6a), 4.11–4.08 (m, 2H, H-5, H-6b), 3.95 (s, 3H, OCH₃), 2.24, 2.07, 2.06, 2.05 ppm (4 s, 12H, 4 OAc); ¹³C NMR (125 MHz, CDCl₃): $\delta=170.45, 169.96, 169.78, 169.65, 166.76$ (5 CO), 152.94, 143.37, 134.59, 130.34, 129.40, 126.79, 126.14, 115.79 (12C, Ar-C), 95.67 (C-1), 69.91 (C-5), 69.15 (C-2), 68.56 (C-3), 65.50 (C-4), 61.97 (C-6), 52.25 (OCH₃), 20.88, 20.71,

20.66 ppm (4C, 4 COCH₃); HRMS: *m/z*: calcd for C₂₉H₂₉F₃NaO₁₂ [M+Na]⁺: 649.1503, found: 649.1503.

Methyl 4'-(2,3,4,6-tetra-O-acetyl- α -D-mannopyranosyloxy)-3'-methoxybiphenyl-4-carboxylate (12d): Prepared according to general procedure B from **10d** (100 mg, 0.188 mmol), **11** (37.1 mg, 0.206 mmol), Pd(dppf)Cl₂·CH₂Cl₂ (4.6 mg, 5.6 μ mol) and K₃PO₄ (59.9 mg, 0.282 mmol). Yield: 91 mg (83%) as white solid. *R*_f=0.25 (PE/EtOAc, 1:0.9); [α]_D²⁰ +50.7 (*c*=1.40, EtOAc); ¹H NMR (500 MHz, CDCl₃): δ =8.10–8.08 (m, 2H, Ar-H), 7.62–7.60 (m, 2H, Ar-H), 7.19–7.13 (m, 3H, Ar-H), 5.64 (dd, *J*=3.5, 10.0 Hz, 1H, H-3), 5.58 (dd, *J*=1.8, 3.5 Hz, 1H, H-2), 5.53 (d, *J*=1.7 Hz, 1H, H-1), 5.38 (t, *J*=10.0 Hz, 1H, H-4), 4.34–4.28 (m, 2H, H-5, H-6a), 4.12 (m, 1H, H-6b), 3.94 (2 s, 6H, 2 OCH₃), 2.21, 2.08, 2.05, 2.04 ppm (4 s, 12H, 4 OAc); ¹³C NMR (125 MHz, CDCl₃): δ =170.61, 170.02, 169.92, 169.83, 166.94 (5 CO), 151.01, 145.06, 144.92, 136.51, 130.13, 128.86, 126.87, 119.72, 119.32, 111.60 (12C, Ar-C), 97.50 (C-1), 69.48 (C-5), 69.43 (C-2), 68.91 (C-3), 66.12 (C-4), 62.29 (C-6), 56.01 (OCH₃), 52.18 (CO₂CH₃), 20.95, 20.76, 20.74, 20.72 ppm (4 COCH₃); HRMS: *m/z*: calcd for C₂₉H₃₂NaO₁₃ [M+Na]⁺: 611.1735, found: 611.1736.

Methyl 4'-(2,3,4,6-tetra-O-acetyl- α -D-mannopyranosyloxy)-3'-cyclopropylbiphenyl-4-carboxylate (12e): Prepared according to general procedure B from **10e** (100 mg, 0.184 mmol), **11** (36.4 mg, 0.202 mmol), Pd(dppf)Cl₂·CH₂Cl₂ (4.5 mg, 5.5 μ mol) and K₃PO₄ (58.6 mg, 0.276 mmol). Yield: 60 mg (55%) as white solid. *R*_f=0.48 (PE/EtOAc, 2:1); [α]_D²⁰ +53.0 (*c*=0.70, EtOAc); ¹H NMR (500 MHz, CDCl₃): δ =8.08–8.07 (m, 2H, Ar-H), 7.59–7.57 (m, 2H, Ar-H), 7.37 (dd, *J*=2.4, 8.5 Hz, 1H, Ar-H), 7.19–7.17 (m, 2H, Ar-H), 5.64 (dd, *J*=3.5, 10.1 Hz, 1H, H-3), 5.61 (d, *J*=1.6 Hz, 1H, H-1), 5.54 (dd, *J*=1.9, 3.4 Hz, 1H, H-2), 5.42 (t, *J*=10.1 Hz, 1H, H-4), 4.31 (dd, *J*=5.3, 12.2 Hz, 1H, H-6a), 4.19–4.10 (m, 2H, H-5, H-6b), 3.94 (s, 3H, OCH₃), 2.22 (s, 3H, OAc), 2.17 (m, 1H, H-cPr), 2.08–2.05 (m, 9H, 3 OAc), 1.06–1.05 (m, 2H, CH₂-cPr), 0.74–0.73 ppm (m, 2H, CH₂-cPr); ¹³C NMR (125 MHz, CDCl₃): δ =170.55, 170.06, 170.02, 169.75, 166.98 (5 CO), 154.76, 145.12, 134.83, 133.56, 130.08, 128.58, 126.71, 125.33, 125.06, 114.84 (12C, Ar-C), 96.04 (C-1), 69.49 (C-5), 69.42 (C-2), 69.02 (C-3), 65.81 (C-4), 62.15 (C-6), 52.12 (OCH₃), 20.91, 20.71 (4C, 4 COCH₃), 9.78, 7.58 ppm (3C, cPr); elemental analysis calcd (%) for C₂₉H₃₂O₁₂: C 62.20, H 5.72, found: C 62.00, H 5.86.

Methyl 4'-(2,3,4,6-tetra-O-acetyl- α -D-mannopyranosyloxy)-3'-cyanobiphenyl-4-carboxylate (12f): Prepared according to general procedure B from **10f** (100 mg, 0.189 mmol), **11** (37.5 mg, 0.208 mmol), Pd(dppf)Cl₂·CH₂Cl₂ (4.6 mg, 5.7 μ mol) and K₃PO₄ (60.2 mg, 0.284 mmol). Yield: 92 mg (84%) as white solid. *R*_f=0.18 (PE/EtOAc, 2:1); [α]_D²⁰ +61.4 (*c*=0.80, EtOAc); ¹H NMR (500 MHz, CDCl₃): δ =8.06–8.05 (m, 2H, Ar-H), 7.80 (d, *J*=2.3 Hz, 1H, Ar-H), 7.72 (dd, *J*=2.3, 8.8 Hz, 1H, Ar-H), 7.53–7.51 (m, 2H, Ar-H), 7.28 (d, *J*=8.8 Hz, 1H, Ar-H), 5.64 (d, *J*=1.7 Hz, 1H, H-1), 5.55 (dd, *J*=3.5, 10.0 Hz, 1H, H-3), 5.49 (dd, *J*=1.9, 3.4 Hz, 1H, H-2), 5.37 (t, *J*=10.0 Hz, 1H, H-4), 4.24 (dd, *J*=5.0, 12.4 Hz, 1H, H-6a), 4.12 (ddd, *J*=2.2, 4.9, 10.0 Hz, 1H, H-5), 4.05 (dd, *J*=2.2, 12.4 Hz, 1H, H-6b), 3.88 (s, 3H, OCH₃), 2.16, 2.01, 1.99, 1.98 ppm (4 s, 12H, 4 OAc); ¹³C NMR (125 MHz, CDCl₃): δ =170.45, 170.01, 169.78, 169.54, 166.65 (5 CO), 156.84, 142.44, 135.67, 132.36, 129.77, 126.76, 115.99, 115.18, 104.47 (13C, Ar-C, CN), 96.63 (C-1), 70.24 (C-5), 69.17 (C-2), 68.49 (C-3), 65.48 (C-4), 60.85 (C-6), 20.88, 20.73, 20.71, 20.64 ppm (4 COCH₃); HRMS: *m/z*: calcd for C₂₉H₂₉NNaO₁₂ [M+Na]⁺: 606.1582, found: 606.1583.

Methyl 3'-fluoro-4'-(α -D-mannopyranosyloxy)biphenyl-4-carboxylate (13a): Prepared according to general procedure C from **12a** (33 mg, 0.057 mmol). Yield: 15 mg (65%). [α]_D²⁰ +114.3 (*c*=0.30, MeOH); ¹H NMR (500 MHz, CD₃OD): δ =7.98–7.97 (m, 2H, Ar-H),

7.63–7.61 (m, 2H, Ar-H), 7.42–7.36 (m, 3H, Ar-H), 5.45 (d, *J*=1.7 Hz, 1H, H-1), 3.99 (dd, *J*=1.9, 3.4 Hz, 1H, H-2), 3.82–3.84 (m, 4H, H-3, OCH₃), 3.71–3.56 ppm (m, 4H, H-4, H-5, H-6); ¹³C NMR (125 MHz, CD₃OD): δ =168.34 (CO), 154.75 (d, *J*=243.8 Hz, Ar-C), 145.6 (2C, Ar-C), 136.37 (d, *J*=6.9 Hz, Ar-C), 130.20, 129.20, 127.80, 124.33, 120.33 (7C, Ar-C), 116.00 (d, *J*=20.0 Hz, Ar-C), 101.40 (C-1), 75.97 (C-5), 72.31 (C-3), 71.82 (C-2), 68.18 (C-4), 62.65 (C-6), 52.65 ppm (OCH₃); HRMS: *m/z*: calcd for C₂₀H₂₁FNaO₈ [M+Na]⁺: 431.1113, found: 431.1112.

Methyl 4'-(α -D-mannopyranosyloxy)-3'-methylbiphenyl-4-carboxylate (13b): Prepared according to general procedure C from **12b** (31 mg, 0.054 mmol). Yield: 16 mg (73%). [α]_D²⁰ +110.5 (*c*=0.35, MeOH); ¹H NMR (500 MHz, CD₃OD): δ =7.96–7.94 (m, 2H, Ar-H), 7.60–7.58 (m, 2H, Ar-H), 7.40–7.37 (m, 2H, Ar-H), 7.22 (d, *J*=8.5 Hz, 1H, Ar-H), 5.47 (d, *J*=1.6 Hz, 1H, H-1), 3.97 (dd, *J*=1.9, 3.4 Hz, 1H, H-2), 3.87 (dd, *J*=3.4, 9.5 Hz, 1H, H-3), 3.82 (s, 3H, OMe), 3.67–3.52 (m, 3H, H-4, H-6), 3.46 (m, 1H, H-5), 2.21 ppm (s, 3H, Me); ¹³C NMR (125 MHz, CD₃OD): δ =168.56 (CO), 156.20, 146.86, 134.70, 131.07, 130.07, 130.54, 129.45, 128.92, 127.63, 126.85, 115.83 (12C, Ar-C), 99.76 (C-1), 75.55 (C-5), 72.64 (C-3), 72.11 (C-2), 68.31 (C-4), 62.68 (C-6), 52.59 ppm (OCH₃), 16.54 (CH₃); HRMS: *m/z*: calcd for C₂₁H₂₄NaO₈ [M+Na]⁺: 427.1363, found: 427.1370.

Methyl 3'-trifluoromethyl-4'-(α -D-mannopyranosyloxy)biphenyl-4-carboxylate (13c): Prepared according to general procedure C from **12c** (30 mg, 0.048 mmol). Yield: 14 mg (64%). [α]_D²⁰ +113.1 (*c*=0.40, MeOH); ¹H NMR (500 MHz, CD₃OD): δ =8.11–8.10 (m, 2H, Ar-H), 7.92–7.90 (m, 2H, Ar-H), 7.75–7.73 (m, 2H, Ar-H), 7.63 (d, *J*=8.4 Hz, 1H, Ar-H), 5.69 (d, *J*=1.5 Hz, 1H, H-1), 4.09 (dd, *J*=1.8, 3.3 Hz, 1H, H-2), 3.98–3.94 (m, 4H, H-3, OMe), 3.79–3.73 (m, 3H, H-4, H-6), 3.61 ppm (ddd, *J*=2.3, 5.7, 9.6 Hz, 1H, H-5); ¹³C NMR (125 MHz, CD₃OD): δ =168.29 (CO), 155.54, 145.13, 134.74, 133.45, 131.36, 131.29, 130.32, 127.91, 127.85, 126.44, 117.80 (Ar-C), 100.27 (C-1), 76.13 (C-5), 72.24 (C-3), 71.74 (C-2), 68.09 (C-4), 62.67 ppm (C-6), 52.69 (OMe); HRMS: *m/z*: calcd for C₂₁H₂₁F₃NaO₈ [M+Na]⁺: 481.1081, found: 481.1082.

Methyl 4'-(α -D-mannopyranosyloxy)-3'-methoxybiphenyl-4-carboxylate (13d): Prepared according to general procedure C from **12d** (32 mg, 0.055 mmol). Yield: 12 mg (52%). [α]_D²⁰ +133.1 (*c*=0.20, MeOH); ¹H NMR (500 MHz, CD₃OD): δ =7.97–7.96 (m, 2H, Ar-H), 7.63–7.61 (m, 2H, Ar-H), 7.21–7.11 (m, 3H, Ar-H), 5.37 (d, *J*=1.7 Hz, 1H, H-1), 4.00 (dd, *J*=1.8, 3.4 Hz, 1H, H-2), 3.86 (dd, *J*=3.5, 8.8 Hz, 1H, H-3), 3.82 (s, 6H, 2 CH₃), 3.70–3.63 ppm (m, 4H, H-4, H-5, H-6); ¹³C NMR (125 MHz, CD₃OD): δ =168.50 (CO), 152.33, 147.40, 146.83, 136.56, 131.08, 129.76, 127.87, 120.86, 120.10, 112.54 (Ar-C), 101.51 (C-1), 75.66 (C-5), 72.40 (C-2), 72.00 (C-3), 68.34 (C-4), 62.70 (C-6), 56.61 (OMe), 52.63 ppm (OMe); HRMS: *m/z*: calcd for C₂₁H₂₄NaO₉ [M+Na]⁺: 443.1313, found: 443.1315.

Methyl 3'-cyclopropyl-4'-(α -D-mannopyranosyloxy)biphenyl-4-carboxylate (13e): Prepared according to general procedure C from **12e** (21 mg, 0.035 mmol). Yield: 10 mg (67%). [α]_D²⁰ +101.6 (*c*=0.24, MeOH); ¹H NMR (500 MHz, CD₃OD): δ =8.07–8.05 (m, 2H, Ar-H), 7.68–7.67 (m, 2H, Ar-H), 7.46 (dd, *J*=2.4, 8.5 Hz, 1H, Ar-H), 7.33 (d, *J*=8.5 Hz, 1H, Ar-H), 7.21 (d, *J*=2.4 Hz, 1H, Ar-H), 5.60 (d, *J*=1.7 Hz, 1H, H-1), 4.13 (dd, *J*=1.9, 3.3 Hz, 1H, H-2), 4.02 (dd, *J*=3.4, 9.5 Hz, 1H, H-3), 3.93 (s, 3H, OMe), 3.81–3.74 (m, 3H, H-4, H-6), 3.69 (m, 1H, H-5), 2.19 (m, 1H, H-cPr), 1.01–0.99 (m, 2H, CH₂-cPr), 0.76–0.74 ppm (m, 2H, CH₂-cPr); ¹³C NMR (125 MHz, CD₃OD): δ =168.54 (CO), 156.92, 146.98, 135.00, 134.59, 131.07, 127.34, 127.67, 126.39, 125.34, 116.29 (12C, Ar-C), 100.14 (C-1), 75.61 (C-5), 72.64 (C-3), 72.14 (C-2), 68.33 (C-4), 62.71 (C-6), 52.60 (OCH₃), 10.93,

8.06 ppm (3C, cPr); HRMS: m/z : calcd for $C_{23}H_{26}NaO_8$ [$M+Na$] $^+$: 453.1520, found: 453.1519.

Methyl 3'-cyano-4'-(α -D-mannopyranosyloxy)biphenyl-4-carboxylate (13f): Prepared according to general procedure C from **12f** (37 mg, 0.063 mmol). Yield: 19 mg (73%). $[\alpha]_D^{20} + 101.1$ ($c=0.30$, MeOH); 1H NMR (500 MHz, CD_3OD): $\delta=8.00$ – 7.99 (m, 2H, Ar-H), 7.90–7.85 (m, 2H, Ar-H), 7.65–7.63 (m, 2H, Ar-H), 7.50 (d, $J=8.8$ Hz, 1H, Ar-H), 5.63 (s, 1H, H-1), 4.03 (m, 1H, H-2), 3.91 (dd, $J=2.8$, 9.4 Hz, 1H, H-3), 3.83 (s, 3H, OMe), 3.69–3.60 (m, 3H, H-4, H-6), 3.50 ppm (m, 1H, H-5); ^{13}C NMR (125 MHz, CD_3OD): $\delta=168.22$ (CO), 159.29, 144.38, 135.61, 134.50, 133.08, 131.31, 130.56, 127.87, 117.36, 116.75, 104.35 (13C, Ar-C, CN), 100.62 (C-1), 76.39 (C-5), 72.27 (C-2), 71.62 (C-3), 68.07 (C-4), 62.64 (C-6), 52.71 ppm (OMe); HRMS: m/z : calcd for $C_{21}H_{21}NNaO_8$ [$M+Na$] $^+$: 438.1159, found: 438.1162.

Sodium 3'-fluoro-4'-(α -D-mannopyranosyloxy)biphenyl-4-carboxylate (14a): Prepared according to general procedure D from **12a** (50 mg, 0.087 mmol). Yield: 21 mg (58%). $[\alpha]_D^{20} + 112.7$ ($c=0.40$, MeOH); 1H NMR (500 MHz, D_2O): $\delta=7.78$ – 7.77 (m, 2H, Ar-H), 7.46–7.45 (m, 2H, Ar-H), 7.30–7.15 (m, 3H, Ar-H), 5.43 (s, 1H, H-1), 4.07 (s, 1H, H-2), 3.93 (d, $J=3.3$ Hz, 1H, H-3), 3.68–3.62 ppm (m, 4H, H-4, H-5, H-6); ^{13}C NMR (125 MHz, D_2O): $\delta=175.19$ (CO), 153.02 (d, $J=242.6$ Hz, Ar-C), 142.52 (d, $J=10.8$ Hz, Ar-C), 141.23 (Ar-C), 135.53 (d, $J=6.4$ Hz, Ar-C), 135.07, 129.43, 126.25, 126.01, 122.96, 119.13 (Ar-C), 114.83 (d, $J=19.4$ Hz, Ar-C), 99.32 (C-1), 73.65 (C-5), 70.23 (C-3), 69.67 (C-2), 66.35 (C-4), 60.52 ppm (C-6); HRMS: m/z : calcd for $C_{19}H_{19}FNaO_8$ [$M+Na$] $^+$: 417.0956, found: 417.0957.

Sodium 4'-(α -D-mannopyranosyloxy)-3'-methylbiphenyl-4-carboxylate (14b): Prepared according to general procedure D from **12b** (46 mg, 0.081 mmol). Yield: 5 mg (15%). $[\alpha]_D^{20} + 85.7$ ($c=0.20$, MeOH); 1H NMR (500 MHz, D_2O): $\delta=7.78$ – 7.76 (m, 2H, Ar-H), 7.53–7.52 (m, 2H, Ar-H), 7.43–7.37 (m, 2H, Ar-H), 7.10 (d, $J=8.6$ Hz, 1H, Ar-H), 5.52 (d, $J=1.6$ Hz, 1H, H-1), 4.07 (dd, $J=1.9$, 3.4 Hz, 1H, H-2), 3.95 (dd, $J=3.5$, 9.6 Hz, 1H, H-3), 3.63–3.50 (m, 4H, H-4, H-5, H-6), 2.14 ppm (s, 3H, CH_3); ^{13}C NMR (125 MHz, D_2O): $\delta=153.33$, 142.57, 134.59, 133.97, 129.47, 128.42, 126.25, 125.43, 114.99 (12C, Ar-C), 97.46 (C-1), 73.39 (C-5), 70.54 (C-3), 69.88 (C-2), 66.53 (C-4), 60.60 (C-6), 15.31 ppm (CH_3); HRMS: m/z : calcd for $C_{20}H_{22}NaO_8$ [$M+Na$] $^+$: 413.1207, found: 413.1209.

Sodium 3'-trifluoromethyl-4'-(α -D-mannopyranosyloxy)biphenyl-4-carboxylate (14c): Prepared according to general procedure D from **12c** (45 mg, 0.072 mmol). Yield: 25 mg (74%). $[\alpha]_D^{20} + 94.2$ ($c=0.30$, MeOH); 1H NMR (500 MHz, D_2O): $\delta=7.83$ – 7.81 (m, 3H, Ar-H), 7.75 (d, $J=8.7$ Hz, 1H, Ar-H), 7.57–7.55 (m, 2H, Ar-H), 7.31 (d, $J=8.8$ Hz, 1H, Ar-H), 5.64 (s, 1H, H-1), 4.09 (d, $J=1.5$ Hz, 1H, H-2), 3.94 (dd, $J=3.4$, 9.7 Hz, 1H, H-3), 3.67–3.60 (m, 3H, H-4, H-6), 3.54 ppm (m, 1H, H-5); ^{13}C NMR (125 MHz, D_2O): $\delta=175.25$ (CO), 152.40, 141.31, 135.09, 133.53, 131.93, 129.46, 126.34, 125.59, 115.86 (12C, Ar-C), 97.20 (C-1), 73.68 (C-5), 70.19 (C-3), 69.58 (C-2), 66.36 (C-4), 60.55 ppm (C-6); HRMS: m/z : calcd for $C_{20}H_{19}F_3NaO_8$ [$M+Na$] $^+$: 467.0924, found: 467.0923.

Sodium 4'-(α -D-mannopyranosyloxy)-3'-methoxybiphenyl-4-carboxylate (14d): Prepared according to general procedure D from **12d** (47 mg, 0.080 mmol). Yield: 10 mg (29%). $[\alpha]_D^{20} + 115.1$ ($c=0.30$, MeOH); 1H NMR (500 MHz, D_2O): $\delta=7.81$ – 7.79 (m, 2H, Ar-H), 7.54–7.53 (m, 2H, Ar-H), 7.19–7.11 (m, 3H, Ar-H), 5.43 (d, $J=1.6$ Hz, 1H, H-1), 4.10 (dd, $J=1.8$, 3.5 Hz, 1H, H-2), 3.96 (dd, $J=3.5$, 9.0 Hz, 1H, H-3), 3.78 (s, 3H, OCH_3), 3.70–3.62 ppm (m, 4H, H-4, H-5, H-6); ^{13}C NMR (125 MHz, D_2O): $\delta=175.24$ (CO), 149.53, 144.24, 142.42, 135.59, 134.75, 129.40, 126.41, 119.86, 118.03, 111.44 (12C, Ar-C), 99.23 (C-1), 73.53 (C-5), 70.32 (C-3), 69.78 (C-2), 66.40 (C-4), 60.54

(C-6), 55.81 ppm (OCH_3); HRMS: m/z : calcd for $C_{20}H_{22}NaO_9$ [$M+Na$] $^+$: 429.1156, found: 429.1154.

Sodium 3'-cyclopropyl-4'-(α -D-mannopyranosyloxy)biphenyl-4-carboxylate (14e): Prepared according to general procedure D from **12e** (28 mg, 0.047 mmol). Yield: 6 mg (26%). $[\alpha]_D^{20} + 149.8$ ($c=0.20$, MeOH); 1H NMR (500 MHz, D_2O): $\delta=7.79$ – 7.77 (m, 2H, Ar-H), 7.48–7.46 (m, 2H, Ar-H), 7.30 (d, $J=7.8$ Hz, 1H, Ar-H), 7.07–7.05 (m, 2H, Ar-H), 5.52 (s, 1H, H-1), 4.10 (m, 1H, H-2), 3.98 (dd, $J=3.4$, 9.5 Hz, 1H, H-3), 3.69–3.62 (m, 4H, H-4, H-5, H-6), 1.99 (m, 1H, H-cPr), 0.86–0.84 (m, 2H, CH_2 -cPr), 0.58–0.56 ppm (m, 2H, CH_2 -cPr); ^{13}C NMR (125 MHz, D_2O): $\delta=175.34$ (CO), 153.82, 142.58, 134.57, 134.34, 133.74, 129.38, 126.26, 125.01, 124.01, 115.47 (12C, Ar-C), 97.88 (C-1), 73.47 (C-5), 70.55 (C-3), 69.93 (C-2), 66.46 (C-4), 60.57 (C-6), 9.16, 7.26, 7.06 ppm (cPr); HRMS: m/z : calcd for $C_{22}H_{24}ONaO_8$ [$M+Na$] $^+$: 439.1363, found: 439.1363.

Sodium 3'-cyano-4'-(α -D-mannopyranosyloxy)biphenyl-4-carboxylate (14f): A two-neck flask was charged with **10f** (150 mg, 0.28 mmol), 4-carboxybenzene boronic acid pinacol ester (**15**) (77 mg, 0.31 mmol), $Pd(dppf)Cl_2 \cdot CH_2Cl_2$ (7 mg, 0.008 mmol), K_3PO_4 (89 mg, 0.42 mmol) and a stirring bar. The flask was evacuated and flushed with argon, then anhydrous DMF (2 mL) was added under a stream of argon. The mixture was degassed in an ultrasonic bath and flushed with argon for 5 min, and then stirred at 80 °C overnight. The reaction mixture was cooled to RT, diluted with EtOAc (50 mL), and washed with H_2O (50 mL) and brine (50 mL). The organic layer was dried over Na_2SO_4 and concentrated in vacuo. The residue was purified by MPLC on silica gel ($CH_2Cl_2/MeOH$, 10:1–8:1) to afford the biphenyl intermediate (162 mg). The intermediate was dissolved in dry MeOH (4 mL) and treated with freshly prepared 1 M NaOMe/MeOH (28 μ L) for 4 h at RT. The reaction mixture was neutralized with Amberlyst-15 (H^+), filtered and concentrated. The crude product was transformed into the sodium salt by passing through a small column of Dowex 50X8 (Na^+ form) ion-exchange resin. After concentration the residue was purified by MPLC (RP-18, H_2O) followed by size-exclusion chromatography (P-2 gel, H_2O) to give **14f** (19 mg, 17%) as a white solid after final lyophilization from H_2O . $[\alpha]_D^{20} + 75.3$ ($c=0.20$, MeOH); 1H NMR (500 MHz, D_2O): $\delta=7.86$ – 7.79 (m, 4H, Ar-H), 7.53–7.52 (m, 2H, Ar-H), 7.31 (d, $J=8.9$ Hz, 1H, Ar-H), 5.64 (d, $J=1.9$ Hz, 1H, H-1), 4.11 (dd, $J=1.9$, 3.4 Hz, 1H, H-2), 4.00 (dd, $J=3.5$, 9.7 Hz, 1H, H-3), 3.73–3.65 (m, 3H, H-4, H-6), 3.58 ppm (ddd, $J=2.4$, 5.5, 9.9 Hz, 1H, H-5); ^{13}C NMR (125 MHz, D_2O): $\delta=175.12$ (CO), 156.82, 140.37, 134.39, 133.56, 131.83, 129.58, 126.25, 116.82, 115.78, 102.08 (13C, Ar-C, CN), 98.09 (C-1), 73.97 (C-5), 70.29 (C-3), 69.54 (C-2), 66.36 (C-4), 60.56 ppm (C-6); HRMS: m/z : calcd for $C_{21}H_{21}NNaO_8$ [$M+Na$] $^+$: 424.1003, found: 424.1003.

3-Bromobenzyl 2,3,4,6-tetra-O-acetyl- α -D-mannopyranoside (17a): Prepared according to general procedure A from **8**^[12] and 3-bromobenzyl alcohol (**16a**). Yield: 100 mg (34%) as colorless oil. $R_f=0.43$ (PE/EtOAc, 2:1); $[\alpha]_D^{20} + 42.0$ ($c=1.40$, EtOAc); 1H NMR (500 MHz, $CDCl_3$): $\delta=7.48$ – 7.46 , 7.30–7.24 (m, 4H, Ar-H), 5.37 (dd, 1H, $J=3.4$, 10.1 Hz, H-3), 5.33–5.29 (m, 2H, H-2, H-4), 4.88 (d, 1H, $J=1.3$ Hz, H-1), 4.68, 4.54 (A, B of AB, $J=12.1$ Hz, 2H, CH_2 Ar), 4.29 (dd, 1H, $J=5.2$, 12.3 Hz, H-6a), 4.07 (dd, 1H, $J=2.3$, 12.3 Hz, H-6b), 3.99 (ddd, 1H, $J=2.4$, 5.2, 9.9 Hz, H-5), 2.15, 2.13, 2.05, 2.00 ppm (4 s, 12H, 4 OAc); ^{13}C NMR (125 MHz, $CDCl_3$): $\delta=170.59$, 169.98, 169.87, 169.69 (4 CO), 138.49, 131.34, 131.09, 130.24, 126.66, 122.57 (Ar-C), 96.83 (C-1), 69.43, 69.02, 68.90, 68.78 (C-2, C-3, C-5, CH_2 Ar), 66.03 (C-4), 62.36 (C-6), 20.86, 20.76, 20.68 ppm (4C, $COCH_3$); ESI-MS: m/z : calcd for $C_{21}H_{25}BrNaO_{10}$ [$M+Na$] $^+$: 539.05, found: 539.14.

5-Bromo-2-chlorobenzyl 2,3,4,6-tetra-O-acetyl- α -D-mannopyranoside (17b): Prepared according to general procedure A from **8**^[12] and 5-bromo-2-chlorobenzyl alcohol (**16b**). Yield: 152 mg (48%) as a white solid. $R_f=0.56$ (PE/EtOAc, 2:1); $[\alpha]_D^{20} + 48.0$ ($c=1.50$, EtOAc); $^1\text{H NMR}$ (500 MHz, CDCl_3): $\delta=7.48$ (t, $J=1.8$ Hz, 1H, Ar-H), 7.38 (s, 1H, Ar-H), 7.35 (d, $J=1.8$ Hz, 1H, Ar), 5.33 (m, 3H, H-2, H-3, H-4), 4.88 (d, $J=1.5$ Hz, 1H, H-1), 4.65, 4.51 (A, B of AB, $J=12.3$ Hz, 2H, CH_2Ar), 4.30 (dd, $J=5.3$, 12.3 Hz, 1H, H-6a), 4.09 (dd, $J=2.4$, 12.3 Hz, 1H, H-6b), 3.98 (ddd, $J=2.4$, 5.2, 9.7 Hz, 1H, H-5), 2.16, 2.13, 2.05, 2.01 ppm (4 s, 12H, 4 OAc); $^{13}\text{C NMR}$ (125 MHz, CDCl_3): $\delta=170.58$, 169.98, 169.89, 169.69 (4 CO), 139.77, 135.35, 129.25, 126.85, 122.91 (6C, Ar-C), 96.96 (C-1), 69.33, 68.93, 68.24 (4C, C-2, C-3, C-5, CH_2Ar), 65.98 (C-4), 62.38 (C-6), 20.86, 20.77, 20.68 ppm (4C, 4COCH₃); ESI-MS: m/z : calcd for $\text{C}_{21}\text{H}_{24}\text{BrClNaO}_{10}$ $[\text{M}+\text{Na}]^+$: 573.01, found: 573.06.

2-Bromobenzyl 2,3,4,6-tetra-O-acetyl- α -D-mannopyranoside (17c): Prepared according to general procedure A from **8**^[12] and 2-bromobenzyl alcohol (**16c**). Yield: 140 mg (47%) as a white solid. $R_f=0.55$ (petrol ether/EtOAc, 2:1); $[\alpha]_D^{20} + 44.6$ ($c=2.10$, EtOAc); $^1\text{H NMR}$ (500 MHz, CDCl_3): $\delta=7.57$ (dd, $J=1.0$, 8.0 Hz, 1H, Ar-H), 7.47 (dd, $J=1.4$, 7.6 Hz, 1H, Ar-H), 7.35 (td, $J=1.1$, 7.5 Hz, 1H, Ar-H), 7.20 (td, $J=1.7$, 7.9 Hz, 1H, Ar-H), 5.41 (dd, $J=3.5$, 10.0 Hz, 1H, H-3), 5.35 (dd, $J=1.8$, 3.5 Hz, 1H, H-2), 5.31 (t, $J=9.9$ Hz, 1H, H-4), 4.98 (d, $J=1.6$ Hz, 1H, H-1), 4.83, 4.61 (A, B of AB, $J=12.7$ Hz, 2H, CH_2Ar), 4.29 (dd, $J=5.8$, 12.6 Hz, 1H, H-6a), 4.10–4.06 (m, 2H, H-6b, H-5), 2.17, 2.12, 2.04, 2.00 ppm (4 s, 12H, 4 OAc); $^{13}\text{C NMR}$ (125 MHz, CDCl_3): $\delta=170.64$, 170.02, 169.88, 169.72 (4 CO), 135.77, 132.69, 129.58, 129.49, 127.64, 122.96 (Ar-C), 97.33 (C-1), 69.48, 69.30, 69.10, 68.84 (C-2, C-3, C-5, CH_2Ar), 66.05 (C-4), 62.35 (C-6), 20.88, 20.76, 20.69 ppm (4C, 4COCH₃); ESI-MS: m/z : calcd for $\text{C}_{21}\text{H}_{25}\text{BrNaO}_{10}$ $[\text{M}+\text{Na}]^+$: 539.05, found: 539.14.

Methyl 3'-[(2,3,4,6-tetra-O-acetyl- α -D-mannopyranosyloxy)methyl]biphenyl-4-carboxylate (18a): Prepared according to general procedure B from **17a** (87.0 mg, 0.167 mmol), **11** (33.1 mg, 0.184 mmol), $\text{Pd}(\text{dppf})\text{Cl}_2\cdot\text{CH}_2\text{Cl}_2$ (4.1 mg, 5.0 μmol) and K_3PO_4 (53.2 mg, 0.251 mmol). Yield: 70 mg (73%) as colorless oil. $R_f=0.30$ (PE/EtOAc, 2:1); $[\alpha]_D^{20} + 41.2$ ($c=1.00$, EtOAc); $^1\text{H NMR}$ (500 MHz, CDCl_3): $\delta=8.13$ –8.11 (m, 2H, Ar-H), 7.68–7.67 (m, 2H, Ar-H), 7.60–7.58 (m, 2H, Ar-H), 7.48 (t, $J=4.7$ Hz, 1H, Ar-H), 7.39 (d, $J=7.7$ Hz, 1H, Ar-H), 5.41 (dd, $J=3.4$, 10.0 Hz, 1H, H-3), 5.33–5.30 (m, 2H, H-2, H-4), 4.94 (d, $J=1.5$ Hz, 1H, H-1), 4.79, 4.64 (A, B of AB, $J=12.0$ Hz, 2H, CH_2Ar), 4.30 (dd, $J=5.0$, 12.1 Hz, 1H, H-6a), 4.09–4.03 (m, 2H, H-6b, H-5), 3.94 (s, 3H, OMe), 2.15, 2.11, 2.04, 2.00 ppm (4 s, 12H, 4 OAc); $^{13}\text{C NMR}$ (125 MHz, CDCl_3): $\delta=170.64$, 170.03, 169.91, 169.73, 166.94 (5 CO), 145.11, 140.41, 136.97, 130.15, 129.27, 129.09, 127.94, 127.22, 127.11 (12C, Ar-C), 96.76 (C-1), 69.57, 69.09, 68.94, 66.12 (C-2, C-3, C-5, CH_2Ar), 62.40 (C-4), 60.38 (C-6), 52.15 (OMe), 20.89, 20.77, 20.69 ppm (4C, 4COCH₃); ESI-MS: m/z : calcd for $\text{C}_{29}\text{H}_{32}\text{NaO}_{12}$ $[\text{M}+\text{Na}]^+$: 595.18, found: 595.21.

Methyl 3'-[(2,3,4,6-tetra-O-acetyl- α -D-mannopyranosyloxy)methyl]-4'-chlorobiphenyl-4-carboxylate (18b): Prepared according to general procedure B from **17b** (143 mg, 0.260 mmol), **11** (51.5 mg, 0.286 mmol), $\text{Pd}(\text{dppf})\text{Cl}_2\cdot\text{CH}_2\text{Cl}_2$ (6.4 mg, 7.8 μmol) and K_3PO_4 (82.8 mg, 0.390 mmol). Yield: 133 mg (84%) as colorless oil. $R_f=0.30$ (PE/EtOAc, 2:1); $[\alpha]_D^{20} + 45.9$ ($c=1.20$, EtOAc); $^1\text{H NMR}$ (500 MHz, CDCl_3): $\delta=8.13$ –8.11 (m, 2H, Ar-H), 7.65–7.64 (m, 2H, Ar-H), 7.57 (t, $J=1.8$ Hz, 1H, Ar-H), 7.47 (s, 1H, Ar-H), 7.37 (s, 1H, Ar-H), 5.40 (dd, $J=3.4$, 10.1 Hz, 1H, H-3), 5.33–5.29 (m, 2H, H-2, H-4), 4.93 (d, $J=1.4$ Hz, 1H, H-1), 4.76, 4.61 (A, B of AB, $J=12.1$ Hz, 2H, CH_2Ar), 4.31 (dd, $J=5.2$, 12.3 Hz, 1H, H-6a), 4.11 (dd, $J=2.3$, 12.3 Hz, 1H, H-6b), 4.03 (ddd, $J=2.4$, 5.2, 9.9 Hz, 1H, H-5), 3.95 (s, 3H, OMe), 2.16, 2.12, 2.05, 2.00 ppm (4 s, 12H, 4OAc); $^{13}\text{C NMR}$

(125 MHz, CDCl_3): $\delta=170.61$, 170.02, 169.90, 169.72, 166.75 (5 CO), 143.68, 142.16, 138.79, 135.11, 130.26, 129.68, 127.14, 125.14 (12C, Ar-C), 96.85 (C-1), 68.99, 68.89, 68.85, 66.07 (C-2, C-3, C-5, CH_2Ar), 62.42 (C-4), 60.39 (C-6), 52.23 (OMe), 20.89, 20.78, 20.71, 20.69 ppm (4COCH₃); ESI-MS: m/z : calcd for $\text{C}_{29}\text{H}_{31}\text{ClNaO}_{12}$ $[\text{M}+\text{Na}]^+$: 629.14, found: 629.10.

Methyl 2'-[(2,3,4,6-tetra-O-acetyl- α -D-mannopyranosyloxy)methyl]biphenyl-4-carboxylate (21): Prepared according to general procedure B from **17c** (115 mg, 0.223 mmol), **11** (44.1 mg, 0.245 mmol), $\text{Pd}(\text{dppf})\text{Cl}_2\cdot\text{CH}_2\text{Cl}_2$ (5.5 mg, 6.7 μmol) and K_3PO_4 (71.0 mg, 0.335 mmol). Yield: 120 mg (94%) as colorless oil. $R_f=0.41$ (PE/EtOAc, 2:1); $[\alpha]_D^{20} + 38.3$ ($c=2.00$, EtOAc); $^1\text{H NMR}$ (500 MHz, CDCl_3): $\delta=8.11$ –8.10 (m, 2H, Ar-H), 7.51–7.48 (m, 1H, Ar-H), 7.45–7.41 (m, 4H, Ar-H), 7.29 (m, 1H, Ar-H), 5.27–5.21 (m, 2H, H-3, H-4), 5.19 (dd, $J=1.9$, 3.3 Hz, 1H, H-2), 4.77 (d, $J=1.4$ Hz, 1H, H-1), 4.67, 4.34 (A, B of AB, $J=11.3$ Hz, 2H, CH_2Ar), 4.13 (dd, $J=5.2$, 12.5 Hz, 1H, H-6a), 3.94 (s, 3H, OMe), 3.90 (dd, $J=2.2$, 12.3 Hz, 1H, H-6a), 3.52 (ddd, $J=2.2$, 5.1, 9.3 Hz, 1H, H-5), 2.13, 2.05, 2.04, 1.99 ppm (4 s, 12H, 4 OAc); $^{13}\text{C NMR}$ (125 MHz, CDCl_3): $\delta=170.52$, 169.95, 169.82, 169.74, 166.77 (5 CO), 145.48, 141.44, 133.46, 129.99, 129.91, 129.58, 129.22, 128.52, 128.21 (12C, Ar-C), 97.20 (C-1), 69.47 (C-2), 68.98 (C-3), 68.48 (C-5), 68.13 (CH_2Ar), 65.88 (C-4), 62.15 (C-6), 52.18 (OMe), 20.85, 20.66, 20.62 ppm (4C, 4COCH₃); ESI-MS: m/z : calcd for $\text{C}_{29}\text{H}_{32}\text{NaO}_{12}$ $[\text{M}+\text{Na}]^+$: 595.18, found: 595.21.

Methyl 3'-[(α -D-mannopyranosyloxy)methyl]biphenyl-4-carboxylate (19a): Prepared according to general procedure C from **18a** (24 mg, 0.042 mmol). Yield: 11 mg (65%). $R_f=0.40$ ($\text{CH}_2\text{Cl}_2/\text{MeOH}$, 8:1); $[\alpha]_D^{20} + 68.0$ ($c=0.34$, MeOH); $^1\text{H NMR}$ (500 MHz, CD_3OD): $\delta=8.11$ –8.09 (m, 2H, Ar-H), 7.77–7.75 (m, 2H, Ar-H), 7.70 (s, 1H, Ar-H), 7.63 (d, $J=7.6$ Hz, 1H, Ar-H), 7.49 (t, $J=7.6$ Hz, 1H, Ar-H), 7.45 (d, $J=7.6$ Hz, 1H, Ar-H), 4.90 (d, $J=1.8$ Hz, 1H, H-1), 4.86, 4.63 (A, B of AB, $J=12.0$ Hz, 2H, CH_2Ar), 3.94 (s, 3H, OMe), 3.89–3.87 (m, 2H, H-2, H-3), 3.79–3.73 (m, 2H, H-4, H-6a), 3.68–3.64 ppm (m, 2H, H-5, H-6b); $^{13}\text{C NMR}$ (125 MHz, CD_3OD): $\delta=168.42$ (CO), 146.91, 141.31, 139.97, 131.13, 130.20, 129.07, 128.17, 127.91, 127.67 (12C, Ar-C), 100.76 (C-1), 75.02 (C-5), 72.65 (C-3), 72.22 (C-2), 69.73 (CH_2Ar), 68.65 (C-4), 62.98 (C-6), 52.66 ppm (OMe); HRMS: m/z : calcd for $\text{C}_{21}\text{H}_{24}\text{NaO}_8$ $[\text{M}+\text{Na}]^+$: 427.1363, found: 427.1361.

Methyl 4'-chloro-3'-[(α -D-mannopyranosyloxy)methyl]biphenyl-4-carboxylate (19b): Prepared according to general procedure C from **18b** (40 mg, 0.066 mmol). Yield: 26 mg (90%). $R_f=0.19$ ($\text{CH}_2\text{Cl}_2/\text{MeOH}$, 8:1); $[\alpha]_D^{20} + 101.8$ ($c=0.50$, MeOH); $^1\text{H NMR}$ (500 MHz, CD_3OD): $\delta=8.06$ (d, $J=8.4$ Hz, 2H, Ar-H), 7.69 (d, $J=8.4$ Hz, 2H, Ar-H), 7.57–7.56 (m, 2H, Ar-H), 7.41 (s, 1H, Ar-H), 4.87 (s, 1H, H-1), 4.80, 4.58 (A, B of AB, $J=12.3$ Hz, 2H, CH_2Ar), 3.91 (s, 3H, OMe), 3.87–3.83 (m, 2H, H-2, H-3), 3.74–3.57 ppm (m, 4H, H-4, H-5, H-6); $^{13}\text{C NMR}$ (125 MHz, CD_3OD): $\delta=168.74$ (CO), 145.78, 143.68, 142.71, 136.55, 131.75, 131.31, 129.02, 128.77, 127.95, 126.63 (12C, Ar-C), 101.47 (C-1), 75.65 (C-5), 73.16 (C-3), 72.65 (C-2), 69.49 (CH_2Ar), 69.13 (C-4), 63.49 (C-6), 53.26 ppm (OMe); HRMS: m/z : calcd for $\text{C}_{21}\text{H}_{23}\text{ClNaO}_8$ $[\text{M}+\text{Na}]^+$: 461.0974, found: 461.0975.

Methyl 2'-[(α -D-mannopyranosyloxy)methyl]biphenyl-4-carboxylate (22): Prepared according to general procedure C from **21** (48 mg, 0.084 mmol). Yield: 16 mg (47%). $R_f=0.42$ ($\text{CH}_2\text{Cl}_2/\text{MeOH}$, 8:1); $[\alpha]_D^{20} + 61.9$ ($c=0.90$, MeOH); $^1\text{H NMR}$ (500 MHz, CD_3OD): $\delta=8.11$ –8.09 (m, 2H, Ar-H), 7.57 (m, 1H, Ar-H), 7.51–7.49 (m, 2H, Ar-H), 7.43–7.40 (m, 2H, Ar-H), 7.31 (m, 1H, Ar-H), 4.71 (A of AB, $J=11.4$ Hz, 1H, CH_2Ar), 4.70 (d, $J=1.5$ Hz, 1H, H-1), 4.38 (B of AB, $J=11.4$ Hz, 1H, CH_2Ar), 3.75–3.60 (m, 5H, H-2, H-3, H-4, H-6), 3.95 (s, 3H, OMe), 3.40 ppm (ddd, $J=3.0$, 5.6, 6.8 Hz, 1H, H-5); $^{13}\text{C NMR}$

(125 MHz, CD₃OD): δ = 168.42 (CO), 147.33, 142.66, 136.03, 130.83, 130.53, 130.47, 129.26, 129.15 (12C, Ar-C), 101.14 (C-1), 74.78 (C-5), 72.60 (C-3), 72.18 (C-2), 68.37 (2C, C-4, CH₂Ar), 62.71 ppm (C-6), 52.69 (OMe); HRMS: m/z : calcd for C₂₁H₂₄NaO₈Na [M+Na]⁺: 427.1363, found: 427.1367.

Sodium 3'-[(α -D-mannopyranosyloxy)methyl]biphenyl-4-carboxylate (6): Prepared according to general procedure D from **18a** (35 mg, 0.061 mmol). Yield: 24 mg (96%). [α]_D²⁰ +64.5 (c = 0.30, MeOH/H₂O 1:1); ¹H NMR (500 MHz, D₂O): δ = 7.80–7.78 (m, 2H, Ar-H), 7.50–7.43 (m, 4H, Ar-H), 7.31–7.24 (m, 2H, Ar-H), 4.82 (s, 1H, H-1), 4.58, 4.40 (A, B of AB, J = 11.5 Hz, 2H, CH₂Ar), 3.82 (m, 1H, H-2), 3.75–3.50 ppm (m, 5H, H-3, H-4, H-5, H-6); ¹³C NMR (125 MHz, D₂O): δ = 175.14 (CO), 142.69, 140.05, 137.34, 135.01, 129.46, 129.28, 127.92, 126.87, 126.64 (12C, Ar-C), 99.40 (C-1), 72.84 (C-5), 70.51 (C-3), 70.01 (C-2), 69.29 (CH₂Ar), 66.61 (C-4), 60.71 ppm (C-6); HRMS: m/z : calcd for C₂₀H₂₂NaO₈ [M+Na]⁺: 413.1207, found: 413.1211.

Sodium 4'-chloro-3'-[(α -D-mannopyranosyloxy)methyl]biphenyl-4-carboxylate (20): Prepared according to general procedure D from **18b** (54 mg, 0.089 mmol). Yield: 4 mg (10%). [α]_D²⁰ +44.7 (c = 0.30, MeOH); ¹H NMR (500 MHz, D₂O): δ = 7.86 (d, J = 7.8 Hz, 2H, Ar-H), 7.58–7.56 (m, 3H, Ar-H), 7.46, 7.34 (2 s, 2H, Ar-H), 4.90 (s, 1H, H-1), 4.58, 4.50 (A, B of AB, J = 12.3 Hz, 2H, CH₂Ar), 3.91 (s, 1H, H-2), 3.78–3.75 (m, 2H, H-3, H-4), 3.71–3.59 ppm (m, 3H, H-5, H-6); ¹³C NMR (125 MHz, D₂O): δ = 174.76 (CO), 141.82, 141.55, 139.40, 134.37, 129.56, 127.34, 126.74, 126.62, 125.15 (12C, Ar-C), 99.99 (C-1), 72.96 (C-5), 70.55 (C-3), 70.04 (C-2), 68.72 (CH₂Ar), 66.66 (C-4), 60.77 ppm (C-6); HRMS: m/z : calcd for C₂₀H₂₁ClNaO₈ [M+Na]⁺: 447.0817, found: 447.0816.

Sodium 2'-[(α -D-mannopyranosyloxy)methyl]biphenyl-4-carboxylate (23): Prepared according to general procedure D from **21** (78 mg, 0.137 mmol). Yield: 26 mg (46%). [α]_D²⁰ +53.2 (c = 0.40, MeOH); ¹H NMR (500 MHz, D₂O): δ = 7.91–7.89 (m, 2H, Ar-H), 7.43–7.34 (m, 5H, Ar-H), 7.26 (m, 1H, Ar-H), 4.68 (s, 1H, H-1), 4.57, 4.31 (A, B of AB, J = 10.8 Hz, 2H, CH₂Ar), 3.57 (m, 1H, H-2), 3.46–3.39 (m, 4H, H-3, H-4, H-6), 2.83 ppm (m, 1H, H-5); ¹³C NMR (125 MHz, D₂O): δ = 173.20 (CO), 144.48, 141.80, 133.47, 132.43, 130.69, 129.95, 129.27, 128.96, 128.32 (12C, Ar-C), 99.90 (C-1), 72.44 (C-5), 70.33 (C-3), 69.82 (C-2), 68.14 (CH₂Ar), 65.99 (C-4), 60.25 ppm (C-6); HRMS: m/z : calcd for C₂₀H₂₂NaO₈ [M+Na]⁺: 413.1207, found: 413.1208.

4-(4,4,5,5-Tetramethyl)-1,3,2-dioxaborolan-2-yl)phenyl 2,3,4,6-tetra-O-acetyl- α -D-mannopyranoside (27): A microwave tube was charged with **26**^[37] (240 mg, 0.55 mmol), KOAc (161 mg, 1.65 mmol), bis(pinacolato)diboron (152 mg, 0.60 mmol) and Pd(dppf)Cl₂·CH₂Cl₂ (13 mg, 0.017 mmol). The tube was closed, evacuated and flushed with argon. Then anhydrous DMF (1 mL) was added under a stream of argon. The mixture was degassed in an ultrasonic bath and flushed with argon for 5 min, and then heated by microwave irradiation at 120 °C for 2 h. The reaction mixture was cooled to RT and diluted with CH₂Cl₂/H₂O (100 mL, 1:1). The organic layer was washed with H₂O (50 mL) and brine (50 mL), dried over Na₂SO₄ and concentrated. The residue was purified by MPLC (toluene/EtOAc, 4:1) to afford **27** (120 mg, 50%) as colorless oil. [α]_D²⁰ +58.1 (c = 0.60, EtOAc); ¹H NMR (500 MHz, CDCl₃): δ = 7.76 (d, J = 8.6 Hz, 2H, Ar-H), 7.08 (d, J = 8.6 Hz, 2H, Ar-H), 5.58–5.55 (m, 2H, H-1, H-3), 5.45 (dd, J = 1.9, 3.4 Hz, 1H, H-2), 5.37 (t, J = 10.0 Hz, 1H, H-4), 4.28 (dd, J = 5.0, 12.0 Hz, 1H, H-6a), 4.05–4.02 (m, 2H, H-6b, H-5), 2.20, 2.05, 2.03 (3 s, 12H, 4 OAc), 1.33 ppm (s, 12H, 4 CH₃); ¹³C NMR (125 MHz, CDCl₃): δ = 170.55, 169.91, 169.74 (4C, 4 CO), 157.98, 136.62, 136.58, 115.67 (5C, Ar-C), 95.44 (C-1), 83.77 (Ar-C), 69.37 (C-2), 69.21 (C-5), 68.87 (C-3), 65.92 (C-4), 62.06 (C-6),

24.86, 24.58 (4C, 4 CH₃), 20.87, 20.69 ppm (4C, 4 COCH₃); ESI-MS: m/z : calcd for C₂₆H₃₅BNaO₁₂ [M+Na]⁺: 573.21, found: 573.32.

Methyl 2-[4'-(2,3,4,6-tetra-O-acetyl- α -D-mannopyranosyloxy)biphenyl-4-yl]acetate (29): Prepared according to general procedure B from methyl 2-(4-bromophenyl)acetate (**28**, 41.2 mg, 0.180 mmol), **27** (109 mg, 0.198 mmol), Pd(dppf)Cl₂·CH₂Cl₂ (4.4 mg, 5.4 μ mol) and K₃PO₄ (57.3 mg, 0.270 mmol). Yield: 35 mg (34%) as yellow oil. R_f = 0.25 (petrol ether/EtOAc 2:1); [α]_D²⁰ +75.09 (c = 0.8, EtOAc); ¹H NMR (500 MHz, CDCl₃): δ = 7.52–7.49 (m, 4H, Ar-H), 7.35–7.33 (m, 2H, Ar-H), 7.17–7.14 (m, 2H, Ar-H), 5.60–5.56 (m, 2H, H-1, H-3), 5.47 (dd, J = 1.8, 3.5 Hz, 1H, H-2), 5.38 (t, J = 10.0 Hz, 1H, H-4), 4.29 (dd, J = 5.0, 11.9 Hz, 1H, H-6a), 4.15–4.08 (m, 2H, H-6b, H-5), 3.71 (s, 3H, OMe), 3.66 (s, 2H, ArCH₂), 2.21, 2.06, 2.05, 2.03 ppm (4 s, 12H, 4 OAc); ¹³C NMR (125 MHz, CDCl₃): δ = 171.99, 170.53, 169.99, 169.95, 169.76 (5 CO), 155.09, 139.26, 135.72, 132.83, 129.73, 128.21, 127.03, 116.82 (12C, Ar-C), 95.87 (C-1), 69.43 (C-2), 69.23 (C-5), 68.91 (C-3), 65.99 (C-4), 62.15 (C-6), 52.11 (OMe), 40.78 (ArCH₂), 20.88, 20.71, 20.70, 20.67 ppm (4COCH₃); ESI-MS: m/z : calcd for C₂₉H₃₂NaO₁₂ [M+Na]⁺: 595.18, found: 595.21.

Methyl 2-[4'-(2,3,4,6-tetra-O-acetyl- α -D-mannopyranosyloxy)biphenyl-4-yl]cyclopropanecarboxylate (33): Prepared according to general procedure B from methyl 1-(4-bromophenyl)cyclopropanecarboxylate (**32**, 42.6 mg, 0.167 mmol), **27** (101 mg, 0.184 mmol), Pd(dppf)Cl₂·CH₂Cl₂ (4.1 mg, 5.0 μ mol) and K₃PO₄ (53.2 mg, 0.251 mmol). Yield: 60 mg (56%) as colorless oil. R_f = 0.31 (PE/EtOAc, 2:1); [α]_D²⁰ +70.2 (c = 1.00, EtOAc); ¹H NMR (500 MHz, CDCl₃): δ = 7.54–7.48 (m, 4H, Ar-H), 7.40–7.39 (m, 2H, Ar-H), 7.17–7.14 (m, 2H, Ar-H), 5.59 (dd, J = 3.55, 10.1 Hz, 1H, H-3), 5.56 (d, J = 1.6 Hz, 1H, H-1), 5.46 (dd, J = 1.9, 3.5 Hz, 1H, H-2), 5.38 (t, J = 10.0 Hz, 1H, H-4), 4.29 (dd, J = 5.1, 12.0 Hz, 1H, H-6a), 4.15–4.09 (m, 2H, H-6b, H-5), 3.65 (s, 3H, OMe), 2.21, 2.06, 2.05, 2.03 (4 s, 12H, 4 OAc), 1.64–1.62 (m, 2H, cPr), 1.27–1.16 ppm (m, 2H, cPr); ¹³C NMR (125 MHz, CDCl₃): δ = 175.04, 170.53, 169.98, 169.95, 169.75 (5 CO), 155.10, 139.25, 138.43, 135.76, 130.94, 128.24, 126.61, 116.80 (12C, Ar-C), 95.89 (C-1), 69.44 (C-5), 69.23 (C-2), 68.90 (C-3), 66.00 (C-4), 62.15 (C-6), 52.42 (OMe), 28.67 (cPr), 20.71, 20.68 (4C, 4COCH₃), 16.75 ppm (cPr); ESI-MS: m/z : calcd for C₃₁H₃₄NaO₁₂ [M+Na]⁺: 621.19, found: 621.26.

Methyl 2-[4'-(α -D-mannopyranosyloxy)biphenyl-4-yl]acetate (30): Prepared according to general procedure C from **29** (30 mg, 0.052 mmol). Yield: 20 mg (95%). R_f = 0.25 (CH₂Cl₂/MeOH, 8:1); [α]_D²⁰ +116.0 (c = 0.50, MeOH); ¹H NMR (500 MHz, CD₃OD): δ = 7.57–7.53 (m, 4H, Ar-H), 7.34–7.33 (m, 2H, Ar-H), 7.22–7.20 (m, 2H, Ar-H), 5.54 (d, J = 1.5 Hz, 1H, H-1), 4.05 (dd, J = 1.8, 3.3 Hz, 1H, H-2), 3.95 (dd, J = 3.4, 9.5 Hz, 1H, H-3), 3.82–3.74 (m, 3H, H-4, H-6), 3.71 (s, 3H, OMe), 3.66 (s, 2H, ArCH₂), 3.65 ppm (ddd, J = 2.5, 5.2, 9.7 Hz, 1H, H-5); ¹³C NMR (125 MHz, CD₃OD): δ = 174.02 (CO), 157.50, 140.77, 136.22, 134.29, 130.81, 129.00, 127.77, 118.13 (12C, Ar-C), 100.23 (C-1), 75.42 (C-5), 72.45 (C-3), 72.03 (C-2), 68.38 (C-4), 62.70 (C-6), 52.49 (OMe), 41.34 ppm (ArCH₂); HRMS: m/z : calcd for C₂₁H₂₄NaO₈ [M+Na]⁺: 427.1363, found: 427.1363.

Methyl 2-[4'-(α -D-mannopyranosyloxy)biphenyl-4-yl]cyclopropanecarboxylate (34): Prepared according to general procedure C from **33** (38 mg, 0.063 mmol). Yield: 9 mg (33%). R_f = 0.33 (CH₂Cl₂/MeOH, 8:1); [α]_D²⁰ +108.0 (c = 0.30, MeOH); ¹H NMR (500 MHz, CD₃OD): δ = 7.46–7.39 (m, 4H, Ar-H), 7.28–7.26 (m, 2H, Ar-H), 7.10–7.07 (m, 2H, Ar-H), 5.42 (d, J = 1.7 Hz, 1H, H-1), 3.93 (dd, J = 1.9, 3.4 Hz, 1H, H-2), 3.82 (dd, J = 3.4, 9.4 Hz, 1H, H-3), 3.69–3.61 (m, 3H, H-4, H-6), 3.53 (m, 4H, OMe, H-5), 1.49–1.47 (m, 2H, cPr), 1.14–1.11 ppm (m, 2H, cPr); ¹³C NMR (125 MHz, CD₃OD): δ = 157.50, 140.87, 139.51, 136.26, 132.03, 129.04, 127.43, 118.11 (12C, Ar-C),

FimH Antagonists

100.20 (C-1), 75.43 (C-5), 72.42 (C-3), 72.02 (C-2), 68.34 (C-4), 62.68 (C-6), 52.81 (OMe), 17.20 ppm (2C, cPr); HRMS: m/z : calcd for $C_{23}H_{26}NaO_8 [M+Na]^+$: 453.1520, found: 453.1523.

Sodium 2-[4'-(α -D-mannopyranosyloxy)biphenyl-4-yl]acetate (31): Prepared according to general procedure D from **29** (59 mg, 0.103 mmol). Yield: 17 mg (40%). $[\alpha]_D^{20} + 94.0$ ($c=0.20$, MeOH/H₂O 1:1); ¹H NMR (500 MHz, D₂O): $\delta=7.61$ (d, $J=8.6$ Hz, 2H, Ar-H), 7.55 (d, $J=8.0$ Hz, 2H, Ar-H), 7.31 (d, $J=8.0$ Hz, 2H, Ar-H), 7.19 (d, $J=8.6$ Hz, 2H, Ar-H), 5.60 (s, 1H, H-1), 4.13 (m, 1H, H-2), 4.00 (dd, $J=3.2$, 8.5 Hz, 1H, H-3), 3.75–3.67 (m, 4H, H-4, H-5, H-6), 3.51 ppm (s, 2H, ArCH₂); ¹³C NMR (125 MHz, D₂O): $\delta=154.94$, 137.93, 136.29, 135.08, 129.76, 128.07, 126.72, 117.49 (12C, Ar-C), 98.20 (C-1), 73.37 (C-5), 70.40 (C-3), 69.89 (C-2), 66.58 (C-4), 60.65 (C-6), 43.89 ppm (ArCH₂); HRMS: m/z : calcd for $C_{20}H_{22}NaO_8 [M+Na]^+$: 413.1207, found: 413.1208.

Sodium 2-[4'-(α -D-mannopyranosyloxy)biphenyl-4-yl]cyclopropa-necarboxylate (35): Prepared according to general procedure D from **33** (59 mg, 0.099 mmol). Yield: 10 mg (23%). $[\alpha]_D^{20} + 95.0$ ($c=0.20$, dioxane/H₂O 1:1); ¹H NMR (500 MHz, D₂O): $\delta=7.62$ –7.60 (m, 2H, Ar-H), 7.54–7.53 (m, 2H, Ar-H), 7.38–7.19 (m, 4H, Ar-H), 5.60 (s, 1H, H-1), 4.13 (m, 1H, H-2), 4.00 (m, 1H, H-3), 3.75–3.67 (4H, H-4, H-5, H-6), 1.33 (s, 2H, cPr), 1.01 ppm (s, 2H, cPr); ¹³C NMR (125 MHz, D₂O): $\delta=128.67$, 126.10, 124.37, 115.47 (12C, Ar-C), 96.18 (C-1), 71.35 (C-5), 68.38 (C-3), 67.87 (C-2), 64.56 (C-4), 58.62 (C-6), 12.66 ppm (2C, cPr); HRMS: m/z : calcd for $C_{22}H_{24}NaO_8 [M+Na]^+$: 439.1363, found: 439.1363.

Competitive binding assay

A recombinant protein consisting of the CRD of FimH linked with a thrombin cleavage site (Th) to a His₆-tag (FimH-CRD-Th-His₆) was expressed in *E. coli* strain HM125 and purified by affinity chromatography.^[16] To determine the affinity of the various FimH antagonists, a competitive binding assay described previously^[16] was applied. Microtiter plates (F96 MaxiSorp, Nunc) were coated with a 10 $\mu\text{g mL}^{-1}$ solution of FimH-CRD-Th-His₆ in 20 mM HEPES, 150 mM NaCl, and 1 mM CaCl₂, pH 7.4 (assay buffer), 100 μL per well, overnight at 4 °C. The coating solution was discarded, and the wells were blocked with 3% BSA in assay buffer (150 μL per well) for 2 h at 4 °C. After three washing steps with assay buffer (150 μL per well), a fourfold serial dilution of the test compound (50 μL per well) in assay buffer containing 5% DMSO and streptavidin-peroxidase coupled Man- α (1–3)[Man- α (1–6)]-Man- β (1–4)-GlcNAc- β (1–4)-GlcNAc β polyacrylamide (TM-PAA) polymer (50 μL per well of a 0.5 $\mu\text{g mL}^{-1}$ solution) were added. On each individual microtiter plate, *n*-heptyl α -D-mannopyranoside (**1**) was tested in parallel. The plates were incubated for 3 h at 25 °C and 350 rpm and then carefully washed four times with 150 μL per well assay buffer. After the addition of 100 μL per well of 2,2'-azino-di-(3-ethylbenzthiazoline-6-sulfonic acid) (ABTS) substrate, the colorimetric reaction was allowed to develop for 4 min and then was stopped by the addition of 2% aqueous oxalic acid before the optical density (OD) was measured at 415 nm on a microplate reader (Spectramax 190, Molecular Devices, CA, USA). The IC₅₀ values of the compounds tested in duplicate were calculated with Prism software (GraphPad Software Inc., La Jolla, CA, USA). The IC₅₀ defines the molar concentration of the test compound that decreases the maximal specific binding of TM-PAA polymer to FimH-CRD by 50%. The relative IC₅₀ (rIC₅₀) is the ratio of the IC₅₀ of the test compound to the IC₅₀ of *n*-heptyl α -D-mannopyranoside (**1**).

Cell-based flow cytometry assay

The assay was performed as described previously.^[17] Briefly, 5637 cells (DSMZ, Braunschweig, Germany) were grown to confluence in 24-well plates. Before infection, a serial dilution of test compound in 5% DMSO, PBS (Sigma–Aldrich) was prepared. GFP-labeled UT189 bacteria (200 μL) in RPMI 1640 medium (Invitrogen, Basel, Switzerland) were pre-incubated with test compound (25 μL) for 10 min at RT. The bacteria–antagonist mixtures were then added to the monolayers of 5637 cells. The multiplicity of infection (MOI) was 1:50 (cell/bacteria). To homogenize the infection, plates were centrifuged at RT for 3 min at 600 *g*. After an incubation time of 1.5 h at 37 °C, infected cells were washed four times with RPMI 1640 medium and suspended in ice-cold PBS for 5–20 min (treatment with ice-cold PBS results in the detachment of the infected cells). Cells were then kept in the dark until analysis. Samples were measured with a CyAn ADP flow cytometer (Beckman–Coulter, Brea, CA, USA) and analyzed by gating on the eukaryotic cells based on forward (FSC) and side scatter (SSC), which excludes unbound labeled bacteria and debris from analysis. A total of 10⁴ cells were measured per sample. Data were acquired in a linear mode for the SSC and logarithmic mode for FSC and the green fluorescent channel FL1-H (GFP). The mean fluorescence intensity (MFI) of GFP was counted as a surrogate marker for the adherence of bacteria. Quantification of adhesion was evaluated with the FlowJo software 9.0.1 (Tree Star Inc., Ashland, OR, USA). IC₅₀ values were determined by plotting the concentration of the antagonist in a logarithmic mode versus the MFI and by fitting the curve with Prism software (GraphPad, inhibition curve, variable slope), ($n=2-3$, in duplicate/triplicate).

Isothermal titration calorimetry (ITC)

For the ITC experiments, the His tag in FimH-CRD-Th-His₆ was cleaved.^[16] Briefly, the protein (1 mg) was incubated with 10 U thrombin (T-6884, Sigma–Aldrich) in 20 mM Tris-HCl, pH 8.4, 150 mM NaCl and 2.5 mM CaCl₂ (cleavage buffer) at 20 °C for 16 h. The mixture was then applied to a gel filtration column (Bio-Prep SE100/17, Bio-Rad) attached to an FPLC system. The chromatography was run with assay buffer and analyzed by SDS-PAGE. The fractions containing FimH-CRD were pooled and concentrated by ultrafiltration (MWCO10, Sartorius AG, Tagelswangen, Switzerland). The ITC experiments were performed using a VP-ITC instrument from MicroCal Inc. (GE Healthcare, Northampton, MA, USA). The measurements were performed at 25 °C. Prior to measurements, the protein was dialyzed in assay buffer (10 mM HEPES, 150 mM NaCl, 1 mM CaCl₂, pH 7.4 (HBS-Ca)). Injections of 3–5 μL ligand solutions (150 μM) were added at an interval of 10 min into the sample cell solution containing FimH-CRD (8–22 μM , sample cell volume 1.4523 mL) with stirring at 307 rpm. Protein concentration was determined by HPLC-UV against a BSA standard.^[38] The quantity $c = Mt(0) K_D^{-1}$, where $Mt(0)$ is the initial macromolecule concentration, is of importance in titration microcalorimetry. The c values ranged between 300 and 3200. Because the smallest reliable volumes were injected, sigmoidal curves were obtained. Control experiments injecting ligand solution into buffer without protein showed that the heat of dilution was small and constant. Baseline correction and peak integration were accomplished using Origin 7 as described by the manufacturer (OriginLab, Northampton, MA, USA). The first injection was always excluded from data analysis because it usually suffers from sample loss during the mounting of the syringe and the equilibration preceding the actual titration. A three-parameter (N (stoichiometry), K_D (dissociation constant) and ΔH° (change in enthalpy) nonlinear least-square data fitting was per-

formed in a Microsoft Excel spreadsheet using the Solver add-in (Frontline System)^[39,40] according to binding isotherms published by Ziegler and Seelig.^[41]

Thermodynamics parameters were calculated from Equation (4).

$$\Delta G = \Delta H - T\Delta S = RT \ln K_D = -RT \ln K_A \quad (4)$$

where ΔG , ΔH , and ΔS are the changes in free energy, enthalpy, and entropy of binding, respectively, T is the absolute temperature, and R is the universal gas constant ($8.314 \text{ J mol}^{-1} \text{ K}^{-1}$).

Determination of pharmacokinetic parameters

Materials: Dimethyl sulfoxide (DMSO), 1-octanol, Dulbecco's modified Eagle's medium (DMEM) high glucose, L-glutamine solution, penicillin-streptomycin solution, Dulbecco's phosphate-buffered saline (DPBS), and trypsin-EDTA solution were purchased from Sigma-Aldrich. MEM nonessential amino acid (MEM-NEAA) solution, fetal bovine serum (FBS), and DMEM without sodium pyruvate and phenol red were bought from Invitrogen. PAMPA System Solution, GIT-0 Lipid Solution, and Acceptor Sink Buffer were ordered from plon (Woburn, MA, USA). Acetonitrile (MeCN) was bought from Acros Organics. The Caco-2 cells were kindly provided by Prof. G. Imanidis, FHNW, Muttenz, Switzerland and originated from the American Type Culture Collection (Rockville, MD, USA).

Parallel artificial membrane permeation assay (PAMPA)

Values of $\log P_e$ were determined in a 96-well format with the PAMPA^[33] permeation assay. For each compound, measurements were performed at three pH values (5.0, 6.2, 7.4) in quadruplicate. For this purpose, 12 wells of a deep-well plate, i.e., four wells per pH value, were filled with 650 μL System Solution. Samples (150 μL) were withdrawn from each well to determine the blank spectra by UV spectroscopy (SpectraMax 190). Then, analyte dissolved in DMSO was added to the remaining System Solution to yield 50 μM solutions. To exclude precipitation, the optical density was measured at 650 nm, with 0.01 being the threshold value. Solutions exceeding this threshold were filtered. Afterward, samples (150 μL) were withdrawn to determine the reference spectra. Further 200 μL were transferred to each well of the donor plate of the PAMPA sandwich P/N 110 163 (plon, Woburn MA, USA). The filter membranes at the bottom of the acceptor plate were impregnated with 5 μL of GIT-0 Lipid Solution, and 200 μL of Acceptor Sink Buffer were filled into each acceptor well. The sandwich was assembled, placed in the GutBox, and left undisturbed for 16 h. It was then disassembled, and samples (150 μL) were transferred from each donor and acceptor well to UV plates. Quantification was performed by both UV spectroscopy and LC-MS; $\log P_e$ values were calculated with the aid of the PAMPA Explorer Software (plon, version 3.5).

Colorectal adenocarcinoma (Caco-2) cell permeation assay

Caco-2 cells were cultivated in tissue culture flasks (BD Biosciences, Franklin Lakes, NJ, USA) with DMEM high-glucose medium containing L-glutamine (2 mM), nonessential amino acids (0.1 mM), penicillin (100 U mL^{-1}), streptomycin (100 $\mu\text{g mL}^{-1}$), and FBS (10%). The cells were kept at 37 °C in humidified air containing 5% CO_2 , and the medium was changed every second day. When ~90% confluence was reached, the cells were split in a 1:10 ratio and distributed to new tissue culture flasks. At passage numbers between 60

and 65, they were seeded at a density of 5.3×10^5 cells per well to Transwell 6-well plates (Corning Inc., Corning, NY, USA) with 2.5 mL culture medium in the basolateral and 1.8 mL in the apical compartment. The medium was renewed on alternate days. Permeation experiments were performed between days 19 and 21 post-seeding. Prior to the experiment, the integrity of the Caco-2 monolayers was evaluated by measuring the transepithelial electrical resistance (TEER) with an Endohm tissue resistance instrument (World Precision Instruments Inc., Sarasota, FL, USA). Only wells with TEER values $> 300 \Omega \text{ cm}^2$ were used. Experiments were performed in the apical-to-basolateral (absorptive) and basolateral-to-apical (secretory) directions in triplicate. Transport medium (DMEM without sodium pyruvate and phenol red) was withdrawn from the donor compartments of three wells and replaced by the same volume of compound stock solutions to reach an initial sample concentration of 62.5 μM . The Transwell plate was then shaken (250 rpm) in the incubator. Samples (40 μL) were withdrawn after 15, 30, and 60 min from the donor and acceptor compartments, and their concentrations were determined by LC-MS. Apparent permeability coefficients (P_{app}) were calculated according to the equation

$$P_{app} = \frac{dQ}{dt} \times \frac{1}{A \times c_0} \quad (5)$$

where dQ/dt is the permeability rate, A the surface area of the monolayer, and c_0 the initial concentration in the donor compartment.^[42] After the experiment, TEER values were assessed again for each well and results from wells with values $< 300 \Omega \text{ cm}^2$ were discarded.

$\log D_{7,4}$ determination

The in silico prediction tool ALOGPS^[43] was used to estimate the $\log P$ values of the compounds. Depending on these values, the compounds were classified into three categories: hydrophilic compounds ($\log P < 0$), moderately lipophilic compounds ($0 \leq \log P \leq 1$) and lipophilic compounds ($\log P > 1$). For each category, two different ratios (volume of 1-octanol to volume of buffer) were defined as experimental parameters (Table 4).

Compound type	$\log P$	Ratio (1-octanol)/buffer
hydrophilic	< 0	30:140, 40:130
moderately lipophilic	0–1	70:110, 110:70
lipophilic	> 1	3:180, 4:180

Equal amounts of phosphate buffer (0.1 M, pH 7.4) and 1-octanol were mixed and shaken vigorously for 5 min to saturate the phases. The mixture was left until separation of the two phases occurred, and the buffer was retrieved. Stock solutions of the test compounds were diluted with buffer to a concentration of 1 μM . For each compound, six determinations, i.e., three determinations per 1-octanol/buffer ratio, were performed in different wells of a 96-well plate. The respective volumes of buffer containing analyte (1 μM) were pipetted to the wells and covered by saturated 1-octanol according to the chosen volume ratio. The plate was sealed with aluminum foil, shaken (1350 rpm, 25 °C, 2 h) on a Heidolph Titramax 1000 plate shaker (Heidolph Instruments GmbH & Co. KG, Schwabach, Germany) and centrifuged (2000 rpm, 25 °C,

FimH Antagonists

5 min, 5804 R Eppendorf centrifuge, Hamburg, Germany). The aqueous phase was transferred to a 96-well plate for analysis by LC-MS.

$\log D_{7.4}$ was calculated from the 1-octanol/buffer ratio (o/b), the initial concentration of the analyte in buffer ($1 \mu\text{M}$), and the concentration of the analyte in the aqueous phase (c_B) with equation:

$$\log D_{7.4} = \log \left(\frac{1 \mu\text{M} - c_B}{c_B} \times \frac{1}{o : b} \right) \quad (6)$$

Solubility

Solubility was determined in a 96-well format using the μSOL Explorer solubility analyzer (plon, version 3.4.0.5). For each compound, measurements were performed at three pH values (3.0, 5.0, 7.4) in triplicates. For this purpose, nine wells of a deep-well plate, that is, three wells per pH value, were filled with 300 μL of an aqueous universal buffer solution. Aliquots (3 μL) of a compound stock solution (10–50 mM in DMSO) were added and thoroughly mixed. The final sample concentration was 0.1–0.5 mM, the residual DMSO concentration was 1.0% (v/v) in the buffer solutions. After 15 h, the solutions were filtered (0.2 μm 96-well filter plates) using a vacuum to collect manifold (Whatman Ltd., Maidstone, UK) to remove any precipitates. Equal amounts of filtrate and *n*-propanol were mixed and transferred to a 96-well plate for UV detection (190–500 nm). The amount of material dissolved was calculated by comparison with UV spectra obtained from reference samples, which were prepared by dissolving compound stock solution in a 1:1 mixture of buffer and *n*-propanol (final concentrations 0.017–0.083 mM).

LC-MS measurements

Analyses were performed using an 1100/1200 Series HPLC System coupled to a 6410 Triple Quadrupole mass detector (Agilent Technologies, Inc., Santa Clara, CA, USA) equipped with electrospray ionization. The system was controlled with the Agilent MassHunter Workstation Data Acquisition software (version B.01.04). The column used was an Atlantis T3 C_{18} column (2.1 \times 50 mm) with a 3 μm particle size (Waters Corp., Milford, MA, USA). The mobile phase consisted of two eluents: solvent A (H_2O , containing 0.1% formic acid, v/v) and solvent B (MeCN, containing 0.1% formic acid, v/v), both delivered at 0.6 mL min^{-1} . The gradient was ramped from 95% A/5% B to 5% A/95% B over 1 min, and then held at 5% A/95% B for 0.1 min. The system was then brought back to 95% A/5% B, resulting in a total duration of 4 min. MS parameters such as fragmentor voltage, collision energy, and polarity were optimized individually for each analyte, and the molecular ion was followed for each compound in the multiple reaction monitoring mode. The concentrations of the analytes were quantified by the Agilent Mass Hunter Quantitative Analysis software (version B.01.04).

Abbreviations

Caco-2 cells, colorectal adenocarcinoma cells; CRD, carbohydrate recognition domain; D , distribution coefficient octanol/ H_2O ; GFP, green fluorescent protein; HPLC, high-performance liquid chromatography; IC_{50} , half-maximal inhibitory concentration; ITC, isothermal titration calorimetry; MFI, mean fluorescence intensity; PAMPA, parallel artificial membrane permeability assay; P_{app} , apparent per-

meability coefficient; P_e , effective permeation value; SAR, structure–activity relationship; SPR, structure–property relationship; UPEC, uropathogenic *E. coli*; UTI, urinary tract infection.

Acknowledgement

Financial support from the Swiss National Science Foundation (SNF interdisciplinary grant K-32K1-120904) is gratefully acknowledged.

Keywords: bacterial adhesin • FimH antagonists • flow cytometry • isothermal titration calorimetry • urinary tract infections

- [1] a) T. M. Hooton, W. E. Stamm, *Infect. Dis. Clin. North Am.* **1997**, *11*, 551–581; b) T. J. Wiles, R. R. Kulesus, M. A. Mulvey, *Exp. Mol. Pathol.* **2008**, *85*, 11–19; c) S. D. Fihn, *N. Engl. J. Med.* **2003**, *349*, 259–266.
- [2] C. Svanborg, G. Godaly, *Infect. Dis. Clin. North Am.* **1997**, *11*, 513–529.
- [3] a) J. D. Schilling, S. J. Hultgren, *Int. J. Antimicro. Ag.* **2002**, *19*, 457–460; b) M. G. Blango, M. A. Mulvey, *Antimicrob. Agents Chemother.* **2010**, *54*, 1855–1863.
- [4] G. Capitani, O. Eidam, R. Glockshuber, M. G. Grutter, *Microbes Infect.* **2006**, *8*, 2284–2290.
- [5] a) M. A. Mulvey, *Cell Microbiol.* **2002**, *4*, 257–271; b) S. G. Gouin, A. Wellens, J. Bouckaert, J. Kovensky, *ChemMedChem* **2009**, *4*, 749–755.
- [6] N. Sharon, *Biochim. Biophys. Acta.* **2006**, *1760*, 527–537.
- [7] a) N. Firon, I. Ofek, N. Sharon, *Biochem. Biophys. Res. Commun.* **1982**, *105*, 1426–1432; b) N. Firon, I. Ofek, N. Sharon, *Carbohydr. Res.* **1983**, *120*, 235–249; c) N. Sharon, *FEBS Lett.* **1987**, *217*, 145–157.
- [8] D. Choudhury, A. Thompson, V. Stojanoff, S. Langermann, J. Pinkner, S. J. Hultgren, S. D. Knight, *Science* **1999**, *285*, 1061–1066.
- [9] a) C. S. Hung, J. Bouckaert, D. Hung, J. Pinkner, C. Widberg, A. DeFusco, C. G. Auguste, R. Strouse, S. Langermann, G. Waksman, S. J. Hultgren, *Mol. Microbiol.* **2002**, *44*, 903–915; b) J. Bouckaert, J. Berglund, M. Schembri, E. D. Genst, L. Cools, M. Wuhler, C. S. Hung, J. Pinkner, R. Slättergard, A. Zavalov, D. Choudhury, S. Langermann, S. J. Hultgren, L. Wyns, P. Klemm, S. Oscarson, S. D. Knight, H. De Greve, *Mol. Microbiol.* **2005**, *55*, 441–455; c) A. Wellens, C. Garofalo, H. Nguyen, N. Van Gerven, R. Slättergard, J.-P. Hemalsteens, L. Wyns, S. Oscarson, H. De Greve, S. Hultgren, J. Bouckaert, *PLoS ONE* **2008**, *3*, e2040.
- [10] a) N. Firon, S. Ashkenazi, D. Mirelman, I. Ofek, N. Sharon, *Infect. Immun.* **1987**, *55*, 472–476; b) T. K. Lindhorst, S. Kötter, J. Kubisch, U. Krallmann-Wenzel, S. Ehlers, V. Kren, *Eur. J. Org. Chem.* **1998**, 1669–1674; c) O. Sperling, A. Fuchs, T. K. Lindhorst, *Org. Biomol. Chem.* **2006**, *4*, 3913–3922; d) Z. Han, J. S. Pinker, B. Ford, R. Obermann, W. Nolan, S. A. Wildman, D. Hobbs, T. Ellenberger, C. K. Cusumano, S. J. Hultgren, J. W. Janetka, *J. Med. Chem.* **2010**, *53*, 4779–4792; e) T. Klein, D. Abgottsson, M. Wittwer, S. Rabbani, J. Herold, X. Jiang, S. Kleeb, C. Lüthi, M. Scharenberg, J. Bezençon, E. Gubler, L. Pang, M. Smieško, B. Cutting, O. Schwardt, B. Ernst, *J. Med. Chem.* **2010**, *53*, 8627–8641; f) O. Schwardt, S. Rabbani, M. Hartmann, D. Abgottsson, M. Wittwer, S. Kleeb, A. Zalewski, M. Smieško, B. Cutting, B. Ernst, *Bioorg. Med. Chem.* **2011**, *19*, 6454–6473; g) C. K. Cusumano, J. S. Pinkner, Z. Han, S. E. Greene, B. A. Ford, J. R. Crowley, J. P. Henderson, J. W. Janetka, S. J. Hultgren, *Sci. Transl. Med.* **2011**, *3*, 109ra115; h) J. Berglund, J. Bouckaert, H. De Greve, S. Knight, *Anti-Adhesive Compounds to Prevent and Treat Bacterial Infections*, Intl. Pat. PCT/US 2005/089733, **2005**.
- [11] Glide, version 5.7, Schrödinger, LLC, New York, NY (USA), **2011**.
- [12] I. L. Scott, R. V. Market, R. J. DeOrazio, H. Meckler, T. P. Kogan, *Carbohydr. Res.* **1999**, *317*, 210–216.
- [13] C. A. Ocasio, T. S. Scanlan, *Bioorg. Med. Chem.* **2008**, *16*, 762–770.
- [14] M. Prieto, E. Zurita, E. Rosa, L. Muñoz, P. Lloyd-Williams, E. Giral, *J. Org. Chem.* **2004**, *69*, 6812–6820.
- [15] M. Ishikawa, Y. Hashimoto, *J. Med. Chem.* **2011**, *54*, 1539–1554.
- [16] S. Rabbani, X. Jiang, O. Schwardt, B. Ernst, *Anal. Biochem.* **2010**, *407*, 188–195.

- [17] M. Scharenberg, D. Abgottspon, E. Cicek, X. Jiang, O. Schwardt, S. Rabani, B. Ernst, *Assay Drug Dev. Technol.* **2011**, *9*, 455–464.
- [18] J. Bouckaert, J. Mackenzie, J. L. de Paz, B. Chipwaza, D. Choudhury, A. Zavialov, K. Mannerstedt, J. Anderson, D. Pierard, L. Wyns, P. H. Seeberger, S. Oscarson, H. De Greve, S. D. Knight, *Mol. Microbiol.* **2006**, *61*, 1556–1568.
- [19] G. Zhou, W. J. Mo, P. Sebbel, G. W. Min, T. A. Neubert, R. Glockshuber, *J. Cell Sci.* **2001**, *114*, 4095–4103.
- [20] P. Aprikian, V. Tchesnokova, B. Kidd, O. Yakovenko, V. Yarov-Yarovoy, E. Trinchina, V. Vogel, W. Thomas, E. Sokurenko, *J. Biol. Chem.* **2007**, *282*, 23437–23446.
- [21] I. Le Trong, P. Aprikian, B. A. Kidd, M. Forero-Shelton, V. Tchesnokova, P. Rajagopal, V. Rodriguez, G. Interlandi, R. Klevit, V. Vogel, R. E. Stenkamp, E. V. Sokurenko, W. E. Thomas, *Cell* **2010**, *141*, 645–655.
- [22] D. Abgottspon, G. Rölli, L. Hosch, A. Steinhuber, X. Jiang, O. Schwardt, B. Cutting, M. Smieško, U. Jenal, B. Ernst, A. Trampuz, *J. Microbiol. Methods* **2010**, *82*, 249–255.
- [23] a) J. E. Ladbury, *Biochem. Soc. Trans.* **2010**, *38*, 888–893; b) G. A. Holdgate, W. H. Ward, *Drug Discovery Today* **2005**, *10*, 1543–1550; c) R. Perozoz, G. Folkers, L. Scapozza, *J. Recept. Signal Transduction Res.* **2004**, *24*, 1–52; d) J. E. Ladbury, G. Klebe, E. Freire, *Nat. Rev. Drug Discovery* **2010**, *9*, 23–27; e) K. P. Murphy, D. Xie, K. S. Thompson, L. M. Amzel, E. Freire, *Proteins* **1994**, *18*, 63–67.
- [24] a) B. Baum, L. Muley, M. Smolinski, A. Heine, D. Hangauer, G. Klebe, *J. Mol. Biol.* **2010**, *397*, 1042–1054; b) M. C. Chervenak, E. J. Toone, *J. Am. Chem. Soc.* **1994**, *116*, 10533–10539; c) J. E. DeLorbe, J. H. Clements, M. G. Teresk, A. P. Benfield, H. R. Plake, L. E. Millsbaugh, S. F. Martin, *J. Am. Chem. Soc.* **2009**, *131*, 16758–16770.
- [25] S. Cabani, P. Gianni, V. Mollica, L. Lepori, *J. Solution Chem.* **1981**, *10*, 563–595.
- [26] A. V. Finkelstein, J. Janin, *Protein Eng.* **1989**, *3*, 1–3.
- [27] K. P. Murphy, *Biophys. Chem.* **1994**, *51*, 311–326.
- [28] E. Freire, *Drug Discovery Today* **2008**, *13*, 869–874.
- [29] a) T. S. G. Olsson, M. A. Williams, W. R. Pitt, J. E. Ladbury, *J. Mol. Biol.* **2008**, *384*, 1002–1017; b) C. Diehl, O. Engstrom, T. Delaine, M. Hakansson, S. Genheden, K. Modig, H. Leffler, U. Ryde, U. J. Nilsson, M. Akke, *J. Am. Chem. Soc.* **2010**, *132*, 14577–14589.
- [30] Phase, version 3.3, Schrödinger, LLC, New York, NY (USA), **2011**.
- [31] a) B. A. Williams, M. C. Chervenak, E. J. Toone, *J. Biol. Chem.* **1992**, *267*, 22907–22911; b) E. J. Toone, *Curr. Opin. Struct. Biol.* **1994**, *4*, 719–728; c) T. K. Dam, C. F. Brewer, *Chem. Rev.* **2002**, *102*, 387–429; d) M. Ambrosi, N. R. Cameron, B. G. Davis, *Org. Biomol. Chem.* **2005**, *3*, 1593–1608; e) E. Garcia-Hernandez, R. A. Zubillaga, E. A. Chavelas-Adame, E. Vazquez-Contreras, A. Rojo-Dominguez, M. Costas, *Protein Sci.* **2003**, *12*, 135–142.
- [32] H. Van de Waterbeemd, D. A. Smith, K. Beaumont, D. K. Walker, *J. Med. Chem.* **2001**, *44*, 1313–1333.
- [33] M. Kansy, F. Senner, K. Gubernator, *J. Med. Chem.* **1998**, *41*, 1007–1010.
- [34] A. Avdeef, S. Bendels, L. Di, B. Faller, M. Kansy, K. Sugano, Y. Yamauchi, *J. Pharm. Sci.* **2007**, *96*, 2893–2909.
- [35] C. A. Lipinski, *J. Pharmacol. Toxicol. Methods* **2000**, *44*, 235–249.
- [36] J. Kasuga, M. Ishikawa, M. Yonehara, M. Makishima, Y. Hashimoto, H. Miyachi, *Bioorg. Med. Chem.* **2010**, *18*, 7164–7173.
- [37] R. Roy, S. K. Das, F. Santoyo-González, F. Hernández-Mateo, T. K. Dam, C. F. Brewer, *Chem. Eur. J.* **2000**, *6*, 1757–1762.
- [38] a) F. Bitsch, R. Aichholz, J. Kallen, S. Geisse, B. Fournier, J. M. Schlaeppi, *Anal. Biochem.* **2003**, *323*, 139–149; b) S. Mesch, K. Lemme, H. Koliwer-Brandl, D. S. Strasser, O. Schwardt, S. Kelm, B. Ernst, *Carbohydr. Res.* **2010**, *345*, 1348–1359.
- [39] G. Kemmer, S. Keller, *Nat. Protoc.* **2010**, *5*, 267–281.
- [40] O. O. Krylova, N. Jahnke, S. Keller, *Biophys. Chem.* **2010**, *150*, 105–111.
- [41] A. Ziegler, J. Seelig, *Biophys. J.* **2004**, *86*, 254–263.
- [42] P. Artursson, J. Karlsson, *Biochem. Biophys. Res. Commun.* **1991**, *175*, 880–885.
- [43] a) VCCLAB, Virtual Computational Chemistry Laboratory, 2005, <http://www.vcclab.org> (accessed May 3, 2012); b) I. V. Tetko, J. Gasteiger, R. Todeschini, A. Mauri, D. Livingstone, P. Ertl, V. A. Palyulin, E. V. Radchenko, N. S. Zefirov, A. S. Makarenko, V. Y. Tanchuk, V. V. Prokopenko, *J. Comput. Aid. Mol. Des.* **2005**, *19*, 453–463.

Received: March 6, 2012

Revised: April 27, 2012

Published online on May 29, 2012



Supporting Information

© Copyright Wiley-VCH Verlag GmbH & Co. KGaA, 69451 Weinheim, 2012

FimH Antagonists: Structure–Activity and Structure–Property Relationships for Biphenyl α -D-Mannopyranosides

Lijuan Pang, Simon Kleeb, Katrin Lemme, Said Rabbani, Meike Scharenberg, Adam Zalewski, Florentina Schädler, Oliver Schwardt, and Beat Ernst*^[a]

cmdc_201200125_sm_miscellaneous_information.pdf

Supporting Information

Contents

HPLC data for the target compounds	S2
HPLC traces for the target compounds	S3
NMR spectra for the synthetic compounds	S13

HPLC data for the target compounds:

System: Beckman Coulter Gold, consisting of pump 126, DAD 168 (190-400 nm) and auto-sampler 508. Column: Waters Atlantis T3, 3 μ m, 2.1 \times 100 mm. A: H₂O + 0.1% TFA; B: MeCN + 0.1% TFA.

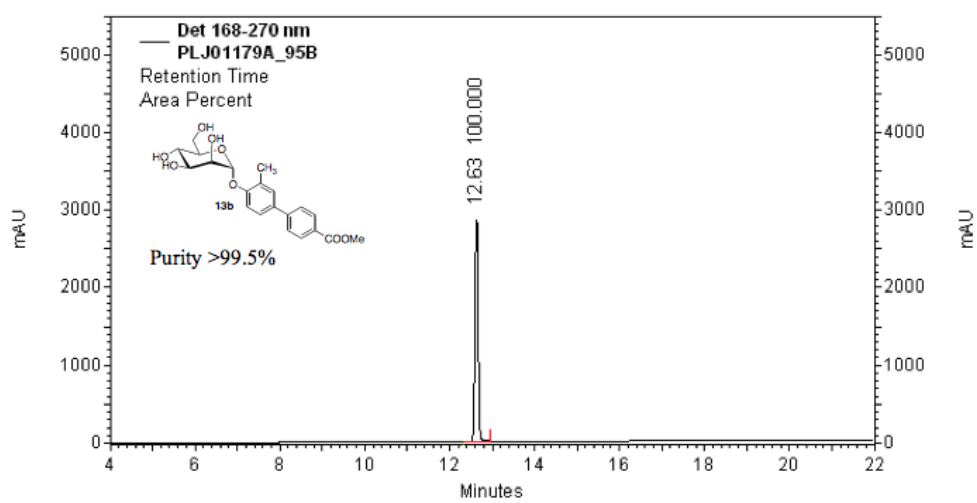
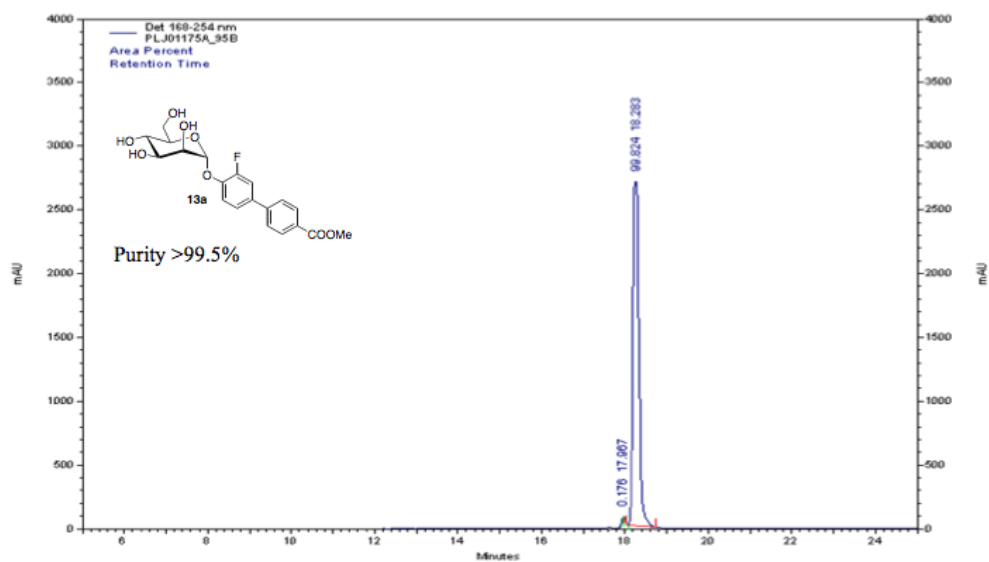
Gradient A: 0% B \rightarrow 95% B (20 min); 95% B (2 min); 95% B \rightarrow 5% B (3 min); 5% B \rightarrow 0% B (2 min); flow rate: 0.5 mL/min.

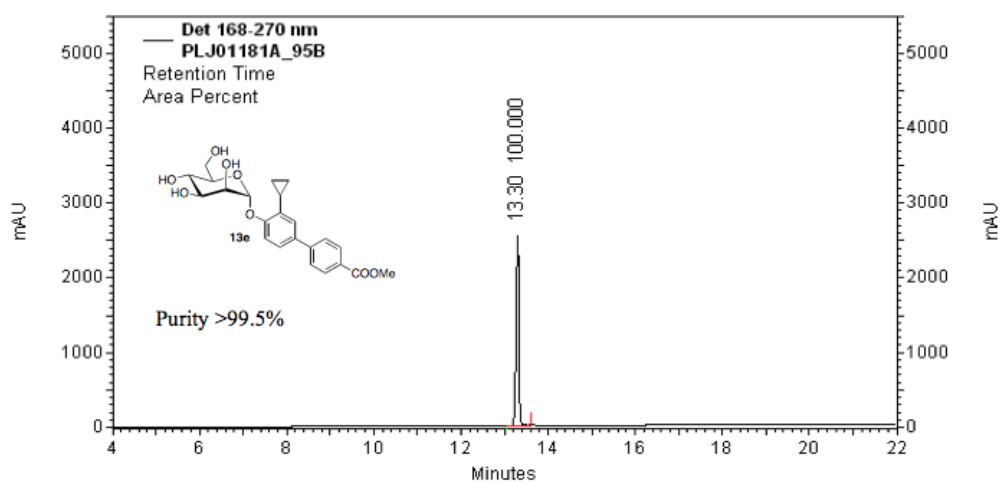
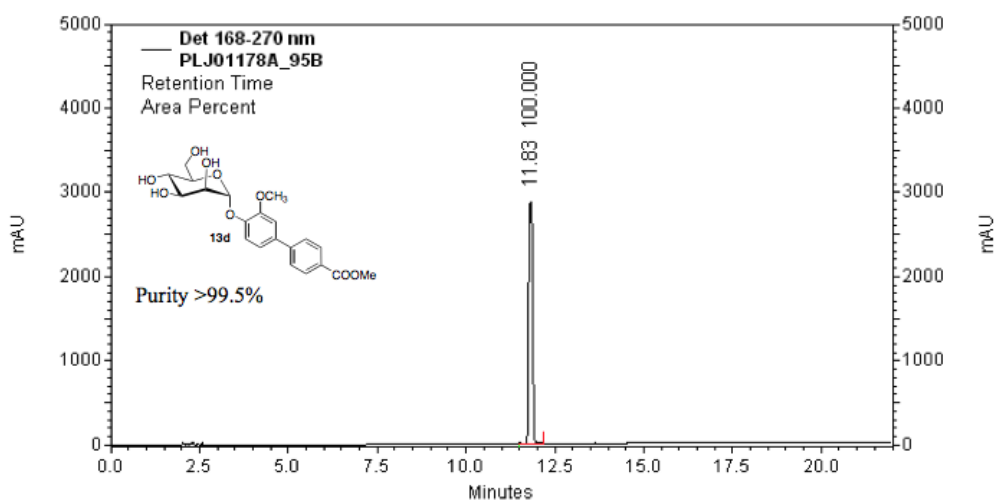
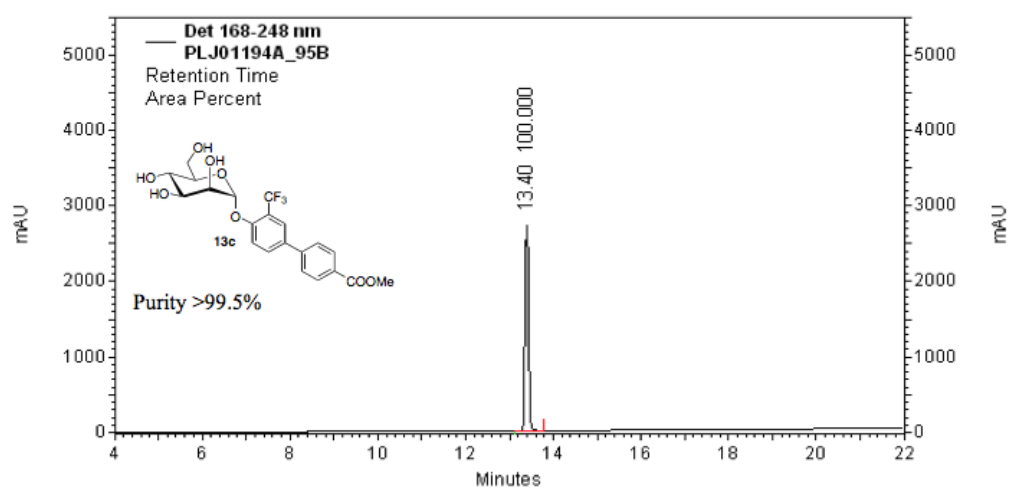
Gradient B: 0% B \rightarrow 5% B (1 min); 5% B \rightarrow 70% B (15 min); 70% B (4min); 70% B \rightarrow 5% B (5 min); 5% B (1min); 5% B \rightarrow 0% B (2 min); flow rate: 0.5 mL/min.

Table S1. HPLC data for the target compounds.

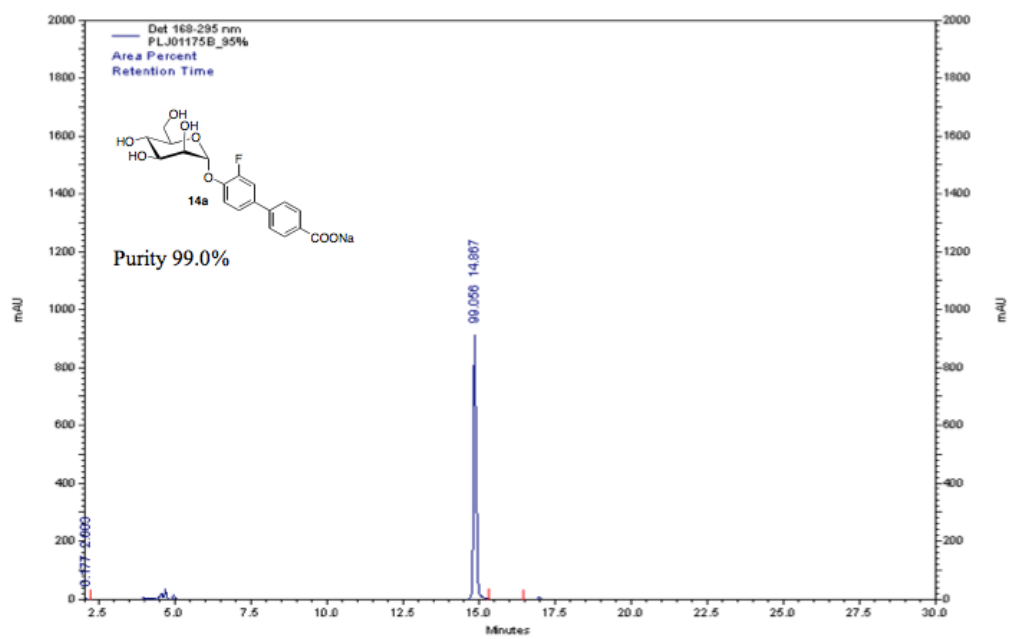
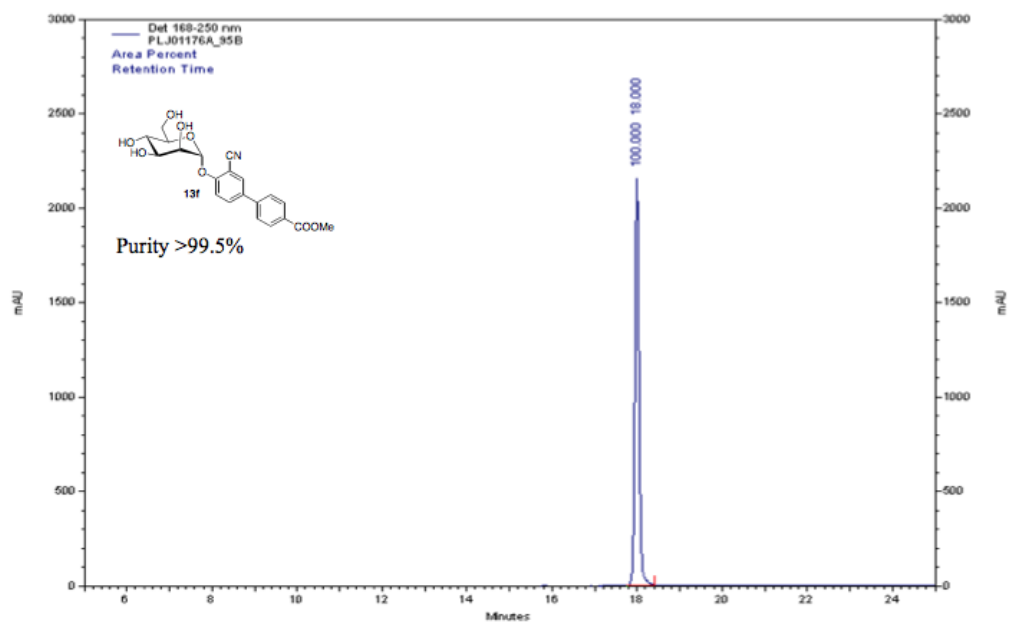
Compound	Formula	Gradient	Retention [min]	Detection	Purity [%]
13a	C ₂₀ H ₂₁ FO ₈	A	18.28	254 nm	99.8
13b	C ₂₁ H ₂₄ O ₈	A	12.63	270 nm	100
13c	C ₂₁ H ₂₁ F ₃ O ₈	A	17.10	250 nm	99.4
13d	C ₂₁ H ₂₄ O ₉	A	11.83	270 nm	100
13e	C ₂₃ H ₂₆ O ₈	A	13.30	270 nm	100
13f	C ₂₁ H ₂₁ NO ₈	A	18.00	250 nm	100
14a	C ₁₉ H ₁₈ FNaO ₈	A	14.87	295 nm	99.0
14b	C ₂₀ H ₂₁ NaO ₈	B	16.37	250 nm	99.9
14c	C ₂₀ H ₁₈ F ₃ NaO ₈	A	17.10	250 nm	99.9
14d	C ₂₀ H ₂₁ NaO ₉	B	15.57	250 nm	100
14e	C ₂₂ H ₂₃ NaO ₈	A	15.70	250 nm	99.9
14f	C ₂₀ H ₁₈ NNaO ₈	B	15.83	256 nm	98.4
19a	C ₂₁ H ₂₄ O ₈	A	16.73	254 nm	97.9
19b	C ₂₁ H ₂₃ ClO ₈	A	13.30	270 nm	97.6
6	C ₂₀ H ₂₁ NaO ₈	A	15.03	254 nm	98.6
20	C ₂₁ H ₂₃ ClO ₈	A	11.53	270 nm	95.1
22	C ₂₁ H ₂₄ O ₈	A	16.65	290 nm	96.8
23	C ₂₀ H ₂₁ NaO ₈	A	15.22	254 nm	98.7
30	C ₂₁ H ₂₄ O ₈	A	11.82	246 nm	96.6
31	C ₂₀ H ₂₁ NaO ₈	A	10.12	265 nm	98.7
34	C ₂₃ H ₂₆ O ₈	A	12.87	270 nm	99.5
35	C ₂₂ H ₂₃ NaO ₈	A	11.17	265 nm	95.5

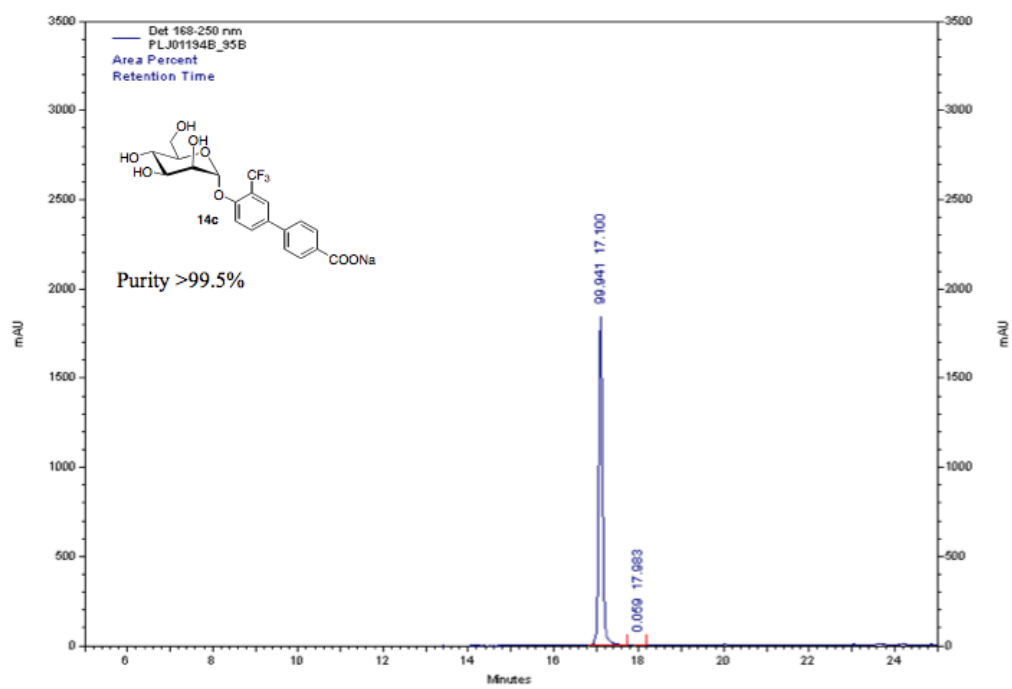
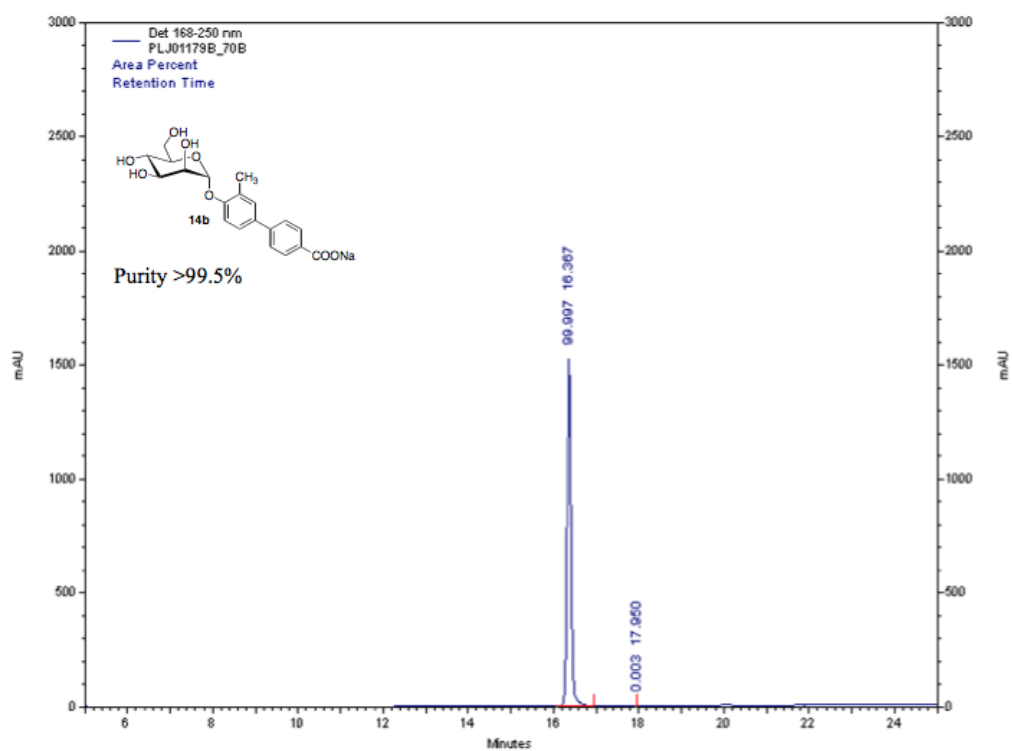
HPLC traces for the target compounds:

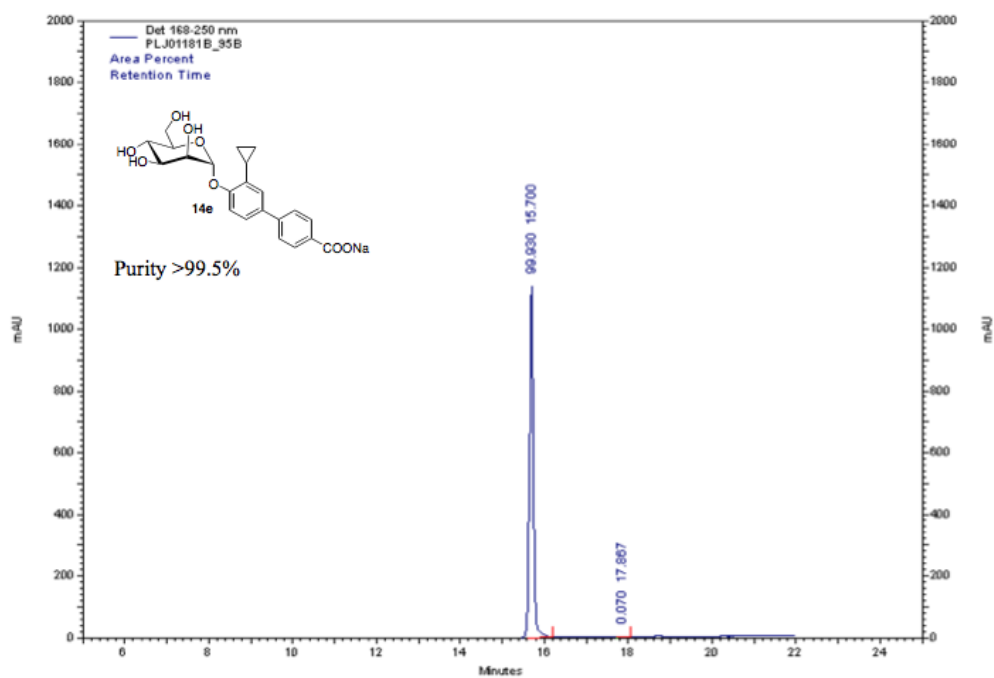
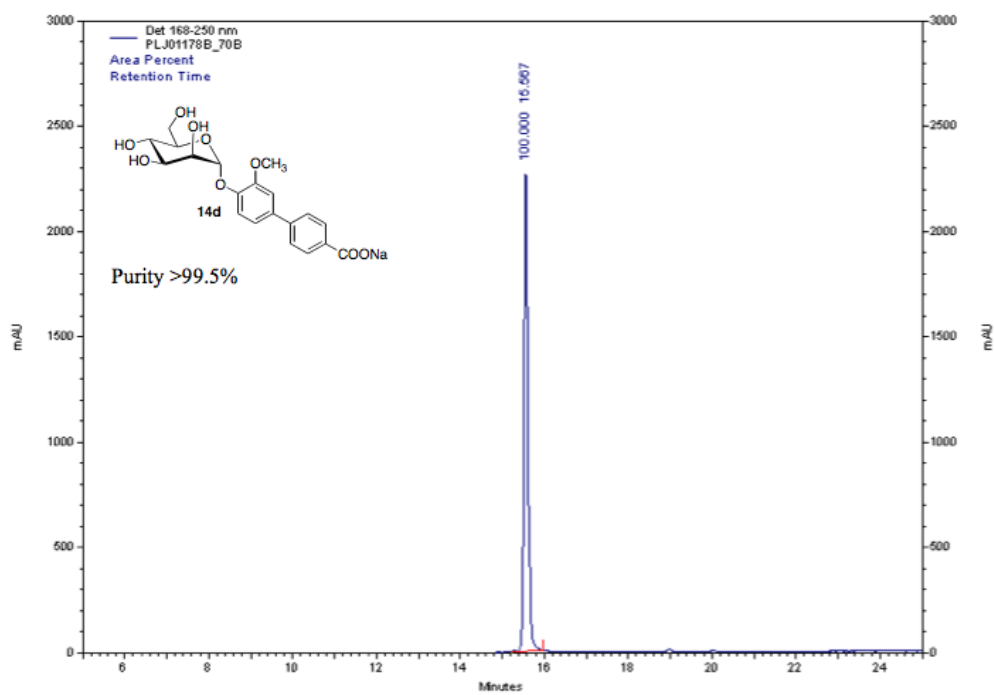




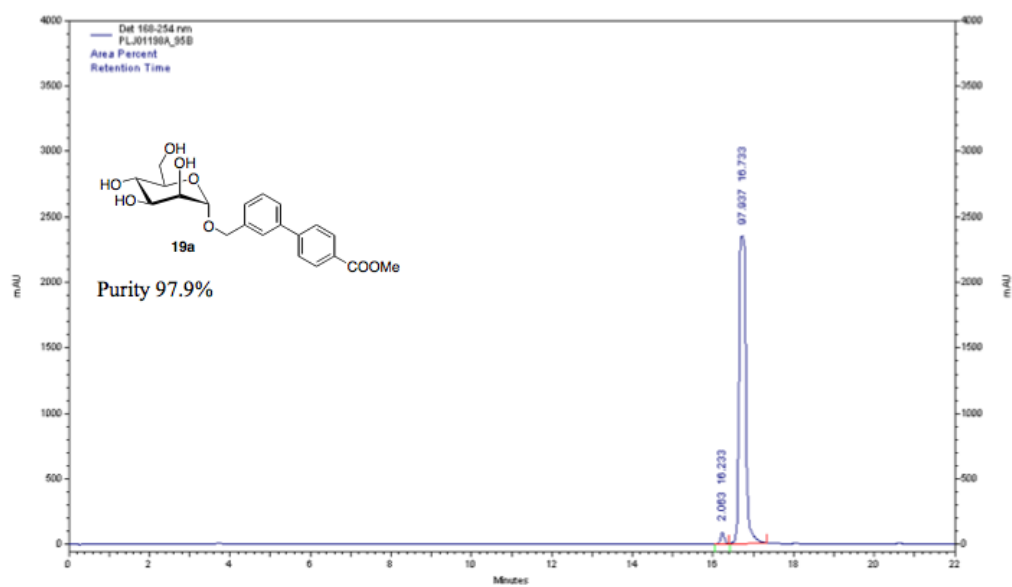
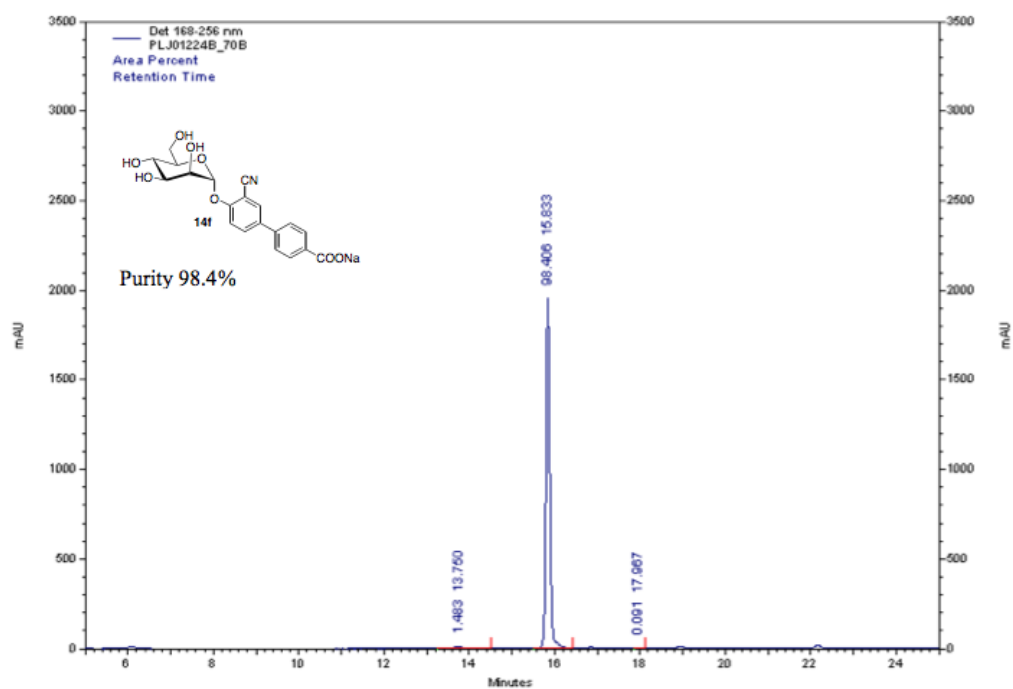
S4

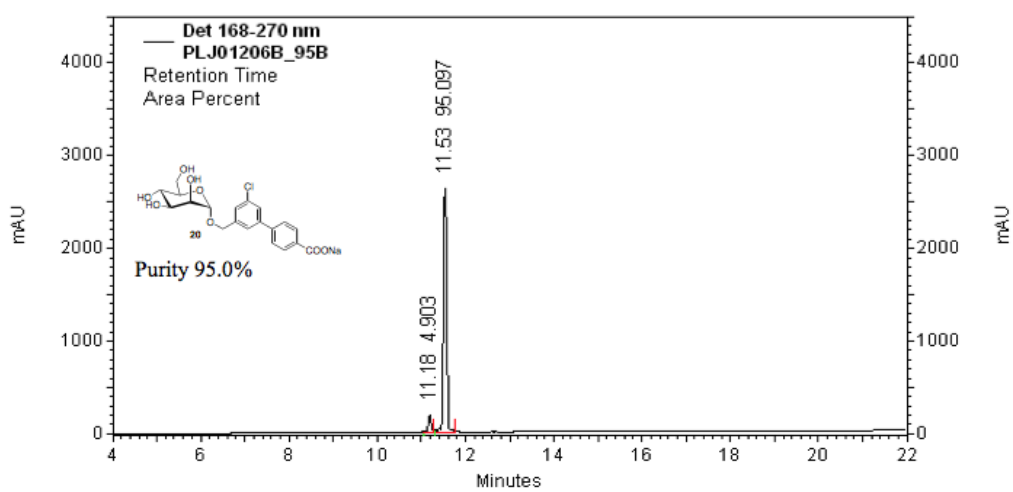
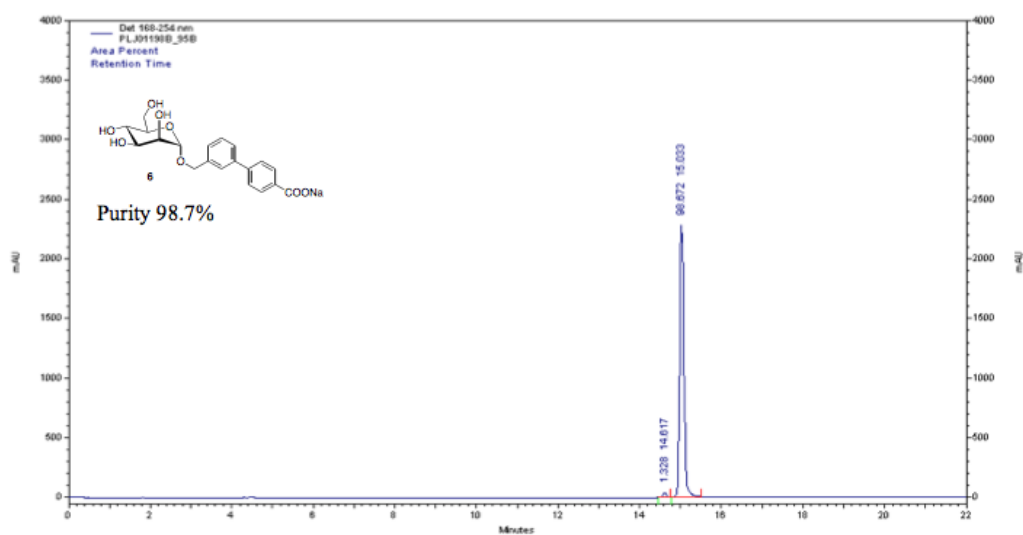
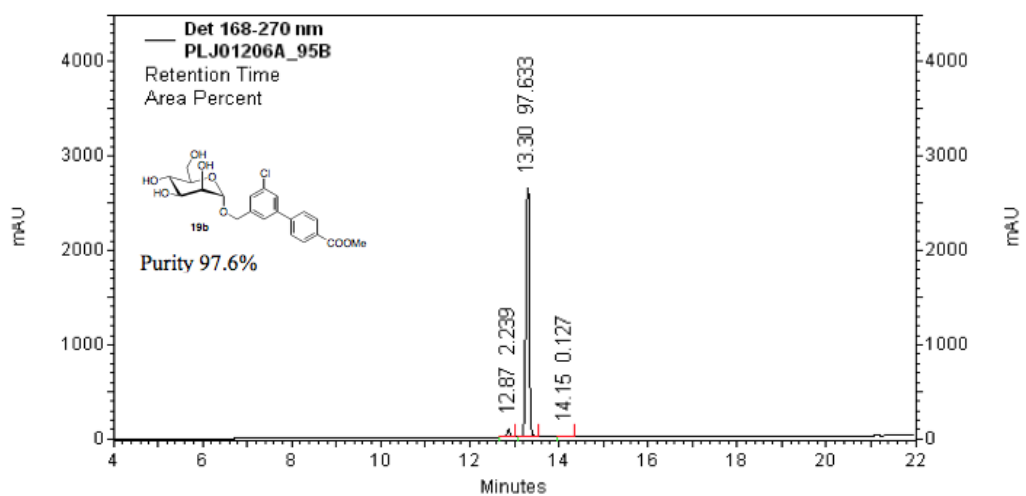


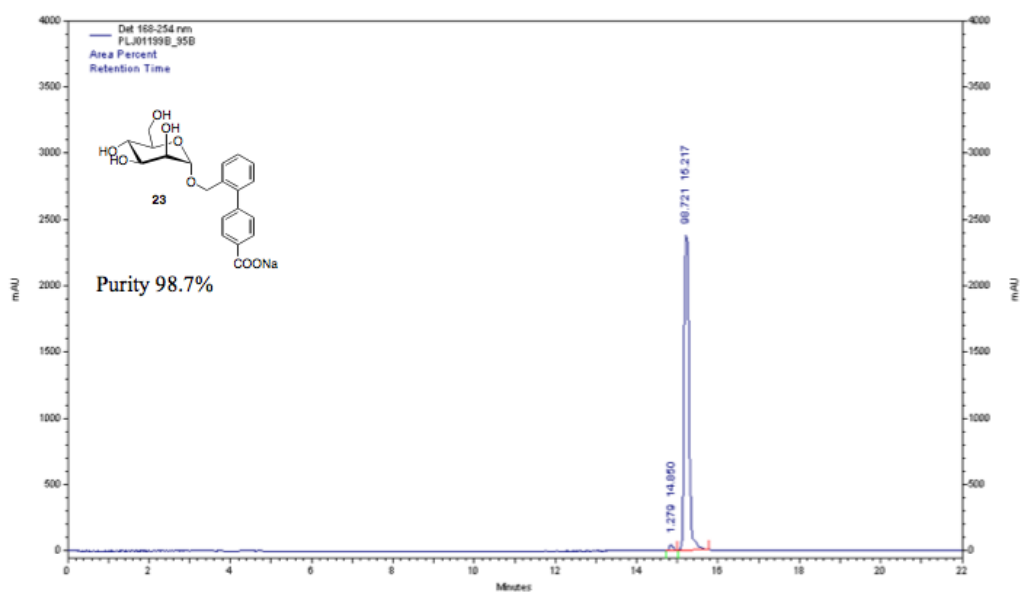
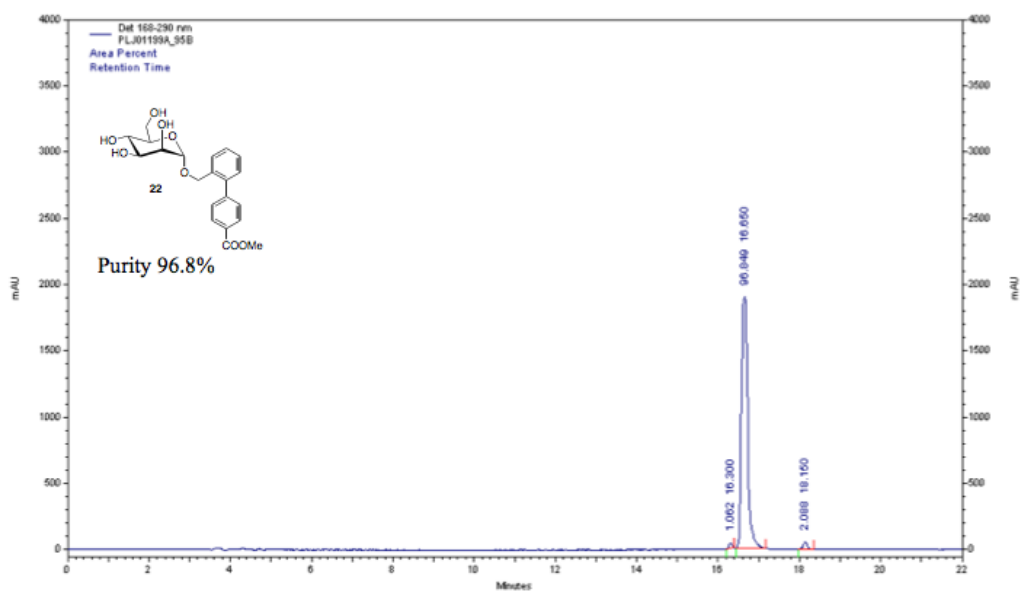


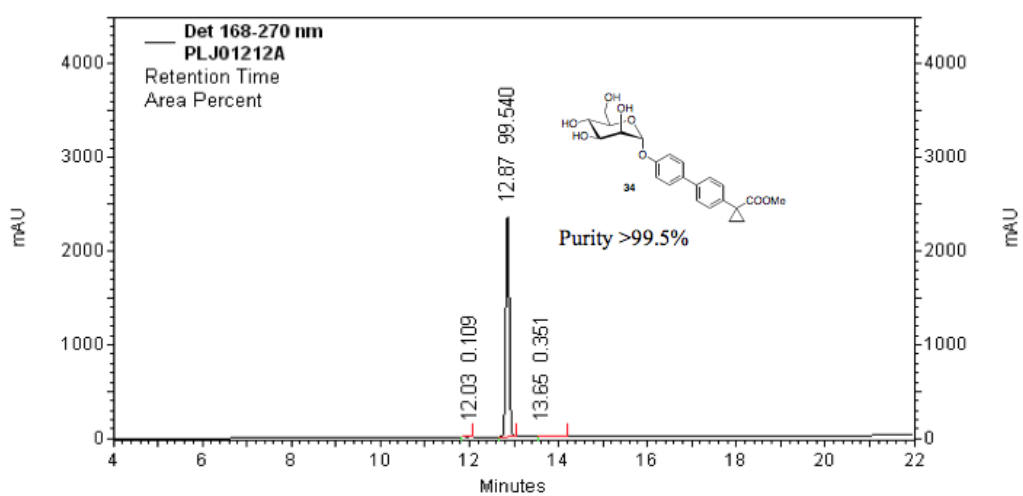
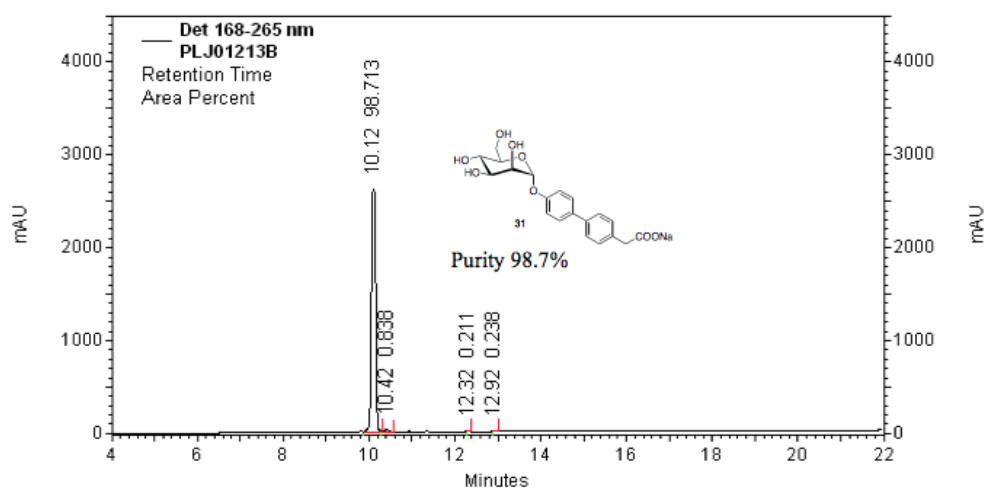
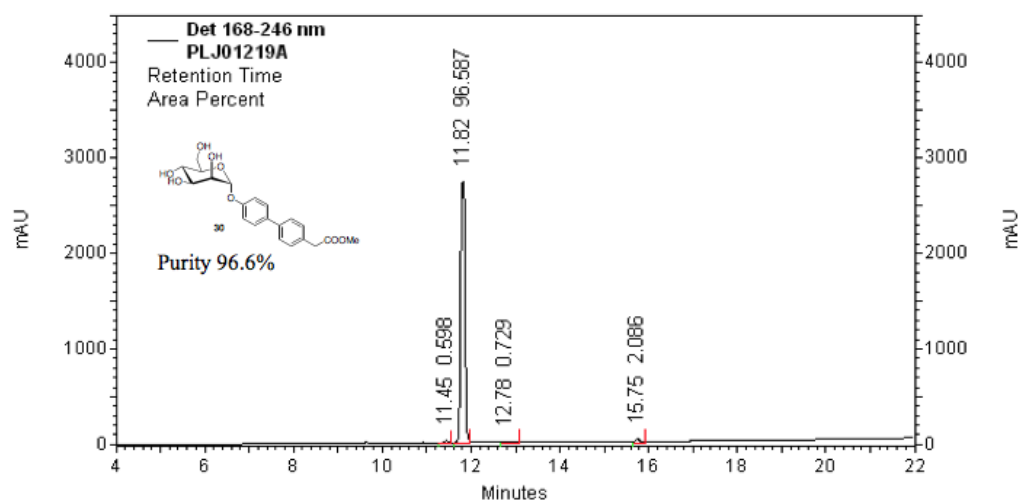


S7

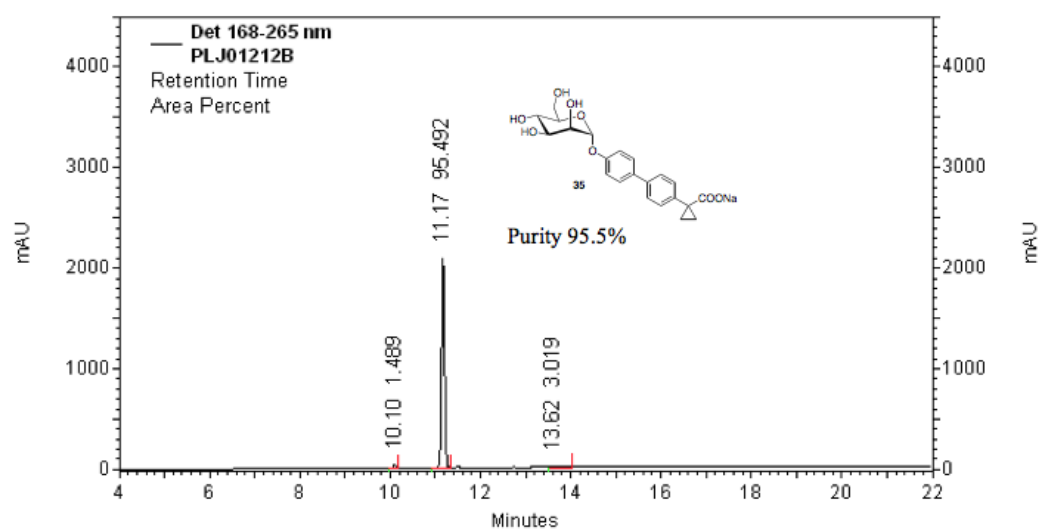


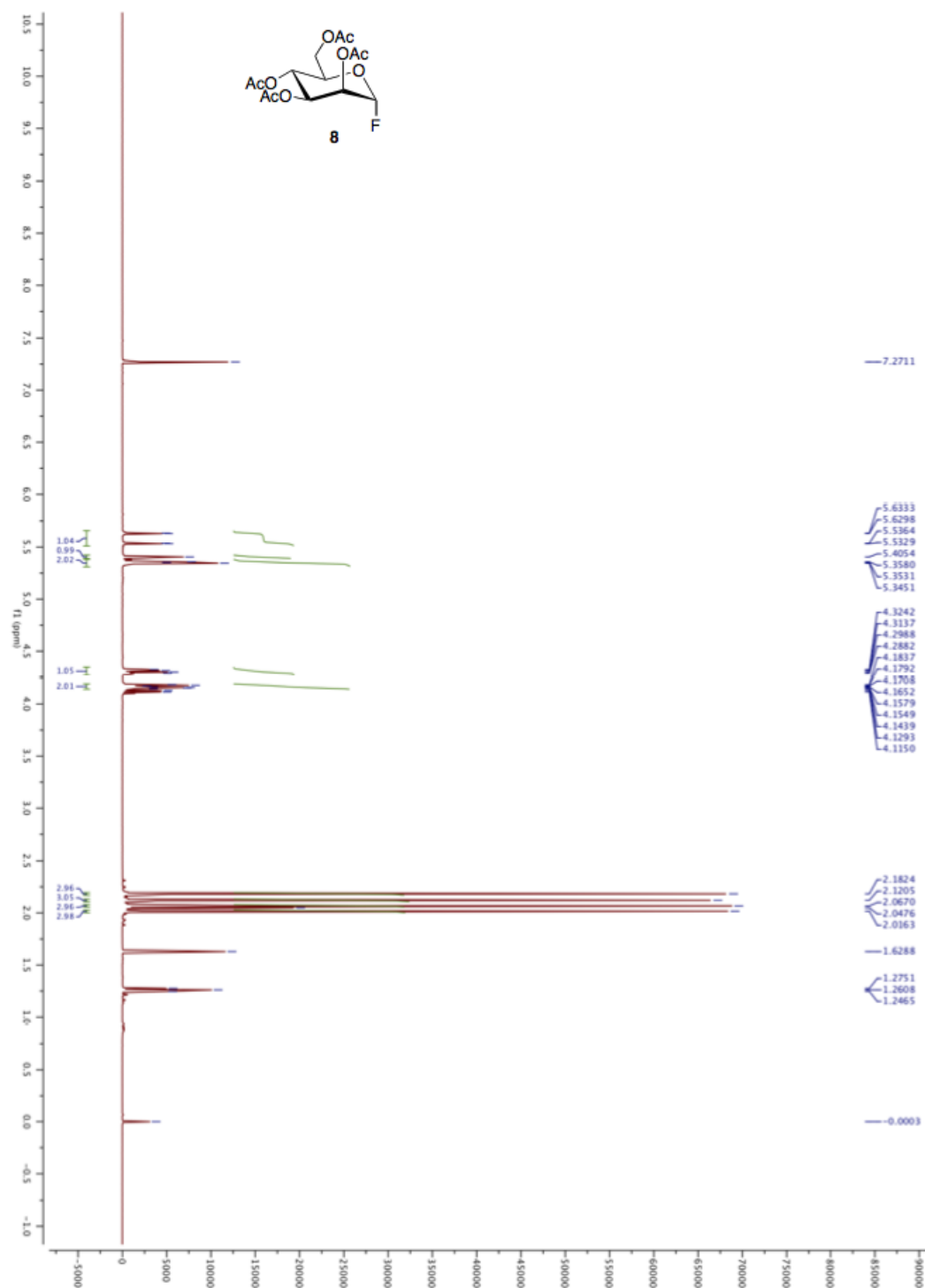


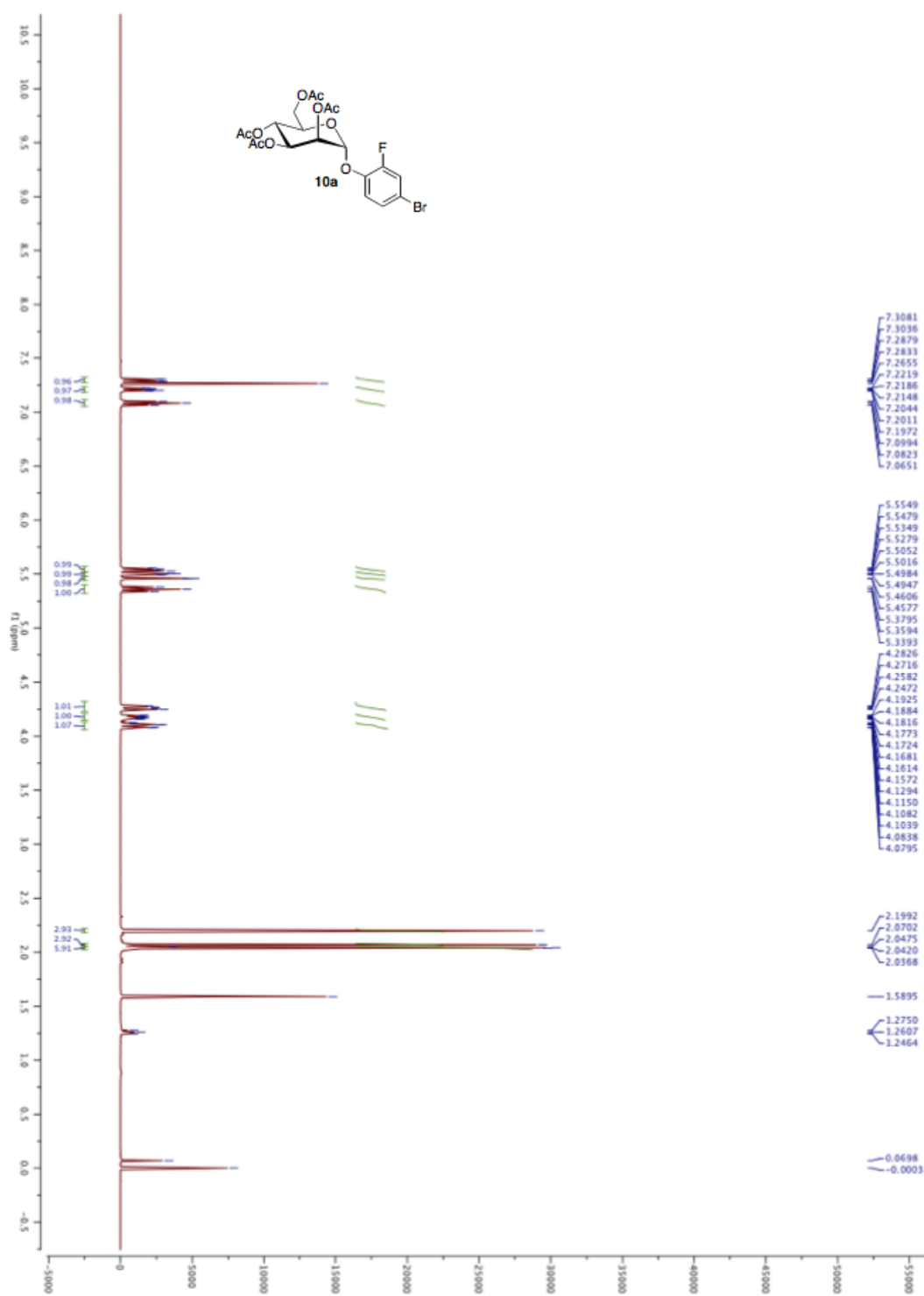


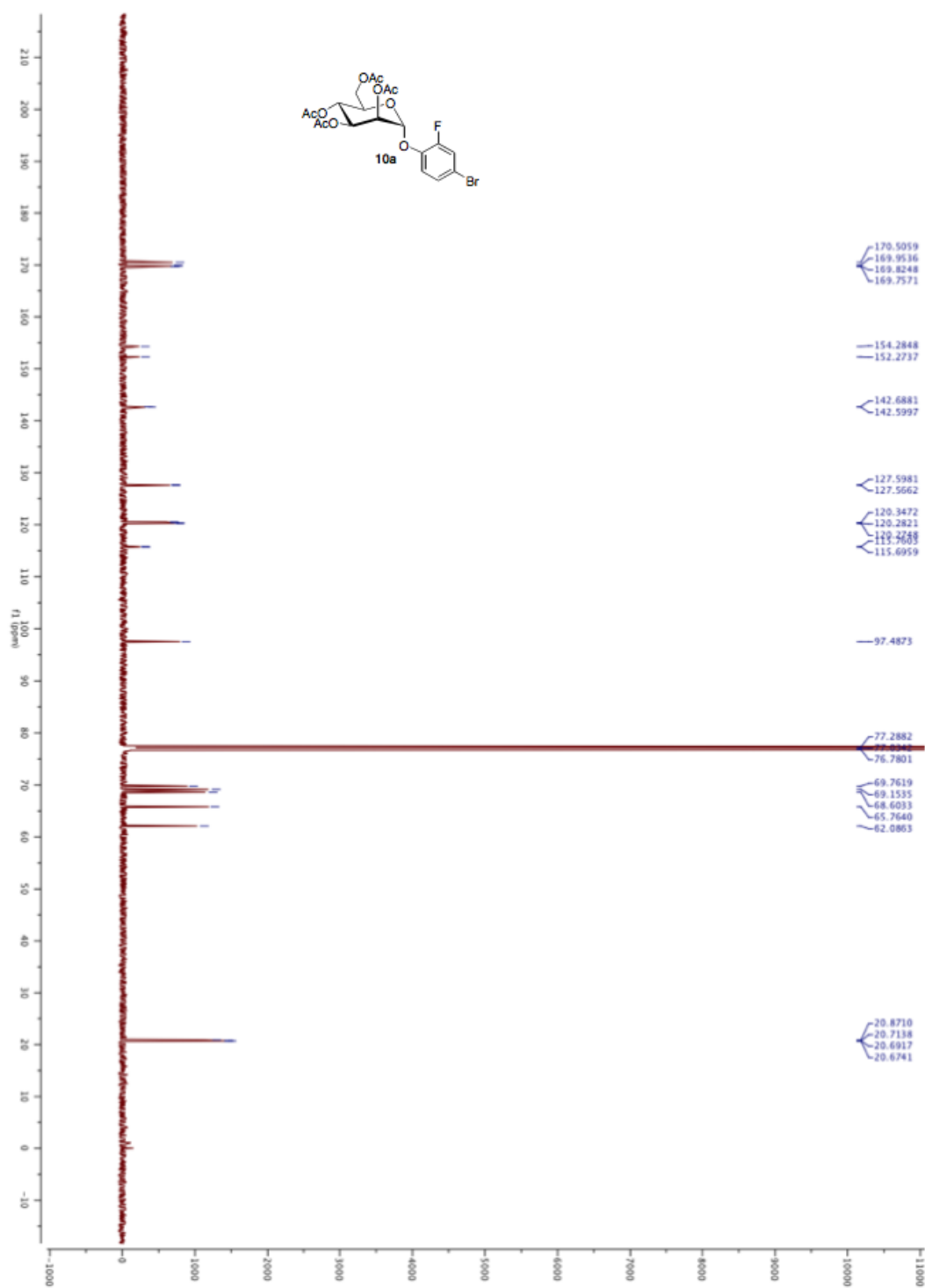


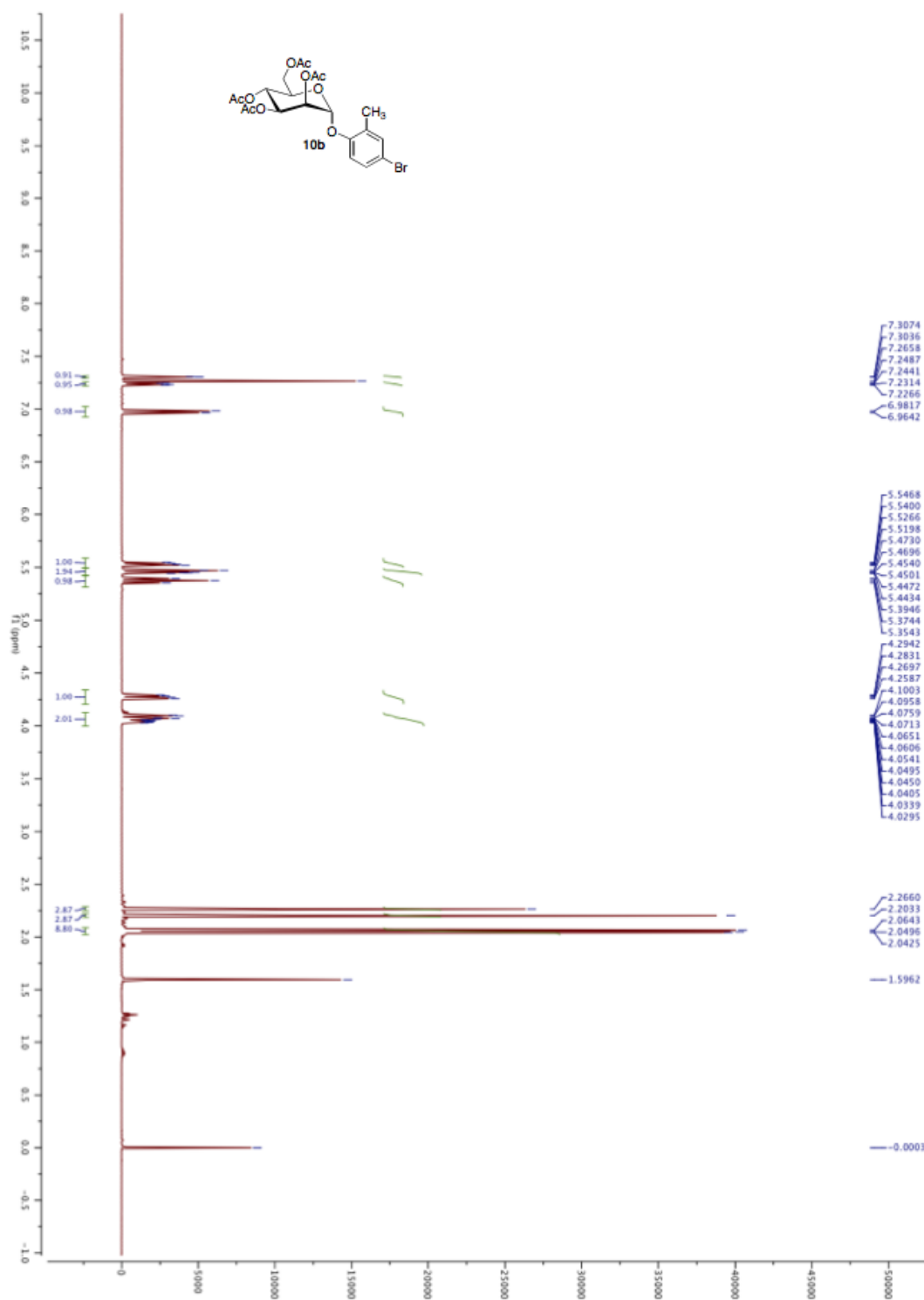
S11

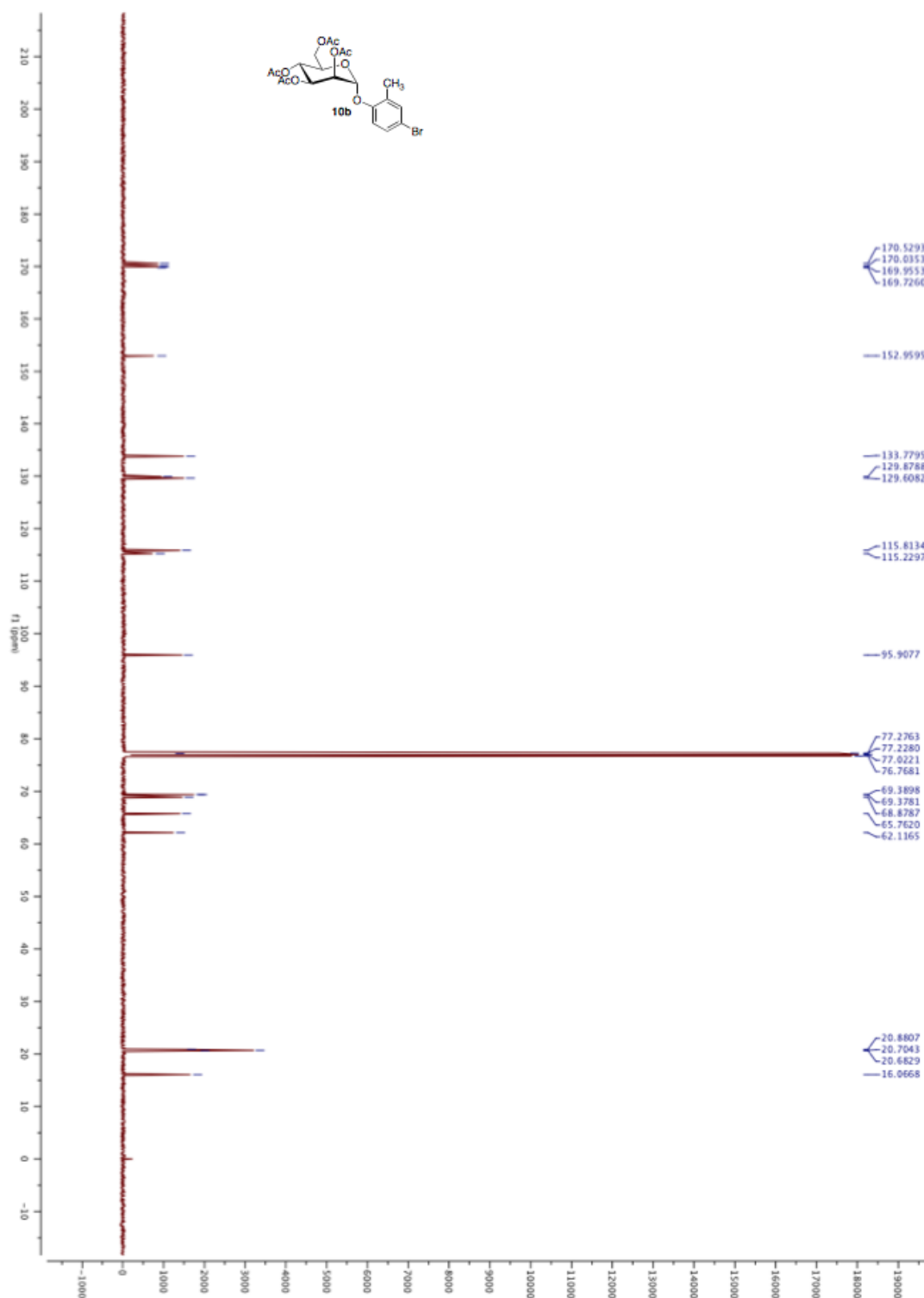


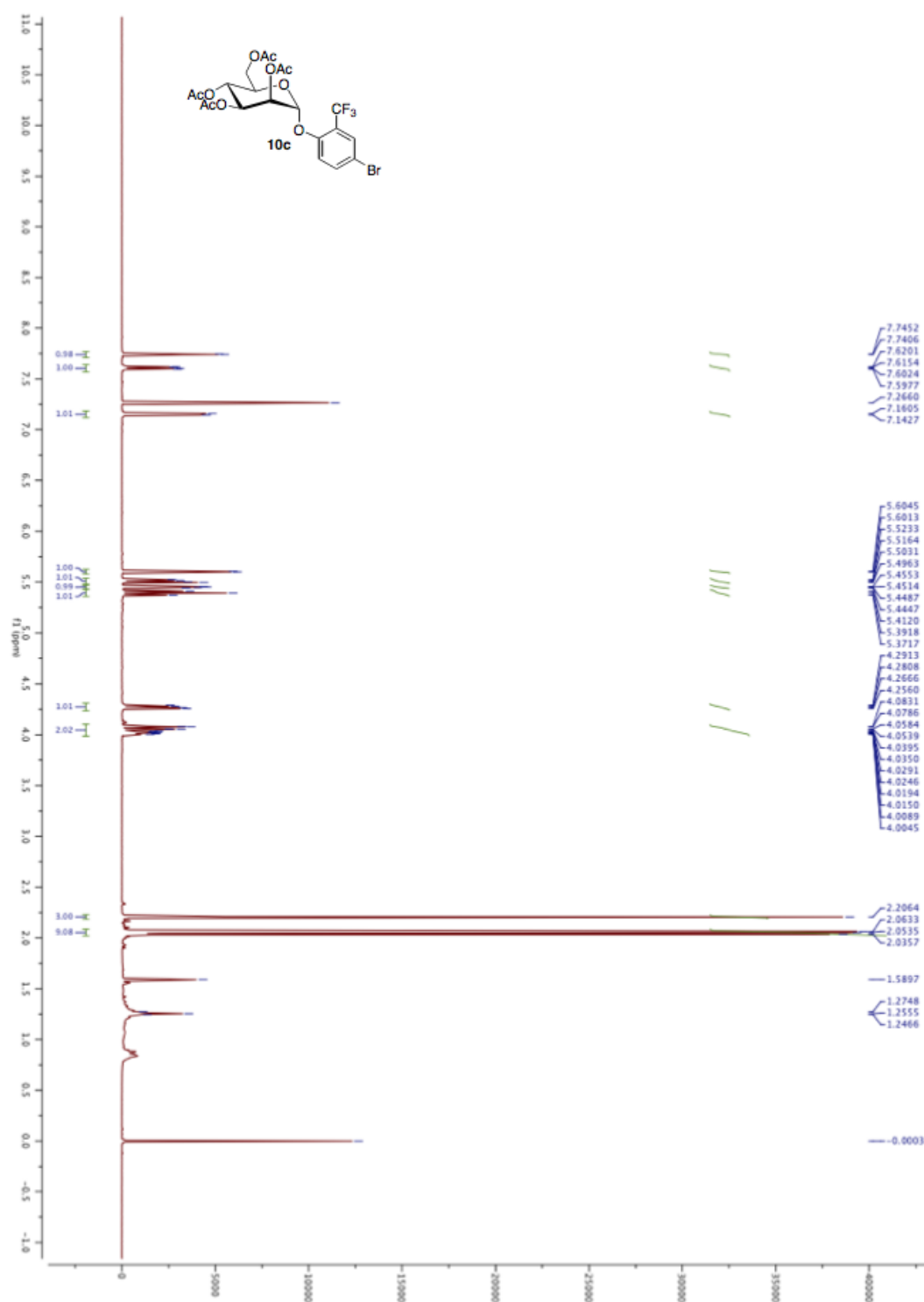
NMR Spectra for the synthetic compounds: ^1H NMR (500 MHz) of **8**

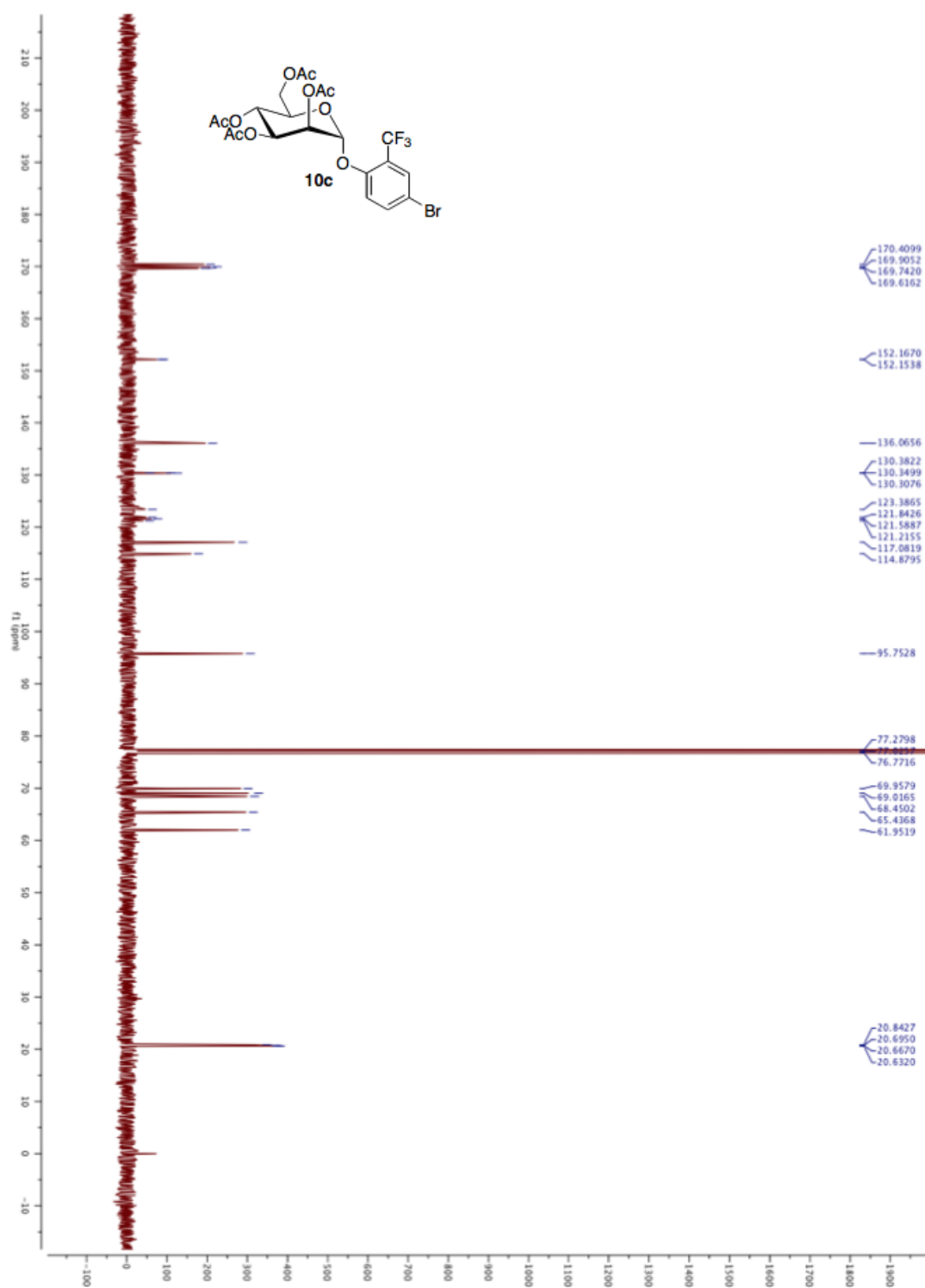
^1H NMR (500 MHz) of 10a

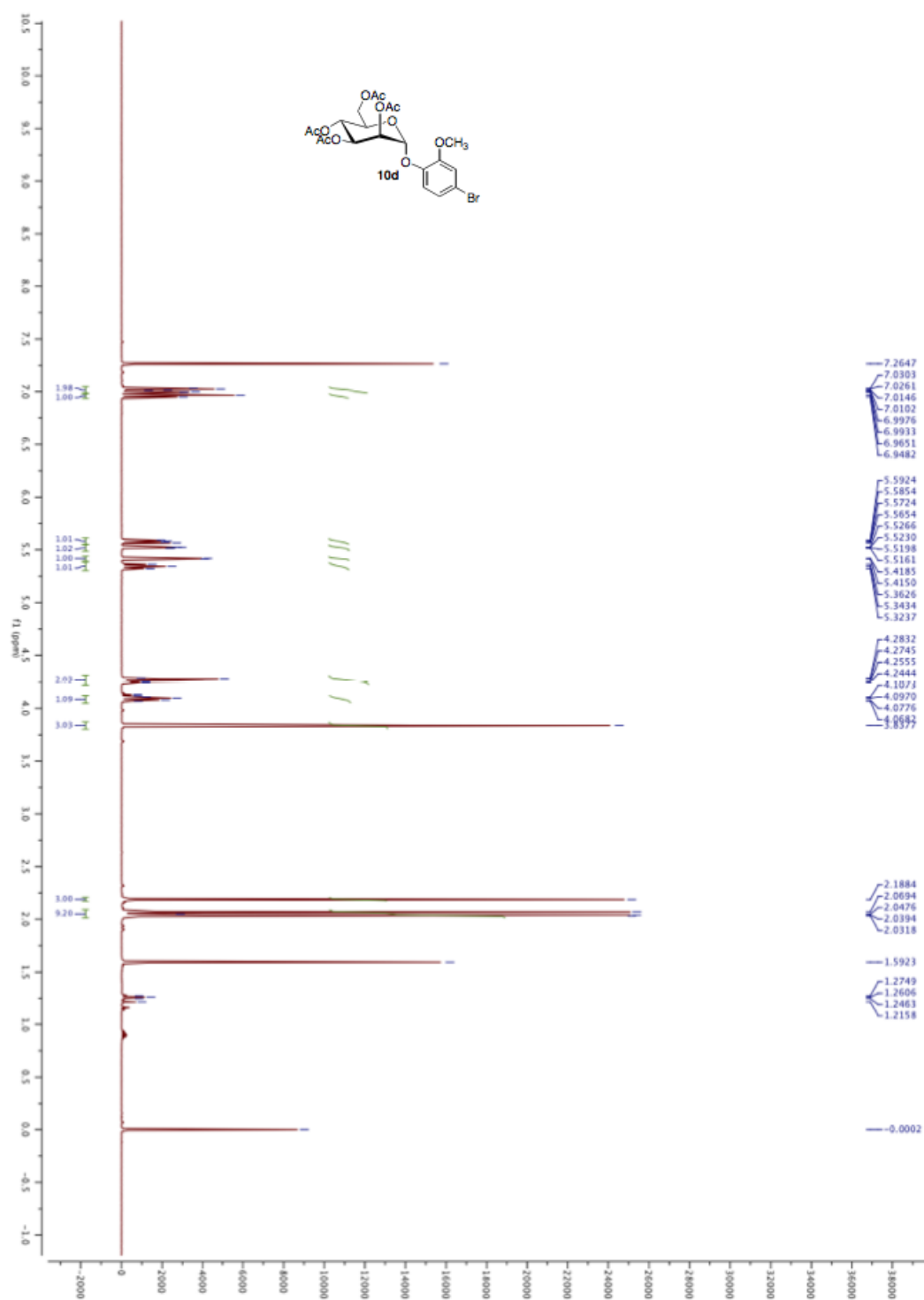
^{13}C NMR (125 MHz) of **10a**

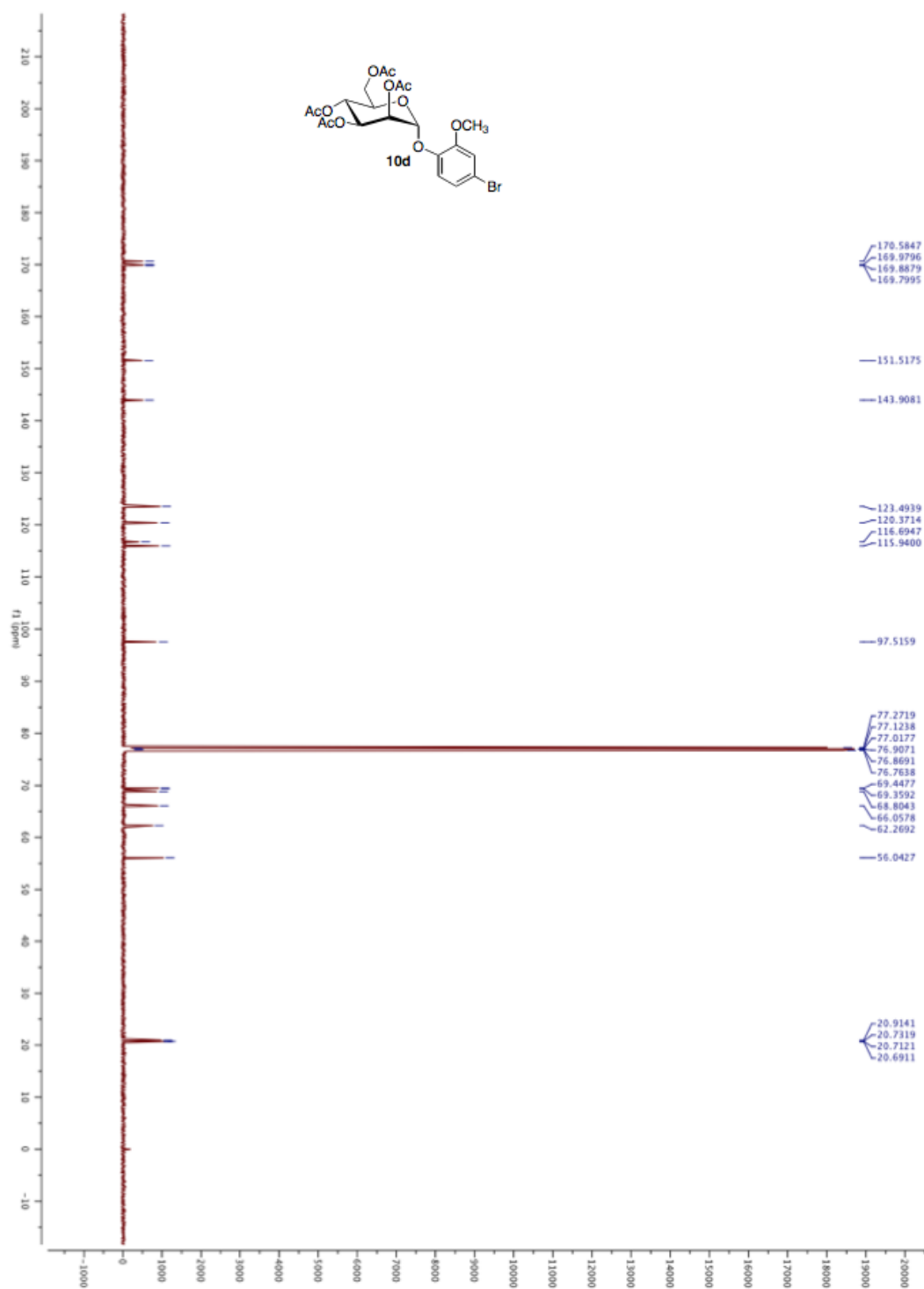
^1H NMR (500 MHz) of **10b**

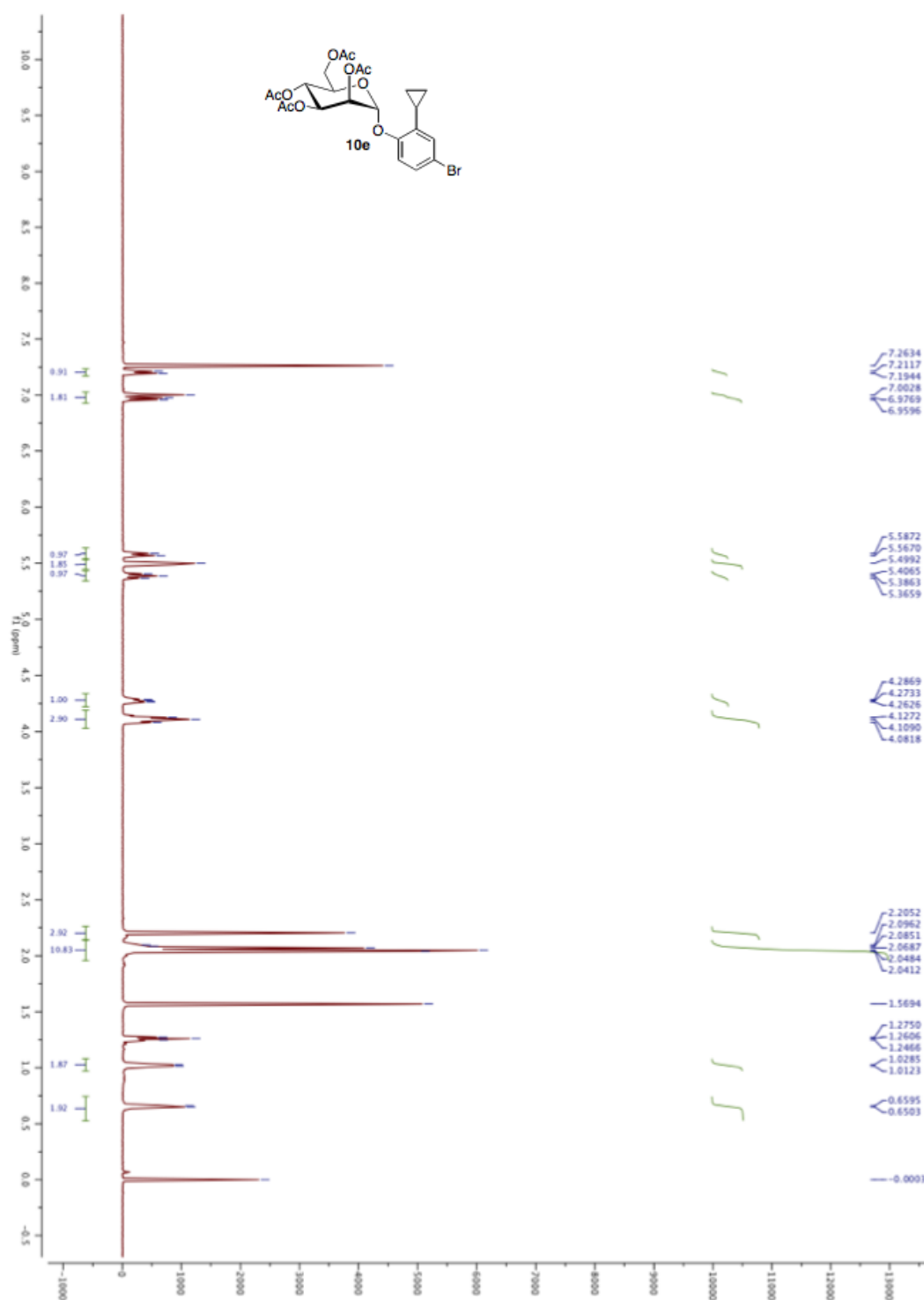
^{13}C NMR (125 MHz) of **10b**

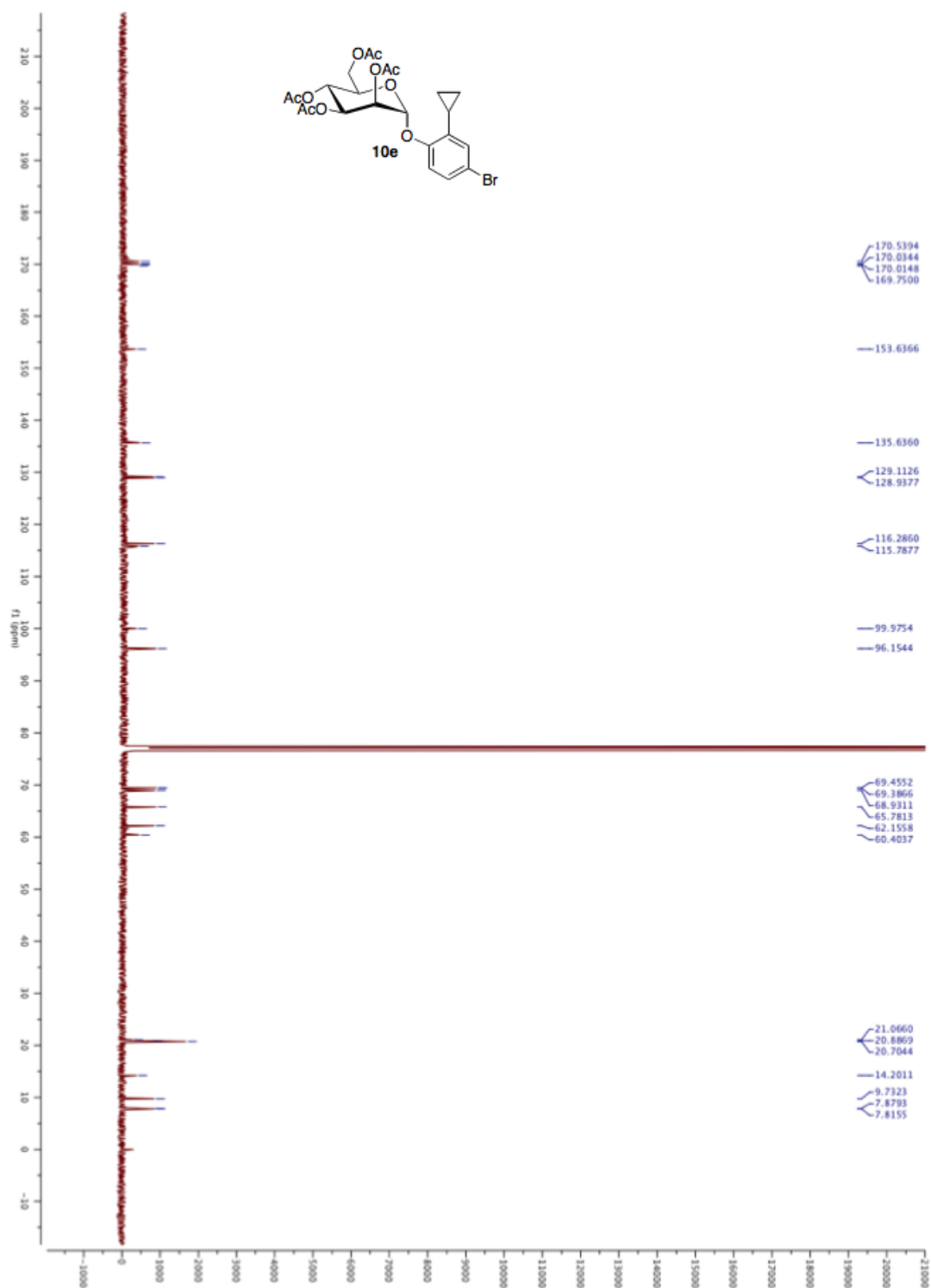
^1H NMR (500 MHz) of **10c**

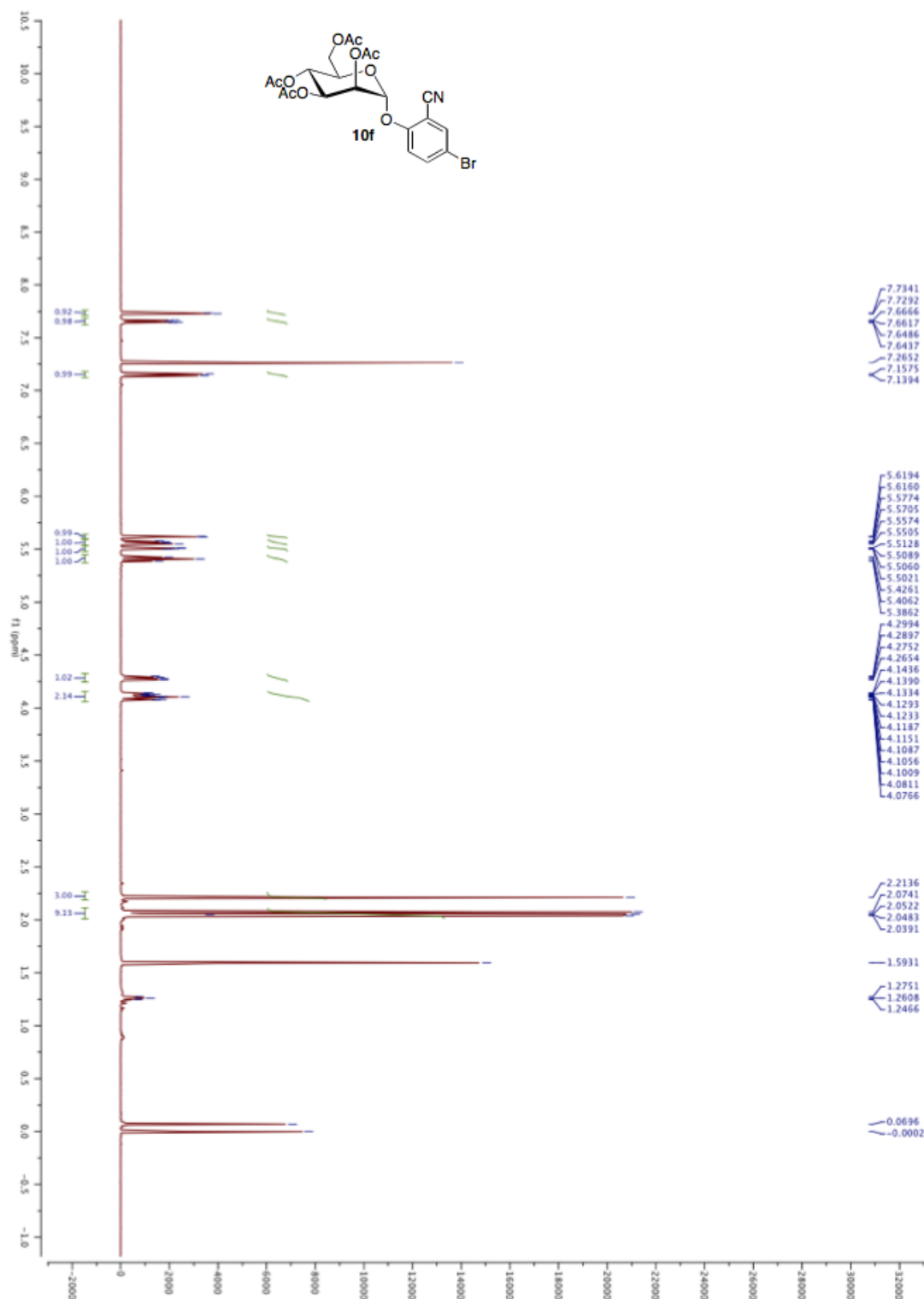
^{13}C NMR (125 MHz) of **10c**

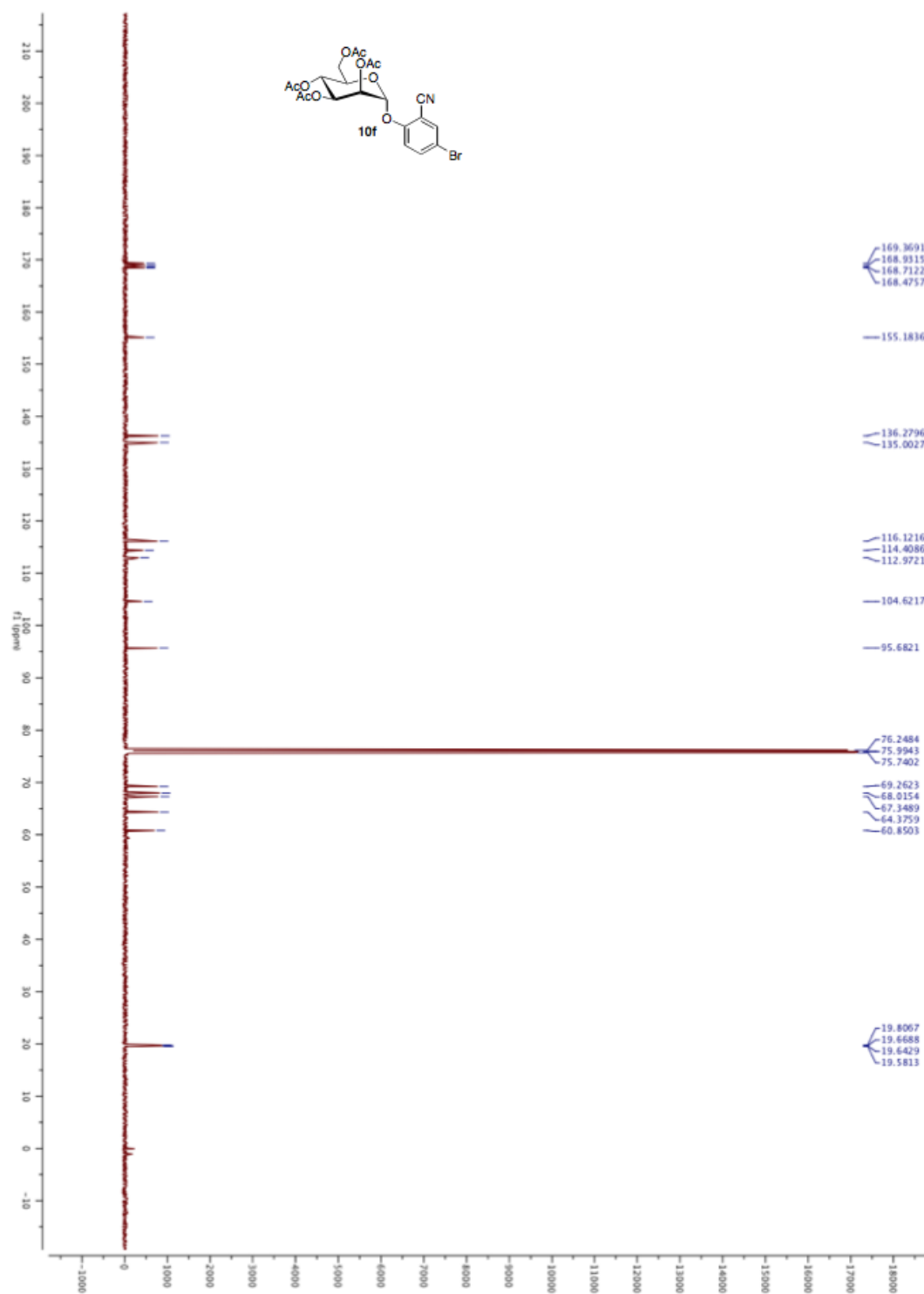
^1H NMR (500 MHz) of **10d**

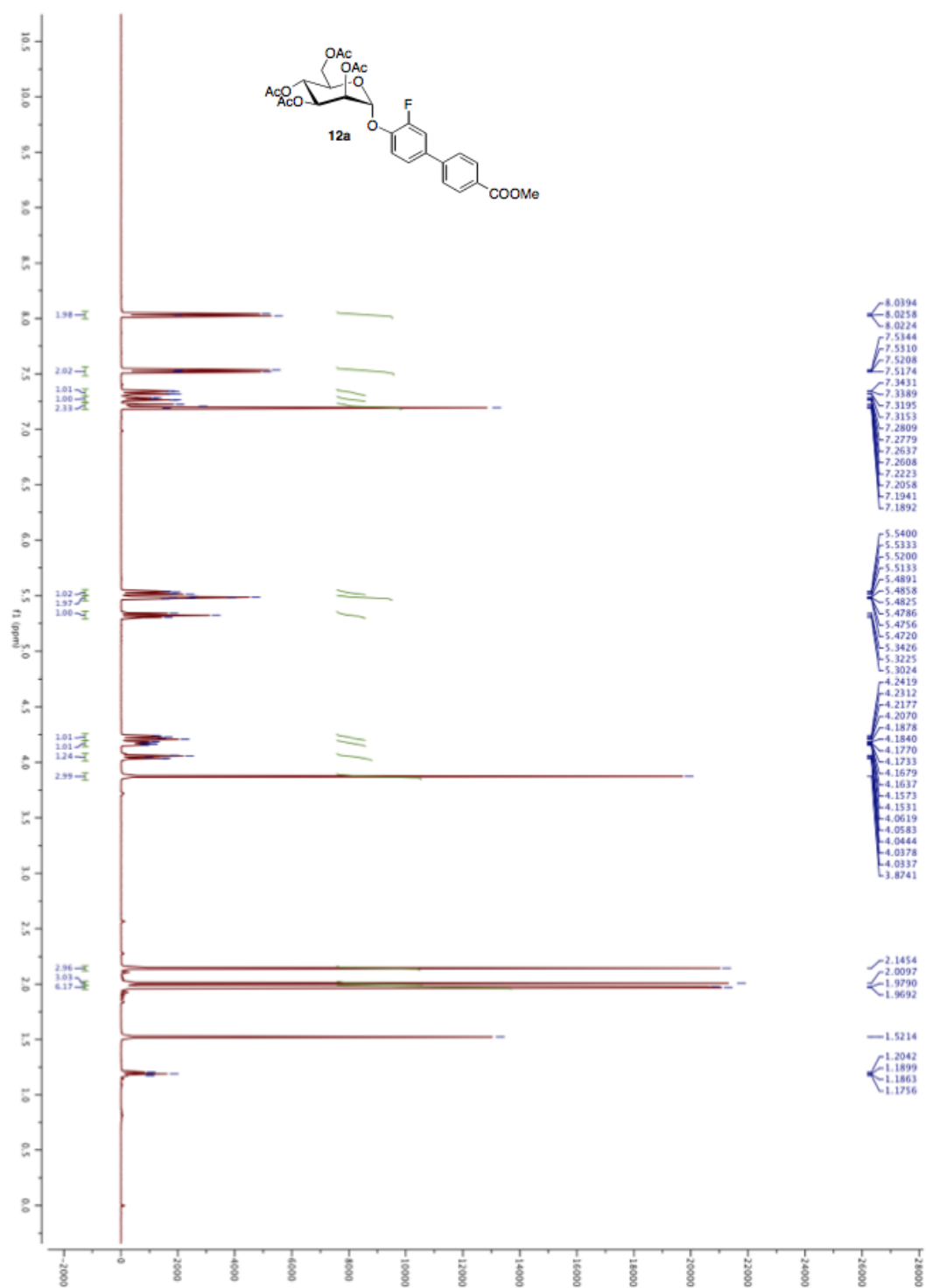
^{13}C NMR (125 MHz) of **10d**

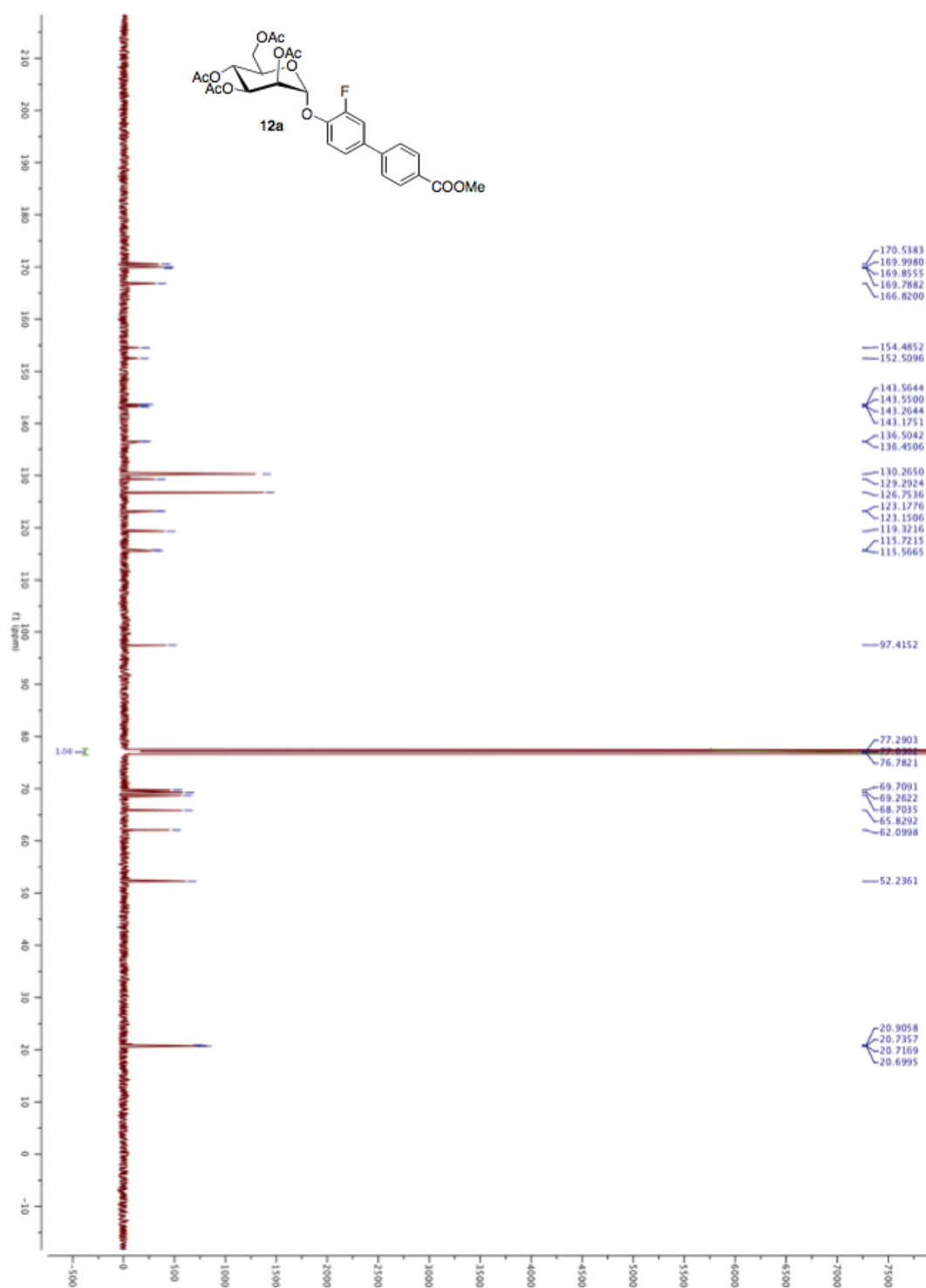
^1H NMR (500 MHz) of **10e**

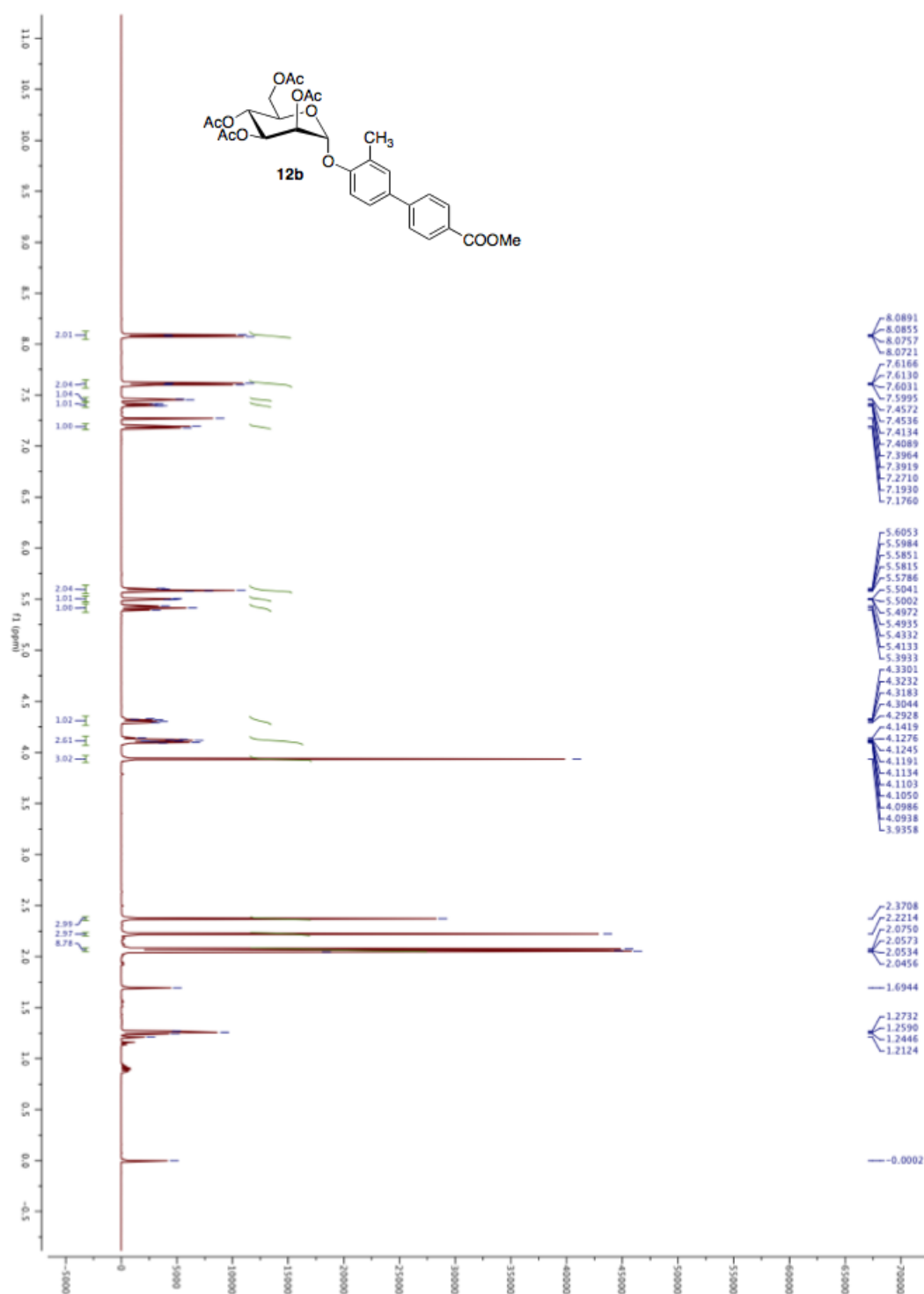
^{13}C NMR (125 MHz) of **10e**

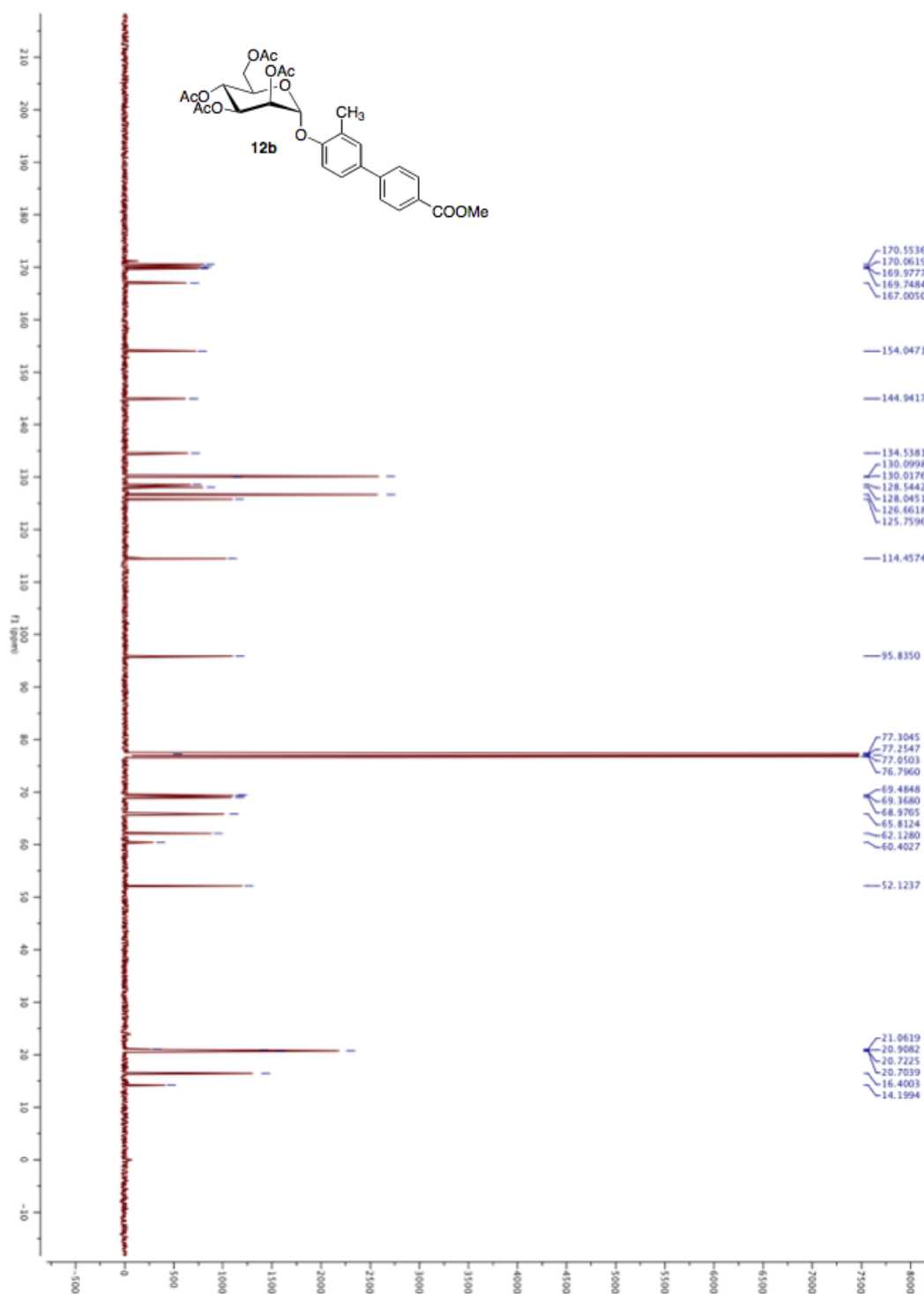
^1H NMR (500 MHz) of **10f**

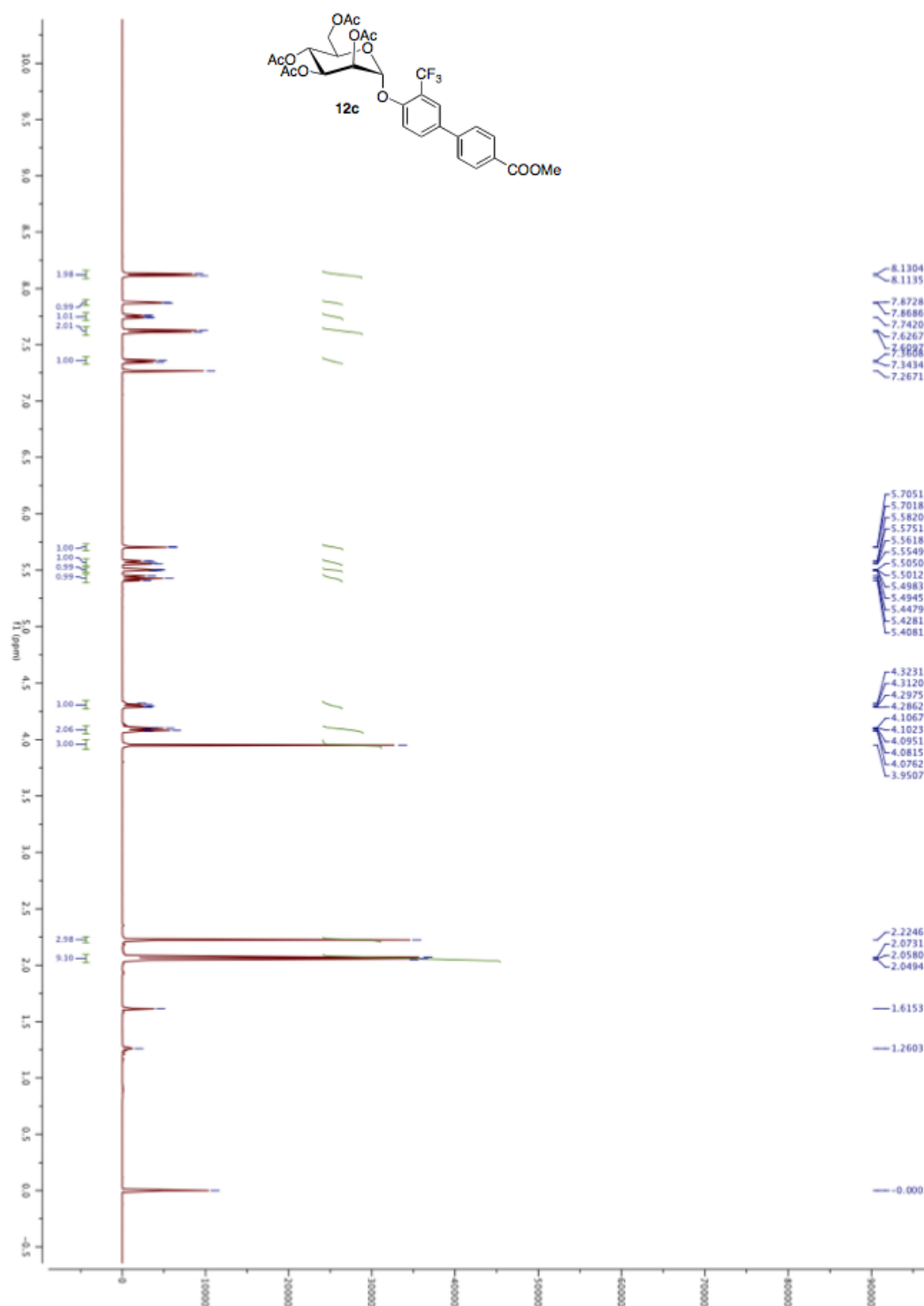
^{13}C NMR (125 MHz) of **10f**

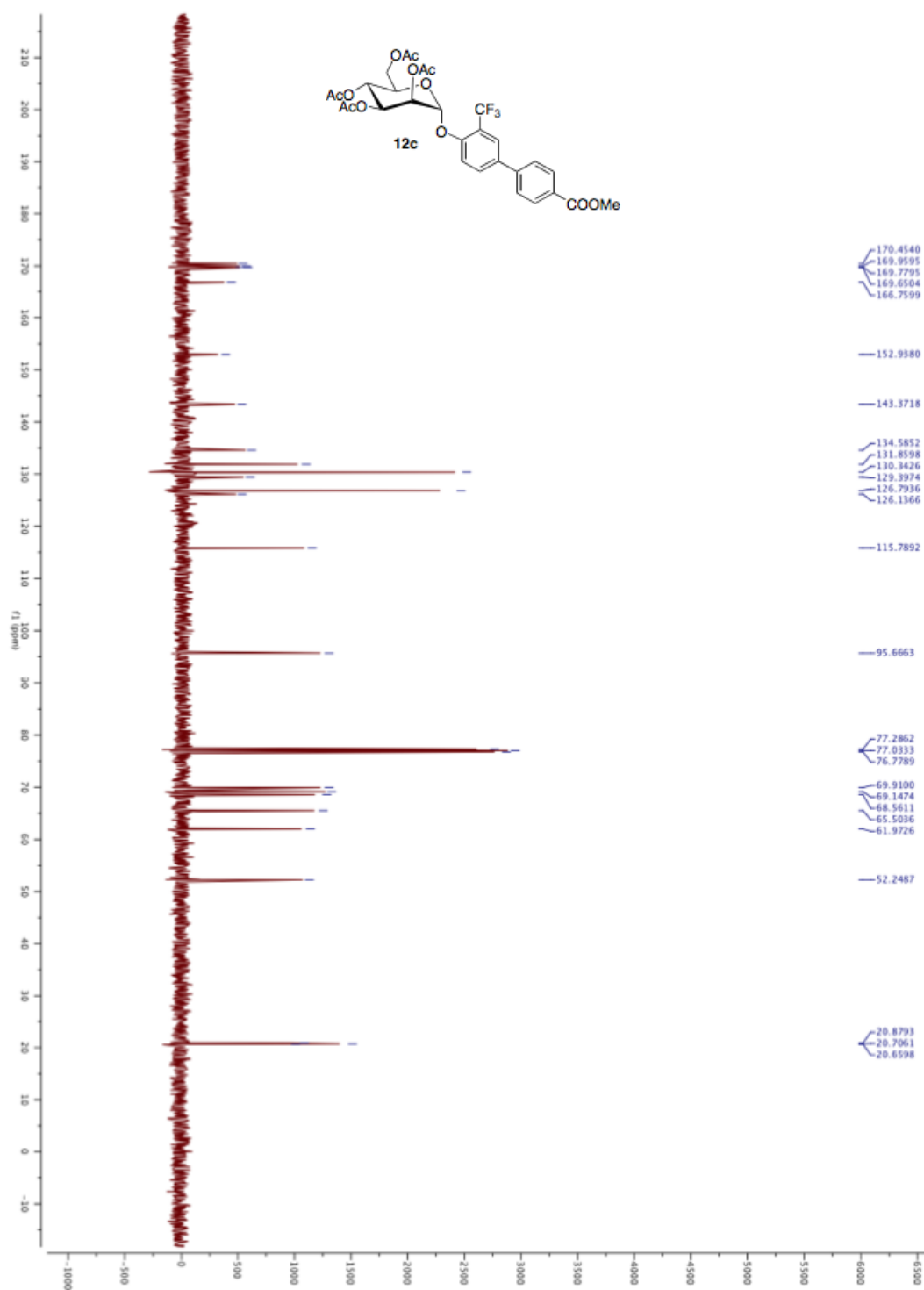
^1H NMR (500 MHz) of **12a**

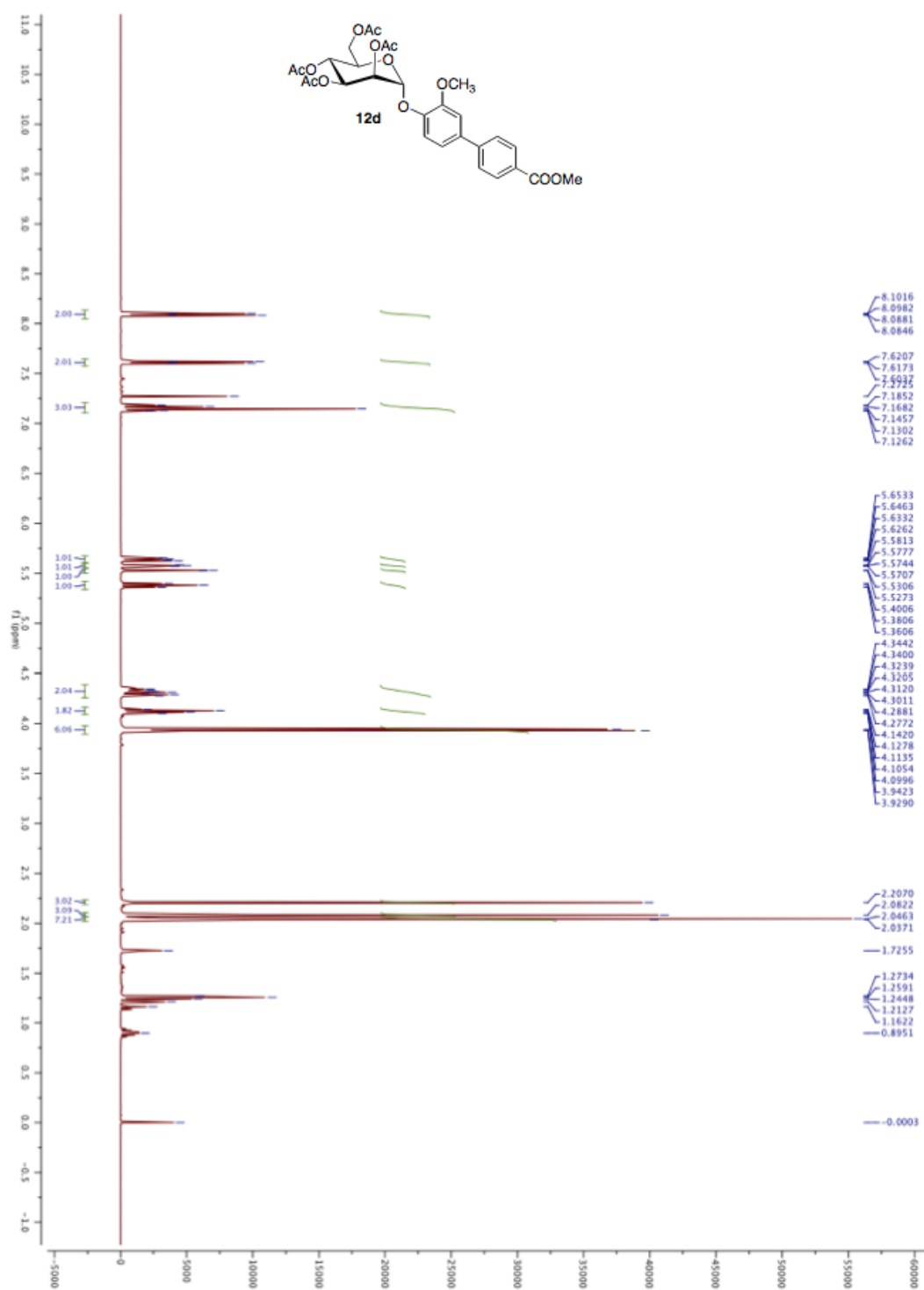
^{13}C NMR (125 MHz) of **12a**

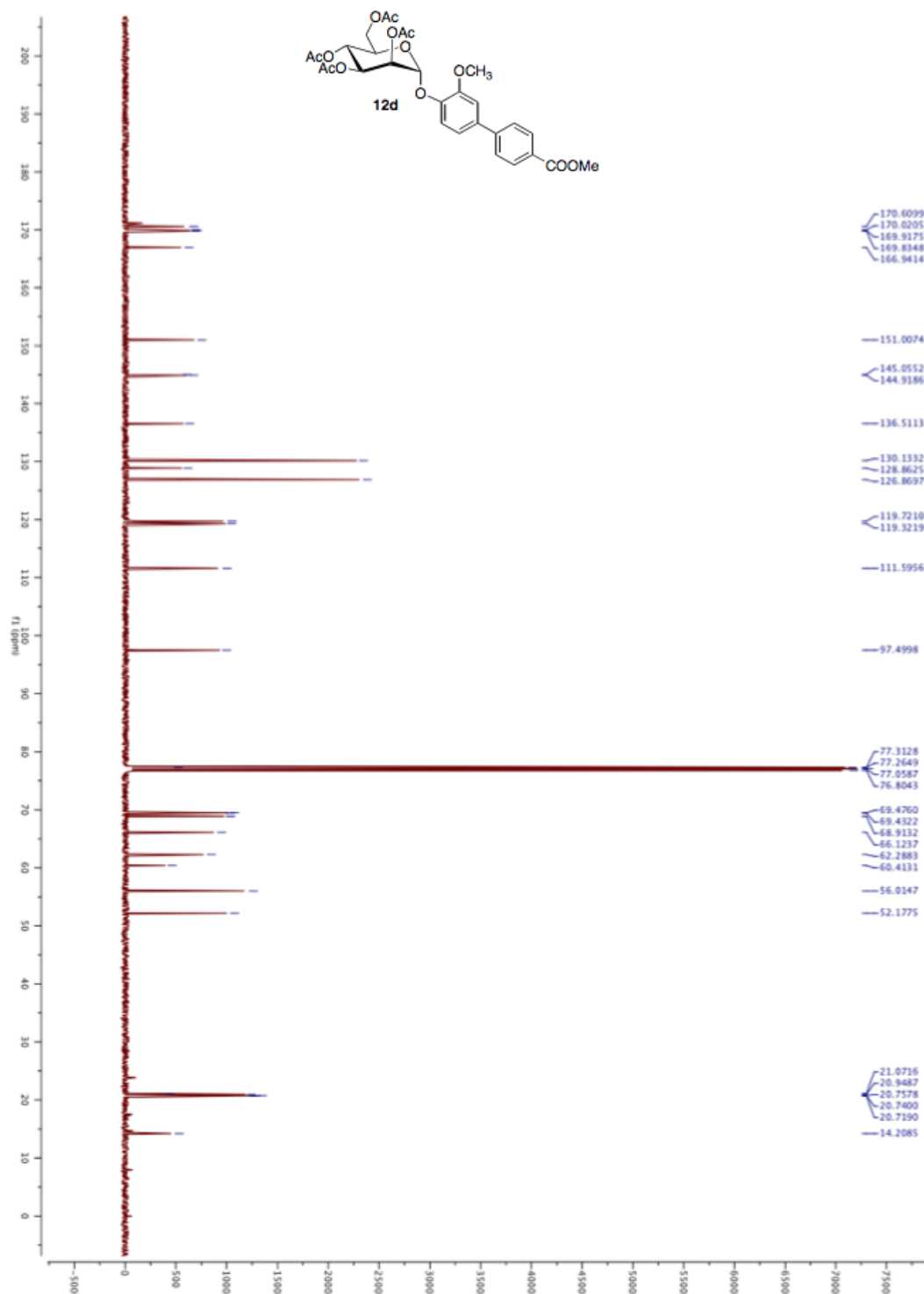
^1H NMR (500 MHz) of **12b**

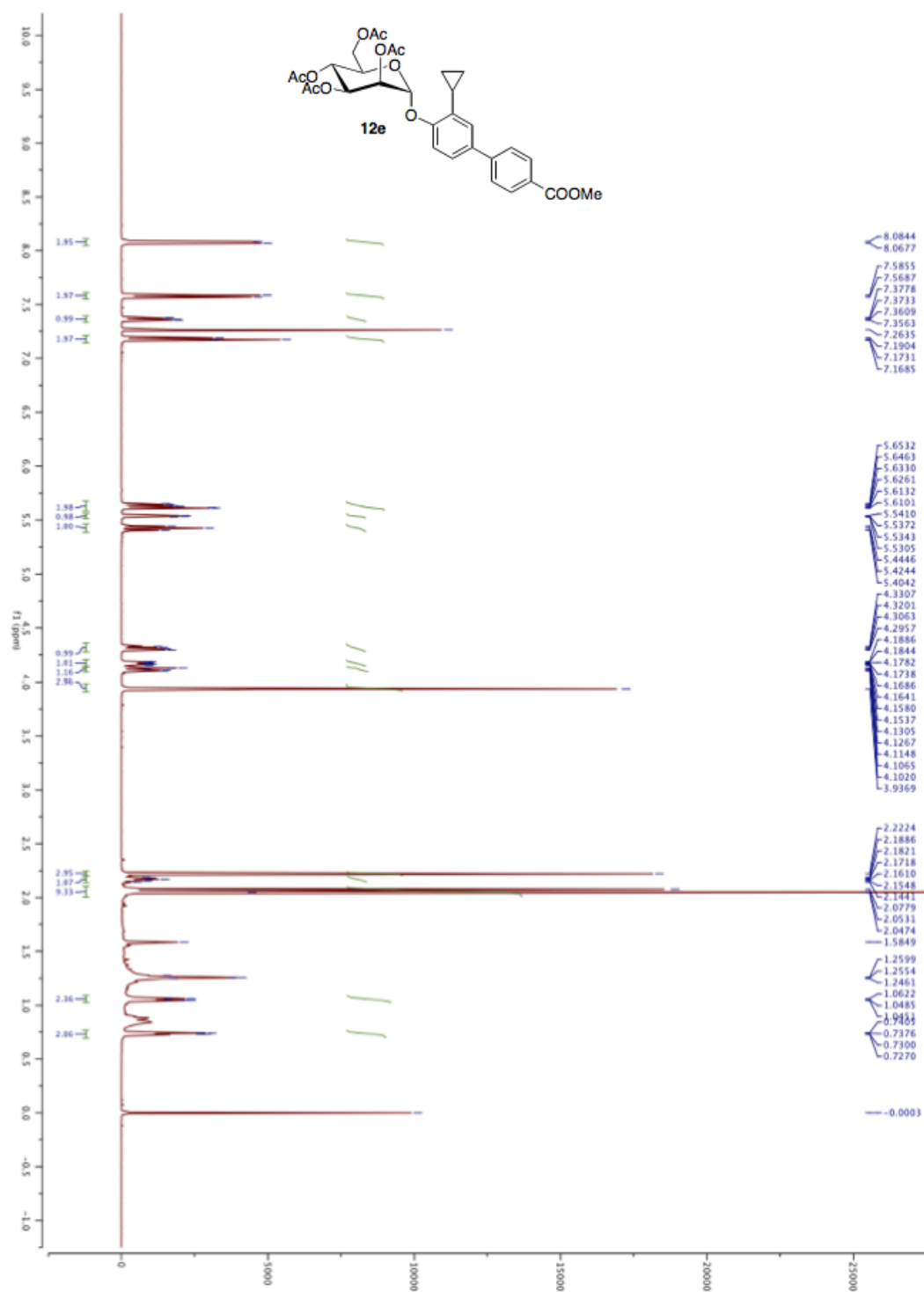
^{13}C NMR (125 MHz) of **12b**

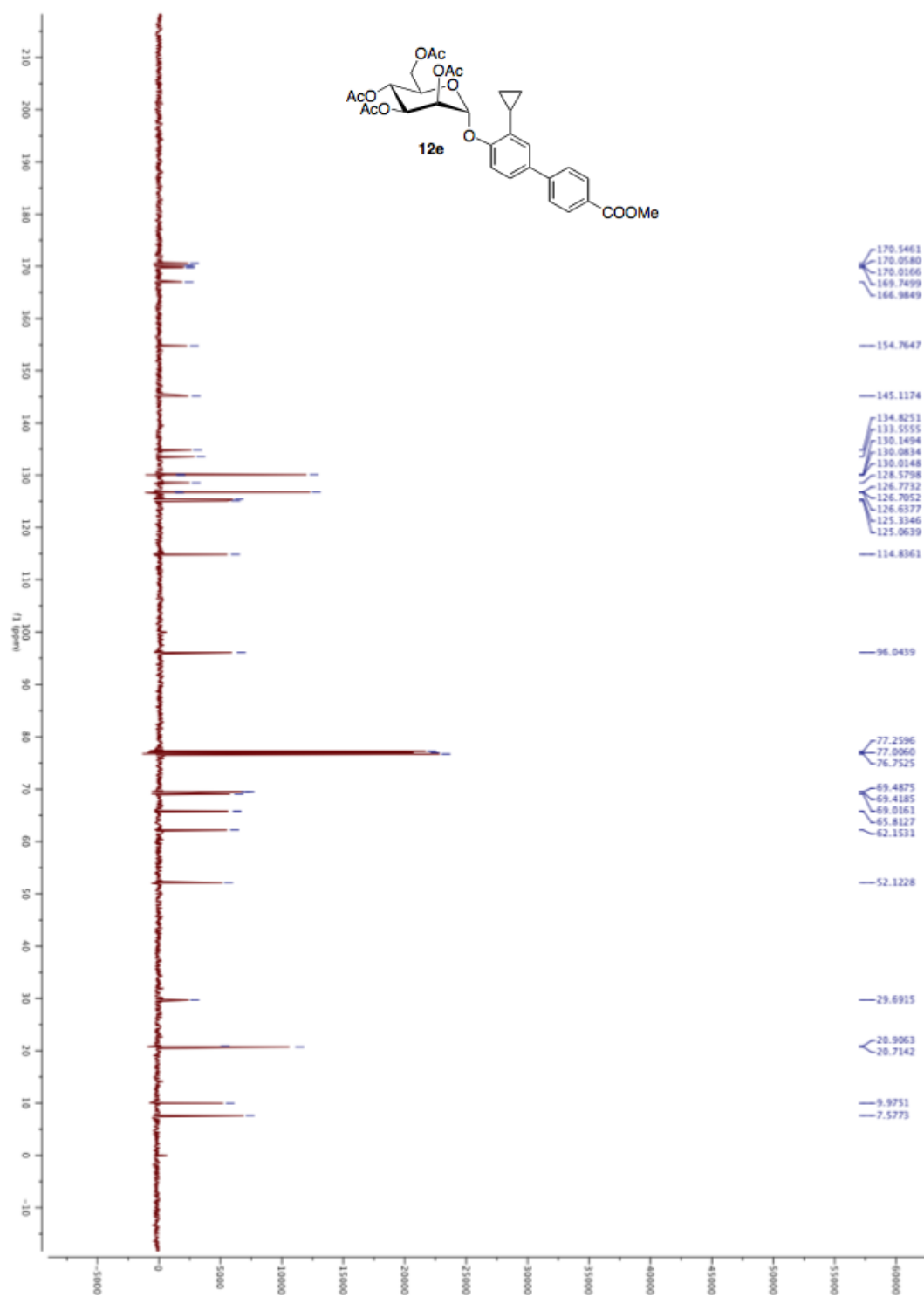
^1H NMR (500 MHz) of **12c**

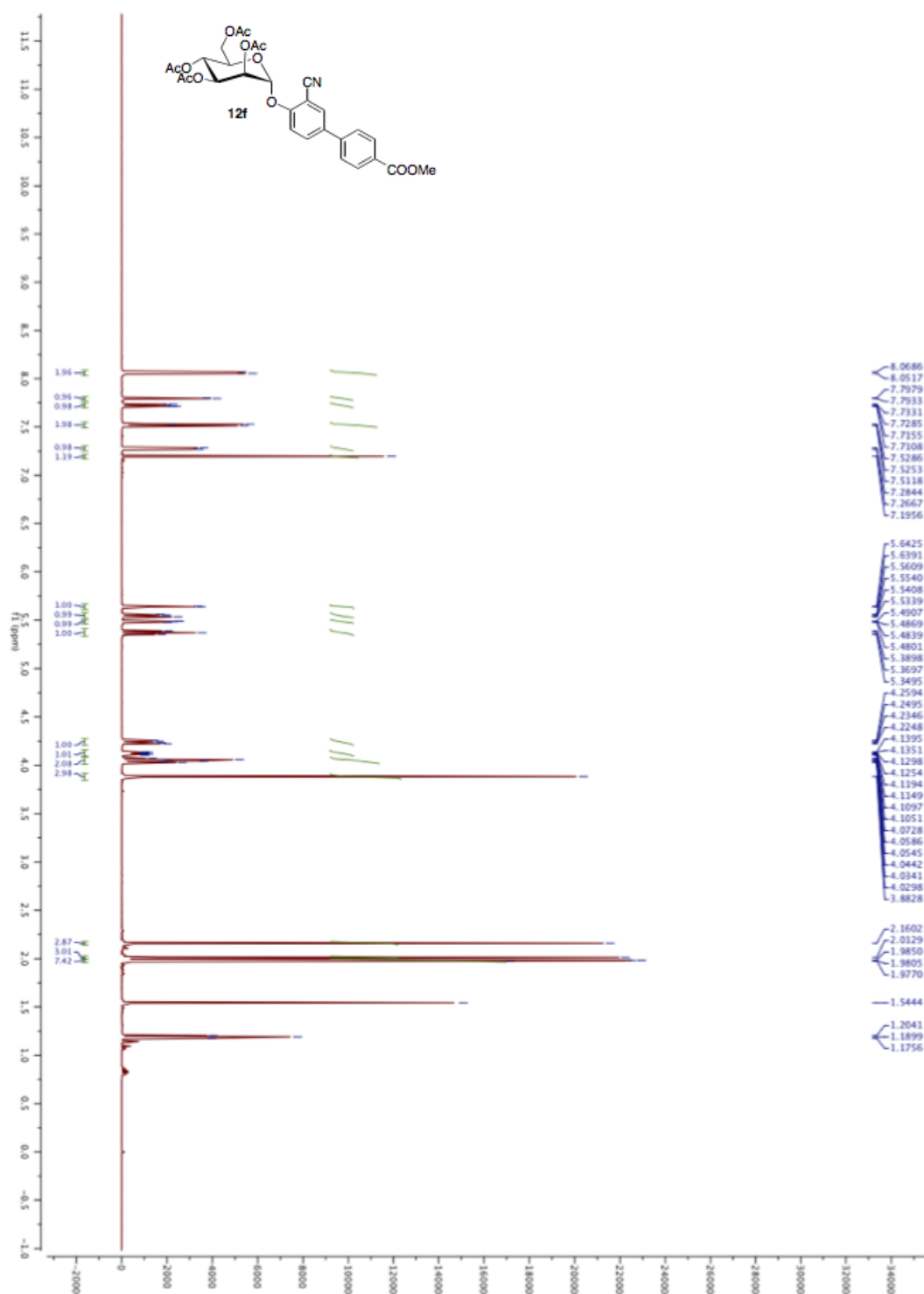
^{13}C NMR (125 MHz) of **12c**

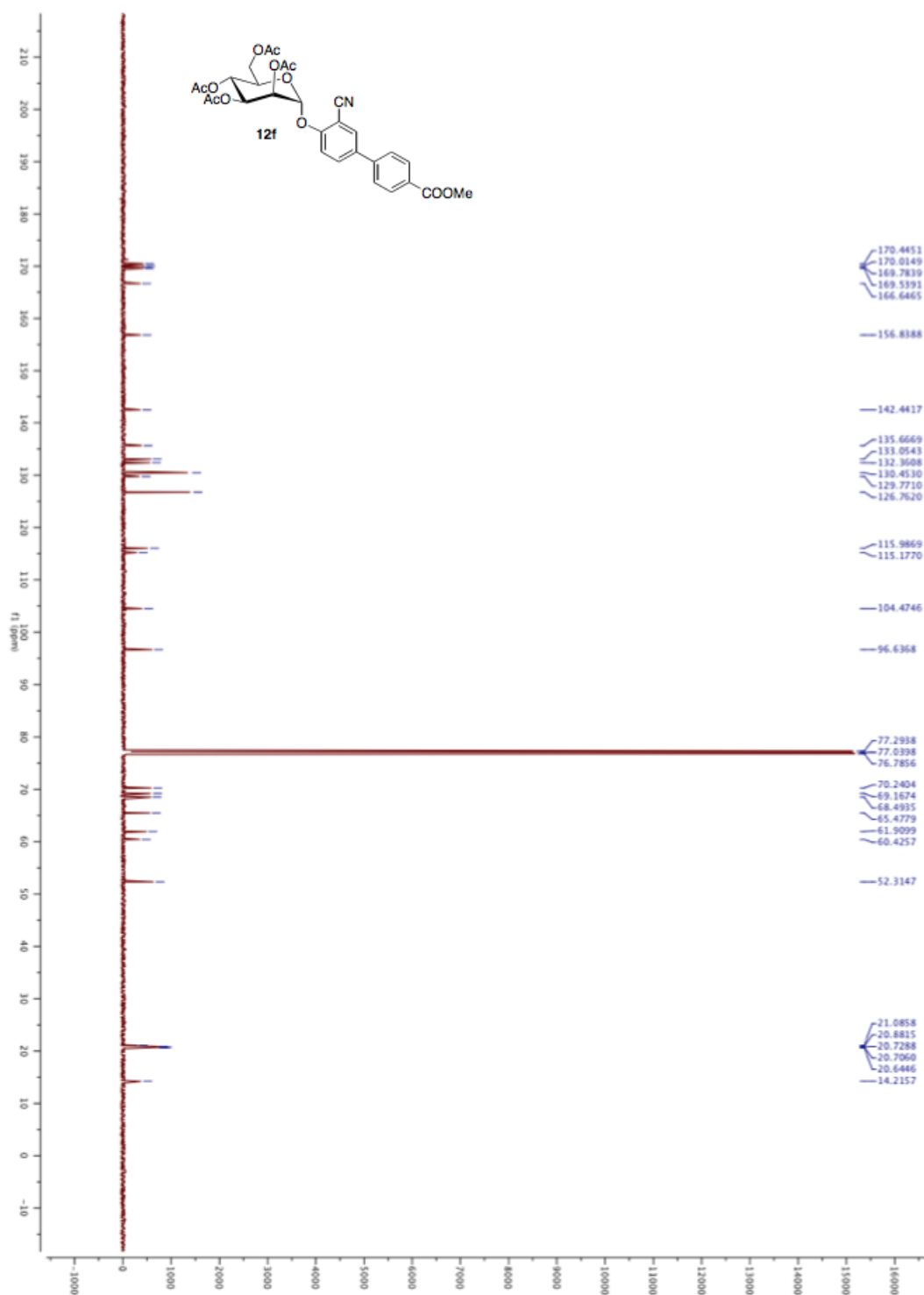
^1H NMR (500 MHz) of 12d

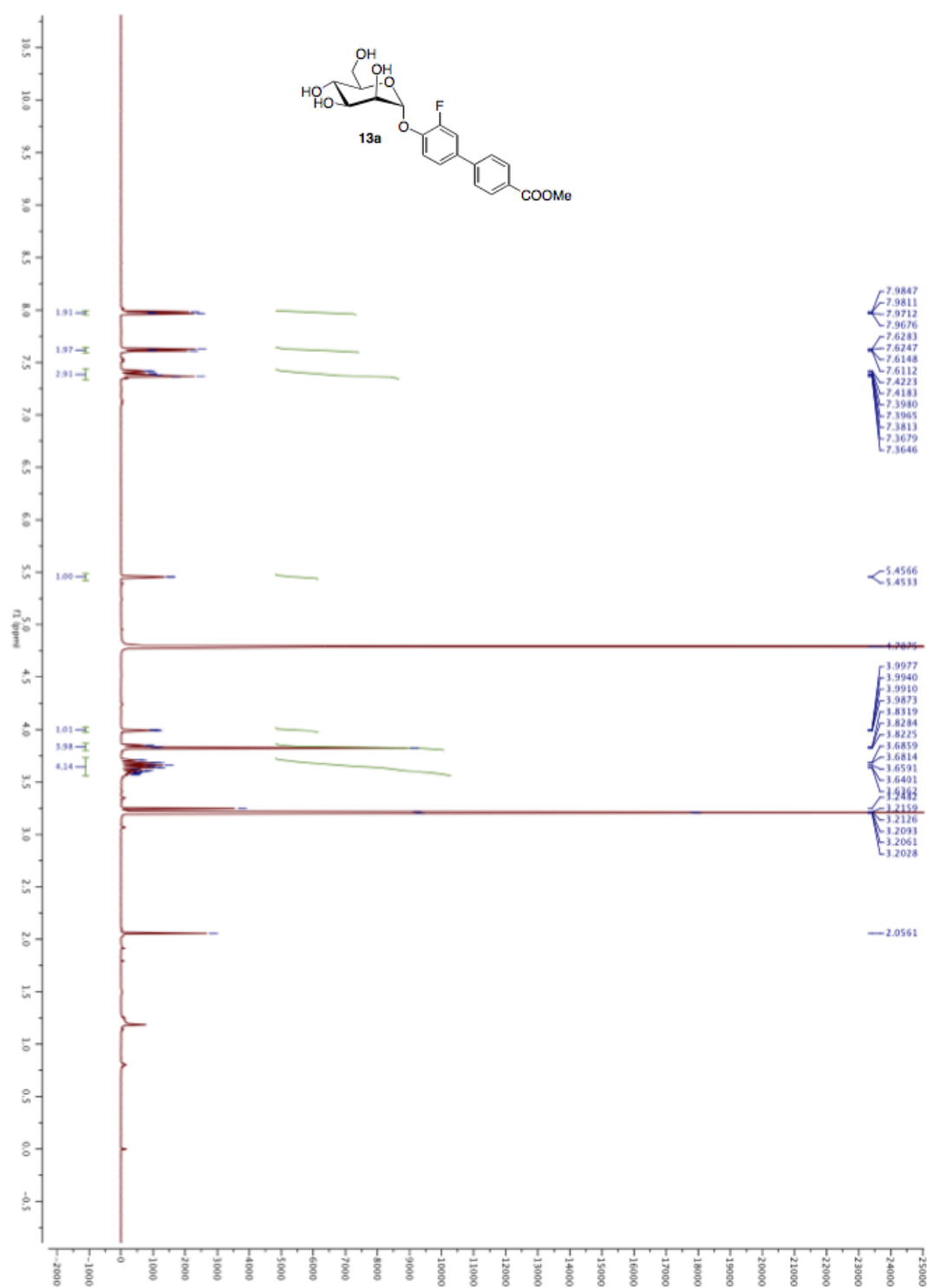
^{13}C NMR (125 MHz) of **12d**

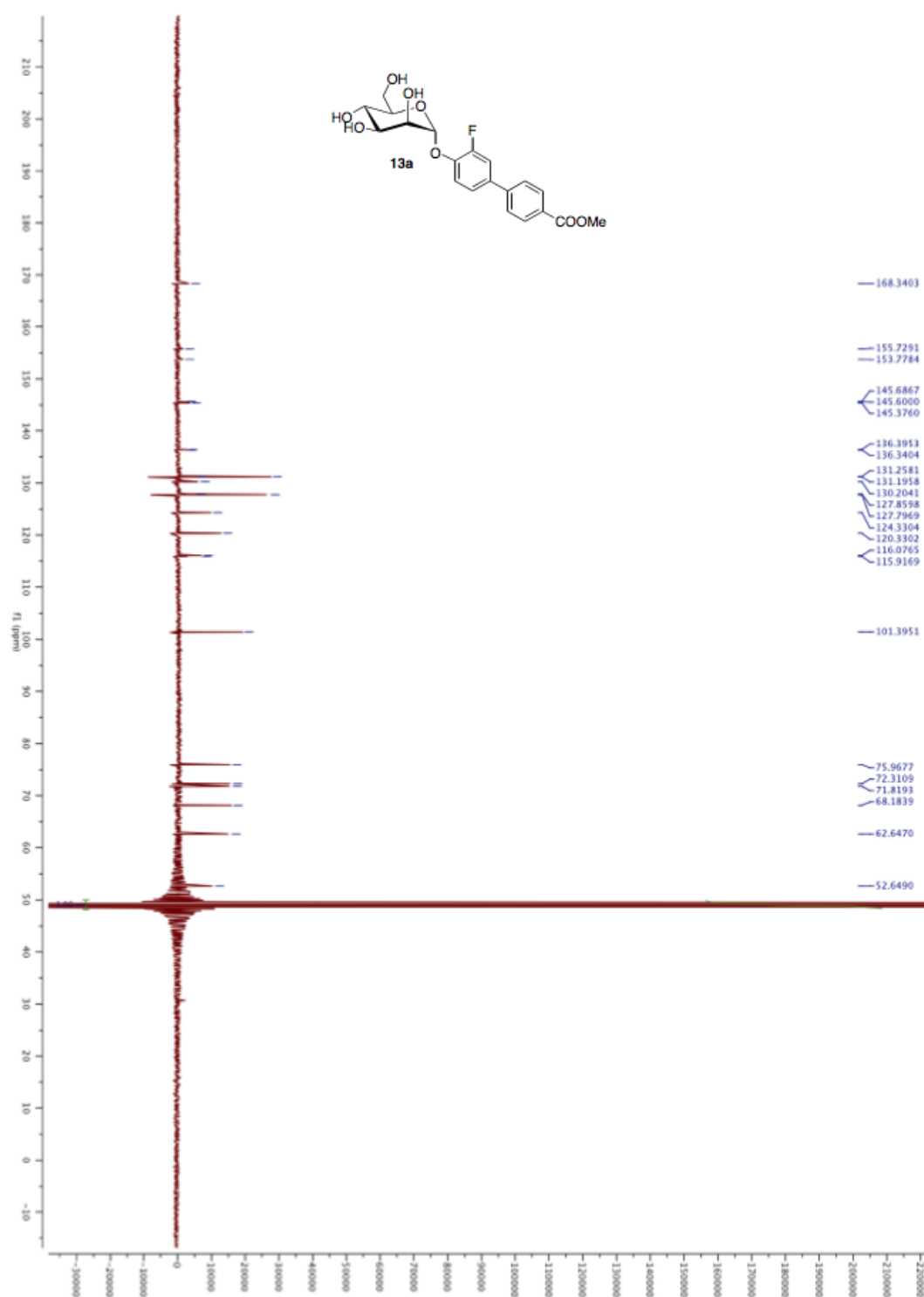
^1H NMR (500 MHz) of **12e**

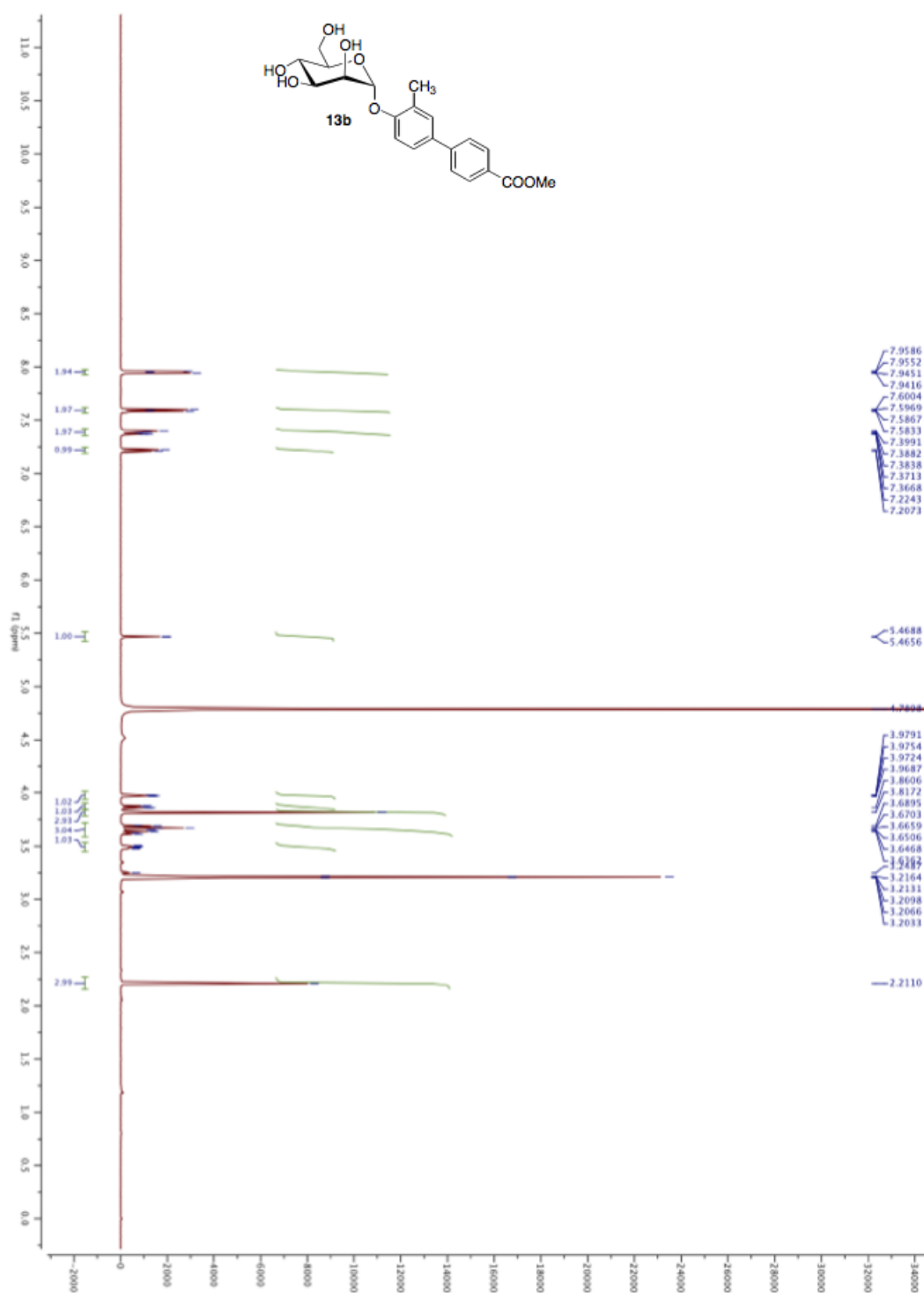
^{13}C NMR (125 MHz) of **12e**

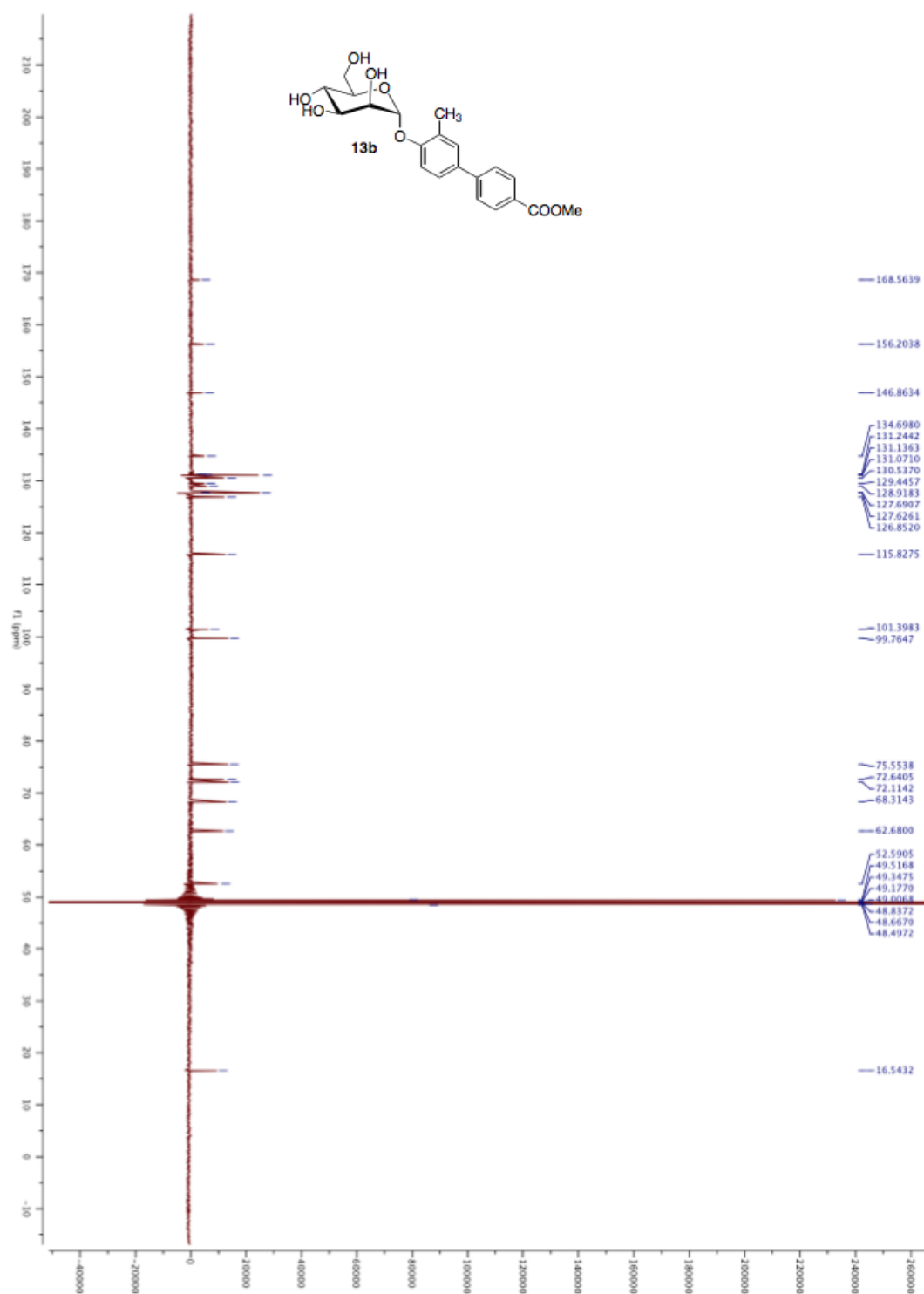
^1H NMR (500 MHz) of **12f**

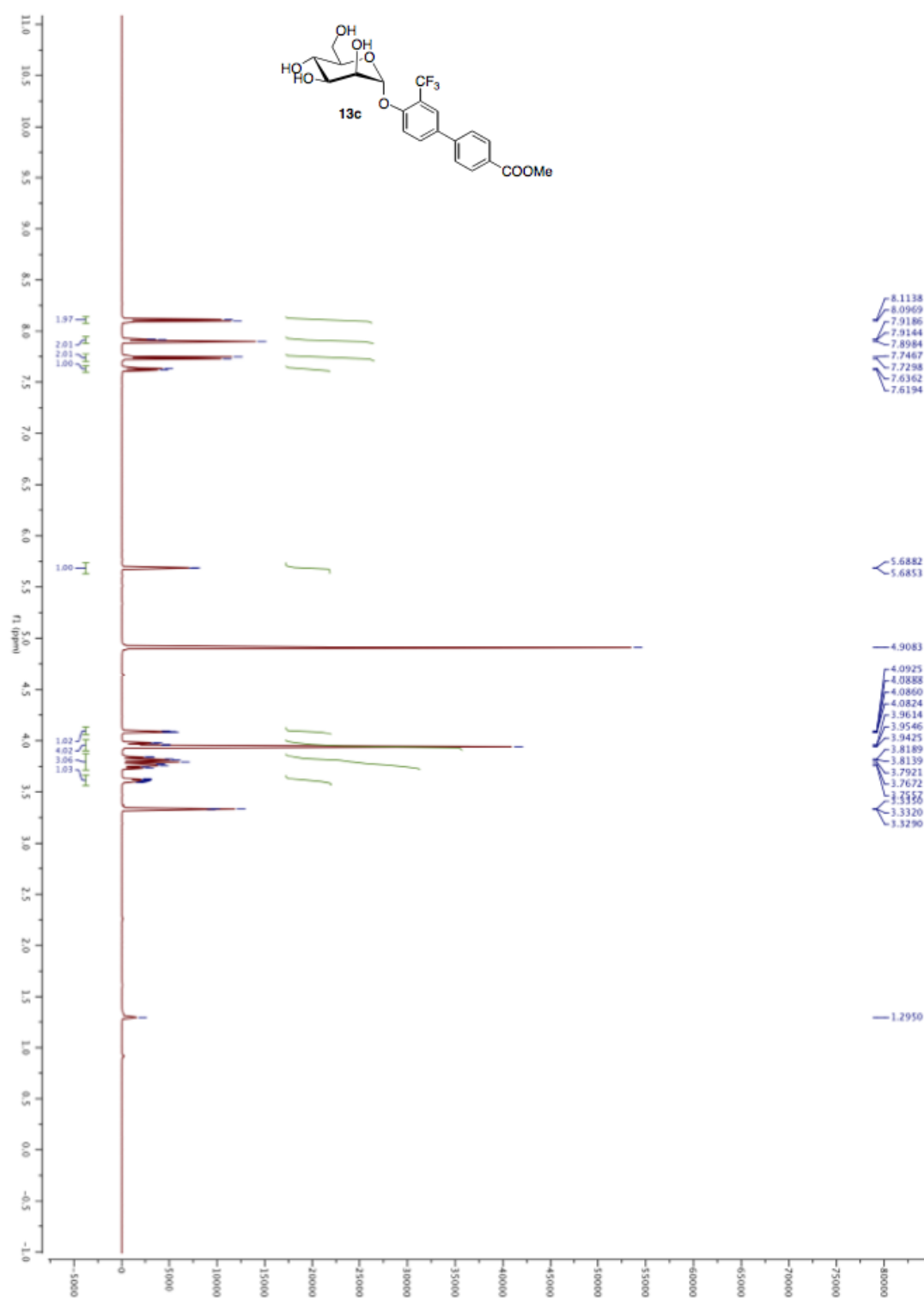
^{13}C NMR (125 MHz) of **12f**

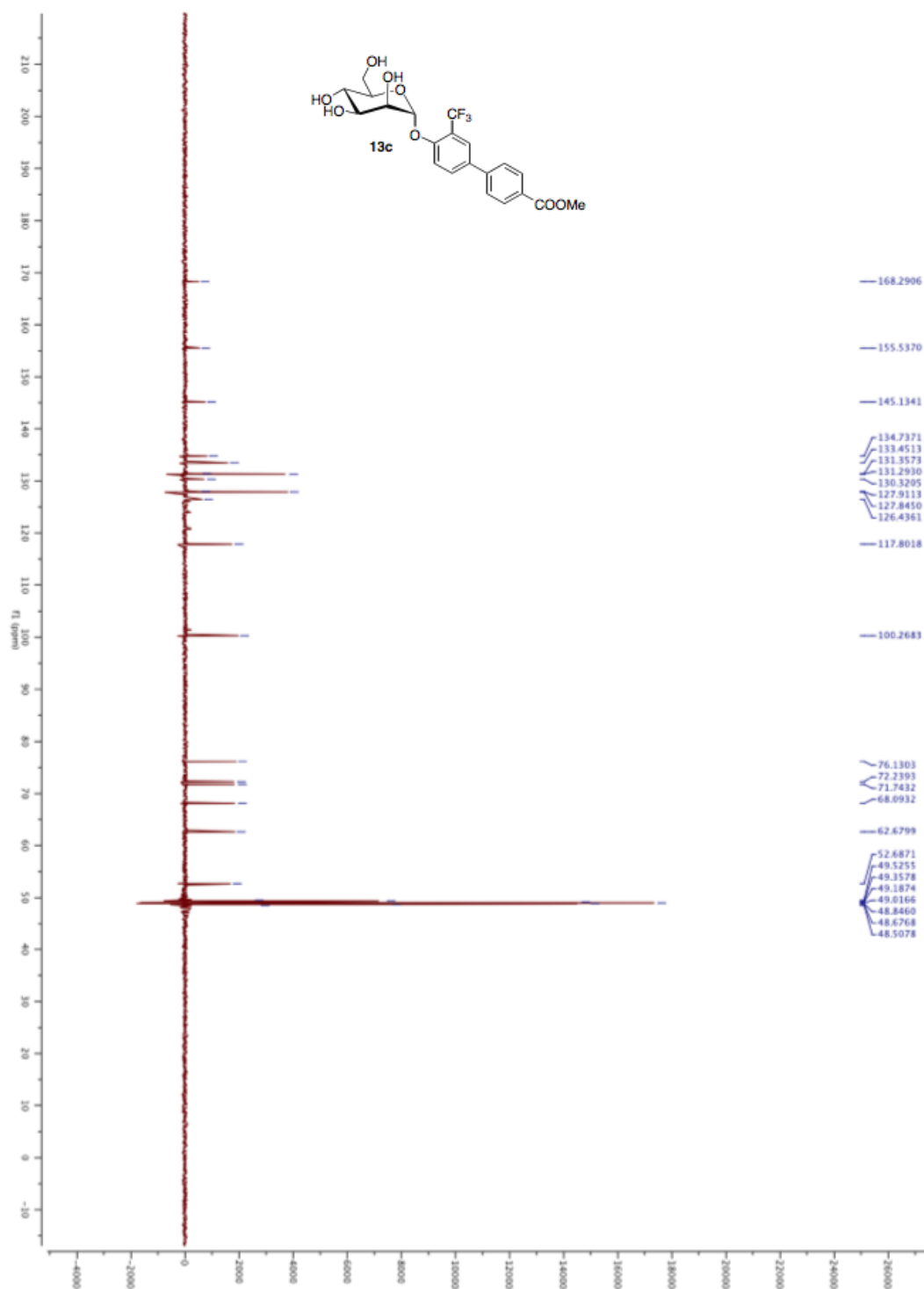
^1H NMR (500 MHz) of **13a**

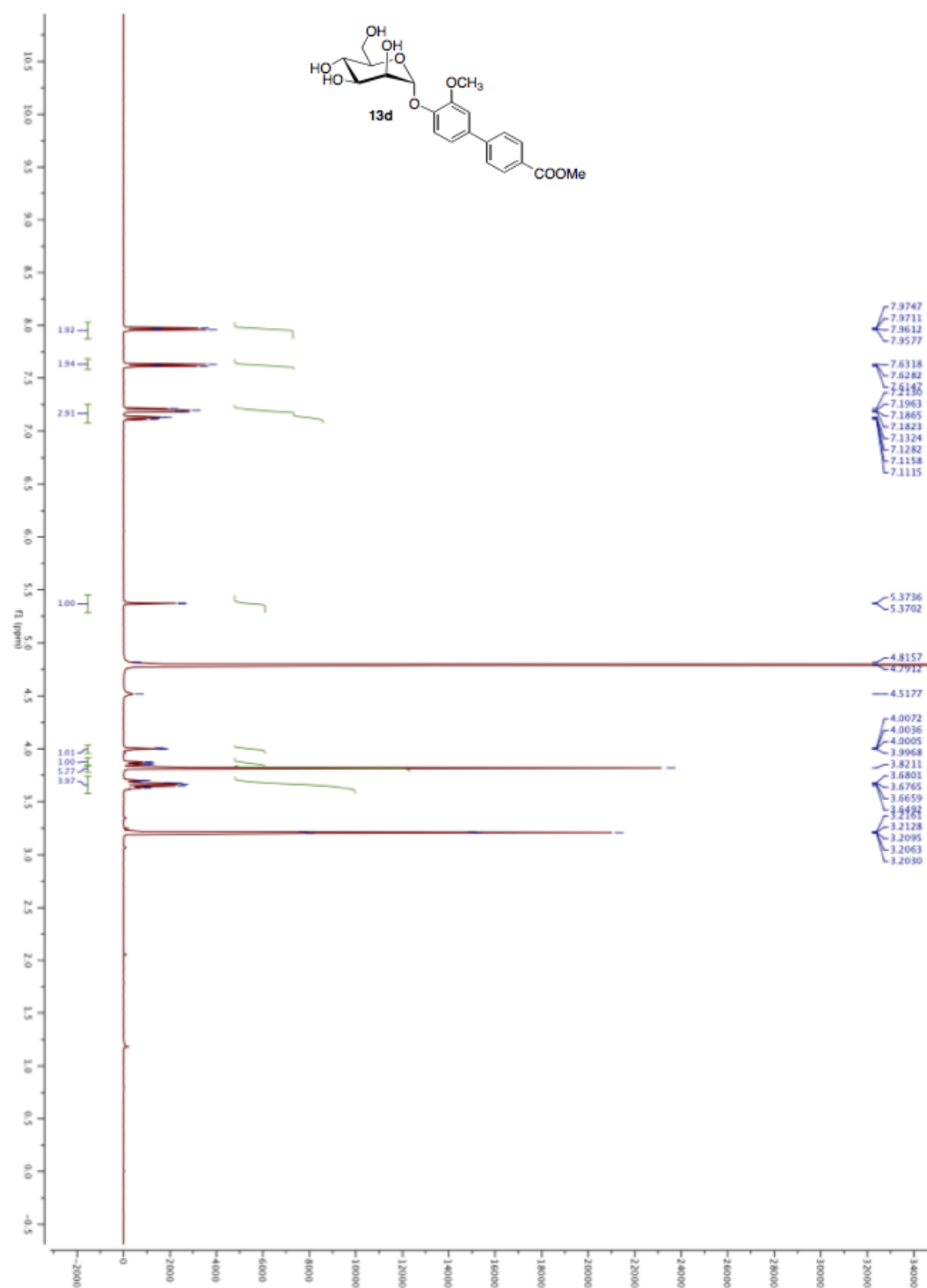
^{13}C NMR (125 MHz) of **13a**

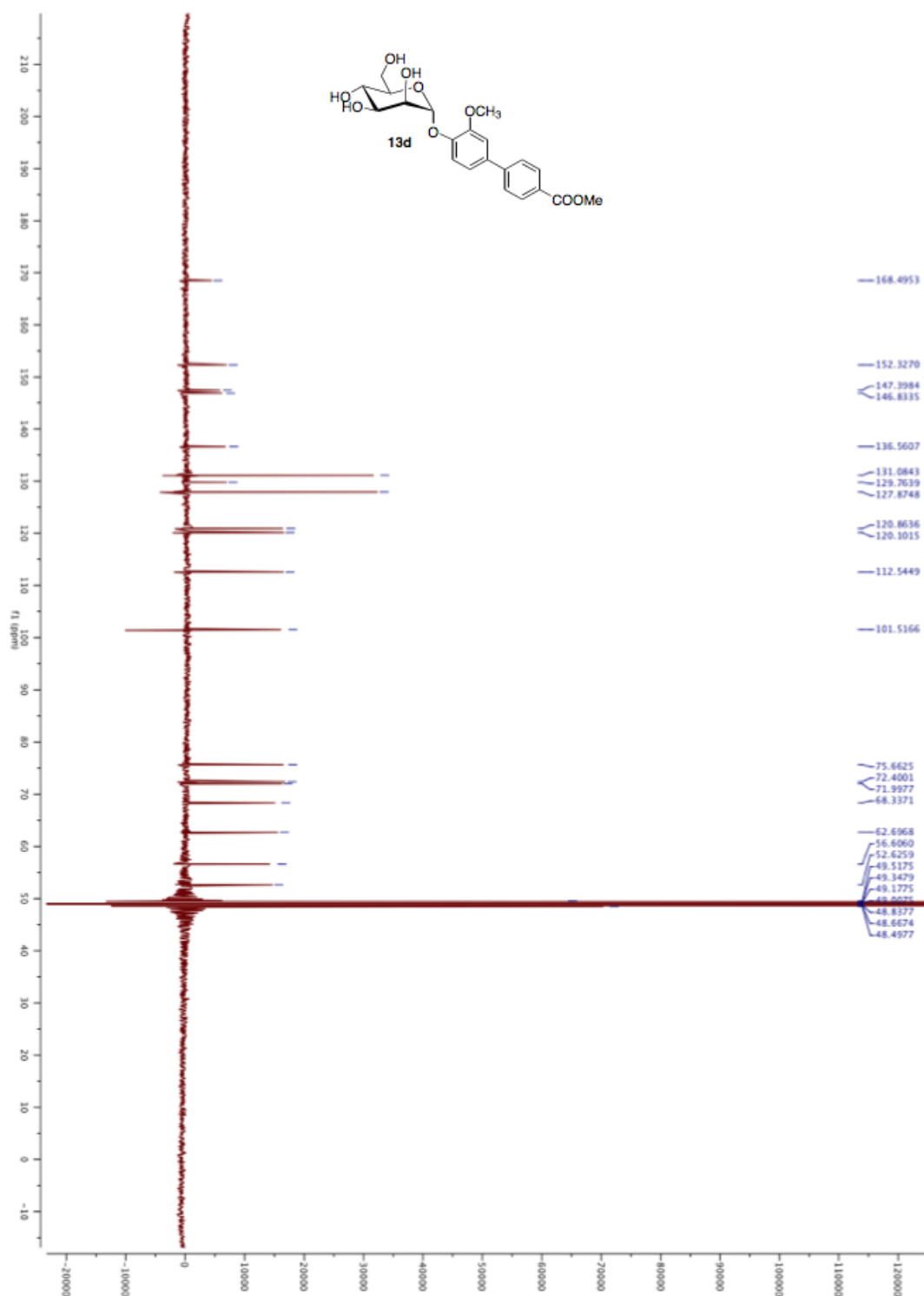
^1H NMR (500 MHz) of **13b**

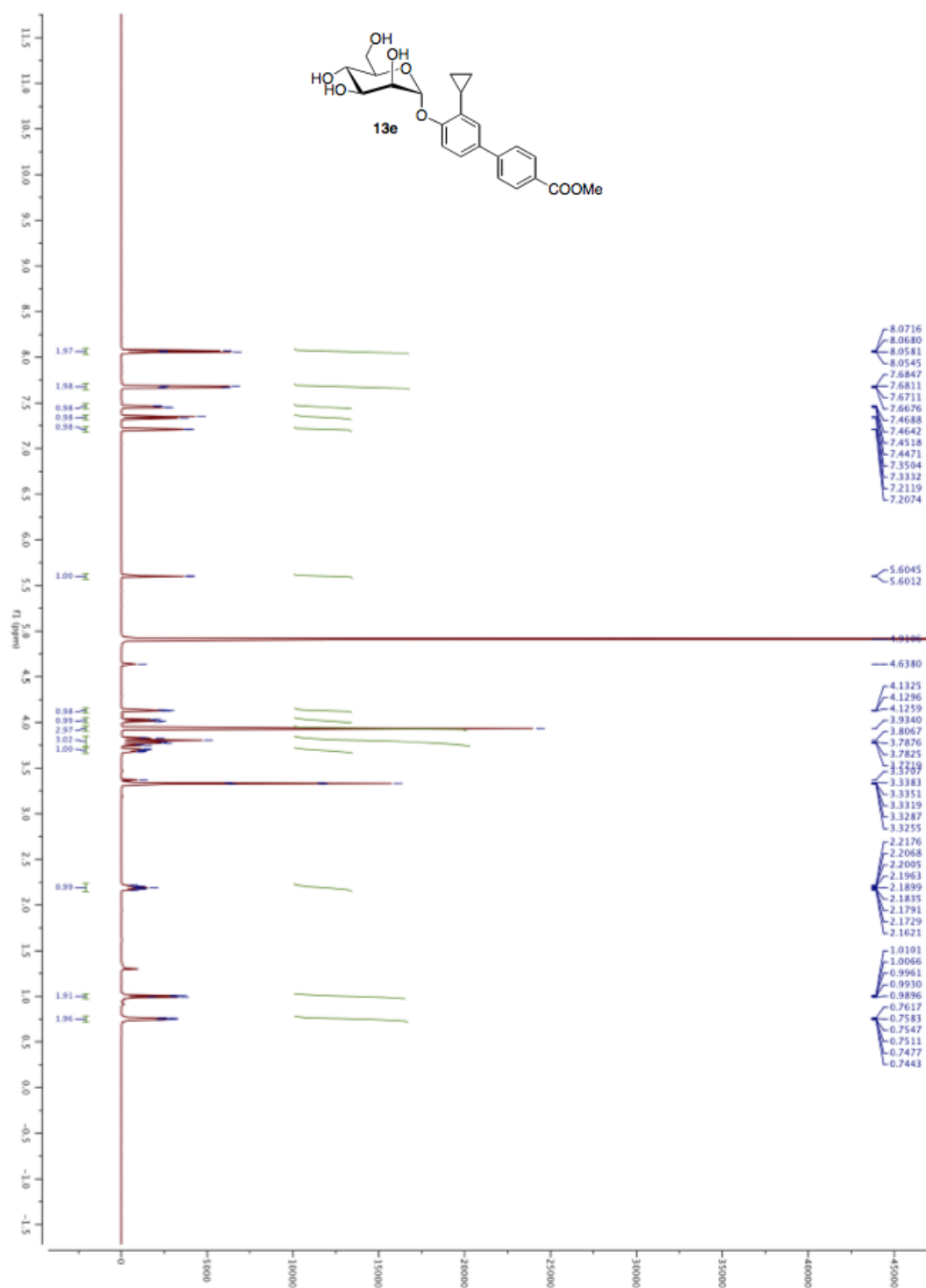
^{13}C NMR (125 MHz) of **13b**

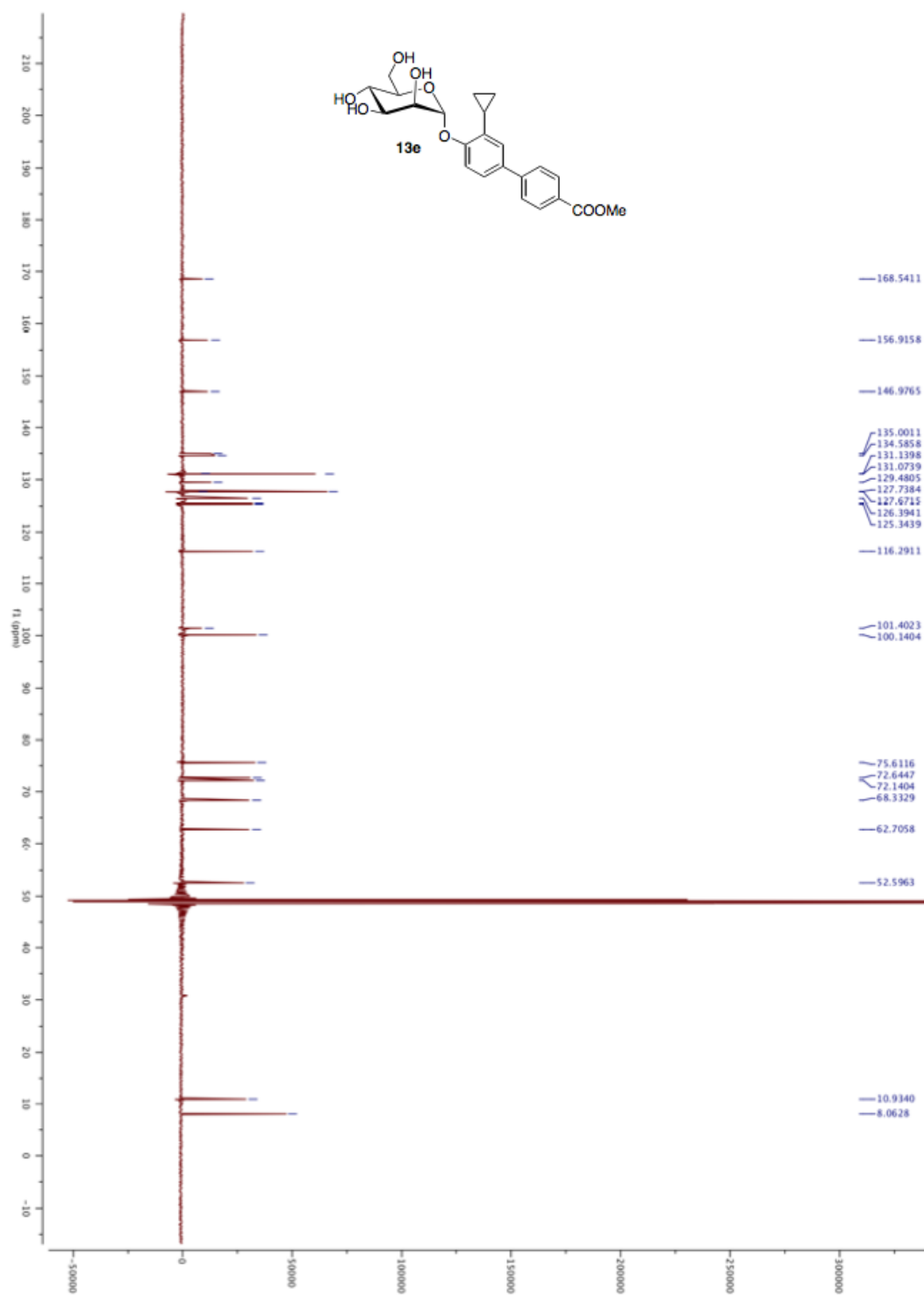
^1H NMR (500 MHz) of **13c**

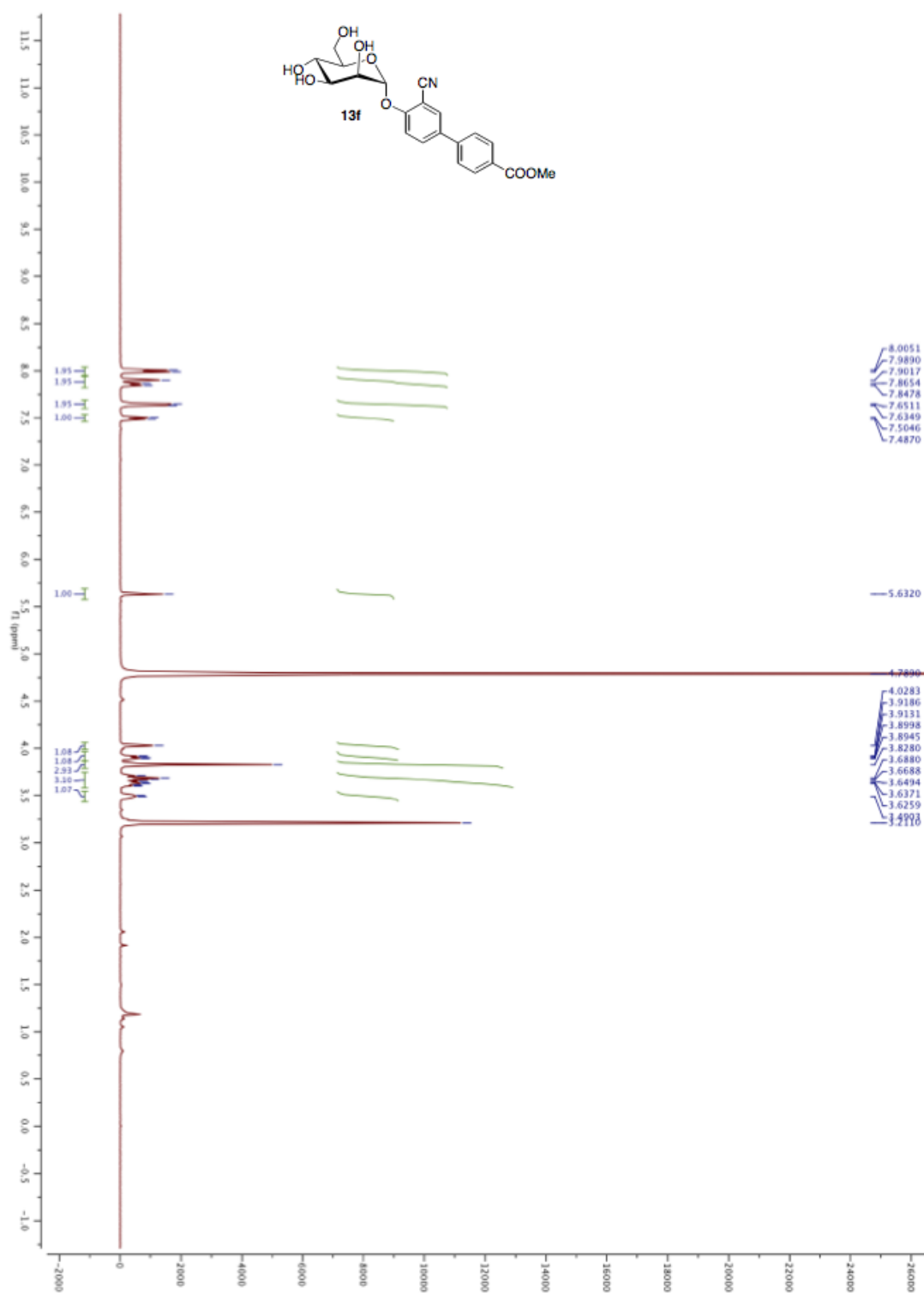
^{13}C NMR (125 MHz) of **13c**

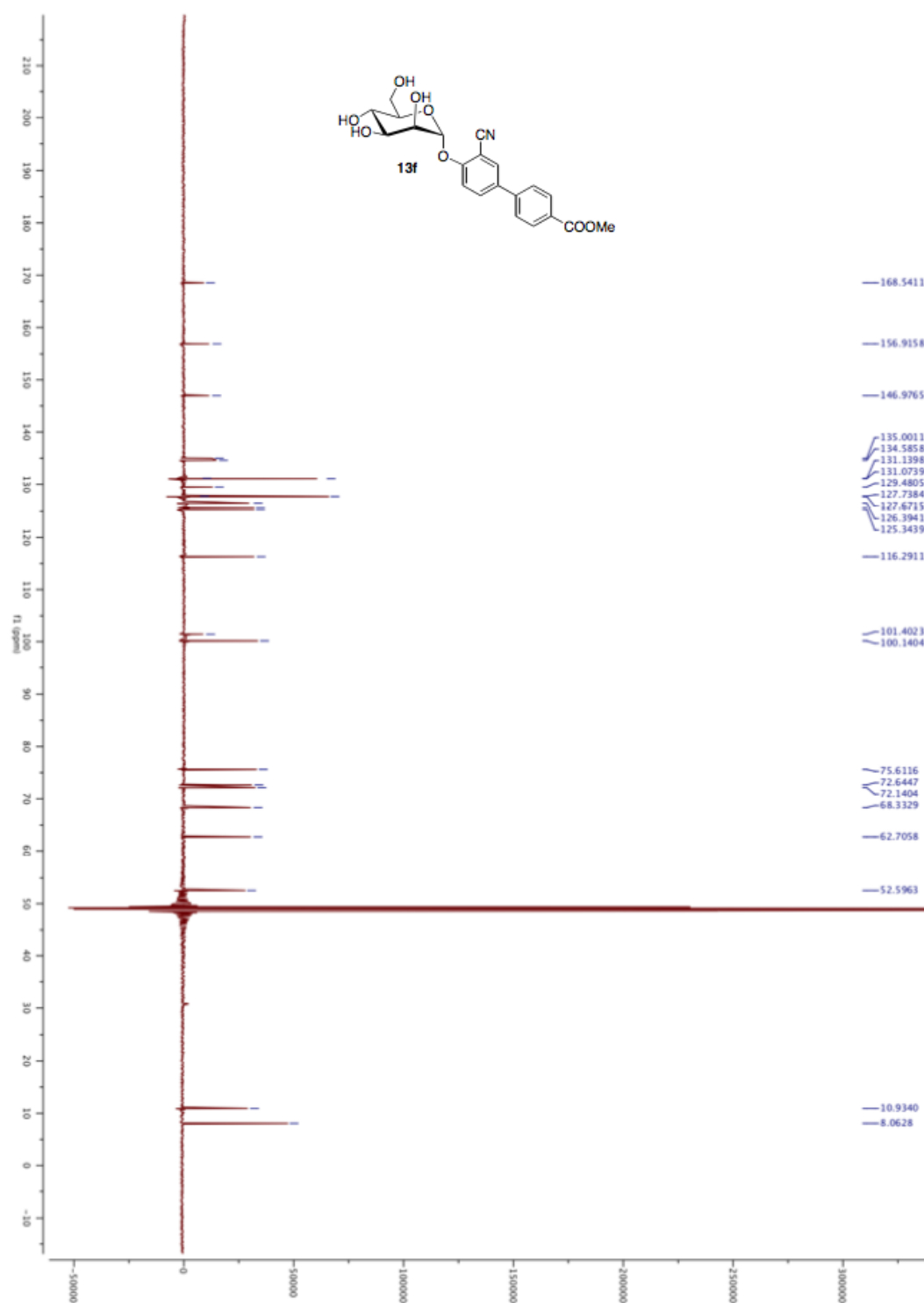
^1H NMR (500 MHz) of **13d**

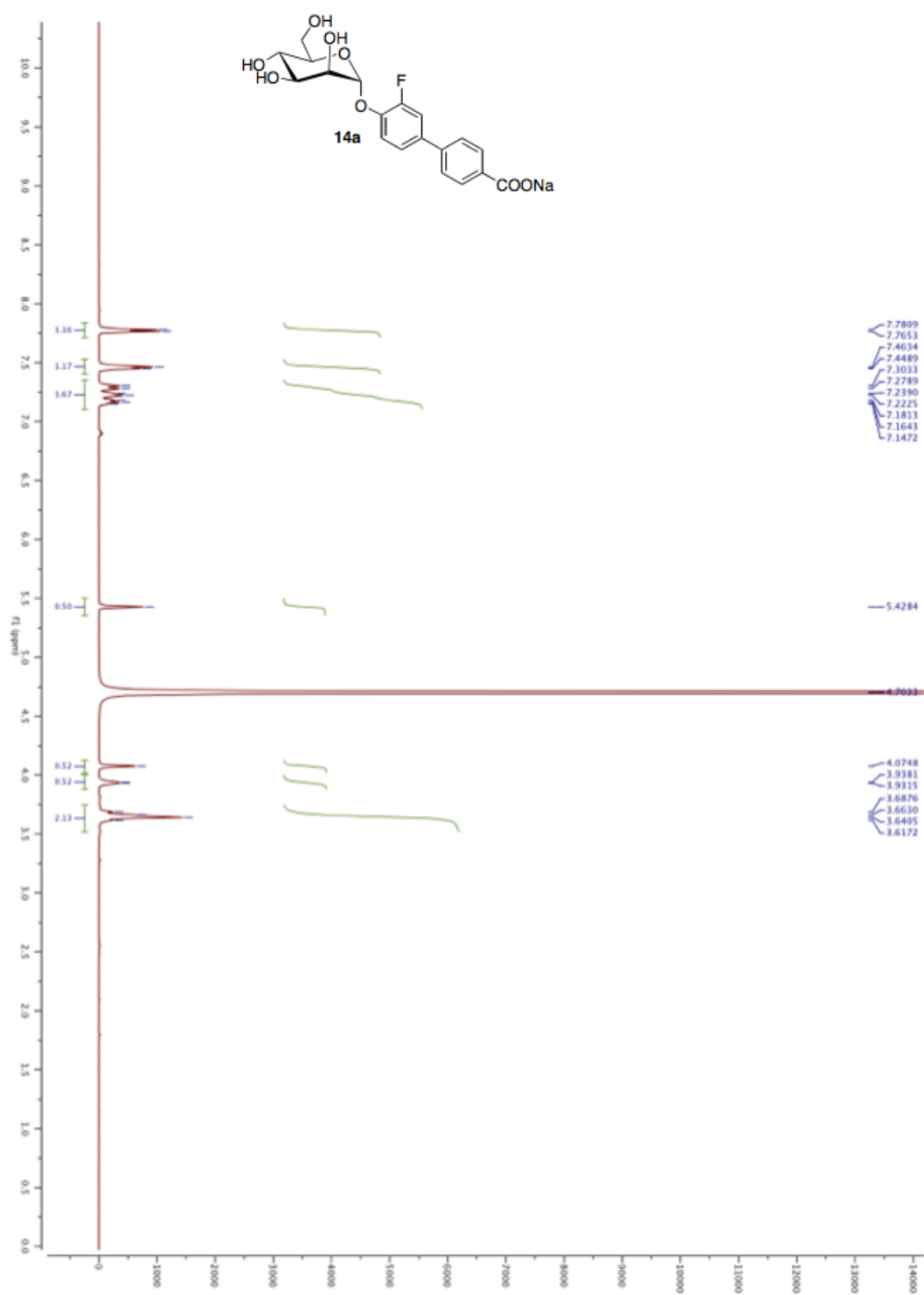
^{13}C NMR (125 MHz) of **13d**

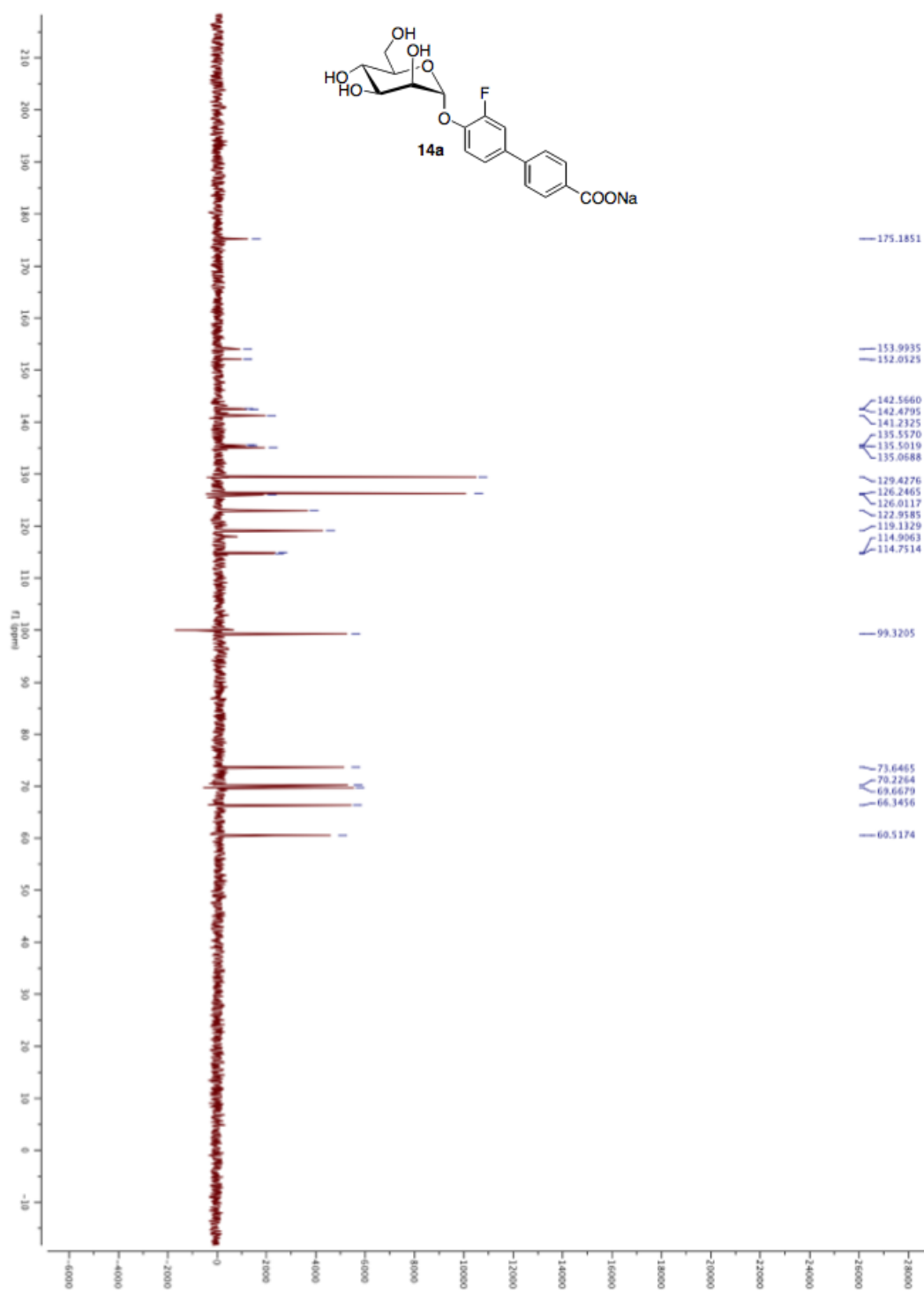
^1H NMR (500 MHz) of **13e**

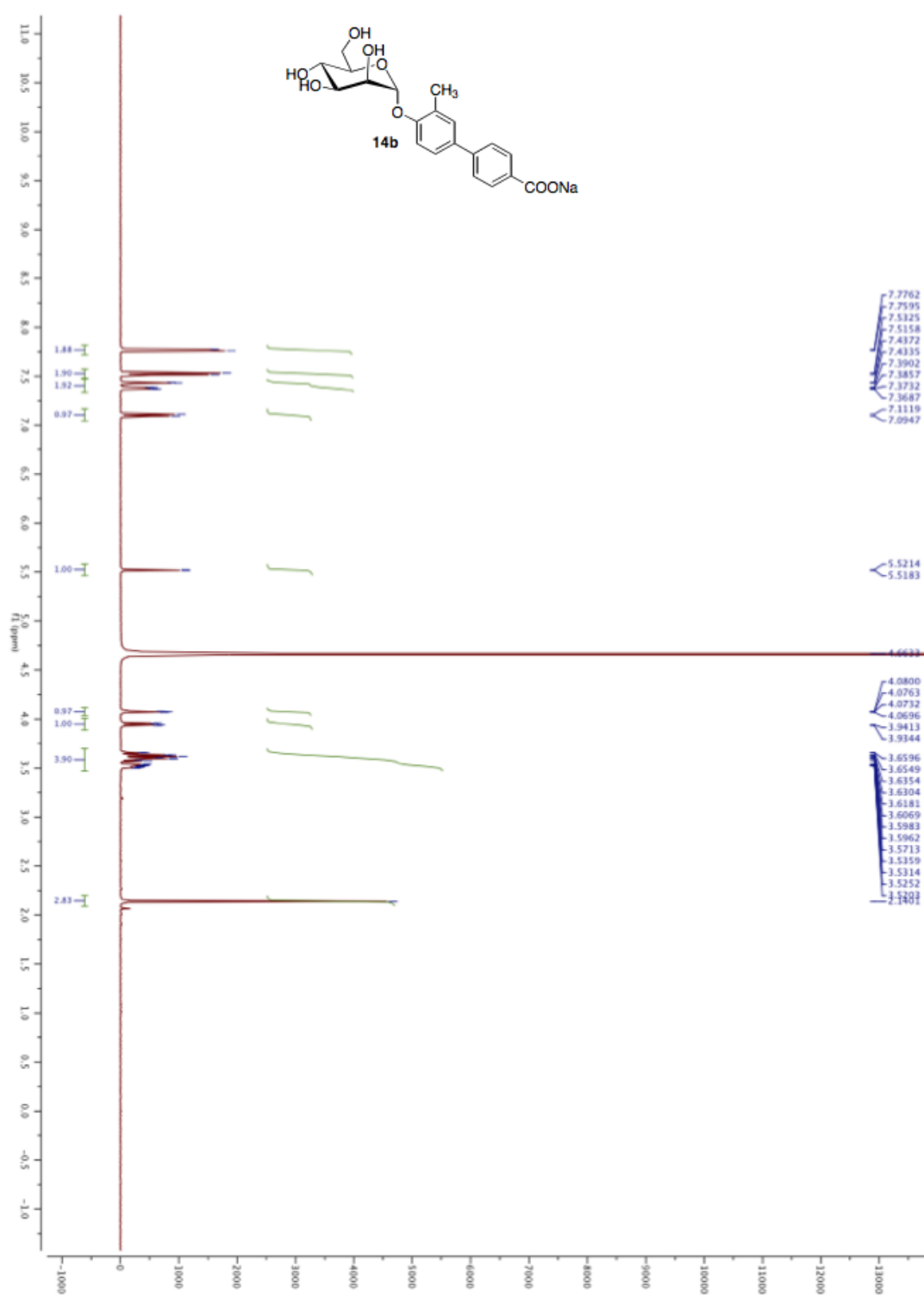
^{13}C NMR (125 MHz) of **13e**

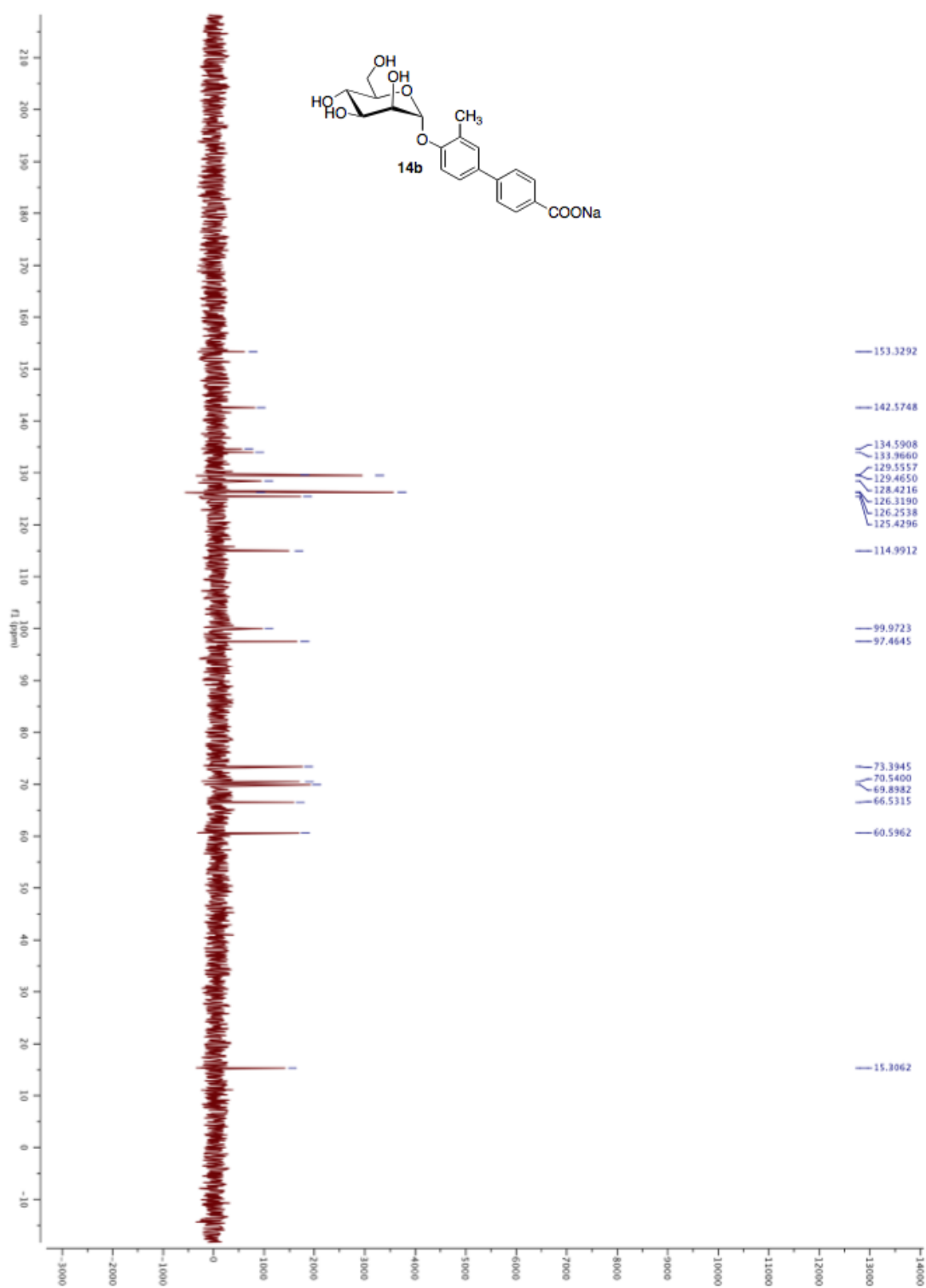
^1H NMR (500 MHz) of **13f**

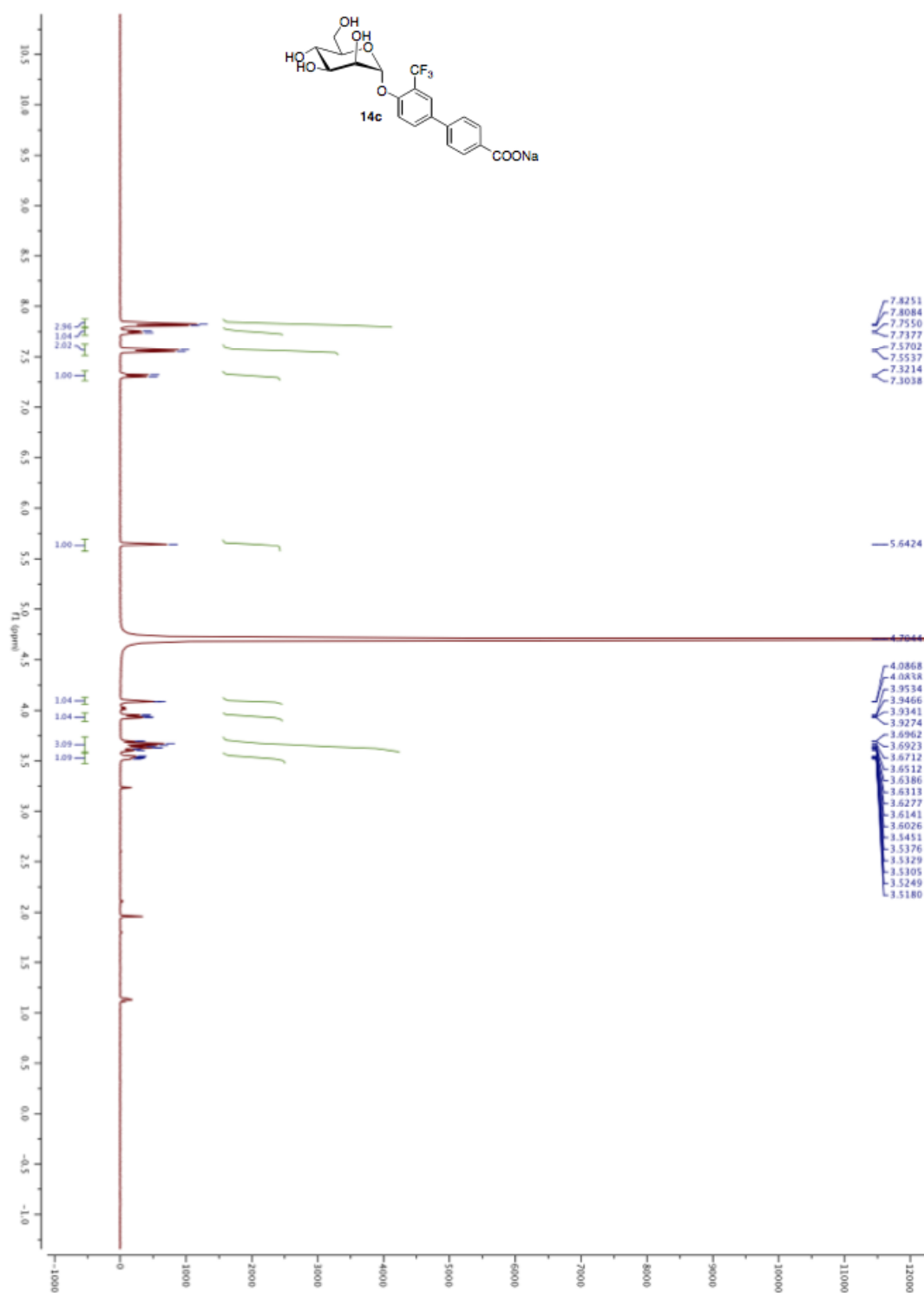
^{13}C NMR (125 MHz) of **13f**

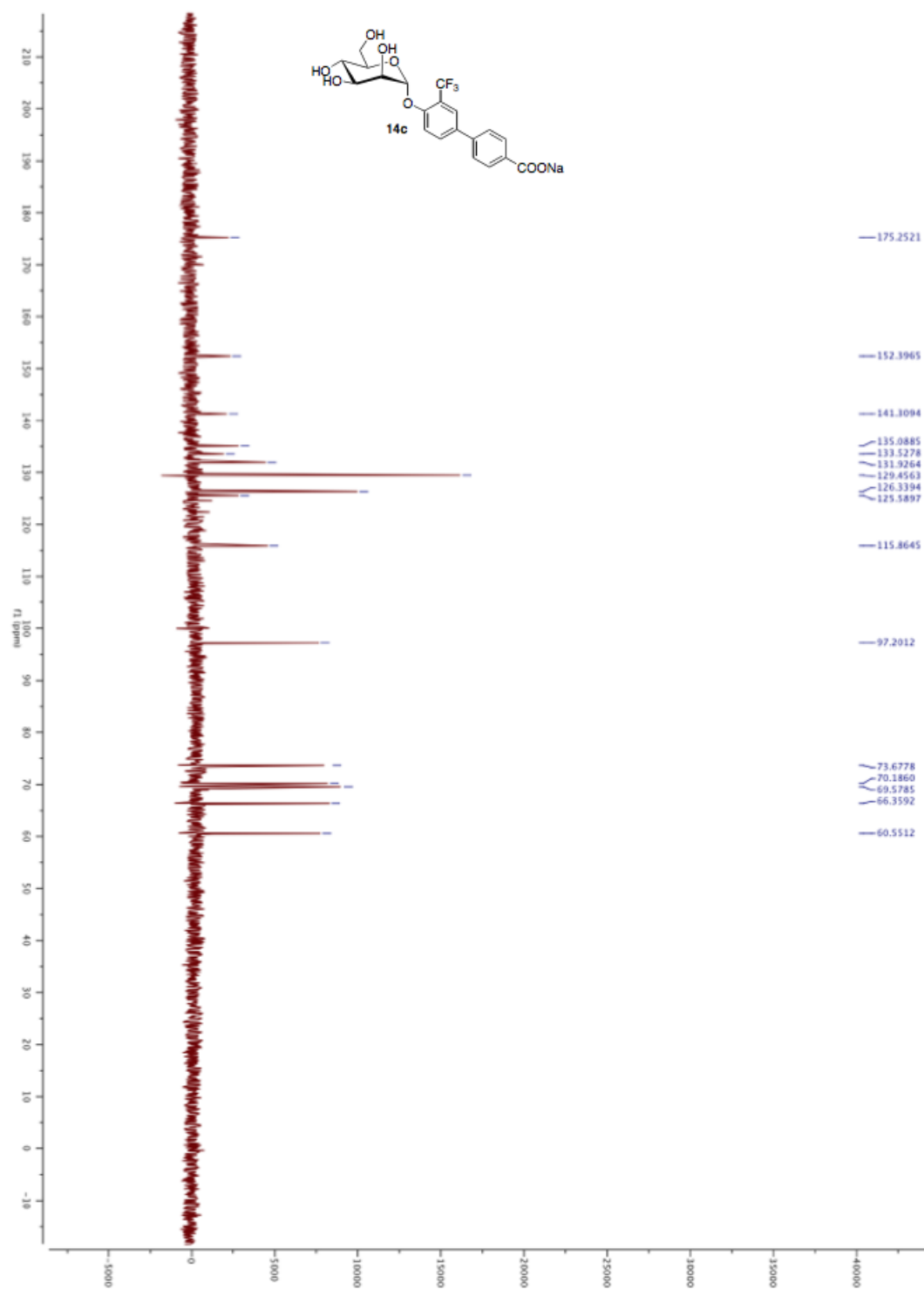
^1H NMR (500 MHz) of **14a**

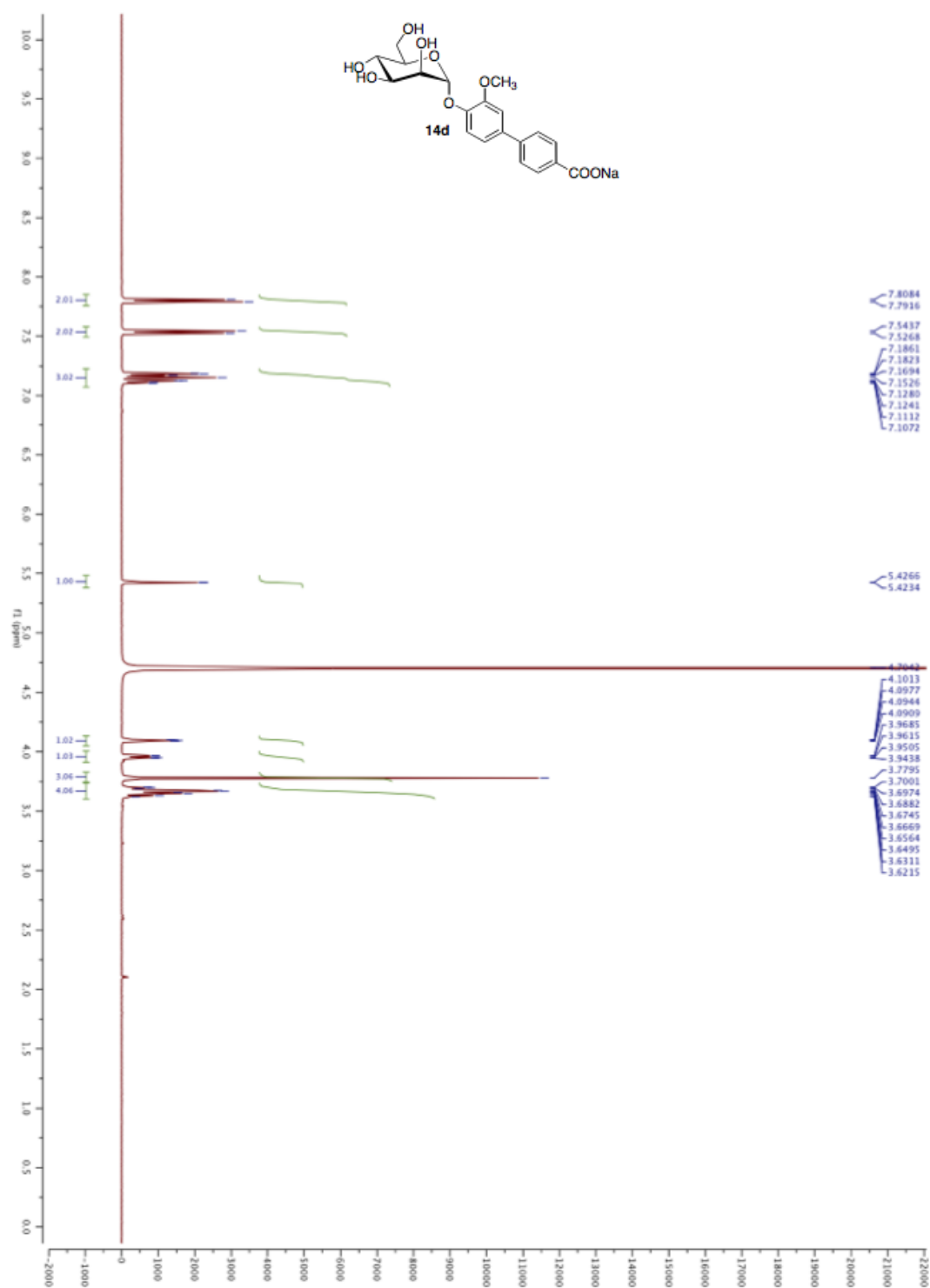
^{13}C NMR (125 MHz) of **14a**

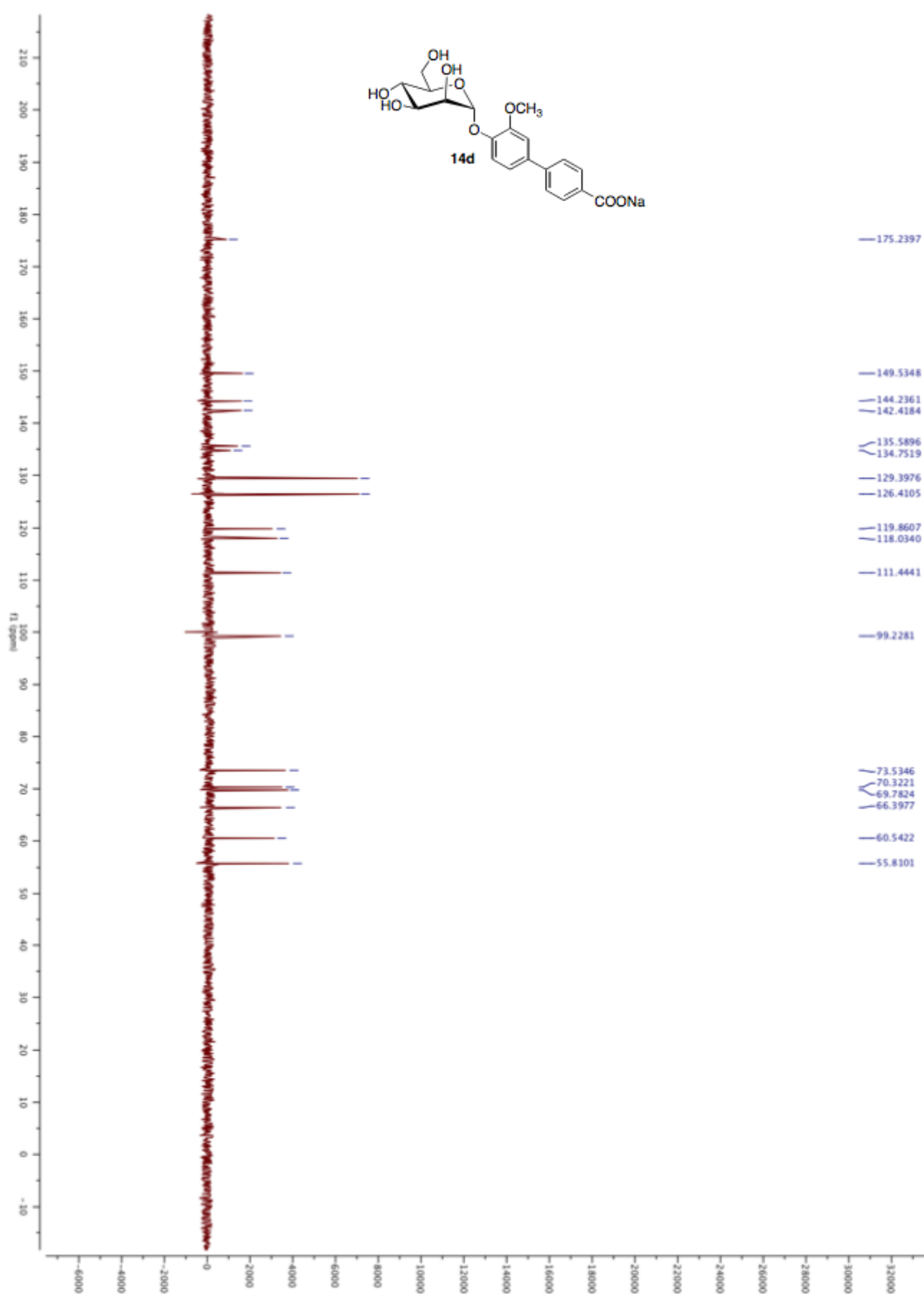
^1H NMR (500 MHz) of **14b**

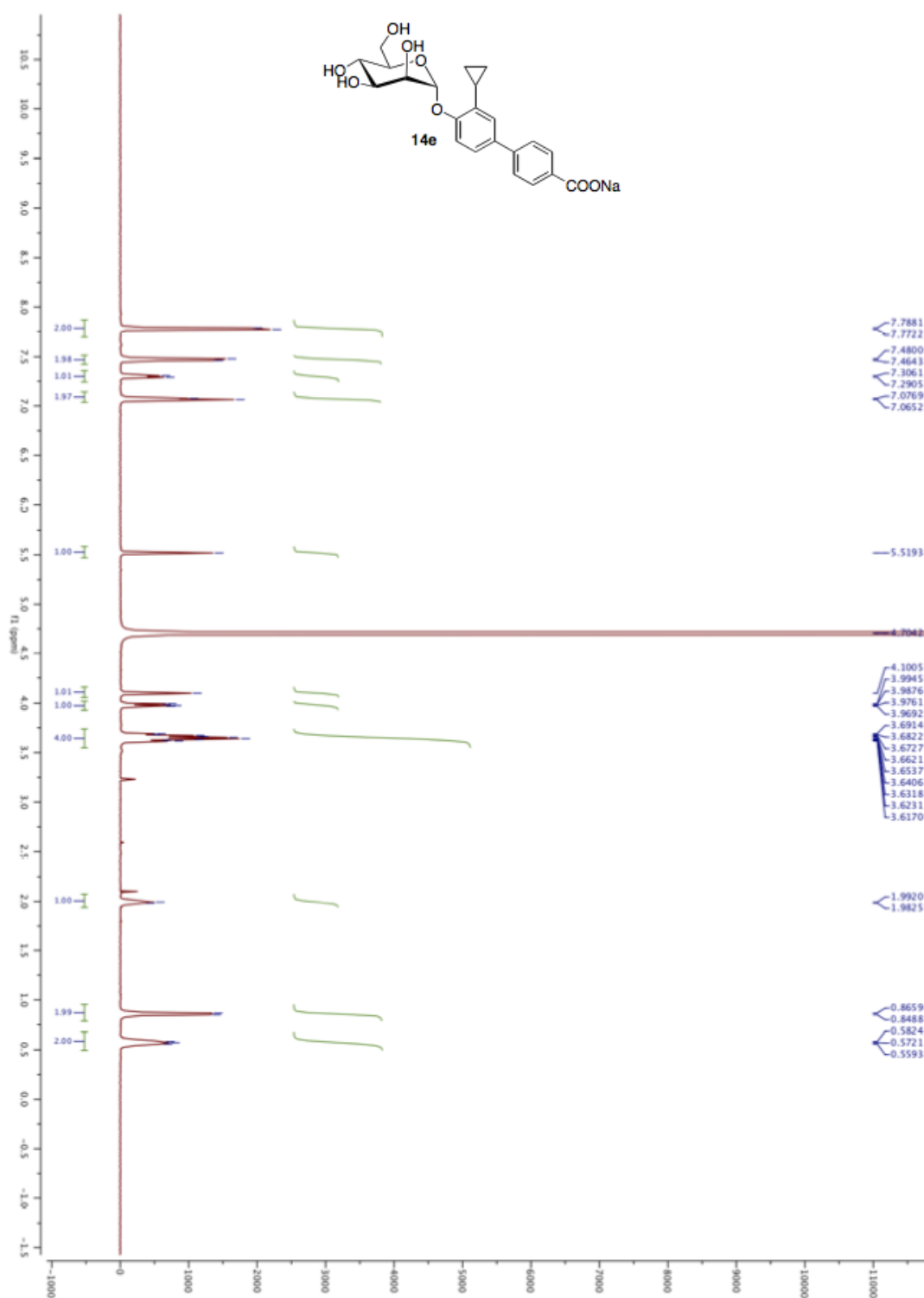
^{13}C NMR (125 MHz) of **14b**

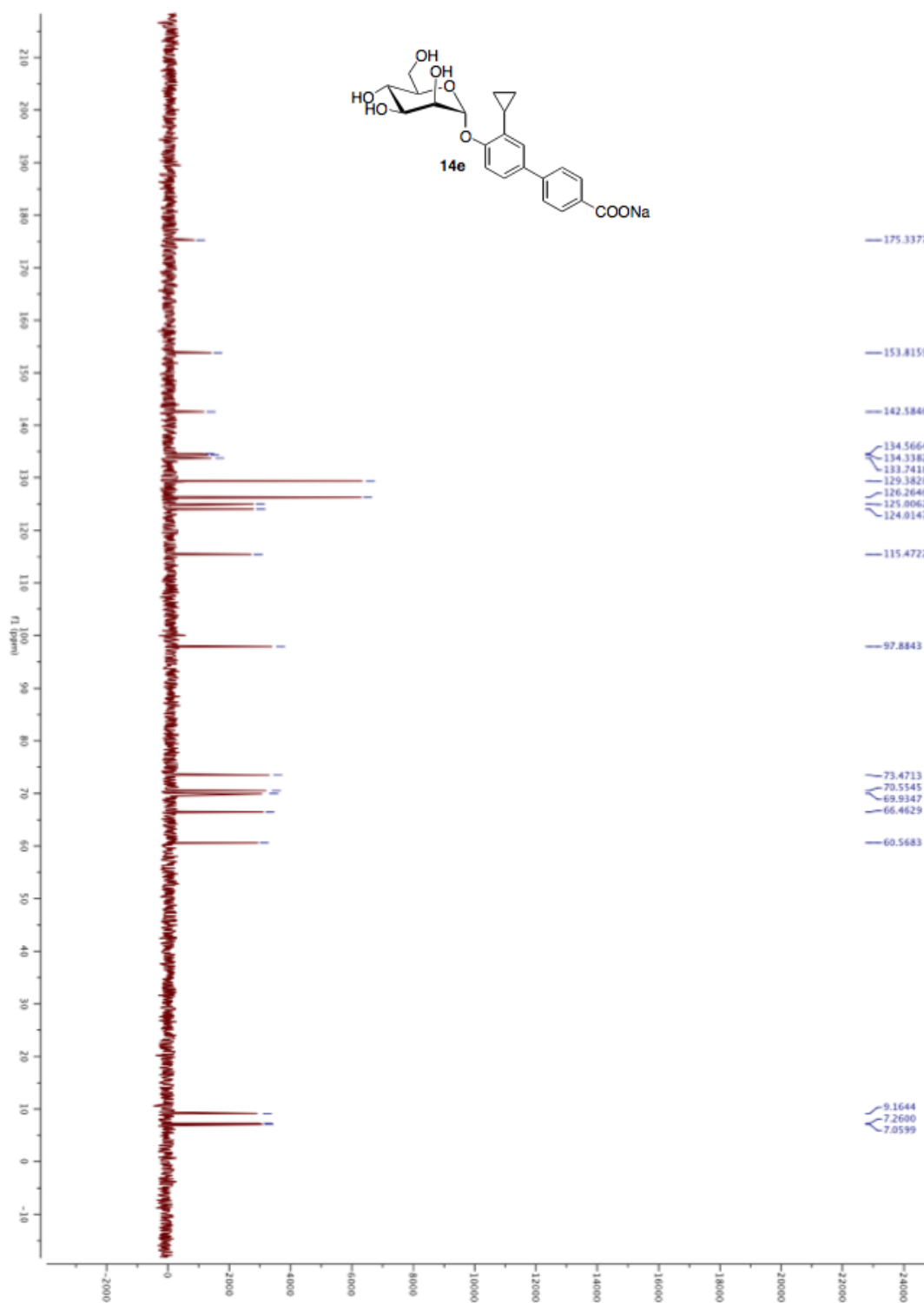
^1H NMR (500 MHz) of **14c**

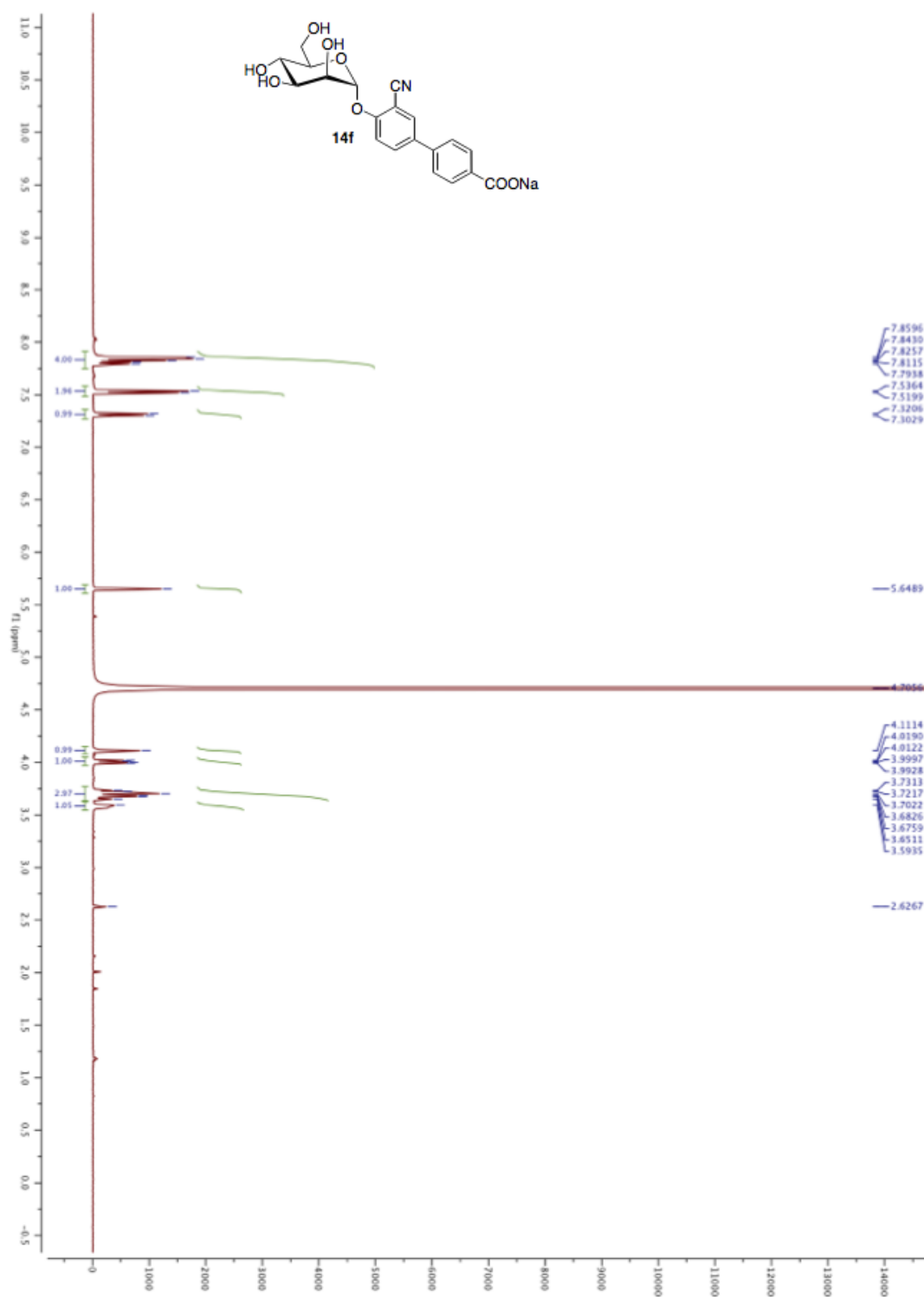
^{13}C NMR (125 MHz) of **14c**

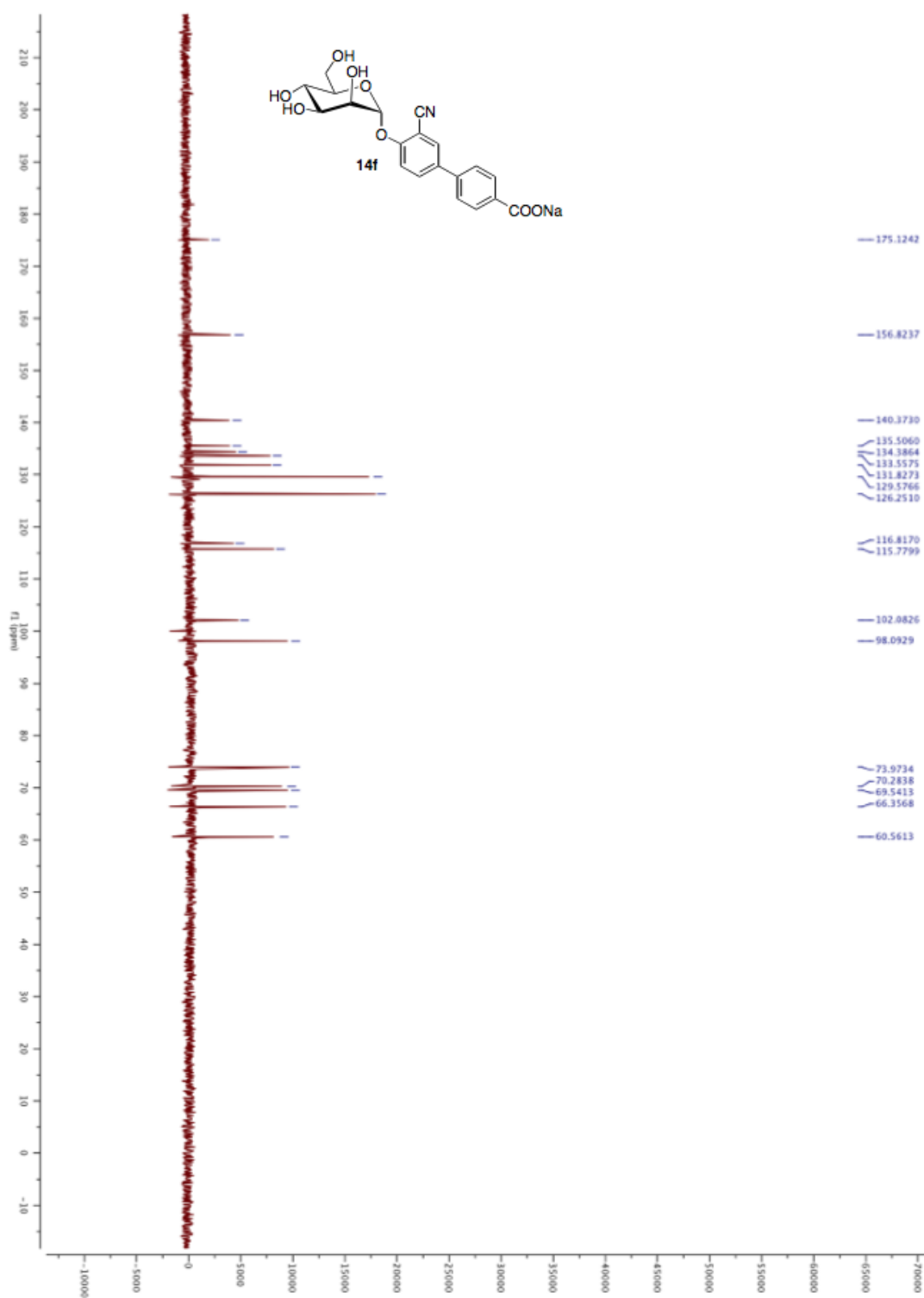
^1H NMR (500 MHz) of **14d**

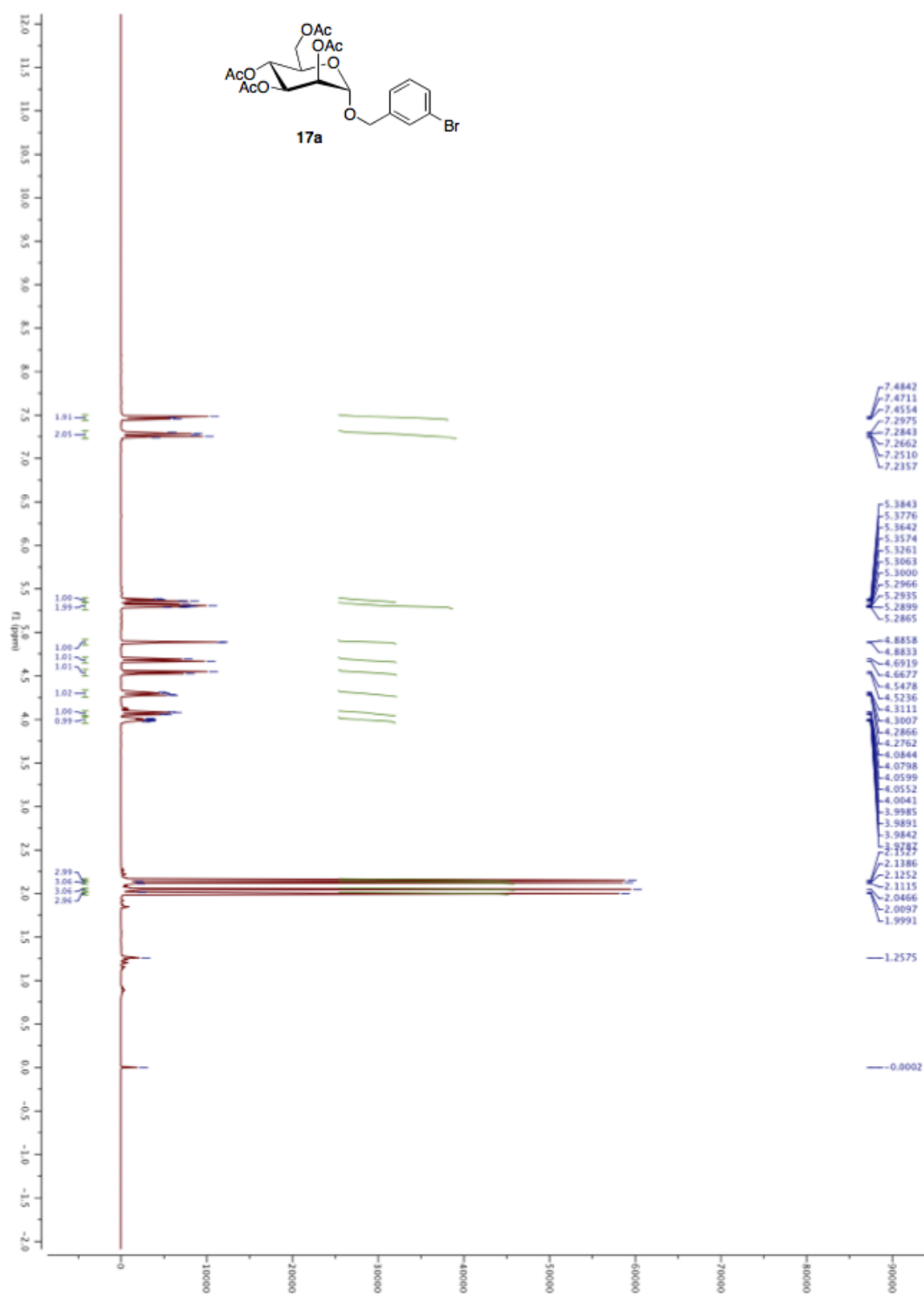
^{13}C NMR (125 MHz) of **14d**

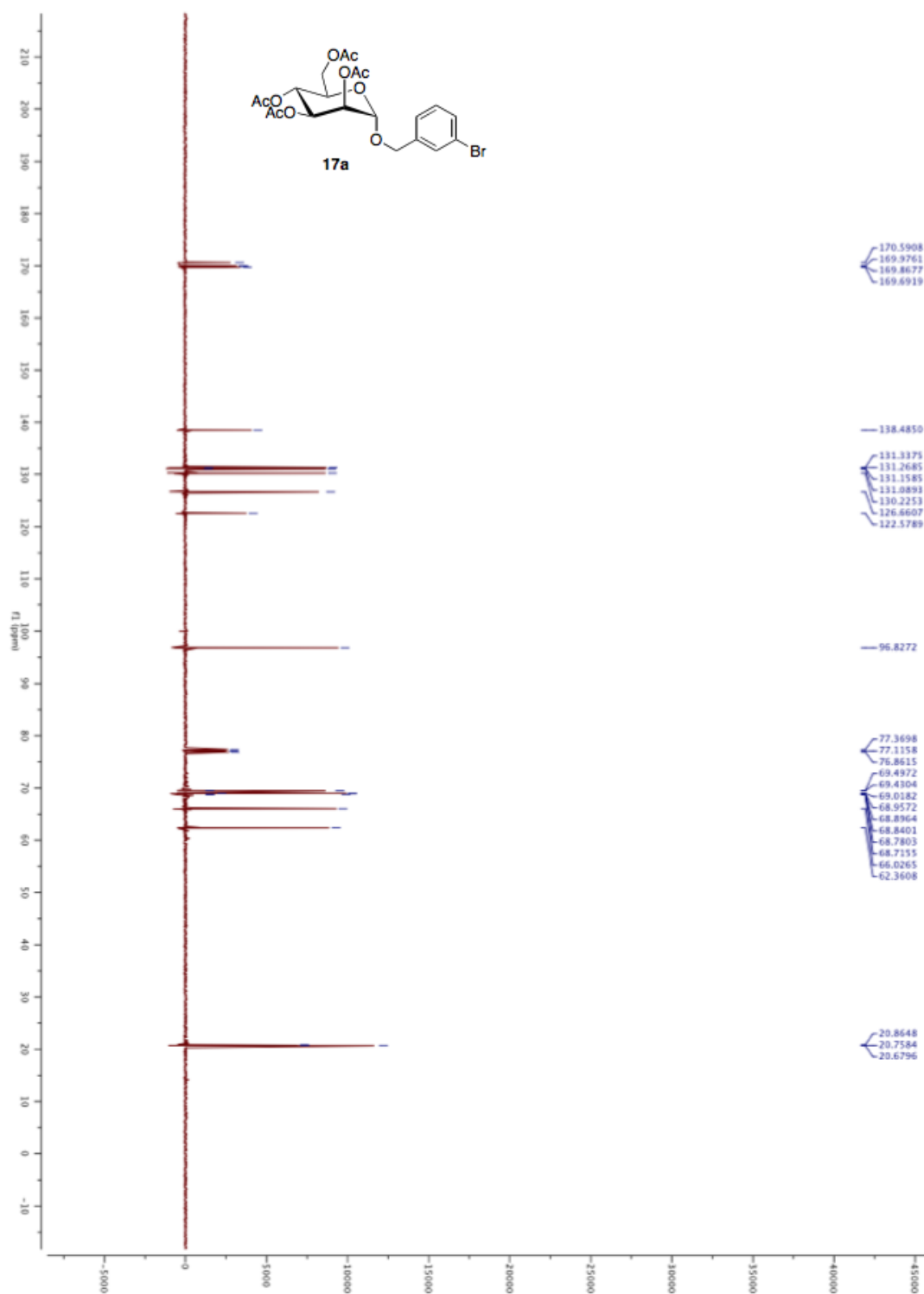
^1H NMR (500 MHz) of **14e**

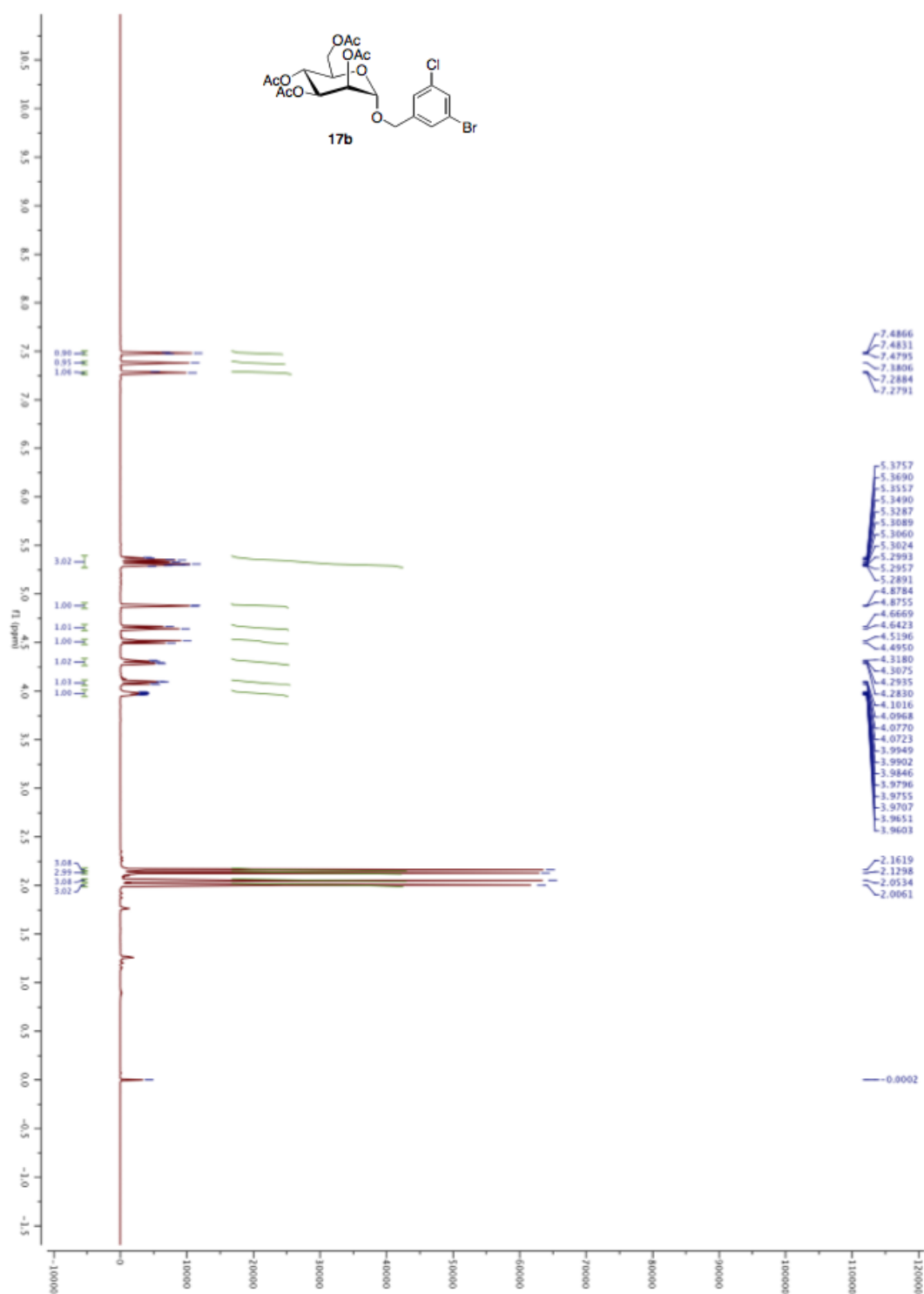
^{13}C NMR (125 MHz) of **14e**

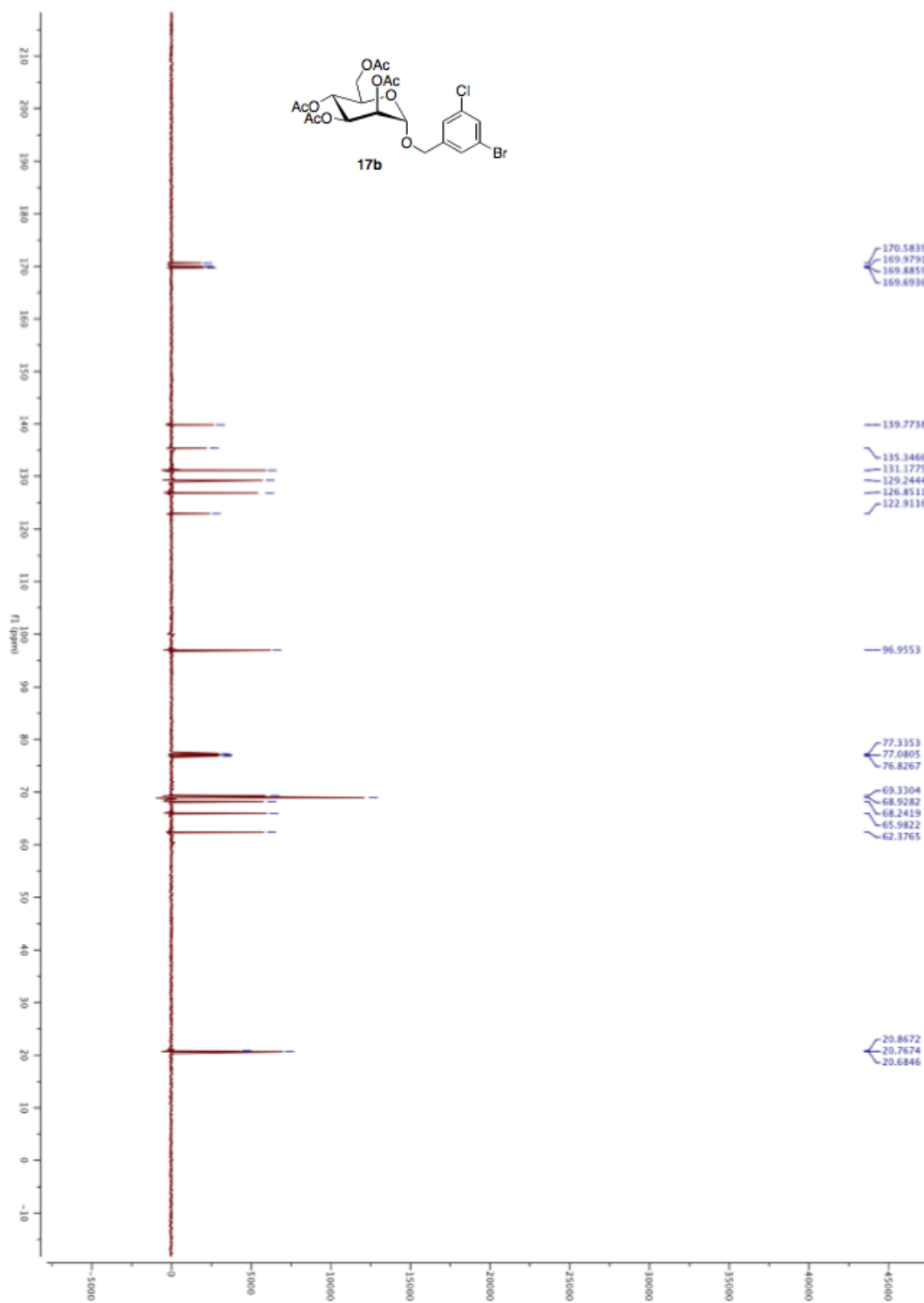
^1H NMR (500 MHz) of **14f**

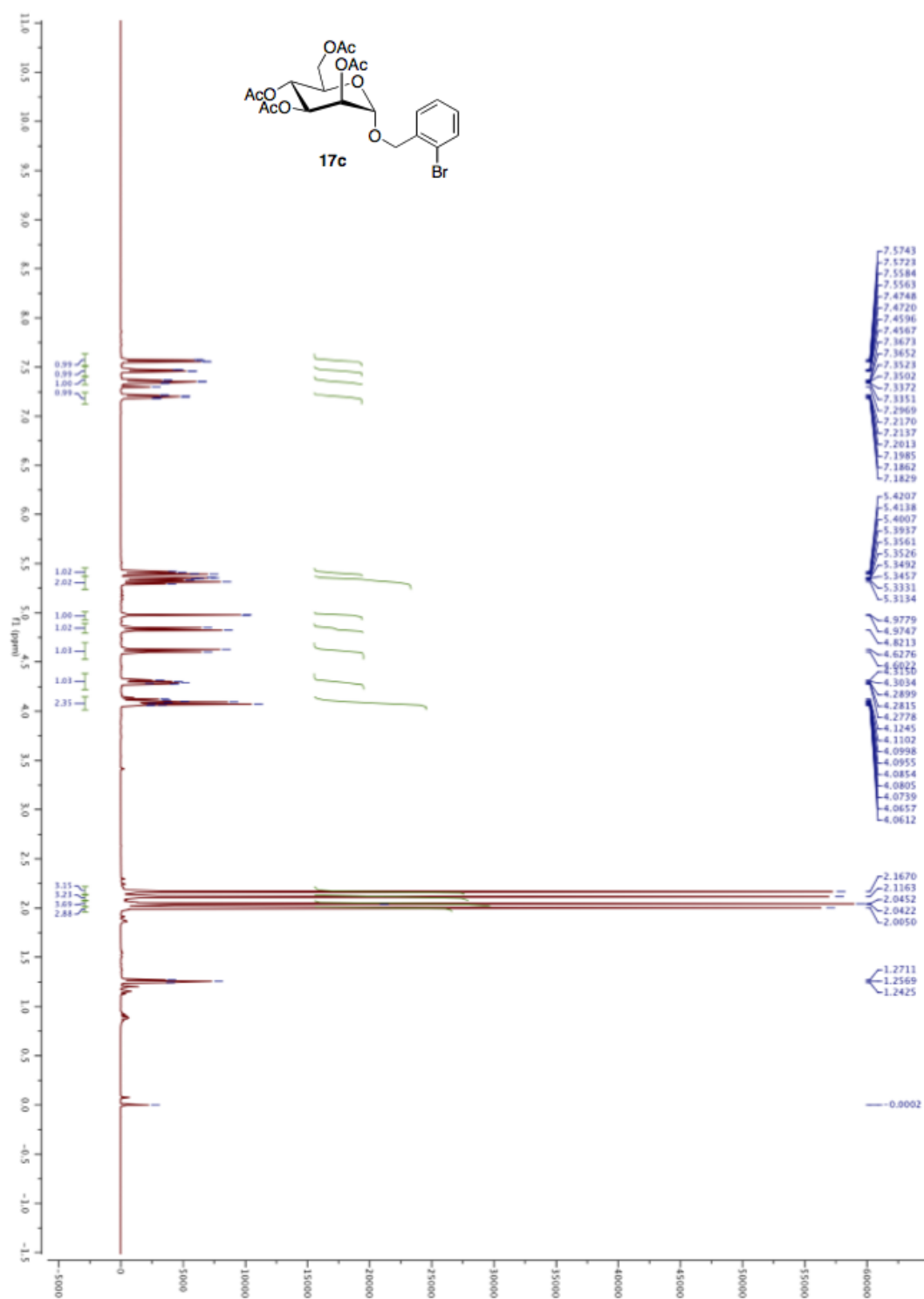
^{13}C NMR (125 MHz) of **14f**

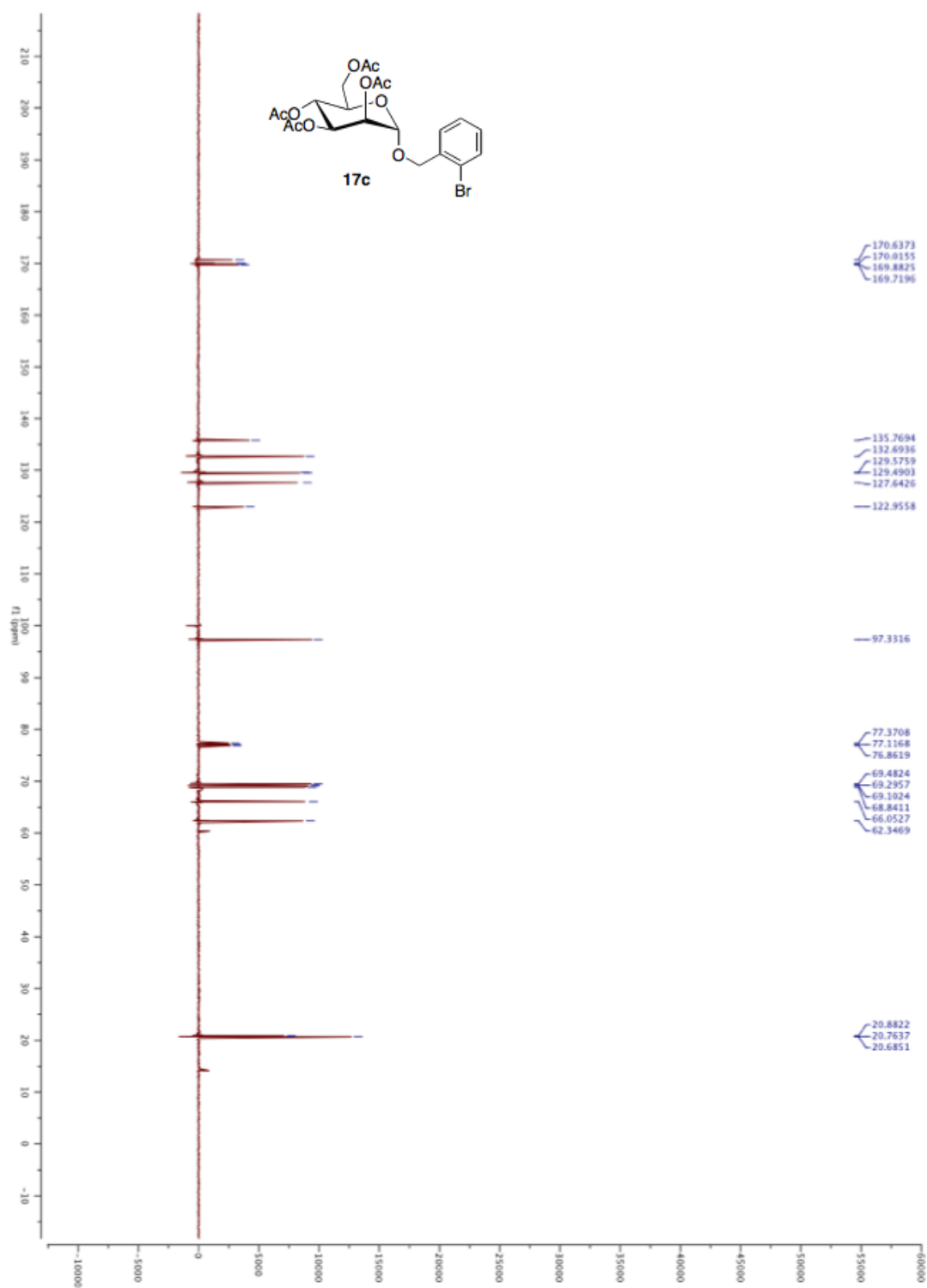
^1H NMR (500 MHz) of **17a**

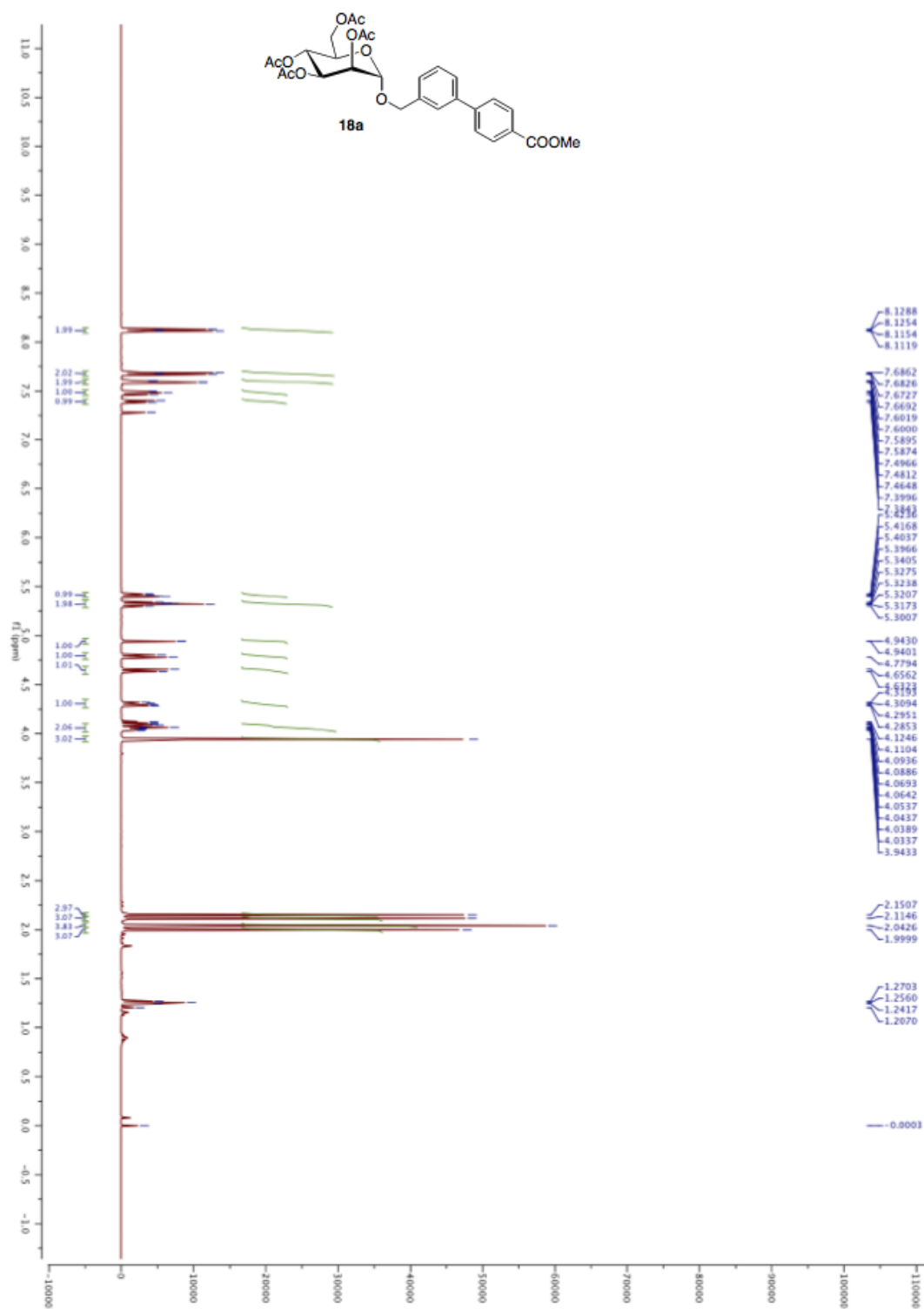
^{13}C NMR (125 MHz) of **17a**

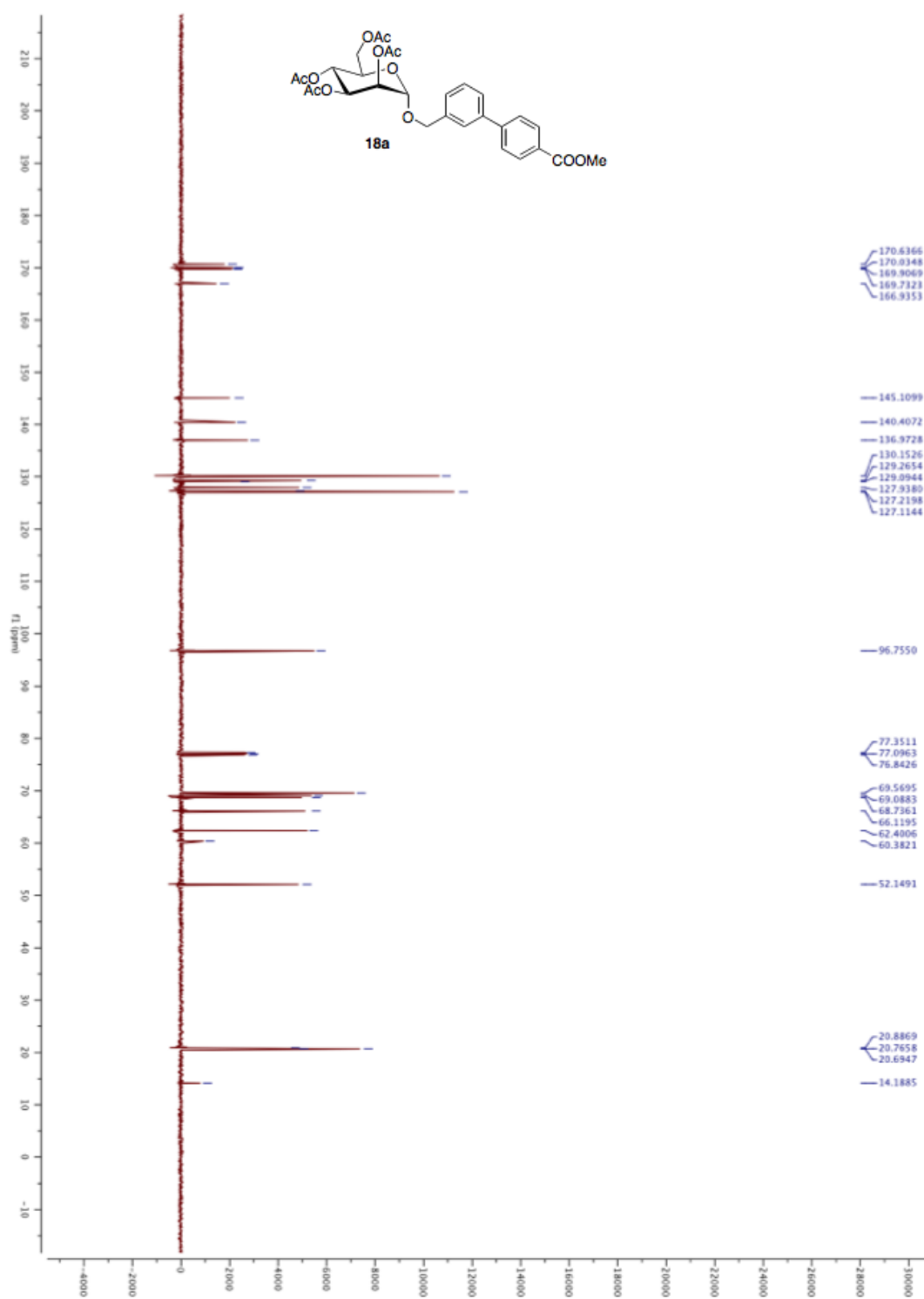
^1H NMR (500 MHz) of **17b**

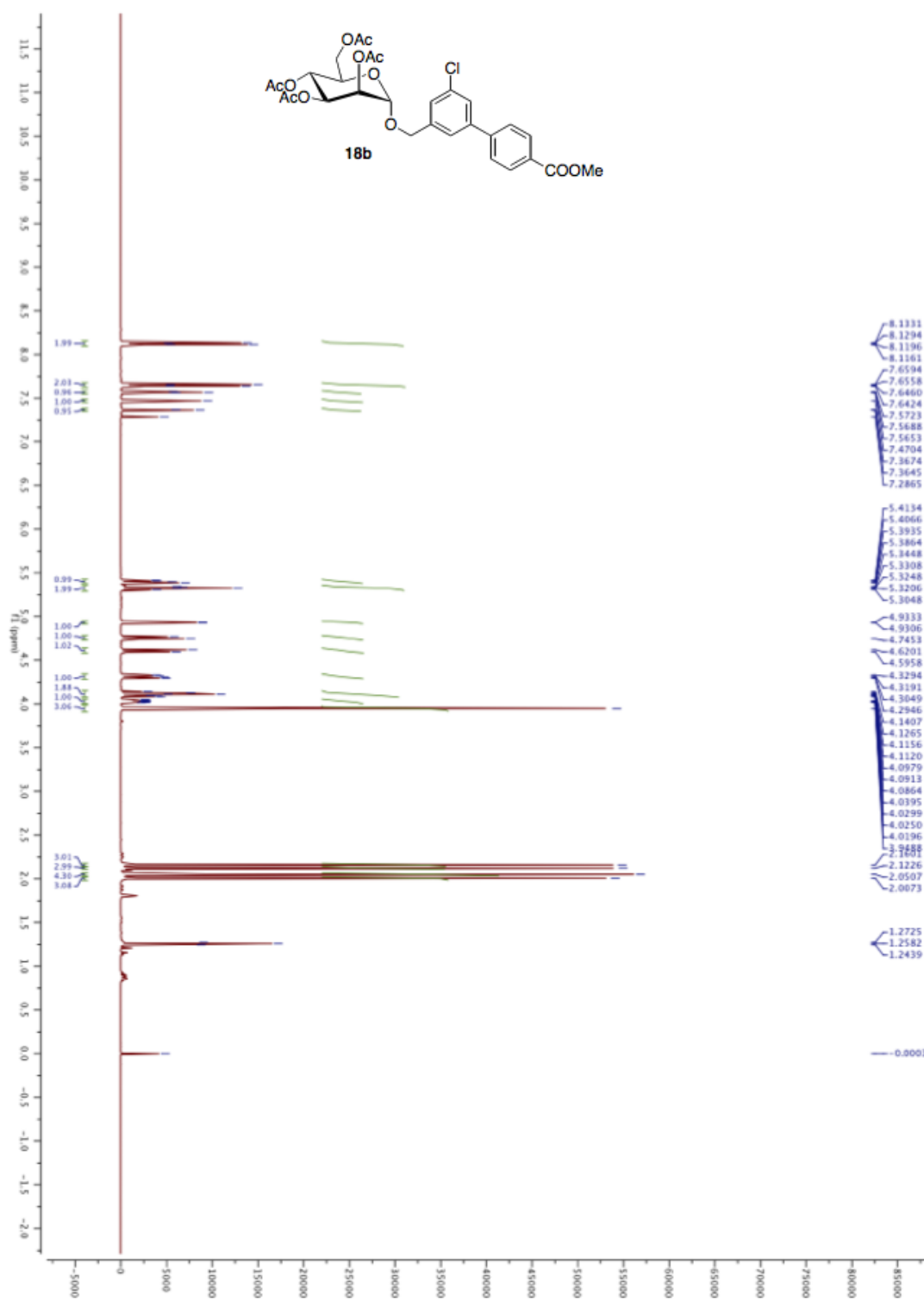
^{13}C NMR (125 MHz) of **17b**

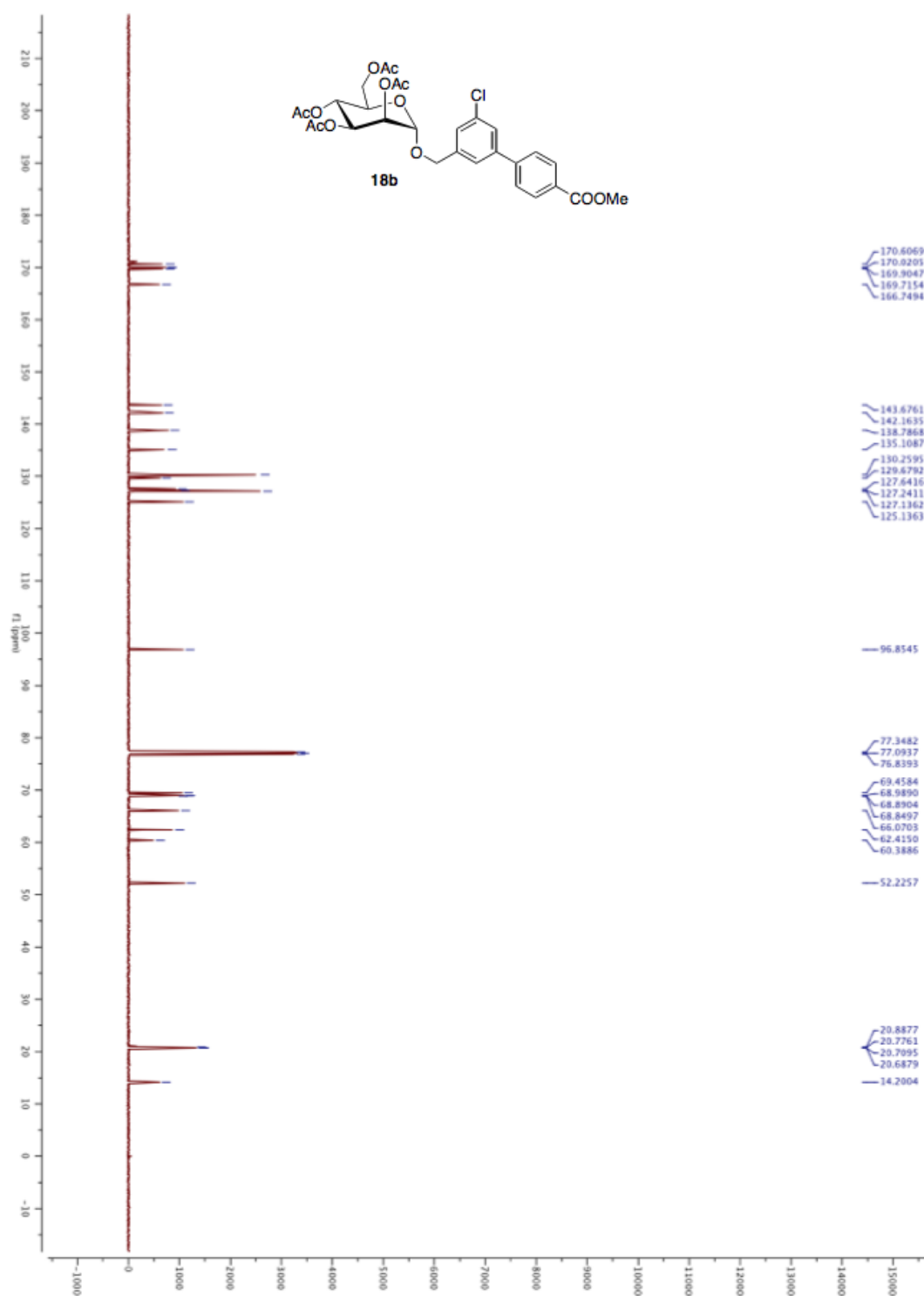
^1H NMR (500 MHz) of **17c**

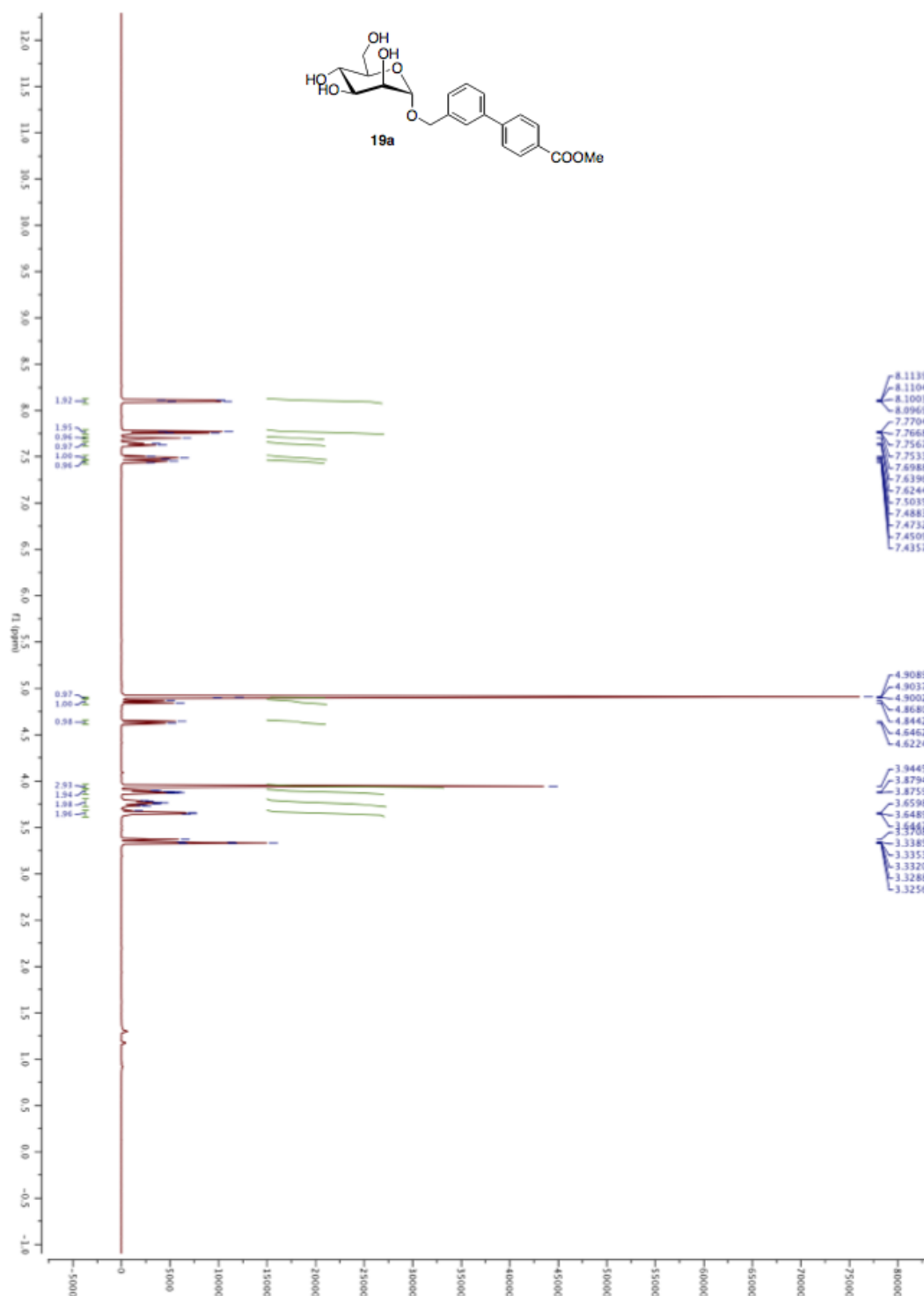
^{13}C NMR (125 MHz) of **17c**

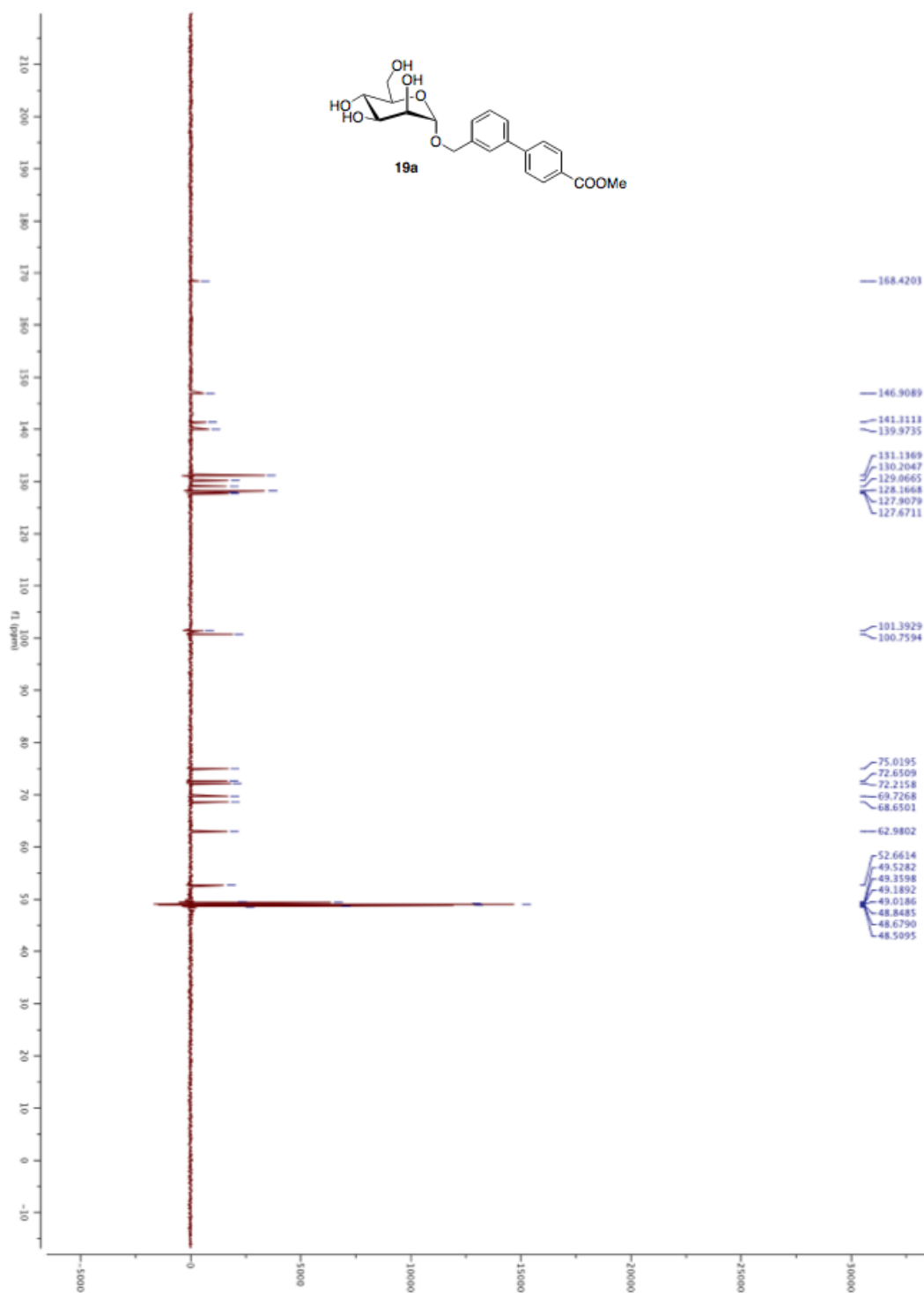
^1H NMR (500 MHz) of **18a**

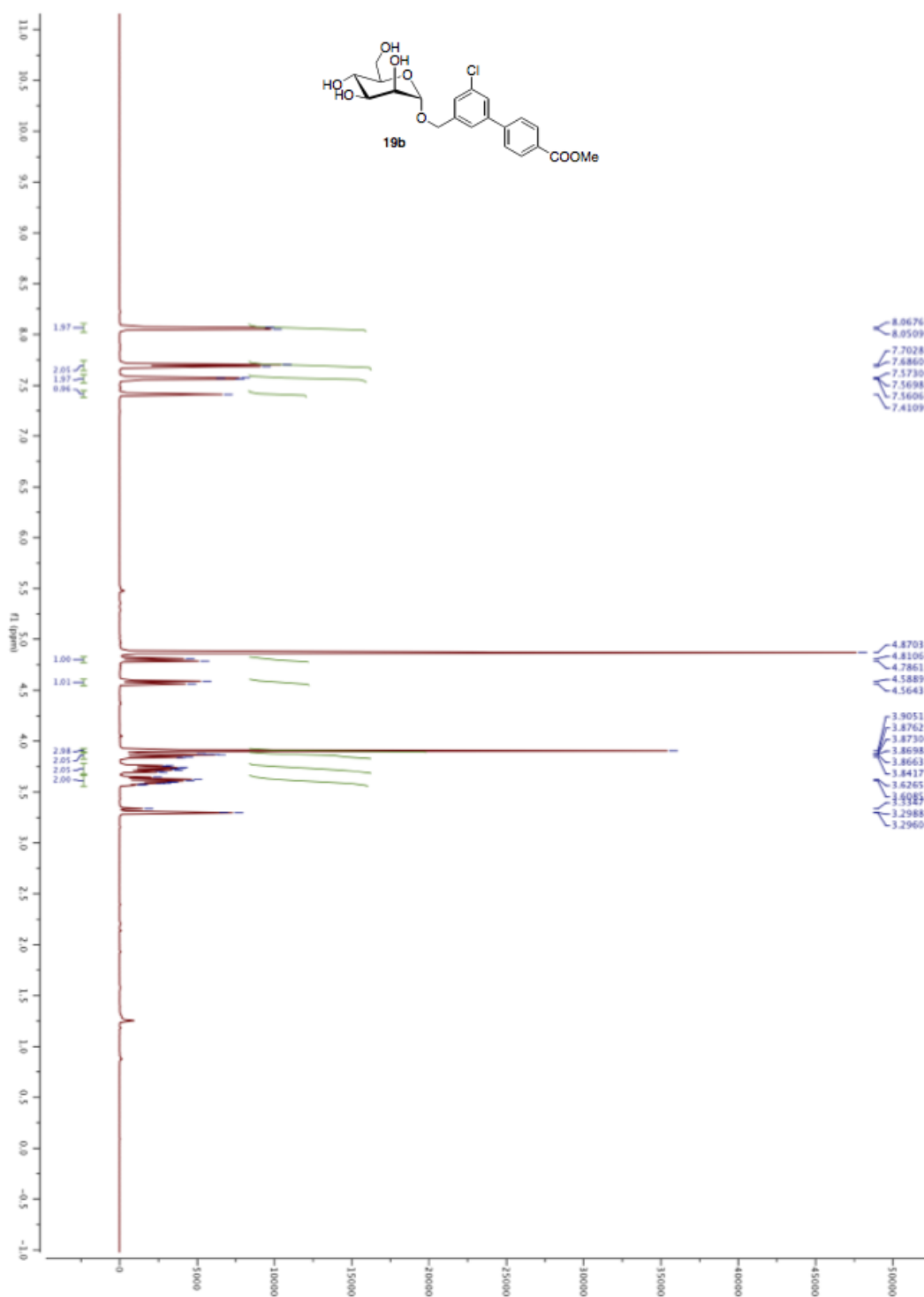
^{13}C NMR (125 MHz) of **18a**

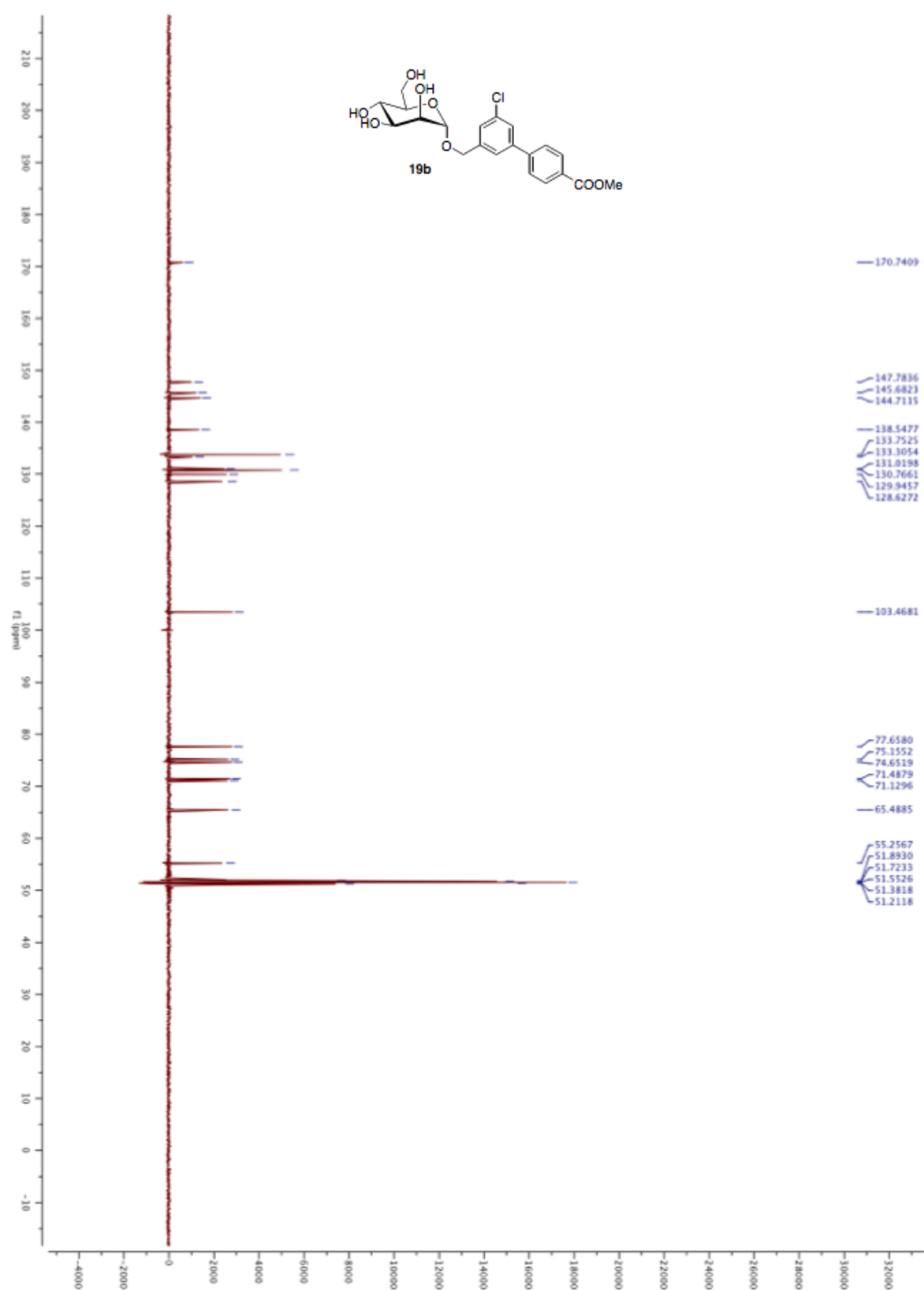
^1H NMR (500 MHz) of **18b**

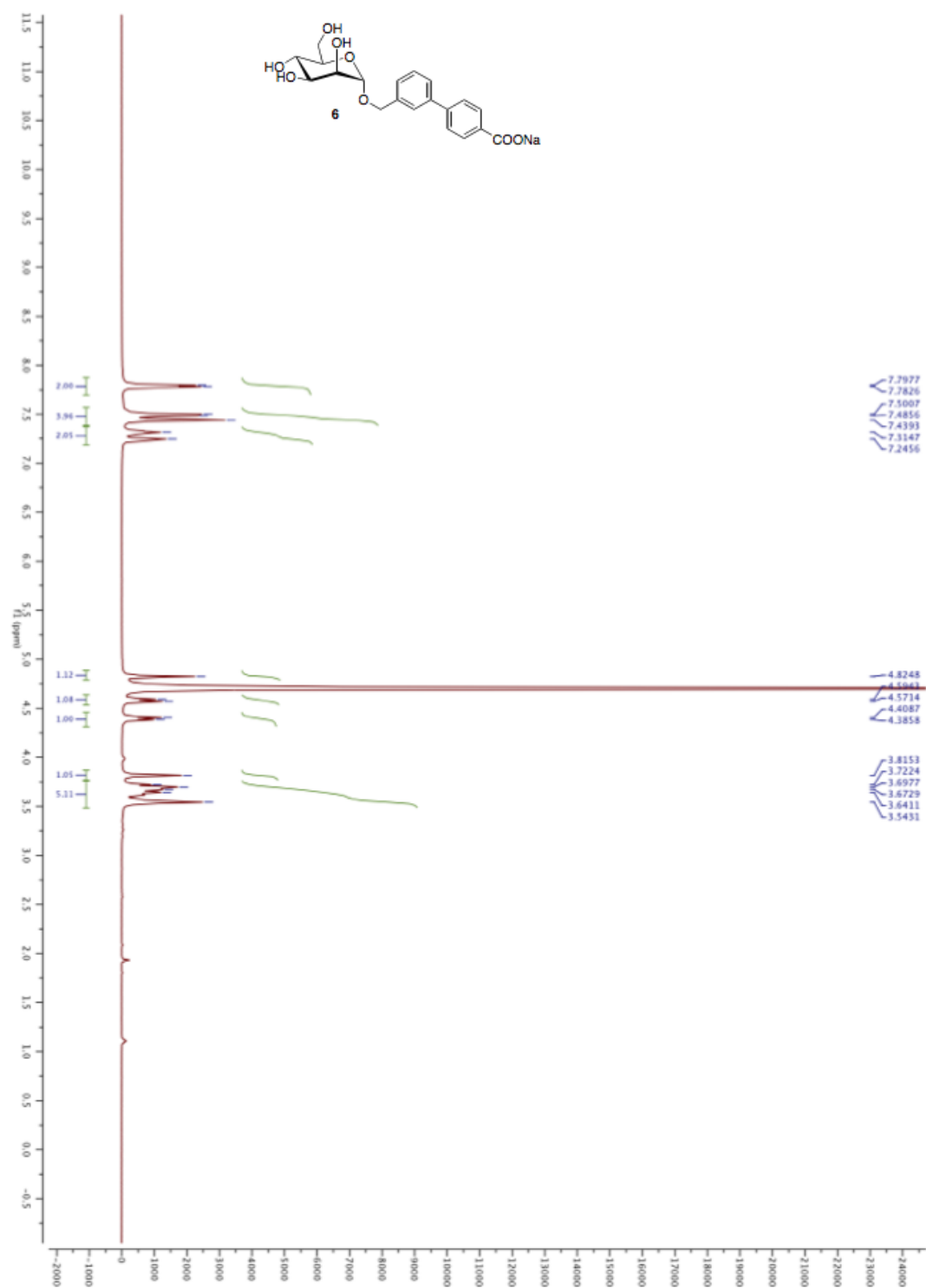
^{13}C NMR (125 MHz) of **18b**

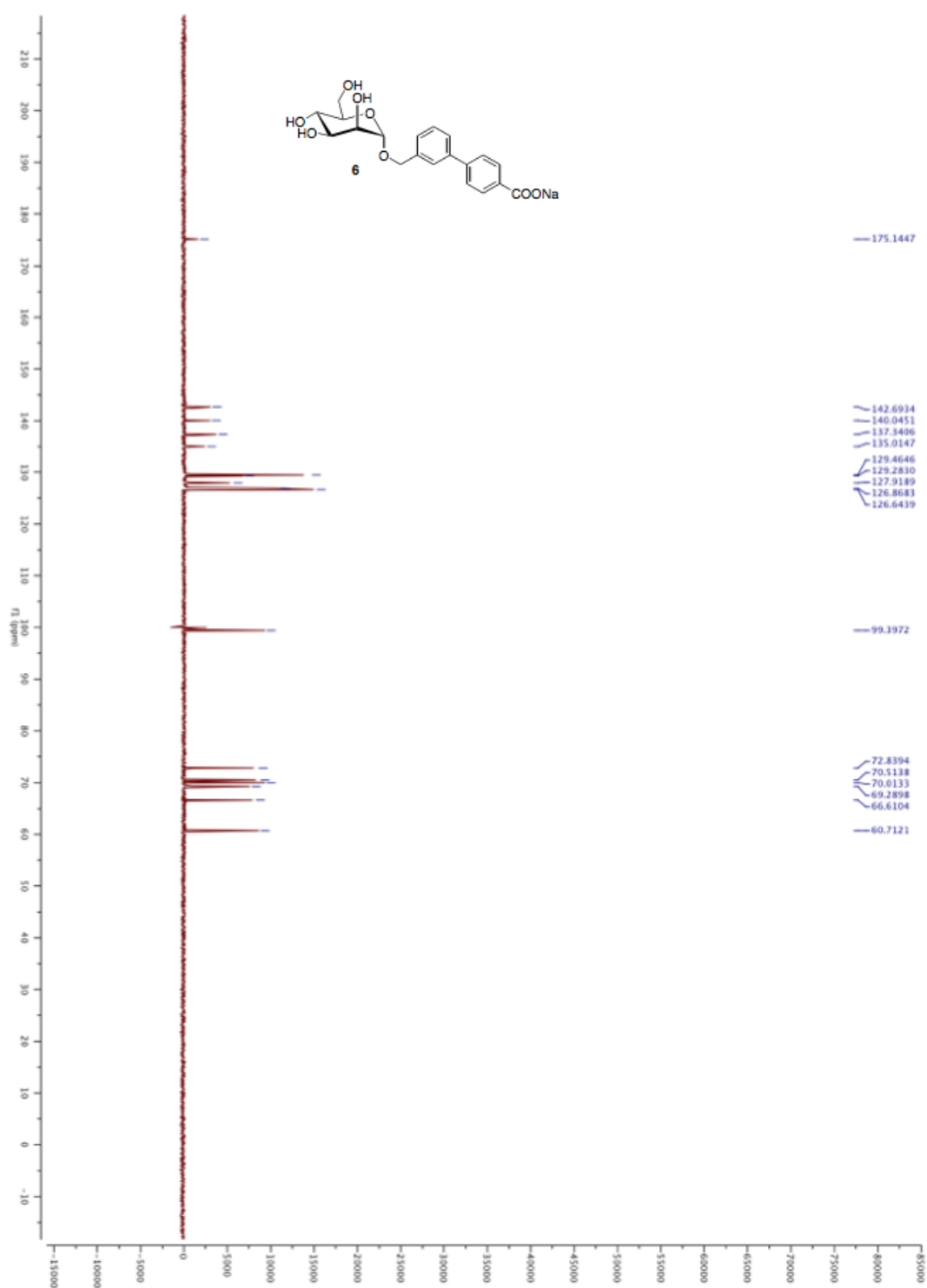
^1H NMR (500 MHz) of **19a**

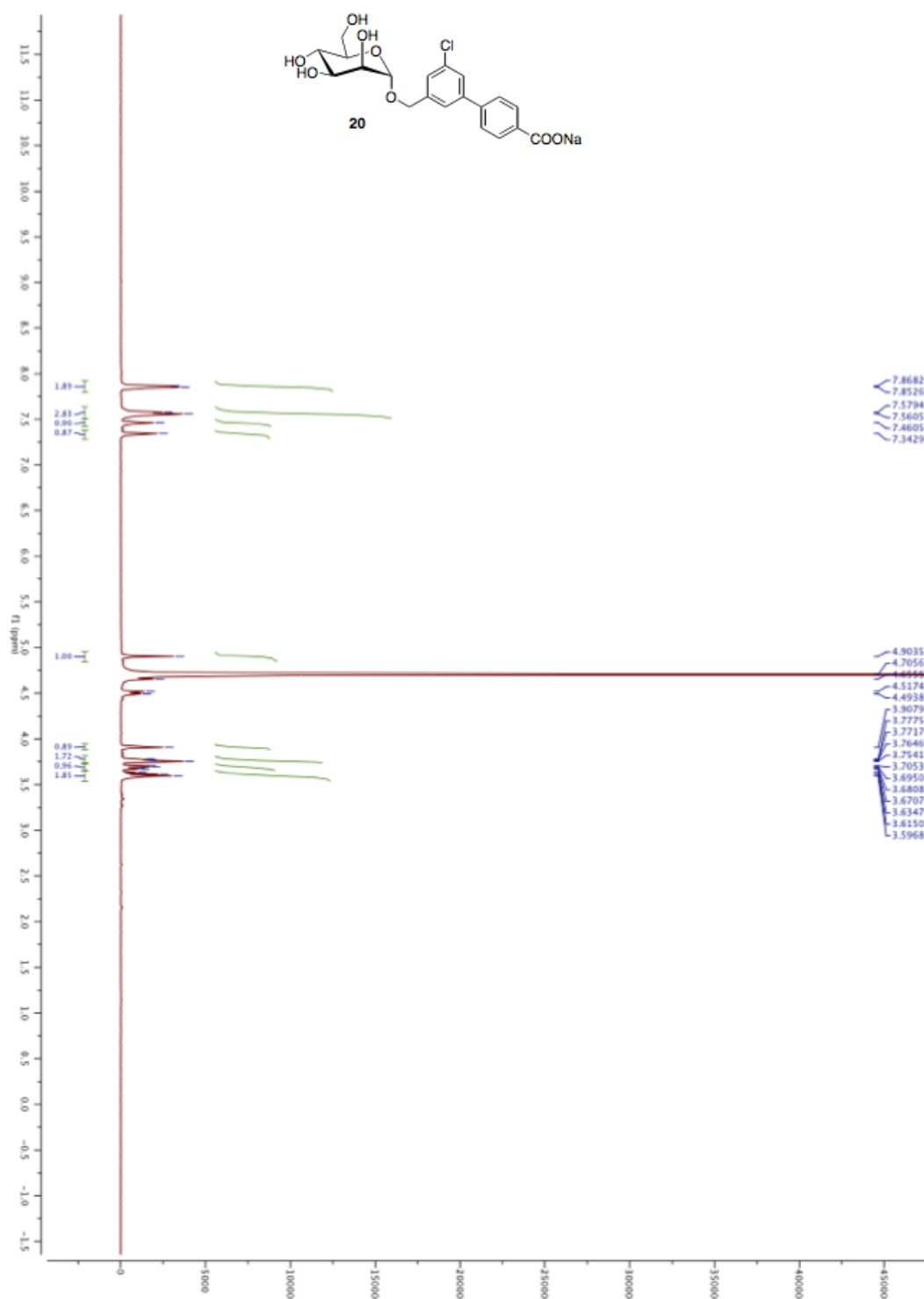
^{13}C NMR (125 MHz) of **19a**

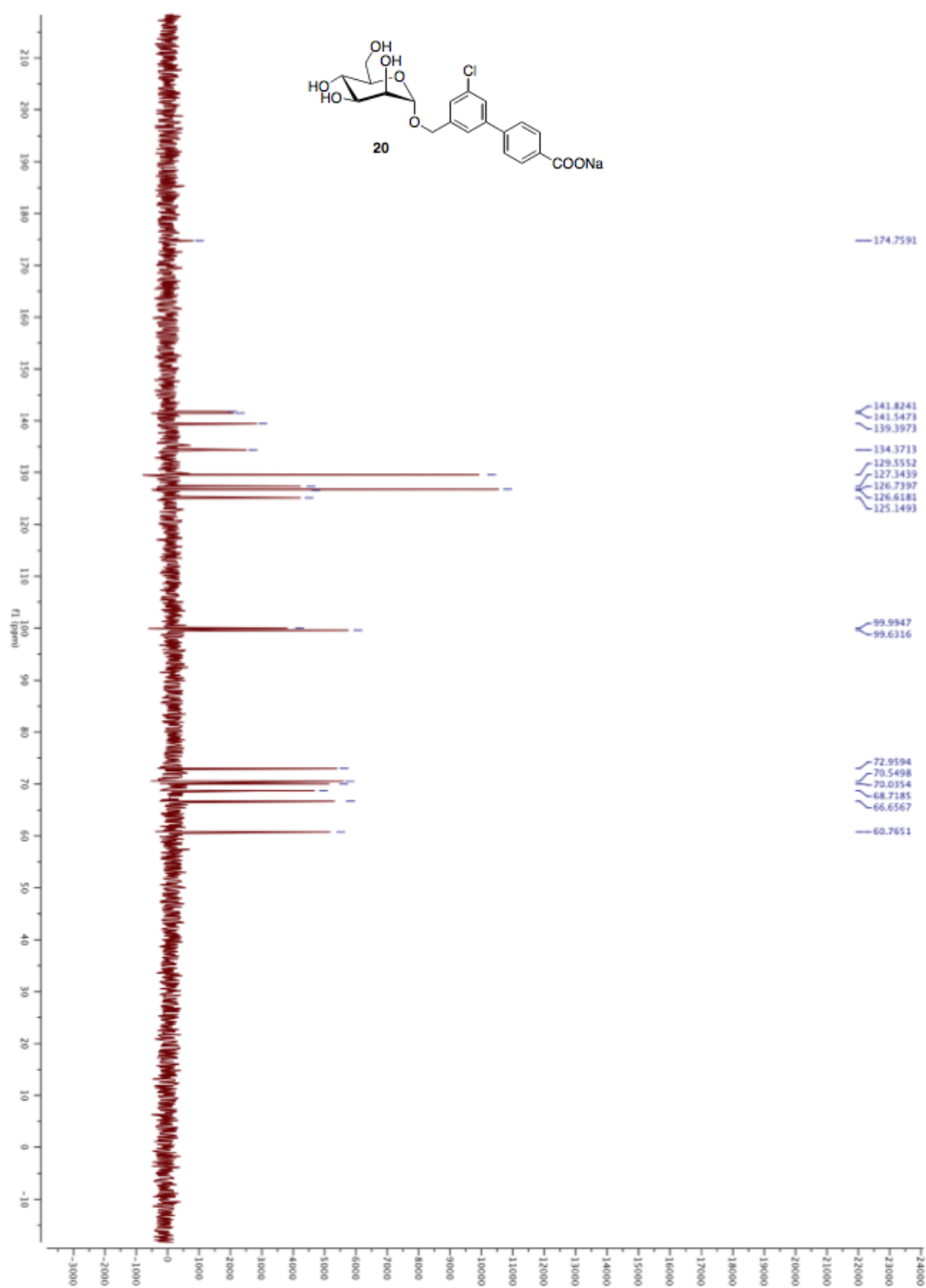
^1H NMR (500 MHz) of **19b**

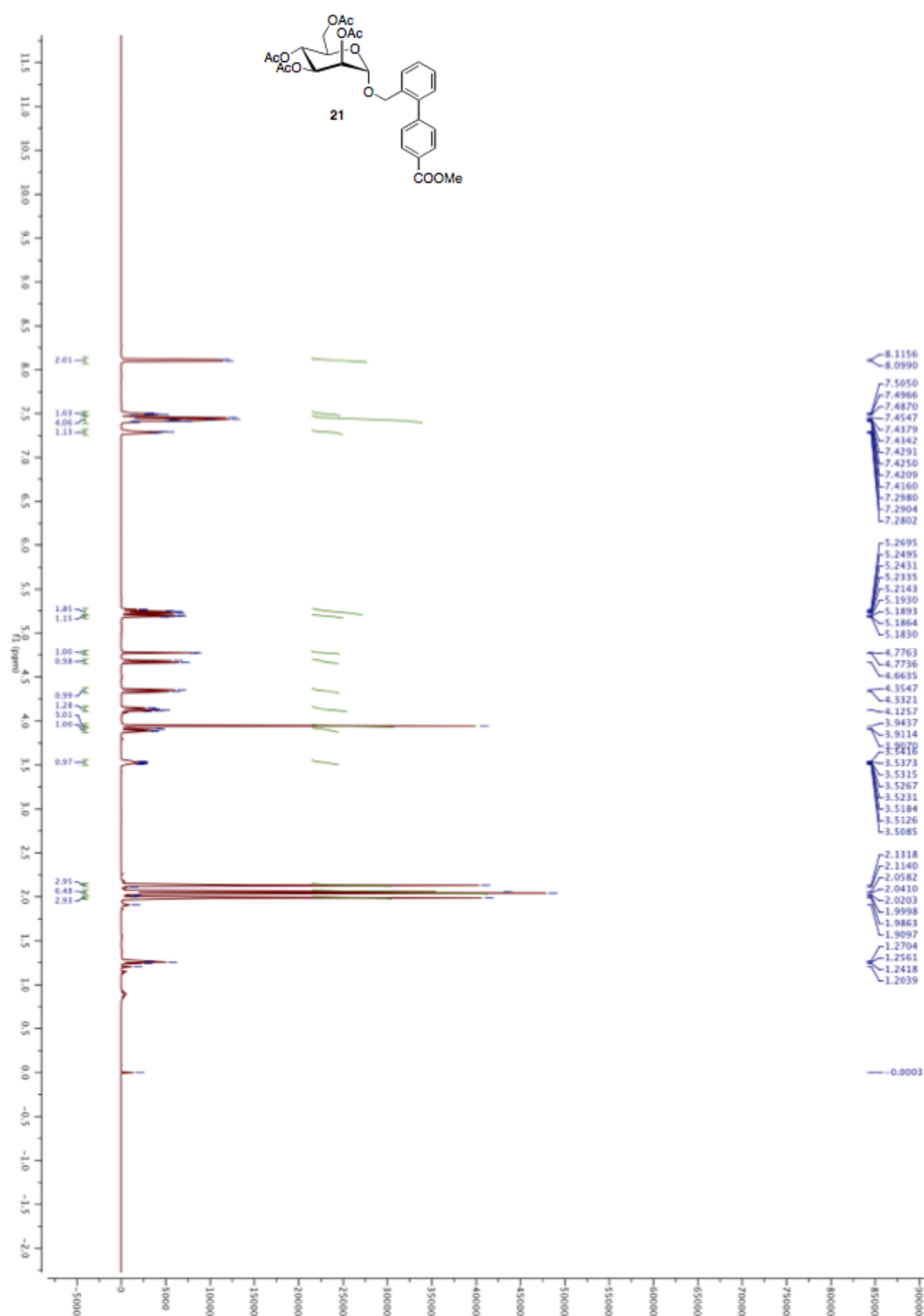
^{13}C NMR (125 MHz) of **19b**

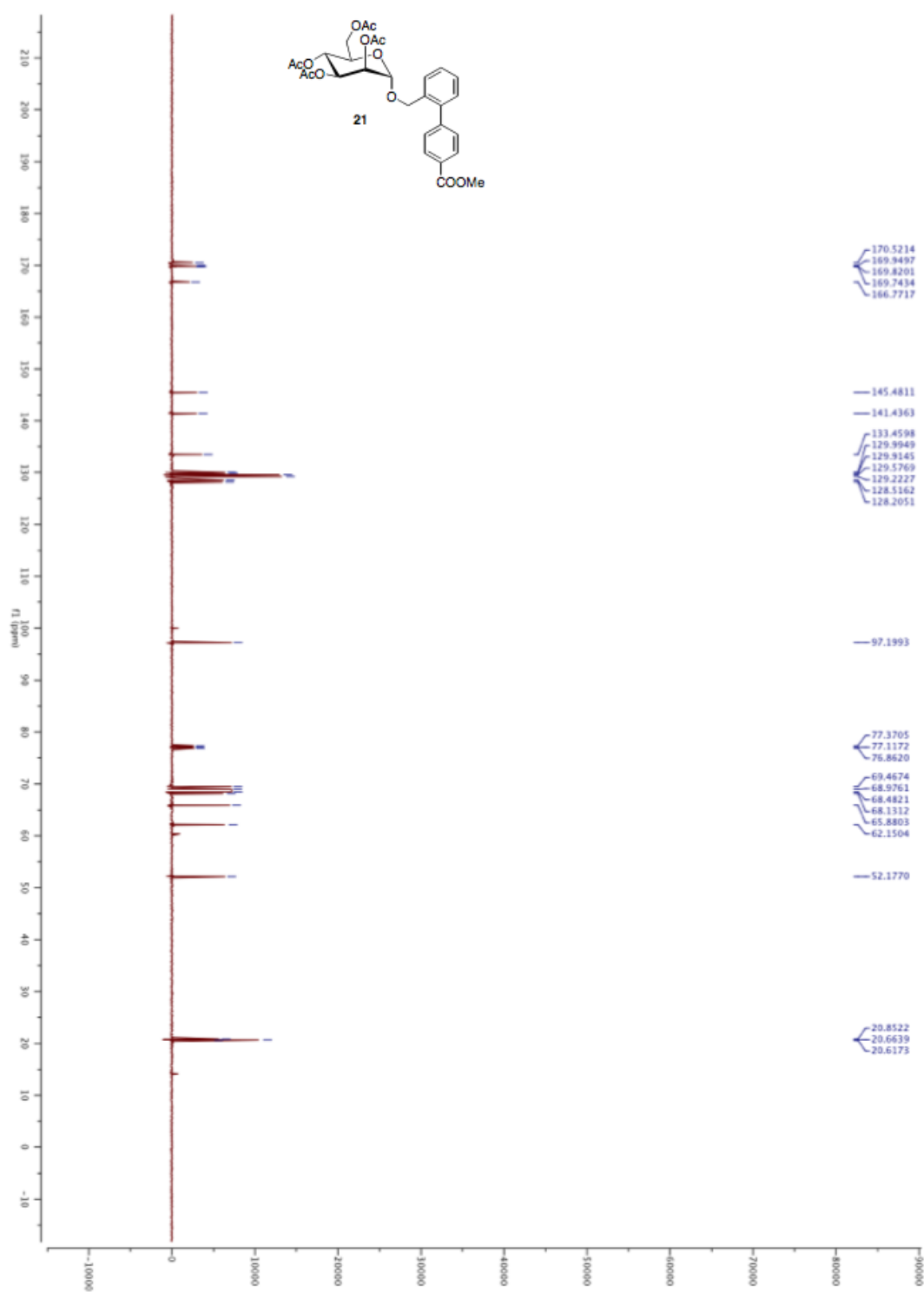
^1H NMR (500 MHz) of **6**

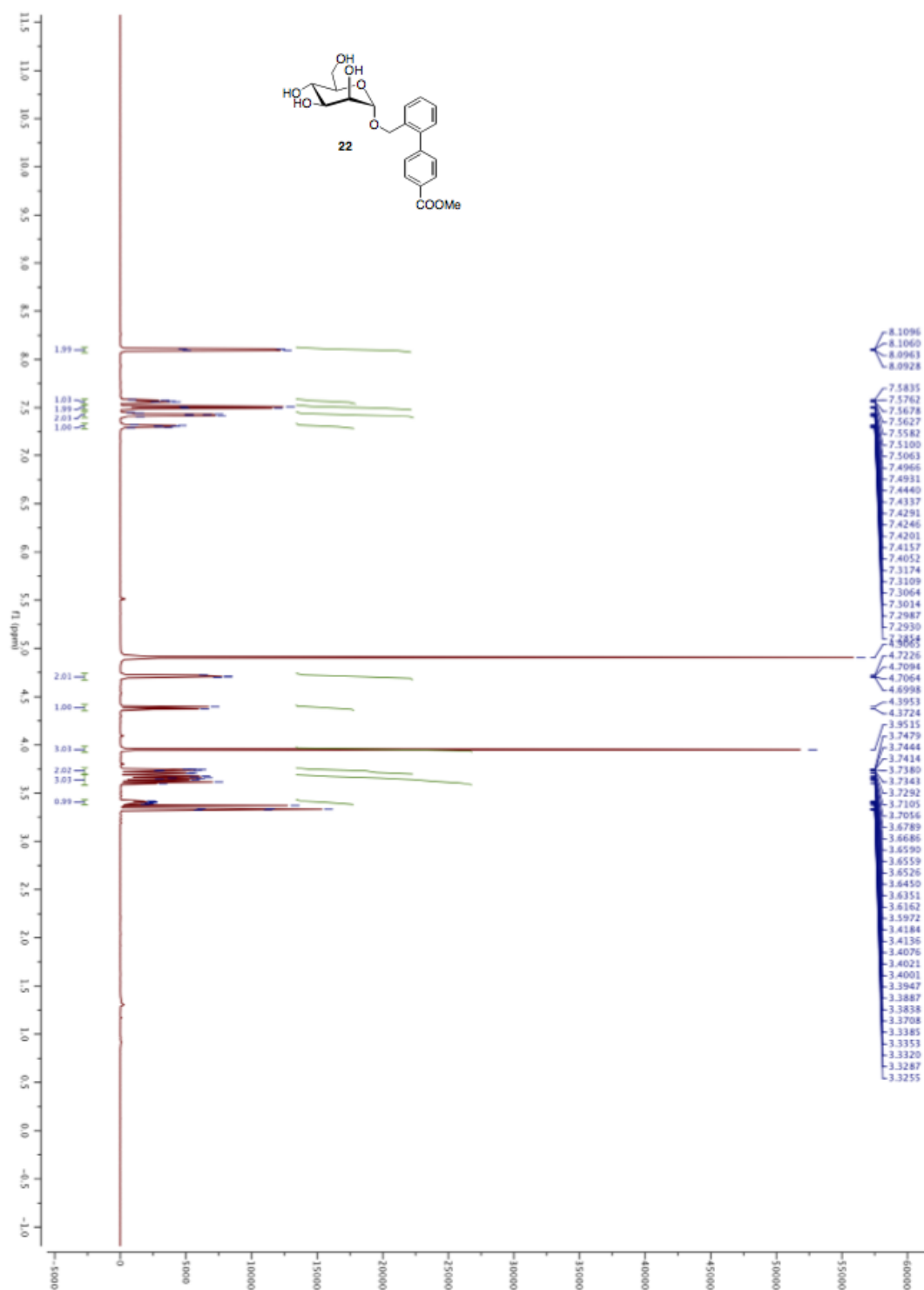
^{13}C NMR (125 MHz) of **6**

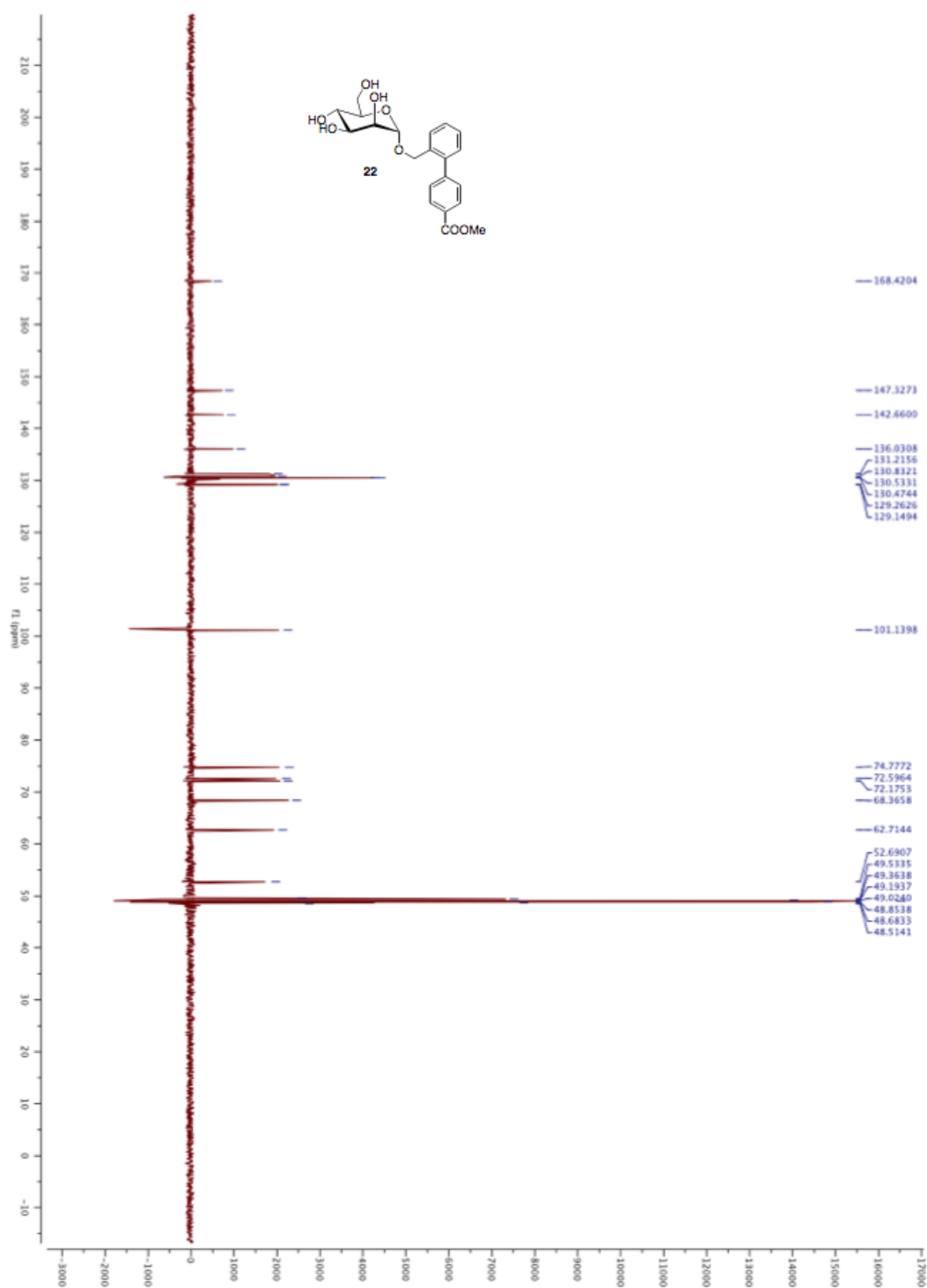
^1H NMR (500 MHz) of **20**

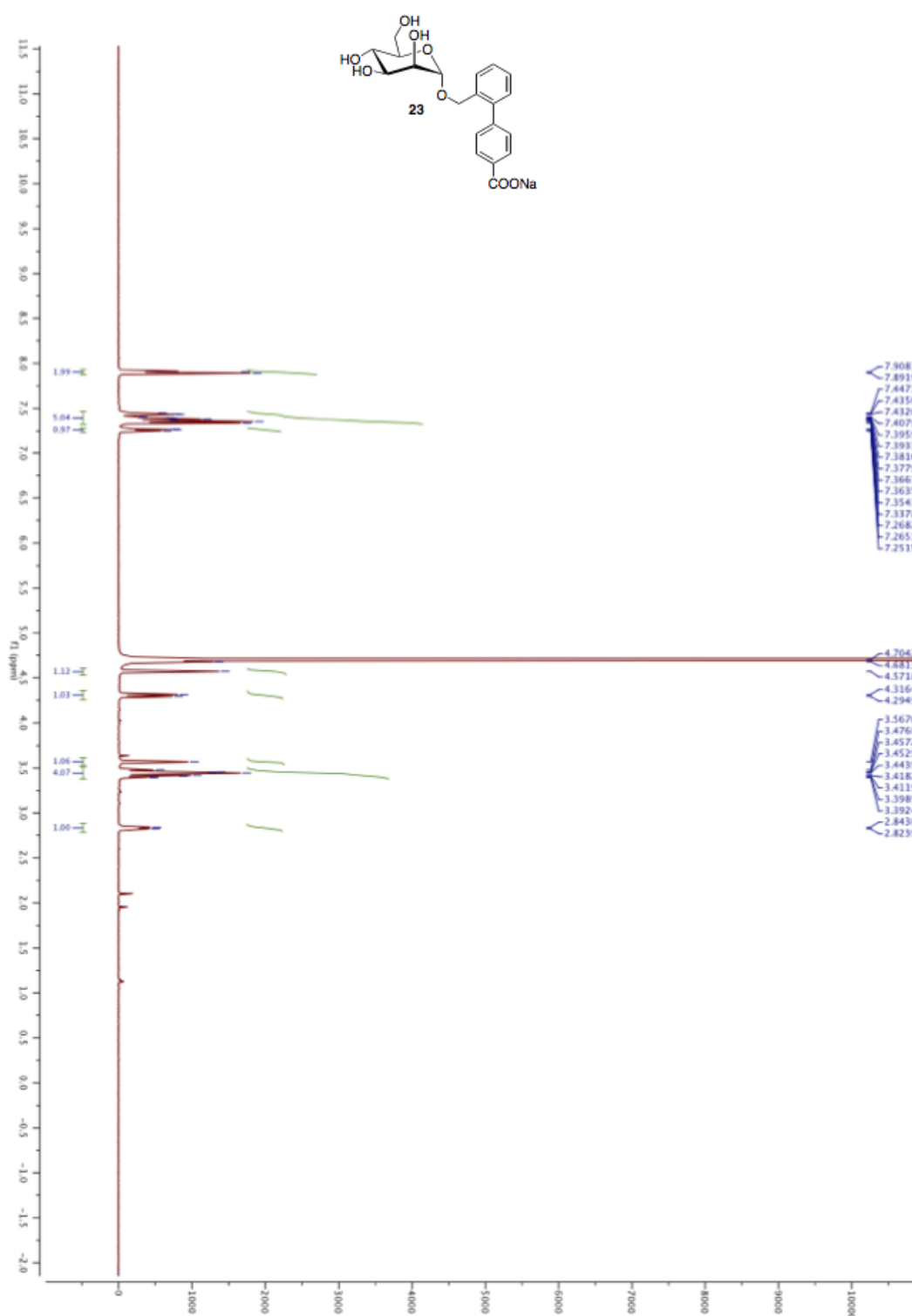
^{13}C NMR (125 MHz) of **20**

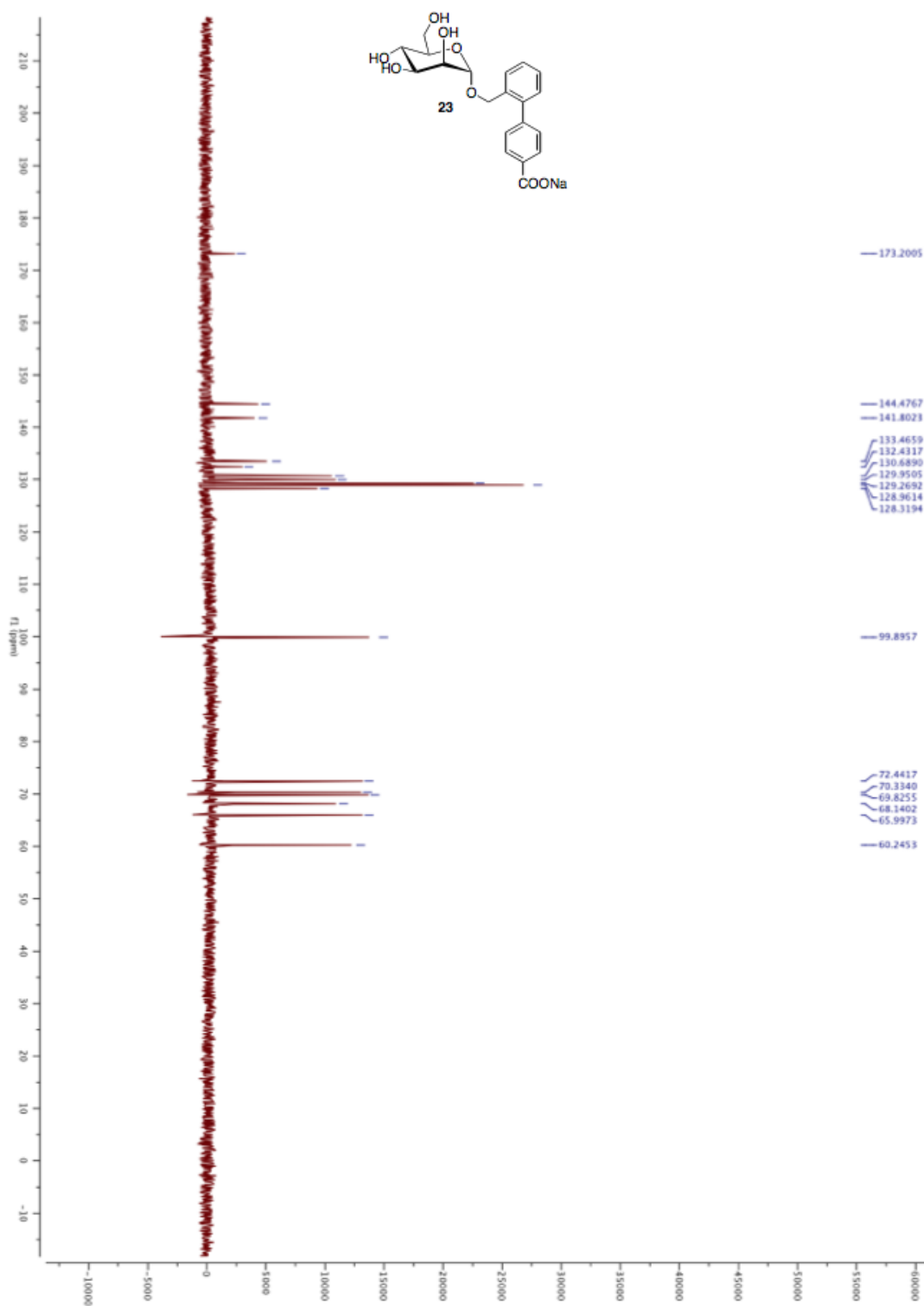
^1H NMR (500 MHz) of **21**

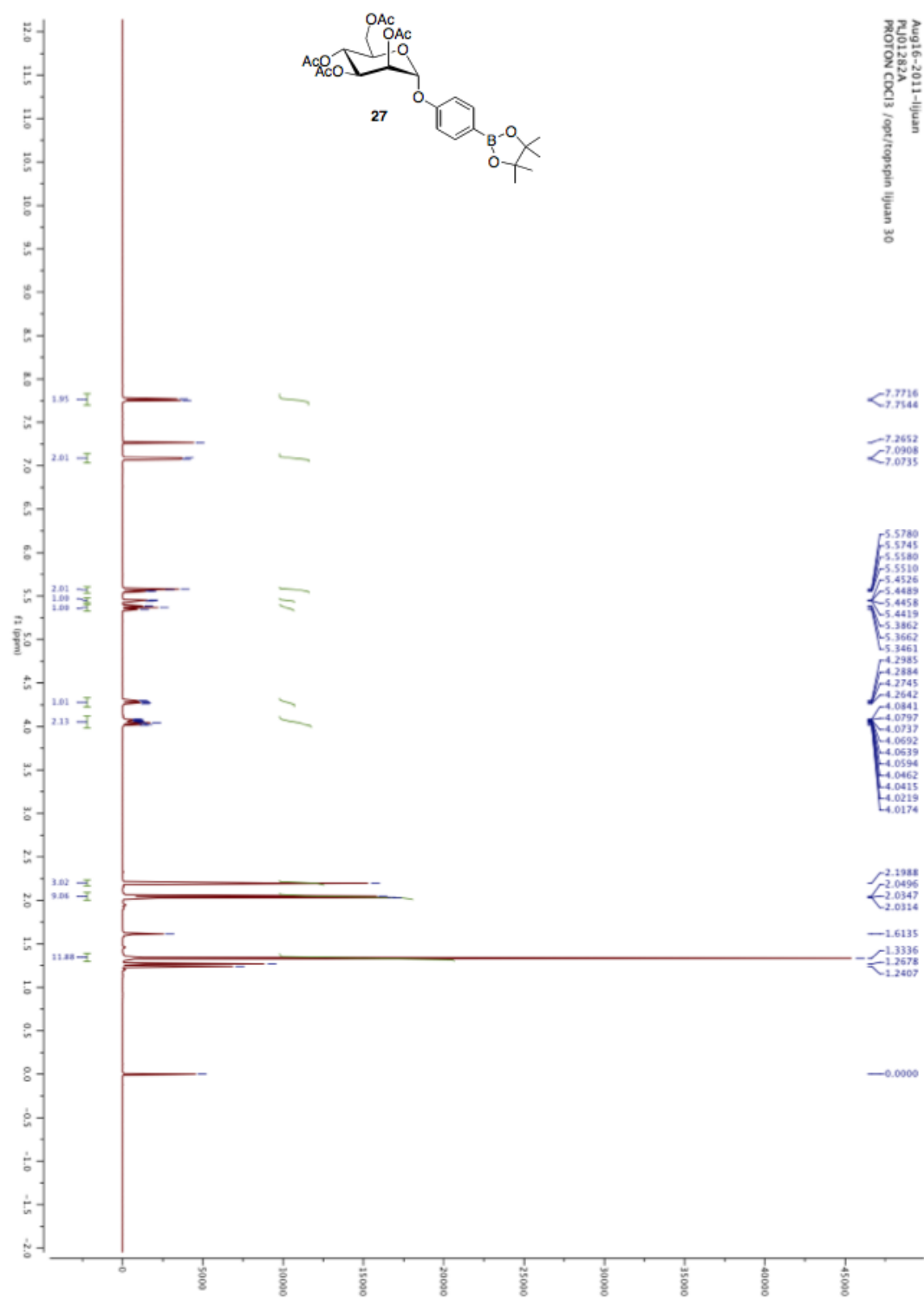
^{13}C NMR (125 MHz) of **21**

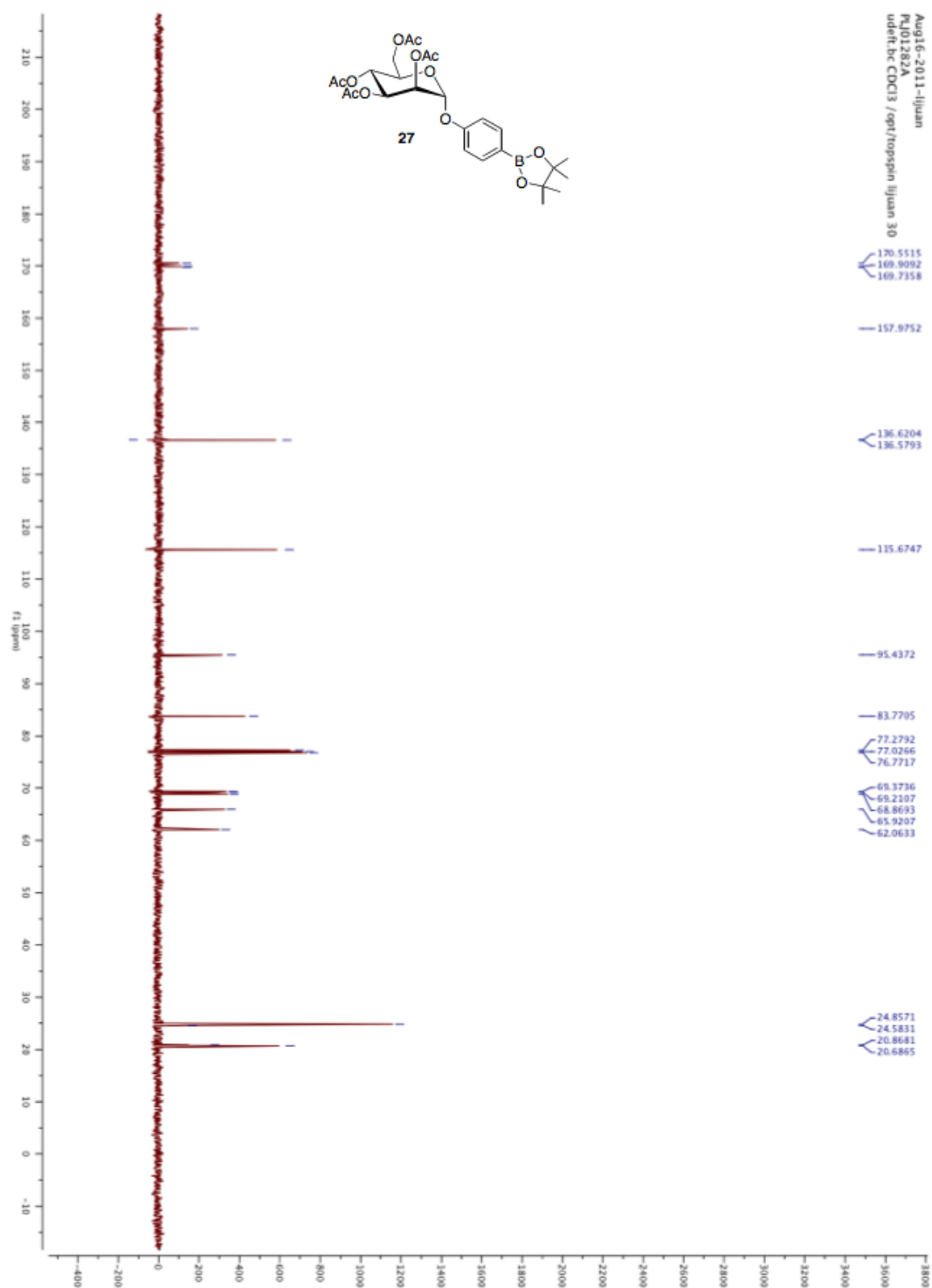
^1H NMR (500 MHz) of **22**

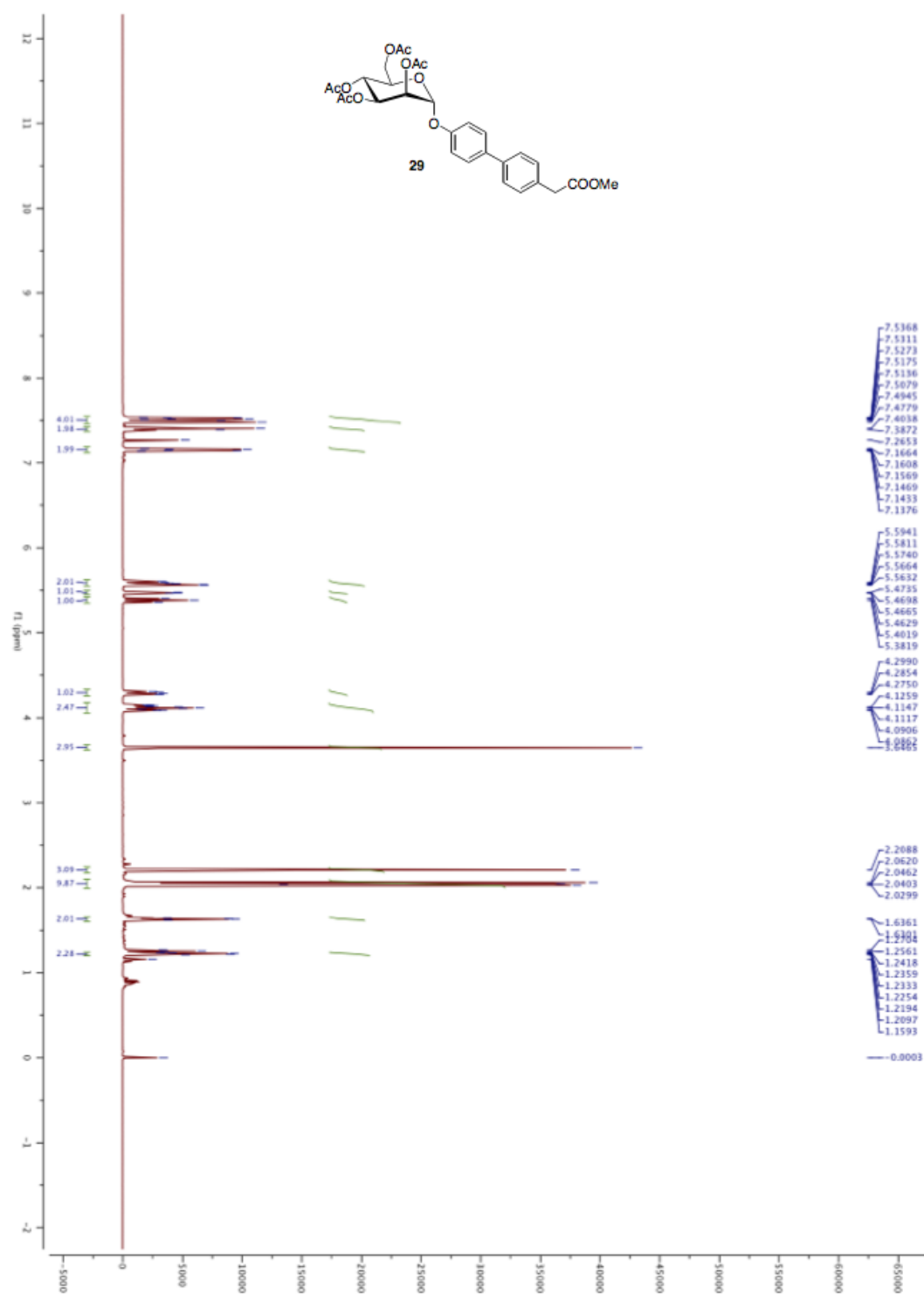
^{13}C NMR (125 MHz) of **22**

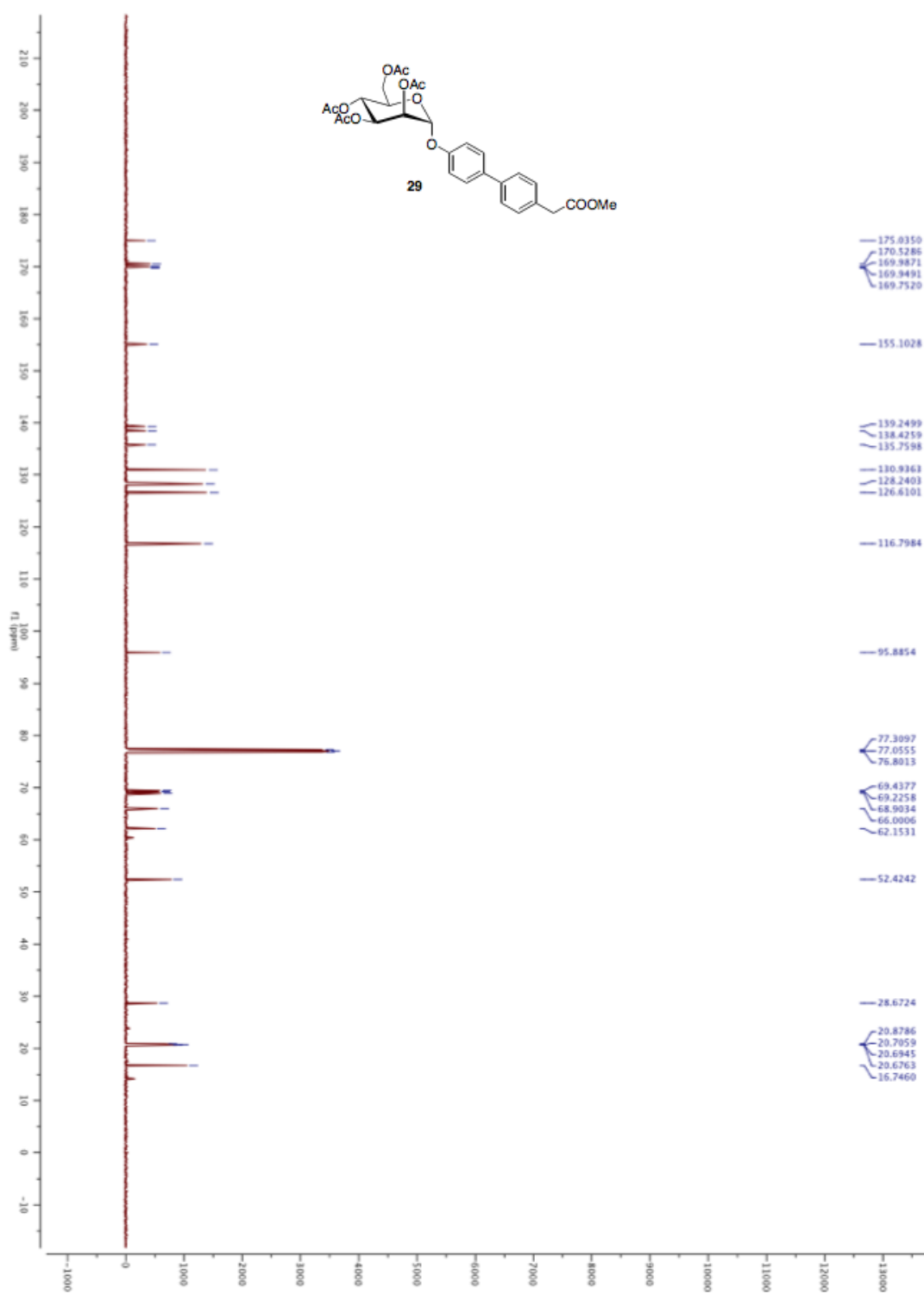
^1H NMR (500 MHz) of **23**

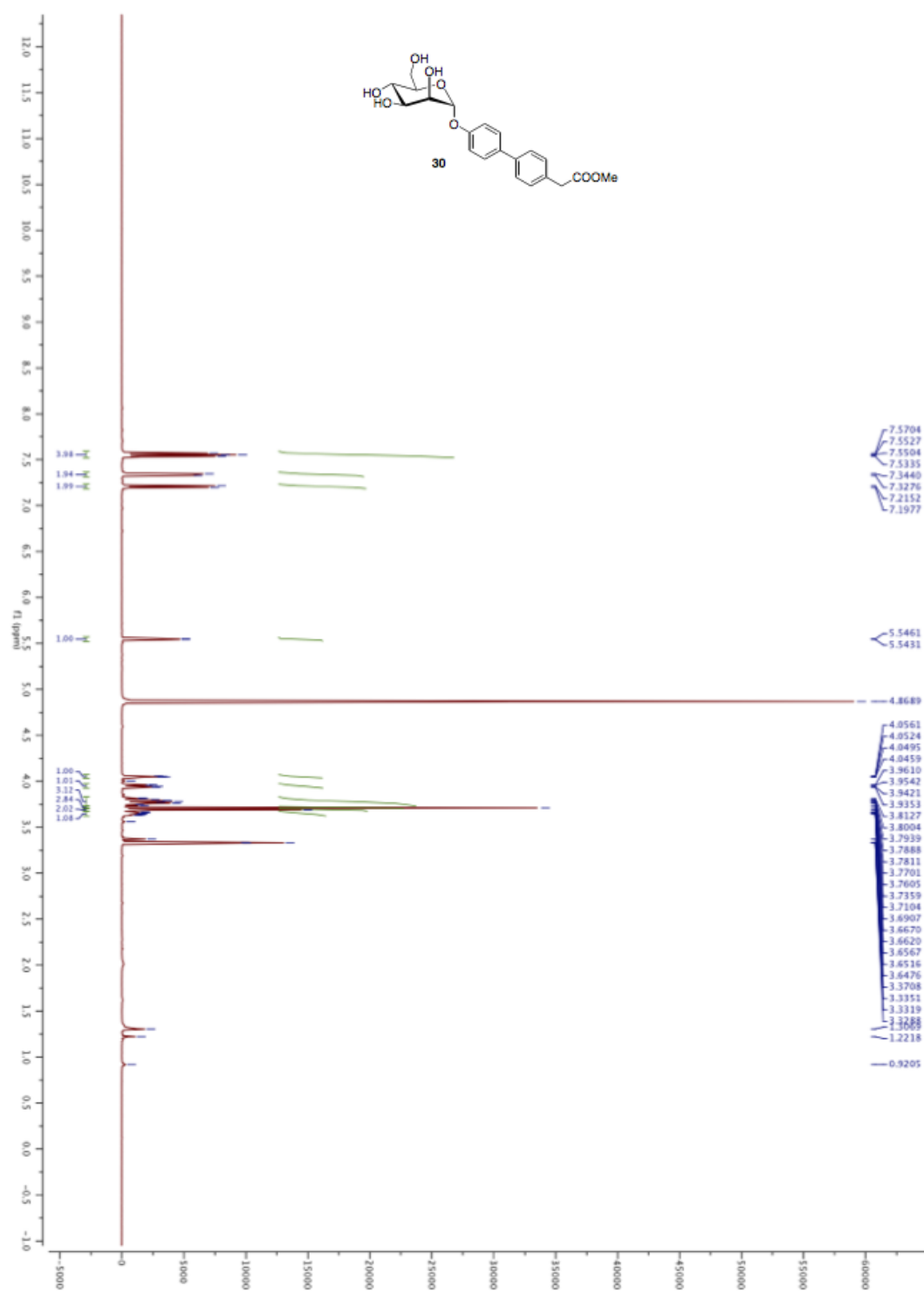
^{13}C NMR (125 MHz) of 23

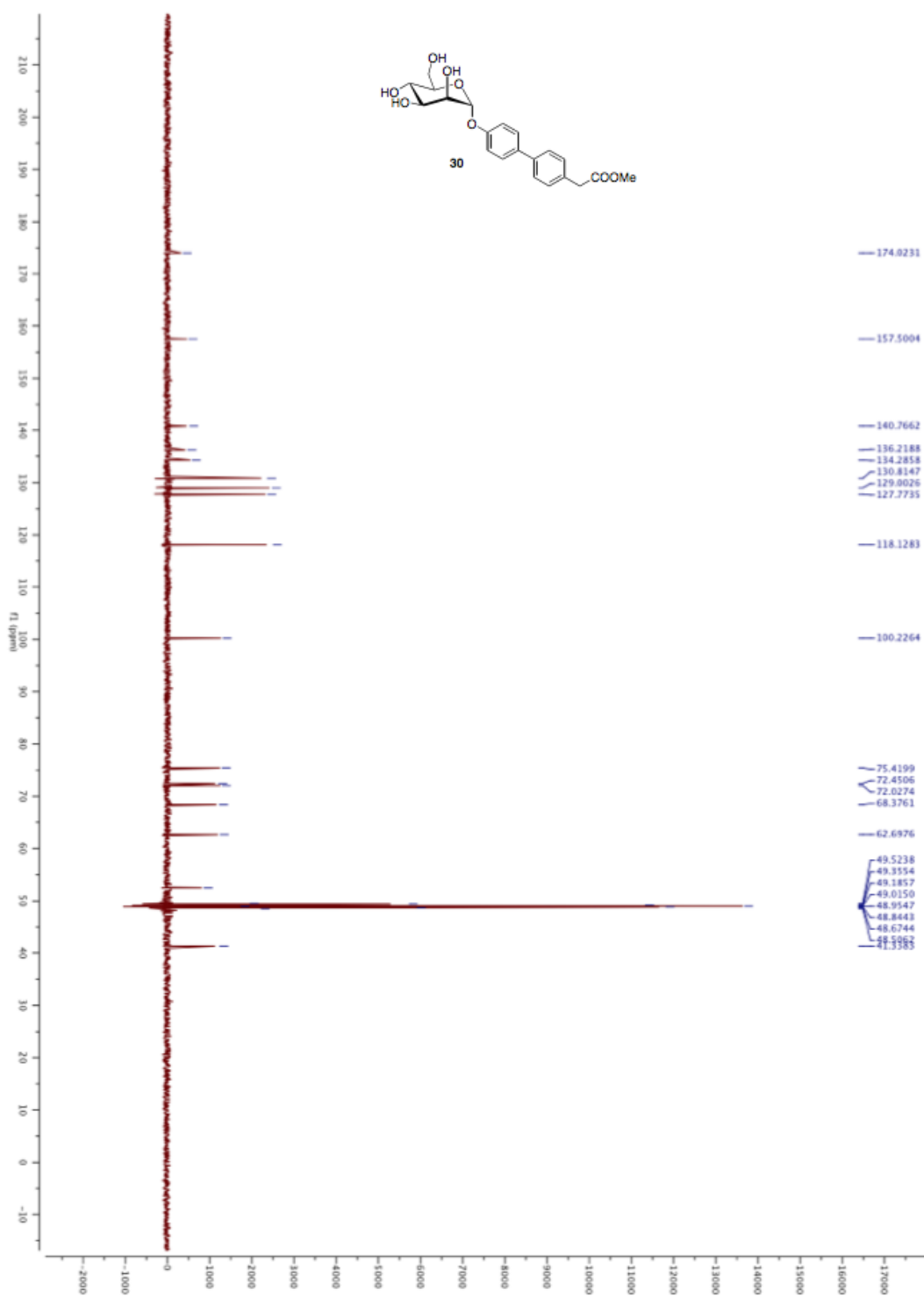
^1H NMR (500 MHz) of **27**

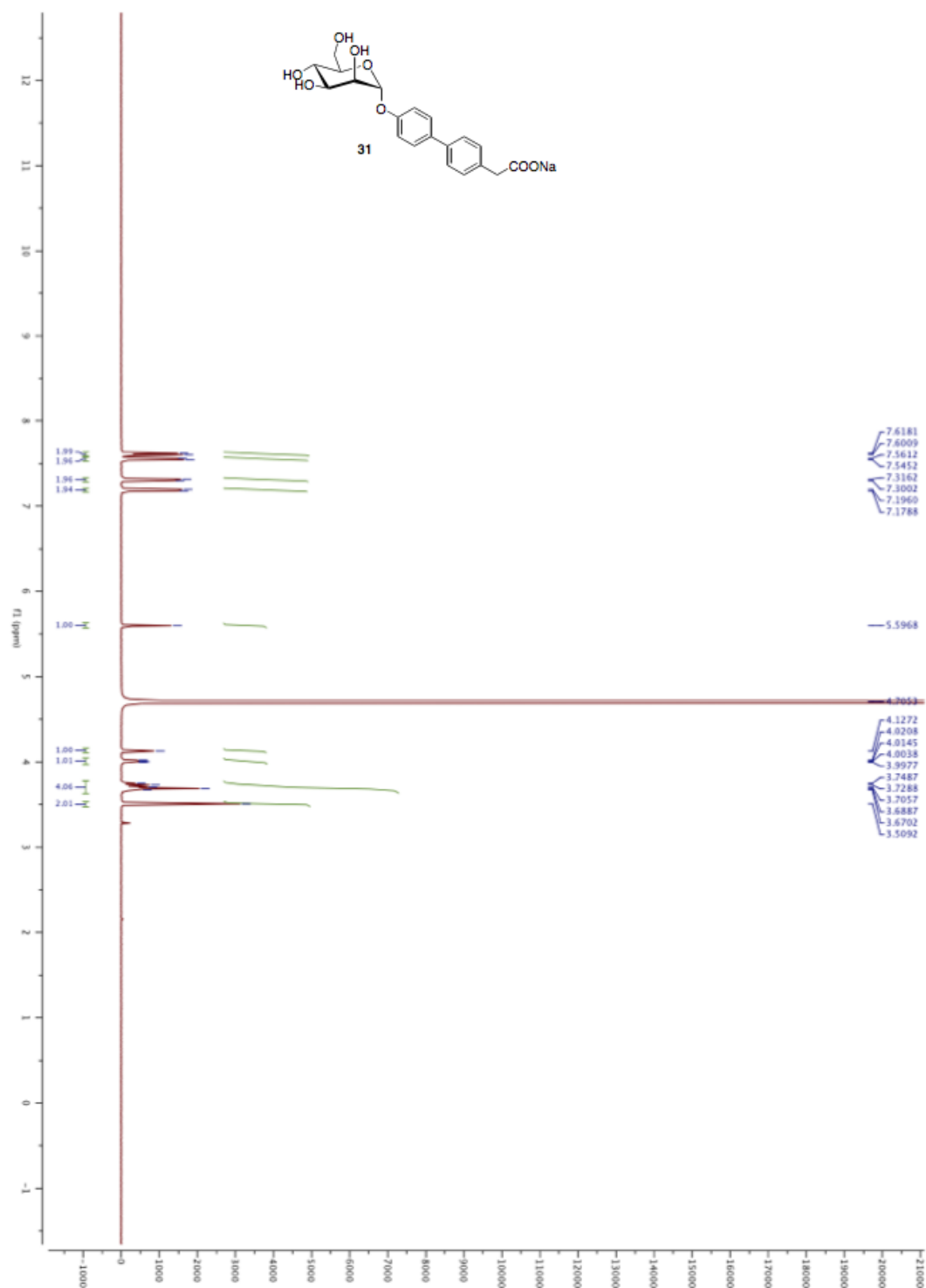
^{13}C NMR (125 MHz) of **27**

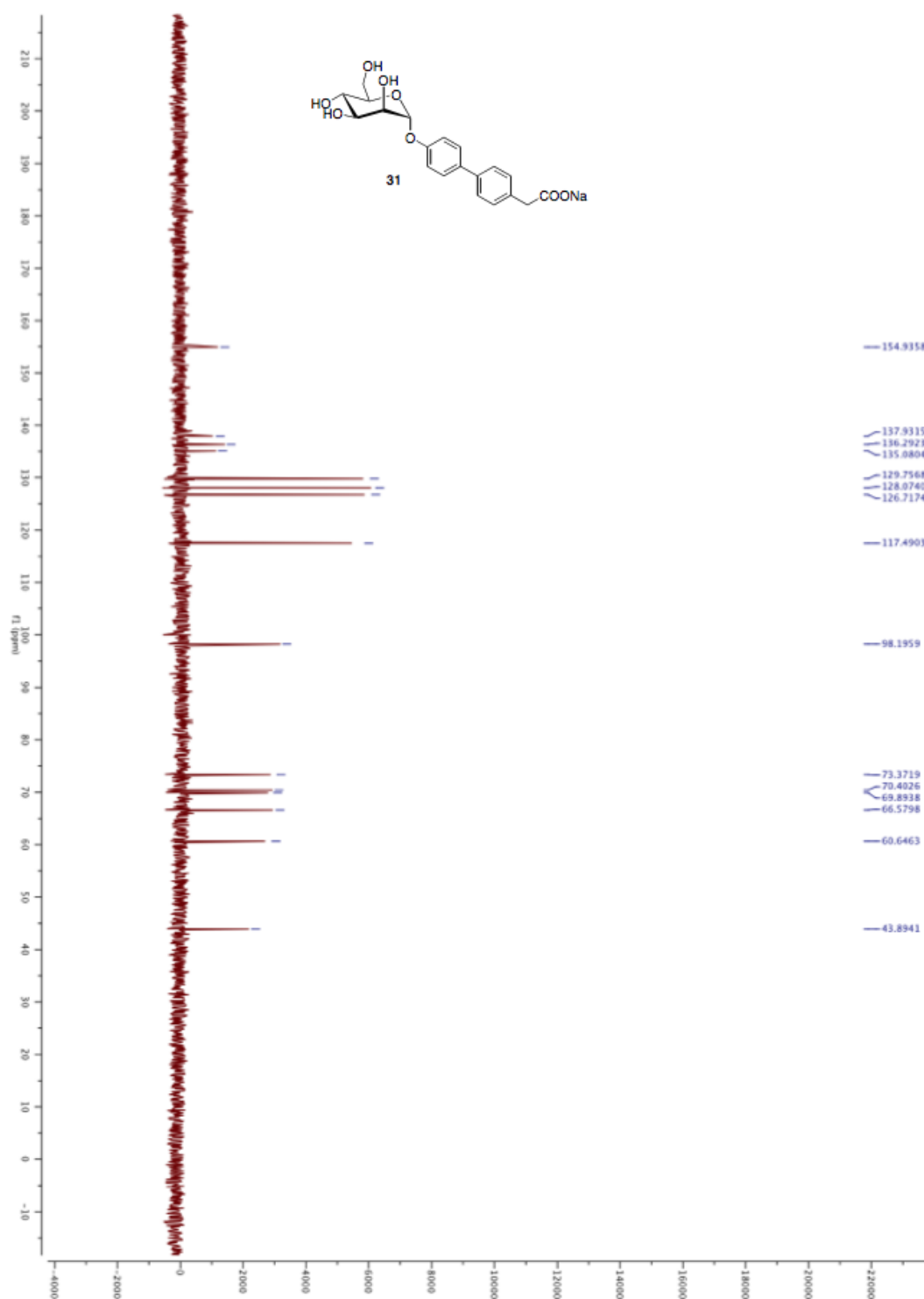
^1H NMR (500 MHz) of **29**

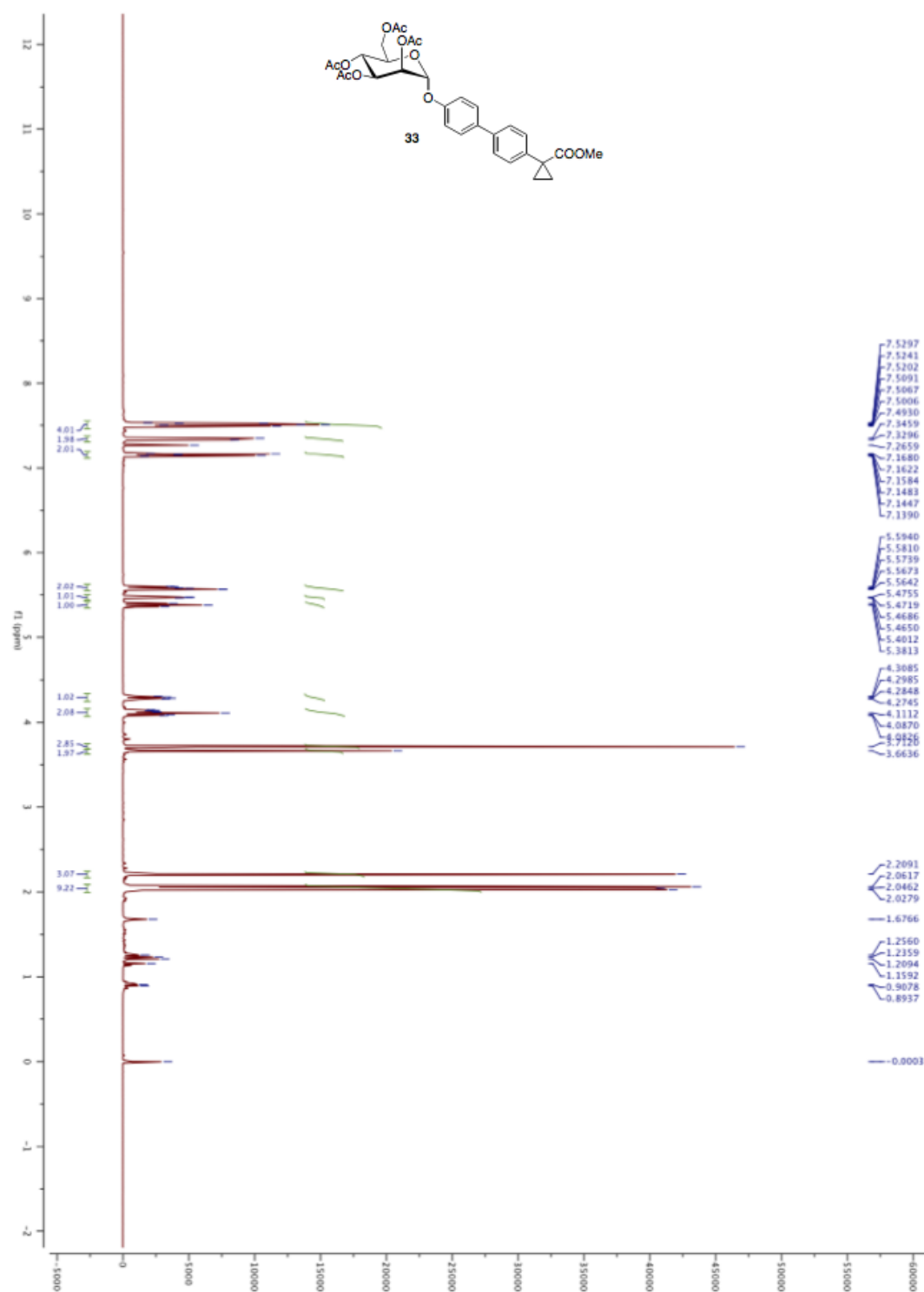
^{13}C NMR (125 MHz) of **29**

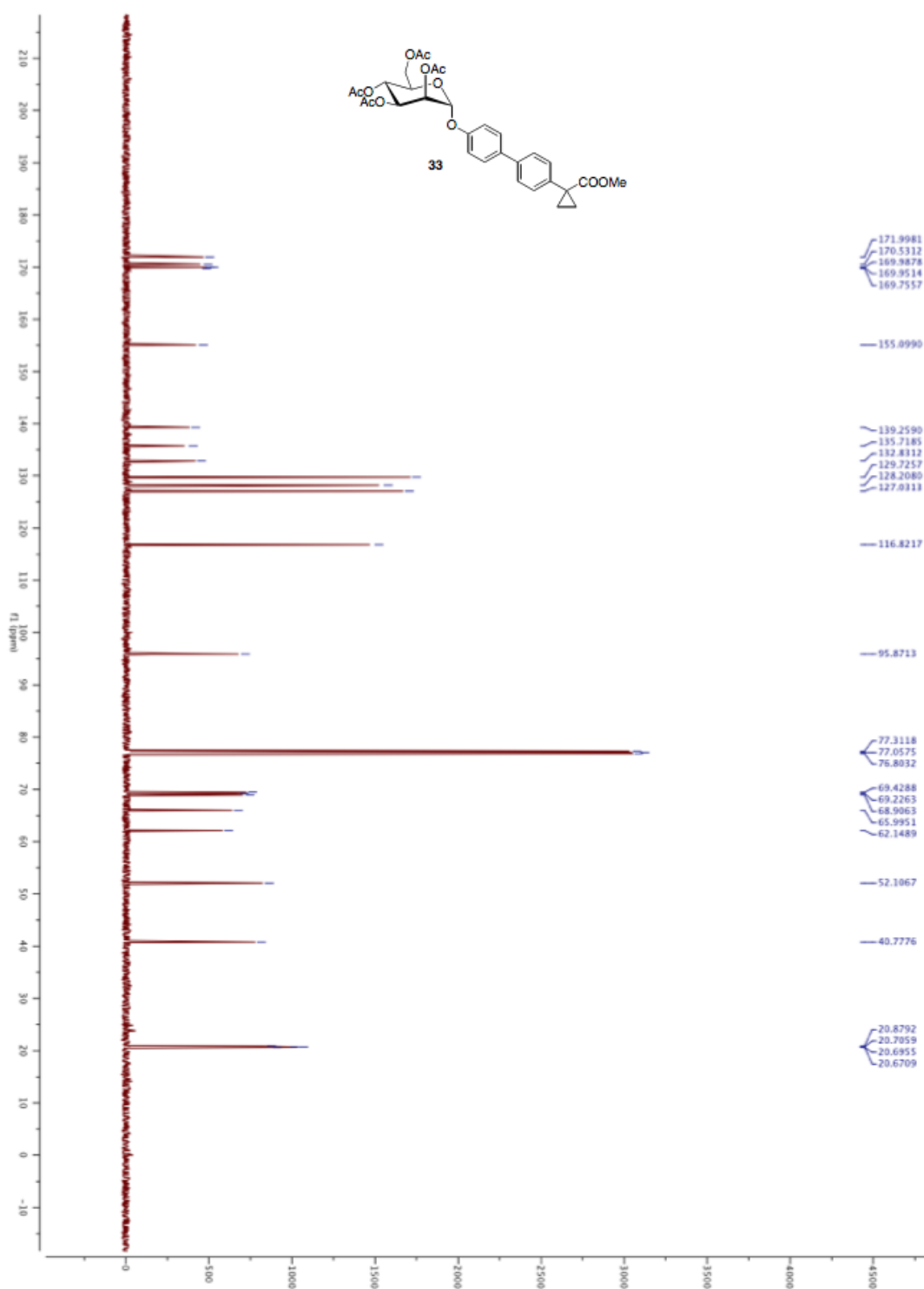
^1H NMR (500 MHz) of **30**

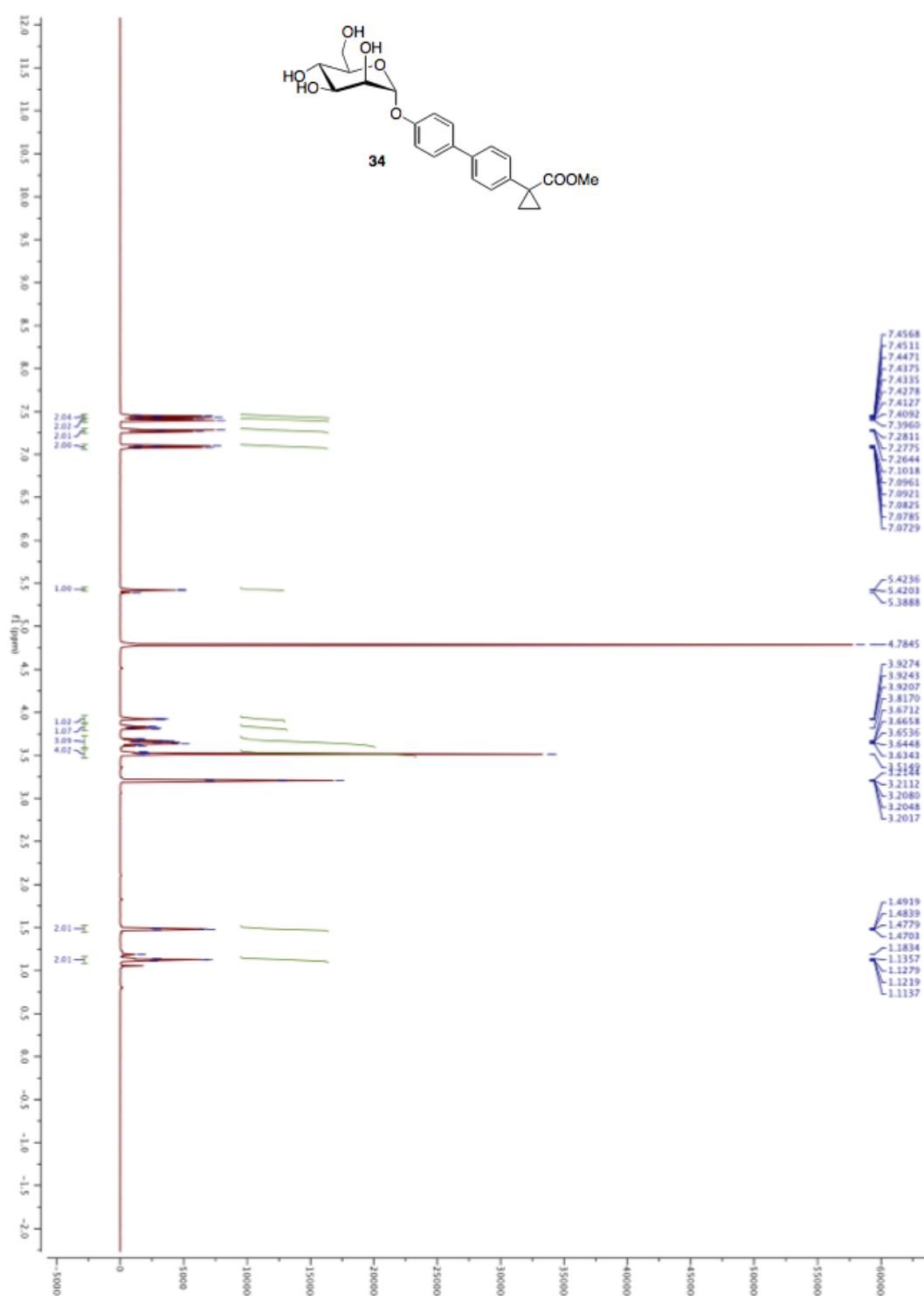
^{13}C NMR (125 MHz) of **30**

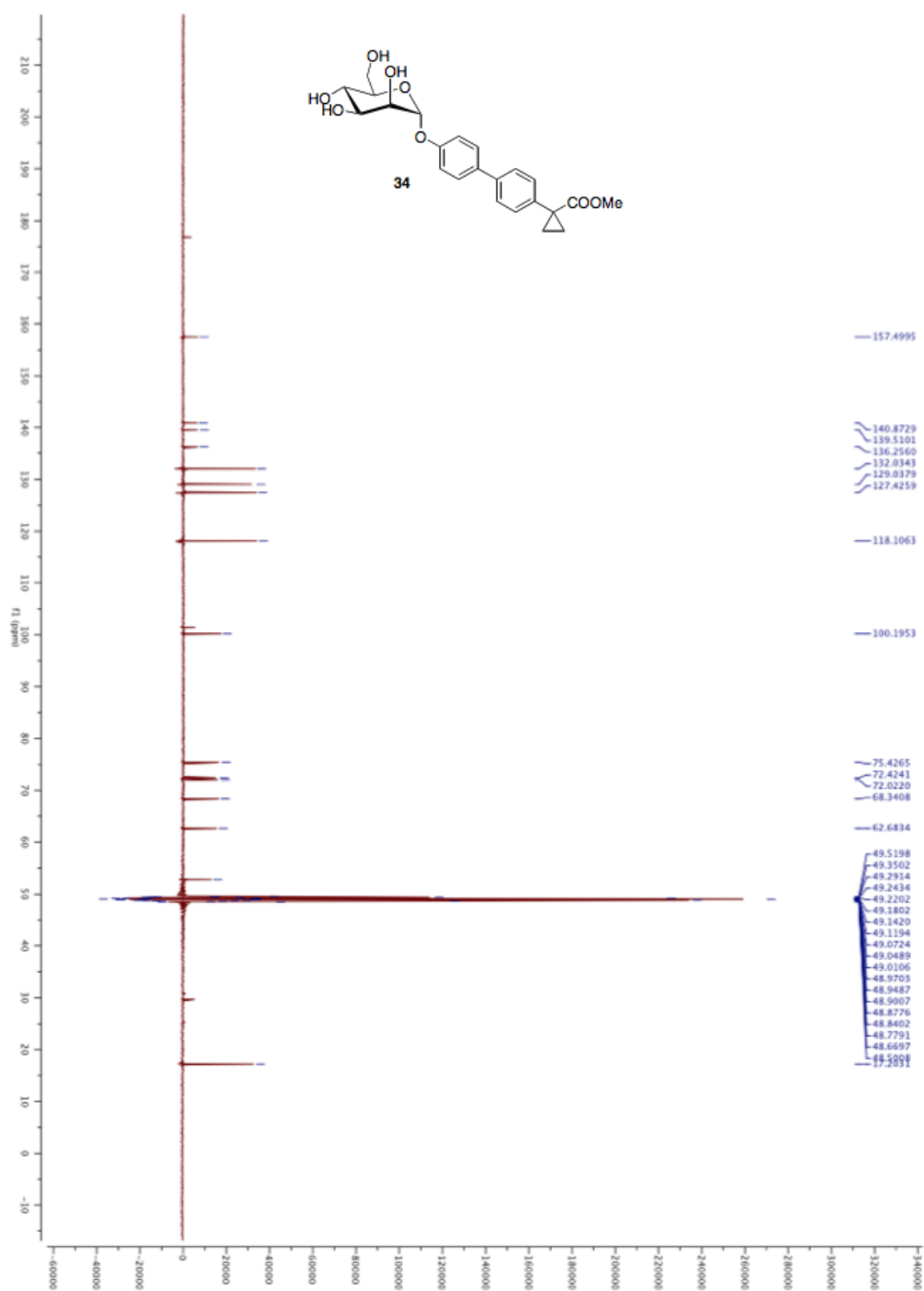
^1H NMR (500 MHz) of **31**

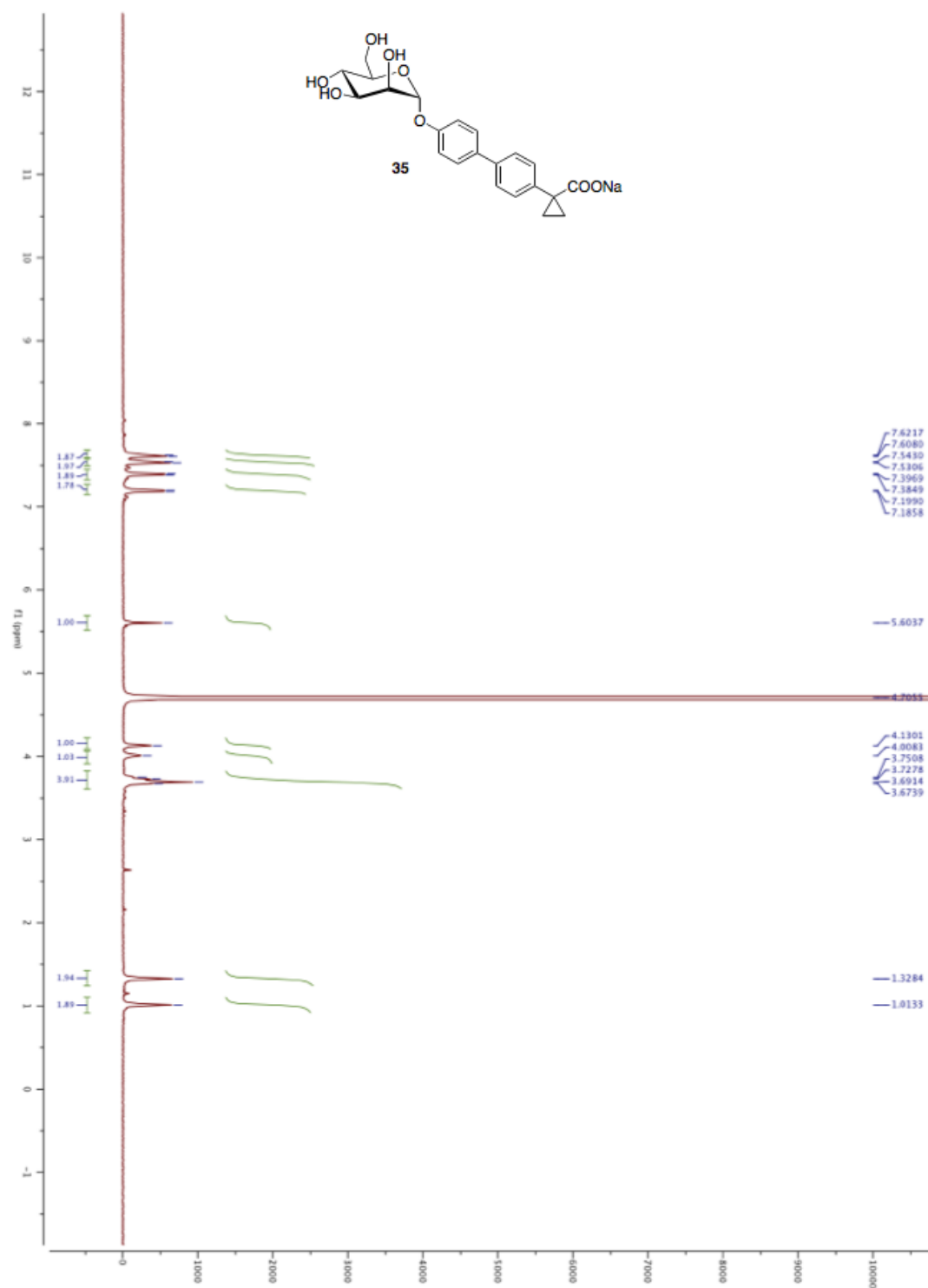
^{13}C NMR (125 MHz) of **31**

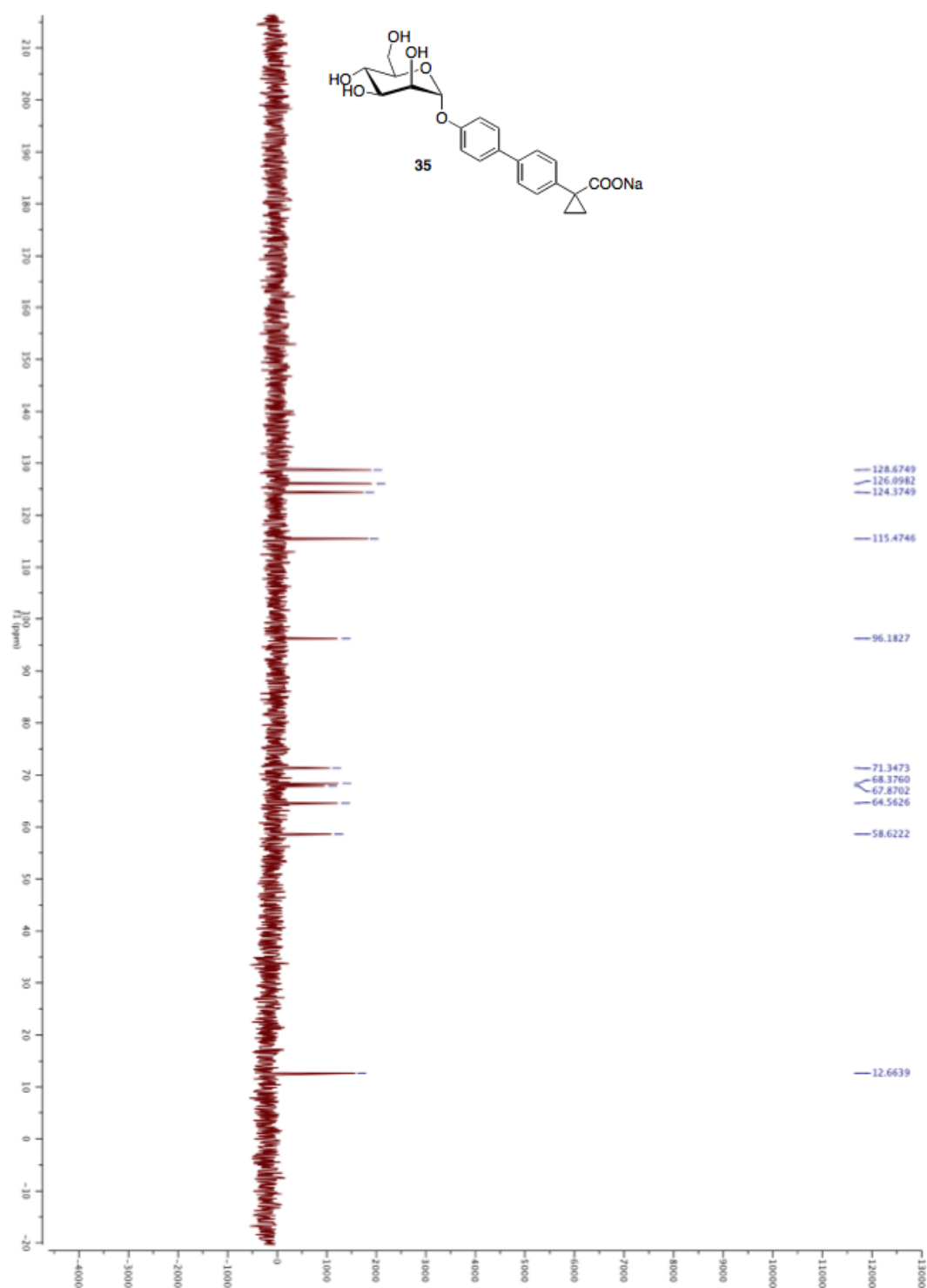
^1H NMR (500 MHz) of **33**

^{13}C NMR (125 MHz) of **33**

^1H NMR (500 MHz) of **34**

^{13}C NMR (125 MHz) of **34**

^1H NMR (500 MHz) of **35**

^{13}C NMR (125 MHz) of **35**

2.4 Paper 3: FimH Antagonists: Bioisosteres to Improve the *in Vitro* and *in Vivo* PK/PD Profile

This article describes the lead optimization efforts for the improvement of oral bioavailability of biphenyl FimH antagonists. By replacing the *para*-carboxylate moiety with various bioisosteres, a series of modified antagonists were designed and synthesized. The *in vitro* and *in vivo* biological evaluations of the target compounds revealed the principles behind the improvement of PK/PD properties.

Contributions to this project:

Lijuan Pang designed the structures of the target compounds with *VirtualDesignLab* (a computational docking program). Furthermore, she synthesized all the target compounds and the reference compounds except **11j**. She evaluated the p*K*_a values of compounds in Table 3. She was also responsible for writing the synthesis sections of this paper.

This paper was published in the *Journal of Medicinal Chemistry*:

Kleeb, S. *; Pang, L. *; Mayer, K. *; Eris, D. *; Sigl, A. *; Preston, R.C.; Zihlmann, P.; Sharpe, T.; Jakob, R.P.; Abgottspon, D.; Hutter, A.S.; Scharenberg, M.; Jiang, X.; Navarra, G.; Rabbani, S.; Smiesko, M.; Lüdin, N.; Bezençon, J.; Schwardt, O.; Maier, T.; Ernst, B. FimH antagonists: Bioisosteres to improve the *in vitro* and *in vivo* PK/PD profile. *J. Med. Chem.* **2015**, 58, 2221-2239.

* These authors contributed equally to the project.

© 2015 American Chemical Society

FimH Antagonists: Bioisosteres To Improve the in Vitro and in Vivo PK/PD Profile

Simon Kleeb,^{†,||} Lijuan Pang,^{†,||} Katharina Mayer,^{†,||} Deniz Eris,^{†,||} Anja Sigl,^{†,||} Roland C. Preston,[†] Pascal Zihlmann,[†] Timothy Sharpe,[§] Roman P. Jakob,[‡] Daniela Abgottspon,[†] Aline S. Hutter,[†] Meike Scharenberg,[†] Xiaohua Jiang,[†] Giulio Navarra,[†] Said Rabbani,[‡] Martin Smiesko,[†] Nathalie Lüdin,[†] Jacqueline Bezençon,[†] Oliver Schwardt,[†] Timm Maier,[‡] and Beat Ernst^{*,†}

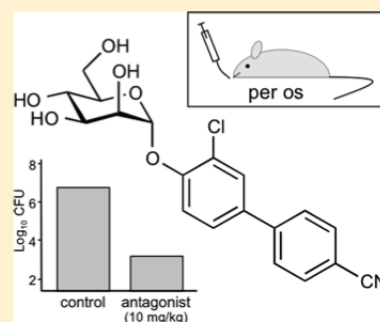
[†]Institute of Molecular Pharmacy, Pharmacenter, University of Basel, Klingelbergstrasse 50, CH-4056 Basel, Switzerland

[‡]Structural Biology, Biocenter, University of Basel, Klingelbergstrasse 70, CH-4056 Basel, Switzerland

[§]Biophysical Facility, Biocenter, University of Basel, Klingelbergstrasse 70, CH-4056 Basel, Switzerland

S Supporting Information

ABSTRACT: Urinary tract infections (UTIs), predominantly caused by uropathogenic *Escherichia coli* (UPEC), belong to the most prevalent infectious diseases worldwide. The attachment of UPEC to host cells is mediated by FimH, a mannose-binding adhesin at the tip of bacterial type 1 pili. To date, UTIs are mainly treated with antibiotics, leading to the ubiquitous problem of increasing resistance against most of the currently available antimicrobials. Therefore, new treatment strategies are urgently needed. Here, we describe the development of an orally available FimH antagonist. Starting from the carboxylate substituted biphenyl α -D-mannoside **9**, affinity and the relevant pharmacokinetic parameters (solubility, permeability, renal excretion) were substantially improved by a bioisosteric approach. With 3'-chloro-4'-(α -D-mannopyranosyloxy)biphenyl-4-carbonitrile (**10j**) a FimH antagonist with an optimal in vitro PK/PD profile was identified. Orally applied, **10j** was effective in a mouse model of UTI by reducing the bacterial load in the bladder by about 1000-fold.



■ INTRODUCTION

Urinary tract infection (UTI) is one of the most frequent infectious diseases worldwide and affects millions of people every year.¹ In more than 70% of the reported cases, uropathogenic *Escherichia coli* (UPEC) is the causal pathogen.² Acute, uncomplicated lower urinary tract infection, commonly referred to as cystitis, requires an antibiotic treatment for symptom relief (i.e., reduction of dysuria, frequent and urgent urination, bacteriuria, pyuria) and for prevention of more devastating or even life threatening complications like pyelonephritis and urosepsis.^{3,4} However, the repeated use of antibacterial chemotherapeutics provokes antimicrobial resistance leading to treatment failure.⁵ Hence, a new approach for the prevention and treatment of UTI with orally applicable therapeutics is urgently needed.⁶

UPEC undergo a well-defined infection cycle within the host.⁷ The key step in pathogenesis is bacterial adhesion to the epithelial cells in the lower urinary tract.⁸ This interaction prevents UPEC from clearance by the bulk flow of urine and enables the bacteria to colonize the epithelial cells. The adhesion is mediated by the virulence factor FimH located at the tip of bacterial type 1 pili.^{9,10} FimH consists of two immunoglobulin-like domains: the N-terminal lectin domain and (connected by a short linker) the C-terminal pilin domain.¹¹ The lectin domain encloses the carbohydrate recognition domain (CRD) that binds

to the oligomannosides of the glycoprotein uroplakin Ia on the epithelial cell surface.¹² The pilin domain anchors the adhesin to the pilus and regulates the switch between two conformational states of the CRD with high and low affinity for mannoses, respectively.

More than 3 decades ago, Sharon and co-workers described various oligomannosides and aryl α -D-mannosides as potential antagonists of the FimH-mediated bacterial adhesion.^{13,14} However, only weak interactions in the milli- to micromolar range were observed. In recent years, several high-affinity monovalent mannose-based FimH antagonists with various aglycones like *n*-alkyl,¹⁵ phenyl,¹⁶ dioxocyclobutenyl-aminophenyl,¹⁷ umbelliferyl,¹⁶ biphenyl,^{18–22} indol(in)-ylphenyl,²³ triazolyl,²⁴ and thiazolylamino²⁵ have been reported. In addition, different multivalent presentations of the mannose have been synthesized^{26–32} and a heptavalent presentation of *n*-heptyl α -D-mannoside (**1**) tethered to β -cyclodextrin proved to be highly effective when applied together with the UTI89 bacterial strain through a catheter into the bladder of C3H/HeN mice.³² Importantly, adverse side effects resulting from nonselective binding of FimH antagonists (they are all α -D-mannopyrano-

Received: October 3, 2014

Published: February 10, 2015

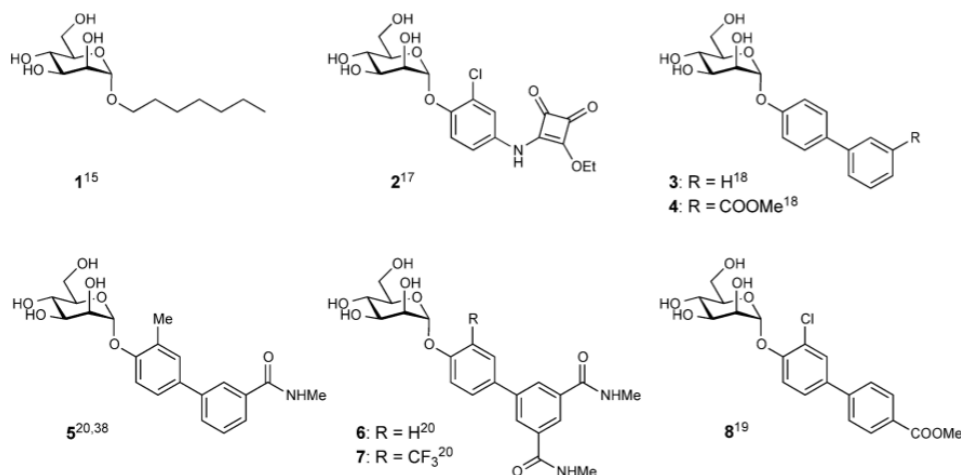


Figure 1. Monovalent FimH antagonists 1–4 acting as reference compounds and 5–8 which have been orally explored in in vivo disease models.

sides) to mannose receptors of the human host system have recently been ruled out.³³

The high affinities of the monovalent α -D-mannopyranosides are based on optimal interactions with the main structural features of the CRD:^{34–37} first, the mannose binding pocket accommodating the mannose moiety by means of an extended hydrogen bond network and, second, the entrance to the binding site composed of three hydrophobic amino acids (Tyr48, Tyr137, and Ile52) and therefore referred to as “tyrosine gate” hosting aliphatic and aromatic aglycones. As an example, *n*-heptyl α -D-mannopyranoside (**1**) exhibits nanomolar affinity due to hydrophobic contacts of the alkyl aglycone with the hydrophobic residues of the tyrosine gate.¹⁵ Furthermore, aromatic aglycones, such as present in mannosides **2** and **3** (Figure 1), provide strong π - π stacking interactions with the tyrosine gate. This interaction is further favored by the addition of an electron withdrawing substituent on the terminal ring of the biaryl portion (\rightarrow **4**).^{18,19}

Recent in vivo PK studies in mice proved the high potential of the biphenyl α -D-mannosides **5**–**8** for an oral treatment, although high doses (≥ 50 mg/kg) were necessary to achieve the minimal concentrations required for the antiadhesive effect in the urinary bladder.^{19–21} Moreover, the therapeutic effect could only be maintained for a few hours, i.e., 4 h for a po (per os) single-dose application of **7** (50 mg/kg), because of rapid elimination by glomerular filtration and low reabsorption from the primary urine in the renal tubules.²⁰

To date, the physicochemical properties affecting the rate of renal excretion, i.e., lipophilicity and plasma protein binding (PPB), or metabolic liabilities promoting nonrenal elimination pathways have been barely investigated for FimH antagonists. The goal of the present study was to optimize the biphenyl α -D-mannoside with respect to oral bioavailability and renal excretion. Starting from antagonist **9**¹⁹ (Figure 2), we synthesized new biphenyl derivatives, characterized their affinity to the CRD, structurally investigated their binding mode, and determined physicochemical and pharmacokinetic parameters predictive for intestinal absorption and renal elimination. Furthermore, we determined in vivo PK (pharmacokinetics) of the most promising new antagonists in a mouse model. After oral administration, the compound with the best PK profile proved effective in reducing the bacterial loads upon bladder infection in a mouse model of UTI.

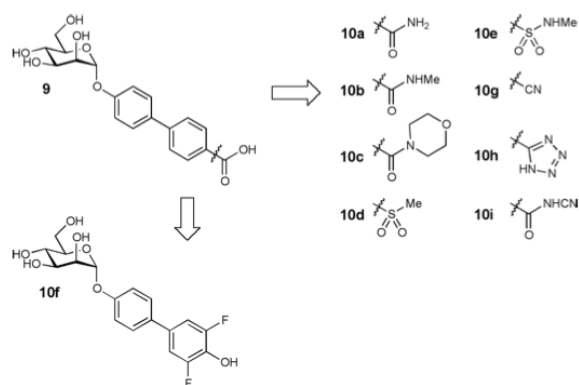


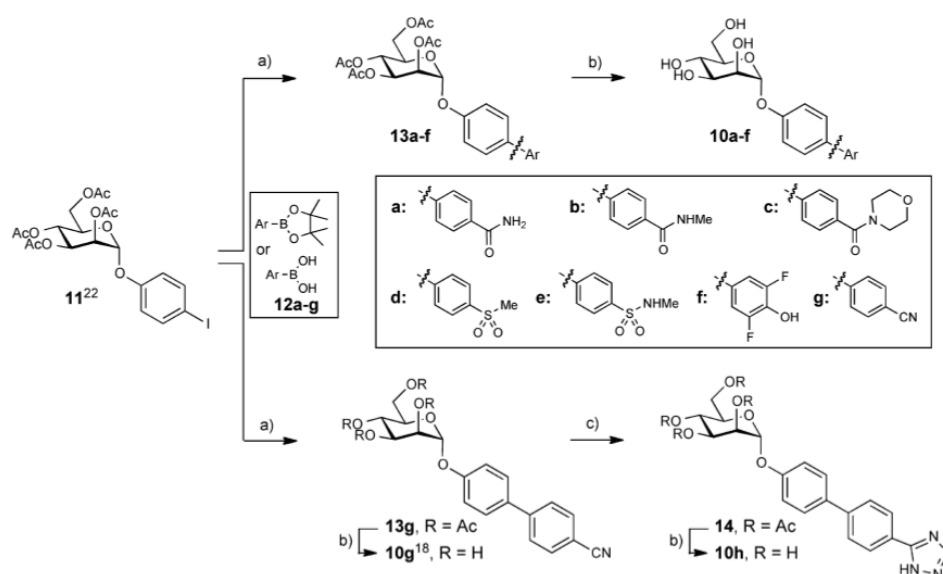
Figure 2. Bioisosteric replacement of the carboxylic acid substituent of biphenyl α -D-mannopyranoside **9**.

RESULTS AND DISCUSSION

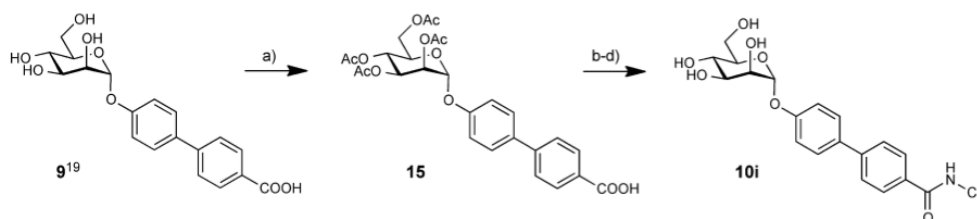
As previously reported, the carboxylate substituent present in the biphenyl mannoside **9** (its electron withdrawing potential being essential for an enhanced drug target interaction) strongly decreases the lipophilicity of the antagonist ($\log D_{7.4} < -1.5$ ¹⁹) in comparison to the *n*-heptyl (\rightarrow **1**, $\log P = 1.7$ ¹⁹) or the unsubstituted biphenyl aglycone (\rightarrow **3**, $\log P = 2.1$ ²²). Since low lipophilicity is a major reason for low intestinal absorption and rapid renal excretion of the systemically available antagonist,^{19,23} we aspired to improve oral bioavailability as well as renal excretion by replacing the carboxylate in **9** with various bioisosteric groups³⁹ (Figure 2).

Synthesis. Iodide **11** was prepared from peracetylated mannose and 4-iodophenol in the presence of $\text{BF}_3 \cdot \text{Et}_2\text{O}$.²² In a palladium-catalyzed Miyaura–Suzuki coupling⁴⁰ with the boronic acid or boronate derivatives **12a–g**, the biphenyl derivatives **13a–g** were obtained in good to excellent yields. Final deprotection yielded the test compounds **10a–g**. When microwave-assisted reaction conditions⁴¹ were utilized, the conversion of aryl nitrile **13g** to tetrazole **14** proceeded rapidly and with good yield. After deprotection of **14** using Zemléen conditions, the test compound **10h** was obtained (Scheme 1).

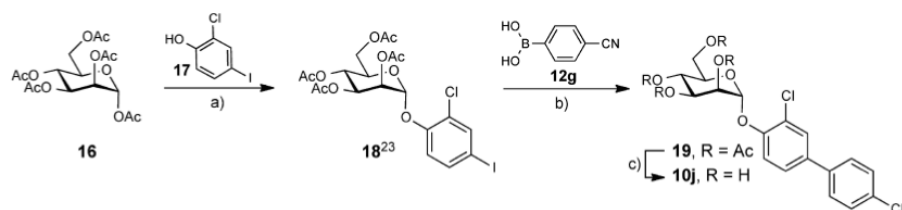
The cyanobenzamide derivative **10i** (Scheme 2) was obtained from **9** by peracetylation (\rightarrow **15**) followed by conversion of the

Scheme 1^a

^a(a) Pd(Cl₂)dppf·CH₂Cl₂, K₃PO₄, DMF, 80 °C, 4 h (13a–g, 44–99%); (b) NaOMe, MeOH, rt, 4 h (10a–h, 29–86%); (c) TMSN₃, Bu₂Sn(O), DME, 150 °C, microwave, 10 min (81%).

Scheme 2^a

^a(a) (i) Ac₂O, DMAP, pyridine, 0 °C to rt, overnight; (ii) sat. NaHCO₃ aq, DCM, rt, 2 h (15, 53%); (b) 1-chloro-*N,N*,2-trimethyl-1-propenylamine, toluene, 0 °C to rt, 2 h; (c) NaH, NH₂CN, DMF, 0 °C to rt, overnight; (d) NaOMe, MeOH, rt, 4 h (10i, 21% for three steps).

Scheme 3^a

^a(a) BF₃·Et₂O, CH₂Cl₂, 40 °C (76%); (b) Pd(Cl₂)dppf·CH₂Cl₂, K₃PO₄, DMF, 80 °C (75%); (c) NaOMe, MeOH, rt, 4 h (48%).

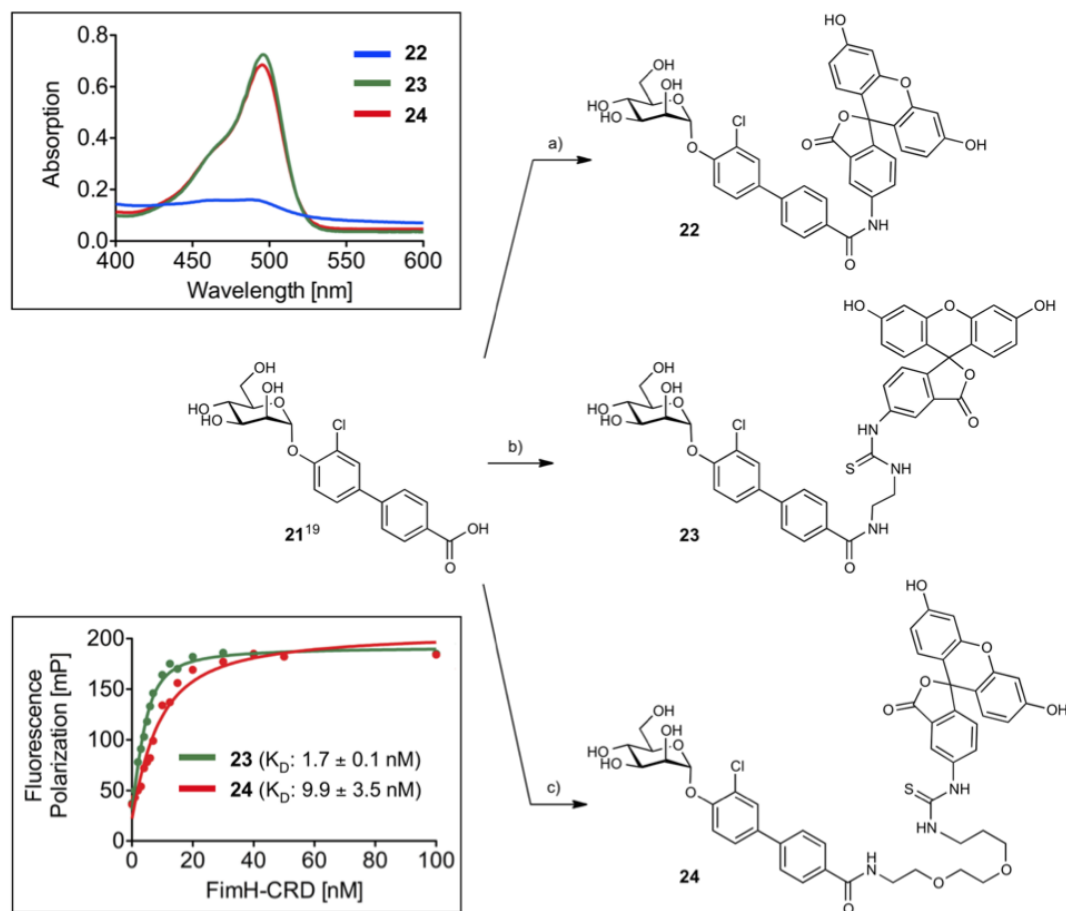
carboxylic acid into its acid chloride with 1-chloro-*N,N*,2-trimethyl-1-propenylamine.⁴² Without isolation, the acid chloride was reacted with sodium hydrogen cyanamide in DMF followed by deacetylation under Zemplén conditions to yield the test compound 10i.

Finally, to further improve the pharmacokinetic properties of mannoside 10g¹⁸ (see Table 3), a chloride substituent was introduced to the ortho-position of the aromatic ring adjacent to the anomeric oxygen. For its synthesis, peracetylated α -D-mannose (16) was coupled with 2-chloro-4-iodophenol (17) using BF₃·Et₂O as promotor (\rightarrow 18, 76%). After the introduction

of the second aromatic ring by Miyaura–Suzuki coupling (\rightarrow 19, 75%), deprotection yielded mannoside 10j (Scheme 3).

Binding Affinity. The binding affinity of heptyl mannoside 1, the biphenyl mannosides 3, 9, 20,¹⁸ and the bioisosteres 10a–j was determined in a competitive fluorescence polarization assay (FP assay) and with isothermal titration calorimetry (ITC). A protein construct consisting of the CRD with a C-terminal His-tag with a thrombin cleavage site (FimH-CRD-Th-His₆) was used for all experiments.⁴³

Competitive Fluorescence Polarization Assay. For the rapid evaluation of binding affinity, we established a competitive

Scheme 4^a

^a(a) 1-[(1-(Cyano-2-ethoxy-2-oxoethylideneaminoxy)dimethylaminomorpholinomethylene)]methanaminium hexafluorophosphate (COMU), NEt_3 , fluoresceinamine, DMF, rt, 7 h (**22**, 19%); b) (i) DIC, NHS, *N*-Boc-ethylenediamine, DMF, rt, 12 h; (ii) TFA, DCM, rt, 10 min (68% over two steps), (iii) fluorescein isothiocyanate (FITC), NEt_3 , DMF, rt, 3 h (**23**, 48%); c) (i) DIC, NHS, *N*-Boc-PEG2- NH_2 , DMF, rt, 14 h; (ii) TFA, DCM, rt, 30 min (62% over two steps); (iii) FITC, DMF, rt (**24**, 65%).

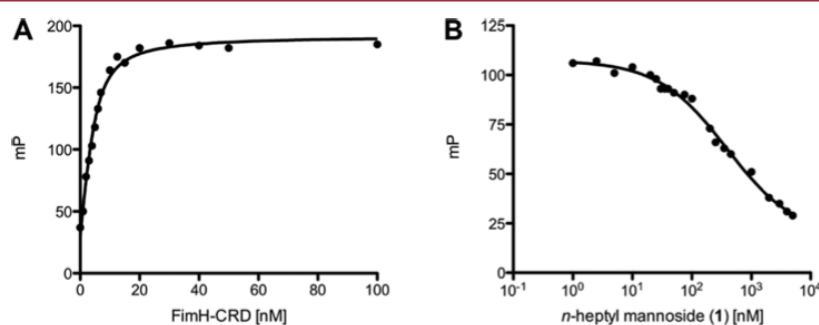


Figure 3. (A) Direct binding curve of the labeled competitor **23** obtained by adding a linear dilution of FimH-CRD (0–100 nM) and a constant concentration of competitor **23** (5 nM). The K_D was determined by fitting the experimental data to a single-site binding fit that accounts for ligand depletion. In three FP based direct binding experiments the K_D of competitor **23** was determined to be 1.7 nM. (B) Inhibition curve of *n*-heptyl mannoside (**1**) from the competitive FP assay. The IC_{50} value was determined by nonlinear least-squares fitting to a standard four-parameter equation. A modified Cheng–Prusoff equation⁴⁵ was used to calculate the corresponding K_D value ($K_D = 28.3$ nM).

binding assay based on fluorescence polarization (FP). Similar formats have been applied before for the detection of carbohydrate–lectin interactions.^{18,44} In this assay, the antagonist of interest displaces a fluorescently labeled competitor from

the binding site, thereby causing a reduction in fluorescence polarization.⁴⁵ To identify the optimal competitor, fluorescein isothiocyanate (FITC) was connected to the FimH ligand **21** by three linkers of different lengths (\rightarrow **22–24**, Scheme 4). For

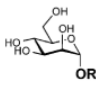
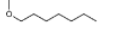
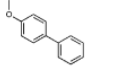
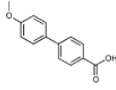
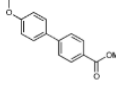
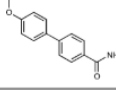
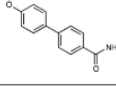
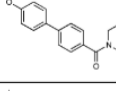
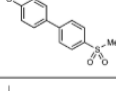
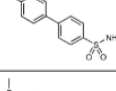
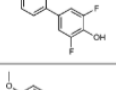
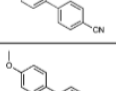
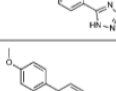
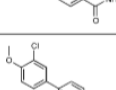
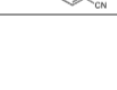
optimal sensitivity and signal-to-noise ratio, three main parameters need to be considered: (i) the affinity of the competitor should not be impaired by the fluorescent label; (ii) the conformational flexibility of the label upon binding of the competitor to the CRD should be low; (iii) the fluorescence properties of the label should not be affected by the connected ligand.^{46–48} A change in fluorescence properties was observed for reporter ligand **22** in which the label was linked to the biphenyl aglycone by an amide bond. The absorption spectrum revealed a lack of the characteristic fluorescein absorption peak at 494 nm (Scheme 4), likely due to an extension of the conjugated system to the biphenyl moiety of the ligand. The elongated saturated spacer groups in competitors **23** and **24** ensured that the expected spectral properties of the dye were retained (Scheme 4).

For the determination of their binding affinity, fixed concentrations of the reporter ligands **23** and **24** were incubated for 24 h with a linear dilution of the FimH-CRD (0–100 nM). FP was measured using a plate reader, with polarized excitation at 485 nm and emission at 528 nm measured through appropriately oriented polarizers. Fitting the single-site binding function of Cooper⁴⁹ to the observed FP data resulted for compound **23** in a dissociation constant ($K_D = 1.7$ nM, Figure 3A) similar to that of the unlabeled parent compound **21**,¹⁹ whereas **24** showed a 5-fold lower affinity (9.9 nM) (Scheme 4). Therefore, the reporter ligand **23** fulfills all characteristics as an optimal competitor and was used for the FP assay.

For the test compounds **1**, **3**, **9**, **20**, and **10a–j**, a 24 h incubation time was applied before FP was measured because of the long residence time of FimH antagonists ($t_{1/2} > 3.5$ h, Figure 3B⁵⁰). The 24 h incubation period was empirically determined to be necessary to reach equilibrium between reporter ligand and compound of interest. IC_{50} values were obtained by nonlinear least-squares regression (standard four-parameter dose–response curve) and converted to K_D values using a modified Cheng–Prusoff equation.⁴⁵ This equation accounts for the ligand depletion effect in competitive titrations involving high-affinity interaction partners present in similar concentrations. Under these conditions, the free concentration of an interacting species cannot be assumed to equal the total concentration.

The K_D values determined for the test compounds **1**, **3**, **9**, **20**, and **10a–j** are summarized in Table 1. Against our expectations, the biphenyl mannosides **3** and **9** exhibit similar affinities (Table 1), despite the presence of an electron withdrawing carboxylate substituent in antagonist **9**. According to the crystal structure of FimH cocrystallized with the sulfonamide derivative **10e** (Figure 4A), the outer aromatic ring of the biphenyl aglycone forms π – π interactions with the electron rich Tyr48, which is part of the tyrosine gate of FimH.¹⁵ A reduction of electron density of the aglycone by the electron withdrawing carboxylate was expected to enforce these π – π stacking interactions and lead to improved affinity. However, this beneficial effect might be compensated by an entropic penalty originating from the improved π – π stacking to Tyr48 that might lead to the reduced flexibility of both protein and antagonist. Furthermore, a beneficial enthalpy effect might be partially compensated by an enthalpy penalty originating from the desolvation of the charged carboxylate in **9**⁵¹ (see also Experimental Section). Although this substituent is solvent exposed, at least a partial desolvation may be necessary upon antagonist binding. To prove this assumption, we replaced the carboxylate by the corresponding methyl ester (\rightarrow **20**)¹⁸ in order to reduce the desolvation penalty and, as predicted by the Hammett constant σ_p ⁵² to further improve the π – π stacking.

Table 1. Affinities (K_D) of FimH Antagonists to FimH-CRD-Th-His₆^b

Entry	Compd		Affinity K_D [nM]
1	1		28.3 ± 5.0
2	3		15.1 ± 2.2
3	9		17.9 ± 1.5
4	20		3.6 ± 0.9
5	10a		2.8 ± 0.3
6	10b		2.9 ± 0.5
7	10c		3.0 ± 0.1
8	10d		1.7 ± 0.2
9	10e		2.7 ± 0.4
10	10f		3.7 ± 0.2
11	10g		2.0 ± 0.6
12	10h		5.7 ± 0.1
13	10i		8.4 ± 0.3
14	10j		< 1 ^{a)}

^aThe K_D value of **10j** was approximated to be in the subnanomolar range. The IC_{50} value obtained in the competitive FP assay was equal to the lowest value that can be resolved by the assay, indicating stoichiometric titration of **10j** due to its high affinity. Consequently, its K_D must be below the K_D of competitor **23**. ^bDissociation constants (K_D) were determined in a competitive fluorescence polarization assay.

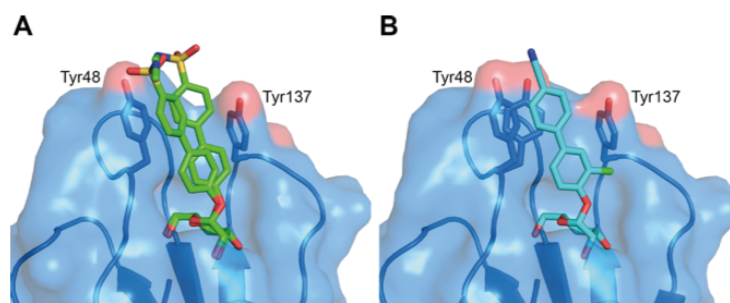


Figure 4. Ligand binding poses determined by X-ray cocrystallization with compounds **10e** resolved to 1.07 Å (A) and **10j** resolved to 1.10 Å (B). The electron density surrounding the aglycone of **10e** indicates flexibility of the aglycone and was modeled in two poses. Both compounds bind in a similar pose with a well-defined hydrogen network surrounding the mannose moiety and π - π stacking interactions between the second aromatic ring and Tyr48 side chain (A). In contrast, in the FimH-CRD/**10j** structure the amino acid side chain of Y48 can be modeled in two distinct rotamers, suggesting flexibility also of the receptor (B).

Indeed, a 6-fold improvement in affinity was achieved. However, since the methyl ester undergoes rapid enzyme-mediated hydrolysis *in vivo*,¹⁹ it will not be available at the place of action in the urinary bladder. The methyl ester was therefore replaced by metabolically stable bioisosteres³⁹ exhibiting comparable electron withdrawing properties⁵² (Table 1, entries 5–13). The most potent derivatives **10d**, **10e**, and **10g** showed affinities in the low nanomolar range.

As previously reported,²² a chloro substituent in the ortho-position of the aromatic ring adjacent to the anomeric oxygen is favorable for affinity and improves the physicochemical properties relevant for oral bioavailability. Indeed, the corresponding antagonist **10j** was the most potent compound tested in this study.

Isothermal Titration Calorimetry (ITC). To further confirm our hypothesis regarding π - π stacking and desolvation, we performed ITC experiments with the reference compound **1**, the unsubstituted biphenyl mannoside **3**, the carboxylic acid **9**, and the bioisosteres **10b–e,g,j** (Table 2). ITC allows the simultaneous determination of the stoichiometry (N), the change in enthalpy (ΔH) and the dissociation constant (K_D) for ligand–protein binding.^{53,54} The reliable determination of these three parameters requires well-defined sigmoidal titration curves characterized by the dimensionless Wiseman parameter c ($c = Mt(0) K_D^{-1}$, where $Mt(0)$ is the initial macromolecule concentration).⁵⁵ To be sure that data can be fitted with confidence, the c -value should be between 1 and 1000 (ideally between 5 and 500),⁵⁶ which could be achieved for the antagonists **3** and **9**. For titrations involving low micromolar $Mt(0)$ and interactions in the low nanomolar or picomolar range, as suggested for the bioisosteres **10b–j**, c -values above 1000 were expected. Since these conditions lead to steep titration curves that do not allow the determination of the curve slope representing $1/K_D$, we applied an alternative, competitive format referred to as displacement assay.^{57,58} First, FimH-CRD-Th-His₆ was preincubated with the low affinity antagonist *n*-heptyl 2-deoxy- α -D-mannopyranoside (**25**, for synthesis see Supporting Information). The high-affinity bioisosteres of interest were titrated into the protein–ligand complex giving well-defined sigmoidal titration curves.

The resulting K_D values (Table 2) correspond well with the data obtained from the FP assay (Table 1). A comparison of the thermodynamic fingerprints of antagonists **3** and **9** reveals that the more favorable enthalpic contribution resulting from facilitated π - π stacking leads to a net enthalpy gain ($\Delta\Delta H =$

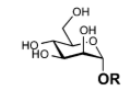
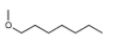
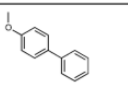
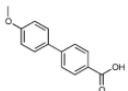
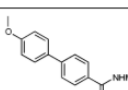
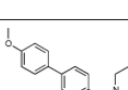
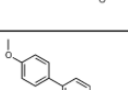
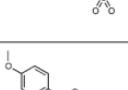
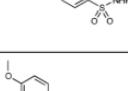
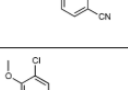
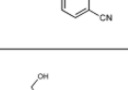
-3.7 kJ/mol). However, an even greater increase in enthalpy is likely countered by the enthalpy costs for desolvation of the electron withdrawing carboxylate.

The gain in enthalpy is in turn compensated by an unfavorable entropy ($-T\Delta\Delta S = 3.2$ kJ/mol) as a result of the reduced flexibility of both the antagonist and the Tyr48 side chain caused by the improved interaction. This is not entirely outweighed by the beneficial entropy contribution related to the partial desolvation of the carboxylate and the related release of water into the bulk. Added together, the enthalpy and entropy contributions of antagonists **3** and **9** result in similar affinities (K_D of 17.7 and 15.0 nM, respectively).

In contrast, the replacement of the carboxylate group by various neutral bioisosteres (entries 4–7) reduces the enthalpy costs for desolvation (see calculated free energies of desolvation, Experimental Section) and therefore leads to a markedly improved enthalpy ($\Delta\Delta H$ from -3.5 to -5.8 kJ/mol). As a result, an up to 5-fold improvement of the K_D values was achieved. Finally, with a cyano substituent (entries 8 and 9), the enthalpy term was further improved ($\Delta\Delta H = -3.7$ kJ/mol) because of a reduced desolvation penalty and improved π - π stacking interactions. However, this beneficial component is again partially compensated by a decrease in entropy. This can be attributed, first, to the loss of flexibility of the tightly bound ligand (Figure 4B) and, second, to the smaller surface area of the cyano substituent compared to amide, sulfonamide, and sulfone, which results in a smaller number of water molecules being released to bulk upon binding.

X-ray Crystallography. To determine the binding poses of the bioisosteres, we cocrystallized the compounds **10e** and **10j** with the FimH-CRD (Figure 4). Atomic resolution crystal structures were obtained at 1.07 Å (**10e**) and 1.10 Å (**10j**). As observed in previous mannoside cocrystal structures,^{15,18,36} the mannose moiety forms an extensive hydrogen bond network to the well-defined binding site with all of its hydroxyl groups. The biphenyl aglycone is located between the tyrosine gate residues (Tyr48/Tyr137). The π - π stacking of the second aromatic ring of the aglycone to the side chain of Tyr48 contributes most to the interaction energy of the aglycone moiety. Interactions to the Tyr137 side chain on the other hand are only limited. Whereas a previously published crystal structure of a biphenyl mannoside in complex with FimH-CRD suffers from crystal contacts of binding site residues (Tyr48 side chain to backbone oxygen of Val27) possibly causing the distortion of the binding site,¹⁸ the binding sites of our structures are mostly solvent exposed. This

Table 2. Thermodynamic Parameters from ITC for Selected FimH Antagonists Binding to FimH-CRD-Th-His^d

Entry	Compd		$K_D^{[a]}$ [nM]	ΔG [kJ/mol]	$\Delta H^{[a]}$ [kJ/mol]	$-T\Delta S$ [kJ/mol]	n	Type of measurement
1	1 ^[b,c]		28.9 (25.8 – 32.3)	-43.0	-50.3 (-50.2 – -50.7)	7.3	1.00	direct
2	3 ^[b]		17.7 (14.1 – 22.3)	-44.2	-45.0 (-44.5 – -45.6)	0.8	1.07	direct
3	9		15.0 (13.4 – 16.7)	-44.7	-48.7 (-48.4 – -49.0)	4.0	1.05	direct
4	10b		4.3 (3.2 – 5.6)	-47.8	-54.5 (-54.1 – -54.9)	6.7	1.02	competitive vs. 25
5	10c		5.0 (3.8 – 6.6)	-47.4	-54.5 (-54.1 – -54.8)	7.1	0.97	competitive vs. 25
6	10d		3.0 (2.1 – 4.2)	-48.7	-52.3 (-51.5 – -53.1)	3.6	0.99	competitive vs. 25
7	10e		3.5 (2.9 – 4.3)	-48.2	-52.2 (-51.6 – -52.8)	3.9	1.06	competitive vs. 25
8	10g		2.8 (2.3 – 3.3)	-48.8	-58.2 (-57.8 – -58.6)	9.4	1.00	competitive vs. 25
9	10j		1.3 (1.1 – 1.6)	-50.7	-60.9 (-60.4 – -61.4)	10.1	1.01	competitive vs. 25
10	25		9*386 (8*555 – 10*287)	-28.7	-19.5 (-19.1 – -20.0)	-9.1	1.00	direct

^a95% confidence interval from fitting in parentheses. ^bGlobal fit including two direct titration measurements. ^cITC data were previously published with an n -value of 0.82.³⁷ ^d n , stoichiometric correction factor.

revealed the flexibility of the aglycone in the FimH-CRD/**10e** structure, since the electron density toward the solvent-exposed sulfonamide indicates that there is not one single orientation. Therefore, the aglycone was modeled in two distinct poses. In contrast, in the FimH-CRD/**10j** structure the amino acid side chain of Y48 can be modeled in two distinct rotamers, suggesting flexibility also of the receptor.

Physicochemical Properties and in Vitro Pharmacokinetics. Intestinal absorption and renal excretion are prerequisites for a successful oral treatment of UTI with FimH

antagonists. Furthermore, reabsorption of antagonist from the renal ultrafiltrate is desirable for maintaining the minimal antiadhesive concentration in the target organ, namely, the bladder, over an extended period of time. To estimate the influence of the bioisostere approach on oral bioavailability and the rate of renal excretion, we determined lipophilicity by means of the octanol–water distribution coefficient ($\log D_{7.4}$),⁵⁹ aqueous solubility, and membrane permeability in the artificial membrane permeability assay (PAMPA)⁶⁰ and the colorectal adenocarcinoma (Caco-2) cell monolayer model.⁶¹

Table 3. Physicochemical and in Vitro Pharmacokinetic Parameters^h

compd	pK _a ^a	log D _{7.4} ^b	solubility [μg/mL]/pH ^c	PAMPA log P _e ^d [cm/s]/pH ^d	Caco-2 P _{app} [10 ⁻⁶ cm/s] ^e		PPB f _b ^f [%] ^f	metabolic stability t _{1/2} ^g [min] ^g
					a → b	b → a		
1		1.65	>3000	-4.89	7.0 ± 0.6	9.4 ± 0.2	81	13
3		2.1 ± 0.1	21 ± 1/7.4	-4.7 ± 0.1/7.4	10.0 ± 0.9	19.0 ± 1.2	93 ± 1	nd
20		2.14	33.8/6.51	-4.7	4.23	nd	93	1.0
9	3.88	<-1.5	>3000/6.61	no permeation	nd	nd	73	>60
10a		0.5 ± 0.1	12 ± 1/7.4	-6.8 ± 0.3/7.4	0.12 ± 0.01	0.61 ± 0.03	nd	nd
10b		0.8 ± 0.0	122 ± 13/7.4	-9.2 ± 1.4/7.4	1.10 ± 0.82	0.87 ± 0.15	nd	nd
10c		0.2 ± 0.1	>250/7.4	-7.8 ± 0.3/7.4	0.18 ± 0.07	1.30 ± 0.03	48 ± 2	>60
10d		0.4 ± 0.0	246 ± 17/7.4	-7.2 ± 0.0/7.4	0.36 ± 0.01	1.76 ± 0.12	99 ± 1	>60
10e		0.7 ± 0.1	>250/7.4	-8.6 ± 0.2/7.4	0.28 ± 0.23	1.82 ± 0.14	>99	>60
10f	6.5	1.1 ± 0.0	>150/3.0	-7.7 ± 0.8/5.0	0.40 ± 0.02	1.90 ± 0.17	nd	nd
			>150/7.4	-8.8 ± 0.1/7.4				
10g		1.4 ± 0.0	186 ± 4/7.6	-5.7 ± 0.0/7.4	2.0 ± 0.1	13.2 ± 2.1	99 ± 0	>60
10h	3.7	-1.4 ± 0.1	11 ± 0/3.0	-9.3 ± 1.4/5.0	0.17 ± 0.00	0.22 ± 0.01	nd	nd
			273 ± 2/7.4	-8.8 ± 1.4/7.4				
10i	2.5	-1.1 ± 0.1	>150/3.0	-6.8 ± 0.2/5.0	0.22 ± 0.14	0.29 ± 0.03	nd	nd
			>150/7.4	-7.0 ± 0.1/7.4				
10j		2.1 ± 0.0	192 ± 5/7.4	-5.2 ± 0.0/7.4	2.2 ± 0.4	22.1 ± 1.5	89 ± 1	>60

^apK_a values were determined by NMR spectroscopy. ^bOctanol–water distribution coefficients (log D_{7.4}) were determined by a miniaturized shake-flask procedure at pH 7.4. Values represent the mean ± SD of sextuplicate measurements.⁵⁹ ^cKinetic solubility was measured in a 96-well format using the μSOL Explorer solubility analyzer at the indicated pH in triplicate. ^dP_e = effective permeability. Passive permeation through an artificial membrane was determined by the parallel artificial membrane permeation assay (PAMPA). Values represent the mean ± SD of quadruplicate measurements performed at the indicated pH.⁶⁰ ^eP_{app} = apparent permeability. Permeation through a Caco-2 cell monolayer was assessed in the absorptive (a → b) and secretory (b → a) directions in triplicate.⁶¹ ^fPlasma protein binding (PPB) was determined by equilibrium dialysis in triplicate.⁶² ^gMetabolic stability was determined by incubating the compounds (2 μM) with pooled rat liver microsomes (RLM, 0.5 mg/mL) in the presence of NADPH (1 mM, compounds 1, 9, 10c–e,g,j) or without NADPH (compound 20).⁶³ ^hnd = not determined.

Oral Bioavailability. Oral bioavailability of a compound relies on solubility, permeation through the membranes lining the intestine, and stability against first pass metabolism.^{64,65} As discussed by Lipinski⁶⁶ and Curatolo,⁶⁷ dose and permeability define the minimum aqueous solubility required for oral administration. Thus, a dose of 1 mg/kg of a moderately permeable compound requires a solubility of at least 52 μg/mL. Whereas sufficient aqueous solubility (>3000 μg/mL) was reported for *n*-heptyl α -mannopyranoside (1),¹⁹ the unsubstituted biphenyl α -D-mannopyranoside 3 and the antagonists bearing a methylcarboxylate, carboxamide, or tetrazole substituent (compounds 20, 10a, and 10h) were found to be scarcely soluble.²² As proposed by Ishikawa,⁶⁸ a possible reason is the apolar and planar aglycone. By contrast, the polar carboxylic acid moiety present in antagonist 9 or the substituents in the bioisosteres 10b–j enhance solubility to 122–273 μg/mL, a level sufficient for in vivo PK studies. For in vivo disease studies, however, dosages of up to 10 mg/kg were foreseen (see below), requiring a solubility of 520 μg/mL.^{66,67} For this reason, surfactant Tween 80 (1%) had to be added.

Furthermore, permeability data derived from PAMPA⁶⁹ and the Caco-2 model⁷⁰ suggest moderate to high permeation of the moderately lipophilic antagonists 1, 3, and 20 (log D_{7.4} > 1.6) through the intestinal membranes. The bioisosteres 10a–f,h,i, although slightly more permeable than the strongly hydrophilic carboxylic acid derivative 9, show only low values of permeability compared to *n*-heptyl α -D-mannopyranoside (1) or the unsubstituted biphenyl mannoside 3. However, the *p*-cyanobiphenyl derivatives 10g and 10j display elevated log D_{7.4} and effective permeability (log P_e) in the range for successful intestinal absorption. Regarding both sufficient aqueous solubility and elevated membrane permeability, the *p*-cyano substituted bioisosteres 10g and 10j are thus the most promising

candidates for oral absorption. Moreover, combining the bioisosteric replacement with the addition of a chloro substituent in the ortho-position of the aromatic ring adjacent to the anomeric oxygen (→10j)²² resulted in the most advantageous physicochemical profile for oral bioavailability.

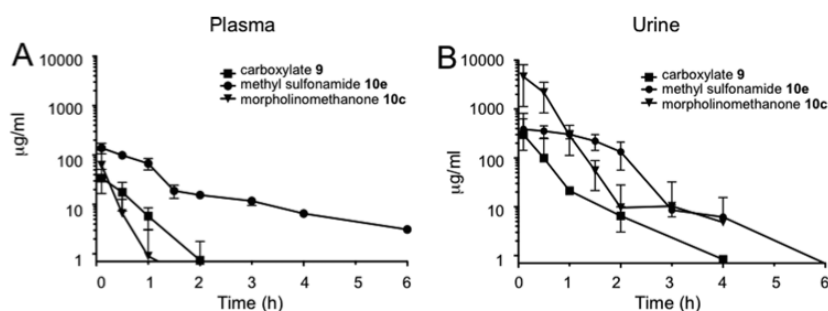
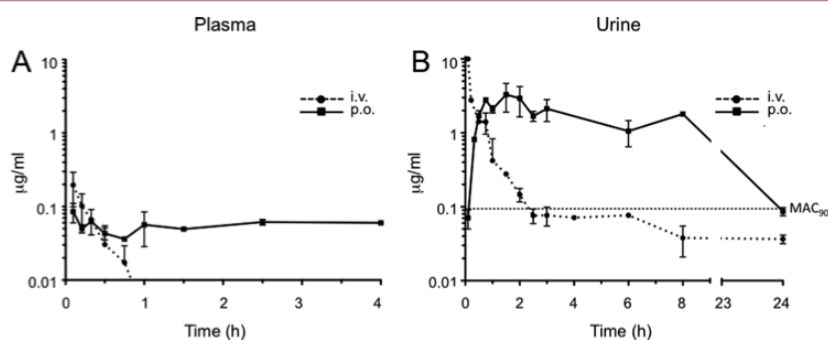
Renal Excretion. The rate of renal excretion depends on the rate of glomerular filtration and the propensity to tubular secretion and reabsorption of an antagonist.⁷¹ Only the fraction that is not bound to plasma proteins is expected to enter the glomerular filtrate.⁷² Plasma protein binding (PPB) data indicating the fraction bound (f_b) are listed in Table 2.⁶² The biphenyls 9 and 10c were identified as moderate binders to plasma proteins (f_b ≤ 65%), which suggests a low impact of PPB on antagonist filtration. The f_b values of the antagonists 1, 3, 20, and 10j were between 80% and 93%, whereas the bioisosteres 10d,e,g showed particularly high protein binding (f_b ≥ 99%) implying slow compound entry into the primary urine. However, the kinetic aspects of PPB, that is, association and dissociation rate constants, remain to be determined to quantify precisely the influence of PPB on filtration.⁷³

Furthermore, log D_{7.4} was identified as key determinant of tubular reabsorption.^{74–76} Accordingly, lipophilic compounds are predominantly reabsorbed from the renal filtrate. Given that renal clearance is the major route of elimination, this will result in a slow but steady excretion into the bladder. In contrast, hydrophilic compounds are poorly reabsorbed and thus quickly renally eliminated, which leads to high initial compound levels in the urine but narrows the time range where the minimal antiadhesive concentration is maintained. Consequently, low log D_{7.4} as shown for the antagonists 9, 10h, and 10i implies low tubular reabsorption and rapid elimination of the filtered molecules by the urine. Otherwise, log D_{7.4} between 0.2 and 0.7, such as determined for the bioisosteres 10a–e, suggests

Table 4. Pharmacokinetic Parameters Determined after a Single iv Application of Compounds 9, 10c, 10e, and 10j in Female C3H/HeN Mice^a

compd	plasma							urine, C_{max} ($\mu\text{g/mL}$)
	C_0 ($\mu\text{g/mL}$)	dose (mg/kg)	V_z (mL)	$t_{1/2}$ (h)	AUC_{0-inf} ($\mu\text{g}\cdot\text{h/mL}$)	CL_{tot} (mL/h)		
9	40	50	25.2	0.33	23.5	53.1	300	
10c	109.7	50	28.3	0.4	25.3	49.4	4611	
10e	151.6	50	19.5	1.9	175.1	7.1	387	
10j	0.36	0.625	52.8	0.17	0.07	218	10	

^aValues were calculated using PKSolver.⁷⁸ C_0 , initial concentration; V_z , volume of distribution in terminal phase; AUC, area under the curve; CL_{tot} , total clearance; C_{max} , maximal concentration.

**Figure 5.** Antagonist concentrations in (A) plasma and (B) urine after a single iv application of 9, 10c, and 10e (50 mg/kg).**Figure 6.** Antagonist concentrations in (A) plasma and (B) urine after a single iv and po application of compound 10j (iv, 0.625 mg/kg; po, 1.25 mg/kg). MAC_{90} is the minimal antiadhesive concentration to inhibit 90% adhesion (0.094 $\mu\text{g/mL}$).

increasing propensity to tubular reuptake, whereas $\log D_{7.4} > 1$ as shown for heptyl mannoside 1 and the biphenyl mannosides 3, 20, 10g, 10f, and 10j is optimal for tubular reabsorption from the glomerular filtrate and thus for slow renal clearance.

Metabolic Stability. Increasing lipophilicity is usually paralleled by increasing susceptibility to metabolism.⁷⁷ Liabilities toward metabolic clearance pathways that prevent the intact antagonist from reaching the target in the bladder were therefore of interest. To assess their propensity to cytochrome P450 (CYP450) mediated metabolism, heptyl mannoside 1, the carboxylic acid derivative 9, and the bioesters 10c–e,g,j were incubated with rat liver microsomes (RLM, 0.5 mg/mL) in the presence of the cofactor β -nicotinamide adenine dinucleotide phosphate (NADPH).⁶³ To confirm the high propensity of the methyl ester present in antagonist 20 to carboxylesterase (CES) mediated hydrolysis, this antagonist was incubated with RLM only. The profiles of unchanged compound versus time revealed high susceptibility of heptyl mannoside 1 to CYP450-mediated metabolism ($t_{1/2} = 13$ min) and rapid hydrolysis of the ester 20 by the hepatic CES ($t_{1/2} = 1.0$ min). Otherwise, the bioesters 10c–e,g,j were stable against enzyme-mediated bioconversion

($t_{1/2} > 60$ min), suggesting lower propensity to metabolic, nonrenal elimination pathways.

Considering PPB, lipophilicity, and metabolic stability data, we therefore expected (i) a steady release of compounds 10d,e,g,j into the bladder because of high PPB decelerating glomerular filtration (10d,e,g) and/or high $\log D_{7.4}$ supporting tubular reabsorption (10g,j), (ii) a fast excretion of antagonists 9 and 10c via the urine due to low PPB and low $\log D_{7.4}$, and (iii) a rapid clearance of heptyl mannoside 1 from the body by renal and metabolic pathways. Compounds featuring high propensity to renal excretion as major route of elimination (10c, 10e and 10j) were selected for in vivo PK studies in a mouse model.

Pharmacokinetic Studies in C3H/HeN Mice. This first part of our study explored the predicted effects of lipophilicity, PPB, and metabolic stability on antagonist disposition and elimination upon a single dose iv application (50 mg/kg) of compounds 10c and 10e. The PK parameters of these applications and those of the previously published carboxylate 9 are summarized in Table 4. The table also contains the results of the iv administration of compound 10j (0.625 mg/kg).

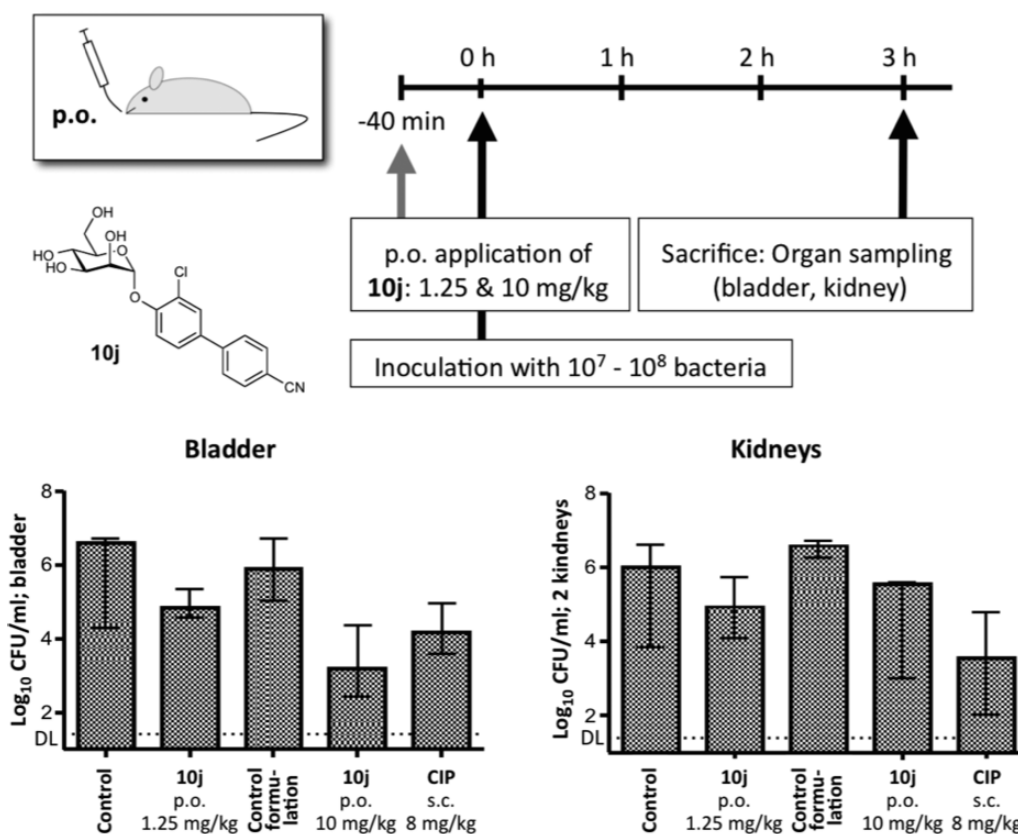


Figure 7. Preventive efficacy of 10j in the UTI mouse model 3 h after infection. The bars depict the median bacterial load with the interquartile range in the different study groups. Shown are the results of the control group (PBS), control group formulation (5% DMSO in PBS containing 1% Tween 80), and the intervention groups with the preventive applications of either 1.25 or 10 mg/kg 10j po or 8 mg/kg CIP sc (representing the murine dose equivalent to a human standard dose).⁸¹ DL, detection limit. CFU, colony forming units.

In contrast to the fast plasma clearance of antagonists **9** and **10c** (Figure 5A), the methylsulfonamide bioisostere **10e** attained higher initial concentration in plasma (C_0) and lower total clearance (CL_{tot}). Therefore, it could be detected until 6 h after application, resulting in markedly higher plasma AUC. The observed high C_0 of compound **10e** may be attributed to a small volume of distribution (V_d) resulting from the high PPB ($f_b \geq 99\%$).⁷² In urine (Figure 5B), the carboxylic acid **9** and the morpholinomethanone **10c** displayed high levels immediately following administration and a rapid concentration decrease within the first 2 h, reflecting the rapid elimination from plasma. Fast renal excretion as major route of elimination can be rationalized by the physicochemical properties of the antagonists **9** and **10c**, that is, moderate PPB and $\log D_{7,4}$, as well as high metabolic stability. Otherwise, the methylsulfonamide bioisostere **10e** showed sustained compound levels in urine over a period of 2 h and subsequent slow decrease until 6 h after administration. This sustained renal excretion is a result of the interplay of the antagonist's elevated PPB and $\log D_{7,4}$.

In a second study, the *p*-cyano bioisostere **10j**, characterized by a high oral absorption potential, was administered as a single dose iv (0.625 mg/kg) and po (1.25 mg/kg). The plasma concentration curve upon iv dosing displays a steep decline within the first hour after application, while the po curve shows a prolonged period where absorption and elimination are in equilibrium (Figure 6A). The urine concentration profiles

(Figure 6B) parallel the plasma curves obtained by the two modes of application; i.e., high plasma clearance upon iv bolus injection led to high initial antagonist levels in urine and a rapid concentration decline. By contrast, sustained plasma concentrations upon po administration resulted in prolonged urine levels.

As a result, urine concentrations exceed the minimum level required for the antiadhesive effect as estimated from the in vitro cell infection model⁷⁹ (minimal antiadhesion concentration, $MAC_{90} = 0.094 \mu\text{g/mL}$) for more than 8 h upon oral single-dose administration (Figure 6B).

Infection Study in C3H/HeN Mice. In a preventive study, six mice were inoculated with UTI89 following an oral application of **10j** (1.25 mg/kg) 40 min prior to infection. Three hours after inoculation, the animals were sacrificed and bladder and kidneys were removed. Organs were homogenized and analyzed for bacterial counts. The effect of the FimH antagonist was compared to a 8 mg/kg dose of ciprofloxacin (CIP), applied subcutaneously (sc) 10 min before infection. CIP is used as standard antibiotic therapy in humans for the treatment of UTI.⁸⁰ In mice, the dose of 8 mg/kg sc was shown to mimic the standard human dose regarding peak levels and the AUC_{24} in serum.⁸¹ The median reductions in bacterial counts in mice treated with **10j** and CIP compared to the control group 3 h after infection are displayed in Figure 7.

The median value in the untreated control group showed bacterial counts of 6.6 log₁₀ colony forming units (CFU) in the bladder and 6 log₁₀ CFU in the kidneys. After oral application of 1.25 mg/kg **10j**, bacterial loads in the bladder decreased by 1.78 log₁₀ CFU and 1.07 log₁₀ CFU in the kidneys. The lower reduction in the kidneys is most likely due to the differing adhesion mechanisms between bladder and kidneys (type 1 pili vs P-pili), which is not targeted by **10j**.⁸² With CIP (8 mg/kg sc) a substantial reduction in both bladder and kidneys (median reductions of 2.44 log₁₀ and 2.47 log₁₀, respectively) was observed. Despite the low oral dose of **10j** (1.25 mg/kg), the approximately 100-fold reduction of CFU in the bladder promised an even higher effect upon dose increase to 10 mg/kg. Since the solubility of **10j** for this increased dose is too low (192 µg/mL), we used 5% DMSO and surfactant Tween 80 (1%) as solubilizer. To effectively compare the effect of a higher dose of **10j**, a control group receiving the formulation only (5% DMSO in PBS containing 1% Tween 80, termed control group formulation) was tested in parallel. When 10 mg/kg **10j** was applied, bacterial loads in the bladder decreased by 2.68 log₁₀ CFU/mL compared to the control group formulation, clearly exceeding the effect of CIP with a reduction of 2.44 log₁₀ CFU/mL. However, only a moderate reduction of 1.04 log₁₀ CFU was achieved in the kidneys.

SUMMARY AND CONCLUSION

Recently, numerous monovalent alkyl and aryl α -D-mannopyranosides have been described as potent FimH antagonists. However, most of them suffer from insufficient pharmacokinetic properties, i.e., modest bioavailability and short duration of the therapeutic effect in the bladder, their site of action. As a consequence, high doses at short intervals are required to achieve antiadhesive effects over an extended period of time. Therefore, the goal of the present study was an appropriate optimization of the pharmacokinetic profile of biphenyl α -D-mannopyranosides while keeping their high affinity to the CRD of FimH. The starting point was the biphenylcarboxylate **9** where the critical carboxylate was replaced by bioisosteres.^{39,83}

With a series of bioisosteres, a 3- to 5-fold improvement of affinity was achieved compared to **9**. Although binding necessitates only partial desolvation of the carboxylate and its bioisosteric replacements, a reduction of the enthalpy penalty for desolvation⁵¹ was identified as the source of the improved affinity exhibited by the bioisosteres. Thermodynamic evaluation of antagonists **10b–e** revealed almost identical enthalpy contribution to binding. However, for antagonists with the *p*-cyano substituent (**10g** and **10j**) an enhancement of up to -8.7 kJ/mol was observed, indicating a reduced desolvation penalty and an improved stacking as derived from the crystal structure of **10j** cocrystallized with the CRD of FimH (Figure 4B). On the other hand, higher affinity originating from a reduction of conformational flexibility of ligand and protein resulted in a concomitant entropy penalty of up to 6.5 kJ/mol.

In addition to the improved pharmacodynamics, the relevant pharmacokinetic parameters (solubility, permeability, renal excretion) were substantially improved. With 3'-chloro-4'-(α -D-mannopyranosyloxy)biphenyl-4-carbonitrile (**10j**), a FimH antagonist with an optimal in vitro PK/PD profile was identified. The *p*-cyano substituent conferred lipophilicity and high binding to plasma proteins, which slowed the rate of renal excretion. Despite higher lipophilicity, antagonist **10j** was unsusceptible to CYP450-mediated metabolism and therefore predominantly eliminated via the renal pathway. In vivo experiments confirmed

the excellent PK profile of **10j** with steady renal excretion for more than 8 h after oral application (1.25 mg/kg), suggesting a long-lasting antiadhesive effect. Finally, the preventive oral application of **10j** (10 mg/kg) reduced the bacterial load in the bladder by almost 1000-fold 3 h after infection. Although the first 3 h of the infection do not represent the complete infection cycle, they represent the time span of bacteria adhering and invading urothelial cells.^{84,85} Nevertheless, the effect of FimH antagonist **10j** within a longer infection time and at higher dosing will be the subject of future investigations.

EXPERIMENTAL SECTION

Synthesis. The synthesis of compounds **10a–d**, **10f**, **10g**, **10i**, **13a–d**, **13f**, **13g**, **15**, **18**, and **25**, including compound characterization data, can be found in the Supporting Information.

General Methods. NMR spectra were recorded on a Bruker Avance DMX-500 (500.1 MHz) spectrometer. Assignment of ¹H and ¹³C NMR spectra was achieved using 2D methods (COSY, HSQC, HMBC). Chemical shifts are expressed in ppm using residual CHCl₃, CHD₂OD, or H₂O as references. Optical rotations were measured using PerkinElmer polarimeter 341. Electron spray ionization mass spectra were obtained on a Waters micromass ZQ. The LC/HRMS analyses were carried out using a Agilent 1100 LC equipped with a photodiode array detector and a Micromass QTOF I equipped with a 4 GHz digital time converter. Microwave-assisted reactions were carried out with a CEM Discover and Explorer. Reactions were monitored by TLC using glass plates coated with silica gel 60 F₂₅₄ (Merck) and visualized by using UV light and/or by charring with a molybdate solution (a 0.02 M solution of ammonium cerium sulfate dihydrate and ammonium molybdate tetrahydrate in aqueous 10% H₂SO₄). MPLC separations were carried out on a CombiFlash Companion or Rf (Teledyne Isco) equipped with RediSep normal-phase or RP-18 reversed-phase flash columns. LC-MS separations were done on a Waters system equipped with sample manager 2767, pump 2525, PDA 2525, and Micromass ZQ. All compounds used for biological assays are at least of 95% purity based on HPLC analytical results. Commercially available reagents were purchased from Fluka, Aldrich, Alfa Aesar, or abcr GmbH & Co. KG (Germany). Solvents were purchased from Sigma-Aldrich or Acros and were dried prior to use where indicated. Methanol (MeOH) was dried by refluxing with sodium methoxide and distilled immediately before use. Dimethoxyethane (DME) was dried by filtration over Al₂O₃ (Fluka, type 5016 A basic).

4'-(2,3,4,6-Tetra-O-acetyl- α -D-mannopyranosyloxy)-N-methylbiphenyl-4-sulfonamide (13e). A Schlenk tube was charged with aryl iodide **11**²² (116 mg, 0.21 mmol), 4-(*N*-methylsulfamoyl)phenylboronic acid (**12e**, 50 mg, 0.23 mmol), Pd(dppf)Cl₂·CH₂Cl₂ (5 mg, 0.006 mmol), K₃PO₄ (67 mg, 0.32 mmol), and a stirring bar. The tube was closed with a rubber septum and was evacuated and flushed with argon. This procedure was repeated once, and then anhydrous DMF (1 mL) was added under a stream of argon. The mixture was degassed in an ultrasonic bath and flushed with argon for 5 min and then stirred at 80 °C overnight. The reaction mixture was cooled to rt, diluted with EtOAc (50 mL), and washed with water (50 mL) and brine (50 mL). The organic layer was dried over Na₂SO₄ and concentrated in vacuo. The residue was purified by MPLC on silica gel (petroleum ether/EtOAc) to afford **13e** (105 mg, 84%) as a white solid. [α]_D²⁰ +56.4 (*c* 0.50, MeOH). ¹H NMR (500 MHz, CDCl₃): δ = 7.92–7.90 (m, 2H, Ar–H), 7.70–7.68 (m, 2H, Ar–H), 7.57–7.55 (m, 2H, Ar–H), 7.21–7.19 (m, 2H, Ar–H), 5.60–5.57 (m, 2H, H-1, H-3), 5.48 (dd, *J* = 1.8, 3.4 Hz, 1H, H-2), 5.40 (t, *J* = 10.0 Hz, 1H, H-4), 4.38 (dd, *J* = 5.4, 10.8 Hz, 1H, NH), 4.30 (dd, *J* = 4.9, 12.3 Hz, 1H, H-6a), 4.13–4.08 (m, 2H, H-5, H-6b), 2.72 (d, *J* = 5.4 Hz, 3H, NCH₃), 2.22, 2.07, 2.05, 2.04 (4 s, 12H, 4 COCH₃). ¹³C NMR (126 MHz, CDCl₃): δ = 170.55, 170.06, 170.03, 169.75 (4 CO), 155.97, 144.81, 137.16, 134.09, 128.62, 127.85, 127.39, 117.01 (Ar–C), 95.78 (C-1), 69.34 (C-5), 69.31 (C-2), 68.81 (C-3), 65.86 (C-4), 62.07 (C-6), 29.44 (NHCH₃), 20.92, 20.74, 20.72 (4C, 4 COCH₃). ESI-MS *m/z*, calcd for C₂₇H₃₁NNaO₁₂S [M + Na]⁺: 616.1. Found: 616.1.

4'-(α -D-Mannopyranosyloxy)-N-methylbiphenyl-4-sulfonamide (10e). To a solution of 13e (40 mg, 0.07 mmol) in dry MeOH (5 mL) was added freshly prepared 1 M NaOMe/MeOH (0.1 equiv) under argon. The mixture was stirred at rt until the reaction was complete (monitored by TLC), then neutralized with Amberlyst-15 (H⁺) ion-exchange resin, filtered, and concentrated in vacuo. The residue was purified by MPLC on silica gel (DCM/MeOH, 10:1 to 7:1) to afford 10e (22 mg, 76%) as white solid. $[\alpha]_D^{20} +105.7$ (c 0.30, MeOH). ¹H NMR (500 MHz, CD₃OD): δ = 7.90–7.88 (m, 2H, Ar–H), 7.80–7.79 (m, 2H, Ar–H), 7.66–7.64 (m, 2H, Ar–H), 7.26–7.25 (m, 2H, Ar–H), 5.58 (d, *J* = 1.7 Hz, 1H, H-1), 4.06 (dd, *J* = 1.8, 3.3 Hz, 1H, H-2), 3.96 (dd, *J* = 3.4, 9.5 Hz, 1H, H-3), 3.79–3.74 (m, 3H, H-4, H-6a, H-6b), 3.63 (ddd, *J* = 2.5, 5.2, 9.7 Hz, 1H, H-5), 2.57 (s, 3H, NHCH₃). ¹³C NMR (126 MHz, CD₃OD): δ = 158.34, 146.13, 138.67, 134.55, 129.53, 128.82, 128.21, 118.29 (Ar–C), 100.09 (C-1), 75.53 (C-5), 72.42 (C-3), 71.96 (C-2), 68.32 (C-4), 62.68 (C-6), 29.31 (NHCH₃). HRMS *m/z*, calcd for C₁₉H₂₃NNaO₈ [M + Na]⁺: 448.1037. Found: 448.1038.

5-(4'-(2,3,4,6-Tetra-O-acetyl- α -D-mannopyranosyloxy)biphenyl-4-yl)-1H-tetrazole (14). A Schlenk tube was charged with 13g (30 mg, 0.06 mmol), trimethylsilyl azide (16 μ L, 0.12 mmol), dibutyltin oxide (2 mg, 0.006 mmol), DME (1 mL), and a stirring bar. The mixture was heated to 150 °C for 10 min by microwave irradiation. The reaction mixture was cooled to rt and then concentrated in vacuo. The residue was purified by MPLC on silica gel (DCM/MeOH, 9:1 to 8:1) to afford 14 (26 mg, 81%) as a colorless oil. $[\alpha]_D^{20} +56.1$ (c 0.3, MeOH). ¹H NMR (500 MHz, CDCl₃): δ = 8.25–8.15 (m, 2H, Ar–H), 7.75–7.65 (m, 2H, Ar–H), 7.60–7.55 (m, 2H, Ar–H), 7.20–7.17 (m, 2H, Ar–H), 5.64–5.55 (m, 2H, H-1, H-3), 5.49 (dd, *J* = 1.7, 3.3 Hz, 1H, H-2), 5.40 (t, *J* = 10.1 Hz, 1H, H-4), 4.31 (dd, *J* = 5.3, 12.4 Hz, 1H, H-6a), 4.17–4.06 (m, 2H, H-5, H-6b), 2.22, 2.07, 2.06, 2.05 (4 s, 12H, 4 COCH₃). ¹³C NMR (126 MHz, CDCl₃): δ = 170.67, 170.14, 170.11, 169.81 (4 CO), 155.61, 128.36, 127.84, 127.49, 116.93 (Ar–C), 95.78 (C-1), 69.36 (C-5), 69.26 (C-2), 68.90 (C-3), 65.89 (C-4), 62.12 (C-6), 20.92, 20.76, 20.73 (4 COCH₃). ESI-MS *m/z*, calcd for C₂₇H₂₈N₄NaO₁₀ [M + Na]⁺: 591.2. Found: 591.1.

5-(4'-(α -D-Mannopyranosyloxy)biphenyl-4-yl)-1H-tetrazole (10h). Prepared according to the procedure described for 10e from 14 (26 mg, 0.03 mmol). Yield: 18 mg (quant) as a white solid. $[\alpha]_D^{20} +112.1$ (c 0.1, MeOH/H₂O, 2:1). ¹H NMR (500 MHz, CD₃OD): δ = 7.98–7.96 (m, 2H, Ar–H), 7.72–7.71 (m, 2H, Ar–H), 7.58–7.54 (m, 2H, Ar–H), 7.16–7.13 (m, 2H, Ar–H), 5.46 (d, *J* = 1.7 Hz, 1H, H-1), 3.94 (dd, *J* = 1.9, 3.5 Hz, 1H, H-2), 3.83 (dd, *J* = 3.4, 9.5 Hz, 1H, H-3), 3.68–3.61 (m, 3H, H-4, H-6a, H-6b), 3.52 (ddd, *J* = 2.5, 5.4, 9.7 Hz, 1H, H-5). ¹³C NMR (126 MHz, CD₃OD): δ = 158.19, 145.07, 134.97, 129.29, 128.74, 128.55, 118.26 (Ar–C), 100.13 (C-1), 75.52 (C-5), 72.42 (C-3), 71.98 (C-2), 68.33 (C-4), 62.69 (C-6). HRMS *m/z*, calcd for C₁₉H₂₁N₄O₆ [M + H]⁺: 401.1456. Found: 401.1450.

4'-(2,3,4,6-Tetra-O-acetyl- α -D-mannopyranosyloxy)-3'-chlorobiphenyl-4-carbonitrile (19). Prepared according to the procedure described for 13e from aryl iodide 18²³ (79 mg, 0.135 mmol), 12g (22 mg, 0.15 mmol), Pd(dppf)Cl₂·CH₂Cl₂ (3.3 mg, 4 μ mol), and K₃PO₄ (57 mg, 0.27 mmol). Yield: 57 mg (75%) as a white solid. $[\alpha]_D^{20} +77.7$ (c 0.5, CHCl₃). ¹H NMR (500 MHz, CDCl₃): δ = 7.72 (d, *J* = 8.3 Hz, 2H, Ar–H), 7.63 (m, 3H, Ar–H), 7.43 (dd, *J* = 2.2, 8.6 Hz, 1H, Ar–H), 7.27 (d, *J* = 8.6 Hz, 1H, Ar–H), 5.64–5.59 (m, 2H, H-1, H-2), 5.54 (dd, *J* = 1.9, 3.2 Hz, 1H, H-3), 5.41 (t, *J* = 10.1 Hz, 1H, H-4), 4.28 (dd, *J* = 5.2, 12.3 Hz, 1H, H-6a), 4.17 (ddd, *J* = 2.1, 5.1, 10.0 Hz, 1H, H-5), 4.10 (dd, *J* = 2.2, 12.3 Hz, 1H, H-6b), 2.21 (s, 3H, COCH₃), 2.12–2.00 (m, 9H, 3 COCH₃). ¹³C NMR (126 MHz, CDCl₃): δ = 170.54, 170.08, 169.90, 169.84, (4C, CO) 151.67, 143.61, 135.29, 132.87, 129.41, 127.53, 126.60, 125.20, 118.79, 117.36, 111.47 (Ar–C, CN), 96.72 (C-1), 70.00 (C-5), 69.39 (C-3), 68.82 (C-2), 65.86 (C-4), 62.16 (C-6), 20.98, 20.81, 20.79, 20.78 (4 COCH₃). ESI-MS *m/z*, calcd for C₂₇H₂₆ClNNaO₁₀ [M + Na]⁺: 582.1. Found: 582.1.

3'-Chloro-4'-(α -D-mannopyranosyloxy)biphenyl-4-carbonitrile (10j). Prepared according to the procedure described for 10e from 19 (36 mg, 0.06 mmol). Yield: 12 mg (48%) as a white solid. $[\alpha]_D^{20} +109.4$ (c 0.23, MeOH). ¹H NMR (500 MHz, CD₃OD): δ = 7.80–7.72 (m, 5H, Ar–H), 7.59 (dd, *J* = 2.2, 8.6 Hz, 1H, Ar–H), 7.48 (d, *J* = 8.7 Hz, 1H, Ar–H), 5.62 (d, *J* = 1.4 Hz, 1H, H-1), 4.12 (dd, *J* = 1.8, 3.3 Hz, 1H,

H-2), 4.00 (dd, *J* = 3.4, 9.5 Hz, 1H, H-3), 3.83–3.68 (m, 3H, H-4, H-6a, H-6b), 3.63 (ddd, *J* = 2.3, 5.4, 9.6 Hz, 1H, H-5). ¹³C NMR (126 MHz, CD₃OD): δ = 153.65, 145.15, 135.42, 133.86, 129.82, 128.53, 127.87, 125.47, 119.70, 118.59 (Ar–C), 111.97 (CN), 100.66 (C-1), 76.05 (C-5), 72.39 (C-3), 71.80 (C-2), 68.20 (C-4), 62.65 (C-6). IR (KBr), ν = 3400 (OH), 2227 (C≡N), 1606, 1487 (Ar–C=C) cm⁻¹. HRMS *m/z*, calcd for C₁₉H₁₈ClNNaO₆ [M + Na]⁺: 414.0715. Found: 414.0721.

3'-Chloro-N-(3',6'-dihydroxy-3-oxo-3H-spiro-[isobenzofuran-1,9'-xanthen]-5-yl)-4'-(α -D-mannopyranosyloxy)biphenyl-4-carboxamide (22). Compound 21 (10.0 mg, 0.024 mmol), fluoresceinamine isomer I (12.7 mg, 0.037 mmol), and COMU (20.9 mg, 0.049 mmol) were dissolved in dry DMF (1 mL). Then NEt₃ (10 μ L, 0.073 mmol) was added and the mixture was stirred at rt for 7 h. 1 N HCl in DMF was added until acid reaction on pH paper and the mixture was concentrated. The residue was dissolved in DCM/MeOH (3:1) and loaded onto a silica gel column. The complex mixture of compounds was only partially resolved. The fractions containing the product were collected, concentrated, and purified by preparative HPLC (gradient H₂O/MeCN, +0.2% HCO₂H) to afford compound 22 (5 mg, 19%). $[\alpha]_D^{20} +21.1$ (c 0.10, MeOH). ¹H NMR (500 MHz, CD₃OD): δ = 8.26 (d, *J* = 8.4 Hz, 2H, Ar–H), 7.88–7.74 (m, 3H, Ar–H), 7.66 (dd, *J* = 2.2, 8.6 Hz, 1H, Ar–H), 7.51 (d, *J* = 8.7 Hz, 1H, Ar–H), 7.29 (dd, *J* = 1.9, 5.3 Hz, 2H, Ar–H), 7.19 (dd, *J* = 2.1, 8.3 Hz, 1H, Ar–H), 7.08–6.99 (m, 2H, Ar–H), 6.95 (d, *J* = 8.7 Hz, 1H, Ar–H), 6.72 (dd, *J* = 5.5, 10.6 Hz, 2H, Ar–H), 6.61 (dd, *J* = 2.3, 8.7 Hz, 1H, Ar–H), 5.65 (s, 1H, H-1), 4.15 (dd, *J* = 1.8, 3.2 Hz, H-2), 4.03 (dd, *J* = 3.4, 9.5 Hz, H-3), 3.87–3.72 (m, 3H, H-4, H-6a, H-6b), 3.65 (m, 1H, H-5). ¹³C NMR (126 MHz, CD₃OD): δ = 137.50, 136.01, 131.90, 130.24, 130.20, 129.87, 129.24, 128.03, 127.91, 125.79, 125.46, 124.73, 118.99, 118.76, 118.65 (Ar–C), 100.73 (C-1), 76.06 (C-5), 72.42 (C-3), 71.85 (C-2), 68.24 (C-4), 62.69 (C-2). ESI-MS *m/z*, calcd for C₃₉H₃₁ClNO₁₂ [M + H]⁺: 740.2. Found: 740.2.

3'-Chloro-N-(2-(3-(3',6'-dihydroxy-3-oxo-3H-spiro-[isobenzofuran-1,9'-xanthen]-5-yl)thioureido)ethyl)-4'-(α -D-mannopyranosyloxy)biphenyl-4-carboxamide (23). To a stirred solution of compound 21 (25 mg, 0.061 mmol) in dry DMF (1 mL), NHS (21 mg, 0.183 mmol) was added, followed by DIC (9.2 mg, 0.073 mmol). The mixture was stirred at rt for 2 h. Then *N*-Boc-ethylendiamine (10.7 mg, 0.067 mmol) was added and the reaction was stirred for 10 h. It was then cooled down to 0 °C, diluted with water, and concentrated. Chromatography on silica gel (DCM/MeOH) yielded 23 mg (0.042 mmol, 68%) of *tert*-butyl (3'-chloro-4'-(α -D-mannopyranosyloxy)biphenyl-4-yl-carboxamido)ethyl)carbamate. This product was dissolved in DCM (3 mL), and TFA (1 mL) was added. The solid dissolved during addition of TFA. After 10 min the reaction was complete. The mixture was evaporated, and excess TFA was removed in high vacuum. The intermediate *N*-(2-aminoethyl)-3'-chloro-4'-(α -D-mannopyranosyloxy)biphenyl-4-carboxamide TFA salt (23 mg, 0.042 mmol, quant) was used directly in the next step. It was dissolved in dry DMF (0.5 mL), and NEt₃ (12.8 mg, 0.127 mmol) was added. The mixture was cooled to 0 °C. Then FITC (14.8 mg, 0.038 mmol) was added and the mixture was stirred for 3 h in the dark. The mixture was then coevaporated with water, taken up in MeOH/10% aq acetic acid and evaporated. Chromatography on silica gel (DCM/MeOH) yielded compound 23, contaminated with triethylammonium acetate. The compound was then redissolved in MeOH, and 0.5 N HCl in MeOH was added. The mixture was evaporated and chromatographed on silica gel to yield pure 23 (15 mg, 47%). $[\alpha]_D^{20} +12.1$ (c 0.30, MeOH). ¹H NMR (500 MHz, CD₃OD): δ = 8.12 (s, 1H), 7.92 (d, *J* = 8.3 Hz, 2H, Ar–H), 7.70 (dd, *J* = 5.0, 13.1 Hz, 2H, Ar–H), 7.64 (d, *J* = 8.3 Hz, 2H, Ar–H), 7.54 (dd, *J* = 2.2, 8.6 Hz, 1H, Ar–H), 7.46 (d, *J* = 8.7 Hz, 1H, Ar–H), 7.09 (d, *J* = 8.2 Hz, 1H, Ar–H), 6.74 (s, 2H), 6.69 (d, *J* = 1.4 Hz, 2H, Ar–H), 6.55 (d, *J* = 8.4 Hz, 2H, Ar–H), 5.63 (d, *J* = 1.3 Hz, H-1), 4.15 (dd, *J* = 1.8, 3.1 Hz, H-2), 4.03 (dd, *J* = 3.4, 9.5 Hz, H-3), 3.94 (s, 2H, CH₂), 3.86–3.64 (m, 6H, H-4, H-5, H-6, CH₂). ¹³C NMR (126 MHz, CD₃OD): δ = 153.21, 143.84, 136.41, 129.66, 129.18, 127.76, 127.70, 125.37, 118.64, 103.62 (Ar–C), 100.75 (C-1), 76.00 (C-5), 72.41 (C-3), 71.86 (C-2), 68.24 (C-4), 62.69 (C-6), 40.76 (CH₂). ESI-MS *m/z*, calcd for C₄₂H₃₇ClN₃O₁₂S [M + H]⁺: 842.2. Found: 842.2.

3'-Chloro-N-(2-(2-(2-(3-(3',6'-dihydroxy-3-oxo-3H-spiro-[isobenzofuran-1,9'-xanthen]-5-yl)thioureido)ethoxy)ethoxy)ethyl)-4'-(α -D-mannopyranosyloxy)biphenyl-4-carboxamide (24). Compound 21 (280 mg, 0.68 mmol) was dissolved in dry DMF (5 mL) under argon. Then NHS (235 mg, 2.04 mmol) was added, followed by DIC (0.12 mL, 0.78 mmol) and the mixture was stirred at rt for 4 h. Then Boc-PEG2-NH₂ (186 mg, 0.75 mmol) was added, and the mixture was stirred at rt under argon for 10 h. It was then slowly diluted with water and concentrated. The residue was purified by chromatography on silica gel (DCM/MeOH) to give *tert*-butyl (2-(2-(2-(3'-chloro-4'-(α -D-mannopyranosyloxy)biphenyl-4-carboxamido)ethoxy)ethoxy)ethyl)-carbamate (300 mg, 0.468 mmol, 69%). Then the carbamate was suspended in DCM (3 mL), and TFA (1 mL) was added dropwise at rt. After 30 min, the solvents were evaporated and the crude mixture was dissolved in CHCl₃/MeOH (6:4, +0.5% conc NH₄OH) and transferred to a silica gel column, eluting with the same solvent mixture, to yield N-(2-(2-(2-aminoethoxy)ethoxy)ethyl)-3'-chloro-4'-(α -D-mannopyranosyloxy)biphenyl-4-carboxamide (228 mg, 90%). A fraction of the amine (10 mg, 0.018 mmol) was dissolved in dry DMF (0.5 mL) and cooled to 0 °C. FITC (6.5 mg, 0.017 mmol) was added, and the mixture was stirred for 1 h. The mixture was concentrated and the residue was purified by chromatography on silica (DCM/MeOH) to yield 24 (10 mg, 65%). ¹H NMR (500 MHz, CD₃OD): δ = 8.21 (d, *J* = 1.4 Hz, 1H, Ar-H), 7.88 (d, *J* = 8.3 Hz, 2H, Ar-H), 7.68 (d, *J* = 2.2 Hz, 2H, Ar-H), 7.63 (d, *J* = 8.3 Hz, 2H, Ar-H), 7.53 (dd, *J* = 2.2, 8.6 Hz, 1H, Ar-H), 7.43 (d, *J* = 8.7 Hz, 1H, Ar-H), 7.09 (d, *J* = 8.2 Hz, 1H, Ar-H), 6.68 (d, *J* = 2.3 Hz, 2H, Ar-H), 6.65 (dd, *J* = 2.6, 8.6 Hz, 2H, Ar-H), 6.53 (dd, *J* = 1.6, 8.7 Hz, 2H, Ar-H), 5.61 (d, *J* = 1.3 Hz, 1H, H-1), 4.14 (dd, *J* = 1.8, 3.2 Hz, 1H, H-2), 4.03 (dd, *J* = 3.4, 9.5 Hz, 1H, H-3), 3.93–3.53 (m, 16H), 3.37 (s, 2H, NCH₂), 1.30 (s, 2H, CH₂). ¹³C NMR (126 MHz, CD₃OD): δ = 170.01 (CO), 153.17, 143.72, 136.37, 134.37, 130.39, 129.69, 129.04, 127.78, 127.73, 125.35, 118.60, 103.60 (Ar-C), 100.72 (C-1), 75.97 (C-5), 72.41 (C-3), 71.86, 71.40, 70.59 (5C, C-2, OCH₂), 68.23 (C-4), 62.64 (C-6), 49.88, 45.49, 40.97 (CH₂). ESI-MS *m/z*, calcd for C₄₆H₄₅ClN₃O₁₄S [M + H]⁺: 930.2. Found: 930.4.

Competitive Fluorescence Polarization Assay. Expression and Purification of CRD of FimH. A recombinant protein consisting of the CRD of FimH linked to a 6His-tag via a thrombin cleavage site (FimH-CRD-Th-His₆) was expressed in *E. coli* strain HM125 and purified by affinity chromatography as previously described.⁴³

K_D Determination of FITC-Labeled Ligands. The functionalized ligands (23, 24) were prepared as a 10 mM stock solution in pure DMSO (Sigma-Aldrich, Buchs, Switzerland). All further dilutions of compounds and FimH-CRD-Th-His₆ protein were prepared in assay buffer (20 mM HEPES, 150 mM NaCl, 50 μ g/mL BSA, pH 7.4). BSA was added to the assay buffer to prevent nonspecific binding of protein to the plastic surface. Binding isotherms for the fluorescent ligands were obtained in direct binding studies by adding a constant concentration of ligand (final concentration 5 nM) and a linear dilution of protein (final concentration 0–100 nM) to a final volume of 200 μ L in 96-well, black, flat bottom NBS plates (Corning Inc., Corning, NY, USA). After incubation of the plate for 24 h at rt with gentle shaking, the fluorescence polarization was measured with the Synergy H1 hybrid multimode microplate reader (BioTek Instruments Inc., Winooski, VT, USA) with polarized excitation at 485 nm and emission measured at 528 nm through polarizing filters parallel and perpendicularly oriented to the incident polarized light. K_D values were determined by plotting the FP readout as a function of the protein concentration and applying the following single-site binding equation (eq 1) that accounts for ligand depletion:

$$S_{\text{obs}} = S_{\text{F}} + (S_{\text{B}} - S_{\text{F}}) \times \left(\frac{C_{\text{P}} + C_{\text{L}} + K_{\text{D}} - \sqrt{(C_{\text{P}} + C_{\text{L}} + K_{\text{D}})^2 - 4C_{\text{P}}C_{\text{L}}}}{2C_{\text{L}}} \right) \quad (1)$$

where S_{obs} is the observed signal from the ligand, S_{F} is the signal from free ligand, S_{B} is the signal from bound ligand, C_{P} is the total concentration of protein, and C_{L} is the total concentration of ligand.⁴⁹

K_D Determination of FimH Antagonists. The fluorescently labeled ligand 23 was used for the competitive fluorescence polarization assay. A linear dilution of nonlabeled FimH antagonist with final concentrations ranging from 0 to 10 μ M was titrated into 96-well, black, flat-bottom NBS plates (Corning Inc.) to a final volume of 200 μ L containing a constant concentration of protein (final concentration 25 nM) and FITC-labeled ligand which was fixed at a higher concentration in competitive binding assays than in direct binding experiments to obtain higher fluorescence intensities (final concentration 20 nM). Prior to measuring the fluorescence polarization, the plates were incubated on a shaker for 24 h at rt until the reaction reached equilibrium. The IC₅₀ value was determined with Prism (GraphPad Software Inc., La Jolla, CA, USA) by applying a standard four-parameter IC₅₀ function. The obtained IC₅₀ values were converted into their corresponding K_D values using the derivation of the Cheng–Prusoff equation.⁴⁵ This variation of the Cheng–Prusoff equation is applied to competition assays with tight-binding inhibitors and includes terms to correct for ligand depletion effects. However, the K_D for antagonists having a higher affinity toward FimH than the labeled ligand could not be accurately determined.⁴⁵

Isothermal Titration Calorimetry (ITC). All ITC experiments were performed with the FimH-CRD-Th-His₆ protein using a VP-ITC instrument from MicroCal, Inc. (Malvern Instruments, Worcestershire, U.K.) with a sample cell volume of 1.4523 mL. The measurements were performed with 0–5% DMSO at 25 °C, a stirring speed of 307 rpm, and 10 μ cal s⁻¹ reference power. The protein samples were dialyzed in assay buffer prior to all experiments. Because of the high protein consumption of ITC, only the experiments for the reference compounds (1, 3, and 25) were measured in duplicates. Compounds 1, 3, 9, and 25 were measured in a direct fashion by titration of ligand (100–2,000 μ M) into protein (8.6–55 μ M) with injections of 3–8 μ L at intervals of 10 min to ensure nonoverlapping peaks. The quantity $c = \text{Mt}(0)K_{\text{D}}^{-1}$, where Mt(0) is the initial macromolecule concentration, is of importance in titration microcalorimetry. The *c*-values of the direct titrations were below 1000 and thus within the reliable range. For the compounds 10b–e, 10g, and 10j additional competitive ITC experiments were performed because of their high affinity resulting in *c*-values above 1000 for direct titrations. These ligands (600 μ M) were titrated into protein (30 μ M), which was preincubated with compound 25 (300 μ M) resulting in sigmoidal titration curves. Because of slow reaction kinetics, titration intervals of 20 min were used.

Baseline correction and peak integration were performed using the Origin 7 software (OriginLab, Northampton, MA, USA). An initial 2 μ L injection was excluded from data analysis. Baseline subtraction and curve-fitting with the three variables *N* (concentration correction factor), *K_D* (dissociation constant), and ΔH° (change in enthalpy) were performed with the SEDPHAT software, version 10.40 (National Institutes of Health).⁸⁶ A global fitting analysis was performed for the competition titration (10b–e, 10g, or 10j) competing for the protein binding site with compound 25 and the direct titration of the competitor (compound 25 binding to protein) to fit for *K_D*, ΔH° and *N* were fitted from direct titrations of 10b–e, 10g, or 10j into protein. For the compounds 3, 9, and 25 binding to protein all variables could be determined from a global analysis of the direct titration.

The thermodynamic parameters were calculated with the following equation (eq 2):

$$\Delta G^{\circ} = \Delta H^{\circ} - T\Delta S^{\circ} = RT \ln K_{\text{D}} = -RT \ln K_{\text{A}} \quad (2)$$

where ΔG° , ΔH° , and ΔS° are the changes in free energy, enthalpy, and entropy of binding, respectively, *T* is the absolute temperature, and *R* is the universal gas constant (8.314 J mol⁻¹ K⁻¹). The 95% confidence intervals of the measurements were calculated for the two variables *K_D* and ΔH° with the one-dimensional error surface projection within the SEDPHAT software.

Calculation of the Free Energy of Desolvation. The three-dimensional representation for each of the aglycons (4-methoxybiphenyl scaffold, Figure 8) was built in the Maestro⁸⁷ modeling environment, and the global minimum conformation was identified by performing 500 iterations of the mixed torsional/low-mode conformational sampling in combination with the OPLS-2005 force-field and the implicit solvent model (water) as implemented in the Macromodel

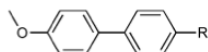


Figure 8. 4-Methoxybiphenyl scaffold of aglycons.

9.9.⁸⁸ The global minimum structures were used as input for the AMSOL 7.1 program⁸⁹ to obtain the free energy of desolvation ΔG_{des} (Table 5) with the SMS.4A solvation model⁹⁰ and the AM1⁹¹ level of theory (used keywords "AM1 SMS.4A SOLVNT=WATER TRUES").

Table 5. Aqueous Free Energy of Desolvation

R	ΔG_{des} [kJ/mol]
neutral	
H	15.6
CONHCH ₃	39.9
COOCH ₃	23.0
SO ₂ NHCH ₃	65.5
SO ₂ CH ₃	56.4
4-morpholineamide	45.3
CN	22.0
deprotonated	
COO ⁻	298.2
SO ₂ N ⁻ -Me	342.0

Determination of the MAC₉₀ by Flow Cytometry. The MAC₉₀ was determined in principle as in the previously published flow cytometry assay⁷⁹ but with some modifications. The human epithelial bladder carcinoma cell line 5637 (DSMZ, Braunschweig, Germany) was grown in RPMI 1640 medium, supplemented with 10% fetal calf serum (FCS), 100 U/mL penicillin, and 100 $\mu\text{g}/\text{mL}$ streptomycin at 37 °C, 5% CO₂. All solutions were purchased from Invitrogen (Basel, Switzerland). The cells were subcultured 1:6 twice per week [using trypsin/EDTA (Sigma-Aldrich) for the detachment]. Two days before infection, 1.8×10^5 cells were seeded in each well of a 24-well plate in RPMI 1640 containing 10% FCS without antibiotics. The cell density was approximately $(3-5) \times 10^5$ cells/well at the assay day.

For infection, the GFP-expressing clinical *E. coli* isolate UTI89⁹² (UTI89 wt) and the GFP-expressing FimA-H knockout strain UTI89 $\Delta\text{fimA-H}$ were used (strains were provided by Prof. Urs Jenal, Biocenter, University of Basel, Switzerland).⁷⁹ Bacteria were cultivated at 37 °C in 10 mL Luria-Bertani (LB) broth (Becton, Dickinson and Company) overnight, harvested by centrifugation (3800 rpm, 10 min), and washed three times in phosphate buffered saline (PBS, Sigma-Aldrich), and a bacterial solution of OD₆₀₀ of 0.75 in RPMI + 10% FCS was prepared. For the determination of the MAC₉₀ value, the IC₉₀, linear dilutions of the FimH antagonist were prepared in 5% DMSO and PBS. Bacteria and antagonists were preincubated for 10 min at 37 °C, before cells were infected with either only 200 μL of bacterial solution of UTI89 or UTI89 $\Delta\text{fimA-H}$ (positive and negative controls), or 225 μL of the preincubated bacteria-antagonist mixture. Infection lasted for 1.5 h. During this time infected cells were incubated at 37 °C. Then, cells were washed with PBS and detached from wells by the addition of 150 μL of trypsin and incubation at 37 °C for 10 min, before flushing from wells PBS containing 2% FCS and transferred to tubes. To dilute the trypsin, cells were centrifuged at 13 000 rpm, 1 min, 600 μL of the supernatant was discarded, and the pellet was resuspended in the remaining 300 μL of PBS containing 2% FCS. Samples were stored on ice until measurement. Before analysis with the flow cytometer (Becton Dickinson, FACSCanto II), the samples were gently mixed and filtered using a 35 μm nylon mesh (Corning Life Sciences) to prevent cellular aggregation. Cells were gated with linear scaling for side scatter (SSC) and forward scatter (FSC) and GFP intensity of live cells was evaluated. IC₉₀ values were determined by plotting the concentration of the antagonist in a logarithmic mode versus the mean fluorescence intensity (MFI) of living cells and by fitting a dose-response curve (variable slope, four parameters) with the Prism software (GraphPad Prism).

X-ray Analysis of the Antagonists 10e and 10j Cocrystallized with FimH-CRD. *FimH-CRD/10e Cocrystallization.* Initial FimH-CRD (18 mg/mL in 20 mM HEPES, pH 7.4) crystals were obtained in complex with 4-(5-nitroindolin-1-yl)phenyl α -D-mannopyranoside (5 mM).²³ Crystals were grown in sitting-drop vapor diffusion at 20 °C with 200 nL of protein-antagonist mixture together with 200 nL of precipitant solution in well D3 (0.2 M sodium phosphate monobasic monohydrate, 20% w/v PEG 3,350) of the PEG/Ion HT screen (Hampton Research, CA, USA). Cubic crystals appeared within 1 week, which served as cross-seeding crystals. A solution of FimH-CRD (20 mg/mL) and 10e (5 mM) was mixed with 0.2 M sodium phosphate monobasic monohydrate, 20% w/v PEG 400 with 0.5 μL of each solution. Streak-seeding was performed after 1 day of incubation. Cubic FimH-CRD/10e crystals formed within 24 h. Crystals were flash cooled to 100 K with perfluoropolyether cryo oil (Hampton Research, CA, USA) as cryoprotectant. Data were collected with synchrotron radiation ($\lambda = 0.99999 \text{ \AA}$) at the PXIII beamline, Swiss Light Source, Switzerland.

FimH-CRD/10j Cocrystallization. Cocrystals were initially grown in sitting-drop vapor diffusion at 20 °C with 0.5 μL of a mixture of FimH-CRD (20 mg/mL) and 10j (5 mM) together with 0.5 μL of 0.1 M HEPES, pH 7.5, 2 M ammonium sulfate. Plate-like crystals formed within 2 weeks and were used as seeds for subsequent crystallization. Diffraction quality crystals were grown by streak-seeding in 0.5 μL of FimH-CRD (10 mg/mL) with 10j (2.5 mM) and 0.5 μL of 0.1 M HEPES, pH 7.5, 1.25 M ammonium sulfate. The drops were covered with perfluoropolyether cryo oil prior to flash cooling to 100 K. Data were collected with synchrotron radiation ($\lambda = 1.00003 \text{ \AA}$) at the PXIII beamline, Swiss Light Source, Switzerland.

Structure Determination and Refinement. Data were indexed and integrated with the XDS package⁹³ for the FimH-CRD/10e cocrystal structure, and with mosflm⁹⁴ for the FimH-CRD/10j cocrystal structure (Table 6). Scaling was performed with XDS and SCALA included in the CCP4 suite, respectively.⁹⁵ Structures were solved by molecular

Table 6. Data Collection and Refinement Statistics for FimH-CRD/10e and FimH-CRD/10j Cocrystals

	FimH-CRD/10e	FimH-CRD/10j
PDB code	4CSS	4CST
space group	$P2_12_12_1$	$P2_12_12_1$
no. of molecules in the asymmetric unit	1	1
Cell Dimensions		
a, b, c (Å)	48.38, 56.23, 61.59	48.84, 55.89, 61.00
α, β, γ (deg)	90, 90, 90	90, 90, 90
Data Collection		
beamline	Swiss Light Source PXIII	Swiss Light Source PXIII
resolution range (Å) ^a	30.0–1.07 (1.13–1.07)	23.5–1.10 (1.12–1.10)
unique observations ^a	72000 (9354)	66470 (2500)
average multiplicity ^a	10.9 (3.7)	5.4 (2.4)
completeness (%)	96.1 (78.0)	97.2 (76.5)
R_{merge} ^a	0.056 (0.57)	0.051 (0.305)
mean $I/\sigma(I)$ ^a	21.5 (2.22)	15.5 (2.9)
Refinement		
resolution range (Å)	15.7–1.07	23.5–1.10
R, R_{free}	11.2, 13.2	11.4, 13.0
rms deviation from ideal bond length (Å)	0.010	0.010
rms deviation from ideal bond angle (deg)	1.170	1.420

^aValues in parentheses are for highest-resolution shell.

replacement with PHASER⁹⁶ using the FimH-CRD-butyl α -D-mannopyranoside complex (PDB code 1UWF) as search model. The structures were iteratively built using the COOT software⁹⁷ and refined with the PHENIX software.⁹⁸ Geometric restraints for **10e** and **10j** were generated with PRODRG.⁹⁹ The models were validated using molprobity.¹⁰⁰ Residues 113–115 were not modeled in the **10e** structure because of disorder. Furthermore, the ligand was modeled in two possible conformations. For both ligands, electron density is reduced on the second aromatic ring because of flexibility of the ligand.

Physicochemical and In Vitro Pharmacokinetic Studies.

Materials. Dimethyl sulfoxide (DMSO), 1-propanol, 1-octanol, Dulbecco's modified Eagle medium (DMEM)–high glucose, L-glutamine solution, penicillin–streptomycin solution, Dulbecco's phosphate buffered saline (DPBS), trypsin–EDTA solution, magnesium chloride hexahydrate, and reduced nicotinamide adenine dinucleotide phosphate (NADPH) were purchased from Sigma-Aldrich. MEM nonessential amino acid (MEM-NEAA) solution, fetal bovine serum (FBS), and DMEM without sodium pyruvate and phenol red were bought from Invitrogen (Carlsbad, CA, USA). PRISMA HT universal buffer, GIT-0 Lipid Solution, and Acceptor Sink Buffer were ordered from pIon (Woburn, MA, USA). Human plasma was bought from Biopredic (Rennes, France), and acetonitrile (MeCN) and methanol (MeOH) were from Acros Organics (Geel, Belgium). Pooled male rat liver microsomes were purchased from BD Bioscience (Franklin Lakes, NJ, USA). Tris(hydroxymethyl)aminomethane (TRIS) was obtained from AppliChem (Darmstadt, Germany). The Caco-2 cells were kindly provided by Prof. G. Imanidis, FHNW, Muttenz, and originated from the American Type Culture Collection (Rockville, MD, USA).

pK_a . The pK_a values were determined as described elsewhere.¹⁰¹ In brief, the pH of a sample solution was gradually changed and the chemical shift of protons adjacent to ionizable centers was monitored by ¹H nuclear magnetic resonance (NMR) spectroscopy. The shift was plotted against the pH of the respective sample, and the pK_a was read out from the inflection point of the resulting sigmoidal curve.

$\log D_{7.4}$. The in silico prediction tool ALOGPS¹⁰² was used to estimate $\log P$ values of the compounds. Depending on these values, the compounds were classified into three categories: hydrophilic compounds ($\log P$ below zero), moderately lipophilic compounds ($\log P$ between zero and one), and lipophilic compounds ($\log P$ above one). For each category, two different ratios (volume of 1-octanol to volume of buffer) were defined as experimental parameters (Table 7).

Table 7. Compound Classification Based on Estimated $\log P$ Values

compd type	$\log P$	ratio (1-octanol/buffer)
hydrophilic	<0	30:140, 40:130
moderately lipophilic	0–1	70:110, 110:70
lipophilic	>1	3:180, 4:180

Equal amounts of phosphate buffer (0.1 M, pH 7.4) and 1-octanol were mixed and shaken vigorously for 5 min to saturate the phases. The mixture was left until separation of the two phases occurred, and the buffer was retrieved. Stock solutions of the test compounds were diluted with buffer to a concentration of 1 μ M. For each compound, six determinations, that is, three determinations per 1-octanol/buffer ratio, were performed in different wells of a 96-well plate. The respective volumes of buffer containing analyte (1 μ M) were pipetted to the wells and covered by saturated 1-octanol according to the chosen volume ratio. The plate was sealed with aluminum foil, shaken (1350 rpm, 25 °C, 2 h) on a Heidolph Titramax 1000 plate-shaker (Heidolph Instruments GmbH & Co. KG, Schwabach, Germany), and centrifuged (2000 rpm, 25 °C, 5 min, 5804 R Eppendorf centrifuge, Hamburg, Germany). The aqueous phase was transferred to a 96-well plate for analysis by LC–MS.

The $\log D_{7.4}$ coefficient was calculated from the 1-octanol/buffer ratio (o/b), the initial concentration of the analyte in buffer (1 μ M), and the concentration of the analyte in buffer (c_B) with eq 3:

$$\log D_{7.4} = \log \left(\frac{1 \mu\text{M} - c_B}{c_B} \frac{1}{o/b} \right) \quad (3)$$

Aqueous Solubility. Solubility was determined in a 96-well format using the μ SOL Explorer solubility analyzer (pIon, version 3.4.0.5). For each compound, measurements were performed at pH 3.0 and 7.4 in triplicate. For this purpose, six wells of a deep well plate, that is, three wells per pH value, were filled with 300 μ L of PRISMA HT universal buffer, adjusted to pH 3.0 or 7.4 by adding the requested amount of NaOH (0.5 M). Aliquots (3 μ L) of a compound stock solution (10–50 mM in DMSO) were added and thoroughly mixed. The final sample concentration was 0.1–0.5 mM, and the residual DMSO concentration was 1.0% (v/v) in the buffer solutions. After 15 h, the solutions were filtered (0.2 μ m 96-well filter plates) using a vacuum to collect manifold (Whatman Ltd., Maidstone, U.K.) to remove the precipitates. Equal amounts of filtrate and 1-propanol were mixed and transferred to a 96-well plate for UV/vis detection (190–500 nm, SpectraMax 190). The amount of material dissolved was calculated by comparison with UV/vis spectra obtained from reference samples, which were prepared by dissolving compound stock solution in a 1:1 mixture of buffer and 1-propanol (final concentrations 0.017–0.083 mM).

Parallel Artificial Membrane Permeation Assay (PAMPA). Effective permeability ($\log P_e$) was determined in a 96-well format with the PAMPA.⁶⁰ For each compound, measurements were performed at pH 5.0 and 7.4 in quadruplicates. Eight wells of a deep well plate, that is, four wells per pH value, were filled with 650 μ L of PRISMA HT universal buffer adjusted to pH 5.0 or 7.4 by adding the requested amount of NaOH (0.5 M). Samples (150 μ L) were withdrawn from each well to determine the blank spectra by UV/vis spectroscopy (190–500 nm, SpectraMax 190). Then analyte dissolved in DMSO was added to the remaining buffer to yield 50 μ M solutions. To exclude precipitation, the optical density was measured at 650 nm, with 0.01 being the threshold value. Solutions exceeding this threshold were filtered. Afterward, samples (150 μ L) were withdrawn to determine the reference spectra. Further 200 μ L was transferred to each well of the donor plate of the PAMPA sandwich (pIon, P/N 110163). The filter membranes at the bottom of the acceptor plate were infused with 5 μ L of GIT-0 lipid solution, and 200 μ L of Acceptor Sink Buffer was filled into each acceptor well. The sandwich was assembled, placed in the GutBox, and left undisturbed for 16 h. Then it was disassembled and samples (150 μ L) were transferred from each donor and acceptor well to UV plates for determination of the UV/vis spectra. Effective permeability ($\log P_e$) was calculated from the compound flux deduced from the spectra, the filter area, and the initial sample concentration in the donor well with the aid of the PAMPA Explorer software (pIon, version 3.5).

Colorectal Adenocarcinoma (Caco-2) Cell Permeation Assay. Caco-2 cells were cultivated in tissue culture flasks (BD Biosciences) with DMEM high glucose medium, containing L-glutamine (2 mM), nonessential amino acids (0.1 mM), penicillin (100 U/mL), streptomycin (100 μ g/mL), and fetal bovine serum (10%). The cells were kept at 37 °C in humidified air containing 5% CO₂, and the medium was changed every second day. When approximately 90% confluence was reached, the cells were split in a 1:10 ratio and distributed to new tissue culture flasks. At passage numbers between 60 and 65, they were seeded at a density of 5.3×10^5 cells per well to Transwell six-well plates (Corning Inc.) with 2.5 mL of culture medium in the basolateral and 1.8 mL in the apical compartment. The medium was renewed on alternate days. Permeation experiments were performed between days 19 and 21 after seeding. Prior to the experiment, the integrity of the Caco-2 monolayers was evaluated by measuring the transepithelial electrical resistance (TEER) with an Endohm tissue resistance instrument (World Precision Instruments Inc., Sarasota, FL, USA). Only wells with TEER values higher than 250 Ω cm² were used. Experiments were performed in the apical-to-basolateral (absorptive) and basolateral-to-apical (secretory) directions in triplicate. Transport medium (DMEM without sodium pyruvate and phenol red) was withdrawn from the donor compartments of three wells and replaced by the same volume of compound stock solution (10 mM in DMSO) to reach an initial sample concentration of 62.5 μ M. The Transwell plate was then shaken (600 rpm, 37 °C) on a Heidolph

Titramax 1000 plate-shaker. Samples (40 μL) were withdrawn from the donor and acceptor compartments 30 min after initiation of the experiment, and the compound concentrations were determined by LC–MS (see below). Apparent permeability (P_{app}) was calculated according to eq 4:

$$P_{\text{app}} = \frac{dQ}{dt} \frac{1}{Ac_0} \quad (4)$$

where dQ/dt is the compound flux (mol s^{-1}), A is the surface area of the monolayer (cm^2), and c_0 is the initial concentration in the donor compartment (mol cm^{-3}).⁶⁰ After the experiment, TEER values were assessed again for each well and results from wells with values below 250 $\Omega \text{ cm}^2$ were discarded.

Plasma Protein Binding (PPB). PPB was determined in a 96-well format using a high throughput dialysis block (HTD96b; HTDialysis LCC, Gales Ferry, CT, USA). For each compound, measurements were performed in triplicate. Dialysis membranes (MWCO 12–14 K; HTDialysis LCC) were hydrated according to the instructions of the manufacturer and placed into the dialysis block. Human plasma was centrifuged (5800 rpm, 5 $^{\circ}\text{C}$, 10 min), the pH of the supernatant (without floating plasma lipids) was adjusted to 7.4 by adding the requested amount of HCl (4 M), and analyte was added to yield a final concentration of 10 μM . Equal volumes (150 μL) of plasma containing the analyte or TRIS-HCl buffer (0.1 M, pH 7.4) were transferred to the compartments separated by the dialysis membrane. The block was covered with a sealing film and left undisturbed (5 h, 37 $^{\circ}\text{C}$). Afterward, samples (90 μL) were withdrawn from the buffer compartments and diluted with plasma (10 μL). From the plasma compartments, samples (10 μL) were withdrawn and diluted with TRIS-HCl buffer (90 μL). The solutions were further diluted with ice-cooled MeCN (300 μL) to precipitate the proteins and centrifuged (3600 rpm, 4 $^{\circ}\text{C}$, 10 min). The supernatants (50 μL) were retrieved, and the analyte concentrations were determined by LC–MS (see below). The fraction bound (f_b) was calculated as follows (eq 5):

$$f_b = 1 - \frac{c_b}{c_p} \quad (5)$$

where c_b is the concentration of the analyte withdrawn from the buffer compartment before dilution and c_p is the concentration in the plasma compartment. The values were accepted if the recovery of analyte was between 80% and 120% of the initial amount.

Cytochrome P450 Mediated Metabolism. Incubations consisted of pooled male rat liver microsomes (0.5 mg microsomal protein/mL), test compound (2 μM), MgCl_2 (2 mM), and NADPH (1 mM) in a total volume of 300 μL TRIS-HCl buffer (0.1 M, pH 7.4) and were performed in a 96-well plate on a Thermomixer Comfort (Eppendorf). Compounds and microsomes were preincubated (37 $^{\circ}\text{C}$, 700 rpm, 10 min) before NADPH was added. Samples (50 μL) at $t = 0$ min and after an incubation time of 5, 10, 20, and 30 min were quenched with 150 μL of ice-cooled MeOH, centrifuged (3600 rpm, 4 $^{\circ}\text{C}$, 10 min), and 80 μL of supernatant was transferred to a 96-well plate for LC–MS analysis (see below). The metabolic half-life ($t_{1/2}$) was calculated from the slope of the linear regression from the log percentage remaining compound versus incubation time relationship. Control experiments without NADPH were performed in parallel.

LC–MS Measurements. Analyses were performed using an 1100/1200 series HPLC system coupled to a 6410 triple quadrupole mass detector (Agilent Technologies, Inc., Santa Clara, CA, USA) equipped with electrospray ionization. The system was controlled with the Agilent MassHunter Workstation Data Acquisition software (version B.01.04). The column used was an Atlantis T3 C18 column (2.1 mm \times 50 mm) with a 3 μm particle size (Waters Corp., Milford, MA, USA). The mobile phase consisted of eluent A (H_2O containing 0.1% formic acid (for 10a–f,h,i), or 10 mM ammonium acetate, pH 5.0 in 95:5, $\text{H}_2\text{O}/\text{MeCN}$ (for 10g,j)) and eluent B (MeCN containing 0.1% formic acid). The flow rate was maintained at 0.6 mL/min. The gradient was ramped from 95% A/5% B to 5% A/95% B over 1 min and then held at 5% A/95% B for 0.1 min. The system was then brought back to 95% A/5% B, resulting in a total duration of 4 min. MS parameters such as fragmentor voltage,

collision energy, polarity were optimized individually for each analyte, and the molecular ion was followed for each compound in the multiple reaction monitoring mode. The concentrations of the analytes were quantified by the Agilent Mass Hunter Quantitative Analysis software (version B.01.04).

In Vivo Studies. Animals. Female C3H/HeN mice weighing between 19 and 25 g were obtained from Charles River Laboratories (Sulzfeld, Germany) or Harlan (Venray, The Netherlands) and were housed three or four per cage. The mice were kept under specific pathogen-free conditions in the Animal House of the Department of Biomedicine, University Hospital of Basel, and animal experimentation guidelines according to the regulations of the Swiss veterinary law were followed. After 7 days of acclimatization, 9- to 10-week-old mice were used for the studies. Animals had free access to chow and water at any time and were kept in a 12 h/12 h light/dark cycle. For administration volumes and sampling the good practice guidelines were followed.¹⁰³

Pharmacokinetic Studies. The single-dose studies for the first experiment set were performed by intravenous application of FimH antagonists at a dosage of 50 mg/kg body weight, followed by plasma and urine sampling. Antagonists were diluted in PBS (Sigma-Aldrich) for injection into the tail vein. Blood and urine samples (10 μL) were taken at 6 and 30 min and at 1, 2, 4, 6, and 8 h after injection. For the PK studies with 10j, the antagonist was dissolved in PBS with 5% DMSO (Sigma-Aldrich) and injected into the tail vein (0.625 mg/kg) or given orally (1.25 mg/kg) using a gavage (syringes from BD Micro Fine, U-100 Insuline, 30 G with BD Microlance 3, 25 G needles, Becton Dickinson and Soft-Ject, 1 mL syringes from Henke Sass Wolf; gavage from Fine Science Tools). Blood and urine were sampled (10 μL) after 7, 13, 20, 30, 45 min and after 1, 1.5, 2, 2.5, 3, 4, 6, 8, and 24 h. Both blood and urine samples were directly diluted after sampling with MeOH (Acros Organics) to precipitate the proteins and centrifuged for 11 min at 13 000 rpm. The supernatants were transferred to a 96-well plate (Agilent Technologies, 0.5 mL, polypropylene), and the analyte concentrations were determined by LC–MS (see above).

Infection Study. For all infection studies, the drinking water of the mice was replaced by water containing 5% glucose (monohydrate from AppliChem, BioChemica), 3 days before the start of the experiment. 10j was dosed at 1.25 mg/kg (in 5% DMSO and PBS) and 10 mg/kg (in 5% DMSO in PBS containing 1% Tween 80, all purchased from Sigma-Aldrich) and applied orally via gavage to six and four mice, respectively, as described in the section Pharmacokinetic Studies, 40 min prior to infection. Ciprofloxacin (Ciproxin solution, 2 mg/mL, Bayer) was dosed with 8 mg/kg, which would correspond to a human dose of 500 mg,⁸¹ subcutaneously 10 min prior to infection with UT189 to 4 mice. The values for the control group (PBS, po) resulted from the infection of 11 mice. Four mice were orally treated with the formulation vehicle for 10j (5% DMSO in PBS containing 1% Tween 80) and termed controls formulation. Before infection, remaining urine in the bladder was expelled by gentle pressure on the abdomen. Mice were anesthetized in 2.5 vol % isoflurane/oxygen mixture (Attane, Minrad Inc., USA) and placed on their back. Infection was performed transurethrally using a polyethylene catheter (Intramedic polyethylene tubing, inner diameter 0.28 mm, outer diameter 0.61 mm, Becton Dickinson), on a syringe (Hamilton Gastight Syringe 50 μL , removable 30G needle, BGB Analytik AG, Switzerland). After gentle insertion of the catheter into the bladder, 50 μL of bacterial suspension of UT189 (5.5×10^9 to 2.25×10^{10} CFU/mL) was slowly injected. This corresponded to approximately 10^7 – 10^8 CFU per mouse. Mice were killed by CO_2 3 h after inoculation, and bladder and kidneys were aseptically removed. Organs were homogenized in 1 mL of PBS using a tissue lyser (Retsch, Germany). Serial dilutions of bladder and kidneys were plated on Levine Eosin Methylene Blue Agar plates (Becton Dickinson), and CFUs were counted after overnight incubation at 37 $^{\circ}\text{C}$.

■ ASSOCIATED CONTENT

● Supporting Information

HPLC data and chromatograms of target compounds and ¹H NMR spectra of the synthetic compounds. This material is available free of charge via the Internet at <http://pubs.acs.org>.

AUTHOR INFORMATION

Corresponding Author

*Phone: +41 61 267 15 51. Fax: +41 61 267 15 52. E-mail: beat.ernst@unibas.ch.

Author Contributions

^{||}S.K., L.P., K.M., D.E., and A.S. contributed equally to the project.

Notes

The authors declare no competing financial interest.

ACKNOWLEDGMENTS

The authors thank Prof. Dr. med. Radek Skoda, Department of Biomedicine, University Hospital Basel, Switzerland, for giving us access to the animal facility. The financial support by the Swiss National Science Foundation (SNF Interdisciplinary Grant K-32K1-120904) is gratefully acknowledged.

ABBREVIATIONS USED

ΔH , change in enthalpy; ΔS , change in entropy; AUC, area under the curve; BSA, bovine serum albumin; C_{max} , maximal concentration; Caco-2, colorectal adenocarcinoma; CFU, colony forming unit; CL_{tot} , total clearance; CRD, carbohydrate recognition domain; C_0 , initial concentration; DL, detection limit; FITC, fluorescein isothiocyanate; FP, fluorescence polarization; ITC, isothermal titration calorimetry; iv, intravenous; K_D , dissociation constant; MAC_{90} , minimal antiadhesion concentration to inhibit 90% adhesion; PAMPA, parallel artificial membrane permeation assay; P_{app} , apparent permeability; PD, pharmacodynamics; P_e , effective permeability; PK, pharmacokinetics; po, per os; sc, subcutaneous; UPEC, uropathogenic *Escherichia coli*; UTI, urinary tract infection; V_z , volume of distribution in terminal phase

REFERENCES

- (1) Foxman, B.; Barlow, R.; D'Arcy, H.; Gillespie, B.; Sobel, J. D. Urinary tract infection: self-reported incidence and associated costs. *Ann. Epidemiol.* **2000**, *10*, 509–515.
- (2) Ronald, A. The etiology of urinary tract infection: traditional and emerging pathogens. *Am. J. Med.* **2002**, *113* (Suppl. 1A), 14S–19S.
- (3) Fihn, S. D. Acute uncomplicated urinary tract infection in women. *N. Engl. J. Med.* **2003**, *349*, 259–266.
- (4) Hooton, T. M.; Besser, R.; Foxman, B.; Fritsche, T. R.; Nicolle, L. E. Acute uncomplicated cystitis in an era of increasing antibiotic resistance: a proposed approach to empirical therapy. *Clin. Infect. Dis.* **2004**, *39*, 75–80.
- (5) Sanchez, G. V.; Master, R. N.; Karlowsky, J. A.; Bordon, J. M. In vitro antimicrobial resistance of urinary *Escherichia coli* isolates among U.S. outpatients from 2000 to 2010. *Antimicrob. Agents Chemother.* **2012**, *56*, 2181–2183.
- (6) Clatworthy, A. E.; Pierson, E.; Hung, D. T. Targeting virulence: a new paradigm for antimicrobial therapy. *Nat. Chem. Biol.* **2007**, *3*, 541–548.
- (7) Mulvey, M. A.; Schilling, J. D.; Martinez, J. J.; Hultgren, S. J. Bad bugs and beleaguered bladders: interplay between uropathogenic *Escherichia coli* and innate host defenses. *Proc. Natl. Acad. Sci. U.S.A.* **2000**, *97*, 8829–8835.
- (8) Schilling, J. D.; Mulvey, M. A.; Hultgren, S. J. Structure and function of *Escherichia coli* type 1 pili: new insight into the pathogenesis of urinary tract infections. *J. Infect. Dis.* **2001**, *183* (Suppl. 1), S36–S40.
- (9) Wiles, T. J.; Kulesus, R. R.; Mulvey, M. A. Origins and virulence mechanisms of uropathogenic *Escherichia coli*. *Exp. Mol. Pathol.* **2008**, *85*, 11–19.
- (10) Capitani, G.; Eidam, O.; Glockshuber, R.; Grütter, M. G. Structural and functional insights into the assembly of type 1 pili from *Escherichia coli*. *Microbes Infect.* **2006**, *8*, 2284–2290.
- (11) Le Trong, I.; Aprikian, P.; Kidd, B. A.; Forero-Shelton, M.; Tchesnokova, V.; Rajagopal, P.; Rodriguez, V.; Interlandi, G.; Klevit, R.; Vogel, V.; Stenkamp, R. E.; Sokurenko, E. V.; Thomas, W. E. Structural basis for mechanical force regulation of the adhesin FimH via finger trap-like β sheet twisting. *Cell* **2010**, *141*, 645–655.
- (12) Sharon, N. Carbohydrates as future anti-adhesion drugs for infectious diseases. *Biochim. Biophys. Acta* **2006**, *1760*, 527–537.
- (13) Firon, N.; Itzhak, O.; Sharon, N. Interaction of mannose-containing oligosaccharides with the fimbrial lectin of *Escherichia coli*. *Biochem. Biophys. Res. Commun.* **1982**, *105*, 1426–1432.
- (14) Firon, N.; Ofek, I.; Sharon, N. Carbohydrate specificity of the surface lectins of *Escherichia coli*, *Klebsiella pneumoniae*, and *Salmonella typhimurium*. *Carbohydr. Res.* **1983**, *120*, 235–249.
- (15) Bouckaert, J.; Berglund, J.; Schembri, M.; De Genst, E.; Cools, L.; Wuhler, M.; Hung, C.-S.; Pinkner, J.; Slättegård, R.; Zavalov, A.; Choudhury, D.; Langermann, S.; Hultgren, S. J.; Wyns, L.; Klemm, P.; Oscarson, S.; Knight, S. D.; De Greve, H. Receptor binding studies disclose a novel class of high-affinity inhibitors of the *Escherichia coli* FimH adhesin. *Mol. Microbiol.* **2005**, *55*, 441–455.
- (16) Firon, N.; Ashkenazi, S.; Mirelman, D.; Ofek, I.; Sharon, N. Aromatic alpha-glycosides of mannose are powerful inhibitors of the adherence of type 1 fimbriated *Escherichia coli* to yeast and intestinal epithelial cells. *Infect. Immun.* **1987**, *55*, 472–476.
- (17) Sperling, O.; Fuchs, A.; Lindhorst, T. K. Evaluation of the carbohydrate recognition domain of the bacterial adhesin FimH. Design, synthesis and binding properties of mannoside ligands. *Org. Biomol. Chem.* **2006**, *4*, 3913–3922.
- (18) Han, Z.; Pinkner, J. S.; Ford, B.; Obermann, R.; Nolan, W.; Wildman, S. A.; Hobbs, D.; Ellenberger, T.; Cusumano, C. K.; Hultgren, S. J.; Janetka, J. W. Structure-based drug design and optimization of mannoside bacterial FimH antagonists. *J. Med. Chem.* **2010**, *53*, 4779–4792.
- (19) Klein, T.; Abgottspon, D.; Wittwer, M.; Rabbani, S.; Herold, J.; Jiang, X.; Kleeb, S.; Lüthi, C.; Scharenberg, M.; Bezençon, J.; Gubler, E.; Pang, L.; Smiesko, M.; Cutting, B.; Schwardt, O.; Ernst, B. FimH antagonists for the oral treatment of urinary tract infections: from design and synthesis to in vitro and in vivo evaluation. *J. Med. Chem.* **2010**, *53*, 8627–8641.
- (20) Cusumano, C. K.; Pinkner, J. S.; Han, Z.; Greene, S. E.; Ford, B. A.; Crowley, J. R.; Henderson, J. P.; Janetka, J. W.; Hultgren, S. J. Treatment and prevention of urinary tract infection with orally active FimH inhibitors. *Sci. Transl. Med.* **2011**, *3*, 109ra115.
- (21) Han, Z.; Pinkner, J. S.; Ford, B.; Chorell, E.; Crowley, J. M.; Cusumano, C. K.; Campbell, S.; Henderson, J. P.; Hultgren, S. J.; Janetka, J. W. Lead optimization studies on FimH antagonists: discovery of potent and orally bioavailable ortho-substituted biphenyl mannosides. *J. Med. Chem.* **2012**, *55*, 3945–3959.
- (22) Pang, L.; Kleeb, S.; Lemme, K.; Rabbani, S.; Scharenberg, M.; Zalewski, A.; Schädler, F.; Schwardt, O.; Ernst, B. FimH antagonists: structure–activity and structure–property relationships for biphenyl α -D-mannopyranosides. *ChemMedChem* **2012**, *7*, 1404–1422.
- (23) Jiang, X.; Abgottspon, D.; Kleeb, S.; Rabbani, S.; Scharenberg, M.; Wittwer, M.; Haug, M.; Schwardt, O.; Ernst, B. Anti-adhesion therapy for urinary tract infections—a balanced PK/PD profile proved to be key for success. *J. Med. Chem.* **2012**, *55*, 4700–4713.
- (24) Schwardt, O.; Rabbani, S.; Hartmann, M.; Abgottspon, D.; Wittwer, M.; Kleeb, S.; Zalewski, A.; Smiesko, M.; Cutting, B.; Ernst, B. Design, synthesis and biological evaluation of mannosyl triazoles as FimH antagonists. *Bioorg. Med. Chem.* **2011**, *19*, 6454–6473.
- (25) Brument, S.; Sivignon, A.; Dumych, T. I.; Moreau, N.; Roos, G.; Guérardel, Y.; Chalopin, T.; Deniaud, D.; Bilyy, R. O.; Darfeuille-Michaud, A.; Bouckaert, J.; Gouin, S. G. Thiazolylaminomannosides as potent antiadhesives of type 1 pilated *Escherichia coli* isolated from Crohn's disease patients. *J. Med. Chem.* **2013**, *56*, 5395–5406.
- (26) Lindhorst, T. K.; Kieburg, C.; Krallmann-Wenzel, U. Inhibition of the type 1 fimbriae-mediated adhesion of *Escherichia coli* to erythrocytes by multiantennary D-mannosyl clusters: the effect of multivalency. *Glycoconjugate J.* **1998**, *15*, 605–613.

- (27) Nagahori, N.; Lee, R. T.; Nishimura, S.-L.; Pagé, S.; Roy, R.; Lee, Y. C. Inhibition of adhesion of type 1 fimbriated *Escherichia coli* to highly mannosylated ligands. *ChemBioChem* **2002**, *3*, 836–844.
- (28) Appeldoorn, C. C. M.; Joosten, J. A. F.; Maate, F. A.; Dobrindt, U.; Hacker, J.; Liskamp, R. M. J.; Khan, A. S.; Pieters, R. J. Novel multivalent mannose compounds and their inhibition of the adhesion of type 1 fimbriated uropathogenic *E. coli*. *Tetrahedron: Asymmetry* **2005**, *16*, 361–372.
- (29) Patel, A.; Lindhorst, T. K. A modular approach for the synthesis of oligosaccharide mimetics. *Carbohydr. Res.* **2006**, *341*, 1657–1668.
- (30) Touaibia, M.; Wellens, A.; Shiao, T. C.; Wang, Q.; Sirois, S.; Bouckaert, J.; Roy, R. Mannosylated G(0) dendrimers with nanomolar affinities to *Escherichia coli* FimH. *ChemMedChem* **2007**, *2*, 1190–1201.
- (31) Durka, M.; Buffet, K.; Iehl, J.; Holler, M.; Nierengarten, J.-F.; Taganna, J.; Bouckaert, J.; Vincent, S. P. The functional valency of dodecamannosylated fullerenes with *Escherichia coli* FimH—towards novel bacterial antiadhesives. *Chem. Commun.* **2011**, *47*, 1321–1323.
- (32) Bouckaert, J.; Li, Z.; Xavier, C.; Almant, M.; Cavelliers, V.; Lahoutte, T.; Weeks, S. D.; Kovensky, J.; Gouin, S. G. Heptyl α -D-mannosides grafted on a β -cyclodextrin core to interfere with *Escherichia coli* adhesion: an in vivo multivalent effect. *Chem.—Eur. J.* **2013**, *19*, 7847–7855.
- (33) Scharenberg, M.; Schwardt, O.; Rabbani, S.; Ernst, B. Target selectivity of FimH antagonists. *J. Med. Chem.* **2012**, *55*, 9810–9816.
- (34) Choudhury, D.; Thompson, A.; Stojanoff, V.; Langermann, S.; Pinkner, J.; Hultgren, S. J.; Knight, S. D. X-ray structure of the FimC-FimH chaperone-adhesin complex from uropathogenic *Escherichia coli*. *Science* **1999**, *285*, 1061–1066.
- (35) Hung, C.-S.; Bouckaert, J.; Hung, D.; Pinkner, J.; Widberg, C.; DeFusco, A.; Auguste, C. G.; Strouse, R.; Langermann, S.; Waksman, G.; Hultgren, S. J. Structural basis of tropism of *Escherichia coli* to the bladder drug in urinary tract infection. *Mol. Microbiol.* **2002**, *44*, 903–915.
- (36) Wellens, A.; Garofalo, C.; Nguyen, H.; Van Gerven, N.; Slättegård, R.; Henalsteens, J.-P.; Wyns, L.; Oscarson, S.; De Greve, H.; Hultgren, S. J.; Bouckaert, J. Intervening with urinary tract infections using anti-adhesives based on the crystal structure of the FimH-oligomannose-3 complex. *PLoS One* **2008**, *3*, e2040.
- (37) Wellens, A.; Lahmann, M.; Touaibia, M.; Vaucher, J.; Oscarson, S.; Roy, R.; Remaut, H.; Bouckaert, J. The tyrosine gate as a potential entropic lever in the receptor-binding site of the bacterial adhesin FimH. *Biochemistry* **2012**, *51*, 4790–4799.
- (38) Totsika, M.; Kostakioti, M.; Hannan, T. J.; Upton, M.; Beatson, S. A.; Janetka, J. W.; Hultgren, S. J.; Schembri, M. A. A FimH inhibitor prevents acute bladder infection and treats chronic cystitis caused by multidrug-resistant uropathogenic *Escherichia coli* ST131. *J. Infect. Dis.* **2013**, *208*, 921–928.
- (39) Meanwell, M. A. Synopsis of some recent tactical application of bioisosteres in drug design. *J. Med. Chem.* **2011**, *54*, 2529–2591.
- (40) Prieto, M.; Zurita, E.; Rosa, E.; Luño, L.; Lloyd-Williams, P.; Giralt, E. Arylboronic acids and arylpinacolboronate esters in Suzuki coupling reactions involving indoles. Partner role swapping and heterocycle protection. *J. Org. Chem.* **2004**, *69*, 6812–6820.
- (41) Schulz, M. J.; Coats, S. J.; Hlasta, D. J. Microwave-assisted preparation of aryltetrazoleboronate esters. *Org. Lett.* **2004**, *6*, 3265–3268.
- (42) Devos, A.; Remion, J.; Frisque-Hesbain, A. M.; Colens, A.; Ghosez, L. Synthesis of acyl halides under very mild conditions. *J. Chem. Soc., Chem. Commun.* **1979**, 1180–1181.
- (43) Rabbani, S.; Jiang, X.; Schwardt, O.; Ernst, B. Expression of the carbohydrate recognition domain of FimH and development of a competitive binding assay. *Anal. Biochem.* **2010**, *407*, 188–195.
- (44) Waetherman, R. V.; Kiessling, L. L. Fluorescence anisotropy assay reveals affinities of C- and O-glycosides for concanavalin A. *J. Org. Chem.* **1996**, *61*, 534–538.
- (45) Cer, R. Z.; Mudunuri, U.; Stephens, R.; Lebeda, F. J. IC50-to-Ki: a web-based tool for converting IC50 to Ki values for inhibitors of enzyme activity and ligand binding. *Nucleic Acids Res.* **2009**, *37*, W441–W445.
- (46) Lynch, B. A.; Loiacono, K. A.; Tiong, C. L.; Adams, S. E.; MacNeil, I. A. A fluorescence polarization based Src-SH2 binding assay. *Anal. Biochem.* **1997**, *247*, 77–82.
- (47) Wu, P.; Brasseur, M.; Schindler, U. A high-throughput STAT binding assay using fluorescence polarization. *Anal. Biochem.* **1997**, *249*, 29–36.
- (48) Huang, X. Fluorescence polarization competition assay: the range of resolvable inhibitor potency is limited by the affinity of the fluorescent ligand. *J. Biomol. Screening* **2003**, *8*, 34–38.
- (49) Cooper, A. *Biophysical Chemistry*, 2nd ed.; RSC Publishing: Cambridge, U.K., 2011; pp 122–123.
- (50) Scharenberg, M.; Jiang, X.; Pang, L.; Navarra, G.; Rabbani, S.; Binder, F.; Schwardt, O.; Ernst, B. Kinetic properties of carbohydrate-lectin interactions: FimH antagonists. *ChemMedChem* **2014**, *9*, 78–83.
- (51) Cabani, S.; Gianni, P.; Mollica, V.; Lepori, L. Group contribution to the thermodynamic properties of non-ionic solutes in dilute aqueous solution. *J. Solution Chem.* **1981**, *10*, S63–S95.
- (52) Hansch, C.; Leo, A.; Taft, R. W. A survey of Hammett substituent constants and resonance and field parameters. *Chem. Rev.* **1991**, *91*, 165–195.
- (53) Chen, A.; Wadso, I. Simultaneous determination of delta G, delta H and delta S by an automatic microcalorimetric titration technique: application to protein ligand binding. *J. Biochem Biophys Methods* **1982**, *6*, 307–316.
- (54) Freire, E.; Mayorga, O. L.; Straume, M. Isothermal titration calorimetry. *Anal. Chem.* **1990**, *62*, 950A–959A.
- (55) Wiseman, T.; Williston, S.; Brandts, J. F.; Lin, L.-N. Rapid measurement of binding constants and heats of binding using a new titration calorimeter. *Anal. Biochem.* **1989**, *179*, 131–137.
- (56) Turnbull, W. B.; Daranas, A. H. On the value of c: can low affinity systems be studied by isothermal titration calorimetry? *J. Am. Chem. Soc.* **2003**, *125*, 14859–14866.
- (57) Sigurskjold, B. W. Exact analysis of competition ligand binding by displacement isothermal titration calorimetry. *Anal. Biochem.* **2000**, *277*, 260–266.
- (58) Velazquez-Campoy, A.; Freire, E. Isothermal titration calorimetry to determine association constants for high-affinity ligands. *Nat. Protoc.* **2006**, *1*, 186–191.
- (59) Dearden, J. C.; Bresnen, G. M. The measurement of partition coefficients. *QSAR Comb. Sci.* **1988**, *7*, 133–144.
- (60) Kansy, M.; Senner, F.; Gubernator, K. Physicochemical high throughput screening: parallel artificial membrane permeation assay in the description of passive absorption processes. *J. Med. Chem.* **1998**, *41*, 1007–1010.
- (61) Hubatsch, L.; Ragnarsson, E. G. E.; Artursson, P. Determination of drug permeability and prediction of drug absorption in Caco-2 monolayers. *Nat. Protoc.* **2007**, *2*, 2111–2119.
- (62) Banker, M. J.; Clark, T. H.; Williams, J. A. Development and validation of a 96-well equilibrium dialysis apparatus for measuring plasma protein binding. *J. Pharm. Sci.* **2003**, *92*, 967–974.
- (63) Obach, R. S. Prediction of human clearance of twenty-nine drugs from hepatic microsomal intrinsic clearance data: an examination of in vitro half-life approach and nonspecific binding to microsomes. *Drug Metab. Dispos.* **1999**, *27*, 1350–1359.
- (64) Chaturvedi, P. R.; Decker, C. J.; Odinecs, A. Prediction of pharmacokinetic properties using experimental approaches during early drug discovery. *Curr. Opin. Chem. Biol.* **2001**, *5*, 452–463.
- (65) Di, L.; Kerns, E. H. Profiling drug-like properties in discovery research. *Curr. Opin. Chem. Biol.* **2003**, *7*, 402–408.
- (66) Lipinski, C. A. Drug-like properties and the causes of poor solubility and poor permeability. *J. Pharmacol. Toxicol. Methods* **2000**, *44*, 235–249.
- (67) Curatolo, W. Physical chemical properties of oral drug candidates in the discovery and exploratory development settings. *Pharm. Sci. Technol. Today* **1998**, *1*, 387–393.
- (68) Ishikawa, M.; Hashimoto, Y. Improvement in aqueous solubility in small molecule drug discovery programs by disruption of molecular planarity and symmetry. *J. Med. Chem.* **2011**, *54*, 1539–1554.

- (69) Avdeef, A.; Bendels, S.; Di, L.; Faller, B.; Kansy, M.; Sugano, K.; Yamauchi, Y. PAMPA – critical factors for better predictions of absorption. *J. Pharm. Sci.* **2007**, *96*, 2893–2909.
- (70) Artursson, P.; Karlsson, J. Correlation between oral drug absorption in humans and apparent drug permeability coefficients in human intestinal epithelial (Caco-2) cells. *Biochem. Biophys. Res. Commun.* **1991**, *175*, 880–885.
- (71) Feng, B.; LaPerle, J. L.; Chang, G.; Varma, M. V. S. Renal clearance in drug discovery and development: molecular descriptors, drug transporters and disease state. *Expert Opin. Drug. Metab. Toxicol.* **2010**, *6*, 939–952.
- (72) Schmidt, S.; Gonzalez, D.; Derendorf, H. Significance of protein binding in pharmacokinetics and pharmacodynamics. *J. Pharm. Sci.* **2010**, *99*, 1107–1122.
- (73) Weisiger, R. A. Dissociation from albumin: A potentially rate-limiting step in the clearance of substances by the liver. *Proc. Natl. Acad. Sci. U.S.A.* **1985**, *82*, 1563–1567.
- (74) Smith, D. A.; Jones, B. C.; Walker, D. K. Design of drugs involving the concepts and theories of drug metabolism and pharmacokinetics. *Med. Res. Rev.* **1996**, *16*, 243–266.
- (75) Van de Waterbeemd, H.; Smith, D. A.; Beaumont, K.; Walker, D. K. Property-based design: optimization of drug absorption and pharmacokinetics. *J. Med. Chem.* **2001**, *44*, 1313–1333.
- (76) Varma, M. V. S.; Feng, B.; Obach, R. S.; Troutman, M. D.; Chupka, J.; Miller, H. R.; El-Kattan, A. Physicochemical determinants of human renal clearance. *J. Med. Chem.* **2009**, *52*, 4844–4852.
- (77) Waring, M. J. Lipophilicity in drug discovery. *Expert Opin. Drug Discovery* **2010**, *5*, 235–248.
- (78) Zhang, Y.; Huo, M.; Solver, P. K. An add-in program for pharmacokinetic and pharmacodynamic data analysis in Microsoft Excel. *Comput. Methods Programs Biomed.* **2010**, *99*, 306–314.
- (79) Scharenberg, M.; Abgottspon, D.; Cicek, E.; Jiang, X.; Schwaradt, O.; Rabbani, S.; Ernst, B. Cytometry-based assay for screening FimH antagonists. *Assay Drug Dev. Technol.* **2011**, *9*, 455–464.
- (80) Hooton, T. M. Fluoroquinolones and resistance in the treatment of uncomplicated urinary tract infection. *Int. J. Antimicrob. Agents* **2003**, *22*, 65–72.
- (81) Jakobsen, L.; Cattoir, V.; Jensen, K. S.; Hammerum, A. M.; Nordmann, P.; Fridmødt-Møller, N. Impact of low-level fluoroquinolone resistance genes *qnrA1*, *qnrB19*, and *qnrS1* on ciprofloxacin treatment of isogenic *Escherichia coli* strains in a murine urinary tract infection model. *J. Antimicrob. Chemother.* **2012**, *67*, 2438–2444.
- (82) Mulvey, M. A. Adhesion and entry of uropathogenic *Escherichia coli*. *Cell. Microbiol.* **2002**, *4*, 257–271.
- (83) Ballatore, C.; Hury, D. M.; Smith, A. B. Carboxylic acid (bio)isosteres in drug design. *ChemMedChem* **2013**, *8*, 385–395.
- (84) Justice, S. S.; Hung, C.; Theriot, J. A.; Fletcher, D. A.; Anderson, G. G.; Footer, M. J.; Hultgren, S. J. Differentiation and developmental pathways of uropathogenic *Escherichia coli* in urinary tract pathogenesis. *Proc. Natl. Acad. Sci. U.S.A.* **2004**, *101*, 1333–1338.
- (85) Mulvey, M. A.; Schilling, J. D.; Hultgren, S. J. Establishment of a persistent *Escherichia coli* reservoir during the acute phase of a bladder infection. *Infect. Immun.* **2001**, *69*, 4572–9.
- (86) Houtman, J. C.; Brown, P. C.; Bowden, B.; Yamaguchi, H.; Appella, E.; Samelson, L. E.; Schuck, P. Studying multisite binary and ternary protein interactions by global analysis of isothermal titration calorimetry data in SEDPHAT: application to adaptor protein complexes in cell signaling. *Protein Sci.* **2007**, *16*, 30–42.
- (87) *Maestro*, version 9.3; Schrödinger, LLC: New York, NY, 2012.
- (88) *MacroModel*, version 9.9; Schrödinger, LLC: New York, NY, 2012.
- (89) Hawkins, G. D.; Giesen, D. J.; Lynch, G. C.; Chambers, C. C.; Rossi, I.; Storer, J. W.; Li, J.; Thompson, J. D.; Winget, P.; Lynch, B. J.; Rinaldi, D.; Liotard, D. A.; Cramer, C. J.; Truhlar, D. G. *AMSOL*, version 7.1; University of Minnesota: Minneapolis, MN, 2003; based in part on the following: Liotard, D. A.; Healy, E. F.; Ruiz, J. M.; Dewar, M. J. S. *AMPAC*, version 2.1; Semicem, Inc.: Shawnee, KS.
- (90) Chambers, C. C.; Hawkins, G. D.; Cramer, C. J.; Truhlar, D. G. Model for aqueous solvation based on class IV atomic charges and first solvation shell effects. *J. Phys. Chem.* **1996**, *100*, 16385–16398.
- (91) Dewar, M. J. S.; Zoebisch, E. G.; Healy, E. F.; Stewart, J. J. P. AM1: a new general purpose quantum mechanical molecular model. *J. Am. Chem. Soc.* **1993**, *115*, 5348–5348 [Erratum to *J. Am. Chem. Soc.* **1985**, *107*, 3902–3909].
- (92) Mulvey, M. A.; Schilling, J. D.; Hultgren, S. J. Establishment of a persistent *Escherichia coli* reservoir during the acute phase of a bladder infection. *Infect. Immun.* **2001**, *69*, 4572–4579.
- (93) Kabsch, W. Automatic processing of rotation diffraction data from crystals of initially unknown symmetry and cell constants. *J. Appl. Crystallogr.* **1993**, *26*, 795–800.
- (94) Leslie, A. G. W. The integration of macromolecular diffraction data. *Acta Crystallogr. D* **2006**, *62*, 48–57.
- (95) Winn, M. D.; Ballard, C. C.; Cowtan, K. D.; Dodson, E. J.; Emsley, P.; Evans, P. R.; Keegan, R. M.; Krissinel, E. B.; Leslie, A. G. W.; McCoy, A.; McNicholas, S. J.; Murshudov, G. N.; Pannu, N. S.; Potterton, E. A.; Powell, H. R.; Read, R. J.; Vagin, A.; Wilson, K. S. Overview of the CCP4 suite and current developments. *Acta Crystallogr. D* **2011**, *67*, 235–242.
- (96) McCoy, A. J. Solving structures of protein complexes by molecular replacement with Phaser. *Acta Crystallogr. D* **2007**, *63*, 32–41.
- (97) Emsley, P.; Cowtan, K. Coot: model-building tools for molecular graphics. *Acta Crystallogr. D* **2004**, *60*, 2126–2132.
- (98) Adams, P. D.; Grosse-Kunstleve, R. W.; Hung, L.-W.; Ioerger, T. R.; McCoy, A. J.; Moriarty, N. W.; Read, R. J.; Sacchettini, J. C.; Sauter, N. K.; Terwilliger, T. C. PHENIX: building new software for automated crystallographic structure determination. *Acta Crystallogr., Sect. D: Biol. Crystallogr.* **2002**, *58*, 1948–1954.
- (99) van Aalten, D. M. F.; Bywater, R.; Findlay, J. B. C.; Hendlich, M.; Hoof, R. W. W.; Vriend, G. PRODRG, a program for generating molecular topologies and unique molecular descriptors from coordinates of small molecules. *J. Comput.-Aided Mol. Des.* **1996**, *10*, 255–262.
- (100) Chen, V. B.; Arendall, W. B.; Headd, J. J.; Keedy, D. A.; Immormino, R. M.; Kapral, G. J.; Murray, L. W.; Richardson, J. S.; Richardson, D. C. MolProbity: all-atom structure validation for macromolecular crystallography. *Acta Crystallogr. D* **2010**, *66*, 12–21.
- (101) Bezençon, J.; Wittwer, M. B.; Cutting, B.; Smiesko, M.; Wagner, B.; Kansy, M.; Ernst, B. pK_a determination by ^1H NMR spectroscopy—an old methodology revisited. *J. Pharm. Biomed. Anal.* **2014**, *93*, 147–155.
- (102) (a) VCCLAB, Virtual Computational Chemistry Laboratory, 2005. <http://www.vcclab.org> (accessed August 14, 2012). (b) Tetko, I. V.; Gasteiger, J.; Todeschini, R.; Mauri, A.; Livingstone, D.; Ertl, P.; Palyulin, V. A.; Radchenko, E. V.; Zefirov, N. S.; Makarenko, A. S.; Tanchuk, V. Y.; Prokopenko, V. V. Virtual computational chemistry laboratory—design and description. *J. Comput.-Aided Mol. Des.* **2005**, *19*, 453–463.
- (103) Diehl, K.-H.; Hull, R. A. Good practice guide to the administration of substances and removal of blood, including routes and volumes. *J. Appl. Toxicol.* **2001**, *21*, 15–23.

Supporting Information

FimH Antagonists - Bioisosteres to Improve the *in vitro* and *in vivo* PK/PD Profile

Simon Kleeb,^{a)} Lijuan Pang,^{a)} Katharina Mayer,^{a)} Deniz Eris,^{a)} Anja Sigl,^{a)} Roland C. Preston,^{a)} Pascal Zihlmann,^{a)} Timothy Sharpe,^{c)} Roman P. Jakob,^{b)} Daniela Abgottspon,^{a)} Aline S. Hutter,^{a)} Meike Scharenberg,^{a)} Xiaohua Jiang,^{a)} Giulio Navarra,^{a)} Said Rabbani,^{a)} Martin Smiesko,^{a)} Nathalie Lüdin,^{a)} Jacqueline Bezençon,^{a)} Oliver Schwardt,^{a)} Timm Maier,^{b)} Beat Ernst^{a)*}

a) Institute of Molecular Pharmacy, Pharmacenter, University of Basel, Klingelbergstrasse 50, CH-4056 Basel, Switzerland

b) Structural Biology, Biocenter, University of Basel, Klingelbergstrasse 70, CH-4056 Basel

c) Biophysical Facility, Biocenter, University of Basel, Klingelbergstrasse 70, CH-4056 Basel

* To whom correspondence should be addressed: Prof. Dr. Beat Ernst, Institute of Molecular Pharmacy, Pharmacenter, University of Basel, Klingelbergstrasse 50, CH-4056 Basel, Switzerland; Tel: +41 61 267 15 51, Fax: +41 61 267 15 52; E-mail: beat.ernst@unibas.ch

Contents

Synthesis	S2
HPLC data of the target compounds	S12
HPLC traces of the target compounds	S13
¹ H NMR spectra of the synthetic compounds	S20
References	S32

Synthesis

General methods. NMR spectra were recorded on a Bruker Avance DMX-500 (500.1 MHz) spectrometer. Assignment of ^1H and ^{13}C NMR spectra was achieved using 2D methods (COSY, HSQC, HMBC). Chemical shifts are expressed in ppm using residual CHCl_3 , CHD_2OD or HDO as references. Optical rotations were measured using Perkin-Elmer Polarimeter 341. Electron spray ionization mass spectra (ESI-MS) were obtained on a Waters micromass ZQ. The LC/HRMS analysis were carried out using a Agilent 1100 LC equipped with a photodiode array detector and a Micromass QTOF I equipped with a 4 GHz digital-time converter. Microwave-assisted reactions were carried out with a CEM Discover and Explorer. Reactions were monitored by TLC using glass plates coated with silica gel 60 F₂₅₄ (Merck) and visualized by using UV light and/or by charring with a molybdate solution (a 0.02 M solution of ammonium cerium sulfate dihydrate and ammonium molybdate tetrahydrate in aqueous 10% H_2SO_4). MPLC separations were carried out on a CombiFlash Companion or Rf (Teledyne Isco) equipped with RediSep normal-phase or RP-18 reversed-phase flash columns. LC-MS separations were done on a Waters system equipped with sample manager 2767, pump 2525, PDA 2525 and micromass ZQ. All compounds used for biological assays are at least of 95% purity based on HPLC analytical results. Commercially available reagents were purchased from Fluka, Aldrich, Alfa Aesar or abcr GmbH & Co. KG (Germany). Solvents were purchased from Sigma-Aldrich or Acros and were dried prior to use where indicated. Methanol (MeOH) was dried by refluxing with sodium methoxide and distilled immediately before use. Dimethoxyethane (DME) was dried by filtration over Al_2O_3 (Fluka, type 5016 A basic).

General procedure A for palladium-catalyzed Miyaura-Suzuki coupling. A Schlenk tube was charged with aryl iodide **11**^{S1} (1.0 eq), boronic acid or boronate **12a-d, f, g** (1.1 eq), $\text{Pd}(\text{dppf})\text{Cl}_2 \cdot \text{CH}_2\text{Cl}_2$ (0.03 eq), K_3PO_4 (1.5 eq) and a stirring bar. The tube was closed with a rubber septum and was evacuated and flushed with argon. This procedure was repeated once, and then anhydrous DMF (2 mL) was added under a stream of argon. The mixture was degassed in an ultrasonic bath and flushed with argon for 5 min, and then stirred at 80 °C overnight. The reaction mixture was cooled to rt, diluted with EtOAc (50 mL), and washed with water (50 mL) and brine (50 mL). The organic layer was dried over Na_2SO_4 and concentrated in vacuo. The residue was purified by MPLC on silica gel (petroleum ether/EtOAc) to afford **13a-d, f, g**.

General procedure B for deacetylation. To a solution of **13a-d, f, g** (1.0 eq) in dry MeOH (5 mL) was added freshly prepared 1 M NaOMe/MeOH (0.1 eq) under argon. The mixture was stirred at rt until the reaction was complete (monitored by TLC), then neutralized with Amberlyst-15 (H⁺) ion-exchange resin, filtered and concentrated in vacuo. The residue was purified by MPLC on silica gel (DCM/MeOH, 10:1-7:1) to afford **10a-d, f, g** as white solids.

4'-(2,3,4,6-Tetra-*O*-acetyl- α -D-mannopyranosyloxy)-biphenyl-4-carboxamide (13a).

Prepared according to general procedure A from **11** (150 mg, 0.27 mmol), (4-carbamoylphenyl)boronic acid (**12a**, 49 mg, 0.30 mmol), Pd(dppf)Cl₂·CH₂Cl₂ (6.6 mg, 0.008 mmol) and K₃PO₄ (86 mg, 0.41 mmol). Yield: 108 mg (73%) as yellow oil. [α]_D²⁰ +70.7 (*c* 0.60, EtOAc); ¹H NMR (500 MHz, CDCl₃): δ = 7.89-7.87 (m, 2H, Ar-H), 7.63-7.62 (m, 2H, Ar-H), 7.57-7.55 (m, 2H, Ar-H), 7.19-7.17 (m, 2H, Ar-H), 6.18 (br, 1H, NH), 5.85 (br, 1H, NH), 5.60-5.57 (m, 2H, H-1, H-3), 5.48 (dd, *J* = 1.8, 3.5 Hz, 1H, H-2), 5.40 (t, *J* = 10.1 Hz, 1H, H-4), 4.30 (dd, *J* = 5.3, 12.4 Hz, 1H, H-6a), 4.17-4.03 (m, 2H, H-5, H-6b), 2.22, 2.07, 2.05, 2.04 (4 s, 12H, 4 COCH₃); ¹³C NMR (126 MHz, CDCl₃): δ = 170.68, 170.17, 170.14, 169.88, 169.12 (5 CO), 155.77, 144.07, 134.85, 131.83, 128.58, 128.10, 127.04, 117.02 (Ar-C), 95.89 (C-1), 69.47 (C-5), 69.38 (C-2), 68.96 (C-3), 66.00 (C-4), 62.20 (C-6), 21.03, 20.86, 20.84, 20.83 (4 COCH₃); ESI-MS: *m/z*: Calcd for C₂₇H₂₉NNaO₁₁ [M+Na]⁺: 566.2, found: 566.2.

4'-(2,3,4,6-Tetra-*O*-acetyl- α -D-mannopyranosyloxy)-*N*-methyl-biphenyl-4-carboxamide (13b).

Prepared according to general procedure A from **11** (50 mg, 0.09 mmol), (4-(methylcarbamoyl)phenyl)boronic acid (**12b**, 18 mg, 0.10 mmol), Pd(dppf)Cl₂·CH₂Cl₂ (3 mg, 0.003 mmol) and K₃PO₄ (29 mg, 0.14 mmol). Yield: 32 mg (63%) as colorless oil. [α]_D²⁰ +76.1 (*c* 0.60, EtOAc); ¹H NMR (500 MHz, CDCl₃): δ = 7.83-7.81 (m, 2H, Ar-H), 7.60-7.53 (m, 4H, Ar-H), 7.17-7.15 (m, 2H, Ar-H), 6.30 (d, *J* = 4.8 Hz, 1H, NH), 5.58-5.56 (m, 2H, H-1, H-3), 5.46 (dd, *J* = 1.8, 3.4 Hz, 1H, H-2), 5.38 (t, *J* = 10.0 Hz, 1H, H-4), 4.28 (dd, *J* = 5.1, 12.1 Hz, 1H, H-6a), 4.12-4.06 (m, 2H, H-5, H-6b), 3.03 (d, *J* = 4.8 Hz, 3H, NHCH₃), 2.20, 2.05, 2.03, 2.02 (4 s, 12H, 4 COCH₃); ¹³C NMR (126 MHz, CDCl₃): δ = 170.66, 170.14, 170.11, 169.86, 167.99 (5 CO), 155.65, 143.36, 134.97, 133.17, 128.51, 127.53, 126.96, 116.98 (Ar-C), 95.88 (C-1), 69.46 (C-5), 69.35 (C-2), 68.96 (C-3), 65.98 (C-4), 62.19 (C-6), 26.99 (NHCH₃), 21.02, 20.84, 20.82, 20.81 (4 COCH₃); ESI-MS: *m/z*: Calcd for C₂₈H₃₂NO₁₁ [M+H]⁺: 558.2, found: 558.3.

4'-(2,3,4,6-Tetra-*O*-acetyl- α -D-mannopyranosyloxy)-biphenyl-4-yl-(morpholino)-methanone (13c). Prepared according to general procedure A from **11** (110 mg, 0.20 mmol), pinacol 4-(morpholine-4-carbonyl)phenylboronate (**12c**, 70 mg, 0.22 mmol), Pd(dppf)Cl₂·CH₂Cl₂ (5 mg, 0.006 mmol) and K₃PO₄ (64 mg, 0.30 mmol). Yield: 139 mg (99%) as yellow oil. $[\alpha]_D^{20} +62.0$ (*c* 0.40, MeOH); ¹H NMR (500 MHz, CDCl₃): δ = 7.60-7.47 (m, 6H, Ar-H), 7.19-7.17 (m, 2H, Ar-H), 5.60-5.58 (m, 2H, H-1, H-3), 5.47 (dd, *J* = 1.9, 3.4 Hz, 1H, H-2), 5.40 (t, *J* = 10.1 Hz, 1H, H-4), 4.30 (dd, *J* = 5.1, 12.2 Hz, 1H, H-6a), 4.14-4.08 (m, 2H, H-6b, H-5), 3.78-3.45 (m, 8H, 4 CH₂), 2.22, 2.09, 2.07, 2.04 (4 s, 12H, 4 COCH₃); ¹³C NMR (126 MHz, CDCl₃): δ = 170.55, 170.26, 170.05, 170.01, 169.76 (5 CO), 155.50, 142.00, 135.03, 133.82, 128.36, 127.80, 126.94, 116.90 (Ar-C), 95.81 (C-1), 69.38 (C-5), 68.85 (C-2), 66.94 (C-3), 65.90 (C-4), 62.09 (C-6), 20.92, 20.74, 20.72, 20.71 (4 COCH₃); ESI-MS: *m/z*: Calcd for C₃₁H₃₅NNaO₁₂ [M+Na]⁺: 636.2, found: 636.3.

4'-(Methylsulfonyl)-biphenyl-4-yl 2,3,4,6-tetra-*O*-acetyl- α -D-mannopyranoside (13d). Prepared according to general procedure A from **11** (50 mg, 0.09 mmol), 4-(methylsulfonyl)-phenylboronic acid (**12d**, 20 mg, 0.10 mmol), Pd(dppf)Cl₂·CH₂Cl₂ (3 mg, 0.003 mmol) and K₃PO₄ (29 mg, 0.14 mmol). Yield: 23 mg (44%) as a yellow solid. $[\alpha]_D^{20} +78.3$ (*c* 0.60, EtOAc); ¹H NMR (500 MHz, CDCl₃): δ = 8.00-7.99 (m, 2H, Ar-H), 7.74-7.72 (m, 2H, Ar-H), 7.59-7.56 (m, 2H, Ar-H), 7.23-7.18 (m, 2H, Ar-H), 5.60-5.56 (m, 2H, H-1, H-3), 5.47 (dd, *J* = 1.8, 3.4 Hz, 1H, H-2), 5.40 (t, *J* = 10.0 Hz, 1H, H-4), 4.30 (dd, *J* = 4.9, 12.0 Hz, 1H, H-6a), 4.13-4.08 (m, 2H, H-5, H-6b), 3.10 (s, 3H, SO₂CH₃), 2.22, 2.07, 2.05, 2.04 (4 s, 12H, 4 COCH₃); ¹³C NMR (126 MHz, CDCl₃): δ = 170.53, 170.05, 170.02, 169.73 (4 CO), 156.11, 145.82, 138.86, 133.89, 128.71, 128.00, 127.61, 117.05 (Ar-C), 95.77 (C-1), 69.32 (2C, C-2, C-5), 68.80 (C-3), 65.84 (C-4), 62.06 (C-6), 44.65 (SO₂CH₃), 20.91, 20.74, 20.72 (4C, 4 COCH₃); ESI-MS: *m/z*: Calcd for C₂₇H₃₀NaO₁₂S [M+Na]⁺: 601.1, found: 601.1.

3',5'-Difluoro-4'-hydroxy-biphenyl-4-yl 2,3,4,6-tetra-*O*-acetyl- α -D-mannopyranoside (13f). Prepared according to general procedure A from **11** (100 mg, 0.18 mmol), pinacol (3,5-difluoro-4-hydroxyphenyl)boronate (**12f**, 51 mg, 0.20 mmol), Pd(dppf)Cl₂·CH₂Cl₂ (5 mg, 0.006 mmol) and K₃PO₄ (57 mg, 0.27 mmol). Yield: 57 mg (52%) as colorless oil. $[\alpha]_D^{20} +64.9$ (*c* 0.70, MeOH); ¹H NMR (500 MHz, CDCl₃): δ = 7.44-7.38 (m, 2H, Ar-H), 7.15-7.11 (m, 2H, Ar-H), 7.10-7.02 (m, 2H, Ar-H), 5.90 (bs, 1H, OH), 5.59 (dd, *J* = 3.6, 10.1 Hz, 1H, H-3), 5.56 (d, *J* = 1.8 Hz, 1H, H-1), 5.47 (dd, *J* = 1.8, 3.5 Hz, 1H, H-2), 5.40 (t, *J* = 10.1 Hz,

1H, H-4), 4.30 (dd, $J = 4.8, 12.0$ Hz, 1H, H-6a), 4.14-4.08 (m, 2H, H-6b, H-5), 2.22, 2.07, 2.06, 2.05 (4 s, 12H, 4 COCH₃); ¹³C NMR (126 MHz, CDCl₃): $\delta = 170.83, 170.31, 170.25, 169.99$ (4 CO), 155.43 (Ar-C), 152.19 (d, $J = 241.0$ Hz, Ar-C), 152.14 (d, $J = 241.0$ Hz, Ar-C), 133.82 (Ar-C), 132.29 (d, $J = 20.6$ Hz, Ar-C), 127.93, 117.02 (Ar-C), 110.04 (d, $J = 6.4$ Hz, Ar-C), 109.91 (d, $J = 6.4$ Hz, Ar-C), 95.90 (C-1), 69.53 (C-5), 69.34 (C-2), 68.97 (C-3), 66.02 (C-4), 62.23 (C-6), 21.02, 20.85, 20.82, 20.81 (4 COCH₃); ESI-MS: m/z : Calcd for C₂₆H₂₆F₂NaO₁₁ [M+Na]⁺: 575.1, found: 575.2.

4'-(2,3,4,6-Tetra-*O*-acetyl- α -D-mannopyranosyloxy)-biphenyl-4-carbonitrile (13g).

Prepared according to general procedure A from **11** (330 mg, 0.60 mmol), 4-cyanophenylboronic acid (**12g**, 96 mg, 0.65 mmol), Pd(dppf)Cl₂·CH₂Cl₂ (15 mg, 0.018 mmol) and K₃PO₄ (192 mg, 0.90 mmol). Yield: 187 mg (59%) as colorless oil. $[\alpha]_D^{20} +72.9$ (*c* 0.80, MeOH); ¹H NMR (500 MHz, CD₃OD): $\delta = 7.73-7.71$ (m, 2H, Ar-H), 7.65-7.64 (m, 2H, Ar-H), 7.57-7.53 (m, 2H, Ar-H), 7.21-7.19 (m, 2H, Ar-H), 5.60-5.57 (m, 2H, H-1, H-3), 5.47 (dd, $J = 1.9, 3.4$ Hz, 1H, H-2), 5.40 (t, $J = 10.1$ Hz, 1H, H-4), 4.30 (dd, $J = 5.1, 12.2$ Hz, 1H, H-6a), 4.14-4.08 (m, 2H, H-6b, H-5), 2.22, 2.07, 2.06, 2.04 (4 s, 12H, 4 COCH₃); ¹³C NMR (126 MHz, CD₃OD): $\delta = 170.62, 170.14, 170.11, 169.83$ (4 CO), 156.16, 144.87, 134.05, 132.77, 128.64, 127.46 (Ar-C), 119.05 (CN), 117.15, 110.77 (Ar-C), 95.86 (C-1), 69.42 (2C, C-2, C-5), 68.90 (C-3), 65.94 (C-4), 62.16 (C-6), 21.01, 20.84, 20.82 (4C, 4 COCH₃); ESI-MS: m/z : Calcd for C₂₇H₂₇NNaO₁₀ [M+Na]⁺: 548.2, found: 548.2.

4'-(α -D-Mannopyranosyloxy)-biphenyl-4-carboxamide (10a).

Prepared according to general procedure B from **13a** (30 mg, 0.05 mmol). Yield: 6 mg (29%) as a white solid. $[\alpha]_D^{20} +133.0$ (*c* 0.30, dioxane/H₂O, 2:1); ¹H NMR (500 MHz, DMSO-*d*₆): $\delta = 7.98-7.94$ (m, 2H, Ar-H), 7.72-7.70 (m, 2H, Ar-H), 7.67-7.64 (m, 2H, Ar-H), 7.27-7.23 (m, 2H, Ar-H), 5.57 (d, $J = 1.6$ Hz, 1H, H-1), 4.05 (dd, $J = 1.8, 3.4$ Hz, 1H, H-2), 3.95 (dd, $J = 3.4, 9.4$ Hz, 1H, H-3), 3.85-3.70 (m, 3H, H-4, H-6a, H-6b), 3.64 (m, 1H, H-5); ¹³C NMR (126 MHz, DMSO-*d*₆): $\delta = 167.80$ (CO), 156.39, 142.33, 132.78, 132.36, 128.13, 127.96, 125.93, 117.16 (Ar-C), 98.73 (C-1), 74.89 (C-5), 70.59 (C-3), 70.00 (C-2), 66.62 (C-4), 60.96 (C-6); HRMS: m/z : Calcd for C₁₉H₂₂NO₇ [M+H]⁺: 376.1391, found: 376.1394.

4'-(α -D-Mannopyranosyloxy)-*N*-methyl-biphenyl-4-carboxamide (10b).

Prepared according to general procedure B from **13b** (30 mg, 0.05 mmol). Yield: 13 mg (62%) as a white solid. $[\alpha]_D^{20} +117.0$ (*c* 0.30, MeOH/H₂O, 5:1); ¹H NMR (500 MHz, CD₃OD): $\delta = 7.85-$

7.83 (m, 2H, Ar-H), 7.66-7.64 (m, 2H, Ar-H), 7.61-7.58 (m, 2H, Ar-H), 7.21-7.19 (m, 2H, Ar-H), 5.52 (d, $J = 1.5$ Hz, 1H, H-1), 4.00 (dd, $J = 1.9, 3.4$ Hz, 1H, H-2), 3.90 (dd, $J = 3.4, 9.5$ Hz, 1H, H-3), 3.75-3.69 (m, 3H, H-4, H-6a, H-6b), 3.59 (ddd, $J = 2.4, 5.1, 9.7$ Hz, 1H, H-5), 2.91 (s, 3H, NHCH_3); ^{13}C NMR (126 MHz, CD_3OD): $\delta = 170.51$ (CO), 158.04, 145.09, 135.28, 133.78, 129.29, 128.80, 127.64, 118.20 (Ar-C), 100.13 (C-1), 75.49 (C-5), 72.41 (C-2), 71.98 (C-3), 68.32 (C-4), 62.67 (C-6), 26.94 (NHCH_3); HRMS: m/z : Calcd for $\text{C}_{20}\text{H}_{24}\text{NO}_7$ $[\text{M}+\text{H}]^+$: 390.1547, found: 390.1551.

4'-(α -D-Mannopyranosyloxy)-biphenyl-4-yl-(morpholino)methanone (10c). Prepared according to general procedure B from **13c** (50 mg, 0.08 mmol). Yield: 27 mg (75%) as a white solid. $[\alpha]_{\text{D}}^{20} +96.5$ (c 0.40, MeOH); ^1H NMR (500 MHz, CD_3OD): $\delta = 7.71$ -7.70 (m, 2H, Ar-H), 7.63-7.63 (m, 2H, Ar-H), 7.52-7.50 (m, 2H, Ar-H), 7.25-7.23 (m, 2H, Ar-H), 5.56 (d, $J = 1.7$ Hz, 1H, H-1), 4.05 (dd, $J = 1.8, 3.4$ Hz, 1H, H-2), 3.95 (dd, $J = 3.5, 9.5$ Hz, 1H, H-3), 3.78-3.54 (m, 12H, H-4, H-5, H-6a, H-6b, 4 CH_2); ^{13}C NMR (126 MHz, CD_3OD): $\delta = 172.29$ (CO), 158.00, 143.86, 135.30, 134.66, 129.25, 128.90, 127.85, 118.23 (Ar-C), 100.14 (C-1), 75.50 (C-5), 72.42 (C-3), 71.99 (C-2), 68.33, 62.69 (6C, C-4, C-6, 4 CH_2); HRMS: m/z : Calcd for $\text{C}_{23}\text{H}_{28}\text{NO}_8$ $[\text{M}+\text{H}]^+$: 446.1809, found: 446.1813.

4'-(Methylsulfonyl)-biphenyl-4-yl α -D-mannopyranoside (10d). Prepared according to general procedure B from **13d** (20 mg, 0.03 mmol). Yield: 12 mg (86%) as a white solid. $[\alpha]_{\text{D}}^{20} +105.8$ (c 0.20, DCM/MeOH, 1:3); ^1H NMR (500 MHz, $\text{DMSO-}d_6$): $\delta = 7.90$ -7.88 (m, 2H, Ar), 7.76-7.74 (m, 2H, Ar), 7.58-7.56 (m, 2H, Ar-H), 7.17-7.15 (m, 2H, Ar-H), 5.46 (d, $J = 1.7$ Hz, 1H, H-1), 3.93 (dd, $J = 1.9, 3.5$ Hz, 1H, H-2), 3.81 (dd, $J = 3.4, 9.5$ Hz, 1H, H-3), 3.69-3.61 (m, 3H, H-4, H-6a, H-6b), 3.50 (ddd, $J = 2.5, 5.4, 9.7$ Hz, 1H, H-5), 3.05 (SO_2CH_3); ^{13}C NMR (126 MHz, $\text{DMSO-}d_6$): $\delta = 156.95, 144.60, 138.94, 131.86, 128.36, 127.57, 126.98, 117.24$ (Ar-C), 98.78 (C-1), 75.07 (C-5), 70.63 (C-3), 70.00 (C-2), 66.67 (C-4), 61.02 (C-6), 43.58 (SO_2CH_3); HRMS: m/z : Calcd for $\text{C}_{19}\text{H}_{22}\text{NaO}_8\text{S}$ $[\text{M}+\text{Na}]^+$: 433.0928, found: 433.0928.

3',5'-Difluoro-4'-hydroxy-biphenyl-4-yl α -D-mannopyranoside (10f). Prepared according to general procedure B from **13f** (40 mg, 0.07 mmol). Yield: 21 mg (78%) as a white solid. $[\alpha]_{\text{D}}^{20} +117.6$ (c 0.40, MeOH); ^1H NMR (500 MHz, CD_3OD): $\delta = 7.52$ -7.49 (m, 2H, Ar-H), 7.19-7.14 (m, 4H, Ar-H), 5.54 (d, $J = 1.7$ Hz, 1H, H-1), 4.04 (dd, $J = 1.8, 3.4$ Hz, 1H, H-2), 3.94 (dd, $J = 3.5, 9.5$ Hz, 1H, H-3), 3.78-3.73 (m, 3H, H-4, H-6a, H-6b), 3.63 (ddd, $J = 2.5, 5.1, 9.8$ Hz, 1H, H-5); ^{13}C NMR (126 MHz, CD_3OD): $\delta = 157.56$ (Ar-C), 154.26 (d, $J = 240.0$

Hz, Ar-C), 154.21 (d, $J = 240.0$ Hz, Ar-C), 134.38 (t, $J = 2.3$ Hz, Ar-C), 132.92, 128.64, 118.16 (Ar-C), 110.59 (d, $J = 6.6$ Hz, Ar-C), 110.46 (d, $J = 6.6$ Hz, Ar-C), 100.15 (C-1), 75.44 (C-5), 72.42 (C-3), 71.99 (C-2), 68.32 (C-4), 62.66 (C-6); HRMS: m/z : Calcd for $C_{18}H_{18}F_2NaO_7 [M+Na]^+$: 407.0913, found: 407.0913.

4'-(α -D-Mannopyranosyloxy)-biphenyl-4-carbonitrile (10g). Prepared according to general procedure B from **13g** (40 mg, 0.08 mmol). Yield: 16 mg (60%) as a white solid. 1H NMR (500 MHz, CD_3OD): $\delta = 7.82$ -7.75 (m, 4H, Ar-H), 7.69-7.63 (m, 2H, Ar-H), 7.30-7.23 (m, 2H, Ar-H), 5.58 (d, $J = 1.7$ Hz, 1H, H-1), 4.05 (dd, $J = 1.8, 3.4$ Hz, 1H, H-2), 3.94 (dd, $J = 3.4, 9.5$ Hz, 1H, H-3), 3.83-3.71 (m, 3H, H-4, H-6a, H-6b), 3.62 (ddd, $J = 2.5, 5.3, 9.8$ Hz, 1H, H-5). The spectroscopic data were in accordance with literature values.^{S2}

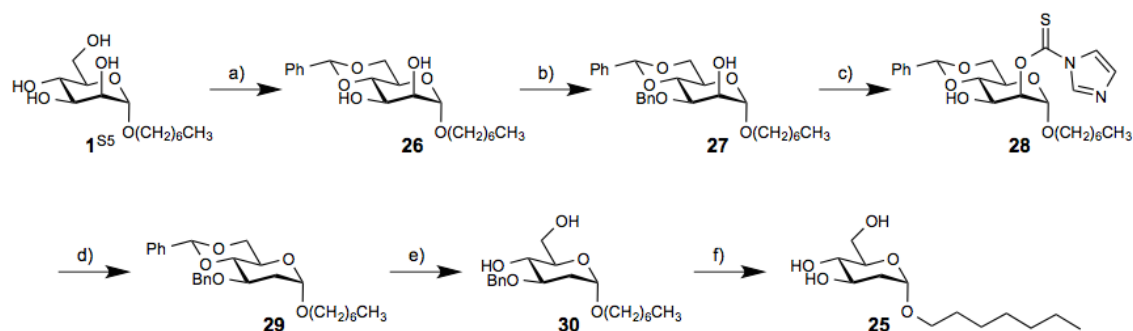
4'-(2,3,4,6-Tetra-*O*-acetyl- α -D-mannopyranosyloxy)-biphenyl-4-carboxylic acid (15). To a solution of **9**^{S3} (59 mg, 0.16 mmol) in pyridine (6 mL) was added acetic anhydride (2 mL) at 0 °C under argon. The mixture was allowed to warm up to rt and stirred overnight. The mixture was concentrated and the residue was treated with DCM/satd. aq. $NaHCO_3$ (1:1, 50 mL) for 1 h. The organic layer was washed subsequently with 1 N aq. HCl (25 mL) and water (25 mL), dried over Na_2SO_4 and concentrated in vacuo. The residue was purified by MPLC on silica gel (DCM/*i*PrOH, 15:1) to afford **15** (45 mg, 53%) as a white solid. $[\alpha]_D^{20} +71.9$ (c 0.40, EtOAc); 1H NMR (500 MHz, $CDCl_3$): $\delta = 8.25$ -8.15 (m, 2H, Ar-H), 7.70 - 7.63 (m, 2H, Ar-H), 7.60-7.55 (m, 2H, Ar-H), 7.20-7.17 (m, 2H, Ar-H), 5.64-5.55 (m, 2H, H-1, H-3), 5.49 (dd, $J = 1.8, 3.4$ Hz, 1H, H-2), 5.41 (t, $J = 10.1$ Hz, 1H, H-4), 4.31 (dd, $J = 5.5, 12.5$ Hz, 1H, H-6a), 4.10-4.08 (m, 2H, H-5, H-6b), 2.22, 2.07, 2.06, 2.05 (4s, 12H, 4 $COCH_3$); ^{13}C NMR (126 MHz, $CDCl_3$): $\delta = 171.72, 170.71, 170.16, 170.14, 169.90$ (5 CO), 155.86, 145.61, 134.75, 130.87, 128.65, 128.49, 127.97, 127.18, 126.84, 122.22, 117.00 (Ar-C), 95.82 (C-1), 69.43 (C-5), 69.34 (C-2), 68.94 (C-3), 65.97 (C-4), 62.18 (C-6), 20.98, 20.80, 20.79, 20.77 (4 $COCH_3$); ESI-MS: m/z : Calcd for $C_{27}H_{28}NaO_{12} [M+Na]^+$: 567.1, found: 567.1.

***N*-Cyano-4'-(α -D-mannopyranosyloxy)-biphenyl-4-carboxamide (10i).** To a solution of **15** (40 mg, 0.07 mmol) in toluene was added 1-chloro-*N,N*-2-trimethyl-1-propenylamine (19 μ L, 0.15 mmol) at 0 °C under argon. The mixture was allowed to warm up to rt in 4 h. Then the reaction mixture was concentrated and dried in vacuo overnight. The residue was dissolved in DMF (1 mL) and treated at 0 °C with a freshly prepared solution of $NaNHCN$ in DMF [NH_2CN (6 mg, 0.15 mmol) and 60% NaH (6 mg, 0.15 mmol) in DMF (0.5 mL)]. The

reaction mixture was stirred at rt overnight and then concentrated in vacuo. The residue was deacetylated according to general procedure B and the crude product was purified by MPLC (H₂O/MeOH, 1:1) on RP18 to afford **10i** (6 mg, 21% for three steps) as a white solid. $[\alpha]_D^{20} +44.7$ (*c* 0.10, MeOH); ¹H NMR (500 MHz, CD₃OD): δ = 8.02-7.95 (m, 2H, Ar-H), 7.80-7.63 (m, 4H, Ar-H), 7.30-7.22 (m, 2H, Ar-H), 5.57 (s, 1H, H-1), 4.05 (s, 1H, H-2), 3.95 (dd, *J* = 3.2, 9.4 Hz, 1H, H-3), 3.84-3.71 (m, 3H, H-4, H-6a, H-6b), 3.66-3.62 (m, 1H, H-5); ¹³C NMR (126 MHz, CD₃OD): δ = 158.37, 134.86, 130.09, 129.46, 127.82, 118.28 (Ar-C), 101.41 (CN), 100.16 (C-1), 75.54 (C-5), 72.44 (C-3), 71.98 (C-2), 68.37 (C-4), 62.71 (C-6); HRMS: *m/z*: Calcd for C₂₀H₂₀N₂NaO₇ [M+Na]⁺: 423.1163, found: 423.1167.

2-Chloro-4-iodophenyl 2,3,4,6-tetra-O-acetyl- α -D-mannopyranoside (18). In a dry flask activated molecular sieves 4Å (300 mg), α -D-mannose pentaacetate (**16**, 390 mg, 0.77 mmol) and 2-chloro-4-iodophenol (**17**, 235 mg, 0.90 mmol) were dissolved in dry CH₂Cl₂ (3 mL) under argon. BF₃·Et₂O (freshly distilled, 290 μ L, 2.3 mmol) was added dropwise and the mixture was stirred for 20 h at 40 °C. After cooling to rt the mixture was diluted with CH₂Cl₂ (75 mL), filtered through celite and subsequently washed with satd. aq. NaHCO₃ (75 mL), water (75 mL) and brine (75 mL). The organic phase was dried over Na₂SO₄ and concentrated under reduced pressure. The crude product was purified via flash column chromatography (petroleum ether/EtOAc, 1:0 to 1:1) to yield **19** (345 mg, 76%). Spectroscopic data were in accordance with reported values.^{S4}

Synthesis of *n*-heptyl 2-deoxy- α -D-mannopyranoside (**25**)



Scheme S1. a) PhCH(OMe)₂, *p*-TsOH, DMF, 50 °C, 5 h (94%); b) Bu₂Sn(O), toluene, TBAB, BnBr, reflux (91%); c) TCDI, DCE, reflux (91%); d) Bu₃SnH, toluene, reflux, 6 h (58%); e) 80% aq. AcOH, 80 °C, 1 h (64%); f) H₂ (4 bar), cat. Pd(OH)₂/C, MeOH, rt, (72%).

***n*-Heptyl 4,6-*O*-benzylidene- α -D-mannopyranoside (**26**).** To a solution of **1**^{SS} (527 mg, 1.89 mmol) in dry DMF (6.0 mL) were added benzaldehyde dimethylacetal (0.56 mL) and *p*-TsOH (18 mg) at rt. The reaction mixture was stirred at 50 °C for 5 h, then diluted with DCM, washed with 5% aq. NaHCO₃ and brine. The organic layer was dried over Na₂SO₄ and concentrated. The residue was purified by flash chromatography on silica gel (petroleum ether/EtOAc, 3:1-3:2) to give **26** (650 mg, 94%) as a glassy solid. ¹H NMR (500 MHz, CD₃OD): δ = 7.51-7.49 (m, 2H Ar-H), 7.37-7.33 (m, 3H, Ar-H), 5.60 (s, 1H, CHPh), 4.77 (d, *J* = 1.0 Hz, 1H, H-1), 4.18 (dd, *J* = 4.5, 10.0 Hz, 1H, H-6a), 3.95-3.90 (m, 2H, H-3, H-4), 3.88 (m, 1H, H-2), 3.81 (t, *J* = 10.0 Hz, 1H, H-6b), 3.76-3.41 (m, 2H, H-5, OCH₂), 3.46 (dt, *J* = 6.5, 9.5 Hz, 1H, OCH₂), 1.62 (m, 2H, CH₂), 1.36 (m, 8H, 4 CH₂), 0.91 (t, *J* = 7.0 Hz, 3H, CH₃); ¹³C NMR (126 MHz; CD₃OD): δ = 139.31, 129.87, 129.02, 127.52 (Ar-C), 103.36 (CHPh), 102.59 (C-1), 80.20 (C-3), 72.74 (C-2), 69.87 (C-6), 69.61 (C-4), 68.77 (OCH₂), 65.25 (C-5), 33.01, 30.57, 30.17, 27.29, 23.70 (5 CH₂), 14.46 (CH₃); ESI-MS: *m/z*: Calcd for C₂₀H₃₀NaO₆ [M+Na]⁺: 389.2, found: 389.1.

***n*-Heptyl 3-*O*-benzyl-4,6-*O*-benzylidene- α -D-mannopyranoside (**27**).** To a solution of **26** (152 mg, 0.414 mmol) in dry toluene (8 mL) was added dibutyltin oxide (112 mg, 0.456 mmol) at rt. The suspension was refluxed for 6 h and concentrated to dryness under reduced pressure. To a solution of the residue in dry toluene (8 mL) were added tetrabutylammonium bromide (TBAB) (147 mg, 0.456 mmol) and benzyl bromide (59 μ L, 0.5 mmol). The mixture was stirred at 95 °C overnight, concentrated to dryness, and purified by flash chromatography

on silica gel (petroleum ether/EtOAc, 9:1-4:1) to give **27** (172 mg, 91%) as colorless oil. $[\alpha]_{\text{D}}^{20} +34.2$ (*c* 1.43, MeOH); $^1\text{H NMR}$ (500 MHz, CDCl_3): $\delta = 7.51\text{--}7.49$ (m, 2H, Ar-H), 7.40-7.33 (m, 8H, Ar-H), 5.62 (s, 1H, PhCH), 4.86 (m, 1H, H-1), 4.87 (d, $J = 11.5$ Hz, 1H, CH_2Ph), 4.73 (d, $J = 11.5$ Hz, 1H, CH_2Ph), 4.27 (m, 1H, H-6a), 4.14-4.06 (m, 2H, H-4, H-2), 3.94 (dd, $J = 3.0, 9.5$ Hz, 1H, H-3), 3.88-3.82 (m, 2H, H-5, H-6b), 3.67 (m, 1H, OCH_2), 3.41 (m, 1H, OCH_2), 2.64 (s, 1H, OH), 1.57 (m, 2H, CH_2), 1.29 (m, 8H, 4 CH_2), 0.89 (t, $J = 7.0$ Hz, 3H, CH_3); $^{13}\text{C NMR}$ (126 MHz, CDCl_3): $\delta = 138.05, 137.53, 128.90, 128.45, 128.22, 127.88, 127.77, 126.01$ (Ar-C), 101.52 (CHPh), 99.87 (C-1), 78.93 (C-4), 75.79 (C-3), 73.04 (CH_2Ph), 70.10 (C-2), 68.92 (C-6), 67.97 (OCH_2), 63.19 (C-5), 32.75, 29.37, 29.05, 26.04, 22.61 (5 CH_2), 14.09 (CH_3); HRMS: m/z : Calcd for $\text{C}_{27}\text{H}_{36}\text{NaO}_6$ $[\text{M}+\text{Na}]^+$: 479.2410, found: 479.2414.

***n*-Heptyl 3-*O*-benzyl-4,6-*O*-benzylidene-2-*O*-(thiocarbonylimidazol-1-yl)- α -D-mannopyranoside (**28**)**. A mixture of **27** (210 mg, 0.46 mmol) and N,N' -thiocarbonyldiimidazole (246 mg, 1.38 mmol) in DCE (5.0 mL) was refluxed overnight. The solution was concentrated in vacuo, the residue was diluted with DCM, and washed with 1 N aq. HCl and brine. The organic layer was dried over Na_2SO_4 and evaporated to dryness. The residue was purified by flash chromatography on silica gel (petroleum ether/EtOAc, 3:1-3:2) to afford **28** (238 mg, 91%) as yellow oil. $[\alpha]_{\text{D}}^{20} -9.8$ (*c* 0.44, CH_2Cl_2); $^1\text{H NMR}$ (500 MHz, CDCl_3): $\delta = 8.39$ (s, 1H, Ar-H), 7.67 (s, 1H, Ar-H), 7.51 (dd, $J = 7.5, 2.5$ Hz, 2H, Ar-H), 7.42-7.36 (m, 3H, Ar-H), 7.29-7.27 (m, 5H, Ar-H), 7.07 (d, $J = 0.5$ Hz, 1H, Ar-H), 5.90 (dd, $J = 1.5, 3.5$ Hz, 1H, H-2), 5.67 (s, 1H, CHPh), 5.01 (d, $J = 1.5$ Hz, 1H, H-1), 4.73 (q, $J = 12.0$ Hz, 2H, CH_2Ph), 4.31 (dd, $J = 4.5, 10.0$ Hz, 1H, H-6a), 4.19 (dd, $J = 3.5, 10.0$ Hz, 1H, H-3), 4.04 (t, $J = 10.0$ Hz, 1H, H-4), 3.94 (td, $J = 4.5, 10.0$ Hz, 1H, H-5), 3.85 (t, $J = 10.0$ Hz, 1H, H-6b), 3.69 (dt, $J = 6.5, 9.5$ Hz, 1H, OCH_2), 3.46 (dt, $J = 6.5, 9.5$ Hz, 1H, OCH_2), 1.61 (m, 2H, CH_2), 1.31 (m, 8H, 4 CH_2), 0.90 (t, $J = 7.0$ Hz, 3H, CH_3); $^{13}\text{C NMR}$ (126 MHz, CDCl_3): $\delta = 183.59$ (CS), 137.65, 137.17, 131.04, 129.05, 128.37, 128.24, 127.77, 127.57, 126.07, 109.96 (Ar-C), 101.75 (PhCH), 97.24 (C-1), 79.24 (C-4), 78.80 (C-2), 73.91 (C-3), 72.87 (CH_2Ph), 68.80 (C-6), 68.54 (OCH_2), 63.68 (C-5), 31.73, 29.24, 29.00, 25.93, 22.60 (5 CH_2), 14.09 (CH_3); HRMS: m/z : Calcd for $\text{C}_{31}\text{H}_{38}\text{N}_2\text{NaO}_6\text{S}$ $[\text{M}+\text{Na}]^+$: 589.2348, found: 589.2351.

***n*-Heptyl 3-*O*-benzyl-4,6-*O*-benzylidene-2-deoxy- α -D-mannopyranoside (**29**)**. A solution of **28** (238 mg, 0.419 mmol) in dry toluene (2 mL) was added dropwise over 10 min to a stirred solution of refluxing toluene (6 mL) and tributylstannane (0.169 mL, 0.63 mmol)

under argon. The reaction mixture was refluxed for 6 h, then the solvent was removed in vacuo and the residue was purified by chromatography on silica gel (petroleum ether/EtOAc, 16:1-4:1) to afford **29** (107 mg, 58%) as colorless oil. $[\alpha]_{\text{D}}^{20} +49.9$ (*c* 1.07, MeOH); ^1H NMR (500 MHz, CDCl_3): δ = 7.52 (dd, *J* = 7.5, 2.5 Hz, 1H, Ar-H), 7.41-7.25 (m, 9H, Ar-H), 5.63 (s, 1H, CHPh), 4.90 (d, *J* = 3.5 Hz, 1H, H-1), 4.86 (d, *J* = 12.0 Hz, 1H, CH₂Ph), 4.69 (d, *J* = 12.0 Hz, 1H, CH₂Ph), 4.26 (dd, *J* = 4.5, 10.0 Hz, 1H, H-6a), 4.05 (ddd, *J* = 5.0, 9.0, 11.0 Hz, 1H, H-3), 3.83 (m, 1H, H-5), 3.77 (t, *J* = 10.0 Hz, 1H, H-6b), 3.70 (t, *J* = 9.0 Hz, 1H, H-4), 3.62 (dt, *J* = 6.5, 9.5 Hz, 1H, OCH₂), 3.35 (dt, *J* = 6.5, 9.5 Hz, 1H, OCH₂), 2.28 (ddd, *J* = 1.0, 5.0, 13.5 Hz, 1H, H-2e), 1.81 (ddd, *J* = 3.5, 11.5, 13.5 Hz, 1H, H-2a), 1.58 (m, 2H, CH₂), 1.30 (m, 8H, 4 CH₂), 0.89 (t, *J* = 7.0 Hz, 3H, CH₃); ^{13}C NMR (126 MHz, CDCl_3): δ = 138.76, 137.63, 128.84, 128.32, 128.21, 127.62, 127.49, 126.02 (Ar-C), 101.29 (CHPh), 97.93 (C-1), 83.99 (C-4), 73.12 (C-3), 72.97 (CH₂Ph), 69.16 (C-6), 67.65 (OCH₂), 62.89 (C-5), 36.58 (C-2), 31.75, 29.49, 29.08, 26.13, 22.61 (5 CH₂), 14.09 (CH₃); HRMS: *m/z*: Calcd for $\text{C}_{27}\text{H}_{36}\text{NaO}_5$ $[\text{M}+\text{Na}]^+$: 463.2460, found: 463.2453.

***n*-Heptyl 3-*O*-benzyl-2-deoxy- α -D-mannopyranoside (30).** A solution of **29** (66 mg, 0.15 mmol) in 80% aq. AcOH (1.25 mL) was stirred at 80 °C for 1 h and then concentrated to dryness. The residue was purified by chromatography on silica gel (petroleum ether/EtOAc, 4:1-3:2) to afford **30** (33.7 mg, 64%), which was directly used in the next step.

***n*-Heptyl 2-deoxy- α -D-mannopyranoside (25).** A suspension of **30** (30 mg, 0.085 mmol) and 10% Pd(OH)₂/C (5.2 mg) in MeOH (5.0 mL) was hydrogenated (4 bar H₂) in a Parr shaker at rt for 5 h. Then, the mixture was filtered through a pad of celite and the filtrate was concentrated in vacuo. The residue was purified by flash chromatography on silica gel (DCM/MeOH, 10:1) to give **25** (18 mg, 72%) as a white solid. $[\alpha]_{\text{D}}^{20} +106.1$ (*c* 0.12, MeOH); ^1H NMR (500 MHz, CD_3OD): δ = 4.87 (d, *J* = 2.5 Hz, 1H, H-1), 3.85-3.79 (m, 2H, H-3, H-6a), 3.70-3.66 (m, 2H, H-6b, OCH₂), 3.52 (m, 1H, H-5), 3.33 (m, 1H, OCH₂), 3.23 (t, *J* = 9.5 Hz, 1H, H-4), 2.04 (dd, *J* = 5.0, 13.0 Hz, 1H, H-2a), 1.62-1.57 (m, 3H, H-2e, CH₂), 1.32 (m, 8H, 4 CH₂), 0.91 (t, *J* = 7.0 Hz, 3H, CH₃); ^{13}C NMR (125 MHz, CD_3OD): δ = 98.58 (C-1), 73.97 (C-5), 73.34 (C-4), 69.99 (C-3), 68.26 (OCH₂), 62.85 (C-6), 39.00 (C-2), 33.02, 30.70, 30.30, 27.40, 23.71 (5 CH₂), 14.43 (CH₃); HRMS: *m/z*: Calcd for $\text{C}_{13}\text{H}_{26}\text{NaO}_5$ $[\text{M}+\text{Na}]^+$: 285.1678, found: 285.1678.

HPLC data of the target compounds:

Method A: System: Beckman Coulter Gold, consisting of pump 126, DAD 168 (190-400 nm) and auto-sampler 508. Column: Waters Atlantis T3, 3 μm , 2.1 \times 100 mm. A: H_2O + 0.1% TFA; B: MeCN + 0.1% TFA. Gradient: 0% B \rightarrow 70% B (20 min); 70% B (2 min); 70% B \rightarrow 5% B (3 min); 5% B \rightarrow 0% B (2 min); flow rate: 0.5 mL/min.

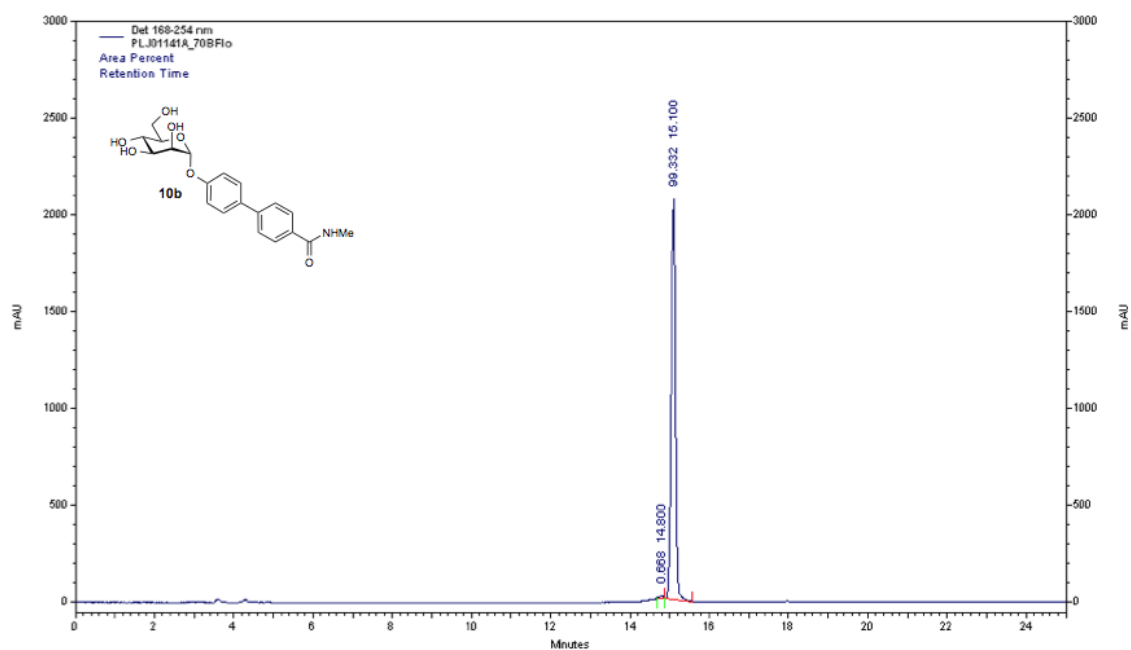
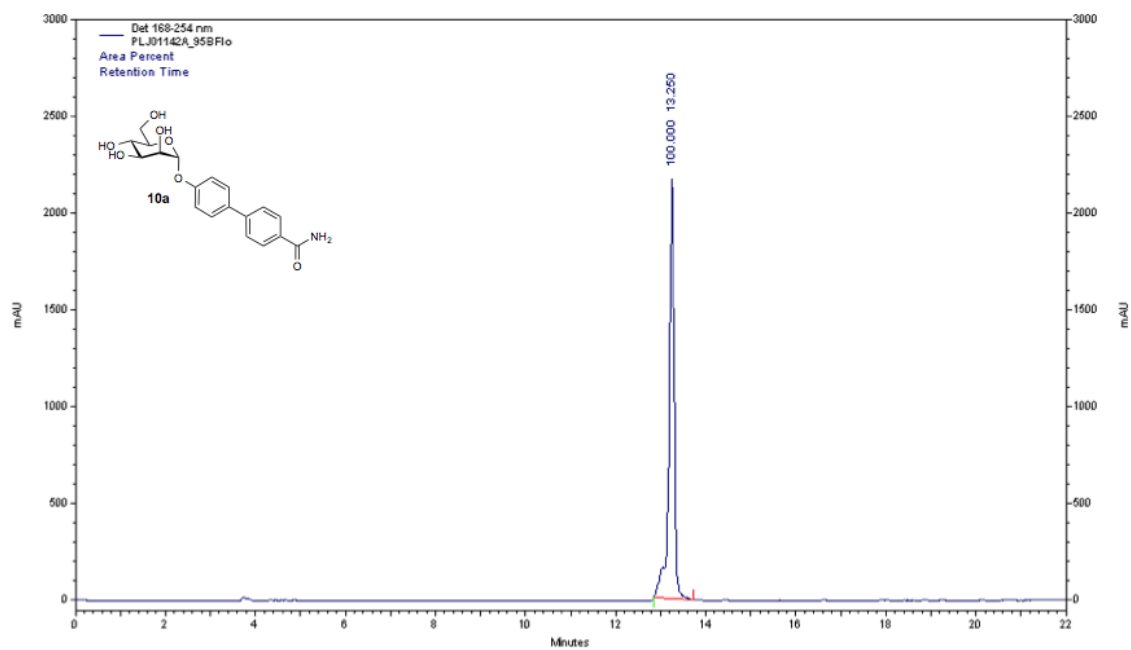
Method B: System: Agilent 1100/1200 with UV detector (190-410 nm) and Waters 2420 ELSD. Column: Waters Atlantis T3, 3 μm , 2.1 \times 100 mm. A: H_2O + 0.1% TFA; B: $\text{H}_2\text{O}/\text{MeCN}$ (90:10) + 0.1% TFA. Detection: UV (214 nm) and light scattering (LS). ELSD parameters: Nebulizer control 70%, drift tube temperature 50°C, gas pressure 50 psi, gain 500. Gradient: 5% B (1 min), 5% B \rightarrow 70% B (15 min), 70% B (1 min), 70% B \rightarrow 5% B (3 min); flow rate: 0.5 mL/min.

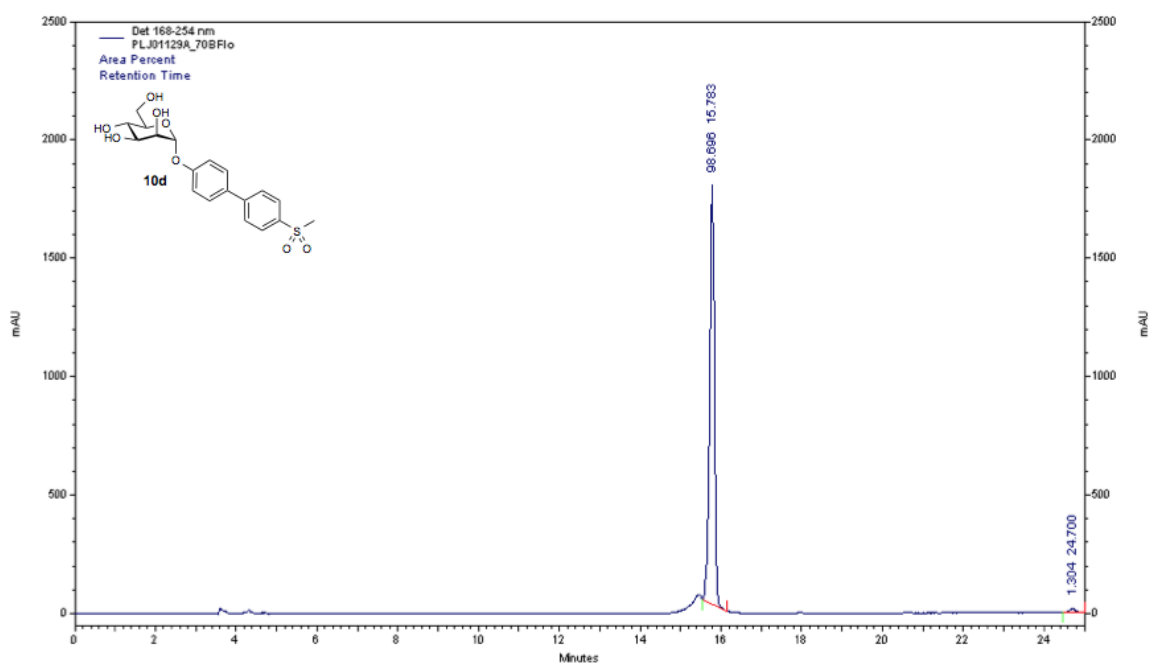
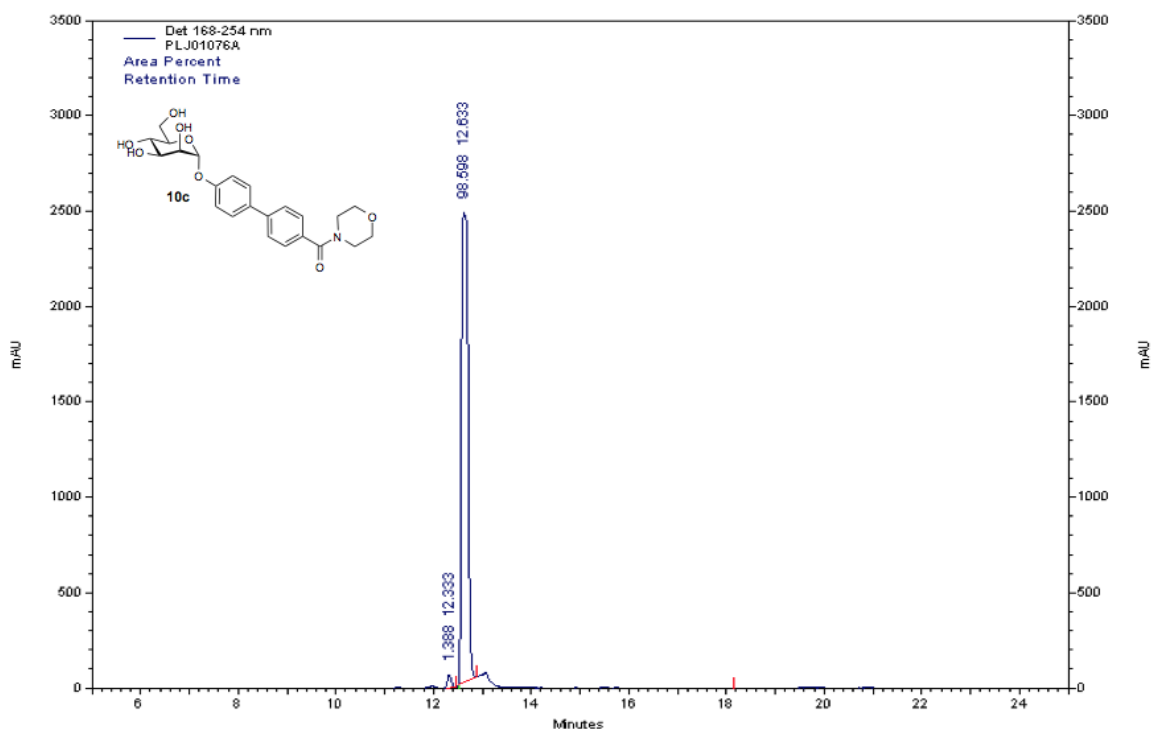
Table S1. HPLC data of the target compounds.

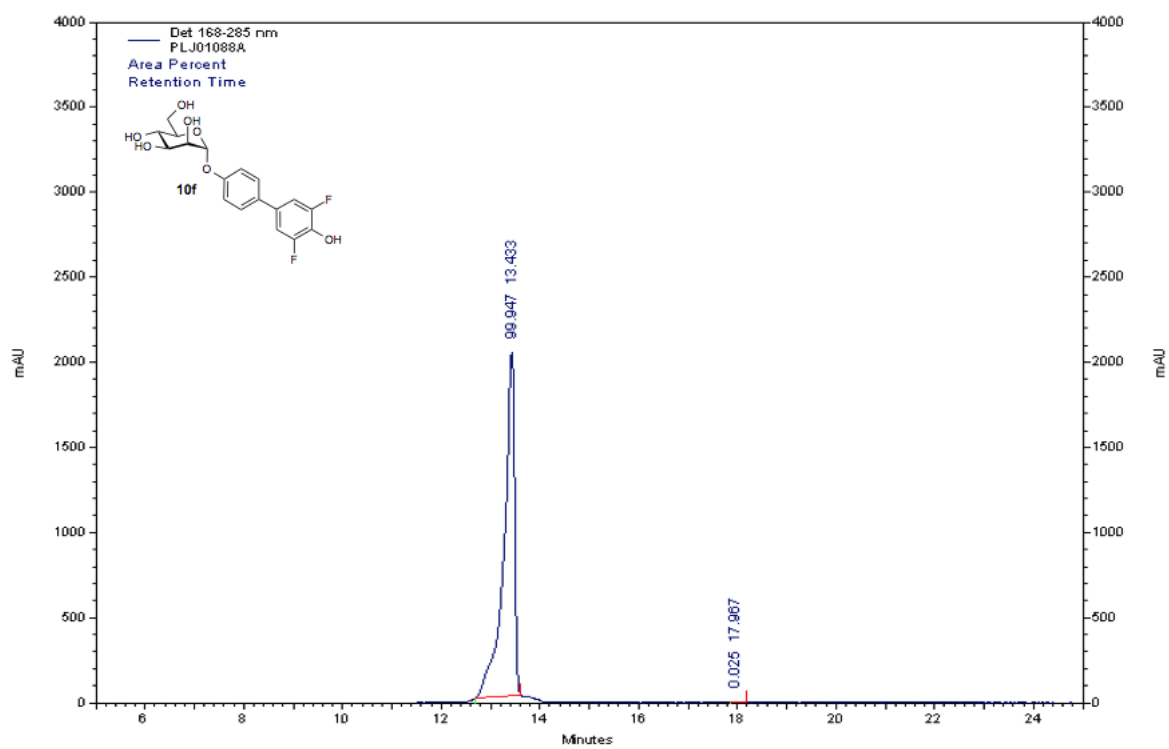
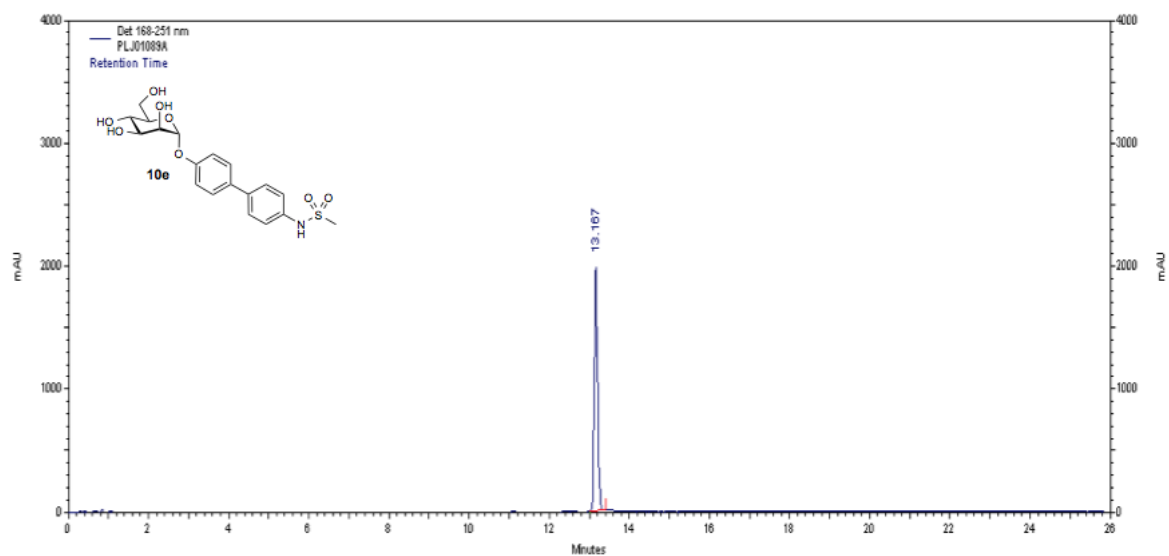
Compound	Formula	Method	Retention [min]	Detection	Purity [%]
10a	$\text{C}_{19}\text{H}_{21}\text{NO}_7$	A	13.25	254 nm	> 99.5
10b	$\text{C}_{20}\text{H}_{23}\text{NO}_7$	A	15.10	254 nm	99.3
10c	$\text{C}_{23}\text{H}_{27}\text{NO}_8$	A	12.63	254 nm	98.6
10d	$\text{C}_{19}\text{H}_{22}\text{O}_8\text{S}$	A	15.78	254 nm	98.7
10e	$\text{C}_{19}\text{H}_{23}\text{NO}_8\text{S}$	A	13.17	285 nm	98.9
10f	$\text{C}_{18}\text{H}_{18}\text{F}_2\text{O}_7$	A	13.43	285 nm	> 99.5
10g	$\text{C}_{19}\text{H}_{19}\text{NO}_6$	B	10.68	LS	> 99.5
10h	$\text{C}_{19}\text{H}_{20}\text{N}_4\text{O}_6$	A	12.73	254 nm	> 99.5
10i	$\text{C}_{20}\text{H}_{20}\text{N}_2\text{O}_7$	A	14.73	296 nm	> 80 ^{a)}
10j	$\text{C}_{19}\text{H}_{18}\text{ClNO}_6$	B	9.79	LS	> 99.5
22	$\text{C}_{39}\text{H}_{30}\text{ClNO}_{12}$	B	12.82	LS	93
23	$\text{C}_{42}\text{H}_{36}\text{ClN}_3\text{O}_{12}\text{S}$	B	9.89	LS	> 99.5
24	$\text{C}_{47}\text{H}_{46}\text{ClN}_3\text{O}_{14}\text{S}$	B	12.10	LS	> 99.5
25	$\text{C}_{13}\text{H}_{26}\text{O}_5$	B	15.12	LS	> 99.5

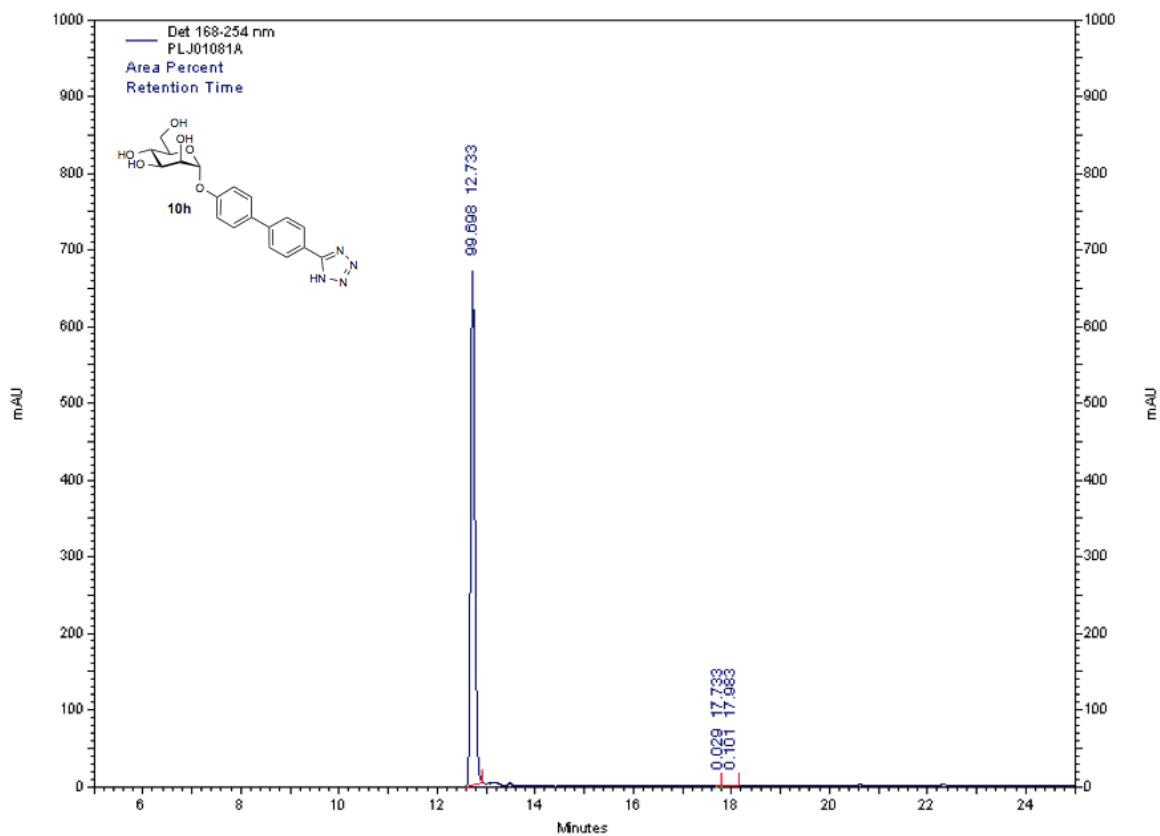
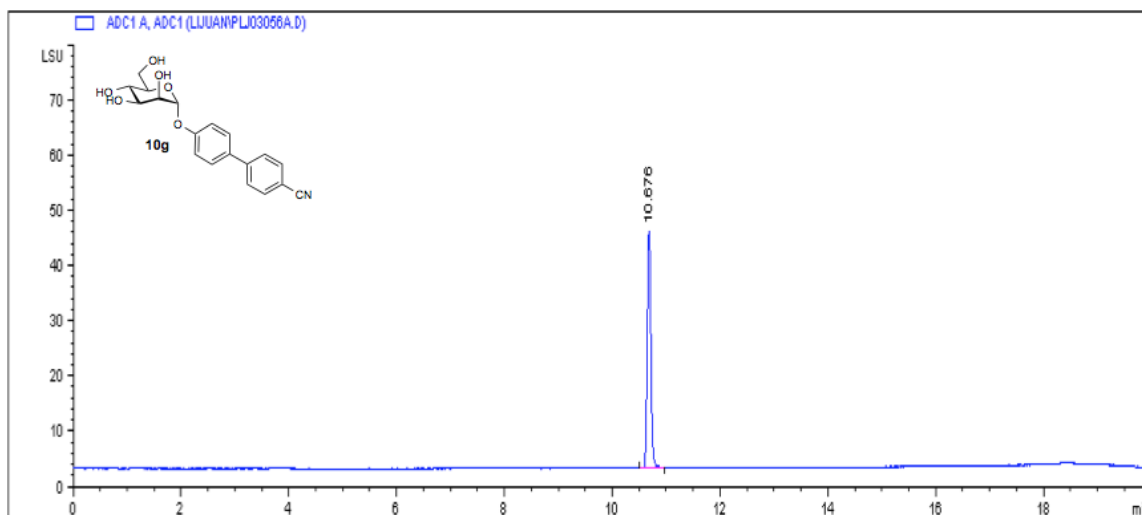
a) The minor peaks presumably stem from the possible tautomers of the cyanamide substituent.

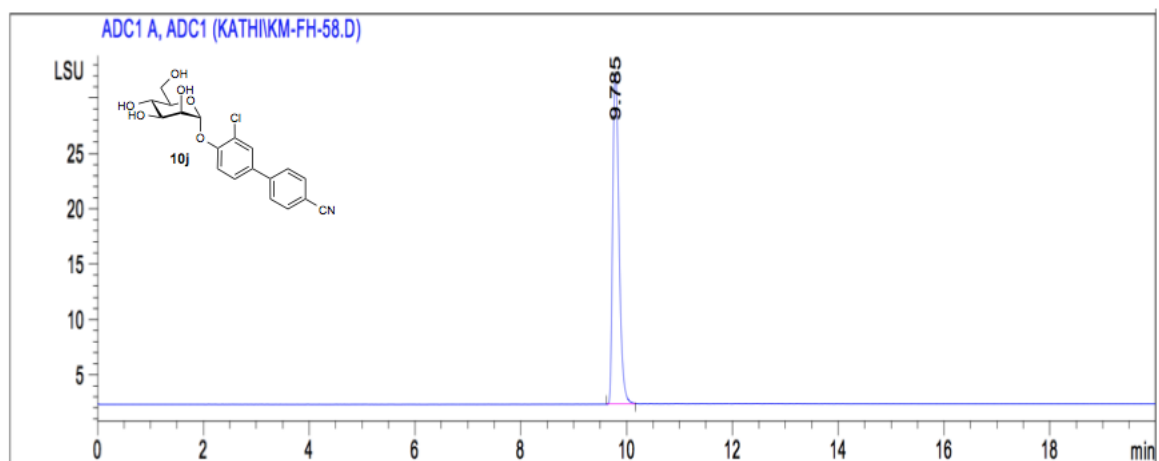
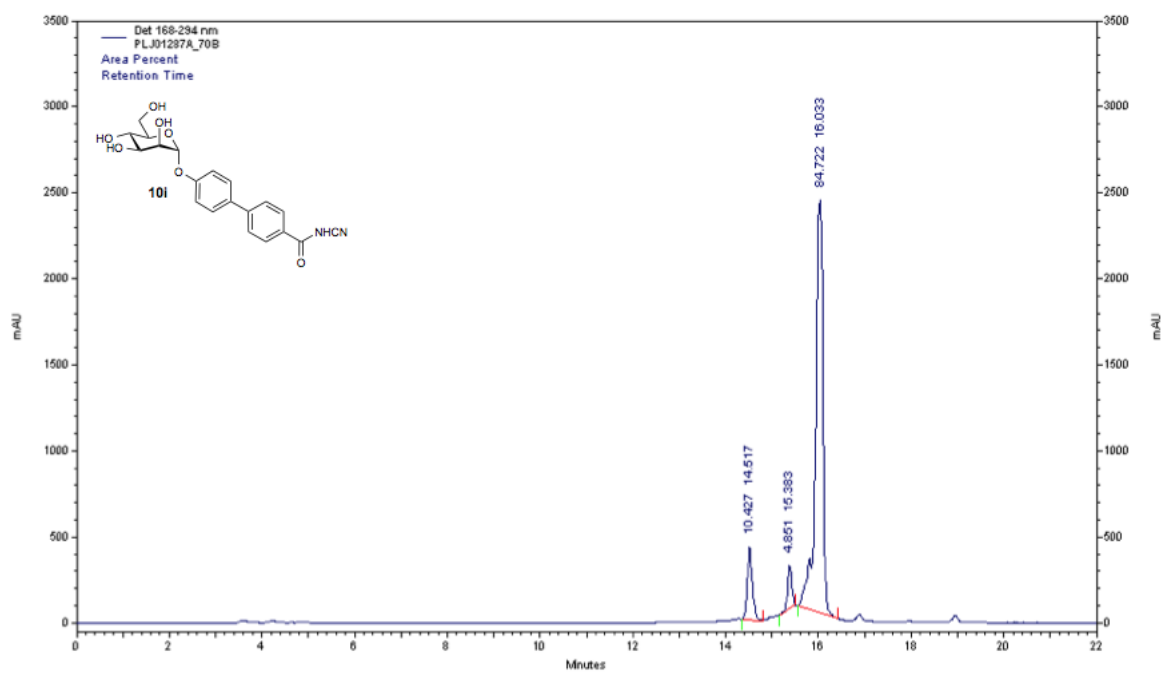
HPLC traces of the target compounds:

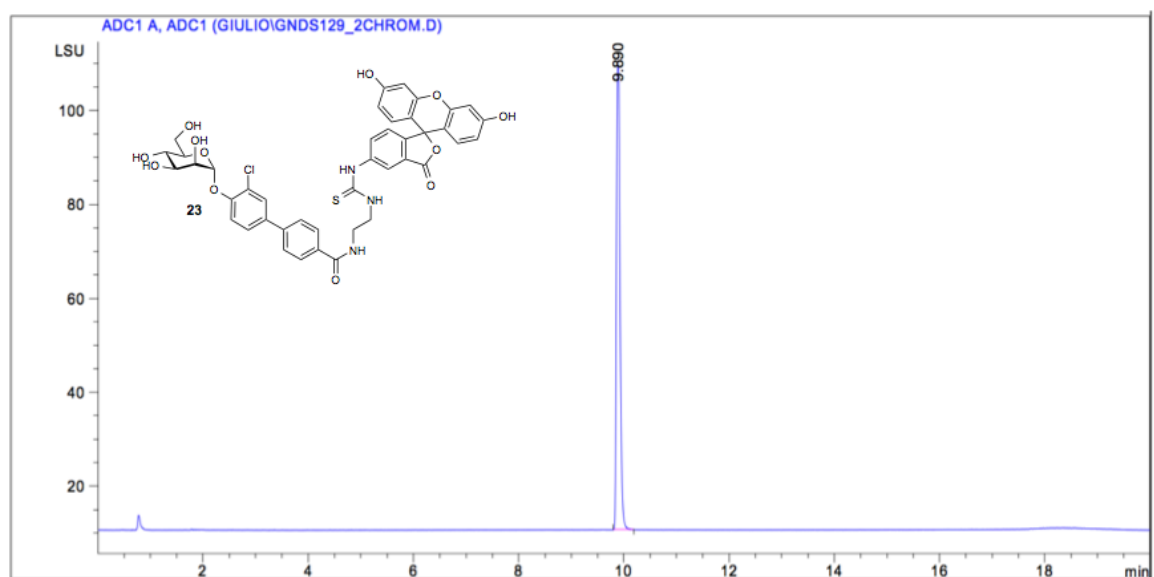
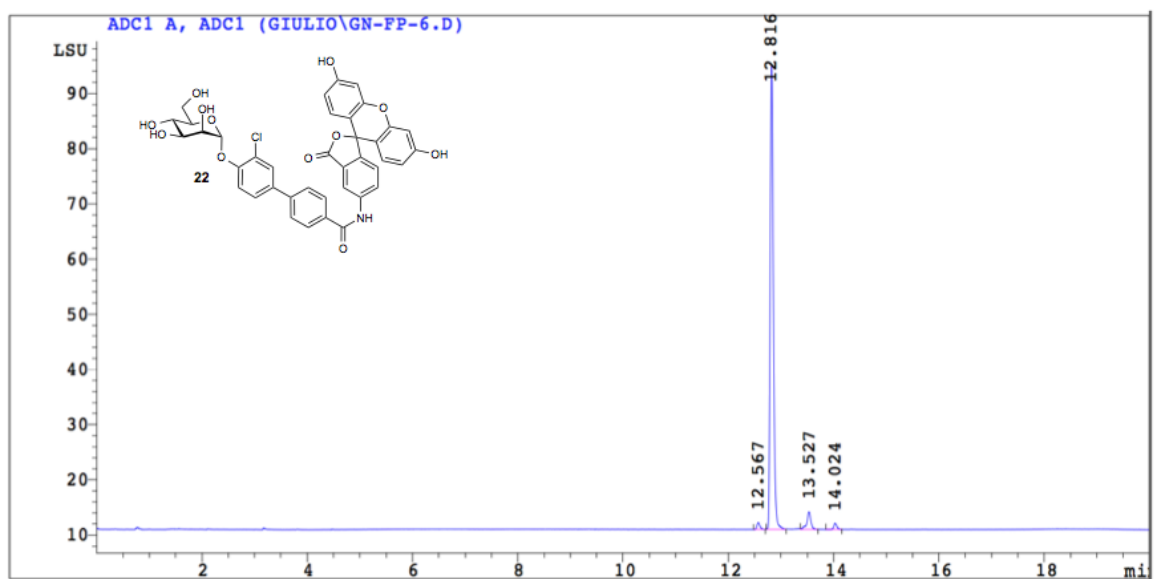


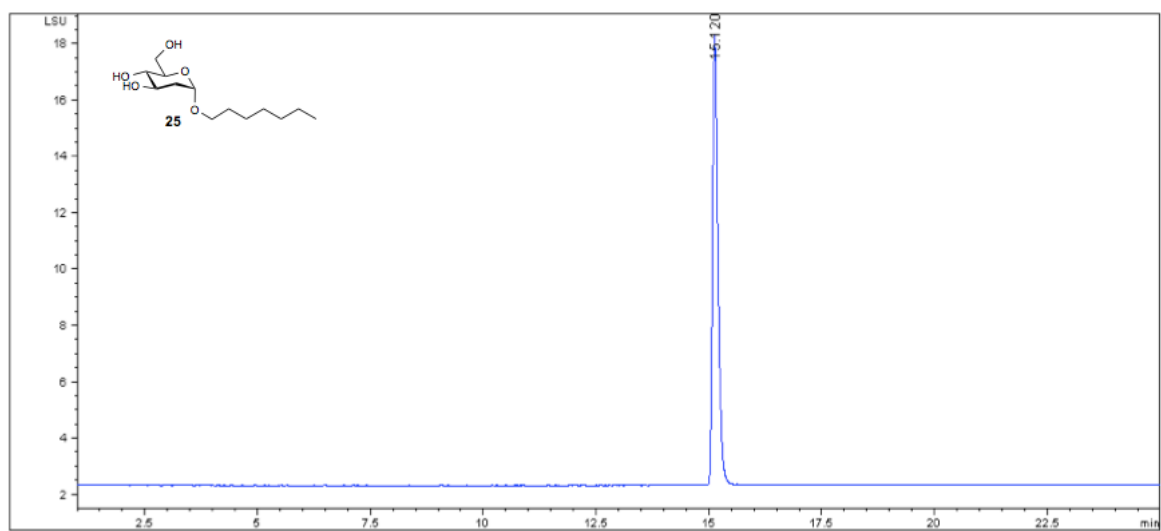
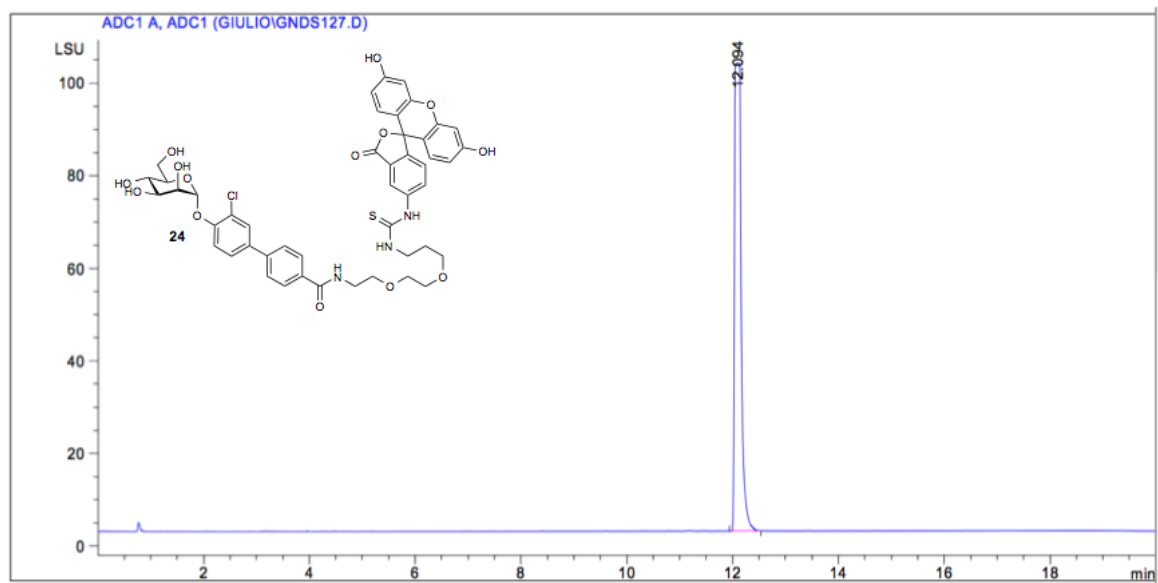


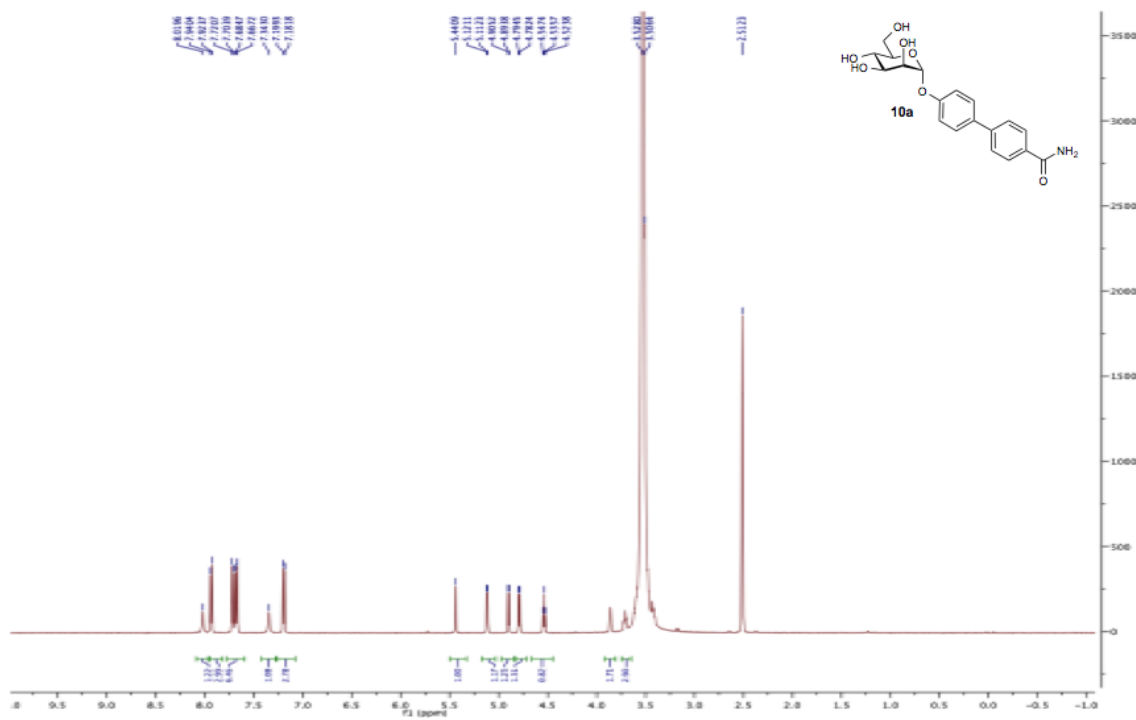
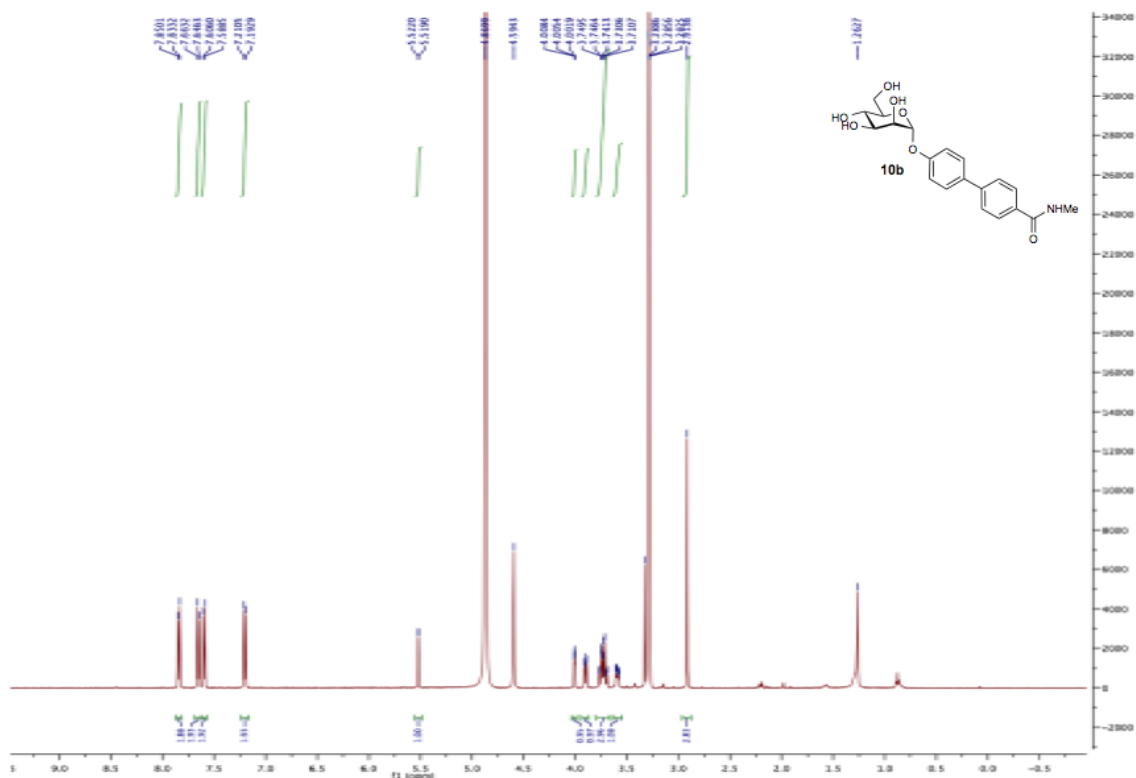


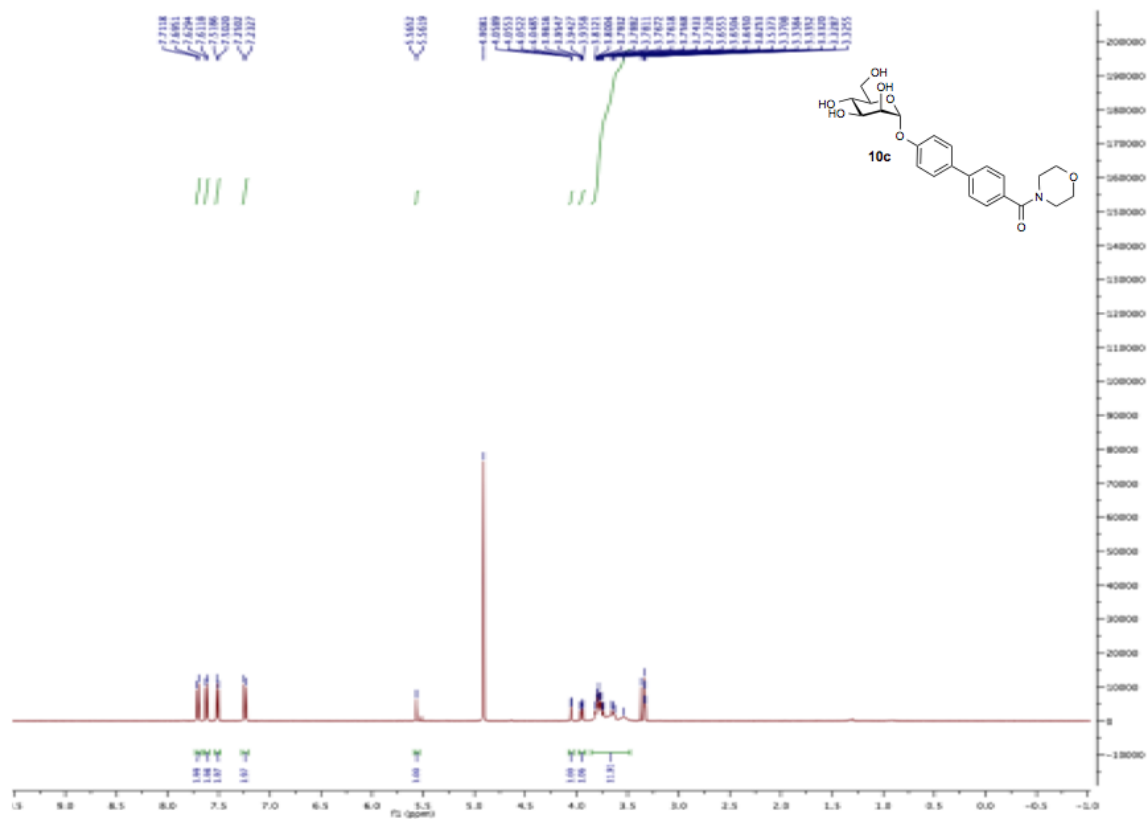
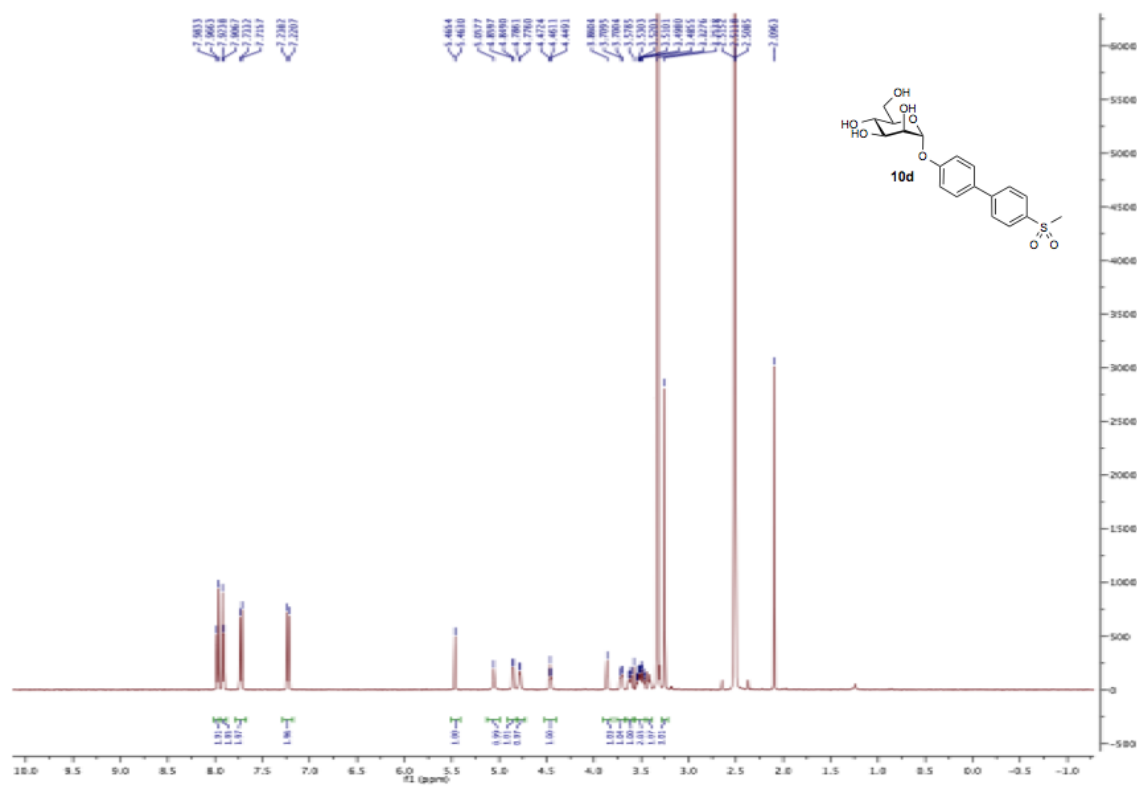


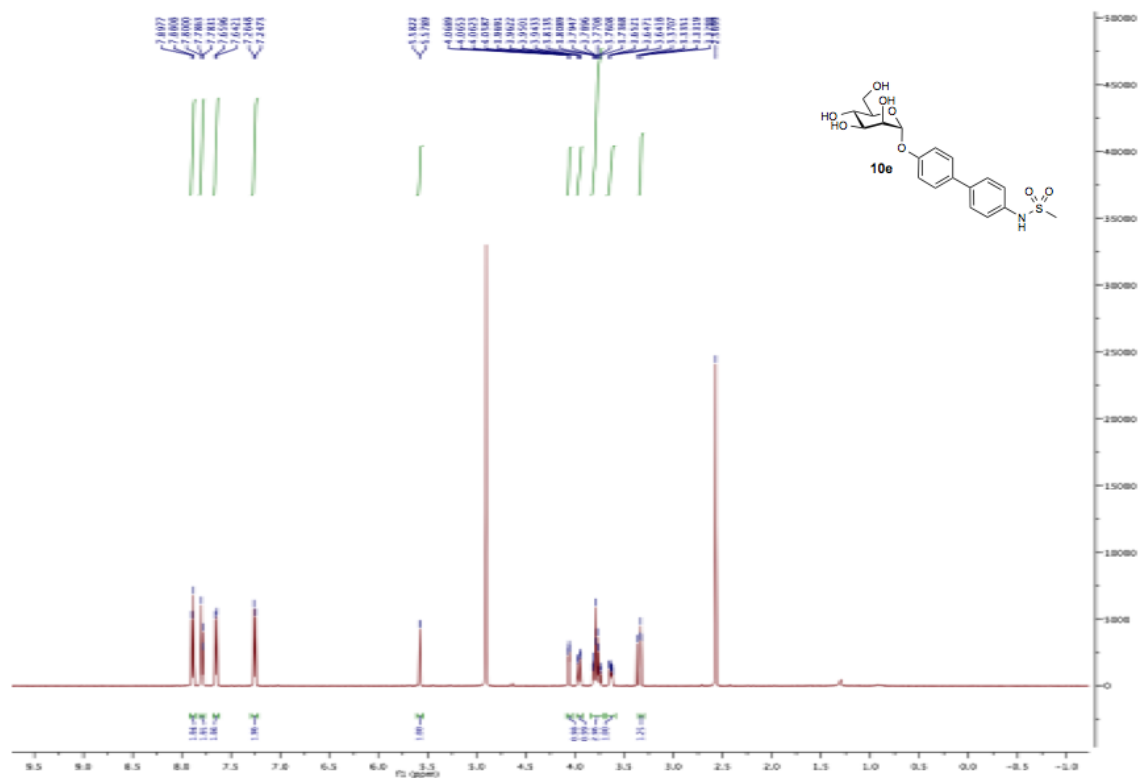
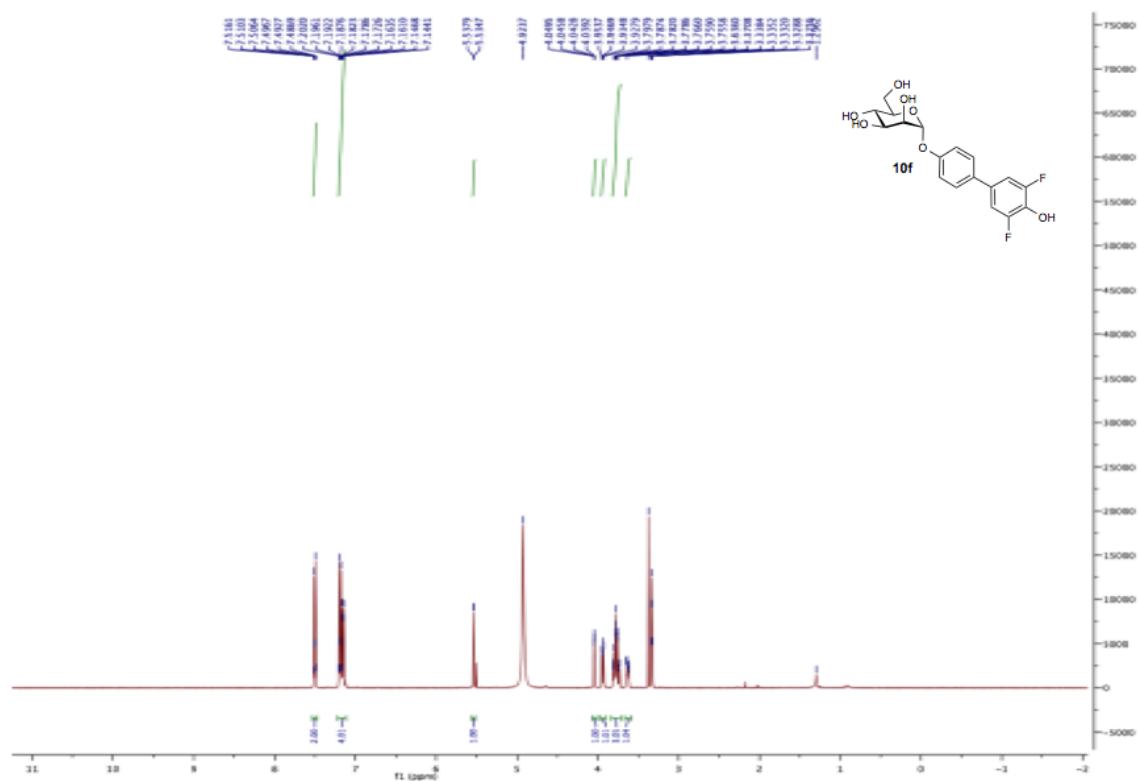


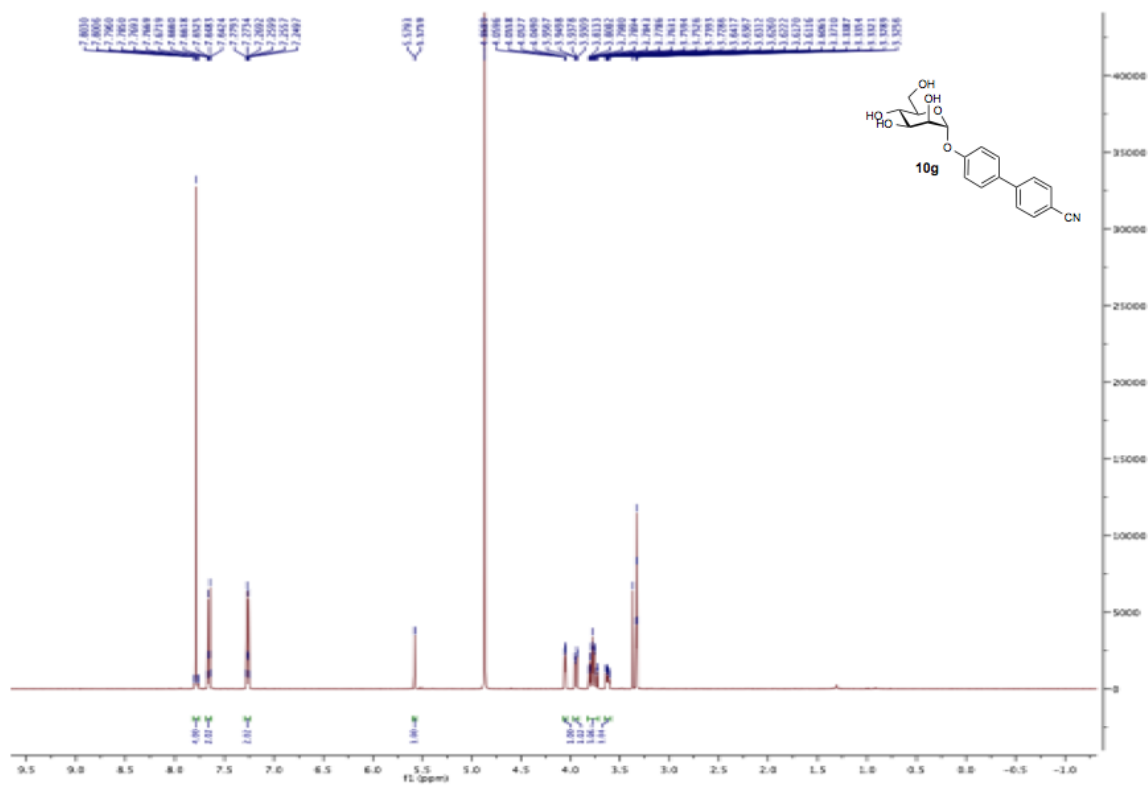
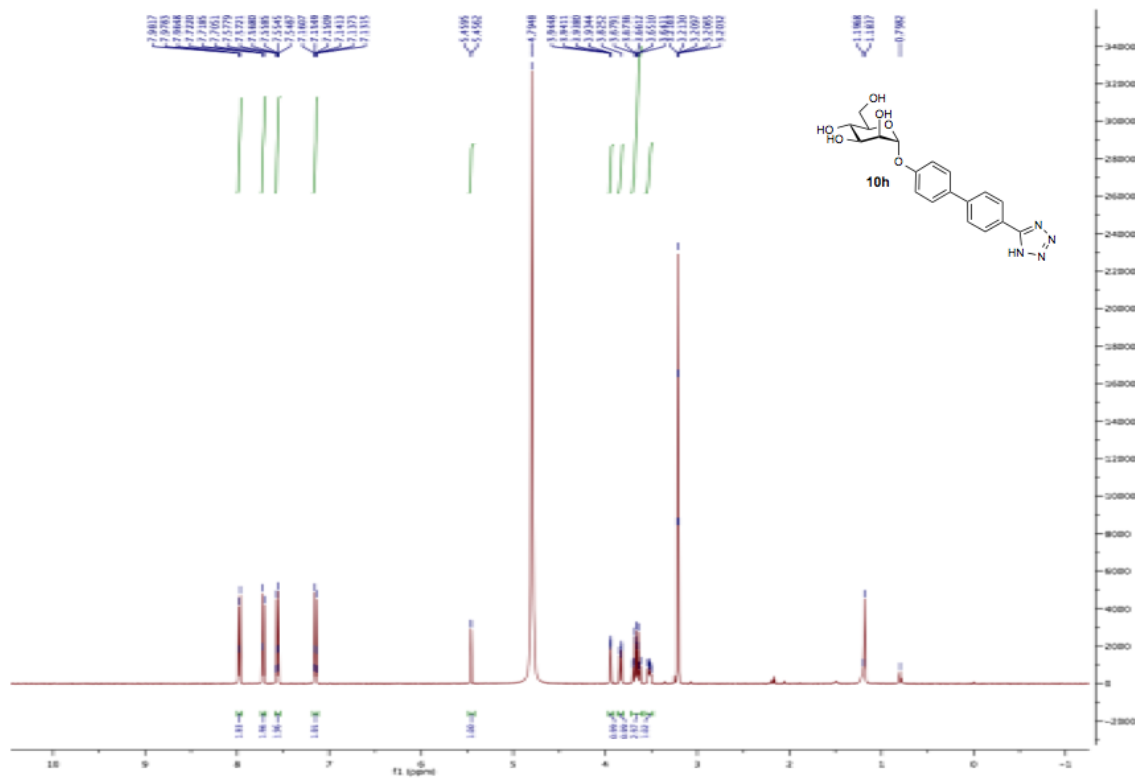


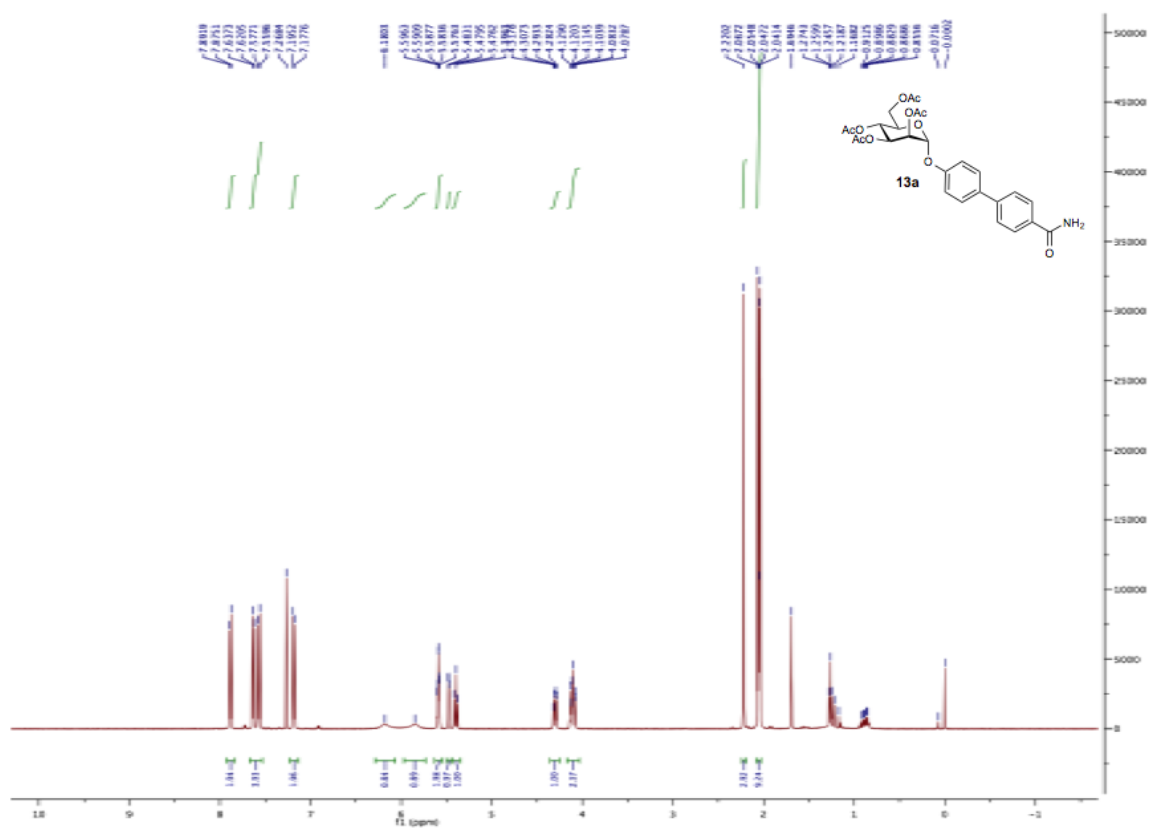
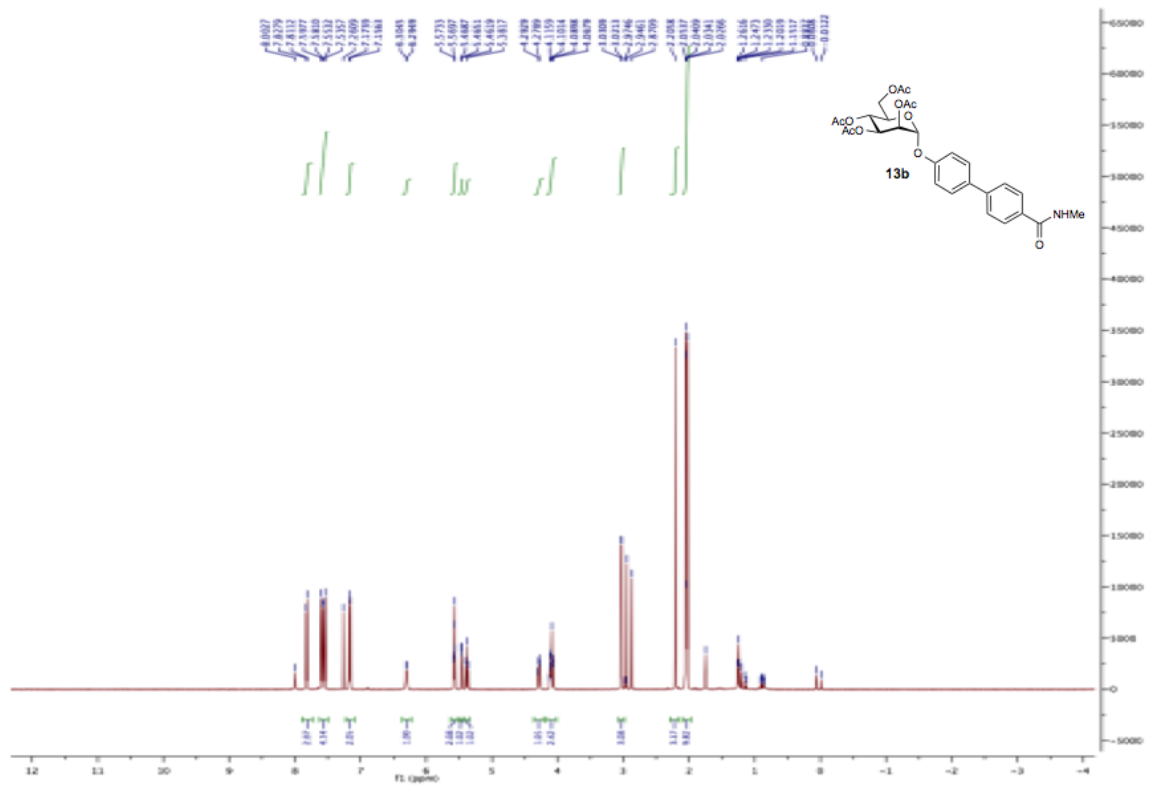


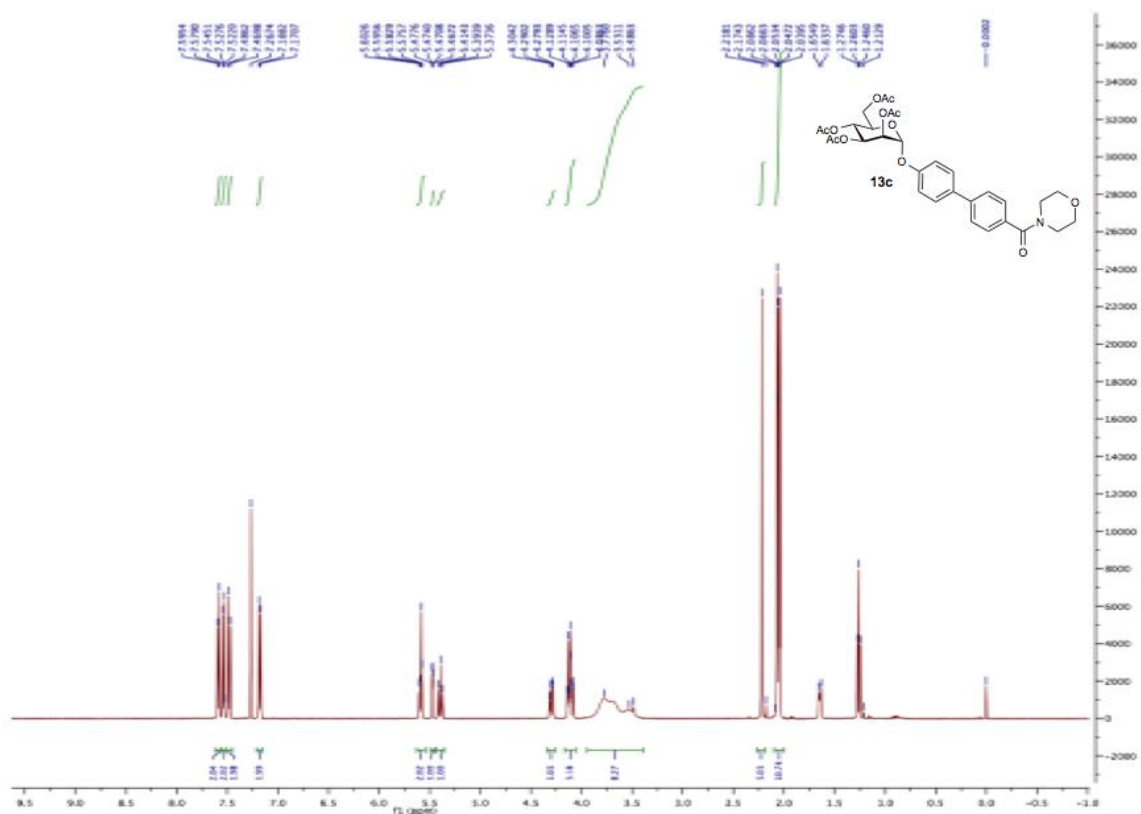
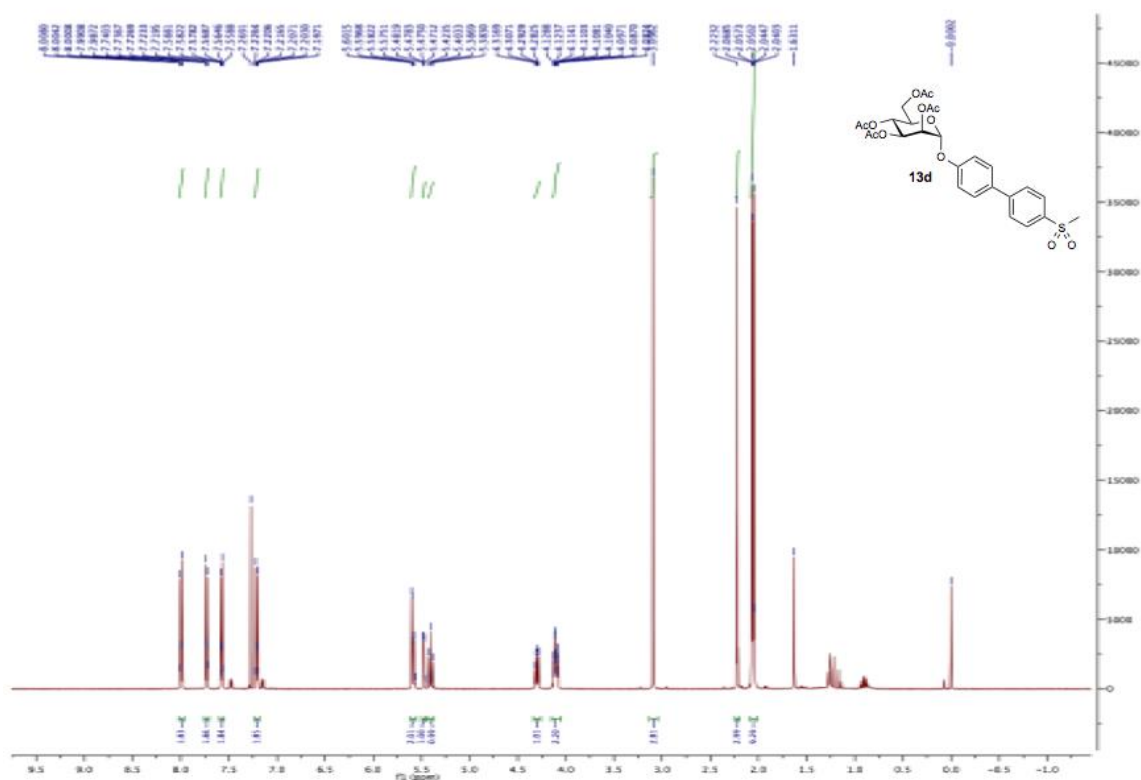
^1H NMR spectra of the synthetic compounds: **^1H NMR (500 MHz) of **10a**** **^1H NMR (500 MHz) of **10b****

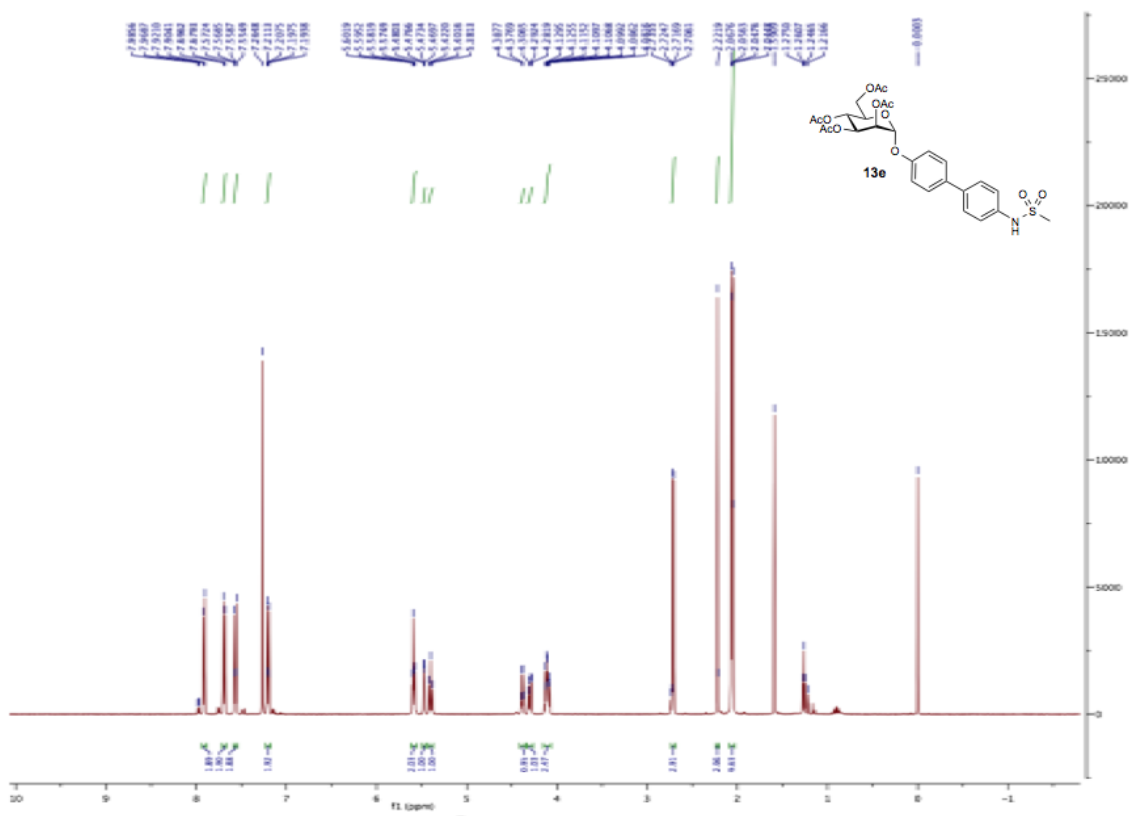
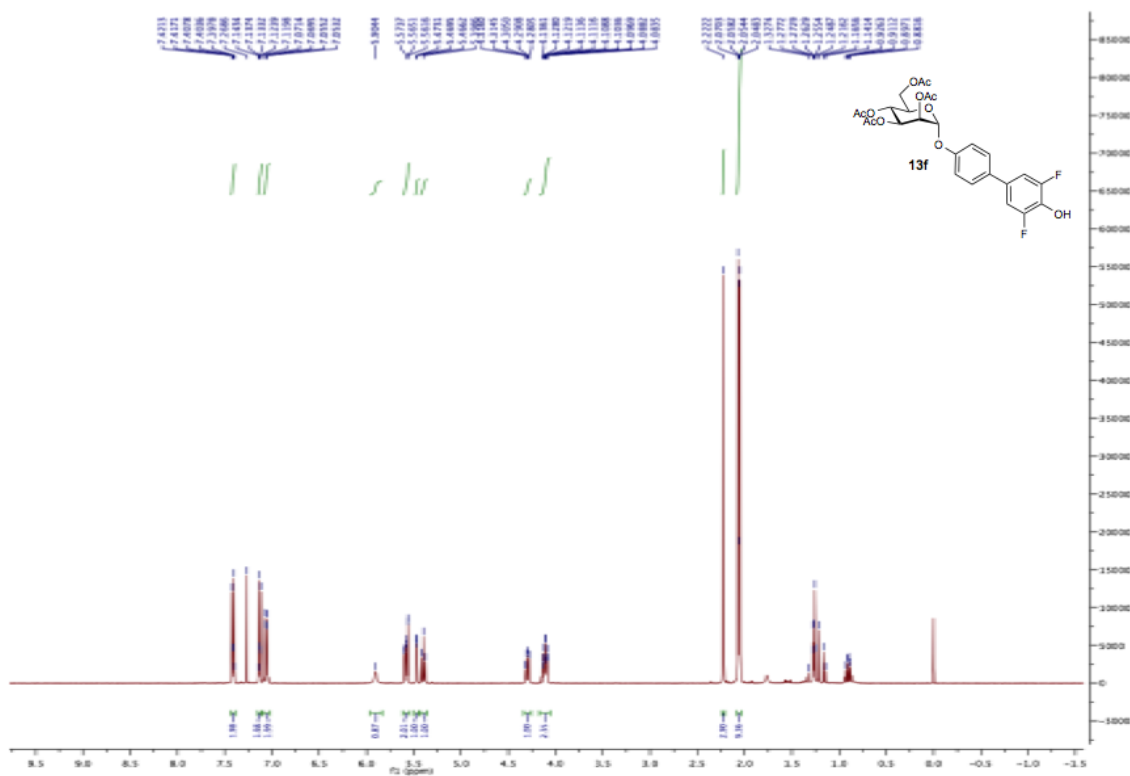
^1H NMR (500 MHz) of **10c** ^1H NMR (500 MHz) of **10d**

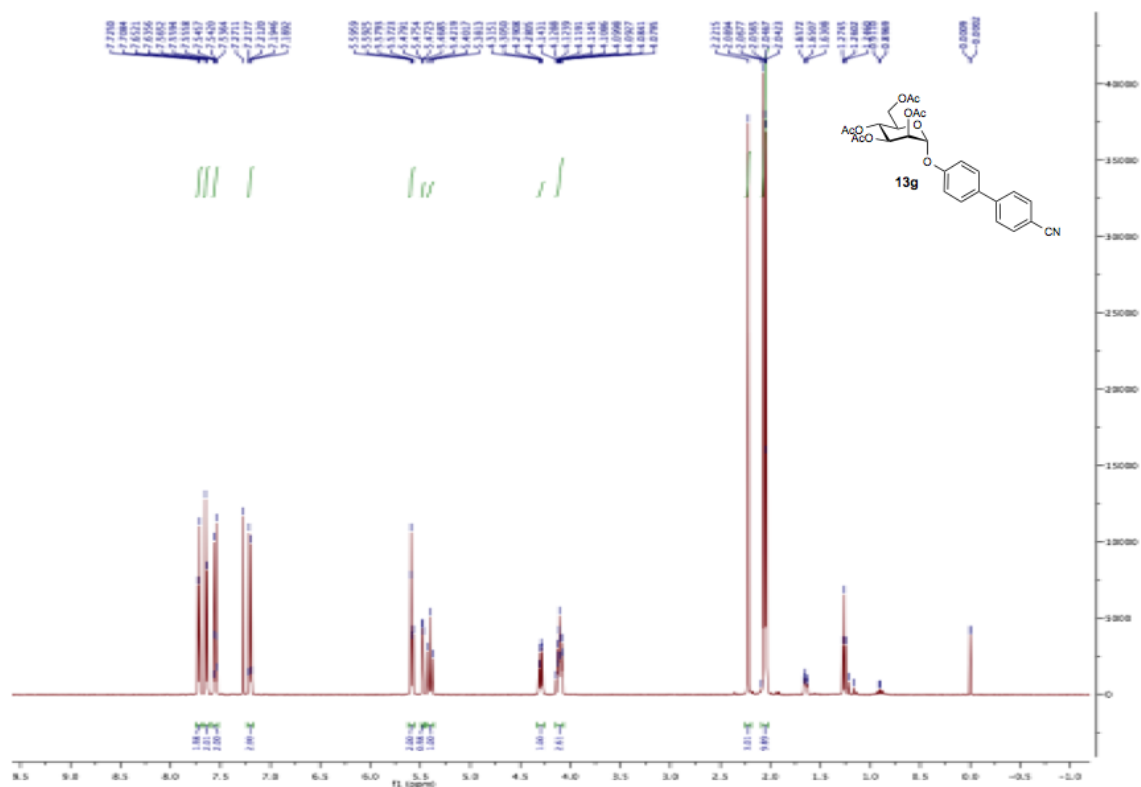
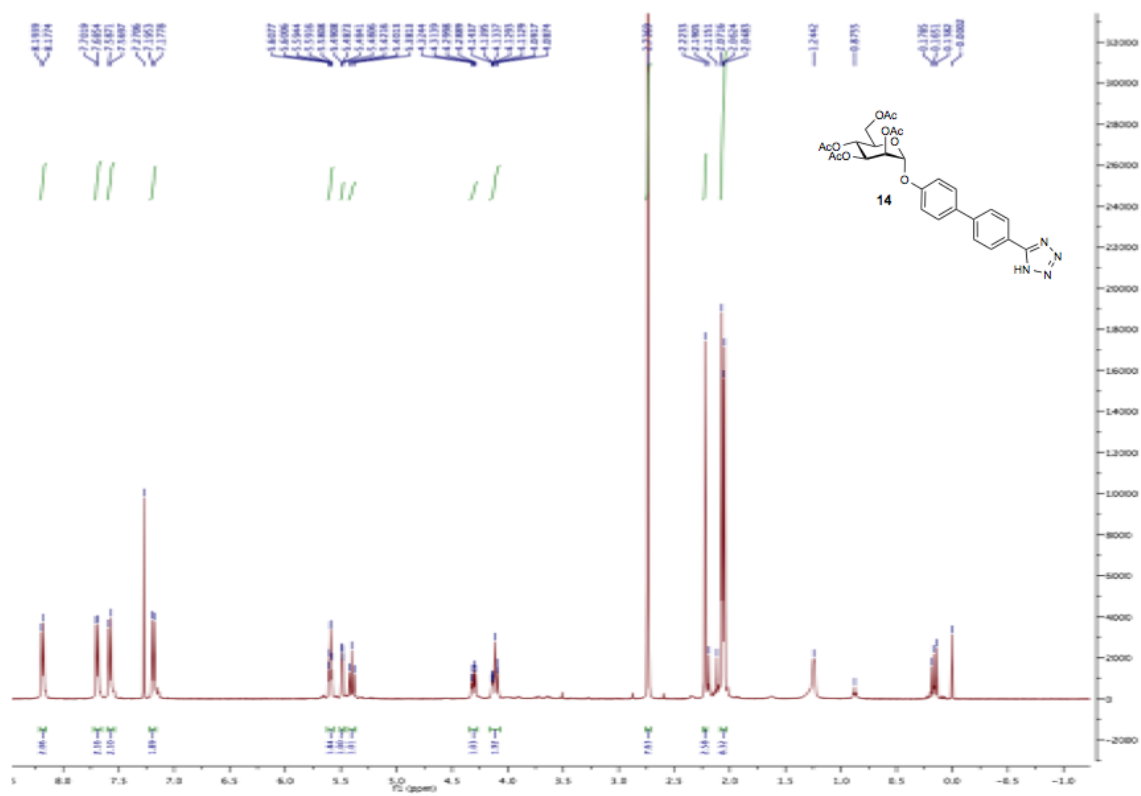
^1H NMR (500 MHz) of **10e** ^1H NMR (500 MHz) of **10f**

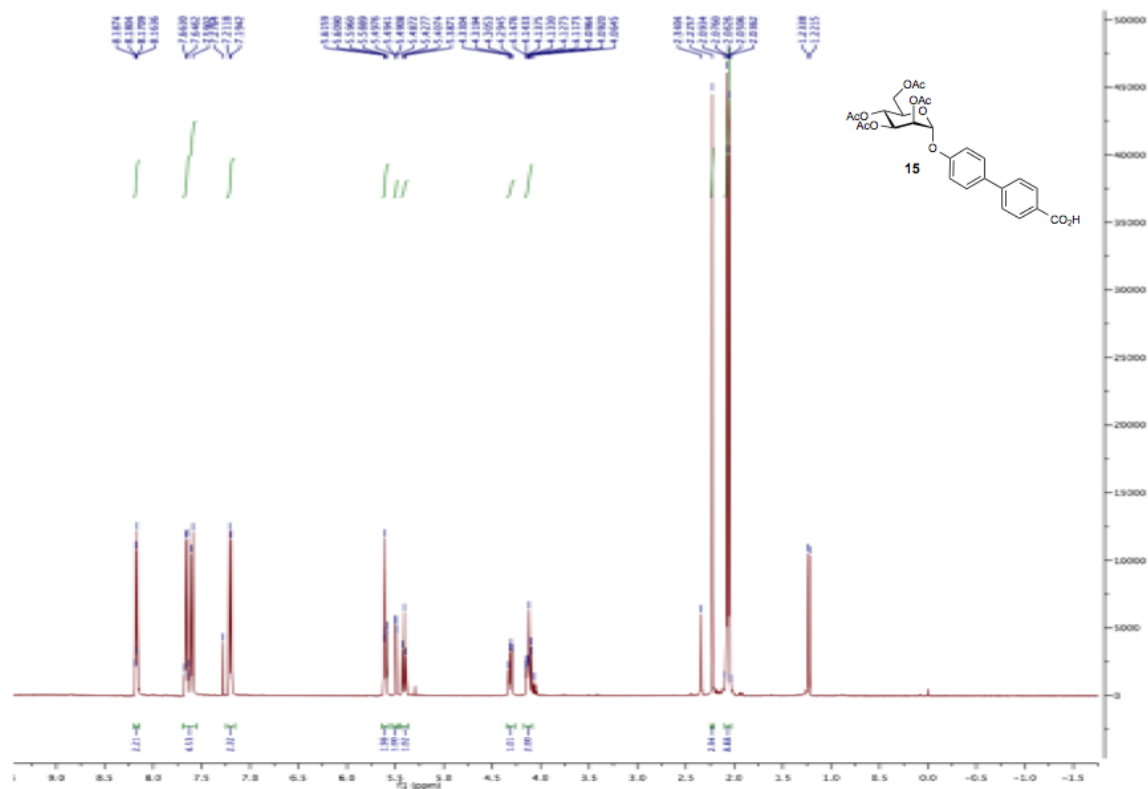
^1H NMR (500 MHz) of **10g** ^1H NMR (500 MHz) of **10h**

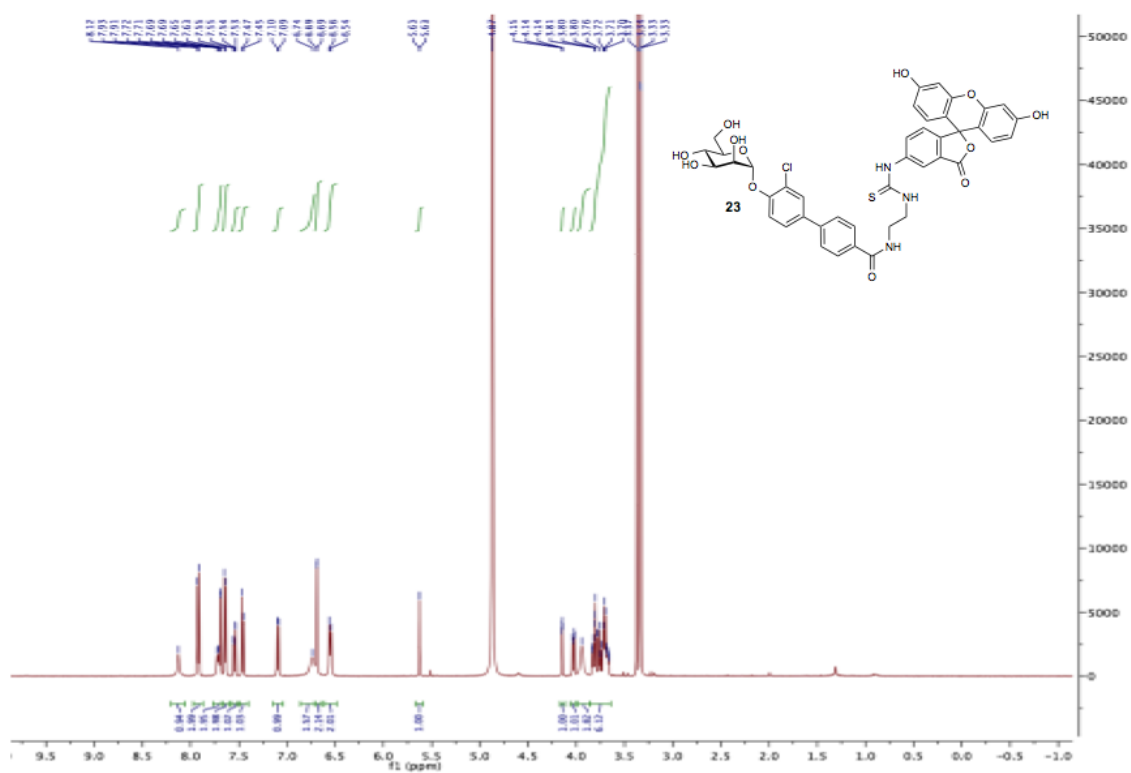
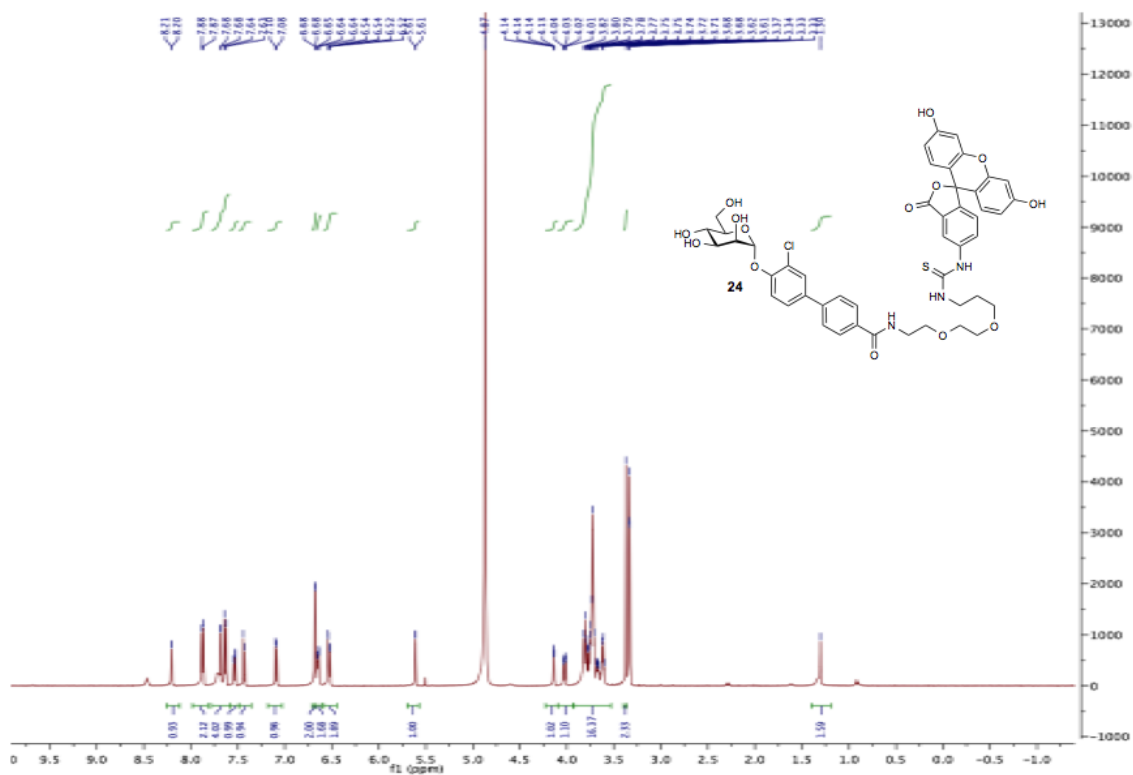
^1H NMR (500 MHz) of **13a** ^1H NMR (500 MHz) of **13b**

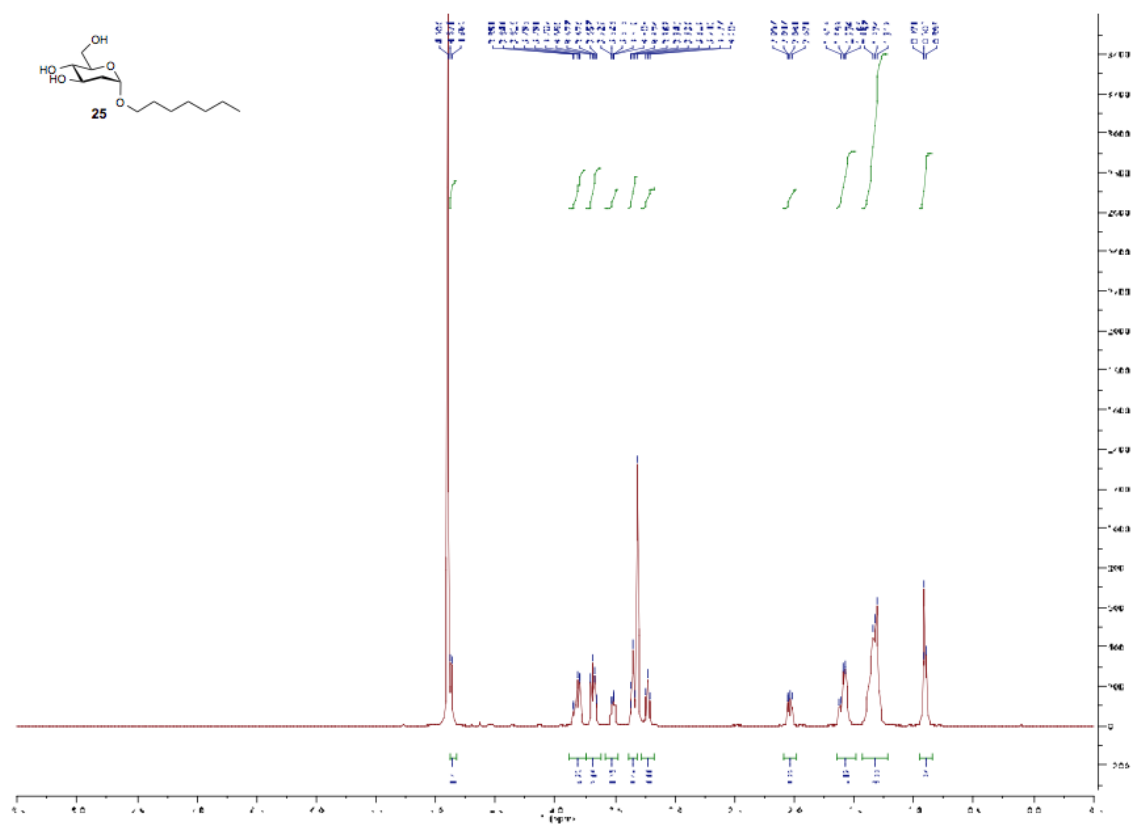
^1H NMR (500 MHz) of **13c** ^1H NMR (500 MHz) of **13d**

^1H NMR (500 MHz) of **13e** ^1H NMR (500 MHz) of **13f**

^1H NMR (500 MHz) of **13g** ^1H NMR (500 MHz) of **14**

^1H NMR (500 MHz) of **15**

^1H NMR (500 MHz) of **23** ^1H NMR (500 MHz) of **24**

^1H NMR (500 MHz) of **25**

References

- (S1) Pang, L.; Kleeb, S.; Lemme, K.; Rabbani, S.; Scharenberg, M.; Zalewski, A.; Schädler, F.; Schwaradt, O.; Ernst, B. FimH antagonists: structure-activity and structure-property relationships for biphenyl α -D-mannopyranosides. *ChemMedChem*. **2012**, *7*, 1404-1422.
- (S2) Han, Z.; Pinkner, J. S.; Ford, B.; Obermann, R.; Nolan, W.; Wildman, S. A.; Hobbs, D.; Ellenberger, T.; Cusumano, C. K.; Hultgren, S. J.; Janetka, J. W. Structure-based drug design and optimization of mannoside bacterial FimH antagonists. *J. Med. Chem.* **2010**, *53*, 4779-4792.
- (S3) Klein, T.; Abgottspon, D.; Wittwer, M.; Rabbani, S.; Herold, J.; Jiang, X.; Kleeb, S.; Lüthi, C.; Scharenberg, M.; Bezençon, J.; Gubler, E.; Pang, L.; Smiesko, M.; Cutting, B.; Schwaradt, O.; Ernst, B. FimH antagonists for the oral treatment of urinary tract infections: from design and synthesis to in vitro and in vivo evaluation. *J. Med. Chem.* **2010**, *53*, 8627-8641.
- (S4) Jiang, X.; Abgottspon, D.; Kleeb, S.; Rabbani, S.; Scharenberg, M.; Wittwer, M.; Haug, M.; Schwaradt, O.; Ernst, B. Antiadhesion therapy for urinary tract infections – a balanced PK/PD profile proved to be key for success. *J. Med. Chem.* **2012**, *55*, 4700-4713.
- (S5) Bouckaert, J.; Berglund, J.; Schembri, M.; De Genst, E.; Cools, L.; Wuhler, M.; Hung, C.-S.; Pinkner, J.; Slättegård, R.; Zavalov, A.; Choudhury, D.; Langermann, S.; Hultgren, S. J.; Wyns, L.; Klemm, P.; Oscarson, S.; Knight, S. D.; De Greve, H. Receptor binding studies disclose a novel class of high-affinity inhibitors of the *Escherichia coli* FimH adhesin. *Mol. Microbiol.* **2005**, *55*, 441-455.

2.5 FimH Antagonists – Solubility vs. Oral Availability

This manuscript describes the optimization of biaryl α -D-mannopyranosides, mainly aiming for improvement of aqueous solubility and oral bioavailability. Two major strategies were applied for structural modifications: 1) the rearrangement of the substitution patterns of the biphenyl aglycone, and 2) the introduction of aromatic heterocycle as terminal ring of the biaryl moiety. The chemical synthesis, binding affinity test and *in vitro* PK studies are described in details.

Contribution to the project:

Lijuan Pang participated in the structure design by computational docking, and performed chemical synthesis for all of the reported compounds. Additionally, she tested the binding affinities with the competitive fluorescence polarization assay for the chosen compounds. Furthermore, she was responsible for writing the entire manuscript except the pharmacokinetic section.

This manuscript is in preparation for *Journal of Medicinal Chemistry*.

Manuscript

FimH Antagonists – Solubility vs. Oral Availability

Lijuan Pang,⁺ Simon Kleeb,⁺ Said Rabbani, Jacqueline Bezençon, Anja Sigl, Deniz Eris, Oliver Schwardt, and Beat Ernst^{*}

Institute of Molecular Pharmacy, Pharmacenter, University of Basel, Klingelbergstr. 50, 4056 Basel, Switzerland

⁺ These authors equally contributed to this work.

^{*} Corresponding author, e-mail: beat.ernst@unibas.ch

Keywords: Aqueous solubility, ester prodrug, FimH antagonist, oral bioavailability

Abbreviations: Caco-2 cells, colorectal adenocarcinoma cells; CES, carboxylesterase; CRD, carbohydrate recognition domain; HPLC, high performance liquid chromatography; IC₅₀, half maximal inhibitory concentration; LC-MS, liquid chromatography mass spectrometry; MAD, maximum absorbable dose; PAMPA, parallel artificial membrane permeability assay; P , octanol-water partition coefficient; P_{app} , apparent permeability; P_e , effective permeability; RLM, rat liver microsomes; UPEC, uropathogenic *Escherichia coli*; UTI, urinary tract infection.

Abstract

Urinary tract infections (UTI) caused by uropathogenic *Escherichia coli* are frequent infectious diseases requiring antibiotic treatment. Since recurrent antibiotic exposure can induce antimicrobial resistance, efficient non-antibiotic prevention and treatment strategies are urgently needed. The first step of the pathogenesis of UTI is the bacterial adherence to the urothelial host cell, mediated by the mannose-binding adhesin FimH, which is located at the tip of bacterial pili. Biphenyl α -D-mannopyranosides with an electron-withdrawing carboxylate on the terminal aromatic ring of the aglycone were identified as potent FimH antagonists. In a preliminary study, oral availability of these charged FimH antagonists could be established by an ester prodrug approach, although for the price of a dramatically reduced solubility. In this article, the solubility problem of the ester prodrug is addressed by disrupting the molecular planarity and symmetry of the biphenyl aglycone by means of the substitution pattern and by introducing heteroatoms. With the parallel artificial membrane permeability assay (PAMPA) and the Caco-2 assay ester prodrugs with oral availability were identified. Surprisingly, those containing a phenyl-*1H*-pyrrole aglycone show high microsomal stability and therefore do not act as prodrugs but are renally excreted unchanged. Their potential for passive reabsorption leads to elevated urine concentration for up to 6 h. The best candidate, the nanomolar FimH antagonist **41f** therefore represents a promising candidate for oral application in UTI treatment.

Introduction

Urinary tract infections (UTIs) – also known as acute cystitis or bladder infections – are among the most prevalent infectious diseases worldwide. UTIs affect millions of people every year and account for significant morbidity and high medical costs.^[1] Complicated UTIs require antibiotic treatment. Since recurrent antibiotic exposure leads to the ubiquitous problem of antimicrobial resistance, efficient non-antibiotic prevention and treatment strategies are urgently needed.^[2] More than 70% of UTIs are caused by uropathogenic *Escherichia coli* (UPEC).^[1a,3] The first step of the infection cycle is the bacterial adherence to the urothelial cell surface, which prevents UPEC from being cleared by micturition but also triggers the invasion into the cells.^[4] This initial contact is mediated by the bacterial adhesin FimH which is located at the tip of type 1 pili.^[5] FimH

consists of an N-terminal carbohydrate recognition domain (CRD) and a C-terminal pilin domain. The CRD specifically recognizes mannosylated uroplakin Ia glycoproteins located on the urinary bladder mucosa, whereas the pilin domain regulates the switch between the low- and high-affinity states of the CRD.^[6] Blocking the FimH-CRD with carbohydrates or mimetics thereof prevents the bacterial adherence as well as the subsequent infection and therefore is regarded as a potential opportunity for prevention and/or treatment of UTIs.^[7]

Over the last three decades, various mannosides and oligomannosides have been tested as potential antagonists for type 1 pili-mediated bacterial adhesion.^[8] The crystal structure of FimH was first solved in 1999,^[9] and since then, numerous crystallographic studies have been published, greatly facilitating the rational design of high-affinity ligands.^[10] As deduced from these studies, the FimH-CRD consists of a deep, negatively charged pocket which accommodates the mannopyranose moiety by an extended hydrogen bond network. At the entrance to this cavity, the amino acids Tyr48, Tyr137, and Ile52 form a hydrophobic rim, the ‘tyrosine gate’, perfectly suited to host aliphatic and aromatic aglycones.^[10a] As a consequence of these hydrophobic contacts, *n*-heptyl α -D-mannopyranoside (**1**, Figure 1) exhibits nanomolar affinity.^[10b] With aromatic aglycones, such as present in the antagonists **2-5**, further improvements were achieved.^[11] The high affinity of α -D-mannopyranosides with biphenyl (\rightarrow **3** & **4**) and indoliny phenyl (\rightarrow **5**) aglycones could be rationalized by optimal π - π stacking interactions between the biaryl aglycone and the tyrosine gate.^[11d,e,11i] Depending on the aglycone, different binding modes have been observed. The alkyl aglycone of *n*-butyl α -D-mannopyranoside interacts with both Tyr48 and Tyr137 of the tyrosine gate.^[10b] By contrast, the biphenyl aglycone present in antagonist **3** was shown to adopt an ‘out-docking mode’,^[11f] that means, it interacts only with Tyr48, probably due to limited flexibility of the biphenyl moiety. Moreover, *ortho*-substituents on ring A of the biphenyl aglycone, such as the *ortho*-chloro substituent in compound **4b**, proved beneficial to binding because of high shape complementarity within the binding pocket and therefore better van der Waals contacts.^[11j]

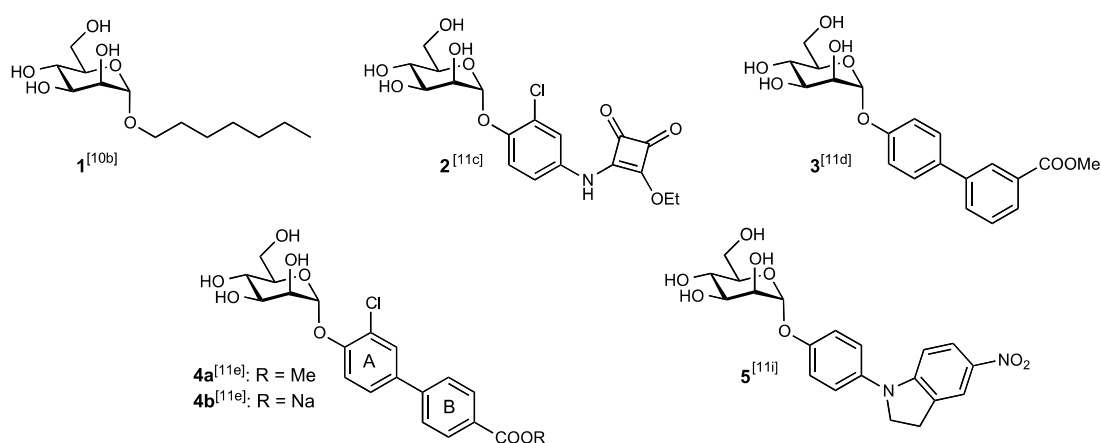


Figure 1. FimH antagonists: *n*-heptyl α -D-mannopyranoside (**1**) is used as reference compound; the squaric acid derivative **2**, the biphenyl derivatives **3-4**, and the indolinyphenyl derivative **5** exhibit nanomolar affinities.

For numerous diseases as e.g. UTI, oral administration of therapeutics is the standard care, because daily therapy is required. As described in our previous publication,^[11e] the carboxylic acid moiety in biphenyl α -D-mannoside **4b** – its electron-withdrawing potential is essential for an enhanced π - π stacking interaction – impairs the membrane permeability and, as a consequence, the potential for oral absorption. Otherwise, ester prodrug **4a** was shown to have markedly increased membrane permeability and to provide – upon absorption and enzyme-mediated hydrolysis – antagonist **4b**, which is perfectly suited for rapid renal excretion. Nonetheless, low aqueous solubility (12 μ g/mL) was identified as a major drawback of prodrug **4a**, limiting the absorptive flux of the prodrug through the intestinal mucosa. According to the maximum absorbable dose (MAD) concept,^[12] aqueous solubility of at least 50 μ g/mL is required to achieve quantitative absorption of a 1 mg/kg dose of prodrug with medium permeability.

Results and Discussion

In the present study, the solubility issue of the ester prodrugs was addressed by two approaches: First, by disrupting the molecular planarity and symmetry with modified substitution pattern on the biphenyl moiety (Figure 2a) and second by increasing the polar surface area (PSA) with heterocyclic biaryl aglycones (Figure 2b).^[13] For improving oral availability, the carboxylic acid was replaced by the bioisosteric cyano group (Figure 2c).^[14]

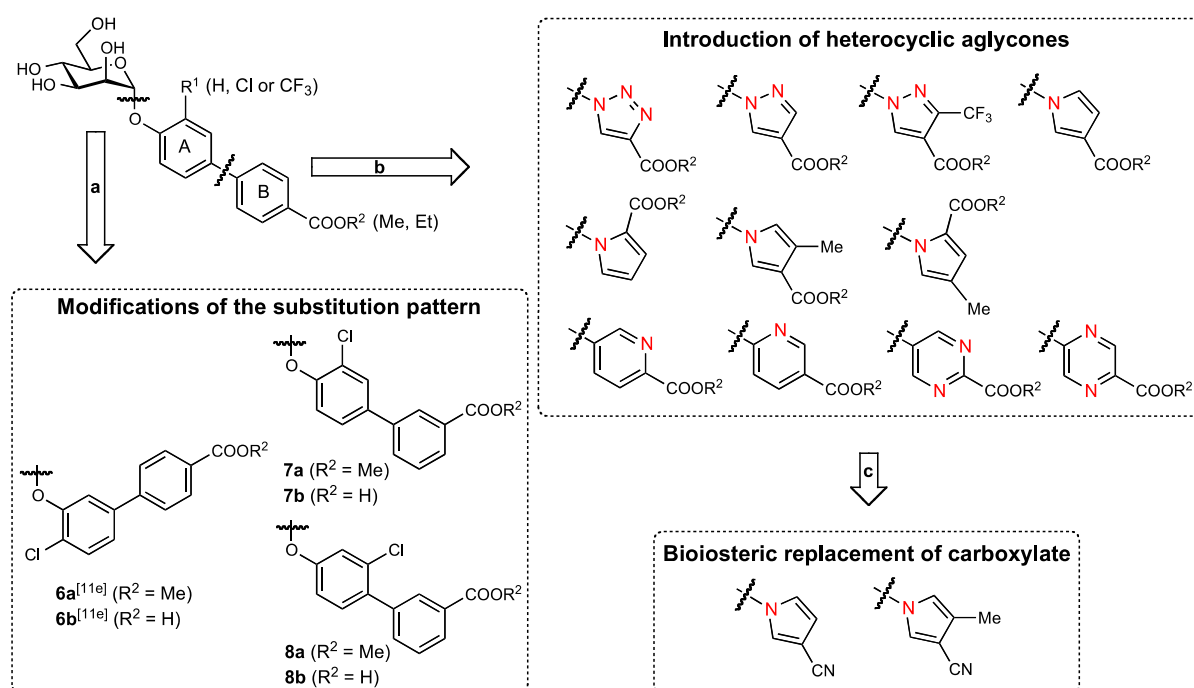


Figure 2. Modifications of the aglycone of FimH antagonists by (a) modifying the substitution pattern, (b) introducing heteroaryl aglycones and (c) replacing the carboxylate moiety with a bioisosteric cyano group.

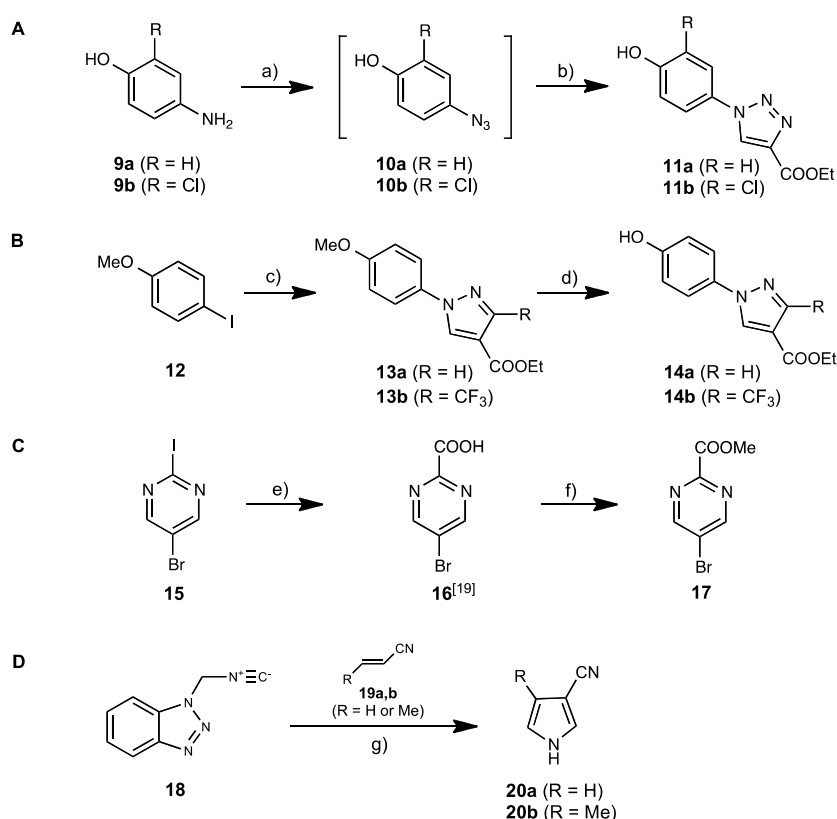
To evaluate the impact of these modifications on PK/PD properties, binding affinity to the FimH-CRD as well as the *in vitro/in vivo* pharmacokinetic properties predictive for oral bioavailability and metabolic stability were studied.

Synthesis

Biphenyl mannosides. Compounds **6a,b**, **7a,b** and **8a,b** (Figure 2a) were synthesized according to a previously described procedure (for synthesis and compound characterization see Supporting Information).^[11e]

Synthesis of heteroaromatic building blocks (Scheme 1). Starting with the commercial aminophenols **9a,b**, the azidophenols **10a,b** were obtained via a diazotransfer reaction using freshly prepared triflyl azide in pyridine and copper (II) sulfate as catalyst.^[15] Because of instability, **10a,b** were used without purification in a subsequent copper (I)-catalyzed Huisgen cycloaddition^[16] with ethyl propiolate, yielding the triazolylphenols **11a,b** with high 1,4-regioselectivity (Scheme 1A). By using an Ullmann-type copper-diamine-catalyzed *N*-arylation,^[17] *1H*-pyrazole-4-carboxylate was coupled with 4-iodoanisole (**12**) in *N*-methyl-2-pyrrolidone (NMP) to furnish **13a**. Because of the low reactivity of the trifluoromethyl-substituted pyrazole, the coupling reaction was carried

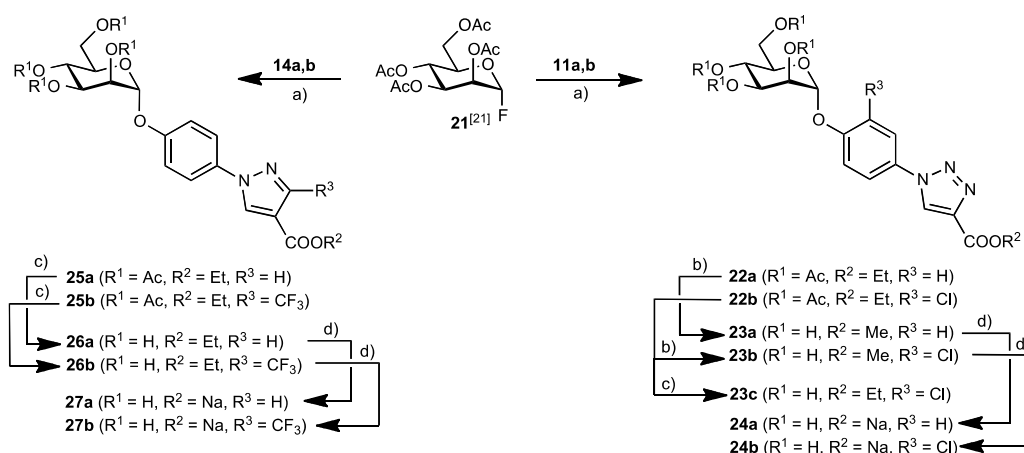
out under solvent-free condition to give **13b** in quantitative yield. Demethylation of **13a,b** with AlCl_3 gave the pyrazolylphenol derivatives **14a,b**. Due to the instability of **14b** under $\text{AlCl}_3/n\text{Bu}_4\text{NI}$ conditions, a AlCl_3 /thiol combination was used to accelerate the reaction and to suppress byproduct formation (Scheme 1B).^[18] The pyrimidinyl derivative **17** was prepared via a $n\text{BuLi}$ -mediated carboxylation with CO_2 followed by esterification (Scheme 1C).^[19] To synthesize the cyano-substituted pyrroles **20a,b**, benzotriazol-1-ylmethyl isocyanide (BetMIC, **18**) was treated with the electron-deficient alkenes **19a,b** under basic heterocyclization conditions (Scheme 1D).^[20]



Scheme 1. Reagents and conditions: a) TfN_3 , CuSO_4 , triethylamine, pyridine, 0 °C to rt, 2 h; b) ethyl propiolate, $\text{CuSO}_4 \cdot 5\text{H}_2\text{O}$, sodium ascorbate, $t\text{BuOH}/\text{H}_2\text{O}$ (1:1), rt, 30 min (yield for two steps: 77% for **11a**, 48% for **11b**); c) ethyl *1H*-pyrazole-4-carboxylate or ethyl 3-trifluoromethyl-*1H*-pyrazole-4-carboxylate, CuI , *trans*-*N,N'*-dimethyl-1,2-cyclohexanediamine, K_2CO_3 , NMP as solvent for **13a** and solvent free for **13b**, 110 °C, 24 h (80% for **13a**, quant. for **13b**); d) AlCl_3 , cat. $n\text{Bu}_4\text{NI}$, DCE (for **14a**), or 1-dodecanethiol without catalyst (for **14b**), 0 °C to rt (60% for **14a**, 26% for **14b**); e) i. $n\text{BuLi}$, hexane, toluene, -78 °C, 1 h; ii. CO_2 (g), -78 °C to rt, 7 h; f) conc. H_2SO_4 (0.8 eq), MeOH, reflux, overnight (37% for two steps); g) nitrile **19a,b**, $t\text{BuOK}$, THF, 0 °C to reflux, 2 h (60% for **20a**, 54% for **20b**).

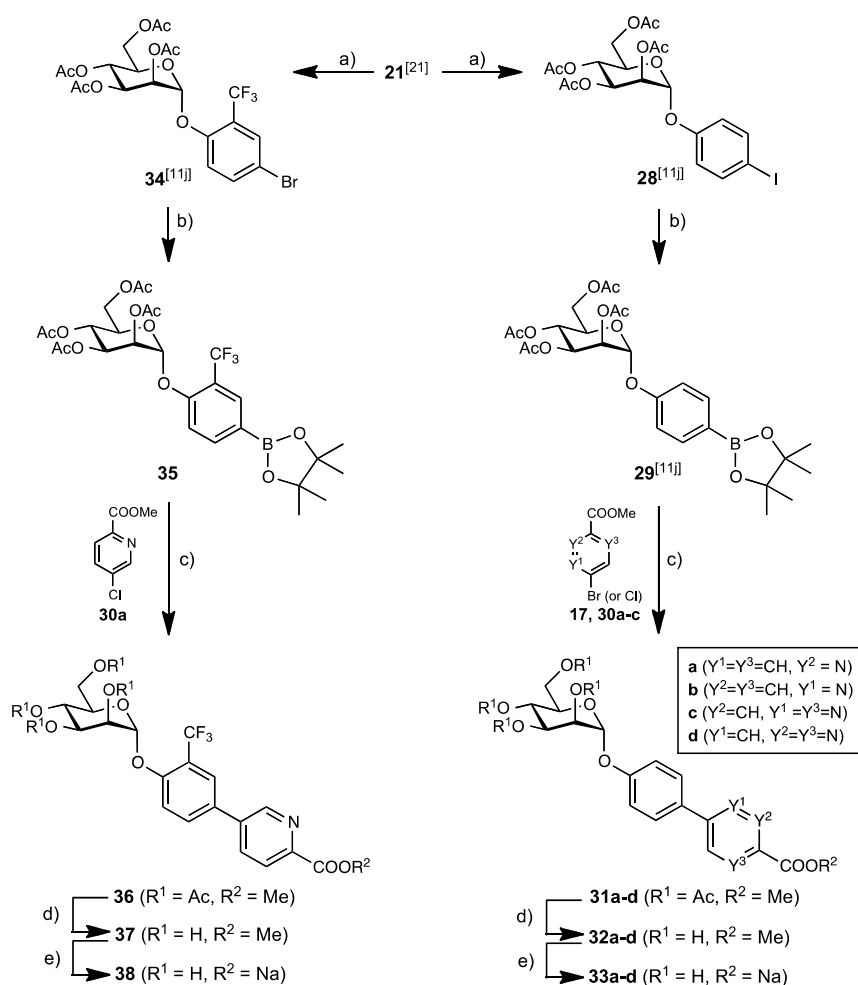
Triazolylphenyl and pyrazolylphenyl mannosides (Schemes 2). Mannosylation of the phenols **11a,b** and **14a,b** (see Scheme 1A & B) with mannosyl fluoride **21** and $\text{BF}_3 \cdot \text{Et}_2\text{O}$

as promoter, yielded exclusively the α -mannosides **22a,b** and **25a,b**.^[21] Deacetylation (\rightarrow **23a-c** and **26a,b**) followed by ester hydrolysis gave the test compounds **24a,b** and **27a,b**.



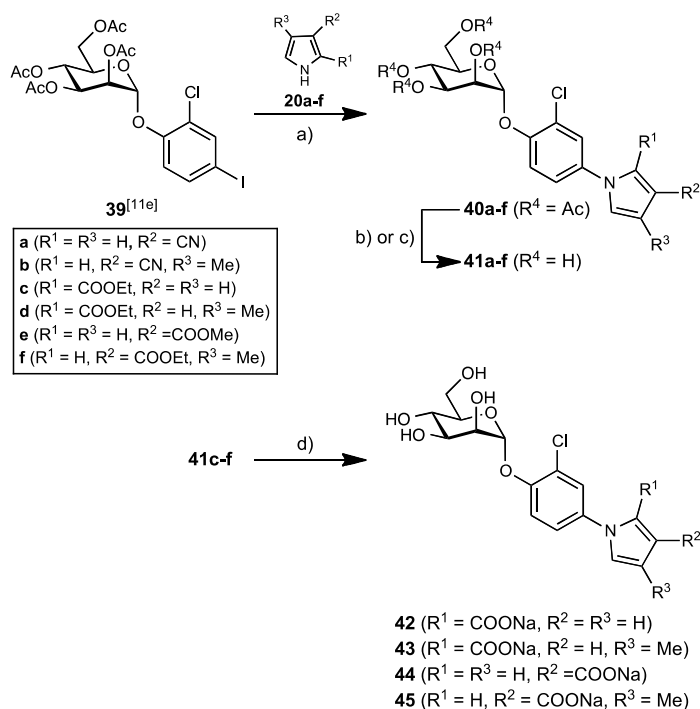
Scheme 2. Reagents and conditions: a) $\text{BF}_3 \cdot \text{Et}_2\text{O}$, DCM, mol. sieves 4 Å, 0 °C to rt, overnight (79% for **22a**, 76% for **22b**, 98% for **25a**, 64% for **25b**); b) NaOMe, MeOH, rt, 4 h (74% for **23a**, 80% for **23b**); c) NaOEt, EtOH, rt, overnight (74% for **23c**, 95% for **26a**, 82% for **26b**); d) 0.2 N aq. NaOH, MeOH, rt, overnight (30% for **24a**, 90% for **24b**, 70% for **27a**, 79% for **27b**).

Pyridinylphenyl, pyrazinylphenyl, and pyrimidinylphenyl mannosides (Scheme 3). Mannosyl fluoride **21** was treated with 4-iodophenol or 4-bromo-2-trifluoromethylphenol in the presence of $\text{BF}_3 \cdot \text{Et}_2\text{O}$. The resulting iodide **28**^[11j] and bromide **34**^[11j] were transformed into the boronic acid pinacol esters **29**^[11j] and **35** under Miyaura-borylation conditions. In a palladium-catalyzed Miyaura-Suzuki coupling^[22] of the heteroaryl halides **17** (see Scheme 1C) and **30a-c** (commercially available) with boronic acid ester **29**, heteroarylphenyl mannosides **31a-d** were obtained in good to excellent yields. Similarly, mannoside **36** was prepared by coupling of ester **35** and pyridinylchloride **30a**. Deacetylation under Zemplén conditions (\rightarrow **32a-d**, **37**) followed by saponification of the methyl ester yielded the sodium salts **33a-d** and **38**.

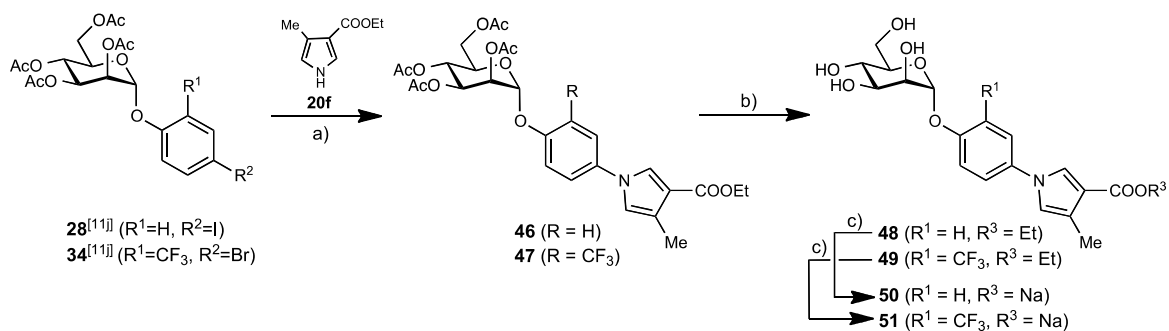


Scheme 3. Reagents and conditions: a) 4-iodophenol or 4-bromo-2-trifluoromethylphenol, $BF_3 \cdot Et_2O$, DCM, mol. sieves 4 Å, 0 °C to rt, overnight (70% for **28**, 80% for **34**); b) bis(pinacolato)diborone, $Pd(Cl_2)dppf \cdot CH_2Cl_2$, KOAc, DMF, 85 °C, overnight (80% for **29**, 83% for **35**); c) $Pd(Cl_2)dppf \cdot CH_2Cl_2$, K_3PO_4 , DMF, 85 °C, overnight (60% for **31a**, 80% for **31b**, 68% for **31c**, 40% for **31d**, 57% for **36**); d) NaOMe, MeOH, rt, 4 h (36% for **32a**, 24% for **32b**, 36% for **32c**, 89% for **32d**, 60% for **37**); e) 0.2 N aq. NaOH, MeOH, rt, overnight (32% for **33a**, 48% for **33b**, 44% for **33c**, 60% for **33d**, 90% for **38**).

Pyrrolylphenyl mannosides (Schemes 4 & 5). In a copper catalyzed *N*-arylation, pyrroles **20a,b** (see Scheme 1D) and **20c-f** (commercial) were coupled with mannoside **39** (*ortho*-Cl) to yield the pyrrolylphenyl mannosides **40a-f** (Scheme 4).^[18] Under similar conditions, mannosides **28** (without *ortho*-substituent) and **34** (*ortho*- CF_3) were coupled with pyrrole **20f** to yield **46** and **47** (Scheme 5). Because of partial deacetylation of the sugar moiety during *N*-arylation, the crude products were reacetylated to facilitate purification. Deacetylation of the mannose moiety (\rightarrow **41a-f**, **48** and **49**) followed by saponification of the alkyl esters gave the test compounds **42-45**, **50** and **51**.



Scheme 4. Reagents and conditions: a) i. CuI, (\pm)-*trans*-1,2-diaminocyclohexane, K₃PO₄, 1,4-dioxane, 110 °C, overnight; ii. Ac₂O, DMAP, pyridine, rt, overnight (44% for **40a**, 92% for **40b**, 33% for **40c**, 64% for **40d**, 99% for **40e**, 77% for **40f**); b) NaOMe, MeOH, rt, 4 h (65% for **41a**, 38% for **41b**, 83% for **41e**); c) NaOEt, EtOH, rt, overnight (91% for **41c**, 61% for **41d**, 93% for **41f**); d) NaOH, MeOH/H₂O (1:2), rt, 12-48 h (58% for **42**, 40% for **43**, 20% for **44**, 57% for **45**).



Scheme 5. Reagents and conditions: a) i. CuI, (\pm)-*trans*-1,2-diaminocyclohexane, K₃PO₄, 1,4-dioxane, 110 °C, overnight; ii. Ac₂O, DMAP, pyridine, rt, overnight (94% for **46**, 49% for **47**); b) NaOEt, EtOH, rt, overnight (46% for **48**, 85% for **49**); c) NaOH, MeOH/H₂O (1:2), rt, 48 h (99% for **50**, 35% for **51**).

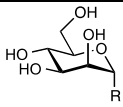
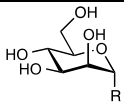
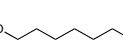
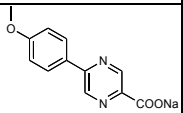
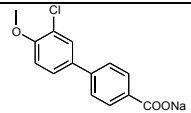
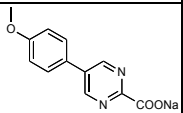
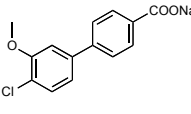
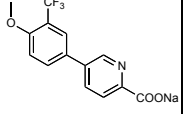
In Vitro binding affinities

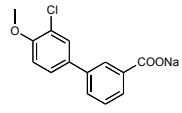
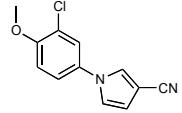
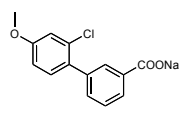
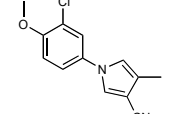
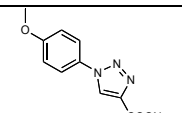
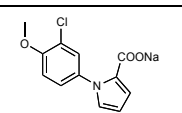
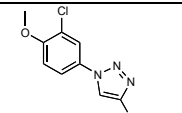
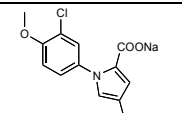
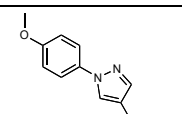
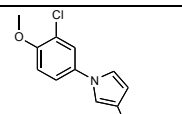
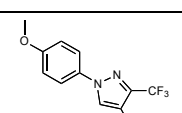
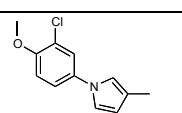
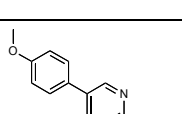
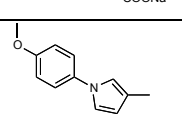
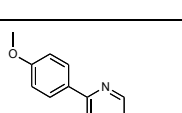
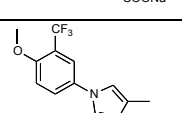
The hydrolyzed prodrugs, i.e. the free carboxylates (**6-8b**, **24a-b**, **27a-b**, **33a-d**, **38**, **42-45**, **50** and **51**) as well as the bioisosteric cyanides (**41a-b**), were evaluated in a cell-free competitive binding assay (Table 1).^[23]

Cell-free competitive binding assay.^[23] The cell-free competitive binding assay is based on the competitive interaction of the compound of interest and the biotinylated polyacrylamide glycopolymer TM-PAA (Man α 1-3(Man α 1-6)Man β 1-4GlcNAc β 1-4GlcNAc β -PAA) with the isolated CRD of FimH. Complexation of the biotinylated glycopolymer with streptavidin coupled to horseradish peroxidase allows for quantification of the binding affinity of the antagonists. For every compound the assay was performed twice with each concentration in duplicate. To ensure comparability between various antagonists, the reference compound *n*-heptyl α -D-mannopyranoside (**1**) was tested each time in parallel. The affinities are reported relative to **1** as rIC₅₀ in Table 1.

A comparison of the biphenyl mannoside antagonist **4b** (entry 2) with the regioisomers **6b**, **7b**, and **8b** (entries 3-5) indicates that changing the position of the carboxylic acid on the terminal ring B of the biphenyl aglycone as well as modifying the substitution pattern on ring A substantially reduced affinity. As previously reported, the *ortho*-chloro substituent present in the antagonists **4b** and **7b** provides additional van der Waals contacts leading to binding affinity in the low nanomolar range.^[11]

Table 1. Pharmacodynamic parameters of FimH antagonists. The IC₅₀ values were determined with a cell-free competitive binding assay.^[23] The rIC₅₀ values were calculated by dividing the IC₅₀ of the compound of interest by the IC₅₀ of reference compound **1**. This leads to rIC₅₀ values below 1.0 for derivatives with higher affinity than reference **1** and rIC₅₀ above 1.0 for compounds with lower affinity than **1**.

Entry	Cpd		IC ₅₀ [nM]	rIC ₅₀	Entry	Cpd		IC ₅₀ [nM]	rIC ₅₀
		R					R		
1	1 ^[10b]		54.9	1	12	33c		39	0.73
2	4b ^[11c]		6.7	0.09	13	33d		35	0.60
3	6b ^[11c]		29	0.40	14	38		20	0.39

4	7b		12	0.19	15	41a		29	0.50
5	8b		53	0.97	16	41b		25	0.43
6	24a		16	0.30	17	42		75	1.37
7	24b		21	0.35	18	43		23	0.41
8	27a		111	2.02	19	44		25	0.45
9	27b		112	2.02	20	45		25	0.44
10	33a		16	0.30	21	50		65	1.18
11	33b		46	0.71	22	51		19	0.33

All heteroaryl mannosides (entries 6-22) showed IC_{50} values in the nanomolar range as well. Nonetheless, they were weaker binders than the optimized biphenyl mannoside **4b**, although *in silico* studies obtained with flexible docking (Glide software package^[24]) to the FimH-CRD suggested a similar ‘out-docking mode’ (Figure 3).

In comparison with the triazolylphenyl mannosides **24a,b** (entries 6 & 7) and the pyrrolylphenyl mannosides **41a,b**, **42-45**, **50** and **51** (entries 15-22), the pyrazolylphenyl analogues **27a,b** (entries 8 & 9) showed markedly lower affinity, even though we expected a similar conformation for all biaryl mannosides containing a five-membered aromatic heterocycle. Furthermore, a high impact of the substitution pattern on the binding affinity was observed for the various pyrrolylphenyl mannosides (entries 15-22). In agreement with previous observations,^[11,j,g] the *ortho*-chloro and the *ortho*-

trifluoromethyl substituents on ring A were beneficial to affinity (**50** vs. **45** & **51**, entries 20-22). The position of the electron-withdrawing carboxylic acid moiety in the heteroaromatic ring furthermore affected the binding affinity. In the 3-position (\rightarrow **44**, entry 19) it conferred three times higher affinity than in the 2-position (\rightarrow **42**, entry 17). *In silico* docking studies indeed suggest that the 2-carboxylate forces the two rings of the aglycone in an orthogonal orientation and therefore disrupts the π - π stacking interactions between the heteroaromatic ring and Tyr48 of the tyrosine gate (\rightarrow **45**, Figure 3B). Otherwise, the additional 4-methyl substituent present in **43** (entry 18) could presumably provide an additional hydrophobic contact (Figure 3A).

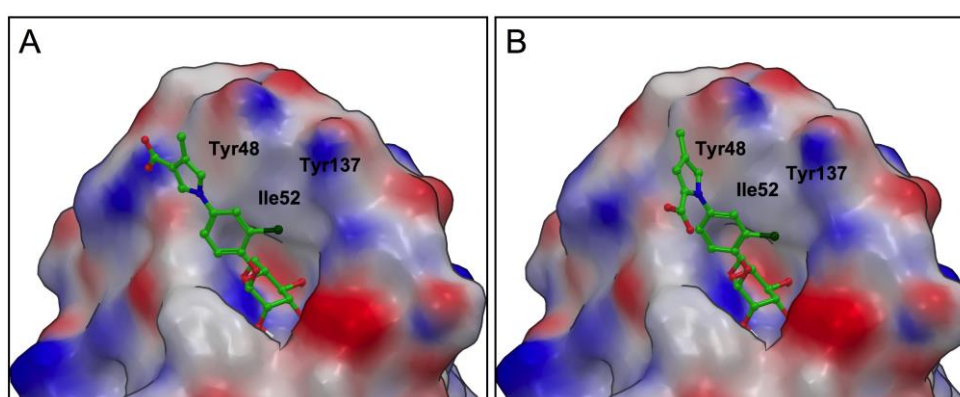
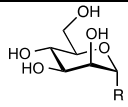


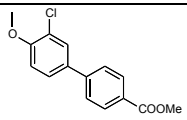
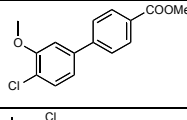
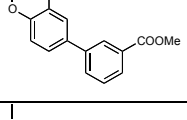
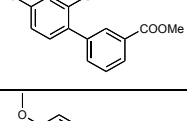
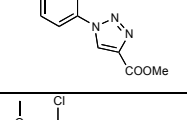
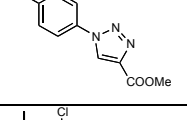
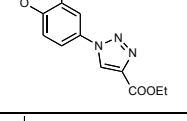
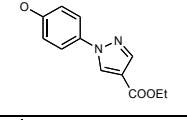
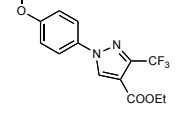
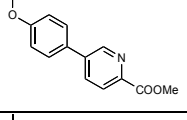
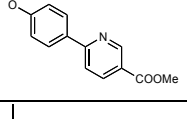
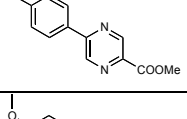
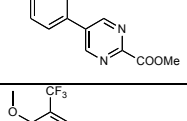
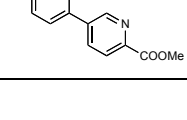
Figure 3. *In silico* docking studies obtained with flexible docking (Glide software package^[24]) to the FimH-CRD (PDB ID: 3MCY); top-scored binding modes of A) **43** (Table 1, entry 18) and B) **45** (entry 20).

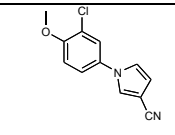
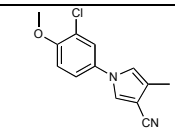
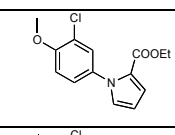
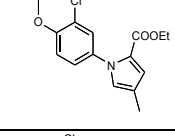
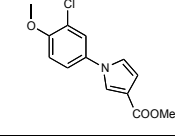
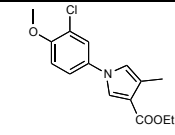
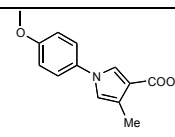
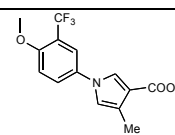
Physicochemical properties and *in vitro* pharmacokinetics

For assessing the potential for intestinal absorption, lipophilicity ($\log P$), aqueous solubility, and permeability through an artificial membrane (PAMPA, $\log P_e$) as well as a Caco-2 cell monolayer (P_{app}) were determined (Table 2).^[25-30] Furthermore, the esters were incubated with rat liver microsomes (RLM) for estimating their susceptibility to carboxylesterase (CES)-mediated hydrolysis.^[31] Mammalian CESs are localized in the endoplasmatic reticulum of the liver and most other organs. Table 2 indicates the metabolic half lives ($t_{1/2}$) as determinants of the rate of bioconversion to the respective acid.

Table 2. Physicochemical and pharmacokinetic parameters of FimH antagonists.

Entry	Cpd		$\log P^a$	Solubility [$\mu\text{g/mL}$] ^b	PAMPA $\log P_e$	Caco-2 P_{app} [10^{-6} cm/s] ^d	Microsomal stability
-------	-----	---	------------	---	---------------------	--	-------------------------

		R			[cm/s] ^c	a→b	b→a	t _{1/2} [min] ^e
1	4a ^[11c]		2.3	11.9	-4.6	5.3 ± 0.6	17.5 ± 1.3	2.1
2	6a ^[11c]		1.7 ± 0.1	14 ± 0	-4.7	6.1 ± 1.2	21.1 ± 1.2	22
3	7a		2.7 ± 0.1	41 ± 3	-4.6 ± 0.2	6.7 ± 0.4	20.7 ± 2.5	84
4	8a		2.7 ± 0.1	134 ± 6	-4.5 ± 0.1	4.5 ± 0.3	10.8 ± 0.7	13
5	23a		-0.6 ± 0.0	> 180	-9.4 ± 0.3	n.d.	n.d.	38
6	23b		0.0 ± 0.0	> 150	-9.1 ± 1.8	n.d.	n.d.	32
7	23c		0.7 ± 0.0	> 150	-10	n.d.	n.d.	42
8	26a		0.9 ± 0.0	> 180	-6.6 ± 0.1	n.d.	n.d.	> 120
9	26b		2.1 ± 0.0	> 180	-5.7 ± 0.1	1.3 ± 0.1	12.4 ± 2.4	113
10	32a		0.2 ± 0.0	> 130	-7.5 ± 0.2	0.22 ± 0.05	2.3 ± 0.1	10
11	32b		1.0 ± 0.0	59 ± 6	-6.3 ± 0.0	0.64 ± 0.06	8.3 ± 0.4	11
12	32c		0.1 ± 0.1	> 150	-7.6 ± 0.0	0.24 ± 0.01	1.8 ± 0.2	11
13	32d		< -1.0	95 ± 6	-8.5 ± 0.1	0.16 ± 0.03	0.22 ± 0.05	24
14	37		1.3 ± 0.1	> 180	-8.6 ± 1.7	0.33 ± 0.04	7.2 ± 0.7	8.2

15	41a		1.5±0.1	>350	-8.8± 2.0	n.d.	n.d.	n.d.
16	41b		2.0±0.1	69 ± 20	-6.3 ± 0.1	n.d.	n.d.	n.d.
17	41c		2.0 ± 0.0	> 180	-5.2 ± 0.0	n.d.	n.d.	> 120
18	41d		2.7 ± 0.0	34 ± 4	-4.8 ± 0.1	5.0 ± 0.2	35.6 ± 1.0	84
19	41e		2.1 ± 0.2	> 180	-6.0 ± 0.1	n.d.	n.d.	> 120
20	41f		2.8 ± 0.1	> 180	-4.8 ± 0.1	6.4 ± 0.7	30.0 ± 2.9	> 120
21	48		2.3 ± 0.0	> 180	-5.1 ± 0.1	1.5 ± 0.5	17.2 ± 0.6	> 120
22	49		3.0 ± 0.1	135 ± 6	-5.0 ± 0.2	5.0 ± 0.3	26.1 ± 1.5	> 120

[a] Octanol-water partition coefficients ($\log P$) were determined by a miniaturized shake flask procedure. The values are indicated as mean \pm SD of sextuplicate determinations.^[25] [b] Kinetic solubility was measured in a 96-well format in triplicate using the μ SOL Explorer solubility analyzer.^[26] [c] Permeation through an artificial membrane ($\log P_e$, effective permeability) was determined by PAMPA (parallel artificial membrane permeability assay) in quadruplicate.^[27] [d] Permeation through a Caco-2 cell monolayer (P_{app} , apparent permeability) was assessed in the absorptive (a \rightarrow b) and secretory (b \rightarrow a) directions in triplicate.^[28] [e] Microsomal stability was determined with pooled male rat liver microsomes (0.125 mg/mL) at pH 7.4 and 37 °C.^[29] n.d., not determined.

Biphenyl mannosides. As observed in our previous study,^[11e] the biphenyl derivatives **4a** and **6a** (Table 2, entries 1 & 2) showed low aqueous solubility probably due to the symmetrical *para-para* substitution pattern. In order to disrupt this symmetry, the carboxylic acid moiety in **4a** was moved from the *para*- to the *meta*-position (\rightarrow **7a**, Table 2, entry 3), leading however only to moderately improved aqueous solubility. Moving the chloro substituent on ring A from the *ortho*- to the *meta*-position (\rightarrow **8a**,

Table 2, entry 4) increased the dihedral angle between the aromatic rings of the bicyclic aglycone (Figure 4A, 60.3° for antagonist **8a** vs. 39.6° for antagonist **7a**, values calculated with MacroModel, version 9.9^[30]), resulting in the disruption of the molecular planarity and markedly enhanced aqueous solubility. Given the elevated solubility (134 $\mu\text{g/mL}$) and the high effective permeability ($\log P_e -4.5$), the prodrug **8a** was identified as the most promising biphenyl derivative for oral administration.

The microsomal incubation with a low initial substrate concentration (2 μM) and a concentration of the microsomal protein of 0.125 mg/mL induced a fast degradation of prodrug **4a** ($t_{1/2}$ 2.1 min, entry 1). The esters in the biphenyl mannosides **6a** ($t_{1/2}$ 22 min, entry 2), **7a** ($t_{1/2}$ 84 min, entry 3), and **8a** ($t_{1/2}$ 13 min, entry 4) were less susceptible to the carboxylesterase (CES)-mediated metabolic turnover. The differing rates of hydrolysis may result from various reasons, i.e. the change in the molecular geometry and therefore in the accessibility of the ester by the catalytic site of the serine hydrolase CES,^[31] and differing electron-density on the carbonyl carbon. Since the first step of the catalytic mechanism relies on the nucleophilic attack by the hydroxyl group of the serine moiety,^[32] increasing electron-deficiency of the carbonyl carbon should lead to a higher propensity for hydrolysis. However, the calculated partial charges (δ) on the carbonyl carbons (Figure 4A, calculated with AMSOL, Version 7.1^[33]) do not correlate with the propensities of the corresponding esters to hydrolysis. We therefore attributed the rate differences of the CES-mediated hydrolysis primarily to the differing geometry of the aglycones, which, in case of **4a**, orients the ester bond within the active site in an optimal position.

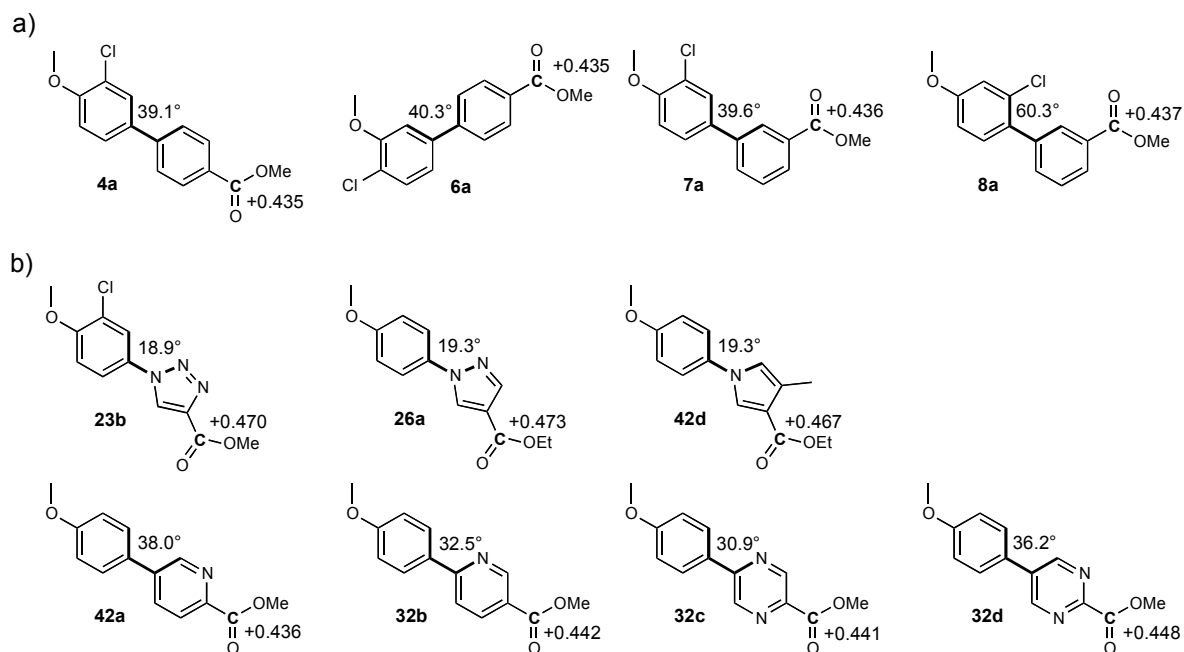


Figure 4. Dihedral angle between the aromatic rings of the bicyclic aglycones and the partial charge (δ) on the carbonyl carbon of A) the biphenyl aglycone and B) the heteroaryl aglycone of prominent biaryl α -D-mannopyranosides. The values were calculated with MacroModel (version 9.9)^[30] and AMSOL (version 7.1).^[33]

Heteroaryl mannosides. The heteroaryl mannosides (Table 2, entries 5-22) exhibited markedly higher aqueous solubility than biphenyl α -D-mannoside **4a**. When the nitrogen atom is moved from the *ortho*- (\rightarrow **32b**, entry 11) to the *meta*-position (\rightarrow **32a**, entry 10) of the heteroaromatic moiety, the dihedral angle between the two aryl rings (Figure 4B, 32.5° for **32b** vs. 38.0° for **32a**) increases, leading to a disruption of the molecular planarity and hence to improved solubility. Furthermore, an additional parameter leading to improved solubility becomes evident from the antagonists **32c** and **32d**. Thus, although **32c** (entry 12) has a smaller dihedral angle than **32d** (entry 13) (Figure 4B, 30.9° for **32c** vs. 36.2° for **32d**) it exhibits higher solubility. One possible rationale is associated with the desymmetrization of the aglycone, reducing compatibility for stacking and therefore increasing solubility. In general, most five-membered heteroaryl mannosides excel in high solubility, either because of the increased polarity [\rightarrow triazoles **23a-c** (entries 5-7) and pyrazoles **26a,b** (entries 8 & 9)] or because of the disruption of molecular symmetry (\rightarrow pyrroles **41a-f**, **48**, **49**, entries 15-22).

As expected, increased polarity (\rightarrow **23a**, $\log P$ -0.6, entry 5) leads to reduced permeability ($\log P_e$ -9.4), i.e. poor oral absorption.^[34] To enhance lipophilicity two strategies were followed: First, an *ortho*-chloro substituent was added to ring A of the biaryl aglycone (\rightarrow **23b**, entry 6) and, second, the methyl ester was replaced by an ethyl ester (\rightarrow **23c**, entry 7). However, both strategies were insufficient to substantially improve the oral absorption potential. For the pyrazolylphenyl derivative **26a** (entry 8), although slightly more lipophilic than the triazolylphenyl **23c** (entry 7), only low effective permeability ($\log P_e$ -6.6) was observed. Introduction of a trifluoromethyl substituent on the pyrazole moiety (\rightarrow **26b**, entry 9) further increased both lipophilicity and permeability but was still not sufficient for successful intestinal uptake.

By contrast, the pyrrolylphenyl mannosides **41a-f**, **48** and **49** (Table 2, entries 15-22) counted among the most lipophilic and the most permeable biaryl derivatives. Lipophilicity and permeability of antagonist **41e** could be successively enhanced by introducing a methyl substituent in the 4-position of the pyrrole moiety (\rightarrow **48**, Table 2, entry 21) and by modifying the *ortho*-substituent on ring A of the biaryl aglycone (\rightarrow **41f** and **49**, entries 20 & 22). For antagonists **41f** and **49**, effective permeability resulting from PAMPA ($\log P_e$ -4.8 and -5.0, respectively) suggested a high oral absorption potential. Moreover, the absorptive flux (apical \rightarrow basal) through the Caco-2 cell monolayer was outstandingly high. Although the ratio $P_{app,b\rightarrow a}/P_{app,a\rightarrow b}$ implied efflux-carrier activity, we expected high systemic availability of **41f** and **49** *in vivo*, notably because efflux transporters at human intestines are considered easily saturable when compounds are administered at elevated doses (e.g. > 100 mg).^[35] In the case of the pyrrolylphenyl derivatives **41c** and **41d** (entries 17 & 18), introducing a 4-methyl substituent increased permeability as well. In turn, it made **41d** the least soluble compound among all assessed heteroaryl mannosides. The bioisosteric replacement of the carboxylic moiety by a cyano group (\rightarrow **41a,b**, entries 15 & 16) resulted in PAMPA data indicating low permeability for both derivatives ($\log P_e$ -8.8 and -6.3, respectively).

Lipophilicity and permeability of the biaryl mannosides with six-membered heterocycles (entries 10-14) could be shown to depend on number and position of the nitrogen atoms in the bicyclic aglycone. The pyridinylphenyl derivative **32a** (entry 10) exhibited low

lipophilicity and permeability, whereas adding a trifluoromethyl substituent on ring A of the aglycone (\rightarrow **37**, entry 14) increased lipophilicity but did not confer higher permeability. By moving the pyridine nitrogen position (\rightarrow **32b**, entry 11), we could moderately increase lipophilicity and permeability. Nonetheless, antagonist **32b** was still too hydrophilic for intestinal absorption, as suggested by PAMPA and the Caco-2 model. The pyrazinylphenyl mannoside **32c** (entry 12) and the pyrimidinylphenyl mannoside **32d** (entry 13) both showed low lipophilicity and low effective permeability, suggesting low oral availability.

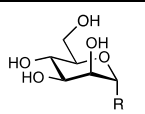
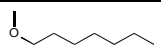
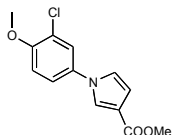
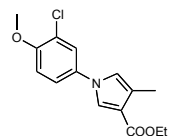
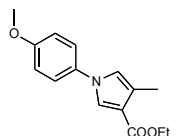
All heteroaryl derivatives with ester functions (Table 2, entries 5-14 and 17-22) were found to be less susceptible to CES-mediated bioconversion than the initial biphenyl mannoside **4a**. Nonetheless, the experimental half-life values suggest a strong relationship between the molecular structure of the heteroaryl portion and the propensity to hydrolysis. The calculated partial charges (δ) on the carbonyl carbon of prominent heteroaryl mannosides are shown in Figure 4B. According to these values, the electron distribution on the antagonists **32a-d**, including six-membered heteroaromatic cycles, is similar to those of the biphenyl mannoside **4a**. This similarity, in combination with the linear molecular geometry, probably explains their considerable propensity to enzyme-mediated hydrolysis. By contrast, the analogs with a five-membered heterocycle were markedly less prone to CES-mediated hydrolysis, probably due to the varying molecular geometries and physicochemical properties affecting the substrate recognition by the CES.^[31]

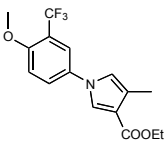
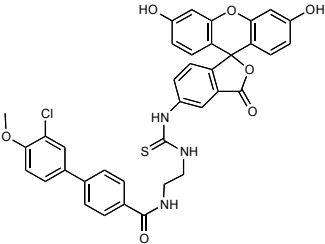
Binding affinity of selected esters

The pyrrolylphenyl esters **41e,f**, **48**, and **49**, which were originally designed as prodrugs, surprisingly proved to be metabolically stable and not hydrolyzable by the carboxylesterases. Since their lipophilicity ($\log P$), solubility, membrane permeation ($\log P_e$ and P_{app}) fulfill the requirements for an oral uptake, the binding affinities of these antagonists were determined in the cell-free competitive assay (see above) as well as in a competitive fluorescence polarization assay (Table 3). In both assays, *n*-heptyl mannoside (**1**) was used as a reference compound.

Competitive Fluorescence Polarization Assay.^[11k] For the rapid evaluation of binding affinity, a previously developed competitive binding assay based on fluorescence polarization (FP) was applied. A FimH variant consisting of the CRD linked to a His-tag by a thrombin cleaving site (FimH-CRD-Th-His₆, expressed and purified as previously described)^[23] was used. The antagonist of interest displaces the fluorescent-labeled competitor **52**^[11k] from the binding site, thereby reducing fluorescence polarization.^[36] Due to the long residence time of FimH antagonists ($t_{1/2} > 3.5$ h),^[37] a 24 h incubation time was applied before measurement of fluorescence polarization. IC₅₀ values were obtained by nonlinear least-squares regression (standard four-parameter IC₅₀ equation) and converted to K_D using a modified Cheng-Prusoff equation.^[36] The K_D values observed for the test compounds **41e,f**, **48** and **49** are summarized in Table 3. In general, the pyrrolylphenyl mannosides (entries 2-5) showed higher affinity than the reference compound **1**. The improved affinity for the *ortho*-substituted biaryls (Cl, **41f** and CF₃, **49**) was confirmed.

Table 3. Affinity of FimH antagonists to FimH-CRD-Th-His₆.^a The IC₅₀ values were determined with a cell-free competitive binding assay.^[23] The rIC₅₀ values were calculated by dividing the IC₅₀ of the compound of interest by the IC₅₀ of reference compound **1**. Dissociation constants (K_D) were determined in a competitive fluorescence polarization assay.^[36] n.d., not determined.

Entry	Cpd		Binding Assay		FP-Assay K_D [nM]
			IC ₅₀ [nM]	rIC ₅₀	
1	1		54.9	1.0	28.3
2	41e		18.5	0.33	4.3
3	41f		25.2	0.46	7.5
4	48		24.9	0.45	24.6

5	49		36.9	0.72	6.0
6	52 ^[11k]		n.d.	n.d.	1.7

In vivo pharmacokinetic study. Antagonist **41f** exhibiting the best *in vitro* PK/PD profile was selected for an *in vivo* pharmacokinetic study. It was orally applied to three mice at a dose of 10 mg/kg. The concentration-time profiles are shown in Figure 5.

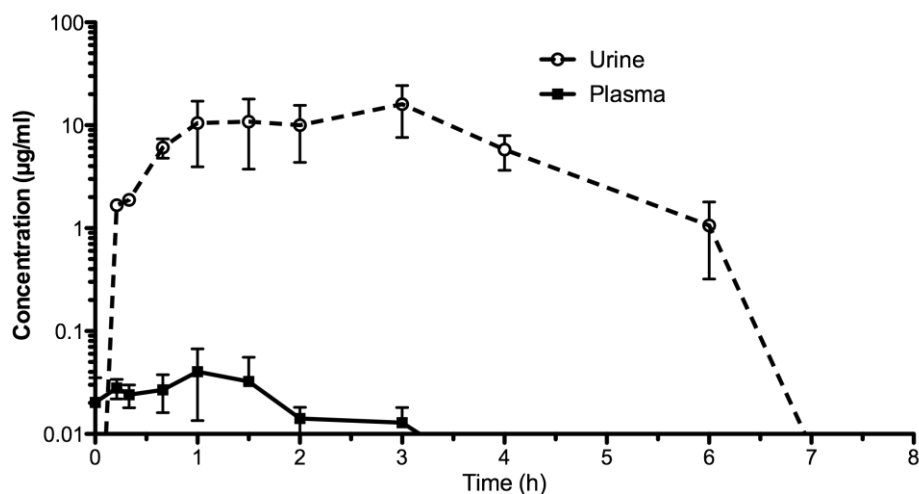


Figure 5. Urine (dashed line) and plasma (continuous line) concentration over time after an application of 10 mg/kg of **41f**. The detection limit for plasma samples was at 0.02 µg/ml, urine samples could be detected down to 0 µg/ml.

Generally, plasma concentrations of **41f** were very low, only barely exceeding the detection limit (0.02 µg/ml), peaking between 40 min and 1.5 h after application with a C_{\max} of only 0.04 µg/ml and subsequently dropping below the detection limit. In contrast, the urine concentration levels show a rapid accumulation of antagonist **41f**, with a C_{\max} ranging from 10 to 16 µg/ml at 1 to 3 h post application, forming a stable concentration plateau, which is slightly shifted in time compared to plasma peak levels. At 8 h, **41f** was not detectable in urine anymore. The dose appearing in urine corresponds to approximately 30% of the oral dose.

The accumulation in the urine, resulting in a relative constant plateau concentration over a time-period of about 3 h, is related to several important interplaying mechanisms. Both, PAMPA^[27] and transport through a Caco-2 cell layer indicate permeability ($\log P_{\text{app}} -4.8$ cm/s, and $P_{\text{app,a-b}} 6.4 \times 10^{-6}$ cm/s, Table 3) for **41f**.^[38,39] However, absorption of **41f** is slowed down by the simultaneous efflux ($P_{\text{app,b-a}} 30 \times 10^{-6}$ cm/s) by P-glycoprotein (P-gp),^[40] exceeding the uptake rate by a factor of about 5. Therefore, **41f** accumulates in the intestinal fluids, leading to P-gp saturation and, consequently, to a prolonged, but slow uptake. As this effect can influence plasma and urine drug levels only for a limited time, further mechanisms come into play. After absorption, the compound only shortly stays in circulation and is rapidly excreted by glomerular filtration in the kidneys. The $\log P$ value of **41f** ($\log P 2.8$, Table 3) implies a high tubular reabsorption from the proximal tubuli, resulting in a delayed renal excretion.^[38,39,41] In summary, the prolonged absorption due to P-gp mediated efflux combined with the delayed elimination via the kidneys due to reabsorption – elimination via the liver can be neglected ($t_{1/2} > 120$ min in RLM, Table 3) – explains the observed PK profile. This PK profile could prove beneficial for UTI treatment, as constant high levels over an extended time would limit dosing to few or even only one application a day.

Conclusions

Starting from prodrug **4a**, the present study aimed at optimizing the pharmacokinetic properties of the biaryl mannoside in order to achieve high oral absorption of the ester prodrug and rapid enzyme-mediated release of the active principle. In this regard, our first approach, i.e. disruption of the molecular planarity and symmetry of the biphenyl mannoside by modifying the substitution pattern, proved successful. Unlike compound **4a**, the ester prodrug **8a** showed solubility and membrane permeability in the range for high oral absorption *in vivo*. Moreover, hepatic esterases were shown to rapidly convert the ester to the polar parent compound **8b**. However, shifting the substituents on the aglycone markedly decreased the affinity to the FimH-CRD, overriding the gain in the intestinal uptake potential.

In a second approach, the improvement of the physicochemical properties by heterocyclic aglycones was studied. Thereby, triazole (**23a-c**), pyrazole (**26a,b**), and six-membered heterocyclic moieties (**32a-d** and **37**) proved highly beneficial to the aqueous solubility but in turn reduced lipophilicity and membrane permeability, which suggests, overall, poor oral absorption. By contrast, the pyrrolylphenyl mannosides – optimized by the introduction of a chloro or trifluoromethyl substituent on ring A and a methyl group on the terminal heterocycle (**41f** and **49**) – exhibited permeability and aqueous solubility in the range for successful oral absorption. Otherwise, incubations with rat liver microsomes, revealing low propensity to enzyme-mediated hydrolysis, predicted erratic conversion of the esters to the free acids in the liver. Despite their high intestinal uptake potential, these esters therefore scarcely act as prodrugs facilitating the delivery of the active principles to the urinary bladder. Nonetheless, the introduction of a pyrrole cycle appears as a promising strategy for optimizing the oral absorption of biaryl mannoside analogues, which do not rely on an ester prodrug approach. Two competitive binding assays indicated high binding affinities for all the heterocyclic derivatives with either free carboxylate or the ester moieties.

In summary, our study exemplifies the benefits of two approaches, that are rearrangement of the substitution pattern and introduction of aromatic heterocycles, on aqueous solubility of the biaryl mannosides. The high microsomal stability of the pyrrole derivatives indicates an action mode rather than a prodrug approach. For the esters **41f** and **49**, an optimal balance of pharmacodynamic, physicochemical and pharmacokinetic properties was obtained. Based on *in vivo* PK studies, **41f** is a promising candidate to be tested in a UTI disease model.

Experimental Section

Synthesis. The synthesis of compounds **11a,b**, **13a,b**, **14a,b**, **17**, **20a,b**, **22b**, **23b,c**, **24b**, **25a,b**, **26a,b**, **27a,b**, **31b-d**, **32b-d**, **33b-d**, **40a-e**, **41a-e**, **42-44**, **47**, **49**, and **51**, including compound characterization data, can be found in the Supporting Information.

General Methods. NMR spectra were recorded on a Bruker Avance DMX-500 (500.1

MHz) spectrometer. Assignment of ^1H and ^{13}C NMR spectra was achieved using 2D methods (COSY, HSQC, HMBC). Chemical shifts are expressed in ppm using residual CHCl_3 , CHD_2OD or HDO as references. Optical rotations were measured using Perkin-Elmer Polarimeter 341. Electron spray ionization mass spectra (ESI-MS) were obtained on a Waters micromass ZQ. The LC/HRMS analysis were carried out using a Agilent 1100 LC equipped with a photodiode array detector and a Micromass QTOF I equipped with a 4 GHz digital-time converter. Microwave-assisted reactions were carried out with a CEM Discover and Explorer. Reactions were monitored by TLC using glass plates coated with silica gel 60 F₂₅₄ (Merck) and visualized by using UV light and/or by charring with a molybdate solution (a 0.02 M solution of ammonium cerium sulfate dihydrate and ammonium molybdate tetrahydrate in aqueous 10% H_2SO_4). MPLC separations were carried out on a CombiFlash Companion or Rf from Teledyne Isco equipped with RediSep normal-phase or RP-18 reversed-phase flash columns. LC-MS separations were done on a Waters system equipped with sample manager 2767, pump 2525, PDA 2525 and micromass ZQ. Size-exclusion chromatography was performed on Bio-Gel[®] P-2 Gel (45-90 mm) from Bio-Rad (Reinach, Switzerland). All compounds used for biological assays are at least of 98% purity based on HPLC analytical results. Commercially available reagents were purchased from Fluka, Aldrich, Alfa Aesar or Iris Biotech (Germany). Solvents were purchased from Sigma-Aldrich (Buchs, Switzerland) or Acros Organics (Geel, Belgium) and were dried prior to use where indicated. Methanol (MeOH) and ethanol (EtOH) were dried by refluxing with sodium methoxide or ethoxide and distilled immediately before use. Dichloromethane (DCM) was dried by filtration over Al_2O_3 (Fluka, type 5016 A basic). Molecular sieves 4Å were activated in vacuo at 500 °C for 1 h immediately before use.

General procedure A for the synthesis of mannosides 22a,b and 25a,b. To an ice-cold suspension of **21**^[21] (1.1 equiv), phenol **11a,b** or **14a,b** (1.0 equiv) and molecular sieves 4 Å (600 mg) in dry DCM (5 mL), $\text{BF}_3 \cdot \text{Et}_2\text{O}$ (4.7 equiv) was added dropwise under argon. The mixture was stirred at 0 °C for 3 h, and then at rt overnight. The reaction mixture was filtered over Celite and the filtrate was diluted with DCM (50 mL), extracted with 0.5 N aq. NaOH (50 mL), water (50 mL) and brine (50 mL). The organic layer was dried over Na_2SO_4 and concentrated in vacuo. The residue was purified by MPLC on silica gel (petrol ether/EtOAc) to yield **22a,b** or **25a,b**.

General procedure B for the coupling of mannosylated phenyls with six-membered heterocyclic halides. A Schlenk tube was charged with heterocyclic halide **30a-c** or **17** (1.0 eq), boronate **29** or **35** (1.1 eq), Pd(dppf)Cl₂·CH₂Cl₂ (0.03 eq), K₃PO₄ (1.5 eq) and a stirring bar. The tube was closed with a rubber septum and was evacuated and flushed with argon. This procedure was repeated once, then anhydrous DMF (2 mL) was added under a stream of argon. The mixture was degassed in an ultrasonic bath and flushed with argon for 5 min, and then stirred at 80-85 °C overnight. The reaction mixture was cooled to rt, diluted with EtOAc (50 mL), and washed with water (50 mL) and brine (50 mL). The organic layer was dried over Na₂SO₄ and concentrated in vacuo. The residue was purified by MPLC on silica gel (petrol ether/EtOAc) to afford heteroarylphenyls **31a-d** or **36**.

General procedure C for the coupling of mannosylated phenyls with substituted pyrrolyl halides. A Schlenk tube was charged with phenyl halide **28**, **34** or **39** (1.0 eq), pyrrolyl halide **20a-f** (1.2 eq), CuI (0.05 eq), (±)-*trans*-1,2-diaminocyclohexane (0.11 eq), K₃PO₄ (2.1 eq) and a stirring bar. The tube was closed with a rubber septum and was evacuated and flushed with argon. This procedure was repeated once, then anhydrous 1,4-dioxane (ca. 0.5 mL, 1 M to phenyl halide) was added under a stream of argon. The mixture was degassed in an ultrasonic bath and flushed with argon for 5 min, and then stirred at 110 °C for 24 h. The reaction mixture was cooled to rt, diluted with EtOAc (50 mL), and filtered through Celite. The filtrate was concentrated in vacuo and co-evaporated with toluene. The residue was acetylated with pyridine/acetic anhydride/DMAP, concentrated and purified by MPLC on silica gel (petrol ether/EtOAc) to afford pyrrolylphenyls **40a-f**, **46** or **47**.

General procedure D for deacetylation: To a solution of **22a,b**, **25a,b**, **31a-d**, **36**, **40a-f**, **46** or **47** (1.0 eq) in dry MeOH (5 mL) for producing methyl ester or in dry EtOH (5 mL) for producing ethyl ester, was added freshly prepared 1 M NaOMe/MeOH or NaOEt/EtOH (0.1 eq) under argon. The mixture was stirred at rt until the reaction was complete (monitored by TLC), then neutralized with Amberlyst-15 (H⁺) ion-exchange resin, filtered and concentrated in vacuo. The residue was purified by MPLC on silica gel

(DCM/MeOH, 10:1 to 8:1 for methyl esters or DCM/EtOH, 3:1 for ethyl esters) to afford **23a-c**, **26a-b**, **32a-d**, **37**, **41a-f**, **48** or **49**.

General procedure E for saponification: To a solution of **22a,b**, **25a,b**, **31a-d**, **36**, **40a-f**, **46** or **47** (1.0 eq) in MeOH (5 mL) was added 1 M NaOMe/MeOH (0.1 eq) at rt. The reaction mixture was stirred at rt for 4 h and concentrated. The residue was treated with 0.5 M aq. NaOH (1 mL) for 24 h at rt. Then the pH was adjusted to 3-4 with Amberlyst-15 (H⁺) and the mixture was filtered and concentrated. The crude product was transformed into the sodium salt by passing through a small column of Dowex 50X8 (Na⁺ form) ion-exchange resin. After concentration the residue was purified by MPLC (RP-18, H₂O/MeOH, 1:0 to 2:1) followed by size-exclusion chromatography (P-2 gel, H₂O) to yield **24a,b**, **27a,b**, **33a-d**, **38**, **42-45**, **50** or **51** as white solids after final lyophilization from water.

Ethyl 1-[4-(2,3,4,6-tetra-*O*-acetyl- α -D-mannopyranosyloxy)phenyl]-1*H*-1,2,3-triazole-4-carboxylate (22a). Prepared according to general procedure A from **21** and **11a**. Yield: 341 mg (79%) as colorless oil. *R*_f 0.30 (petrol ether/EtOAc, 1:1); [α]_D²⁰ +76.7 (*c* 0.90, MeOH); ¹H NMR (500 MHz, CDCl₃): δ = 8.47 (s, 1H, triazole), 7.72-7.70 (m, 2H, Ar-H), 7.29-7.27 (m, 2H, Ar-H), 5.60 (d, *J* = 1.7 Hz, 1H, H-1), 5.56 (dd, *J* = 3.0, 10.0 Hz, 1H, H-3), 5.48 (dd, *J* = 1.9, 3.0 Hz, 1H, H-2), 5.40 (t, *J* = 10.0 Hz, 1H, H-4), 4.47 (dd, *J* = 7.2, 14.2 Hz, 2H, OCH₂), 4.29 (dd, *J* = 5.4, 12.4 Hz, 1H, H-6a), 4.11-4.07 (m, 2H, H-5, H-6b), 2.22, 2.07, 2.06, 2.05 (4 s, 12H, 4 COCH₃), 1.44 (t, *J* = 7.2 Hz, 3H, CH₃); ¹³C NMR (126 MHz, CDCl₃): δ = 170.48, 170.01, 169.99, 169.69, 160.61 (5 CO), 156.17, 140.87, 131.60, 125.52, 122.46, 117.62 (8C, Ar-C), 95.89 (C-1), 69.54 (C-5), 69.14 (C-2), 68.66 (C-3), 65.71 (C-4), 62.03 (C-6), 61.55 (OCH₂), 20.88, 20.71, 20.70 (4C, 4 COCH₃), 14.34 (CH₃); ESI-MS: *m/z*: Calcd for C₂₅H₃₀N₃O₁₂ [M+H]⁺: 564.18, found: 564.20.

Methyl 1-[4-(α -D-mannopyranosyloxy)phenyl]-1*H*-1,2,3-triazole-4-carboxylate (23a). Prepared according to general procedure D from **22a**. Yield: 28 mg (74%) as white solid. *R*_f 0.20 (DCM/MeOH, 8:1); [α]_D²⁰ +99.8 (*c* 0.30, MeOH); ¹H NMR (500 MHz, CD₃OD): δ = 8.94 (s, 1H, Ar-H), 7.72-7.69 (m, 2H, Ar-H), 7.25-7.23 (m, 2H, Ar-H), 5.48 (d, *J* = 1.7 Hz, 1H, H-1), 3.94 (dd, *J* = 1.9, 3.4 Hz, 1H, H-2), 3.85 (s, 3H, OCH₃), 3.81

(dd, $J = 3.5, 9.5$ Hz, 1H, H-3), 3.70-3.60 (m, 3H, H-4, H-6), 3.48 (ddd, $J = 2.4, 5.5, 9.7$ Hz, 1H, H-5); ^{13}C NMR (126 MHz, CD_3OD): $\delta = 162.33$ (CO), 158.64, 141.14, 132.38, 127.77, 123.47, 118.81 (8C, Ar-C), 100.26 (C-1), 75.77 (C-5), 72.34 (C-3), 71.82 (C-2), 68.27 (C-4), 62.68 (C-6), 52.66 (OCH_3); HRMS: m/z : Calcd for $\text{C}_{16}\text{H}_{19}\text{N}_3\text{NaO}_8$ $[\text{M}+\text{Na}]^+$: 404.1064, found: 404.1068.

Sodium 1-[4-(α -D-mannopyranosyloxy)phenyl]-1H-1,2,3-triazole-4-carboxylate (24a). Prepared according to general procedure E from **22a**. Yield: 5 mg (30%) as white solid. $[\alpha]_{\text{D}}^{20} +92.0$ (c 0.20, $\text{MeOH}/\text{H}_2\text{O}$, 1:1); ^1H NMR (500 MHz, D_2O): $\delta = 8.40$ (s, 1H, Ar-H), 7.58-7.56 (m, 2H, Ar-H), 7.18-7.16 (m, 2H, Ar-H), 5.55 (d, $J = 1.4$ Hz, 1H, H-1), 4.08 (dd, $J = 1.9, 3.4$ Hz, 1H, H-2), 3.95 (dd, $J = 3.5, 9.5$ Hz, 1H, H-3), 3.73-3.57 (m, 4H, H-4, H-5, H-6); ^{13}C NMR (126 MHz, D_2O): $\delta = 167.44$ (CO), 156.00, 145.08, 131.02, 125.53, 122.73, 117.65 (8C, Ar-C), 97.98 (C-1), 73.41 (C-5), 70.26, 69.72, 66.51 (C-2, C-3, C-4), 60.60 (C-6); HRMS: m/z : Calcd for $\text{C}_{15}\text{H}_{17}\text{N}_3\text{NaO}_8$ $[\text{M}+\text{H}]^+$: 390.0908, found: 390.0905.

Methyl 5-[4-(2,3,4,6-tetra-*O*-acetyl- α -D-mannopyranosyloxy)phenyl]-picolinate (31a). Prepared according to general procedure B from **29** (120 mg, 0.21 mmol) and methyl 5-bromopicolinate (**30a**, 40 mg, 0.19 mmol). Yield: 62 mg (60%) as white solid. R_f 0.33 (petrol ether/EtOAc, 2:3); $[\alpha]_{\text{D}}^{20} +47.3$ (c 0.60, MeOH); ^1H NMR (500 MHz, CDCl_3): $\delta = 8.93$ (dd, $J = 0.5, 2.2$ Hz, 1H, Ar-H), 8.20 (dd, $J = 0.6, 8.2$ Hz, 1H, Ar-H), 7.99 (dd, $J = 2.4, 8.2$ Hz, 1H, Ar-H), 7.61-7.58 (m, 2H, Ar-H), 7.25-7.23 (m, 2H, Ar-H), 5.60 (d, $J = 1.8$ Hz, 1H, H-1), 5.59 (dd, $J = 3.6, 10.1$ Hz, 1H, H-3), 5.48 (dd, $J = 1.9, 3.5$ Hz, 1H, H-2), 5.41 (t, $J = 10.1$ Hz, 1H, H-4), 4.30 (dd, $J = 5.0, 12.4$ Hz, 1H, H-6a), 4.11-4.08 (m, 2H, H-5, H-6b), 4.04 (s, 3H, OCH_3), 2.23, 2.07, 2.06, 2.05 (4 s, 12H, 4 COCH_3); ^{13}C NMR (126 MHz, CDCl_3): $\delta = 170.49, 170.01, 169.99, 169.70, 165.61$ (5 CO), 156.25, 147.93, 146.20, 138.97, 134.70, 131.35, 128.69, 125.25, 117.22 (11C, Ar-C), 95.71 (C-1), 69.34 (C-2), 69.25 (C-5), 68.78 (C-3), 65.79 (C-4), 62.02 (C-6), 52.94 (OCH_3), 20.89, 20.71, 20.69, 20.68 (4 COCH_3); ESI-MS: m/z : Calcd for $\text{C}_{27}\text{H}_{30}\text{NO}_{12}$ $[\text{M}+\text{H}]^+$: 560.18, found: 560.27.

Methyl 5-[4-(α -D-mannopyranosyloxy)phenyl]-picolinate (32a). Prepared according to general procedure D from **31a**. Yield: 15 mg (36%) as white solid. R_f 0.13 (DCM/MeOH ,

8:1); $[\alpha]_{\text{D}}^{20} +113.4$ (*c* 0.20, MeOH); ^1H NMR (500 MHz, DMSO-*d*₆): δ = 9.18 (d, *J* = 2.2 Hz, 1H, Ar-H), 8.37 (dd, *J* = 2.2, 8.4 Hz, 1H, Ar-H), 8.20 (d, *J* = 8.9 Hz, 2H, Ar-H), 8.14 (d, *J* = 8.4 Hz, 1H, Ar-H), 7.29 (t, *J* = 5.8 Hz, 2H, Ar-H), 5.55 (d, *J* = 1.6 Hz, 1H, H-1), 5.15 (d, *J* = 4.2 Hz, 1H), 4.93 (d, *J* = 5.7 Hz, 1H), 4.87 (d, *J* = 5.6 Hz, 1H), 4.54 (t, *J* = 6.0 Hz, 1H), 3.96 (s, 3H, OCH₃), 3.92 (s, 1H), 3.76 (m, 1H), 3.66 (ddd, *J* = 1.9, 5.8, 11.6 Hz, 1H), 3.61-3.49 (m, 2H), 3.45 (m, 1H); ^{13}C NMR (126 MHz, DMSO-*d*₆): δ = 165.20 (CO), 159.29, 158.04, 150.07, 137.81, 130.95, 128.57, 123.30, 119.25, 116.83 (11C, Ar-C), 98.55 (C-1), 75.10 (C-5), 70.59, 69.94, 66.59 (C-2, C-3, C-4), 60.94 (C-6), 52.32 (OCH₃); HRMS: *m/z*: Calcd for C₁₉H₂₁NNaO₈ [M+Na]⁺: 414.1159, found: 414.1162.

Sodium 5-[4-(α -D-mannopyranosyloxy)phenyl]-picolinate (33a). Prepared according to general procedure E from **31a**. Yield: 3 mg (32%) as white solid. $[\alpha]_{\text{D}}^{20} +99.3$ (*c* 0.20, MeOH/H₂O, 1:1); ^1H NMR (500 MHz, D₂O): δ = 8.63 (s, 1H, Ar-H), 7.96 (d, *J* = 8.0 Hz, 1H, Ar-H), 7.82 (d, *J* = 6.6 Hz, 1H, Ar-H), 7.56-7.54 (m, 2H, Ar-H), 7.13-7.11 (m, 2H, Ar-H), 5.54 (d, *J* = 1.4 Hz, 1H, H-1), 4.07 (m, 1H, H-2), 3.96 (dd, *J* = 3.5, 9.2 Hz, H-3), 3.70-3.58 (m, 4H, H-4, H-5, H-6); ^{13}C NMR (126 MHz, D₂O): δ = 155.75, 146.29, 135.43, 131.05, 128.42, 123.82, 117.39 (11C, Ar-C), 97.91 (C-1), 73.33 (C-5), 70.31, 69.80, 66.51 (C-2, C-3, C-4), 60.59 (C-6); HRMS: *m/z*: Calcd for C₁₈H₁₉NNaO₈ [M+Na]⁺: 400.1003, found: 400.1003.

Methyl 5-[4-(2,3,4,6-tetra-*O*-acetyl- α -D-mannopyranosyloxy)-3-trifluoromethylphenyl]-picolinate (36). A Schlenk tube was charged with **34**^[10j] (394 mg, 0.69 mmol), KOAc (203 mg, 2.07 mmol), bis(pinacolato)diborane (193 mg, 0.76 mmol) and Pd(dppf)Cl₂·CH₂Cl₂ (17 mg, 0.021 mmol). The tube was closed, evacuated and flushed with argon. Then anhydrous DMF (4 mL) was added under a stream of argon. The mixture was degassed in an ultrasonic bath and flushed with argon for 5 min, and then stirred at 85 °C overnight. The reaction mixture was cooled to rt and diluted with DCM/H₂O (100 mL, 1:1). The organic layer was washed with H₂O (50 mL) and brine (50 mL), dried over Na₂SO₄ and concentrated. The residue was passed through a short silica gel column (petrol ether/EtOAc, 2:1) to afford crude **35** (352 mg), which was used directly in the next step. Compound **36** was prepared according to general procedure B from crude **35** (352 mg, 0.57 mmol) and methyl 5-chloropyrazine-2-carboxylate (**30a**, 108 mg, 0.63 mmol). Yield: 205 mg (57%) as colorless oil. *R_f* 0.38 (petrol ether/EtOAc,

2:3); $[\alpha]_{\text{D}}^{20} +64.5$ (*c* 1.00, EtOAc); $^1\text{H NMR}$ (500 MHz, CDCl_3): $\delta = 8.92$ (d, $J = 2.1$ Hz, 1H, Ar-H), 8.23 (d, $J = 8.1$ Hz, 1H, Ar-H), 8.00 (dd, $J = 2.3, 8.1$ Hz, 1H, Ar-H), 7.87 (d, $J = 2.1$ Hz, 1H, Ar-H), 7.77 (dd, $J = 2.2, 8.6$ Hz, 1H, Ar-H), 7.41 (d, $J = 8.7$ Hz, 1H, Ar-H), 5.72 (d, $J = 1.7$ Hz, 1H, H-1), 5.56 (dd, $J = 3.4, 10.1$ Hz, 1H, H-3), 5.50 (dd, $J = 1.9, 3.4$ Hz, 1H, H-2), 5.43 (t, $J = 10.1$ Hz, 1H, H-4), 4.30 (dd, $J = 5.1, 12.5$ Hz, 1H, H-6a), 4.16-4.02 (m, 6H, H-6b, H-5, OCH_3), 2.23, 2.06 (2s, 12H, 4 COCH_3); $^{13}\text{C NMR}$ (126 MHz, CDCl_3): $\delta = 170.40, 169.94, 169.73, 169.62, 165.41$ (5 CO), 153.59, 147.93, 146.98, 137.80, 134.99, 132.06, 131.21, 126.32, 125.33, 116.15 (12C, Ar-C, CF_3), 95.71 (C-1), 70.06 (C-5), 69.10 (C-2), 68.52 (C-3), 65.48 (C-4), 61.95 (C-6), 53.03 (OCH_3), 20.85, 20.68 (4C, 4 COCH_3); ESI-MS: m/z : Calcd for $\text{C}_{28}\text{H}_{29}\text{F}_3\text{NO}_{12}$ $[\text{M}+\text{H}]^+$: 628.16, found: 628.19.

Methyl 5-[4-(α -D-mannopyranosyloxy)-3-trifluoromethyl-phenyl]-picolinate (37).

Prepared according to general procedure D from **36**. Yield: 15 mg (60%) as white solid. R_f 0.20 (DCM/MeOH, 8:1); $[\alpha]_{\text{D}}^{20} +104.9$ (*c* 0.40, MeOH); $^1\text{H NMR}$ (500 MHz, CD_3OD): $\delta = 8.95$ (dd, $J = 0.7, 2.1$ Hz, 1H, Ar-H), 8.25 (qd, $J = 1.5, 8.2$ Hz, 2H, Ar-H), 8.06-7.92 (m, 2H, Ar-H), 7.68 (m, 1H, Ar-H), 5.72 (d, $J = 1.6$ Hz, 1H, H-1), 4.09 (dd, $J = 1.8, 3.4$ Hz, 1H, H-2), 4.02 (s, 3H, OCH_3), 3.96 (dd, $J = 3.4, 9.5$ Hz, 1H, H-3), 3.86-3.69 (m, 3H, H-4, H-6), 3.60 (ddd, $J = 2.3, 5.7, 9.7$ Hz, 1H, H-5); $^{13}\text{C NMR}$ (126 MHz, CD_3OD): $\delta = 166.43$ (CO), 156.19, 148.61, 147.34, 139.82, 136.84, 133.76, 131.17, 126.81, 126.58, 118.09 (12C, Ar-C, CF_3), 100.31 (C-1), 76.24 (C-5), 72.25 (C-3), 71.71 (C-2), 68.11 (C-4), 62.70 (C-6), 53.28 (OCH_3); HRMS: m/z : Calcd for $\text{C}_{20}\text{H}_{20}\text{F}_3\text{NNaO}_8$ $[\text{M}+\text{Na}]^+$: 482.1033, found: 482.0135.

Sodium 5-[4-(α -D-mannopyranosyloxy)-3-trifluoromethyl-phenyl]-picolinate (38).

Prepared according to general procedure E from **36**. Yield: 40 mg (90%) as white solid. $[\alpha]_{\text{D}}^{20} +71.4$ (*c* 0.50, MeOH/ H_2O , 1:1); $^1\text{H NMR}$ (500 MHz, CD_3OD): $\delta = 8.70$ (s, 1H, Ar-H), 8.00 (s, 2H, Ar-H), 7.86-7.77 (m, 2H, Ar-H), 7.53 (m, 1H, Ar-H), 5.58 (d, $J = 1.3$ Hz, 1H, H-1), 3.97 (dd, $J = 1.8, 3.3$ Hz, 1H, H-2), 3.85 (dd, $J = 3.4, 9.5$ Hz, 1H, H-3), 3.73-3.59 (m, 3H, H-4, H-6), 3.49 (m, 1H, H-5); $^{13}\text{C NMR}$ (126 MHz, CD_3OD): $\delta = 172.52$ (CO), 155.69, 155.16, 147.65, 137.21, 136.17, 133.48, 132.31, 132.21, 126.48, 125.22, 118.01, 101.40 (12C, Ar-C, CF_3), 100.33 (C-1), 76.15 (C-5), 72.26 (C-3), 71.75

(C-2), 68.12 (C-4), 62.66 (C-6); HRMS: m/z : Calcd for $C_{19}H_{18}F_3NNa_2O_8$ $[M+Na]^+$: 490.0696, found: 490.0713.

Ethyl 1-[4-(2,3,4,6-tetra-*O*-acetyl- α -D-mannopyranosyloxy)-3-chlorophenyl]-4-methyl-1*H*-pyrrole-3-carboxylate (40f). Prepared according to general procedure C from **39** and methyl 4-methyl-1*H*-pyrrole-3-carboxylate (**20f**). Yield: 240 mg (77%) as colorless oil. R_f 0.34 (petrol ether/EtOAc, 3:2); $[\alpha]_D^{20}$ +64.5 (c 1.00, EtOAc); 1H NMR (500 MHz, $CDCl_3$): δ = 7.55 (d, J = 2.5 Hz, 1H, Ar-H), 7.46 (m, 1H, Ar-H), 7.28-7.20 (m, 2H, Ar-H), 6.76 (dd, J = 1.0, 2.4 Hz, 1H, Ar-H), 5.61 (dd, J = 3.4, 10.0 Hz, 1H, H-3), 5.57 (d, J = 1.7 Hz, 1H, H-1), 5.54 (dd, J = 1.9, 3.4 Hz, 1H, H-2), 5.41 (t, J = 10.1 Hz, 1H, H-4), 4.33-4.26 (m, 3H, H-6b, OCH_2), 4.19 (ddd, J = 2.2, 5.3, 10.1 Hz, 1H, H-5), 4.12 (m, 1H, H-6a), 2.31 (d, J = 0.8 Hz, 3H, CH_3), 2.21, 2.08, 2.05 (3 s, 12H, 4 $COCH_3$), 2.04 (s, 1H), 1.36 (t, J = 7.1 Hz, 3H, CH_3); ^{13}C NMR (126 MHz, $CDCl_3$): δ = 170.41, 169.93, 169.77, 169.73, 164.95 (5 CO), 149.71, 135.88, 125.46, 124.71, 123.48, 122.80, 119.68, 118.99, 117.93, 117.13 (Ar-C), 96.98 (C-1), 69.92 (C-5), 69.26 (C-2), 68.71 (C-3), 65.79 (C-4), 62.13 (C-6), 59.58 (OCH_2), 21.03, 20.85, 20.70, 20.68 (4 $COCH_3$), 14.51 (CH_3), 11.72 (CH_3); ESI-MS: m/z : Calcd for $C_{28}H_{32}ClNNaO_{12}$ $[M+Na]^+$: 632.15, found: 632.15.

Ethyl 1-[3-chloro-4-(α -D-mannopyranosyloxy)phenyl]-4-methyl-1*H*-pyrrole-3-carboxylate (41f). Prepared according to general procedure D from **40f**. Yield: 55 mg (93%) as white solid. R_f 0.29 (DCM/MeOH, 9:1); $[\alpha]_D^{20}$ +89.1 (c 0.50, MeOH); 1H NMR (500 MHz, CD_3OD): δ = 7.68 (d, J = 2.5 Hz, 1H, Ar-H), 7.58 (d, J = 2.7 Hz, 1H, Ar-H), 7.47 (d, J = 8.9 Hz, 1H, Ar-H), 7.39 (dd, J = 2.7, 8.9 Hz, 1H, Ar-H), 6.95 (d, J = 1.0 Hz, 1H, Ar-H), 5.58 (d, J = 1.4 Hz, 1H, H-1), 4.28 (q, J = 7.1 Hz, 2H, OCH_2), 4.14 (dd, J = 1.8, 3.2 Hz, 1H, H-2), 4.01 (dd, J = 3.4, 9.5 Hz, 1H, H-3), 3.86-3.72 (m, 3H, H-4, H-6), 3.67 (m, 1H, H-5), 2.29 (s, 3H, CH_3), 1.37 (t, J = 7.1 Hz, 3H, CH_3); ^{13}C NMR (126 MHz, CD_3OD): δ = 166.98 (CO), 151.75, 136.28, 126.11, 125.75, 124.16, 123.19, 120.88, 120.51, 119.26, 117.60 (Ar-C), 101.01 (C-1), 76.04 (C-5), 72.36 (C-3), 71.78 (C-2), 68.19 (C-4), 62.66 (C-6), 60.74 (OCH_2), 14.77 (CH_3), 11.96 (CH_3); HRMS: m/z : Calcd for $C_{20}H_{24}ClNNaO_8$ $[M+Na]^+$: 464.1083, found: 464.1086.

Sodium 1-[3-chloro-4-(α -D-mannopyranosyloxy)phenyl]-4-methyl-1*H*-pyrrole-3-carboxylate (45). Prepared according to general procedure E from **40f**. Yield: 30 mg (57%) as white solid. ^1H NMR (500 MHz, CD_3OD): δ = 7.69 (d, J = 2.5 Hz, 1H, Ar-H), 7.60 (d, J = 2.6 Hz, 1H, Ar-H), 7.48 (d, J = 8.9 Hz, 1H, Ar-H), 7.42 (dd, J = 2.7, 8.9 Hz, 1H, Ar-H), 6.97 (d, J = 1.2 Hz, 1H, Ar-H), 5.57 (d, J = 1.4 Hz, 1H, H-1), 4.13 (dd, J = 1.8, 3.2 Hz, 1H, H-2), 4.00 (dd, J = 3.4, 9.5 Hz, 1H, H-3), 3.87-3.70 (m, 3H, H-4, H-6), 3.66 (ddd, J = 2.2, 5.5, 9.6 Hz, 1H, H-5), 2.30 (s, 3H, CH_3); ^{13}C NMR (126 MHz, CD_3OD): δ = 168.95 (CO), 151.77, 136.47, 126.41, 125.80, 124.42, 123.25, 120.95, 120.51, 119.34, 118.09 (Ar-C), 101.08 (C-1), 76.08 (C-5), 72.39 (C-3), 71.82 (C-2), 68.23 (C-4), 62.69 (C-6), 11.92 (CH_3); HRMS: m/z : Calcd for $\text{C}_{18}\text{H}_{20}\text{ClNNaO}_8$ $[\text{M}+\text{H}]^+$: 436.0770, found: 436.0773.

Ethyl 1-[4-(2,3,4,6-tetra-*O*-acetyl- α -D-mannopyranosyloxy)phenyl]-4-methyl-1*H*-pyrrole-3-carboxylate (46). Prepared according to general procedure C from **28** and methyl 4-methyl-1*H*-pyrrole-3-carboxylate (**20f**). Yield: 293 mg (94%) as colorless oil. R_f 0.47 (petrol ether/EtOAc, 3:2); $[\alpha]_{\text{D}}^{20}$ +63.7 (c 2.20, EtOAc); ^1H NMR (500 MHz, CDCl_3): δ = 7.36 (d, J = 2.4 Hz, 1H, Ar-H), 7.20 (d, J = 8.8 Hz, 1H, Ar-H), 7.15 (dd, J = 2.5, 8.7 Hz, 1H, Ar-H), 6.91 (d, J = 1.6 Hz, 1H, Ar-H), 6.67 (d, J = 0.9 Hz, 1H, Ar-H), 5.62 (dd, J = 3.5, 10.0 Hz, 1H, H-3), 5.57 (d, J = 1.6 Hz, 1H, H-1), 5.53 (dd, J = 1.9, 3.4 Hz, 1H, H-2), 5.40 (t, J = 10.1 Hz, 1H, H-4), 4.31 (dd, J = 5.3, 12.3 Hz, 1H, H-6a), 4.20 (ddd, J = 2.2, 5.2, 10.1 Hz, 1H, H-5), 4.18-4.08 (m, 3H, OCH_2 , H-6b), 2.21, 2.11, 2.08, 2.07, 2.05 (5 s, 15H, 4 COCH_3 , CH_3), 1.23 (t, J = 7.1 Hz, 3H, CH_3); ^{13}C NMR (126 MHz, CDCl_3): δ = 170.52, 169.91, 169.75, 160.32 (5C, 5 CO), 150.69, 136.26, 128.55, 128.10, 125.80, 123.86, 123.18, 120.00, 119.90, 116.17 (Ar-C), 96.86 (C-1), 69.83 (C-5), 69.32 (C-2), 68.75 (C-3), 65.81 (C-4), 62.08 (C-6), 59.90 (OCH_2), 20.85, 20.71, 20.68, 14.27, 11.43 (6C, 4 COCH_3 , 2 CH_3); ESI-MS: m/z : Calcd for $\text{C}_{28}\text{H}_{33}\text{NNaO}_{12}$ $[\text{M}+\text{Na}]^+$: 598.19, found: 598.16.

Ethyl 1-[4-(α -D-mannopyranosyloxy)phenyl]-4-methyl-1*H*-pyrrole-3-carboxylate (48). Prepared according to general procedure D from **46**. Yield: 87 mg (46%) as white solid. R_f 0.30 (DCM/MeOH, 8:1); $[\alpha]_{\text{D}}^{20}$ +109.7 (c 0.80, MeOH); ^1H NMR (500 MHz, CD_3OD): δ = 7.67 (d, J = 2.5 Hz, 1H, Ar-H), 7.46-7.41 (m, 2H, Ar-H), 7.27-7.22 (m, 2H, Ar-H), 6.95 (dd, J = 1.0, 2.4 Hz, 1H, Ar-H), 5.52 (d, J = 1.6 Hz, 1H, H-1), 4.29 (q, J = 7.1

Hz, 2H, OCH₂), 4.04 (dd, $J = 1.8, 3.4$ Hz, 1H, H-2), 3.92 (dd, $J = 3.4, 9.4$ Hz, 1H, H-3), 3.84-3.70 (m, 3H, H-4, H-6), 3.62 (ddd, $J = 2.4, 5.4, 9.7$ Hz, 1H, H-5), 2.30 (d, $J = 0.9$ Hz, 3H, CH₃), 1.37 (t, $J = 7.1$ Hz, 3H, CH₃); ¹³C NMR (126 MHz, CD₃OD): $\delta = 167.22$ (CO), 156.53, 135.97, 126.23, 123.86, 122.85, 120.73, 118.92, 117.13 (8C, Ar-C), 100.47 (C-1), 75.57 (C-5), 72.41 (C-3), 71.95 (C-2), 68.35 (C-4), 62.72 (C-6), 60.68 (OCH₂), 14.80, 11.98 (2 CH₃); HRMS: m/z : Calcd for C₂₀H₂₅NNaO₈ [M+Na]⁺: 430.1472, found: 430.1474.

Sodium 1-[4-(α -D-mannopyranosyloxy)phenyl]-4-methyl-1*H*-pyrrole-3-carboxylate (50). Prepared according to general procedure E from **46**. Yield: 93 mg (99%) as white solid. $[\alpha]_D^{20} +97.0$ (c 0.70, MeOH/H₂O, 1:2); ¹H NMR (500 MHz, D₂O): $\delta = 7.51$ (d, $J = 2.4$ Hz, 1H, Ar-H), 7.42 (d, $J = 8.9$ Hz, 2H, Ar-H), 7.22 (d, $J = 8.9$ Hz, 2H, Ar-H), 6.93 (s, 1H, Ar-H), 5.60 (s, 1H, H-1), 4.19 (m, 1H, H-2), 4.07 (dd, $J = 3.4, 8.9$ Hz, 1H, H-3), 3.90-3.68 (m, 4H, H-4, H-5, H-6), 2.27 (s, 3H, CH₃); ¹³C NMR (125 MHz, D₂O): $\delta = 174.29$ (CO), 153.52, 135.00, 123.89, 121.84, 121.78, 121.56, 119.09, 118.07 (10C, Ar-C), 98.45 (C-1), 73.40 (C-5), 70.39 (C-3), 69.88 (C-2), 66.58 (C-4), 60.65 (C-6), 10.97 (CH₃); HRMS: m/z : Calcd for C₁₈H₂₁NNaO₈ [M+Na]⁺: 402.1159, found: 402.1159.

Cell-free competitive binding assay.

A recombinant protein consisting of the CRD of FimH linked with a thrombin cleavage site to a 6His-tag (FimH-CRD-Th-6His) was expressed in *E. coli* strain HM125 and purified by affinity chromatography.^[23] To determine the affinity of the various FimH antagonists, a competitive binding assay as described previously was applied.^[23] Microtiter plates (F96 MaxiSorp, Nunc) were coated with 100 μ L/well of a 10 μ g/mL solution of FimH-CRD-Th-6His in 20 mM HEPES, 150 mM NaCl, and 1 mM CaCl₂, pH 7.4 (assay buffer) overnight at 4 °C. The coating solution was discarded and the wells were blocked with 150 μ L/well of 3% BSA in assay buffer for 2 h at 4 °C. After three washing steps with assay buffer (150 μ L/well), a 4-fold serial dilution of the test compound (50 μ L/well) in assay buffer containing 5% DMSO and streptavidin-peroxidase coupled to Man- α (1-3)[Man- α (1-6)]-Man- β (1-4)-GlcNAc- β (1-4)-GlcNAc β polyacrylamide (TM-PAA) polymer (50 μ L/well of a 0.5 μ g/mL solution) were added. On each individual microtiter plate, *n*-heptyl α -D-mannopyranoside (**1**) was tested in

parallel. The plates were incubated for 3 h at 25 °C and 350 rpm and then carefully washed four times with 150 μL /well assay buffer. After the addition of 100 μL /well of 2,2'-azino-di-(3-ethylbenzthiazoline-6-sulfonic acid) (ABTS)-substrate, the colorimetric reaction was allowed to develop for 4 min and then was stopped by the addition of 2% aq. oxalic acid before the optical density (OD) was measured at 415 nm on a microplate-reader (Spectramax 190, Molecular Devices, Silicon Valley, CA, USA). The IC_{50} values of the compounds tested in duplicates were calculated with prism software (GraphPad Software, Inc., La Jolla, CA, USA). The IC_{50} defines the molar concentration of the test compound that reduces the maximal specific binding of TM-PAA polymer to FimH-CRD by 50%. The relative IC_{50} (rIC_{50}) is the ratio of the IC_{50} of the test compound to the IC_{50} of *n*-heptyl α -D-mannopyranoside (**1**).

K_D determination with fluorescence polarization assay.

The fluorescently labeled ligand **52**^[11k] was used for the competitive fluorescence polarization assay. A serial dilution of non-labeled FimH antagonist with final concentrations ranging from 0-10 μM was titrated into 96-well NBSTM plates to a final volume of 200 μL containing a constant concentration of protein (final concentration 25 nM) and FITC-labeled ligand **52** which was fixed at a higher concentration in competitive binding assays to obtain higher fluorescence intensities (final concentration 20 nM). Prior to measuring the fluorescence polarization, the plates were incubated on a shaker for 24 h at rt until the reaction reached its equilibrium. The IC_{50} value was determined with Prism (GraphPad Software Inc., La Jolla, CA, USA) by applying a standard four-parameter IC_{50} function. The obtained IC_{50} values were converted into their corresponding K_D values using the following derivation of the Cheng-Prusoff equation (Equation 1):^[25]

$$K_D = \frac{I_{50}}{\frac{L_{50}}{K_D} + \frac{P_0}{K_D} + 1} \quad (1)$$

where I_{50} and L_{50} are the concentrations of inhibitor and ligand at half-maximal inhibition, respectively, and P_0 is the free concentration of protein in the absence of inhibitor. This variation of the Cheng-Prusoff equation is applied to competition assays with tight-binding inhibitors. However, the K_D for antagonists, which have a higher affinity towards FimH than the labeled ligand could not be accurately determined with this equation.^[25]

Physicochemical properties and in vitro pharmacokinetics

Materials. Dimethyl sulfoxide (DMSO), 1-propanol, 1-octanol, Dulbecco's Modified Eagle's Medium (DMEM) high glucose, penicillin-streptomycin (solution stabilized, with 10'000 units penicillin and 10 mg streptomycin/mL), L-glutamine solution (200 mM), magnesium chloride, ammonium acetate, and bis(4-nitrophenyl) phosphate (BNPP) were purchased from Sigma-Aldrich (Buchs, Switzerland). PRISMA HT universal buffer, GIT-0 Lipid Solution, and Acceptor Sink Buffer were ordered from pIon (Woburn, MA, USA). MEM non-essential amino acids solution 10 mM (100X), fetal bovine serum (FBS), and DMEM without sodium pyruvate and phenol red were bought from Invitrogen (Carlsbad, CA, USA). Acetonitrile (MeCN) and methanol (MeOH) were ordered from Acros Organics (Geel, Belgium). Pooled male rat liver microsomes (Sprague Dawley) were ordered from BD Bioscience (Franklin Lakes, NJ, USA). The Caco-2 cells were kindly provided by Prof G. Imanidis, FHNW, Muttens, Switzerland and originated from the American Type Culture Collection (Rockville, MD, USA).

log P determination. The in silico prediction tool ALOGPS^[42] was used to estimate the octanol-water partition coefficient ($\log P$) of the compounds. Depending on these values, the compounds were classified into three categories: hydrophilic compounds ($\log P < 0$), moderately lipophilic compounds ($\log P$ between 0 and 1) and lipophilic compounds ($\log P > 1$). For each category, two different ratios (volume of 1-octanol to volume of buffer) were defined as experimental parameters (Table 4).

Table 4. Parameters for the experimental determination of lipophilicity.

Compound type	$\log P$	ratios (1-octanol: buffer)
hydrophilic	< 0	30:140, 40:130
moderately lipophilic	0 - 1	70:110, 110:70
lipophilic	> 1	3:180, 4:180

Equal amounts of phosphate buffer (0.1 M, pH 7.4) and 1-octanol were mixed and shaken vigorously for 5 min to saturate the phases. The mixture was left until separation of the two phases occurred, and the buffer was retrieved. Stock solutions of the test compounds were diluted with buffer to a concentration of 1 μ M. For each compound, six determinations, i.e. three determinations per 1-octanol:buffer ratio, were performed in

different wells of a 96-well plate. The respective volumes of buffer containing analyte (1 μM) were pipetted to the wells and covered by saturated 1-octanol according to the chosen volume ratio. The plate was sealed with aluminium foil, shaken (1350 rpm, 25 °C, 2 h) on a Heidolph Titramax 1000 plate-shaker (Heidolph Instruments GmbH & Co. KG, Schwabach, Germany) and centrifuged (2000 rpm, 25 °C, 5 min, 5804R Eppendorf centrifuge, Hamburg, Germany). The aqueous phase was transferred to a 96-well plate for analysis by liquid chromatography-mass spectrometry (LC-MS, see below). The partition coefficient ($\log P$) was calculated from the 1-octanol:buffer ratio (o:b), the initial concentration of the analyte in buffer (1 μM), and the concentration of the analyte in buffer (c_B) according to Equation 2:

$$\log P = \log \frac{1}{c_B} \frac{M}{o:b} \quad (2)$$

The average of the three $\log P$ values per 1-octanol:buffer ratio was calculated. If the two means obtained for a compound did not differ by more than 0.1 units, the results were accepted.

Aqueous solubility. Solubility was determined in a 96-well format using the μSOL Explorer solubility analyzer (pIon, version 3.4.0.5). For each compound, measurements were performed in triplicate. Three wells of a deep well plate were filled with 300 μL of PRISMA HT universal buffer, adjusted to pH 7.4 by adding the requested amount of NaOH (0.5 M). Aliquots (3 μL) of a compound stock solution (40-100 mM in DMSO) were added and thoroughly mixed. The final sample concentration was 0.4-1.0 mM, the residual DMSO concentration was 1.0% (v/v). Fifteen hours after initiation of the experiment, the solutions were filtrated (0.2 μm 96-well filter plates) using a vacuum to collect manifold (Whatman Ltd., Maidstone, UK) and to remove any precipitates. Equal amounts of filtrate and 1-propanol were mixed and transferred to a 96-well plate for UV/Vis detection (190 to 500 nm, SpectraMax 190, Molecular Devices, Silicon Valley, CA, USA). The amount of material dissolved was calculated by comparison with the spectra obtained from reference samples, which were prepared by dissolving the compound stock solution in a 1:1 mixture of buffer and 1-propanol (final concentrations 0.067-0.167 mM).

Parallel artificial membrane permeability assay (PAMPA). Effective permeability ($\log P_e$) was determined in a 96-well format with PAMPA.^[29] For each compound, measurements were performed in quadruplicate. Four wells of a deep well plate were filled with 650 μL of PRISMA HT universal buffer, adjusted to pH 7.4 by adding the requested amount of NaOH (0.5 M). Samples (150 μL) were withdrawn from each well to determine the blank spectra by UV/Vis-spectroscopy (190 to 500 nm, SpectraMax 190). The analyte dissolved in DMSO was added to the remaining buffer to yield 50 μM solutions. To exclude precipitation, the optical density (OD) was measured at 650 nm, and solutions exceeding OD 0.01 were filtrated. Afterwards, samples (150 μL) were withdrawn to determine the reference spectra. Further 200 μL were transferred to each well of the donor plate of the PAMPA sandwich (pIon, P/N 110 163). The filter membranes at the bottom of the acceptor plate were infused with 5 μL of GIT-0 Lipid Solution, and 200 μL of Acceptor Sink Buffer were filled into each acceptor well. The sandwich was assembled, placed in the GutBoxTM, and left undisturbed for 16 h. Then, it was disassembled and samples (150 μL) were withdrawn from each donor and acceptor well for detection of the UV/Vis spectra. Effective permeability ($\log P_e$) was calculated from the compound flux deduced from the spectra, the filter area, and the initial sample concentration in the donor well with the aid of the PAMPA Explorer Software (pIon, version 3.5).

Colorectal adenocarcinoma (Caco-2) cell permeation assay. Caco-2 cells were cultivated in tissue culture flasks (BD Biosciences, Franklin Lakes, NJ, USA) with DMEM high glucose medium, containing L-glutamine (2 mM), non-essential amino acids (0.1 mM), penicillin (100 U/mL), streptomycin (100 $\mu\text{g/mL}$), and fetal bovine serum (10%). The cells were kept at 37 °C in humidified air containing 5% CO₂, and the medium was changed every second day. When approximately 90% confluence was reached, the cells were split in a 1:10 ratio and distributed to new tissue culture flasks. At passage numbers between 60 and 65, they were seeded at a density of 5.3×10^5 cells per well to Transwell 6-well plates (Corning Inc., Corning, NY, USA) with 2.5 mL of culture medium in the basolateral and 2 mL in the apical compartment. The medium was renewed on alternate days. Permeation experiments were performed between days 19 and 21 post seeding. Previously to the experiment, the integrity of the Caco-2 monolayers was evaluated by measuring the transepithelial electrical resistance (TEER) with an Endohm

tissue resistance instrument (World Precision Instruments Inc., Sarasota, FL, USA). Only wells with TEER values higher than $250 \Omega \text{ cm}^2$ were used. To inhibit carboxylesterase activity, the Caco-2 cell monolayers were pre-incubated with bis(4-nitrophenyl) phosphate (BNPP, $200 \mu\text{M}$) dissolved in transport medium (DMEM without sodium pyruvate and phenol red) for 40 min.^[43] Experiments were performed in the apical-to-basolateral (absorptive) and basolateral-to-apical (secretory) directions in triplicates. Transport medium was withdrawn from the donor compartments and replaced by the same volume of compound stock solution (10 mM in DMSO) to reach an initial sample concentration of $62.5 \mu\text{M}$. The Transwell plate was shaken (600 rpm , $37 \text{ }^\circ\text{C}$) on a Heidolph Titramax 1000 plate-shaker. Samples ($40 \mu\text{L}$) were withdrawn from the donor and acceptor compartments 30 min after initiation of the experiment and the concentrations were determined by LC-MS (see below). Apparent permeability (P_{app}) was calculated according to Equation 3:

$$P_{\text{app}} = \frac{dQ}{dt} \frac{1}{A c_0} \quad (3)$$

where dQ/dt is the compound flux (in mol s^{-1}), A is the surface area of the monolayer (in cm^2), and c_0 is the initial concentration in the donor compartment (in mol cm^{-3}).^[44] After the experiment, TEER values were assessed again and results from wells with values below $250 \Omega \text{ cm}^2$ were discarded.

Microsomal stability assay. Incubations were performed in duplicate in a 96-well format on an Eppendorf Thermomixer Comfort. The reaction mixture ($270 \mu\text{L}$) consisting of liver microsomes ($0.139 \mu\text{g/mL}$), TRIS-HCl buffer (0.1 M , $\text{pH } 7.4$) and MgCl_2 (2 mM) was preheated ($37 \text{ }^\circ\text{C}$, 500 rpm , 10 min), and the incubation was initiated by adding $30 \mu\text{L}$ of compound solution ($20 \mu\text{M}$ in TRIS-HCl buffer). The final concentration of the compound was $2 \mu\text{M}$, and the microsomal concentration was 0.125 mg/mL . At the beginning of the experiment ($t = 0 \text{ min}$) and after an incubation time of 5, 10, 20, 40, and 60 min, samples ($40 \mu\text{L}$) were transferred to $120 \mu\text{L}$ of ice-cooled MeOH and centrifuged (3600 rpm , $4 \text{ }^\circ\text{C}$, 10 min , 5804 R Eppendorf centrifuge). Then, $80 \mu\text{L}$ of supernatant was transferred to a 96-well plate for analysis by LC-MS (see below). The metabolic half-life ($t_{1/2}$) was calculated from the slope of the linear regression from the log percentage remaining compound versus incubation time relationship. Control experiments were performed in parallel by preincubating the microsomes with the specific carboxylesterase inhibitor BNPP (1 mM) for 5 min before addition of the compound solution.^[45]

LC-MS measurements. Analyses were performed using an 1100/1200 Series HPLC System coupled to a 6410 Triple Quadrupole mass detector (Agilent Technologies, Inc., Santa Clara, CA, USA) equipped with electrospray ionization. The system was controlled with the Agilent MassHunter Workstation Data Acquisition software (version B.01.04). The column used was an Atlantis[®] T3 C18 column (2.1 × 50 mm) with a 3 μm particle size (Waters Corp., Milford, MA, USA). The mobile phase consisted of eluent A: H₂O containing 0.1% formic acid (for **23a-c**, **26a**, **32a-d**, **37**, **42a-f**) or 10 mM ammonium acetate, pH 5.0 in 95:5, H₂O:MeCN (for **4a**, **6-8a**, **26b**); and eluent B: MeCN, containing 0.1% formic acid. The flow rate was maintained at 0.6 mL/min. The gradient was ramped from 95% A/5% B to 5% A/95% B over 1 min, and then hold at 5% A/95% B for 0.1 min. The system was then brought back to 95% A/5% B, resulting in a total duration of 4 min. MS parameters such as fragmentor voltage, collision energy, polarity were optimized individually for each drug, and the molecular ion was followed for each compound in the multiple reaction monitoring mode. The concentrations of the analytes were quantified by the Agilent Mass Hunter Quantitative Analysis software (version B.01.04).

In vivo pharmacokinetic studies.

Eight-week-old female C3H/HeN mice from Harlan (Venray, The Netherlands) weighing between 19 and 25 g were used for the PK study. Three mice were put in one cage and kept under specific pathogen-free conditions in the Animal House of the Department of Biomedicine, University Hospital of Basel. All animal experimentation guidelines according to the regulations of the Swiss veterinary law were followed. The animals had free access to chow and water ad libitum and were kept in a 12 h/12 h light/dark cycle. After one week of acclimatization, the mice were used for the pharmacokinetic study. Compound **41f** was diluted in 5% DMSO in 1% Tween 80 in PBS and applied using an oral gavage at a dose of 10 mg/kg. Blood and urine samples (10 μL) were taken before the experiment (0 min) and at 6, 13, 20, 40 min, 1, 1.5, 2, 3, 4, 6, 8, and 24 h after administration. Samples were diluted in MeOH directly after sampling in a ratio of 1:5 to precipitate proteins. After centrifugation (11 min, 13000 rpm) the supernatant was

transferred to a 96-well plate and analyzed by LC-MS as described before. The samples at 0 min were used to define the detection limit in plasma and urine.

Acknowledgement

The authors gratefully acknowledge the financial support by the Swiss National Science Foundation (grant no. xy).

References

- [1] a) Hooton, T. M.; Stamm, W. E. Diagnosis and treatment of uncomplicated urinary tract infection. *Infect. Dis. Clin. North Am.* **1997**, *11*, 551-581; b) Wiles, T. J.; Kulesus, R. R.; Mulvey, M. A. Origins and virulence mechanisms of uropathogenic *Escherichia coli*. *Exp. Mol. Pathol.* **2008**, *85*, 11-19; c) Fihn, S. D. Acute uncomplicated urinary tract infection in women. *N. Engl. J. Med.* **2003**, *349*, 259-266.
- [2] a) Schilling, J. D.; Hultgren, S. J. Recent advances into the pathogenesis of recurrent urinary tract infections: the bladder as a reservoir for uropathogenic *Escherichia coli*. *Int. J. Antimicrob. Agents* **2002**, *19*, 457-460; b) Blango, M.; Mulvey, M. Persistence of uropathogenic *Escherichia coli* in the face of multiple antibiotics. *Agents Chemother.* **2010**, *54*, 1855-1863.
- [3] Svanborg, C.; Godaly, G. Bacterial virulence in urinary tract infection. *Infect. Dis. Clin. North Am.* **1997**, *11*, 513-529.
- [4] a) Mulvey, M. A. Adhesion and entry of uropathogenic *Escherichia coli*. *Cell Microbiol.* **2002**, *4*, 257-271; b) Eto, D. S.; Jones, T. A.; Sundsbak, J. L.; Mulvey, M. A. Integrin-mediated host cell invasion by type 1-piliated uropathogenic *Escherichia coli*. *PLoS Pathog.* **2007**, *3*, e100.
- [5] Capitani, G.; Eidam, O.; Glockshuber, R.; Grütter, M. G. Structural and functional insights into the assembly of type 1 pili from *Escherichia coli*. *Microbes Infect.* **2006**, *8*, 2284-2290.
- [6] Le Trong, I.; Aprikian, P.; Kidd, B. A.; Forero-Shelton, M.; Tchesnokova, V.; Rajagopal, P.; Rodriguez, V.; Interlandi, G.; Klevit, R.; Vogel, V.; Stenkamp, R. E.; Sokurenko, E. V.; Thomas, W. E. Structural basis for mechanical force regulation of the adhesin FimH via finger trap-like β sheet twisting. *Cell* **2010**, *141*, 645-655.

- [7] Sharon, N. Carbohydrates as future anti-adhesion drugs for infectious diseases. *Biochim. Biophys. Acta* **2006**, *1760*, 527-537.
- [8] a) Firon, N.; Ofek, I.; Sharon, N. Interaction of mannose-containing oligosaccharides with the fimbrial lectin of *Escherichia coli*. *Biochem. Biophys. Res. Commun.* **1982**, *105*, 1426-1432; b) Firon, N.; Ofek, I.; Sharon, N. Carbohydrate specificity of the surface lectins of *Escherichia coli*, *Klebsiella pneumoniae*, and *Salmonella typhimurium*. *Carbohydr. Res.* **1983**, *120*, 235-249; c) Sharon, N. Bacterial lectins, cell-cell recognition and infectious disease. *FEBS Lett.* **1987**, *217*, 145-157.
- [9] Choudhury, D.; Thompson, A.; Stojanoff, V.; Langermann, S.; Pinkner, J.; Hultgren, S. J.; Knight, S. D. X-ray structure of the FimC-FimH chaperone-adhesin complex from uropathogenic *Escherichia coli*. *Science* **1999**, *285*, 1061-1066.
- [10] a) Hung, C. S.; Bouckaert, J.; Hung, D.; Pinkner, J.; Widberg, C.; DeFusco, A.; Auguste, C. G.; Strouse, R.; Langermann, S.; Waksman, G.; Hultgren, S. J. Structural basis of tropism of *Escherichia coli* to the bladder during urinary tract infection. *Mol. Microbiol.* **2002**, *44*, 903-915; b) Bouckaert, J.; Berglund, J.; Schembri, M.; De Genst, E.; Cools, L.; Wuhrer, M.; Hung, C. S.; Pinkner, J.; Slattegard, R.; Zavialov, A.; Choudhury, D.; Langermann, S.; Hultgren, S. J.; Wyns, L.; Klemm, P.; Oscarson, S.; Knight, S. D.; De Greve, H. Receptor binding studies disclose a novel class of high-affinity inhibitors of the *Escherichia coli* FimH adhesin. *Mol. Microbiol.* **2005**, *55*, 441-455; c) Wellens, A.; Garofalo, C.; Nguyen, H.; Van Gerven, N.; Slattegard, R.; Hernalsteens, J. P.; Wyns, L.; Oscarson, S.; De Greve, H.; Hultgren, S.; Bouckaert, J. Intervening with urinary tract infections using anti-adhesives based on the crystal structure of the FimH-oligomannose-3 complex. *PLoS ONE* **2008**, *3*, e2040; d) Wellens, A.; Lahmann, M.; Touaibia, M.; Vaucher, J.; Oscarson, S.; Roy, R.; Remaut, H.; Bouckaert, J. The tyrosine gate as a potential entropic lever in the receptor-binding site of the bacterial adhesin FimH. *Biochemistry* **2012**, *51*, 4790-4799.
- [11] a) Firon, N.; Ashkenazi, S.; Mirelman, D.; Ofek, I.; Sharon, N. Aromatic alpha-glycosides of mannose are powerful inhibitors of the adherence of type-1 fimbriated *Escherichia coli* to yeast and intestinal epithelial-cells. *Infect. Immun.* **1987**, *55*, 472-476; b) Lindhorst, T.; Kotter, S.; Kubisch, J.; Krallmann-Wenzel, U.; Ehlers, S.; Kren, V. Effect of p-substitution of aryl α -D-mannosides on inhibiting mannose-sensitive adhesion of *Escherichia coli* - Syntheses and testing. *Eur. J. Org. Chem.*

1998, 1669-1674; c) Sperling, O.; Fuchs, A.; Lindhorst, T. K. Evaluation of the carbohydrate recognition domain of the bacterial adhesin FimH: Design, synthesis and binding properties of mannoside ligands. *Org. Biomol. Chem.* **2006**, *4*, 3913-3922; d) Han, Z. F.; Pinkner, J. S.; Ford, B.; Obermann, R.; Nolan, W.; Wildman, S. A.; Hobbs, D.; Ellenberger, T.; Cusumano, C. K.; Hultgren, S. J.; Janetka, J. W. Structure-based drug design and optimization of mannoside bacterial FimH antagonists. *J. Med. Chem.* **2010**, *53*, 4779-4792; e) Klein, T.; Abgottspon, D.; Wittwer, M.; Rabbani, S.; Herold, J.; Jiang, X. H.; Kleeb, S.; Luthi, C.; Scharenberg, M.; Bezencon, J.; Gubler, E.; Pang, L. J.; Smiesko, M.; Cutting, B.; Schwaradt, O.; Ernst, B. FimH antagonists for the oral treatment of urinary tract infections: From design and synthesis to in vitro and in vivo evaluation. *J. Med. Chem.* **2010**, *53*, 8627-8641; f) Schwaradt, O.; Rabbani, S.; Hartmann, M.; Abgottspon, D.; Wittwer, M.; Kleeb, S.; Zalewski, A.; Smiesko, M.; Cutting, B.; Ernst, B. Design, synthesis and biological evaluation of mannosyl triazoles as FimH antagonists. *Bioorg. Med. Chem.* **2011**, *19*, 6454-6473; g) Cusumano, C. K.; Pinkner, J. S.; Han, Z.; Greene, S. E.; Ford, B. A.; Crowley, J. R.; Henderson, J. P.; Janetka, J. W.; Hultgren, S. J. Treatment and prevention of urinary tract infection with orally active FimH inhibitors. *Sci. Transl. Med.* **2011**, *3*, 109ra115; h) Han, Z. F.; Pinkner, J. S.; Ford, B.; Chorell, E.; Crowley, J. M.; Cusumano, C. K.; Campbell, S.; Henderson, J. P.; Hultgren, S. J.; Janetka, J. W. Lead optimization studies on FimH antagonists: Discovery of potent and orally bioavailable ortho-substituted biphenyl mannosides. *J. Med. Chem.* **2012**, *55*, 3945-3959; i) Jiang, X. H.; Abgottspon, D.; Kleeb, S.; Rabbani, S.; Scharenberg, M.; Wittwer, M.; Haug, M.; Schwaradt, O.; Ernst, B. Antiadhesion therapy for urinary tract infections—a balanced PK/PD profile proved to be key for success. *J. Med. Chem.* **2012**, *55*, 4700-4713; j) Pang, L.; Kleeb, S.; Lemme, K.; Rabbani, S.; Scharenberg, M.; Zalewski, A.; Schadler, F.; Schwaradt, O.; Ernst, B. FimH antagonists: Structure-activity and structure-property relationships for biphenyl α -D-mannopyranosides. *ChemMedChem* **2012**, *7*, 1404-1422; k) Kleeb, S.; Pang, L.; Mayer, K.; Eris, D.; Sigl, A.; Preston, R. C.; Zihlmann, P.; Abgottspon, D.; Hutter, A.; Scharenberg, M.; Jiang, X.; Navarra, G.; Rabbani, S.; Smiesko, M.; Lüdin, N.; Jakob, R. P.; Schwaradt, O.; Maier, T.; Sharpe, T.; Ernst, B. FimH Antagonists: Bioisosteres of a Carboxylate to Improve PK/PD Properties, submitted.

- [12] a) Johnson, K. C.; Swindell, A. C. Guidance in the setting of drug particle size specifications to minimize variability in absorption. *Pharm. Res.* **1996**, *13*, 1795-1798; b) Lipinski, C. A. Drug-like properties and the causes of poor solubility and poor permeability. *J. Pharmacol. Toxicol. Methods* **2000**, *44*, 235-249.
- [13] Ishikawa, M.; Hashimoto, Y. Improvement in aqueous solubility in small molecule drug discovery programs by disruption of molecular planarity and symmetry. *J. Med. Chem.* **2011**, *54*, 1539-1554.
- [14] Meanwell, N. A. Synopsis of some recent tactical application of bioisosteres in drug design. *J. Med. Chem.* **2011**, *54*, 2529-2591.
- [15] Yan, R.; Yang, F.; Wu, Y.; Zhang, L.; Ye, X. An efficient and improved procedure for preparation of triflyl azide and application in catalytic diazotransfer reaction. *Tetrahedron Lett.* **2005**, *46*, 8993-8995.
- [16] Rostovtsev, V.; Green, L.; Fokin, V.; Sharpless, K. A stepwise Huisgen cycloaddition process: Copper(I)-catalyzed regioselective "ligation" of azides and terminal alkynes. *Angew. Chem. Int. Ed.* **2002**, *41*, 2596-2599.
- [17] Antilla, J.; Baskin, J.; Barder, T.; Buchwald, S. Copper-diamine-catalyzed *N*-arylation of pyrroles, pyrazoles, indazoles, imidazoles, and triazoles. *J. Org. Chem.* **2004**, *69*, 5578-5587.
- [18] a) Node, M.; Nishide, K.; Fuji, K.; Fujita, E. Hard acid and soft nucleophile system. 2. Demethylation of methyl esters of alcohol and phenol with an aluminum halide-thiol system. *J. Org. Chem.* **1980**, *45*, 4275-4277; b) Node, M.; Kumar, K.; Nishide, K.; Ohsugi, S.; Miyamoto, T. Odorless substitutes for foul-smelling thiols: Syntheses and applications. *Tetrahedron Lett.* **2001**, *42*, 9207-9210.
- [19] Le Bourdonnec, B.; Windh, R.; Leister, L.; Zhou, Q.; Ajello, C.; Gu, M.; Chu, G.; Tuthill, P.; Barker, W.; Koblish, M.; Wiant, D.; Graczyk, T.; Belanger, S.; Cassel, J.; Feschenko, M.; Brogdon, B.; Smith, S.; Derelanko, M.; Kutz, S.; Little, P.; DeHaven, R.; DeHaven-Hudkins, D.; Dolle, R. Spirocyclic delta opioid receptor agonists for the treatment of pain: Discovery of *N,N*-diethyl-3-hydroxy-4-(spiro[chromene-2,4'-piperidine]-4-yl) benzamide (ADL5747). *J. Med. Chem.* **2009**, *52*, 5685-5702.
- [20] Katritzky, A.; Cheng, D.; Musgrave, R. Syntheses of imidazoles and pyrroles: BetMIC and TosMIC as complementary reagents. *Heterocycles* **1997**, *44*, 67-70.
- [21] Scott, I. L.; Market, R. V.; DeOrazio, R. J.; Meckler, H.; Kogan, T. P. Stereospecific α -D-mannosylation. *Carbohydr. Res.* **1999**, *317*, 210-216.

- [22] Prieto, M.; Zurita, E.; Rosa, E.; Munoz, L.; Lloyd-Williams, P.; Giralt, E. Arylboronic acids and arylpinacolboronate esters in Suzuki coupling reactions involving indoles. Partner role swapping and heterocycle protection. *J. Org. Chem.* **2004**, *69*, 6812-6820.
- [23] Rabbani, S.; Jiang, X. H.; Schwardt, O.; Ernst, B. Expression of the carbohydrate recognition domain of FimH and development of a competitive binding assay. *Anal. Biochem.* **2010**, *407*, 188-195.
- [24] Glide, version 5.7, Schrödinger, LLC, New York, NY, **2011**.
- [25] Dearden, J. C.; Bresnen, G. M. The Measurement of Partition Coefficients. *Quant. Struct.-Act. Rel.* **1988**, *7*, 133-144.
- [26] A. Avdeef in *Pharmacokinetic Optimization in Drug Research; Biological, Physicochemical and Computational Strategies* (Eds.: B. Testa, H. van de Waterbeemd, G. Folkers, R. Guy), Verlag Helvetica Chimica Acta, Zurich, **2001**, pp 305-326.
- [27] Kansy, M.; Senner, F.; Gubernator, K. Physicochemical high throughput screening: Parallel artificial membrane permeation assay in the description of passive absorption processes. *J. Med. Chem.* **1998**, *41*, 1007-1010.
- [28] Artursson, P.; Karlsson, J. Correlation between oral-drug absorption in humans and apparent drug permeability coefficients in human intestinal epithelial (Caco-2) cells. *Biochem. Biophys. Res. Commun.* **1991**, *175*, 880-885.
- [29] Imai, T.; Taketani, M.; Shii, M.; Hosokawa, M.; Chiba, K. Substrate specificity of carboxylesterase isozymes and their contribution to hydrolase activity in human liver and small intestine. *Drug Metab. Dispos.* **2006**, *34*, 1734-1741.
- [30] MacroModel, version 9.9, Schrödinger, LLC, New York, NY, **2012**. Torsion angle measurements are based on the lowest-energy conformers.
- [31] a) Wadkins, R. M.; Morton, C. L.; Weeks, J. K.; Oliver, L.; Wierdl, M.; Danks, M. K.; Potter, P. M. Structural constraints affect the metabolism of 7-ethyl-10-[4-(1-piperidino)-1-piperidino]carbonyloxycamptothecin (CPT-11) by carboxylesterases. *Mol. Pharmacol.* **2001**, *60*, 355-362; b) Hatfield, J. M.; Wierdl, M.; Wadkins, R. M.; Potter, P. M. Modifications of human carboxylesterase for improved prodrug activation. *Expert Opin. Drug Metab. Toxicol.* **2008**, *4*, 1153-1165; c) Vistoli, G.; Pedretti, A.; Mazzolari, A.; Testa, B. In silico prediction of human carboxylesterase-1 (hCES1) metabolism combining docking analyses and MD simulations. *Bioorg. Med. Chem.* **2010**, *18*, 320-329.

- [32] Satoh, T.; Hosokawa, M. Structure, function and regulation of carboxylesterases. *Chem. Bio. Interact.* **2006**, *162*, 195-211.
- [33] a) AMSOL, version 7.1, by Hawkins, G. D.; Giesen, D. J.; Lynch, G. C.; Chambers, C. C.; Rossi, I.; Storer, J. W.; Li, J.; Thompson, J. D.; Winget, P.; Lynch, B. J.; Rinaldi, D.; Liotard, D. A.; Cramer, C. J.; Truhlar, D. G. University of Minnesota, Minneapolis, **2003**, based in part on AMPAC, version 2.1 by Liotard, D. A.; Healy, E. F.; Ruiz, J. M.; Dewar, M. J. S.; b) Storer, J.; Giesen, D.; Cramer, C.; Truhlar, D. Class-IV charge models – a new semiempirical approach in quantum-chemistry. *J. Comput. Aided Mol. Des.* **1995**, *9*, 87-110; c) Dewar, M.; Zoebisch, E.; Healy, E.; Stewart, J. The development and use of quantum mechanical molecular models. 76. AM1: A new general-purpose quantum mechanical molecular model. *J. Am Chem. Soc.* **1985**, *107*, 3902-3909.
- [34] Avdeef, A.; Bendels, S.; Di, L.; Faller, B.; Kansy, M.; Sugano, K.; Yamauchi, Y. PAMPA – critical factors for better predictions of absorption. *J. Pharm. Sci.* **2007**, *96*, 2893-2909.
- [35] Lin, J. H. Drug-drug interaction mediated by inhibition and induction of P-glycoprotein. *Adv. Drug Deliv. Rev.* **2003**, *21*, 53-81.
- [36] Nikolovska-Coleska, Z.; Wang, R.; Fang, X.; Pan, H.; Tomita, Y.; Li, P.; Roller, P.; Krajewski, K.; Saito, N.; Stuckey, J.; Wang, S. Development and optimization of a binding assay for the XIAP BIR3 domain using fluorescence polarization. *Anal. Biochem.* **2004**, *332*, 261-273.
- [37] Scharenberg, M.; Jiang, X.; Pang, L.; Navarra, G.; Rabbani, S.; Binder, F.; Schwardt, O.; Ernst, B. Kinetic properties of carbohydrate-lectin interactions: FimH antagonists. *ChemMedChem* **2014**, *1*, 78-83.
- [38] Smith, D. A.; Jones, B. C.; Walker, D. K. Design of drugs involving the concepts and theories of drug metabolism and pharmacokinetics. *Med. Res. Rev.* **1996**, *16*, 243-266.
- [39] van de Waterbeemd, H.; Smith, D.; Beaumont, K.; Walker, D. Property-based design: Optimization of drug absorption and pharmacokinetics. *J. Med. Chem.* **2001**, *44*, 1313-1333.
- [40] van Breemen, R. B.; Li, Y. Caco-2 cell permeability assays to measure drug absorption. *Expert Opin. Drug. Metab. Toxicol.* **2005**, *1*, 175-185.

-
- [41] Varma, M. V.; Feng, B.; Obach, R. S.; Troutman, M. D.; Chupka, J.; Miller, H. R.; El-Kattan, A. Physicochemical determinants of human renal clearance. *J. Med. Chem.* **2009**, *52*, 4844-4852.
- [42] a) VCCLAB, Virtual Computational Chemistry Laboratory, **2005**, <http://www.vcclab.org> (accessed March 25, 2013); b) Tetko, I. V.; Gasteiger, J.; Todeschini, R.; Mauri, A.; Livingstone, D.; Ertl, P.; Palyulin, V. A.; Radchenko, E. V.; Zefirov, N. S.; Makarenko, A. S.; Tanchuk, V. Y.; Prokopenko, V. V. Virtual computational chemistry laboratory-design and description. *J. Comput. Aided Mol. Des.* **2005**, *19*, 453-463.
- [43] Ohura, K.; Sakamoto, H.; Ninomiya, S.; Imai, T. Development of a novel system for estimating human intestinal absorption using Caco-2 cells in the absence of esterase activity. *Drug Metab. Dispos.* **2010**, *38*, 323-331.
- [44] Hubatsch, I.; Ragnarsson, E. G.; Artursson, P. Determination of drug permeability and prediction of drug absorption in Caco-2 monolayers. *Nat. Protoc.* **2007**, *2*, 2111-2119.
- [45] Taketani, M.; Shii, M.; Ohura, K.; Ninomiya, S.; Imai, T. Carboxylesterase in the liver and small intestine of experimental animals and human. *Life Sci.* **2007**, *81*, 924-932.

Supporting Information

FimH Antagonists – Solubility vs. Oral Availability

Lijuan Pang, Simon Kleeb, Said Rabbani, Jacqueline Bezençon, Anja Sigl, Deniz Eris, Oliver Schwardt, and Beat Ernst*

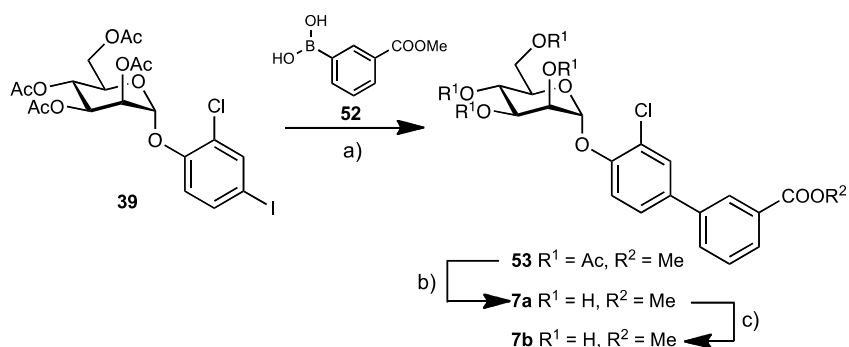
Institute of Molecular Pharmacy, Pharmacenter, University of Basel, Klingelbergstrasse 50, CH-4056 Basel, Switzerland

* To whom correspondence should be addressed: Prof. Dr. Beat Ernst, Institute of Molecular Pharmacy, Pharmacenter, University of Basel, Klingelbergstrasse 50, CH-4056 Basel, Switzerland; Tel: +41 61 267 15 51, Fax: +41 61 267 15 52; E-mail: beat.erst@unibas.ch

Contents

Synthesis	S2
HPLC data for the target compounds	S21
HPLC traces of the target compounds	S23
¹ H NMR Spectra of the target compounds	S36
References	S73

Synthesis

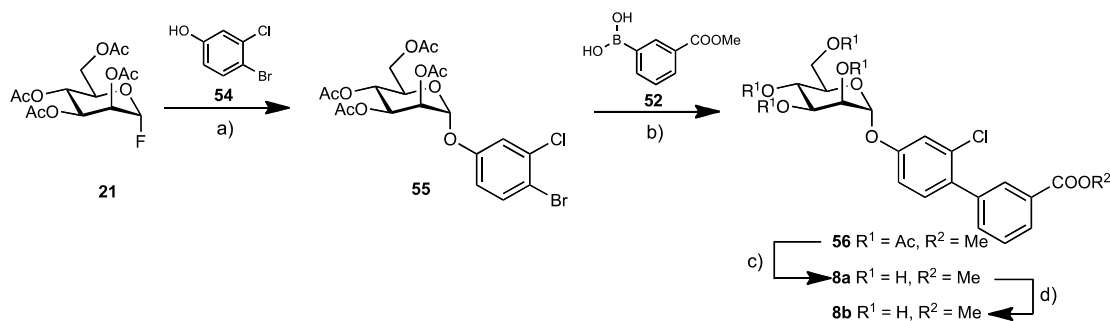


Scheme S1. Reagents and conditions: a) Pd(Cl₂)dppf·CH₂Cl₂, K₃PO₄, DMF, 80 °C, overnight (70%); b) NaOMe, MeOH, rt, 4 h (quant.); c) 0.2 N aq. NaOH, MeOH, rt, overnight (50%).

Methyl 4'-(2,3,4,6-tetra-*O*-acetyl- α -D-mannopyranosyloxy)-3'-chlorobiphenyl-3-carboxylate (53**).** A Schlenk tube was charged with **39** (100 mg, 0.17 mmol), **52** (31 mg, 0.17 mmol), Pd(Cl₂)dppf·CH₂Cl₂ (4 mg, 0.0051 mmol), K₃PO₄ (54 mg, 0.26 mmol) and a stirring bar. The tube was closed, evacuated and flushed with argon. This procedure was repeated twice, then anhydrous DMF (2 mL) was added under a stream of argon. The mixture was degassed in an ultrasonic bath and flushed with argon for 5 min, then stirred at 80 °C overnight. The reaction mixture was cooled to rt, diluted with EtOAc (20 mL), and washed with H₂O (20 mL) and brine (20 mL). The organic layer was dried over Na₂SO₄ and concentrated in vacuo. The residue was purified by MPLC on silica gel (petroleum ether/EtOAc) to afford **53** (70 mg, 69%) as a white solid. $[\alpha]_D^{20} +62.8$ (*c* 0.7, EtOAc); ¹H NMR (500 MHz, CDCl₃): δ = 8.20 (s, 1H, Ar-H), 8.03 (d, *J* = 7.8 Hz, 1H, Ar-H), 7.72 (d, *J* = 7.9 Hz, 1H, Ar-H), 7.67 (d, *J* = 2.2 Hz, 1H, Ar-H), 7.51 (t, *J* = 7.8 Hz, 1H, Ar-H), 7.46 (dd, *J* = 8.5, 2.3 Hz, 1H, Ar-H), 5.64 (dd, *J* = 10.0, 3.5 Hz, 1H, H-3), 5.61 (d, *J* = 1.6 Hz, 1H, H-1), 5.56 (dd, *J* = 3.4, 1.9 Hz, 1H, H-2), 5.41 (t, *J* = 10.1 Hz, 1H, H-4), 4.30 (dd, *J* = 12.3, 5.3 Hz, 1H, H-6a), 4.24-4.18 (m, 1H, H-5), 4.11 (m, 1H, H-6b), 3.96 (s, 3H, OCH₃), 2.22-2.08, 2.04, 2.05 (4s, 12H, 4 OAc); ¹³C NMR (126 MHz, CDCl₃): δ = 170.51, 169.80 (5C, 5 CO), 150.91, 139.44, 131.18, 129.20, 129.08, 128.73, 127.95, 126.37, 117.31 (12C, Ar-C), 96.70 (C-1), 69.82 (C-5), 69.35 (C-2), 68.79 (C-3), 65.85 (C-4), 62.12 (C-6), 52.30 (OCH₃), 20.89, 20.70 (4C, 4 COCH₃); ESI-MS: *m/z*: Calcd for C₂₈H₂₉ClNaO₁₂ [M+Na]⁺: 615.12, found: 615.17.

Methyl 3'-chloro-4'-(α -D-mannopyranosyloxy)biphenyl-3-carboxylate (7a). To a solution of **53** (28 mg, 0.05 mmol) in dry MeOH (5 mL) was added freshly prepared 1 M NaOH/MeOH (50 μ L) under argon. The mixture was stirred at rt for 4 h, then neutralized with Amberlyst-15 (H^+) ion-exchange resin, filtered and concentrated in vacuo. The residue was purified by MPLC on silica gel (DCM/MeOH, 10:1-7:1) to afford **7a** (20 mg, quant.) as a white solid after lyophilization from H_2O . $[\alpha]_D^{20} +110.7$ (c 0.3, MeOH); 1H NMR (500 MHz, CD_3OD): $\delta = 8.22$ (s, 1H, Ar-H), 8.01 (d, $J = 7.8$ Hz, 1H, Ar-H), 7.85 (d, $J = 7.8$ Hz, 1H, Ar-H), 7.71 (d, $J = 2.2$ Hz, 1H, Ar-H), 7.62-7.54 (m, 2H, Ar-H), 7.49 (d, $J = 8.6$ Hz, 1H, Ar-H), 5.63 (d, $J = 1.2$ Hz, 1H, H-1), 4.14 (dd, $J = 3.2, 1.8$ Hz, 1H, H-2), 4.03 (dd, $J = 9.5, 3.4$ Hz, 1H, H-3), 3.96 (s, 3H, OMe), 3.86-3.71 (m, 3H, H-4, H-6b, H-6a), 3.68 ppm (ddd, $J = 9.6, 5.4, 2.2$ Hz, 1H, H-5); ^{13}C NMR (126 MHz, CD_3OD): $\delta = 168.38$ (CO), 153.11, 141.12, 136.54, 132.38, 132.10, 130.35, 129.59, 129.42, 128.59, 127.62, 125.40, 118.74 (Ar-C), 100.79 (C-1), 76.02 (C-5), 72.42 (C-3), 71.87 (C-2), 68.25 (C-4), 62.69 (C-6), 52.78 (OMe); HRMS: m/z : Calcd for $C_{20}H_{21}ClNaO_8$ $[M+Na]^+$: 447.0817, found: 447.0817.

Sodium 3'-chloro-4'-(α -D-mannopyranosyloxy)biphenyl-3-carboxylate (7b). To a solution of **53** (30 mg, 0.05 mmol) in MeOH (5 mL) was added 1M NaOH/MeOH (50 μ L). The mixture was stirred at RT for 4h and concentrated. The residue was treated with 0.5 M aq. NaOH (1 mL) for 24 h at rt. The solution was then adjusted to pH 3-4 with Amberlyst-15 (H^+), and the mixture was filtered and concentrated. The crude product was transformed into the sodium salt by passing through a small column of Dowex 50X8 (Na^+ form) ion-exchange resin. After concentration, the residue was purified by MPLC (RP-18, $H_2O/MeOH$, 1:0-2:1) followed by size-exclusion chromatography (P-2 gel, H_2O) to give **7b** (11 mg, 50%) as a white solid after lyophilization from H_2O . $[\alpha]_D^{20} +88.9$ (c 0.3, MeOH); 1H NMR (500 MHz, D_2O): $\delta = 7.98$ (s, 1H, Ar-H), 7.77 (d, $J = 7.7$ Hz, 1H, Ar-H), 7.62, 7.53-7.37 (m, 4H, Ar-H), 7.25 (d, $J = 8.6$ Hz, 1H, Ar-H), 5.60 (s, 1H, H-1), 4.17 (dd, $J = 3.2, 1.8$ Hz, 1H, H-2), 4.05 (dd, $J = 8.7, 3.4$ Hz, 1H, H-3), 3.81-3.57 (m, 4H, H-4, H-5, H-6); ^{13}C NMR (126 MHz, D_2O): $\delta = 175.29$ (CO), 150.10, 138.58, 137.02, 135.96, 129.16, 128.93, 128.52, 127.95, 126.94, 126.40, 123.99, 117.85 (Ar-C), 98.60 (C-1), 73.87 (C-5), 70.41 (C-3), 69.73 (C-2), 66.47 (C-4), 60.59 (C-6); HRMS: m/z : Calcd for $C_{19}H_{19}ClNaO_8$ $[M+H]^+$: 433.0661, found: 433.0661.



Scheme S2. Reagents and conditions: a) $\text{BF}_3 \cdot \text{Et}_2\text{O}$, DCM, mol. sieves 4\AA , $0\text{ }^\circ\text{C}$ to rt, overnight (90%); b) $\text{Pd}(\text{Cl}_2)\text{dppf} \cdot \text{CH}_2\text{Cl}_2$, K_3PO_4 , DMF, $80\text{ }^\circ\text{C}$, overnight (76%); c) NaOMe, MeOH, rt, 4 h (quant.); d) 0.2 N aq. NaOH, MeOH, rt, overnight (61%).

4-Bromo-3-chlorophenyl 2,3,4,6-tetra-O-acetyl- α -D-mannopyranoside (55). To an ice-cold suspension of **21** (200 mg, 0.57 mmol), phenol **54** (107 mg, 0.52 mmol), and molecular sieves (4\AA , 600 mg) in dry DCM (5 mL), $\text{BF}_3 \cdot \text{Et}_2\text{O}$ (0.3 mL, 2.44 mmol) was added dropwise under argon. The mixture was stirred at $0\text{ }^\circ\text{C}$ for 3 h, and then at rt overnight. The reaction mixture was filtered over Celite, and the filtrate was diluted with DCM (50 mL), extracted with 0.5 N aq. NaOH (50 mL), H_2O (50 mL), and brine (50 mL). The organic layer was dried over Na_2SO_4 and concentrated in vacuo. The residue was purified by MPLC on silica gel (petrol ether/EtOAc) to yield **55** (250 mg, 90%) as a white solid. $[\alpha]_{\text{D}}^{20} +75.8$ (c 0.5, EtOAc); ^1H NMR (500 MHz, CDCl_3): δ = 7.53 (d, J = 8.9 Hz, 1H, Ar-H), 7.29 (d, J = 2.8 Hz, 1H, Ar-H), 6.89 (dd, J = 8.9, 2.8 Hz, 1H, Ar-H), 5.53-5.45 (m, 2H, H-3, H-1), 5.42 (dd, J = 3.4, 1.8 Hz, 1H, H-2), 5.34 (t, J = 10.1 Hz, 1H, H-4), 4.27 (dd, J = 12.2, 6.0 Hz, 1H, H-6a), 4.11-4.00 (m, 2H, H-5, H-6b), 2.20, 2.06, 2.05, 2.04 (4s, 12H, 4 COCH_3); ^{13}C NMR (126 MHz, CDCl_3): δ = 170.49, 169.91, 169.68 (4 CO), 155.16, 135.17, 134.16, 118.62, 116.77, 115.84 (Ar-C), 96.05 (C-1), 69.50 (C-5), 69.09 (C-2), 68.62 (C-3), 65.82 (C-4), 62.16 (C-6), 20.83, 20.66 (4C, 4 COCH_3); ESI-MS: m/z : Calcd for $\text{C}_{20}\text{H}_{22}\text{BrClNaO}_{10}$ $[\text{M}+\text{Na}]^+$: 559.00, found: 559.10.

Methyl 4'-(2,3,4,6-tetra-O-acetyl- α -D-mannopyranosyloxy)-2'-chlorobiphenyl-3-carboxylate (56). Prepared according to the procedure for **53** from **55** (100 mg, 0.19 mmol), **52** (33 mg, 0.19 mmol), $\text{Pd}(\text{Cl}_2)\text{dppf} \cdot \text{CH}_2\text{Cl}_2$ (5 mg, 0.0057 mmol), and K_3PO_4 (60 mg, 0.29 mmol). Yield: 84 mg (76%) as colorless oil. $[\alpha]_{\text{D}}^{20} +76.1$ (c 0.8, EtOAc); ^1H NMR (500 MHz, CDCl_3): δ = 8.10-8.01 (m, 2H, Ar-H), 7.62 (m, 1H, Ar-H), 7.50 (t, J = 7.7 Hz, 1H, Ar-H), 7.34-7.25 (m, 2H, Ar-H), 7.08 (dd, J = 8.5, 2.5 Hz, 1H, Ar-H), 5.57-5.55 (m, 2H, H-1, H-3), 5.47 (dd, J = 3.5, 1.8 Hz, 1H, H-2), 5.38 (t, J = 10.0 Hz, 1H, H-

4), 4.31 (dd, $J = 12.7, 6.4$ Hz, 1H, H-6a), 4.14-4.09 (m, 2H, H-5, H-6b), 3.93 (s, 3H, OCH₃), 2.22, 2.07, 2.05, 2.04 (4s, 12H, 4 COCH₃); ¹³C NMR (126 MHz, CDCl₃): $\delta = 170.61, 170.01, 169.79$ (4C, 4 CO), 155.56, 139.05, 134.49, 134.08, 133.24, 132.08, 130.68, 130.29, 128.83, 128.27, 118.12, 115.61 (Ar-C), 96.10 (C-1), 69.52 (C-5), 69.30 (C-2), 68.81 (C-3), 65.98 (C-4), 62.27 (C-6), 52.29 (OCH₃), 20.93, 20.76 (4C, 4 COCH₃); ESI-MS: m/z : Calcd for C₂₈H₂₉ClNaO₁₂ [M+Na]⁺: 615.12, found: 615.14.

Methyl 2'-chloro-4'-(α -D-mannopyranosyloxy)biphenyl-3-carboxylate (8a). Prepared according to the procedure for **7a** from **56** (45 mg, 0.07 mmol). Yield: 32 mg (quant.) as white solid. $[\alpha]_D^{20} +112.9$ (c 0.7, MeOH); ¹H NMR (500 MHz, CD₃OD): $\delta = 8.03$ (dd, $J = 7.4, 4.6$ Hz, 2H, Ar-H), 7.65 (m, 1H, Ar-H), 7.55 (t, $J = 7.7$ Hz, 1H, Ar-H), 7.36-7.28 (m, 2H, Ar-H), 7.19 (dd, $J = 8.5, 2.5$ Hz, 1H, Ar-H), 5.58 (d, $J = 1.6$ Hz, 1H, H-1), 4.06 (dd, $J = 3.3, 1.8$ Hz, 1H, H-2), 3.98-3.90 (m, 4H, H-3, OCH₃), 3.87-3.72 (m, 3H, H-4, H-6), 3.62 (ddd, $J = 9.7, 5.3, 2.4$ Hz, 1H, H-5); ¹³C NMR (126 MHz, CD₃OD): $\delta = 168.36$ (CO), 158.03, 140.83, 135.33, 134.70, 133.86, 133.10, 131.57, 131.29, 129.50, 129.48, 119.14, 116.87 (Ar-C), 100.31 (C-1), 75.73 (C-5), 72.36 (C-3), 71.82 (C-2), 68.29 (C-4), 62.66 (C-6), 52.77 (OCH₃); HRMS: m/z : Calcd for C₂₀H₂₁ClNaO₈ [M+Na]⁺: 447.0817, found: 447.0815.

Sodium 2'-chloro-4'-(α -D-mannopyranosyloxy)biphenyl-3-carboxylate (8b). Prepared according to the procedure for **7b** from **56** (25 mg, 0.04 mmol). Yield: 11 mg (61%) as white solid. $[\alpha]_D^{20} +94.1$ (c 0.7, MeOH/H₂O, 1:1); ¹H NMR (500 MHz, D₂O): $\delta = 7.95$ -7.87, 7.60-7.51, 7.38-7.33 (m, 6H, Ar-H), 7.16 (dd, $J = 8.6, 2.5$ Hz, 1H, Ar-H), 5.63 (d, $J = 1.6$ Hz, 1H, H-1), 4.17 (dd, $J = 3.4, 1.8$ Hz, 1H, H-2), 4.06 (dd, $J = 9.5, 3.5$ Hz, 1H, H-3), 3.85-3.73 (m, 3H, H-4, H-6), 3.70 (m, 1H, H-5); ¹³C NMR (126 MHz, D₂O): $\delta = 175.16$ (CO), 155.29, 138.57, 136.31, 134.02, 132.26, 132.12, 132.08, 129.86, 128.14, 128.03, 118.11, 115.82 (Ar-C), 98.15 (C-1), 73.47 (C-5), 70.34 (C-3), 69.79 (C-2), 66.51 (C-4), 60.60 (C-6); ESI-MS: m/z : Calcd for C₁₉H₁₉ClNaO₈ [M+H]⁺: 433.0661, found: 433.0661.

Ethyl 1-(4-hydroxyphenyl)-1H-1,2,3-triazole-4-carboxylate (11a). To an ice-cold suspension of sodium azide (429 mg, 6.60 mmol) in pyridine (8 mL), was added dropwise triflic anhydride (1.55 g, 0.9 mL, 5.5 mmol). The mixture was stirred at 0 °C for 2 h, then

this TfN₃-containing solution directly was added dropwise to an ice-cold mixture of 4-aminophenol (**9a**, 500 mg, 4.58 mmol), copper(II) sulfate (6 mg, 0.04 mmol), and NEt₃ (1.3 mL, 9.16 mmol) in pyridine (2 mL). The reaction mixture was stirred at 0 °C for 2 h, then concentrated, dissolved in EtOAc (50 mL), and extracted with H₂O (50 mL) and brine (50 mL). The organic layer was concentrated in vacuo. The residue (crude **10a**) was dissolved in *t*BuOH/water (1:1, 20 mL) and directly used in the next step. To the above solution containing **10a** were added subsequently ethyl propiolate (0.46 mL, 4.58 mmol), sodium ascorbate (89 mg, 0.45 mmol) and CuSO₄·5H₂O (12 mg, 0.05 mmol) at rt. After stirring for 30 min, the reaction mixture was filtered over Celite, the precipitate was washed with water, and then dried under vacuum to yield **11a** (821 mg, 77% for two steps) as brown solid. *R_f* 0.42 (petrol ether/EtOAc, 1:1); ¹H NMR (500 MHz, CD₃OD): δ = 8.98 (s, 1H, Ar-H), 7.69 (d, *J* = 8.0 Hz, 2H, Ar-H), 6.98 (d, *J* = 8.0 Hz, 2H, Ar-H), 4.44 (dd, *J* = 7.0, 7.1 Hz, 2H, OCH₂), 1.43 (t, *J* = 7.0 Hz, 3H, CH₃); ¹³C NMR (126 MHz, CD₃OD): δ = 161.97 (CO), 160.14, 141.26, 130.08, 127.56, 123.68, 117.23 (8C, Ar-C), 62.38 (OCH₂), 14.59 (CH₃); ESI-MS: *m/z*: Calcd for C₁₁H₁₁N₃NaO₃ [M+Na]⁺: 256.07, found: 256.09.

Ethyl 1-(2-chloro-4-hydroxyphenyl)-1*H*-1,2,3-triazole-4-carboxylate (11b). Prepared according to the procedure for **11a** from **9b** (200 mg, 1.4 mmol). Yield: 180 mg (48%). *R_f* 0.52 (petrol ether/EtOAc, 1:1); ¹H NMR (500 MHz, CD₃OD): δ = 8.90 (s, 1H, Ar-H), 7.79 (d, *J* = 2.6 Hz, 1H, Ar-H), 7.55 (dd, *J* = 8.8, 2.6 Hz, 1H, Ar-H), 6.99 (d, *J* = 8.8 Hz, 1H, Ar-H), 4.32 (q, *J* = 7.1 Hz, 1H, OCH₂), 1.31 (t, *J* = 7.1 Hz, 3H, CH₃); ¹³C NMR (126 MHz, CD₃OD): δ = 161.90 (CO), 127.71, 123.99, 121.92, 118.21, 101.40 (8C, Ar-C), 62.42 (OCH₂), 14.56 (CH₃); ESI-MS: *m/z*: Calcd for C₁₁H₁₀ClN₃NaO₂ [M+Na]⁺: 290.03, found: 289.85.

Ethyl 1-(4-methoxyphenyl)-1*H*-pyrazole-4-carboxylate (13a). To a sealable Schlenk tube were added CuI (16 mg, 0.082 mmol), ethyl *1H*-pyrazole-4-carboxylate (230 mg, 1.64 mmol), Cs₂CO₃ (2.10 mmol), and a stirring bar. The reaction vessel was closed with a rubber septum, evacuated and back-filled with argon. This sequence was repeated once. Then, 1-iodo-4-methoxybenzene (**12**, 461 mg, 1.97 mmol), *trans*-*N,N'*-dimethyl-1,2-cyclohexanediamine (52 μL, 0.33 mmol) and NMP (2 mL) were added successively under a stream of argon. The reaction tube was sealed and stirred in a preheated oil bath

at 110 °C for 24 h. The reaction mixture was allowed to reach rt, diluted with EtOAc (5 mL), filtered over Celite, and eluted with additional EtOAc (20 mL). The filtrate was concentrated and the resulting residue was purified by MPLC on silica gel (petrol ether/EtOAc, 4:1) to afford **13a** (325 mg, 80%) as white solid. R_f 0.43 (petrol ether/EtOAc, 4:1); ^1H NMR (500 MHz, CDCl_3): δ = 8.30, 8.07 (2 s, 2H, Ar-H), 7.60 (d, J = 8.8 Hz, 2H, Ar-H), 6.98 (d, J = 8.8 Hz, 2H, Ar-H), 4.33 (q, J = 7.0 Hz, 2H, OCH_2), 1.37 (t, J = 7.1 Hz, 3H, CH_3); ^{13}C NMR (126 MHz, CDCl_3): δ = 162.93 (CO), 158.99, 141.86, 133.08, 129.96, 121.24, 116.55, 114.65 (9C, Ar-C), 60.36 (OCH_2), 55.59 (OCH_3), 14.40 (CH_3); ESI-MS: m/z : Calcd for $\text{C}_{13}\text{H}_{15}\text{N}_2\text{O}_3$ $[\text{M}+\text{H}]^+$: 247.11, found: 246.89.

Ethyl 1-(4-methoxyphenyl)-3-(trifluoromethyl)-1H-pyrazole-4-carboxylate (13b).

Prepared according to the procedure for **13a** from 1-iodo-4-methoxybenzene (**12**, 733 mg, 3.13 mmol), CuI (8 mg, 0.039 mmol), ethyl 3-trifluoromethyl-1H-pyrazole-4-carboxylate (162 mg, 0.78 mmol), K_2CO_3 (226 mg, 1.64 mmol), and trans-*N,N'*-dimethyl-1,2-cyclohexanediamine (20 μL , 0.16 mmol). Yield: 260 mg (quant.). R_f 0.45 (petrol ether/EtOAc, 4:1); ^1H NMR (500 MHz, CDCl_3): δ = 8.37 (s, 1H, Ar-H), 7.61 (d, J = 9.0 Hz, 2H, Ar-H), 7.00 (d, J = 9.0 Hz, 2H, Ar-H), 4.36 (q, J = 7.1 Hz, 2H, OCH_2), 1.38 (t, J = 7.1 Hz, 3H, CH_3); ^{13}C NMR (126 MHz, CDCl_3): δ = 160.83, 159.69, 132.91, 132.12, 121.70, 114.78 (10C, CO, Ar-C), 61.08 (OCH_2), 55.64 (OCH_3), 14.09 (CH_3); ESI-MS: m/z : Calcd for $\text{C}_{14}\text{H}_{14}\text{F}_3\text{N}_2\text{O}_3$ $[\text{M}+\text{H}]^+$: 315.10, found: 315.06.

Ethyl 1-(4-hydroxyphenyl)-1H-pyrazole-4-carboxylate (14a). To a stirred ice-cold solution of **13a** (36 mg, 0.15 mmol) in DCE were added AlCl_3 (200 mg, 1.5 mmol) and *n*Bu₄NI (550 mg, 1.5 mmol). After stirring overnight at rt, the reaction mixture was poured into ice-water, and extracted with DCM (20 mL). The organic layer was washed with satd. aq. $\text{Na}_2\text{S}_2\text{O}_3$ (2 \times 20 mL), dried over Na_2SO_4 and concentrated in vacuo. The residue was purified by MPLC on silica gel (petrol ether/EtOAc, 2:1) to yield **14a** (20 mg, 60%) as yellow solid. R_f 0.32 (petrol ether/EtOAc, 2:1); ^1H NMR (500 MHz, CD_3OD): δ = 8.56, 8.04 (2 s, 2H, Ar-H), 7.66-7.49, 7.01-6.83 (m, 4H, Ar-H), 4.33 (q, J = 7.1 Hz, 2H, OCH_2), 1.38 (t, J = 7.1 Hz, 3H, CH_3); ^{13}C NMR (126 MHz, CD_3OD): δ = 164.60 (CO), 158.62, 142.53, 133.28, 131.96, 122.77, 117.40, 116.98 (9C, Ar-C), 61.57 (OCH_2), 14.69 (CH_3); ESI-MS: m/z : Calcd for $\text{C}_{12}\text{H}_{13}\text{N}_2\text{O}_3$ $[\text{M}+\text{H}]^+$: 233.09, found: 232.84.

Ethyl 1-(4-hydroxyphenyl)-3-(trifluoromethyl)-1H-pyrazole-4-carboxylate (14b). To a solution of **13b** (60 mg, 0.25 mmol) in 1-dodecanethiol (1 mL) was added AlCl₃ (170 mg, 1.27 mmol) at rt. The reaction mixture was stirred for 2 h at rt, then the reaction mixture was poured into ice-water and extracted with DCM (20 mL). The organic layer was washed with H₂O (20 mL) and brine (20 mL), dried over Na₂SO₄ and concentrated in vacuo. The residue was purified by MPLC on silica gel (petrol ether/EtOAc, 2:1) to yield **14b** (15 mg, 26%, with 9% impurities, which were removed in the next step). ¹H NMR (500 MHz, CD₃OD): δ = 8.75 (s, 1H, Ar-H), 7.64 (d, *J* = 8.9 Hz, 2H, Ar-H), 6.94 (d, *J* = 8.9 Hz, 2H, Ar-H), 4.35 (dd, *J* = 14.3, 7.1 Hz, 2H, OCH₂), 1.38 (t, *J* = 7.1 Hz, 3H, CH₃).

Methyl 5-bromopyrimidine-2-carboxylate (17). To a mixture of a of *n*-butyl lithium (1.6 M in hexanes, 1.3 mL, 2.1 mmol) and toluene (4 mL) at -78 °C was added a solution of **15** (0.57 g, 2.0 mmol) in toluene (2 mL). The reaction mixture was stirred for 1 h at -78 °C. The reaction was quenched with freshly crushed dry ice. The mixture was warmed slowly to rt and stirred for 2 h at rt. The mixture was concentrated under reduced pressure, and the resulting solid was treated with acetic acid. Solid **16**^[S1] was collected by filtration, dried under vacuum, and used for the next step without further purification. To a solution of **16** in dry MeOH (15 mL) was added conc. H₂SO₄ (109 μ L, 2.04 mmol). The reaction mixture was refluxed at 70 °C for 5 h, and then quenched with ice-water (50 mL). After stirring for 20 min, the reaction mixture was extracted with DCM (50 mL). The organic layer was dried over Na₂SO₄ and concentrated in vacuo. The residue was purified by MPLC on silica gel (petrol ether/EtOAc 2:1) to afford **17** (160 mg, 37% for two steps) as yellow solid. *R*_f 0.31 (petrol ether/EtOAc, 2:1); ¹H NMR (500 MHz, CDCl₃): δ = 9.00 (s, 2H, Ar-H), 4.08 (s, 3H, OCH₃); ¹³C NMR (126 MHz, CDCl₃): δ = 163.12 (CO), 158.68, 154.30, 123.50 (Ar-C), 53.79 (OCH₃); ESI-MS: *m/z*: Calcd for C₆H₆BrN₂O₂ [M+H]⁺: 216.96, found: 216.99.

3-Cyano-1H-pyrrole (20a). To a stirred solution of BetMIC (**18**, 200 mg, 1.26 mmol) and alkene **19a** (83 μ l, 1.26 mmol) in THF (5 mL) at 0 °C was added *t*BuOK (284 mg, 2.53 mmol). The reaction mixture was heated to reflux for 2 h, then cooled, diluted with water (5 mL), adjusted to pH 5 with 10% aq. HCl, and extracted with Et₂O (30 mL). The organic layer was dried with MgSO₄, filtered and concentrated. The residue was purified

by MPLC on silica (petrol ether/ EtOAc, 1:1) to give **20a** (70 mg, 60%) as yellow solid. R_f 0.35 (petrol ether/EtOAc, 1:1); ^1H NMR (500 MHz, CDCl_3): δ = 9.18-8.51 (m, 1H, NH), 7.33 (dt, J = 3.2, 1.8 Hz, 1H, Ar-H), 6.83 (dd, J = 4.8, 2.6 Hz, 1H, Ar-H), 6.52 (dd, J = 4.1, 2.7 Hz, 1H, Ar-H); ^{13}C NMR (126 MHz, CDCl_3): δ 125.65, 119.19, 116.80, 111.83, 93.34 (Ar-C, CN). The spectroscopic data were in accordance with literature values.^[S2]

3-Cyano-4-methyl-1H-pyrrole (20b). Prepared according to the procedure for **20a** from BetMIC (**18**, 200 mg, 1.26 mmol) and alkene **19b** (101 μl , 1.26 mmol). Yield: 72 mg (54%) as yellow solid. R_f 0.64 (petrol ether/EtOAc, 1:1); ^1H NMR (500 MHz, CDCl_3): δ = 8.54 (br s, 1H, NH), 7.23 (dd, J = 3.1, 2.2 Hz, 1H, Ar-H), 6.59 (td, J = 2.2, 1.0 Hz, 1H, Ar-H), 2.22 (d, J = 1.0 Hz, 3H, CH_3); ^{13}C NMR (126 MHz, CDCl_3): δ = 125.22, 122.36, 116.65, 116.51, 94.60 (Ar-C, CN), 10.37 (CH_3). The spectroscopic data were in accordance with literature values.^[S3]

Ethyl 1-[4-(2,3,4,6-tetra-*O*-acetyl- α -D-mannopyranosyloxy)-2-chlorophenyl]-1H-1,2,3-triazole-4-carboxylate (22b). Prepared according to general procedure A from **21** and **11b**. Yield: 170 mg (76%) as colorless oil. R_f 0.48 (petrol ether/EtOAc, 1:1); $[\alpha]_D^{20}$ +68.6 (c 0.5, EtOAc); ^1H NMR (500 MHz, CDCl_3): δ = 8.45 (s, 1H, Ar-H), 7.87 (d, J = 2.6 Hz, 1H, Ar-H), 7.64 (dd, J = 8.9, 2.6 Hz, 1H, Ar-H), 7.36 (d, J = 9.0 Hz, 1H, Ar-H), 5.66-5.58 (m, 2H, H-1, H-3), 5.55 (dd, J = 3.4, 1.9 Hz, 1H, H-2), 5.41 (t, J = 10.0 Hz, 1H, H-4), 4.47 (q, J = 7.1 Hz, 2H, OCH_2), 4.29 (dd, J = 12.2, 5.1 Hz, 1H, H-6a), 4.19-4.06 (m, 2H, H-5, H-6b), 2.22, 2.08, 2.05, 2.04 (4 s, 12H, 4 COCH_3), 1.44 (t, J = 7.1 Hz, 3H, CH_3); ^{13}C NMR (126 MHz, CDCl_3): δ = 169.76, 160.39 (5C, 5 CO), 151.98, 131.88, 125.39, 123.22, 120.13, 117.38 (8C, Ar-C), 96.72 (C-1), 70.10 (C-5), 69.12 (C-2), 68.58 (C-3), 65.64 (C-4), 62.02 (C-6), 61.62 (OCH_2), 20.84, 20.67 (4C, 4 COCH_3), 14.32 (CH_3); ESI-MS: m/z : Calcd for $\text{C}_{25}\text{H}_{28}\text{ClN}_3\text{NaO}_{12}$ $[\text{M}+\text{Na}]^+$: 620.13, found: 620.13.

Methyl 1-[2-chloro-4-(α -D-mannopyranosyloxy)phenyl]-1H-1,2,3-triazole-4-carboxylate (23b). Prepared according to general procedure D from **22b**. Yield: 5 mg (80%) as white solid. R_f 0.22 (DCM/MeOH, 8:1); $[\alpha]_D^{20}$ +86.2 (c 0.2, MeOH); ^1H NMR (500 MHz, CD_3OD): δ = 8.99 (s, 1H, Ar-H), 7.91 (d, J = 2.6 Hz, 1H, Ar-H), 7.70 (dd, J = 9.0, 2.7 Hz, 1H, Ar-H), 7.48 (t, J = 9.1 Hz, 1H, Ar-H), 5.56 (d, J = 1.5 Hz, 1H, H-1), 4.02

(dd, $J = 3.3, 1.8$ Hz, 1H, H-2), 3.89 (dd, $J = 9.5, 3.4$ Hz, 1H, H-3), 3.85 (s, 3H, OCH₃), 3.73-3.57 (m, 3H, H-4, H-6), 3.50 (ddd, $J = 9.6, 5.7, 2.3$ Hz, 1H, H-5); ¹³C NMR (126 MHz, CD₃OD): $\delta = 162.25$ (CO), 154.00, 141.30, 132.60, 127.90, 125.79, 123.90, 121.67, 118.77, 101.40 (Ar-C), 100.83 (C-1), 76.27 (C-5), 72.37 (C-3), 71.70 (C-2), 68.17 (C-4), 62.66 (C-6), 52.68 (OCH₃); HRMS: m/z : Calcd for C₁₆H₁₈ClN₃NaO₈ [M+Na]⁺: 438.0675, found: 438.0674.

Ethyl 1-[2-chloro-4-(α -D-mannopyranosyloxy)phenyl]-1H-1,2,3-triazole-4-carboxylate (23c). Prepared according to general procedure D from **22b**. Yield: 64 mg (74%) as white solid. R_f 0.30 (DCM/MeOH, 8:1); $[\alpha]_D^{20} +86.7$ (c 0.5, MeOH); ¹H NMR (500 MHz, CD₃OD): $\delta = 9.08$ (s, 1H, Ar-H), 8.00 (d, $J = 2.6$ Hz, 1H, Ar-H), 7.81 (dd, $J = 9.0, 2.6$ Hz, 1H, Ar-H), 7.59 (d, $J = 9.0$ Hz, 1H, Ar-H), 5.69 (d, $J = 1.1$ Hz, 1H, H-1), 4.45 (q, $J = 7.1$ Hz, 2H, OCH₂), 4.17 (dd, $J = 3.0, 1.7$ Hz, 1H, H-2), 4.03 (dd, $J = 9.5, 3.4$ Hz, 1H, H-3), 3.90-3.69 (m, 3H, H-4, H-6), 3.64 (ddd, $J = 9.5, 5.6, 2.2$ Hz, 1H, H-5), 1.44 (t, $J = 7.1$ Hz, 3H, CH₃); ¹³C NMR (126 MHz, CD₃OD): $\delta = 161.76$ (CO), 153.86, 141.50, 132.48, 127.68, 125.69, 123.71, 121.50, 118.70 (Ar-C), 100.75 (C-1), 76.19 (C-5), 72.32 (C-3), 71.64 (C-2), 68.13 (C-4), 62.61, 62.46 (C-6, OCH₂), 14.55 (CH₃); HRMS: m/z : Calcd for C₁₇H₂₀ClN₃NaO₈ [M+Na]⁺: 452.0831, found: 452.0835.

Sodium 1-[2-chloro-4-(α -D-mannopyranosyloxy)phenyl]-1H-1,2,3-triazole-4-carboxylate (24b). Prepared according to general procedure E from **22b**. Yield: 76 mg (90%) as white solid. $[\alpha]_D^{20} +60.6$ (c 0.3, MeOH/H₂O, 1:1); ¹H NMR (500 MHz, D₂O): $\delta = 8.48$ (s, 1H, Ar-H), 7.82 (d, $J = 2.0$ Hz, 1H, Ar-H), 7.59 (dd, $J = 8.9, 2.0$ Hz, 1H, Ar-H), 7.36 (d, $J = 8.9$ Hz, 1H, Ar-H), 5.65 (s, 1H, H-1), 4.18 (m, 1H, H-2), 4.03 (dd, $J = 9.4, 3.4$ Hz, 1H, H-3), 3.78-3.53 (m, 4H, H-4, H-5, H-6); ¹³C NMR (126 MHz, D₂O): $\delta = 151.34, 125.55, 124.46, 123.25, 120.88, 117.82, 99.99$ (Ar-C), 98.52 (C-1), 73.99 (C-5), 70.36 (C-3), 69.62 (C-2), 66.47 (C-4), 60.62 (C-6); HRMS: m/z : Calcd for C₁₅H₁₆ClN₃NaO₈ [M+H]⁺: 424.0518, found: 424.0518.

Ethyl 1-[4-(2,3,4,6-tetra-*O*-acetyl- α -D-mannopyranosyloxy)phenyl]-1H-pyrazole-4-carboxylate (25a). Prepared according to general procedure A from **21** and **14a**. Yield: 198 mg (98%) as yellow oil. R_f 0.27 (petrol ether/EtOAc, 2:1); $[\alpha]_D^{20} +67.5$ (c 2.0, EtOAc); ¹H NMR (500 MHz, CDCl₃): $\delta = 8.35, 8.08$ (2 s, 2H, Ar-H), 7.65 (t, $J = 6.1$ Hz,

2H, Ar-H), 7.21 (d, $J = 9.0$ Hz, 2H, Ar-H), 5.60-5.53 (m, 2H, H-1, H-3), 5.47 (dd, $J = 3.3$, 1.8 Hz, 1H, H-2), 5.39 (t, $J = 10.1$ Hz, 1H, H-4), 4.38-4.25 (m, 3H, H-6a, OCH₂), 4.15-4.07 (m, 2H, H-5, H-6b), 2.21, 2.07, 2.05, 2.04 (4 s, 12H, 4 COCH₃), 1.38 (t, $J = 7.1$ Hz, 3H, CH₃); ¹³C NMR (126 MHz, CDCl₃): $\delta = 170.42$, 169.92, 169.89, 169.66, 162.74 (5 CO), 154.76, 142.07, 134.89, 129.92, 121.07, 117.43, 116.88 (9C, Ar-C), 95.99 (C-1), 69.39 (C-5), 69.23 (C-2), 68.74 (C-3), 65.83 (C-4), 62.08 (C-6), 60.40 (OCH₂), 20.82, 20.65 (4C, 4 COCH₃), 14.37 (CH₃); ESI-MS: m/z : Calcd for C₂₆H₃₀N₂NaO₁₂ [M+Na]⁺: 585.17, found: 585.23.

Ethyl 1-[4-(2,3,4,6-tetra-*O*-acetyl- α -D-mannopyranosyloxy)phenyl]-3-trifluoromethyl-1*H*-pyrazole-4-carboxylate (25b). Prepared according to general procedure A from **21** and **14b**. Yield: 43 mg (64%). R_f 0.20 (petrol ether/EtOAc, 2:1); $[\alpha]_D^{20} +67.0$ (c 0.9, EtOAc); ¹H NMR (500 MHz, CDCl₃): $\delta = 8.41$ (s, 1H, Ar-H), 7.70-7.63 (m, 2H, Ar-H), 7.26-7.20 (m, 2H, Ar-H), 5.59-5.54 (m, 2H, H-1, H-3), 5.47 (dd, $J = 3.3$, 1.8 Hz, 1H, H-2), 5.39 (t, $J = 10.0$ Hz, 1H, H-4), 4.37 (q, $J = 7.1$ Hz, 2H, OCH₂), 4.29 (dd, $J = 12.8$, 5.8 Hz, 1H, H-6a), 4.11-4.05 (m, 2H, H-5, H-6b), 2.22, 2.06, 2.05, 2.04 (4 s, 12H, 4 COCH₃), 1.38 (t, $J = 7.1$ Hz, 3H, CH₃); ¹³C NMR (126 MHz, CDCl₃): $\delta = 170.45$, 169.97, 169.95, 169.67, 160.68 (5 CO), 155.49, 133.95, 132.88, 121.61, 117.52, 114.72 (9C, Ar-C), 95.96 (C-1), 69.51 (C-5), 69.20 (C-2), 68.71 (C-3), 65.79 (C-4), 62.06 (C-6), 61.16 (OCH₂), 20.85, 20.68, 20.67 (4C, 4 COCH₃), 14.09 (CH₃); ESI-MS: m/z : Calcd for C₂₇H₂₉F₃N₂NaO₁₂ [M+Na]⁺: 653.16, found: 653.33.

Ethyl 1-[4-(α -D-mannopyranosyloxy)phenyl]-1*H*-pyrazole-4-carboxylate (26a). Prepared according to general procedure D from **25a**. Yield: 30 mg (95%) as white solid. R_f 0.26 (DCM/MeOH, 8:1); $[\alpha]_D^{20} +110.4$ (c 0.4, MeOH); ¹H NMR (500 MHz, CD₃OD): $\delta = 8.65$ (s, 1H, Ar-H), 8.06 (s, 1H, Ar-H), 7.76-7.68 (m, 2H, Ar-H), 7.32-7.24 (m, 2H, Ar-H), 5.55 (d, $J = 1.5$ Hz, 1H, H-1), 4.34 (q, $J = 7.1$ Hz, 2H, OCH₂), 4.06 (dd, $J = 3.3$, 1.8 Hz, 1H, H-2), 3.94 (dd, $J = 9.5$, 3.4 Hz, 1H, H-3), 3.84-3.71 (m, 3H, H-4, H-6), 3.63 (ddd, $J = 7.3$, 5.9, 3.0 Hz, 1H, H-5), 1.38 (t, $J = 7.1$ Hz, 3H, CH₃); ¹³C NMR (126 MHz, CD₃OD): $\delta = 164.51$ (CO), 157.34, 142.82, 135.53, 132.01, 122.35, 118.67, 117.73 (9C, Ar-C), 100.39 (C-1), 75.63 (C-5), 72.40 (C-3), 71.91 (C-2), 68.34 (C-4), 62.70 (C-6), 61.62 (OCH₂), 14.70 (CH₃); HRMS: m/z : Calcd for C₁₈H₂₂N₂NaO₈ [M+Na]⁺: 417.1268, found: 417.1274.

Ethyl 1-[4-(α -D-mannopyranosyloxy)phenyl]-3-trifluoromethyl-1H-pyrazole-4-carboxylate (26b). Prepared according to general procedure D from **25b**. Yield: 12 mg (82%) as white solid. R_f 0.59 (DCM/MeOH, 7:1); $[\alpha]_D^{20}$ +84.1 (*c* 0.4, MeOH); ^1H NMR (500 MHz, CD_3OD): δ = 8.74 (d, J = 0.7 Hz, 1H, Ar-H), 7.71-7.63, 7.23-7.16 (m, 4H, Ar-H), 5.45 (d, J = 1.6 Hz, 1H, H-1), 4.24 (q, J = 7.1 Hz, 2H, OCH_2), 3.93 (dd, J = 3.4, 1.8 Hz, 1H, H-2), 3.81 (dd, J = 9.4, 3.4 Hz, 1H, H-3), 3.72-3.58 (m, 3H, H-4, H-6), 3.49 (ddd, J = 9.6, 5.4, 2.3 Hz, 1H, H-5), 1.27 (t, J = 7.1 Hz, 3H, CH_3); ^{13}C NMR (126 MHz, CD_3OD): δ = 162.13 (CO), 157.93, 135.12, 134.77, 122.62, 118.71, 115.32 (9C, Ar-C), 100.36 (C-1), 75.71 (C-5), 72.38 (C-3), 71.87 (C-2), 68.31 (C-4), 62.70 (C-6), 62.11 (OCH_2), 14.47 (CH_3); HRMS: m/z : Calcd for $\text{C}_{19}\text{H}_{21}\text{F}_3\text{N}_2\text{NaO}_8$ $[\text{M}+\text{Na}]^+$: 485.1142, found: 485.1141.

Sodium 1-[4-(α -D-mannopyranosyloxy)phenyl]-1H-pyrazole-4-carboxylate (27a). Prepared according to general procedure E from **25a**. Yield: 82 mg (70%) as white solid. $[\alpha]_D^{20}$ +118.61 (*c* 0.4, MeOH); ^1H NMR (500 MHz, CD_3OD): δ = 8.61, 8.06 (2 s, 2H, Ar-H), 7.75-7.70, 7.33-7.25 (m, 4H, Ar-H), 5.56 (d, J = 1.4 Hz, 1H, H-1), 4.06 (dd, J = 3.3, 1.8 Hz, 1H, H-2), 3.94 (dd, J = 9.4, 3.4 Hz, 1H, H-3), 3.84-3.72 (m, 3H, H-4, H-6), 3.62 (ddd, J = 9.6, 5.3, 2.4 Hz, 1H, H-5); ^{13}C NMR (126 MHz, CD_3OD): δ = 157.32, 143.18, 135.65, 132.19, 122.38, 118.67 (9C, Ar-C), 100.41 (C-1), 75.63 (C-5), 72.40 (C-3), 71.91 (C-2), 68.34 (C-4), 62.70 (C-6); HRMS: m/z : Calcd for $\text{C}_{16}\text{H}_{18}\text{N}_2\text{NaO}_8$ $[\text{M}+\text{H}]^+$: 389.0955, found: 389.0956.

Sodium 1-[4-(α -D-mannopyranosyloxy)phenyl]-3-trifluoromethyl-1H-pyrazole-4-carboxylate (27b). Prepared according to general procedure E from **25b**. Yield: 11 mg (79%) as white solid. $[\alpha]_D^{20}$ +85.8 (*c* 0.4, MeOH); ^1H NMR (500 MHz, CD_3OD): δ = 8.52 (s, 1H, Ar-H), 7.69-7.60, 7.22-7.15 (m, 4H, Ar-H), 5.45 (d, J = 1.3 Hz, 1H, H-1), 3.93 (dd, J = 3.2, 1.8 Hz, 1H, H-2), 3.81 (dd, J = 9.4, 3.4 Hz, 1H, H-3), 3.71-3.59 (m, 3H, H-4, H-6), 3.49 (ddd, J = 9.7, 5.3, 2.4 Hz, 1H, H-5); ^{13}C NMR (126 MHz, CD_3OD): δ = 156.18, 132.78, 121.00, 117.18 (9C, Ar-C), 98.87 (C-1), 74.15 (C-5), 70.87 (C-3), 70.38 (C-2), 66.80 (C-4), 61.16 (C-6); HRMS: m/z : Calcd for $\text{C}_{17}\text{H}_{17}\text{F}_3\text{N}_2\text{NaO}_8$ $[\text{M}+\text{H}]^+$: 457.0829, found: 457.0829.

Methyl 5-[4-(2,3,4,6-tetra-*O*-acetyl- α -D-mannopyranosyloxy)phenyl]-nicotinate (31b). Prepared according to general procedure B from **29** (50 mg, 0.09 mmol) and methyl 6-chloronicotinate (**30b**, 14 mg, 0.08 mmol). Yield: 40 mg (80%) as white solid. R_f 0.32 (petrol ether/EtOAc, 1:1); $[\alpha]_D^{20}$ +82.8 (c 0.8, EtOAc); ^1H NMR (500 MHz, CDCl_3): δ = 9.25 (dd, J = 0.7, 2.2 Hz, 1H, Ar-H), 8.33 (dd, J = 2.2, 8.3 Hz, 1H, Ar-H), 8.06-8.03 (m, 2H, Ar-H), 7.77 (dd, J = 0.6, 8.4 Hz, 1H, Ar-H), 7.23-7.20 (m, 2H, Ar-H), 5.62 (d, J = 1.7 Hz, 1H, H-1), 5.59 (dd, J = 3.6, 10.1 Hz, 1H, H-3), 5.48 (dd, J = 1.8, 3.5 Hz, 1H, H-2), 5.40 (t, J = 10.0 Hz, 1H, H-4), 4.31 (dd, J = 4.8, 12.0 Hz, 1H, H-6a), 4.12-4.06 (m, 2H, H-5, H-6b), 3.97 (s, 3H, OCH_3), 2.22, 2.07, 2.05, 2.04 (4 s, 12H, 4 COCH_3); ^{13}C NMR (126 MHz, CDCl_3): δ = 170.56, 170.01, 169.98, 169.74, 165.89 (5 CO), 160.02, 157.03, 151.00, 137.92, 133.10, 128.88, 123.89, 119.26, 116.71 (11C, Ar-C), 95.62 (C-1), 69.33 (C-5), 69.29 (C-2), 68.82 (C-3), 65.83 (C-4), 62.04 (C-6), 52.37 (OCH_3), 20.91, 20.73, 20.71 (4C, 4 COCH_3); ESI-MS: m/z : Calcd for $\text{C}_{27}\text{H}_{30}\text{NO}_{12}$ $[\text{M}+\text{H}]^+$: 560.18, found: 560.20.

Methyl 5-[4-(2,3,4,6-tetra-*O*-acetyl- α -D-mannopyranosyloxy)phenyl]-pyrazine-2-carboxylate (31c). Prepared according to general procedure B from **29** (70 mg, 0.13 mmol) and methyl 5-chloropyrazine-2-carboxylate (**30c**, 28 mg, 0.12 mmol). Yield: 48 mg (68%) as white solid. R_f 0.31 (petrol ether/EtOAc, 2:3); $[\alpha]_D^{20}$ +88.1 (c 1.0, EtOAc); ^1H NMR (500 MHz, CDCl_3): δ = 9.30 (d, J = 1.4 Hz, 1H, Ar-H), 9.09 (d, J = 1.4 Hz, 1H, Ar-H), 8.11-8.09, 7.27-7.25 (m, 4H, Ar-H), 5.64 (d, J = 1.7 Hz, 1H, H-1), 5.60 (dd, J = 3.6, 10.1 Hz, 1H, H-3), 5.49 (dd, J = 1.9, 3.5 Hz, 1H, H-2), 5.40 (t, J = 10.1 Hz, 1H, H-4), 4.30 (dd, J = 5.2, 12.4 Hz, 1H, H-6a), 4.13-4.07 (m, 5H, H-5, H-6b, OCH_3), 2.23, 2.07, 2.06, 2.04 (4 s, 12H, 4 COCH_3); ^{13}C NMR (126 MHz, CDCl_3): δ = 170.52, 170.01, 169.99, 169.72, 164.60 (5 CO), 157.80, 154.42, 145.68, 140.85, 140.58, 130.03, 129.18, 117.05 (10C, Ar-C), 95.59 (C-1), 69.45 (C-5), 69.21(C-2), 68.75 (C-3), 65.76 (C-4), 65.76 (C-6), 53.09 (OCH_3), 20.91, 20.73, 20.71 (4C, 4 COCH_3); ESI-MS: m/z : Calcd for $\text{C}_{26}\text{H}_{29}\text{N}_2\text{O}_{12}$ $[\text{M}+\text{H}]^+$: 561.17, found: 561.23.

Methyl 5-[4-(2,3,4,6-tetra-*O*-acetyl- α -D-mannopyranosyloxy)phenyl]-pyrimidine-2-carboxylate (31d). Prepared according to general procedure B from **29** (149 mg, 0.27 mmol) and **17** (53 mg, 0.25 mmol). Yield: 54 mg (40%) as white solid. R_f 0.25 (petrol ether/EtOAc, 1:2); $[\alpha]_D^{20}$ +91.9 (c 0.6, MeOH); ^1H NMR (500 MHz, CDCl_3): δ = 9.02 (s,

2H, Ar-H), 7.54 (d, $J = 8.8$ Hz, 2H, Ar-H), 7.21 (d, $J = 8.5$ Hz, 2H, Ar-H), 5.54 (d, $J = 1.7$ Hz, 1H, H-1), 5.51 (dd, $J = 3.5, 10.0$ Hz, 1H, H-3), 5.41 (dd, $J = 1.8, 3.5$ Hz, 1H, H-2), 5.34 (t, $J = 10.0$ Hz, 1H, H-4), 4.22 (dd, $J = 5.5, 12.8$ Hz, 1H, H-6a), 4.05-3.99 (m, 5H, H-5, H-6a, OCH₃), 2.16, 2.00, 1.99, 1.98 (4 s, 12H, 4 COCH₃); ¹³C NMR (126 MHz, CDCl₃): $\delta = 170.47, 170.01, 170.00, 169.68, 163.65$ (5 CO), 156.91, 155.22, 154.54, 135.13, 128.70, 127.73, 117.55 (10C, Ar-C), 95.68 (C-1), 69.44 (C-5), 69.19 (C-2), 68.72 (C-3), 65.71 (C-4), 61.97 (C-6), 53.65 (OCH₃), 29.69, 20.89, 20.71, 20.69 (4 COCH₃); ESI-MS: m/z : Calcd for C₂₆H₂₉N₂O₁₂ [M+H]⁺: 561.17, found: 561.23.

Methyl 5-[4-(α -D-mannopyranosyloxy)phenyl]-nicotinate (32b). Prepared according to general procedure D from **31b**. Yield: 6 mg (24%) as white solid. R_f 0.40 (DCM/MeOH, 5:1); $[\alpha]_D^{20} +142.6$ (c 0.1, MeOH); ¹H NMR (500 MHz, CD₃OD): $\delta = 9.04$ (dd, $J = 0.7, 2.2$ Hz, 1H, Ar-H), 8.28 (dd, $J = 2.2, 8.4$ Hz, 1H, Ar-H), 7.96-7.93 (m, 2H, Ar-H), 7.85 (dd, $J = 0.7, 8.4$ Hz, 1H, Ar-H), 7.18-7.16 (m, 2H, Ar-H), 5.49 (d, $J = 1.7$ Hz, 1H, H-1), 3.93 (dd, $J = 1.9, 3.4$ Hz, 1H, H-2), 3.86 (s, 3H, OCH₃), 3.82 (dd, $J = 3.5, 9.5$ Hz, 1H, H-3), 3.67-3.60 (m, 3H, H-4, H-6), 3.49 (ddd, $J = 2.7, 5.5, 9.5$ Hz, 1H, H-5); ¹³C NMR (126 MHz, CD₃OD): $\delta = 151.50, 139.33, 133.28, 130.00, 125.38, 121.05, 117.96, 101.40$ (10C, Ar-C), 100.04 (C-1), 75.59 (C-5), 72.42 (C-3), 71.92 (C-2), 68.33 (C-4), 62.69 (C-6), 52.85 (OCH₃); HRMS: m/z : Calcd for C₁₉H₂₁NNaO₈ [M+Na]⁺: 414.1159, found: 414.1159.

Methyl 5-[4-(α -D-mannopyranosyloxy)phenyl]-pyrazine-2-carboxylate (32c). Prepared according to general procedure D from **31c**. Yield: 5 mg (36%) as white solid. R_f 0.42 (DCM/MeOH, 5:1); $[\alpha]_D^{20} +138.4$ (c 0.2, MeOH); ¹H NMR (500 MHz, CD₃OD): $\delta = 9.14$ (t, $J = 1.2$ Hz, 1H, Ar-H), 9.09 (t, $J = 1.2$ Hz, 1H, Ar-H), 8.10-8.08, 7.21-7.20 (m, 4H, Ar), 5.51 (d, $J = 1.5$ Hz, 1H, H-1), 3.94 (dd, $J = 1.9, 3.3$ Hz, 1H, H-2), 3.92 (s, 3H, OCH₃), 3.81 (dd, $J = 3.5, 9.5$ Hz, 1H, H-3), 3.66-3.60 (m, 3H, H-4, H-6), 3.47 (ddd, $J = 2.5, 5.2, 9.5$ Hz, 1H, H-5); ¹³C NMR (126 MHz, CD₃OD): $\delta = 165.88$ (CO), 160.43, 156.27, 146.57, 142.09, 141.46, 130.40, 130.27, 118.23 (10C, Ar-C), 99.95 (C-1), 75.72 (C-5), 72.36 (C-2), 71.85 (C-3), 68.26 (C-4), 62.66 (C-6), 53.33 (OCH₃); HRMS: m/z : Calcd for C₁₈H₂₀N₂NaO₈ [M+Na]⁺: 415.1112, found: 414.1106.

Methyl 5-[4-(α -D-mannopyranosyloxy)phenyl]-pyrimidine-2-carboxylate (32d).

Prepared according to general procedure D from **31d**. Yield: 8 mg (89%) as white solid. R_f 0.40 (DCM/MeOH, 5:1); $[\alpha]_D^{20} +134.7$ (c 0.1, dioxane/H₂O, 1:1); ¹H NMR (500 MHz, DMSO-*d*₆): δ = 9.30 (s, 2H, Ar-H), 7.88 (d, J = 8.7 Hz, 2H, Ar-H), 7.28 (d, J = 8.7 Hz, 2H, Ar-H), 5.50 (s, 1H, H-1), 5.09 (s, 1H, OH), 4.87 (s, 1H, OH), 4.80 (s, 1H, OH), 4.47 (t, J = 5.3 Hz, 1H, OH), 3.94 (s, 3H, OCH₃), 3.87 (m, 1H, H-2), 3.72 (m, 1H, H-3), 3.61 (m, 1H, H-6a), 3.57-3.44 (m, 2H, H-4, H-6b), 3.41 (m, 1H, H-5), 3.18 (d, J = 4.9 Hz, 1H); ¹³C NMR (126 MHz, DMSO-*d*₆): δ = 163.60 (CO), 157.60, 154.79, 154.20, 134.05, 128.60, 126.22, 117.48 (10C, Ar-C), 98.68 (C-1), 75.11 (C-5), 70.61, 69.94 (C-2, C-3), 66.65 (C-4), 60.99 (C-6), 52.76 (OCH₃); HRMS: m/z : Calcd for C₁₈H₂₀N₂NaO₈ [M+Na]⁺: 415.1112, found: 414.1113.

Sodium 5-[4-(α -D-mannopyranosyloxy)phenyl]-nicotinate (33b). Prepared according to general procedure E from **31b**. Yield: 10 mg (48%) as white solid. $[\alpha]_D^{20} +138.0$ (c 0.5, MeOH/H₂O, 1:1); ¹H NMR (500 MHz, D₂O): δ = 8.66 (s, 1H, Ar-H), 7.94 (d, J = 8.0 Hz, 1H, Ar-H), 7.46 (d, J = 8.4 Hz, 2H, Ar-H), 7.38 (d, J = 8.1 Hz, 1H, Ar-H), 6.88 (d, J = 8.4 Hz, 2H, Ar-H), 5.40 (s, 1H, H-1), 3.98 (m, 1H, H-2), 3.88 (dd, J = 9.6, 3.4 Hz, 1H, H-3), 3.67-3.54 (m, 3H, H-4, H-6), 3.50 (ddd, J = 9.8, 5.0, 2.2 Hz, 1H, H-5); ¹³C NMR (126 MHz, D₂O): δ = 157.78, 156.56, 149.30, 138.34, 132.14, 128.56, 120.63, 116.86 (10C, Ar-C), 97.83 (C-1), 73.39 (C-5), 70.37 (C-3), 69.87 (C-2), 66.59 (C-4), 60.67 (C-6); HRMS: m/z : Calcd for C₁₈H₁₉NNaO₈ [M+H]⁺: 400.1003, found: 400.0993.

Sodium 5-[4-(α -D-mannopyranosyloxy)phenyl]-pyrazine-2-carboxylate (33c).

Prepared according to general procedure E from **31c**. Yield: 6 mg (44%) as white solid. $[\alpha]_D^{20} +90.3$ (c 0.2, MeOH/H₂O, 1:1); ¹H NMR (500 MHz, D₂O): δ = 8.94, 8.89 (2 s, 2H, Ar-H), 7.85-7.83, 7.19-7.17 (m, 4H, Ar-H), 5.64 (d, J = 1.7 Hz, 1H, H-1), 4.17 (dd, J = 1.8, 3.5 Hz, 1H, H-2), 4.05 (dd, J = 3.5, 9.4 Hz, H-3), 3.78-3.67 (m, 4H, H-4, H-5, H-6); ¹³C NMR (126 MHz, D₂O): δ = 157.23, 152.73, 145.68, 143.73, 141.21, 129.32, 128.86, 117.12 (10C, Ar-C), 97.65 (C-1), 73.38 (C-5), 69.74 (2C, C-2, C-3), 66.53 (C-4), 60.61 (C-6); HRMS: m/z : Calcd for C₁₇H₁₇N₂Na₂O₈ [M+Na]⁺: 423.0775, found: 423.0774.

Sodium 5-[4-(α -D-mannopyranosyloxy)phenyl]-pyrimidine-2-carboxylate (33d). Prepared according to general procedure E from **32d**. Yield: 17 mg (60%) as white solid.

$[\alpha]_{\text{D}}^{20} +89.5$ (*c* 0.2, MeOH/H₂O, 3:1); ¹H NMR (500 MHz, D₂O): δ = 8.91 (bs, 2H, Ar-H), 7.60-7.58, 7.17-7.16 (m, 4H, Ar-H), 5.55 (d, *J* = 1.7 Hz, 1H, H-1), 4.05 (dd, *J* = 1.9, 3.5 Hz, 1H, H-2), 3.93 (dd, *J* = 3.5, 9.1 Hz, H-3), 3.66-3.55 (m, 4H, H-4, H-5, H-6); ¹³C NMR (126 MHz, D₂O): δ = 128.54, 117.60 (Ar-C), 97.85 (C-1), 73.38 (C-5), 70.30 (C-3), 69.77 (C-2), 66.51 (C-4), 60.59 (C-6); HRMS: *m/z*: Calcd for C₁₇H₁₉N₂O₈ [M+H]⁺: 379.1136, found: 379.1136.

1-[4-(2,3,4,6-Tetra-*O*-acetyl- α -D-mannopyranosyloxy)-3-chlorophenyl]-1*H*-pyrrole-3-carbonitrile (40a). Prepared according to general procedure C from **39** (86 mg, 0.15 mmol) and **20a** (16 mg, 0.17 mmole). Yield: 35 mg (44%) as yellow oil. *R_f* 0.37 (petrol ether/EtOAc, 2:1); $[\alpha]_{\text{D}}^{20} +56.3$ (*c* 1.7, EtOAc); ¹H NMR (500 MHz, CDCl₃): δ = 7.45 (d, *J* = 2.6 Hz, 1H, Ar-H), 7.42 (m, 1H, Ar-H), 7.26 (d, *J* = 3.3 Hz, 1H, Ar-H), 7.23 (dd, *J* = 8.8, 2.6 Hz, 1H, Ar-H), 6.95 (dd, *J* = 3.0, 2.3 Hz, 1H, Ar-H), 6.59 (dd, *J* = 3.0, 1.6 Hz, 1H, Ar-H), 5.59 (dd, *J* = 10.1, 3.5 Hz, 1H, H-3), 5.57 (d, *J* = 1.8 Hz, 1H, H-1), 5.52 (dd, *J* = 3.5, 1.9 Hz, 1H, H-2), 5.40 (t, *J* = 10.1 Hz, 1H, H-4), 4.28 (dd, *J* = 12.3, 5.1 Hz, 1H, H-6a), 4.16 (m, 1H, H-5), 4.10 (m, 1H, H-6b), 2.21, 2.07, 2.04, 2.04 (4 s, 12H, 4 COCH₃); ¹³C NMR (126 MHz, CDCl₃): δ = 170.40, 169.97, 169.80, 169.69 (4 CO), 150.66, 135.03, 126.48, 125.68, 123.88, 121.21, 120.74, 117.78, 115.91, 113.73 (11C, Ar-C, CN), 95.61 (C-1), 69.99 (C-5), 69.20 (C-2), 68.62 (C-3), 65.69 (C-4), 62.05 (C-6), 20.85, 20.68, 20.67 (4C, 4 COCH₃); ESI-MS: *m/z*: Calcd for C₂₅H₂₅ClN₂NaO₁₀ [M+Na]⁺: 571.11, found: 571.18.

1-[4-(2,3,4,6-Tetra-*O*-acetyl- α -D-mannopyranosyloxy)-3-chlorophenyl]-4-methyl-1*H*-pyrrole-3-carbonitrile (40b). Prepared according to general procedure C from **39** (50 mg, 0.09 mmol) and **20b** (11 mg, 0.11 mmole). Yield: 44 mg (92%) as yellow oil. *R_f* 0.29 (petrol ether/EtOAc, 2:1); $[\alpha]_{\text{D}}^{20} +63.2$ (*c* 1.0, EtOAc); ¹H NMR (500 MHz, CDCl₃): δ = 7.35 (d, *J* = 2.6 Hz, 1H, Ar-H), 7.27 (d, *J* = 2.4 Hz, 1H, Ar-H), 7.20 (t, *J* = 8.2 Hz, 1H, Ar-H), 7.13 (m, 1H, Ar-H), 6.69 (dd, *J* = 2.2, 1.1 Hz, 1H, Ar-H), 5.54 (m, 1H, H-3), 5.49 (d, *J* = 1.7 Hz, 1H, H-1), 5.46 (dd, *J* = 3.4, 1.9 Hz, 1H, H-2), 5.34 (t, *J* = 10.1 Hz, 1H, H-4), 4.22 (dd, *J* = 12.3, 5.2 Hz, 1H, H-6a), 4.11 (m, 1H, H-5), 4.04 (dd, *J* = 12.2, 3.3 Hz, 1H, H-6b), 2.16 (d, *J* = 0.8 Hz, 3H, CH₃), 2.14, 2.01, 1.99, 1.98 (4 s, 12H, 4 COCH₃); ¹³C NMR (126 MHz, CDCl₃): δ = 170.41, 169.97, 169.80, 169.70 (4 CO), 150.35, 135.20, 125.73, 125.63, 124.52, 123.43, 120.26, 118.72, 117.82, 115.60 (11C, Ar-C, CN),

96.94 (C-1), 69.96 (C-5), 69.22 (C-2), 68.63 (C-3), 65.71 (C-4), 62.07 (C-6), 20.85, 20.68, 20.67 (4C, 4 COCH₃), 10.52 (CH₃); ESI-MS: *m/z*: Calcd for C₂₆H₂₇ClN₂NaO₁₀ [M+Na]⁺: 585.12, found: 585.03.

Ethyl 1-[4-(2,3,4,6-tetra-*O*-acetyl- α -D-mannopyranosyloxy)-3-chlorophenyl]-*1H*-pyrrole-2-carboxylate (40c). Prepared according to general procedure C from **39** and methyl *1H*-pyrrole-2-carboxylate (**20c**). Yield: 34 mg (33%) as colorless oil. *R_f* 0.43 (petrol ether/EtOAc, 3:2); [α]_D²⁰ + 61.0 (*c* 0.7, EtOAc); ¹H NMR (500 MHz, CDCl₃): δ 7.39 (d, *J* = 2.4 Hz, 1H, Ar-H), 7.22 (d, *J* = 8.8 Hz, 1H, Ar-H), 7.18 (dd, *J* = 8.7, 2.5 Hz, 1H, Ar-H), 7.09 (dd, *J* = 3.9, 1.8 Hz, 1H, Ar-H), 6.88 (dd, *J* = 2.5, 1.9 Hz, 1H, Ar-H), 6.28 (dd, *J* = 3.8, 2.7 Hz, 1H, Ar-H), 5.62 (dd, *J* = 10.0, 3.5 Hz, 1H, H-3), 5.59 (d, *J* = 1.6 Hz, 1H, H-1), 5.54 (dd, *J* = 3.4, 1.9 Hz, 1H, H-2), 5.41 (t, *J* = 10.1 Hz, 1H, H-4), 4.31 (dd, *J* = 12.3, 5.2 Hz, 1H, H-6a), 4.23-4.14 (m, 3H, OCH₂, H-5), 4.11 (dd, *J* = 12.3, 2.2 Hz, 1H, H-6b), 2.21, 2.08, 2.07, 2.05 (4 s, 12H, 4 COCH₃), 1.24 (t, *J* = 7.1 Hz, 3H, CH₃); ¹³C NMR (126 MHz, CDCl₃): δ = 170.51, 169.91, 169.76, 169.75, 160.31 (5 CO), 150.88, 136.14, 129.59, 128.64, 125.88, 123.93, 123.78, 119.04, 116.18, 109.46 (C-Ar), 96.83 (C-1), 69.85 (C-5), 69.30 (C-2), 68.73 (C-3), 65.79 (C-4), 62.07 (C-6), 60.02 (OCH₂), 20.85, 20.71, 20.67 (4C, 4 COCH₃), 14.26 (CH₃); ESI-MS: *m/z*: Calcd for C₂₇H₃₀ClN₂NaO₁₂ [M+Na]⁺: 618.13, found: 618.18.

Ethyl 1-[4-(2,3,4,6-tetra-*O*-acetyl- α -D-mannopyranosyloxy)-3-chlorophenyl]-4-methyl-*1H*-pyrrole-2-carboxylate (40d). Prepared according to general procedure C from **39** and methyl 4-methyl-*1H*-pyrrole-2-carboxylate (**20d**). Yield: 67 mg (64%) as colorless oil. *R_f* 0.30 (petrol ether/EtOAc, 2:1); [α]_D²⁰ + 47.8 (*c* 0.7, EtOAc); ¹H NMR (500 MHz, CDCl₃): δ = 7.36 (d, *J* = 2.4 Hz, 1H, Ar-H), 7.20 (d, *J* = 8.8 Hz, 1H, Ar-H), 7.15 (dd, *J* = 8.7, 2.5 Hz, 1H, Ar-H), 6.91 (d, *J* = 1.6 Hz, 1H, Ar-H), 6.67 (d, *J* = 0.9 Hz, 1H, Ar-H), 5.62 (dd, *J* = 10.0, 3.5 Hz, 1H, H-3), 5.57 (d, *J* = 1.6 Hz, 1H, H-1), 5.53 (dd, *J* = 3.4, 1.9 Hz, 1H, H-2), 5.40 (t, *J* = 10.1 Hz, 1H, H-4), 4.31 (dd, *J* = 12.3, 5.3 Hz, 1H, H-6a), 4.20 (ddd, *J* = 10.1, 5.2, 2.2 Hz, 1H, H-5), 4.18-4.08 (m, 3H, OCH₂, H-6b), 2.21, 2.11, 2.08, 2.07, 2.05 (5 s, 15H, 5 CH₃), 1.23 (t, *J* = 7.1 Hz, 3H, CH₃); ¹³C NMR (126 MHz, CDCl₃): δ = 170.52, 169.91, 169.75, 160.32 (5C, 5 CO), 150.69, 136.26, 128.55, 128.10, 125.80, 123.86, 123.18, 120.00, 119.90, 116.17 (C-Ar), 96.86 (C-1), 69.83 (C-5), 69.32 (C-2), 68.75 (C-3), 65.81 (C-4), 62.08 (C-6), 59.90 (OCH₂), 20.85, 20.71, 20.68

(4C, 4 COCH₃), 14.27, 11.43 (2 CH₃); ESI-MS: *m/z*: Calcd for C₂₈H₃₂ClNNaO₁₂ [M+Na]⁺: 632.15, found: 632.16.

Methyl 1-[4-(2,3,4,6-tetra-*O*-acetyl- α -D-mannopyranosyloxy)-3-chlorophenyl]-*1H*-pyrrole-3-carboxylate (40e). Prepared according to general procedure C from **39** and methyl *1H*-pyrrole-3-carboxylate (**20e**). Yield: 87 mg (99 %) as colorless oil. *R_f* 0.42 (petrol ether/EtOAc, 3:2); [α]_D²⁰ +62.5 (*c* 0.8, EtOAc); ¹H NMR (500 MHz, CDCl₃): δ = 7.60 (m, 1H, Ar-H), 7.48 (d, *J* = 1.4 Hz, 1H, Ar-H), 7.26 (d, *J* = 0.9 Hz, 2H, Ar-H), 6.95 (m, 1H, Ar-H), 6.74 (dd, *J* = 3.0, 1.6 Hz, 1H, Ar-H), 5.61 (dd, *J* = 10.0, 3.5 Hz, 1H, H-3), 5.57 (d, *J* = 1.6 Hz, 1H, H-1), 5.54 (dd, *J* = 3.4, 1.9 Hz, 1H, H-2), 5.41 (t, *J* = 10.1 Hz, 1H, H-4), 4.29 (dd, *J* = 12.3, 5.3 Hz, 1H, H-6a), 4.19 (ddd, *J* = 10.1, 5.2, 2.2 Hz, 1H, H-5), 4.11 (m, 1H, H-6b), 3.84 (s, 3H, OCH₃), 2.22, 2.08, 2.05 (3s, 12H, 4 COCH₃); ¹³C NMR (126 MHz, CDCl₃): δ = 170.39, 169.92, 169.76, 169.70, 164.82 (5 CO), 150.06, 135.81, 125.51, 124.30, 123.31, 120.62, 120.18, 118.29, 117.85, 111.92 (C-Ar), 96.93 (C-1), 69.92 (C-5), 69.22 (C-2), 68.66 (C-3), 65.74 (C-4), 62.08 (C-6), 51.25 (OCH₃), 20.83, 20.68, 20.66 (4C, 4 COCH₃); ESI-MS: *m/z*: Calcd for C₂₆H₂₈ClNNaO₁₂ [M+Na]⁺: 604.12, found: 604.21.

1-[3-Chloro-4-(α -D-mannopyranosyloxy)phenyl]-*1H*-pyrrole-3-carbonitrile (41a). Prepared according to general procedure D from **40a**. Yield: 15 mg (65%) as white solid. *R_f* 0.33 (DCM/MeOH, 8:1); [α]_D²⁰ +65.8 (*c* 1.1, MeOH); ¹H NMR (500 MHz, CD₃OD): δ = 7.86 (m, 1H, Ar-H), 7.68 (d, *J* = 2.6 Hz, 1H, Ar-H), 7.52 (d, *J* = 8.9 Hz, 1H, Ar-H), 7.47 (dd, *J* = 8.9, 2.7 Hz, 1H, Ar-H), 7.28 (dd, *J* = 3.0, 2.3 Hz, 1H, Ar-H), 6.63 (dd, *J* = 1.6, 3.0 Hz, 1H, Ar-H), 5.61 (d, *J* = 1.7 Hz, 1H, H-1), 4.13 (dd, *J* = 3.4, 1.8 Hz, 1H, H-2), 4.00 (dd, *J* = 9.5, 3.4 Hz, 1H, H-3), 3.84-3.70 (m, 3H, H-4, H-6), 3.64 (ddd, *J* = 9.7, 5.6, 2.3 Hz, 1H, H-5); ¹³C NMR (126 MHz, CD₃OD): δ = 152.48, 135.71, 128.46, 125.83, 124.14, 122.82, 121.82, 119.17, 117.18, 114.15 (Ar-C, CN), 100.97 (C-1), 95.65 (Ar-C), 76.15 (C-5), 72.38 (C-3), 71.78 (C-2), 68.20 (C-4), 62.68 (C-6); ESI-MS: *m/z*: Calcd for C₁₇H₁₇ClN₂NaO₆ [M+Na]⁺: 403.0667, found: 403.0669.

1-[3-Chloro-4-(α -D-mannopyranosyloxy)phenyl]-4-methyl-*1H*-pyrrole-3-carbonitrile (41b). Prepared according to general procedure D from **40b**. Yield: 6 mg (38%) as white solid. *R_f* 0.32 (DCM/MeOH, 8:1); [α]_D²⁰ +50.0 (*c* 0.3, MeOH); ¹H NMR (500 MHz,

CD₃OD): δ = 7.63 (d, J = 2.4 Hz, 1H, Ar-H), 7.52 (d, J = 2.7 Hz, 1H, Ar-H), 7.37 (d, J = 8.9 Hz, 1H, Ar-H), 7.31 (dd, J = 8.9, 2.7 Hz, 1H, Ar-H), 6.96 (dd, J = 2.3, 1.1 Hz, 1H, Ar-H), 5.47 (d, J = 1.7 Hz, 1H, H-1), 4.00 (dd, J = 3.4, 1.8 Hz, 1H, H-2), 3.87 (dd, J = 9.5, 3.4 Hz, 1H, H-3), 3.72-3.57 (m, 3H, H-4, H-6), 3.52 (ddd, J = 9.7, 5.6, 2.3 Hz, 1H, H-5), 2.11 (d, J = 0.9 Hz, 3H, CH₃); ¹³C NMR (126 MHz, CD₃OD): δ = 152.22, 135.83, 127.72, 125.82, 125.01, 123.71, 121.39, 120.31, 119.21, 116.77 (Ar-C, CN), 101.00 (C-1), 96.96 (Ar-C), 76.12 (C-5), 72.38 (C-3), 71.79 (C-2), 68.21 (C-4), 62.68 (C-6), 10.44 (CH₃); ESI-MS: m/z : Calcd for C₁₈H₁₉ClN₂NaO₆ [M+Na]⁺: 417.0824, found: 417.0824.

Ethyl 1-[3-chloro-4-(α -D-mannopyranosyloxy)phenyl]-1H-pyrrole-2-carboxylate (41c). Prepared according to general procedure D from **40c**. Yield: 21 mg (91%) as white solid. R_f 0.32 (DCM/MeOH, 8:1); $[\alpha]_D^{20}$ +77.6 (c 0.4, MeOH); ¹H NMR (500 MHz, CD₃OD): δ = 7.32 (d, J = 8.8 Hz, 1H, Ar-H), 7.27 (d, J = 2.5 Hz, 1H, Ar-H), 7.10 (dd, J = 8.8, 2.6 Hz, 1H, Ar-H), 6.97 (dd, J = 3.9, 1.7 Hz, 1H, Ar-H), 6.92 (m, 1H, Ar-H), 6.19 (dd, J = 3.9, 2.7 Hz, 1H, Ar-H), 5.49 (d, J = 1.5 Hz, 1H, H-1), 4.06-3.98 (m, 3H, H-2, OCH₂), 3.90 (dd, J = 9.5, 3.4 Hz, 1H, H-3), 3.73-3.60 (m, 3H, H-4, H-6), 3.55 (ddd, J = 9.7, 5.3, 2.4 Hz, 1H, H-5), 1.08 (t, J = 7.1 Hz, 3H, CH₃); ¹³C NMR (126 MHz, CD₃OD): δ = 162.04 (CO), 152.92, 136.88, 131.36, 129.36, 127.08, 124.87, 124.35, 120.38, 117.82, 110.44 (Ar-C), 100.99 (C-1), 76.06 (C-5), 72.41 (C-3), 71.84 (C-2), 68.19 (C-4), 62.66 (C-6), 61.15 (OCH₂), 14.52 (CH₃); HRMS: m/z : Calcd for C₁₉H₂₂ClNNaO₈ [M+Na]⁺: 450.0926, found: 450.0926.

Ethyl 1-[3-chloro-4-(α -D-mannopyranosyloxy)phenyl]-4-methyl-1H-pyrrole-2-carboxylate (41d). Prepared according to general procedure D from **40d**. Yield: 14 mg (61%) as white solid. R_f 0.21 (DCM/MeOH, 8:1); $[\alpha]_D^{20}$ +71.2 (c 0.4, MeOH); ¹H NMR (500 MHz, CD₃OD): δ = 7.30 (d, J = 8.8 Hz, 1H, Ar-H), 7.23 (d, J = 2.5 Hz, 1H, Ar-H), 7.06 (dd, J = 8.8, 2.6 Hz, 1H, Ar-H), 6.79 (d, J = 1.5 Hz, 1H, Ar-H), 6.70 (d, J = 0.9 Hz, 1H, Ar-H), 5.48 (d, J = 1.4 Hz, 1H, H-1), 4.05-3.95 (m, 3H, H-2, OCH₂), 3.89 (dd, J = 9.5, 3.4 Hz, 1H, H-3), 3.73-3.59 (m, 3H, H-4, H-6), 3.55 (ddd, J = 9.7, 5.3, 2.4 Hz, 1H, H-5), 1.07 (t, J = 7.1 Hz, 3H, CH₃); ¹³C NMR (126 MHz, CD₃OD): δ = 162.08 (CO), 152.74, 137.00, 129.86, 129.27, 126.98, 124.31, 124.30, 121.32, 121.14, 117.82 (Ar-C), 101.01 (C-1), 76.04 (C-5), 72.41 (C-3), 71.85 (C-2), 68.19 (C-4), 62.65 (C-6), 61.05

(OCH₂), 14.53, 11.47 (2 CH₃); HRMS: *m/z*: Calcd for C₂₀H₂₄ClNNaO₈ [M+Na]⁺: 464.1083, found: 464.1083.

Methyl 1-[3-chloro-4-(α -D-mannopyranosyloxy)phenyl]-1*H*-pyrrole-3-carboxylate (41e). Prepared according to general procedure D from **40e**. Yield: 24 mg (83%) as white solid. *R_f* 0.27 (DCM/MeOH, 8:1); [α]_D²⁰ +82.0 (*c* 0.4, MeOH); ¹H NMR (500 MHz, CD₃OD): δ = 7.77 (m, 1H, Ar-H), 7.63 (d, *J* = 2.6 Hz, 1H, Ar-H), 7.49 (d, *J* = 8.9 Hz, 1H, Ar-H), 7.43 (dd, *J* = 8.9, 2.7 Hz, 1H, Ar-H), 7.17 (m, 1H, Ar-H), 6.70 (dd, *J* = 3.0, 1.6 Hz, 1H, Ar-H), 5.59 (d, *J* = 1.4 Hz, 1H, H-1), 4.14 (dd, *J* = 3.2, 1.8 Hz, 1H, H-2), 4.01 (dd, *J* = 9.5, 3.4 Hz, 1H, H-3), 3.89-3.70 (m, 6H, OCH₃, H-4, H-6), 3.66 (ddd, *J* = 9.6, 5.5, 2.2 Hz, 1H, H-5); ¹³C NMR (126 MHz, CD₃OD): δ = 167.05 (CO), 152.10, 136.30, 125.80, 125.77, 123.74, 122.21, 121.45, 119.25, 118.82, 112.50 (Ar-C), 101.01 (C-1), 76.11 (C-5), 72.40 (C-3), 71.80 (C-2), 68.23 (C-4), 62.69 (C-6), 51.76 (OCH₃); HRMS: *m/z*: Calcd for C₁₈H₂₀ClNNaO₈ [M+Na]⁺: 436.0770, found: 436.0768.

Sodium 1-[3-chloro-4-(α -D-mannopyranosyloxy)phenyl]-1*H*-pyrrole-2-carboxylate (42). Prepared according to general procedure E from **40c**. Yield: 14 mg (58%) as white solid. [α]_D²⁰ +73.8 (*c* 0.4, MeOH); ¹H NMR (500 MHz, CD₃OD): δ = 7.42 (d, *J* = 8.8 Hz, 1H, Ar-H), 7.39 (d, *J* = 2.5 Hz, 1H, Ar-H), 7.23 (dd, *J* = 8.8, 2.6 Hz, 1H, Ar-H), 7.02 (dd, *J* = 3.8, 1.7 Hz, 1H, Ar-H), 6.98 (m, 1H, Ar-H), 6.27 (dd, *J* = 3.7, 2.8 Hz, 1H, Ar-H), 5.59 (d, *J* = 1.4 Hz, 1H, H-1), 4.13 (dd, *J* = 3.2, 1.8 Hz, 1H, H-2), 4.01 (dd, *J* = 9.5, 3.4 Hz, 1H, H-3), 3.87-3.72 (m, 3H, H-4, H-6), 3.68 (ddd, *J* = 9.8, 5.3, 2.3 Hz, 1H, H-5); ¹³C NMR (126 MHz, CD₃OD): δ = 152.63, 137.37, 130.26, 129.02, 126.80, 124.31, 119.52, 117.95, 110.01, 101.39 (Ar-C), 101.09 (C-1), 76.01 (C-5), 72.41 (C-3), 71.87 (C-2), 68.22 (C-4), 62.67 (C-6); HRMS: *m/z*: Calcd for C₁₇H₁₈ClNNaO₈ [M+Na]⁺: 422.0613, found: 422.0614.

Sodium 1-[3-chloro-4-(α -D-mannopyranosyloxy)phenyl]-4-methyl-1*H*-pyrrole-2-carboxylate (43). Prepared according to general procedure E from **40d**. Yield: 8 mg (40%) as white solid. [α]_D²⁰ +74.5 (*c* 0.4, MeOH); ¹H NMR (500 MHz, CD₃OD): δ = 7.39-7.30 (m, 2H, Ar-H), 7.19 (dd, *J* = 8.7, 2.6 Hz, 1H, Ar-H), 6.63 (d, *J* = 1.6 Hz, 1H, Ar-H), 6.59 (d, *J* = 0.9 Hz, 1H, Ar-H), 5.54 (d, *J* = 1.5 Hz, 1H, H-1), 4.12 (dd, *J* = 3.3, 1.8 Hz, 1H, H-2), 4.00 (dd, *J* = 9.5, 3.4 Hz, 1H, H-3), 3.85-3.72 (m, 3H, H-4, H-6), 3.69

(ddd, $J = 9.7, 5.0, 2.4$ Hz, 1H, H-5), 2.09 (s, 3H, CH₃); ¹³C NMR (126 MHz, CD₃OD): $\delta = 151.72, 138.57, 128.27, 126.05, 125.42, 124.18, 119.79, 117.99$ (10C, Ar-C), 101.40 (C-1), 75.89 (C-5), 72.41 (C-3), 71.91 (C-2), 68.28 (C-4), 62.62 (C-6), 11.72 (CH₃); HRMS: m/z : Calcd for C₁₈H₂₀ClNNaO₈ [M+H]⁺: 436.0770, found: 436.0774.

Sodium 1-[3-chloro-4-(α -D-mannopyranosyloxy)phenyl]-1H-pyrrole-3-carboxylate (44). Prepared according to general procedure E from **41e**. Yield: 6 mg (20%) as white solid. $[\alpha]_D^{20} +92.6$ (c 0.4, MeOH); ¹H NMR (500 MHz, CD₃OD): $\delta = 7.74$ (t, $J = 1.9$ Hz, 1H, Ar-H), 7.66 (d, $J = 2.6$ Hz, 1H, Ar-H), 7.51 (d, $J = 8.9$ Hz, 1H, Ar-H), 7.46 (dd, $J = 8.9, 2.6$ Hz, 1H, Ar-H), 7.17 (t, $J = 2.7$ Hz, 1H, Ar-H), 6.71 (dd, $J = 3.0, 1.6$ Hz, 1H, Ar-H), 5.59 (d, $J = 1.4$ Hz, 1H, H-1), 4.13 (dd, $J = 3.2, 1.8$ Hz, 1H, H-2), 4.00 (dd, $J = 9.5, 3.4$ Hz, 1H, H-3), 3.86-3.70 (m, 3H, H-4, H-6), 3.66 (m, 1H, H-5); ¹³C NMR (126 MHz, CD₃OD): $\delta = 152.03, 136.54, 125.81, 125.70, 123.72, 121.96, 121.43, 119.29, 112.84$ (10C, Ar-C), 101.06 (C-1), 76.11 (C-5), 72.39 (C-3), 71.82 (C-2), 68.23 (C-4), 62.69 (C-6); HRMS: m/z : Calcd for C₁₇H₁₈ClNNaO₈ [M+H]⁺: 422.0613, found: 422.0612.

Ethyl 1-[4-(2,3,4,6-tetra-*O*-acetyl- α -D-mannopyranosyloxy)-3-(trifluoromethyl)phenyl]-4-methyl-1H-pyrrole-3-carboxylate (47). Prepared according to general procedure C from **34** and methyl 4-methyl-1H-pyrrole-3-carboxylate (**20f**). Yield: 55 mg (49%) as colorless oil. R_f 0.48 (petrol ether/EtOAc, 3:2); $[\alpha]_D^{20} + 60.9$ (c 1.1, EtOAc); ¹H NMR (500 MHz, CDCl₃): $\delta = 7.63$ (d, $J = 2.6$ Hz, 1H, Ar-H), 7.58 (d, $J = 2.5$ Hz, 1H, Ar-H), 7.51 (dd, $J = 8.9, 2.6$ Hz, 1H, Ar-H), 7.34 (d, $J = 8.9$ Hz, 1H, Ar-H), 6.78 (d, $J = 1.3$ Hz, 1H, Ar-H), 5.65 (d, $J = 1.5$ Hz, 1H, H-1), 5.54 (dd, $J = 10.1, 3.4$ Hz, 1H, H-3), 5.48 (dd, $J = 3.3, 1.9$ Hz, 1H, H-2), 5.42 (t, $J = 10.1$ Hz, 1H, H-4), 4.35-4.25 (m, 3H, OCH₂, H-6a), 4.13-4.04 (m, 2H, H-5, H-6b), 2.33 (d, $J = 0.5$ Hz, 3H, CH₃), 2.22, 2.07, 2.06, 2.05 (4 s, 12H, 4 COCH₃), 1.36 (t, $J = 7.1$ Hz, 3H, CH₃); ¹³C NMR (126 MHz, CDCl₃): $\delta = 170.49, 170.01, 169.83, 169.72, 165.04$ (5 CO), 151.44, 134.91, 125.23, 124.86, 123.82, 121.65, 121.48, 121.23, 119.93, 119.89, 119.13, 117.48, 116.89 (Ar-C, CF₃), 96.15 (C-1), 70.12 (C-5), 69.20 (C-2), 68.60 (C-3), 65.63 (C-4), 62.12 (C-6), 59.76 (OCH₂), 20.93, 20.78, 20.73 (4C, 4 COCH₃), 14.60, 11.81 (2 CH₃); ESI-MS: m/z : Calcd for C₂₉H₃₂F₃NNaO₁₂ [M+Na]⁺: 666.18, found: 666.22.

Ethyl 1-[4-(α -D-mannopyranosyloxy)-3-(trifluoromethyl)phenyl]-4-methyl-1H-pyrrole-3-carboxylate (49). Prepared according to general procedure D from **47**. Yield: 17 mg (85%) as white solid. R_f 0.41 (DCM/MeOH, 8:1); $[\alpha]_D^{20} +84.6$ (c 0.4, MeOH); ^1H NMR (500 MHz, CD_3OD): $\delta = 7.74$ (dd, $J = 4.9, 2.7$ Hz, 3H, Ar-H), 7.64 (m, 1H, Ar-H), 7.02 (d, $J = 1.3$ Hz, 1H, Ar-H), 5.64 (d, $J = 1.3$ Hz, 1H, H-1), 4.29 (q, $J = 7.1$ Hz, 2H, OCH_2), 4.07 (dd, $J = 3.3, 1.8$ Hz, 1H, H-2), 3.94 (dd, $J = 9.5, 3.4$ Hz, 1H, H-3), 3.83 (dd, $J = 12.0, 2.3$ Hz, 1H, H-6a), 3.80-3.71 (m, 2H, H-4, H-6b), 3.60 (m, 1H, H-5), 2.31 (s, 3H, CH_3), 1.38 (t, $J = 7.1$ Hz, 3H, CH_3); ^{13}C NMR (126 MHz, CD_3OD): $\delta = 166.97$ (CO), 135.32, 126.78, 126.29, 124.35, 120.70, 118.75, 117.82 (11C, Ar-C, CF_3), 100.59 (C-1), 76.17 (C-5), 72.22 (C-3), 71.70 (C-2), 68.11 (C-4), 62.71 (C-6), 60.76 (OCH_2), 14.77, 11.92 (2 CH_3); HRMS: m/z : Calcd for $\text{C}_{21}\text{H}_{24}\text{F}_3\text{NNaO}_8$ $[\text{M}+\text{Na}]^+$: 498.1346, found: 498.1347.

Sodium 1-[4-(α -D-mannopyranosyloxy)-3-(trifluoromethyl)phenyl]-4-methyl-1H-pyrrole-3-carboxylate (51). Prepared according to general procedure E from **49**. Yield: 7 mg (35%) as white solid. $[\alpha]_D^{20} +96.6$ (c 0.4, MeOH); ^1H NMR (500 MHz, CD_3OD): $\delta = 7.77$ -7.69 (m, 3H, Ar-H), 7.63 (d, $J = 9.8$ Hz, 1H, Ar-H), 7.01 (d, $J = 1.2$ Hz, 1H, Ar-H), 5.64 (d, $J = 1.2$ Hz, 1H, H-1), 4.07 (dd, $J = 3.2, 1.8$ Hz, 1H, H-2), 3.94 (dd, $J = 9.5, 3.4$ Hz, 1H, H-3), 3.88-3.70 (m, 3H, H-4, H-6), 3.61 (m, 1H, H-5), 2.31 (s, 3H, CH_3); ^{13}C NMR (126 MHz, CD_3OD): $\delta = 135.42, 126.76, 126.55, 124.58, 120.63, 118.77$ (11C, Ar-C, CF_3), 100.62 (C-1), 76.18 (C-5), 72.23 (C-3), 71.71 (C-2), 68.13 (C-4), 62.72 (C-6), 11.90 (CH_3); HRMS: m/z : Calcd for $\text{C}_{19}\text{H}_{20}\text{F}_3\text{NNaO}_8$ $[\text{M}+\text{H}]^+$: 470.1033, found: 470.1039.

HPLC data for the target compounds:

System: Beckman Coulter Gold, consisting of pump 126, DAD 168 (190-400 nm) and auto-sampler 508. Column: Waters Atlantis T3, 3 μm , 2.1 \times 100 mm. A: $\text{H}_2\text{O} + 0.1\%$ TFA; B: MeCN + 0.1% TFA.

Gradient A: 0% B \rightarrow 95% B (20 min); 95% B (2 min); 95% B \rightarrow 5% B (3 min); 5% B \rightarrow 0% B (2 min); flow rate: 0.5 mL/min.

Gradient B: 0% B \rightarrow 70% B (20 min); 70% B (2 min); 70% B \rightarrow 5% B (3 min); 5% B \rightarrow 0% B (2 min); flow rate: 0.5 mL/min.

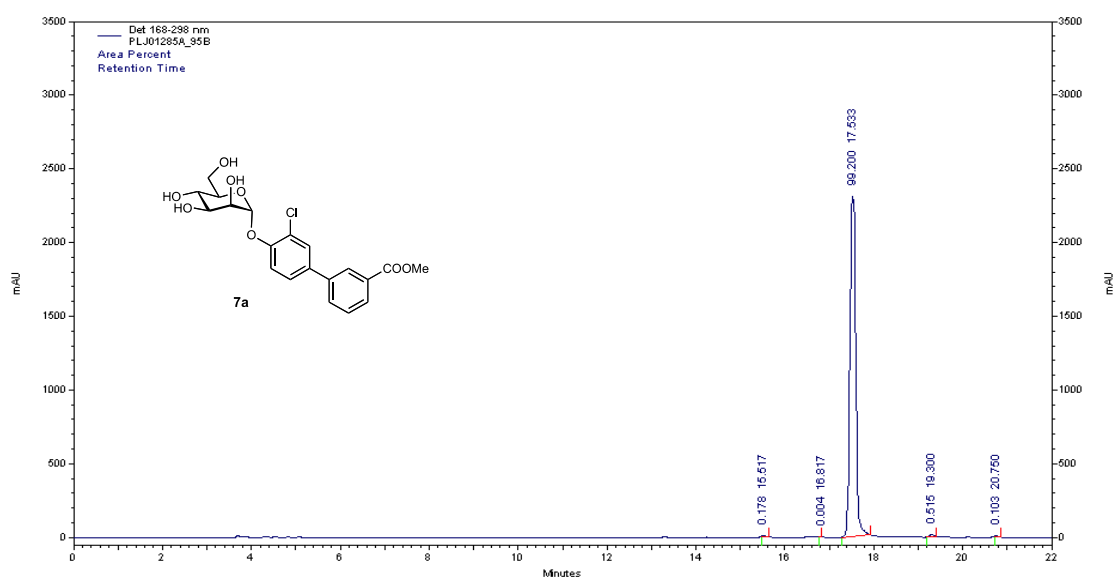
Gradient C: 0% B → 50% B (20 min); 50% B (2 min); 50% B → 5% B (3 min); 5% B → 0% B (2 min); flow rate: 0.5 mL/min.

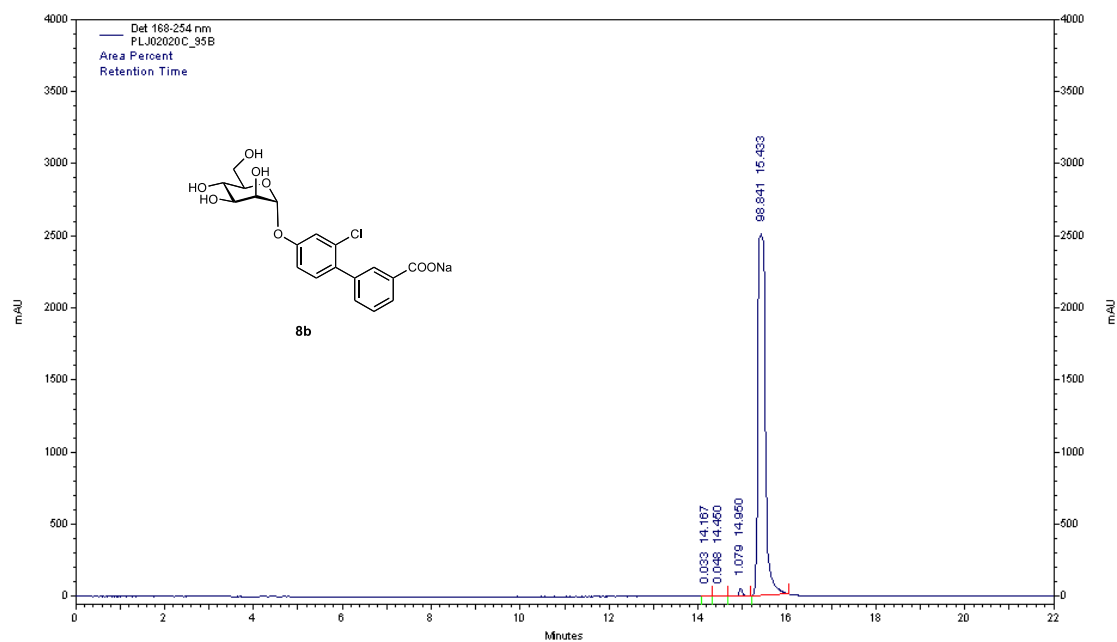
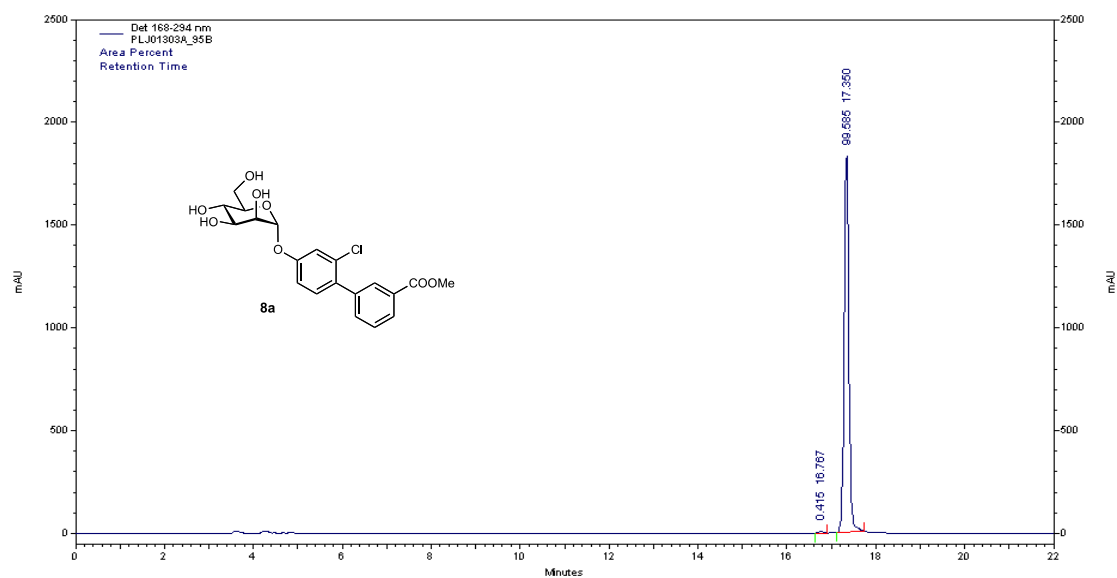
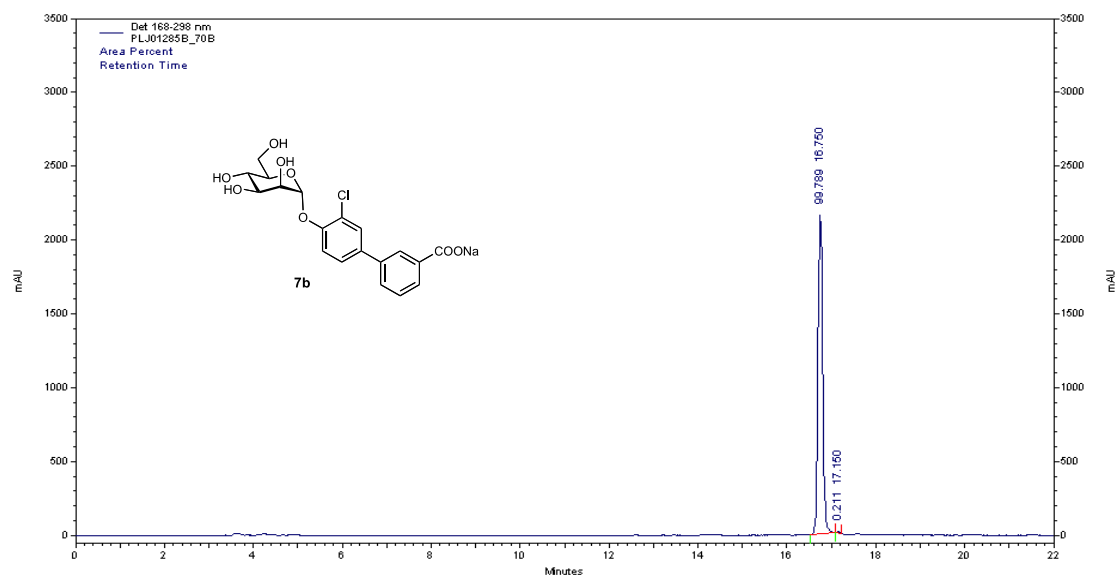
Table S1. HPLC data for the target compounds.

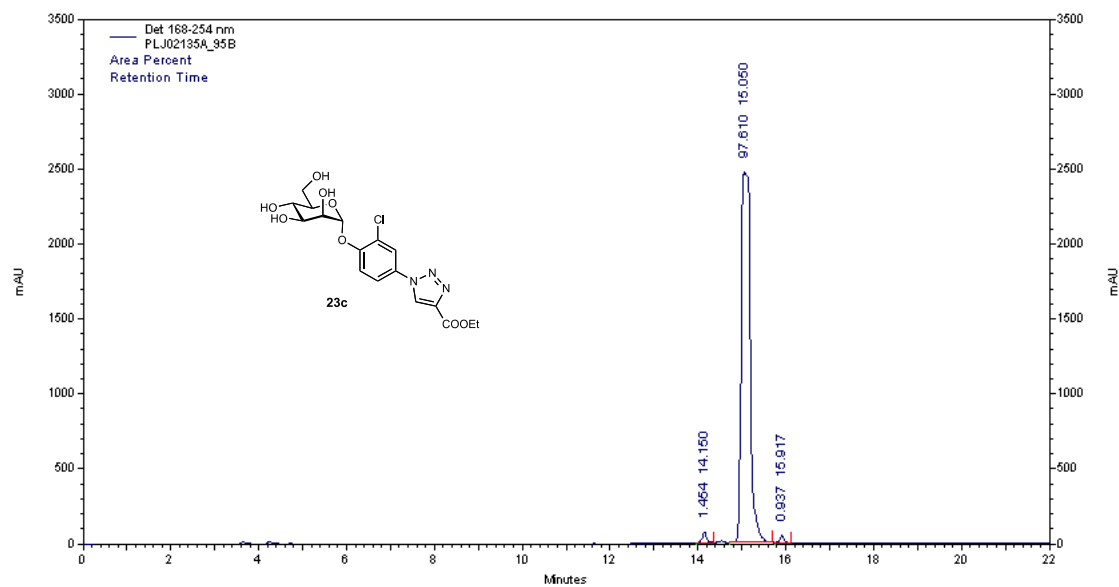
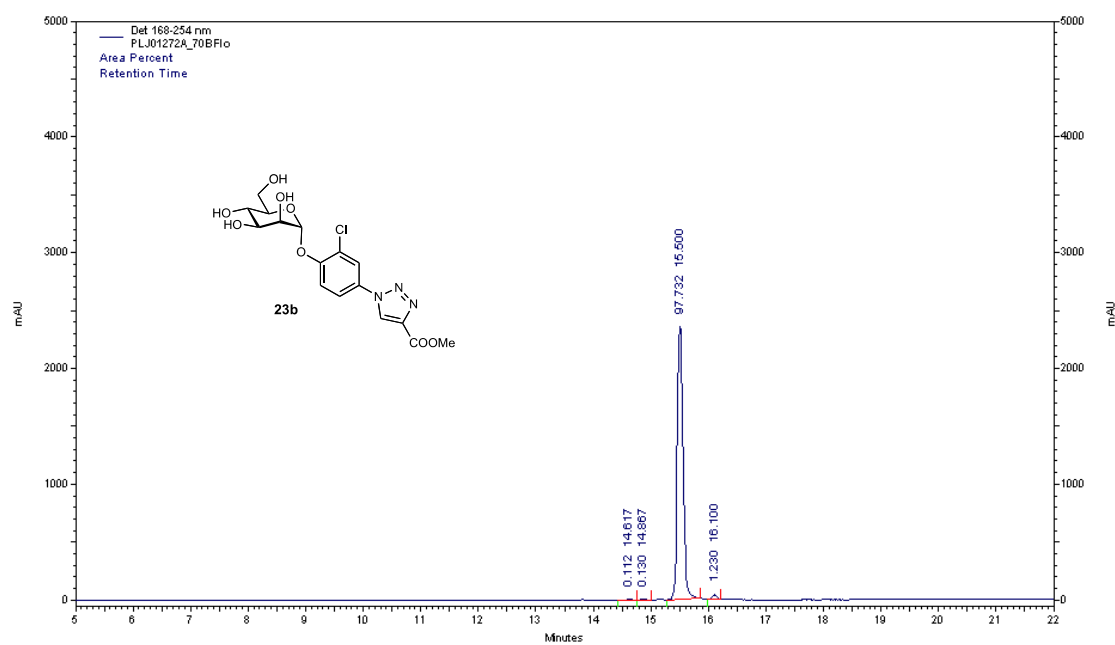
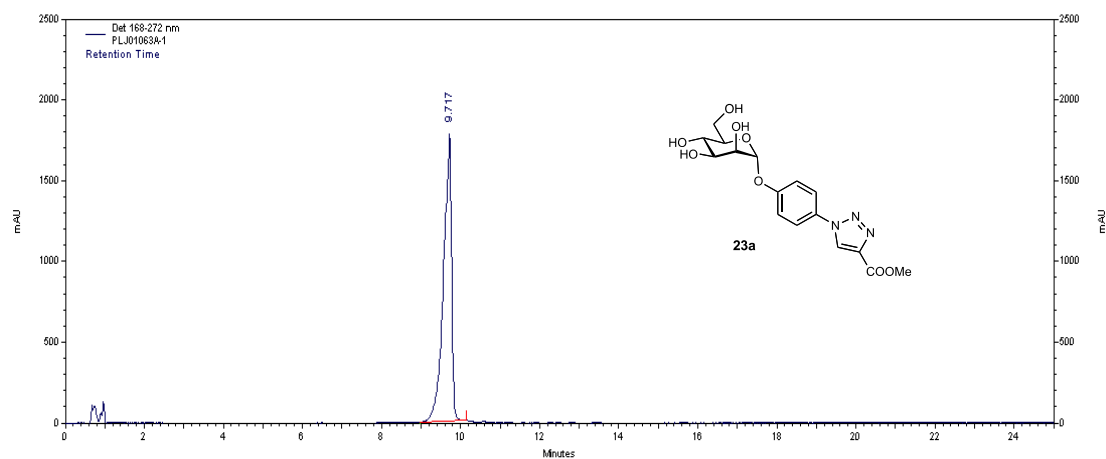
Compound	Formula	Gradient	Retention [min]	Detection	Purity [%]
7a	C ₂₀ H ₂₁ ClO ₈	A	17.53	298 nm	99.2
7b	C ₁₉ H ₁₈ ClNaO ₈	B	16.75	298 nm	99.8
8a	C ₂₀ H ₂₁ ClO ₈	A	17.35	294 nm	99.6
8b	C ₁₉ H ₁₈ ClNaO ₈	A	15.43	254 nm	98.8
23a	C ₁₆ H ₁₉ N ₃ O ₈	C	9.72	272 nm	100
23b	C ₁₆ H ₁₈ ClN ₃ O ₈	B	15.50	254 nm	97.7
23c	C ₁₇ H ₂₀ ClN ₃ O ₈	A	15.05	254 nm	97.6
24a	C ₁₅ H ₁₆ N ₃ NaO ₈	C	5.88	252 nm	100
24b	C ₁₅ H ₁₅ ClN ₃ NaO ₈	A	12.58	254 nm	99.1
26a	C ₁₈ H ₂₂ N ₂ O ₈	A	10.45	270 nm	95.0
26b	C ₁₉ H ₂₁ F ₃ N ₂ O ₈	A	12.98	254 nm	100
27a	C ₁₆ H ₁₇ N ₂ NaO ₈	A	7.75	254 nm	100
27b	C ₁₇ H ₁₆ F ₃ N ₂ NaO ₈	A	10.15	254 nm	94.7
32a	C ₁₉ H ₂₁ NO ₈	C	12.07	312 nm	100
32b	C ₁₉ H ₂₁ NO ₈	B	15.82	328 nm	99.7
32c	C ₁₈ H ₂₀ N ₂ O ₈	B	15.08	328 nm	100
32d	C ₁₈ H ₂₀ N ₂ O ₈	C	9.42	308 nm	100
33a	C ₁₈ H ₁₈ NNaO ₈	C	2.37	248 nm	100
33b	C ₁₈ H ₁₈ NNaO ₈	A	12.25	270 nm	97.9
33c	C ₁₇ H ₁₇ N ₂ NaO ₈	B	13.58	328 nm	100
33d	C ₁₇ H ₁₇ N ₂ NaO ₈	C	7.28	248 nm	100
37	C ₂₀ H ₂₀ F ₃ NO ₈	A	10.70	254 nm	98.9
38	C ₁₉ H ₁₇ F ₃ NNaO ₈	A	8.10	257 nm	96.6
41a	C ₁₇ H ₁₇ ClN ₂ O ₆	A	15.90	271 nm	100
41b	C ₁₈ H ₁₉ ClN ₂ O ₆	A	16.73	271 nm	99.2
41c	C ₁₉ H ₂₂ ClNO ₈	A	12.42	254 nm	97.7
41d	C ₂₀ H ₂₄ ClNO ₈	A	13.33	254 nm	100

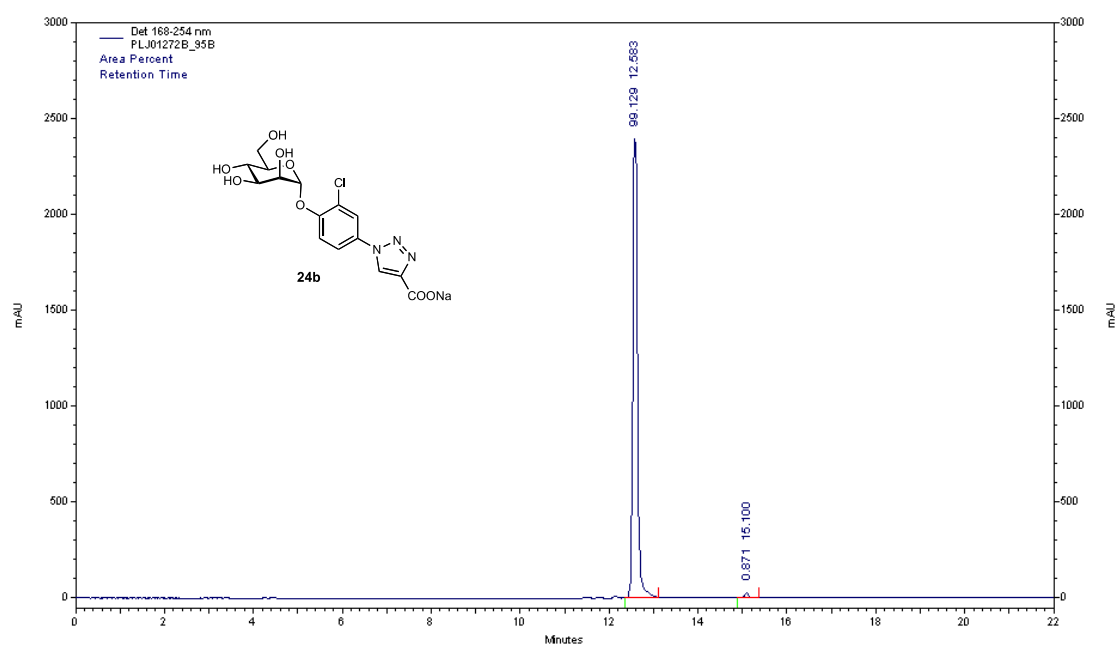
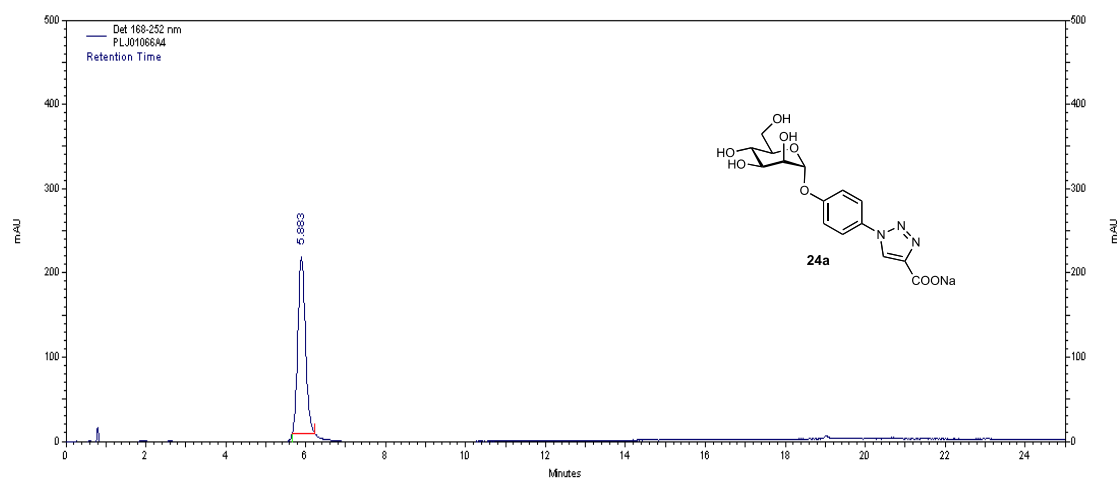
41e	$C_{18}H_{20}ClNO_8$	A	11.37	254 nm	98.6
41f	$C_{20}H_{24}ClNO_8$	A	17.90	254 nm	99.0
42	$C_{17}H_{17}ClNNaO_8$	A	10.27	254 nm	98.1
43	$C_{18}H_{19}ClNNaO_8$	A	11.15	254 nm	98.8
44	$C_{17}H_{17}ClNNaO_8$	A	9.65	254 nm	99.8
45	$C_{18}H_{19}ClNNaO_8$	A	15.10	254 nm	98.4
48	$C_{20}H_{25}NO_8$	A	12.37	254 nm	99.7
49	$C_{21}H_{24}F_3NO_8$	A	13.68	290 nm	100
50	$C_{18}H_{20}NNaO_8$	A	9.72	254 nm	100
51	$C_{19}H_{19}F_3NNaO_8$	A	11.10	254 nm	98.6

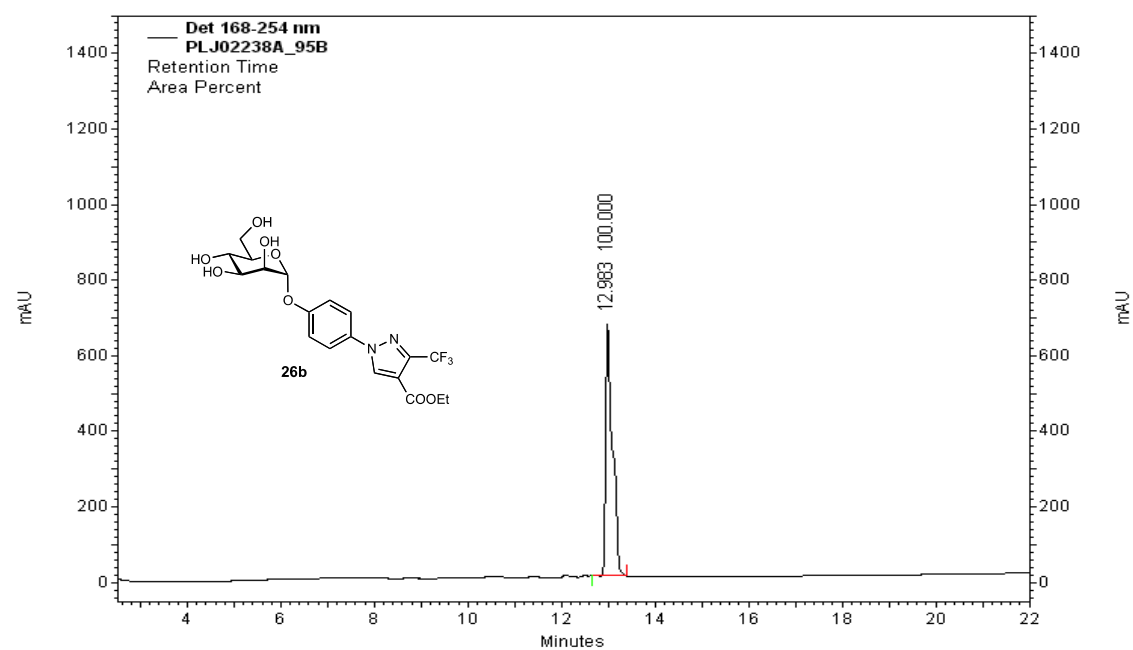
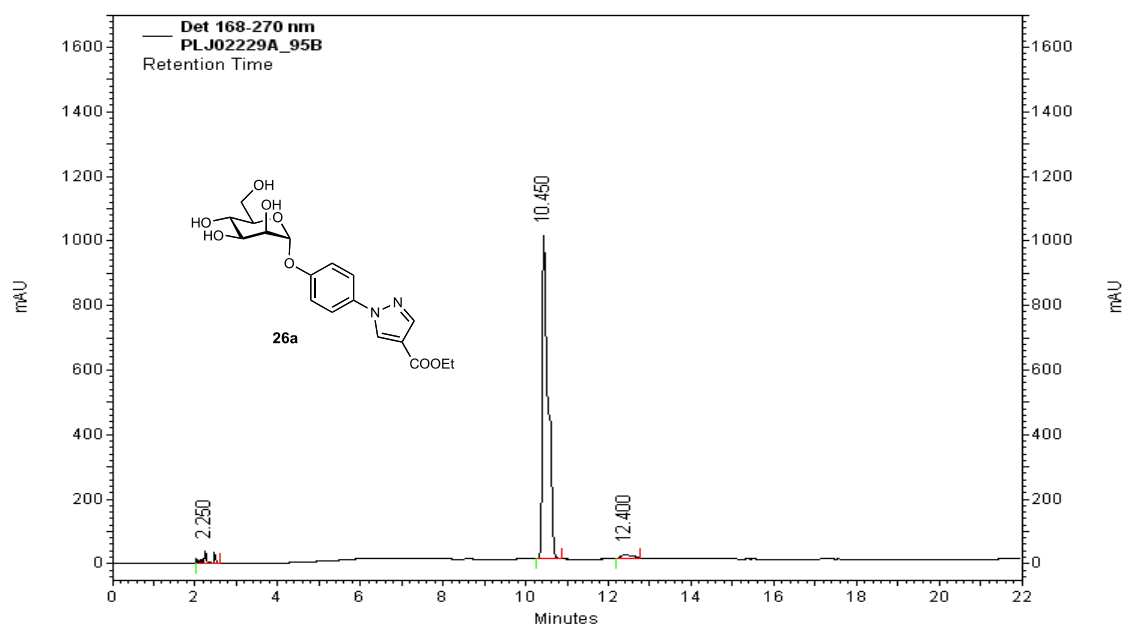
HPLC traces of the target compounds:

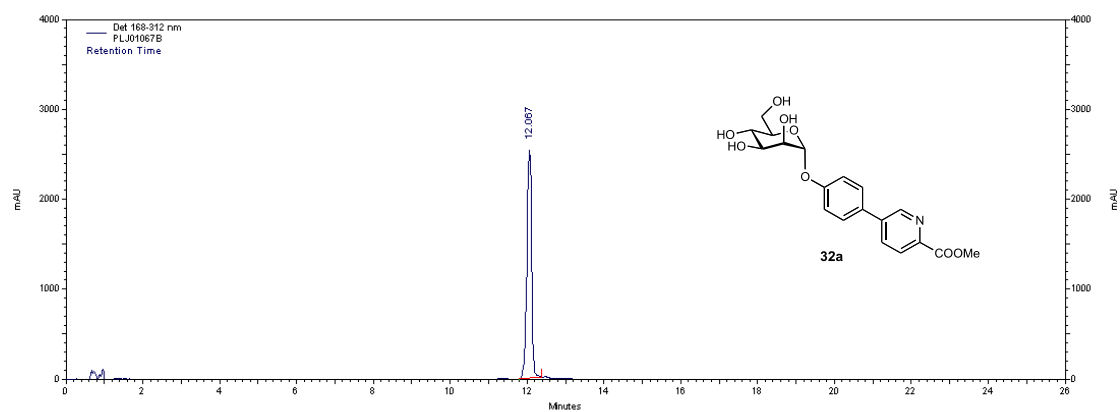
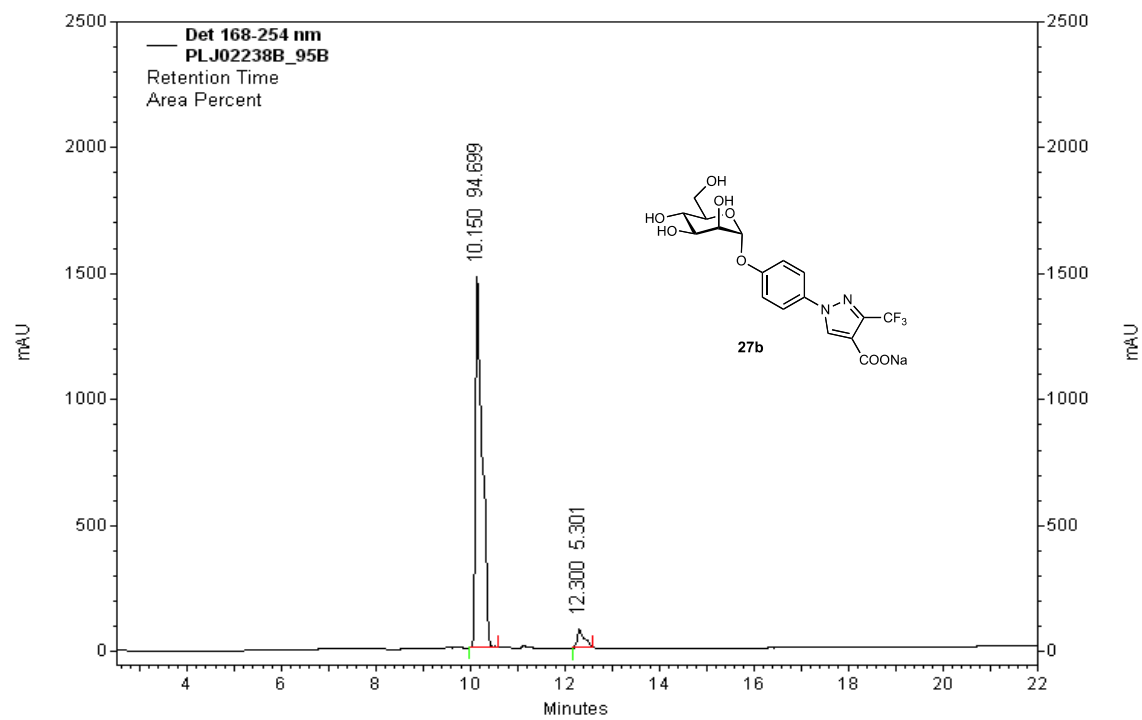
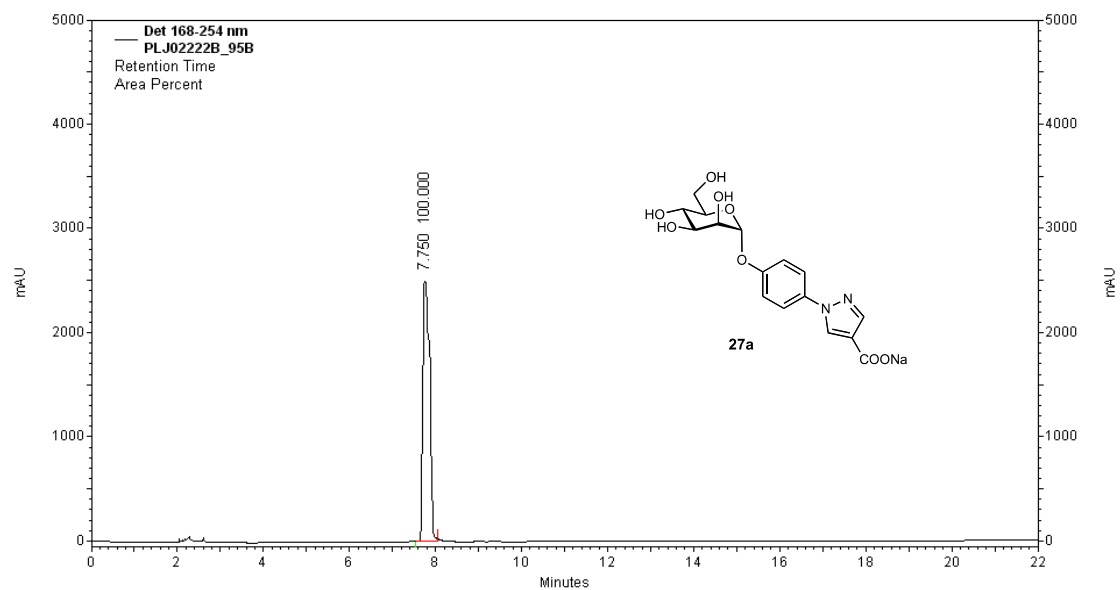


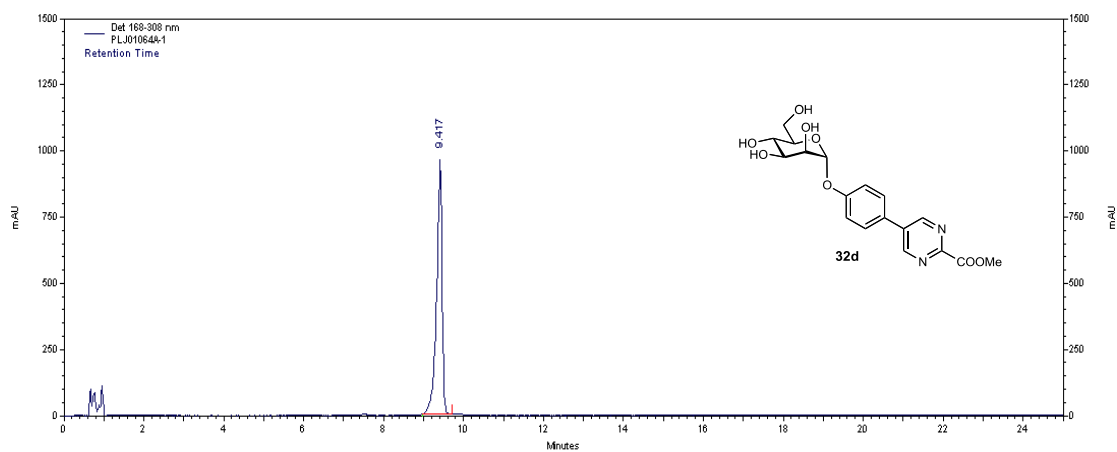
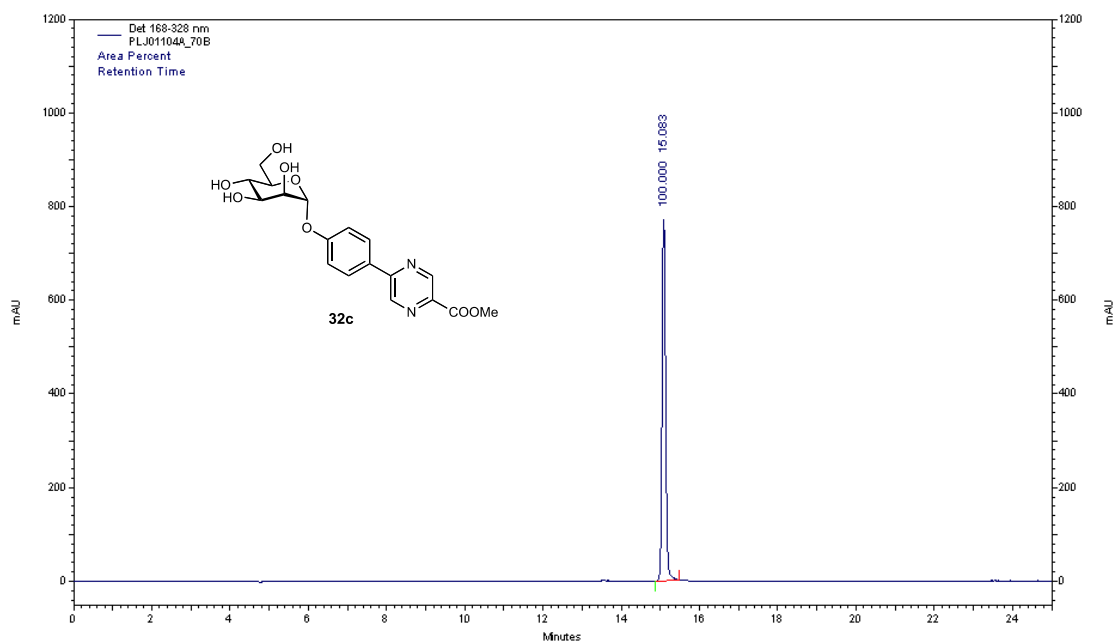
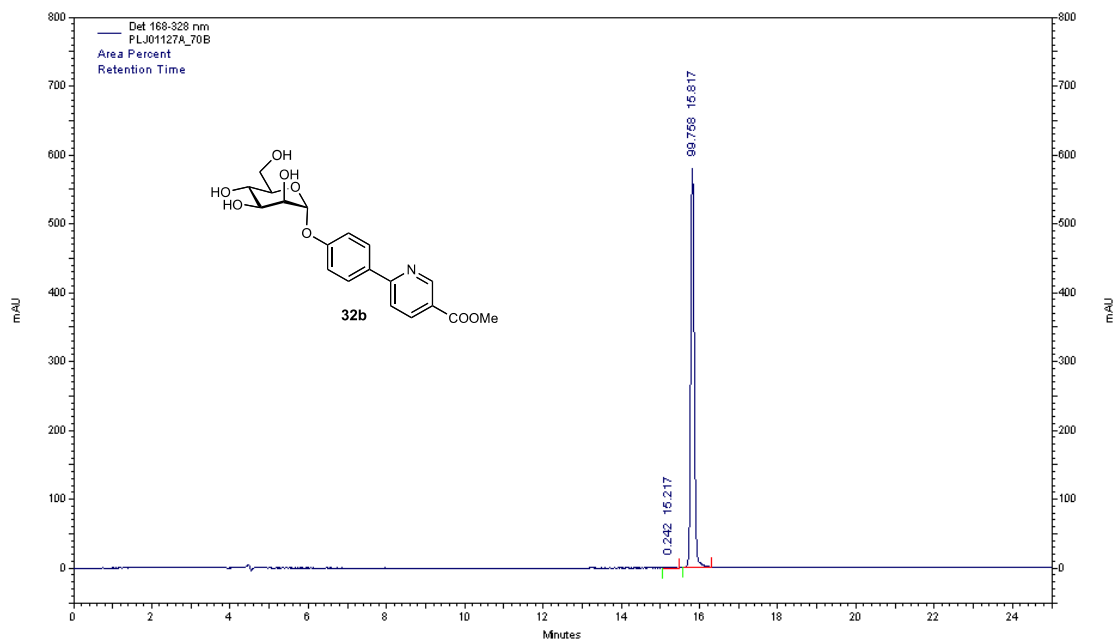


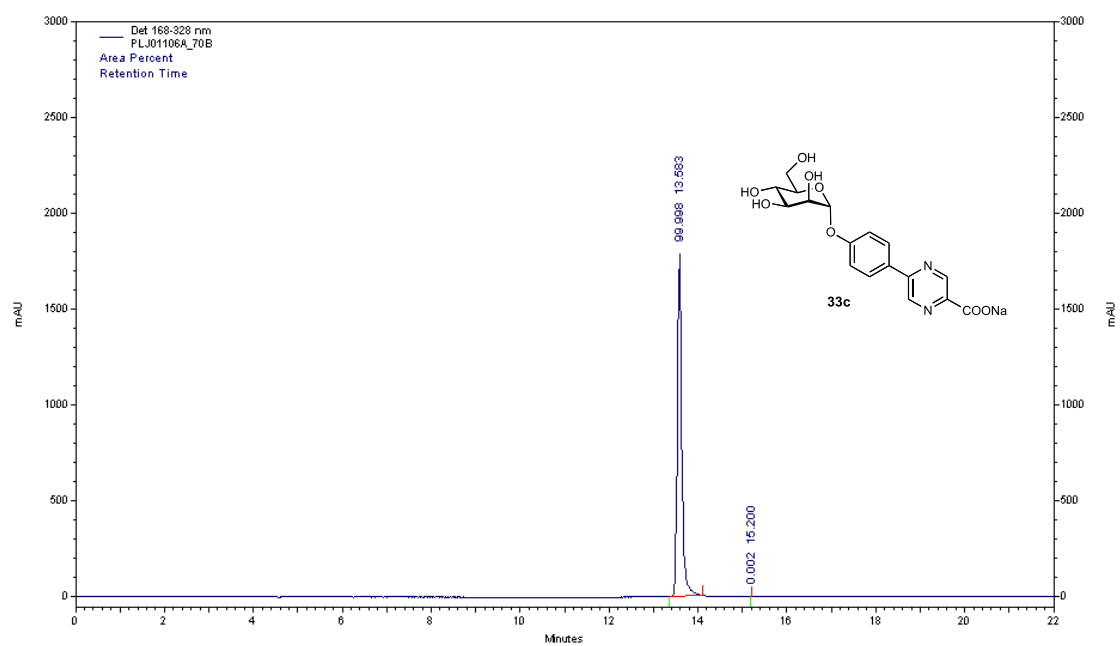
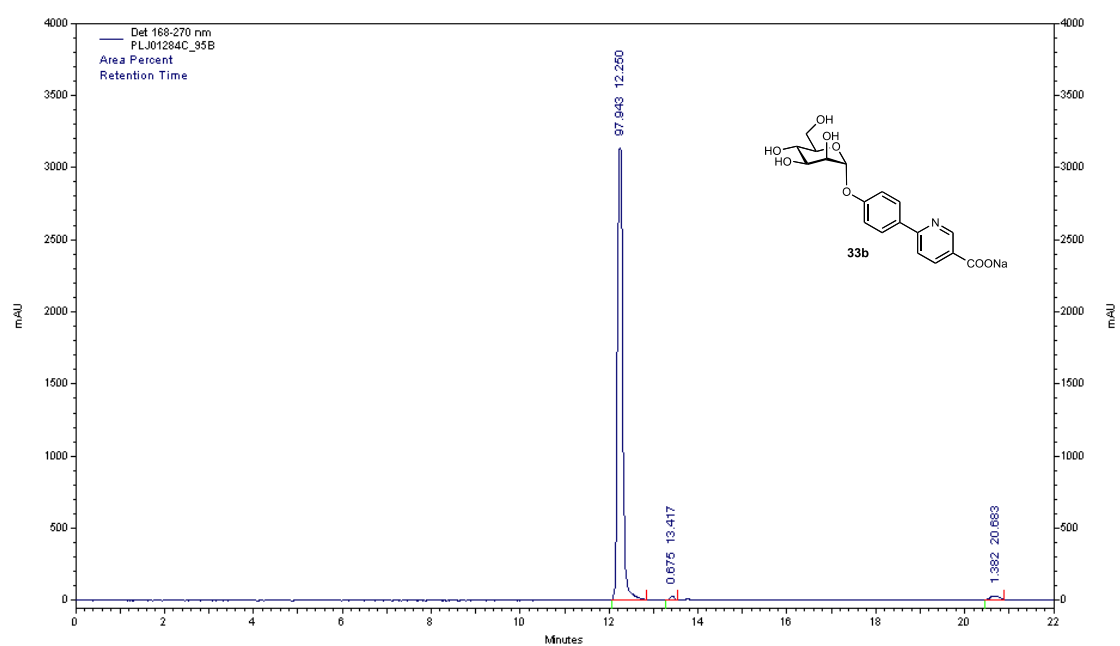
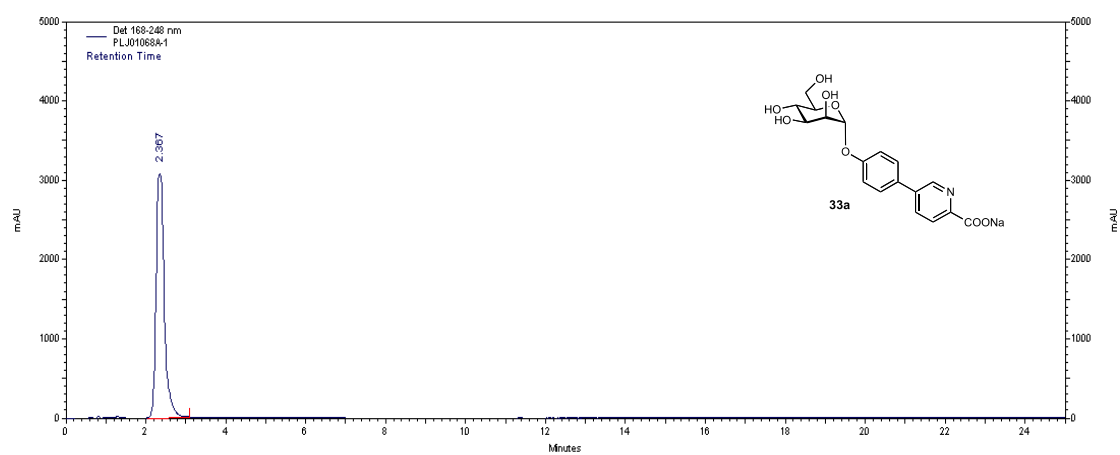


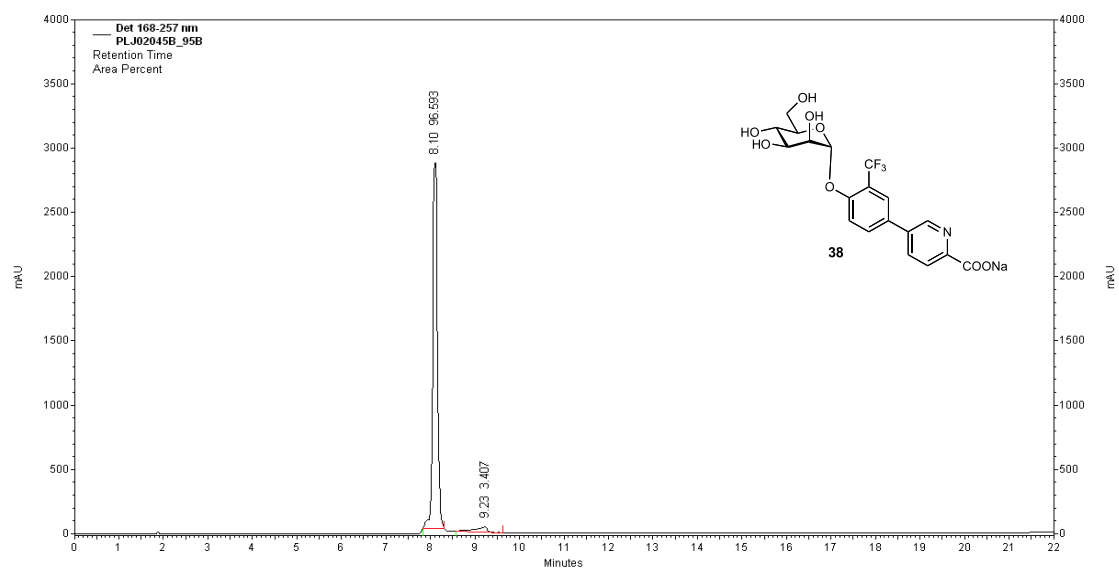
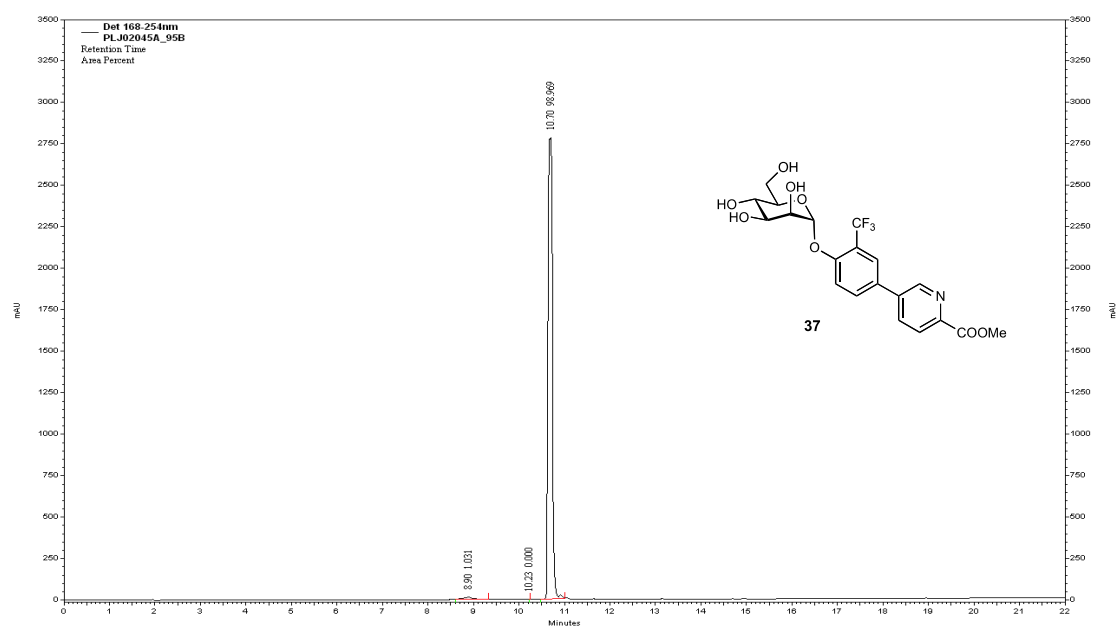
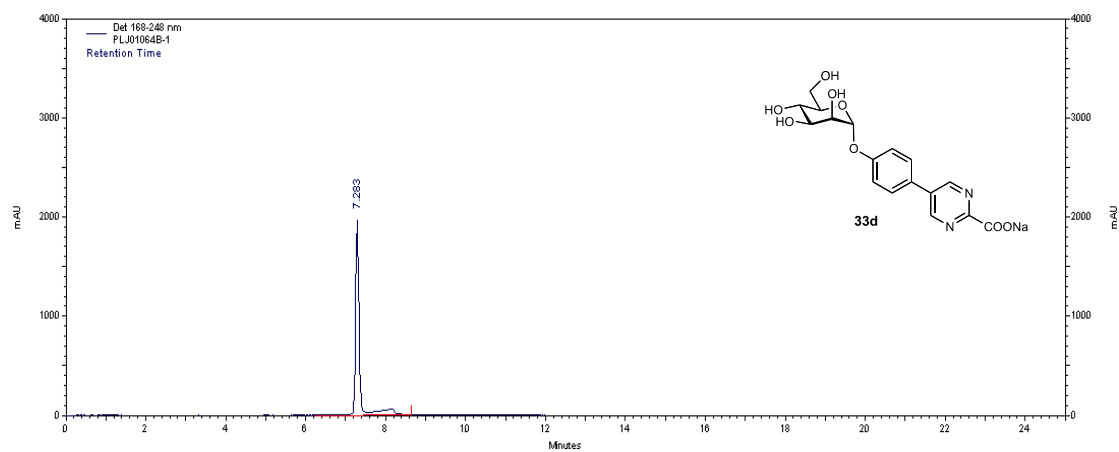


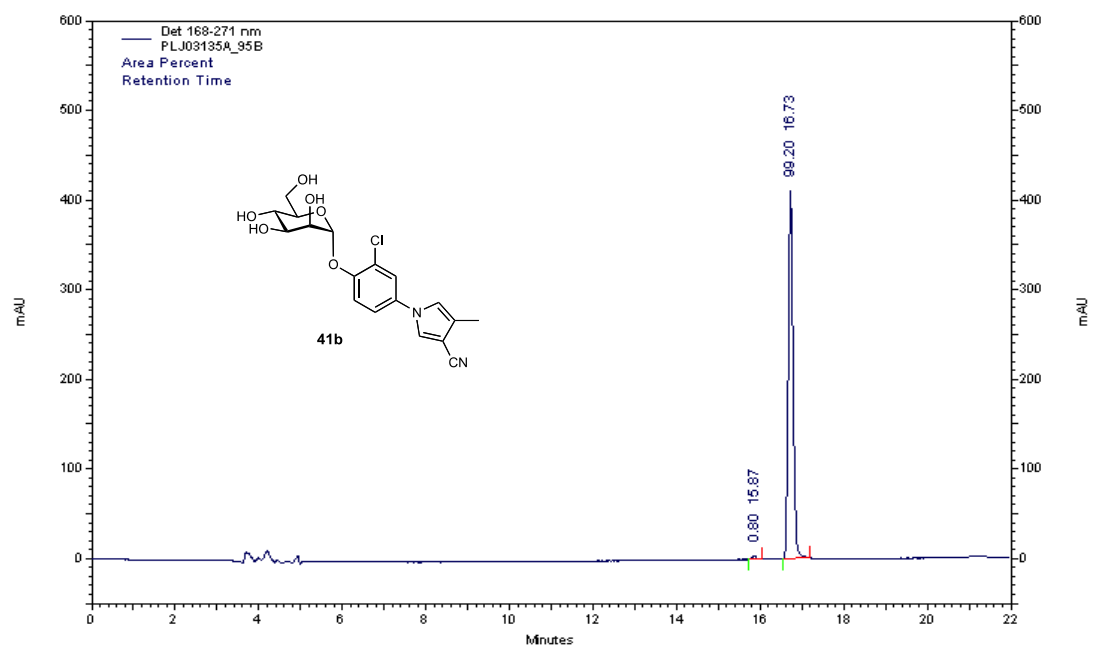
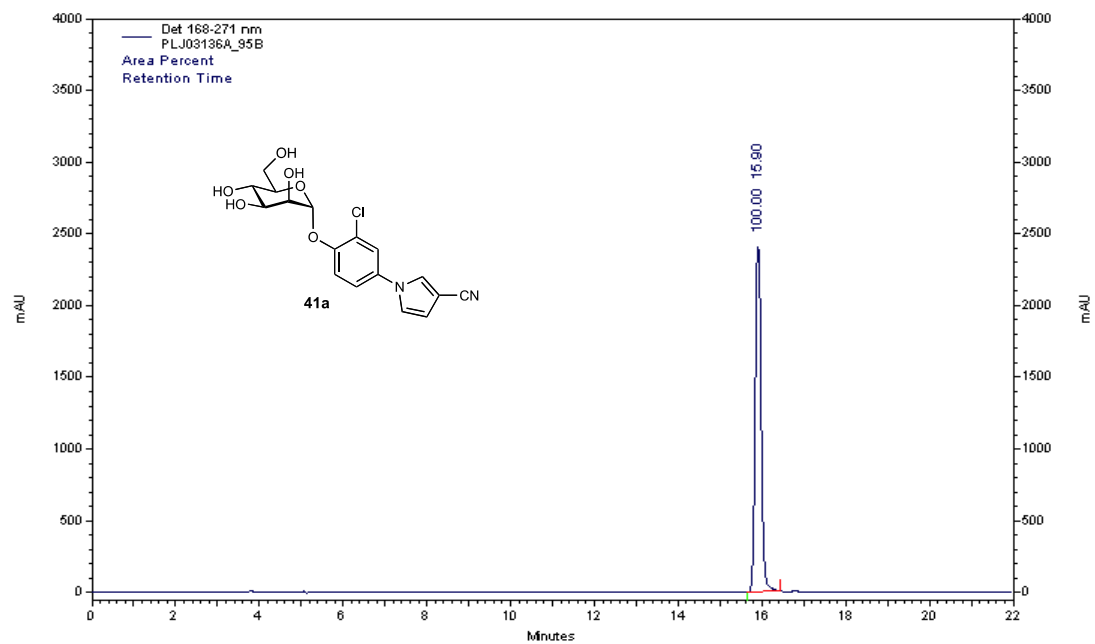


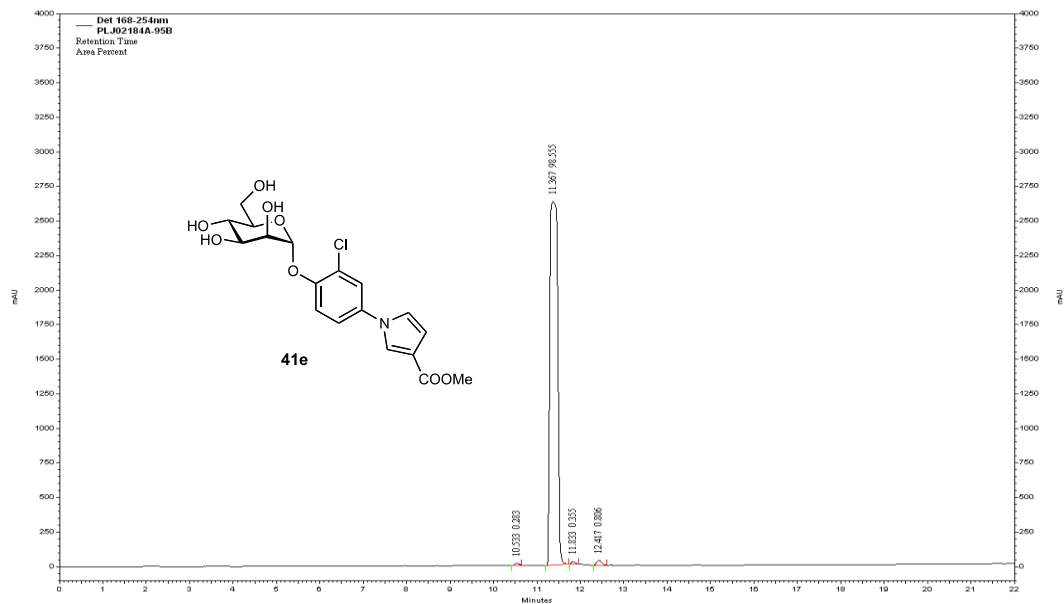
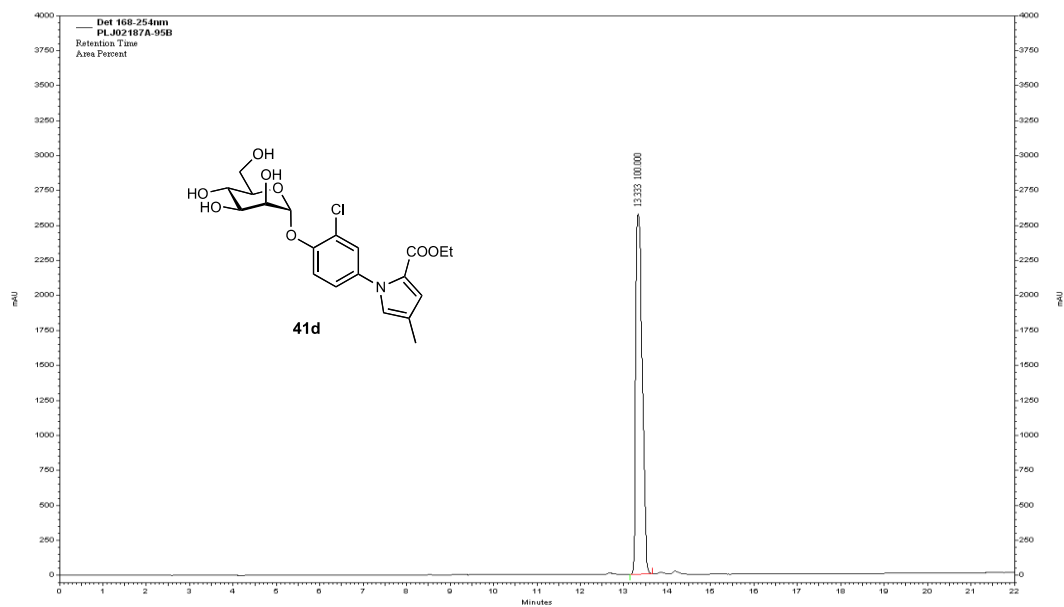
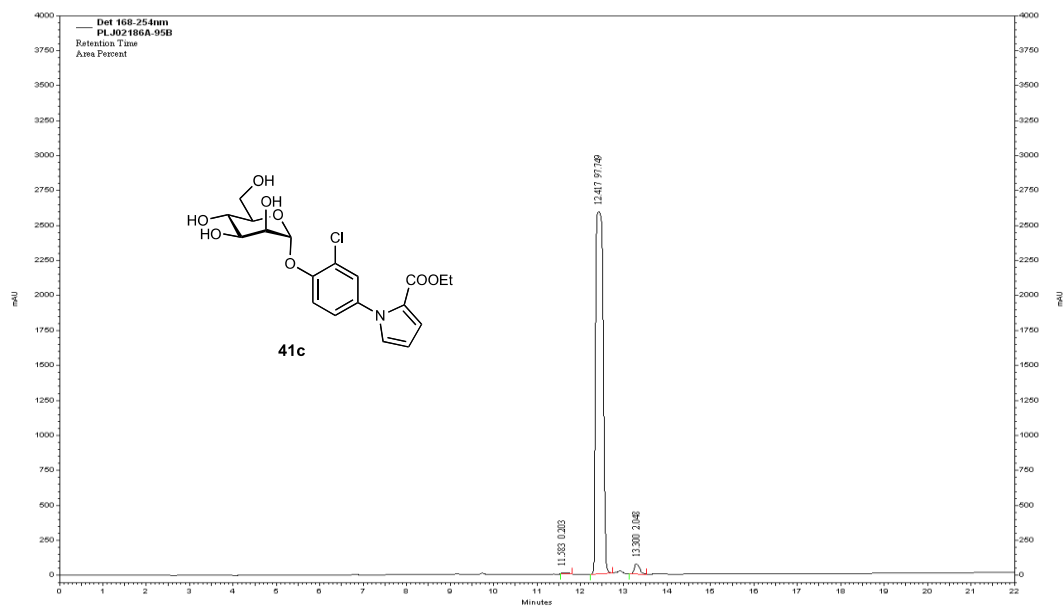


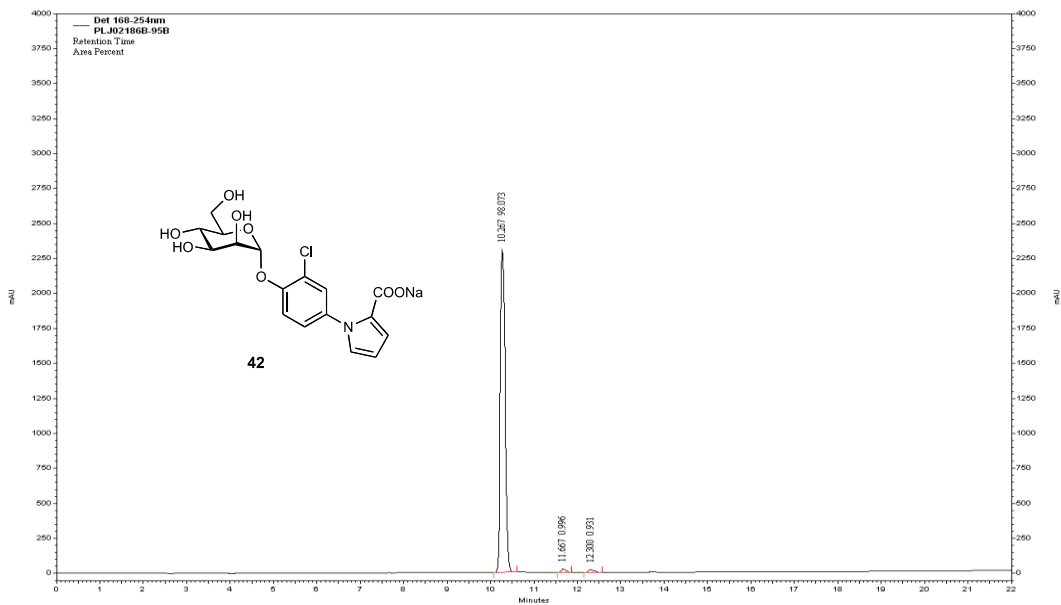
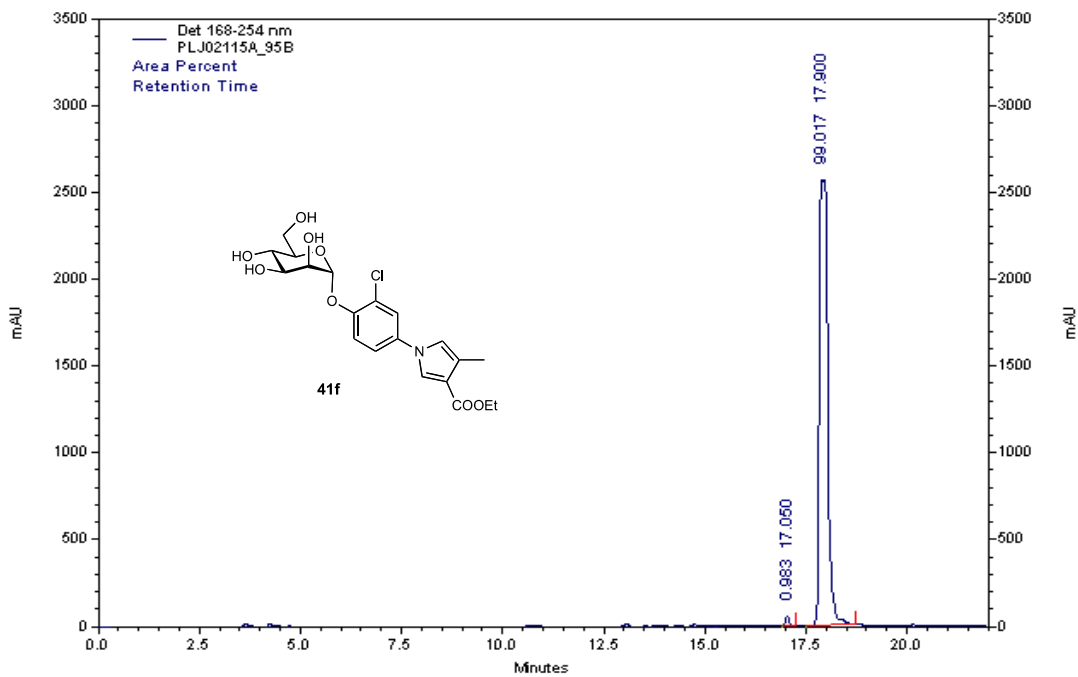


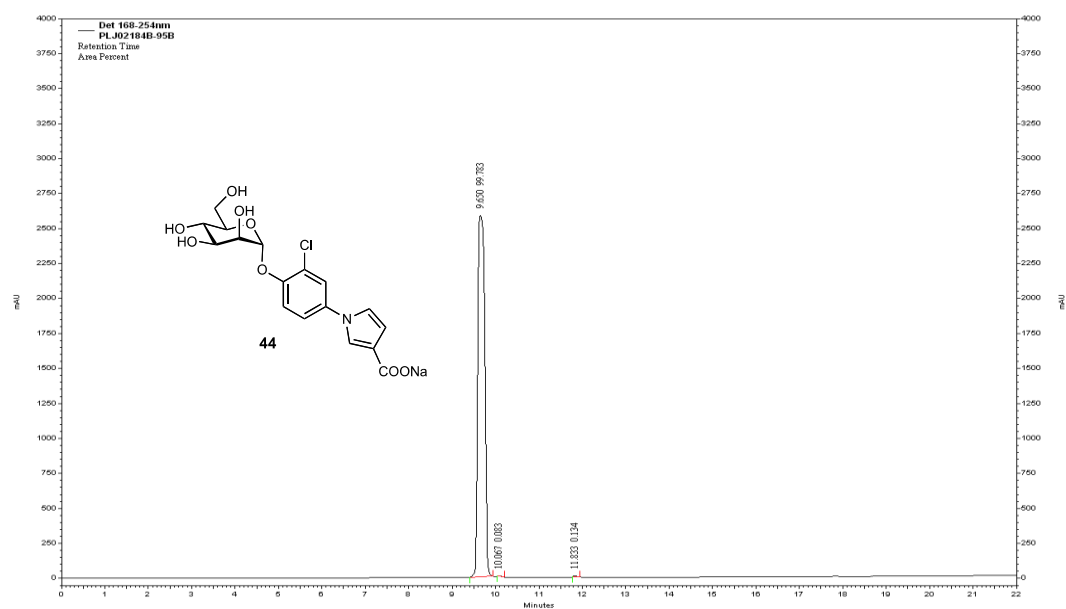
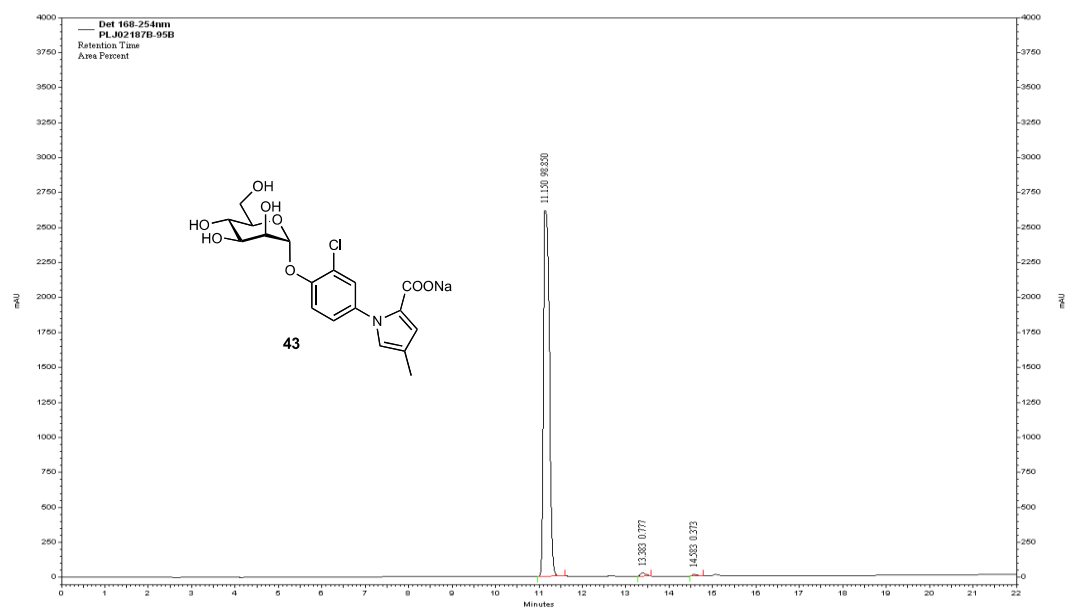


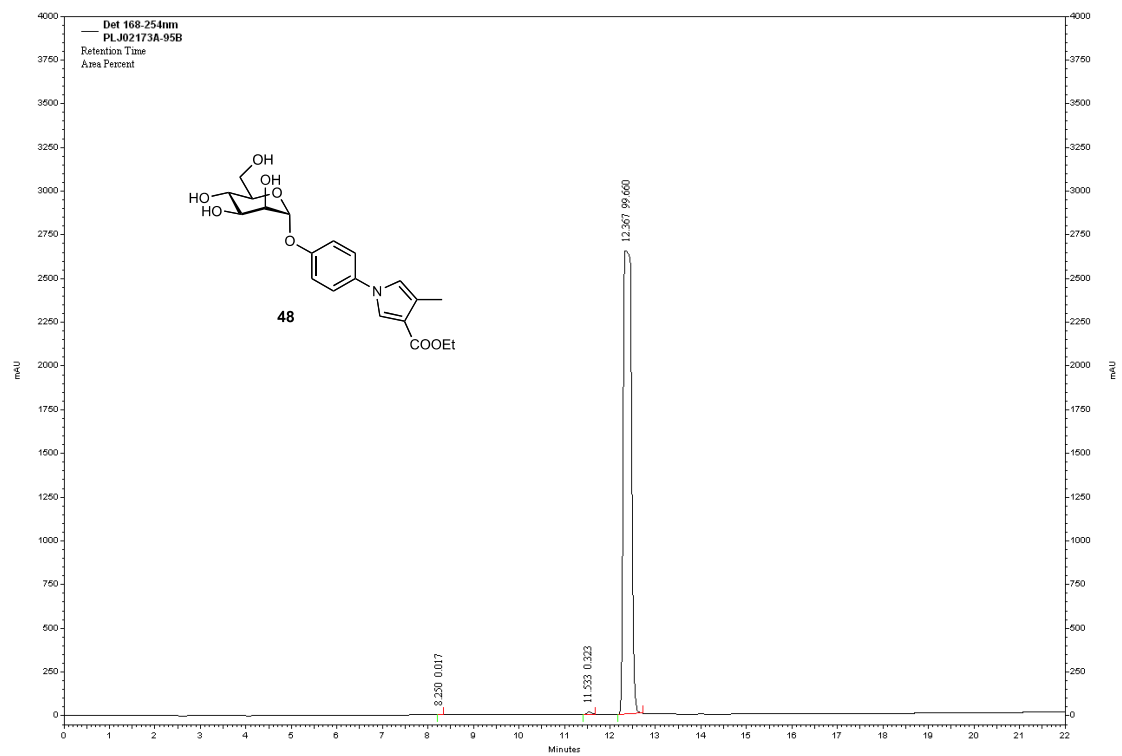
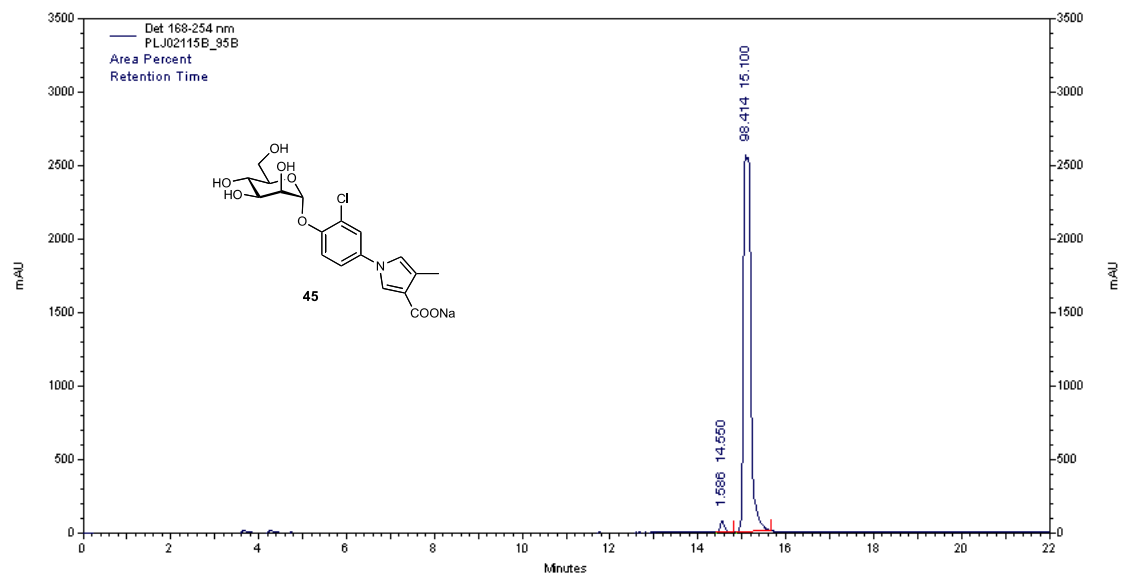


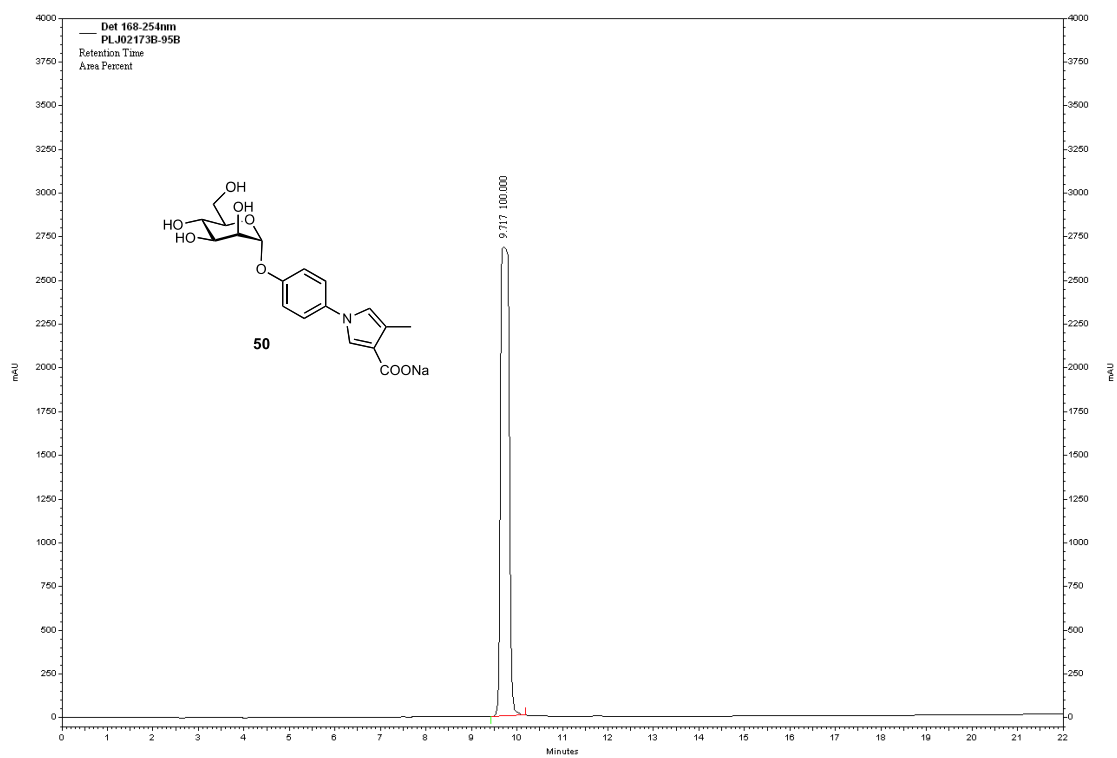
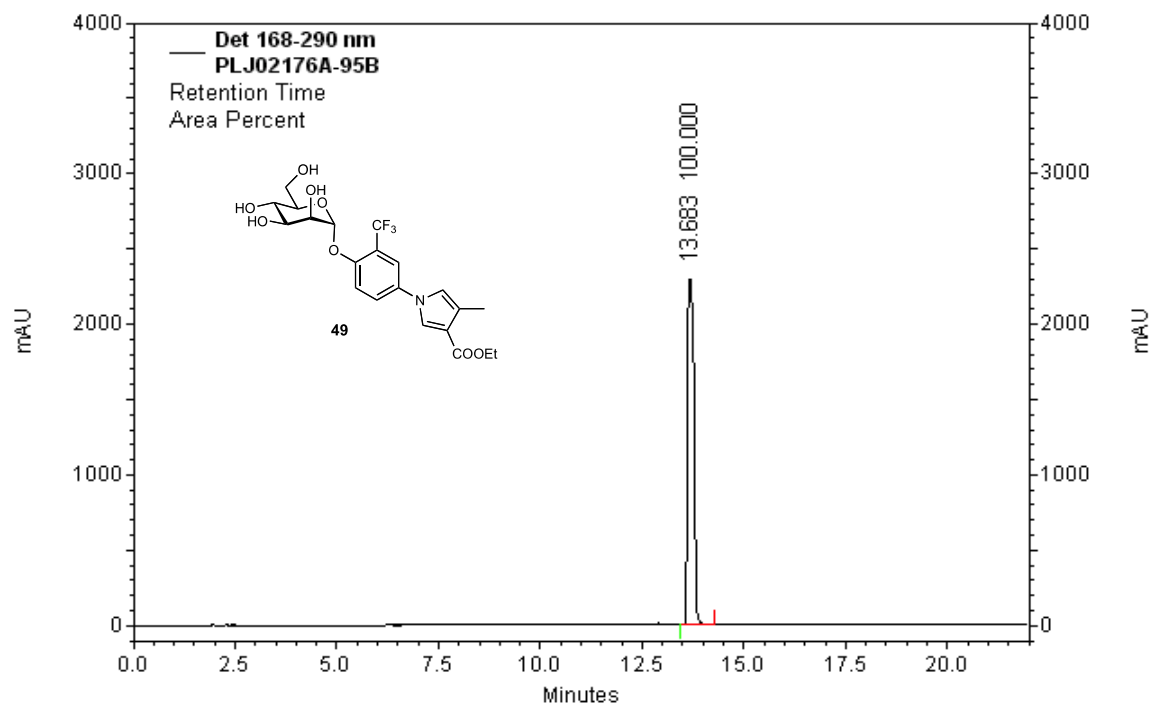


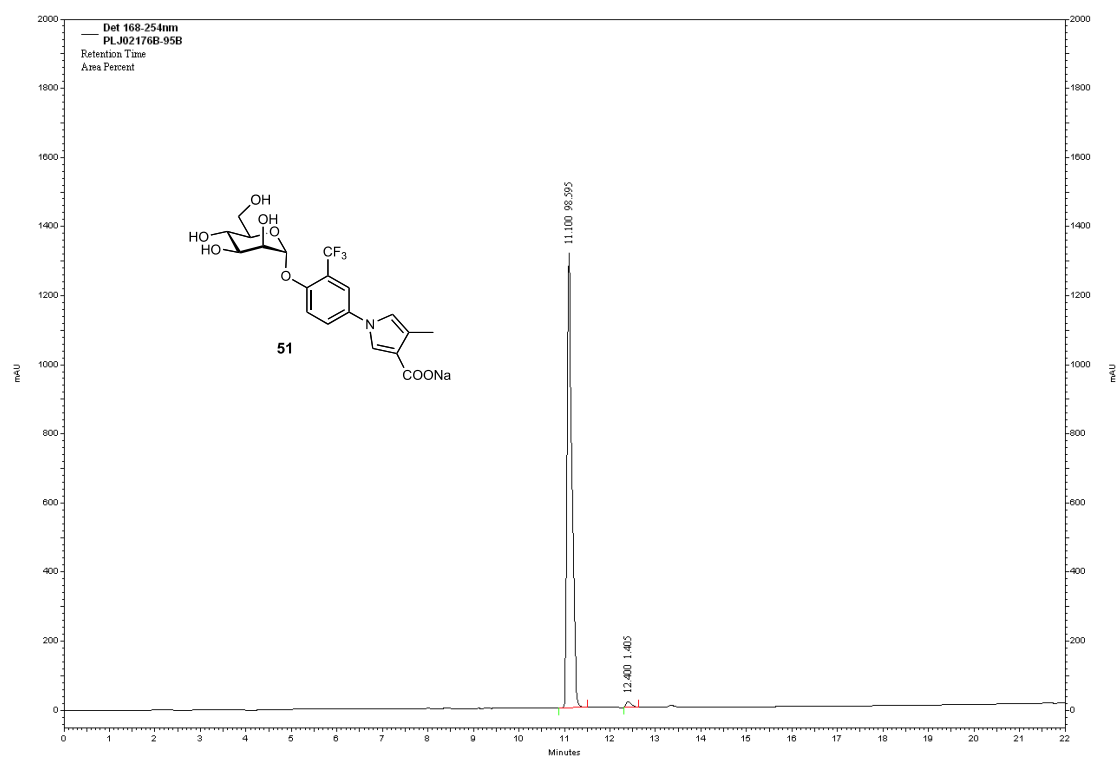


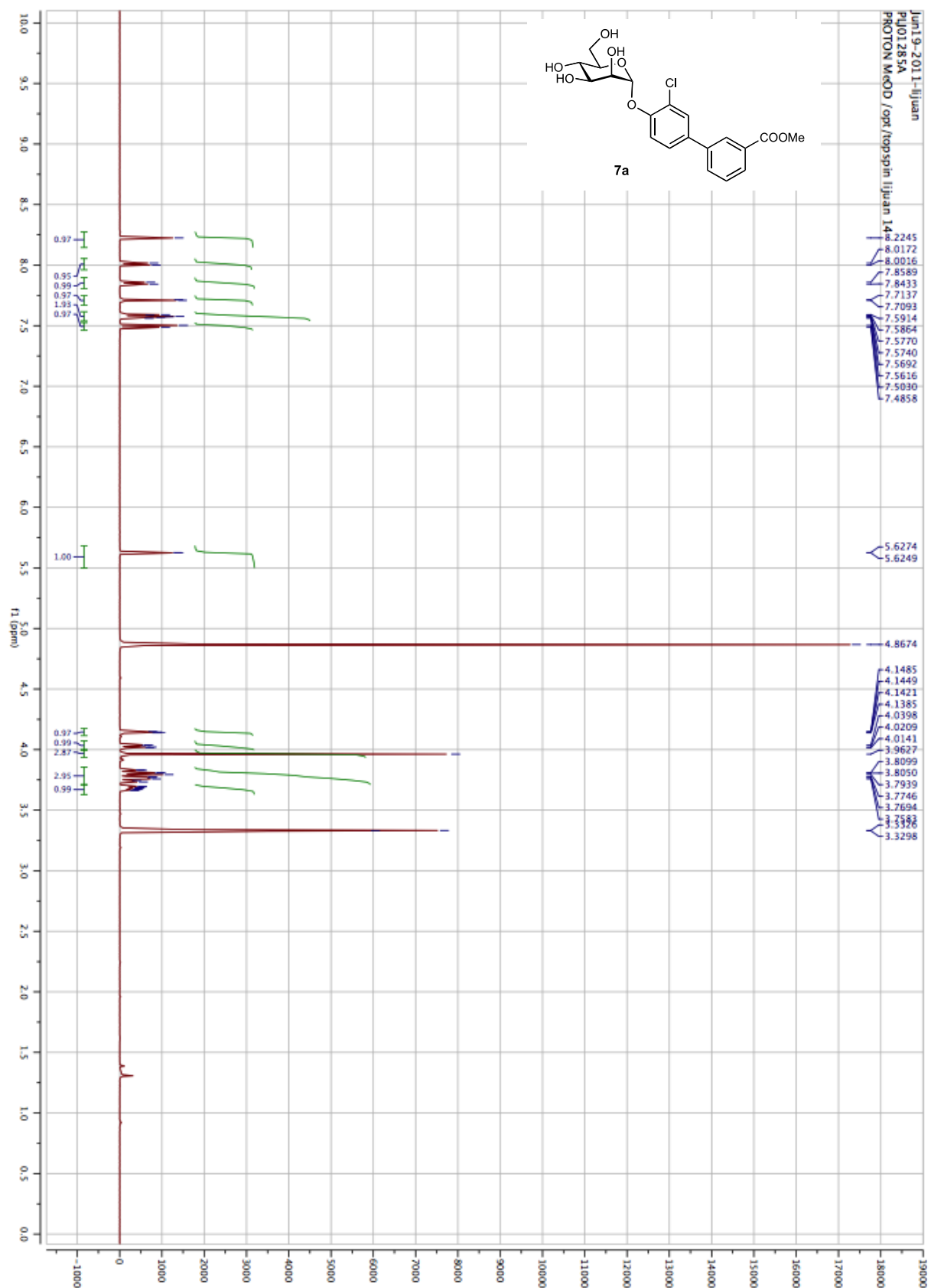


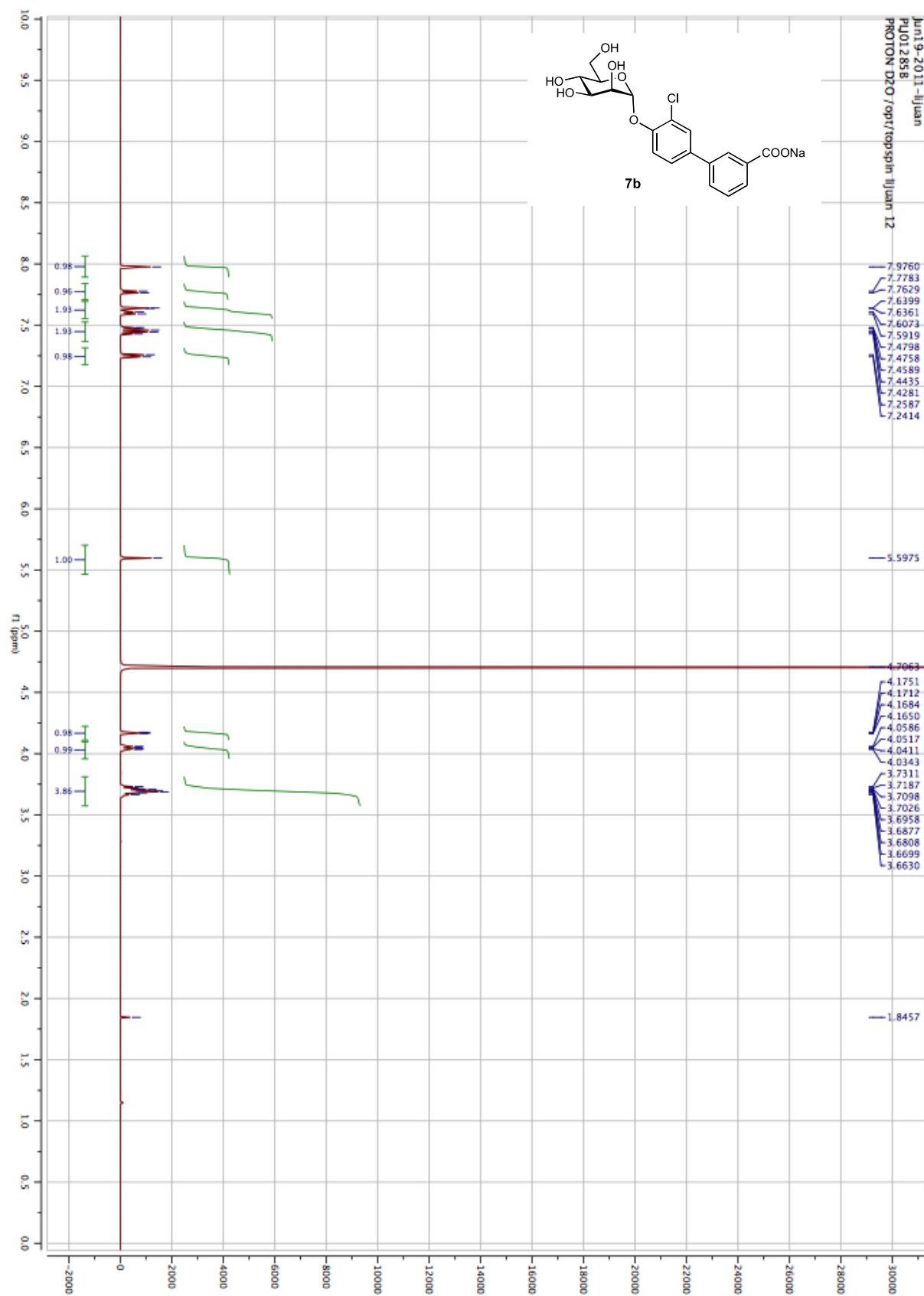


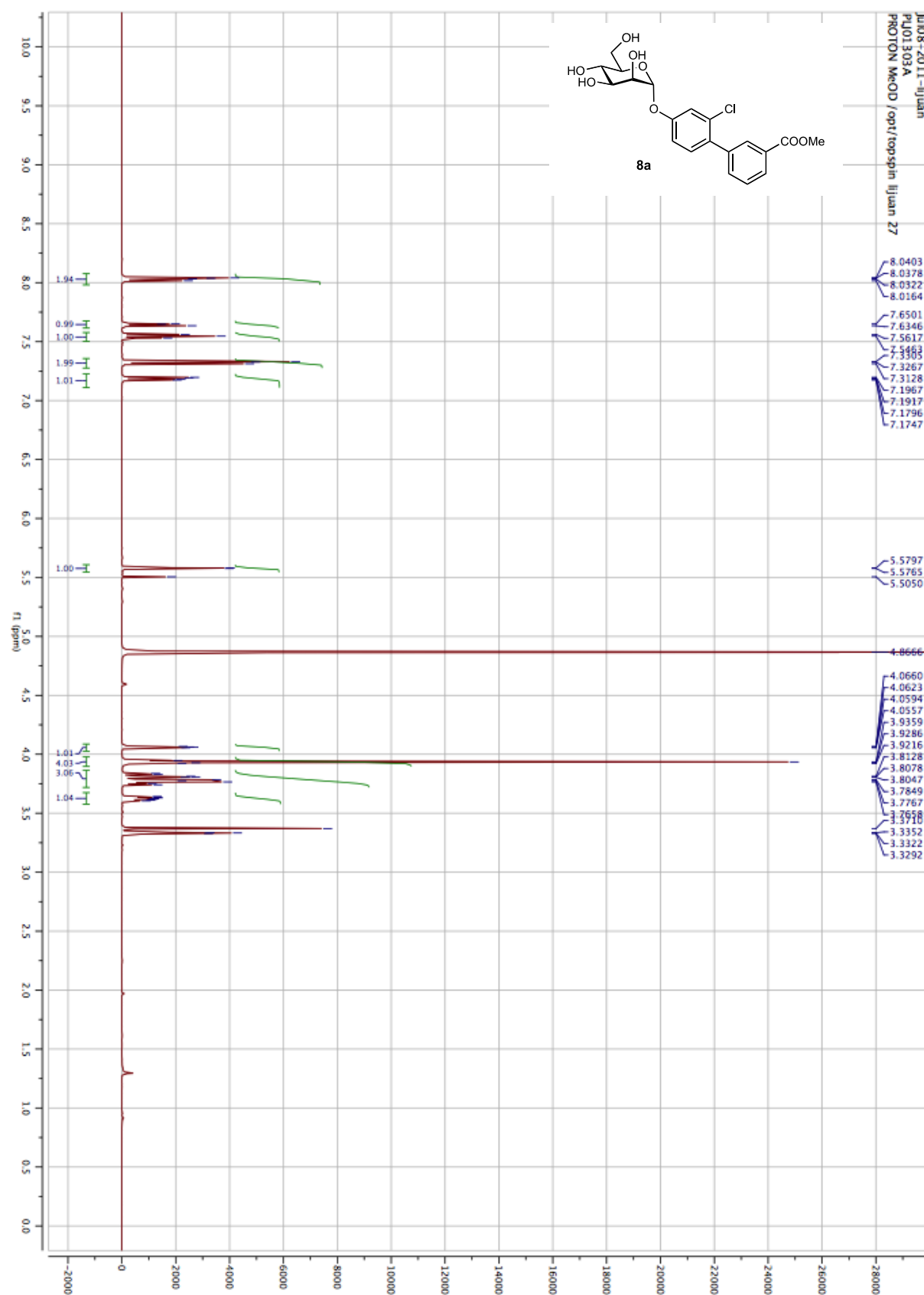


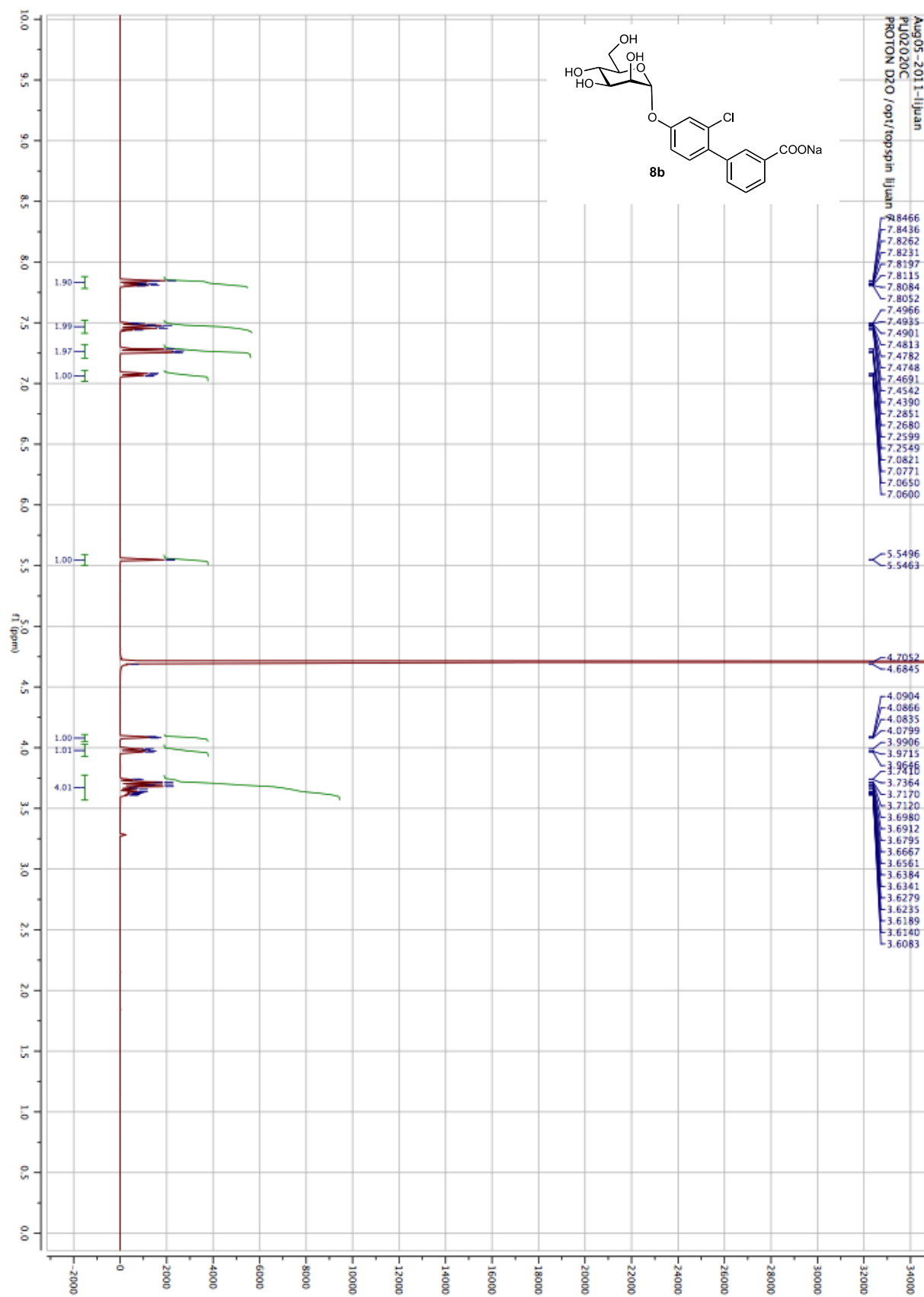


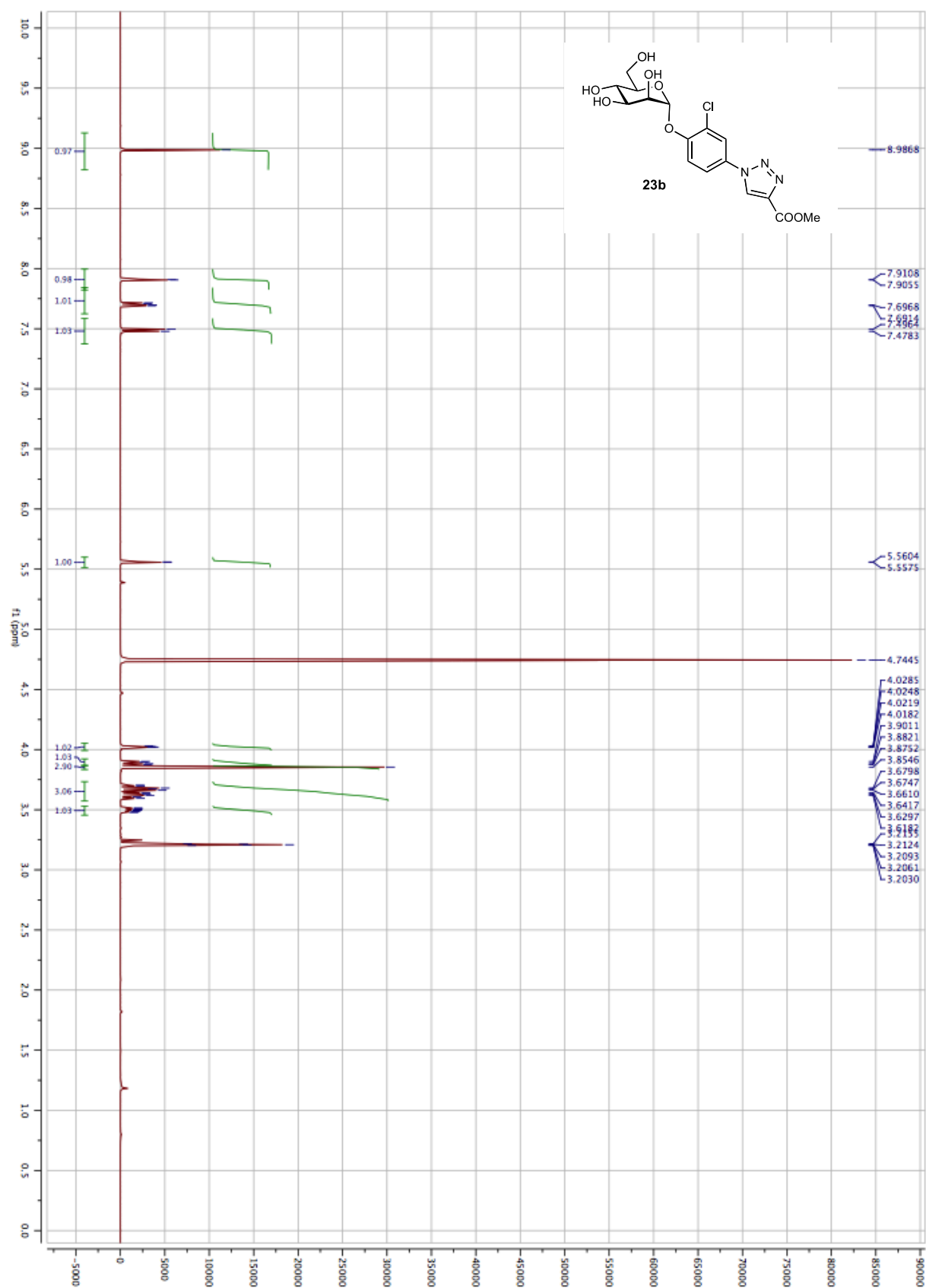


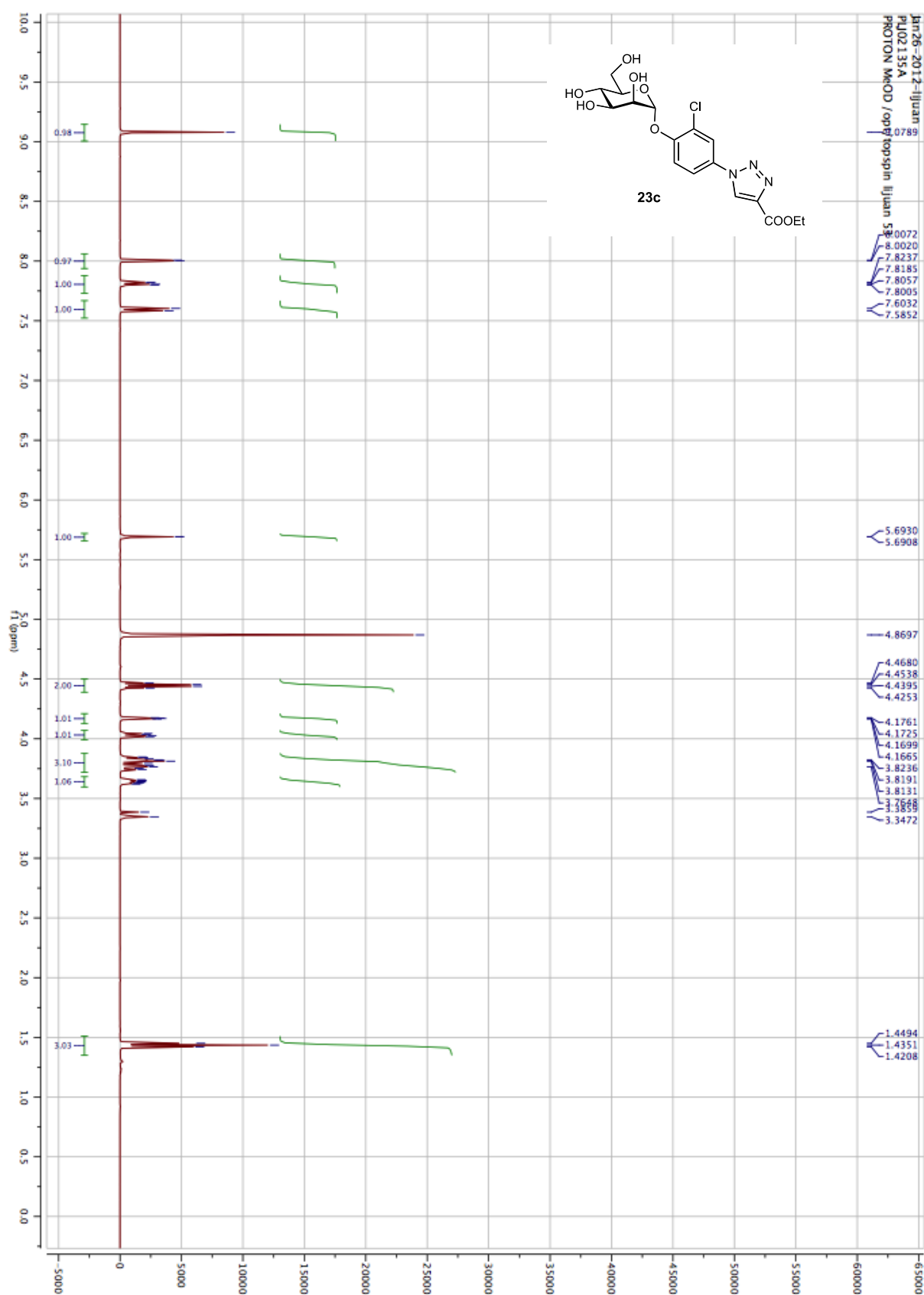
^1H NMR spectra of the target compounds: **^1H NMR (500 MHz) of 7a**

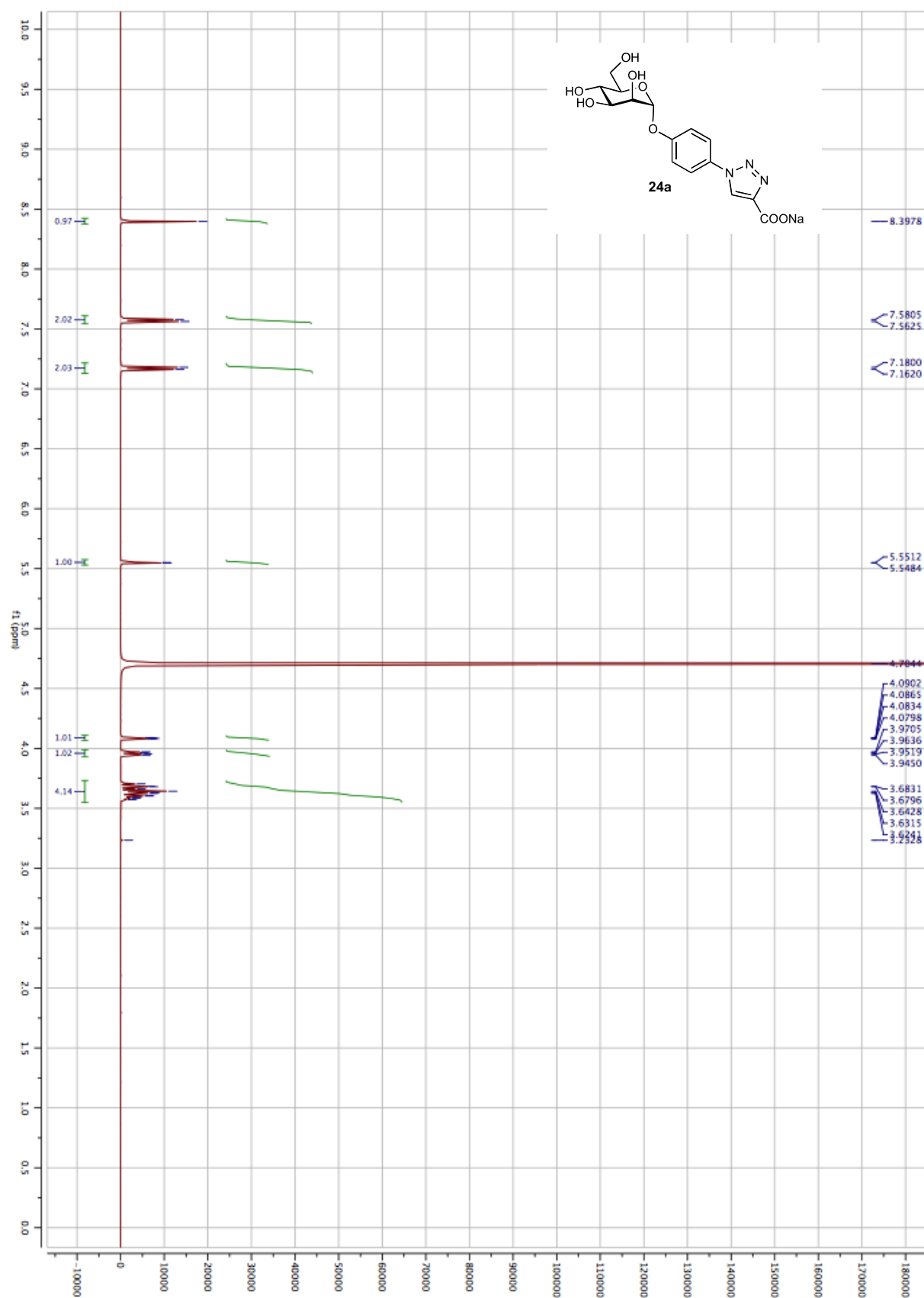
^1H NMR (500 MHz) of **7b**

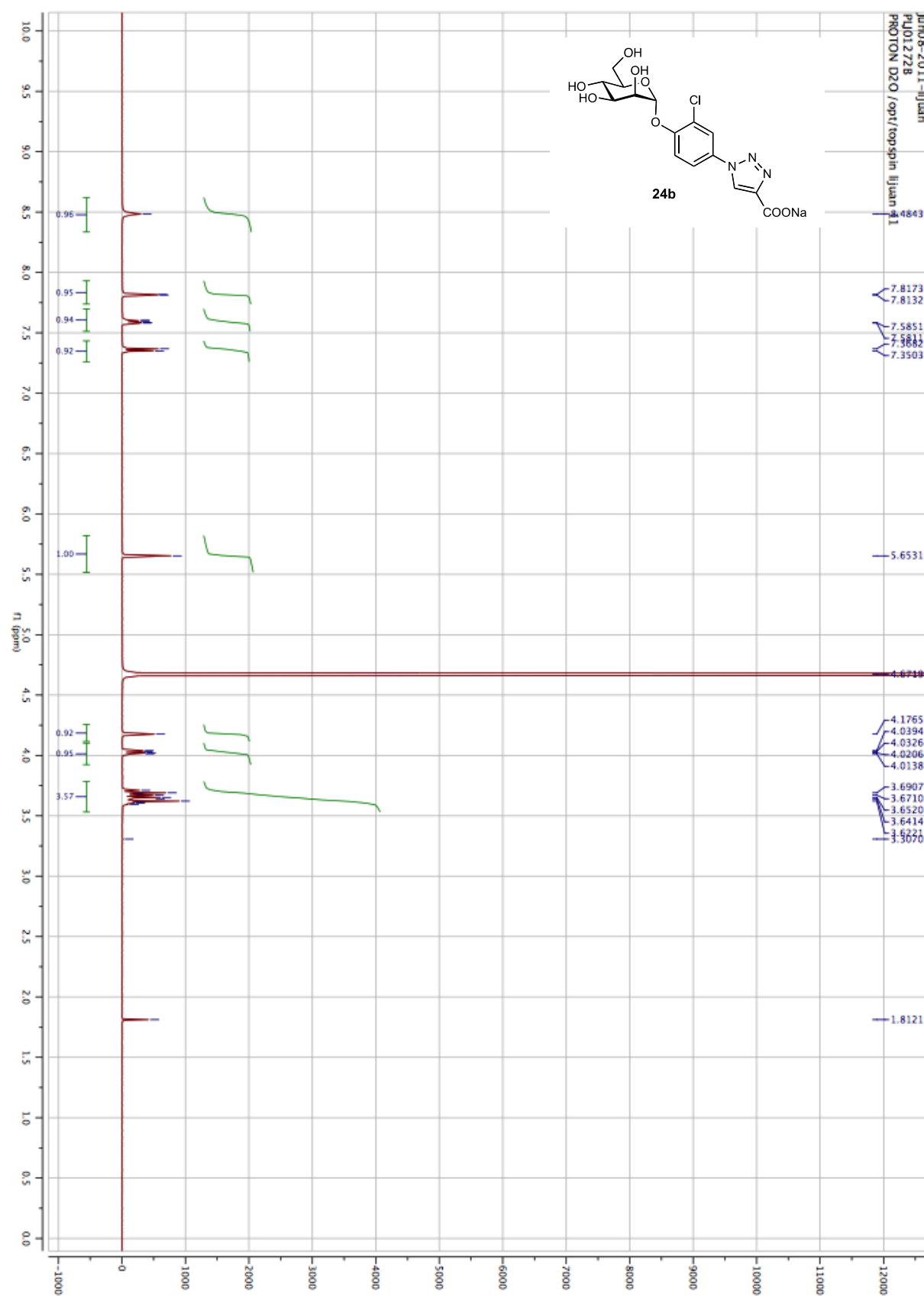
^1H NMR (500 MHz) of **8a**

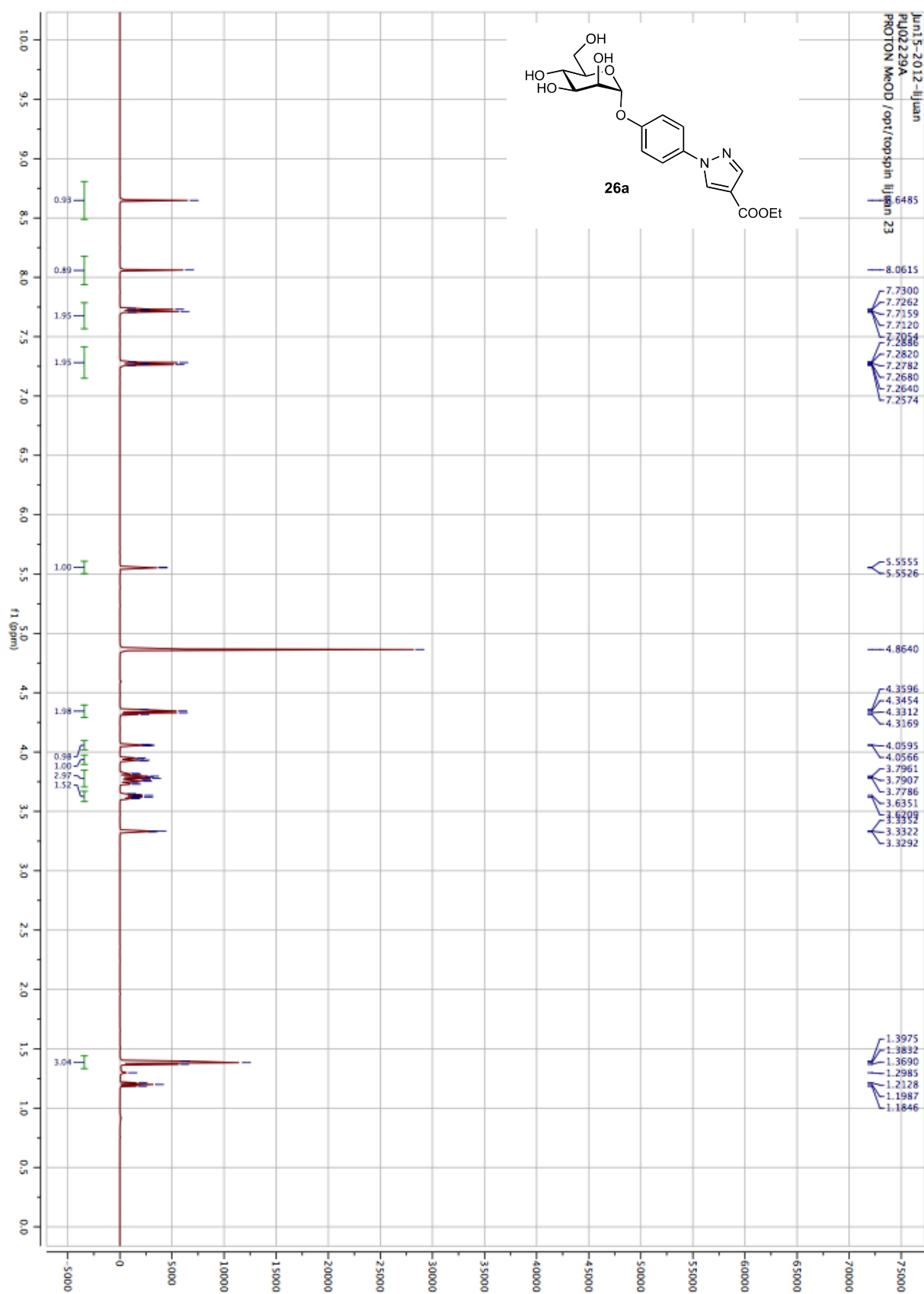
^1H NMR (500 MHz) of **8b**

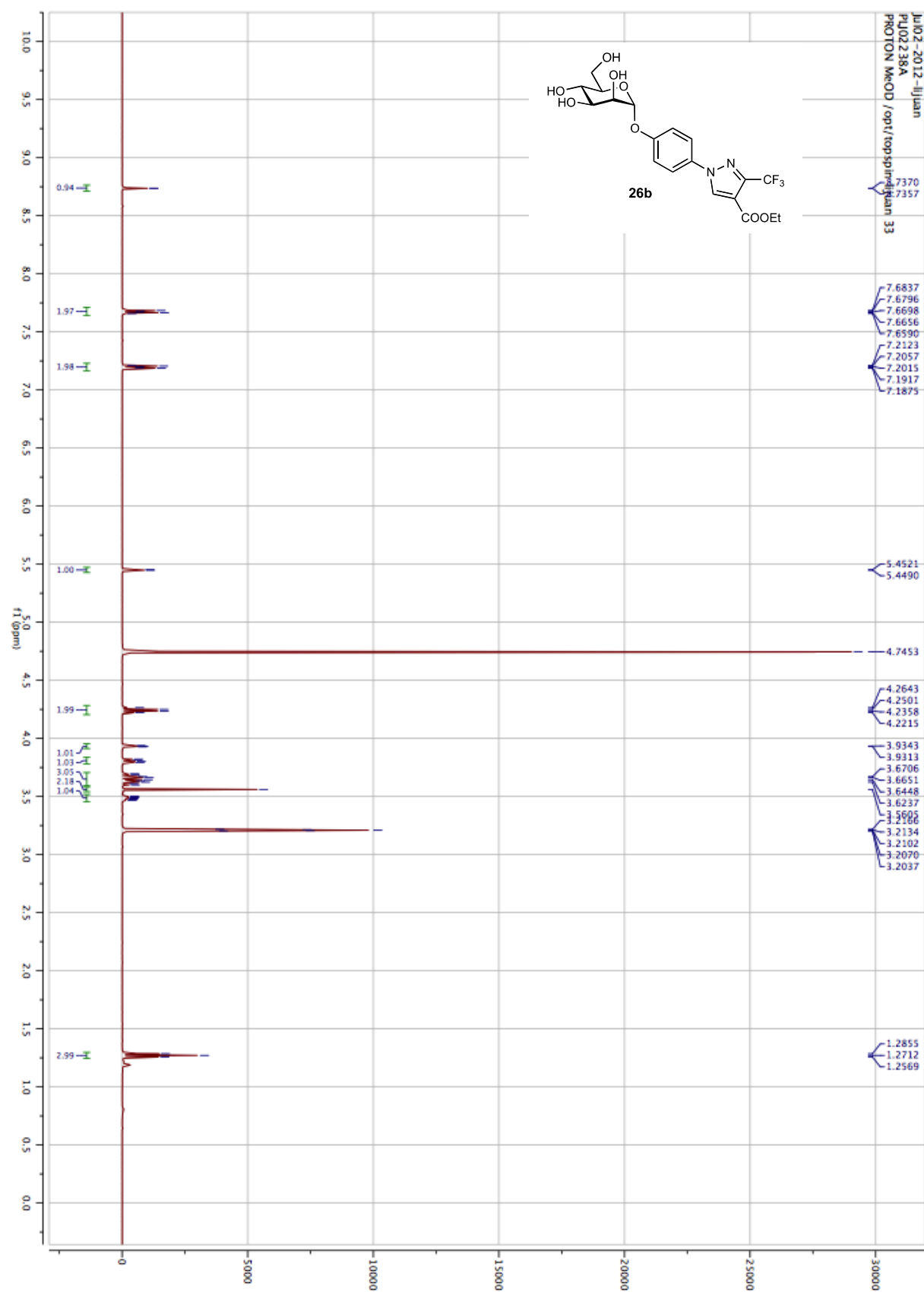
^1H NMR (500 MHz) of **23b**

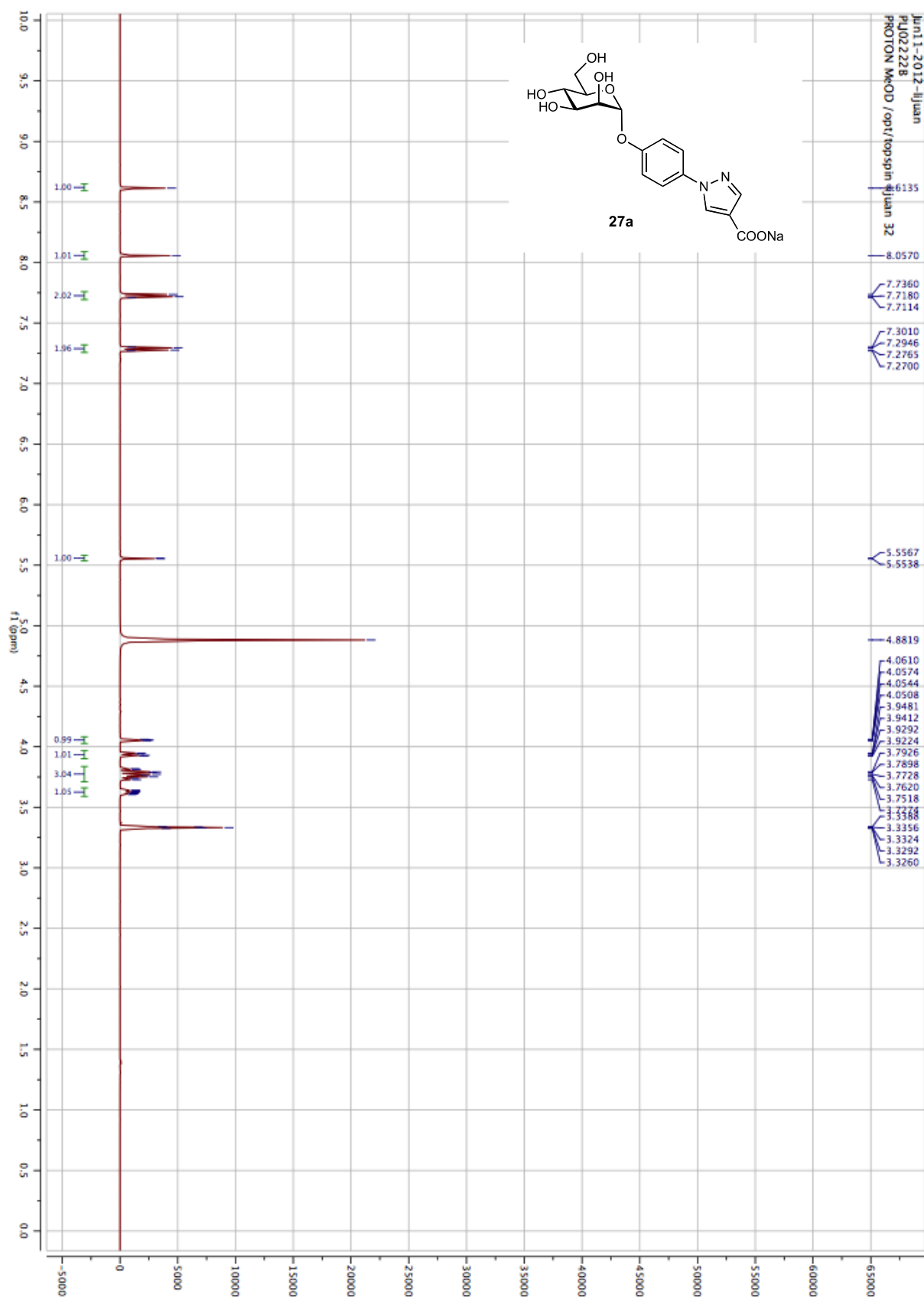
^1H NMR (500 MHz) of **23c**

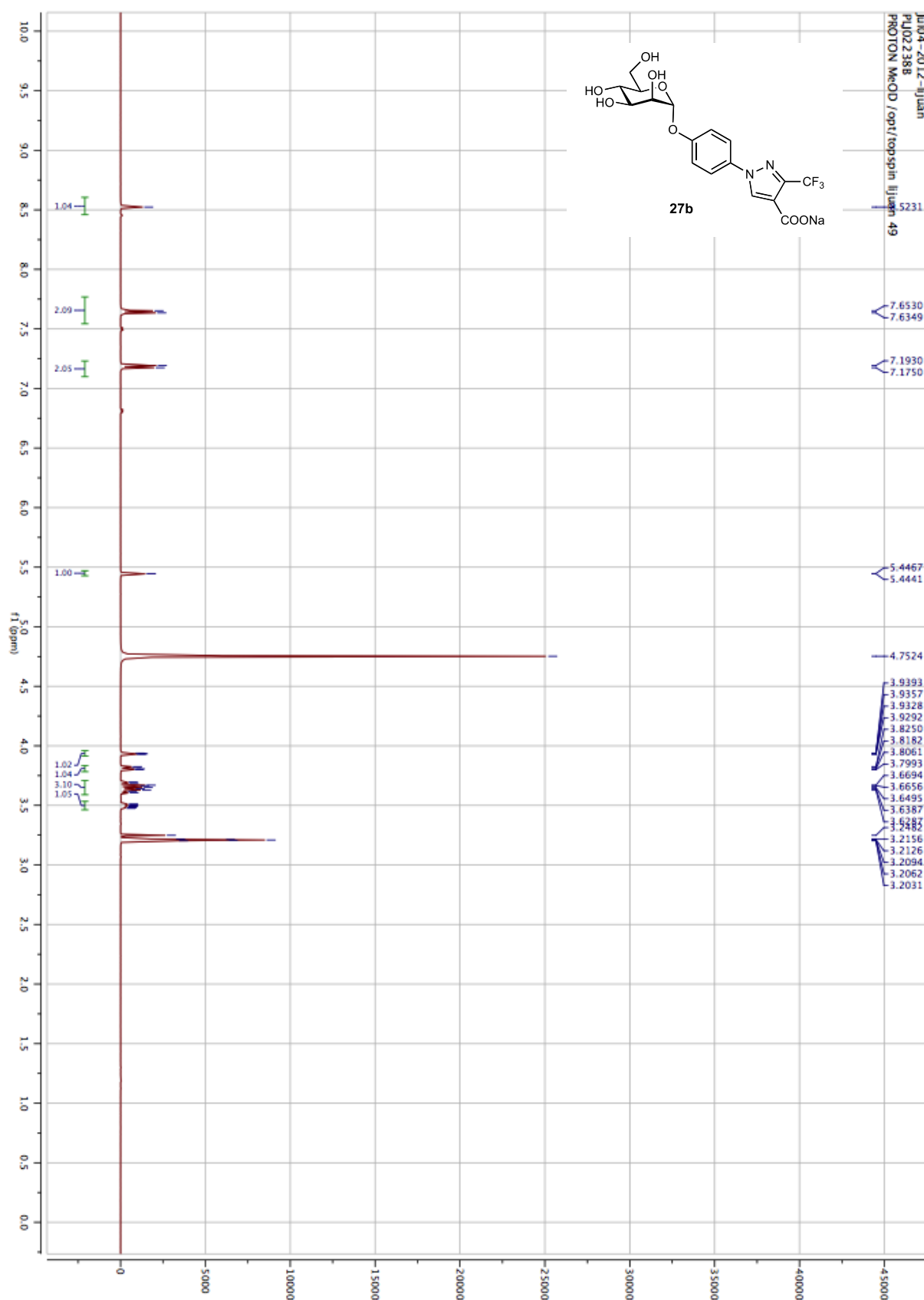
^1H NMR (500 MHz) of **24a**

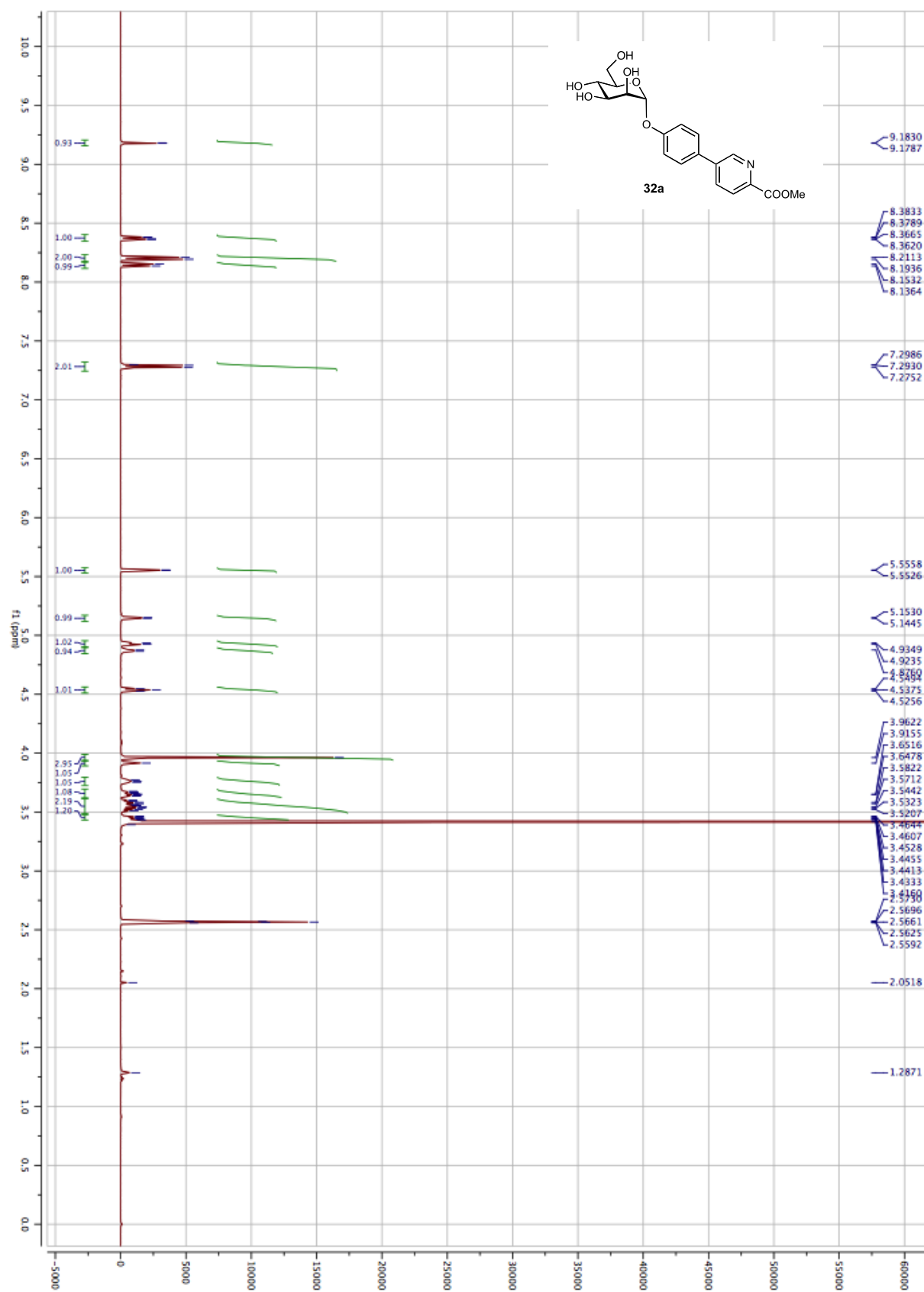
^1H NMR (500 MHz) of **24b**

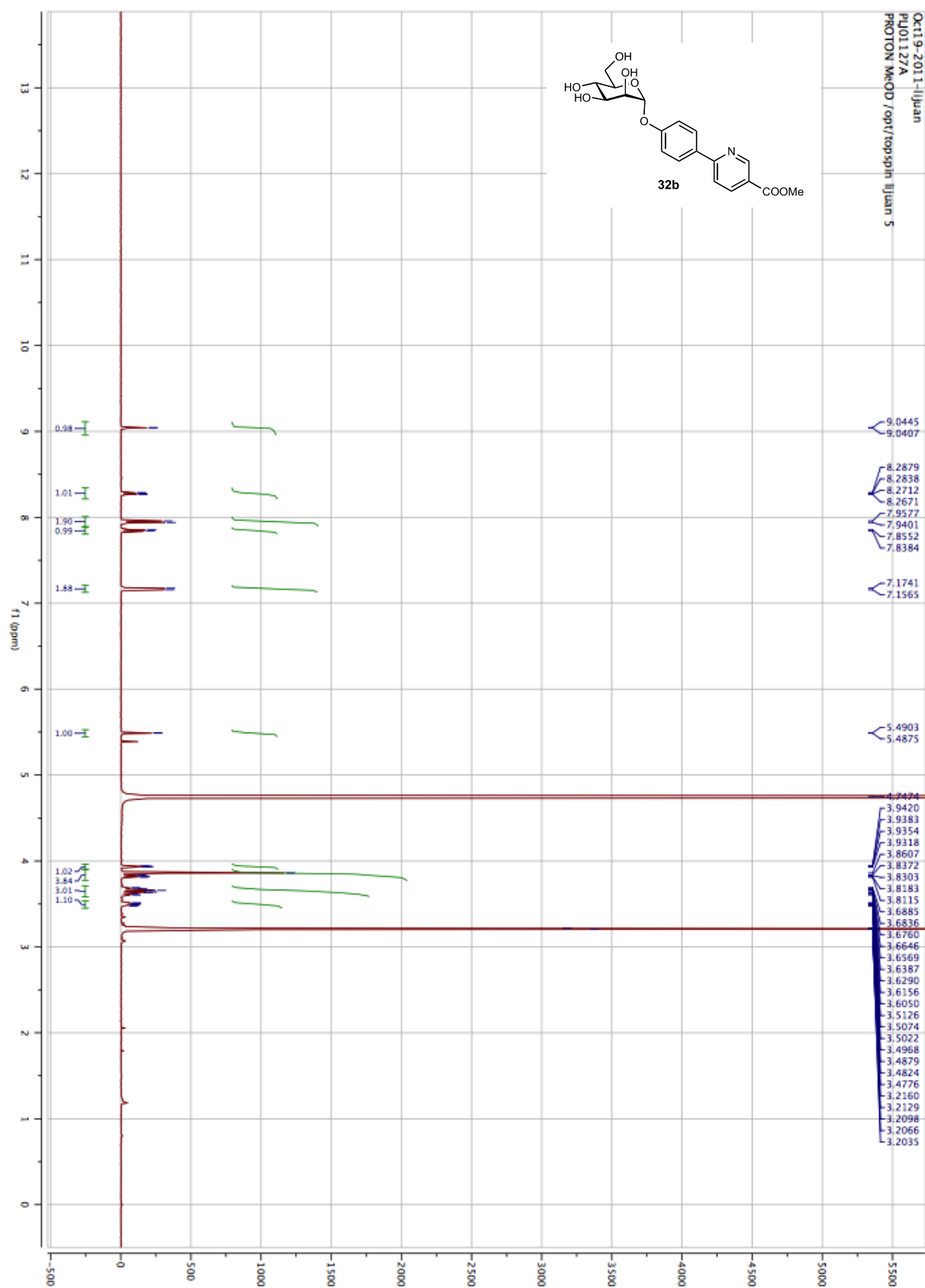
^1H NMR (500 MHz) of **26a**

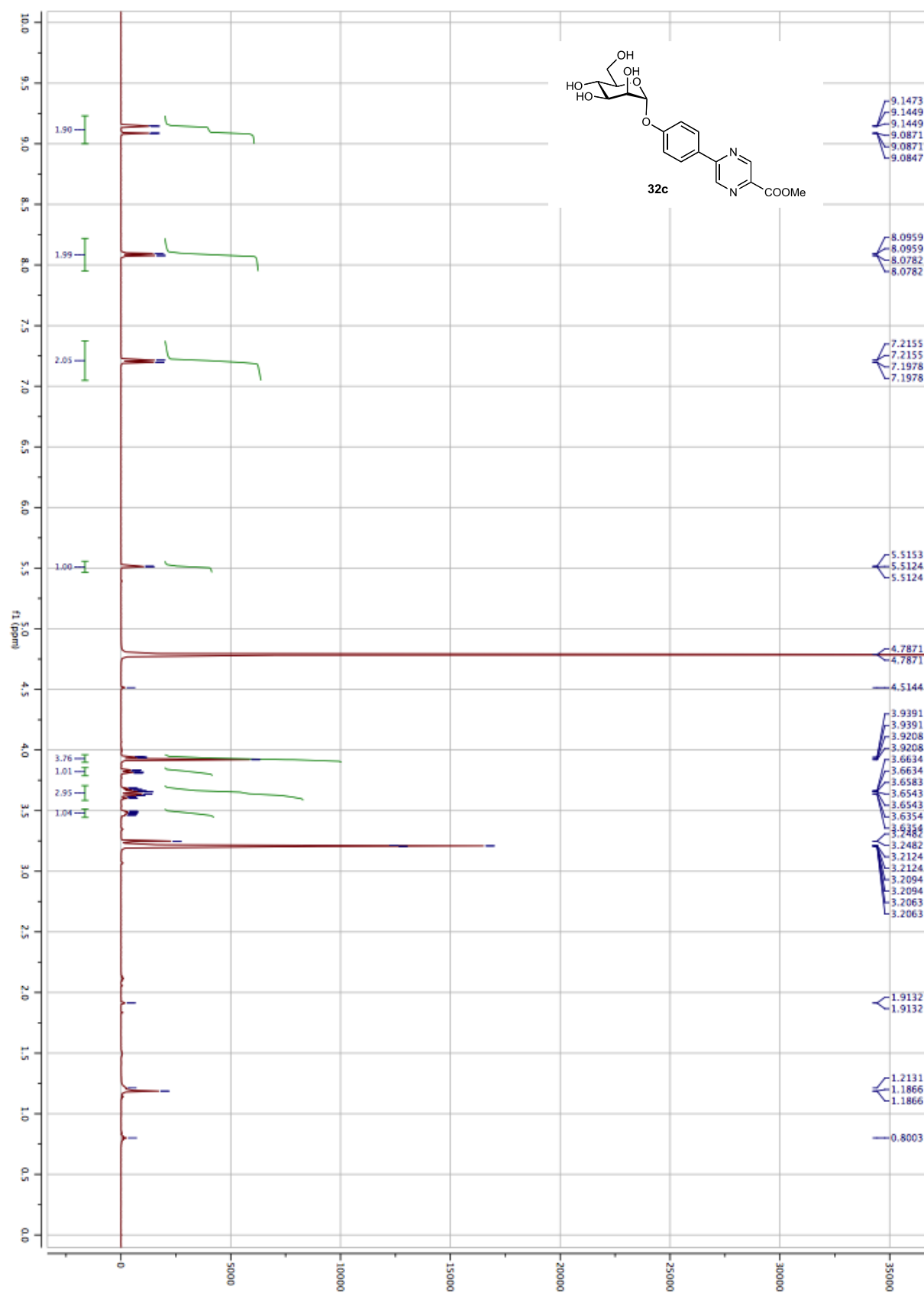
^1H NMR (500 MHz) of **26b**

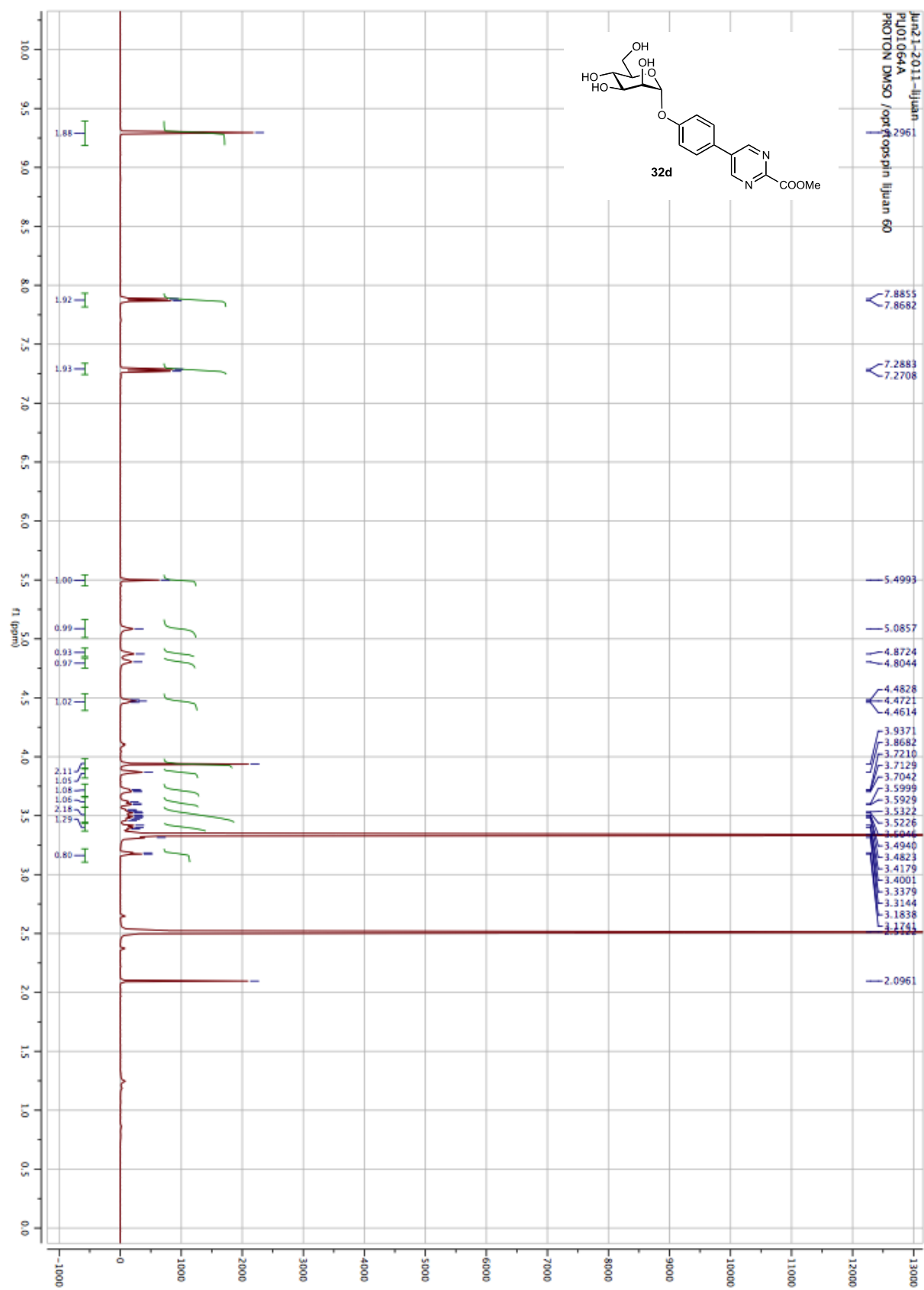
^1H NMR (500 MHz) of **27a**

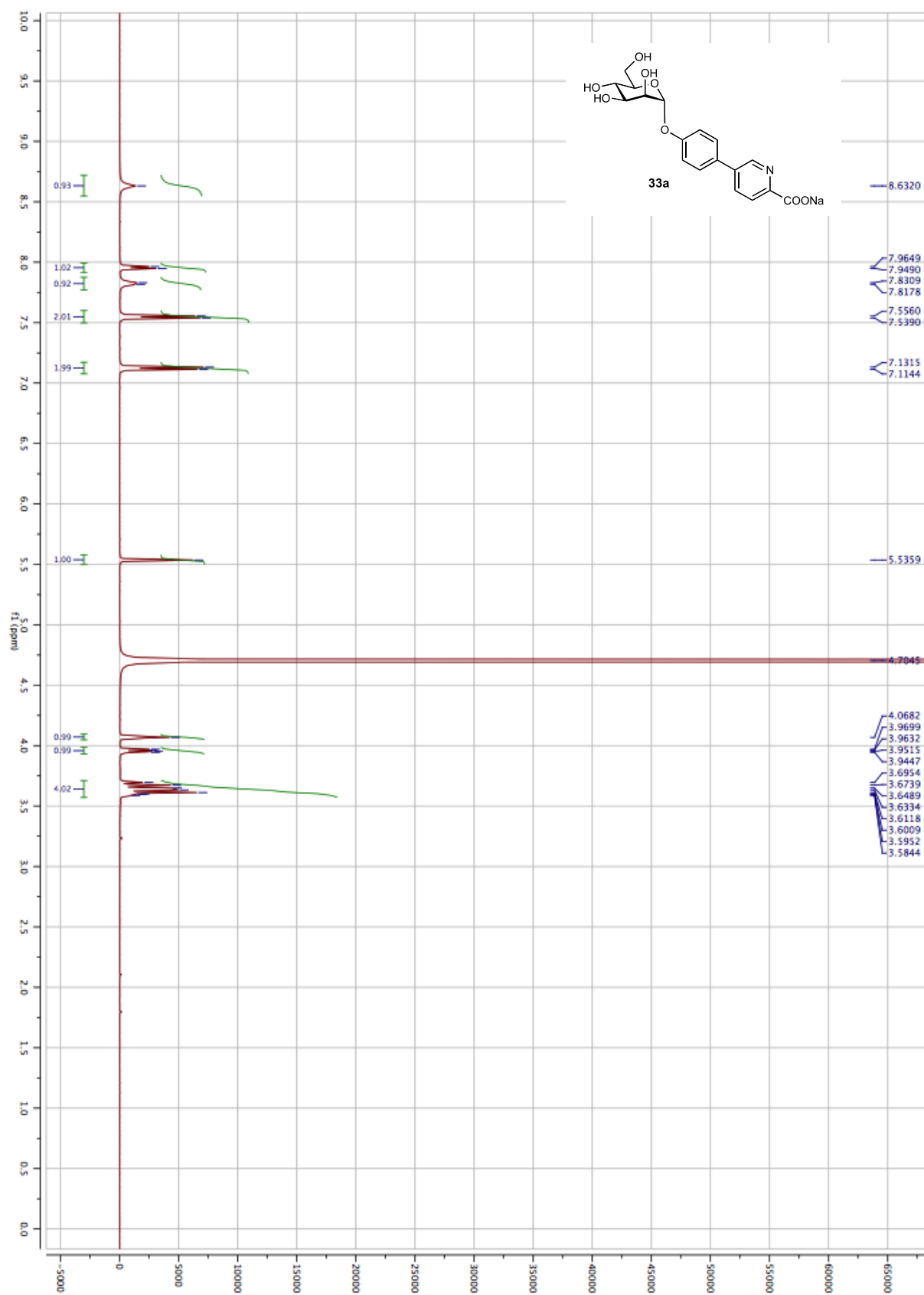
^1H NMR (500 MHz) of **27b**

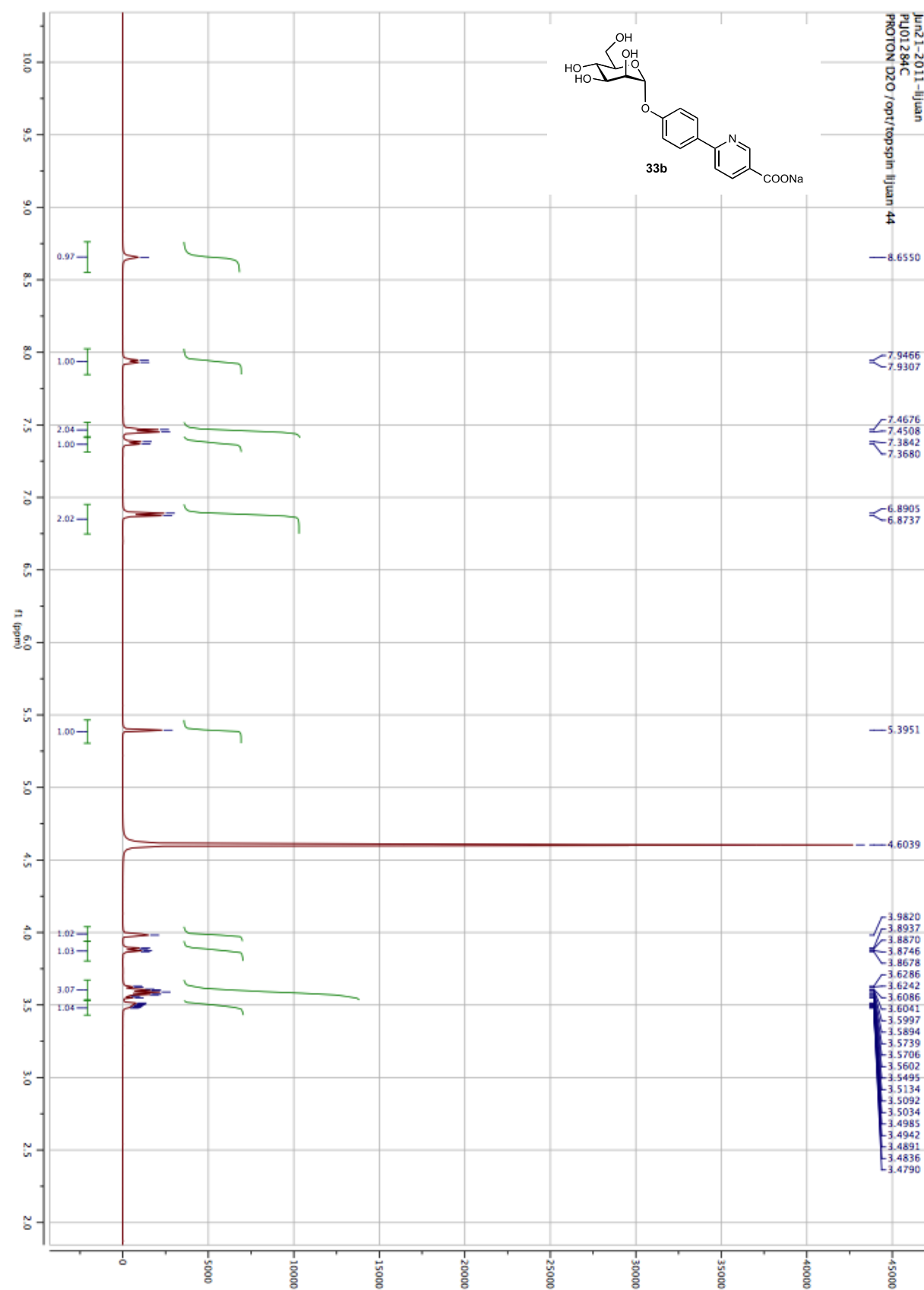
^1H NMR (500 MHz) of **32a**

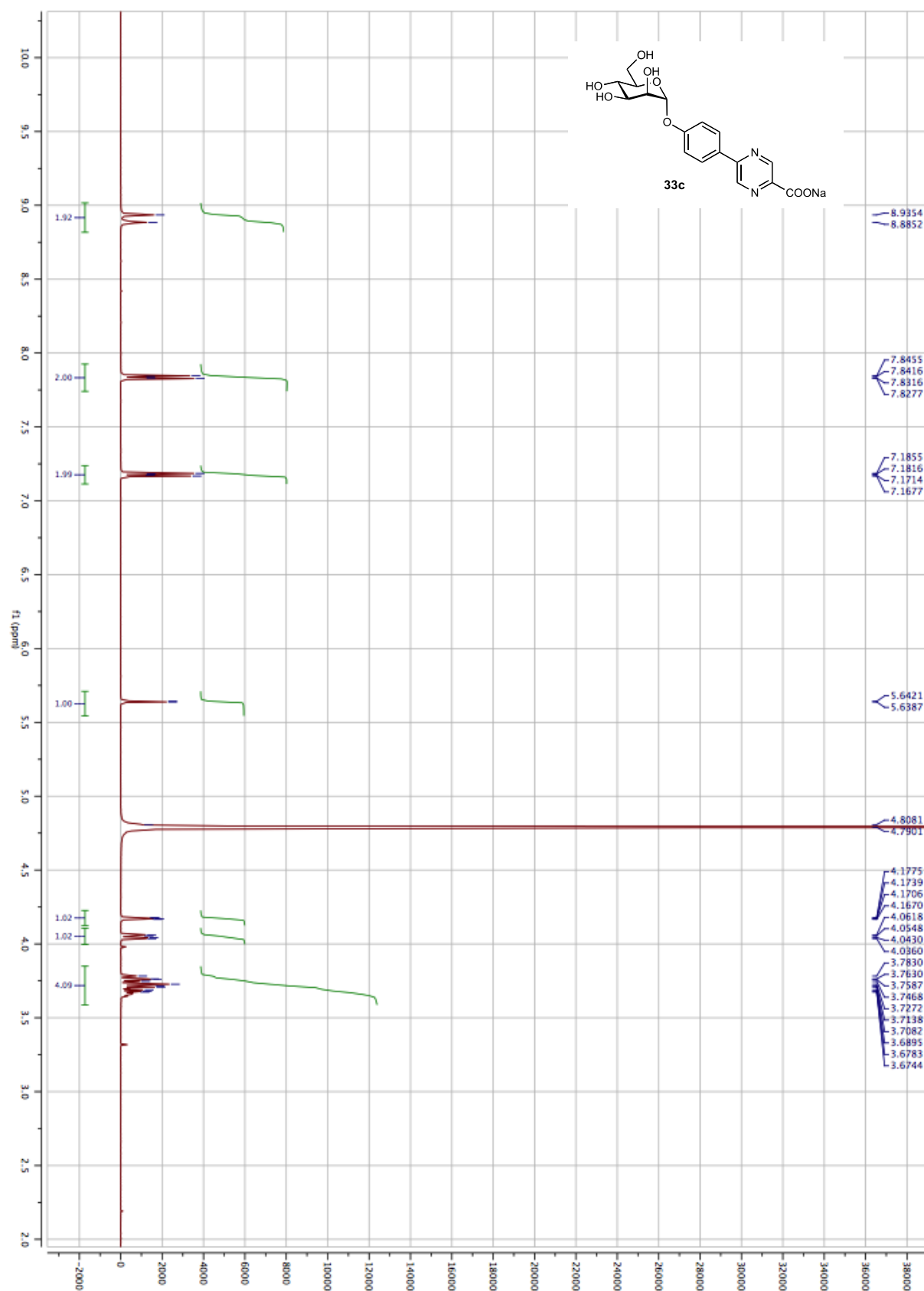
^1H NMR (500 MHz) of **32b**

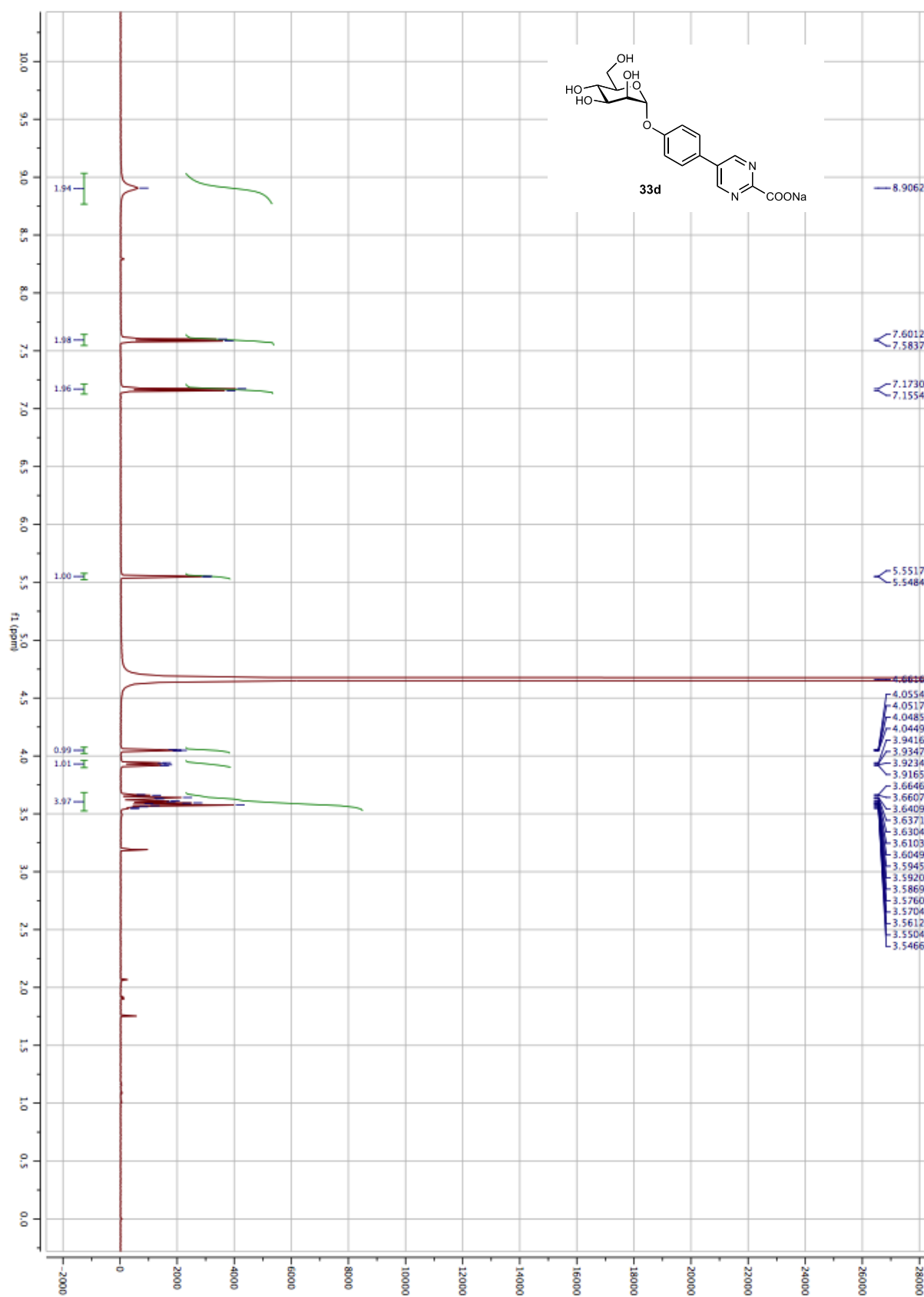
^1H NMR (500 MHz) of **32c**

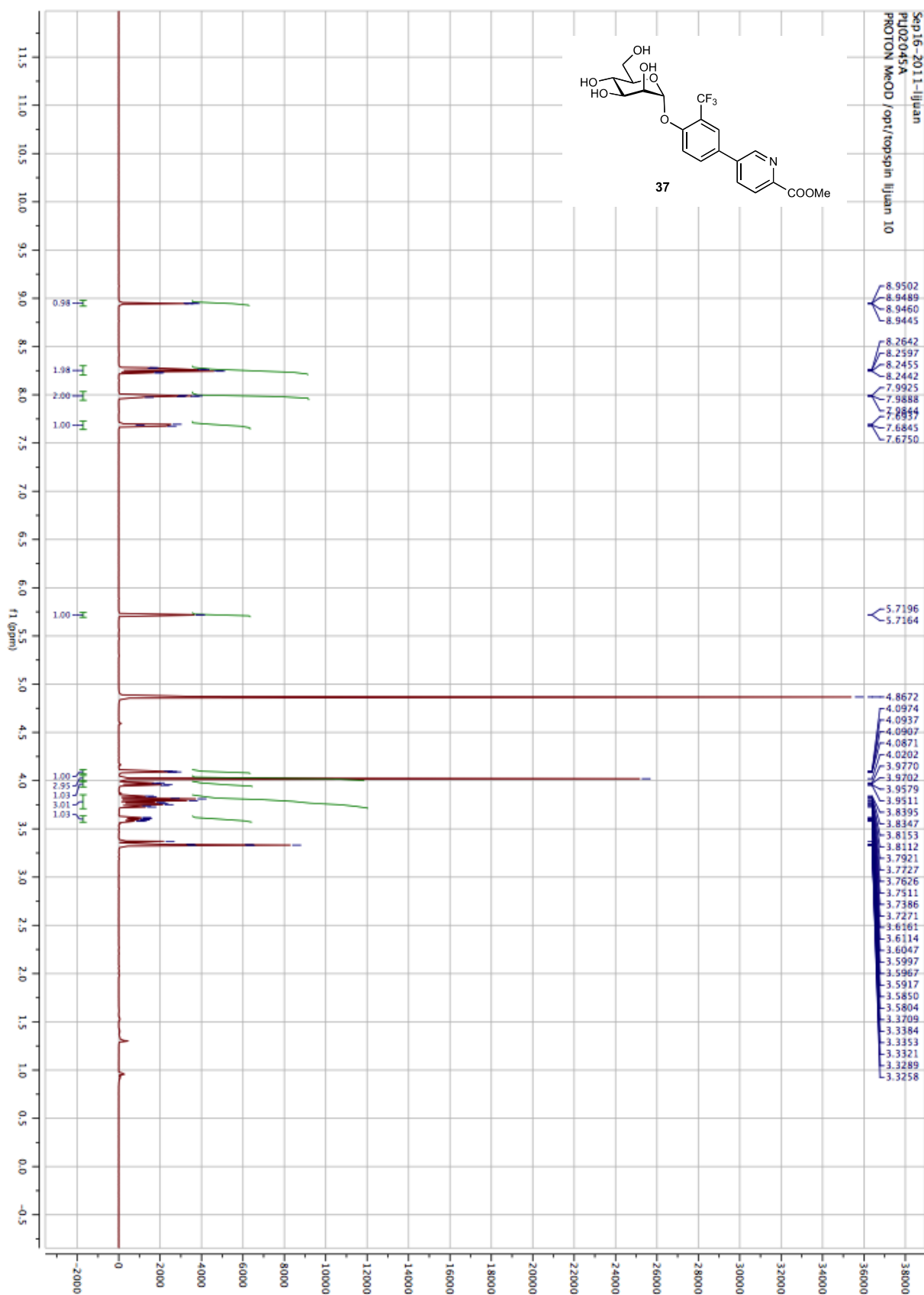
^1H NMR (500 MHz) of **32d**

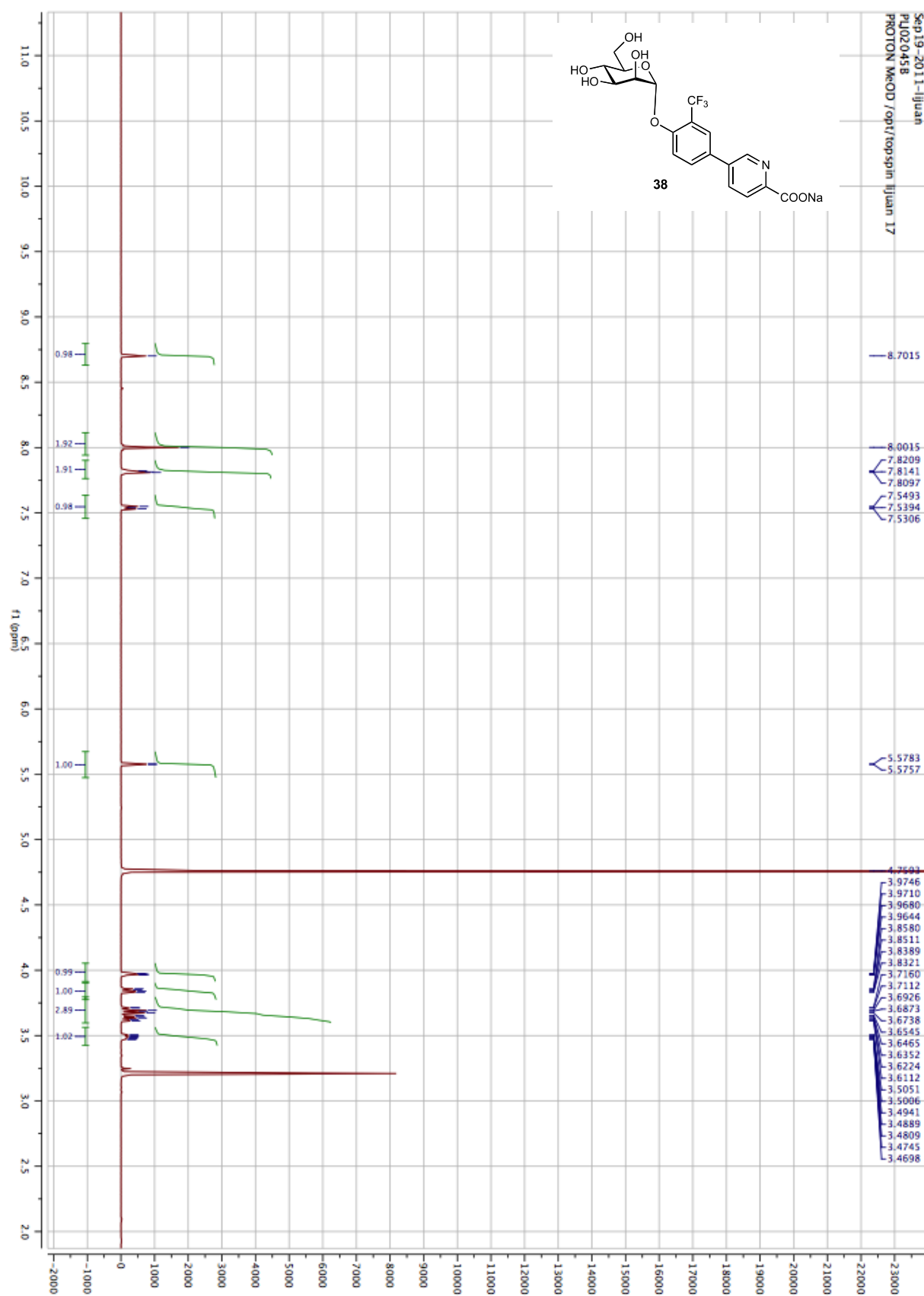
^1H NMR (500 MHz) of **33a**

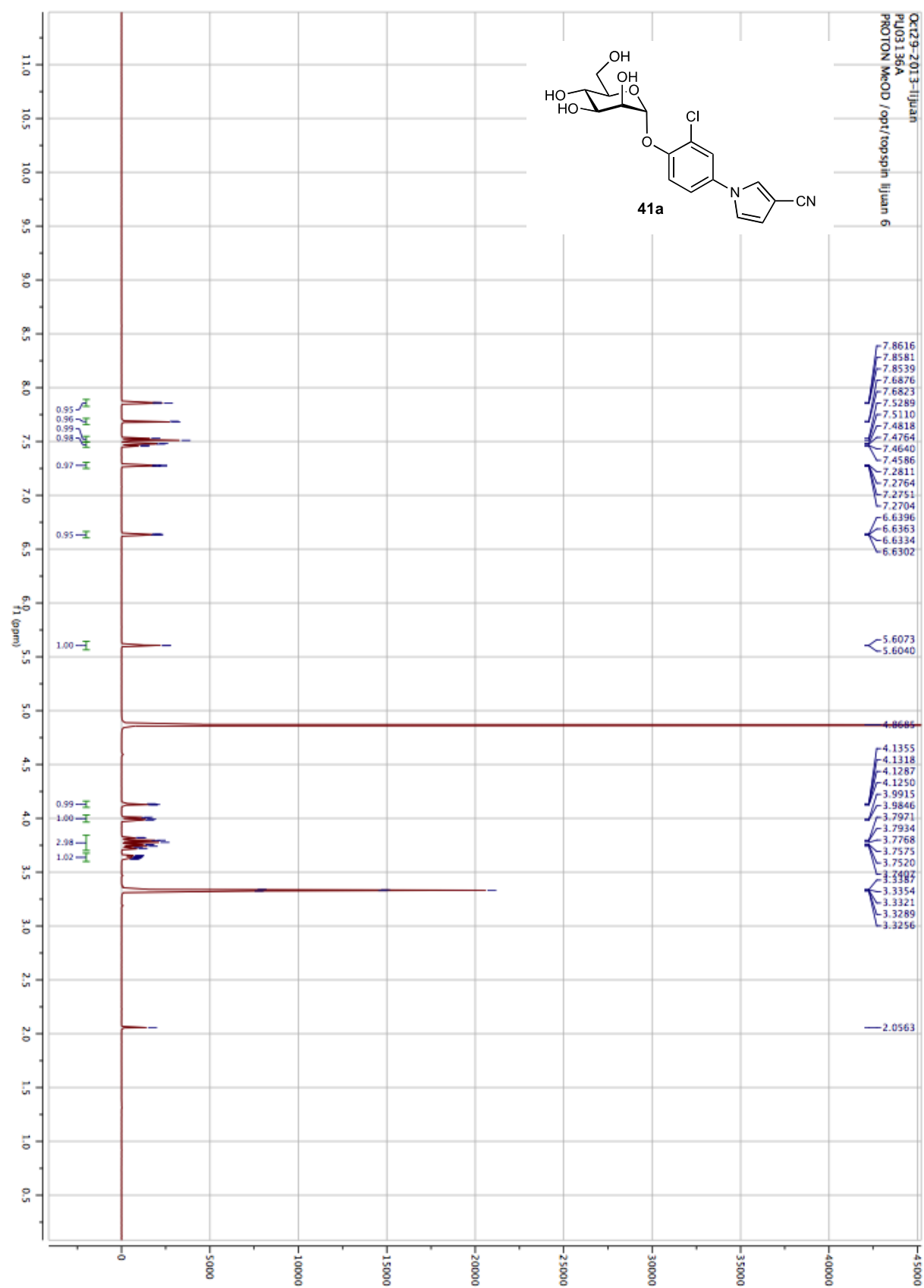
^1H NMR (500 MHz) of **33b**

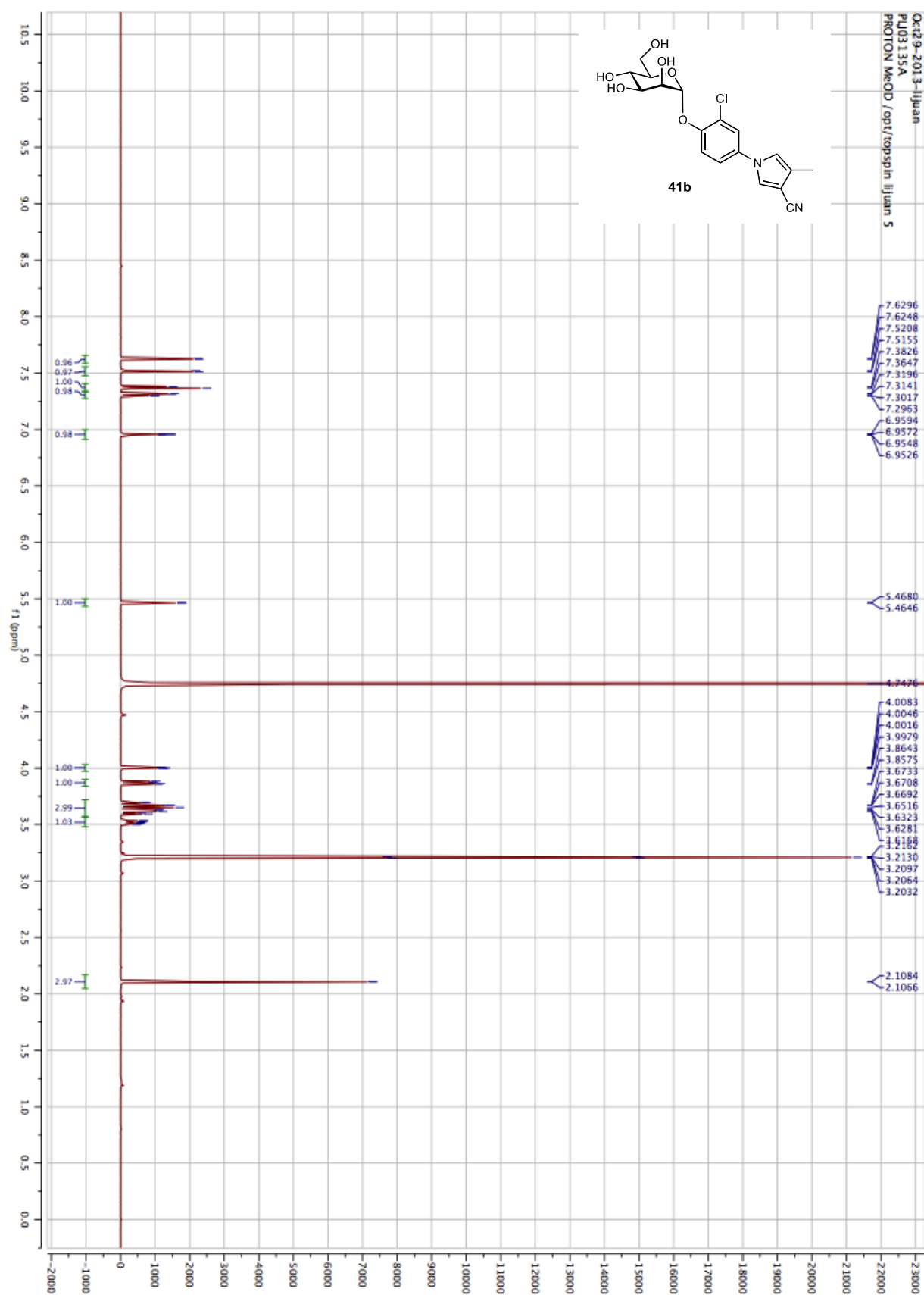
^1H NMR (500 MHz) of **33c**

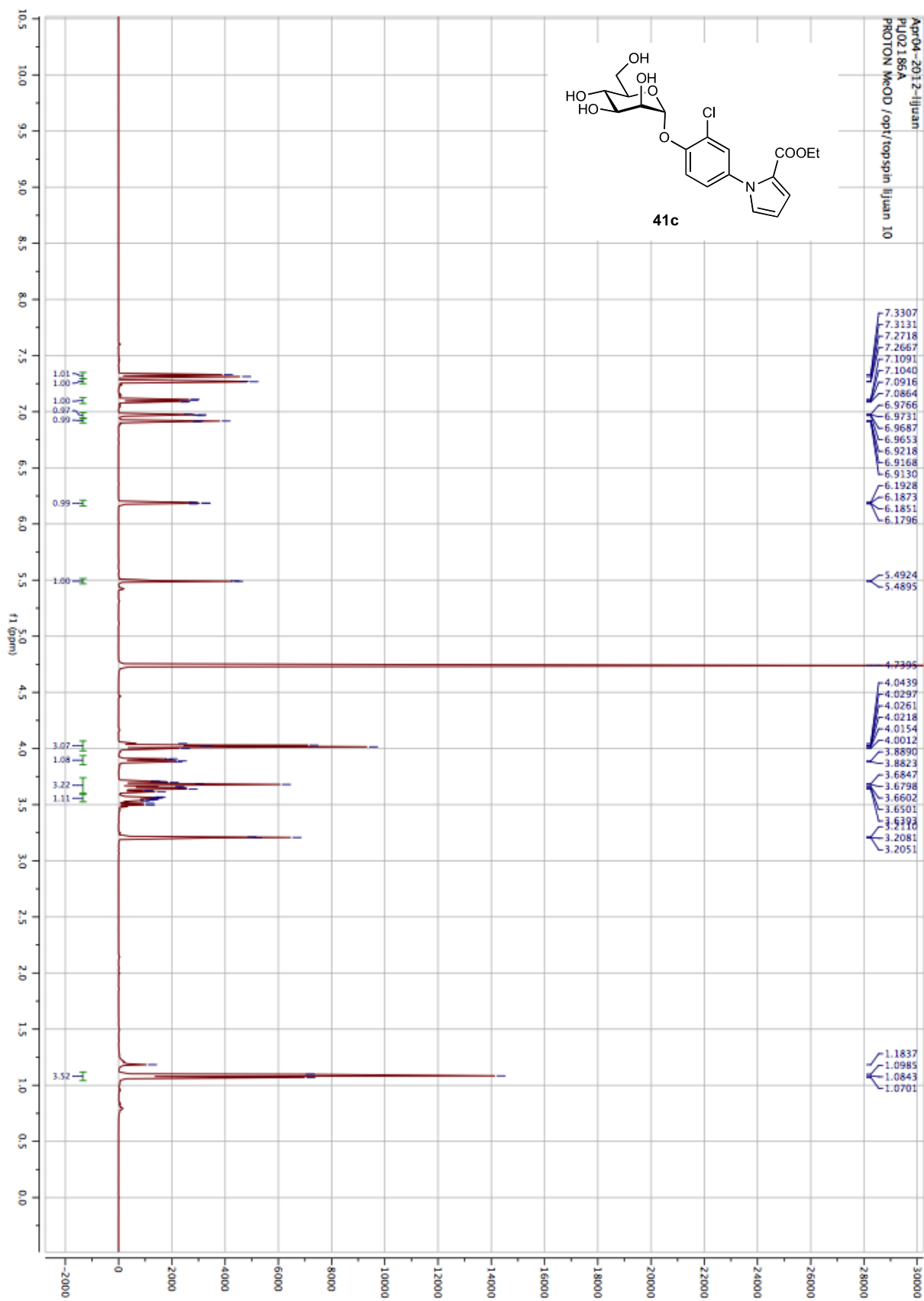
^1H NMR (500 MHz) of **33d**

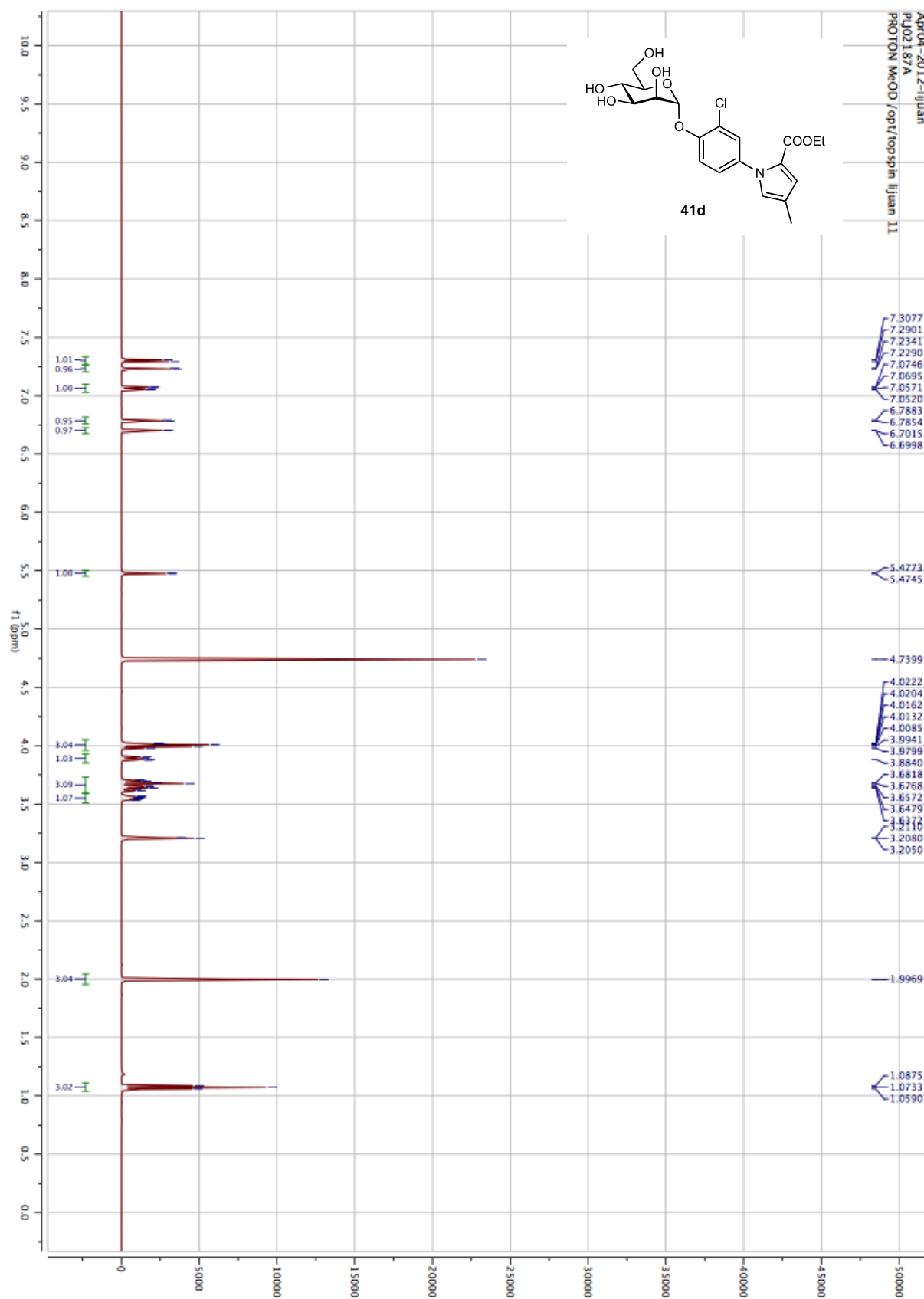
^1H NMR (500 MHz) of **37**

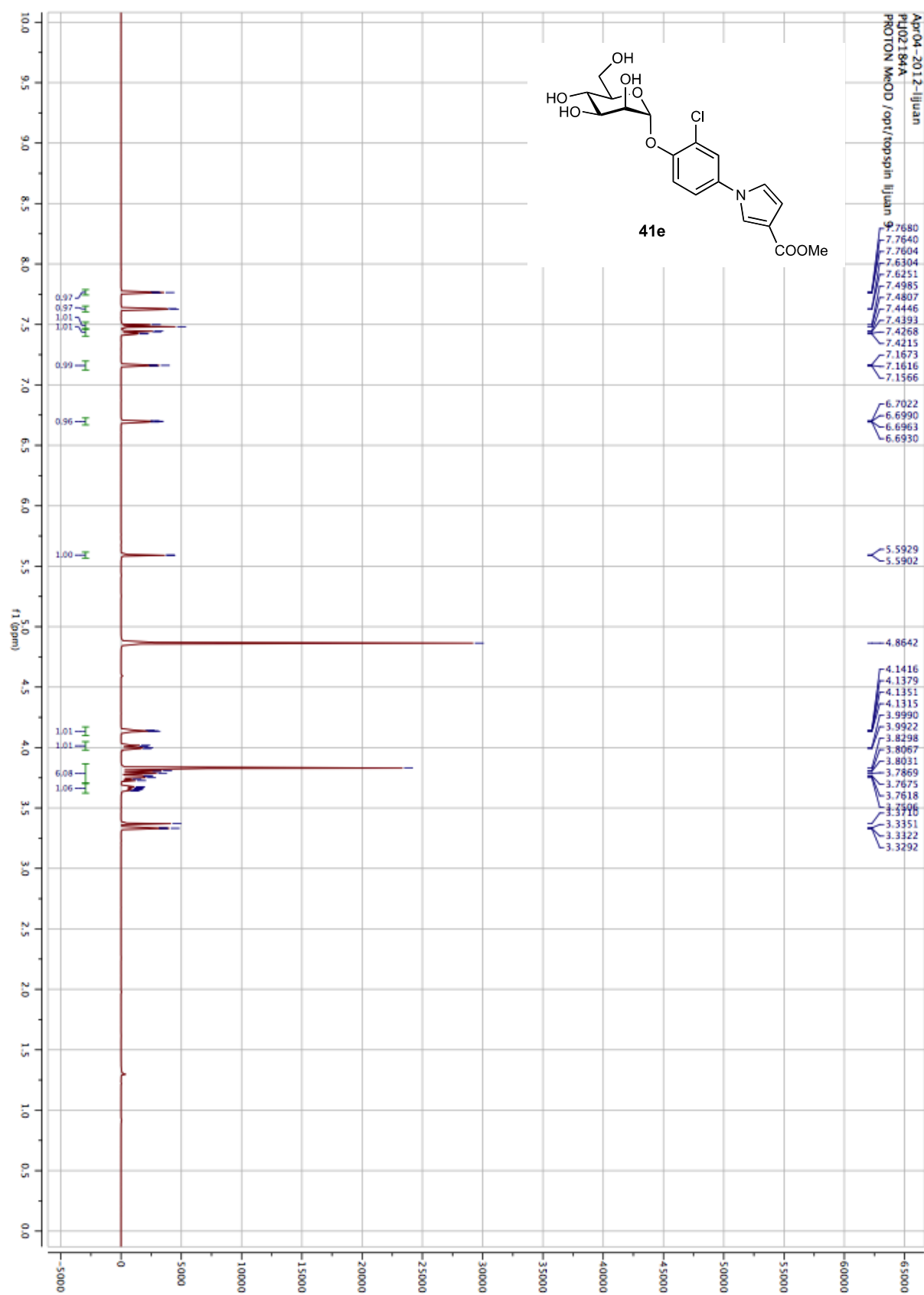
^1H NMR (500 MHz) of **38**

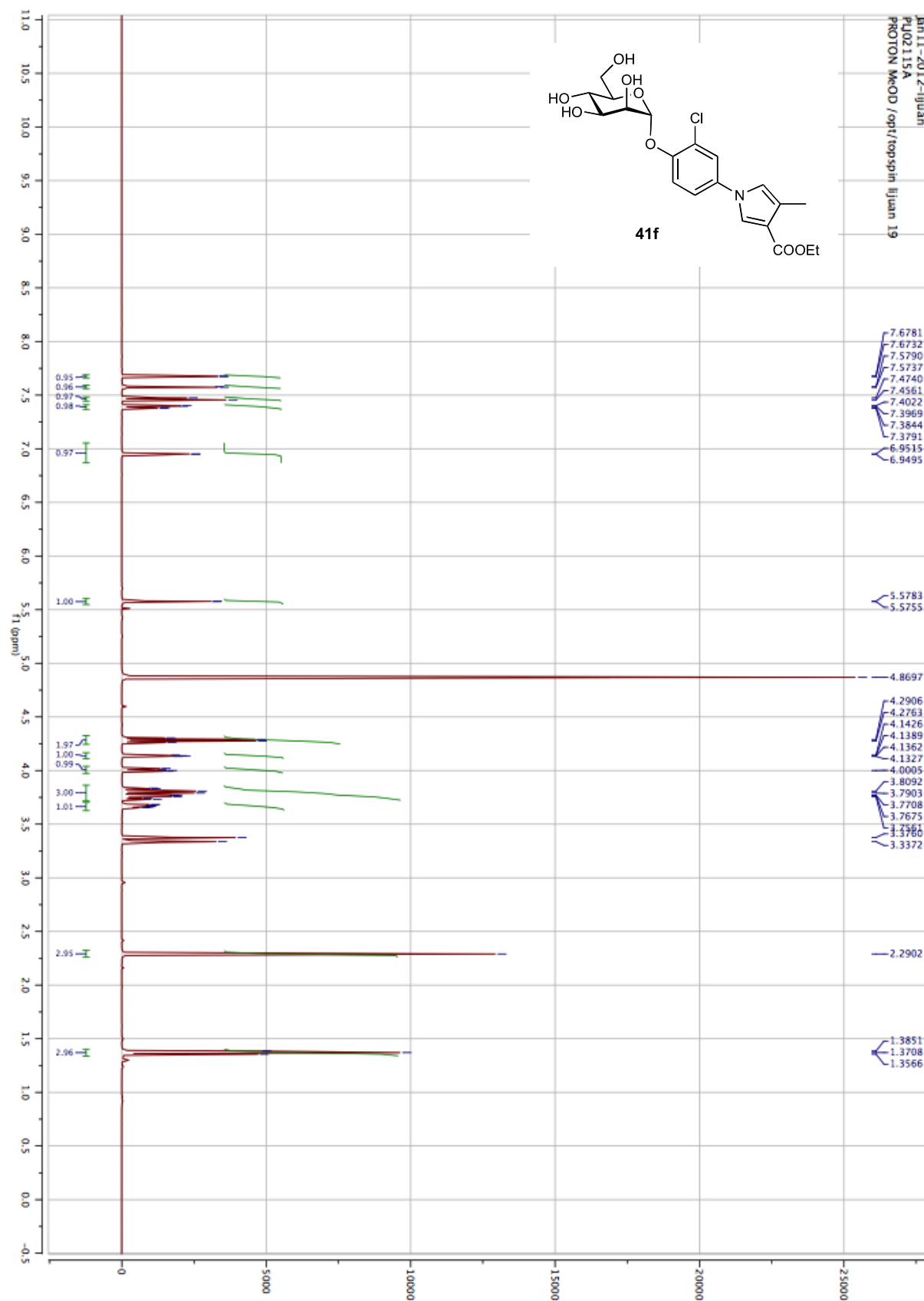
^1H NMR (500 MHz) of **41a**

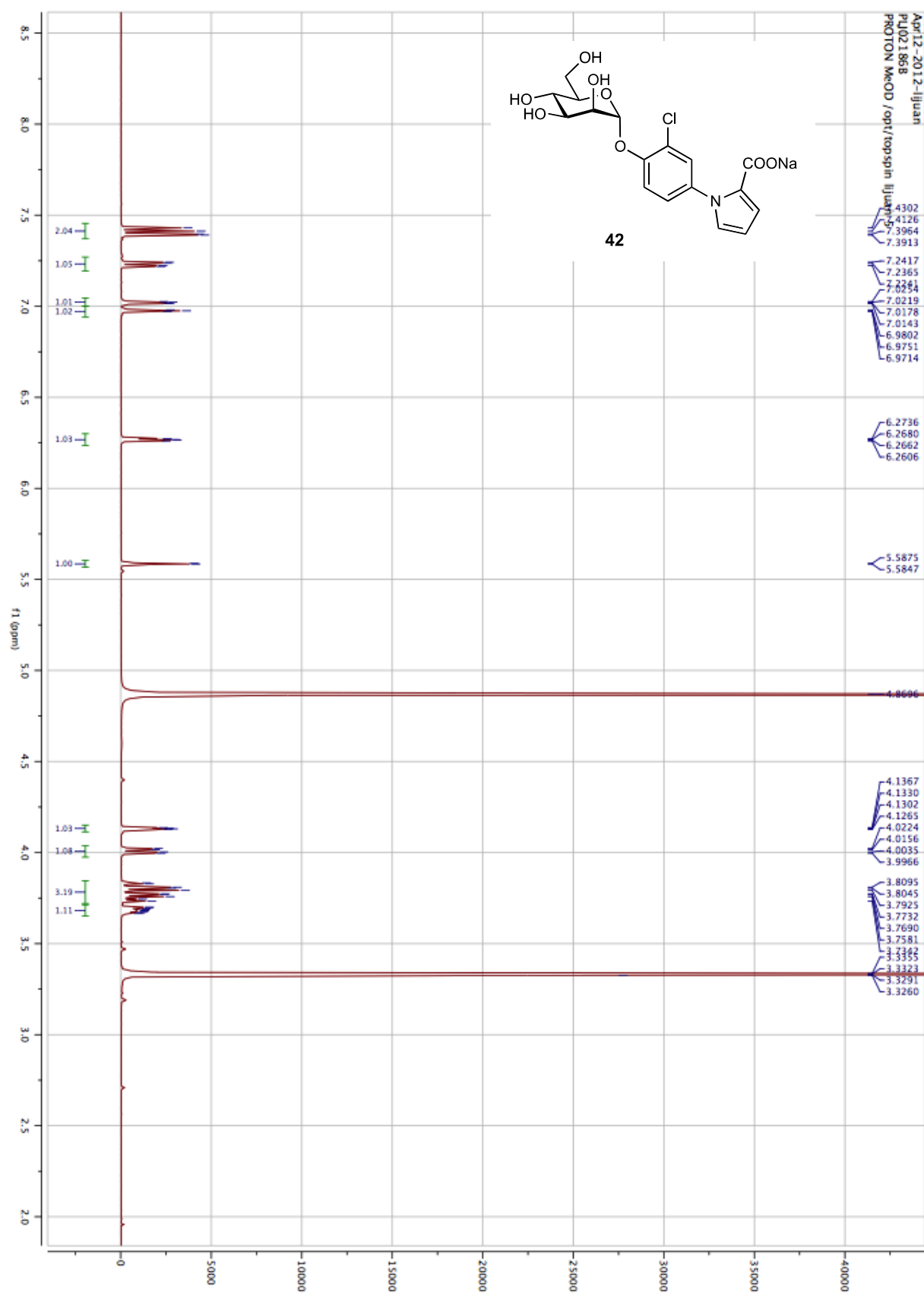
^1H NMR (500 MHz) of **41b**

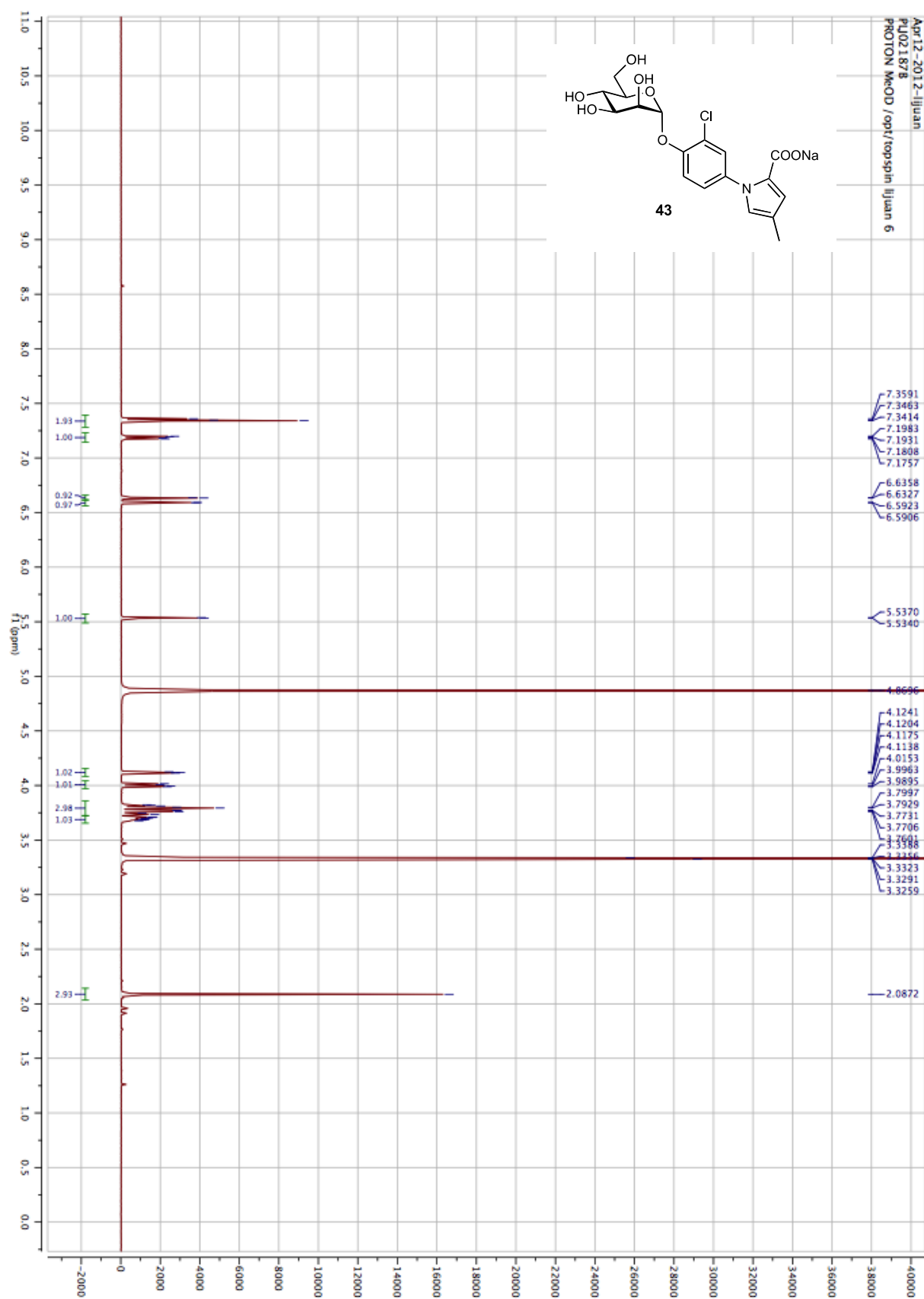
^1H NMR (500 MHz) of **41c**

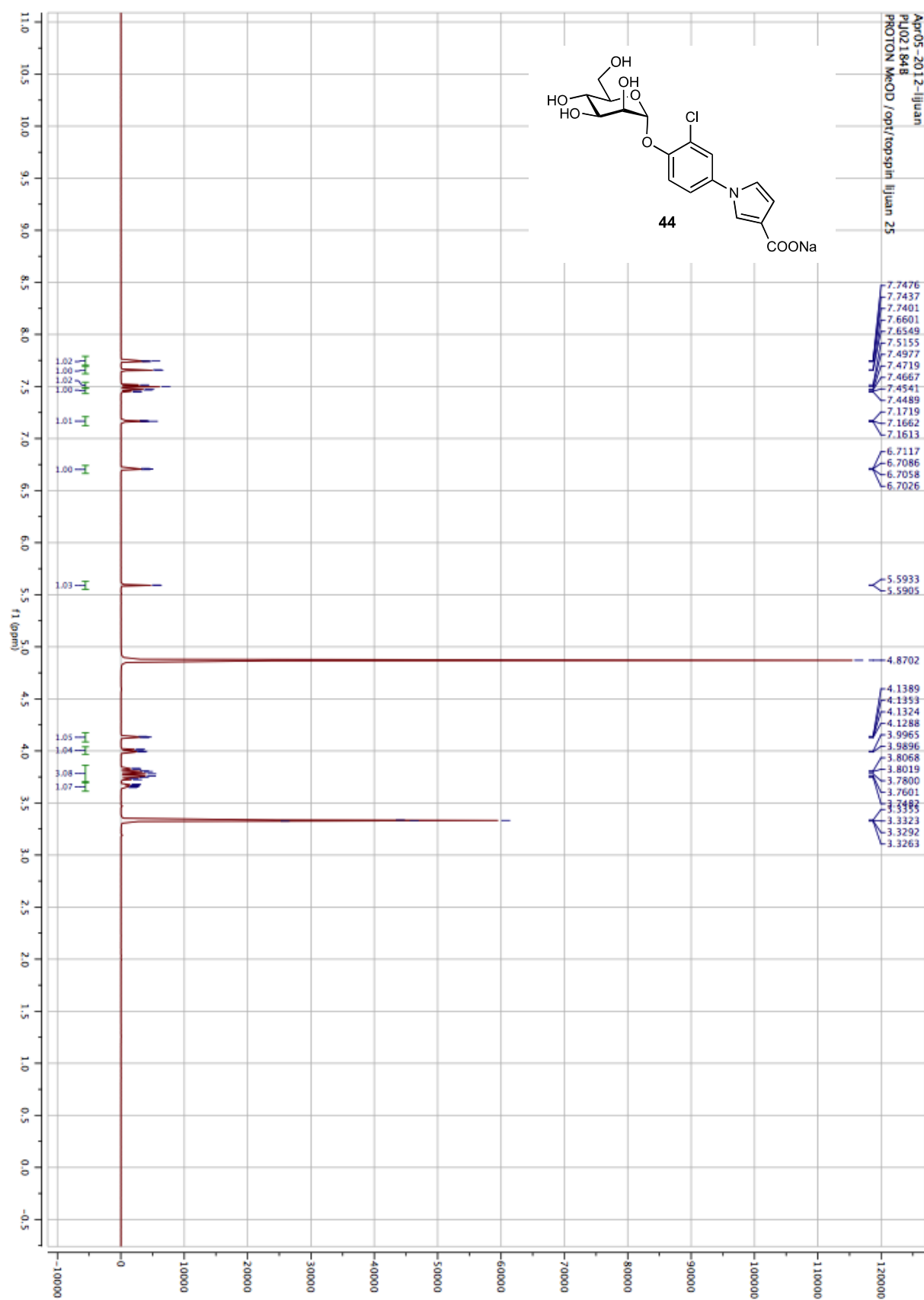
^1H NMR (500 MHz) of **41d**

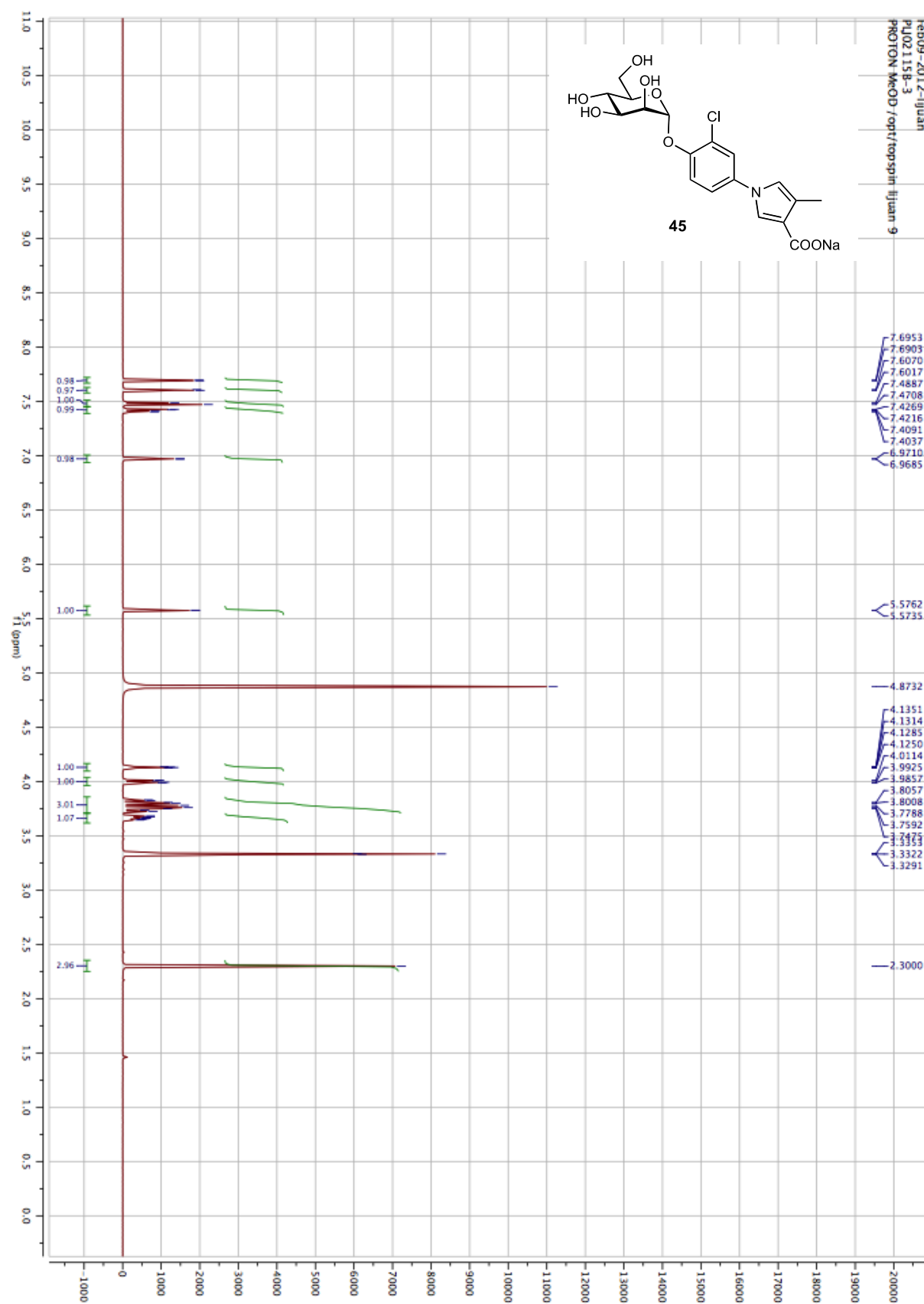
^1H NMR (500 MHz) of **41e**

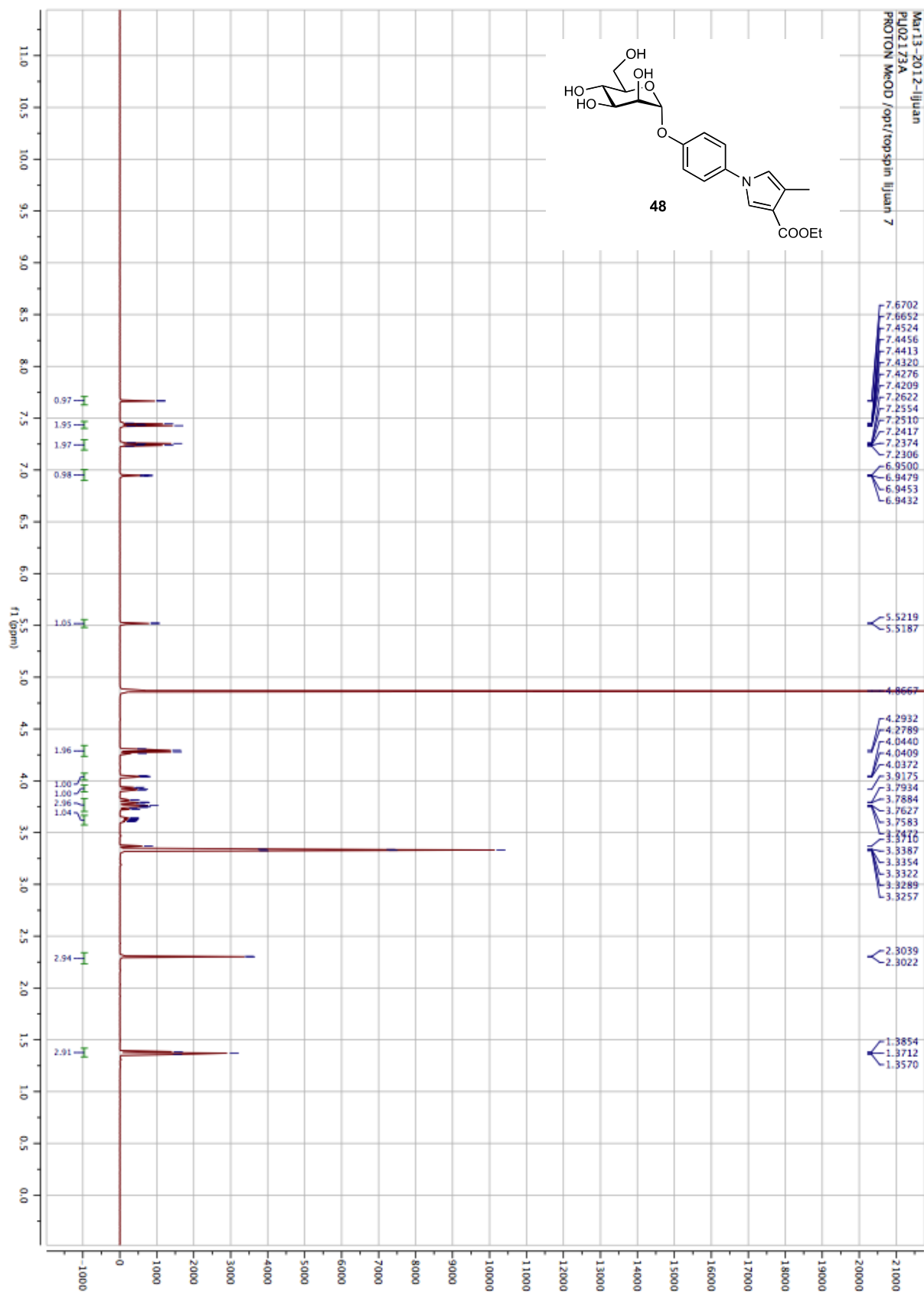
^1H NMR (500 MHz) of **41f**

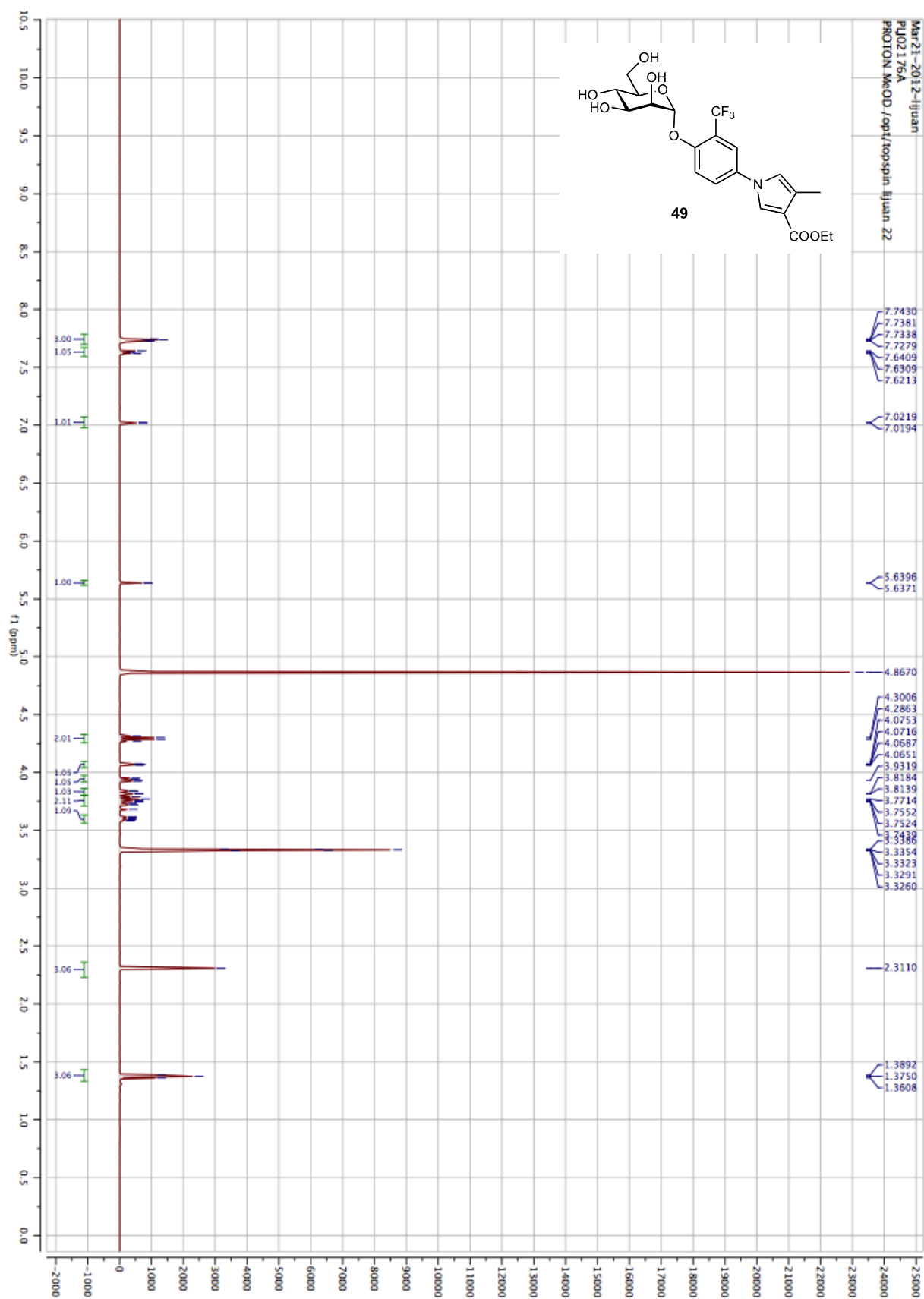
^1H NMR (500 MHz) of **42**

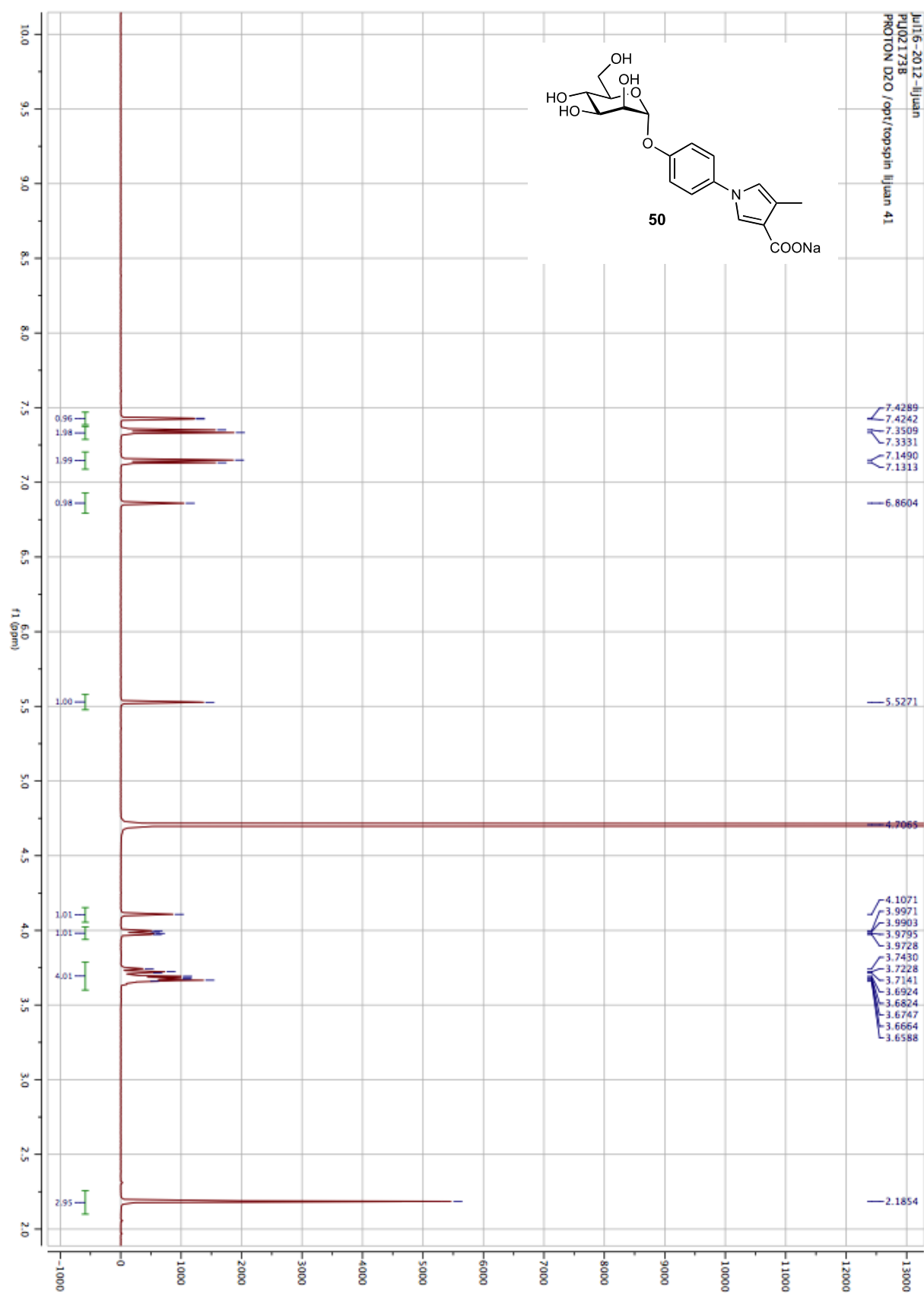
^1H NMR (500 MHz) of **43**

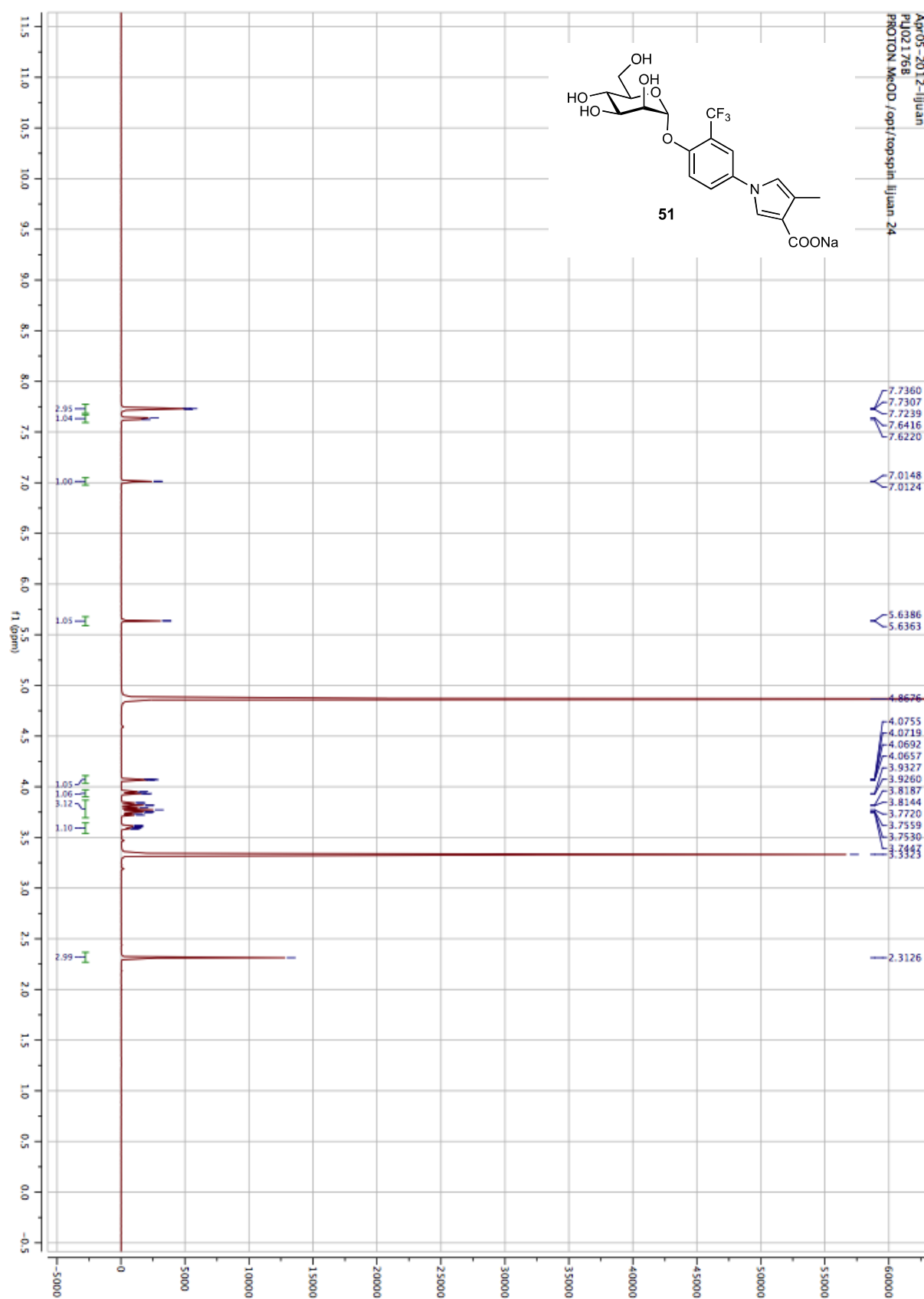
^1H NMR (500 MHz) of **44**

^1H NMR (500 MHz) of **45**

^1H NMR (500 MHz) of **48**

^1H NMR (500 MHz) of **49**

^1H NMR (500 MHz) of **50**

^1H NMR (500 MHz) of **51**

References:

- [S1] Le Bourdonnec, B.; Windh, R.; Leister, L.; Zhou, Q.; Ajello, C.; Gu, M.; Chu, G.; Tuthill, P.; Barker, W.; Koblish, M.; Wiant, D.; Graczyk, T.; Belanger, S.; Cassel, J.; Feschenko, M.; Brogdon, B.; Smith, S.; Derelanko, M.; Kutz, S.; Little, P.; DeHaven, R.; DeHaven-Hudkins, D.; Dolle, R. Spirocyclic delta opioid receptor agonists for the treatment of pain: Discovery of *N,N*-diethyl-3-hydroxy-4-(spiro[chromene-2,4'-piperidine]-4-yl) benzamide (ADL5747). *J. Med. Chem.* **2009**, *52*, 5685-5702.
- [S2] McCluskey, A.; Wentrup, C. 2-Pyridylnitrene from tetrazolo[1,5-a]pyridine and pyrido[2,3-a][1,2,4]oxadiazol-2-one. *J. Org. Chem.* **2008**, *73*, 6265-6267.
- [S3] Dawadi, P.; Lugtenburg, J. Efficient preparation of [1-(15)N]-3-Cyano-4-methyl-1H-pyrrole by a Wittig-based strategy. *Eur. J. Org. Chem.* **2008**, 2288-2292.

2.6 Paper 4: Kinetic Properties of Carbohydrate – Lectin Interactions: FimH Antagonists

This report describes the kinetic study on the interactions between FimH and the synthesized FimH antagonists. Three lead structures were chosen and immobilized on sensor chips via amine-coupling procedure. The kinetic properties of FimH antagonists were examined by surface plasmon resonance.

Contributions to this project:

Lijuan Pang synthesized the amide-chain functionalized compound **2** and the test compounds **8-13**.

This paper was published in *ChemMedChem*:

Scharenberg, M.; Jiang, X.; Pang, L.; Navarra, G.; Rabbani, S.; Binder, F.; Schwardt, O.; Ernst, B. Kinetic properties of carbohydrate – lectin interactions: FimH antagonists. *ChemMedChem* **2014**, *9*, 78-83.

© 2014 Wiley-VCH Verlag GmbH & Co. KGaA, Weinheim

DOI: 10.1002/cmdc.201300349

Kinetic Properties of Carbohydrate–Lectin Interactions: FimH Antagonists

Meike Scharenberg, Xiaohua Jiang, Lijuan Pang, Giulio Navarra, Said Rabbani, Florian Binder, Oliver Schwardt, and Beat Ernst^{*[a]}

The lectin FimH is terminally expressed on type 1 pili of uropathogenic *Escherichia coli* (UPEC), which is the main cause of urinary tract infections (UTIs). FimH enables bacterial adhesion to urothelial cells, the initial step of infection. Various mannose derivatives have been shown to antagonize FimH and are therefore considered to be promising therapeutic agents for the treatment of UTIs. As part of the preclinical development process, when the kinetic properties of FimH antagonists were examined by surface plasmon resonance, extremely low dissociation rates (k_{off}) were found, which is uncommon for carbohydrate–lectin interactions. As a consequence, the corresponding half-lives ($t_{1/2}$) of the FimH antagonist complexes are above 3.6 h. For a therapeutic application, extended $t_{1/2}$ values are a prerequisite for success, since the target occupancy time directly influences the in vivo drug efficacy. The long $t_{1/2}$ value of the tested FimH antagonists further confirms their drug-like properties and their high therapeutic potential.

Urinary tract infections (UTIs) are among the most prevalent infections and affect millions of people each year. In 70–95% of all cases, the UTI is caused by uropathogenic *Escherichia coli* (UPEC).^[1] These bacteria express type 1 pili with a terminally located adhesive protein called FimH. FimH-mediated adhesion to the surface of urothelial cells by binding to oligomannoside residues of the glycoprotein uroplakin Ia (UPIa)^[2–5] is a prerequisite for the invasion of the host cells leading to a UTI.^[2,3] Therefore, efforts have been made to identify orally available FimH antagonists to interfere with the attachment of UPEC to urothelial cells. From these studies, α -D-mannopyranosides have emerged providing a novel therapeutic opportunity for prevention and treatment of UTIs as an alternative to antibiotics.^[6–8] To date, several mannose-based FimH antagonists have been validated in various in vitro and in vivo studies.^[9–20]

As part of their pharmacodynamic characterization, not only equilibrium dissociation constants (K_D) or half-maximal inhibitory concentrations (IC_{50}) but also the kinetics of the binding process are studied.^[21–23] One crucial factor for a sustained in vivo efficacy is the half-life ($t_{1/2}$) of the drug–receptor complex, especially when drugs compete with endogenous ligands.

The $t_{1/2}$ of a drug–receptor complex depends on the dissociation rate (k_{off}). Slow off-rates are beneficial for the in vivo efficacy, as prolonged occupancy of the target by the drug results in an extended duration of the pharmacological effect. Consequently, lower drug concentrations are required to obtain high efficacy, decreasing the risk of off-target toxicity.^[21–23] The importance of long target occupancy is reflected in the long $t_{1/2}$ of many drugs reaching the market, such as the HIV-1 protease inhibitor Darunavir ($t_{1/2} > 240$ h),^[24] the CCR5 receptor antagonist Maraviroc ($t_{1/2} = 10.5$ h),^[25] or the viral neuraminidase inhibitor Zanamivir ($t_{1/2} > 33$ min), which was developed from a carbohydrate-based lead structure.^[26]

For carbohydrate–lectin interactions, only a few studies describing the kinetic properties are available. For the lectins, myelin-associated glycoprotein (MAG),^[27,28] E-, L- and P-selectin,^[29–31] galectin-1 and -3,^[32] mannose-binding protein (MBP),^[33] concanavalin A (ConA),^[34] and calreticulin^[35] surface plasmon resonance (SPR) experiments revealed fast association and dissociation kinetics with k_{off} rates between 2.6×10^{-3} and $> 10 \text{ s}^{-1}$, resulting in short $t_{1/2}$ values ranging from 266 to 0.07 seconds (Table 1). These fast binding kinetics, typical for carbohydrate–lectin interactions, strongly hamper the development of carbohydrate-derived drugs. The determination of the kinetic parameters of FimH antagonists is therefore of utmost importance for successful lead optimization.

Beside K_D values, dissociation rates (k_{off}) of the complex between the antagonist and the target protein FimH are of special interest. To study these parameters, SPR is widely applied, including for carbohydrate–lectin^[37] and carbohydrate–antibody^[36] interactions. For the lectin domain of FimH, different affinity states are known.^[38] In this study, the lectin domain in the high-affinity state was used.^[39] Immobilization attempts by standard amine coupling failed, presumably due to accessible amino groups in and close to the ligand binding site. Thus, the N-terminal phenylalanine is part of the binding site. Immobilization via a C-terminal His-tag onto a nickel(II)–nitrilotriacetate (Ni-NTA) chip or indirect coupling via an anti-His-tag antibody failed due to instability of the base line, resulting from a slow detachment of the noncovalently immobilized FimH. Furthermore, harsh regenerating conditions (50 mM NaOH), necessary for the dissociation of the antagonist–lectin complex, caused the inactivation of the protein. Consequently, we immobilized FimH antagonists functionalized with an amino- (1 and 2) or N-hydroxy- (3a,b) succinimide via an amine-coupling procedure on CM4 dextran sensor surface chips (Scheme 1).

To determine the kinetic parameters of the FimH–antagonist interaction, a direct binding assay was performed. FimH was

[a] Dr. M. Scharenberg, Dr. X. Jiang, L. Pang, G. Navarra, Dr. S. Rabbani, Dr. F. Binder, Dr. O. Schwardt, Prof. Dr. B. Ernst
Institute of Molecular Pharmacy, Pharmcenter, University of Basel
Klingelbergstrasse 50, 4056 Basel (Switzerland)
E-mail: beat.ernst@unibas.ch

Supporting information for this article is available on the WWW under <http://dx.doi.org/10.1002/cmdc.201300349>.

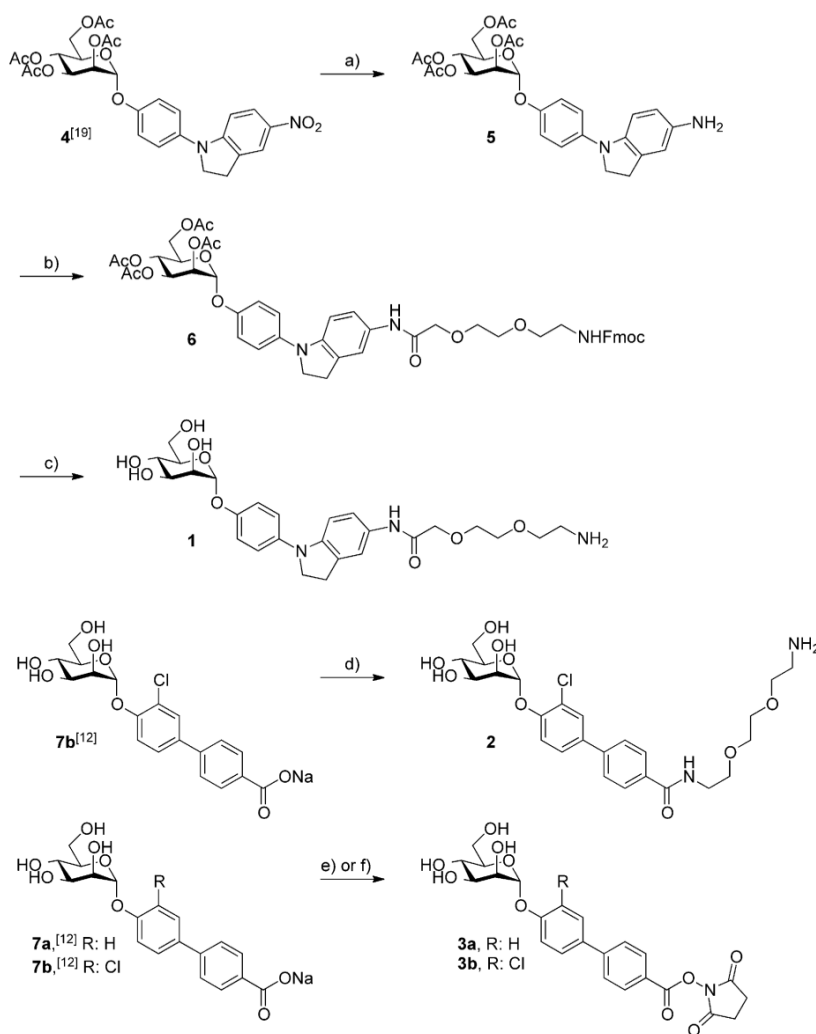
Table 1. Typical kinetic binding parameters of carbohydrate–protein interactions.

Protein	Ligand	K_D [μM]	k_{on} [$\text{M}^{-1}/\text{s}^{-1}$]	k_{off} [s^{-1}]	$t_{1/2}$ [s]	Ref.
L-selectin	GlyCAM1	108	$> 10^5$	> 10	0.07	[30]
E-selectin	ESL 1	62	4×10^4	3.0	0.2	[29]
P-selectin	PSGL 1	0.3	4×10^6	1.4	0.5	[31]
GSLA-2 mAB	sialyl Lewis ^a	4.3	1.1×10^5	8×10^{-1}	0.9	[36]
MAG	D-Neu5Ac derivative	2.8	3.5×10^5	0.8×10^{-1}	0.9	[27]
Galectin-1	D-Lactose derivative	1010	1.9×10^2	2.1×10^{-1}	3.3	[32]
Galectin-3	D-Lactose derivative	280	7.3×10^2	2.0×10^{-1}	3.4	[32]
CG-1A (avian galectin)	D-Lactose derivative	83.5	2.5×10^3	2.1×10^{-1}	3.3	[32]
Calreticulin	Glc ₁ Man ₃ -GlcNAc ₂	2	3.9×10^4	8×10^{-2}	8.6	[35]
Con A	D-Man derivative	65	1.43×10^2	9.4×10^{-3}	73.7	[34]
MBP	D-Man ₁₆ /BSA	13.3	3.47×10^4	2.6×10^{-3}	266.6	[33]

Abbreviations: myelin-associated glycoprotein (MAG); concanavalin A (Con A); mannose-binding protein (MBP).

passed at concentrations between 0–200 nM over the flow cells (CM4 chip) equipped with covalently linked antagonists (Figure 1a). A reference cell without antagonist but treated with *N*-hydroxysuccinimide (NHS)/*N*-(3-dimethylaminopropyl)-*N*-ethylcarbodiimide hydrochloride (EDC) and ethanolamine (EA) was used to account for nonspecific binding of the protein to the dextran matrix. The kinetic parameters k_{on} and k_{off} were obtained by applying a global fit to the sensorgrams, using a 1:1 (Langmuir-type) binding-model (Scrubber 2.0c). The fitted sensorgrams of compounds **1**, **2**, **3a** and **3b** are shown in Figure 1b.

Mass transfer limitations, which might occur when using proteins as analytes (FimH: MW=18.6 kD), can falsify the measured kinetic parameters. They depend on the cell dimension, the flow rate, and the diffusion coefficient of the analyte. Proteins having smaller diffusion coefficients than low-molecular-weight compounds are prone to show mass transfer limitations. To rule out these limitations, we used high flow rates (20–30 $\mu\text{L}\cdot\text{min}^{-1}$) and a low surface antagonist density (usage of CM4 chips instead of CM5 chips). Furthermore, we immobilized antagonist **1** at three different immobilization levels (differ-



Scheme 1. Synthesis of the amino- or *N*-hydroxyl-succinimide-functionalized FimH antagonists **1**–**3**. *Reagents and conditions:* a) H₂ (1 atm), PtO₂, morpholine, EtOAc/MeOH (1:1), RT, 1 h (97%); b) 8-(Fmoc-amino)-3,6-dioxaoctanoic acid, PyBOP, DIPEA, DMF, RT, overnight; c) NaOMe, MeOH, RT, 2 h (47% over two steps); d) EBE, COMU, DIPEA, DMF, 0 °C → RT, overnight (20%); e) EDC, NHS, H₂O, RT, 30 min (**3a**: 98%); f) EDC, NHS, MES buffer (pH 5.6), RT, 30 min (**3b**: 99%).

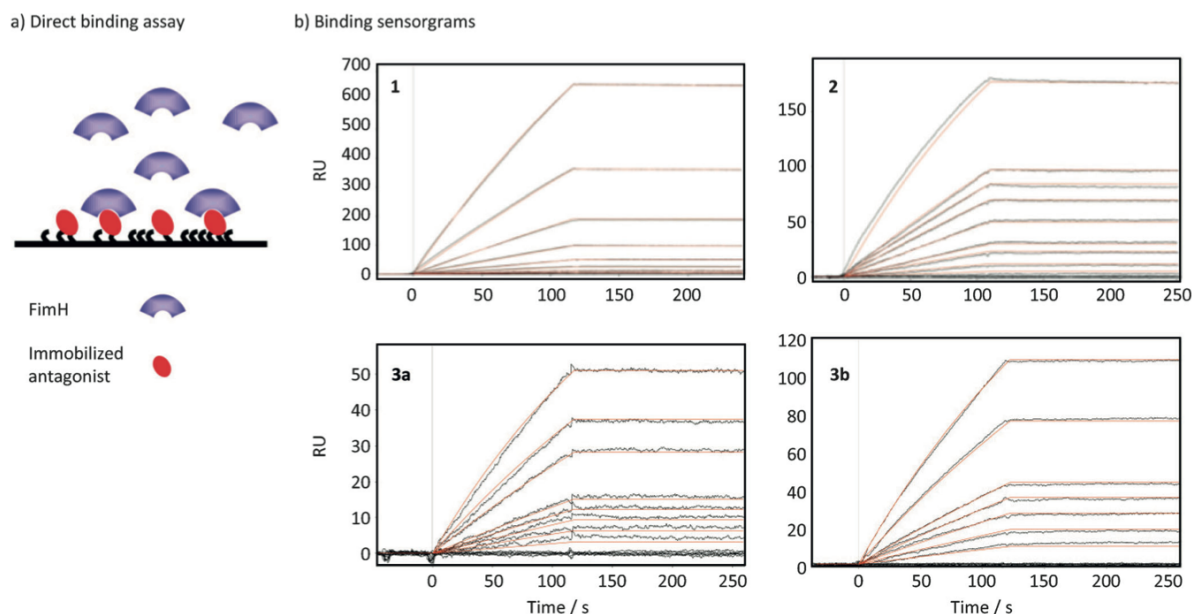


Figure 1. a) Schematic representation of a direct binding assay format. FimH binds to test compound (i.e., **1**, **2**, **3a,b**) immobilized on the chip. b) Sensorgrams obtained by kinetic fits of FimH binding to immobilized antagonists **1**, **2**, **3a** and **3b**. Solutions of FimH ranging between 0–200 nM were passed over the surface. For the fitting of the sensorgrams, Scrubber 2.0c was applied.

ent ratios between **1** and EA used for the immobilization) on the same sensor chip. FimH was screened simultaneously on all three surfaces, and the kinetic parameters and affinities were evaluated. Since all three surfaces showed similar kinetic rates and affinities, mass transfer effects are negligible. The obtained kinetic parameters are summarized in Table 2.

Association rates (k_{on}) between 1.4×10^4 and $4.8 \times 10^4 \text{ M}^{-1} \text{ s}^{-1}$ were obtained and are in the expected range for low-molecular-weight compounds. The dissociation rates (k_{off}) were $5.2 \times 10^{-5} \text{ s}^{-1}$ for **1**, $3.5 \times 10^{-5} \text{ s}^{-1}$ for **2**, and $2.0 \times 10^{-5} \text{ s}^{-1}$ for **3a**. For compound **3b**, the detection limit of k_{off} ($< 10^{-6} \text{ s}^{-1}$) was reached and consequently the K_D value was not determinable. The small dissociation constants resulted in $t_{1/2}$ values between 3.6 h and > 19 h, representing extraordinary long $t_{1/2}$ values for carbohydrate–lectin interactions, which are usually in the

range of seconds (see Table 1). Consistent with the long $t_{1/2}$ values, the equilibrium state of the interactions can only be reached after an extended period of time, conditions that were not applicable to our SPR experiments. The affinity (K_D) of the antagonists was therefore calculated from the kinetic parameters ($K_D = k_{off}/k_{on}$) and not determined from steady state measurements. As expected,^[12,19] affinities in the low nanomolar range (0.7–3.5 nM) were obtained. Furthermore, the three-fold higher affinity of compound **2** compared with compound **3a** is consistent with published data, confirming that a chloro substituent in the *ortho* position of the aromatic ring adjacent to the anomeric center enhances binding affinity to FimH.^[12] The off-rate of compound **2** was already close to the detection limit of the method applied. Compound **3b**, which differs from **2** only by a shorter linker length, did not reveal reliable kinetic data, due to its immeasurable k_{off} value ($\leq 10^{-6} \text{ s}^{-1}$), indicating that the linker length presumably has a small effect on the binding affinity.

FimH can exhibit two conformations, a low-affinity conformation and a high-affinity conformation. The switch from the low-affinity state to the high-affinity state can be triggered by applying a mechanical force along the molecule. This behavior is characteristic for the catch-bond mechanism found for the FimH–ligand interaction.^[38] It enables the bacteria to firmly attach to oligomannosides on bladder epithelial cells, even under the harsh conditions of the urinary tract (i.e., flow of urine). In the high-affinity state, the binding site of FimH forms a deep, narrow, and negatively charged pocket, unlike mammalian lectins, often characterized by shallow and water-accessible binding sites (see for example, selectins,^[40] galectins,^[41]

Table 2. Kinetic binding parameters for the interaction of FimH with antagonists **1**, **2** and **3a,b**.

Compd	Ligand/EA ratio ^[a]	K_D [nM]	k_{on} [$10^4 \text{ M}^{-1} \text{ s}^{-1}$]	k_{off} [10^{-5} s^{-1}]	$t_{1/2}$ [h]
1	1:0 (high)	3.5	1.4	5.2	3.7
1	1:10 (middle)	2.5	2.0	5.1	3.8
1	1:100 (low)	2.0	2.6	5.3	3.6
2	1:0	0.7	4.8	3.5	5.5
3a	1:0	2.3	1.1	2.0	9.6
3b	1:0	n.d. ^[b]	1.4	$\leq 10^{-6}$ ^[c]	> 19

[a] Molar ratio of ligand/ethanolamine (EA); density is given in parentheses; [b] not determinable (n.d.) due to $k_{off} \leq 10^{-6} \text{ s}^{-1}$; [c] k_{off} value for **3b** out of limit.

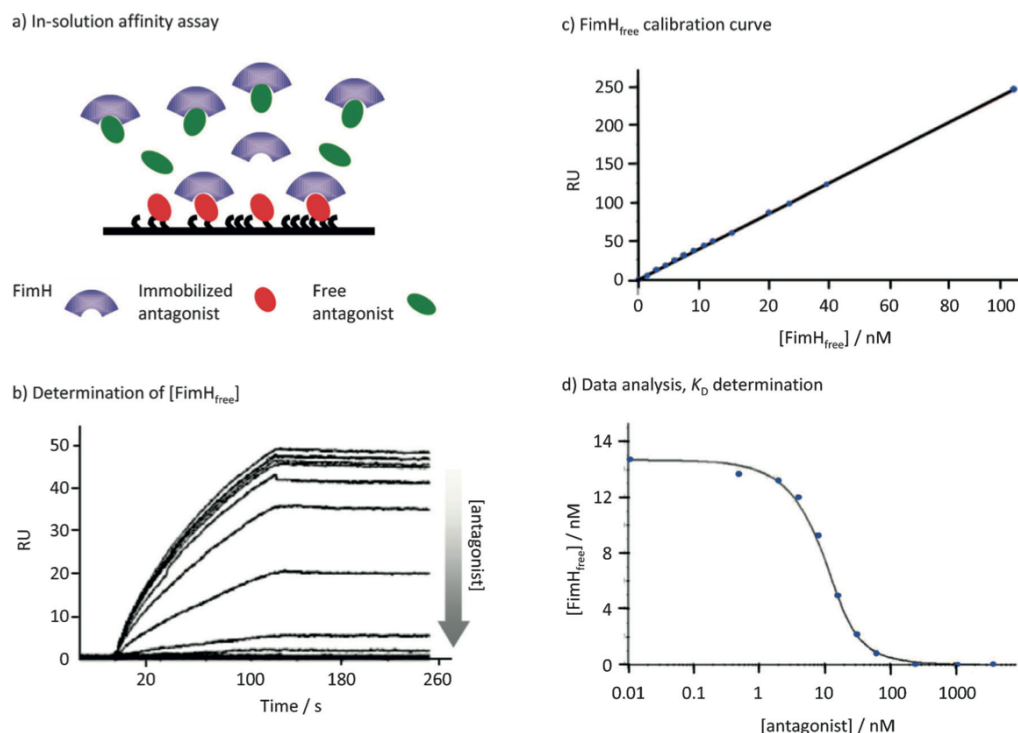


Figure 2. Results from the in-solution affinity assay with *n*-heptyl α -D-mannopyranoside **8** (see Table 3, entry 1). a) Schematic representation of the in-solution affinity assay. $FimH_{free}$ after equilibration binds to **1**, which is immobilized on the chip. b) Sensorgrams obtained after passing over the equilibrated mixtures of compound **8** and $FimH$. c) $FimH$ calibration curve ($FimH$: 0–120 nM) and d) K_D determination by in-solution affinity-fit algorithm of the BiaEvaluation software.

mannose-binding protein^[42] or DC-SIGN).^[43] The hydrophilic side chains of amino acids lining the $FimH$ binding pocket establish a perfect network of hydrogen bonds with the hydroxy groups of α -D-mannopyranosides.^[44] Consequently, the slow dissociation of the carbohydrate– $FimH$ complex found in this study can be explained by the binding mode of $FimH$ ligands to the high-affinity $FimH$ conformation. As the pathogenicity of the bacteria depends on the interaction between $FimH$ and its physiological ligand on the urothelial surface, a long $t_{1/2}$ value for $FimH$ antagonists is of utmost importance for successful treatment.

Due to the high affinity of $FimH$ antagonists and their small dissociation rate, in-solution affinity experiments (as described by Durka et al. in Ref. [45]) can be applied to determine K_D values of antagonists. For these experiments, we used the CM4 sensor chip coated with compound **1** (chip 1). For an accurate determination of K_D values, a constant concentration of $FimH$ (10–15 nM) in the range of the K_D value to prevent stoichiometric titration conditions was equilibrated with a dilution series of the antagonists **7b–13**.^[46] After equilibration, the unbound $FimH$ ($FimH_{free}$) binds to the immobilized antagonist **1** (Figure 2a) and can therefore be determined by SPR (Figure 2b) using a calibration curve (Figure 2c). Finally, $[FimH_{free}]$ was plotted versus the antagonist concentration, and the curve was fitted with the in-solution affinity-fit algorithm of the BiaEvalu-

ation software (Figure 2d). The obtained K_D values are summarized in Table 3.

n-Heptyl α -D-mannopyranoside **8** and the biphenyl-substituted mannose antagonists **7b** and **9–13** with different substitutions in the *ortho* position of the aromatic ring adjacent to the anomeric position showed affinities in the low nanomolar range, which are in good agreement with data obtained from isothermal titration calorimetry (ITC) experiments.^[46] To further validate the assay, we additionally tested compound **7b** on a chip functionalized with compound **2** (chip 2), and we obtained a similar K_D value (0.5 vs 0.7 nM). Furthermore, the K_D value of **7b** determined by the in-solution affinity approach is equal to the K_D value of **2** found by a direct binding assay ($K_D = 0.7$ nM; Table 2). Compounds **2** and **7b** share identical structure with the only difference that **2** was immobilized on the chip via a linker (for the direct binding approach) whereas the K_D for **7b** was determined by the in-solution affinity assay. The comparable affinities derived from the two approaches confirm that the attachment of a linker and the immobilization process do not significantly influence the affinity of the antagonist.

In conclusion, for most medical applications, half-lives ($t_{1/2}$) of the drug–target complex of several tens of minutes or even hours are of utmost importance, since long $t_{1/2}$ values translate into higher in vivo efficacies and decrease adverse side effects

Table 3. K_D values of FimH antagonists^[46] determined by an in-solution affinity assay.

Entry	Compd	R	K_D [nM] ^[a]	rK_D ^[b]
1	8	–	5.21 ± 1.6	1
2	7b	Cl	0.71 ± 0.01	0.13
			0.5 ± 0.05 ^[c]	0.10 ^[c]
3	9	F	1.63 ± 0.9	0.32
4	10	OCH ₃	1.08 ± 0.18	0.21
5	11	CH ₃	0.44 ± 0.22	0.09
6	12	Cyclopropyl	2.19 ± 0.1	0.42
7	13	CF ₃	1.1 ± 0.34	0.21

[a] Determined on chip 1 (CM4 chip functionalized with compound 1). Data represent the mean ± SD of $n=3$ independent experiments performed in triplicate. [b] The relative K_D (rK_D) values were calculated by dividing the K_D of the antagonist of interest by the K_D of *n*-heptyl α -D-mannopyranoside (**8**). [c] Determined on chip 2 (CM4 chip functionalized with compound 2, $n=3$).

resulting from off-target toxicity.^[21,22] However, carbohydrate-lectin interactions often exhibit low affinities and fast off-rates—properties that hamper the development of carbohydrate-derived drugs. Therefore, as part of the preclinical development process of FimH antagonists, we examined their kinetic characteristics by surface plasmon resonance (SPR). In this study, the lectin domain of FimH in the high-affinity state was used. The surprisingly small dissociation rates for FimH–antagonist complexes resulting in long $t_{1/2}$ values in the range of several hours (> 3.6 h) are indicators for high in vivo efficacy. This is a further indication that the corresponding ester prodrugs not only have a beneficial pharmacokinetic profile,^[46] but also fulfill the pharmacodynamic requirements for therapeutic application, that is, high affinity and long residence time. However, whether the investigated high-affinity state of FimH investigated in our study^[39] is the only pathophysiologically relevant state remains to be demonstrated. Therefore, studies with FimH lectin in other affinity states are planned.

Experimental Section

Synthesis: For synthesis and spectroscopic details of antagonists **1**, **2** and **3a,b**, see the Supporting Information. The synthesis and characterization of compounds **9–13** are described in Ref. [46].

Chemical abbreviations used in Scheme 1 and elsewhere: (benzotriazol-1-yloxy)tripyrrolidinophosphonium hexafluorophosphate (PyBOP), (1-cyano-2-ethoxy-2-oxoethylideneaminoxy)dimethylamino-morpholino-carbenium hexafluorophosphate (COMU), *N,N*-diisopropylethylamine (DIPEA), *N*-(3-dimethylaminopropyl)-*N*-ethylcarbodiimide hydrochloride (EDC), 2,2'-(ethylenedioxy)bis(ethylamine) (EBE), ethanolamine (EA), 2-[4-(2-hydroxyethyl)piperazin-1-yl]etha-

nesulfonic acid (HEPES), *N*-hydroxysuccinimide (NHS), 2-(*N*-morpholino)ethanesulfonic acid (MES).

FimH-CRD-6His protein expression: The FimH carbohydrate recognition domain (CRD) with a thrombin cleavage site linked to a 6His tag (FimH-CRD-Th-6His) was expressed in *E. coli* strain HM125 and purified by affinity chromatography as described by Rabbani et al.^[39]

Surface plasmon resonance (SPR) analysis: SPR measurements were performed on a Biacore 3000 SPR-based optical biosensor (Biacore, GE Healthcare, Uppsala, Sweden). Sensor chips (CM4), immobilization kits, maintenance supply and HBS-P buffer were purchased from GE Healthcare (Uppsala). The amino-functionalized monovalent compounds **1** and **2** were covalently attached to the activated dextrane matrix on CM4 chips by the standard amine-coupling method (GE Healthcare, Uppsala). The surface was activated by NHS and EDC. To obtain different ligand densities on the chip, compound **1** (1 mM in borate buffer) was mixed with EA (1 M) in different molar ratios prior to the coupling process (1/EA ratios: 1:0, 1:10, and 1:100). Pure compound **2** (1 mM in borate buffer) was coupled to the chip. After coupling, the matrix was capped with EA. For the coupling of the *N*-hydroxy-succinimide-functionalized compounds **3** and **4**, the free carboxyl groups on the chip were activated with NHS and EDC and reacted with 1,2-diaminoethane (0.1 M in borate buffer, pH 8.5) to give free amino groups. The next steps were followed as described above. A reference cell without immobilized ligand was prepared and the system equilibrated with HEPES-buffered saline (HBS)-P buffer (10 mM HEPES, 150 mM NaCl, 0.005% P20, pH 7.4). The activity of the chips was confirmed by FimH binding at a constant concentration of 50 nM in HBS-P buffer. All binding experiments were performed at 25 °C at a flow rate of 20 or 30 $\mu\text{L}\cdot\text{min}^{-1}$ using HBS-P buffer. For kinetic studies, a dilution series of FimH with concentrations ranging from 0–200 nM in HBS-P buffer was used. Contact time was 120 s, and the dissociation time was 1200 s. The surface was regenerated with a single injection of 50 mM NaOH for 120 s. Data processing as well as k_{on} , k_{off} , and K_D determinations were accomplished with the Scrubber software (BioLogic Software, Version 2.0c, Campbell, Australia). Double referencing (subtraction of reference and blank injection) was applied to correct for bulk effects and other systematic artifacts.

In-solution affinity inhibition experiments: FimH (10–15 nM in HBS-P buffer) was inhibited with a series of test compound solutions of increasing concentrations (0–1 μM) overnight at RT to allow the equilibration of the system. The mixtures were run over a sensor surface coated with compound **1**, and the resonance units (RU) after an association time of 110 s were detected. The non-inhibited FimH concentration ($[\text{FimH}_{\text{free}}]$) in the protein–compound mixtures was determined by means of a FimH calibration curve using free FimH concentrations ranging from 0–120 nM. The K_D values of the compounds were calculated by plotting $[\text{FimH}_{\text{free}}]$ versus $[\text{compound}]$, and fitting the curve with the in-solution affinity fit.

Acknowledgements

The authors gratefully acknowledge the financial support for G.N. by Nano-Tera (grant no. NT.ch 611_61).

Keywords: antagonists • carbohydrate–lectin interactions • FimH • kinetics • urinary tract infections • uropathogenic *Escherichia coli*

- [1] A. Ronald, *Am. J. Med.* **2002**, *113*, 145–195.
- [2] M. A. Mulvey, *Cell. Microbiol.* **2002**, *4*, 257–271.
- [3] T. J. Wiles, R. R. Kulesus, M. A. Mulvey, *Exp. Mol. Pathol.* **2008**, *85*, 11–19.
- [4] B. Xie, G. Zhou, S. Y. Chan, E. Shapiro, X. P. Kong, X. R. Wu, T. T. Sun, C. E. Costello, *J. Biol. Chem.* **2006**, *281*, 14644–14653.
- [5] G. Zhou, W. J. Mo, P. Sebbel, G. W. Min, T. A. Neubert, R. Glockshuber, X. R. Wu, T. T. Sun, X. P. Kong, *Cell Sci.* **2001**, *114*, 4095–4103.
- [6] I. Ofek, D. L. Hasy, N. Sharon, *FEMS Immunol. Med. Microbiol.* **2003**, *38*, 181–191.
- [7] N. Sharon, *Biochim. Biophys. Acta Gen. Subj.* **2006**, *1760*, 527–537.
- [8] B. Ernst, J. L. Magnani, *Nat. Rev. Drug Discovery* **2009**, *8*, 661–677.
- [9] J. Bouckaert, J. Berglund, M. Schembri, E. De Genst, L. Cools, M. Wuhrer, C. S. Hung, J. Pinkner, R. Slättegård, A. Zavalov, D. Choudhury, S. Langermann, S. J. Hultgren, L. Wyns, P. Klemm, S. Oscarson, S. D. Knight, H. De Greve, *Mol. Microbiol.* **2005**, *55*, 441–455.
- [10] T. K. Lindhorst, C. Kieburg, U. Krallmann-Wenzel, *Glycoconjugate J.* **1998**, *15*, 605–613.
- [11] O. Sperling, A. Fuchs, T. K. Lindhorst, *Org. Biomol. Chem.* **2006**, *4*, 3913–3922.
- [12] T. Klein, D. Abgottspon, M. Wittwer, S. Rabbani, J. Herold, X. Jiang, S. Kleeb, C. Lüthi, M. Scharenberg, J. Bezençon, E. Gubler, L. Pang, M. Smiesko, B. Cutting, O. Schwardt, B. Ernst, *J. Med. Chem.* **2010**, *53*, 8627–8641.
- [13] D. Abgottspon, G. Roelli, L. Hosch, A. Steinhuber, X. Jiang, O. Schwardt, B. Cutting, M. Smiesko, U. Jenal, B. Ernst, A. Trampuz, *J. Microbiol. Methods* **2010**, *82*, 249–255.
- [14] Z. Han, J. S. Pinkner, B. Ford, R. Obermann, W. Nolan, S. A. Wildman, D. Hobbs, T. Ellenberger, C. K. Cusumano, S. J. Hultgren, J. W. Janetka, *J. Med. Chem.* **2010**, *53*, 4779–4792.
- [15] A. Wellens, C. Garofalo, H. Nguyen, N. Van Gerven, R. Slättegård, J.-P. Hernalsteens, L. Wyns, S. Oscarson, H. De Greve, S. Hultgren, J. Bouckaert, *PLoS One* **2008**, *3*, e2040.
- [16] C. S. Edén, R. Freter, L. Hagberg, R. Hull, S. Hull, H. Leffler, G. Schoolnik, *Nature* **1982**, *298*, 560–562.
- [17] M. Aronson, O. Medalia, L. Schori, D. Mirelman, N. Sharon, I. Ofek, *J. Infect. Dis.* **1979**, *139*, 329–332.
- [18] M. Scharenberg, D. Abgottspon, E. Cicek, X. Jiang, O. Schwardt, S. Rabbani, B. Ernst, *Assay Drug Dev. Technol.* **2011**, *9*, 455–464.
- [19] X. Jiang, D. Abgottspon, S. Kleeb, S. Rabbani, M. Scharenberg, M. Wittwer, M. Haug, O. Schwardt, B. Ernst, *J. Med. Chem.* **2012**, *55*, 4700–4713.
- [20] M. Hartmann, T. K. Lindhorst, *Eur. J. Org. Chem.* **2011**, 3583–3609.
- [21] R. A. Copeland, D. L. Pompliano, T. D. Meek, *Nat. Rev. Drug Discovery* **2006**, *5*, 730–739.
- [22] D. C. Swinney, *Nat. Rev. Drug Discovery* **2004**, *3*, 801–808.
- [23] H. Lu, P. J. Tonge, *Curr. Opin. Chem. Biol.* **2010**, *14*, 467–474.
- [24] C. Napier, H. Sale, M. Mosley, G. Rickett, P. Dorr, R. Mansfield, M. Holbrook, *Biochem. Pharmacol.* **2005**, *71*, 163–172.
- [25] I. Dierynck, M. De Wit, E. Gustin, I. Keuleers, J. Vandersmissen, S. Hallenberger, K. Hertogs, *J. Virol.* **2007**, *81*, 13845–13851.
- [26] W. M. Kati, D. Montgomery, R. Carrick, L. Gubareva, C. Maring, K. McDaniel, K. Steffy, A. Molla, F. Hayden, D. Kempf, W. Kohlbrenner, *Antimicrob. Agents Chemother.* **2002**, *46*, 1014–1021.
- [27] O. Schwardt, H. Gähje, A. Vedani, S. Mesch, G.-P. Gao, M. Spreafico, J. von Orelli, S. Kelm, B. Ernst, *J. Med. Chem.* **2009**, *52*, 989–1004.
- [28] S. Mesch, K. Lemme, H. Koliwer-Brandl, D. S. Strasser, O. Schwardt, S. Kelm, B. Ernst, *Carbohydr. Res.* **2010**, *345*, 1348–1359.
- [29] M. K. Wild, M. C. Huang, U. Schulze-Horsel, P. A. van der Merwe, D. Vestweber, *J. Biol. Chem.* **2001**, *276*, 31602–31612.
- [30] M. W. Nicholson, A. N. Barclay, M. S. Singer, S. D. Rosen, P. A. van der Merwe, *J. Biol. Chem.* **1998**, *273*, 763–770.
- [31] P. Mehta, R. D. Cummings, R. P. McEver, *J. Biol. Chem.* **1998**, *273*, 32506–32513.
- [32] G. J. Muñoz, J. I. Santos, A. Ardá, S. André, H.-J. Gabius, J. V. Sinisterra, J. Jiménez-Barbero, M. J. Hernáiz, *Org. Biomol. Chem.* **2010**, *8*, 2986–2992.
- [33] T. Terada, M. Nishikawa, F. Yamashita, M. Hashida, *Int. J. Pharm.* **2006**, *316*, 117–123.
- [34] B. N. Murthy, S. Sinha, A. Suroliá, S. S. Indi, N. Jayaraman, *Glycoconjugate J.* **2008**, *25*, 313–321.
- [35] A. R. Patil, C. J. Thomas, A. Suroliá, *J. Biol. Chem.* **2000**, *275*, 24348–24356.
- [36] L. Herfurth, B. Ernst, B. Wagner, D. Ricklin, D. S. Strasser, J. L. Magnani, A. J. Benie, T. Peters, *J. Med. Chem.* **2005**, *48*, 6879–6886.
- [37] E. Duverger, N. Frison, A. C. Roche, M. Monsigny, *Biochimie* **2003**, *85*, 167–179.
- [38] I. Le Trong, P. Aprikian, B. A. Kidd, M. Forero-Shelton, V. Tchesnokova, P. Rajagopal, V. Rodríguez, G. Interlandi, R. Klevit, V. Vogel, R. E. Stenkamp, E. V. Sokurenko, W. E. Thomas, *Cell* **2010**, *141*, 645–655.
- [39] S. Rabbani, X. Jiang, O. Schwardt, B. Ernst, *Anal. Biochem.* **2010**, *407*, 188–195.
- [40] a) W. S. Somers, J. Tang, G. D. Shaw, R. T. Camphausen, *Cell* **2000**, *103*, 467–479; b) B. J. Graves, R. L. Crowther, C. Chandran, J. M. Rumberger, S. Li, K. S. Huang, D. H. Presky, P. C. Famillett, B. A. Wolitzky, D. K. Burns, *Nature* **1994**, *367*, 532–538.
- [41] P. M. Collins, C. T. Öberg, H. Leffler, U. J. Nilsson, H. Blanchard, *Chem. Biol. Drug Des.* **2012**, *79*, 339–346.
- [42] K. S. Kenneth, K. Drickamer, W. I. Weis, *J. Biol. Chem.* **1996**, *271*, 663–674.
- [43] Y. Guo, H. Feinberg, E. Conroy, D. Mitchell, R. Alvarez, O. Blixt, M. Taylor, W. I. Weis, K. Drickamer, *Nat. Struct. Mol. Biol.* **2004**, *11*, 591–598.
- [44] C. Hung, J. Bouckaert, D. L. Hung, J. Pinkner, C. Widberg, A. DeFusco, G. Auguste, R. Strouse, S. Langermann, S. J. Hultgren, *Abstr. Gen. Meeting Am. Soc. Microbiol.* **2002**, *102*, 41.
- [45] M. Durka, K. Buffet, J. Iehl, M. Holler, J. F. Nierengarten, J. Taganna, J. Bouckaert, S. P. Vincent, *Chem. Commun.* **2011**, *47*, 1321–1323.
- [46] L. Pang, S. Kleeb, K. Lemme, S. Rabbani, M. Scharenberg, A. Zalewski, F. Schädler, O. Schwardt, B. Ernst, *ChemMedChem* **2012**, *7*, 1404–1422.

Received: August 29, 2013

Published online on December 2, 2013



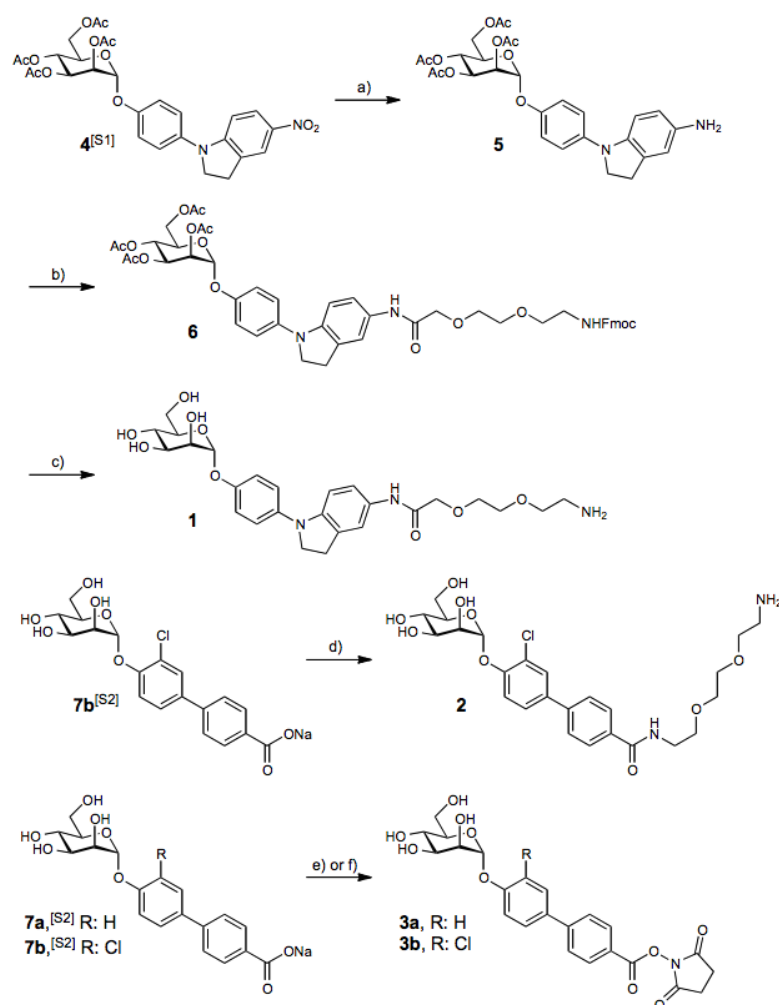
Supporting Information

© Copyright Wiley-VCH Verlag GmbH & Co. KGaA, 69451 Weinheim, 2013

Kinetic Properties of Carbohydrate–Lectin Interactions: FimH Antagonists

Meike Scharenberg, Xiaohua Jiang, Lijuan Pang, Giulio Navarra, Said Rabbani,
Florian Binder, Oliver Schwardt, and Beat Ernst*^[a]

cmdc_201300349_sm_miscellaneous_information.pdf

Synthesis and spectroscopic details of antagonists **1**, **2** and **3a,b**

Scheme S1. Synthesis of the amino- or *N*-hydroxyl-succinimide functionalized FimH antagonists **1**, **2**, **3a** and **3b**. a) H_2 (1 atm), PtO_2 , morpholine, EtOAc/MeOH (1:1) (97%); b) 8-(Fmoc-amino)-3,6-dioxa-octanoic acid, PyBOP, DIPEA, DMF, rt; c) NaOMe, MeOH, rt (47% over two steps); d) EBE, COMU, DIPEA, DMF, 0 °C to rt (20%); e) EDC, NHS, H_2O , rt (**3a**: 98%); f) EDC, NHS, MES buffer (pH 5.6), rt (**3b**: 99%).

General methods. NMR spectra were recorded on a Bruker Avance DMX-500 (500 MHz) spectrometer. Assignment of ^1H and ^{13}C NMR spectra was achieved using 2D methods (COSY, HSQC, TOCSY). Chemical shifts are expressed in ppm using residual CHCl_3 , CHD_2OD and HDO as references. Optical rotations were measured using Perkin-Elmer Polarimeter 341. Electron spray ionization mass spectra (ESI-MS) were obtained on a Waters micromass ZQ. HRMS analysis was carried out using a Bruker Daltonics micrOTOF spectrometer equipped with a TOF hexapole detector. Reactions were monitored by TLC using glass plates coated with silica gel 60 F_{254} (Merck) and visualized by using UV light and/or by heating to $150\text{ }^\circ\text{C}$ for 5 min with a molybdate solution (a 0.02 M solution of ammonium cerium sulfate dihydrate and ammonium molybdate tetrahydrate in aqueous 10% H_2SO_4). Column chromatography was performed on a CombiFlash Companion (Teledyne-ISCO, Inc.) using RediSep[®] normal phase disposable flash columns (silica gel). Reversed phase chromatography was performed on LiChroprep[®]RP-18 (Merck, 40-63 μm). Commercially available reagents were purchased from Fluka, Aldrich or Acros. Methanol (MeOH) was dried by refluxing with sodium methoxide and distilled immediately before use. Dichloromethane (DCM) and ethyl acetate (EtOAc) were dried by filtration over Al_2O_3 (Fluka, type 5016 A basic).

4-(5-Aminoindolin-1-yl)phenyl 2,3,4,6-tetra-*O*-acetyl- α -D-mannopyranoside (5). To a solution of **4**^[S1] (47.8 mg, 0.08 mmol) in MeOH/EtOAc (1:1, 5 mL) PtO_2 (5 mg) and morpholine (10 μL) were added. The reaction mixture was stirred at rt under hydrogen (1 atm) for 1 h, then filtrated through a pad of celite and the celite was washed thoroughly with EtOAc. The filtrate was concentrated in vacuo to give **5** (44 mg, 97%) as off-white foam, which was used in the next step without further purification.

2-(2-(2-Fmoc-aminoethoxy)ethoxy)-*N*-(4-(2,3,4,6-tetra-*O*-acetyl- α -D-mannopyranosyloxy)phenyl)-indolin-5-yl)-acetamide (6). To a mixture of **5** (45 mg, 0.08 mmol), PyBoP (50 mg, 0.096 mmol) and 8-(Fmoc-amino)-3,6-dioxa-octanoic acid (39 mg, 0.1 mmol) in dry DMF (1.5 mL) was added DIPEA (32 μL , 0.19 mmol) at rt. The reaction mixture was stirred at rt overnight, then diluted with EtOAc, and washed with water and brine. The organic layer was dried over Na_2SO_4 and the solvent was removed under reduced pressure. The residue was purified by silica gel chromatography (DCM/MeOH 24:1) to provide crude **6** as black oil, which contained some DMF. ^1H NMR (500 MHz, CDCl_3): δ = 2.05, 2.06, 2.08, 2.21 (4s, 12H, 4 OAc), 3.19 (t, J = 8.4 Hz, 2H, CH_2), 3.42 (dd, J = 5.2, 10.4 Hz, 2H, CH_2), 3.62 (t, J = 5.0 Hz, 2H, CH_2), 3.70 (m, 2H, CH_2), 3.80 (m, 2H, CH_2), 4.08-4.16 (m, 4H, H-5, H-6a, CH_2), 4.33 (d, J = 7.1 Hz, 2H, CH_2), 4.29 (dd, J = 5.2, 12.2 Hz, 1H, H-6b), 5.15 (t, J = 5.3 Hz, 1H, NH), 5.37 (t, J = 10.0 Hz, 1H, H-4), 5.44 (m, 2H, H-1, H-2), 5.56 (dd, J = 3.0, 10.0 Hz, 1H, H-3), 6.88 (d, J = 8.5 Hz, 1H), 7.01-7.07 (m, 4H, Ar-H), 7.27 (m, 1H, Ar-H), 7.36 (m, 2H, Ar-H), 7.46 (s, 1H, Ar-H), 7.52 (d, J = 7.0 Hz, 2H, Ar-H), 7.74 (d, J = 8.0 Hz, 2H, Ar-H), 8.47 (s, 1H, Ar-H); ^{13}C NMR (125 MHz, CDCl_3): δ 20.52, 20.71, 20.89 (4C, 4 OAc), 28.12, 40.74, 47.12, 52.70 (4 CH_2), 62.14 (C-6), 65.96 (C-4), 66.72 (CH_2), 68.90 (C-3), 68.99 (C-5), 69.43 (C-2), 70.02, 70.23, 70.61, 71.06 (CH_2 , CH), 96.35 (C-1), 107.29, 117.44, 118.47, 119.15, 119.43, 119.93, 124.85, 125.01, 126.99, 127.65, 128.44, 131.83, 139.72, 141.23, 144.82, 150.04, 156.40 (Ar-C), 167.63, 169.76, 169.97, 170.02, 170.57, 174.43 (6 CO); ESI-MS: m/z : Calcd for $\text{C}_{28}\text{H}_{31}\text{N}_2\text{O}_{12}$ [$\text{M}+\text{Na}$]⁺: 946.34, found 946.30.

2-(2-(2-Aminoethoxy)ethoxy)-*N*-(4-(α -D-mannopyranosyloxy)phenyl)-indolin-5-yl)-acetamide (1). Crude **6** was dissolved in dry MeOH and treated at rt with 0.5 M NaOMe/MeOH (0.2 mL) until completion of the reaction. The reaction mixture was neutralized with Amberlyst-15 (H^+) ion-exchange resin and filtered. The filtrate was concentrated and the residue was purified by silica gel chromatography

(DCM/MeOH/H₂O 50:50:6) to afford amine **1** (20 mg, 47% over two steps from **5**) as an off-white solid. $[\alpha]_D^{20} +70.7$ (*c* 0.095, MeOH); ¹H NMR (500 MHz, CD₃OD): δ = 2.84 (t, *J* = 5.5 Hz, 2H, CH₂), 3.10 (t, *J* = 8.0 Hz, 2H, CH₂), 3.59 (t, *J* = 5.5 Hz, 2H, CH₂), 3.67 (m, 3H, H-5, CH₂), 3.73 (m, 4H, H-4, H-6a, CH₂), 3.78 (m, 3H, H-6b, CH₂), 3.89 (m, 3H, H-3, CH₂), 4.01 (dd, *J* = 2.0, 3.5 Hz, 1H, H-2), 5.41 (d, *J* = 2.0 Hz, 1H, H-1), 6.88 (d, *J* = 8.5 Hz, 1H, Ar-H), 7.12-7.18 (m, 5H, Ar-h), 7.39 (d, *J* = 1.5 Hz, 1H, Ar-H); ¹³C NMR (125 MHz, CD₃OD): δ = 29.09, 41.87, 54.10 (3 CH₂), 62.73 (C-6), 68.39 (C-4), 71.28 (C-2), 71.53, 72.10 (2 CH₂), 72.42 (C-3), 73.03 (CH₂), 75.33 (C-5), 100.84 (C-1), 108.11, 118.90, 119.96, 120.88, 121.28, 129.79, 132.90, 140.76, 146.81, 152.86 (Ar-C), 170.56 (CO); ESI-MS: *m/z*: Calcd for C₂₁H₂₀ClNO₈ [M+H]⁺: 534.24, found 534.20.

N-(2-(2-(2-Aminoethoxy)ethoxy)ethyl)-3'-chloro-4'-(α -D-mannopyranosyloxy)-biphenyl-4-carboxamide (2). COMU was added at 0 °C to a mixture of **7b**^[S2] (20 mg, 0.05 mmol) and DIPEA (9 μ L, 0.05 mmol) in dry DMF (0.5 mL). The reaction mixture was activated for 5 min, then EBE (14 μ L, 0.1 mmol) and DIPEA (9 μ L, 0.05 mmol) were added. The reaction mixture was stirred at 0 °C for 1 h and at rt overnight. Water (0.5 mL) was added to the mixture and stirring continued for 5 min. The reaction was concentrated under reduced pressure, then the yellow residue was loaded onto a RP-18 chromatography column and eluted with MeOH (0 to 100%) in 0.01 N aqueous ammonia to give **2** (5.0 mg, 20%). ¹H NMR (500 MHz, CD₃OD): δ = 3.42-3.68 (m, 16H, H-4, H-5, H-6a, H-6b, 6 CH₂), 3.90 (dd, *J* = 3.4, 9.5 Hz, 1H, H-3), 4.02 (dd, *J* = 1.8, 3.4 Hz, 1H, H-2), 5.50 (d, *J* = 1.6 Hz, 1H, H-1), 7.37 (d, *J* = 8.7 Hz, 1H, Ar-H), 7.49 (dd, *J* = 2.3, 8.6 Hz, 1H, Ar-H), 7.58-7.63 (m, 3H, Ar-H), 7.76-7.85 (m, 2H, Ar-H); ESI-MS: *m/z*: Calcd for C₂₅H₃₄ClN₂O₉ [M+H]⁺: 541.19, found: 541.24.

2,5-Dioxopyrrolidin-1-yl 4'-(α -D-mannopyranosyloxy)-biphenyl-4-carboxylate (3a). Compound **7a**^[S2] (3.0 mg, 7.5 μ mol) was added to a stirred solution of NHS (4.3 mg, 37 μ mol) and EDC (538 mg, 2.8 mmol) in water (37.5 mL) resulting in the formation of a white precipitate. After stirring for 30 min, the reaction mixture was diluted with satd aq. NH₄Cl, filtered (syringe filter) and the filter was washed with DCM (2 x 3 mL). The product was recovered from the filter by washing with MeOH several times. Evaporation of the volatiles under reduced pressure gave the activated acid **3a** (3.5 mg, 98%) as a white solid. ¹H NMR (500 MHz, CD₃OD): δ = 2.92 (s, 4H, 2 CH₂), 3.61 (ddd, *J* = 2.7, 5.0, 9.8 Hz, 1H, H-5), 3.71-3.80 (m, 3H, H-4, H-6a, H-6b), 3.93 (dd, *J* = 3.4, 9.5 Hz, 1H, H-3), 4.04 (dd, *J* = 1.8, 3.4 Hz, 1H, H-2), 5.57 (d, *J* = 1.6 Hz, 1H, H-1), 7.26 (d, *J* = 8.8 Hz, 2H, Ar-H), 7.70 (d, *J* = 8.8 Hz, 2H, Ar-H), 7.83 (d, *J* = 8.5 Hz, 2H, Ar-H), 8.18 (d, *J* = 8.5 Hz, 2H, Ar-H); ¹³C NMR (125 MHz, CD₃OD): δ = 26.55 (2 CH₂), 62.16 (C-6), 67.69 (C-4), 71.44 (C-2), 72.01 (C-3), 75.00 (C-5), 99.56 (C-1), 117.64, 127.64, 128.95, 131.17 (Ar-C); ESI-MS: *m/z*: Calcd for C₂₃H₂₃NNaO₁₀ [M+Na]⁺: 496.12, found: 496.16 [M+Na]⁺.

2,5-Dioxopyrrolidin-1-yl 3'-chloro-4'-(α -D-mannopyranosyloxy)-biphenyl-4-carboxylate (3b). NHS (160 mg, 1.38 mmol) and EDC (532 mg, 2.77 mmol) were dissolved in 0.1 M MES buffer (pH 5.6, 10 mL). After stirring for 10 min **7b**^[S2] (300 mg, 0.693 mmol) was added. The solution became turbid, then clear, and then a precipitate started to form. After 20 min the solid was collected by filtration on a frittered-glass G4 filter, and washed with satd aq. NH₄Cl and DCM. The solid was recovered with MeOH, the solvent was evaporated, and the residue dried under high vacuum to yield **3b** (350 mg, 99%) as a white solid. ¹H NMR (500 MHz, CD₃OD): δ = 2.94 (s, 4H, 2 CH₂), 3.68-3.82 (m, 4H, H-4, H-5, H-6a, H-6b), 4.03 (dd, *J* = 3.3, 9.3 Hz, 1H, H-3), 4.15 (dd, *J* = 1.3, 3.3 Hz, 1H, H-2), 5.66 (d, *J* = 1.6 Hz, 1H, H-1), 7.53 (d, *J* = 10.0 Hz, 1H, Ar-H), 7.68 (dd, *J* = 10.5 Hz, 1H, Ar-H), 7.83-7.87 (m, 3H, Ar-H), 7.76 (m, 1H, Ar-H), 8.21 (m, 1H, Ar-H); ¹³C NMR (125 MHz, CD₃OD): δ = 26.63 (2 CH₂), 62.64 (C-6), 68.21 (C-4),

71.83 (C-2), 72.41 (C-3), 76.06 (C-5), 100.70 (C-1), 118.61, 128.01, 128.30, 129.96, 132.03 (Ar-C), 171.88 (CO); ESI-MS: m/z : Calcd for $C_{23}H_{22}ClNNaO_{10}$ $[M+Na^+]$: 530.09, found: 530.00 $[M+Na^+]$.

References

- [S1] X. Jiang, D. Abgottspon, S. Kleeb, S. Rabbani, M. Scharenberg, M. Wittwer, M. Haug, O. Schwardt, B. Ernst, *J. Med. Chem.* **2012**, *55*, 4700-4713.
- [S2] T. Klein, D. Abgottspon, M. Wittwer, S. Rabbani, J. Herold, X. Jiang, S. Kleeb, C. Lüthi, M. Scharenberg, J. Bezençon, E. Gubler, L. Pang, M. Smiesko, B. Cutting, O. Schwardt, B. Ernst, *J. Med. Chem.* **2010**, *53*, 8627-8641.

2.7 Combinatorial Library Screening of FimH Antagonists: an Application of Protein-Directed Dynamic Strategy

This chapter describes an extensive exploration on structural diversity of FimH antagonists. The structural modifications were carried out for both the sugar moiety and the aglycone. Acylhydrazone formation reaction was applied for the establishment of combinatorial libraries of FimH antagonists. Furthermore, the dynamic combinatorial libraries were *in situ* generated and screened against both the native full-length FimH and its lectin domain.

As a result, thiophene derivatives **42/43c** with an acylhydrazone linkage were demonstrated to be highly effective candidates for further *in vitro* and *in vivo* studies.

Contributions to this project:

Lijuan Pang designed the structural modifications and synthesized all the reported compounds except compound **13a**. She also designed and performed the dynamic combinatorial experiments for *in situ* generation and screening of FimH antagonists. Furthermore, she tested the binding affinity of all the target compounds with a competitive fluorescence polarization assay.

Keywords: Urinary tract infections, uropathogenic *Escherichia coli*, native full-length FimH, FimH antagonists, lead discovery, lead optimization, dynamic combinatorial chemistry, dynamic combinatorial library, fluorescence polarization assay, isothermal titration calorimetry.

2.7.1 Introduction

Urinary tract infections (UTIs) are among the most prevalent infectious diseases affecting millions of people each year.^{1, 2} The leading cause of UTI is uropathogenic *Escherichia coli* (UPEC), which make up 70-95% of diagnosed cases.³ UTIs are treated with antibiotics,^{4, 5} however, recurrent infections of UPEC followed by repeated antibiotic exposure often lead to the emergence of antimicrobial resistance, and consequently to treatment failure.^{6, 7}

UPEC express filamentous surface organelles, called type 1 pili (fimbriae), which act as highly efficient adhesion tools for UPEC inhabiting in host cells.⁸ At the tips of these pili, a bacterial lectin, FimH, is located. FimH binds to oligomannoside containing glycoproteins, mainly uroplakin-Ia (UPIa), and thus mediates UPEC adhesion to the urinary bladder mucosa.⁹ This adhesion prevents the clearance of *E. coli* by the flow of urine and facilitates UPEC invasion.^{10, 11} Blocking FimH with carbohydrates or glycomimetics inhibits UPEC adhesion and therefore prevents bacterial infection.¹² The anti-adhesive agent doesn't act by killing or preventing growth of bacteria, thus unlikely causing bacterial resistance. FimH antagonist therefore offers a great therapeutic potential in prevention and/or treatment of UTI.

The development of FimH antagonists as anti-adhesive agents started more than two decades ago when Sharon and co-workers reported their pioneering work.^{13, 14} They explored various mono- and oligomannosides as potential antagonists for type 1 pili-mediated bacterial adhesion and observed interactions in the micro- to millimolar range. In 1999, the first crystal structure of FimH was solved,¹⁵ since then numerous crystallographic studies have been published, greatly facilitating the discovery of high-affinity FimH antagonists.¹⁶⁻¹⁸ So far, the reported FimH antagonists lead to two major classes of structures (Figure 2.7.1), including the long-chain alkyl mannosides (**1**)¹⁷ and the mannosides with extended aromatic aglycones (**2-5**).¹⁹⁻²²

Based on the reported crystal structures, the high affinity can be rationalized^{17, 20}: First, the hydroxyl groups on mannose interact extensively with the binding pocket by forming

direct and indirect hydrogen bonds; second, the aliphatic or aromatic aglycones can be hosted in the “tyrosine gate” (Tyr48, Tyr137, and Ile 52) through hydrophobic interactions. Co-crystallization of *n*-butyl α -D-mannoside¹⁷ (Figure 2.7.2A) and biphenyl mannoside **3**²⁰ (Figure 2.7.2B) suggested two docking modes²³: One is the “in-docking mode”, that is the aliphatic aglycone inserts into the tyrosine gate and interact with both tyrosines (Tyr48 and Tyr137); the other is the “out-docking mode”, that is the biphenyl aglycone interacts only with Tyr48, and the π - π stacking of the outer aromatic ring of the biphenyl aglycone with Tyr48 is effected by induced fit. Whereas the optimized structures with extended aromatic aglycones showed nanomolar affinities toward the lectin domain of FimH, the reported *in vitro* screening assays were complicated by the high- and low-affinity states of FimH.²⁴ More recently, a crystal structure of native full-length FimH, reported by Le Trong and co-workers, elucidated that the pilin domain stabilizes the lectin domain in the low-affinity state, whereas the isolated lectin domain adopts the high-affinity state.²⁵ These findings explained a loss of affinity of the developed FimH antagonists toward full-length FimH, when compared to the lectin domain alone.

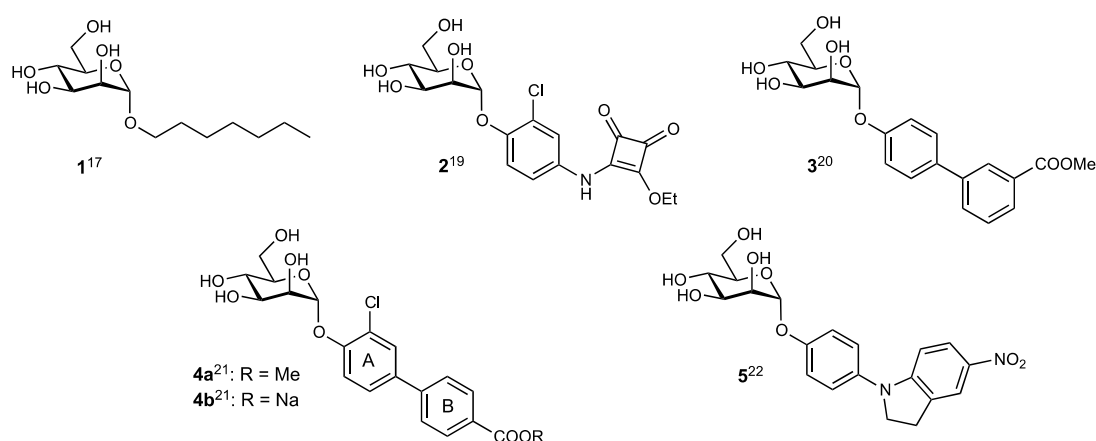


Figure 2.7.1. FimH antagonists: *n*-heptyl α -D-mannoside (**1**)¹⁷ used as reference compound; the squaric acid derivative **2**¹⁹, biphenyl derivatives **3-4**^{20, 21}, and indolinyphenyl mannoside **5**²² exhibit nanomolar affinities.

To further explore the structural scope and to improve binding affinities of FimH antagonists, we synthesized a series of modified α -D-mannosides with aliphatic or aromatic aglycones. Moreover, we investigated *in situ* generation and screening of

dynamic combinatorial libraries of FimH antagonists to boost the *in vitro* screening and lead optimization process.

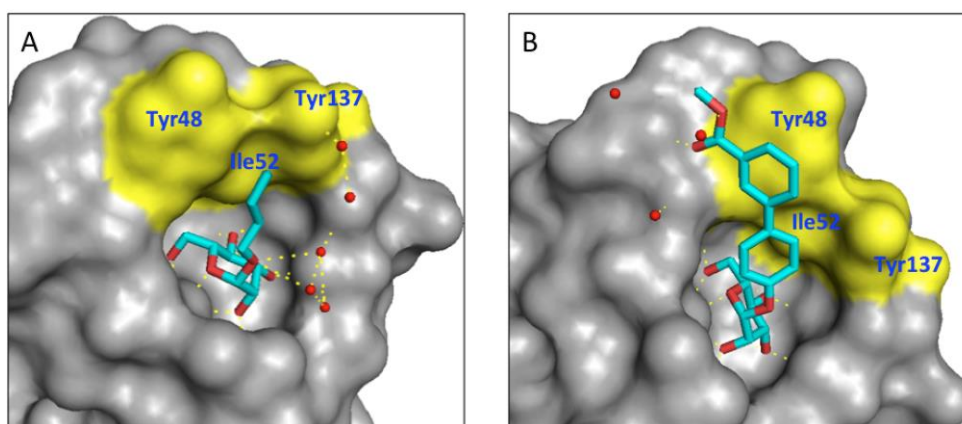


Figure 2.7.2. Crystal structure of A) *n*-butyl α -D-mannoside (PDB ID: 1UWF)¹⁷ and B) biphenyl **3** (PDB ID: 3MCY)²⁰ bound to the FimH CRD. Pictures were generated with PyMOL²⁶; the red ball represents water molecule; yellow dashed line represents hydrogen bonds in the ligand site.

2.7.2 *In Silico* Docking and Structural Design

In most of the reported FimH antagonists, the sugar ring is a conservative structure – mannose. According to the crystal structures, all of the hydroxyls on mannose are involved in the hydrogen-bonding network. Hence modifications on mannose ring could break the ligand-protein interactions and decrease the binding affinity. However, from a thermodynamic point of view the hydroxyl group increases desolvation penalty and unfavorable binding enthalpy as well. Compared to hydroxyl, halogen atoms are less polar, exhibiting low desolvation penalty.²⁷ *In silico* docking studies with 2-halogen substituents on mannose showed that 2-F could form possible polar C-F bond-protein interaction in the binding pocket (Figure 2.7.3A).²⁸ Moreover, 2-Cl and 2-Br could displace the water molecule and interact with the carbonyl of Phe1 by forming a halogen bond (Figure 2.7.3B, 2-Cl).

Further *in silico* docking studies with various aglycone structures suggested either an “in-docking mode” or an “out-docking mode” with the aliphatic or aromatic ring systems. Whereas the aromatic aglcones are more rigid than the aliphatic aglycones therefore could decrease the entropic penalty upon binding, with the aliphatic rings we could further explore the binding pocket and the two binding modes. Different substitution

patterns were introduced through a hydrazone linkage in order to detect the optimal orientations of the aglycones (Figure 2.7.3C, *para*-substitution; Figure 2.7.3D, *meta*-substitution).

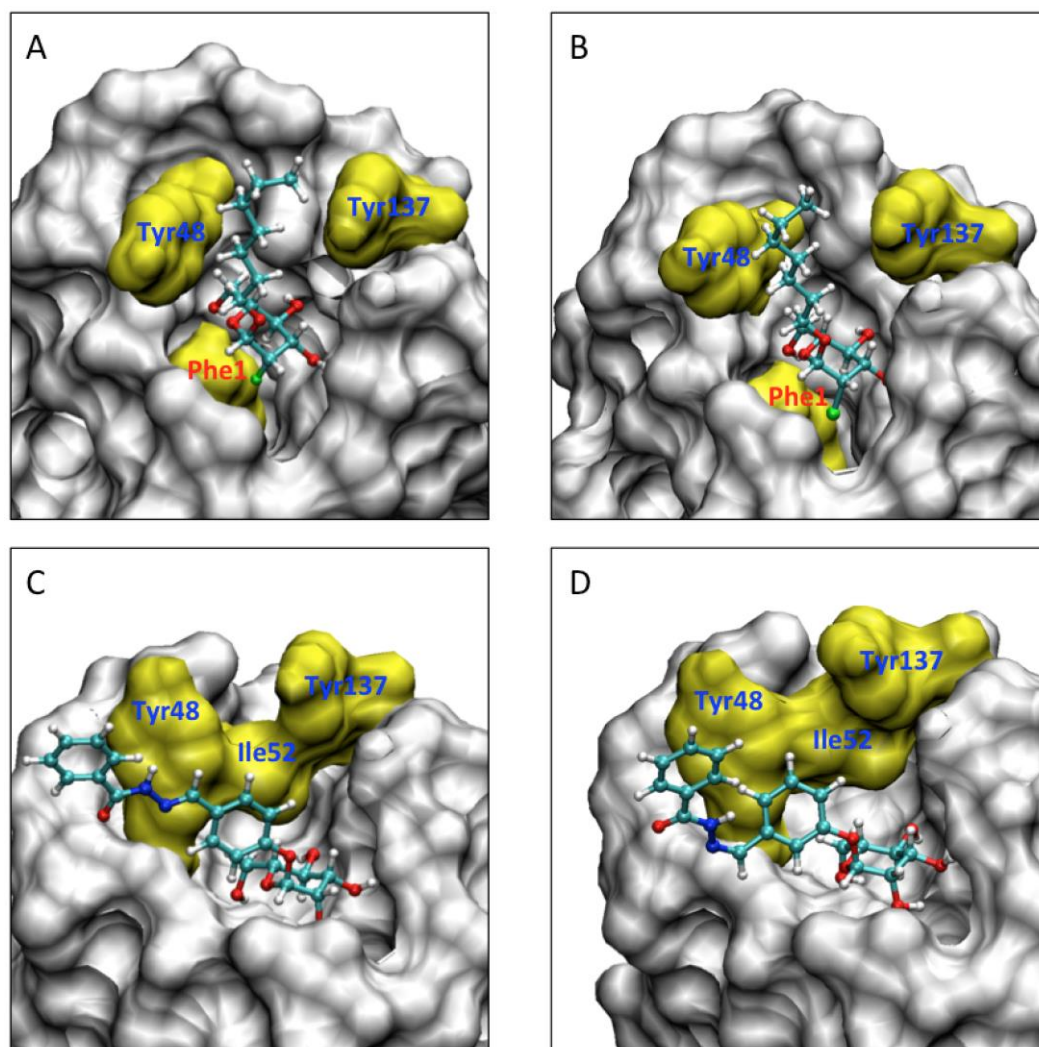


Figure 2.7.3. *In silico* docking studies obtained with flexible docking (VirtualDesignLab²⁸) to the same FimH CRD structure; top-scored binding mode of A) heptyl 2-fluoro- α -D-mannopyranoside (**13a**), B) heptyl 2-chloro- α -D-mannopyranoside (**13b**), C) representative of the *para*-substituted acylhydrazone aglycone (**32a**), D) representative of the *meta*-substituted acylhydrazone aglycone (**36**).

Starting from *n*-heptyl α -D-mannoside (**1**), we explored the modifications on both sugar ring and the aglycone moiety (Figure 2.7.4):

- 1) To investigate the modifications on mannose ring, we replaced the 2-hydroxyl with halogen substituents – F, Cl and Br – to enable either a polar interaction or halogen bonding.
- 2) To expand the structural diversity of the aglycone and further study the binding modes, we introduced a series of aglycones with either aliphatic chain, or aliphatic /aromatic ring system.
- 3) To facilitate the *in vitro* screening and lead optimization process, acylhydrazone linkages were applied, evaluated and optimized with *in situ* generation and screening of DCLs.^{29, 30}

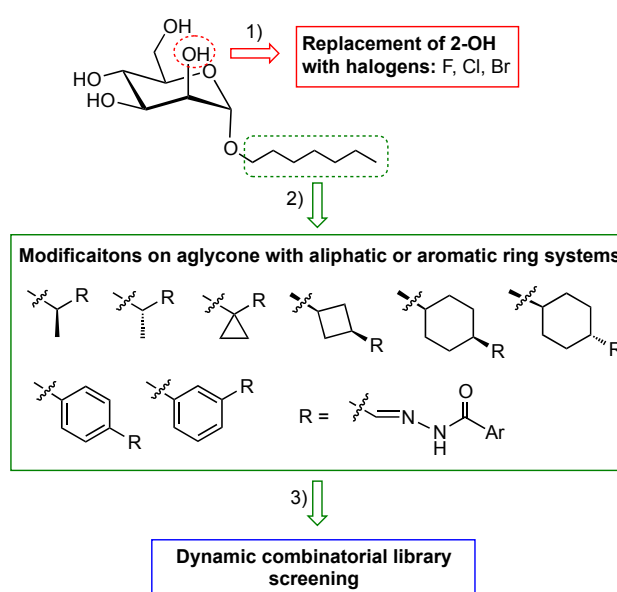


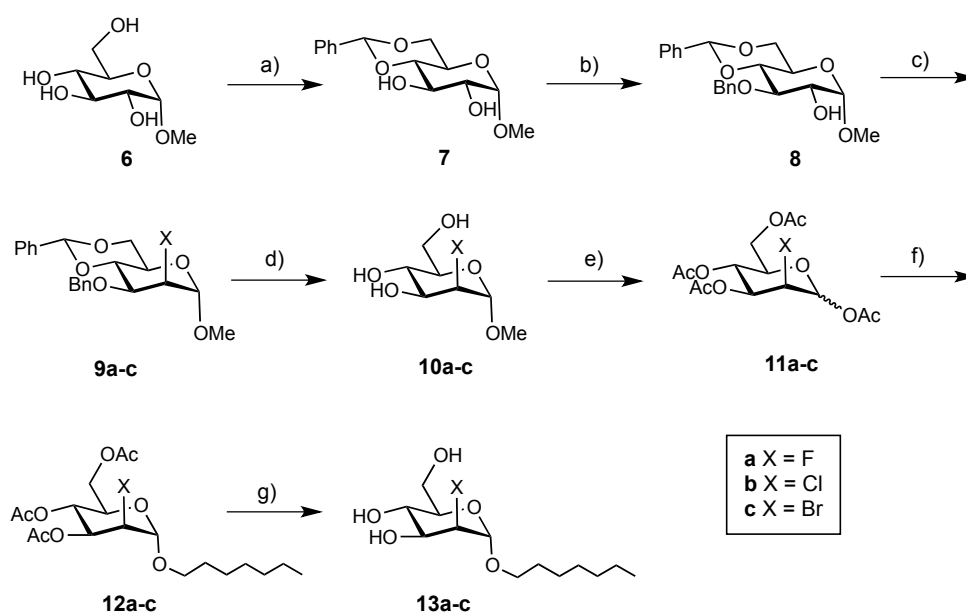
Figure 2.7.4. Modifications to the sugar moiety and the aglycone of FimH antagonists by 1) replacement of 2-OH on mannose with halogen atoms, 2) modifications on aglycone with both aliphatic and aromatic ring systems, 3) DCL screening of acylhydrazones.

2.7.3 Chemical Synthesis

2.7.3.1 Replacement of 2-OH with halogens (Scheme 2.7.1)

The benzylidene protecting derivative **7** was prepared from α -D-glucose derivative **6** in the presence of camphorsulfonic acid and benzaldehyde dimethyl acetal in acetonitrile.³¹ In a regioselective benzylation of **7**, mannoside **8** with free 2-OH was obtained.³² Triflation of the 2-OH of **8** followed by nucleophilic substitutions with ammonium or lithium halides gave the 2-halogen substituted compounds **9a-c**.³³ Compared to the

substitution with fluoride, the substitution with chloride and bromide proceeded more slowly and the reaction was not complete even after two days. Due to the same polarity of the triflate intermediate and the chloride/bromide products, crude **9b-c** were used directly in the next step. Removal of benzylidene and benzyl protection yielded mannosides **10a-c**, which were acetylated under acetic anhydride/sulfuric acid condition to give acetates **11a-c**. Selective deacetylation of the anomeric hydroxyls, followed by trichloroacetimidation, and then mannosylation afforded the heptyl mannoside derivatives **12a-c**. Final deacetylation using Zemplén conditions gave the test compounds **13a-c**.

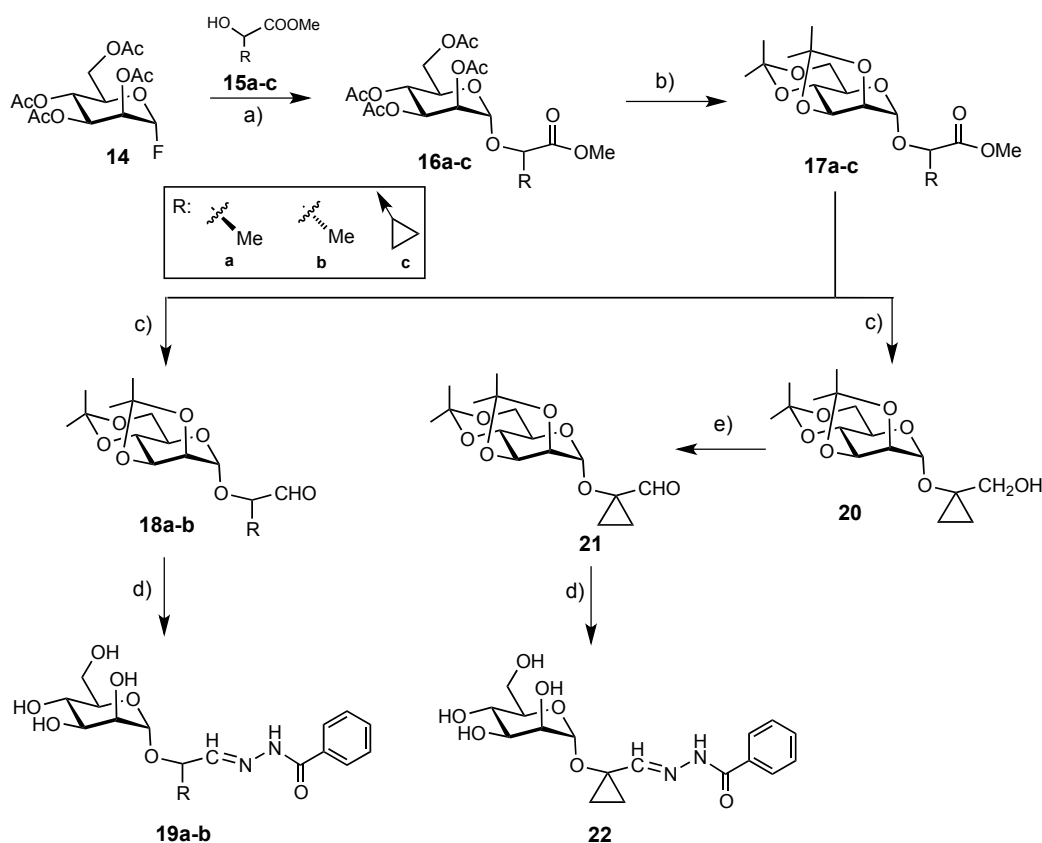


Scheme 2.7.1. Reagents and conditions: a) PhCH(OMe)₂, camphorsulfonic acid, CH₃CN, 50°C, overnight (81%); b) i. nBu₂SnO, toluene, reflux, 3h; ii. BnBr, CsF, DMF, rt, overnight (50%); c) i. Tf₂O, pyridine, DCM, -20°C, 2h; ii. TBAF, THF, 50°C, overnight for **9a** (50%); LiCl, NMP, rt, 2 days for **9b**; TBAB, DMF, 60°C, 2 days for **9c**; d) i. 80% AcOH/H₂O, 60°C; ii. 10% Pd/C, H₂ (g), MeOH/EtOAc/DCM (3:1:1), rt, 1h, **10a-c** (90-94%); e) conc. H₂SO₄, Ac₂O, rt, 3h, **11a-c** (98% to quant.); f) i. NH₄OAc, DMF, rt, overnight; ii. NaH, trichloroacetonitrile, DCM, rt, 2h; iii. *n*-heptanol, TMSOTf, DCM, 0°C to rt, 6h, **12a-c** (70-80%); g) NaOMe, MeOH, rt, 4h, **13a-c** (67-70%).

2.7.3.2 Modifications with aliphatic aglycones (Scheme 2.7.2-3)

Mannosylation of alcohols **15a-c**, with mannosyl fluoride **23** as donor and BF₃·Et₂O as promoter, yielded α-mannosides **16a-c** stereo specifically. Deacetylation of **16a-c** followed by selective protection with 2-methoxypropene and catalytic amount of *p*-

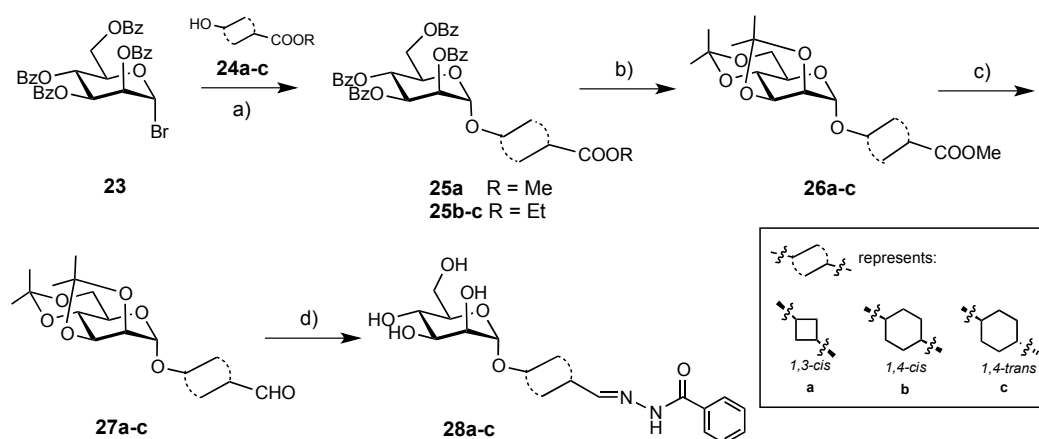
toluenesulfonic acid formed 2,3:4,6-di-*O*-isopropylidene mannosides **17a-c**. Reduction of the methyl ester moiety of **17a-b** in the presence of diisobutylaluminium hydride afforded the aldehydes **18a-b**, whereas the ester **17c** was reduced to alcohol **20** due to high reactivity. Under Swern Oxidation condition alcohol **20** was converted to aldehyde **21** in good yield. Deprotection of isopropylidene followed by hydrazone formation under acidic conditions yielded the test compounds **19a-b** and **22**.



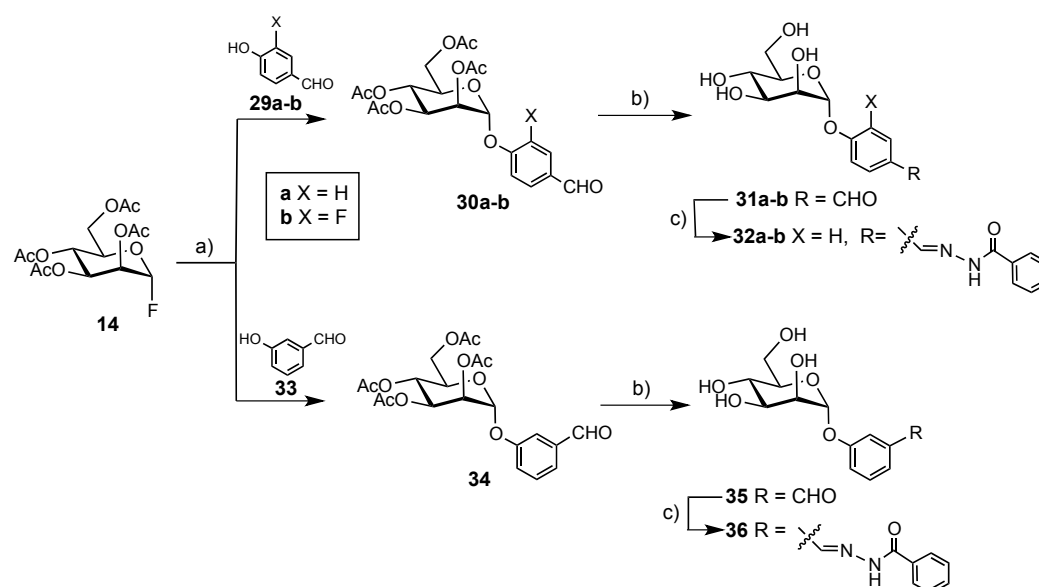
Scheme 2.7.2. *Reagents and conditions:* a) $\text{BF}_3 \cdot \text{Et}_2\text{O}$, hydroxycarboxylate **15a-c**, DCM, 0°C to rt, overnight (83% for **16a**, 78% for **16b**, 63% for **16c**); b) i. NaOMe, MeOH, rt, 4h; ii. 2,2-dimethyl propanone, TsOH, DMF, rt, overnight (62% for **17a**, 81% for **17b**, 78% for **17c**); c) DIBAL-H, DCM, -78°C (70% for **18a**, 71% for **18b**, 85% for **20**); d) i. 80% AcOH/ H_2O , 60°C , 1h; ii. benzohydrazide, AcOH, acetonitrile/ H_2O (3:7), rt, overnight (87% for **19a**, 92% for **19b**, 50% for **22**); e) $(\text{COCl})_2$, DMSO, TEA, DCM, -78°C to rt (89%).

As described above, similar synthetic route was applied to introduce the 4- and 6-membered ring systems (Scheme 2.7.3). Mannosylation of alcohols **24a-c** with mannosyl fluoride **14** could afford the expected mannosides, however, low yields ($< 25\%$) due to partially deacetylation of **14** hampered the scale-up of the reactions. Therefore, we

changed the mannosylation donor to perbenzoylated mannosyl bromide **23**, which gave acceptable yields for the synthesis of **25a-c**. After a series of protecting and functional group manipulations, the test compounds **28a-c** were obtained in good to excellent yields.



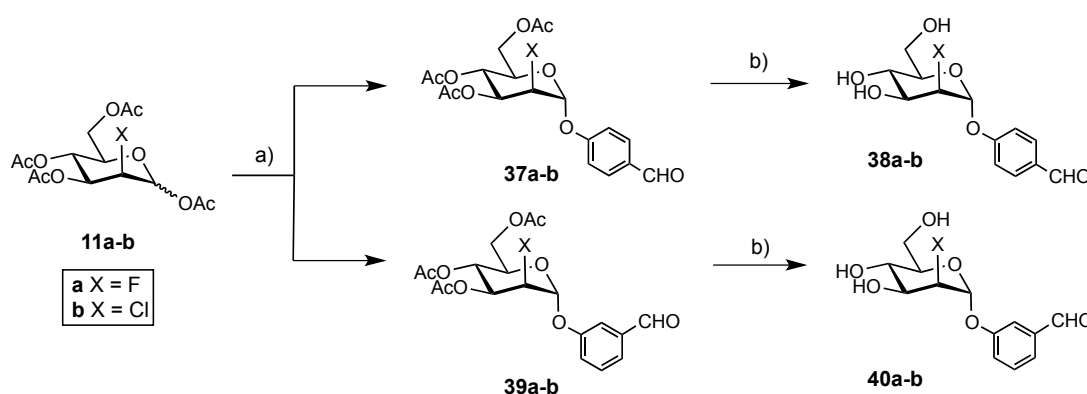
Scheme 2.7.3. Reagents and conditions: a) hydroxycycloalkane carboxylate **24a-c**, HgBr_2 , $\text{Hg}(\text{CN})_2$, DCM, rt, overnight (69% for **25a**, 85% for **25b**, 75% for **25c**); b) i. NaOMe, MeOH, rt, 4h; ii. 2,2-dimethylpropanone, TsOH, DMF, rt, overnight (86% for **26a**, 61% for **26b**, 60% for **26c**); c) DIBAL-H, DCM, -78°C (74% for **27a**, 54% for **27b**, 98% for **27c**); d) i. 80% AcOH/ H_2O , 60°C , 1h; ii. benzohydrazide, AcOH, acetonitrile/ H_2O (3:7), rt, 2h (quant. for **28a-c**).



Scheme 2.7.4. Reagents and conditions: a) $\text{BF}_3 \cdot \text{Et}_2\text{O}$, DCM, 4-hydroxybenzaldehyde **29a-b** or 3-hydroxybenzaldehyde **33**, 0°C to rt, overnight (82% for **30a**, 72% for **30b**, 95% for **34**); b) NaOMe, MeOH, rt, 4h (quant.); c) benzohydrazide, AcOH, acetonitrile/ H_2O (3:7), rt, 2h (quant.).

2.7.3.3 Modifications with aromatic aglycones (Scheme 2.7.4-5)

Hydroxylbenzaldehydes **29a-b** and **33** were mannosylated with donor **14** to yield the benzyl mannosides **30a-b** and **34** (Scheme 2.7.4). Subsequent deacetylation yielded the aldehydes **31a-b** and **34**. In the hydrazone formation reactions test compounds **32a-b** and **36** were synthesized. To synthesize the 2-F and 2-Cl aryl mannosides, peracetylated mannose **11a-b** were firstly treated with HBr to prepare the bromide donors, which were mannosylated with hydroxyl benzaldehydes **29a** and **33** in the presence of Ag₂O to yield **37a-b** and **39a-b** (Scheme 2.7.5). Deacetylation with sodium methoxide yielded the aldehydes **38a-b** and **40a-b** respectively for dynamic combinatorial screening.

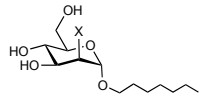


Scheme 2.7.5. Reagents and conditions: a) i. HBr (30% in AcOH), Ac₂O, AcOH, RT, overnight; ii. **29a** or **33**, Ag₂O, acetonitrile, 38°C, 1h (46% for **37a**, 40% for **37b**, 38% for **39a**, 39% for **39b**); g) NaOMe, MeOH, rt, 4h (96% for **38a**, 14% for **38b**, 73% for **40a**, 64% for **40b**).

2.7.4 Biological Evaluation

2.7.4.1 Isothermal titration calorimetry (ITC) with 2-halogenated mannosides.

Table 2.7.1. Thermodynamic parameters of the interaction of selected FimH-antagonists with FimH-CRD-Th-His6.

Entry	Compd	 X =	K _D [nM]	ΔG [KJ/mol]	ΔH [KJ/mol]	-TΔS [KJ/mol]	Desolvation Penalty (ΔH) [KJ/mol]
1	1	OH	28	-43.1	-47.1	3.9	36.38
2	13a	F	637	-35.4	-28.2	-7.1	1.87
3	13b	Cl	1452	-33.3	-24.1	-9.3	6.90

4	13c	Br	2142	-32.4	-21.7	-10.7	9.27
---	------------	----	------	-------	-------	-------	------

To test our hypothesis regarding halogen replacement at 2-position of mannose and desolvation, we performed ITC experiments with compounds **1** and **13a-c** (Table 2.7.1). ITC allows the simultaneous determination of the change in enthalpy (ΔH) and the dissociation constant (K_D) for ligand-protein binding.^{34, 35} The measured thermodynamic parameters showed that 2-halogenated heptyl mannosides (**13a-c**) have lower binding affinities than the reference compound (**1**), and the ranking of enthalpic term indicated that there is no halogen bonding with 2-Cl or 2-Br. According to previous study published by Cabani and coworkers, the desolvation penalty of polar groups is enthalpic driven.²⁷ Subtracting the desolvation penalties described in Cabani's report showed that all halogen-substituents interacted comparably with FimH, again indicating no halogen bonding at the 2-position.

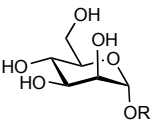
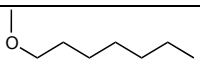
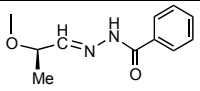
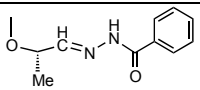
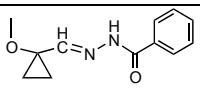
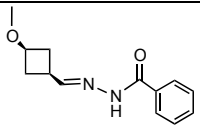
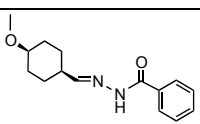
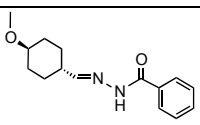
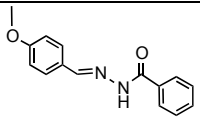
2.7.4.2 Competitive fluorescence polarization assay.

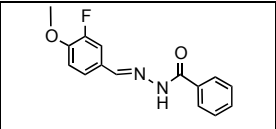
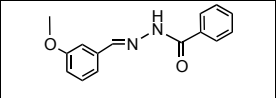
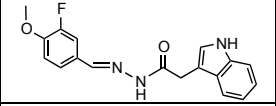
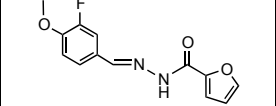
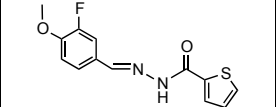
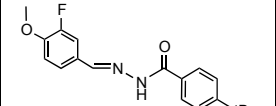
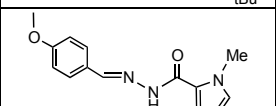
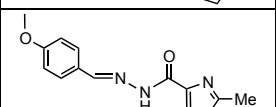
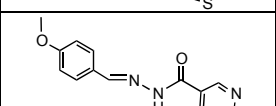
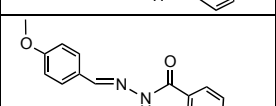
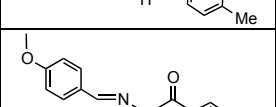
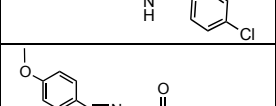
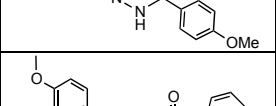
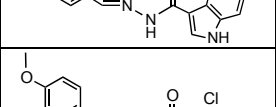
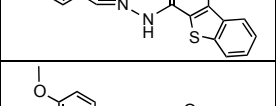
For a rapid evaluation of binding affinity of the modified aglycones (**19a-b**, **22**, **28a-c**, **32a-b**, **36**), we used a competitive binding assay based on fluorescence polarization (FP) as described in Chapter 2.4. In the FP-assay, the antagonist of interest displaces a fluorescent-labeled competitor from the binding site, thereby reducing fluorescence polarization.³⁶ Before the measurement of fluorescence polarization, a 24 h incubation time was applied in the presence of the lectin domain of FimH due to the long residence time of FimH antagonists ($t_{1/2} > 3.5$ h),³⁷ whereas a 3 h incubation time was used in the presence of the native full-length FimH due to a shorter half-life (in millisecond range).³⁸ These assays were performed twice for every compound with each concentration in duplicate. IC_{50} values were obtained by nonlinear least-squares regression (standard four-parameter IC_{50} equation) and converted to K_D using a modified Cheng-Prusoff equation.³⁶ The K_D values observed for the test compounds **1**, **19a-b**, **22**, **28a-c**, **32a-b** and **36** are summarized in Table 2.7.2.

A comparison of the affinities between compounds **19a-b**, **22** and **28a-c** clearly indicates that both the orientation and the size of the aglycones are important factors upon binding. More linear structures **19a** and **28a** showed better affinities than the folded structures **19b** and **28b**. With the same orientation, the optimal size of the aliphatic aglycone is six-

membered ring system (\rightarrow **28b**), which gave eight-fold higher affinity than four-membered ring (\rightarrow **28a**). Furthermore, affinity improvement with aromatic aglycones (\rightarrow **32a-b**) clearly indicates an optimal size and rigidity of the aglycone moieties. However, an affinity loss was observed with *meta*-substituted phenyl (**36**) indicating an unfavorable orientation. Combined the optimal size and orientation, the elongated aromatic aglycones with *para*-substituted hydrazone moiety (\rightarrow **32a-b**) showed highest affinities. Additionally, an electron-withdrawing fluoro-substituent at *ortho*-position slightly increased affinity probably because of the decreased electron density of the phenyl ring and enhanced π - π interaction with Tyr48. To further optimize the acylhydrazone moiety, **32a-b** were chosen as the lead structures for *in situ* dynamic combinatorial screening.

Table 2.7.2. Binding affinity of FimH antagonists determined by fluorescence polarization assay.³⁶

Entry	Compd	 R=	Against the lectin domain of FimH K_D [nM]	Against the full-length FimH K_D [μ M]
1	1		28.4	2.3
2	19a		652.3	n.d.
3	19b		3548.7	n.d.
4	22		1479.1	n.d.
5	28a		853.0	n.d.
6	28b		106.3	n.d.
7	28c		236.6	n.d.
8	32a		17.7	n.d.

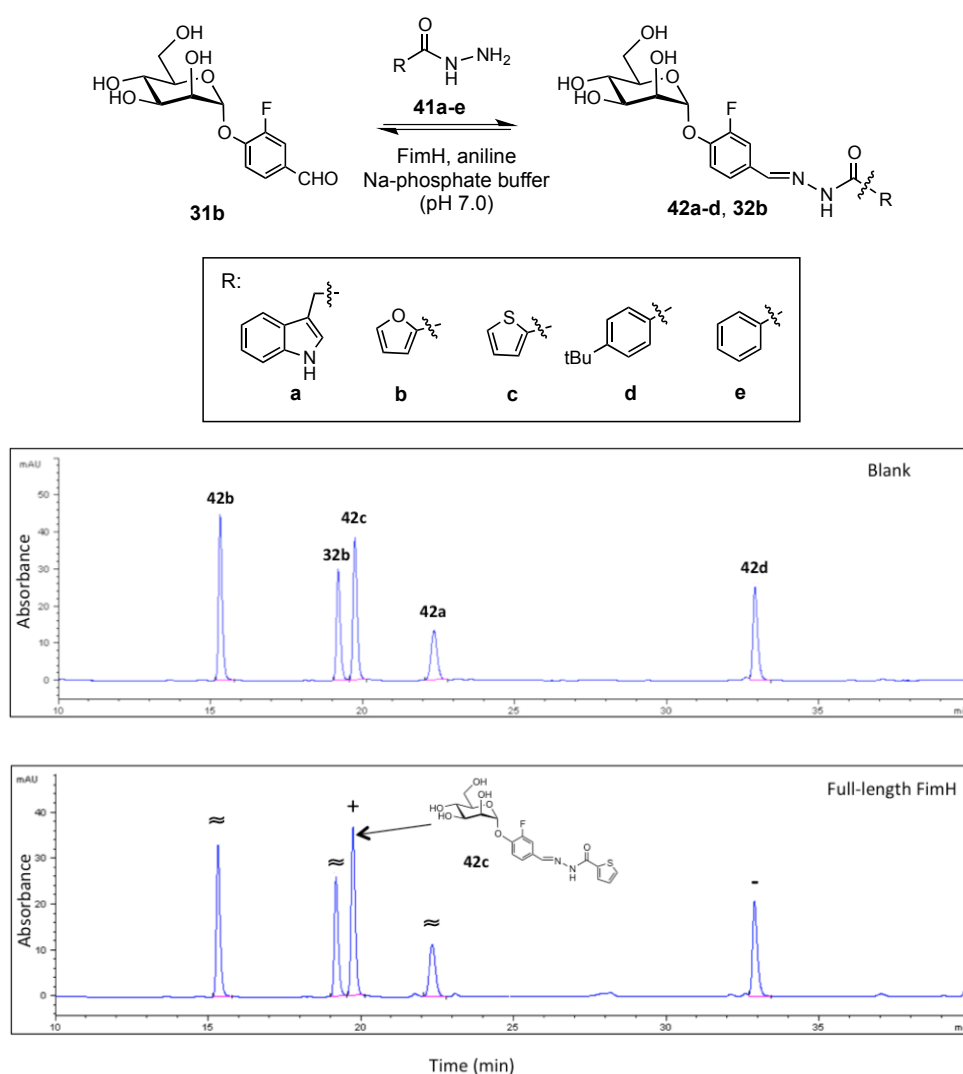
9	32b		11.7±0.1	0.29±0.01
10	36		97.5	n.d.
11	42a		12.3±0.4	0.41±0.03
12	42b		9.0±3.5	0.14±0.01
13	42c		6.0±0.9	0.13±0.01
14	42d		31.2±1.2	0.58±0.07
15	50a		n.d.	0.47±0.04
16	50b		n.d.	0.36±0.05
17	50c		n.d.	0.35±0.01
18	50d		n.d.	0.40±0.15
19	50e		n.d.	0.64±0.07
20	50f		n.d.	0.40±0.01
21	50g		n.d.	0.42±0.02
22	50h		n.d.	0.68±0.04
23	43c		n.d.	0.21±0.02

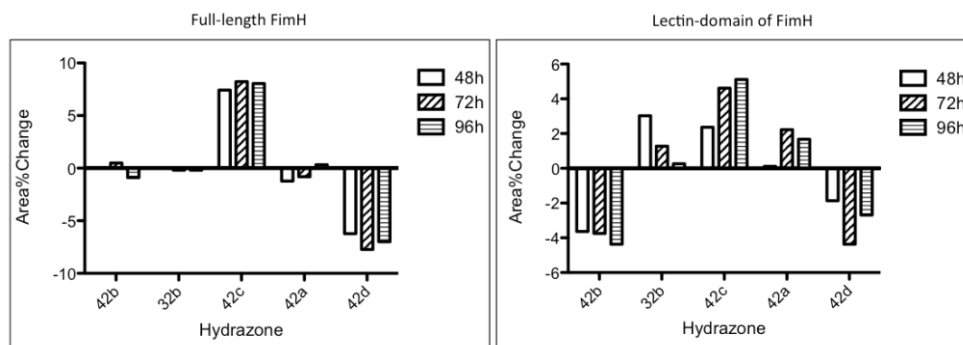
2.7.5 Dynamic Combinatorial Screening

To further optimize the lead structures and to explore the binding pocket of FimH, we applied the synthesized aldehydes (**31a-b**, **35**, **38a-b** and **40a-b**) to generate DCLs.²⁹ The equilibrium between aldehydes, hydrazides and acylhydrazones was established through the formation of acylhydrazone linkages. The reversible reaction was accelerated by aniline, a nucleophilic catalyst, which allows the reaction to reach equilibrium in 24 h under neutral conditions.³⁰ Adaptive DCLs were synthesized in the presence of full-length FimH or its lectin domain. The protein-template DCLs were incubated at room temperature for at least 48 h before HPLC analysis. Raising the pH with aqueous NaOH stopped the reversible reaction, at the same time, denatured the protein FimH. Compared with other denaturing methods, such as urea or acidic conditions, NaOH provided an optimal condition for quenching the reaction and releasing up to 80% of the bound ligands. Using a centrifuge filter, the denatured protein was filtered off and the filtrate was ready for HPLC analysis. Sub-libraries or individual products were synthesized for the HPLC assignment. Peak changes were calculated by subtracting the peak percentages of the blank DCL composition. Synthesizing the DCLs in the presence of bovine serum albumin (BSA) as control experiments produced no measurable amplification, indicating FimH proteins as being responsible for the component amplifications.

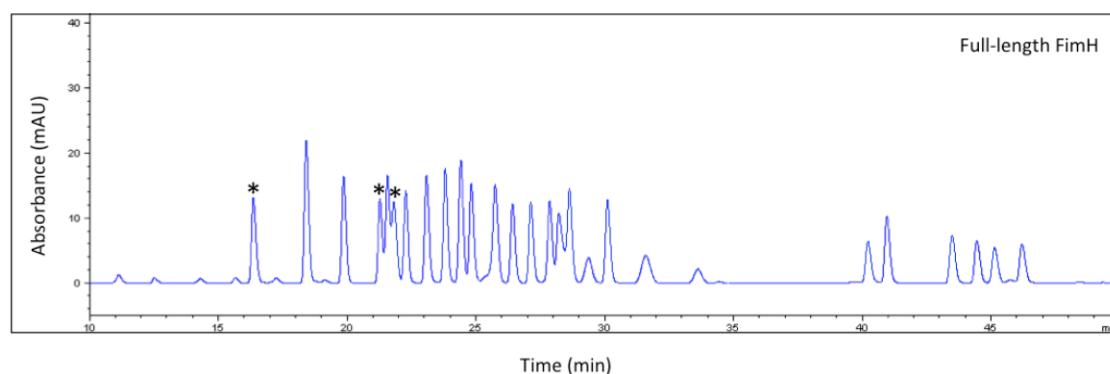
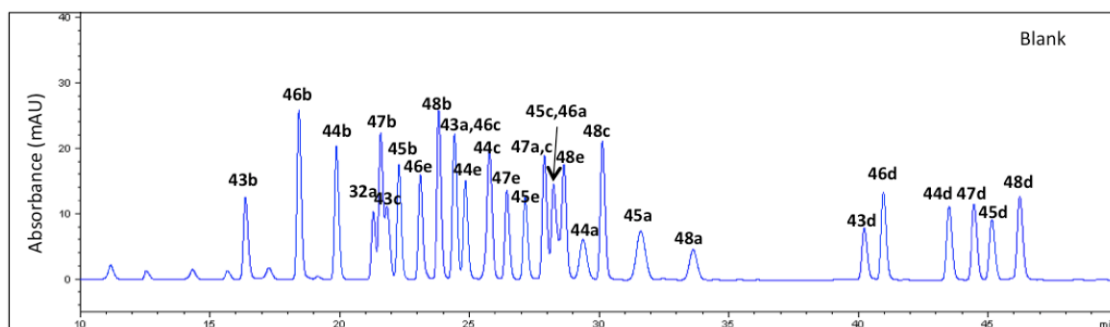
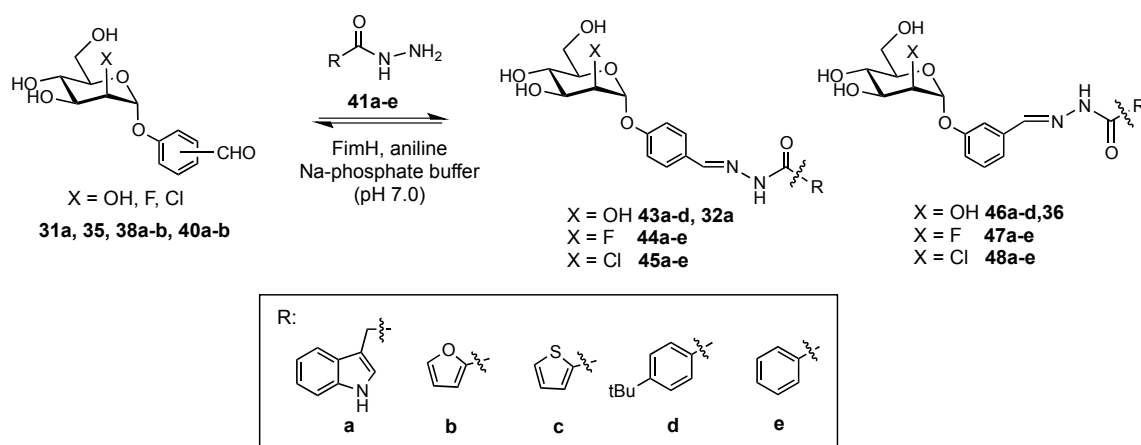
Initial DCL experiments using aldehyde **32b** and five hydrazides **41a-e** were carried out in the presence of either native full-length FimH or its lectin domain (Scheme 2.7.6). The equilibration was complete in 48 h in the presence of full-length FimH. However, with the lectin domain of FimH the distribution of DCL-1 components were shifting after more than 72 h incubation time, which could be explained by the long residence time of FimH ligands to the lectin domain alone. To verify that the amplifications were not due to a kinetic selection, the lectin-domain of FimH was added to a pre-equilibrated DCL and similar equilibrium was achieved after 96 h. After 72 h, clear amplifications could be observed for both FimH targets: in each case the same acylhydrazone (**42c**) was selected as the best binder, which was amplified to ~30% of its concentration in the blank DCL, at the expense of nearly 30% of **42d** in the DCL of full-length FimH (Scheme 2.7.6). To confirm the DCL-1 composition reflecting the affinity ranking, **42a-d** were individually

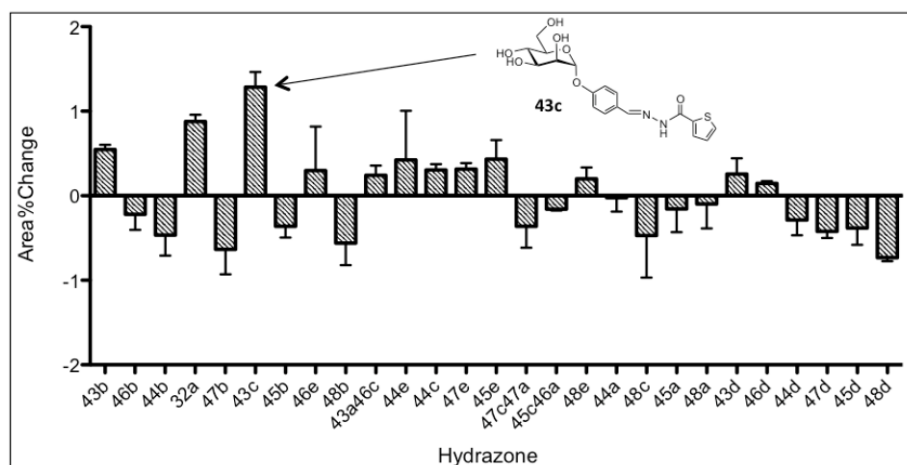
synthesized, and their binding affinities towards both full-length FimH and its lectin domain were evaluated with a competitive fluorescence polarization assay (Entry 11-14, Table 2.7.2). Because the lectin domain of FimH represents the high-affinity state of FimH, the K_D values towards the lectin domain are higher compared to the native full-length protein. For both FimH targets, the DCL-1 amplified hydrazone **42c** as the most active (K_D : 6.0 ± 0.9 nM vs. lectin domain of FimH, 0.13 ± 0.01 μ M vs. full-length FimH), and hydrazone **42d** as the least active (K_D : 31.2 ± 1.2 nM vs. lectin domain of FimH, 0.58 ± 0.07 μ M vs. full-length FimH) among the library members.



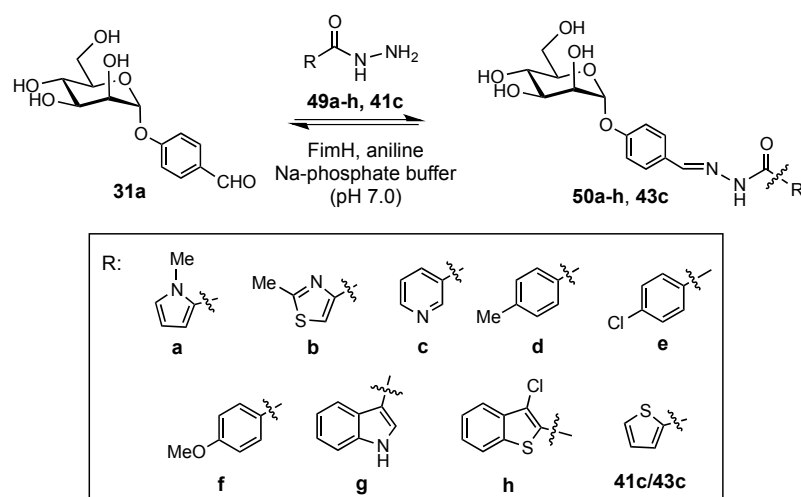


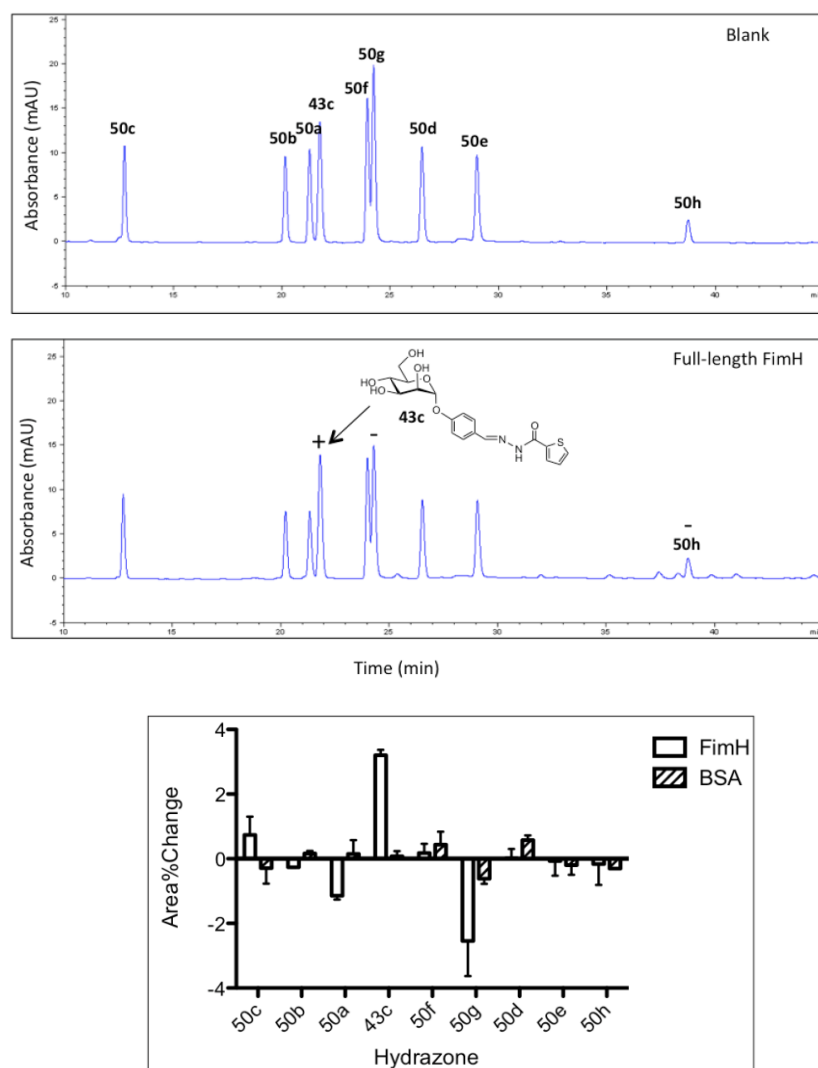
Scheme 2.7.6. FimH-templated DCL-1. DCL conditions: the native full-length FimH or the lectin domain of FimH, aldehyde **31b**, acylhydrazides **41a-e** (25 μ M each), and aniline (10 mM) in Na-phosphate buffer (50mM, pH 7.0) containing <3% DMSO for 96h.





Scheme 2.7.7. FimH-templated DCL-2. DCL conditions: the native full-length FimH (25 μ M), aldehydes **31a**, **35**, **38a-b**, **40a-b** and acylhydrazides **41a-e** (25 μ M each), and aniline (10 mM) in Na-phosphate buffer (50mM, pH 7.0) containing <3% DMSO for 48h.





Scheme 2.7.8. FimH-templated DCL-3. DCL conditions: the native full-length FimH, aldehyde **31a**, acylhydrazides **49a-h**, **41c** (25 μM each), and aniline (10 mM) in Na-phosphate buffer (50mM, pH 7.0) containing <3% DMSO for 48h.

Further DCL experiments were investigated to study the modifications on mannose and substitution patterns on the aromatic aglycones. The full-length FimH-directed DCL-2 was synthesized in the presence of aldehydes **31a**, **35**, **38a-b** (2-F) and **40a-b** (2-Cl) and five hydrazides **41a-e** (Scheme 2.7.7). Three components marked by asterisks (**32a**, **43b** and **43c**) were clearly amplified, indicating the mannose with 2-OH and the *para*-substituted benzaldehyde (**31a**) as an optimal precursor and **43c** as the best binder among the DCL-2 components.

Subsequently, a lead optimization DCL was synthesized with aldehyde **31a** and nine hydrazides (**41c** and **49a-h**) in the presence of full-length FimH (Scheme 2.7.8, DCL-3).

As a result, thiophene hydrazide **41c** was the most positively selected fragment, indicating **43c** as the optimized structure. Further control experiment involved BSA showed no clear amplification of any DCL members, indicating the positive selection coming from the template protein – FimH. Competitive fluorescence polarization assay was then performed to establish whether the amplified ligand in the FimH-directed lead-optimization DCL indeed has high affinity toward full-length FimH (Entry 15-23, Table 2.7.2). In the FP-assay, thiophene **43c** showed the lowest K_D value ($0.21 \pm 0.02 \mu\text{M}$), correlating with the DCL screening results.

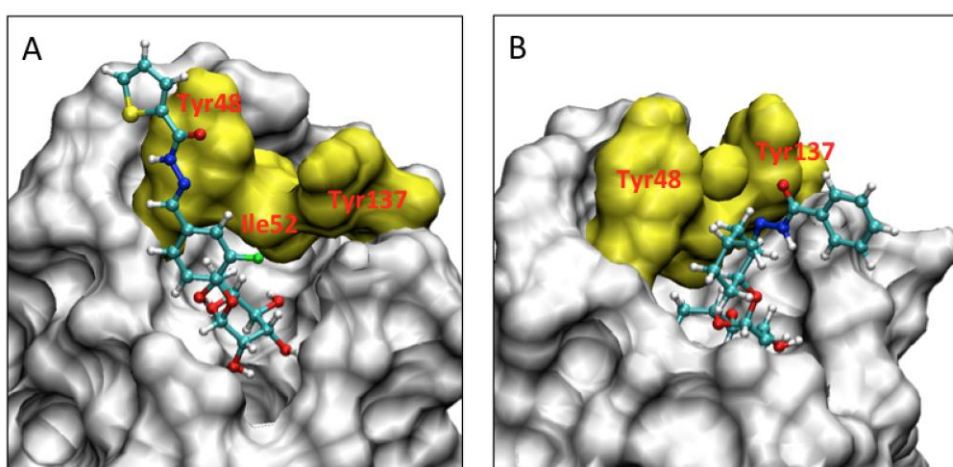


Figure 2.7.5. *In silico* docking studies obtained with flexible docking (VirtualDesignLab²⁸) to the same FimH CRD structure; top-scored binding mode of A) **42c** and B) **28b**.

To gain a molecular insight into the affinity difference between the hydrazones we carried out further *in silico* docking studies with VirtualDesignLab.²⁸ An “out-docking mode” was revealed for thiophenes **42/43c**, and a strong π - π stacking of the acylhydrazone linkage with Tyr48 was observed (Figure 2.7.5A). As previously reported,³⁹ an *ortho*-substitution on the phenyl moiety adjacent to the anomeric center could interact with the empty space of the protein surface, which explained the affinity improvement of the substituted ligand **42c** (*ortho*-F, K_D : $0.13 \pm 0.01 \mu\text{M}$ vs. full-length FimH) comparing to **43c** (*ortho*-H, K_D : $0.21 \pm 0.02 \mu\text{M}$ vs. full-length FimH). With the aliphatic ring system, neither the acylhydrazone nor the outer phenyl ring of **28b** could form π - π interaction with the tyrosine gate, and the binding was between the “in” and “out” docking mode due to an unfavorable shape of the cyclohexane moiety (Figure 2.7.5B).

2.7.6 Conclusion

In this study, we have investigated a series of structurally diversified α -D-mannosides, aiming at exploring the binding pocket of FimH and optimizing the lead structures as FimH antagonists. In this regard, we firstly modified the mannose ring by replacement of the 2-OH with halogen atoms in order to achieve the possible polar interaction (2-F) and halogen bonding (2-Cl, Br). Subsequent ITC measurements of the thermodynamic parameters indicated unfavorable enthalpy contributions for all the halogen-replaced antagonists therefore confirmed mannose ring as a conservative structure for antagonizing FimH. Further modifications on the aglycone, i.e. introduction of the aliphatic or aromatic aglycones with various lengths, sizes, rigidity, and orientations, were implemented. Binding affinities were evaluated with a competitive fluorescence polarization assay, which allowed a rapid screening for the synthesized antagonists. A comparison of the affinities revealed the importance of the size and orientation of the aglycone, and the best combination was observed with the *para*-substituted aromatic moieties (**32a-b**).

Introduction of the acylhydrazone linkages to the aglycone moieties enabled *in situ* generation and screening of DCLs, further extended the structural scope of FimH antagonists. The reversible formation of acylhydrazones was demonstrated to be compatible with the protein target FimH, and the adaptive DCLs allowed amplification effects directly related to the structures presented at equilibrium. The difference between half-lives of the antagonists toward the lectin domain and the full-length FimH resulted in varied reaction rates to reach the equilibrium in DCLs. Denaturing conditions were optimized to ensure the release of the high-affinity antagonists. To optimize the structures for antagonizing full-length FimH, three DCLs were applied, and 43 acylhydrazones were screened. As indicated in all the DCLs, the thiophene fragment (**41c**) was selected to form the best binders (**42/43c**). The high affinity of ligands **42/43c** was further confirmed by the pharmacodynamic evaluation with a FP-assay, and supported by *in silico* docking results.

In summary, our study explored the structural diversity of α -D-mannosides as FimH antagonists in a broad range and further confirmed the optimal substitution patterns on mannose and the aglycone moiety. An application of acylhydrazone DCC demonstrated the effectiveness of the strategy for both lead discovery and leads optimization process,

and thus offered a powerful tool for structural modifications of FimH antagonist and other lectin-targeting ligands. The optimized ligands, thiophene derivatives **42/43c**, represent promising candidates for future *in vitro* and *in vivo* studies.

2.7.7 Experimental Section

General methods: NMR spectra were recorded on a Bruker Avance DMX-500 (500.1 MHz) spectrometer. Assignment of ^1H and ^{13}C NMR spectra was achieved using 2D methods (COSY, HSQC, HMBC). Chemical shifts are expressed in ppm using residual CHCl_3 , CHD_2OD or HDO as references. Optical rotations were measured using Perkin-Elmer Polarimeter 341. Electron spray ionization mass spectra (ESI-MS) were obtained on a Waters micromass ZQ. The LC/HRMS analysis were carried out using a Agilent 1100 LC equipped with a photodiode array detector and a Micromass QTOF I equipped with a 4 GHz digital-time converter. Microwave-assisted reactions were carried out with a CEM Discover and Explorer. Reactions were monitored by TLC using glass plates coated with silica gel 60 F₂₅₄ (Merck) and visualized by using UV light and/or by charring with a molybdate solution (a 0.02 M solution of ammonium cerium sulfate dihydrate and ammonium molybdate tetrahydrate in aqueous 10% H_2SO_4). MPLC separations were carried out on a CombiFlash Companion or Rf from Teledyne Isco equipped with RediSep normal-phase or RP-18 reversed-phase flash columns. LC-MS separations were done on a Waters system equipped with sample manager 2767, pump 2525, PDA 2525 and micromass ZQ. Size-exclusion chromatography was performed on Bio-Gel[®] P-2 Gel (45-90 mm) from Bio-Rad (Reinach, Switzerland). All compounds used for biological assays are at least of 98% purity based on HPLC analytical results. Commercially available reagents were purchased from Fluka, Aldrich, Alfa Aesar or Iris Biotech (Germany). Solvents were purchased from Sigma-Aldrich (Buchs, Switzerland) or Acros Organics (Geel, Belgium) and were dried prior to use where indicated. Methanol (MeOH) and ethanol (EtOH) were dried by refluxing with sodium methoxide and distilled immediately before use. Dichloromethane (DCM) was dried by filtration over Al_2O_3 (Fluka, type 5016 A basic). Molecular sieves 4Å were activated in vacuo at 500°C for 1 h immediately before use.

General procedure A for the preparation of mannosides 12a-c: To a solution of **11a-c**

(1.0 equiv) in DMF (2 mL), NH₄OAc (2.0 equiv) was added. The mixture was stirred at RT overnight. The reaction mixture was extracted with EtOAc (10 mL) and washed with water (10 mL). The organic layer was dried over Na₂SO₄ and concentrated in vacuo. The residue was dissolved with DCM (2 mL), and added with 60% NaH in mineral oil (0.15 equiv) and trichloroacetonitrile (10 equiv) at RT. The reaction mixture was stirred at RT for 1.5h. The mixture was concentrated and dried in vacuo to give the crude trichloroacetimidate donor. To a suspension of the crude trichloroacetimidate, *n*-heptanol (2 equiv), and molecular sieves (4 Å, 600 mg) in dry DCM (5 mL), TMSOTf (0.15 equiv) was added dropwise under argon. The mixture was stirred at RT for 5h, then filtered over Celite and concentrated. The residue was purified by MPLC on silica gel (PE/EtOAc) to yield **12a-c**.

General procedure B for deacetylation: To a solution of **12a-c**, (1.0 equiv) in dry MeOH (5 mL) was added freshly prepared 1M NaOMe/MeOH (0.1 equiv) under argon. The mixture was stirred at RT until the reaction was complete (monitored by TLC), then neutralized with Amberlyst-15 (H⁺) ion-exchange resin, filtered and concentrated in vacuo. The residue was purified by MPLC on silica gel (DCM/MeOH 10:1-8:1) to afford **13a-c**.

General procedure C for the synthesis of 16a-c, 30a-b, 34. To an ice-cold suspension of **14** (200 mg, 0.57 mmol, 1.0 equiv), alcohol **15a-c** or phenol **29a-b, 33** (0.52 mmol, 1.0 equiv), and molecular sieves (4Å, 600 mg) in dry DCM (5 mL), BF₃·Et₂O (0.3 mL, 2.44 mmol, 4.7 equiv) was added dropwise under argon. The mixture was stirred at 0°C for 3h, and then at RT overnight. The reaction mixture was filtered through Celite, and then the filtrate was diluted with DCM (50 mL), extracted with 0.5 N aq. NaOH (50 mL), water (50 mL) and brine (50 mL). The organic layer was dried over Na₂SO₄ and concentrated in vacuo. The residue was purified by MPLC on silica gel (petroleum ether/EtOAc) to yield **16a-c, 30a-b** and **34**.

General procedure D for the synthesis of 17a-c and 26a-c. **16a-c** or **25a-c** was firstly deacetylated according to general procedure B and concentrated to afford the deacetylated mannosides. To a solution of the deacetylated mannoside (1.0 equiv) in 2,2-dimethylpropanone/DMF (2:1), TsOH (0.01 equiv) was added at RT. The mixture was

stirred at RT overnight, diluted with EtOAc (20 mL), and washed with water (20 mL). The organic layer was dried over Na₂SO₄ and concentrated. The residue was purified by MPLC on silica gel (PE/EtOAc 4:1) to give **17a-c** and **26a-c** as colorless oil.

General procedure E for DIBAL-H reduction: To a solution of **17a-c** or **26a-c** (0.2 mmol, 1 equiv) in dry DCM (5 mL) at -78 °C, DIBAL-H (1M in DCM, 0.22 mL, 0.22 mmol) was added dropwise. The reaction mixture was stirred at -78 °C for 1h, and then quenched with a saturated solution of potassium sodium tartrate (10 mL). The mixture was extracted with DCM (15 mL). The organic layer was dried over Na₂SO₄ and concentrated. The residue was purified by MPLC on silica gel (PE/EtOAc 4:1) to give **18a-b**, **20** and **27a-c**.

General procedure F for preparation of hydrazones 19a-b, 22, 28a-c: A solution of **18a-b**, **21**, **27a-c** in 80% AcOH/H₂O was stirred at 60 °C for 1h. The reaction mixture was concentrated in vacuo to give the crude aldehyde. To a solution of aldehyde (0.02 mmol, 1 equiv) in a mixture of acetonitrile/H₂O (3:7, 2 mL), benzohydrazide (3 mg, 0.022 mmol, 1.1 equiv) was added. The reaction mixture was stirred at RT overnight. The mixture was concentrated and the residue was purified by MPLC (RP-18, H₂O/MeOH 1:0 – 1:1) to give **19a-b**, **22**, **28a-c** as white solids after final lyophilization from H₂O.

General procedure G for preparation of mannosides 25a-c: To a suspension of **23** (1.0 equiv), alcohol **24a-c** (1.0-1.5 equiv) and molecular sieves (4Å, 1.2 g) in dry DCM, HgBr₂ (1.3 equiv) and Hg(CN)₂ (1.3 equiv) was added under argon. The reaction mixture was stirred at RT overnight. The reaction mixture was filtered through Celite and concentrated in vacuo. The residue was purified by MPLC on silica gel (petroleum ether/EtOAc) to yield **25a-c**.

General procedure H for preparation of mannosides 37a-b and 39a-b: To a solution of **11a-b** (0.30 mmol, 1 equiv) in acetic acid (1.5 mL), hydrobromic acid solution (33 wt. % in acetic acid, 0.5 mL) was added at RT. The reaction mixture was stirred at RT overnight. The reaction mixture was poured into ice-water (20 mL), extracted with DCM (20 mL). The organic phase was washed with saturated NaHCO₃ aqueous solution (20 mL), dried with Na₂SO₄, and concentrated in vacuo to give the bromide intermediate. To

a solution of the bromide intermediate in acetonitrile (5 mL), phenol (0.36 mmol, 1.2 equiv) and freshly prepared Ag₂O (0.45 mmol, 1.5 equiv) were added. Then the mixture was stirred at 38 °C for 1h. The reaction mixture was filtered through Celite and concentrated. The residue was purified by MPLC (PE/EtOAc 1:1) to give **37a-b** and **39a-b**.

General procedure I for the preparation of hydrazones 32a-b, 36, 42a-d and 50a-h:

To a mixture of the aldehyde **31a-b** or **35** (5 mg, 1 equiv.) and the corresponding hydrazide (1 equiv.) in ethanol, a few drops of glacial acetic acid was added at RT. The mixture was stirred at RT overnight, and then concentrated. The residue was purified by MPLC (MeOH/H₂O 1:2) to give **32a-b** and **36**. Compound **42a-d** and **50a-h** were purified directly by preparative HPLC-MS (HPLC conditions: Column: SunFire™ 5 μ prepC18 19 \times 150 mm, flow rate = 15 mL \cdot min⁻¹, gradient H₂O / MeCN (0.1% formic acid) from 95% to 5% over 20 min).

Methyl 4,6-O-benzylidene- α -D-glucopyranoside (7). Prepared according to the similar procedure as described in literature. ¹H NMR (500 MHz, CDCl₃): δ 7.49 (d, J = 5.6 Hz, 2H, Ph), 7.37 (d, J = 4.7 Hz, 3H, Ph), 5.53 (s, 1H, PhCHO₂), 4.79 (d, J = 2.9 Hz, 1H, H-1), 4.29 (dd, J = 9.8, 4.3 Hz, 1H, H-6a), 3.93 (t, J = 9.2 Hz, 1H, H-3), 3.86 - 3.77 (m, 2H, H-5 and H-6b), 3.74 (t, J = 10.2 Hz, 1H, H-4), 3.63 (t, J = 7.5 Hz, 1H, H-2), 3.53 - 3.43 (m, 4H, H-4, -OCH₃), 2.77 (s, 1H, OH), 2.31 (d, J = 9.4 Hz, 1H, OH). The proton NMR was consistent with literature data.³¹

Methyl 3-O-benzyl-4,6-O-benzylidene- α -D-glucopyranoside (8). Prepared according to the similar procedure as described in literature. ¹H NMR (500 MHz, CDCl₃): δ 7.49 (d, J = 5.8 Hz, 2H, Ph), 7.42 - 7.28 (m, 8H, Ph), 5.51 (s, 1H, PhCHO₂), 4.78 (d, J = 12.2 Hz, 1H, PhCHH), 4.70 (d, J = 12.2 Hz, 1H, PhCHH), 4.61 (d, J = 3.3 Hz, 1H, H-1), 4.26 (dd, J = 10.1, 4.8 Hz, 1H, H-6a), 4.15 (t, J = 9.3 Hz, 1H, H-3), 3.81 (td, J = 9.9, 4.8 Hz, 1H, H-5), 3.70 (t, J = 10.3 Hz, 1H, H-6b), 3.54 - 3.44 (m, 2H, H-2, H-4), 3.37 (s, 3H, OCH₃). The proton NMR was consistent with literature data.³²

Methyl 2-deoxy-2-fluoro-3-O-benzyl-4,6-O-benzylidene- α -D-mannopyranoside (9a).

A solution of α -D-glucopyranoside **8** (800 mg, 2.15 mmol) in CH₂Cl₂ (10 mL) and

pyridine (0.9 mL, 10.8 mmol) was cooled to $-20\text{ }^{\circ}\text{C}$, treated with Tf_2O (0.43 mL, 2.60 mmol), stirred for 15 min at $-20\text{ }^{\circ}\text{C}$ for 2 h. A solution of the residue in CH_2Cl_2 was washed with sat. NaHCO_3 aq. solution (10 mL). The organic layer was dried over Na_2SO_4 and concentrated in vacuo. The triflate residue was then treated with TBAF (1M solution in THF, 10 mL), stirred at $50\text{ }^{\circ}\text{C}$ for 48 h, cooled to room temperature, concentrated and purified by MPLC (petrol ether (PE)/EtOAc 3:1) to yield **9a** (540 mg, 50%) as a colorless oil. ^1H NMR (500 MHz, CDCl_3): δ 7.49 (dt, $J = 4.5, 2.5$ Hz, 2H, Ar), 7.43 - 7.26 (m, 8H, Ar), 5.63 (s, 1H, PhCHO_2), 4.86 (dd, $J = 7.0, 5.3$ Hz, 2H, PhCHH , H-1), 4.74 (dt, $^2J_{\text{H,F}} = 48.8$, $J = 2.2$ Hz, 1H, H-2), 4.76 (d, $J = 12.2$, PhCHH), 4.33 - 4.26 (m, 1H, H-6a), 4.15 - 4.08 (m, 1H, H-6b), 3.92 (ddd, $^3J_{\text{H,F}} = 27.8$, $J = 10.0, 2.7$ Hz, 1H, H-3), 3.88 - 3.77 (m, 2H, H-5, H-6b), 3.39 (s, 3H, OCH_3). The proton NMR was consistent with literature data.³³

Methyl 2-deoxy-2-chloro- α -D-mannopyranoside (10b): According to the similar procedure for the preparation of **9a**, **9b** was prepared by treatment of the triflate intermediate (478 mg, 0.95 mmol) with LiCl (201 mg, 4.75 mmol) in *N*-methyl-2-pyrrolidone (2 mL) at RT overnight. The reaction mixture was then diluted with EtOAc (20 mL), and washed with water (20 mL) and brine (20 mL). The organic layer was dried over Na_2SO_4 , concentrated and purified by MPLC (PE/EtOAc 8:1) to give crude **9b** (393 mg). The crude **9b** was treated with 80% AcOH in water (5 mL) at $60\text{ }^{\circ}\text{C}$ for 1h, and then concentrated in vacuo. The residue was dissolved in a mixed solvent of MeOH/EtOAc/DCM (3:1:1), added with 10% Pd/C (60 mg), and stirred under hydrogen atmosphere at RT for 1h. The reaction mixture was filtered and concentrated. The residue was purified by MPLC (DCM/MeOH 9:1) to yield **10b** (60 mg, 32% over two steps) as colorless oil. $[\alpha]_{\text{D}} = +80.22$ ($c = 1.5$, MeOH); ^1H NMR (500 MHz, MeOD): δ 4.85 (s, 1H, H-1), 4.22 (d, $J = 2.0$ Hz, 1H, H-2), 3.99 (dd, $J = 9.1, 3.3$ Hz, 1H, H-3), 3.87 (d, $J = 11.8$ Hz, 1H, H-6a), 3.71 (dd, $J = 11.8, 6.1$ Hz, 1H, H-6b), 3.66 (t, $J = 9.5$ Hz, 1H, H-4), 3.60 - 3.53 (m, 1H, H-5), 3.42 (s, 3H); ^{13}C NMR (126 MHz, MeOD): δ 102.43 (C-1), 75.22 (C-5), 71.00 (C-3), 68.30 (C-4), 63.00 (C-2), 62.84 (C-6), 55.58 (OCH_3); ESI-MS: m/z : calcd for $\text{C}_7\text{H}_{13}\text{ClNaO}_5$ $[\text{M}+\text{Na}]^+$: 235.03, found: 234.76.

Methyl 2-deoxy-2-bromo- α -D-mannopyranoside (10c): According to the similar procedure for the preparation of **9a**, **9c** was prepared by treatment of the triflate

intermediate (540 mg, 1.07 mmol) with $n\text{Bu}_4\text{NBr}$ (700 mg, 2.14 mmol) in DMF (5 mL) at 60°C for 48h. The reaction mixture was then diluted with EtOAc (50 mL), and washed with water (50 mL) and brine (50 mL). The organic layer was dried over Na_2SO_4 , concentrated and purified by MPLC (PE/EtOAc 5:1) to give the crude **9c** (280 mg). The crude product **9c** was treated with 80% AcOH in water (5 mL) at 60°C for 1h, and then concentrated in vacuo. The residue was dissolved in a mixed solvent of MeOH/EtOAc/DCM (3:1:1), added with 10% Pd/C (150 mg), and stirred under hydrogen atmosphere at RT for 1h. The reaction mixture was filtered and concentrated. The residue was purified by MPLC (DCM/MeOH 10:1) to yield **10b** (150 mg, 55% over two steps) as colorless oil. $[\alpha]_{\text{D}} = +53.47$ ($c = 0.8$, EtOAc); $^1\text{H NMR}$ (500 MHz, MeOD): δ 4.96 (s, 1H), 4.31 (dd, $J = 3.8, 1.3$ Hz, 1H, H-2), 3.87 (dd, $J = 11.8, 2.3$ Hz, 1H, H-6a), 3.82 (dd, $J = 9.0, 3.9$ Hz, 1H, H-3), 3.71 (dd, $J = 11.8, 6.1$ Hz, 1H, H-6b), 3.66 (t, $J = 9.4$ Hz, 1H, H-4), 3.62 - 3.57 (m, 1H, H-5), 3.42 (s, 3H, CH_3); $^{13}\text{C NMR}$ (126 MHz, MeOD): δ 102.65 (C-1), 75.35 (C-5), 70.44 (C-3), 69.12 (C-4), 62.88 (C-6), 56.37 (C-6), 55.60 (C-2); ESI-MS: m/z : calcd for $\text{C}_7\text{H}_{13}\text{BrNaO}_5$ $[\text{M}+\text{Na}]^+$: 278.98, found 278.79.

2-Deoxy-2-fluoro-1,3,4,6-tetra-O-acetyl- α -D-mannopyranoside (11a): **9a** (350 mg, 0.93 mmol) was treated with 80% AcOH in water (5 mL) at 60°C for 1h, and then concentrated in vacuo. The residue was dissolved in a mixed solvent of MeOH/EtOAc/DCM (3:1:1), added with 10% Pd/C, and stirred under hydrogen atmosphere at RT for 1h. The reaction mixture was filtered and concentrated to afford crude **10a**. The crude product **10a** was mixed with acetic anhydride (2 mL) and conc. H_2SO_4 (63 μl , 1.19 mmol). The reaction mixture was stirred at RT overnight, and then diluted with DCM (20 mL). After being washed with sat. NaHCO_3 aq. solution (20 mL) and brine (50 mL), the organic layer was dried over Na_2SO_4 and concentrated in vacuo. The residue was purified by MPLC (PE/EtOAc 2:1) to yield **11a** (276 mg, 84%) as colorless oil. $[\alpha]_{\text{D}} = +53.17$ ($c = 0.9$, EtOAc); $^1\text{H NMR}$ (500 MHz, CDCl_3): δ 6.27 (dd, $^3J_{\text{H,F}} = 6.5$ Hz, $J = 2.1$ Hz, 1H, H-1), 5.41 (t, $J = 10.1$ Hz, 1H, H-4), 5.26 (ddd, $^3J_{\text{H,F}} = 27.9$ Hz, $J = 10.2, 2.6$ Hz, 1H, H-3), 4.75 (dt, $^2J_{\text{H,F}} = 48.7$ Hz, $J = 2.4$ Hz, 1H, H-2), 4.27 (dd, $J = 12.5, 4.5$ Hz, 1H, H-6a), 4.11 (dd, $J = 12.4, 2.4$ Hz, 1H, H-6b), 4.05 (ddd, $J = 10.1, 4.4, 2.3$ Hz, 1H, H-5), 2.17, 2.11, 2.09, 2.05 (4s, 12H, 4 COOCH_3); $^{13}\text{C NMR}$ (126 MHz, CDCl_3) δ : 170.72, 170.24, 169.30, 168.04 (4 CO), 90.15 ($J_{\text{C,F}} = 31.07$ Hz, C-1), 85.93 ($J_{\text{C,F}} = 182.09$ Hz, H-2), 70.75 (C-5), 69.50 ($J_{\text{C,F}} = 17.0$ Hz, C-3), 65.17 (C-4),

61.75 (C-6), 20.84, 20.71, 20.70, 20.59 (4C, COOCH₃). ESI-MS: m/z : calcd for C₁₄H₁₉FNao₉ [M+Na]⁺: 373.09, found: 372.98.

2-Deoxy-2-chloro-1,3,4,6-tetra-O-acetyl- α -D-mannopyranoside (11b): **10b** (20 mg, 0.09 mmol) was mixed with acetic anhydride (0.25 mL) and conc. H₂SO₄ (7.5 μ l, 0.14 mmol). The reaction mixture was stirred at RT overnight, and then diluted with DCM (10 mL). After being washed with sat. NaHCO₃ aq. solution (10 mL) and brine (10 mL), the organic layer was dried over Na₂SO₄ and concentrated in vacuo. The residue was purified by MPLC (PE/EtOAc 2:1) to yield **11b** (34 mg, 99%) as colorless oil. $[\alpha]_D = +27.51$ ($c = 1.7$, EtOAc); ¹H NMR (500 MHz, CDCl₃): δ 6.24 (s, 1H, H-1), 5.48 (t, $J = 9.9$ Hz, 1H, H-4), 5.36 (dd, $J = 9.8, 3.1$ Hz, 1H, H-3), 4.40 (s, 1H, H-2), 4.25 (dd, $J = 12.4, 4.3$ Hz, 1H, H-6a), 4.14 (d, $J = 12.7$ Hz, 1H, H-6b), 4.09 (d, $J = 10.0$ Hz, 1H, H-5), 2.18, 2.11, 2.10, 2.07 (4 s, 12H, 4 COOCH₃); ¹³C NMR (126 MHz, CDCl₃): δ 170.68, 170.12, 169.27, 168.10 (4 CO), 92.91 (C-1), 71.19 (C-5), 69.24 (C-3), 64.91 (C-4), 61.88 (C-6), 56.36 (C-2), 20.87, 20.71, 20.69, 20.61 (4 COOCH₃). ESI-MS: m/z : calcd for C₁₄H₁₉ClNaO₉ [M+Na]⁺: 389.06, found: 388.97.

2-Deoxy-2-bromo-1,3,4,6-tetra-O-acetyl- α -D-mannopyranoside (11c): Prepared according to the similar procedure of **11b** from **10c** (100mg, 0.39 mmol). Yield: 136 mg (85%). $[\alpha]_D = +20.13$ ($c = 0.9$, EtOAc); ¹H NMR (500 MHz, CDCl₃): δ 6.32 (d, $J = 1.7$ Hz, 1H, H-1), 5.49 (t, $J = 9.9$ Hz, 1H, H-4), 5.20 (dd, $J = 9.7, 4.0$ Hz, 1H, H-3), 4.44 (dd, $J = 4.0, 1.7$ Hz, 1H, H-2), 4.24 (dd, $J = 12.4, 4.6$ Hz, 1H, H-6a), 4.16 (dd, $J = 12.4, 2.4$ Hz, 1H, H-6b), 4.10 (ddd, $J = 10.0, 4.5, 2.6$ Hz, 1H, H-5), 2.17, 2.11, 2.11, 2.07 (4 s, 12H, 4 COOCH₃); ¹³C NMR (126 MHz, CDCl₃): δ 170.70, 170.07, 169.28, 168.12 (4 CO), 93.19 (C-1), 71.33 (C-5), 68.82 (C-3), 65.63 (C-4), 61.89 (C-6), 47.82 (C-2), 20.88, 20.77, 20.71, 20.62 (4 COOCH₃). ESI-MS: m/z : calcd for C₁₄H₁₉BrNaO₉ [M+Na]⁺: 433.01, found: 432.91.

Heptyl 2-deoxy-2-fluoro-3,4,6-tetra-O-acetyl- α -D-mannopyranoside (12a): Prepared according to general procedure A from **11a** (176 mg, 0.57 mmol). Yield: 122 mg (60%) as colorless oil. ¹H NMR (500 MHz, CDCl₃): δ 5.31 (t, $J = 10.0$ Hz, 1H, H-4), 5.25 (ddd, $J = 28.0, 10.0, 2.5$ Hz, 1H, H-3), 4.98 (dd, $J = 7.0, 1.5$ Hz, 1H, H-1), 4.73 (dt, $J = 50.0, 2.5$ Hz, 1H, H-2), 4.27 (dd, $J = 12.0, 5.0$, 1H, H-6a), 4.12 (dd, $J = 12.0, 2.0$ Hz, 1H, H-

6b), 3.97 (ddd, $J = 9.5, 4.5, 2.0$ Hz, 1H, H-5), 3.71 (dt, $J = 9.5, 6.5$ Hz, 1H, H-OCH₂C₆H₁₃), 3.47 (dt, $J = 9.5, 6.5$ Hz, 1H, H-OCH₂C₆H₁₃), 2.10, 2.09, 2.04 (3s, 3 COCH₃), 1.58 (m, 2H), 1.31 (m, 8H), 0.87 (m, 3H, CH₃); ¹³C NMR (126 MHz, CDCl₃): δ 170.75, 170.17, 169.53 (3 COCH₃), 97.12 (d, $J = 28.63$ Hz, C-1), 87.05 (d, $J = 178.25$ Hz, C-2), 69.99 (d, $J = 16.5$ Hz, C-3), 68.67 (OCH₂C₆H₁₃), 68.41 (C-5), 65.91 (C-4), 62.18 (C-6), 32.79, 31.71, 28.98, 25.99, 22.58, 14.06 (OCH₂C₆H₁₃), 20.78, 20.74, 20.65 (3C, COCH₃); HR-MS: m/z : calcd for C₁₉H₃₁FN₁O₈ [M+Na]⁺: 429.1901, found: 429.1905.

Heptyl 2-deoxy-2-chloro-3,4,6-tetra-O-acetyl- α -D-mannopyranoside (12b): Prepared according to general procedure A from **11b** (60 mg, 0.28mmol). Yield: 42 mg (35%) as colorless oil. $[\alpha]_D = +35.0$ ($c = 1.3$, EtOAc); ¹H NMR (500 MHz, CDCl₃): δ 5.43 - 5.34 (m, 2H, H-3, H-4), 4.96 (s, 1H, H-1), 4.38 (s, 1H, H-2), 4.25 (dd, $J = 12.2, 4.9$ Hz, 1H, H-6a), 4.14 (d, $J = 12.1$ Hz, 1H, H-6b), 3.99 (s, 1H, H-5), 3.68 (dd, $J = 16.3, 6.9$ Hz, 1H, -OCH- of heptyl), 3.48 (dd, $J = 16.1, 6.7$ Hz, 1H, -OCH- of heptyl), 2.10, 2.09, 2.05 (3 s, 9H, 3COOCH₃), 1.67 - 1.55 (m, 2H, CH₂), 1.30 (d, $J = 12.6$ Hz, 8H, 4 CH₂), 0.89 (d, $J = 6.9$ Hz, 3H, CH₃); ¹³C NMR (126 MHz, CDCl₃): δ 170.72, 170.07, 169.50 (3 CO), 99.72 (C-1), 69.77 (C-3), 68.88 (CH₂), 68.83 (C-5), 65.60 (C-4), 62.34 (C-6), 57.70 (C-2), 31.74, 29.28, 29.00, 26.03, 22.60 (5C, CH₂), 20.79, 20.73, 20.67 (4C, CO), 14.07 (CH₃); ESI-MS: m/z : calcd for C₁₉H₃₁ClNaO₈ [M+Na]⁺: 445.16, found: 445.12.

Heptyl 2-deoxy-2-bromo-3,4,6-tetra-O-acetyl- α -D-mannopyranoside (12c): Prepared according to general procedure A from **11c** (207 mg, 0.52 mmol). Yield: 60 mg (26%) as colorless oil. $[\alpha]_D = +38.2$ ($c = 0.4$, EtOAc); ¹H NMR (500 MHz, CDCl₃): δ 5.40 (t, $J = 9.9$ Hz, 1H, H-4), 5.23 (dd, $J = 9.7, 4.0$ Hz, 1H, H-3), 5.06 (s, 1H, H-1), 4.44 (dd, $J = 4.0, 1.3$ Hz, 1H, H-2), 4.24 (dd, $J = 12.2, 5.0$ Hz, 1H, H-6a), 4.14 (dd, $J = 12.2, 2.4$ Hz, 1H, H-6b), 4.00 (ddd, $J = 10.0, 4.9, 2.4$ Hz, 1H, H-5), 3.68 (dt, $J = 9.6, 6.8$ Hz, 1H, -OCH-), 3.47 (dt, $J = 9.6, 6.6$ Hz, 1H, -OCH-), 2.11, 2.09, 2.05 (3 s, 9H, 3 COOCH₃), 1.60 (dd, $J = 14.1, 6.9$ Hz, 2H, CH₂), 1.37 - 1.27 (m, 8H, 4 CH₂), 0.89 (t, $J = 6.9$ Hz, 3H, CH₃); ¹³C NMR (126 MHz, CDCl₃): δ 170.72, 170.01, 169.50 (3 CO), 99.95 ($J = 9.43$ Hz, C-1), 69.34 (C-3), 68.98 (C-5), 68.87 (OCH₂), 66.28 (C-4), 62.34 (C-6), 49.71 (C-2), 31.74, 29.31, 29.01, 26.04, 22.60 (5C, 5 CH₂), 20.83, 20.74, 20.67 (3 CH₃ of OAc), 14.07 (CH₃); ESI-MS: m/z : calcd for C₁₉H₃₁BrNaO₈ [M+Na]⁺: 489.11, found: 489.04.

Heptyl 2-deoxy-2-fluoro- α -D-mannopyranoside (13a): Prepared according to general procedure B from **12a** (134 mg, 0.33 mmol). Yield: 71 mg (77%). $[\alpha]_D = +75.4$ ($c = 0.4$, DCM); $^1\text{H NMR}$ (500 MHz, CDCl_3): δ 4.93 (dd, $J = 7.5, 1.5$ Hz, 1H, H-1), 4.66 (d, $J = 50.0$ Hz, 1H, H-2), 3.92 – 3.82 (m, 4H, H-6a, H-6b, H-4, H-3), 3.68 (dt, $J = 9.5, 6.5$ Hz, 1H, H-OCH₂C₆H₁₃), 3.59 (m, 1H, H-5), 3.41 (dt, $J = 9.5, 6.5$ Hz, 1H, H-OCH₂C₆H₁₃), 4.21, 3.03, 2.10 (3, 4, 6-OH), 1.56 (m, 2H), 1.27 (m, 8H), 0.88 (t, $J = 7.0$ Hz, 3H, CH₃); $^{13}\text{C NMR}$ (126 MHz, CDCl_3): δ 97.41 (d, $J = 29.13$ Hz, C-1), 89.71 (d, $J = 172.63$ Hz, C-2), 71.91 (C-5), 70.82 (d, $J = 17.5$ Hz, C-3), 68.22 (OCH₂C₆H₁₃), 67.66 (C-4), 61.73 (C-6), 31.73, 29.30, 29.02, 25.98, 22.59, 14.06 (OCH₂C₆H₁₃); HR-MS: m/z : calcd for C₁₉H₃₁FNao₈ [M+Na]⁺: 303.1584, found: 303.1585.

Heptyl 2-deoxy-2-chloro- α -D-mannopyranoside (13b): Prepared according to general procedure B from **12b** (30 mg, 0.07 mmol). Yield: 14 mg (67%) as a white solid. $[\alpha]_D = +60.9$ ($c = 0.6$, MeOH); $^1\text{H NMR}$ (500 MHz, MeOD): δ 4.94 (s, 1H, H-1), 4.22 (s, 1H, H-2), 4.02 (dd, $J = 8.9, 2.9$ Hz, 1H, H-3), 3.85 (d, $J = 11.7$ Hz, 1H, H-6a), 3.77 (dd, $J = 15.8, 6.9$ Hz, 1H, -OCH- of heptyl), 3.74 - 3.63 (m, 2H, H-4, H-6b), 3.63 - 3.56 (m, 1H, H-5), 3.47 (dd, $J = 15.6, 6.5$ Hz, 1H, -OCH- of heptyl), 1.62 (d, $J = 6.7$ Hz, 2H, CH₂), 1.45 - 1.28 (m, 8H, 4 CH₂), 0.93 (t, $J = 6.3$ Hz, 3H, CH₃); $^{13}\text{C NMR}$ (126 MHz, MeOD): δ 101.31 (C-1), 75.33 (C-5), 71.09 (C-3), 69.10 (CH₂), 68.35 (C-4), 63.24 (C-6), 62.86 (C-2), 32.99, 30.62, 30.25, 27.30, 23.70 (5 CH₂), 14.44 (CH₃); ESI-MS: m/z : calcd for C₁₃H₂₅ClNaO₅ [M+Na]⁺: 319.13, found: 318.86.

Heptyl 2-deoxy-2-bromo- α -D-mannopyranoside (13c): Prepared according to general procedure B from **12c** (60 mg, 0.13 mmol). Yield: 26 mg (60 %) as a white solid. $[\alpha]_D = +67.5$ ($c = 0.8$, MeOH); $^1\text{H NMR}$ (500 MHz, MeOD): δ 5.05 (s, 1H, H-1), 4.31 (dd, $J = 3.8, 1.3$ Hz, 1H, H-2), 3.88 - 3.82 (m, 2H, H-3, H-6a), 3.76 (dt, $J = 9.5, 6.7$ Hz, 1H, -OCH-), 3.73 - 3.60 (m, 3H, H-4, H-5, H-6b), 3.47 (dt, $J = 9.5, 6.4$ Hz, 1H, -OCH-), 1.67 - 1.58 (m, 2H, CH₂), 1.44 - 1.30 (m, 8H, 4 CH₂), 0.93 (t, $J = 7.0$ Hz, 3H, CH₃); $^{13}\text{C NMR}$ (126 MHz, MeOD): δ 101.54 (C-1), 75.46 (C-5), 70.53 (C-3), 69.18 (C-4), 69.15 (OCH₂), 62.90 (C-6), 56.66 (C-2), 33.00, 30.66, 30.25, 27.30, 23.70 (5 CH₂), 14.45 (CH₃); ESI-MS: m/z : calcd for C₁₃H₂₅BrNaO₅ [M+Na]⁺: 363.08, found: 362.94.

(R)-Methyl 2-(2,3,4,6-tetra-O-acetyl- α -D-mannopyranosyloxy)propanoate (16a):

Prepared according to general procedure C from **14** and methyl D-(+) lactate **15a**. Yield: 187 mg (83%) as yellow oil. $[\alpha]_D = +68.8$ ($c = 1.4$, EtOAc); $^1\text{H NMR}$ (500 MHz, CDCl_3): δ 5.42 - 5.34 (m, 2H, H-2, H-3), 5.28 (t, $J = 10.0$ Hz, 1H, H-4), 4.97 (s, 1H, H-1), 4.35 (d, $J = 7.0$ Hz, 1H, -CH(CH₃)-), 4.27 (dd, $J = 12.2, 5.5$ Hz, 1H, H-6b), 4.17 - 4.09 (m, 1H, H-6a), 4.00 (ddd, $J = 9.9, 5.4, 2.4$ Hz, 1H, H-5), 2.15, 2.10, 2.05, 2.00 (4s, 12H, 4 OAc), 1.48 (d, $J = 7.0$ Hz, 3H, CH₃); $^{13}\text{C NMR}$ (126 MHz, CDCl_3): δ 172.17, 170.73, 169.97, 169.91, 169.85 (5 C=O), 96.96 (C-1), 71.19 (-CH(CH₃)-), 69.50 (C-5), 69.22 (C-2), 68.95 (C-3), 66.41 (C-4), 62.65 (C-6), 52.40 (COOCH₃), 21.00, 20.83 (4 OAc), 18.56 (CH₃); ESI-MS: m/z : calcd for C₁₈H₂₆NaO₁₂ [M+Na]⁺: 457.13, found: 457.15.

(S)-Methyl 2-(2,3,4,6-tetra-O-acetyl- α -D-mannopyranosyloxy)propanoate (16b):

Prepared according to general procedure C from **14** and methyl L-(-) lactate **15b**. Yield: 165 mg (73%) as colorless oil. $[\alpha]_D = +24.9$ ($c = 2.8$, EtOAc); $^1\text{H NMR}$ (500 MHz, CDCl_3): δ 5.39 (dd, $J = 10.1, 3.4$ Hz, 1H, H-3), 5.32 (t, $J = 10.0$ Hz, 1H, H-4), 5.27 (dd, $J = 3.4, 1.8$ Hz, 1H, H-2), 4.90 (d, $J = 1.6$ Hz, 1H, H-1), 4.31 (ddd, $J = 9.9, 4.3, 2.1$ Hz, 1H, H-5), 4.26 (dd, $J = 12.3, 4.3$ Hz, 1H, H-6b), 4.16 (q, $J = 6.8$ Hz, 1H, -CH(Me)COOMe), 4.01 (dd, $J = 12.3, 2.1$ Hz, 1H, H-6a), 3.74 (s, 3H, COOCH₃), 2.16, 2.10, 2.05, 2.00 (4s, 12H), 1.44 (d, $J = 6.8$ Hz, 3H, CH₃); $^{13}\text{C NMR}$ (126 MHz, CDCl_3): δ 172.58, 170.76, 170.12, 169.91, 169.84 (5C, 4 OAc, COOMe), 98.41 (C-1), 74.81 (-CH(Me)COOMe), 69.84 (C-2), 69.20 (C-5), 69.08 (C-3), 65.93 (C-4), 62.20 (C-6), 52.23 (COOCH₃), 20.95, 20.82, 20.76 (4C, 4 OAc), 18.34 (CH₃); ESI-MS: m/z : calcd for C₁₈H₂₆NaO₁₂ [M+Na]⁺: 457.13, found: 457.15.

Methyl 1-(2,3,4,6-tetra-O-acetyl- α -D-mannopyranosyloxy)cyclopropanecarboxylate (16c):

Prepared according to general procedure C from **14** and methyl 1-hydroxycyclopropanecarboxylate **15c**. $[\alpha]_D = +33.4$ ($c = 0.7$, EtOAc); $^1\text{H NMR}$ (500 MHz, CDCl_3): δ 5.37-5.32 (m, 2H, H-2, H-3), 5.26 (t, $J = 9.9$ Hz, 1H, H-4), 5.10 (d, $J = 1.7$ Hz, 1H, H-1), 4.24 (dd, $J = 12.2, 5.9$ Hz, 1H, H-6b), 4.15 - 4.04 (m, 2H, H-5, H-6a), 3.74 (s, 3H, COOCH₃), 2.15, 2.10, 2.04, 2.00 (4s, 12H, 4 OAc), 1.49 (ddd, $J = 10.8, 7.9, 4.7$ Hz, 1H, H-cyclopropyl), 1.40 (ddd, $J = 10.4, 7.9, 4.9$ Hz, 1H, H-cyclopropyl), 1.32 - 1.27 (m, 1H, H-cyclopropyl), 1.19 (ddd, $J = 10.8, 8.0, 4.9$ Hz, 1H, H-cyclopropyl); $^{13}\text{C NMR}$ (126 MHz, CDCl_3): δ 172.83, 170.72, 170.06, 170.00, 169.89 (5 C=O), 98.90 (C-

1), 69.90 (C-2), 69.36 (C-5), 68.84 (C-3), 66.35 (C-4), 62.77 (C-6), 52.63 (COOCH₃), 21.04, 20.84 (4 OAc), 16.27, 15.60 (C-cyclopropyl); ESI-MS: *m/z*: calcd for C₁₉H₂₆NaO₁₂ [M+Na]⁺: 469.13, found: 469.11.

(R)-Methyl 2-(2,3:4,6-bis-O-methylethylidene- α -D-mannopyranosyloxy)propanoate

(17a): Prepared according to general procedure D from **16a** (200 mg, 0.46 mmol). Yield: 99 mg (62%) as colorless oil. [α]_D = +15.3 (*c* = 1.5, EtOAc); ¹H NMR (500 MHz, CDCl₃): δ 5.15 (s, 1H, H-1), 4.38 (q, *J* = 7.0 Hz, 1H, -CH(CH₃)-), 4.29 (d, *J* = 5.6 Hz, 1H, H-2), 4.17 (dd, *J* = 8.0, 5.6 Hz, 1H, H-3), 3.87 (dd, *J* = 10.8, 5.6 Hz, 1H, H-6b), 3.79 - 3.71 (m, 5H, H-4, H-6a, COOCH₃), 3.62 - 3.53 (m, 1H, H-5), 1.55, 1.52, (2s, 2 CH₃), 1.43 (d, *J* = 7.0 Hz, 6H, 2 CH₃), 1.36 (s, 3H, CH₃); ¹³C NMR (126 MHz, CDCl₃): δ 172.85 (C=O), 109.63, 100.13, 99.88, 96.99 (C-1), 75.97 (C-2), 74.75 (C-3), 72.81 (C-4), 70.30 (-CH(CH₃)-), 62.11(C-5), 62.04 (C-6), 52.26 (COOCH₃), 29.15, 28.30, 26.29, 18.88, 18.84 (5 CH₃); ESI-MS: *m/z*: calcd for C₁₆H₂₆NaO₈ [M+Na]⁺: 369.15, found: 369.04.

(S)-Methyl 2-(2,3:4,6-bis-O-methylethylidene- α -D-mannopyranosyloxy)propanoate

(17b): Prepared according to general procedure D from **16b** (160 mg, 0.37 mmol). Yield: 103 mg (81%) as yellow oil. [α]_D = -25.3 (*c* = 1.3, EtOAc); ¹H NMR (500 MHz, CDCl₃): δ 5.08 (s, 1H, H-1), 4.25 - 4.09 (m, 4H), 3.78 - 3.63 (m, 7H), 1.54 (s, 3H), 1.50 (s, 3H), 1.45 - 1.39 (m, 6H), 1.35 (s, 3H); ¹³C NMR (126 MHz, CDCl₃): δ 173.14 (C=O), 109.50, 99.74, 98.63 (C-1), 76.27 (C-2), 75.06 (C-3), 73.63 (C-4), 72.55 (-CH(CH₃)-), 62.18 (C-5), 61.94 (C-6), 52.23 (COOCH₃), 29.14, 28.26, 26.23, 18.96, 18.19 (5 CH₃); ESI-MS: *m/z*: calcd for C₁₆H₂₆NaO₈ [M+Na]⁺: 369.15, found: 368.80.

Methyl

1-(2,3:4,6-bis-O-methylethylidene- α -D-

mannopyranosyloxy)cyclopropanecarboxylate (17c): Prepared according to general procedure D from **16c** (175 mg, 0.39 mmol). Yield: 96 mg (68 %) as colorless oil. [α]_D = +61.1 (*c* = 1.4, EtOAc); ¹H NMR (500 MHz, CDCl₃): δ 5.27 (s, 1H, H-1), 4.30 (d, *J* = 5.6 Hz, 1H, H-2), 4.15 (dd, *J* = 7.6, 5.7 Hz, 1H, H-3), 3.80 (dd, *J* = 10.0, 5.0 Hz, 1H, H-6b), 3.74 (s, 3H, COOCH₃), 3.73 - 3.61 (m, 3H, H-4, H-5, H-6a), 1.55 (s, 3H, CH₃), 1.51 (s, 3H, CH₃), 1.45 - 1.35 (m, 8H, 2H from cyclopropyl and 2 CH₃), 1.33 - 1.28 (m, 1H, cyclopropyl), 1.19 - 1.14 (m, 1H, cyclopropyl); ¹³C NMR (126 MHz, CDCl₃): δ 173.21

(C=O), 109.51, 99.78, 99.08 (C-1), 76.32 (C-2), 74.90 (C-3), 72.62 (C-4), 62.40 (C-5), 62.04 (C-6), 60.10, 52.50 (COOCH₃), 29.14, 28.27, 26.30, 18.90, 16.78, 15.01 (2 -CH₂- and 4 CH₃); ESI-MS: *m/z*: calcd for C₁₇H₂₆NaO₈ [M+Na]⁺: 381.15, found: 381.09.

(R)-2-(α-D-Mannopyranosyloxy)propanal (deprotected 18a): Prepared according to general procedure E and F from **17a** (84 mg). Yield: 28 mg (49% for two steps) as white solid. [α]_D = +90.4 (*c* = 0.7, MeOH); ¹H NMR (500 MHz, CDCl₃): δ 5.08 (d, *J* = 1.4 Hz, 1H, H-1), 4.96 (d, *J* = 4.3 Hz, 1H, -CH(CH₃-), 4.00 (dd, *J* = 3.3, 1.7 Hz, 1H, H-2), 3.91 (d, *J* = 10.0 Hz, 1H, H-6b), 3.84 (dd, *J* = 9.6, 3.4 Hz, 1H, H-3), 3.83-3.73 (m, 3H, H-4, H-5, H-6a), 3.66 (t, *J* = 9.6 Hz, 1H, -CH(OH)₂-), 1.25 (d, *J* = 6.5 Hz, 3H, CH₃); ¹³C NMR (126 MHz, CDCl₃): δ 100.67 (C-1), 91.38 (-CH(CH₃-), 76.65 (C-5), 73.08 (C-4), 70.40 (C-3), 70.13 (C-2), 66.84 (-CH(OH)₂-), 60.99 (C-6), 15.41 (CH₃); ESI-MS: *m/z*: calcd for C₉H₁₆NaO₇ [M+Na]⁺: 259.08, found: 258.91.

(S)-2-(2,3:4,6-Bis-O-methylethylidene-α-D-mannopyranosyloxy)propanal (18b): Prepared according to general procedure E from **17b** (70 mg). Yield: 45 mg (71%) as colorless oil. [α]_D = -9.4 (*c* = 1.1, EtOAc); ¹H NMR (500 MHz, CDCl₃): δ 9.60 (d, *J* = 1.7 Hz, 1H, CHO), 5.13 (s, 1H, C-1), 4.25 (d, *J* = 5.8 Hz, 1H), 4.20 (dd, *J* = 7.6, 5.9 Hz, 1H), 4.04 (qd, *J* = 6.9, 1.7 Hz, 1H), 3.83 - 3.77 (m, 1H), 3.77 - 3.71 (m, 1H), 3.71 - 3.62 (m, 2H), 1.54, 1.50, 1.42, 1.36 (4s, 12H, 4 CH₃), 1.31 (d, *J* = 6.9 Hz, 3H, CH₃); ¹³C NMR (126 MHz, CDCl₃): δ 201.33 (CHO), 109.66, 100.12, 99.87, 97.91 (C-1), 78.80, 76.16, 74.93, 72.51, 62.25, 61.76, 29.12, 28.22, 26.20, 18.88, 14.84; ESI-MS: *m/z*: calcd for C₁₅H₂₄NaO₇ [M+Na]⁺: 339.14, found: 339.02.

(1-(2,3:4,6-Bis-O-methylethylidene-α-D-mannopyranosyloxy)cyclopropyl)

methanol (20): Prepared according to general procedure E from **17c** (72 mg, 0.2 mmol). Yield: 56 mg (85%) as a white solid. [α]_D = +13.0 (*c* = 0.5, EtOAc); ¹H NMR (500 MHz, CDCl₃): δ 5.21 (d, *J* = 0.4 Hz, 1H, H-1), 4.15 (t, *J* = 6.4 Hz, 1H, H-3), 4.03 (dd, *J* = 5.7, 1.0 Hz, 1H, H-2), 3.90 (dd, *J* = 8.3, 6.3 Hz, 2H, H-6a, -CHOH), 3.82 - 3.70 (m, 3H, H-4, H-5, H-6b), 3.34 (dd, *J* = 12.6, 8.5 Hz, 1H, -CHOH), 2.94 (d, *J* = 6.7 Hz, 1H, -OH), 1.53, 1.51, 1.42, 1.33 (4 s, 12H, 4 CH₃), 1.00 (dd, *J* = 11.0, 5.4 Hz, 1H), 0.91 - 0.81 (m, 1H), 0.75 (ddd, *J* = 10.1, 6.7, 5.7 Hz, 1H), 0.67 (ddd, *J* = 10.1, 6.4, 5.1 Hz, 1H) (4 *H* on cyclopropyl); ¹³C NMR (126 MHz, CDCl₃): δ 109.72, 100.13, 99.88, 98.28 (C-1), 76.68

(C-2), 75.01 (C-3), 72.53 (C-5), 67.91 (-CH₂OH), 65.26, 62.65 (C-4), 61.90 (C-6), 29.12, 28.19, 26.21, 18.89 (4 CH₃), 13.14, 10.04 (2C on cyclopropyl); ESI-MS: *m/z*: calcd for C₁₆H₂₆NaO₇ [M+Na]⁺: 353.16, found: 353.12.

1-(2,3:4,6-Bis-*O*-methylethylidene- α -D-

mannopyranosyloxy)cyclopropanecarbaldehyde (21): To a solution of oxalyl chloride (10 μ L, 0.12 mmol) in CH₂Cl₂ (1 mL) cooled at -78 ° C was added dropwise a solution of DMSO (7.6 μ L, 0.11 mmol) in CH₂Cl₂ (0.5 mL). After 5 min, a solution of **20** (32 mg, 0.10 mmol) in CH₂Cl₂ (0.5 mL) was added. The reaction mixture was then stirred for 15 min at -78 °C and triethylamine (67 μ L, 0.49 mmol) was added. After 10 min at -78 °C, the mixture was allowed to warm to RT and diluted with CH₂Cl₂ (20 mL). The organic layer was successively washed with a saturated aqueous solution of NH₄Cl (10 mL) and brine (10 mL). The combined organic extracts were dried over Na₂SO₄, and concentrated in vacuo. The residue was purified by MPLC on silica gel (PE/EtOAc 2:1) to give **21** (29 mg, 94%) as yellow oil. [α]_D = +44.3 (*c* = 0.5, EtOAc); ¹H NMR (500 MHz, CDCl₃): δ 9.36 (s, 1H, CHO), 5.15 (s, 1H, H-1), 4.23 (d, *J* = 5.8 Hz, 1H, H-2), 4.17 (t, *J* = 6.5 Hz, 1H, H-3), 3.88 - 3.81 (m, 1H, H-6a), 3.73 (tt, *J* = 19.8, 7.7 Hz, 3H, H-4, H-5, H-6b), 1.58 - 1.28 (m, 16H, 4 CH₃, 2 CH₂); ¹³C NMR (126 MHz, CDCl₃): δ 199.56 (CO), 109.54, 99.73, 99.03 (C-1), 76.09 (C-2), 74.81 (C-3), 72.37 (C-5), 67.71 (C-4), 62.49 (C-6), 61.72, 29.00, 28.09, 26.10, 18.76, 17.88, 14.53; ESI-MS: *m/z*: calcd for C₁₆H₂₄NaO₇ [M+Na]⁺: 351.14, found: 351.09.

(*R,E*)-*N'*-(2-(α -D-Mannopyranosyloxy)propylidene)benzohydrazide (19a): Prepared according to general procedure F from **18a** (5 mg, 0.02 mmol). Yield: 4.8 mg (87%). [α]_D = +158.7 (*c* = 0.2, MeOH); ¹H NMR (500 MHz, MeOD): δ 7.90 (d, *J* = 7.4 Hz, 2H, H-Ar), 7.70 (d, *J* = 6.0 Hz, 1H, H-Ar), 7.61 (t, *J* = 7.4 Hz, 1H, H-Ar), 7.52 (t, *J* = 7.6 Hz, 2H, H-Ar), 4.98 (s, 1H, H-1), 4.53 - 4.43 (m, 1H, -CH(CH₃-), 3.91 - 3.80 (m, 2H, H-2, H-6b), 3.77 - 3.69 (m, 2H, H-3, H-6a), 3.67-3.60 (m, 2H, H-4, H-5), 1.42 (d, *J* = 6.5 Hz, 3H, CH₃); ¹³C NMR (126 MHz, MeOD): δ 154.72 (CHO), 133.32, 129.73, 128.72 (6C, Ar), 101.10 (C-1), 75.31 (C-5), 75.12 (-CH(CH₃-), 72.47 (C-2), 72.34 (C-3), 68.58 (C-4), 62.96 (C-6), 18.55 (CH₃); ESI-MS: *m/z*: calcd for C₁₆H₂₂N₂NaO₇ [M+Na]⁺: 377.13, found 377.02.

(*S,E*)-*N'*-(2-(α -D-Mannopyranosyloxy)propylidene)benzohydrazide (19b): Prepared according to general procedure F from **18b** (5 mg, 0.02 mmol). Yield: 5.2 mg (90%). $[\alpha]_D = +32.9$ ($c = 0.4$, MeOH); $^1\text{H NMR}$ (500 MHz, D_2O): δ 7.76 (d, $J = 7.4$ Hz, 2H, Ar), 7.64 - 7.54 (m, 2H, Ar, CHO), 7.49 (dd, $J = 16.0, 8.2$ Hz, 2H, Ar), 4.90 (s, 1H, H-1), 4.51 (p, $J = 6.5$ Hz, 1H, $\text{CH}(\text{CH}_3)\text{CHO}$), 3.91 (dd, $J = 3.2, 1.7$ Hz, 1H, H-2), 3.90 - 3.83 (m, 1H, H-6a), 3.79 (dd, $J = 9.3, 3.4$ Hz, 1H, H-3), 3.71 (dd, $J = 12.1, 6.1$ Hz, 1H, H-6b), 3.68 - 3.55 (m, 2H, H-5, H-4), 1.38 (d, $J = 6.7$ Hz, 3H, CH_3); $^{13}\text{C NMR}$ (126 MHz, D_2O): δ 153.53 (CHO), 132.86, 128.91, 127.54 (6C, Ar), 97.76 (C-1), 73.19 (C-5), 71.13 ($\text{CH}(\text{CH}_3)\text{CHO}$), 70.41 (C-3), 70.03 (C-2), 66.80 (C-4), 61.00 (C-6), 18.17 (CH_3); ESI-MS: m/z : calcd for $\text{C}_{16}\text{H}_{22}\text{N}_2\text{NaO}_7$ $[\text{M}+\text{Na}]^+$: 377.13, found 377.04.

(*E*)-*N'*-((1- α -D-Mannopyranosyloxycyclopropyl)methylene)benzohydrazide (22): Prepared according to general procedure F from **21** (25 mg, 0.07 mmol). Yield: 3 mg (11%). $[\alpha]_D = +70.8$ ($c = 0.2$, MeOH); $^1\text{H NMR}$ (500 MHz, CDCl_3): δ 7.70 (dd, $J = 28.9, 6.7$ Hz, 5H), 7.63 - 7.53 (m, 2H), 7.48 (dt, $J = 12.5, 7.7$ Hz, 4H), 5.12 (d, $J = 1.5$ Hz, 1H, H-1), 4.05 - 3.99 (m, 1H, H-2), 3.81 (d, $J = 9.9$ Hz, 1H, H, H-4), 3.78 - 3.65 (m, 3H, H-3, H-5, H-6a), 3.60 (dd, $J = 12.7, 6.5$ Hz, 1H, H-6b), 1.60 - 1.49 (m, 1H), 1.34 - 1.17 (m, 2H), 1.17 - 1.05 (m, 1H); $^{13}\text{C NMR}$ (126 MHz, D_2O): δ 167.29 (CO), 156.01, 132.68, 132.21, 128.88, 128.82, 127.44, 126.98 (C-Ar), 100.74 (C-1), 73.50 (C-5), 70.23 (C-3), 70.18 (C-2), 66.69 (C-4), 61.44 ($=\text{C}(\text{COOMe})\text{O}-$), 60.95 (C-6), 15.21, 12.98 (2 CH_2); ESI-MS: m/z : calcd for $\text{C}_{17}\text{H}_{22}\text{N}_2\text{NaO}_7$ $[\text{M}+\text{Na}]^+$: 389.13, found: 389.00.

(*1S,3S*)-Methyl 3-(2,3,4,6-tetra-*O*-benzoyl- α -D-mannopyranosyloxy)cyclobutanecarboxylate (25a): Prepared according to general procedure G from **23** (337 mg, 0.51 mmol) and cyclobutanecarboxylate **24a** (100 mg, 0.77 mmol). Yield: 250 mg (69%) as colorless oil. $[\alpha]_D = +37.9$ ($c = 1.0$, EtOAc); $^1\text{H NMR}$ (500 MHz, CDCl_3): δ 8.15 - 8.07 (m, 2H, Ar), 8.08 - 8.03 (m, 2H, Ar), 8.01 - 7.94 (m, 2H, Ar), 7.88 - 7.80 (m, 2H, Ar), 7.58 (dd, $J = 16.5, 7.6$ Hz, 2H, Ar), 7.50 (t, $J = 7.4$ Hz, 1H, Ar), 7.45 - 7.32 (m, 7H, Ar), 7.26 (t, $J = 7.8$ Hz, 2H, Ar), 6.13 (t, $J = 9.8$ Hz, 1H, H-4), 5.93 (dd, $J = 10.1, 3.3$ Hz, 1H, H-3), 5.67 (dd, $J = 3.0, 1.9$ Hz, 1H, H-2), 5.12 (d, $J = 1.5$ Hz, 1H, H-1), 4.67 (dd, $J = 13.8, 4.0$ Hz, 1H, H-6a), 4.54 - 4.45 (m, 2H, H-6b, H-5), 4.23 (t, $J = 7.1$ Hz, 1H, $\text{OCH}(\text{CH}_2)_2$), 2.74 - 2.55 (m, 3H, cyclobutyl), 2.47 (ddd, $J = 18.1, 13.7, 5.2$ Hz, 2H, cyclobutyl); $^{13}\text{C NMR}$ (126 MHz, CDCl_3): δ 174.46, 170.69, 170.12,

169.95, 169.83 (5 CO), 96.77 (C-1), 69.75 (C-2), 69.02 (C-3), 69.00 (C-5), 68.39 (OCH(CH₂)₂), 66.31 (C-4), 62.60 (C-6), 52.05 (COOCH₃), 34.72, 33.83, 29.33 (3 C-cyclobutyl); ESI-MS: *m/z*: calcd for C₄₀H₃₆NaO₁₂ [M+Na]⁺: 731.21, found: 731.27.

(1*S*,4*S*)-Ethyl**4-(2,3,4,6-tetra-*O*-benzoyl- α -D-**

mannopyranosyloxy)cyclohexanecarboxylate (25b): Prepared according to general procedure G from **23** (400 mg, 0.61 mmol) and cyclohexanecarboxylate **24b** (157 mg, 0.91 mmol). Yield: 354 mg (78%). [α]_D = -35.8 (*c* = 1.9, EtOAc); ¹H NMR (500 MHz, CDCl₃): δ 8.08 (ddd, *J* = 12.2, 8.2, 1.2 Hz, 4H, Ar), 7.98 (dd, *J* = 8.3, 1.1 Hz, 2H, Ar), 7.84 (dd, *J* = 8.3, 1.2 Hz, 2H, Ar), 7.64 - 7.23 (m, 12H, Ar), 6.09 (dd, *J* = 12.5, 7.5 Hz, 1H, H-4), 5.93 (dd, *J* = 10.1, 3.3 Hz, 1H, H-3), 5.66 (dd, *J* = 3.2, 1.8 Hz, 1H, H-2), 5.21 (d, *J* = 1.7 Hz, 1H, H-1), 4.67 (dt, *J* = 3.7, 3.1 Hz, 1H, H-6a), 4.54 - 4.45 (m, 2H, H-5, H-6b), 4.23 - 4.14 (m, 2H, COOCH₂CH₃), 3.95 - 3.86 (m, 1H, OCH(CH₂)₂), 2.46 - 1.60 (m, 9H, cyclohexyl), 1.30 (t, *J* = 7.1 Hz, 3H, COOCH₂CH₃); ¹³C NMR (126 MHz, CDCl₃): δ 174.98, 166.18, 165.58, 165.53, 165.48 (5CO), 133.45, 133.15, 133.06, 129.88, 129.86, 129.74, 129.42, 129.16, 129.00, 128.59, 128.44, 128.43, 128.31 (Ar), 96.32 (C-1), 74.13 (OCH(CH₂)₂), 71.18 (C-2), 70.12 (C-3), 69.13 (C-5), 67.12 (C-4), 63.05 (C-6), 60.38 (CO₂CH₂CH₃), 41.20 (CH(CH₂)₂(CO₂)), 30.51, 28.64, 24.26, 24.04 (4C on cyclohexyl), 14.30 (CO₂CH₂CH₃); ESI-MS: *m/z*: calcd for C₄₃H₄₂NaO₁₂ [M+Na]⁺: 773.26, found: 773.45.

(1*R*,4*R*)-Ethyl**4-(2,3,4,6-tetra-*O*-benzoyl- α -D-**

mannopyranosyloxy)cyclohexanecarboxylate (25c): Prepared according to general procedure G from **23** (382 mg, 0.58 mmol) and cyclohexanecarboxylate **25c** (100 mg, 0.58 mmol). Yield: 328 mg (75%). [α]_D = -33.3 (*c* = 1.0, EtOAc); ¹H NMR (500 MHz, CDCl₃): δ 8.07 (ddd, *J* = 10.6, 8.2, 1.1 Hz, 4H, Ar), 7.97 (dd, *J* = 8.3, 1.1 Hz, 2H, Ar), 7.83 (dd, *J* = 8.3, 1.1 Hz, 2H, Ar), 7.64 - 7.20 (m, 14H, Ar), 6.05 (t, *J* = 10.0 Hz, 1H, H-4), 5.92 (dd, *J* = 10.1, 3.3 Hz, 1H, H-3), 5.64 (dd, *J* = 3.2, 1.8 Hz, 1H, H-2), 5.25 (d, *J* = 1.7 Hz, 1H, H-1), 4.72 - 4.63 (m, 1H, H-6a), 4.56 - 4.43 (m, 2H, H-5, H-6b), 4.13 (q, *J* = 7.1 Hz, 2H, COOCH₂CH₃), 3.71 (td, *J* = 10.1, 5.0 Hz, 1H, OCH(CH₂)₂), 2.28 (ddd, *J* = 14.8, 7.4, 3.6 Hz, 1H, CH(CH₂)₂(CHO)), 2.23 - 1.37 (m, 10H, cyclohexyl), 1.26 (t, *J* = 7.1 Hz, 3H, COOCH₂CH₃); ¹³C NMR (126 MHz, CDCl₃): δ 175.42, 166.31, 165.69 (5CO), 133.62, 133.59, 133.32, 133.26, 130.00, 129.98, 129.88, 129.84, 129.51, 129.26,

129.13, 128.74, 128.61, 128.59, 128.45 (Ar), 96.24 (C-1), 76.69 (OCH(CH₂)₂), 71.26 (C-2), 70.23 (C-3), 69.17 (C-5), 67.32 (C-4), 63.27 (C-6), 60.47 (CO₂CH₂CH₃), 42.30 (CH(CH₂)₂(CO₂)), 32.48, 30.80, 27.17, 27.04 (4C on cyclohexyl), 14.38 (CO₂CH₂CH₃); ESI-MS: *m/z*: calcd for C₄₃H₄₂NaO₁₂ [M+Na]⁺: 773.26, found: 773.45.

(1*S*,3*S*)-Methyl 3-(2,3:4,6-bis-*O*-methylethylidene- α -D-mannopyranosyloxy)cyclobutanecarboxylate (26a): Prepared according to general procedure D from **25a** (290 mg, 0.41 mmol). Yield: 132 mg (86%). [α]_D = + 15.2 (*c* = 1.1, EtOAc); ¹H NMR (500 MHz, CDCl₃): δ 5.02 (s, 1H, H-1, H-1), 4.15 (d, *J* = 3.0 Hz, 2H, H-2, H-3), 4.12 - 4.03 (m, 1H, H-cyclobutyl), 3.82 (dd, *J* = 10.7, 5.6 Hz, 1H, H-6a), 3.77 - 3.65 (m, 5H, H-4, H-5, COOCH₃), 3.59 (td, *J* = 10.2, 5.6 Hz, 1H, H-6b), 2.72 - 2.59 (m, 1H, H-cyclobutyl), 2.59 - 2.45 (m, 2H, H-cyclobutyl), 2.36 - 2.21 (m, 2H, H-cyclobutyl), 1.54, 1.51, 1.43, 1.35 (4 s, 12H, 4 CH₃); ¹³C NMR (126 MHz, CDCl₃): δ 174.57 (CO), 109.43, 99.68, 96.87 (C-1), 76.05 (C-2), 74.85 (C-3), 72.68 (C-5), 67.33 (C-cyclobutyl), 61.92 (C-4), 61.63 (C-6), 51.91 (COOCH₃), 35.06, 33.51, 29.40 (3 C-cyclobutyl), 29.05, 28.17, 26.12, 18.77 (4 CH₃); ESI-MS: *m/z*: calcd for C₁₈H₂₈NaO₈ [M+Na]⁺: 395.17, found: 395.03.

(1*S*,4*S*)-Methyl 4-(2,3:4,6-bis-*O*-methylethylidene- α -D-mannopyranosyloxy)cyclohexanecarboxylate (26b): Prepared according to general procedure D from **25b** (438 mg, 0.58 mmol). Yield: 140 mg (60%). [α]_D = + 14.4 (*c* = 1.7, EtOAc); ¹H NMR (500 MHz, CDCl₃): δ 5.11 (s, 1H, H-1), 4.21 - 4.09 (m, 2H, H-2, H-3), 3.87 - 3.79 (m, 2H, H-6a, OCH(CH₂)₂), 3.77 - 3.69 (m, 2H, H-4, H-5), 3.67 (s, 3H, COOCH₃), 3.60 (td, *J* = 10.2, 5.6 Hz, 1H, H-6b), 2.41 - 2.31 (m, 1H, CH(CH₂)₂(CO₂)), 1.93 - 1.44 (m, 14H, cyclohexyl, 2CH₃), 1.42 (s, 3H, CH₃), 1.35 (s, 3H, CH₃); ¹³C NMR (126 MHz, CDCl₃): δ 175.77 (CO), 109.37 (C(O)₂(CH₃)₂), 99.69 (C(O)₂(CH₃)₂), 95.70 (C-1), 76.60 (C-3), 74.88 (C-2), 72.89 (C-4), 71.01 (OCH(CH₂)₂), 62.08 (C-5), 61.43 (C-6), 51.61 (COOCH₃), 41.57 (CH(CH₂)₂(CO₂)), 30.68 (1C on cyclohexyl), 29.06 (CH₃), 28.24 (CH₃), 27.88 (1C on cyclohexyl), 26.23 (CH₃), 23.94, 23.60 (2C on cyclohexyl), 18.79 (CH₃); ESI-MS: *m/z*: calcd for C₂₀H₃₂NaO₈ [M+Na]⁺: 423.20, found: 423.19.

(1*R*,4*R*)-Methyl 4-(2,3:4,6-bis-*O*-methylethylidene- α -D-mannopyranosyloxy)cyclohexanecarboxylate (26c): Prepared according to general

procedure D from **25c** (300 mg, 0.40 mmol). Yield: 89 mg (56%). $[\alpha]_D = +37.0$ ($c = 1.7$, EtOAc); $^1\text{H NMR}$ (500 MHz, CDCl_3): δ 5.15 (s, 1H, H-1), 4.17 - 4.08 (m, 2H, H-2, H-3), 3.85 (dt, $J = 7.6, 3.8$ Hz, 1H, H-6a), 3.77 - 3.70 (m, 2H, H-4, H-5), 3.66 (s, 3H, COOCH_3), 3.64 - 3.53 (m, 2H, H-6b, $\text{OCH}(\text{CH}_2)_2$), 2.31 - 2.22 (m, 1H, $\text{CH}(\text{CH}_2)_2(\text{CO}_2)$), 2.10 - 1.94 (m, 4H, cyclohexyl), 1.58 - 1.20 (m, 16H, 4 CH_3 , 4H on cyclohexyl); $^{13}\text{C NMR}$ (126 MHz, CDCl_3): δ 175.78 (CO), 109.38 ($\text{C}(\text{O})_2(\text{CH}_3)_2$), 99.70 ($\text{C}(\text{O})_2(\text{CH}_3)_2$), 95.85 (C-1), 76.54 (C-3), 74.89 (C-2), 74.56 ($\text{OCH}(\text{CH}_2)_2$), 72.86 (C-4), 62.07 (C-5), 61.43 (C-6), 51.63 (COOCH_3), 42.09 ($\text{CH}(\text{CH}_2)_2(\text{CO}_2)$), 32.39, 30.34 (2C on cyclohexyl), 29.08 (CH_3), 28.21 (CH_3), 27.09, 26.85 (2C on cyclohexyl), 26.18 (CH_3), 18.79 (CH_3); ESI-MS: m/z : calcd for $\text{C}_{20}\text{H}_{32}\text{NaO}_8$ $[\text{M}+\text{Na}]^+$: 423.20, found: 423.31.

(1*S*,3*S*)-3-(2,3:4,6-Bis-*O*-methylethylidene- α -D-

mannopyranosyloxy)cyclobutanecarbaldehyde (27a): Prepared according to general procedure E from **26a** (132 mg, 0.35 mmol). Yield: 90 mg (74%). $[\alpha]_D = +63.9$ ($c = 0.7$, DCM/MeOH 2:1); $^1\text{H NMR}$ (500 MHz, CDCl_3): δ 9.68 (d, $J = 2.4$ Hz, 1H, -CHO), 5.03 (s, 1H, H-1), 4.21 (t, $J = 7.5$ Hz, 1H, H-cyclobutyl), 4.16 - 4.10 (m, 2H, H-2, H-3), 3.83 (dd, $J = 10.8, 5.7$ Hz, 1H, H-6a), 3.79 - 3.68 (m, 2H, H-4, H-5), 3.63 - 3.52 (m, 1H, H-6b), 2.82 - 2.70 (m, 1H, H-cyclobutyl), 2.47 (dtd, $J = 9.9, 7.5, 2.7$ Hz, 2H, H-cyclobutyl), 2.24 (tdd, $J = 11.6, 6.8, 4.9$ Hz, 2H, H-cyclobutyl), 1.54, 1.51, 1.43, 1.35 (4 s, 12H, 4 CH_3); $^{13}\text{C NMR}$ (126 MHz, CDCl_3): δ 173.14 (C=O), 109.50, 99.74, 98.63 (C-1), 76.27 (C-2), 75.06 (C-3), 73.63 (C-5), 72.55 (C-cyclobutyl), 62.18 (C-4), 61.94 (C-6), 52.23 (COOCH_3), 29.14, 28.26, 26.23 (C-cyclobutyl), 18.96, 18.19 (4 CH_3); ESI-MS: m/z : calcd for $\text{C}_{17}\text{H}_{26}\text{NaO}_7$ $[\text{M}+\text{Na}]^+$: 365.16, found: 364.96.

(1*S*,4*S*)-4-(2,3:4,6-Bis-*O*-methylethylidene- α -D-

mannopyranosyloxy)cyclohexanecarbaldehyde (27b): Prepared according to general procedure E from **26b** (140 mg, 0.35 mmol). Yield: 70 mg (54%). $[\alpha]_D = +16.0$ ($c = 3.5$, EtOAc); $^1\text{H NMR}$ (500 MHz, CDCl_3): δ 9.66 (s, 1H, CHO), 5.14 (s, 1H, C-1), 4.22 - 4.11 (m, 2H, H-2, H-3), 3.92 - 3.81 (m, 2H, H-6a, $\text{OCH}(\text{CH}_2)_2$), 3.80 - 3.72 (m, 2H, H-4, H-5), 3.61 (td, $J = 10.3, 5.6$ Hz, 1H, H-6b), 2.35 - 2.26 (m, 1H, $\text{CH}(\text{CH}_2)_2(\text{CHO})$), 1.93 - 1.51 (m, 14H, 2 CH_3 , 8H on cyclohexyl), 1.45 (s, 3H, CH_3), 1.38 (s, 3H, CH_3); $^{13}\text{C NMR}$ (126 MHz, CDCl_3): δ 204.29 (CHO), 109.40 ($\text{C}(\text{O})_2(\text{CH}_3)_2$), 99.71 ($\text{C}(\text{O})_2(\text{CH}_3)_2$), 95.70 (C-1), 76.55 (C-3), 74.87 (C-2), 72.84 (C-4), 71.45 ($\text{OCH}(\text{CH}_2)_2$), 62.06 (C-5), 61.48 (C-

6), 48.31 (CH(CH₂)₂(CHO)), 30.44 (C on cyclohexyl), 29.05 (CH₃), 28.22 (CH₃), 27.71 (C on cyclohexyl), 26.21 (CH₃), 21.32, 20.99 (2C on cyclohexyl), 18.78 (CH₃); ESI-MS: *m/z*: calcd for C₁₉H₃₀NaO₇ [M+Na]⁺: 393.19, found: 393.08.

(1*R*,4*R*)-4-(2,3:4,6-Bis-*O*-methylethylidene- α -D-

mannopyranosyloxy)cyclohexanecarbaldehyde (27c): Prepared according to general procedure E from **26c** (70 mg, 0.18 mmol). Yield: 64 mg (98%). [α]_D = + 22.8 (*c* = 2.3, EtOAc); ¹H NMR (500 MHz, CDCl₃): δ 9.61 (d, *J* = 1.1 Hz, 1H, CHO), 5.13 (s, 1H, H-1), 4.14 - 4.09 (m, 2H, H-2, H-3), 3.83 (dd, *J* = 10.8, 5.6 Hz, 1H, H-6a), 3.75 - 3.67 (m, 2H, H-4, H-6b), 3.64 - 3.52 (m, 2H, H-5, OCH(CH₂)₂), 2.24 - 2.15 (m, 1H, CH(CH₂)₂(CHO)), 2.07 - 1.94 (m, 4H, cyclohexyl), 1.52, 1.49 (2s, 6H, 2CH₃), 1.44 - 1.28 (m, 10H, 2CH₃ and cyclohexyl); ¹³C NMR (126 MHz, CDCl₃): δ 203.74 (CHO), 109.37 (C(O)₂(CH₃)₂), 99.68 (C(O)₂(CH₃)₂), 95.90 (C-1), 76.51 (C-3), 74.86 (C-2), 74.38 (C-4), 72.81 (OCH(CH₂)₂), 62.03 (C-5), 61.47 (C-6), 48.89 (CH(CH₂)₂(CHO)), 31.84, 29.75 (2C on cyclohexyl), 29.06, 28.20, 26.17 (3CH₃), 23.77, 23.52 (2C on cyclohexyl), 18.77 (CH₃); ESI-MS: *m/z*: calcd for C₁₉H₃₀NaO₇ [M+Na]⁺: 393.19, found: 393.22.

(*E*)-*N*'-((1*S*,3*S*)-3-(α -D-Mannopyranosyloxycyclobutyl)methylene)benzohydrazide

(28a): Prepared according to general procedure F from **27a** (25 mg, 0.09 mmol). Yield: 10 mg (28%). [α]_D = + 28.3 (*c* = 0.6, MeOH); ¹H NMR (500 MHz, D₂O): δ 7.72 (d, *J* = 7.6 Hz, 2H), 7.69 - 7.64 (m, 1H), 7.56 (dt, *J* = 15.1, 7.4 Hz, 1H), 7.47 (dd, *J* = 16.8, 8.8 Hz, 2H), 4.84 (s, 1H), 4.22 (t, *J* = 7.4 Hz, 1H), 3.85 (s, 1H), 3.83 - 3.78 (m, 1H), 3.71 (ddd, *J* = 17.5, 10.5, 4.4 Hz, 2H), 3.65 - 3.56 (m, 2H), 2.80 - 2.70 (m, 1H), 2.52 (dt, *J* = 11.4, 6.8 Hz, 2H), 2.17 - 2.02 (m, 2H); ¹³C NMR (126 MHz, D₂O): δ 158.05 (CO), 132.64, 132.20, 128.85, 128.81, 127.43, 126.97 (C-Ar), 98.81 (C-1), 73.05 (C-5), 70.46 (C-3), 70.08 (C-2), 68.33 (-CH(CH₂)₂-), 66.71 (C-4), 60.86 (C-6), 34.67, 33.53, 27.88 (3 CH₂); ESI-MS: *m/z*: calcd for C₁₈H₂₄N₂NaO₇ [M+Na]⁺: 403.15, found: 403.10.

(*E*)-*N*'-((1*S*,4*S*)-4-(α -D-Mannopyranosyloxycyclohexyl)methylene)benzohydrazide

(28b): Prepared according to general procedure F from **27b** (18 mg, 0.05 mmol). Yield: 7 mg (37%). [α]_D = + 41.1 (*c* = 1.6, MeOH); ¹H NMR (500 MHz, MeOD): δ 7.89 (d, *J* = 7.4 Hz, 2H, Ar), 7.61 (dd, *J* = 17.3, 6.6 Hz, 2H, Ar, CH=N), 7.51 (t, *J* = 7.6 Hz, 2H, Ar), 4.91 (d, *J* = 1.2 Hz, 1H, H-1), 3.98 (s, 1H, OCH(CH₂)₂), 3.85 (d, *J* = 11.2 Hz, 1H, H-6a),

3.82 (dd, $J = 3.2, 1.7$ Hz, 1H, H-2), 3.79 - 3.70 (m, 2H, H-5, H-6b), 3.68 - 3.61 (m, 2H, H-3, H-4), 2.45 (dd, $J = 9.8, 4.3$ Hz, 1H, $CH(CH_2)_2(CH=N)$), 2.02 - 1.51 (m, 8H, cyclohexyl); ^{13}C NMR (126 MHz, MeOD): δ 166.88 (CONH), 158.48, 134.32 (CH=N), 133.17, 129.71, 128.66 (C-Ar), 99.70 (C-1), 74.92 (C-3), 72.78 (C-2), 72.71 (C-5), 72.24 ($OCH(CH_2)_2$), 68.79 (C-4), 63.01 (C-6), 40.99 ($CH(CH_2)_2(CH=N)$), 31.39, 28.96, 25.93, 25.53 (4 CH_2); ESI-MS: m/z : calcd for $C_{20}H_{28}N_2NaO_7$ $[M+Na]^+$: 431.18, found: 431.17.

(E)-N'-((1R,4R)-4-(α -D-Mannopyranosyloxycyclohexyl)methylene)benzohydrazide

(28c): Prepared according to general procedure F from **27c** (15 mg, 0.04 mmol). Yield: 11 mg (68%). $[\alpha]_D = +193.1$ ($c = 0.3$, MeOH); 1H NMR (500 MHz, MeOD): δ 7.91 - 7.85 (m, 2H, Ar), 7.63 - 7.56 (m, 2H, Ar, $CH=N$), 7.51 (t, $J = 7.6$ Hz, 2H, Ar), 4.96 (d, $J = 1.4$ Hz, 1H, H-1), 3.88 - 3.83 (m, 1H, H-6a), 3.77 (dd, $J = 3.3, 1.7$ Hz, 1H, H-2), 3.76 - 3.59 (m, 5H, H-3,4,5,6b, and $OCH(CH_2)_2$), 2.40 - 2.30 (m, 1H, $CH(CH_2)_2(CH=N)$), 2.22 - 1.29 (m, 8H, cyclohexyl); ^{13}C NMR (126 MHz, MeOD): δ 166.87 (CONH), 158.08, 134.28, 133.19 (CH=N), 129.71, 128.65 (5C-Ar), 99.61 (C-1), 75.96 (C-3), 74.80 (C-2), 72.72 (C-5), 72.60 ($OCH(CH_2)_2$), 68.80 (C-4), 63.04 (C-6), 41.42 ($CH(CH_2)_2(CH=N)$), 33.55, 31.70, 29.35, 29.08 (4 CH_2); ESI-MS: m/z : calcd for $C_{20}H_{28}N_2NaO_7$ $[M+Na]^+$: 431.18, found: 431.11.

4-(2,3,4,6-Tetra-O-acetyl- α -D-mannopyranosyloxy)benzaldehyde (30a): Prepared according to general procedure C from **14** (100mg, 0.28 mmol) and 4-hydroxybenzaldehyde (**29a**) (38 mg, 0.31 mmol). Yield: 106 mg (82%). $[\alpha]_D = +82.5$ ($c = 1.94$, EtOAc); 1H NMR (500 MHz, $CDCl_3$): δ 9.93 (s, 1H, CHO), 8.08 - 7.71 (m, 2H, H-Ar), 7.27 - 7.17 (m, 2H, H-Ar), 5.64 (d, $J = 1.7$ Hz, 1H, H-1), 5.56 (dd, $J = 10.0, 3.5$ Hz, 1H, H-3), 5.46 (dd, $J = 3.5, 1.9$ Hz, 1H, H-2), 5.38 (t, $J = 10.0$ Hz, 1H, H-4), 4.28 (dd, $J = 12.2, 5.3$ Hz, 1H, H-6b), 4.09 - 4.01 (m, 2H, H-5, H-6a), 2.22, 2.06, 2.05, 2.02 (4s, 12H, 4OAc); ^{13}C NMR (126 MHz, $CDCl_3$): δ 190.78 (CHO), 170.52, 170.03, 169.76, 160.26 (4COOCH₃), 131.95, 131.83, 116.75 (C-Ar), 95.60 (C-1), 69.73 (C-5), 69.21 (C-2), 68.75 (C-3), 65.84 (C-4), 62.10 (C-6), 20.93, 20.76 (4 OAc); ESI-MS: m/z : calcd for $C_{21}H_{24}NaO_{11}$ $[M+Na]^+$: 475.12, found: 475.16.

3-Fluoro-4-(2,3,4,6-tetra-O-acetyl- α -D-mannopyranosyloxy)benzaldehyde (30b):

Prepared according to general procedure C from **14** (200 mg, 0.57 mmol) and 3-fluoro-4-

hydroxybenzaldehyde (**29b**) (88 mg, 0.63 mmol). Yield: 193 mg (72%). $[\alpha]_D = +147.9$ ($c = 0.6$, EtOAc); $^1\text{H NMR}$ (500 MHz, CDCl_3): δ 9.90 (s, 1H, -CHO), 7.65 (t, $J = 10.3$ Hz, 2H, H-Ph), 7.36 (t, $J = 7.8$ Hz, 1H, H-Ph), 5.64 (s, 1H, H-1), 5.57 (d, $J = 10.1$ Hz, H-3), 5.52 (s, 1H, H-2), 5.39 (t, $J = 10.0$ Hz, 1H, H-4), 4.28 (dd, $J = 12.0, 5.0$ Hz, 1H, H-6a), 4.17 - 4.03 (m, 2H, H-5, H-6b), 2.22, 2.07, 2.05, 2.02 (4s, 12H, 4 COOCH_3); $^{13}\text{C NMR}$ (126 MHz, CDCl_3): δ 189.67 (CHO), 170.39, 169.90, 169.75, 169.68 (4 CO from COOCH_3), 153.16 (d, $J_{F-C} = 252.0$ Hz), 148.42 (d, $J_{F-C} = 11.3$ Hz), 132.45 (d, $J_{F-C} = 5.1$ Hz), 127.27 (d, $J_{F-C} = 3.3$ Hz), 117.76, 116.76 (d, $J_{F-C} = 18.9$ Hz) (6C-Ph), 96.74 (C-1), 70.01 (C-5), 69.04 (C-2), 68.50 (C-3), 65.68 (C-4), 61.98 (C-6), 20.83, 20.67, 20.66, 20.63 (4 COOCH_3); ESI-MS: m/z : calcd for $\text{C}_{21}\text{H}_{23}\text{FNaO}_{11}$ $[\text{M}+\text{Na}]^+$: 493.11, found: 493.12.

4-(α -D-Mannopyranosyloxy)benzaldehyde (31a): Prepared according to general procedure B from **30a** (106mg, 0.23 mmol). Yield: 50 mg (75%). $[\alpha]_D = +41.1$ ($c = 1.6$, MeOH); $^1\text{H NMR}$ (500 MHz, MeOD): δ 9.89 (s, 1H, CHO), 7.95 - 7.84 (m, 2H, Ar), 7.35 - 7.26 (m, 2H, Ar), 5.66 (d, $J = 1.7$ Hz, 1H, H-1), 4.05 (dd, $J = 3.4, 1.9$ Hz, 1H, H-2), 3.93 (dd, $J = 9.5, 3.4$ Hz, 1H, H-3), 3.80 - 3.70 (m, 3H, H-4, H-6a, H-6b), 3.55 (ddd, $J = 9.8, 5.4, 2.5$ Hz, 1H, H-5); $^{13}\text{C NMR}$ (126 MHz, MeOD): δ 192.92 (CO), 162.92, 132.94, 132.55, 117.89 (Ar), 99.89 (C-1), 75.89 (C-5), 72.32 (C-2), 71.72 (C-3), 68.22 (C-4), 62.64 (C-6); ESI-MS: m/z : calcd for $\text{C}_{13}\text{H}_{16}\text{NaO}_7$ $[\text{M}+\text{Na}]^+$: 307.08, found: 306.84.

3-Fluoro-4-(α -D-mannopyranosyloxy)benzaldehyde (31b): Prepared according to general procedure B from **30b** (100mg, 0.21 mmol). Yield: 62 mg (96%). $[\alpha]_D = +144.0$ ($c = 0.6$, MeOH); $^1\text{H NMR}$ (500 MHz, DMSO- d_6): δ 9.89 (d, $J = 1.8$ Hz, 1H, CHO), 7.83 - 7.68 (m, 2H, H-Ar), 7.59 (t, $J = 8.3$ Hz, 1H, H-Ar), 5.63 (d, $J = 1.6$ Hz, 1H, H-1), 5.19 (d, $J = 4.5$ Hz, 1H, OH-2), 4.91 (d, $J = 5.8$ Hz, 1H, OH-4), 4.87 (d, $J = 5.9$ Hz, 1H, OH-3), 4.48 (t, $J = 6.0$ Hz, 1H, OH-6), 3.90 (t, $J = 4.8$ Hz, 1H, H-2), 3.70 (ddd, $J = 9.1, 5.7, 3.4$ Hz, 1H, H-3), 3.60 (ddd, $J = 12.4, 6.2, 2.3$ Hz, 1H, H-6b), 3.52 (td, $J = 9.5, 5.8$ Hz, 1H, H-4), 3.46 (dt, $J = 11.9, 6.1$ Hz, 1H, H-6a), 3.40 - 3.34 (m, 1H, H-5, overlap with DMSO); $^{13}\text{C NMR}$ (126 MHz, DMSO- d_6): 190.97 (CO), 152.12 ($J_{C,F} = 247.1$ Hz), 149.0 ($J_{C,F} = 10.8$ Hz), 130.78 ($J_{C,F} = 5.1$ Hz), 127.72 ($J_{C,F} = 2.9$ Hz), 117.82, 115.76 ($J_{C,F} = 18.7$ Hz), 99.35 (C-1), 75.68 (C-5), 70.46 (C-3), 69.66 (C-2), 66.37 (C-4), 60.87 (C-6); ESI-MS: m/z : calcd for $\text{C}_{13}\text{H}_{15}\text{FNaO}_7$ $[\text{M}+\text{Na}]^+$: 325.07, found: 324.93.

(E)-N'-(4-(α -D-Mannopyranosyloxy)benzylidene)benzohydrazide (32a): Prepared according to general procedure I from **31a** (100 mg, 0.22 mmol). Yield: 67 mg (75%). $[\alpha]_{\text{D}} = +128.2$ ($c = 0.3$, MeOH); $^1\text{H NMR}$ (500 MHz, DMSO- d_6): δ 11.76 (s, 1H, -CH=N-), 8.42 (s, 1H, -CONH-), 7.92 (d, $J = 7.5$ Hz, 2H, H-Ar), 7.68 (d, $J = 8.5$ Hz, 2H, H-Ar), 7.60 (t, $J = 7.2$ Hz, 1H, H-Ar), 7.54 (t, $J = 7.5$ Hz, 2H, H-Ar), 7.18 (d, $J = 8.5$ Hz, 2H, H-Ar), 5.47 (s, 1H, H-1), 5.06 (d, $J = 4.2$ Hz, 1H, OH-2), 4.84 (d, $J = 5.7$ Hz, 1H, OH-4), 4.77 (d, $J = 5.9$ Hz, 1H, OH-3), 4.46 (t, $J = 5.9$ Hz, 1H, OH-6), 3.85 (s, 1H, H-2), 3.70 (t, $J = 9.0$ Hz, 1H, H-3), 3.66 - 3.58 (m, 1H, H-6a), 3.56 - 3.44 (m, 2H, H-4, H-6b), 3.43 - 3.36 (m, 1H, H-5, overlap with DMSO); $^{13}\text{C NMR}$ (126 MHz, DMSO- d_6): δ 162.95 (CO), 157.85 (C-Ar), 147.47 (-CH=N-), 133.51, 131.64, 128.55, 128.43, 128.06, 127.54, 116.89 (C-Ar), 98.64 (C-1), 75.09 (C-5), 70.61 (C-3), 69.95 (C-2), 66.64 (C-4), 60.98 (C-6); ESI-MS: m/z : calcd for $\text{C}_{20}\text{H}_{22}\text{N}_2\text{NaO}_7$ $[\text{M}+\text{Na}]^+$: 425.13, found: 425.10.

(E)-N'-(3-Fluoro-4-(α -D-mannopyranosyloxy)benzylidene)benzohydrazide (32b): Prepared according to general procedure I from **31b** (5 mg, 0.017 mmol). Yield: 5 mg (71%). $[\alpha]_{\text{D}} = +100.1$ ($c = 0.2$, MeOH); $^1\text{H NMR}$ (500 MHz, MeOD): δ 8.29 (s, 1H, -CH=N-), 7.99 - 7.92 (m, 2H, H-Ar), 7.80 (dd, $J = 12.0, 1.8$ Hz, 1H, H-Ar), 7.62 (d, $J = 7.4$ Hz, 1H, H-Ar), 7.59 - 7.50 (m, 3H, H-Ar), 7.47 (t, $J = 8.3$ Hz, 1H, H-Ar), 5.60 (d, $J = 1.4$ Hz, 1H, H-1), 4.10 (dd, $J = 3.3, 1.8$ Hz, 1H, H-2), 3.95 (dd, $J = 9.4, 3.4$ Hz, 1H, H-3), 3.85 - 3.71 (m, 3H, H-4, H-6a, H-6b), 3.66 (ddd, $J = 9.7, 5.4, 2.3$ Hz, 1H, H-5); $^{13}\text{C NMR}$ (126 MHz, MeOD): δ 167.12 (CO), 155.58 (C-Ar), 149.06 (-CH=N-), 134.14, 133.38, 129.78, 128.76, 126.20, 119.46, 115.46 ($J_{\text{C,F}} = 20.13$ Hz), 101.18 (C-1), 76.06 (C-5), 72.30 (C-3), 71.76 (C-2), 68.18 (C-4), 62.65 (C-6); ESI-MS: m/z : calcd for $\text{C}_{20}\text{H}_{22}\text{FN}_2\text{O}_7$ $[\text{M}+\text{H}]^+$: 421.14, found: 421.13.

3-(2,3,4,6-Tetra-O-acetyl- α -D-mannopyranosyloxy)benzaldehyde (34): Prepared according to general procedure C from **14** (200mg, 0.57 mmol) and 3-hydroxybenzaldehyde (**33**) (77 mg, 0.63 mmol). Yield: 245 mg (95%). $[\alpha]_{\text{D}} = +35.70$ ($c = 0.7$, EtOAc); $^1\text{H NMR}$ (500 MHz, CDCl_3): δ 9.98 (s, 1H, H-CHO), 7.64 (dd, $J = 2.4, 1.4$ Hz, 1H, H-Ar), 7.60 (dt, $J = 7.5, 1.1$ Hz, 1H, H-Ar), 7.50 (t, $J = 7.8$ Hz, 1H, H-Ar), 7.36 (ddd, $J = 8.2, 2.6, 1.0$ Hz, 1H, H-Ar), 5.59 (d, $J = 1.7$ Hz, 1H, H-1), 5.56 (dd, $J = 10.0, 3.5$ Hz, 1H, H-3), 5.46 (dd, $J = 3.5, 1.9$ Hz, 1H, H-2), 5.37 (t, $J = 10.1$ Hz, 1H, H-4),

4.32 - 4.24 (dd, $J = 6.1, 12.5$ Hz, 1H, H-6b), 4.10 - 4.05 (m, 2H, H-5, H-6a), 2.21, 2.06, 2.05, 2.01 (4s, 12H, 4 OAc); ^{13}C NMR (126 MHz, CDCl_3): δ 191.55 (CHO), 170.66, 170.12, 170.08, 169.84 (4 COOCH_3), 156.32, 138.17, 130.52, 125.16, 123.17, 116.31 (C-Ar), 96.00 (C-1), 69.57 (C-5), 69.38 (C-2), 68.87 (C-3), 66.05 (C-4), 62.30 (C-6), 20.99, 20.82, 20.74 (4C, 4 OAc); ESI-MS: m/z : calcd for $\text{C}_{21}\text{H}_{24}\text{NaO}_{11}$ $[\text{M}+\text{Na}]^+$: 475.12, found: 475.13.

3-(α -D-Mannopyranosyloxy)benzaldehyde (35): Prepared according to general procedure B from **34** (160 mg, 0.35 mmol). Yield: 103 mg (quant.). $[\alpha]_{\text{D}} = +131.9$ ($c = 0.3$, MeOH); ^1H NMR (500 MHz, DMSO- d_6): δ 9.98 (s, 1H, CHO), 7.65 - 7.50 (m, 3H H-Ar), 7.42 (ddd, $J = 7.9, 2.5, 1.4$ Hz, 1H, H-Ar), 5.49 (d, $J = 1.7$ Hz, 1H, H-1), 5.08 (s, 1H, OH-2), 4.87 (s, 1H, OH-4), 4.82 (s, 1H, OH-3), 4.47 (s, 1H, OH-6), 3.86 (dd, $J = 3.2, 1.9$ Hz, 1H, H-2), 3.70 (dd, $J = 9.2, 3.2$ Hz, 1H, H-3), 3.62 - 3.43 (m, 3H, H-4, H-6a, H-6b), 3.43 - 3.36 (m, 1H, H-5, overlap with DMSO); ^{13}C NMR (126 MHz, DMSO- d_6): δ 192.88 (CO), 156.77, 137.58, 130.37, 123.24, 123.12, 116.63 (C-Ar), 98.80 (C-1), 75.14 (C-5), 70.61 (C-3), 69.90 (C-2), 66.60 (C-4), 60.91 (C-6); ESI-MS: m/z : calcd for $\text{C}_{13}\text{H}_{16}\text{NaO}_7$ $[\text{M}+\text{Na}]^+$: 307.08, found: 306.91.

(E)-N'-(3-(α -D-Mannopyranosyloxy)benzylidene)benzohydrazide (36): Prepared according to general procedure F from **35** (26 mg, 0.06 mmol). Yield: 19 mg (53%). $[\alpha]_{\text{D}} = +110.8$ ($c = 0.3$, MeOH); ^1H NMR (500 MHz, MeOD): δ 8.33 (s, 1H, $-\text{CH}=\text{N}-$), 8.00 - 7.90 (m, 2H, H-Ar), 7.70 (s, 1H, H-Ar), 7.62 (t, $J = 7.4$ Hz, 1H, H-Ar), 7.54 (t, $J = 7.6$ Hz, 2H, H-Ar), 7.45 (d, $J = 7.6$ Hz, 1H, H-Ar), 7.37 (t, $J = 7.9$ Hz, 1H, H-Ar), 7.20 (dd, $J = 8.1, 1.7$ Hz, 1H, H-Ar), 5.61 (d, $J = 1.4$ Hz, 1H, H-1), 4.06 (dd, $J = 3.3, 1.8$ Hz, 1H, H-2), 3.96 (dd, $J = 9.4, 3.4$ Hz, 1H, H-3), 3.85 - 3.70 (m, 3H, H-4, H-6a, H-6b), 3.65 (ddd, $J = 9.6, 5.4, 2.4$ Hz, 1H, H-5); ^{13}C NMR (126 MHz, MeOD): δ 167.11 (C=O), 158.23 (C-Ar), 150.35 ($-\text{N}=\text{CH}-$), 137.00, 134.10, 133.35, 130.94, 129.74, 128.76, 123.44, 120.38, 115.97 (C-Ar), 100.06 (C-1), 75.55 (C-5), 72.40 (C-3), 71.93 (C-2), 68.42 (C-4), 62.76 (C-6); ESI-MS: m/z : calcd for $\text{C}_{20}\text{H}_{22}\text{N}_2\text{NaO}_7$ $[\text{M}+\text{Na}]^+$: 425.13, found: 425.03.

4-(2-Deoxy-2-fluoro-3,4,6-tetra-O-acetyl- α -D-mannopyranosyloxy)benzaldehyde (37a): Prepared according to general procedure H from **11a** (106 mg, 0.30 mmol). Yield: 57 mg (46%). $[\alpha]_{\text{D}} = +137.82$ ($c = 0.9$, EtOAc); ^1H NMR (500 MHz, CDCl_3): δ 9.94 (s,

1H, -CHO), 7.99 - 7.78 (m, 2H, Ar), 7.36 - 7.14 (m, 2H, Ar), 5.81 (dd, $J = 6.6, 1.8$ Hz, 1H, H-1), 5.53 - 5.40 (m, 2H, H-3, H-4), 5.00 (dt, $J = 48.8, 2.1$ Hz, 1H, H-2), 4.26 (dd, $J = 12.4, 5.0$ Hz, 1H, H-6a), 4.09 (dd, $J = 12.4, 2.3$ Hz, 1H, H-6b), 4.04 (ddd, $J = 9.5, 5.0, 2.2$ Hz, 1H, H-5), 2.15, 2.06, 2.02 (3 s, 9H, 3 COOCH₃); ¹³C NMR (126 MHz, CDCl₃): δ 190.63 (CHO), 170.51, 170.19, 169.42 (3 COOCH₃), 159.96, 131.91, 131.88, 116.60 (C-Ar), 95.06 (d, $J = 30.7$ Hz, C-1), 86.35 (d, $J = 180.9$ Hz, C-2), 69.67 (C-5), 69.53 (d, $J = 16.8$ Hz, C-3), 65.35 (C-4), 61.68 (C-6), 20.75, 20.63, 20.60 (3 COOCH₃); ESI-MS: m/z : calcd for C₁₉H₂₁FNaO₉ [M+Na]⁺: 435.11, found: 435.04.

4-(2-Deoxy-2-chloro-3,4,6-tetra-O-acetyl- α -D-mannopyranosyloxy)benzaldehyde

(37b): Prepared according to general procedure H from **11b** (110 mg, 0.30 mmol). Yield: 42 mg (36%). $[\alpha]_D = +143.47$ ($c = 1.0$, EtOAc); ¹H NMR (500 MHz, CDCl₃): δ 9.94 (s, 1H, -CHO), 7.91 - 7.85 (m, 2H, Ar), 7.26 - 7.21 (m, 2H, Ar), 5.77 (d, $J = 1.5$ Hz, 1H, H-1), 5.57 (dd, $J = 9.8, 3.9$ Hz, 1H, H-3), 5.49 (t, $J = 9.9$ Hz, 1H, H-4), 4.64 (dd, $J = 3.8, 1.6$ Hz, 1H, H-2), 4.23 (dd, $J = 12.4, 5.1$ Hz, 1H, H-6a), 4.10 (dd, $J = 12.4, 2.3$ Hz, 1H, H-6b), 4.04 (ddd, $J = 9.9, 5.1, 2.2$ Hz, 1H, H-5), 2.14, 2.07, 2.03 (3s, 9H, 3 COOCH₃); ¹³C NMR (126 MHz, CDCl₃): δ 190.66 (CHO), 170.51, 170.13, 169.41 (3 COOCH₃), 160.08, 131.91, 116.60 (C-Ar), 97.73 (C-1), 70.06 (C-5), 69.31 (C-3), 65.02 (C-4), 61.80 (C-6), 56.89 (C-2), 20.76, 20.63 (3C, 3 COOCH₃); ESI-MS: m/z : calcd for C₁₉H₂₁ClNaO₉ [M+Na]⁺: 451.08, found: 451.10.

4-(2-Deoxy-2-fluoro- α -D-mannopyranosyloxy)benzaldehyde (**38a**): Prepared according to general procedure B from **37a** (18 mg, 0.04 mmol). Yield: 12 mg (96%). $[\alpha]_D = +111.0$ ($c = 1.0$, MeOH); ¹H NMR (500 MHz, MeOD): δ 9.90 (s, 1H), 7.97 - 7.85 (m, 2H), 7.37 - 7.27 (m, 2H), 5.90 (dd, $J = 6.9, 1.9$ Hz, 1H, H-1), 4.87 (dt, 49.1, 2.4 Hz, 1H, H-2), 3.99 (ddd, $J = 30.8, 9.6, 2.7$ Hz, 1H, H-3), 3.83 - 3.69 (m, 3H, H-4, H-6a, H-6b), 3.63 - 3.56 (m, 1H, H-5); ¹³C NMR (126 MHz, MeOD): δ 192.88 (CHO), 162.42, 132.92, 132.88, 118.01 (C-Ar), 97.06 (d, $J = 31.3$ Hz, C-1), 90.61 (d, $J = 175.6$ Hz, C-2), 76.01 (C-5), 71.45 (d, $J = 17.5$ Hz, C-3), 68.22 (C-4), 62.33 (C-6); ESI-MS: m/z : calcd for C₁₃H₁₅FNaO₆ [M+Na]⁺: 309.07, found: 308.93.

4-(2-Deoxy-2-chloro- α -D-mannopyranosyloxy)benzaldehyde (**38b**): Prepared according to general procedure B from **37b** (31 mg, 0.07 mmol). Yield: 3 mg (14%). $[\alpha]_D$

= +169.5 ($c = 0.2$, MeOH); ^1H NMR (500 MHz, MeOD): δ 9.81 (s, 1H, CHO), 7.86 - 7.80 (m, 2H, Ar), 7.27 - 7.20 (m, 2H, Ar), 5.79 (d, $J = 1.5$ Hz, 1H, H-1), 4.41 (dd, $J = 3.8$, 1.6 Hz, 1H, H-2), 4.15 (dd, $J = 9.2$, 3.8 Hz, 1H, H-3), 3.76 - 3.67 (m, 2H, H-4, H-6a), 3.63 (dd, $J = 12.1$, 5.5 Hz, 1H, H-6b), 3.53 (ddd, $J = 9.7$, 5.5, 2.4 Hz, 1H, H-5); ^{13}C NMR (126 MHz, MeOD): δ 192.88 (CO), 162.51, 132.93, 132.83, 117.96 (C-Ar), 99.69 (C-1), 76.55 (C-5), 70.76 (C-3), 67.86 (C-4), 62.43 (C-6), 62.36 (C-2); ESI-MS: m/z : calcd for $\text{C}_{13}\text{H}_{15}\text{ClNaO}_6$ $[\text{M}+\text{Na}]^+$: 325.04, found: 324.93.

3-(2-Deoxy-2-fluoro-3,4,6-tetra-*O*-acetyl- α -D-mannopyranosyloxy)benzaldehyde

(39a): Prepared according to general procedure H from **11a** (106 mg, 0.30 mmol). Yield: 47 mg (38%). $[\alpha]_{\text{D}} = +91.9$ ($c = 0.8$, EtOAc); ^1H NMR (500 MHz, CDCl_3): δ 10.00 (s, 1H, CHO), 7.67 - 7.58 (m, 2H, Ar), 7.51 (t, $J = 7.8$ Hz, 1H, Ar), 7.40 - 7.34 (m, 1H, Ar), 5.76 (dd, $^3J_{\text{H,F}} = 6.6$ Hz, $J = 1.9$ Hz, 1H, H-1), 5.53 - 5.38 (m, 2H, H-3, H-4), 4.99 (dt, $^2J_{\text{H,F}} = 48.9$ Hz, $J = 2.1$ Hz, 1H, H-2), 4.27 (dd, $J = 12.7$, 5.7 Hz, 1H, H-6a), 4.11 - 4.04 (m, 2H, H-5, H-6b), 2.15, 2.06, 2.02 (3 s, 9H, 3COOCH₃); ^{13}C NMR (126 MHz, CDCl_3): δ 191.34 (CHO), 170.59, 170.20, 169.45 (3CO(O)), 156.01, 138.09, 130.48, 125.15, 122.80, 116.26 (6C, Ar), 95.44 (C-1, $^2J_{\text{C,F}} = 48.9$ Hz), 86.45 (C-2, $^1J_{\text{C,F}} = 180.9$ Hz), 69.61 (C-3, $^3J_{\text{C,F}} = 16.8$ Hz), 69.49 (C-5), 65.50 (C-4), 61.84 (C-6), 20.76, 20.61 (3C, CH₃); ESI-MS: m/z : calcd for $\text{C}_{19}\text{H}_{21}\text{FNaO}_9$ $[\text{M}+\text{Na}]^+$: 435.11, found: 435.04.

3-(2-Deoxy-2-chloro-3,4,6-tetra-*O*-acetyl- α -D-mannopyranosyloxy)benzaldehyde

(39b): Prepared according to general procedure H from **11b** (110 mg, 0.30 mmol). Yield: 50 mg (39%). $[\alpha]_{\text{D}} = +68.02$ ($c = 1.0$, EtOAc); ^1H NMR (500 MHz, CDCl_3): δ 9.99 (s, 1H, CHO), 7.64 (dd, $J = 2.4$, 1.4 Hz, 1H, Ar), 7.61 (dt, $J = 7.5$, 1.1 Hz, 1H, Ar), 7.51 (t, $J = 7.9$ Hz, 1H, Ar), 7.37 (ddd, $J = 8.2$, 2.6, 1.0 Hz, 1H, Ar), 5.73 (d, $J = 1.5$ Hz, 1H, H-1), 5.58 (dd, $J = 9.8$, 3.9 Hz, 1H, H-3), 5.48 (t, $J = 9.9$ Hz, 1H, H-4), 4.64 (dd, $J = 3.8$, 1.6 Hz, 1H, H-2), 4.24 (dd, $J = 12.5$, 5.6 Hz, 1H, H-6a), 4.13 - 4.06 (m, 2H, H-6b, H-5), 2.14, 2.07, 2.02 (3s, 9H, 3 COOCH₃); ^{13}C NMR (126 MHz, CDCl_3): δ 191.38 (CHO), 170.58, 170.12, 169.43 (3 COOCH₃), 156.10, 138.07, 130.45, 125.07, 122.83, 116.28 (C-Ar), 98.10 (C-1), 69.87 (C-5), 69.39 (C-3), 65.17 (C-4), 61.96 (C-6), 57.02 (C-2), 20.77, 20.63, 20.60 (3C, 3 COOCH₃); ESI-MS: m/z : calcd for $\text{C}_{19}\text{H}_{21}\text{ClNaO}_9$ $[\text{M}+\text{Na}]^+$: 451.08, found: 451.12.

3-(2-Deoxy-2-fluoro- α -D-mannopyranosyloxy)benzaldehyde (40a): Prepared according to general procedure B from **39a** (16 mg, 0.04 mmol). Yield: 8 mg (73%). $[\alpha]_D = +119.3$ ($c = 0.7$, MeOH); $^1\text{H NMR}$ (500 MHz, MeOD): δ 9.98 (s, 1H, CHO), 7.70 (s, 1H), 7.63 (d, $J = 7.5$ Hz, 1H, H-Ar), 7.55 (t, $J = 7.8$ Hz, 1H, H-Ar), 7.47 (dd, $J = 8.1, 1.6$ Hz, 1H, H-Ar), 5.83 (d, $J = 5.7$ Hz, 1H, H-1), 4.98 – 4.75 (m, 1H, H-2), 4.00 (ddd, $J = 30.9, 9.6, 2.6$ Hz, 1H, H-3), 3.86 – 3.67 (m, 3H, H-4, H-6a, H-6b), 3.69 - 3.58 (m, 1H, H-5); $^{13}\text{C NMR}$ (126 MHz, MeOD): δ 193.75 (CO), 158.10, 139.56, 131.52, 125.32, 124.35, 117.83 (C-Ar), 97.47 ($J = 31.0$ Hz, C-1), 90.76 ($J = 175.4$ Hz, C-2), 75.83 (C-5), 71.51 ($J = 17.5$ Hz, C-4), 68.24 ($J = 20.6$ Hz, C-6); ESI-MS: m/z : calcd for $\text{C}_{13}\text{H}_{15}\text{FNaO}_6$ $[\text{M}+\text{Na}]^+$: 309.07, found: 308.93.

3-(2-Deoxy-2-chloro- α -D-mannopyranosyloxy)benzaldehyde (40b): Prepared according to general procedure B from **39b** (16 mg, 0.04 mmol). Yield: 7 mg (64%). $[\alpha]_D = +111.2$ ($c = 0.6$, MeOH); $^1\text{H NMR}$ (500 MHz, MeOD): δ 9.98 (s, 1H), 7.69 (dd, $J = 2.4, 1.4$ Hz, 1H, Ar), 7.63 (dt, $J = 7.5, 1.2$ Hz, 1H, Ar), 7.55 (t, $J = 7.8$ Hz, 1H, Ar), 7.46 (ddd, $J = 8.2, 2.6, 1.1$ Hz, 1H, Ar), 5.81 (d, $J = 1.5$ Hz, 1H, H-1), 4.50 (dd, $J = 3.8, 1.6$ Hz, 1H, H-2), 4.25 (dd, $J = 9.2, 3.8$ Hz, 1H, H-3), 3.85 - 3.77 (m, 2H, H-4, H-6a), 3.72 (dd, $J = 12.0, 5.6$ Hz, 1H, H-6b), 3.70 - 3.64 (m, 1H, H-5); $^{13}\text{C NMR}$ (126 MHz, MeOD): δ 193.74 (CHO), 158.21, 139.56, 131.51, 125.22, 124.30, 117.83 (C-Ar), 100.10 (C-1), 76.40 (C-5), 70.82 (C-3), 67.96 (C-4), 62.54 (C-6), 62.47 (C-2); ESI-MS: m/z : calcd for $\text{C}_{13}\text{H}_{15}\text{ClNaO}_6$ $[\text{M}+\text{Na}]^+$: 325.04, found: 324.81.

Hydrazones 42a-d: Prepared according to general procedure I from **31b** (5 mg, 0.017 mmol, 1 equiv.) and the corresponding hydrazide (1 equiv.). Compounds **42a-d** were purified with preparative HPLC-MS, and the yields were calculated after lyophilization.

42a: Yield: 5 mg (71%). $^1\text{H NMR}$ (500 MHz, MeOD): δ 8.29 (s, 1H, -CH=N-), 8.01 - 7.91 (m, 2H, H-Ar), 7.80 (dd, $J = 12.0, 1.8$ Hz, 1H, H-Ar), 7.63 (t, $J = 7.4$ Hz, 1H, H-Ar), 3.59 – 3.51 (m, 3H, H-Ar), 7.47 (t, $J = 8.3$ Hz, 1H, H-Ar), 5.60 (d, $J = 1.5$ Hz, 1H, H-1), 4.10 (dd, $J = 3.4, 1.8$ Hz, 1H, H-2), 3.95 (dd, $J = 9.4, 3.4$ Hz, 1H, H-3), 3.87 – 3.70 (m, 3H, H-4, H-6a, H-6b), 3.66 (ddd, $J = 9.7, 5.4, 2.4$ Hz, 1H, H-5), 3.36 – 3.33 (m, 2H, -CH₂-); ESI-MS: m/z : calcd for $\text{C}_{23}\text{H}_{25}\text{FN}_3\text{O}_7$ $[\text{M}+\text{H}]^+$: 474.17, found: 474.06.

42b: Yield: 4 mg (67%). ^1H NMR (500 MHz, MeOD): δ 8.29 (s, 1H, -CH=N-), 7.83 – 7.74 (m, 2H, H-Ar), 7.57 – 7.43 (m, 2H, H-Ar), 7.33 (d, $J = 3.4$ Hz, 1H, H-Ar) 6.68 (s, 1H, H-Ar), 5.59 (s, 1H, H-1), 4.10 (dd, $J = 3.4, 1.8$ Hz, 1H, H-2), 3.95 (dd, $J = 9.4, 3.5$ Hz, 1H, H-3), 3.85 – 3.71 (m, 3H, H-4, H-6a, H-6b), 3.70 – 3.63 (m, 1H, H-5); ESI-MS: m/z : calcd for $\text{C}_{18}\text{H}_{20}\text{FN}_2\text{O}_8$ $[\text{M}+\text{H}]^+$: 411.12, found: 410.99.

42c: Yield: 5 mg (62%). ^1H NMR (500 MHz, MeOD): δ 8.32 - 7.41 (m, 6H, -CH=N-, H-Ar), 7.23 (dd, $J = 11.1, 6.8$ Hz, 1H, H-Ar), 5.60 (s, 1H, H-1), 4.12 - 4.08 (m, 1H, H-2), 3.95 (dd, $J = 9.4, 3.4$ Hz, 1H, H-3), 3.90 - 3.72 (m, 3H, H-4, H-6a, H-6b), 3.71 – 3.61 (m, 1H, H-5); ESI-MS: m/z : calcd for $\text{C}_{18}\text{H}_{20}\text{FN}_2\text{O}_7\text{S}$ $[\text{M}+\text{H}]^+$: 427.10, found: 426.99.

42d: Yield: 2 mg (30%). ^1H NMR (500 MHz, MeOD): δ 8.29 (s, 1H, -CH=N-), 7.96 – 7.77 (m, 3H, H-Ar), 7.60 (d, $J = 8.5$ Hz, 2H, H-Ar), 7.56 - 7.43 (m, 2H, H-Ar), 5.60 (s, 1H, H-1), 4.10 (dd, $J = 3.2, 1.7$ Hz, 1H, H-2), 3.95 (dd, $J = 9.4, 3.4$ Hz, 1H, H-3), 3.86 - 3.70 (m, 3H, H-4, H-6a, H-6b), 3.70 - 3.62 (m, 1H, H-5), 1.39 (s, 9H, H-tBu); ESI-MS: m/z : calcd for $\text{C}_{24}\text{H}_{30}\text{FN}_2\text{O}_7$ $[\text{M}+\text{H}]^+$: 477.20, found: 477.09.

Hydrazones 43c and 50a-h: Prepared according to general procedure I from **31a** (2 mg, 1 equiv.) and the corresponding hydrazide (1 equiv.). Compounds **43c** and **50a-h** were purified with preparative HPLC-MS. Yield: 50-60%.

43c: ^1H NMR (500 MHz, MeOD): δ 7.94 - 7.71 (m, 5H, -CH=N-, H-Ar), 7.29 - 7.17 (m, 3H, H-Ar), 5.59 (s, 1H, H-1), 4.04 (s, 1H, H-2), 3.93 (dd, $J = 9.5, 3.4$ Hz, 1H, H-3), 3.84 - 3.70 (m, 3H, H-4, H-6a, H-6b), 3.65 – 3.54 (m, 1H, H-5); ESI-MS: m/z : calcd for $\text{C}_{18}\text{H}_{21}\text{N}_2\text{O}_7\text{S}$ $[\text{M}+\text{H}]^+$: 409.11, found: 409.04.

50a: ^1H NMR (500 MHz, MeOD): δ 8.21 (s, 1H, -CH=N-), 7.78 (d, $J = 8.7$ Hz, 2H, H-Ph), 7.20 (d, $J = 8.8$ Hz, 2H, H-Ph), 6.95 (d, $J = 2.3$ Hz, 2H, H-Pyrrole), 6.22 - 6.10 (m, 1H, H-Pyrrole), 5.57 (d, $J = 1.7$ Hz, 1H, H-1), 4.04 (dd, $J = 3.4, 1.8$ Hz, 1H, H-2), 3.98 (s, 3H, CH₃), 3.93 (dd, $J = 9.5, 3.4$ Hz, 1H, H-3), 3.83 - 3.70 (m, 3H, H-4, H-6a, H-6b), 3.64 - 3.57 (m, 1H, H-5); ESI-MS: m/z : calcd for $\text{C}_{19}\text{H}_{24}\text{N}_3\text{O}_7$ $[\text{M}+\text{H}]^+$: 406.16, found: 406.09.

50b: ^1H NMR (500 MHz, MeOD): δ 8.37 (s, 1H, -CH=N-), 8.24 (s, 1H, H-thiazole), 7.83 (d, $J = 8.8$ Hz, 2H, H-Ph), 7.22 (d, $J = 8.8$ Hz, 2H, H-Ph), 5.59 (d, $J = 1.6$ Hz, 1H, H-1), 4.04 (dd, $J = 3.4, 1.8$ Hz, 1H, H-2), 3.93 (dd, $J = 9.5, 3.5$ Hz, 1H, H-3), 3.83 - 3.70 (m, 3H, H-4, H-6a, H-6b), 3.59 (ddd, $J = 9.8, 5.2, 2.6$ Hz, 1H, H-5), 2.80 (s, 3H, CH_3); ESI-MS: m/z : calcd for $\text{C}_{18}\text{H}_{22}\text{N}_3\text{O}_7\text{S}$ $[\text{M}+\text{H}]^+$: 424.12, found: 424.08.

50c: ^1H NMR (500 MHz, MeOD): δ 9.10 (s, 1H, -CH=N-), 8.77 (dd, $J = 4.9, 1.5$ Hz, 1H, H-Py), 8.38 (dt, $J = 8.0, 1.9$ Hz, 1H, H-Py), 8.33 (s, 1H, H-Py), 7.83 (d, $J = 8.8$ Hz, 2H, H-Ph), 7.63 (dd, $J = 7.9, 4.9$ Hz, 1H, H-Py), 7.23 (d, $J = 8.8$ Hz, 2H, H-Ph), 5.59 (d, $J = 1.5$ Hz, 1H, H-1), 4.05 (dd, $J = 3.3, 1.8$ Hz, 1H, H-2), 3.93 (dd, $J = 9.5, 3.4$ Hz, 1H, H-3), 3.83 - 3.70 (m, 3H, H-4, H-6a, H-6b), 3.59 (ddd, $J = 9.7, 5.2, 2.5$ Hz, 1H, H-5); ESI-MS: m/z : calcd for $\text{C}_{19}\text{H}_{22}\text{N}_3\text{O}_7$ $[\text{M}+\text{H}]^+$: 404.15, found: 404.11.

50d: ^1H NMR (500 MHz, MeOD): δ 8.30 (s, 1H, -CH=N-), 7.83 (dd, $J = 15.5, 8.4$ Hz, 4H, H-Ar), 7.36 (d, $J = 8.1$ Hz, 2H, H-Ar), 7.21 (d, $J = 8.7$ Hz, 2H, H-Ar), 5.58 (d, $J = 1.4$ Hz, 1H, H-1), 4.04 (dd, $J = 3.3, 1.8$ Hz, 1H, H-2), 3.93 (dd, $J = 9.5, 3.4$ Hz, 1H, H-3), 3.84 - 3.70 (m, 3H, H-4, H-6a, H-6b), 3.60 (ddd, $J = 9.7, 5.2, 2.5$ Hz, 1H, H-5), 2.45 (s, 3H, CH_3); ESI-MS: m/z : calcd for $\text{C}_{22}\text{H}_{24}\text{N}_3\text{O}_7$ $[\text{M}+\text{H}]^+$: 442.16, found: 442.14.

50e: ^1H NMR (500 MHz, MeOD): δ 8.31 (s, 1H, -CH=N-), 7.94 (d, $J = 8.5$ Hz, 2H, H-Ar), 7.82 (d, $J = 8.7$ Hz, 2H, H-Ar), 7.56 (d, $J = 8.5$ Hz, 2H, H-Ar), 7.22 (d, $J = 8.7$ Hz, 2H, H-Ar), 5.59 (d, $J = 1.3$ Hz, 1H, H-1), 4.04 (dd, $J = 3.3, 1.8$ Hz, 1H, H-2), 3.93 (dd, $J = 9.5, 3.4$ Hz, 1H, H-3), 3.83 - 3.70 (m, 3H, H-4, H-6a, H-6b), 3.59 (ddd, $J = 9.7, 5.2, 2.5$ Hz, 1H, H-5); ESI-MS: m/z : calcd for $\text{C}_{20}\text{H}_{22}\text{ClN}_2\text{O}_7$ $[\text{M}+\text{H}]^+$: 437.11, found: 437.15.

50f: ^1H NMR (500 MHz, MeOD): δ 8.30 (s, 1H, -CH=N-), 7.94 (d, $J = 8.8$ Hz, 2H, H-Ar), 7.81 (d, $J = 8.7$ Hz, 2H, H-Ar), 7.21 (d, $J = 8.7$ Hz, 2H, H-Ar), 7.07 (d, $J = 8.9$ Hz, 2H, H-Ar), 5.58 (d, $J = 1.3$ Hz, 1H, H-1), 4.04 (dd, $J = 3.3, 1.8$ Hz, 1H, H-2), 3.93 (dd, $J = 9.5, 3.4$ Hz, 1H, H-3), 3.90 (s, 3H, CH_3), 3.83 - 3.71 (m, 3H, H-4, H-6a, H-6b), 3.60 (ddd, $J = 9.7, 5.2, 2.5$ Hz, 1H, H-5); ESI-MS: m/z : calcd for $\text{C}_{21}\text{H}_{25}\text{N}_2\text{O}_8$ $[\text{M}+\text{H}]^+$: 433.16, found: 433.11.

50g: ^1H NMR (500 MHz, MeOD): δ 8.23 (s, 2H, H-Ar), 8.07 (s, 1H, -CH=N-), 7.80 (d, $J = 6.5$ Hz, 2H, H-Ar), 7.48 (d, $J = 7.7$ Hz, 1H, H-Ar), 7.31 - 7.16 (m, 4H, H-Ar), 5.58 (d, $J = 1.6$ Hz, 1H, H-1), 4.05 (dd, $J = 3.4, 1.8$ Hz, 1H, H-2), 3.94 (dd, $J = 9.5, 3.4$ Hz, 1H, H-3), 3.85 - 3.71 (m, 3H, H-4, H-6a, H-6b), 3.61 (ddd, $J = 9.8, 5.2, 2.6$ Hz, 1H, H-5); ESI-MS: m/z : calcd for $\text{C}_{22}\text{H}_{24}\text{N}_3\text{O}_7$ $[\text{M}+\text{H}]^+$: 442.16, found: 442.14.

50h: ^1H NMR (500 MHz, MeOD): δ 8.33 (s, 1H, -CH=N-), 8.06 - 7.94 (m, 2H, H-Ar), 7.84 (d, $J = 8.5$ Hz, 2H, H-Ar), 7.61 (dd, $J = 6.0, 3.2$ Hz, 2H, H-Ar), 7.24 (d, $J = 8.6$ Hz, 2H, H-Ar), 5.60 (s, 1H, H-1), 4.05 (s, 1H, H-2), 3.93 (dd, $J = 9.5, 3.2$ Hz, 1H, H-3), 3.85 - 3.69 (m, 3H, H-4, H-6a, H-6b), 3.64 - 3.55 (m, 1H, H-5); ESI-MS: m/z : calcd for $\text{C}_{22}\text{H}_{21}\text{ClN}_2\text{NaO}_7\text{S}$ $[\text{M}+\text{Na}]^+$: 515.07, found: 515.06.

Isothermal Titration Calorimetry (ITC). All thermodynamic experiments were performed with the FimH-CRD-Th-His₆ protein using a VP-ITC instrument from MicroCal, Inc. (GE Healthcare, Northampton, MA, USA) with a sample cell volume of 1.4523 mL. The measurements were performed with 2.5 or 5% DMSO at 25 °C, a stirring speed of 307 rpm, and 10 $\mu\text{cal s}^{-1}$ reference power. The protein samples were dialyzed in assay buffer prior to all experiments. Compounds **1** and **13a-c** were measured in a direct fashion by titration of ligand (120-2000 μM) into protein (10-55 μM) with injections of 3-6 μL at intervals of 10 min to ensure non-overlapping peaks. The quantity $c = \text{Mt}(0)/K_D$, where $\text{Mt}(0)$ is the initial macromolecule concentration, is of importance in titration microcalorimetry. The c -values of the direct titrations were below 1000 and thus within the reliable range. Baseline correction and peak integration was achieved with the Origin 7 software (OriginLab, Northampton, MA, USA). An initial 2 μL -injection was excluded from data analysis. Baseline subtraction and curve fitting with the three variables N (concentration correction factor), K_D (dissociation constant), and ΔH° (change in enthalpy) was performed with the SEDPHAT software version 10.40 (National Institute of Health). A binary complex model was employed. The thermodynamic parameters were calculated with the following equation (Equation 1)³⁵:

$$\Delta G^\circ = \Delta H^\circ - T\Delta S^\circ = RT \ln K_D = -RT \ln K_A \quad (1)$$

where ΔG° , ΔH° , and ΔS° are the changes in free energy, enthalpy, and entropy of binding, respectively, T is the absolute temperature, and R is the universal gas constant ($8.314 \text{ J mol}^{-1} \text{ K}^{-1}$).

K_D Determination of FimH Antagonists. The fluorescently previously reported labeled ligand was used for the competitive fluorescence polarization assay. A serial dilution of non-labeled FimH antagonist with final concentrations ranging from 0-10 μM was titrated into 96-well NBSTM plates to a final volume of 200 μL containing a constant concentration of protein (final concentration: 25 nM for the lectin domain of FimH; 250 nM for the native full-length FimH) and FITC-labeled ligand which was fixed at a higher concentration in competitive binding assays to obtain higher fluorescence intensities (final concentration: 20 nM when tested against the lectin domain of FimH; 25 nM when tested against the native full-length FimH). Prior to measuring the fluorescence polarization, the plates were incubated for 24 h (in the presence of the lectin domain) or 3 h (in the presence of the full-length FimH) at RT until the reaction reached its equilibrium. The IC_{50} value was determined with Prism (GraphPad Software Inc., La Jolla, CA, USA) by applying a standard four-parameter IC_{50} function. The obtained IC_{50} values were converted into their corresponding K_D values using the following derivation of the Cheng-Prusoff equation (Equation 2)³⁶:

$$K_D = \frac{I_{50}}{\frac{L_{50}}{K_D} + \frac{P_0}{K_D} + 1} \quad (2)$$

where I_{50} and L_{50} are the concentrations of inhibitor and ligand at half-maximal inhibition, respectively, and P_0 is the free concentration of protein in the absence of inhibitor. This variation of the Cheng-Prusoff equation is applied to competition assays with tight-binding inhibitors.³⁶

FimH-templated DCLs. The aldehyde (1.26 μL each if more than one aldehyde, 10 mM, DMSO), hydrazides (1.26 μL each, 10 mM, DMSO), and aniline (5 μL , 1M, DMSO) were added to the protein solution (500 μL , 25-30 μM in sodium phosphate buffer 50 mM, pH 7.0). For native full-length FimH, the lectin domain of FimH, and the BSA control, the protein concentrations are 25.0 μM , 30.5 μM and 0.44 $\text{mg} \cdot \text{mL}^{-1}$, respectively. The amount of DMSO should be adjusted to less than 3%. To establish a blank DCL composition, same buffer solution was used to set up the reaction accordingly. The DCL was allowed to stand at room temperature, and was monitored periodically by

HPLC. At the set-up time points, the pH of the reaction was raised to 13 by adding NaOH (10 μ L, 10M, aqueous) to 100 μ L reaction system, and the denatured protein was removed by ultrafiltration using 5,000 MWCO filter (Spin-X). HPLC analysis was performed and the traces were compared with the blank composition (HPLC conditions: column, Atlantis T3 3 μ m, C18, 21 \times 150 mm; flow rate, 0.5 mL \cdot min⁻¹; wavelength, 310 nm; temperature, 30 $^{\circ}$ C; gradient H₂O/MeCN (0.01% TFA) from 95% to 55% over 53 min). All of the experiments were performed in triplicate.

REFERENCES

1. Foxman, B. Recurring urinary-tract infection - incidence and risk-factors. *Am. J. Public Health.* **1990**, *80*, 331-333.
2. Foxman, B.; Barlow, R.; D'Arcy, H.; Gillespie, B.; Sobel, J. D. Urinary tract infection: self reported incidence and associated costs. *Ann. Epidemiol.* **2000**, *10*, 509-515.
3. Cegelski, L.; Marshall, G. R.; Eldridge, G. R.; Hultgren, S. J. The biology and future prospects of antivirulence therapies. *Nat. Rev. Microbiol.* **2008**, *6*, 17-27.
4. Hooton, T. Fluoroquinolones and resistance in the treatment of uncomplicated urinary tract infection. *Int. J. Antimicrob. Agents.* **2003**, *22*, 65-72.
5. Hooton, T. The current management strategies for community-acquired urinary tract infection. *Infect. Dis. Clin. North Am.* **2003**, *17*, 303-332.
6. Franco, A. V. M. Recurrent urinary tract infections. *Best Pract. Res. Clin. Obstet. Gynaecol.* **2005**, *19*, 861-873.
7. Sanchez, G. V.; Master, R. N.; Bordon, J. Trimethoprim-sulfamethoxazole may no longer be acceptable for the treatment of acute uncomplicated cystitis in the United States. *Clin. Infect. Dis.* **2011**, *53*, 316-7.
8. Capitani, G.; Eidam, O.; Glockshuber, R.; Grütter, M. G. Structural and functional insights into the assembly of type 1 pili from *Escherichia coli*. *Microbes. Infect.* **2006**, *8*, 2284-90.
9. Wiles, T. J.; Kulesus, R. R.; Mulvey, M. A. Origins and virulence mechanisms of uropathogenic *Escherichia coli*. *Exp. Mol. Pathol.* **2008**, *85*, 11-19.

10. Martinez, J. J.; Mulvey, M. A.; Schilling, J. D.; Pinkner, J. S.; Hultgren, S. J. Type 1 pilus-mediated bacterial invasion of bladder epithelial cells. *Embo J.* **2000**, *19*, 2803-2812.
11. Mulvey, M. A. Adhesion and entry of uropathogenic Escherichia coli. *Cell Microbiol.* **2002**, *4*, 257-271.
12. Sharon, N. Carbohydrates as future anti-adhesion drugs for infectious diseases. *Biochim. Biophys. Acta.* **2006**, *1760*, 527-37.
13. Firon, N.; Ofek, I.; Sharon, N. Carbohydrate specificity of the surface lectins of Escherichia coli, Klebsiella pneumoniae, and Salmonella typhimurium. *Carbohydr. Res.* **1983**, *120*, 235-249.
14. Firon, N.; Ashkenazi, S.; Mirelman, D.; Ofek, I.; Sharon, N. Aromatic α -glycosides of mannose are powerful inhibitors of the adherence of type-1 fimbriated Escherichia coli to yeast and intestinal epithelial-cells. *Infect. Immun.* **1987**, *55*, 472-476.
15. Choudhury, D.; Thompson, A.; Stojanoff, V.; Langermann, S.; Pinkner, J.; Hultgren, S. J.; Knight, S. D. X-ray structure of the FimC-FimH chaperone-adhesin complex from uropathogenic Escherichia coli. *Science* **1999**, *285*, 1061-1066.
16. Hung, C. S.; Bouckaert, J.; Hung, D.; Pinkner, J.; Widberg, C.; DeFusco, A.; Auguste, C. G.; Strouse, R.; Langermann, S.; Waksman, G.; Hultgren, S. J. Structural basis of tropism of Escherichia coli to the bladder during urinary tract infection. *Mol. Microbiol.* **2002**, *44*, 903-915.
17. Bouckaert, J.; Berglund, J.; Schembri, M.; De Genst, E.; Cools, L.; Wuhrer, M.; Hung, C. S.; Pinkner, J.; Slattegard, R.; Zavialov, A.; Choudhury, D.; Langermann, S.; Hultgren, S. J.; Wyns, L.; Klemm, P.; Oscarson, S.; Knight, S. D.; De Greve, H. Receptor binding studies disclose a novel class of high-affinity inhibitors of the Escherichia coli FimH adhesin. *Mol. Microbiol.* **2005**, *55*, 441-455.
18. Wellens, A.; Garofalo, C.; Nguyen, H.; Van Gerven, N.; Slattegard, R.; Hernalsteens, J. P.; Wyns, L.; Oscarson, S.; De Greve, H.; Hultgren, S.; Bouckaert, J. Intervening with urinary tract infections using anti-adhesives based on the crystal structure of the FimH-oligomannose-3 complex. *PLoS One* **2008**, *3*.
19. Sperling, O.; Fuchs, A.; Lindhorst, T. K. Evaluation of the carbohydrate recognition domain of the bacterial adhesin FimH: design, synthesis and binding properties of mannoside ligands. *Org. Biomol. Chem.* **2006**, *4*, 3913-22.

20. Han, Z. F.; Pinkner, J. S.; Ford, B.; Obermann, R.; Nolan, W.; Wildman, S. A.; Hobbs, D.; Ellenberger, T.; Cusumano, C. K.; Hultgren, S. J.; Janetka, J. W. Structure-based drug design and optimization of mannoside bacterial FimH antagonists. *J. Med. Chem.* **2010**, *53*, 4779-4792.
21. Klein, T.; Abgottspon, D.; Wittwer, M.; Rabbani, S.; Herold, J.; Jiang, X. H.; Kleeb, S.; Luthi, C.; Scharenberg, M.; Bezencon, J.; Gubler, E.; Pang, L. J.; Smiesko, M.; Cutting, B.; Schwardt, O.; Ernst, B. FimH antagonists for the oral treatment of urinary tract infections: from design and synthesis to in vitro and in vivo evaluation. *J. Med. Chem.* **2010**, *53*, 8627-8641.
22. Jiang, X. H.; Abgottspon, D.; Kleeb, S.; Rabbani, S.; Scharenberg, M.; Wittwer, M.; Haug, M.; Schwardt, O.; Ernst, B. Antiadhesion therapy for urinary tract infections- a balanced PK/PD profile proved to be key for success. *J. Med. Chem.* **2012**, *55*, 4700-4713.
23. Schwardt, O.; Rabbani, S.; Hartmann, M.; Abgottspon, D.; Wittwer, M.; Kleeb, S.; Zalewski, A.; Smieško, M.; Cutting, B.; Ernst, B. Design, synthesis and biological evaluation of mannosyl triazoles as FimH antagonists. *Bioorg. Med. Chem.* **2011**, *19*, 6454-73.
24. Aprikian, P.; Tchesnokova, V.; Kidd, B.; Yakovenko, O.; Yarov-Yarovoy, V.; Trinchina, E.; Vogel, V.; Thomas, W.; Sokurenko, E. Interdomain interaction in the FimH adhesin of Escherichia coli regulates the affinity to mannose. *J. Biol. Chem.* **2007**, *282*, 23437-46.
25. Le Trong, I.; Aprikian, P.; Kidd, B. A.; Forero-Shelton, M.; Tchesnokova, V.; Rajagopal, P.; Rodriguez, V.; Interlandi, G.; Klevit, R.; Vogel, V.; Stenkamp, R. E.; Sokurenko, E. V.; Thomas, W. E. Structural basis for mechanical force regulation of the adhesin FimH via finger tap-like β -sheet twisting. *Cell* **2010**, *141*, 645-655.
26. The PyMOL Molecular Graphics System, Version 1.5.0.4 Schrödinger, LLC.
27. Cabani, S.; Gianni, P.; Mollica, V.; Lepori, L. Group contributions to the thermodynamic properties of non-ionic organic solutes in dilute aqueous-solution. *J. Solution Chem.* **1981**, *10*, 563-595.
28. Eid, S.; Zalewski, A.; Smiesko, M.; Ernst, B.; Vedani, A. A molecular-modeling toolbox aimed at bridging the gap between medicinal chemistry and computational sciences. *Int. J. Mol. Sci.* **2013**, *14*, 684-700.

29. Ramstrom, O.; Lehn, J. Drug discovery by dynamic combinatorial libraries. *Nat. Rev. Drug Discov.* **2002**, *1*, 26-36.
30. Bhat, V.; Caniard, A.; Luksch, T.; Brenk, R.; Campopiano, D.; Greaney, M. Nucleophilic catalysis of acylhydrazone equilibration for protein-directed dynamic covalent chemistry. *Nat. Chem.* **2010**, *2*, 490-497.
31. Elchert, B.; Li, J.; Wang, J.; Hui, Y.; Rai, R.; Ptak, R.; Ward, P.; Takemoto, J. Y.; Bensaci, M.; Chang, C. W. Application of the synthetic aminosugars for glycodiversification: synthesis and antimicrobial studies of pyranmycin. *J. Org. Chem.* **2004**, *69*, 1513-23.
32. Matwiejuk, M.; Thiem, J. Defining oxyanion reactivities in base-promoted glycosylations. *Chem. Commun. (Camb)* **2011**, *47*, 8379-81.
33. Giuffredi, G.; Jennings, L.; Bernet, B.; Gouverneur, V. Facile synthesis of 4-deoxy-4-fluoro- α -D-talopyranoside, 4-deoxy-4-fluoro- α -D-idopyranoside and 2,4-dideoxy-2,4-difluoro- α -D-talopyranoside. *J. Fluorine Chem.* **2011**, *132*, 772-778.
34. Chen, A.; Wadsö, I. Simultaneous determination of ΔG , ΔH and ΔS by an automatic microcalorimetric titration technique. Application to protein ligand binding. *J. Biochem. Biophys. Methods* **1982**, *6*, 307-316.
35. Freire, E.; Mayorga, O.; Straume, M. Isothermal titration calorimetry. *Anal. Chem.* **1990**, *62*, 950-959.
36. Nikolovska-Coleska, Z.; Wang, R.; Fang, X.; Pan, H.; Tomita, Y.; Li, P.; Roller, P.; Krajewski, K.; Saito, N.; Stuckey, J.; Wang, S. Development and optimization of a binding assay for the XIAP BIR3 domain using fluorescence polarization. *Anal. Biochem.* **2004**, *332*, 261-273.
37. Scharenberg, M.; Jiang, X.; Pang, L.; Navarra, G.; Rabbani, S.; Binder, F.; Schwardt, O.; Ernst, B. Kinetic properties of carbohydrate-lectin interactions: FimH antagonists. *ChemMedChem* **2014**, *9*, 78-83.
38. Thomas, W.; Forero, M.; Yakovenko, O.; Nilsson, L.; Vicini, P.; Sokurenko, E.; Vogel, V. Catch-bond model derived from allostery explains force-activated bacterial adhesion. *Biophys. J.* **2006**, *90*, 753-764.
39. Pang, L. J.; Kleeb, S.; Lemme, K.; Rabbani, S.; Scharenberg, M.; Zalewski, A.; Schadler, F.; Schwardt, O.; Ernst, B. FimH antagonists: Structure-activity and structure-property relationships for biphenyl α -D-mannopyranosides. *ChemMedChem* **2012**, *7*, 1404-1422.

2.8 Synthesis and Evaluation of 6-Modified Mannosides as FimH Antagonists

This chapter describes structural modifications on *n*-heptyl mannoside by either stereochemically locking 6-hydroxyl group with a cyclopropane unit or introducing a 6-methyl, aiming at exploring possible interactions within the binding pocket and expanding the structural scope of FimH ligands. The chemical structures of the synthesized ligands were characterized by NMR and Mosher's analysis. The binding affinity of the synthesized ligands was evaluated by fluorescence polarization (FP) assay. As a result, the direction of 6-hydroxyl indeed affects ligand-FimH protein interaction. Furthermore, the cyclopropane derivatives provide new scaffolds for other receptors that bind to ¹C₄ conformational mannosides.

Contribution to the project:

Lijuan Pang synthesized and characterized all the reported compounds.

Keywords

Uropathogenic *Escherichia coli*, urinary tract infection, bacterial adhesin FimH, FimH antagonists, *n*-heptyl mannoside, NMR, Mosher's analysis, fluorescence polarization assay

2.8.1 Introduction

Urinary tract infections (UTIs), among the most prevalent infectious diseases, are primarily caused by gram-negative uropathogenic *Escherichia coli* (UPEC).¹ Most UPEC isolates express type 1 pili, where bacterial lectin FimH is located.² The carbohydrate recognition domain (CRD) of FimH binds to mannose-containing receptors on human bladder epithelial cells and thus mediates UPEC adherence and invasion.³ FimH-CRD consists of amino acids with hydrophilic side chains therefore can establish extensive hydrogen-bond network with the hydroxyl groups of D-mannose.⁴ In addition, at the entrance of the binding pocket, three hydrophobic amino acids (Tyr48, Ile52, and Tyr137) form the so called “tyrosine gate”, which can accommodate aliphatic or aromatic aglycones.^{5, 6} Based on the crystal structures, numerous FimH antagonists have been developed for the prevention and treatment of UTIs.⁷

So far, the reported FimH antagonists can be categorized into two major classes: long-chain alkyl mannosides⁶ and mannosides with extended aromatic aglycones⁸⁻¹² (Figure 2.8.1). Although the aglycones of FimH antagonists were extensively modified, few studies on the sugar moiety were reported.¹⁰ *n*-Heptyl mannoside (**1**), commonly used reference in bioassays, was chosen as a model compound in this study. To further extend the structural scope, we modified the mannose by either stereochemically locking 6-hydroxyl group with a cyclopropane unit or introducing a methyl group at C-6 (Figure 2.8.2). Here we used NMR-based methods and Mosher’s analysis¹³ to characterize the chemical structures of 6-modified ligands and fluorescence polarization assay¹⁴ to evaluate their binding affinities.

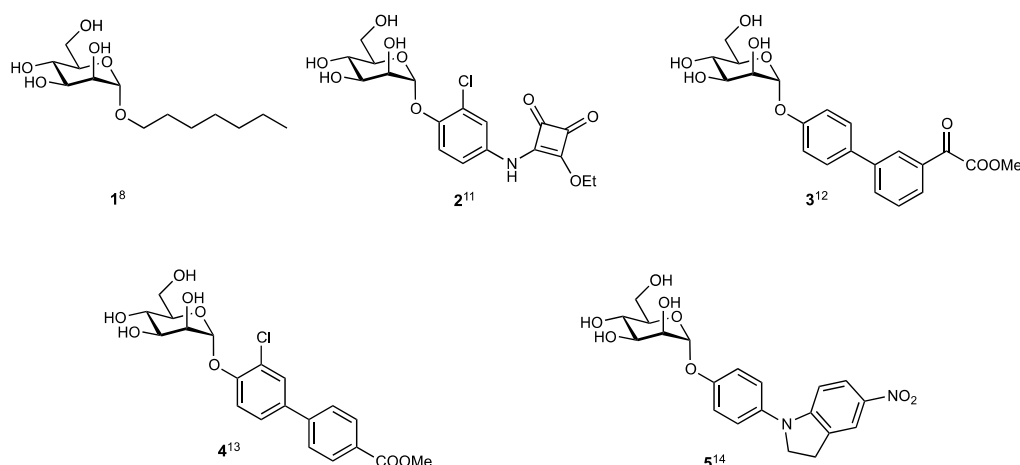


Figure 2.8.1. FimH antagonists: *n*-heptyl α -D-mannoside (**1**)⁶; the squaric acid derivative (**2**)⁹, biphenyl derivatives (**3-4**)^{10, 11}, and indolinyphenyl mannoside (**5**)¹².

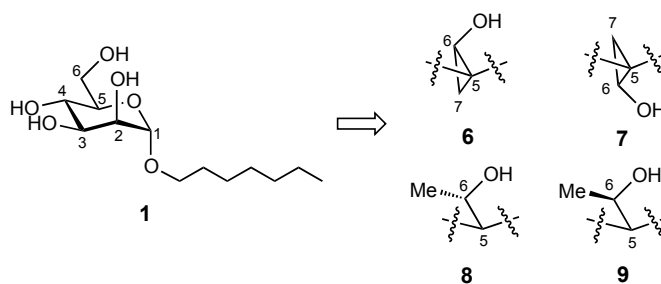


Figure 2.8.2. Structure design of 6-modified *n*-heptyl mannoside (**1**).

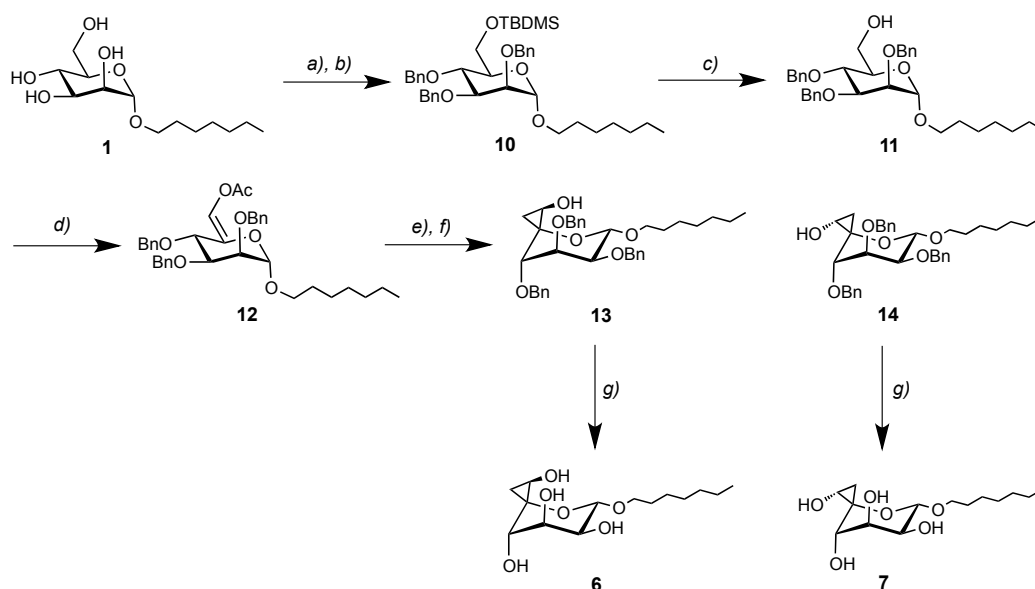
2.8.2 Chemical Synthesis

2.8.2.1 Synthesis of cyclopropane derivatives **6** and **7** (Scheme 2.8.1)

Our starting point of synthesis was *n*-heptyl mannoside (**1**) that was efficiently protected with *tert*-butyldimethylsilyl (TBDMS) at 6-position followed by global benzylation to yield **10**. TBDMS deprotection under acidic condition gave **11**. Swern oxidation of 6-hydroxyl afforded aldehyde intermediate, which was subsequently transformed into enol acetate **12** in the presence of acetic anhydride and potassium carbonate.¹⁵ The structure of (*Z*)-configured **12** was characterized by 2D-NMR and NOESY experiments. In a Simmons-Smith-Furukawa reaction¹⁶, olefin **12** was transformed into C-5 cyclopropane derivatives. The resulting diastereoisomers were separated after deacetylation under Zemplén conditions to afford **13** and **14**. Conformational analysis by ¹H NMR and 2D-NMR experiments revealed that in contrast to *n*-heptyl mannoside (**1**), the cyclopropanes **13** and **14** did not adopt the common ⁴C₁ but a ¹C₄ chair conformation (Figure 2.8.3). Hydrogenolysis afforded the cyclopropanated mannosides **6** and **7**.

2.8.2.2. Synthesis of 6-methyl derivatives **8** and **9** (Scheme 2.8.2)

Previously synthesized compound **11** was subjected to a Swern oxidation reaction followed by carbonyl addition in the presence of methyl lithium. The 6-methylated **15** and **16** were obtained in a ratio of 1:1 and could be separated by careful chromatography. Hydrogenolysis afforded the modified mannosides **8** and **9** in good yields. The absolute configuration of the newly generated 6-carbinol was deduced by Mosher's analysis.¹³



Scheme 2.8.1. Reagents and conditions: a) TBDMSCl, triethylamine, DMAP, DMF, 0°C to rt, overnight; b) BnBr, NaH, TBAI, THF, 0°C to rt, overnight (60% for two steps); c) H₂SO₄, MeOH, rt, overnight (90%); d) i. oxalyl chloride, DMSO, triethylamine, DCM, -78°C to rt, 4h; ii. K₂CO₃, Ac₂O, acetonitrile, reflux, overnight (80%); e) ZnEt₂, CH₂I₂, 1,2-dichloroethane, 50°C, overnight (40%); f) NaOMe, MeOH, rt, 1h (74% for **13**, 43% for **14**); g) Pd/C, H₂ (g), MeOH/DCM/EtOAc (3:1:1), rt, 1h (85% for **6**, 83% for **7**).

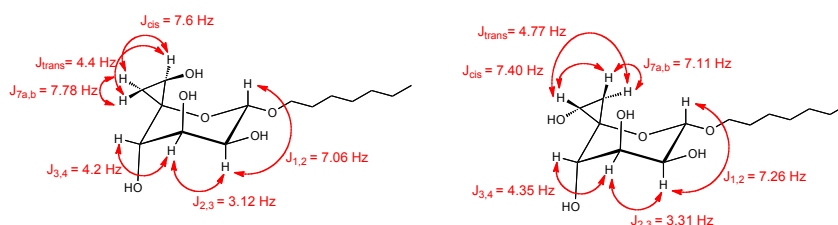
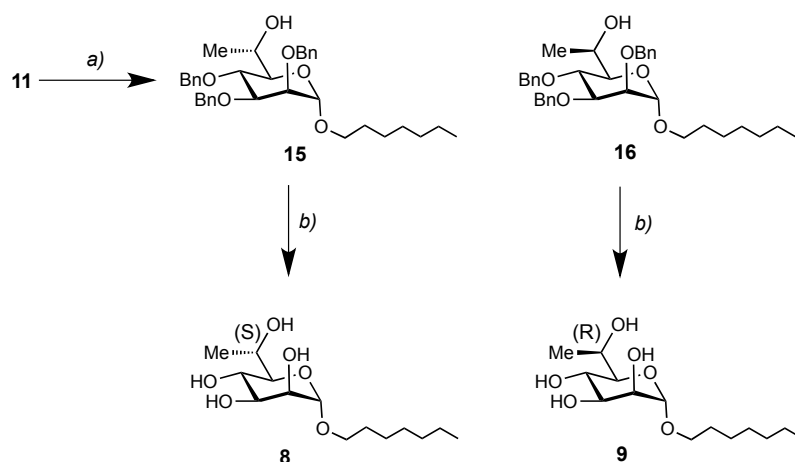


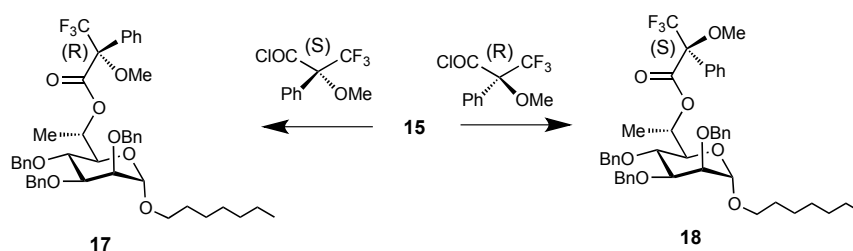
Figure 2.8.3. Coupling constants determined by ¹H NMR and 2D-COSY in D₂O.

2.8.2.3 Synthesis of 6-methyl derivatives **8** and **9** (Scheme 2.8.2)

Previously synthesized compound **11** was subjected to a Swern oxidation reaction followed by carbonyl addition in the presence of methyl lithium. The 6-methylated **15** and **16** were obtained in a ratio of 1:1 and could be separated by careful chromatography. Hydrogenolysis afforded the modified mannosides **8** and **9** in good yields. The absolute configuration of the newly generated 6-carbinol was deduced by Mosher's analysis.¹³



Scheme 2.8.2. Reagents and conditions: a) i. oxalyl chloride, DMSO, triethylamine, DCM, -78°C to rt, 4h; ii. MeLi, THF, -78°C to 0°C , 6h (**15/16** 1:1, 40%); b) Pd/C, H_2 (g), MeOH/DCM/EtOAc (3:1:1), rt, 1h (83% for **8**, 88% for **9**).



Scheme 2.8.3. Reagents and conditions: *S*-(+)- or *R*-(-)-MTPA-Cl, pyridine, DCM, rt, overnight (40%).

2.8.3 Structural Characterization - Mosher's Analysis

R- and *S*-Mosher esters (**17** and **18**) were synthesized from **15** and *S*-(+)-/*R*-(-)-MTPA chloride (Scheme 2.8.3), respectively.¹³ The phenyl substituent in each of the MTPA esters imposes a magnetic shielding effect on protons residing above/below the phenyl ring, resulting in a more upper field chemical shift for the affected protons in the NMR spectrum. ^1H NMR spectral data of the diastereomeric esters (**17** and **18**) were comparatively analyzed, and the chemical shifts were listed in Table 2.8.1. $\Delta\delta^{SR}$ values (defined, by convention, to be $\delta_S - \delta_R$) were calculated. By observing a positive $\Delta\delta^{SR}$ of 5-proton versus a negative value of 6-methyl, we can deduce that 5-proton is shielded in *R*-ester (**17**) and 6-methyl is shielded in *S*-ester (**18**), therefore the absolute configuration of C-6 in **15** is *S*. Thus the absolute configuration of C-6 in **16** is *R*.

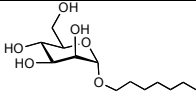
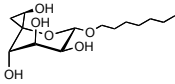
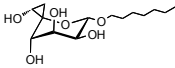
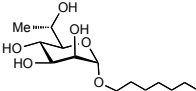
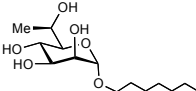
Table 2.8.1. $\Delta\delta(=\delta_S - \delta_R)$ data for the *R*- and *S*-MTPA Mosher esters (**17** and **18**).¹³

	δ_R -ester (17) (ppm)	δ_S -ester (18) (ppm)	$\Delta\delta^{SR}(=\delta_S - \delta_R)$	
			ppm	Hz (500 MHz)
6-Me	1.47	1.34	-0.13	-65
H-6	5.61	5.70	+0.09	45
H-5	3.55	3.59	+0.04	20
H-4	3.76	3.86	+0.10	50
H-3	3.87	3.91	+0.04	20
H-2	3.71	3.76	+0.05	25
H-1	4.85	4.86	+0.01	5

2.8.4 Biological Evaluation

To evaluate the binding affinity of modified n-heptyl mannosides (**6-9**), we used a competitive binding assay based on fluorescence polarization (FP) as described in Chapter 2.4. In a FP-assay, the test compound displaces a fluorescent-labeled competitor from the binding site, thereby reducing fluorescence polarization. Before the measurement of fluorescence polarization, a 24 h incubation time was applied in the presence of FimH-CRD. The assay was performed twice for each compound with each concentration in duplicate. IC_{50} values were obtained by nonlinear least-squares regression (standard four-parameter IC_{50} equation) and converted to K_D using a modified Cheng-Prusoff equation. The K_D values observed for the test compounds are summarized in Table 2.8.2.

Table 2.8.2. Affinity of synthesized antagonists to FimH-CRD-Th-His₆. Dissociation constants (K_d) were determined in a competitive fluorescence polarization assay.

Entry	Cpd	Structure	K_d [μ M]
1	1		0.028
2	6		> 30
3	7		--- ^a
4	8		7.5
5	9		2.6

a. The binding affinity was not detectable.

In general, the modified compounds (**6-9**) have shown lower affinity than *n*-heptyl mannoside (**1**) toward FimH-CRD. More than 1000-fold affinity decrease was observed with **6** and **7** due to conformational change of the sugar ring. The affinity difference between **8** and **9** shows that the direction of 6-hydroxyl group affects the binding affinity, and the decreased affinity indicates that the methyl group might be too bulky to fit into the binding pocket.

2.8.5 Conclusion

The modified heptyl mannosides **6-9** have shown different binding affinities, indicating that the direction of 6-hydroxyl indeed affects the ligand-protein interaction. However, 6-methyl is too bulky to maintain the high affinity; a fine tune of 6-substituent could be beneficial for further development of FimH antagonists. NMR analysis of derivatives **6** and **7** revealed the structural details of the stereochemically locked mannosides. Locking 6-hydroxyl of D-mannoses with cyclopropane unit provide new scaffolds for other protein targets that bind to ¹C₄ conformational mannosides.¹⁷

2.8.6 Experimental Section

General methods. NMR spectra were recorded on a Bruker Avance DMX-500 (500.1 MHz) spectrometer. Assignment of ¹H and ¹³C NMR spectra was achieved using 2D methods (COSY, HSQC, HMBC). Chemical shifts are expressed in ppm using residual CHCl₃, CHD₂OD or HDO as references. Optical rotations were measured using Perkin-Elmer Polarimeter 341. Electron spray ionization mass spectra (ESI-MS) were obtained on a Waters micromass ZQ. Reactions were monitored by TLC using glass plates coated with silica gel 60 F₂₅₄ (Merck) and visualized by using UV light and/or by charring with a molybdate solution (a 0.02 M solution of ammonium cerium sulfate dihydrate and ammonium molybdate tetrahydrate in aqueous 10% H₂SO₄). MPLC separations were carried out on a CombiFlash Companion or Rf from Teledyne Isco equipped with RediSep normal-phase or RP-18 reversed-phase flash columns. Commercially available reagents were purchased from Fluka, Aldrich, or Alfa Aesar. Solvents were purchased from Sigma-Aldrich (Buchs, Switzerland) or Acros Organics (Geel, Belgium) and were dried prior to use where indicated. Methanol (MeOH) was dried by refluxing with sodium

methoxide and distilled immediately before use. Dichloromethane (DCM) and acetonitrile were dried by filtration over Al₂O₃ (Fluka, type 5016 A basic). Molecular sieves 4Å were activated in vacuo at 500°C for 1 h immediately before use.

Compound 10: TBDMSCl (0.91g, 6.04 mmol), triethylamine (2.5 mL, 17.6 mmol), and DMAP (31 mg, 0.25 mmol) were added to a solution of *n*-heptyl mannoside (**1**)⁶ (1.4 g, 5.03 mmol) in DMF (5 mL) cooled at 0 °C. The mixture was stirred at 0°C for 1h, and then at rt overnight. The reaction mixture was diluted with EtOAc (50 mL), filtered over celite, and then the filtrate was extracted with water (50 mL) and brine (50 mL). The organic layer was dried over Na₂SO₄, filtered and concentrated in vacuo to give the crude intermediate, which was then used directly. To a solution of the intermediate in dry THF (10 mL) at 0°C, NaH (60%, 0.8 g, 20 mmol), BnBr (1.6 mL, 13.3 mmol) and tetrabutylammonium iodide (61 mg, 0.17 mmol) were added. The reaction mixture was then stirred at 0°C to rt overnight. The reaction was diluted with EtOAc (50 mL), extracted with water (50 mL × 3). The organic layer was dried over Na₂SO₄, filtered and concentrated. The residue was purified by MPLC on silica gel (petrol ether (PE)/EtOAc 10:1) to afford compound **10** (1.9 g, 60% for two steps) as colorless oil. R_f = 0.61 (PE/EtOAc, 10:1); [α]_D²⁰ +22.9 (*c* 2.0, EtOAc); ¹H NMR (500 MHz, CDCl₃): δ 7.37 - 7.20 (m, 15H, H-Ar), 4.86 (d, *J* = 10.9 Hz, 1H, CHPh), 4.74 (d, *J* = 1.3 Hz, 1H, H-1), 4.68 (d, *J* = 12.4 Hz, 1H, CHPh), 4.64 - 4.53 (m, 4H, 4 CHPh), 3.88 - 3.82 (m, 2H, H-3, H-4), 3.82 - 3.74 (m, 2H, H-6a, H-6b), 3.69 (s, 1H, H-2), 3.61 - 3.50 (m, 2H, H-5, OCH-heptyl), 3.25 (dt, *J* = 9.6, 6.6 Hz, 1H, OCH-heptyl), 1.48 - 1.39 (m, 2H, CH₂-heptyl), 1.28 - 1.13 (m, 8H, 4 CH₂-heptyl), 0.88 - 0.79 (m, 12H, CH₃-heptyl, tBu), 0.01 (d, *J* = 5.6 Hz, 6H, 2 SiCH₃); ¹³C NMR (126 MHz, CDCl₃): δ 138.77, 138.71, 138.61, 128.34, 128.31, 128.24, 128.02, 127.67, 127.65, 127.57, 127.47, 127.43 (C-Ar), 97.49 (C-1), 80.39 (C-3), 75.29 (C-2), 75.12 (CH₂Ph), 75.08 (C-4), 73.22 (C-5), 72.49, 72.18 (2 CH₂Ph), 67.35 (OCH₂), 62.89 (C-6), 31.78, 29.43, 29.10, 26.11, 25.94 (5 CH₂), 22.61, 18.31, 14.09, -5.12, -5.27 (6 CH₃); ESI-MS: *m/z*: calcd for C₄₀H₅₈NaO₆Si [M + Na]⁺: 685.39, found: 685.46.

Compound 11: To a solution of **10** (0.85 g, 1.3 mmol) in MeOH (7 mL) at rt was added 1N H₂SO₄ in MeOH (130 μL, 0.13 mmol). The reaction mixture was stirred at rt overnight and then concentrated. The residue was purified by MPLC on silica gel (PE/EtOAc 4:1) to afford compound **11** (0.64 g, 90%) as colorless oil. R_f = 0.42

(PE/EtOAc, 4:1); $[\alpha]_{\text{D}}^{20} +16.5$ (*c* 0.4, EtOAc); $^1\text{H NMR}$ (500 MHz, CDCl_3): δ 7.42 - 7.26 (m, 15H, H-Ar), 4.94 (d, $J = 10.9$ Hz, 1H, *CHPh*), 4.81 - 4.76 (m, 2H, 2 *CHPh*), 4.74 - 4.61 (m, 4H, H-1, 3 *CHPh*), 4.01 - 3.90 (m, 2H, H-3, H-4), 3.89 - 3.68 (m, 3H, H-2, H-6a, H-6b), 3.70 - 3.53 (m, 2H, H-5, *OCH*-heptyl), 3.32 (dt, $J = 9.6, 6.6$ Hz, 1H, *OCH*-heptyl), 1.54 - 1.44 (m, 2H, CH_2 -heptyl), 1.35-1.18 (m, 8H, 4 CH_2 -heptyl), 0.91 - 0.82 (m, 3H, CH_3); $^{13}\text{C NMR}$ (126 MHz, CDCl_3): δ 138.53, 138.41, 138.37, 128.43, 128.37, 128.11, 127.81, 127.75, 127.67, 127.62, 127.57 (C-Ar), 98.19 (C-1), 80.32 (C-3), 75.27 (C-4), 75.04 (2C, C-2, CH_2Ph), 72.92, 72.27 (2 CH_2Ph), 72.08 (C-5), 67.73 (OCH_2), 62.49 (C-6), 31.75, 29.40, 29.07, 26.06, 22.62 (5 CH_2), 14.09 (CH_3); ESI-MS: m/z : calcd for $\text{C}_{34}\text{H}_{44}\text{NaO}_6$ $[\text{M} + \text{Na}]^+$: 571.30, found: 571.38.

Compound 12: To a solution of oxalyl chloride (37 μL , 0.43 mmol) in DCM (1 mL) at -78°C , a solution of DMSO (28 μL , 0.40 mmol) in DCM (0.5 mL) was added. After 5 min, a solution of **11** (196 mg, 0.36 mmol) in DCM (1 mL) was added to the reaction mixture. After 15 min, triethylamine (0.25 mL, 1.8 mmol) was added at -78°C . The reaction mixture was stirred at -78°C for another 10 min, and then allowed to warm up to rt. The reaction mixture was diluted with DCM (10 mL), extracted with sat. NH_4Cl (10 mL) and brine (10 mL). The organic layer was concentrated, azeotroped with toluene (5 mL \times 3), and then dried in vacuo for 3h. The residue was dissolved with dry acetonitrile (5 mL), mixed with K_2CO_3 (100 mg, 0.72 mmol) and Ac_2O (70 μL , 0.72 mmol) at rt. And then the reaction mixture was stirred at 80°C overnight. The reaction mixture was then filtered through celite, concentrated and purified by MPLC on silica gel (PE/EtOAc, 6:1) to afford the enol ether **12** (119 mg, 57%) as colorless oil. $R_f = 0.42$ (PE/EtOAc, 6:1); $[\alpha]_{\text{D}}^{20} -19.3$ (*c* 1.0, EtOAc); $^1\text{H NMR}$ (500 MHz, CDCl_3): δ 7.37 - 7.26 (m, 15H, H-Ar), 7.02 (d, $J = 0.7$ Hz, 1H, H-6), 4.97 (d, $J = 4.4$ Hz, 1H, H-1), 4.79 - 4.56 (m, 6H, 6 *CHPh*), 4.18 (d, $J = 7.2$ Hz, 1H, H-4), 3.94 - 3.88 (m, 2H, H-3, *OCH*-heptyl), 3.86 - 3.81 (m, 1H, H-2), 3.50 (dt, $J = 9.3, 6.7$ Hz, 1H, *OCH*-heptyl), 2.16 (s, 3H, OAc), 1.61 - 1.55 (m, 2H, CH_2 -heptyl), 1.34 - 1.20 (m, 8H, 4 CH_2 -heptyl), 0.88 (t, $J = 6.9$ Hz, 3H, CH_3); $^{13}\text{C NMR}$ (126 MHz, CDCl_3): δ 167.47 (CO), 138.41, 138.36, 137.85, 135.71, 128.41, 128.33, 127.85, 127.72, 127.70, 127.62, 122.75 (C-Ar), 100.77 (C-1), 78.14 (C-3), 75.88 (C-2), 74.41 (C-4), 73.33, 72.95, 72.52 (3 CH_2Ph), 69.25 (OCH_2), 31.79, 29.45, 29.08, 26.04, 22.61 (5 CH_2), 20.68 (COCH_3), 14.09 (CH_3); ESI-MS: m/z : calcd for $\text{C}_{36}\text{H}_{44}\text{NaO}_7$ $[\text{M} + \text{Na}]^+$: 611.30, found: 611.16.

Compound 13 and 14: A two-neck flash was charged with **12** (650 mg, 1.1 mmol), CH_2I_2 (0.89 mL, 11.1 mmol), 4Å sieves (1.3 g), dry 1,2-dichloroethane (11 mL) and a stirring bar. The reaction mixture was stirred at 50°C under argon atmosphere for 2h. Then the reaction mixture was cooled with ice-bath, and added with ZnEt_2 (1M in Hexane, 5.5 mL, 5.5 mmol) dropwise. After 5 min at rt, the reaction mixture was stirred at 50°C overnight. The reaction mixture was cooled to rt, diluted with DCM (50 mL), extracted with sat. NaHCO_3 (50 mL \times 3). The organic layer was dried over Na_2SO_4 , filtered and concentrated in vacuo. The residue was purified by MPLC on silica gel (PE/EtOAc, 8:1) to give the acetate intermediates (265 mg, isomer ratio 2:1, 40%). The isomers were dissolved in MeOH (2 mL) and added with freshly prepared 0.5 M NaOMe/MeOH (0.1 equiv) under argon. The mixture was stirred at rt for 1h, and then neutralized with Amberlyst-15 (H^+) ion-exchange resin, filtered and concentrated in vacuo. The residue was purified by MPLC (PE/EtOAc 4:1) to give the products as colorless oil.

Compound 13: Yield: 127 mg, 73%. $R_f = 0.33$ (PE/EtOAc, 4:1); $[\alpha]_{\text{D}}^{20} +15.2$ (c 1.0, EtOAc); $^1\text{H NMR}$ (500 MHz, CDCl_3): δ 7.40 - 7.22 (m, 13H, H-Ar), 7.21 - 7.15 (m, 2H, H-Ar), 4.90 (d, $J = 4.6$ Hz, 1H, H-1), 4.79 (d, $J = 12.1$ Hz, 1H, *CHPh*), 4.74 (d, $J = 12.1$ Hz, 1H, *CHPh*), 4.72-4.60 (m, 3H, 3 *CHPh*), 4.50 (d, $J = 11.7$ Hz, 1H, *CHPh*), 3.91 (dd, $J = 6.8, 3.0$ Hz, 1H, H-3), 3.80 (dd, $J = 4.4, 3.2$ Hz, 1H, H-2), 3.74 (dt, $J = 9.3, 6.7$ Hz, 1H, *OCH-heptyl*), 3.60 (s, 1H, H-4), 3.39 (dt, $J = 9.4, 6.7$ Hz, 1H, *OCH-heptyl*), 3.34 (dt, $J = 7.4, 3.9$ Hz, 1H, H-6), 2.02 (d, $J = 4.7$ Hz, 1H, OH), 1.59 - 1.50 (m, 2H, CH_2 -heptyl), 1.29 (td, $J = 12.5, 5.9$ Hz, 8H, 4 CH_2 -heptyl), 1.04 (t, $J = 7.3$ Hz, 1H, H-7a), 0.88 (t, $J = 6.9$ Hz, 3H, CH_3), 0.69 (dd, $J = 7.4, 4.2$ Hz, 1H, H-7b); $^{13}\text{C NMR}$ (126 MHz, CDCl_3): δ 138.58, 138.30, 128.39, 128.35, 127.88, 127.66, 127.63, 127.60 (C-Ar), 100.42 (C-1), 78.25 (C-3), 76.36 (C-2), 75.89 (C-4), 73.44, 72.91(3 CH_2Ph), 69.18 (OCH_2), 57.02 (C-5), 50.29 (C-6), 31.81, 29.55, 29.15, 26.04, 22.63 (5 CH_2), 16.43 (C-7), 14.12 (CH_3); ESI-MS: m/z : calcd for $\text{C}_{35}\text{H}_{44}\text{NaO}_6$ [$\text{M} + \text{Na}$] $^+$: 583.30, found: 583.34.

Compound 14: Yield: 35 mg, 43%. $R_f = 0.33$ (PE/EtOAc, 4:1); $[\alpha]_{\text{D}}^{20} +20.7$ (c 1.3, EtOAc); $^1\text{H NMR}$ (500 MHz, CDCl_3): δ 7.40 - 7.24 (m, 13H, H-Ar), 7.21 - 7.17 (m, 2H, H-Ar), 4.80 - 4.74 (m, 3H, H-1, 2 *CHPh*), 4.67 (s, 2H, 2 *CHPh*), 4.65 - 4.59 (m, 1H, *CHPh*), 4.47 (d, $J = 11.7$ Hz, 1H, *CHPh*), 3.87 (dd, $J = 6.3, 3.0$ Hz, 1H, H-3), 3.79 - 3.61 (m, 3H, H-2, H-4, *OCH-heptyl*), 3.50 - 3.43 (m, 1H, H-6), 3.37 (dt, $J = 9.4, 6.9$ Hz, 1H,

OCH-heptyl), 2.96 (d, $J = 2.6$ Hz, 1H, OH), 1.56 – 1.45 (m, 2H, CH₂-heptyl), 1.34 - 1.20 (m, 8H, 4 CH₂-heptyl), 0.93 (t, $J = 7.2$ Hz, 1H, H-7a), 0.88 (t, $J = 7.0$ Hz, 3H, CH₃), 0.83 (dd, $J = 7.3, 4.3$ Hz, 1H, H-7b); ¹³C NMR (126 MHz, CDCl₃): δ 138.43, 138.35, 138.12, 128.39, 128.38, 128.36, 127.97, 127.79, 127.74, 127.69, 127.66, 127.49 (C-Ar), 101.14 (C-1), 78.02 (C-3), 76.39 (C-4), 76.10 (C-2), 73.48, 73.19, 73.06 (3 CH₂Ph), 70.12 (OCH₂), 59.43 (C-5), 49.81 (C-6), 31.72, 29.59, 28.98, 25.88, 22.59 (5 CH₂), 18.16 (C-7), 14.07 (CH₃); ESI-MS: m/z : calcd for C₃₅H₄₄NaO₆ [M + Na]⁺: 583.30, found: 583.34.

Compound 6 and 7: To a solution of **13** or **14** (10 mg, 0.017 mmol, 1.0 eq.) in a mixture of MeOH/DCM/EtOAc (3:1:1, 0.5 mL) Pd/C (10 wt.% on activated carbon, 10 mg) was added under argon atmosphere. The argon was exchange by a hydrogen atmosphere and the reaction mixture was stirred at rt for 1h. The reaction mixture was filtered through celite and concentrated. The residue was purified by MPLC on silica gel (DCM/MeOH 8:1) to afford **6** or **7** as colorless oil.

Compound 6: $R_f = 0.26$ (DCM/MeOH, 8:1); $[\alpha]_D^{20} +68.4$ (c 0.1, MeOH); ¹H NMR (500 MHz, D₂O): δ 4.75 (d, $J = 7.1$ Hz, 1H, H-1), 3.98 (t, $J = 3.4$ Hz, 1H, H-3), 3.82 – 3.76 (dd, $J = 16.7, 7.1$ Hz, 1H, OCH-heptyl); 3.72 (dd, $J = 6.9, 3.2$ Hz, 1H, H-2), 3.55 (dd, $J = 16.7, 7.1$ Hz, 1H, OCH-heptyl), 3.41 (dd, $J = 7.5, 4.5$ Hz, 1H, H-6), 3.27 (d, $J = 4.2$ Hz, 1H, H-4), 1.61 - 1.48 (m, 2H, CH₂), 1.32-1.14 (m, 8H, 4 CH₂), 0.96 (t, $J = 7.8$ Hz, 1H, H-7a), 0.79 (t, $J = 7.0$ Hz, 3H, CH₃), 0.73 (dd, $J = 7.6, 4.5$ Hz, 1H, H-7b); ¹³C NMR (126 MHz, D₂O): δ 99.88 (C-1), 71.79 (C-4), 70.97 (C-3), 70.28 (OCH₂), 68.30 (C-2), 58.99 (C-5), 51.26 (C-6), 31.00, 28.61, 28.19, 25.02, 21.95 (5 CH₂), 13.64 (C-7), 13.36 (CH₃); ESI-MS: m/z : calcd for C₁₄H₂₆NaO₆ [M + Na]⁺: 313.1622, found: 313.1622.

Compound 7: $R_f = 0.35$ (DCM/MeOH, 8:1); $[\alpha]_D^{20} +93.8$ (c 0.1, MeOH); ¹H NMR (500 MHz, D₂O): δ 4.75 (d, $J = 7.3$ Hz, 1H, H-1), 4.00 (t, $J = 3.8$ Hz, 1H, H-3), 3.85 - 3.73 (m, 2H, H-2, OCH-heptyl), 3.56 (dt, $J = 10.7, 6.9$ Hz, 1H, OCH-heptyl), 3.44 (dd, $J = 7.4, 4.8$ Hz, 1H, H-6), 3.28 (d, $J = 4.3$ Hz, 1H, H-4), 1.61 – 1.48 (m, 2H, CH₂), 1.34 – 1.14 (m, 8H, 4 CH₂), 1.03 (t, $J = 7.1$ Hz, 1H, H-7a), 0.90 - 0.84 (m, 1H, H-7b), 0.80 (t, $J = 6.7$ Hz, 3H, CH₃); ¹³C NMR (126 MHz, D₂O): δ 100.54 (C-1), 72.09 (C-4), 71.46 (C-3), 70.51 (OCH₂), 68.59 (C-2), 59.52 (C-5), 49.81 (C-6), 31.02, 28.69, 28.18, 25.03, 21.95 (5 CH₂), 17.30 (C-7), 13.36 (CH₃); ESI-MS: m/z : calcd for C₁₄H₂₆NaO₆ [M + Na]⁺: 313.1622, found: 313.1622.

Compound 15 and 16: To a solution of oxalyl chloride (37 μ L, 0.43 mmol) in DCM (1 mL) at -78°C , a solution of DMSO (28 μ L, 0.40 mmol) in DCM (0.5 mL) was added. After 5 min, a solution of **11** (200 mg, 0.36 mmol) in DCM (1 mL) was added to the reaction mixture. After 15 min, triethylamine (0.26 mL, 1.8 mmol) was added at -78°C . The reaction mixture was stirred at -78°C for another 10 min, and then allowed to warm up to rt. The reaction mixture was diluted with DCM (10 mL), extracted with sat. NH_4Cl (10 mL) and brine (10 mL). The organic layer was concentrated, azeotroped with toluene (5 mL \times 3), and then dried in vacuo for 3h. To a solution of the residue in dry THF (2 mL) at -78°C was added MeLi (1.6 M in diethyl ether, 0.36 mL, 0.36 mmol). The reaction mixture was stirred at -78°C to rt for 6h. The reaction mixture was quenched with ice water (10 mL), and then extracted with DCM (10 mL \times 2). The organic layer was dried over Na_2SO_4 , filtered and concentrated in vacuo. The residue was purified by MPLC on silica gel (PE/EtOAc 4:1) to give compound **15** and **16** (1:1, 40 mg, 40%) as colorless oil. Compound **15**: $R_f = 0.40$ (PE/EtOAc 4:1); $[\alpha]_{\text{D}}^{20} +19.2$ (c 0.9, EtOAc); ^1H NMR (500 MHz, CDCl_3): δ 7.38 - 7.26 (m, 15H, H-Ar), 4.95 (d, $J = 10.7$ Hz, 1H, *CHPh*), 4.82 (d, $J = 1.4$ Hz, 1H, H-1), 4.79 (d, $J = 12.2$ Hz, 1H, *CHPh*), 4.70 (d, $J = 4.1$ Hz, 1H, *CHPh*), 4.68 (d, $J = 5.8$ Hz, 1H, *CHPh*), 4.66 (d, $J = 1.8$ Hz, 2H, *CHPh*), 4.09 (t, $J = 9.5$ Hz, 2H, H-4, H-6), 3.90 (dd, $J = 9.4, 3.0$ Hz, 1H, H-3), 3.78 - 3.76 (m, 1H, H-2), 3.58 (dt, $J = 9.5, 6.8$ Hz, 1H, *OCH*-heptyl), 3.40 (dd, $J = 9.7, 1.0$ Hz, 1H, H-5), 3.32 (dt, $J = 9.6, 6.4$ Hz, 1H, *OCH*-heptyl), 1.54 - 1.47 (m, 2H, CH_2), 1.29 (dd, $J = 15.3, 6.9$ Hz, 11H, 4 CH_2 , CH_3 -6), 0.88 (t, $J = 6.8$ Hz, 3H, CH_3 -heptyl); ^{13}C NMR (126 MHz, CDCl_3): δ 138.61, 138.55, 138.46, 128.42, 128.40, 128.36, 128.14, 127.76, 127.70, 127.67, 127.63, 127.62, 127.54 (C-Ar), 98.22 (C-1), 80.45 (C-3), 75.33 (CH_2Ph), 75.14 (C-2), 75.09 (C-4), 74.37 (C-5), 72.86, 72.25 (2 CH_2Ph), 67.60 (OCH_2), 65.62 (C-6), 31.76, 29.41, 29.08, 26.16, 22.63 (5 CH_2), 20.33 (CH_3 -6), 14.10 (CH_3 -heptyl); ESI-MS: m/z : calcd for $\text{C}_{35}\text{H}_{46}\text{NaO}_6$ [$\text{M} + \text{Na}$] $^+$: 585.32, found: 585.36.

Compound **16**: $R_f = 0.45$ (PE/EtOAc 4:1); $[\alpha]_{\text{D}}^{20} +29.2$ (c 0.8, EtOAc); ^1H NMR (500 MHz, CDCl_3): δ 7.40 - 7.25 (m, 15H, H-Ar), 4.99 (d, $J = 10.9$ Hz, 1H, *CHPh*), 4.79 (d, $J = 1.6$ Hz, 1H, H-1), 4.75 (d, $J = 12.4$ Hz, 1H, *CHPh*), 4.71 - 4.59 (m, 4H, *CHPh*), 4.04 (s, 1H, H-6), 3.97 - 3.89 (m, 2H, H-3, H-4), 3.77 (s, 1H, H-2), 3.62 (dt, $J = 9.5, 6.8$ Hz, 1H, *OCH*-heptyl), 3.54 (dd, $J = 8.5, 5.1$ Hz, 1H, H-5), 3.31 (dt, $J = 9.5, 6.5$ Hz, 1H, *OCH*-heptyl), 2.83 (d, $J = 3.5$ Hz, 1H, OH), 1.56 - 1.48 (m, 2H, CH_2), 1.33 - 1.23 (m, 8H, 4 CH_2), 1.21 (d, $J = 6.3$ Hz, 3H, CH_3 -6), 0.88 (t, $J = 6.2$ Hz, 3H, CH_3 -heptyl); ^{13}C NMR

(126 MHz, CDCl₃): δ 138.38, 138.32, 138.00, 128.50, 128.42, 128.37, 128.14, 127.87, 127.73, 127.66 (C-Ar), 97.88 (C-1), 80.61 (C-4), 74.98 (C-3), 74.91 (C-2), 73.71 (CH₂Ph), 72.76 (C-5), 72.03 (2 CH₂Ph), 68.82 (C-6), 67.63 (OCH₂), 31.78, 29.40, 29.10, 26.12, 22.63 (5 CH₂), 18.16 (CH₃-6), 14.11(CH₃-heptyl); ESI-MS: m/z : calcd for C₃₅H₄₆NaO₆ [M + Na]⁺: 585.32, found: 585.36.

Compound 8 and 9: To a solution of **15** or **16** (7 mg, 0.012 mmol) in a mixture of MeOH/DCM/EtOAc (3:1:1, 0.5 mL) Pd/C (10 wt.% on activated carbon, 7 mg) was added under argon atmosphere. The argon was exchange by a hydrogen atmosphere and the reaction mixture was stirred at rt for 1h. The reaction mixture was filtered through celite and concentrated. The residue was purified by MPLC on silica gel (DCM/MeOH 8:1) to afford **8** or **9** as colorless oil.

Compound **8**: Yield: 3 mg, 83%; R_f = 0.40 (DCM/MeOH 8:1); $[\alpha]_D^{20}$ +77.3 (c 0.8, MeOH); ¹H NMR (500 MHz, MeOD): δ 4.79 (s, 1H, H-1), 4.13 (q, J = 6.4 Hz, 1H, H-5), 3.87 - 3.75 (m, 2H, H-2, H-4), 3.70 (t, J = 8.2 Hz, 2H, H-3, OCH-heptyl), 3.44 (dd, J = 15.5, 6.5 Hz, 1H, OCH-heptyl), 3.30 (1H, H-6), 1.61 (s, 2H, CH₂), 1.45 - 1.32 (m, 8H, 4 CH₂), 1.29 (d, J = 6.6 Hz, 3H, CH₃-6), 0.93 (t, J = 6.3 Hz, 3H, CH₃-heptyl); ¹³C NMR (126 MHz, MeOD): δ 101.70 (C-1), 76.09 (C-6), 72.99 (C-3), 72.37 (C-2), 68.60 (C-4), 68.41 (OCH₂), 65.99 (C-5), 32.98, 30.62, 30.24, 27.41, 23.70 (5 CH₂), 20.37 (CH₃-6), 14.42 (CH₃-heptyl); ESI-MS: m/z : calcd for C₁₄H₂₈NaO₆ [M + Na]⁺: 315.1778, found: 315.1779.

Compound **9**: Yield: 3.2 mg, 88%; R_f = 0.42 (DCM/MeOH 8:1); $[\alpha]_D^{20}$ +80.8 (c 0.86, MeOH); ¹H NMR (500 MHz, MeOD): δ 4.74 (d, J = 1.2 Hz, 1H, H-1), 4.07 - 4.02 (m, 1H, H-5), 3.79 (dd, J = 3.1, 1.6 Hz, 1H, H-2), 3.76 (dt, J = 9.5, 6.7 Hz, 1H, OCH-heptyl), 3.70 (dd, J = 9.3, 3.3 Hz, 1H, H-3), 3.65 (t, J = 9.4 Hz, 1H, H-4), 3.47 (dd, J = 9.4, 4.3 Hz, 1H, H-6), 3.41 (dt, J = 9.6, 6.3 Hz, 1H, OCH-heptyl), 1.66 - 1.57 (m, 2H, CH₂), 1.45 - 1.30 (m, 8H, 4 CH₂), 1.27 (d, J = 6.4 Hz, 3H, CH₃-6), 0.93 (t, J = 6.9 Hz, 3H, CH₃-heptyl); ¹³C NMR (126 MHz, MeOD): δ 101.52 (C-1), 75.89 (C-6), 72.80 (C-3), 72.15 (C-2), 70.87 (C-4), 69.37 (C-5), 68.48 (OCH₂), 33.02, 30.62, 30.28, 27.38, 23.70 (5 CH₂), 17.99 (CH₃-6), 14.43 (CH₃-heptyl); ESI-MS: m/z : calcd for C₁₄H₂₈NaO₆ [M + Na]⁺: 315.1778, found: 315.1779.

Compound 17 and 18: To a solution of **15** (19 mg, 0.03 mmol) in dry DCM (1 mL) was added S-(+)- MTPA chloride or R-(-)-MTPA chloride (17 mg, 0.06 mmol) and pyridine (8 μ L, 0.10 mmol) at rt. The reaction mixture was stirred at rt for 2h. The reaction mixture was then diluted with ethyl ether (10 mL) and extracted with water (10 mL \times 2). The organic layer was dried over Na₂SO₄, filtered and concentrated in vacuo. The residue was purified by MPLC on silica gel (PE/EtOAc 4:1) to give compound **17** or **18** (10 mg, 40%) as colorless oil.

Compound **17**: R_f = 0.66 (PE/EtOAc 4:1); $[\alpha]_D^{20}$ +44.4 (c 1.0, EtOAc); ¹H NMR (500 MHz, CDCl₃): δ 7.61 (d, J = 7.2 Hz, 2H, H-Ar), 7.38 - 7.21 (m, 18H, H-Ar), 5.65 - 5.57 (m, 1H, H-6), 4.85 (d, J = 1.5 Hz, 1H, H-1), 4.78 (d, J = 10.2 Hz, 1H, *CHPh*), 4.68 (d, J = 12.1 Hz, 1H, *CHPh*), 4.62 (d, J = 2.4 Hz, 2H, *CHPh*), 4.58 (d, J = 12.1 Hz, 1H, *CHPh*), 4.28 (d, J = 10.2 Hz, 1H, *CHPh*), 3.87 (dd, J = 9.2, 3.0 Hz, 1H, H-3), 3.76 (t, J = 9.5 Hz, 1H, H-4), 3.73 - 3.70 (m, 1H, H-2), 3.59 - 3.51 (m, 2H, H-5, *OCH*-heptyl), 3.48 (s, 3H, OCH₃), 3.32 (dt, J = 9.6, 6.5 Hz, 1H, *OCH*-heptyl), 1.51 - 1.44 (m, 4H, CH₂, CH₃-6), 1.34 - 1.19 (m, 8H, 4 CH₂), 0.88 (t, J = 6.8 Hz, 3H, CH₃-heptyl); ¹³C NMR (126 MHz, CDCl₃): δ 166.54 (CO), 138.60, 138.55, 138.35, 131.97, 129.67, 128.61, 128.57, 128.51, 128.34, 127.94, 127.85, 127.75, 127.64, 127.59 (C-Ar), 97.87 (C-1), 80.66 (C-3), 75.35 (*CHPh*), 75.28 (C-2), 74.84 (C-4), 73.21 (C-5), 72.80, 72.11 (2 *CHPh*), 71.15 (C-6), 67.82 (*OCH*-heptyl), 55.67 (OCH₃), 31.88, 29.58, 29.22, 26.30, 22.76 (5 CH₂), 16.45 (CH₃-6), 14.23 (CH₃-heptyl); ESI-MS: m/z : calcd for C₄₅H₅₃F₃NaO₈ [M + Na]⁺: 801.36, found: 801.46.

Compound **18**: R_f = 0.66 (PE/EtOAc 4:1); $[\alpha]_D^{20}$ -16.0 (c 0.6, EtOAc); ¹H NMR (500 MHz, CDCl₃): δ 7.60 - 7.53 (m, 2H, H-Ar), 7.40 - 7.26 (m, 18H, H-Ar), 5.75 - 5.67 (m, 1H, H-6), 4.88 (d, J = 10.0 Hz, 1H, *CHPh*), 4.86 (d, J = 1.6 Hz, 1H, H-1), 4.72 (d, J = 11.9 Hz, 1H, *CHPh*), 4.67 (s, 1H, *CHPh*), 4.62 (d, J = 12.0 Hz, 1H, *CHPh*), 4.44 (d, J = 10.0 Hz, 1H, *CHPh*), 3.91 (dd, J = 9.2, 2.9 Hz, 1H, H-3), 3.86 (t, J = 9.4 Hz, 1H, H-4), 3.78 - 3.74 (m, 1H, H-2), 3.59 - 3.52 (m, 2H, H-5, *OCH*-heptyl), 3.47 (s, 3H, OCH₃), 3.32 (dt, J = 9.6, 6.5 Hz, 1H, *OCH*-heptyl), 1.52 - 1.44 (m, 2H, CH₂), 1.34 (d, J = 6.6 Hz, 3H, CH₃-6), 1.31 - 1.20 (m, 8H, 4 CH₂), 0.87 (t, J = 6.9 Hz, 3H, CH₃-heptyl); ¹³C NMR (126 MHz, CDCl₃): δ 166.54 (CO), 138.41, 138.34, 138.24, 131.81, 129.50, 128.48, 128.45, 128.42, 128.37, 128.30, 127.81, 127.79, 127.72, 127.65 (C-Ar), 97.83 (C-1), 80.62 (C-3), 75.36 (*CHPh*), 75.23 (C-2), 74.82 (C-4), 73.14 (C-5), 73.00, 72.07 (2 *CHPh*), 70.31 (C-6), 67.72 (*OCH*-heptyl), 55.74 (OCH₃), 31.73, 29.42, 29.07, 26.15, 22.62 (5 CH₂), 16.46

(CH₃-6), 14.08 (CH₃-heptyl); ESI-MS: *m/z*: calcd for C₄₅H₅₃F₃NaO₈ [M + Na]⁺: 801.36, found: 801.52.

REFERENCES

1. a) Foxman, B.; Barlow, R.; D'Arcy, H.; Gillespie, B.; Sobel, J. D., Urinary tract infection: Self reported incidence and associated costs. *Ann. Epidemiol.* **2000**, *10*, 509-515; b) Ronald, A., The etiology of urinary tract infection: Traditional and emerging pathogens. *Am. J. Med.* **2002**, *113*, 14S-19S.
2. Wiles, T. J.; Kulesus, R. R.; Mulvey, M. A., Origins and virulence mechanisms of uropathogenic Escherichia coli. *Exp. Mol. Pathol.* **2008**, *85*, 11-19.
3. Capitani, G.; Eidam, O.; Glockshuber, R.; Grütter, M. G., Structural and functional insights into the assembly of type 1 pili from Escherichia coli. *Microbes. Infect.* **2006**, *8*, 2284-2290.
4. a) Choudhury, D.; Thompson, A.; Stojanoff, V.; Langermann, S.; Pinkner, J.; Hultgren, S. J.; Knight, S. D., X-ray structure of the FimC-FimH chaperone-adhesin complex from uropathogenic Escherichia coli. *Science* **1999**, *285*, 1061-1066.; b) Wellens, A.; Garofalo, C.; Nguyen, H.; Van Gerven, N.; Slattegard, R.; Hernalsteens, J. P.; Wyns, L.; Oscarson, S.; De Greve, H.; Hultgren, S.; Bouckaert, J., Intervening with Urinary Tract Infections Using Anti-Adhesives Based on the Crystal Structure of the FimH-Oligomannose-3 Complex. *PLoS One* **2008**, *3*, e2040.
5. Wellens, A.; Lahmann, M.; Touaibia, M.; Vaucher, J.; Oscarson, S.; Roy, R.; Remaut, H.; Bouckaert, J., The Tyrosine Gate as a Potential Entropic Lever in the Receptor-Binding Site of the Bacterial Adhesin FimH. *Biochemistry* **2012**, *51*, 4790-4799.
6. Bouckaert, J.; Berglund, J.; Schembri, M.; De Genst, E.; Cools, L.; Wuhrer, M.; Hung, C. S.; Pinkner, J.; Slattegard, R.; Zavialov, A.; Choudhury, D.; Langermann, S.; Hultgren, S. J.; Wyns, L.; Klemm, P.; Oscarson, S.; Knight, S. D.; De Greve, H., Receptor binding studies disclose a novel class of high-affinity inhibitors of the Escherichia coli FimH adhesin. *Mol. Microbiol.* **2005**, *55*, 441-455.

7. Sharon, N., Carbohydrates as future anti-adhesion drugs for infectious diseases. *Biochim. Biophys. Acta.* **2006**, *1760*, 527-537.
8. a) Firon, N.; Ashkenazi, S.; Mirelman, D.; Ofek, I.; Sharon, N., Aromatic Alpha-Glycosides of Mannose Are Powerful Inhibitors of the Adherence of Type-1 Fimbriated Escherichia-Coli to Yeast and Intestinal Epithelial-Cells. *Infect. Immun.* **1987**, *55*, 472-476.; b) Pang, L. J.; Kleeb, S.; Lemme, K.; Rabbani, S.; Scharenberg, M.; Zalewski, A.; Schadler, F.; Schwardt, O.; Ernst, B., FimH Antagonists: Structure-Activity and Structure-Property Relationships for Biphenyl a-D-Mannopyranosides. *ChemMedChem* **2012**, *7*, 1404-1422.
9. Sperling, O.; Fuchs, A.; Lindhorst, T. K., Evaluation of the carbohydrate recognition domain of the bacterial adhesin FimH: Design, synthesis and binding properties of mannoside ligands. *Org. Biomol. Chem.* **2006**, *4*, 3913-3922.
10. Han, Z. F.; Pinkner, J. S.; Ford, B.; Obermann, R.; Nolan, W.; Wildman, S. A.; Hobbs, D.; Ellenberger, T.; Cusumano, C. K.; Hultgren, S. J.; Janetka, J. W., Structure-Based Drug Design and Optimization of Mannoside Bacterial FimH Antagonists. *J. Med. Chem.* **2010**, *53*, 4779-4792.
11. Klein, T.; Abgottspon, D.; Wittwer, M.; Rabbani, S.; Herold, J.; Jiang, X. H.; Kleeb, S.; Luthi, C.; Scharenberg, M.; Bezencon, J.; Gubler, E.; Pang, L. J.; Smiesko, M.; Cutting, B.; Schwardt, O.; Ernst, B., FimH Antagonists for the Oral Treatment of Urinary Tract Infections: From Design and Synthesis to in Vitro and in Vivo Evaluation. *J. Med. Chem.* **2010**, *53*, 8627-8641.
12. Jiang, X. H.; Abgottspon, D.; Kleeb, S.; Rabbani, S.; Scharenberg, M.; Wittwer, M.; Haug, M.; Schwardt, O.; Ernst, B., Antiadhesion Therapy for Urinary Tract Infections-A Balanced PK/PD Profile Proved To Be Key for Success. *J. Med. Chem.* **2012**, *55*, 4700-4713.
13. Hoye, T. R.; Jeffrey, C. S.; Shao, F., Mosher ester analysis for the determination of absolute configuration of stereogenic (chiral) carbinol carbons. *Nat. Protoc.* **2007**, *2*, 2451-2458.
14. Nikolovska-Coleska, Z.; Wang, R.; Fang, X.; Pan, H.; Tomita, Y.; Li, P.; Roller, P.; Krajewski, K.; Saito, N.; Stuckey, J.; Wang, S., Development and optimization of a binding assay for the XIAP BIR3 domain using fluorescence polarization. *Anal. Biochem.* **2004**, *332*, 261-273.
15. a) Brand, C.; Granitzka, M.; Stalke, D.; Werz, D. B., Reducing the conformational flexibility of carbohydrates: locking the 6-hydroxyl group by cyclopropanes. *Chem.*

-
- Commun.* **2011**, *47*, 10782-10784.; b) Brand, C.; Kettelhoit, K.; Werz, D. B., Glycosylations of cyclopropyl-modified carbohydrates: remarkable β -selectivity using a mannose building block. *Org. Lett.* **2012**, *14*, 5126-5129.
16. Kim, H. Y.; Walsh, P. J., Efficient approaches to the stereoselective synthesis of cyclopropyl alcohols. *Acc. Chem. Res.* **2012**, *45*, 1533-1547.
17. Karaveg, K.; Siriwardena, A.; Tempel, W.; Liu, Z. J.; Glushka, J.; Wang, B. C.; Moremen, K. W., Mechanism of class 1 (glycosylhydrolase family 47) α -mannosidases involved in N-glycan processing and endoplasmic reticulum quality control. *J. Biol. Chem.* **2005**, *280*, 16197-16207.

3. Summary and Outlook

The goal of the present thesis was to optimize the lead structures of carbohydrate mimetics, to develop highly potent, orally available FimH antagonists for the treatment of urinary tract infections. For this purpose, various structural modifications were performed, being guided by computational modeling and biological evaluation results. Diverse strategies were implemented in order to improve the binding affinity, to explore the binding mode, and to optimize the pharmacokinetic (PK) properties of FimH antagonists (Figure 3.1). The structures of the synthesized compounds were designed based on crystal structures of the ligand-protein complexes and *in silico* docking studies. Divergent synthetic procedures were carried out and optimized. Both traditional synthetic strategies and dynamic combinatorial techniques were applied for establishing the designed compound libraries.

Starting from highly potent biphenyl α -D-mannopyranoside with a *para*-carboxylate on the terminal aromatic ring of the aglycone, an ester prodrug approach was successfully applied for masking the polar carboxylate and, hence, for increasing the membrane permeability.¹ However, the aqueous solubility of the initially developed antagonists was in the low $\mu\text{g/mL}$ range, which hampered their oral application and complicated their *in vivo* evaluation. To solve the solubility problem, we firstly introduced different substitution patterns to the aglycone moiety in order to decrease the crystal packing energy by disruption of the molecular planarity and symmetry. Further modifications included introduction of heterocyclic aryl aglycones, and bioisosteric replacement of the carboxylic ester moiety to improve both PD and PK properties. All above approaches indeed increased the solubility and PD/PK properties of a series of biaryl FimH antagonists, according to *in vitro* results. *In vivo* evaluation of the selected candidates will be performed in a further step.

While the optimized PK profile is a prerequisite for achieving oral bioavailability, the binding affinity plays another crucial role for a successful treatment. As previously reported, the binding mode of an antagonist to the CRD of FimH can switch from an “in-docking mode” to an “out-docking mode”, depending on the structure of the antagonist.² Moreover, the “catch bond” behavior of FimH, that is the lectin domain of FimH is stabilized in a low-affinity state by the pili domain and the isolated lectin domain adopts a

high-affinity state, further complicated the binding affinity of FimH antagonists.^{3, 4} To study the binding mode, to optimize the potency, and to explore the CRD of FimH, we investigated the structure-activity relationships (SARs) for diversified compound libraries. By introducing *ortho* substituents on ring A (Figure 3.1), we demonstrated the correlation between vdW volumes of the substituents and the enthalpy term, which indicated the importance of shape complementarity.⁵ With a series of bioisosteric replacement of the *para*-carboxylic ester on ring B, a four- to five-fold improvement of affinity was achieved, resulting from reduced desolvation penalty and improved fit in the binding pocket.⁶ *In situ* generation and screening of dynamic combinatorial libraries (DCLs) further boosted the lead optimization process toward the native full-length FimH, and provided a rapid and efficient platform of the ligand screening.

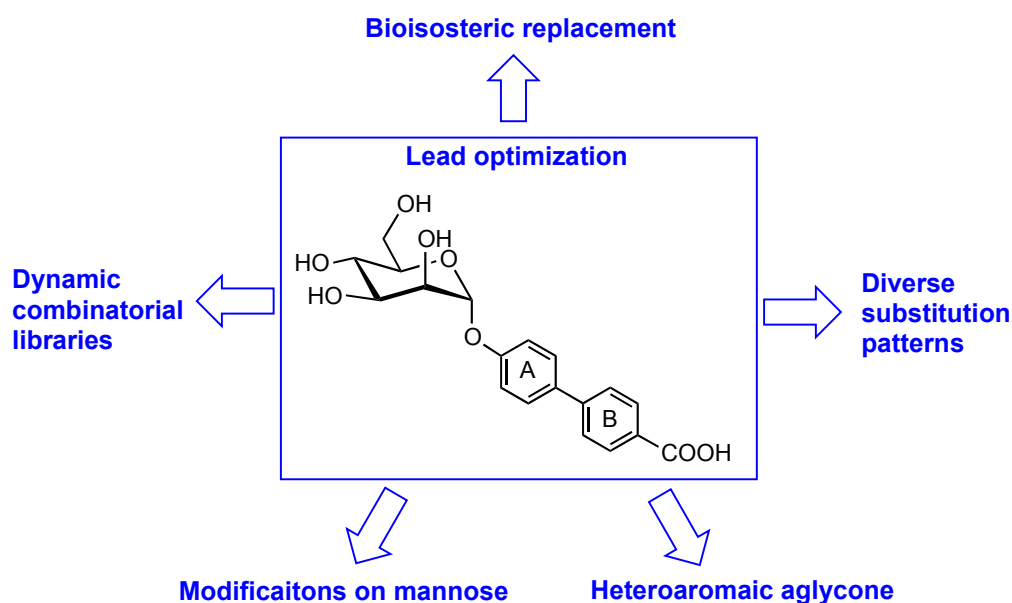


Figure 3.1. Lead optimization strategies for the development of FimH antagonists.

In summary, our studies established structural-activity and structure-property relationships for a series of structurally diversified α -D-mannosides. Balancing between the PD and PK properties to make a best compromise is critical for lead optimization of FimH antagonists. Further *in vitro* and *in vivo* pharmacokinetic studies provided insightful understanding of the anti-adhesive efficiency of biaryl FimH antagonists. The thorough lead optimization studies will further support the development of biaryl α -D-

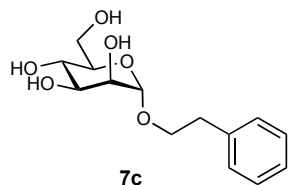
mannosides towards a marketed drug for the prevention and treatment of urinary tract infections.

REFERENCES

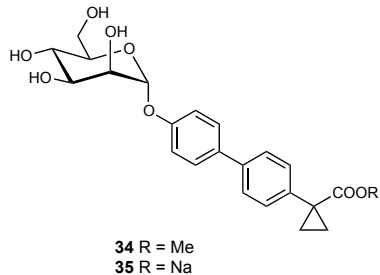
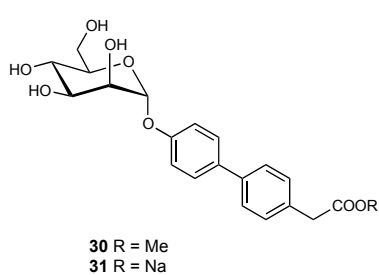
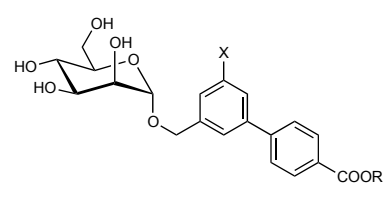
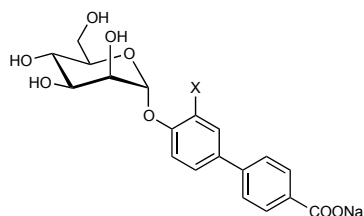
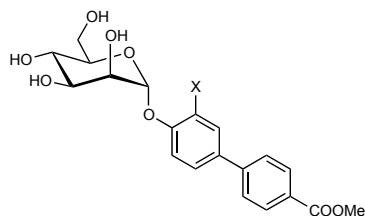
1. Klein, T.; Abgottspon, D.; Wittwer, M.; Rabbani, S.; Herold, J.; Jiang, X.; Kleeb, S.; Lüthi, C.; Scharenberg, M.; Bezençon, J.; Gubler, E.; Pang, L.; Smiesko, M.; Cutting, B.; Schwardt, O.; Ernst, B. FimH antagonists for the oral treatment of urinary tract infections: from design and synthesis to in vitro and in vivo evaluation. *J. Med. Chem.* **2010**, *53*, 8627-41.
2. Schwardt, O.; Rabbani, S.; Hartmann, M.; Abgottspon, D.; Wittwer, M.; Kleeb, S.; Zalewski, A.; Smiesko, M.; Cutting, B.; Ernst, B. Design, synthesis and biological evaluation of mannosyl triazoles as FimH antagonists. *Bioorg. Med. Chem.* **2011**, *19*, 6454-6473.
3. Le Trong, I.; Aprikian, P.; Kidd, B. A.; Forero-Shelton, M.; Tchesnokova, V.; Rajagopal, P.; Rodriguez, V.; Interlandi, G.; Klevit, R.; Vogel, V.; Stenkamp, R. E.; Sokurenko, E. V.; Thomas, W. E. Structural basis for mechanical force regulation of the adhesin fimH via finger trap-like beta sheet twisting. *Cell* **2010**, *141*, 645-655.
4. Scharenberg, M.; Jiang, X.; Pang, L.; Navarra, G.; Rabbani, S.; Binder, F.; Schwardt, O.; Ernst, B. Kinetic properties of carbohydrate-lectin interactions: FimH antagonists. *ChemMedChem* **2014**, *9*, 78-83.
5. Pang, L.; Kleeb, S.; Lemme, K.; Rabbani, S.; Scharenberg, M.; Zalewski, A.; Schädler, F.; Schwardt, O.; Ernst, B. FimH antagonists: structure-activity and structure-property relationships for biphenyl α -D-mannopyranosides. *ChemMedChem* **2012**, *7*, 1404-22.
6. Kleeb, S.; Pang, L.; Mayer, K.; Eris, D.; Sigl, A.; Preston, R.C.; Zihlmann, P.; Sharpe, T.; Jakob, R.P.; Abgottspon, D.; Hutter, A.S.; Scharenberg, M.; Jiang, X.; Navarra, G.; Rabbani, S.; Smiesko, M.; Lüdin, N.; Bezençon, J.; Schwardt, O.; Maier, T.; Ernst, B. FimH antagonists: Bioisosteres to improve the in vitro and in vivo PK/PD profile. *J. Med. Chem.* **2015**, *58*, 2221-2239.

4. Formula Index

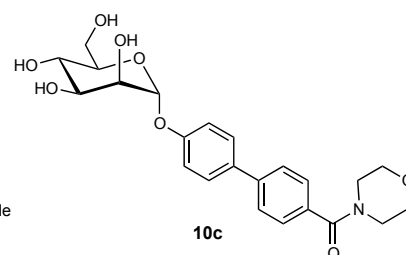
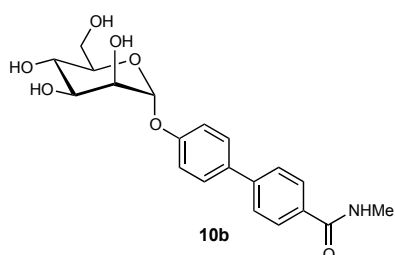
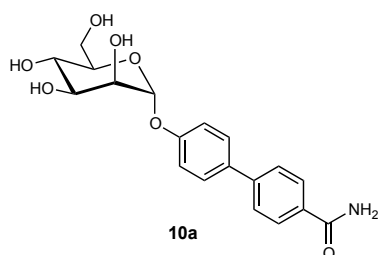
Chapter 2.2

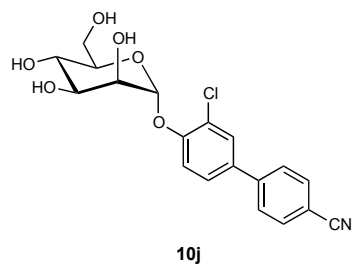
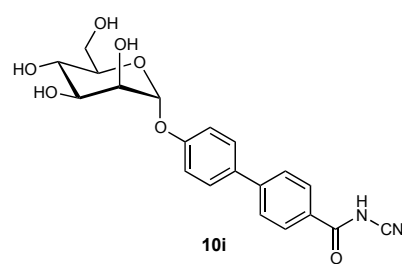
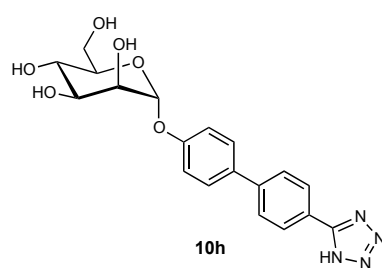
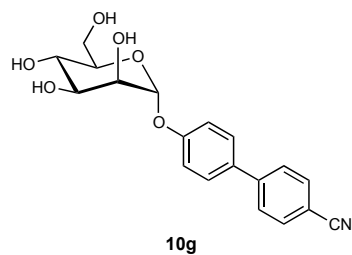
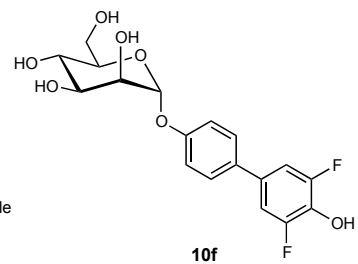
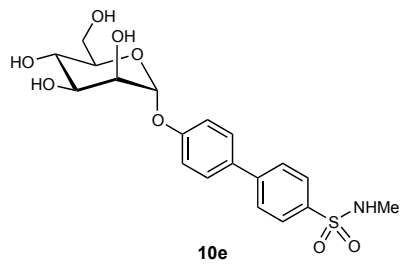
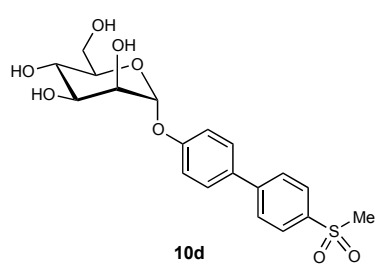


Chapter 2.3

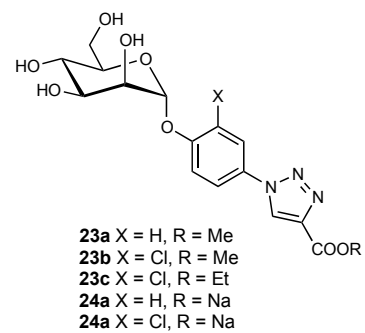
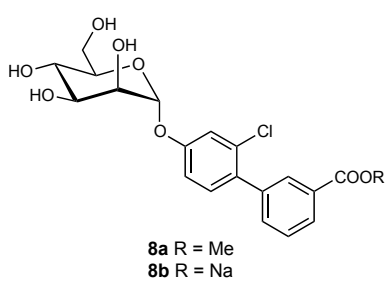
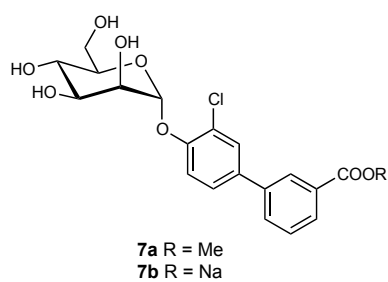


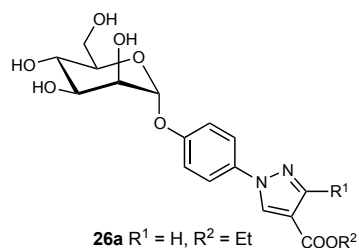
Chapter 2.4



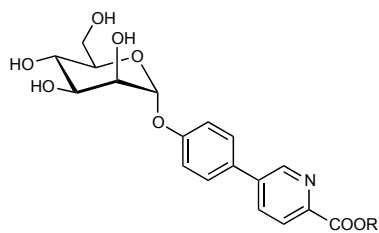


Chapter 2.5

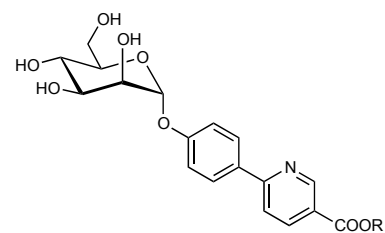




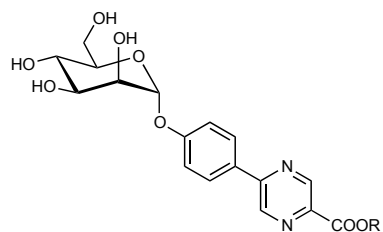
26a R¹ = H, R² = Et
26b R¹ = CF₃, R² = Et
27a R¹ = H, R² = Na
27b R¹ = CF₃, R² = Na



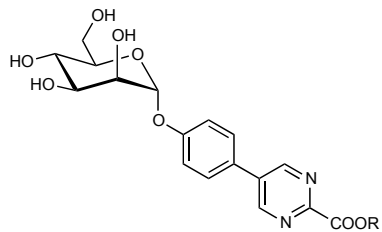
32a R = Me
33a R = Na



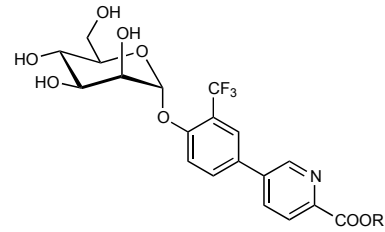
32b R = Me
33b R = Na



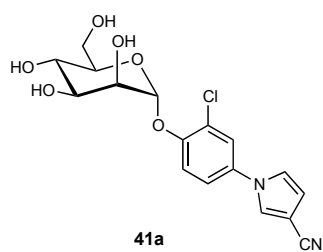
32c R = Me
33c R = Na



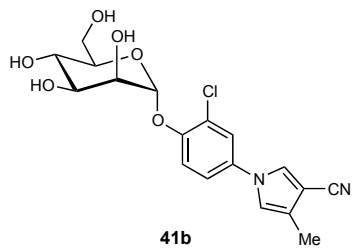
32d R = Me
33d R = Na



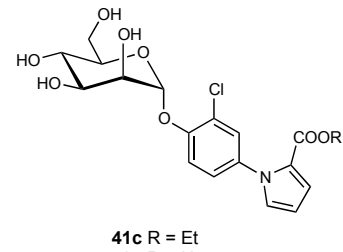
37 R = Me
38 R = Na



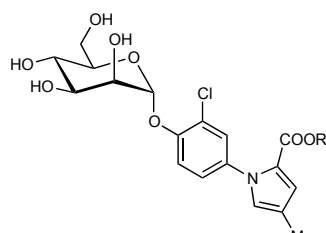
41a



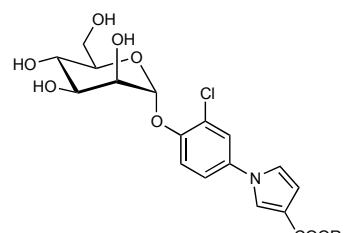
41b



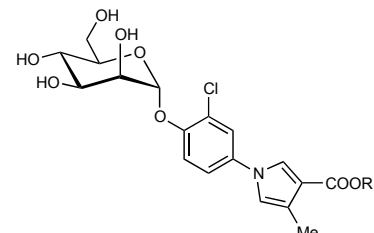
41c R = Et
42 R = Na



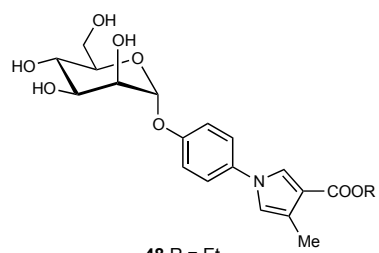
41d R = Et
43 R = Na



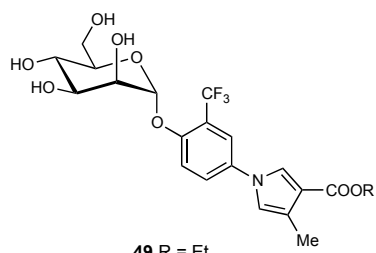
41e R = Me
44 R = Na



41f R = Et
45 R = Na

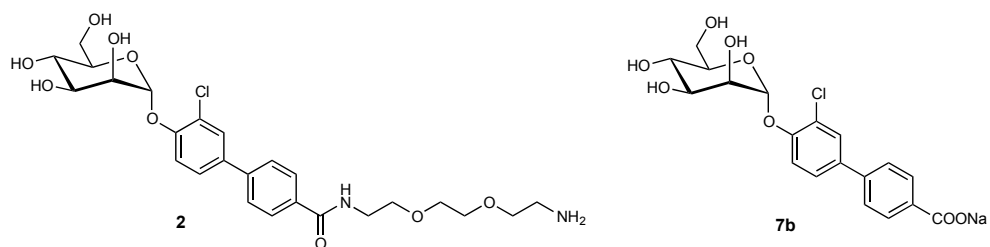


48 R = Et
50 R = Na

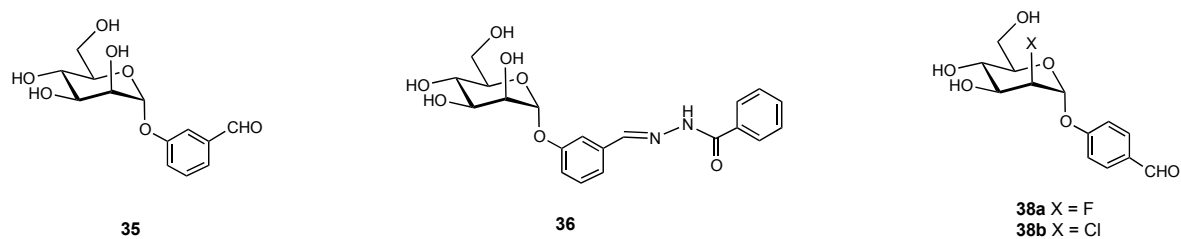
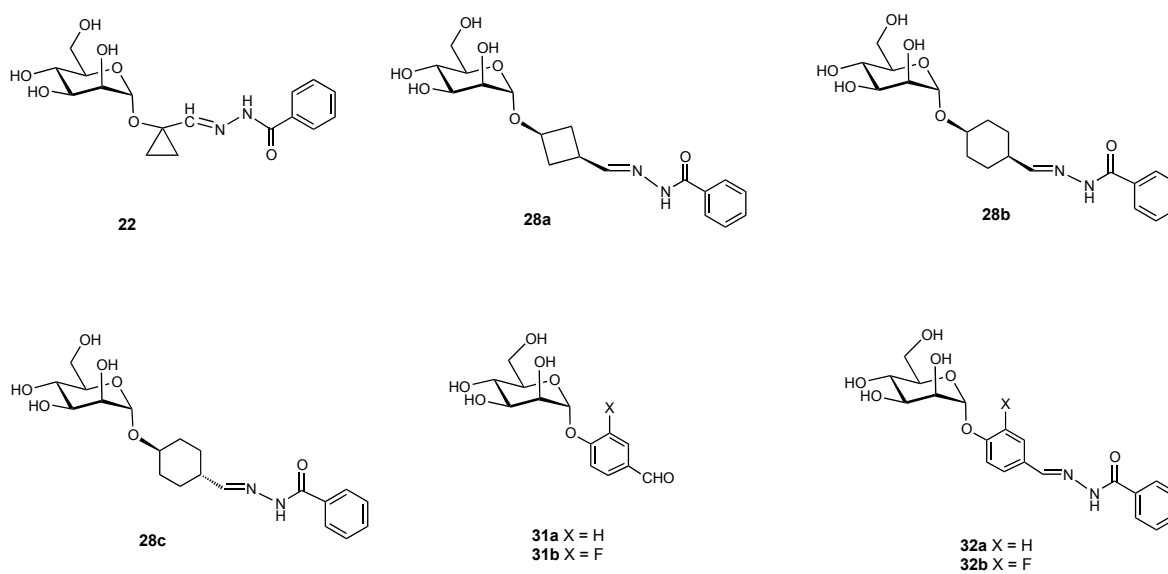
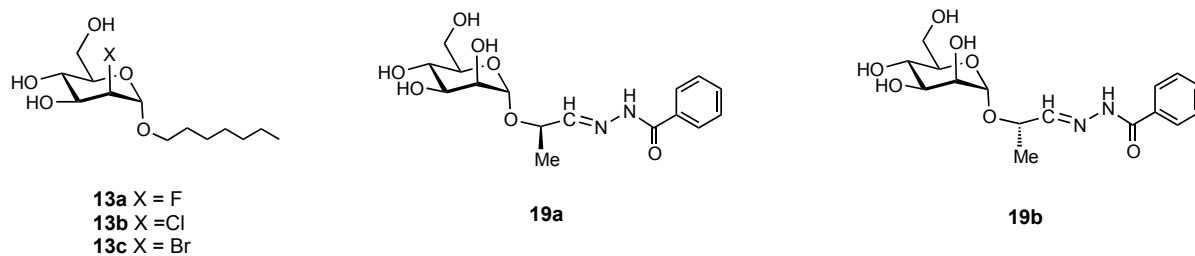


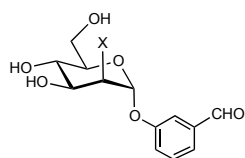
49 R = Et
51 R = Na

Chapter 2.6

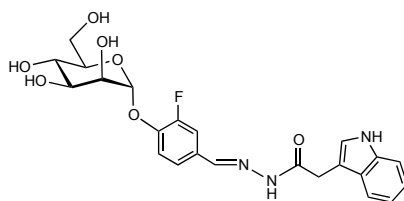


Chapter 2.7

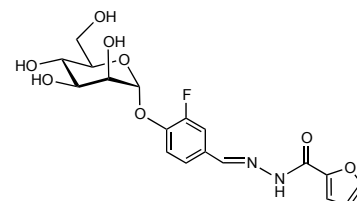




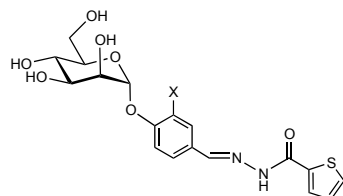
40a X = F
40b X = Cl



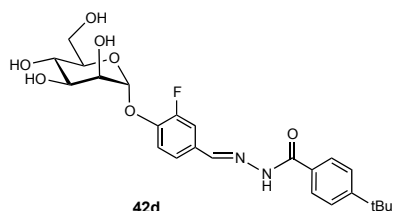
42a



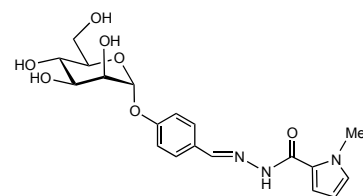
42b



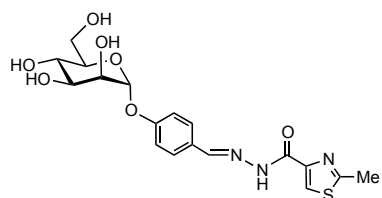
42c X = F
43c X = H



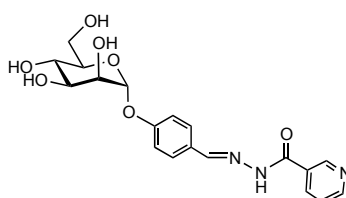
42d



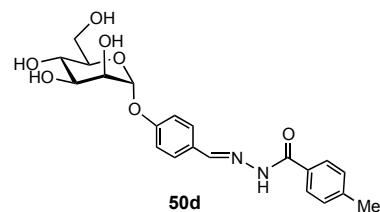
50a



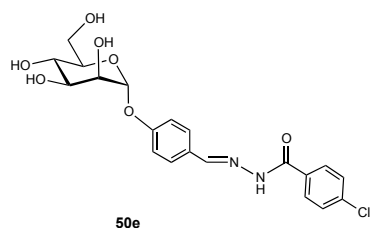
50b



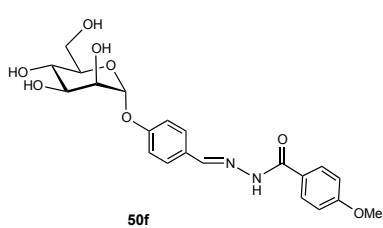
50c



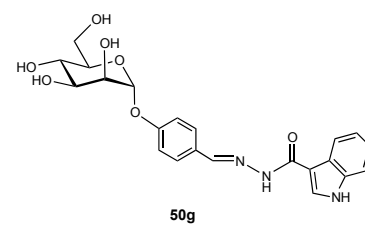
50d



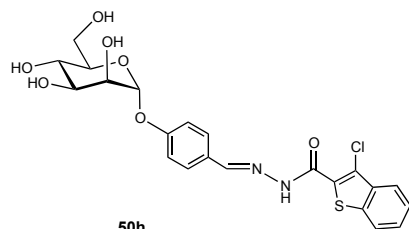
50e



50f

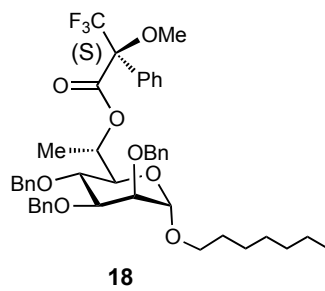
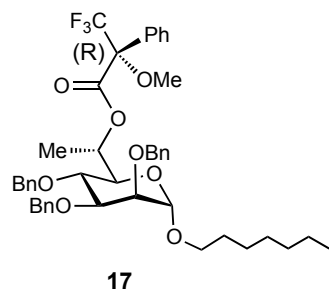
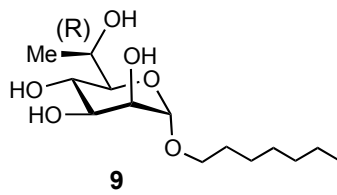
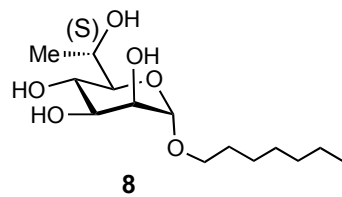
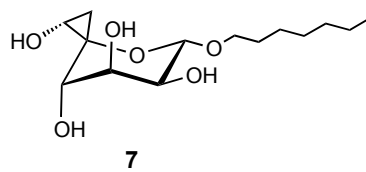
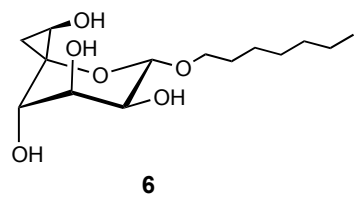


50g



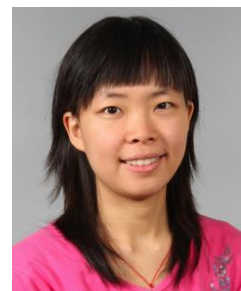
50h

Chapter 2.8



CURRICULUM VITAE**PANG LIJUAN**

Institute of Molecular Pharmacy, University of Basel
 Klingelbergstrasse 50 CH-4056 Basel Switzerland
 Email: lijuan.pang@unibas.ch
 Date of Birth: 03/01/1983
 Nationality: China
 Marital Status: Married

**EDUCATION**

- 05.2010-present **University of Basel**, Basel, Switzerland
 Ph.D. Candidate in Medicinal Chemistry, Thesis advisor: Prof. Dr. Beat Ernst
- 09.2005-01.2008 **Peking University**, Beijing, China
 M.Sc. in Chemical Biology, Thesis advisor: Prof. Dr. Xin-Shan Ye
- 09.2001-07.2005 **Peking University**, Beijing, China
 B.Sc. in Pharmacy

WORK EXPERIENCE

- 08.2009-04.2010 **Bioduro (Beijing) Inc.**, Beijing, China
 R&D Chemist II of drug discovery and development
- 04.2008-04.2009 **Apotex Pharmachem (Tianjin) Inc.**, Tianjin, China
 R&D Assistant Researcher of organic process research & development

PUBLICATIONS

Pang, L.J.; Wang, D.; Zhou, J.; Zhang, L.H.; Ye, X.S. Synthesis of neamine-derived pseudodisaccharides by stereo- and region-selective functional group transformations. *Org. Biomol. Chem.* **2009**, *7*, 4252-4266.

Klein, T.; Abgottspon, D.; Wittwer, M.; Rabbani, S.; Herold, J.; Jiang, X.; Kleeb, S.; Luethi, C.; Scharenberg, M.; Bezençon, J.; Gubler, E.; **Pang, L.**; Smiesko, M.; Cutting, B.; Schwardt, O.; Ernst, B. FimH antagonists for the oral treatment of urinary tract infections: from design and synthesis to in vitro and in vivo evaluation. *J. Med. Chem.* **2010**, *53*, 8627-8641.

Pang, L.; Kleeb, S.; Lemme, K.; Rabbani, S.; Scharenberg, M.; Zalewski, A.; Schädler, F.; Schwardt, O.; Ernst, B. FimH antagonists: structure-activity and structure-property relationships for biphenyl α -D-mannopyranosides. *ChemMedChem* **2012**, *7*, 1404-1422. (VIP Paper and a Back Cover Paper)

Scharenberg, M.; Jiang, X.; **Pang, L.**; Navarra, G.; Rabbani, S.; Binder, F.; Schwardt, O.; Ernst, B. Kinetic properties of carbohydrate – lectin interactions: FimH antagonists. *ChemMedChem* **2014**, *9*, 78-83.

Kleeb, S.; **Pang, L.** (co-first author); Mayer, K.; Eris, D.; Sigl, A.; Preston, R.C.; Zihlmann, P.; Sharpe, T.; Jakob, R.P.; Abgottspon, D.; Hutter, A.S.; Scharenberg, M.; Jiang, X.; Navarra, G.; Rabbani, S.; Smiesko, M.; Lüdin, N.; Bezençon, J.; Schwardt, O.; Maier, T.; Ernst, B. FimH antagonists: Bioisosteres to improve the in vitro and in vivo PK/PD profile. *J. Med. Chem.* **2015**, *58*, 2221-2239.

PRESENTATIONS

“Anti-adhesion therapy for urinary tract infections: A Study on lead optimization of FimH antagonists”, Oral Presentation, *Joint Meeting of the Society for Glycobiology (SFG) and the Japanese Society of Carbohydrate Research (JSCR) - 2014*, Honolulu, Hawaii, USA, November 2014.

“FimH antagonists for the treatment of urinary tract infections”, Oral Presentation, *Swiss Chemical Society – 2012 Fall Meeting*, Zürich, Switzerland, September 2012.

“FimH antagonists: structural-activity relationship (SAR) on biphenyl α -D-mannopyranosides”, Poster Presentation, *Annual Research Meeting of Department of Pharmaceutical Sciences - 2014*, University of Basel, Basel, Switzerland, February 2014.

“Bioisosteric modifications to extend the anti-adhesive effect of FimH antagonists”, Poster Presentation, *Swiss Chemical Society – 2013 Fall Meeting*, Zürich, Switzerland, September 2013.

“Lead optimization: bioisosteric modifications on FimH antagonists”, Poster Presentation, *Gordon Research Conference Carbohydrates – 2013*, West Dover, Vermont, USA, June 2013.

“FimH antagonists for the treatment of urinary tract infections”, Poster Presentation, *26th International Carbohydrate Symposium*, Madrid, Spain, July 2012.

“FimH antagonists: structural-activity and structure-property relationships for biphenyl α -D-mannopyranosides”, Poster Presentation, *Annual Research Meeting of Department of Pharmaceutical Sciences - 2012*, University of Basel, Basel, Switzerland, February 2012.

PROFESSIONAL TRAINING

10th Swiss Course on Medicinal Chemistry, Division for Medicinal Chemistry of the Swiss Chemical Society, Leysin, Switzerland, October 14-19, 2012.

Graduate Course “Key Issues in Drug Discovery & Development”, Basel, Switzerland, January 13-February 04, 2011.

Project Management Course “Introduction into Project-Management”, Project-Management Basic Training, University of Basel, Basel, Switzerland, January 23-24, 2014.

TEACHING EXPERIENCE

01.2011-06.2011 **University of Basel**, Institute of Molecular Pharmacy
Tutor of master thesis, Thesis Title: Development of a rapid diagnostic system for the detection of bacterial infections

2010-2013
(Fall semesters) **University of Basel**, Department of Pharmaceutical Sciences
Assistant of Practical Course, Course Name: Pharm. Chem. II CombiChem

HONORS AND AWARDS

12.2013 **Swiss National Science Foundation**, EarlyPostdoc. Fellowship

05.2011, 08.2013 **University of Basel**, Awarded Travel Fund for Young Academics

10.2005 **Ministry of Public Health of China**, Scholarship for Outstanding Medical Students

2002-2005 **Peking University**, Prize of Annual Outstanding Medical Students, Scholarship for Outstanding Medical Students

LANGUAGE AND ADDITIONAL SKILLS

Languages: Mandarin Chinese (mother tongue), English (C1 level), German (A2/B1 level)

Computer literacy: experienced with Microsoft Office, ChemOffice, SciFinder, Beilstein, MestReNova (NMR analysis), PyMOL, BioX, VMD (molecular graphics), VirtualToxLab, VirtualDesignLab (molecular modeling)